Advances in Experimental Medicine and Biology 854

Catherine Bowes Rickman
Matthew M. LaVail
Robert E. Anderson
Christian Grimm
Joe Hollyfield
John Ash *Editors*

Retinal Degenerative Diseases

Mechanisms and Experimental Therapy

Springer

Advances in Experimental Medicine and Biology

Volume 854

Advances in Experimental Medicine and Biology presents multidisciplinary and dynamic findings in the broad fields of experimental medicine and biology. The wide variety in topics it presents offers readers multiple perspectives on a variety of disciplines including neuroscience, microbiology, immunology, biochemistry, biomedical engineering and cancer research. *Advances in Experimental Medicine and Biology* has been publishing exceptional works in the field for over 30 years and is indexed in Medline, Scopus, EMBASE, BIOSIS, Biological Abstracts, CSA, Biological Sciences and Living Resources (ASFA-1), and Biological Sciences. The series also provides scientists with up to date information on emerging topics and techniques.
2013 Impact Factor: 2.012.

More information about this series at http://www.springer.com/series/5584

Catherine Bowes Rickman • Matthew M. LaVail
Robert E. Anderson • Christian Grimm
Joe Hollyfield • John Ash
Editors

Retinal Degenerative Diseases

Mechanisms and Experimental Therapy

Springer

Editors
Catherine Bowes Rickman
Department of Ophthalmology
Duke University Medical Center
Durham
North Carolina
USA

Matthew M. LaVail
Beckman Vision Center
University of California, San Francisco
School of Medicine
San Francisco
California
USA

Robert E. Anderson
Dean A. McGee Eye Inst.
University of Oklahoma Health Science Center
Oklahoma City
Oklahoma
USA

Christian Grimm
University Hospital Zurich
Zurich
Switzerland

Joe Hollyfield
Case Western Reserve University Cleveland Clinic Lerner College of Med
Cleveland
Ohio
USA

John Ash
Univ of Florida Dept of Ophthalmology/Arb R112
Gainesville
Florida
USA

Supplementary material to this book can be accessed at http://link.springer.com/book/10.1007/978-3-319-17121-0

ISSN 0065-2598 ISSN 2214-8019 (electronic)
Advances in Experimental Medicine and Biology
ISBN 978-3-319-17120-3 ISBN 978-3-319-17121-0 (eBook)
DOI 10.1007/978-3-319-17121-0

Library of Congress Control Number: 2015938602

Springer Cham Heidelberg New York Dordrecht London

Printed on acid-free paper

Springer International Publishing AG Switzerland is part of Springer Science+Business Media (www.springer.com)

Dedication

Holly Jo Whiteside

Holly Whiteside has been an extraordinary RD Symposium Coordinator for 16 years, from RD2000 through the RD2014 meeting. For most of these symposia, she managed all aspects of the meetings, their selection sites, the design and maintenance of the meeting website, all interactions with participants and Travel Awardees, as well as assisting the preparation and submission of the conference grant from the NEI and the proceedings volume. For many, Holly has been the face of the meetings, and she showed remarkable dedication to the meetings and their participants, often giving much of her personal time to be sure the symposia were successful. In so doing, she helped mostly during the period of doubling the size of the biennial meeting. Holly has decided to step down from her involvement with the RD Symposia to devote her time to other aspects of her research and administrative tasks and her personal interests. We will miss her and are honored to dedicate this proceedings volume to her.

Preface

The International Symposia on Retinal Degeneration have been held in conjunction with the biennial meeting of the International Society of Eye Research (ISER) since 1984. These RD Symposia have allowed basic and clinician scientists from around the world to convene and present their new research findings. They have been organized to allow substantial time for discussions and one-on-one interactions in a relaxed atmosphere, where international friendships and collaborations can be fostered.

The XVI International Symposium on Retinal Degeneration (also known as RD2014) was held from July 13–18, 2014 at the Asilomar Conference Center in the beautiful city of Pacific Grove, California, USA. The meeting brought together 272 basic and clinician scientists, retinal specialists in ophthalmology, and trainees in the field from all parts of the world. In the course of the meeting, 43 platform and 159 poster presentations were given, and a majority of these are presented in this proceedings volume. New discoveries and state of the art findings from most research areas in the field of retinal degenerations were presented. This was the largest of all of the RD Symposia, with the greatest number of attendees and presentations.

The RD2014 meeting was highlighted by three special keynote lectures. The first was given by **John Flannery,** PhD, of the University of California, Berkeley, Berkeley, CA. Dr. Flannery discussed "Engineering AAV vectors to target specific functional subclasses of retinal neurons and glia." Dr. Flannery's talk was the first named keynote lecture of the RD Symposia in 32 years, the Edward H. Gollob Lecture, named for the President of the Foundation Fighting Blindness. The second keynote lecture was given by **Sally Temple,** PhD, Director of the Neural Stem Cell Institute, Regenerative Research Foundation, Rensselaer, NY. Dr. Temple discussed "Endogenous RPE stem cells, their surprising plasticity and implications for therapeutic applications." The third keynote lecture was given by **Samuel G. Jacobson,** MD, PhD, of the University of Pennsylvania, Philadelphia, PA. Dr. Jacobson discussed "A treatment trial for an inherited retinal degeneration: what have we learned?"

The scientific meeting ended with a "Welcome to RD2016" by Prof. Nagahisa Yoshimura of Kyoto, Japan, along with the organizers primarily responsible for the meeting, Drs. John Ash and Robert E. Anderson.

We thank the outstanding management and staff of the beautiful Asilomar Conference Center for their assistance in making this an exceptionally smooth-running conference and a truly memorable experience for all of the attendees. These included, in particular, **Suzan Carabarin**, **Vivian Garcia, Sammy Ramos** and **Carlene Miller**. We also thank **Kelly Gilford** and **Jason McIntosh** for providing audio/visual equipment and services that resulted in a flawless flow of platform presentations. We thank **Steve Henry** of Associated Hosts, Inc. for planning and implementing transportation of most of the attendees to and from the Asilomar meeting venue, the memorable whale watching excursion, as well as for providing the dynamic "Beach Boys Band" for the end-of-meeting Gala for a truly California experience. Lastly, we thank **Franz Badura** of Pro Retina Germany for serenading the attendees at the Gala with his beautiful trumpet solos.

The Symposium received international financial support from a number of organizations. We are particularly pleased to thank The Foundation Fighting Blindness, Columbia, Maryland, for its continuing support of this and all previous biennial Symposia, without which we could not have held these important meetings. In addition, for the seventh time, the National Eye Institute of the National Institutes of Health contributed in a major way to the meeting. In the past, funds from these two organizations allowed us to provide 25–35 Travel Awards to young investigators and trainees working in the field of retinal degenerations. However, the response to the Travel Awards program was extraordinary, with 110 applicants, many more than in the past. For this reason, we sought additional support for the Travel Awards program. We are extremely appreciative for the contributions from Pro Retina Germany, the Fritz Tobler Foundation Switzerland and from Ed and Sandy Gollob. In total, we were able to fund 49 Travel Awards, the largest number ever an RD Symposia held in North America. We are grateful to the BrightFocus Foundation, which supported the important poster sessions. Many of the contributing foundations sent members of their organizations to attend the meeting. Their participation and comments in the scientific sessions were instructive to many, offering new perspectives to some of the problems being discussed. The Travel Awardees were selected on the basis of 9 independent scores of their submitted abstracts, 6 from each of the organizers and 3 from the other members of the Travel Awards Committee for RD2014, Drs. Jacque Duncan, Machelle Pardue and XianJie Yang.

We also acknowledge the diligent and outstanding efforts of Ms. **Holly Whiteside,** who along with Dr. **John Ash**, carried out most of the administrative aspects of the RD2014 Symposium, and designed and maintained the meeting website. Holly is the Administrative Manager of Dr. Anderson's laboratory at the University of Oklahoma Health Sciences Center. For this Symposium, Ms. **Melody Marcum**, Director of Development of the Dean McGee Eye Institute, worked closely and extensively in selecting and negotiating the meeting venue, and in planning the meals, entertainment and various events. Melody and Holly were crucial to the success of the RD2014 symposium. Also, Dr. **Michael Matthes** in Dr. LaVail's laboratory

played a major role in all aspects in the production of this volume, along with the assistance of Ms. **Cathy Lau-Villacorta**, also in Dr. LaVail's laboratory.

Finally, we honor the monumental efforts of Holly Whiteside. Holly has been the RD Symposium Coordinator since 2000, and during that time she has been the "face" of the RD Symposia. She has been responsible for virtually all of the administrative aspects of the RD Symposia for 16 years, and most repeat attendees feel a close relationship with Holly. She is now stepping back from the efforts of the RD Symposia to pursue personal and professional avenues. We have valued Holly's efforts enormously over these years, and we are proud to dedicate this volume to her.

Catherine Bowes Rickman
Matthew M. LaVail
Robert E. Anderson
Christian Grimm
Joe G. Hollyfield
John D. Ash

Travel Awards

We gratefully acknowledge National Eye Institute, NIH, USA; the Foundation Fighting Blindness, USA; Pro Retina Germany; the Fritz Tobler Foundation, Switzerland; and Ed and Sandy Gollob for their generous support of 49 Travel Awards to allow young investigators and trainees to attend this meeting. Eligibility was restricted to graduate students, postdoctoral fellows, instructors and assistant professors actively involved in retinal degeneration research. These awards were based on the quality of the abstract submitted by each application. Catherine Bowes Rickman chaired the Travel Awards Committee of 9 senior retinal degeneration investigators, the 6 organizers and Drs. Jacque Duncan, Machelle Pardue and Xian-Jie Yang. The travel awardees are listed below.

Carolina Abrahan
University of Florida, Gainesville, USA

Martin-Paul Agbaga
University of Oklahoma HSC, Oklahoma City, USA

Monica Aguila
University College of London, London, United Kingdom

Marcel Alavi
University of California, San Francisco, San Francisco, USA

Seifollah Azadi
University of Oklahoma HSC, Oklahoma City, USA

Emran Bashar
University of British Columbia, Vancouver, Canada

Lea Bennett
Retina Foundation of the Southwest, Dallas, USA

Manas Biswal
University of Florida, College of Medicine, Gainesville, USA

Shannon Boye
University of Florida, Gainesville, USA

Melissa Calton
Stanford University School of Medicine, San Francisco, USA

Livia Carvalho
Schepens Eye Research Institute/MEEI, Boston, USA

Wei-Chieh Chiang
University of California, San Diego, LaJolla, USA

Rob Collin
Radboud University Medical Centre, Nijmegen, Netherlands

Janise Deming
University of Southern California, Los Angeles, USA

Louise Downs
University of Pennsylvania, Philadelphia, USA

Lindsey Ebke
Cleveland Clinic Cole Eye Institute, Cleveland, USA

Michael Elliott
University of Oklahoma HSC, Oklahoma City, USA

Michael Gale
Oregon Health and Science University, Portland, USA

Xavier Gerard
Institut Imagine, Paris, France

Rosario Fernandez Godino
MEEI-Harvard Medical School, Boston, USA

Christin Hanke
University of Utah, Salt Lake City, USA

Stefanie Hauck
Helmholtz Zentrum Müchen, Neuherberg, Germany

Roni Hazim
University of California, Los Angeles, Los Angeles, USA

Claire Hippert
UCL Institute of Ophthalmology, London, United Kingdom

John Hulleman
Univ. of Texas Southwestern Medical Center, Dallas, USA

Xiaojie Ji
The Jackson Laboratory, Bar Harbor, USA

Mark Kleinman
University of Kentucky, Lexington, USA

Elod Kortvely
Universität Tübingen, Tübingen, Germany

Ruanne Lai
University of British Columbia, Vancouver, Canada

Christopher Langlo
Medical College of Wisconsin, Milwaukee, USA

Jennifer Lentz
Louisiana State University HSC, New Orleans, USA

Yao Li
Columbia University, New York City, USA

Hongwei Ma
University of Oklahoma HSC, Oklahoma City, USA

Alexander Marneros
Massachusetts General Hospital, Charlestown, USA

Alex McKeown
University of Alabama at Birmingham, Birmingham, USA

Claudia Müller
Fordham University, New York City, USA

Celia Parinot
Institut de la Vision, Paris, France

David Parfitt
UCL Institute of Ophthalmology, London, United Kingdom

Diana Pauly
Universität Regensburg, Regensburg, Germany

Beryl Royer-Bertrand
University of Lausanne, Lausanne, Switzerland

Matt Rutar
The Australian National University, Canberra, Australia

Marijana Samardzija
University of Zurich, Schlieren, Switzerland

Kimberly Toops
University of Wisconsin—Madison, Madison, USA

Christopher Tracy
University of Missouri, School of Medicine, Columbia, USA

Mallika Valapala
Johns Hopkins University School of Medicine, Baltimore, USA

Lei Wang
Johns Hopkins University, Baltimore, USA

Qingjie Wang
Regenerative Research Foundation, Rensselaer, USA

Wenjun Xiong
Harvard Medical School, Boston, USA

Lei Xu
University of Florida, Gainesville, USA

Contents

Contributors

Toshiaki Abe Division of Clinical Cell Therapy, Center for Advanced Medical Research and Development (ART), Tohoku University Graduate School of Medicine, Sendai, Japan

Mortada A. Abozaid Department of Ophthalmology, The Eye Institute, Medical College of Wisconsin, Milwaukee, WI, USA

Department of Ophthalmology, Sohag University, Sohag, Egypt

Carolina Abrahan Department of Environmental Horticulture Research, University of Florida, Gainesville, FL, USA

Martin-Paul Agbaga Department of Ophthalmology, Dean McGee Eye Institute, University of Oklahoma Health Sciences Center, Oklahoma City, OK, USA

Mònica Aguilà Department of Ocular Biology and Therapeutics, UCL Institute of Ophthalmology, London, UK

Gustavo D Aguirre Section of Ophthalmology, Department of Clinical Studies, School of Veterinary Medicine, University of Pennsylvania, Philadelphia, PA, USA

Kelly Ahern Department of Ophthalmology, University of California, San Francisco, CA, USA

Chulbul M. Ahmed Department of Molecular Genetics and Microbiology, University of Florida College of Medicine, Gainesville, FL, USA

Marcel V. Alavi Department of Ophthalmology, University of California, San Francisco, San Francisco, CA, USA

Muayyad R. Al-Ubaidi Department of Cell Biology, University of Oklahoma Health Sciences Center, Oklahoma city, OK, USA

Robert E. Anderson Department of Cell Biology and Ophthalmology, University of Oklahoma Health Sciences Center, Oklahoma City, OK, USA

Dean A. McGee Eye Institute, Oklahoma City, OK, USA

Departments of Ophthalmology and Cell Biology, Dean McGee Eye Institute, University of Oklahoma Health Sciences Center, Oklahoma City, OK, USA

Yvan Arsenijevic Unit of Gene Therapy and Stem Cell Biology, Department of Ophthalmology, University of Lausanne, Lausanne, Switzerland

John D. Ash Department of Ophthalmology Research, University of Florida, Gainesville, FL, USA

Adrian Au Department of Ophthalmic Research-i31, Cole Eye Institute, Cleveland Clinic, Cleveland, OH, USA

Moe H. Aung Department of Ophthalmology, Emory University School of Medicine, Atlanta, GA, USA

Rehab R&D Center, Research Service (151Oph), Atlanta VA Medical Center, Decatur, GA, USA

Alberto Auricchio Telethon Institute of Genetics and Medicine (TIGEM), Naples, Italy

Cheryl E. Avery Human Genetics Center, School of Public Health, The University of Texas HSC, Houston, TX, USA

Seifollah Azadi Departments of Ophthalmology, Dean McGee Eye Institute, University of Oklahoma Health Sciences Center, Oklahoma City, OK, USA

Wolfgang Baehr Department of Ophthalmology, John A. Moran Eye Center, University of Utah Health Science Center, Salt Lake City, UT, USA

Department of Neurobiology and Anatomy, University of Utah Health Science Center, Salt Lake City, UT, USA

Department of Biology, University of Utah, Salt Lake City, UT, USA

Adam Baker Ottawa Hospital Research Institute, Regenerative Medicine, Ottawa, ON, Canada

Mausumi Bandyopadhyay Departments of Ophthalmology, Medical University of South Carolina, Charleston, SC, USA

Peter Barabas Department of Ophthalmology and Visual Sciences, John A. Moran Eye Institute, University of Utah School of Medicine, Salt Lake City, UT, USA

Maya Barben Laboratory for Retinal Cell Biology, Department of Ophthalmology, University of Zurich, Schlieren, Switzerland

Nicolas G. Bazan Neuroscience Center of Excellence, School of Medicine, Louisiana State University Health Sciences Center, New Orleans, LA, USA

S. Patricia Becerra Section of Protein Structure and Function, Laboratory of Retinal Cell and Molecular Biology, NEI, National Institutes of Health, Bethesda, MD, USA

Craig Beeson MitoChem Therapeutics Inc, Charleston, SC, USA

Departments of Drug Discovery and Biomedical Sciences, Medical University of South Carolina, Charleston, SC, USA

Jean Bennett Scheie Eye Institute, F.M. Kirby Center for Molecular Ophthalmology, University of Pennsylvania, Philadelphia, PA, USA

Lea D. Bennett Retina Foundation of the Southwest, Dallas, TX, USA

Cynthia A. Berlinicke Ophthalmology, Molecular Biology & Genetics, Neuroscience, and Institute of Genetic Medicine, Wilmer Eye Institute, Johns Hopkins University School of Medicine, Baltimore, MD, USA

Andre K. Berner Lexington, KY, USA

Paul S Bernstein Department of Ophthalmology and Visual Sciences, John A. Moran Eye Institute, University of Utah School of Medicine, Salt Lake City, UT, USA

Shagun K. Bhatia Department of Ophthalmology, Emory University School of Medicine, Atlanta, GA, USA

Rehab R&D Center, Research Service (151Oph), Atlanta VA Medical Center, Decatur, GA, USA

Shagun K. Bhatia Ophthalmology, Emory University, Atlanta, GA, USA

David G. Birch The Retina Foundation of the Southwest, Dallas, TX, USA

Manas R Biswal Department of Molecular Genetics and Microbiology, College of Medicine, University of Florida, Gainesville, FL, USA

Susan H. Blanton John P. Hussman Institute for Human Genomics, University of Miami Miller School of Medicine, Miami, FL, USA

Timothy A. Blenkinsop Department of Development and Regenerative Biology, Icahn School of Medicine at Mount Sinai, New York, NY, USA

Jeffrey H. Boatright Department of Ophthalmology, Emory University School of Medicine, Atlanta, GA, USA

Atlanta VA Center of Excellence for Visual and Neurocognitive Rehabilitation, Atlanta VA Medical Center, Decatur, GA, USA

Jeffrey H. Boatright Ophthalmology, Emory University, Atlanta, GA, USA

Dean Bok Jules Stein Eye Institute, University of California, Los Angeles, CA, USA

Michael E Boulton Department of Ophthalmology, Indiana University, Indianapolis, IN, USA

Catherine Bowes Rickman Departments of Ophthalmology and of Cell Biology, Duke University Medical Center, Durham, NC, USA

Sara J. Bowne Human Genetics Center, School of Public Health, The University of Texas HSC, Houston, TX, USA

Shannon E. Boye Departments of Ophthalmology and Molecular Genetics and Microbiology, University of Florida, Gainesville, FL, USA

Barbara M. Braunger Institute of Human Anatomy and Embryology, University of Regensburg, Regensburg, Germany

Russell L. Bromley Translational Research Acceleration Consulting, Templeton, CA, USA

Richard S. Brush Departments of Ophthalmology, Dean McGee Eye Institute, University of Oklahoma Health Sciences Center, Oklahoma City, OK, USA

Jeffrey N. Bryan Department of Veterinary Medicine and Surgery, University of Missouri College of Veterinary Medicine, Columbia, MO, USA

Marie E. Burns Department of Ophthalmology and Vision Science, University of California Davis, Davis, CA, USA

Center for Neuroscience, University of California Davis, Davis, CA, USA

Cell Biology and Human Anatomy, University of California Davis, Davis, CA, USA

Elizabeth D. Cadena Human Genetics Center, School of Public Health, The University of Texas HSC, Houston, TX, USA

Xue Cai Department of Ophthalmology, Dean McGee Eye Institute, University of Oklahoma Health Sciences Center, Oklahoma City, OK, USA

Melissa A. Calton Department of Genetics, Stanford University School of Medicine, Stanford, CA, USA

Marisol Cano Wilmer Eye Institute, Johns Hopkins School of Medicine, Baltimore, MD, USA

Guangwen Cao Department of Epidemiology, Second Military Medical University, Shanghai, China

Joseph Carroll Department of Ophthalmology, The Eye Institute, Medical College of Wisconsin, Milwaukee, WI, USA

Department of Cell Biology, Neurobiology and Anatomy, Medical College of Wisconsin, Milwaukee, WI, USA

Department of Biophysics, Medical College of Wisconsin, Milwaukee, WI, USA

Livia S. Carvalho Department of Ophthalmology, Ocular Genomics Institute, Schepens Eye Research Institute, Massachusetts Eye and Ear Infirmary, Harvard Medical School, Harvard University, Boston, MA, USA

Leilani J. Castaner Department of Ophthalmology, University of Missouri School of Medicine, Mason Eye Institute, Columbia, MO, USA

Constance Cepko Departments of Genetics and Ophthalmology, Howard Hughes Medical Institute, Harvard Medical School, Boston, MA, USA

Lawrence Chan Department of Ophthalmology, Columbia University Medical Center, Columbia University, New York, NY, USA

Bo Chang The Jackson Laboratory, Bar Harbor, ME, USA

Jeremy R. Charette The Jackson Laboratory, Bar Harbor, ME, USA

Michael E. Cheetham Department of Ophthalmology, Indiana University, London, UK

Ocular Bioloy and Therapeutics, UCL Institute of Ophthalmology, London, UK

Wei-Chieh Chiang Department of Pathology, University of California, San Diego, CA, USA

Mayur Choudhary Departments of Ophthalmology and Pathology, Albert Eye Research Institute, Duke University, Durham, NC, USA

Micah A. Chrenek Department of Ophthalmology, Emory University School of Medicine, Atlanta, GA, USA

Ophthalmology, Emory University, Atlanta, GA, USA

Michelle Chyn Wilmer Eye Institute, Johns Hopkins School of Medicine, Baltimore, MD, USA

Vincent Ciavatta Department of Ophthalmology, Emory University School of Medicine, Atlanta, GA, USA

Rehab R&D Center, Research Service (151Oph), Atlanta VA Medical Center, Decatur, GA, USA

Vincent T. Ciavatta Department of Ophthalmology, Emory University School of Medicine, Atlanta, GA, USA

Atlanta VA Center of Excellence for Visual and Neurocognitive Rehabilitation, Atlanta VA Medical Center, Decatur, GA, USA

Artur V. Cideciyan Scheie Eye Institute, Department of Ophthalmology, Perelman School of Medicine, University of Pennsylvania, Philadelphia, PA, USA

Rob W. J. Collin Department of Human Genetics (855), Radboud Institute for Molecular Life Sciences Radboud University Medical Center, Nijmegen, GA, The Netherlands

Shannon M. Conley Department of Cell Biology, University of Oklahoma Health Sciences Center, Oklahoma City, OK, USA

Stuart G. Coupland Ottawa Hospital Research Institute, Regenerative Medicine, Ottawa, ON, Canada

Department of Cellular and Molecular Medicine, University of Ottawa, Ottawa, ON, Canada

Department of Ophthalmology, University of Ottawa, Ottawa, ON, Canada

Cheryl Mae Craft Departments of Ophthalmology and Cell & Neurobiology, USC Eye Institute, Keck School of Medicine of the University of Southern California, Institute for Genetic Medicine, Los Angeles, CA, USA

Priscila P. Cunha Department of Ophthalmology, Emory University School of Medicine, Atlanta, GA, USA

Stephen P. Daiger Human Genetics Center, School of Public Health, The University of Texas HSC, Houston, TX, USA

Ruiz Department of Ophthalmology and Visual Science, Medical School, The University of Texas Health Science Center, Houston, TX, USA

School of Public Health, University of Texas Health Science Center, Houston, TX, USA

Conor Daly School of Biomolecular and Biomedical Science, Conway Institute, University College Dublin, Dublin, Ireland

Monte A Del Monte Department of Ophthalmology, University of Michigan Medical Center, Ann Arbor, MI, USA

François C. Delori Department of Ophthalmology, Harvard Medical School, Schepens Eye Research Institute, Boston, MA, USA

Janise D. Deming Departments of Ophthalmology, USC Eye Institute, Keck School of Medicine of the University of Southern California, Institute for Genetic Medicine, Los Angeles, CA, USA

Wen-Tao Deng Department of Ophthalmology, College of Medicine, University of Florida, Gainesville, FL, USA

Kristin Denton Department of Biology, Texas A&M University, College Station, TX, USA

Tanja Diemer UCLA School of Medicine, Jules Stein Eye Institute, Los Angeles, CA, USA

Xi-Qin Ding The Department of Cell Biology, University of Oklahoma Health Sciences Center, Oklahoma City, OK, USA

Louise M Downs Section of Ophthalmology, Department of Clinical Studies, School of Veterinary Medicine, University of Pennsylvania, Philadelphia, PA, USA

Adam M. Dubis UCL Institute of Ophthalmology, University College London, London, UK

Moorfields Eye Hospital, London, UK

Tobias Duncker Department of Ophthalmology, Harkness Eye Institute, Columbia University Medical Center, New York, NY, USA

Lindsey A. Ebke Department of Ophthalmic Research-i31, Cole Eye Institute, Cleveland Clinic, Cleveland, OH, USA

Katayoon B Ebrahimi Wilmer Eye Institute, Johns Hopkins School of Medicine, Baltimore, MD, USA

Janis T. Eells Department of Biomedical Sciences, University of Wisconsin-Milwaukee, Milwaukee, WI, USA

Michael H. Elliott Department of Ophthalmology, University of Oklahoma Health Sciences Center, Oklahoma City, OK, USA

Oklahoma Center for Neuroscience, University of Oklahoma Health Sciences Center, Oklahoma City, OK, USA

Department of Physiology, University of Oklahoma Health Sciences Center, Oklahoma City, OK, USA

Dean A. McGee Eye Institute, University of Oklahoma Health Sciences Center, Oklahoma City, OK, USA

Yun Sung Eom Biomedical Engineering, Viterbi School of Engineering, University of Southern California, Los Angeles, CA, USA

Victor V. Ermilov Department of Forensic Medicine and Pathology, Volgograd State Medical University, Volgograd, Russia

Julian Esteve-Rudd UCLA School of Medicine, Jules Stein Eye Institute, Los Angeles, CA, USA

Abigail T. Fahim Department of Ophthalmology and Visual Sciences, University of Michigan, Ann Arbor, MI, USA

Debora B. Farber Stein Eye Institute, David Geffen School of Medicine, University of California Los Angeles, Los Angeles, CA, USA

Department of Ophthalmology, David Geffen School of Medicine, University of California Los Angeles, Los Angeles, CA, USA

Molecular Biology Institute, Paul Boyer Hall, University of California Los Angeles, Los Angeles, CA, USA

Brain Research Institute, University of California Los Angeles, Los Angeles, CA, USA

Tatiana Favez IRO—Institute for Research in Ophthalmology, Sion, Switzerland

Shu Feng Department of Ophthalmology, Casey Eye Institute, Oregon Health & Science University, Portland, OR, USA

Rosario Fernandez-Godino Ocular Genomics Institute, Massachusetts Eye and Ear Infirmary, Harvard Medical School, Boston, MA, USA

Silvia C. Finnemann Department of Biological Sciences, Center for Cancer, Genetic Diseases and Gene Regulation, Fordham University, Bronx, NY, USA

Joan K. Fisher Foundation Fighting Blindness, Columbia, MD, USA

Joseph Fogerty Department of Ophthalmic Research, Cole Eye Institute, Cleveland Clinic, Cleveland, OH, USA

Jeanne M. Frederick Department of Ophthalmology, John A. Moran Eye Center, University of Utah Health Science Center, Salt Lake City, UT, USA

John A. Fuller Ophthalmology, Molecular Biology & Genetics, Neuroscience, and Institute of Genetic Medicine, Wilmer Eye Institute, Johns Hopkins University School of Medicine, Baltimore, MD, USA

Robert S. Fulton The Genome Institute, Washington University School of Medicine, St. Louis, MO, USA

Yuka Furutani Department of Ophthalmology and Visual Sciences, Kyoto University Graduate School of Medicine, Kyoto, Japan

Michael J. Gale Department of Ophthalmology, Casey Eye Institute, Oregon Health & Science University, Portland, OR, USA

Alejandro Garanto Department of Human Genetics, Radboud Institute for Molecular Life Sciences Radboud University Medical Center, Nijmegen, The Netherlands

Donita L. Garland Ocular Genomics Institute, Massachusetts Eye and Ear Infirmary, Harvard Medical School, Boston, MA, USA

Philipp Geiger Laboratory for Retinal Cell Biology, Department of Ophthalmology, University of Zurich, Schlieren, Switzerland

Xavier Gerard Laboratory of Genetics in Ophthalmology, INSERM UMR1163 - Imagine Institute, Paris Descartes - Sorbonne Paris Cité University, Paris, France

Preston E. Girardot Department of Ophthalmology, Emory University School of Medicine, Atlanta, GA, USA

Marissa A. Gogniat Department of Ophthalmology, Emory University School of Medicine, Atlanta, GA, USA

Atlanta VA Center of Excellence for Visual and Neurocognitive Rehabilitation, Atlanta VA Medical Center, Decatur, GA, USA

Nestor Mas Gomez Department of Anatomy and Cell Biology, School of Dental Medicine, University of Pennsylvania, Philadelphia, PA, USA

Sandeep Gopalakrishnan College of Nursing, University of Wisconsin-Milwaukee, Milwaukee, WI, USA

Marina S. Gorbatyuk Department of Vision Sciences, University of Alabama at Birmingham, Birmingham, AL, USA

Aruna Gorusupudi Department of Ophthalmology and Visual Sciences, John A. Moran Eye Institute, University of Utah School of Medicine, Salt Lake City, UT, USA

Norimoto Gotoh Department of Ophthalmology and Visual Sciences, Kyoto University Graduate School of Medicine, Kyoto, Japan

Anna B. Graca F. Hoffman La Roche, Basel, Switzerland

Maria B. Grant Department of Ophthalmology, Indiana University, Indianapolis, IN, USA

Christian Grimm Laboratory for Retinal Cell Biology, Department of Ophthalmology, University of Zurich, Schlieren, Switzerland

Hans E. Grossniklaus Ophthalmology, Emory University, Atlanta, GA, USA

Fabian Gruhn Research Unit Protein Science, Helmholtz Zentrum München, German Research Center for Environmental Health GmbH, Munich, Germany

Xiaowu Gu Department of Ophthalmology, University of Oklahoma Health Sciences Center, Oklahoma City, OK, USA

Oklahoma Center for Neuroscience, University of Oklahoma Health Sciences Center, Oklahoma City, OK, USA

Dean A. McGee Eye Institute, University of Oklahoma Health Sciences Center, Oklahoma City, OK, USA

Stephanie A. Hagstrom Department of Ophthalmic Research-i31, Cole Eye Institute, Cleveland Clinic, Cleveland, OH, USA

Department of Ophthalmology, Cleveland Clinic Lerner College of Medicine of Case Western Reserve University, Cleveland, OH, USA

Stephanie A. Hagstrom Department of Ophthalmic Research, Cole Eye Institute, Cleveland Clinic, Cleveland, OH, USA

Department of Ophthalmology, Cleveland Clinic Lerner College of Medicine of Case Western Reserve University, Cleveland, OH, USA

John Hamilton Ottawa Hospital Research Institute, Regenerative Medicine, Ottawa, ON, Canada

Hans-Peter Hammes 5th Medical Clinic, Medical Faculty Mannheim, University of Heidelberg, Mannheim, Germany

Moon K. Han Rehab R&D Center, Research Service (151Oph), Atlanta VA Medical Center, Decatur, GA, USA

Department of Ophthalmology, Emory University School of Medicine, Atlanta, GA, USA

Atlanta VA Center of Excellence for Visual and Neurocognitive Rehabilitation, Atlanta VA Medical Center, Decatur, GA, USA

James T Handa Wilmer Eye Institute, Johns Hopkins School of Medicine, Baltimore, MD, USA

Adam Hanif Department of Ophthalmology, Emory University School of Medicine, Atlanta, GA, USA

Atlanta VA Center of Excellence for Visual and Neurocognitive Rehabilitation, Atlanta VA Medical Center, Decatur, GA, USA

Christin Hanke-Gogokhia Department of Physical Biochemistry, University of Potsdam, Potsdam, Germany

Department of Ophthalmology, John A. Moran Eye Center, University of Utah Health Science Center, Salt Lake City, UT, USA

Stefanie M Hauck Research Unit Protein Science, Helmholtz Zentrum München, German Research Center for Environmental Health GmbH, Munich, Germany

Research Unit Protein Science, Helmoltz Zentrum München, Neuherberg, Germany

William W. Hauswirth Department of Ophthalmology, College of Medicine, University of Florida, Gainesville, FL, USA

Roni Hazim UCLA School of Medicine, Jules Stein Eye Institute, Los Angeles, CA, USA

Wanda Hicks The Jackson Laboratory, Bar Harbor, ME, USA

Claire Hippert F. Hoffman La Roche, Basel, Switzerland

Suguru Hisano Department of Clinical Laboratory Sciences, Department of Molecular Neurobiology, Graduate School of Medical Science, Kanazawa University, Kanazawa, Japan

Suguru Hisano Department of Clinical Laboratory

Sciences, Graduate School of Medical Science, Kanazawa University, Kanazawa, Japan

Stacey Hose Department of Ophthalmology, Johns Hopkins University School of Medicine, Baltimore, MD, USA

Jane Hu Jules Stein Eye Institute, University of California, Los Angeles, CA, USA

Wei Chieh Huang Scheie Eye Institute, Department of Ophthalmology, Perelman School of Medicine, University of Pennsylvania, Philadelphia, PA, USA

John D. Hulleman Departments of Ophthalmology and Pharmacology, University of Texas Southwestern Medical Center, Dallas, TX, USA

David R. Hyde Department of Biological Sciences and the Center for Zebrafish Research, University of Notre Dame, Notre Dame, IN, USA

Cristhian J Ildefonso Department of Molecular Genetics and Microbiology, College of Medicine, University of Florida, Gainesville, FL, USA

James Inglese NCATS, NHGRI, National Institutes of Health, Rockville, MD, USA

Samuel G. Jacobson Scheie Eye Institute, Department of Ophthalmology, Perelman School of Medicine, University of Pennsylvania, Philadelphia, PA, USA

Cheryl A. Jensen Department of Ophthalmology, University of Missouri School of Medicine, Mason Eye Institute, Columbia, MO, USA

Xiaojie Ji The Jackson Laboratory, Bar Harbor, ME, USA

Graduate School of Biomedical Sciences and Engineering, University of Maine, Orono, USA

Mei Jiang UCLA School of Medicine, Jules Stein Eye Institute, Los Angeles, CA, USA

Yi Jiang Mathematics and Statistics, Georgia State University, Atlanta, GA, USA

Heather H. Jin Department of Biology, Washington University, St. Louis, MO, USA

Minghao Jin Department of Ophthalmology and Neuroscience Center, Louisiana State University Health Sciences Center, New Orleans, LA, USA

Jessica L. Johnson Department of Ophthalmology, Emory University School of Medicine, Atlanta, GA, USA

Victory Joseph Department of Pathology, University of California, San Diego, CA, USA

Hirokazu Kaji Department of Bioengineering and Robotics, Tohoku University Graduate School of Engineering, Sendai, Japan

Yogita Kanan Department of Cell Biology, University of Oklahoma Health Sciences Center, Oklahoma City, OK, USA

Satoru Kato Department of Molecular Neurobiology, Graduate School of Medical Science, Kanazawa University, Kanazawa, Japan

Diana Katsman Stein Eye Institute, David Geffen School of Medicine, University of California Los Angeles, Los Angeles, CA, USA

Department of Ophthalmology, David Geffen School of Medicine, University of California Los Angeles, Los Angeles, CA, USA

Martin L. Katz Department of Ophthalmology, University of Missouri School of Medicine, Mason Eye Institute, Columbia, MO, USA

Ryan A. Kelley Department of Cell Biology, University of Oklahoma Health Sciences Center, Oklahoma city, OK, USA

Cristina Kendall Department of Ophthalmology, Emory University School of Medicine, Atlanta, GA, USA

Breandán N. Kennedy School of Biomolecular and Biomedical Science, Conway Institute, University College Dublin, Dublin, Ireland

Mark D. Kirk Division of Biological Sciences, University of Missouri, Columbia, MO, USA

Mark E. Kleinman Department of Ophthalmology and Visual Sciences, University of Kentucky, Lexington, KY, USA

Daniel C. Koboldt The Genome Institute, Washington University School of Medicine, St. Louis, MO, USA

Robert K. Koenekoop McGill Ocular Genetics Laboratory, Departments of Paediatric Surgery, Human Genetics and Ophthalmology, Montreal Children's Hospital, McGill University Health Center, Montreal, QC, Canada

Yoshiki Koriyama Graduate School and Faculty of Pharmaceutical Sciences, Suzuka University of Medical Science, Suzuka, Japan

Graduate School and Faculty of Pharmaceutical Sciences, 3500-3 Minamitamagaki, Suzuka University of Medical Sciences, Suzuka, Mie, Japan

Elod Kortvely Division of Experimental Ophthalmology, University of Tuebingen, Tuebingen, Germany

Piyush C Kothary Department of Ophthalmology, University of Michigan Medical Center, Ann Arbor, MI, USA

Mark P. Krebs The Jackson Laboratory, Bar Harbor, ME, USA

David Krizaj Department of Ophthalmology and Visual Sciences, John A. Moran Eye Institute, University of Utah School of Medicine, Salt Lake City, UT, USA

Departments of Ophthalmology & Visual Sciences, John A. Moran Eye Institute and Neurobiology & Anatomy, Univ. of Utah School of Medicine, Salt Lake City, UT, USA

Laura B. Kuhn Institute of Human Genetics, University of Regensburg, Regensburg, Germany

Masafumi Kurimoto Department of Ophthalmology, Kyoto Katsura Hospital, Kyoto, Japan

Manuela Lahne Department of Biological Sciences and the Center for Zebrafish Research, University of Notre Dame, Notre Dame, IN, USA

Aparna Lakkaraju Department of Ophthalmology and Visual Sciences, School of Medicine and Public Health, University of Wisconsin-Madison, Madison, WI, USA

McPherson Eye Research Institute, University of Wisconsin-Madison, Madison, WI, USA

Division of Pharmaceutical Sciences, School of Pharmacy, University of Wisconsin-Madison, Madison, WI, USA

Mandy L. Lambros Free Radical Biology and Aging Program, Oklahoma Medical Research Foundation, Oklahoma City, OK, USA

Department of Cell Biology, University of Oklahoma Health Sciences Center, Oklahoma City, OK, USA

Christopher S. Langlo Department of Cell Biology, Neurobiology and Anatomy, Medical College of Wisconsin, Milwaukee, WI, USA

Matthew M. LaVail Departments of Anatomy and Ophthalmology, University of California, San Francisco, CA, USA

Beckman Vision Center, UCSF School of Medicine, San Francisco, CA, USA

Eric C. Lawson Department of Ophthalmology, Emory University School of Medicine, Atlanta, GA, USA

Rehab R&D Center, Research Service (151Oph), Atlanta VA Medical Center, Decatur, GA, USA

Eric C. Lawson Department of Ophthalmology, Emory University School of Medicine, Atlanta, GA, USA

Atlanta VA Center of Excellence for Visual and Neurocognitive Rehabilitation, Atlanta VA Medical Center, Decatur, GA, USA

Yun Z. Le Department of Endocrinology and Diabetes, University of Oklahoma Health Science Center, Oklahoma city, OK, USA

Yun-Zheng Le Departments of Medicine Endocrinology and Cell Biology, and Harold Hamm Diabetes Center, University of Oklahoma Health Sciences Center, Oklahoma City, OK, USA

Eun-Jin Lee Biomedical Engineering, Viterbi School of Engineering, University of Southern California, Los Angeles, CA, USA

Sarah V. Leimbeck Institute of Human Anatomy and Embryology, University of Regensburg, Regensburg, Germany

Brian C. Leonard Ottawa Hospital Research Institute, Regenerative Medicine, Ottawa, ON, Canada

Department of Ophthalmology, University of Ottawa, Ottawa, ON, Canada

Emily S. Levine Cell Biology and Human Anatomy, University of California Davis, Davis, CA, USA

Alfred S. Lewin Department of Molecular Genetics and Microbiology, College of Medicine, University of Florida, Gainesville, FL, USA

Department of Molecular Genetics and Microbiology, University of Florida College of Medicine, Gainesville, FL, USA

Richard A. Lewis Departments of Ophthalmology, Medicine, Pediatrics and Molecular and Human Genetics, Baylor College of Medicine, Houston, TX, USA

Hong Li Department of Molecular Genetics and Microbiology, College of Medicine, University of Florida, Gainesville, FL, USA

Songhua Li Department of Ophthalmology and Neuroscience Center, Louisiana State University Health Sciences Center, New Orleans, LA, USA

Yao Li Department of Ophthalmology, Columbia University Medical Center, Columbia University, New York, NY, USA

Jonathan H. Lin Department of Pathology, University of California, San Diego, CA, USA

VA San Diego Healthcare System, San Diego, CA, USA

Chris Lindsey MitoChem Therapeutics Inc, Charleston, SC, USA

Departments of Drug Discovery and Biomedical Sciences, Medical University of South Carolina, Charleston, SC, USA

Qianyong Liu Departments of Biological Science, Allergan Inc, Irvine, CA, USA

Qin Liu Ocular Genomics Institute, and Berman-Gund Laboratory for the Study of Retinal Degenerations, Department of Ophthalmology, Massachusetts Eye and Ear Infirmary, Harvard Medical School, Boston, MA, USA

Glenn P. Lobo Department of Ophthalmic Research-i31, Cole Eye Institute, Cleveland Clinic, Cleveland, OH, USA

Vanda S. Lopes UCLA School of Medicine, Jules Stein Eye Institute, Los Angeles, CA, USA

Hongwei Ma The Department of Cell Biology, University of Oklahoma Health Sciences Center, Oklahoma City, OK, USA

Wenxin Ma Unit on Neuron-Glia Interactions in Retinal Diseases, National Eye Institute, National Institutes of Health, Bethesda, MD, USA

Albert M Maguire Scheie Eye Institute, F.M. Kirby Center for Molecular Ophthalmology, University of Pennsylvania, Philadelphia, PA, USA

Yukiko Makiyama Department of Ophthalmology and Visual Sciences, Kyoto University Graduate School of Medicine, Kyoto, Japan

Goldis Malek Department of Ophthalmology, Duke University School of Medicine, Durham, NC, USA

Brian C. Mansfield Foundation Fighting Blindness, Columbia, MD, USA

Haoyu Mao Department of Molecular Genetics and Microbiology, College of Medicine, University of Florida, Gainesville, FL, USA

Yingyu Mao Department of Biological Sciences, Center for Cancer, Genetic Diseases and Gene Regulation, Fordham University, Bronx, NY, USA

Alexander G. Marneros Department of Dermatology, Cutaneous Biology Research Center, Massachusetts General Hospital, Harvard Medical School, Charlestown, MA, USA

Kathleen Marshall Center for Cellular and Molecular Therapeutics, The Children's Hospital of Philadelphia, Philadelphia, PA, USA

Michael T. Matthes Department of Ophthalmology, University of California, San Francisco, CA, USA

Beckman Vision Center, UCSF School of Medicine, San Francisco, CA, USA

Karina I. Mazzitello CONICET, Universidad Nacional de Mar del Plata, Mar del Plata, Argentina

James F. McGinnis Department of Ophthalmology, Dean McGee Eye Institute, University of Oklahoma Health Sciences Center, Oklahoma City, OK, USA

Department of Ophthalmology, Dean McGee Eye Institute,

Department of Cell Biology, Oklahoma Center for Neuroscience, University of Oklahoma Health Sciences Center, Oklahoma City, OK, USA

Paolo Melillo Eye Clinic, Multidisciplinary Department of Medical, Surgical and Dental Sciences, Second University of Naples, Naples, Italy

Juliane Merl-Pham Research Unit Protein Science, Helmholtz Zentrum München, German Research Center for Environmental Health GmbH, Munich, Germany

Michel Michaelides UCL Institute of Ophthalmology, University College London, London, UK

Moorfields Eye Hospital, London, UK

Stylianos Michalakis Center for Integrated Protein Science Munich, CIPSM and Department of Pharmacy-Center for Drug Research, Ludwig-Maximilians-Universität München, Munich, Germany

Eric B. Miller Center for Neuroscience, University of California Davis, Davis, CA, USA

Rajendra N. Mitra Department of Cell Biology, University of Oklahoma Health Sciences Center, Oklahoma City, OK, USA

Sayak K. Mitter Department of Ophthalmology, Indiana University, Indianapolis, IN, USA

Satoshi Morooka Departments of Ophthalmology and Visual Sciences, Kyoto University Graduate School of Medicine, Kyoto, Japan

Claudia Müller Department of Biological Sciences, Center for Cancer, Genetic Diseases and Gene Regulation, Fordham University, Bronx, NY, USA

Akira Murakami Department of Ophthalmology, Graduate School of Medicine, Juntendo University, Tokyo, Japan

Muna I. Naash Department of Cell Biology, University of Oklahoma Health Sciences Center, Oklahoma City, OK, USA

Nobuhiro Nagai Division of Clinical Cell Therapy, Center for Advanced Medical Research and Development (ART), Tohoku University Graduate School of Medicine, Sendai, Japan

Jürgen K. Naggert The Jackson Laboratory, Bar Harbor, ME, USA

Toru Nakazawa Department of Ophthalmology, Tohoku University Graduate School of Medicine, Sendai, Japan

Hyun Ju Nam Scheie Eye Institute, Department of Ophthalmology, Perelman School of Medicine, University of Pennsylvania, Philadelphia, PA, USA

Emeline F. Nandrot Institut de la Vision, INSERM, U968, Sorbonne Universités, UPMC Univ Paris 06, UMR_S968, CNRS, UMR_7210, Paris, France

Cecile Nasarre Departments of Ophthalmology, Medical University of South Carolina, Charleston, SC, USA

Alla A. Nesterova Department of Histology, Embryology, Cytology, Volgograd State Medical University, Volgograd, Russia

Huy V Nguyen Columbia University College of Physicians and Surgeons, New York, NY, USA

John M. Nickerson Department of Ophthalmology, Emory University School of Medicine, Atlanta, GA, USA

Emory Eye Center, Atlanta, GA, USA

Patsy M. Nishina The Jackson Laboratory, Bar Harbor, ME, USA

Matsuhiko Nishizawa Department of Bioengineering and Robotics, Tohoku University Graduate School of Engineering, Sendai, Japan

Kazuhiro Ogai Wellness Promotion Science Center, Institute of Medical, Pharmaceutical and Health Sciences, Kanazawa University, Kanazawa, Japan

Ken Ogino Department of Ophthalmology and Visual Sciences, Kyoto University Graduate School of Medicine, Kyoto, Japan

Akio Oishi Department of Ophthalmology and Visual Sciences, Kyoto University Graduate School of Medicine, Kyoto, Japan

Maho Oishi Department of Ophthalmology and Visual Sciences, Kyoto University Graduate School of Medicine, Kyoto, Japan

Machelle T. Pardue Department of Ophthalmology, Emory University School of Medicine, Atlanta, GA, USA

Rehab R&D Center, Research Service (151Oph), Atlanta VA Medical Center, Decatur, GA, USA

Machelle T. Pardue Department of Ophthalmology, Emory University School of Medicine, Atlanta, GA, USA

Atlanta VA Center of Excellence for Visual and Neurocognitive Rehabilitation, Atlanta VA Medical Center, Decatur, GA, USA

David A. Parfitt Ocular Bioloy and Therapeutics, UCL Institute of Ophthalmology, London, UK

Célia Parinot Institut de la Vision, INSERM, U968, Sorbonne Universités, UPMC Univ Paris 06, UMR_S968, CNRS, UMR_7210, Paris, France

Gayle J.T. Pauer Department of Ophthalmic Research, Cole Eye Institute, Cleveland Clinic, Cleveland, OH, USA

Diana Pauly Institute of Human Genetics, University of Regensburg, Regensburg, Germany

S. Louise Pay Department of Ophthalmology, Indiana University, Indianapolis, IN, USA

Department of Medical and Molecular Genetics, Indiana University School of Medicine, Indianapolis, IN, USA

Neal S. Peachey Louis Stokes Cleveland VA Medical Center, Cleveland, OH, USA

Cole Eye Institute, Cleveland Clinic, Cleveland, OH, USA

Department of Ophthalmology, Cleveland Clinic Lerner College of Medicine of Case Western Reserve University, Cleveland, OH, USA

Rachael A. Pearson F. Hoffman La Roche, Basel, Switzerland

Mark E. Pennesi Department of Ophthalmology, Casey Eye Institute, Oregon Health & Science University, Portland, OR, USA

Brian D. Perkins Department of Ophthalmic Research, Cole Eye Institute, Cleveland Clinic, Cleveland, OH, USA

Department of Biology, Texas A&M University, College Station, TX, USA

Nathan Perron Departments of Ophthalmology, Medical University of South Carolina, Charleston, SC, USA

Eric A. Pierce Ocular Genomics Institute, Massachusetts Eye and Ear Infirmary, Harvard Medical School, Boston, MA, USA

Scott M. Plafker Free Radical Biology and Aging Program, Oklahoma Medical Research Foundation, Oklahoma City, OK, USA

Federica Polato Section of Protein Structure and Function, Laboratory of Retinal Cell and Molecular Biology, NEI, National Institutes of Health, Bethesda, MD, USA

Constantin J. Pournaras Department of Ophthalmology, Geneva University Hospitals, Geneva, Switzerland

Nathalie Produit-Zengaffinen IRO—Institute for Research in Ophthalmology, Sion, Switzerland

Edward N. Pugh Department of Ophthalmology and Vision Science, University of California Davis, Davis, CA, USA

Cell Biology and Human Anatomy, University of California Davis, Davis, CA, USA

Luciana M. Pujol-Lereis Institute of Human Genetics, University of Regensburg, Regensburg, Germany

Xiaoping Qi Department of Ophthalmology, Indiana University, Indianapolis, IN, USA

Qingwen Qian Department of Ophthalmology, Indiana University, Indianapolis, IN, USA

Suofu Qin Retinal Disease Research, Department of Biological Sciences, Allergan, Inc., Irvine, CA, USA

Raju V.S. Rajala Departments of Cell Biology, Physiology and Ophthalmology, Dean McGee Eye Institute, University of Oklahoma Health Sciences Center, Oklahoma City, OK, USA

Department of Ophthalmology, University of Oklahoma Health Sciences Center, Oklahoma City, OK, USA

Department of Physiology, University of Oklahoma Health Sciences Center, Oklahoma City, OK, USA

Department of Cell Biology, University of Oklahoma Health Sciences Center, Oklahoma City, OK, USA

Dean McGee Eye Institute, University of Oklahoma Health Sciences Center, Oklahoma City, OK, USA

Alia Rashid Ophthalmology, Emory University, Atlanta, GA, USA

Alaina Reagan Department of Ophthalmology, University of Oklahoma Health Sciences Center, Oklahoma City, OK, USA

Oklahoma Center for Neuroscience, University of Oklahoma Health Sciences Center, Oklahoma City, OK, USA

Dean A. McGee Eye Institute, University of Oklahoma Health Sciences Center, Oklahoma City, OK, USA

Nadine Reichhart Experimental Ophthalmology, Department of Ophthalmology, Charite University Medicine Berlin, Berlin, Germany

Bärbel Rohrer Department of Ophthalmology, Ralph H. Johnson VA Medical Center, Medical University of South Carolina and Research Service, Charleston, SC, USA

Departments of Ophthalmology, Medical University of South Carolina, Charleston, SC, USA

Division of Research, Ralph H. Johnson VA Medical Center, Charleston, SC, USA

Benjamin Rossi Department of Ophthalmology, University of Michigan Medical Center, Ann Arbor, MI, USA

Settimio Rossi Eye Clinic, Multidisciplinary Department of Medical, Surgical and Dental Sciences, Second University of Naples, Naples, Italy

Sheldon Rowan USDA-JM Human Nutrition Research Center on Aging (HNRCA), Tufts University, Boston, MA, USA

Department of Ophthalmology, Tufts University School of Medicine, Boston, MA, USA

Jean-Michel Rozet Laboratory of Genetics in Ophthalmology, INSERM UMR1163 - Imagine Institute, Paris Descartes - Sorbonne Paris Cité University, Paris, France

Matt Rutar John Curtin School of Medical Research, The Australian National University, Canberra, ACT, Australia

Leonide Saad Alkeus Pharmaceuticals, Inc., Boston, MA, USA

Janmeet S. Saini Neural Stem Cell Institute, Regenerative Research Foundation, Rensselaer, NY, USA

Department of Biomedical Sciences, University at Albany, Albany, NY, USA

Marijana Samardzija Laboratory for Retinal Cell Biology, Department of Ophthalmology, University of Zurich, Schlieren, Switzerland

Ivy S. Samuels Louis Stokes Cleveland VA Medical Center, Cleveland, OH, USA

Douglas N. Sanders Department of Ophthalmology, University of Missouri School of Medicine, Mason Eye Institute, Columbia, MO, USA

Department of Diagnostics Division, Novartis Pharmaceutical Inc., Cambridge, MA, USA

Nicole Schäfer Institute of Human Genetics, University of Regensburg, Regensburg, Germany

Anja Schlecht Institute of Human Anatomy and Embryology, University of Regensburg, Regensburg, Germany

Daniel F. Schorderet IRO—Institute for Research in Ophthalmology, Sion, Switzerland

Department of Ophthalmology, University of Lausanne, Lausanne, Switzerland

Faculty of Life Sciences, Swiss Federal Institute of Technology, Lausanne, Switzerland

Sharon B. Schwartz Scheie Eye Institute, Department of Ophthalmology, Perelman School of Medicine, University of Pennsylvania, Philadelphia, PA, USA

Mathias W. Seeliger Division of Ocular Neurodegeneration, Institute for Ophthalmic Research, Centre for Ophthalmology, Eberhard Karls University, Tübingen, Germany

Jana T. Sellers Department of Ophthalmology, Emory University School of Medicine, Atlanta, GA, USA

Soo Jung Seo Department of Molecular Genetics and Microbiology, College of Medicine, University of Florida, Gainesville, FL, USA

Yuri Sergeev National Health Institute, Bathesda, MD, USA

Rebecca Sheplock Scheie Eye Institute, Department of Ophthalmology, Perelman School of Medicine, University of Pennsylvania, Philadelphia, PA, USA

Lan Ying Shi The Jackson Laboratory, Bar Harbor, ME, USA

Francesca Simonelli Eye Clinic, Multidisciplinary Department of Medical, Surgical and Dental Sciences, Second University of Naples, Naples, Italy

Napoli, Italy

Debasish Sinha Department of Ophthalmology, Johns Hopkins University School of Medicine, Baltimore, MD, USA

Travis B. Smith Department of Ophthalmology, Casey Eye Institute, Oregon Health & Science University, Portland, OR, USA

Janet R. Sparrow Department of Ophthalmology, Harkness Eye Institute, Columbia University Medical Center, New York, NY, USA

Department of Pathology and Cell Biology, Columbia University Medical Center, New York, NY, USA

Jeffrey H. Stern Neural Stem Cell Institute, Regenerative Research Foundation, Rensselaer, NY, USA

Neural Stem Cell institute, Rensselaer, NY, USA

Lisa Stone The Jackson Laboratory, Bar Harbor, ME, USA

Olaf Strauß Experimental Ophthalmology, Department of Ophthalmology, Charite University Medicine Berlin, Berlin, Germany

Michael W. Stuck Department of Cell Biology, University of Oklahoma Health Sciences Center, Oklahoma City, OK, USA

Kayo Sugitani Department of Clinical Laboratory Sciences, Graduate School of Medical Science, Kanazawa University, Kanazawa, Japan

Lori S. Sullivan Human Genetics Center, School of Public Health, The University of Texas HSC, Houston, TX, USA

Alexander Sumaroka Scheie Eye Institute, Department of Ophthalmology, Perelman School of Medicine, University of Pennsylvania, Philadelphia, PA, USA

Aixu Sun Departments of Biological Science, Allergan Inc, Irvine, CA, USA

Isamu Tachibana Department of Ophthalmology, University of Texas Southwestern Medical Center, Dallas, TX, USA

Ernst R. Tamm Institute of Human Anatomy and Embryology, University of Regensburg, Regensburg, Germany

Li Xuan Tan Department of Ophthalmology and Visual Sciences, School of Medicine and Public Health, University of Wisconsin-Madison, Madison, WI, USA

Yue-Qing Tan Department of Community Medicine, University of North Texas Health Science Center, Fort Worth, TX, USA

Naoyuki Tanimoto Division of Ocular Neurodegeneration, Institute for Ophthalmic Research, Centre for Ophthalmology, Eberhard Karls University, Tübingen, Germany

Sergey Tarima Division of Biostatistics, Institute for Health and Society, Medical College of Wisconsin, Milwaukee, WI, USA

Daniel G. Taub Ocular Genomics Institute, and Berman-Gund Laboratory for the Study of Retinal Degenerations, Department of Ophthalmology, Massachusetts Eye and Ear Infirmary, Harvard Medical School, Boston, MA, USA

Allen Taylor USDA-JM Human Nutrition Research Center on Aging (HNRCA), Tufts University, Boston, MA, USA

Department of Ophthalmology, Tufts University School of Medicine, Boston, MA, USA

Friedman School of Nutrition Science and Policy, Tufts University, Boston, MA, USA

Sally Temple Neural Stem Cell Institute, Regenerative Research Foundation, Rensselaer, NY, USA

Francesco Testa Eye Clinic, Multidisciplinary Department of Medical, Surgical and Dental Sciences, Second University of Naples, Naples, Italy

Timothy C. Thompson Department of Genitourinary Medical Oncology-Research, MD Anderson Cancer Center, The University of Texas, Houston, TX, USA

Hope E. Titus Department of Ophthalmology, Casey Eye Institute, Oregon Health & Science University, Portland, OR, USA

Kimberly A Toops Department of Ophthalmology and Visual Sciences, School of Medicine and Public Health, University of Wisconsin-Madison, Madison, WI, USA

Renée Torlone Ottawa Hospital General Division, Eye Institute, Ottawa, ON, Canada

Christopher J. Tracy Department of Ophthalmology, University of Missouri School of Medicine, Mason Eye Institute, Columbia, MO, USA

Genetics Area Program, University of Missouri, Columbia, USA

Stephen H Tsang New York Presbyterian Hospital/Columbia University Medical Center, New York, NY, USA

Department of Pathology and Cell Biology, Department of Ophthalmology, Edward Harkness Eye Institute, Columbia University, New York, NY, USA

Catherine Tsilfidis Ottawa Hospital Research Institute, Regenerative Medicine, Ottawa, ON, Canada

Department of Cellular and Molecular Medicine, University of Ottawa, Ottawa, ON, Canada

Department of Ophthalmology, University of Ottawa, Ottawa, ON, Canada

Marius Ueffing Division of Experimental Ophthalmology, University of Tuebingen, Tuebingen, Germany

Mallika Valapala Department of Ophthalmology, Johns Hopkins University School of Medicine, Baltimore, MD, USA

Krisztina Valter Divsion of Biomedical Sciences, Research School of Biology, Australian National University, Acton, Australia

Kathleen Van Craenenbroeck University of Ghent, Gent, Belgium

Luk H. Vandenberghe Department of Ophthalmology, Ocular Genomics Institute, Schepens Eye Research Institute, Massachusetts Eye and Ear Infirmary, Harvard Medical School, Harvard University, Boston, MA, USA

Douglas Vollrath Department of Genetics, Stanford University School of Medicine, Stanford, CA, USA

Christian A. Wahl-Schott Center for Integrated Protein Science Munich, CIPSM and Department of Pharmacy-Center for Drug Research, Ludwig-Maximilians-Universität München, Munich, Germany

Keisuke Wakasugi Department of Life Sciences, Graduate School of Arts and Sciences, The University of Tokyo, Meguro-ku, Japan

Lei Wang Wilmer Eye Institute, Johns Hopkins School of Medicine, Baltimore, MD, USA

Qingjie Wang Neural Stem Cell Institute, Regenerative Research Foundation, Rensselaer, NY, USA

Zhaoyang Wang Department of Molecular Genetics and Microbiology, College of Medicine, University of Florida, Gainesville, FL, USA

Ilyas Washington Department of Ophthalmology, Columbia University Medical Center, New York, NY, USA

Sarah Wassmer Ottawa Hospital Research Institute, Regenerative Medicine, Ottawa, ON, Canada

Department of Cellular and Molecular Medicine, University of Ottawa, Ottawa, ON, Canada

Sumiko Watanabe Division of Molecular and Developmental Biology, Institute of Medical Science, University of Tokyo, Tokyo, Japan

Eric Wawrousek National Eye Institute, Bathesda, MD, USA

Bernhard H. F. Weber Institute of Human Genetics, University of Regensburg, Regensburg, Germany

Cynthia X. Wei Department of Ophthalmology, University of Texas Southwestern Medical Center, Dallas, TX, USA

Ji-Ye Wei Departments of Biological Science, Allergan Inc, Irvine, CA, USA

George M. Weinstock Microbial Genomics, The Jackson Laboratory for Genomic Medicine, Farmington, CT, USA

Patrick Whalen Department of Molecular Genetics and Microbiology, University of Florida, Gainesville, FL, USA

Dianna K. Wheaton The Retina Foundation of the Southwest, Dallas, TX, USA

Belinda Willard Proteomics Core Services, Lerner Research Institute, Cleveland Clinic, Cleveland, OH, USA

David S. Williams UCLA School of Medicine, Jules Stein Eye Institute, Los Angeles, CA, USA

Richard K. Wilson The Genome Institute, Washington University School of Medicine, St. Louis, MO, USA

Wai T. Wong Unit on Neuron-Glia Interactions in Retinal Diseases, National Eye Institute, National Institutes of Health, Bethesda, MD, USA

Russell Woods Department of Ophthalmology, Harvard Medical School, Schepens Eye Research Institute, Boston, MA, USA

Wenjun Xiong Departments of Genetics and Ophthalmology, Howard Hughes Medical Institute, Harvard Medical School, Boston, MA, USA

Lei Xu Department of Ophthalmology, University of Florida, Gainesville, FL, USA

Haidong Yang Beckman Vision Center, UCSF School of Medicine, San Francisco, CA, USA

Douglas Yasumura Department of Ophthalmology, University of California, San Francisco, CA, USA

Beckman Vision Center, UCSF School of Medicine, San Francisco, CA, USA

Jun Yin Department of Genetics, Yale University School of Medicine, New Haven, CT, USA

Nagahisa Yoshimura Department of Ophthalmology and Visual Sciences, Kyoto University Graduate School of Medicine, Kyoto, Japan

Minzhong Yu Cole Eye Institute, Cleveland Clinic, Cleveland, OH, USA

Ying Yu Departments of Biological Science, Allergan Inc, Irvine, CA, USA

Donald J. Zack Ophthalmology, Molecular Biology & Genetics, Neuroscience, and Institute of Genetic Medicine, Wilmer Eye Institute, Johns Hopkins University School of Medicine, Baltimore, MD, USA

David N. Zacks Department of Ophthalmology and Visual Sciences, Kellogg Eye Center, University of Michigan Medical School, Ann Arbor, MI, USA

Azhar Zam Cell Biology and Human Anatomy, University of California Davis, Davis, CA, USA

Robert J. Zawadzki Department of Ophthalmology and Vision Science, University of California Davis, Davis, CA, USA

Cell Biology and Human Anatomy, University of California Davis, Davis, CA, USA

Hong Zeng University of Houston College of Optometry, Houston, TX, USA

Houbin Zhang Sichuan Academy of Medical Sciences & Sichuan Provincial People's Hospital, Chengdu, Sichuan, China

Pengfei Zhang Cell Biology and Human Anatomy, University of California Davis, Davis, CA, USA

Qing Zhang Ophthalmology, Emory University, Atlanta, GA, USA

Meili Zhu Department of Medicine Endocrinology, University of Oklahoma Health Sciences Center, Oklahoma City, OK, USA

J Samuel Zigler Department of Ophthalmology, Johns Hopkins University School of Medicine, Baltimore, MD, USA

About the Editors

Catherine Bowes Rickman PhD is a tenured Associate Professor of Ophthalmology and of Cell Biology at Duke University located in Durham, NC. Dr. Bowes Rickman leads a team of researchers focused on developing and using mouse models to understand the pathobiology of age-related macular degeneration (AMD) and on developing and testing therapeutic targets for AMD. Dr. Bowes Rickman received her undergraduate degree at the University of California at Santa Barbara, specializing in Biochemistry/Molecular Biology and Aquatic Biology. She earned a PhD from the University of California at Los Angeles and postdoctoral fellowship at the Jules Stein Eye Institute, California, where she focused on mouse models of retinitis pigmentosa. Dr. Bowes Rickman has a long-standing interest in the molecular and cell biology and pathology of the retina. Amongst her seminal discoveries was the identification of the gene responsible for retinal degeneration in the *rd* mouse. She has applied her expertise in mouse genetics to develop models to study age-related macular degeneration (AMD). Currently, she is using several mouse models developed by her group that faithfully recapitulate many aspects of the human AMD phenotype to provide *in vivo* means to examine the pathogenic contribution of genetic, inflammatory and environmental factors to AMD onset and progression. Recently, she successfully demonstrated therapeutic rescue from dry AMD in one of these models. The last few years has been dedicated towards better understanding the impact of the complement system on the onset and progression of AMD using novel mouse models. Dr. Bowes Rickman's research program has been continually funded by the NIH since 1995 and she has also received support from Research to Prevent Blindness (RPB) Foundation, the Foundation Fighting Blindness, the Macular Degeneration program of the American Health Assistance Foundation, Macula Vision Research Foundation, and The Ruth and Milton Steinbach Fund. Dr. Bowes Rickman has received a RPB Career Development Award, a RPB William and Mary Greve Special Scholars Award and an Edward N. & Della L. Thome Memorial Foundation Award. She has published more than 40 original research and review articles and has edited two books on inherited and environmentally induced retinal degenerations. She currently serves on the Scientific Advisory Boards of the Foundation Fighting Blindness (Owings Mills, Maryland), the Beckman Initiative for Macular Research (Irvine, California) and the Macular Degeneration program of the BrightFocus Foundation (Clarksburg, Maryland) and is a consultant for GlaxoSmithKline and Pfizer.

Matthew M. LaVail PhD is Professor of Anatomy and Ophthalmology at the University of California, San Francisco School of Medicine. He received his PhD degree in Anatomy (1969) from the University of Texas Medical Branch in Galveston and was subsequently a postdoctoral fellow at Harvard Medical School. Dr. LaVail was appointed Assistant Professor of Neurology-Neuropathology at Harvard Medical School in 1973. In 1976, he moved to UCSF, where he was appointed Associate Professor of Anatomy. He was appointed to his current position in 1982, and in 1988, he also became Director of the Retinitis Pigmentosa Research Center at UCSF, later named the Kearn Family Center for the Study of Retinal Degeneration. Dr. LaVail has published extensively in the research areas of photoreceptor-retinal pigment epithelial cell interactions, retinal development, circadian events in the retina, genetics of pigmentation and ocular abnormalities, inherited retinal degenerations, light-induced retinal degeneration, and neuroprotective and gene therapy for retinal degenerative diseases. He has identified several naturally occurring murine models of human retinal degenerations and has developed transgenic mouse and rat models of others. He is the author of more than 180 research publications and has edited 16 books on inherited and environmentally induced retinal degenerations. Dr. LaVail has received the Fight for Sight Citation (1976); the Sundial Award from the Retina Foundation (1976); the Friedenwald Award from the Association for Research in Vision and Ophthalmology (ARVO, 1981); two Senior Scientific Investigators Awards from Research to Prevent Blindness (1988 and 1998); a MERIT Award from the National Eye Institute (1989); an Award for Outstanding Contributions to Vision Research from the Alcon Research Institute (1990); the Award of Merit from the Retina Research Foundation (1990); the first John A. Moran Prize for Vision Research from the University of Utah (1997); the first Trustee Award from The Foundation Fighting Blindness (1998); the fourth Llura Liggett Gund Award from the Foundation Fighting Blindness (2007); and he has received the Distinguished Alumnus Award from both his university (University of North Texas) and his graduate school (University of Texas Medical Branch). He has served on the editorial boards of *Investigative Ophthalmology and Visual Science* and *Experimental Eye Research*. Dr. LaVail has been an active participant in the program committee of ARVO and has served as a Trustee (Retinal Cell Biology Section) of ARVO. In 2009, he was appointed an inaugural ARVO Fellow, Gold, of the 12,000-member organization. Dr. LaVail has been a member of the program committee and a Vice President of the International Society for Eye research. He also served on the Scientific Advisory Board of the Foundation Fighting Blindness from 1973–2011. Dr. LaVail retired from the University of California on July 1, 2014, but continues his laboratory research at UCSF as a Recall Emeritus Professor.

Robert E. Anderson MD, PhD is George Lynn Cross Research Professor, Dean A. McGee Professor of Ophthalmology, Professor of Cell Biology, and Adjunct Professor of Geriatric Medicine at The University of Oklahoma Health Sciences Center in Oklahoma City, Oklahoma. He is also Director of Research at the Dean A. McGee Eye Institute. He received his PhD in Biochemistry (1968) from Texas A&M University and his MD from Baylor College of Medicine in 1975. In 1968, he was a postdoctoral fellow at Oak Ridge Associated Universities. At Baylor, he

was appointed Assistant Professor in 1969, Associate Professor in 1976, and Professor in 1981. He joined the faculty of the University of Oklahoma Health Sciences Center in January of 1995. Dr. Anderson served as director of the Oklahoma Center for Neuroscience (1995–1999) and chairman of the Department of Cell Biology (1998–2007). He has received several honorary appointments including Visiting Professor, West China School of Medicine, Sichuan University, Chengdu, China; Honorary Professorship, Xi'an Jiaotong University, Xi'an, China; and Honorary Professor of Sichuan Medical Science Academy, Sichuan Provincial People's Hospital, Sichuan, China. Dr. Anderson has received the Sam and Bertha Brochstein Award for Outstanding Achievement in Retina Research from the Retina Research Foundation (1980), and the Dolly Green Award (1982) and two Senior Scientific Investigator Awards (1990 and 1997) from Research to Prevent Blindness, Inc. He received an Award for Outstanding Contributions to Vision Research from the Alcon Research Institute (1985), and the Marjorie Margolin Prize (1994). He has served on the editorial boards of Investigative Ophthalmology and Visual Science, Journal of Neuroscience Research, Neurochemistry International, Current Eye Research, and Experimental Eye Research. Dr. Anderson has published extensively in the areas of lipid metabolism in the retina and biochemistry of retinal degenerations. He has edited 17 books, 16 on retinal degenerations and one on the biochemistry of the eye. Dr. Anderson has received grants from the National Institutes of Health, The Retina Research Foundation, the Foundation Fighting Blindness, and Research to Prevent Blindness, Inc. He has been an active participant in the program committees of the Association for Research in Vision and Ophthalmology (ARVO) and was a trustee representing the Biochemistry and Molecular Biology section. He was named a Gold Fellow by ARVO in 2009 and received the Proctor Medal from ARVO in 2011. He received the Llura Liggett Gund Lifetime Achievement Award from the Foundation Fighting Blindness in June 2011. In 2012, he received the Paul A. Kayser International Award, Retina Research Foundation. He has served on the Vision Research Program Committee and Board of Scientific Counselors of the National Eye Institute and the Board of the Basic and Clinical Science Series of The American Academy of Ophthalmology. Dr. Anderson is a past Councilor, Treasurer, and President of the International Society for Eye Research.

Christian Grimm PhD is Professor for Experimental Ophthalmology at the University of Zurich, Switzerland. He received his Ph.D. degree at the Institute for General Microbiology at the University of Berne in 1990. After an initial postdoc position in the field of snRNP maturation, Dr. Grimm conducted research at the University of Wisconsin in Madison, WI, where he studied nucleo-cytoplasmic transport of small RNAs. In 1997 Dr. Grimm moved back to Switzerland where he joined the Lab for Retinal Cell Biology in the department of Ophthalmology at the University of Zurich. Dr. Grimm has led the Lab for Retinal Cell Biology since 2006 and was appointed Professor for Experimental Ophthalmology and joined the medical faculty in 2008. Dr. Grimm has published more than 100 original research and review articles, more than 90 in the field of retinal degeneration. His research focuses on molecular mechanisms of photoreceptor cell death, neuroprotection and hypoxic signaling. Dr. Grimm has received the Alfred Vogt Award (2000), the

Retinitis Pigmentosa Award of Pro Retina Germany (2003) and the Pfizer Research Award in Neuroscience (2004). He serves on the Editorial Boards of *Current Eye Research, Experimental Eye Research* and *Molecular Vision*, is Honorary Board member of *Hypoxic Signaling* and acts as a Scientific Review Associate for the *European Journal of Neuroscience*. Dr. Grimm has received research grants from the Swiss National Science Foundation, the European Union, the University of Zurich and several private funding organizations. He serves on the Scientific Advisory Board of the Foundation Fighting Blindness, ProRetina Germany, Retina Suisse and the Swiss Society of Ophthalmology, is member of the committee of the PhD program in integrative molecular medicine (imMed) and is Vice Chairman of the Center for Integrative Human Physiology, a priority research program of the University of Zurich.

Joe G. Hollyfield PhD is Chairman of Ophthalmic Research and the Llura and Gordon Gund Professor of Ophthalmology Research in the Cole Eye Institute at the Cleveland Clinic, Cleveland, Ohio. He received a PhD from the University of Texas at Austin and did postdoctoral work at the Hubrecht Laboratory in Utrecht, The Netherlands. He has held faculty positions at Columbia University College of Physicians and Surgeons in New York City and at Baylor College of Medicine in Houston, Texas. He was Director of the Retinitis Pigmentosa Research Center in The Cullen Eye Institute at Baylor from 1978 until his move to The Cleveland Clinic Foundation in 1995. He is currently Director of the Foundation Fighting Blindness Research Center at the Cleveland Clinic and oversees activity of the Foundation Fighting Blindness Histopathology Center and Donor Eye Program. He has been an annual Visiting Professor in the Department of Ophthalmology at the University of Puerto Rico, Centro Medico, San Juan, Puerto Rico since 1974, where he and his wife, Mary E. Rayborn, teach the development and anatomy of the eye in the "Guillermo Pico Basic Science Course In Ophthalmology", given for ophthalmology residents in Puerto Rico and 18 other countries in Central and South America. Dr. Hollyfield has published over 200 papers in the area of cell and developmental biology of the retina and retinal pigment epithelium in health and disease. He has edited 17 books, 16 on retinal degenerations and one on the structure of the eye. Dr. Hollyfield received the Marjorie W. Margolin Prize (1981, 1994), the Sam and Bertha Brochstein Award (1985) and the Award of Merit in Retina Research (1998) from the Retina Research Foundation, Houston, Texas; the Olga Keith Weiss Distinguished Scholars' Award (1981) and two Senior Scientific Investigator Awards (1988, 1994) from Research to Prevent Blindness, Inc., New York, New York; an award from the Alcon Research Institute (1987), Fort Worth, Texas; the Distinguished Alumnus Award (1991) from Hendrix College, Conway, Arkansas; the Endre A. Balazs Prize (1994) from the International Society for Eye Research (ISER); the Proctor Medal (2009) from the Association for Research in Vision and Ophthalmology (ARVO), and the 2009 Cless "Best of the Best" Award, given by the University of Illinois Eye and Ear Infirmary, Chicago, Illinois. He was an inaugural Gold Fellow of ARVO when this award was established in 2009. Since 1991 he has been Editor-in-Chief of the journal, *Experimental Eye Research*

published by Elsevier, Amsterdam, The Netherlands. Dr. Hollyfield has been active in ARVO since 1971, serving on the Program Committee (1976), as Trustee (Retinal Cell Biology, 1989–1994), as President (1993–1994) and as Immediate Past President (1994–1995). He also served as President (1988–1991) and Secretary (1984–1987) of the International Society of Eye Research. He is Chairman of the scientific review panel for the Macular Degeneration program of the BrightFocus Foundation (Clarksburg, Maryland), serves on the scientific advisory boards of the Foundation Fighting Blindness (Owings Mills, Maryland), the Helen Keller Eye Research Foundation (Birmingham, Alabama), the South Africa Retinitis Pigmentosa Foundation (Johannesburg, South Africa), is Co-Chairman of the Medical and Scientific Advisory Board of Retina International (Zurich, Switzerland), and is a member of the Board of Trustees of Hendrix College.

John D. Ash PhD Francis M. Bullard Eminent Scholar Chair in Ophthalmological Sciences, Department of Ophthalmology, College of Medicine at the University of Florida. Dr. Ash received his PhD from the Ohio State University Biochemistry Program in 1994, and completed postdoctoral training in the Cell Biology Department at Baylor College of Medicine, in Houston, Texas, and began his faculty career at the University of Oklahoma Health Sciences Center, Oklahoma. Dr. Ash is also a Visiting Professor of the Dalian Medical University, Dalian China. Dr. Ash has written and published 56 manuscripts including research articles, book chapters and invited reviews. He is currently an Executive editor for *Experimental Eye research*, and a Scientific Review Editor for *Molecular Vision*. Dr. Ash is an active reviewer for these journals as well as *Investigative Ophthalmology & Visual Science*. In 2009, Dr. Ash received a research award from Hope for Vision, and in 2010 he received a Lew R. Wasserman Merit award from Research to Prevent Blindness, Inc. Dr. Ash has received grants from the National Institutes of Health, the Foundation Fighting Blindness, Research to Prevent Blindness, Inc., Hope for Vision, and the American Diabetes Association. Dr. Ash has served on the Program and Advocacy committees of the Association for Research in Vision and Ophthalmology. Dr. Ash has served on the scientific review panel for Fight For Sight (2005–2008), and is currently serving on the Scientific Advisory Board of the Foundation Fighting Blindness (Columbia, MD) where he chairs the review committee on Novel Medical Therapies Program. He also serves on the scientific review panel for the Macular Degeneration program of the BrightFocus Foundation (formally the American Health Assistance Foundation, Clarksburg, MD).

Part I
Age-Related Macular Degeneration (AMD)

Chapter 1
Apolipoprotein E Isoforms and AMD

Kimberly A Toops, Li Xuan Tan and Aparna Lakkaraju

Abstract The cholesterol transporting protein apolipoprotein E (ApoE) occurs in three allelic variants in humans unlike in other species. The resulting protein isoforms E2, E3 and E4 exhibit differences in lipid binding, integrating into lipoprotein particles and affinity for lipoprotein receptors. ApoE isoforms confer genetic risk for several diseases of aging including atherosclerosis, Alzheimer's disease, and age-related macular degeneration (AMD). A single E4 allele increases the risk of developing Alzheimer's disease, whereas the E2 allele is protective. Intriguingly, the E4 allele is protective in AMD. Current thinking about different functions of ApoE isoforms comes largely from studies on Alzheimer's disease. These data cannot be directly extrapolated to AMD since the primary cells affected in these diseases (neurons vs. retinal pigment epithelium) are so different. Here, we propose that ApoE serves a fundamentally different purpose in regulating cholesterol homeostasis in the retinal pigment epithelium and this could explain why allelic risk factors are flipped for AMD compared to Alzheimer's disease.

Keywords Apolipoprotein E · ApoE isoforms · Age-related macular degeneration · Retinal pigment epithelium · Cholesterol

A. Lakkaraju (✉) · K. A. Toops · L. X. Tan
Department of Ophthalmology and Visual Sciences, School of Medicine and Public Health, University of Wisconsin-Madison, 1300 University Ave, SMI 677, Madison, WI 53706, USA
e-mail: lakkaraju@wisc.edu

K. A. Toops · A. Lakkaraju
McPherson Eye Research Institute, University of Wisconsin-Madison, Madison, WI 53706, USA

L. X. Tan · A. Lakkaraju
Division of Pharmaceutical Sciences, School of Pharmacy, University of Wisconsin-Madison, Madison, WI 53706, USA

K. A. Toops
e-mail: toops@wisc.edu

L. X. Tan
e-mail: ltan8@wisc.edu

C. Bowes Rickman et al. (eds.), *Retinal Degenerative Diseases,* Advances in Experimental Medicine and Biology 854, DOI 10.1007/978-3-319-17121-0_1

1.1 Introduction

Age-related macular degeneration (AMD), like other multifactorial diseases of aging, has no simple genetic underpinning. A complex mixture of environmental factors, lifestyle choices, and genes influence whether AMD will develop, how rapidly it will advance, and how severe the resulting visual dysfunction will be (Fritsche et al. 2014). Vision loss in AMD results from death of the photoreceptors, particularly in the macula. Photoreceptor loss reflects the terminal step in a cascading pathology whose genesis is in the posterior-most portion of the retina: the RPE, Bruch's membrane (BM) and choroid complex.

The tissue that is the initial site of damage in AMD, the RPE, forms the outer blood-retinal barrier and is responsible for the health and maintenance of the photoreceptors and the choriocapillaris (Toops et al. 2014). One of the many functions of the RPE is to act as the central organizing hub for cholesterol homeostasis for the outer retina (Fliesler and Bretillon 2010; Pikuleva and Curcio 2014). Several independent lines of evidence indicate that cholesterol homeostasis in the RPE and adjacent Bruch's membrane is dysregulated in AMD: one, cholesterol-rich lesions with material at least partly derived from the RPE are found in both sub-retinal and sub-RPE deposits (Bowes Rickman et al. 2013; Pikuleva and Curcio 2014). Two, several critical members of the cholesterol homeostasis pathway including hepatic lipase (LIPC), cholesteryl ester transfer protein (CETP), ATP-binding cassette subfamily A member 1 (ABCA1), and apolipoprotein E (ApoE) have been implicated in modulating AMD susceptibility (Katta et al. 2009; Liu et al. 2012; Fritsche et al. 2014). Of these, how ApoE gene variants alter AMD risk is especially intriguing because of the opposite allele-risk associations between AMD and Alzheimer's disease (AD) (Thakkinstian et al. 2006; McKay et al. 2011; Sivak 2013).

1.2 ApoE Isoforms Structure and Function

The human ApoE gene occurs in three allelic variants E2, E3 and E4 that vary by just two nucleotides resulting in three protein isoforms with amino acid variations at positions 112 and 158. These single amino acid changes profoundly effect protein function because they modify salt bridges within different helices of ApoE leading to altered receptor binding and lipid binding (Mahley and Rall 2000; Huang 2010). Key differences between the three ApoE isoforms are summarized in Table 1.1. The E2 isoform binds poorly to the low-density lipoprotein receptor (LDL-R) compared to E3 or E4 (<2%). E4 associates preferentially with very low-density lipoproteins (VLDL) whereas E2 and E3 associate with high-density lipoproteins (HDL) (Mahley and Rall 2000; Huang 2010). Humans are the only known species that express multiple ApoE isoforms. ApoE expressed by non-human primates and mice is structurally homologous to human ApoE4 with Arg at positions 112 and 158; however, these sequences have Thr at position 61 instead of Arg. This single amino acid switch prevents the formation of an N- and C- terminal domain interaction and results in non-human ApoE functioning more like human ApoE3 (Mahley and Rall 2000; Raffai et al. 2001).

Table 1.1 General properties of the three different human ApoE isoforms are summarized. [a]Population frequency is reported for having at least one allele of a given isoform; total estimated frequencies of the six possible ApoE phenotypes are 55% E3/E3, 25% E3/E4, 15% E3/E2, with E4/E4, E2/2, and E4/E2 being rare phenotypes with 1–2% occurrence (Mahley and Rall 2000). [b]Single polymorphisms lead to alternate amino acids at positions 112 and 158 in the human ApoE isoforms protein primary sequence. [c] ApoE2 has been reported to have less than 2% of the binding capability to LDL-R compared to E3 or E4 (Mahley and Rall 2000)

Properties of human ApoE isoforms				
Isoform	Population frequency (%)[a]	Sequence[b] 112 158	LDL-R affinity	Lipoprotein binding
ApoE2	7	Cys Cys	Very low[c]	HDL
ApoE3	78	Cys Arg	High	HDL
ApoE4	15	Arg Arg	High	VLDL, HDL

1.3 Evidence for ApoE in Human Diseases

1.3.1 Hyperlipidemia

ApoE was first implicated in regulating the balance of serum cholesterol and triglyceride levels (Huang 2010). In this context, ApoE, a component of lipoproteins (primarily chylomicrons, VLDL, and a subset of HDL particles), facilitates entry into cells by acting as a ligand for the low-density lipoprotein receptor (LDL-R), LDL-R like protein (LRP), heparan sulfate proteoglycans, and additional non-canonical receptors (Mahley and Rall 2000; Carlo et al. 2013). E4 is highly enriched in VLDL particles due to its altered lipid-binding region that shows a preference for binding triglyceride-enriched particles. E2 and E3 are more common in HDL particles due to a preference in their lipid-binding regions for phospholipids (Huang 2010). Both E2 and E4 alleles are associated with the development of hyperlipidemia and downstream atherosclerotic lesions, but for different reasons (Mahley and Rall 2000; Huang 2010). Because E2 is a much poorer ligand than E4 for LDL-R, effective uptake of HDL particles is prevented, leading to hyperlipidemia type III in E2 homozygotes. The preferential binding of E4 to VLDL particles leads to a feedback loop of decreased cellular uptake of LDL particles, which can result in hyperlipidemia.

1.3.2 Alzheimer's Disease

In contrast to the above scenario, in individuals with either one or two copies of E4 the risk of developing AD increases by 4- or 12-fold respectively compared to E3 homozygotes (Huang 2010). ApoE4 is the best-characterized risk factor for early-onset familial AD and an estimated 65–80% of AD patients have at least one E4 allele (Carter 2007). Conversely, ApoE2 has been proposed to be mildly protective for AD, although this remains a weak association without a clear mechanism (Maezawa et al. 2004). ApoE4 is thought to contribute to AD mainly by altering how neurons

process the amyloid precursor protein (APP) through a cholesterol-mediated pathway. This pathway results in the accumulation of intra- and extra- neuronal toxic amyloid beta (Aβ) fragments, which eventually kill hippocampal neurons (Carter 2007; de Chaves and Narayanaswami 2008; Huang 2010; Leduc et al. 2010). The mechanism for this is complex and depends on interactions between ApoE, ApoE cell surface receptors, cholesterol, APP and Aβ, within neurons and in the surrounding astrocytes and extracellular space. E4 appears to stabilize toxic Aβ oligomers, which renders them resistant to lysosomal degradation (Cerf et al. 2011). E4 contributes to AD via other mechanisms that are independent of Aβ: one, E4 is a poor supplier of cholesterol for membrane repair in damaged neurons (Rapp et al. 2006; de Chaves and Narayanaswami 2008; Leduc et al. 2010); and two, E4 acts as a pro-inflammatory molecule to exacerbate neuronal damage (Guo et al. 2004).

1.3.3 Age-Related Macular Degeneration

Epidemiological studies suggest that ApoE2 confers risk in AMD, whereas ApoE4 appears to be protective, although the association of E4 with protection is stronger than E2 with risk (McKay et al. 2011). ApoE and its cargo, cholesterol, are abundant components of drusen, the protein- and lipid-rich lesions in the Bruch's membrane characteristic of AMD (Anderson et al. 2001; Curcio et al. 2011; Bowes Rickman et al. 2013; Pikuleva and Curcio 2014). ApoE in drusen could originate from either the retina or the choroidal circulation (or both, since these sources are not mutually exclusive). However, mounting evidence indicates that the material that forms drusen, including ApoE, is secreted from the RPE (even if it is initially transported into the retina from the circulation, as may be the case for certain lipids) (Pikuleva and Curcio 2014). Thus, the retina is an active cholesterol producing and processing tissue and cholesterol efflux mechanisms are critical for maintaining retinal cholesterol homeostasis (Fliesler and Bretillon 2010; Pikuleva and Curcio 2014).

1.4 Cellular Identity and Differential ApoE Function Contributing to Risk

How ApoE4 can be detrimental to neuronal health has been studied extensively in AD. Little is currently known regarding isoform-specific functions of ApoE in the RPE and how these could contribute to AMD. Local sources of ApoE within the retina are the RPE and the Muller glia, indicating that ApoE is a major cholesterol transport in the retina (Anderson et al. 2001; Li et al. 2006; Johnson et al. 2011). RPE cells express the uptake receptors for ApoE (LDL-R and LRP) as well as the machinery for cholesterol efflux (ABCA1 and ABCG1) (Ebrahimi and Handa 2011; Pikuleva and Curcio 2014). Since cholesterol (free, esterified, and oxidized) is a core component of drusen (Curcio et al. 2005), dysregulation of cholesterol

homeostasis seems to be a key player in AMD pathology (Curcio et al. 2011; Ebrahimi and Handa 2011; Pikuleva and Curcio 2014). And it is in this characteristic that hippocampal neurons and RPE cells most likely diverge.

First, whereas RPE have the capacity to synthesize and take up ApoE-containing lipoproteins, neurons are largely at the mercy of the astrocytes for ApoE production and lipid transport (Leduc et al. 2010). This is a critical distinction since very little cholesterol enters the CNS from the circulation and neurons rely on local synthesis and transport of cholesterol to generate and maintain their long membrane-rich axons. As a reflection of this, neuronal plasma membrane has high levels of lipoprotein receptors particularly LRP, which has a strong preference for ApoE2 and E3 (Rapp et al. 2006). On the other hand, although RPE cells express ApoE receptors, they seem to be spatially discreet (i.e., apical vs. basolateral distributions) and with a different abundance (Tserentsoodol et al. 2006a; Tserentsoodol et al. 2006b; Zheng et al. 2012). A comprehensive analysis of this expression remains to be done.

The RPE therefore acts as a hub for ingress and egress of ApoE-cholesterol, while neurons are largely a terminal acceptor. This implies that as far as ApoE is concerned, RPE may be more similar to astrocytes then neurons. Astrocytes are also active producers of ApoE-cholesterol particles and like the RPE, express ABCA1 and ABCG1, which participate in efflux of ApoE rich pseudo-HDL particles (Wu et al. 2010; Johnson et al. 2011; Ito et al. 2014). Astrocytes express LDL-R and LRP but appear to preferentially bind and uptake ApoE4 and E3 containing lipoproteins (Rapp et al. 2006). Astrocytes exposed to ApoE2-, E3- or E4-loaded cholesterol exhibited ApoE isoform-dependent uptake (E4 = E3 > E2) that was exactly opposite to that seen in neurons (E2 = E3 > E4). Further, astrocytes internalized their cholesterol efficiently, whereas in neurons, the cholesterol was retained on the plasma membrane.

1.5 Implications

If the RPE is functionally similar to astrocytes with regard to cholesterol handling, rather than neurons, then the reversed risk alleles for AD and AMD may not be such a puzzle after all. The RPE and astrocytes can preferentially efflux ApoE containing pseudo-HDL particles for efficient intercellular cholesterol transport. In the brain, this becomes problematic for neurons in ApoE4 expressors because poor cholesterol efflux both increases Aβ generation and decreases its degradation. In the retina, a different balance is struck because the RPE is capable of both efflux and re-uptake. This will be more efficient for E4 than E2 due to the presence of LDL-R in RPE, which avidly binds E3 and E4 but has almost no affinity for E2. Experiments aimed at testing how efficiently different ApoE isoforms traffic cholesterol in and out of the RPE will help establish a cellular, mechanistic basis for puzzling epidemiological data.

References

Anderson DH, Ozaki S, Nealon M et al (2001) Local cellular sources of apolipoprotein E in the human retina and retinal pigmented epithelium: implications for the process of drusen formation. Am J Ophthalmol 131:767–781

Bowes Rickman C, Farsiu S, Toth CA et al (2013) Dry age-related macular degeneration: mechanisms, therapeutic targets, and imaging. Invest Ophthalmol Vis Sci 54:ORSF68–80

Carlo AS, Gustafsen C, Mastrobuoni G et al (2013) The pro-neurotrophin receptor sortilin is a major neuronal apolipoprotein E receptor for catabolism of amyloid-beta peptide in the brain. J Neurosci 33:358–370

Carter CJ (2007) Convergence of genes implicated in Alzheimer's disease on the cerebral cholesterol shuttle: APP, cholesterol, lipoproteins, and atherosclerosis. Neurochem Int 50:12–38

Cerf E, Gustot A, Goormaghtigh E et al (2011) High ability of apolipoprotein E4 to stabilize amyloid-beta peptide oligomers, the pathological entities responsible for Alzheimer's disease. Faseb J 25:1585–1595

Curcio CA, Presley JB, Malek G et al (2005) Esterified and unesterified cholesterol in drusen and basal deposits of eyes with age-related maculopathy. Exp Eye Res 81:731–741

Curcio CA, Johnson M, Rudolf M et al (2011) The oil spill in ageing Bruch membrane. Br J Ophthalmol 95:1638–1645

de Chaves EP, Narayanaswami V (2008) Apolipoprotein E and cholesterol in aging and disease in the brain. Future Lipidol 3:505–530

Ebrahimi KB, Handa JT (2011) Lipids, lipoproteins, and age-related macular degeneration. J Lipids 2011:802059

Fliesler SJ, Bretillon L (2010) The ins and outs of cholesterol in the vertebrate retina. J Lipid Res 51:3399–3413

Fritsche LG, Fariss RN, Stambolian D et al (2014) Age-related macular degeneration: genetics and biology coming together. Annu Rev Genomics Hum Genet 15:151–71

Guo L, LaDu MJ, Van Eldik LJ (2004) A dual role for apolipoprotein e in neuroinflammation: anti- and pro-inflammatory activity. J Mol Neurosci: MN 23:205–212

Huang Y (2010) Mechanisms linking apolipoprotein E isoforms with cardiovascular and neurological diseases. Curr Opin Lipidol 21:337–345

Ito J, Nagayasu Y, Miura Y et al (2014) Astrocytes endogenous apoE generates HDL-like lipoproteins using previously synthesized cholesterol through interaction with ABCA1. Brain Res 1570:1–12

Johnson LV, Forest DL, Banna CD et al (2011) Cell culture model that mimics drusen formation and triggers complement activation associated with age-related macular degeneration. Proc Natl Acad Sci U S A 108:18277–18282

Katta S, Kaur I, Chakrabarti S (2009) The molecular genetic basis of age-related macular degeneration: an overview. J Genet 88:425–449

Leduc V, Jasmin-Belanger S, Poirier J (2010) APOE and cholesterol homeostasis in Alzheimer's disease. Trends Mol Med 16:469–477

Li CM, Clark ME, Chimento MF et al (2006) Apolipoprotein localization in isolated drusen and retinal apolipoprotein gene expression. Invest Ophthalmol Vis Sci 47:3119–3128

Liu MM, Chan CC, Tuo J (2012) Genetic mechanisms and age-related macular degeneration: common variants, rare variants, copy number variations, epigenetics, and mitochondrial genetics. Hum Genomics 6:13

Maezawa I, Jin LW, Woltjer RL et al (2004) Apolipoprotein E isoforms and apolipoprotein AI protect from amyloid precursor protein carboxy terminal fragment-associated cytotoxicity. J Neurochem 91:1312–1321

Mahley RW, Rall SC, Jr. (2000) Apolipoprotein E: far more than a lipid transport protein. Annu Rev Genomics Hum Genet 1:507–537

McKay GJ, Patterson CC, Chakravarthy U et al (2011) Evidence of association of APOE with age-related macular degeneration: a pooled analysis of 15 studies. Hum Mutat 32:1407–1416

Pikuleva IA, Curcio CA (2014) Cholesterol in the retina: the best is yet to come. Prog Retin Eye Res 41C:64–89

Raffai RL, Dong LM, Farese RV, Jr. et al (2001) Introduction of human apolipoprotein E4 "domain interaction" into mouse apolipoprotein E. Proc Natl Acad Sci U S A 98:11587–11591

Rapp A, Gmeiner B, Huttinger M (2006) Implication of apoE isoforms in cholesterol metabolism by primary rat hippocampal neurons and astrocytes. Biochimie 88:473–483

Sivak JM (2013) The aging eye: common degenerative mechanisms between the Alzheimer's brain and retinal disease. Invest Ophthalmol Vis Sci 54:871–880

Thakkinstian A, Bowe S, McEvoy M et al (2006) Association between apolipoprotein E polymorphisms and age-related macular degeneration: A HuGE review and meta-analysis. Ame J Epidemiol 164:813–822

Toops KA, Tan LX, Lakkaraju A (2014) A detailed three-step protocol for live imaging of intracellular traffic in polarized primary porcine RPE monolayers. Exp Eye Res 124:74–85

Tserentsoodol N, Gordiyenko NV, Pascual I et al (2006a) Intraretinal lipid transport is dependent on high density lipoprotein-like particles and class B scavenger receptors. Mol Vis 12:1319–1333

Tserentsoodol N, Sztein J, Campos M et al (2006b) Uptake of cholesterol by the retina occurs primarily via a low density lipoprotein receptor-mediated process. Mol Vis 12:1306–1318

Wu T, Fujihara M, Tian J et al (2010) Apolipoprotein B100 secretion by cultured ARPE-19 cells is modulated by alteration of cholesterol levels. J Neurochem 114:1734–1744

Zheng W, Reem RE, Omarova S et al (2012) Spatial distribution of the pathways of cholesterol homeostasis in human retina. PLoS ONE 7:e37926

Chapter 2
Role of Chemokines in Shaping Macrophage Activity in AMD

Matt Rutar and Jan M Provis

Abstract Age-related macular degeneration (AMD) is a multifactorial disorder that affects millions of individuals worldwide. While the advent of anti-VEGF therapy has allowed for effective treatment of neovascular 'wet' AMD, no treatments are available to mitigate the more prevalent 'dry' forms of the disease. A role for inflammatory processes in the progression of AMD has emerged over a period of many years, particularly the characterisation of leukocyte infiltrates in AMD-affected eyes, as well as in animal models. This review focuses on the burgeoning understanding of chemokines in the retina, and their potential role in shaping the recruitment and activation of macrophages in AMD. Understanding the mechanisms which promote macrophage activity in the degenerating retina may be key to controlling the potentially devastating consequences of inflammation in diseases such as AMD.

Keywords Retinal degenerations · Age-related macular degeneration (AMD) · Inflammation · Macrophages · Microglia · Chemokines

2.1 Introduction

Age-related macular degeneration (AMD) affects millions of individuals worldwide, and is the leading cause of blindness in the industrialised world (Ambati et al. 2003a). AMD is a multifactorial disorder, involving complex interaction between environmental and genetic factors. Evidence for a role of inflammation

M. Rutar (✉) · J. M. Provis
John Curtin School of Medical Research, The Australian National University, Building 131, Garran Rd, Canberra, ACT 2601, Australia
e-mail: matt.rutar@anu.edu.au

J. M. Provis
ANU Medical School, The Australian National University, Canberra, ACT 2601, Australia
e-mail: jan.provis@anu.edu.au

C. Bowes Rickman et al. (eds.), *Retinal Degenerative Diseases,* Advances in Experimental Medicine and Biology 854, DOI 10.1007/978-3-319-17121-0_2

in progression AMD has been accruing over a period of many years, particularly through the observations of leukocyte infiltrates within AMD-affected eyes (Penfold et al. 2001; Forrester 2003).

2.2 Macrophage Recruitment in AMD

The involvement of inflammatory processes in the histopathology of AMD was first noted almost 100 years ago (Hegner 1916), and several histological studies since have established the presence of aggregations of choroidal leukocyte infiltrates in association with disciform macular lesions (Hegner 1916; Paul 1927; Green and Key 1977).

Those early observations were confirmed and extended in a number of electron microscopical investigations which demonstrated the involvement of a number of inflammatory cells—including macrophages, lymphocytes, and mast cells—in RPE atrophy, and breakdown of Bruch's membrane (Penfold et al. 1984, 1985). Macrophages and other leukocytes have also been described in excised neovascular membranes (Lopez et al. 1991; Gehrs et al. 1992; Seregard et al. 1994). Ultrastructural studies also identified a close relationship between macrophages and the formation of choroidal neovascular membranes in wet AMD (Penfold et al. 1987). Multinucleated giant cells—which may form through union of multiple macrophages or microglia (Dickson 1986)—have also been found to correlate spatially with regions of breakdown in Bruch's membrane and with CNV (choroidal neovascularisation) (Penfold et al. 1985). Chronic involvement of macrophages and giant cells has also been shown in atrophic AMD lesions, and on the expanding edges (Penfold et al. 1987; Cherepanoff et al. 2009). Other investigations have shown changes in parenchymal microglia in association with early AMD, including increased MHC-II expression and morphological changes suggestive of activation (Penfold et al. 1997). In advanced AMD, activated amoeboid microglia infiltrate the ONL and subretinal space in the degenerating outer retina, where they are associated with neovascular structures (Combadiere et al. 2007), and appear to have a role in the phagocytosis of photoreceptor debris (Gupta et al. 2003; Combadiere et al. 2007).

2.3 Role of Chemokines

First discovered in 1987 (Walz et al. 1987; Yoshimura et al. 1987), chemokines are a large, growing family comprising more than 50 molecules interacting with at least 20 chemokine receptors, that play an important role in the chemotactic guidance of leukocyte migration and activation (Moser and Loetscher 2001; Bajetto et al. 2002). Chemokines are small molecules grouped according to the relative position of their first N-terminal cysteine residues, comprising C (γ chemokines), CC (β chemokines), CXC (α chemokines), and CX3C (δ chemokines) families (Loetscher et al.

2000; Murphy et al. 2000; Zlotnik and Yoshie 2000; Bajetto et al. 2002). These may be expressed by endothelial cells, resident macrophages (including microglia), as well as infiltrating leukocytes (Crane and Liversidge 2008). Chemokines exert their biological activity through binding cell surface chemokine receptors, which are part of the superfamily of seven transmembrane domain receptors that signal through coupled heterotrimeric G-proteins, consisting of C, CC, CXC, CX3C receptor subclasses (Bajetto et al. 2002). Many of these receptors show a degree of redundancy, as multiple chemokines may bind several receptors; although interactions are mainly restricted to within particular subclasses (Bajetto et al. 2002). Chemokine expression typically generates chemical ligand gradients, which serve as directional cues for guidance of leukocytes bearing the appropriate chemokine receptors to sites of injury, and are also thought to aid in extravasation of leukocytes (Luster 1998).

The expression of chemokines in the guidance and activation of macrophages has garnered considerable interest in AMD. Retinas from human donors show increased expression of both α (Cxcl1, Cxcl1) and β (Ccl2) chemokine genes in 'wet' and 'dry' AMD (Newman et al. 2012), while elevated levels of Ccl2 protein—a potent chemoattractant for monocytes (Matsushima et al. 1989; Yoshimura et al. 1989)—have been detected in aqueous humour samples taken from patients in advanced stages of AMD (Jonas et al. 2010; Kramer et al. 2011). Additionally, elevation in Ccl2 is evident within atrophic 'dry' AMD lesions and is accompanied by influxes of monocytes expressing Ccr2 (Sennlaub et al. 2013), which is the receptor for Ccl2 signalling (Yoshimura and Leonard 1990).

A direct for role of chemokines has been elucidated with animal models of AMD (Patel and Chan 2008). Investigations using laser-induced CNV in mice have focused on the role of β chemokine signalling in neovascular AMD. Ablation of Ccl2 using target gene knockout has been shown to inhibit the infiltration of macrophages and results in reduced lesion size following laser-induced CNV compared to controls (Luhmann et al. 2009). Moreover, a mouse knockout of the receptor Ccr2 exhibits decreased macrophage recruitment and vastly reduced neovascularisation following experimental laser-induced CNV (Tsutsumi et al. 2003). In models of atrophic 'dry' AMD which utilise bright light as a damaging stimulus (Marc et al. 2008; Rutar et al. 2010), the suppression of Ccl2 using either ablation or siRNA-mediated knockdown reduces macrophage recruitment and the extent of cell death (Rutar et al. 2012; Sennlaub et al. 2013). Conversely, other studies suggest that a degree of β chemokine signalling may be necessary for the maintenance retinal homeostasis, and prevention of AMD. An investigation in aged, dual Ccl2/Ccr2 knockout mice showed retinal features similar to AMD including formation of lipofuscin, drusen, photoreceptor degeneration, and neovascularisation (Ambati et al. 2003b), although the AMD-like phenotype in this model has been questioned (Luhmann et al. 2009). Ccl2/Ccr2 knockout results in the accumulation of hypertrophied subretinal macrophages, possibly because of impaired monocyte trafficking (Luhmann et al. 2009).

The only δ chemokine receptor characterised, Cx3cr1, has also been implicated in maintenance of homeostasis and genesis of AMD-like pathology. Cx3cr1 is a chemokine receptor found on microglia, macrophages, astrocytes, and T-cells (Patel

and Chan 2008), whose ligand chemokine Cx3cl1 is constitutively expressed on many cell types in the retina, and together are thought to mediate the trafficking of microglia and macrophages in the clearance of extracellular deposits (Fong et al. 1998; Silverman et al. 2003). Targeted knockout of Cx3cr1 in light-stressed mice induces progressive degeneration of photoreceptors in correlation with an accumulation of engorged subretinal microglia/macrophages and other AMD-like features (Combadiere et al. 2007). Moreover, ablation of Cx3cr1 is associated with an increase in lesion size following experimental neovascularisation (Combadiere et al. 2007).

2.4 Summary

Over a period of many years, the role of inflammation in AMD has gradually emerged as an important factor underpinning its pathogenesis. This is exemplified by traditional histological examinations and electron microscopy identifying macrophage/microglial infiltration in AMD-effected eyes, and more recently through investigations utilising animal models. The expression of chemokine-related genes is prodigious in all forms of AMD pathology, and animal models of both and 'dry' and 'wet' AMD indicate that chemokine expression modulates both the recruitment and activation of macrophages, as well as the extent of retinal degeneration. Reducing inflammation by altering macrophage activity in retina may prove an important therapeutic tool in ameliorating degeneration in AMD.

References

Ambati J, Ambati BK, Yoo SH et al (2003a) Age-related macular degeneration: etiology, pathogenesis, and therapeutic strategies. Surv Ophthalmol 48:257–293

Ambati J, Anand A, Fernandez S et al (2003b) An animal model of age-related macular degeneration in senescent Ccl-2- or Ccr-2-deficient mice. Nat Med 9:1390–1397

Bajetto A, Bonavia R, Barbero S et al (2002) Characterization of chemokines and their receptors in the central nervous system: physiopathological implications. J Neurochem 82:1311–1329

Cherepanoff S, McMenamin P, Gillies MC et al (2009) Bruch's membrane and choroidal macrophages in early and advanced age-related macular degeneration. Br J Ophthalmol 94:918–925

Combadiere C, Feumi C, Raoul W et al (2007) CX3CR1-dependent subretinal microglia cell accumulation is associated with cardinal features of age-related macular degeneration. J Clin Invest 117:2920–2928

Crane IJ, Liversidge J (2008) Mechanisms of leukocyte migration across the blood-retina barrier. Semin Immunopathol 30:165–177

Dickson DW (1986) Multinucleated giant cells in acquired immunodeficiency syndrome encephalopathy. Origin from endogenous microglia? Arch Pathol Lab Med 110:967–968

Fong AM, Robinson LA, Steeber DA et al (1998) Fractalkine and CX3CR1 mediate a novel mechanism of leukocyte capture, firm adhesion, and activation under physiologic flow. J Exp Med 188:1413–1419

Forrester JV (2003) Macrophages eyed in macular degeneration. Nat Med 9:1350–1351

Gehrs KM, Heriot WJ, de Juan E, Jr. (1992) Transmission electron microscopic study of a subretinal choroidal neovascular membrane due to age-related macular degeneration. Arch Ophthalmol 110:833–837

Green WR, Key SN, 3rd (1977) Senile macular degeneration: a histopathologic study. Trans Am Ophthalmol Soc 75:180–254

Gupta N, Brown KE, Milam AH (2003) Activated microglia in human retinitis pigmentosa, late-onset retinal degeneration, and age-related macular degeneration. Exp Eye Res 76:463–471

Hegner CA (1916) Retinitis exsudativa bei Lymphogranulomatosis. Klin Monatsbl Augenheil 57:27–48

Jonas JB, Tao Y, Neumaier M et al (2010) Monocyte chemoattractant protein 1, intercellular adhesion molecule 1, and vascular cell adhesion molecule 1 in exudative age-related macular degeneration. Arch Ophthalmol 128:1281–1286

Kramer M, Hasanreisoglu M, Feldman A et al (2012) Monocyte chemoattractant protein-1 in the aqueous humor of patients with age-related macular degeneration. Clin Experiment Ophthalmol 40(6):617–25

Loetscher P, Moser B, Baggiolini M (2000) Chemokines and their receptors in lymphocyte traffic and HIV infection. Adv Immunol 74:127–180

Lopez PF, Grossniklaus HE, Lambert HM et al (1991) Pathologic features of surgically excised subretinal neovascular membranes in age-related macular degeneration. Am J Ophthalmol 112:647–656

Luhmann UF, Robbie S, Munro PM et al (2009) The drusenlike phenotype in aging Ccl2-knockout mice is caused by an accelerated accumulation of swollen autofluorescent subretinal macrophages. Invest Ophthalmol Vis Sci 50:5934–5943

Luster AD (1998) Chemokines–chemotactic cytokines that mediate inflammation. N Engl J Med 338:436–445

Marc RE, Jones BW, Watt CB et al (2008) Extreme retinal remodeling triggered by light damage: implications for age related macular degeneration. Mol Vis 14:782–806

Matsushima K, Larsen CG, DuBois GC et al (1989) Purification and characterization of a novel monocyte chemotactic and activating factor produced by a human myelomonocytic cell line. J Exp Med 169:1485–1490

Moser B, Loetscher P (2001) Lymphocyte traffic control by chemokines. Nat Immunol 2:123–128

Murphy PM, Baggiolini M, Charo IF et al (2000) International union of pharmacology. XXII. Nomenclature for chemokine receptors. Pharmacol Rev 52:145–176

Newman AM, Gallo NB, Hancox LS et al (2012) Systems-level analysis of age-related macular degeneration reveals global biomarkers and phenotype-specific functional networks. Genome Med 4:16

Patel M, Chan CC (2008) Immunopathological aspects of age-related macular degeneration. Semin Immunopathol 30:97–110

Paul LA (1927) Choroiditis exsudativa under dem bilde der scheibenformigen entartung der-netzhautmitte. Z Augenh 63:205–223

Penfold P, Killingsworth M, Sarks S (1984) An ultrastructural study of the role of leucoytes and fibroblasts in the breakdown of Bruch's membrane. Aust J Ophthalmol 12:23–31

Penfold PL, Killingsworth MC, Sarks SH (1985) Senile macular degeneration: the involvement of immunocompetent cells. Graefes Arch Clin Exp Ophthalmol 223:69–76

Penfold PL, Provis JM, Billson FA (1987) Age-related macular degeneration: ultrastructural studies of the relationship of leucocytes to angiogenesis. Graefes Arch Clin Exp Ophthalmol 225:70–76

Penfold PL, Liew SC, Madigan MC et al (1997) Modulation of major histocompatibility complex class II expression in retinas with age-related macular degeneration. Invest Ophthalmol Vis Sci 38:2125–2133

Penfold PL, Madigan MC, Gillies MC et al (2001) Immunological and aetiological aspects of macular degeneration. Prog Ret Eye Res 20:385–414

Rutar M, Provis JM, Valter K (2010) Brief exposure to damaging light causes focal recruitment of macrophages, and long-term destabilization of photoreceptors in the albino rat retina. Curr Eye Res 35:631–643

Rutar MV, Natoli RC, Provis JM (2012) Small interfering RNA-mediated suppression of Ccl2 in Muller cells attenuates microglial recruitment and photoreceptor death following retinal degeneration. J Neuroinflammation 9:221

Sennlaub F, Auvynet C, Calippe B et al (2013) CCR2(+) monocytes infiltrate atrophic lesions in age-related macular disease and mediate photoreceptor degeneration in experimental subretinal inflammation in Cx3cr1 deficient mice. EMBO Mol Med 5:1775–1793

Seregard S, Algvere PV, Berglin L (1994) Immunohistochemical characterization of surgically removed subfoveal fibrovascular membranes. Graefes Arch Clin Exp Ophthalmol 232:325–329

Silverman MD, Zamora DO, Pan Y et al (2003) Constitutive and inflammatory mediator-regulated fractalkine expression in human ocular tissues and cultured cells. Invest Ophthalmol Vis Sci 44:1608–1615

Tsutsumi C, Sonoda KH, Egashira K et al (2003) The critical role of ocular-infiltrating macrophages in the development of choroidal neovascularization. J Leukoc Biol 74:25–32

Walz A, Peveri P, Aschauer H et al (1987) Purification and amino acid sequencing of NAF, a novel neutrophil-activating factor produced by monocytes. Biochem Biophys Res Commun 149:755–761

Yoshimura T, Leonard EJ (1990) Identification of high affinity receptors for human monocyte chemoattractant protein-1 on human monocytes. J Immunol 145:292–297

Yoshimura T, Matsushima K, Oppenheim JJ et al (1987) Neutrophil chemotactic factor produced by lipopolysaccharide (LPS)-stimulated human blood mononuclear leukocytes: partial characterization and separation from interleukin 1 (IL 1). J Immunol 139:788–793

Yoshimura T, Robinson EA, Tanaka S et al (1989) Purification and amino acid analysis of two human glioma-derived monocyte chemoattractants. J Exp Med 169:1449–1459

Zlotnik A, Yoshie O (2000) Chemokines: a new classification system and their role in immunity. Immunity 12:121–127

Chapter 3
Biology of p62/sequestosome-1 in Age-Related Macular Degeneration (AMD)

Lei Wang, Katayoon B Ebrahimi, Michelle Chyn, Marisol Cano and James T Handa

Abstract p62/sequestosome-1 is a multidimensional protein that interacts with many signaling factors, and regulates a variety of cellular functions including inflammation, apoptosis, and autophagy. Our previous work has revealed in the retinal pigment epithelium (RPE) that p62 promotes autophagy and simultaneously enhances an Nrf2-mediated antioxidant response to protect against acute oxidative stress. Several recent studies demonstrated that p62 contributes to NFkB mediated inflammation and inflammasome activation under certain circumstances, raising the question of whether p62 protects against or contributes to tissue injury. Herein, we will review the general characteristics of p62, focusing on its pro- and anti-cell survival roles within different physiological/pathological contexts, and discuss the potential of p62 as a therapeutic target for AMD.

Keywords AMD · RPE · p62 · sqstm1 · Autophagy · Nrf2 · Neurodegeneration · NFκB · PB1

L. Wang (✉) · K. B. Ebrahimi · M. Chyn · M. Cano · J. T. Handa
Wilmer Eye Institute, Johns Hopkins School of Medicine, 400 N Broadway, Rm 3001-D, the Smith Building, Baltimore, MD 21287, USA
e-mail: leiwang.011@gmail.com

K. B. Ebrahimi
e-mail: kebrahi2@jhmi.edu

M. Chyn
e-mail: mchyn1@jhu.edu

M. Cano
e-mail: mcano1@jhmi.edu

J. T. Handa
e-mail: jthanda@jhmi.edu

C. Bowes Rickman et al. (eds.), *Retinal Degenerative Diseases,* Advances in Experimental Medicine and Biology 854, DOI 10.1007/978-3-319-17121-0_3

3.1 Introduction

AMD is the most common cause of blindness among the elderly in western countries (Kaarniranta et al. 2011), and is characterized by dysfunction of the retinal pigment epithelium (RPE). The RPE is under constant oxidative challenge due to phagocytosis and exposure to UV light. Removal of oxidized/misfolded proteins relies on the proteasome and autophagy. We showed that acute stress inhibits the proteasome, but up-regulates anti-oxidant and autophagy related genes, including p62 (Cano et al. 2014). We also confirmed p62's protective role in the RPE, via both autophagic clearance and activation of Nrf2 antioxidant signaling (Wang et al. 2014). As AMD shares pathological and mechanistic features with other adult-onset neurodegenerative diseases (Glass et al. 2010; Kaarniranta et al. 2011), our studies on p62's role in AMD could contribute to the understanding of these diseases.

3.2 Structure and Functions of p62

p62 was initially discovered as an interacting partner of atypical protein kinase C (aPKC) (Puls et al. 1997; Sanchez et al. 1998) via its N-terminal Phox/Bem 1p (PB1) domain, and mediating the activation of NFkB signaling. The following ZZ zinc-finger domain binds receptor interacting protein (RIP), also linking p62 to NFkB signaling. The TRAF6 binding (TB) domain binds TRAF6, which is relevant in osteoclastogenesis, as well as Ras-induced tumorigenesis (Nakamura et al. 2010). Downstream of TB domain, the LC3-interacting region (LIR) interacts with autophagosome protein Atg8/LC3, and the Keap1-interacting region (KIR) is involved with Nrf2 regulation. At the C-terminus, the ubiquitin-associated (UBA) domain regulates p62's interaction with polyubiquitinated proteins targeted for autophagic degradation (Matsumoto et al. 2011). As Table 3.1 shows, p62 is rich in protein-interacting sequences. Its N-terminal region mainly regulates inflammatory responses, and the C-terminal domains mostly contribute to stress reduction. (See Fig. 3.1)

Multiple p62 isoforms have been identified in different species. The rat expresses three p62 protein isoforms (Gong 1999; Croci et al. 2003). The ratio of rat p62

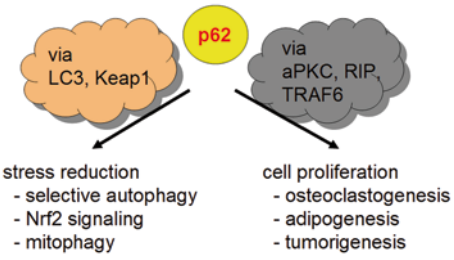

Fig. 3.1 p62 can be either protective or damaging. Its role is determined by its interacting partners, in different pathological context and tissue types

Table 3.1 Studies on p62 functional domains and covalent modifications

References	Studies on individual domain or mutation
(Puls et al. 1997)	p62 interacts with aPKC via the N-terminal PB1 domain
(Bjorkoy et al. 2005)	LC3 interacts with p62
(Jain et al. 2010)	KIR (keap1 interacting region) is mapped
(Linares et al. 2011)	Phosphorylation at T269, S272 influences mitosis and cell proliferation
(Matsumoto et al. 2011)	Phosphorylation at S403 determines its affinity for ubiquitinated cargo
(Ichimura et al. 2013)	Phosphorylation at S351 in an mTORC-1 dependent manner determines its affinity to Keap1
(Shi et al. 2013)	p62 cleavage at TB disrupts autophagy and impairs NFkB signaling

isoform1/isoform2 is tissue specific, and is dynamically regulated in response to stimulation. Humans express two p62 isoforms, of which isoform2 is 84 amino acids shorter at the N-terminus, equivalent to the loss of PB1 domain. Our studies demonstrated that all p62 mRNA species are expressed in cultured human RPE cells, but isoform2 is barely translated (Wang et al. 2014), thus its functional role requires further investigation in AMD patients.

3.3 p62 Protects by Enhancing Autophagic Clearance and Activating Nrf2 Signaling

Aggregates of misfolded/damaged proteins are transported to the autophagy machinery for degradation (Matsumoto et al. 2011). p62 functions as a cargo receptor, binding to polyubiquitinated proteins and guiding them to the autophagosome. Our studies confirmed in RPE cells, that p62 silencing caused cargo loading failure and inefficient autophagy, as demonstrated by a reduced LC3 conversion ratio. Overexpression of p62 gave the opposite results. Interestingly, p62's influence on selective autophagy was observed only when cells were under oxidative stress. We speculate that under basal conditions, RPE cells rely on other protective mechanisms such as the proteasome, and that p62 mediated autophagy is recruited to deal with overwhelming stress.

Along with the p62 mediated autophagic clearance, the antioxidant transcription factor Nrf2 is activated to help maintaining redox homeostasis. Keap1, known to sequester Nrf2 in the cytosol and inhibit its activity, is bound by p62, thus releasing Nrf2 to activate the antioxidant genes (Komatsu et al. 2010). Our studies confirmed in RPE that p62 enhanced Nrf2 activity, and Nrf2 upregulated p62 expression at transcriptional level, thus forming a positive feedback loop. These findings indicate that in response to an acute stress, p62 provides dual cytoprotection to RPE, via autophagic clearance of insoluble proteins and activation of Nrf2 signaling.

3.4 p62, A Double Edged Sword

With aging, the p62 promoter undergoes oxidative damage (Du et al. 2009b; Du et al. 2009a), consistent with our observation of reduced p62 mRNA expression in elderly mouse RPE (unpublished data). We would predict a decline of p62 in the AMD mouse model (Cano et al. 2010) and AMD patients, but p62 accumulation was observed instead (unpublished data). Similar observations were made in neurodegenerative patients (see Table 3.2). This contradiction could result from post-transcriptional up-regulation of p62 to rescue damaged cells, but it is questionable whether p62 can still promote clearance of protein aggregates when the whole autophagy machinery undergoes irreversible failure. It was reported that in autophagy-deficient livers, p62 ablation actually reduced toxicity and prevented cell death (Komatsu et al. 2007).

In vitro studies revealed p62's role in NFkB signaling and inflammasome activation (Takeda-Watanabe et al. 2012; Park et al. 2013). p62 could be a double edged sword - it fights against stress, yet it can promote inflammation, exacerbating cellular crisis. (see Fig. 3.1) Since autophagy failure and a weakened Nrf2 response in the RPE is a component of AMD, the accumulated p62 in disease area possibly exerts a harmful effect by aggravating chronic inflammation, a common feature of neurodegenerative diseases.

Table 3.2 p62 dysregulation is associated with a number of diseases

References	Studies on p62 function	Disease
(Rea et al. 2006)	K378X mutation in p62 is associated with increased NFkB signaling and osteoclast formation	Paget's disease of bone
(Ramesh Babu et al. 2008)	p62 KO leads to accumulation of hyperphosphorylated tau	Alzheimer's disease
(Daroszewska et al. 2011)	p62 mutation (P394L) is associated with bone lesions	Paget's disease of bone
(Braak et al. 2011)	p62 immunostaining in the neurosecretory cells of the paraventricular nucleus	Parkinson's disease
(Salminen et al. 2012)	Lack of p62 provokes the tau pathology; reduced p62 levels were observed in the frontal cortex of AD patients	Alzheimer's disease
(Hirano et al. 2013)	p62 mutations (Ala53Thr, Pro439Leu) are associated with ALS	Amyotrophic lateral sclerosis
(Rue et al. 2013)	p62 accumulation occurs in neuronal nuclei, colocalizing with huntingtin inclusions	Huntington's disease

3.5 Future Experimental Approaches

To evaluate p62's potential as a therapeutic target for AMD, we must elucidate its role under chronic stress (Cano et al. 2010; Wang and Neufeld 2010), to determine:

1) if p62 undergoes posttranscriptional alteration, such as mRNA splicing;
2) if p62 activity is regulated by novel covalent modifications;
3) if p62 has unidentified interacting protein partners under pathological conditions.

A thorough understanding of p62's regulatory mechanism could lead to new therapeutic methods for AMD.

Acknowledgments Funding for this work was provided by NIH EY019904 (JTH), Beckman Foundation AMD Grant (JTH), Thome Foundation (JTH), Research to Prevent Blindness Senior Scientist Award (JTH), NIH P30EY001765 core grant, the Robert Bond Welch Professorship (JTH), a gift from the Merlau family, and an unrestricted grant from RPB to the Wilmer Eye Institute.

References

Bjorkoy G, Lamark T, Brech A et al (2005) p62/SQSTM1 forms protein aggregates degraded by autophagy and has a protective effect on huntingtin-induced cell death. J Cell Biol 171:603–614

Braak H, Thal DR, Del Tredici K (2011) Nerve cells immunoreactive for p62 in select hypothalamic and brainstem nuclei of controls and Parkinson's disease cases. J Neural Trans 118:809–819

Cano M, Thimmalappula R, Fujihara M et al (2010) Cigarette smoking, oxidative stress, the anti-oxidant response through Nrf2 signaling, and Age-related Macular Degeneration. Vision Res 50:652–664

Cano M, Wang L, Wan J et al (2014) Oxidative stress induces mitochondrial dysfunction and a protective unfolded protein response in RPE cells. Free Rad Biol Med 69:1–14

Croci C, Brandstatter JH, Enz R (2003) ZIP3, a new splice variant of the PKC-zeta-interacting protein family, binds to GABAC receptors, PKC-zeta, and Kv beta 2. J Biol Chem 278:6128–6135

Daroszewska A, van 't Hof RJ, Rojas JA et al (2011) A point mutation in the ubiquitin-associated domain of SQSMT1 is sufficient to cause a Paget's disease-like disorder in mice. Hum Mol Genet 20:2734–2744

Du Y, Wooten MC, Wooten MW (2009a) Oxidative damage to the promoter region of SQSTM1/p62 is common to neurodegenerative disease. Neurobiol Dis 35:302–310

Du Y, Wooten MC, Gearing M et al (2009b) Age-associated oxidative damage to the p62 promoter: implications for Alzheimer disease. Free Rad Biol Med 46:492–501

Glass CK, Saijo K, Winner B et al (2010) Mechanisms underlying inflammation in neurodegeneration. Cell 140:918–934

Gong J (1999) Differential stimulation of PKC phosphorylation of potassium channels by ZIP1 and ZIP2. Science 285:1565–1569

Hirano M, Nakamura Y, Saigoh K et al (2013) Mutations in the gene encoding p62 in Japanese patients with amyotrophic lateral sclerosis. Neurology 80:458–463

Ichimura Y, Waguri S, Sou YS et al (2013) Phosphorylation of p62 activates the Keap1-Nrf2 pathway during selective autophagy. Mol Cell 51:618–631

Jain A, Lamark T, Sjottem E et al (2010) p62/SQSTM1 is a target gene for transcription factor NRF2 and creates a positive feedback loop by inducing antioxidant response element-driven gene transcription. J Biol Chem 285:22576–22591

Kaarniranta K, Salminen A, Haapasalo A et al (2011) Age-related macular degeneration (AMD): Alzheimer's disease in the eye? J Alzheimers Dis: JAD 24:615–631
Komatsu M, Waguri S, Koike M et al (2007) Homeostatic levels of p62 control cytoplasmic inclusion body formation in autophagy-deficient mice. Cell 131:1149–1163
Komatsu M, Kurokawa H, Waguri S et al (2010) The selective autophagy substrate p62 activates the stress responsive transcription factor Nrf2 through inactivation of Keap1. Nature Cell Biol 12:213–223
Linares JF, Amanchy R, Greis K et al (2011) Phosphorylation of p62 by cdk1 controls the timely transit of cells through mitosis and tumor cell proliferation. Mol Cell Biol 31:105–117
Matsumoto G, Wada K, Okuno M et al (2011) Serine 403 phosphorylation of p62/SQSTM1 regulates selective autophagic clearance of ubiquitinated proteins. Mol Cell 44:279–289
Nakamura K, Kimple AJ, Siderovski DP et al (2010) PB1 domain interaction of p62/sequestosome 1 and MEKK3 regulates NF-kappaB activation. J Biol Chem 285:2077–2089
Park S, Ha SD, Coleman M et al (2013) p62/SQSTM1 enhances NOD2-mediated signaling and cytokine production through stabilizing NOD2 oligomerization. PLoS One 8:e57138
Puls A, Schmidt S, Grawe F et al (1997) Interaction of protein kinase C zeta with ZIP, a novel protein kinase C-binding protein. Proc Natl Acad Sci USA 94:6191–6196
Ramesh Babu J, Lamar Seibenhener M, Peng J et al (2008) Genetic inactivation of p62 leads to accumulation of hyperphosphorylated tau and neurodegeneration. J Neurochem 106:107–120
Rea SL, Walsh JP, Ward L et al (2006) A novel mutation (K378X) in the sequestosome 1 gene associated with increased NF-kappaB signaling and Paget's disease of bone with a severe phenotype. J Bone Mineral Res 21:1136–1145
Rue L, Lopez-Soop G, Gelpi E et al (2013) Brain region- and age-dependent dysregulation of p62 and NBR1 in a mouse model of Huntington's disease. Neurobiol Dis 52:219–228
Salminen A, Kaarniranta K, Haapasalo A et al (2012) Emerging role of p62/sequestosome-1 in the pathogenesis of Alzheimer's disease. Prog Neurobiol 96:87–95
Sanchez P, De Carcer G, Sandoval IV et al (1998) Localization of atypical protein kinase C isoforms into lysosome-targeted endosomes through interaction with p62. Mol Cell Biol 18: 3069–3080
Shi J, Wong J, Piesik P et al (2013) Cleavage of sequestosome 1/p62 by an enteroviral protease results in disrupted selective autophagy and impaired NFKB signaling. Autophagy 9:1591–1603
Takeda-Watanabe A, Kitada M, Kanasaki K et al (2012) SIRT1 inactivation induces inflammation through the dysregulation of autophagy in human THP-1 cells. Biochem Biophys Res Comm 427:191–196
Wang AL, Neufeld AH (2010) Smoking mice: a potential model for studying accumulation of drusen-like material on Bruch's membrane. Vision Res 50:638–642
Wang L, Cano M, Handa JT (2014) p62 provides dual cytoprotection against oxidative stress in the retinal pigment epithelium. Biochim Biophys Acta 1843:1248–1258

Chapter 4
Gene Structure of the 10q26 Locus: A Clue to Cracking the ARMS2/HTRA1 Riddle?

Elod Kortvely and Marius Ueffing

Abstract Age-related macular degeneration (AMD) is a sight-threatening disorder of the central retina. Being the leading cause of visual impairment in senior citizens, it represents a major public health issue in developed countries. Genetic studies of AMD identified two major susceptibility loci on chromosomes 1 and 10. The high-risk allele of the 10q26 locus encompasses three genes, PLEKHA1, ARMS2, and HTRA1 with high linkage disequilibrium and the individual contribution of the encoded proteins to disease etiology remains controversial. While PLEKHA1 and HTRA1 are highly conserved proteins, ARMS2 is only present in primates and can be detected by using RT-PCR. On the other hand, there is no unequivocal evidence for the existence of the encoded protein. However, it has been reported that risk haplotypes only affect the expression of ARMS2 (but not of HTRA1), making ARMS2 the best candidate for being the genuine AMD gene within this locus. Yet, homozygous carriers of a common haplotype carry a premature stop codon in the ARMS2 gene (R38X) and therefore lack ARMS2, but this variant is not associated with AMD. In this work we aimed at characterizing the diversity of transcripts originating from this locus, in order to find new hints on how to resolve this perplexing paradox. We found chimeric transcripts originating from the PLEKHA1 gene but ending in ARMS2. This finding may give a new explanation as to how variants in this locus contribute to AMD.

Keywords Age-related macular degeneration · HTRA1 · ARMS2 · PLEKHA1 · Chimeric transcripts · Gene transcription · Alternative splicing · rs10490924 · rs11200638 · rs2736911

E. Kortvely (✉) · M. Ueffing
Division of Experimental Ophthalmology, University of Tuebingen, Roentgenweg 11, 72076 Tuebingen, Germany
e-mail: eloed.koertvely@uni-tuebingen.de

M. Ueffing
e-mail: marius.ueffing@uni-tuebingen.de

C. Bowes Rickman et al. (eds.), *Retinal Degenerative Diseases,* Advances in Experimental Medicine and Biology 854, DOI 10.1007/978-3-319-17121-0_4

4.1 Introduction

Age-related macular degeneration (AMD) is a common blinding disease of the elderly with an exceedingly intricate etiology. An interplay of non-modifiable (i.e. multiple genetic variants) and modifiable (i.e. environmental) factors contribute to disease risk (Seddon and Chen 2004).

The involvement of the complement system had been already proposed in 2001 (Hageman et al. 2001), and four years later genome-wide linkage scans indeed identified complement factor H (CFH) as the first major susceptibility gene for AMD (Edwards et al. 2005; Haines et al. 2005; Klein et al. 2005). The second major susceptibility locus was identified shortly after the publication of the above results (Jakobsdottir et al. 2005). This locus on chromosome 10q26 exhibits an even stronger association signal overlying three genes: Pleckstrin Homology Domain Containing, Family A Member 1 (PLEKHA1), Age-Related Maculopathy Susceptibility 2 (ARMS2), and HtrA serine peptidase 1 (HTRA1). Because of the close vicinity of these genes, association studies lack the required discriminative power to determine the causative gene/variant. PLEKHA1 is apparently outside the linkage disequilibrium block exhibiting the peak association. In contrast, there are numerous papers suggesting a role for ARMS2 (Rivera et al. 2005; Fritsche et al. 2008) or for HTRA1 (Dewan et al. 2006; Yang et al. 2006) in AMD. Furthermore, Yang et al. suggests a two-hit model, claiming that both genes are simultaneously affected by the risk haplotype (Yang et al. 2010).

It has been reported in numerous Mendelian diseases that protein products of causal genes tend to physically interact (Brunner and van Driel 2004; Franke et al. 2006). Similarly, growing evidence suggests that products of genes in complex trait-associated loci establish functional protein-protein bindings. The dominance of components belonging to the alternative complement pathway among the proteins implicated in AMD strongly supports this concept. Taking this idea one step further, the sought-after gene within the PLEKHA1/ARMS2/HTRA1 locus should code for a protein that is linked to one of the few disease pathways implicated in AMD (Kortvely and Ueffing 2012). From this vantage point, HTRA1 seems to be the most attracting candidate, because it is involved in the remodeling of the extracellular matrix and participates in TGF beta signaling hinting toward involvement in choroidal neovascularization, a hallmark of the wet form of AMD (Clausen et al. 2011).

In this work we set out to characterize the transcripts generated from the 10q26 locus in order to disentangle the individual effects of these genes on AMD risk. Understanding the regulation of gene expression within this chromosomal region may offer a new explanatory framework to resolve the debate about the AMD gene conferring the highest risk.

4.2 Materials and Methods

4.2.1 Phylogenetic Analysis

To identify the potential homologs/paralogs for the ARMS2 gene and the corresponding putative protein, BLAST searches were performed on the public databases at NIH. Alignments of deduced protein sequences were carried out with the multiple alignment software Geneious (version 7.1). The evolutionary dendrogram (unrooted tree) was calculated by using the Neighbor-Joining method.

4.2.2 RT-PCR

Total RNA was extracted from human term placenta. The RT reaction was performed using 2 ∝g RNA with an oligo(dT) primer using the Omniscript RT kit (Qiagen, GmbH, Hilden, Germany) according to the manufacturer's manual. The following primers were used to detect chimeric transcripts: 5'-ATAACCTAAGTCGCCATGGTG-3' (PLEKHA1 forward), 5'-CAGTTGAGGCAGCTGGAGGG-3' (ARMS2, reverse). Amplified products were cloned and sequenced.

4.3 Results and Discussion

4.3.1 Phylogeny of ARMS2

While the other two genes (PLEKHA1 and HTRA1) of the 10q26 locus are conserved throughout the vertebrates and beyond, ARMS2 is only found in higher primates (more precisely in simians, Fig. 4.1). Strikingly, the evolutionary appearance of ARMS2 parallels the anatomical specialization of the macula. Most importantly, this specialization represents a tradeoff between performance and vulnerability. The restricted blood supply and the concomitant metabolic stress may even play a role in macular differentiation (Provis et al. 2005; Yu et al. 2010). Like humans, macaque monkeys possess a macula and develop age-related macular pathologies and share risk variants with humans (Francis et al. 2008).

Although the vast majority of genes present in any species descend from a gene present in an ancestor, some genes originate from ancestrally non-genic sequences (Carvunis et al. 2012). In fact, de novo gene birth from a pool of pre-existing open reading frames may be more prevalent than sporadic gene duplication. Accordingly, ARMS2 may be evolved from a placeholder sequence separating PLEKHA1 and

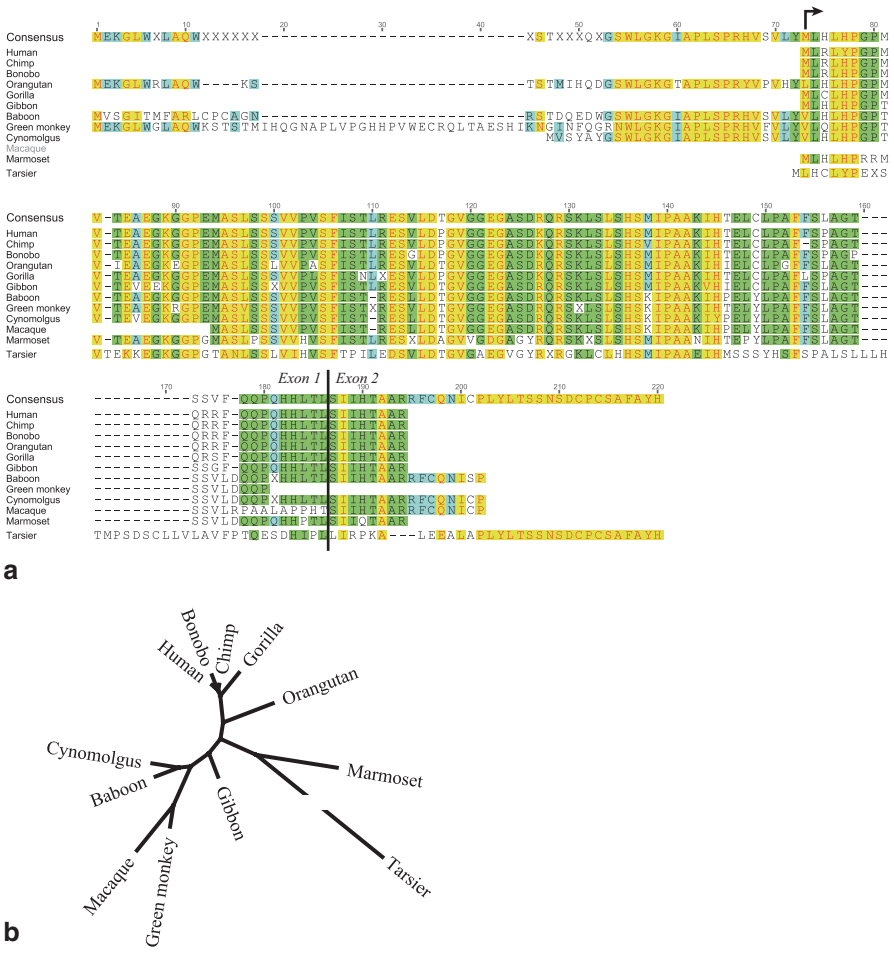

Fig. 4.1 **a** Multiple alignment of predicted ARMS2 amino acid sequences. The putative transcription initiation site in human is marked with a broken *arrow*. Identical residues are indicated by *red* letters on *yellow* background and similar residues are indicated by *green* background. A vertical *line* shows the boundary between the regions encoded by exon 1 and 2. Note that the deduced tarsier sequence (a species not belonging to the simian infraorder) only exhibits a weak similarity to the consensus, thus it is unlikely to exist at protein level. **b** Evolutionary dendrograms of ARMS2 orthologs generated using the Geneious program. Shorter branches indicate larger similarities Tarsier seems to be diverged before the appearance of the functional ARMS2 gene

HTRA1. Primate-specific transcriptional units were found (1) to have transcript lengths comparable with the average length of human cDNAs, and few exons, (2) preferentially expressed in the reproductive system, and (3) to be frequently intercalated in the introns of known protein-coding genes (Tay et al. 2009). To what extent does ARMS2 fit this profile? ARMS2 is indeed composed of only two exons, though the length of the transcript is below the average. Studies suggest that

ARMS2 is primarily expressed in the placenta, being a part of the female reproductive system. Furthermore, we found chimeric transcripts containing exons from both PLEKHA1 and ARMS2 (see below).

4.3.2 Transcript Diversity Originating from the 10q26 Locus

Since it can be easily amplified by RT-PCR, it is generally accepted that ARMS2 exists at RNA level. Beside moderate expression in the placenta, weak expression was detected in the retina (Rivera et al. 2005). Similarly, the transcript was detected in various cell lines (Kanda et al. 2007) and its characteristics fulfill the definition of being a messenger RNA: It possesses a well-defined transcription start site (Fritsche et al. 2008), 5′- and 3′-untranslated regions, two exons separated by a GT-AG intron, and finally a canonical polyadenylation signal and a poly (A) tail. Nevertheless, the detection of the native transcript by Northern analysis still has to be done.

Notably, it has been hypothesized that the defective processing of ARMS2 pre-mRNA due to the removal of the polyadenylation signal by an insertion/deletion in carriers of the risk haplotype is the underlying cause for AMD (Fritsche et al. 2008). Adding to the confusion is the fact that yet another haplotype (R38X) also leads to the failure of ARMS2 synthesis (Fig. 4.2), but this variant is neutral in AMD, thereby contradicting the degradation hypothesis (Allikmets and Dean 2008). Furthermore, in-depth reporter gene assays and the analysis of a large series of human post-mortem retina/RPE samples revealed that the risk haplotype affects ARMS2 but not HTRA1 mRNA expression (Friedrich et al. 2011). Because the lack of ARMS2 does not necessarily leads to AMD and the expression of HTRA1 is not changed in risk vs. non-risk haplotypes, the authors conclude that currently unknown mechanisms mediate the pathogenic effects of the risk-associated variants at the 10q26 AMD locus. It has been also speculated that ARMS2 exists as a non-coding mRNA only. However, antibodies against different epitopes of ARMS2

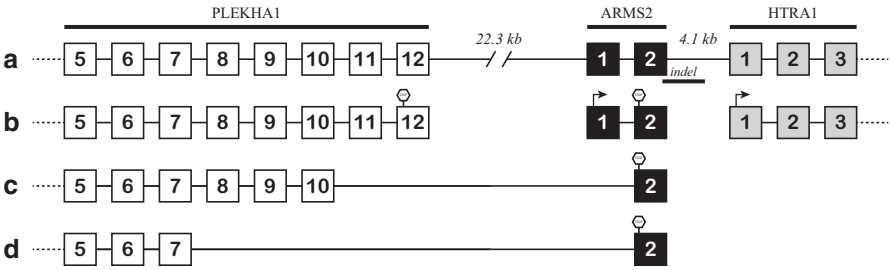

Fig. 4.2 Schematic representation of PLEKHA1/ARMS2 transcript chimerism. Transcription start and stop signals are marked with *broken arrows* and stop signs, respectively. **a** Genomic organization of the 10q26 locus. Only distal exons of PLEKHA1 and proximal exons of HTRA1 are shown. **b** Canonical transcripts of the three genes. **c** and **d** Different spliced isoforms. Note that the indel variant most probably influences the expression of these mRNAs, while the R38X mutation in the first exon of ARMS2 does not

gave rise to identical staining pattern in the choroid layer of human eyes (Kortvely et al. 2010) and Western analyses using the same monoclonals also reveal a single band of the expected size in placental lysates (our unpublished data), supporting the presence of ARMS2 proteins.

Here we propose that the phylogeny of ARMS2 may hold the key to resolve this controversy. Alternative transcript variants have already been described for ARMS2 (Wang et al. 2012). We also examined the exon-intron structure of the transcripts for the entire 10q26 region aimed at finding novel alternative variants also affected by the presence of the risk haplotype. This approach has led to the identification of PLEKHA1/ARMS2 chimeric transcripts (Fig. 4.2). With respect to chimeric proteins, the ENCODE project discovered that gene boundaries extend well beyond the annotated termini in 65 % of cases, often encompassing parts of neighboring genes and at least 4–5 % of the tandem genes in the human genome can be transcribed into a single RNA sequence (Gingeras 2009). Such chimeric mRNAs can augment the number of gene products (Akiva et al. 2006; Parra et al. 2006).

PLEKHA1 and ARMS2 are two adjacent genes in the same orientation that are usually transcribed independently, but occasionally transcribed into a single RNA sequence whose splicing product encodes a protein including coding exons from the two genes. Consequently, the risk variants of the 10q26 locus may also affect the expression of these fusion transcripts, even if the majority of the corresponding gene is outside the linkage block. Since these chimeric RNAs are significantly more tissue-specific than non-chimeric transcripts (Frenkel-Morgenstern et al. 2012), they can exert their biological function restricted, for example, to the eye.

It is of note that we could not detect transcripts containing exons from both ARMS2 and HTRA1, although the intergenic segment is significantly shorter than the one between PLEKHA1 and ARMS2.

In conclusion, the risk variant of the 10q26 locus may influence the expression of these chimeric transcripts and this can exert a pathogenic effect in the eye. Further experiments are warranted to determine the relevance of the corresponding putative chimeric proteins in AMD pathology.

References

Akiva P, Toporik A, Edelheit S et al (2006) Transcription-mediated gene fusion in the human genome. Genome Res 16:30–36

Allikmets R, Dean M (2008) Bringing age-related macular degeneration into focus. Nat Genet 40:820–821

Brunner HG, van Driel MA (2004) From syndrome families to functional genomics. Nat Rev Genet 5:545–551

Carvunis AR, Rolland T, Wapinski I et al (2012) Proto-genes and de novo gene birth. Nature 487:370–374

Clausen T, Kaiser M, Huber R et al (2011) HTRA proteases: regulated proteolysis in protein quality control. Nat Rev Mol Cell Biol 12:152–162

Dewan A, Liu M, Hartman S et al (2006) HTRA1 promoter polymorphism in wet age-related macular degeneration. Science 314:989–992

Edwards AO, Ritter R, 3rd, Abel KJ et al (2005) Complement factor H polymorphism and age-related macular degeneration. Science 308:421–424
Francis PJ, Appukuttan B, Simmons E et al (2008) Rhesus monkeys and humans share common susceptibility genes for age-related macular disease. Hum Mol Genet 17:2673–2680
Franke L, van Bakel H, Fokkens L et al (2006) Reconstruction of a functional human gene network, with an application for prioritizing positional candidate genes. Am J Hum Genet 78:1011–1025
Frenkel-Morgenstern M, Lacroix V, Ezkurdia I et al (2012) Chimeras taking shape: potential functions of proteins encoded by chimeric RNA transcripts. Genome Res 22:1231–1242
Friedrich U, Myers CA, Fritsche LG et al (2011) Risk- and non-risk-associated variants at the 10q26 AMD locus influence ARMS2 mRNA expression but exclude pathogenic effects due to protein deficiency. Hum Mol Genet 20:1387–1399
Fritsche LG, Loenhardt T, Janssen A et al (2008) Age-related macular degeneration is associated with an unstable ARMS2 (LOC387715) mRNA. Nat Genet 40:892–896
Gingeras TR (2009) Implications of chimaeric non-co-linear transcripts. Nature 461:206–211
Hageman GS, Luthert PJ, Victor Chong NH et al (2001) An integrated hypothesis that considers drusen as biomarkers of immune-mediated processes at the RPE-Bruch's membrane interface in aging and age-related macular degeneration. Prog Retin Eye Res 20:705–732
Haines JL, Hauser MA, Schmidt S et al (2005) Complement factor H variant increases the risk of age-related macular degeneration. Science 308:419–421
Jakobsdottir J, Conley YP, Weeks DE et al (2005) Susceptibility genes for age-related maculopathy on chromosome 10q26. Am J Hum Genet 77:389–407
Kanda A, Chen W, Othman M et al (2007) A variant of mitochondrial protein LOC387715/ARMS2, not HTRA1, is strongly associated with age-related macular degeneration. Proc Natl Acad Sci USA 104:16227–16232
Klein RJ, Zeiss C, Chew EY et al (2005) Complement factor H polymorphism in age-related macular degeneration. Science 308:385–389
Kortvely E, Ueffing M (2012) Common mechanisms for separate maculopathies? Adv Exp Med Biol 723:61–66
Kortvely E, Hauck SM, Duetsch G et al (2010) ARMS2 is a constituent of the extracellular matrix providing a link between familial and sporadic age-related macular degenerations. Invest Ophthalmol Vis Sci 51:79–88
Parra G, Reymond A, Dabbouseh N et al (2006) Tandem chimerism as a means to increase protein complexity in the human genome. Genome Res 16:37–44
Provis JM, Penfold PL, Cornish EE et al (2005) Anatomy and development of the macula: specialisation and the vulnerability to macular degeneration. Clin Exp Optom 88:269–281
Rivera A, Fisher SA, Fritsche LG et al (2005) Hypothetical LOC387715 is a second major susceptibility gene for age-related macular degeneration, contributing independently of complement factor H to disease risk. Hum Mol Genet 14:3227–3236
Seddon JM, Chen CA (2004) The epidemiology of age-related macular degeneration. Int Ophthalmol Clin 44:17–39
Tay SK, Blythe J, Lipovich L (2009) Global discovery of primate-specific genes in the human genome. Proc Natl Acad Sci U S A 106:12019–12024
Wang G, Scott WK, Whitehead P et al (2012) A novel ARMS2 splice variant is identified in human retina. Exp Eye Res 94:187–191
Yang Z, Camp NJ, Sun H et al (2006) A variant of the HTRA1 gene increases susceptibility to age-related macular degeneration. Science 314:992–993
Yang Z, Tong Z, Chen Y et al (2010) Genetic and functional dissection of HTRA1 and LOC387715 in age-related macular degeneration. PLoS Genet 6:e1000836
Yu PK, Balaratnasingam C, Cringle SJ et al (2010) Microstructure and network organization of the microvasculature in the human macula. Invest Ophthalmol Vis Sci 51:6735–6743

Chapter 5
Conditional Induction of Oxidative Stress in RPE: A Mouse Model of Progressive Retinal Degeneration

Manas R Biswal, Cristhian J Ildefonso, Haoyu Mao, Soo Jung Seo, Zhaoyang Wang, Hong Li, Yun Z. Le and Alfred S. Lewin

Abstract An appropriate animal model is essential to screening drugs or designing a treatment strategy for geographic atrophy. Since oxidative stress contributes to the pathological changes of the retinal pigment epithelium (RPE), we are reporting a new mouse AMD model of retinal degeneration by inducing mitochondrial oxidative stress in RPE. *Sod2* the gene for manganese superoxide dismutase (MnSOD) was deleted in RPE layer using conditional knockout strategy. Fundus microscopy, SD-OCT and electroretinography were used to monitor retinal structure and function in living animals and microscopy was used to assess pathology *post mortem*. Tissue specific deletion of *Sod2* caused elevated signs of oxidative stress, RPE dysfunction and showed some key features of AMD. Due to induction of oxidative stress, the conditional knockout mice show progressive reduction in ERG responses and thinning of outer nuclear layer (ONL) compared to non-induced littermates.

Keywords Retinal degeneration · Oxidative stress · Geographic atrophy · Retinal pigment epithelium · Superoxide dismutase · Age related macular degeneration · Knockout mice

M. R. Biswal (✉) · C. J. Ildefonso · H. Mao · S. J. Seo · Z. Wang · H. Li · A. S. Lewin
Department of Molecular Genetics and Microbiology, College of Medicine, University of Florida, PO Box 100266-MGM 1200 Newell Drive, Gainesville, FL 32610-0266, USA
e-mail: biswal@ufl.edu

C. J. Ildefonso
e-mail: ildefons@ufl.edu

Z. Wang
e-mail: zhaokekewzy@hotmail.com

Y. Z. Le
Department of Endocrinology and Diabetes, University of Oklahoma Health Science Center, Oklahoma city, OK 73104, USA
e-mail: yun-le@ouhsc.edu

A. S. Lewin
e-mail: lewin@ufl.edu

C. Bowes Rickman et al. (eds.), *Retinal Degenerative Diseases,* Advances in Experimental Medicine and Biology 854, DOI 10.1007/978-3-319-17121-0_5

5.1 Introduction

Age related macular degeneration (AMD) is one of the major causes of vision loss among the elderly population in industrialized nations (de Jong 2006). Degeneration of the neural retina and of the retinal pigment epithelium (RPE) is associated with the advanced dry form of AMD, while vascular leakage and scarring characterize the neovascular form of the disease. Mitochondrial oxidative stress and RPE dysfunction may contribute the disease phenotype (Khandhadia and Lotery 2010) (Jarrett and Boulton 2012). The RPE is considered as one of the critical sites for oxidative injury to cause retinal degeneration in AMD (Cai et al. 2000; Hageman et al. 2001; Liang and Godley 2003). Geographic atrophy is the term used to describe the degeneration of the RPE and overlying photoreceptors in the advanced form of dry AMD (Holz et al. 2014). Anti-oxidant enzymes including manganese superoxide dismutase (MnSOD, coded for by the mouse *Sod2* gene) and catalase play an important role in regulating oxidative stress by reducing the levels of superoxide and hydrogen peroxide, respectively. Developing a mouse model of oxidative stress leading to geographic atrophy will enhance to understand the mechanisms of retinal degeneration and help to develop therapeutic strategy to prevent AMD. Previously, ribozyme mediated knockdown of MnSOD (*Sod2*) mice model was developed to study retinal degeneration (Justilien et al. 2007), but was subject to variability associated with subretinal injections. Using a cre/*lox* system, we developed a mouse model of RPE specific mitochondrial oxidative stress by deleting *Sod2* in RPE. This deletion results progressive retinal degeneration due to induction of oxidative stress in RPE.

5.2 Materials and Methods

5.2.1 Experimental Animals

All animal handling procedures and protocols were followed the guidelines of ARVO statement and approved by the IACUC of University of Florida. In order to generate transgenic mice, two different mice strains were used. One was inducible RPE-specific *cre* mice carrying RPE-specific *VMD2* promoter to drive tetracycline-inducible transactivator gene (rtTA), which, in turn, controlled the expression of *cre* (Le et al. 2008). These mice were crossed with $Sod2^{flox/flox}$ mice in which exon 3 of *Sod2* gene is flanked by *loxP* sites (Strassburger et al. 2005c). In order to maintain pure lines, both the strains were back-crossed to C57Bl/6J mice up to 10 generations. Mutations in rd1 and rd8 were regularly monitored, to maintain good breeding lines. To obtain mice homozygous for the floxed *Sod2* gene and hemizygous the *cre* transgene ($Sod2^{flox/flox}$-*VMD2-cre*), males heterozygous for *VMD2-cre* and for $Sod2^{flox}$ were bred with $Sod2^{flox/flox}$ females. Rodent chow containing doxycycline (dox) at 200 mg/kg was fed to nursing dams from P1 (postnatal day 1) to P14 to induce *cre* expression.

5.2.2 Genotyping and PCR Analysis

To determine the genotype of mice, tail samples were processed to obtain genomic DNA using Sigma REDExtract-N-Amp™ Tissue PCR Kit. PCR analysis using genomic DNA was used to differentiate VMD2-*cre* mice from non-transgenic mice. To determine the *Sod2* genotype, the following primers were used: forward 5′-CTTGTGACATCTGGCTGACG-3′ and reverse 5′-CCCAGATCTGCAATTTCCAA-3′. Genetic deletion of exon 3 of SOD2 gene in *Sod2* $^{flox/flox}$*-VMD2-cre* mice (with or without doxycline food) was verified using genomic DNA isolated from RPE/choroid. The primers to verify *Sod2* deletions were designed from the available sequences located in intron 2 and intron 3 of the *Sod2* gene.

5.2.3 RPE Flat Mount and Staining For Oxidative Stress Marker

In order to process RPE for flat mount, the eyes were enucleated and fixed in 4 % paraformaldehyde for 15–30 min on ice. Cornea, lens, retina and extraocular tissue were removed, and only the RPE was collected in PBS by careful dissection. A rabbit polyclonal zona occludens (ZO-1) antibody (Invitrogen, 1:200) was used to analyze morphologic changes in both control and dox-induced mice. Using RPE flat mount, immunohistochemistry for MnSOD (Millipore, 1:300) was performed to detect changes in *Sod2* level in both no-dox control and dox-fed experimental mice. RPE flat mounts were stained with antibody to 8-hydroxydeoxyguanosine (8-OHdG, Abcam, 1:200 dilution), an oxidative stress marker to study induction of oxidative stress in experimental mice.

5.2.4 Monitoring Structural and Functional Changes

In order to measure functional and structural changes in dox-induced experimental mice in comparison with control, electronretinography (ERG), fundus imaging and spectral-domain optical coherence tomography (SD-OCT) were used. Using an LKC visual electrodiagnostic system, ERG was recorded on dark adapted mice following dilation with 2.5 % phenylephrine. Scotopic ERGs were recorded with 10-ms flashes of white light at following intensity of light 0 db (2.68cds/m^2), 10dB (0.18cds/m^2) and −20 dB (0.02cds/m^2). Structural abnormalities in retina of living mice were analyzed by Micron III fundus imaging system. In order to measure subretinal morphology and changes in outer nuclear thickness (ONL), an ultra-high resolution instrument (Bioptigen) was used. Linear B-scans (around 300) were obtained from an anesthetized mouse and 30 images were averaged to get better resolution. To determine the changes in ONL thickness, measurements were done at four different points around the optic nerve maintaining same distance.

5.3 Results

5.3.1 Generation of Sod2 Knockout Transgenic Mice

In *Sod2*$^{flox/flox}$*VMD2-cre* mice cre was induced by feeding doxycylcine chow to the nursing dam and led to deletion of exon 3 of *Sod2* as evident in PCR analysis of genomic DNA isolated from 5 week old mice (Fig. 5.1a). Dox fed *Sod2*$^{flox/flox}$/*VMD2-cre* mouse produced only a 400 bp product characteristic of the deleted allele, whereas the no-dox control produced 1100 bp band signifying no

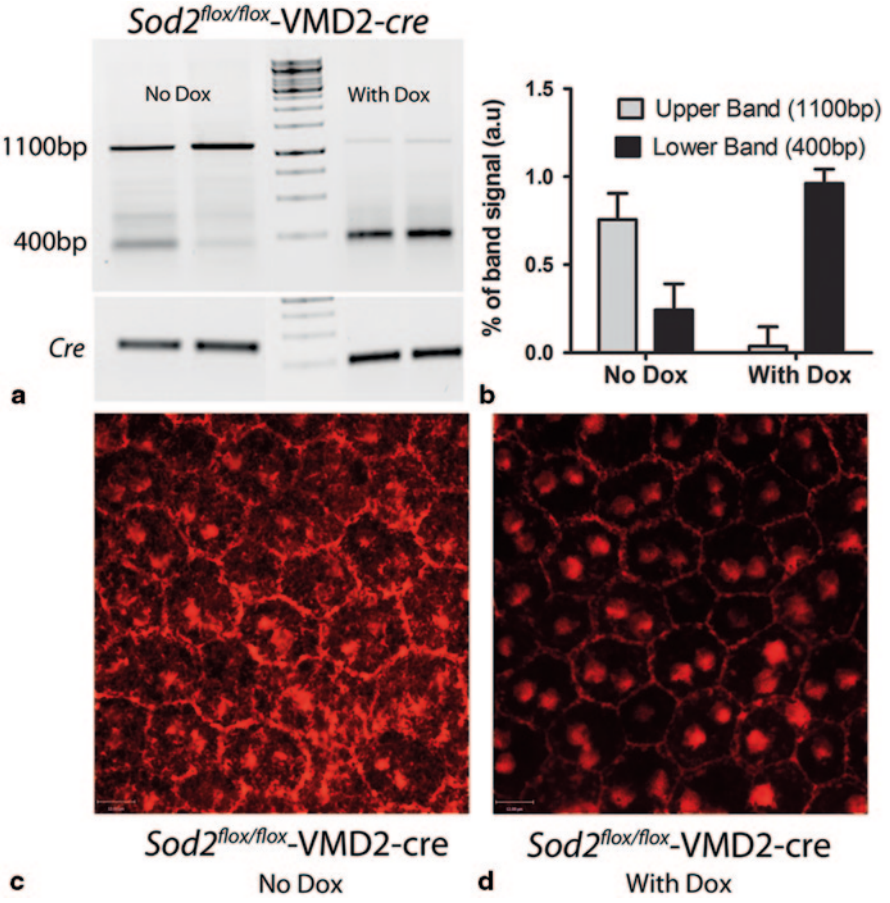

Fig. 5.1 RPE Specific *sod2* deletion in *Sod2*$^{flox/flox}$*VMD2-cre* mice. **a** Image of PCR analysis using genomic DNA from RPE/choroid from 5 week old *Sod2*$^{flox/flox}$*VMD2-cre* mice on doxycline (dox) chow (P0-P14) deleted allele (400 bp) and the full length *Sod2* product is 1100 bp **c** Representative image of *Sod2* immuno-staining of an RPE flat-mount from 2 month old no dox mouse; D: *Sod2* staining of a flat mount from a dox fed mouse

deletion. Quantification of the signal strength of amplified bands in both groups indicated more than 90% deletion of exon-3 in dox-induced mice occurred compared to the no-dox group (Fig. 5.1b). Extensive immunostaining of MnSOD on RPE flatmount was seen in *Sod2*$^{flox/flox}$/VMD2-*cre* mouse without dox food (Fig. 5.1c), whereas the immunostaining was significantly reduced in the dox-fed group (Fig. 5.1d).

5.3.2 Functional and Structural Abnormality

Deletion of *Sod2* in RPE caused elevated level of oxidative damage to the DNA. Flat mounts of 6-week old *Sod2*$^{flox/flox}$*/VMD2-cre* (no dox) mouse showed minimal immunostaining for 8-OHdG (Fig. 5.2a), while dox fed mice of that genotype revealed strong immunostaining, signifying the extent of oxidative injury in the RPE (Fig. 5.2b) due to deletion of *Sod2*. Increase in autofluorescence in aging retina is one of the characteristics of AMD (Lois N 2002). The frozen sections of four month old dox fed *Sod2* $^{flox/flox}$*/VMD2-cre* showed the increased level of fluorescence in choroid and RPE compared to control no dox group (data not shown). Fundus imaging of the experimental mice showed retinal atrophy that was apparent after 6 and 9 months (Fig. 5.2c and d). ERG responses (both a- and b-wave) from the dox treated group progressively declined, and differed significantly from the control (no-dox)

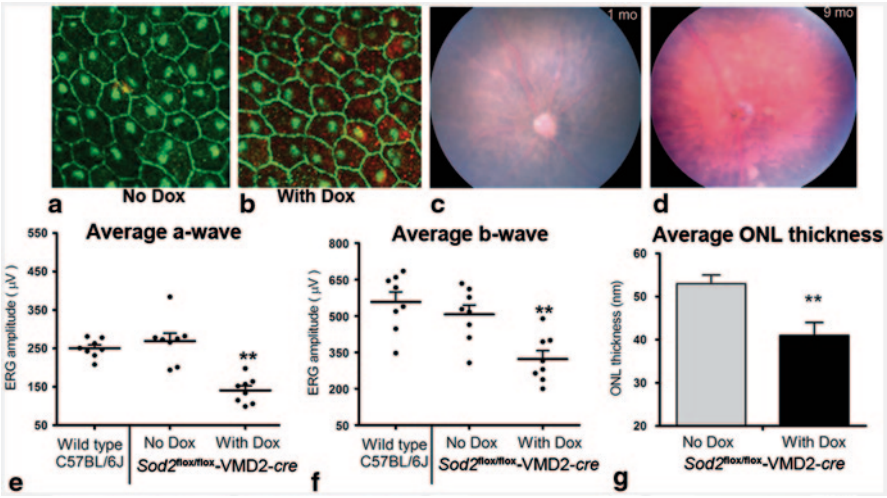

Fig. 5.2 Functional and structural abnormalities due to *sod2* deletion. **a, b** Representative images of RPE flat mount stained for ZO-1 (*green*) and 8-OHdG (*red*). **c, d** Representative fundus images from a dox induced transgenic mice shows extensive degenerated retina in 9 month old mice, **d** compared to a one month old, **c** Average a-wave amplitude, **e** and b-wave, **f** at 2.7 cds/m^2 (ERG responses are significantly reduced in 9 month old dox fed transgenic mice compared to no dox treated transgenic group and wild type C57BL/6J mice). OCT measurement shows the significant reduction, **g** in the thickness of outer nuclear layer in the dox treated group compared to no dox group

group by the age of 6 months. By 9 months, a major loss of a-wave and b-wave was observed (Fig. 5.2e, f) revealing functional abnormalities in *Sod2* deleted mice. SD-OCT on those mice showed the thinning of ONL that was clearly significant by the age of 9 months (Fig. 5.2g).

5.4 Discussion

Reactive oxygen species generated in mitochondria are thought to contribute to the development of AMD (Jarrett and Boulton 2012), and oxidative stress stimulates inflammatory pathways that may become uncontrolled in this disease (Kauppinen et al. 2012; Suzuki et al. 2012). Oxidized lipids and proteins are deposited in the form of lipofuscin in the RPE and eventually as drusen beneath the RPE (Delori et al. 2000; Handa 2012). Several groups have generated mouse models lacking protective enzymes, such as *Sod1* (Imamura et al. 2006)*)*, or regulators of antioxidant pathways, such as *Nrf2* (Zhao et al. 2011). Developing a mouse model to test the role of mitochondrial oxidative stress in the RPE required cre*/lox* technology. Genetic deletion of exon 3 of *Sod2* led to significant reduction of MnSOD in the RPE. We observed increased oxidative stress in RPE as evident from 8-OHdG staining. Progressive reduction of the ERG a-wave and b-wave in *Sod2* deleted mice reflected retinal degeneration that was documented the thinning of outer nuclear layer as measured by SD-OCT.

In summary, inducible genetic defect only in RPE to promote oxidative stress allows this model to recapitulate RPE and retinal degeneration similar to that occurring in geographic atrophy. This model can be used to study drug-based or gene-based treatment approaches that may attenuate oxidative stress directly or the inflammatory processes arising from reactive oxygen species.

Acknowledgments Our work was supported by NIH grant R01EY020825 and P30-EY021721.

References

Cai J, Nelson KC, Wu M et al (2000) Oxidative damage and protection of the RPE. Prog Retin Eye Res 19:205–221.

De Jong PTVM (2006) Age-related macular degeneration. N Engl J Med 355:1474–1485.

Delori FC, Fleckner MR, Goger DG et al (2000) Autofluorescence distribution associated with drusen in age-related macular degeneration. Invest Ophthalmol Vis Sci 41:496–504.

Hageman GS, Luthert PJ, Victor Chong NH et al (2001) An integrated hypothesis that considers drusen as biomarkers of immune-mediated processes at the RPE-Bruch's membrane interface in aging and age-related macular degeneration. Prog Retin Eye Res 20:705–732.

Handa JT (2012) How does the macula protect itself from oxidative stress? Mol Aspects Med 33:418–435.

Holz FG, Schmitz-Valckenberg S, Fleckenstein M (2014) Recent developments in the treatment of age-related macular degeneration. J Clin Invest 124:1430–1438.

Imamura Y, Noda S, Hashizume K et al (2006) Drusen, choroidal neovascularization, and retinal pigment epithelium dysfunction in SOD1-deficient mice: a model of age-related macular degeneration. Proc Natl Acad Sci U S A 103:11282–11287.

Jarrett SG, Boulton ME (2012) Consequences of oxidative stress in age-related macular degeneration. Mol Aspects Med 33:399–417.

Justilien V, Pang J-J, Renganathan K et al (2007) SOD2 knockdown mouse model of early AMD. Invest Ophthalmol Vis Sci 48:4407–4420.

Kauppinen A, Niskanen H, Suuronen T et al (2012) Oxidative stress activates NLRP3 inflammasomes in ARPE-19 cells-implications for age-related macular degeneration (AMD). Immunol Lett 147:29–33.

Khandhadia S, Lotery A (2010) Oxidation and age-related macular degeneration: insights from molecular biology. Expert Rev Mol Med 12:e34.

Le Y-Z, Zheng W, Rao P-C et al (2008) Inducible expression of cre recombinase in the retinal pigmented epithelium. Invest Ophthalmol Vis Sci 49:1248–1253.

Liang F-Q, Godley BF (2003) Oxidative stress-induced mitochondrial DNA damage in human retinal pigment epithelial cells: a possible mechanism for RPE aging and age-related macular degeneration. Exp Eye Res 76:397–403.

Strassburger M, Bloch W, Sulyok S et al (2005) Heterozygous deficiency of manganese superoxide dismutase results in severe lipid peroxidation and spontaneous apoptosis in murine myocardium in vivo. Free Radic Biol Med 38:1458–1470.

Suzuki M, Tsujikawa M, Itabe H et al (2012) Chronic photo-oxidative stress and subsequent MCP-1 activation as causative factors for age-related macular degeneration. J Cell Sci 125:2407–2415.

Zhao Z, Chen Y, Wang J et al (2011) Age-related retinopathy in NRF2-deficient mice. PloS ONE 6:e19456.

Chapter 6
Therapeutic Approaches to Histone Reprogramming in Retinal Degeneration

Andre K. Berner and Mark E. Kleinman

Abstract Recent data have revealed epigenetic derangements and subsequent chromatin remodeling as a potent biologic switch for chronic inflammation and cell survival which are important therapeutic targets in the pathogenesis of several retinal degenerations. Histone deacetylases (HDACs) are a major component of this system and serve as a unique control of the chromatin remodeling process. With a multitude of targeted HDAC inhibitors now available, their use in both basic science and clinical studies has widened substantially. In the field of ocular biology, there are data to suggest that HDAC inhibition may suppress neovascularization and may be a possible treatment for retinitis pigmentosa and dry age-related macular degeneration (AMD). However, the effects of these inhibitors on cell survival and chemokine expression in the chorioretinal tissues remain very unclear. Here, we review the multifaceted biology of HDAC activity and pharmacologic inhibition while offering further insight into the importance of this epigenetic pathway in retinal degenerations. Our laboratory investigations aim to open translational avenues to advance dry AMD therapeutics while exploring the role of acetylation on inflammatory gene expression in the aging and degenerating retina.

Keywords Retinal degeneration · Acetylome · Lysine deacetylases · Histone deacetylases · Valproic acid · Apoptosis · Inflammation · Aging Electronic supplementary material

A. K. Berner (✉)
740 S. Limestone St., Suite E-300, Lexington, KY 40536, USA
e-mail: andrekberner@gmail.com

M. E. Kleinman
Department of Ophthalmology and Visual Sciences, University of Kentucky, Lexington, KY 40536, USA
e-mail: mark.kleinman@uky.edu

C. Bowes Rickman et al. (eds.), *Retinal Degenerative Diseases,* Advances in Experimental Medicine and Biology 854, DOI 10.1007/978-3-319-17121-0_6

6.1 Post-translational Acetylation Controls Gene Expression and Protein Activity

Acetylation is a reversible post-translational modification that was first discovered in histones and occurs in a wide range of organisms. Histone proteins (H2A, H2B, H3 and H4) are integrated with 147 base-pairs of DNA in a complex called the nucleosome (Luger et al. 1997). Lysine acetylation and deacetylation of histones are carried out by two groups of enzymes: acetyl group addition by HATs (or lysine acetyltransferases KATs) and acetyl group removal by HDACs (or KDACs), respectively. A generalized epigenetic principle is that histone acetylation results in an open structure of the DNA enabling gene transcription whereas histone deacetylase activity tightens the nucleosome and compacts the chromatin making those sites inaccessible for transcription (de Ruijter et al. 2003). While this model has not applied to all systems, it is clear from current studies that there is a delicate balance of (de)acetyltransferase activity which may be dysregulated in aging diseases. Lysine acetylation is not limited to histones but are also present in innumerous other protein substrates giving acetylation a wider significance in developmental and disease states (Peserico and Simone 2011). Nuclear receptors (estrogen receptor, p300), proliferating factors (E2F/RB), hypoxia induced factors (HIF-1α), transcription factors (NFκB, p53, STAT3 and c-MYC) and other cellular proteins (αTubulin, Ku70 and Hsp90) are all known non-histone targets of HATs and HDACs (Glozak et al. 2005).

Histone deacetylases are a family of 18 known members, classified in four groups based on their homology to yeast proteins (Dokmanovic et al. 2007). Class I consists of HDAC1, 2, 3 and 8. HDAC1 and HDAC2 are ubiquitously expressed, strongly localized to nuclei and predominantly associated in megadalton complexes (Bantscheff et al. 2011; Di Marcotullio et al. 2011). Members of the Class II-family of HDACs are separated into Class IIa (HDAC4, 5, 7 and 9) which localize to both nuclear and cytosolic compartments and IIb (HDAC6 and 10) which are predominantly cytosolic. Class I/II HDACs are zinc dependent. Class III HDACs, also known as sirtuins (SIRTs), are evolutionarily unrelated to the other HDAC classes. SIRTs require NAD^+ as a co-factor making them highly sensitive to oxidative stress (Balaiya et al. 2012) and a hotly pursued potential therapeutic target for age-related and metabolic diseases (Imai and Guarente 2014). There is only one Class IV HDAC (HDAC11) which is also zinc dependent, localized to the nucleus and is heavily conserved in all living eukaryotes other than fungi (Gao et al. 2002).

6.2 Context and Tissue Dependent Effects of Histone Deacetylases

Expression levels of HATs and HDACs as well as targeted acetylation sites and proteins can dramatically change between tissues and within varying developmental, normal adult, and diseased states. There are several models of neuronal

cell death in which HDAC inhibition (HDACi) exhibits a protective benefit whereas targeting identical pathways in cancer cells is pro-apoptotic. With the highly specialized and multicellular architecture of the eye, the dominant effects of HDAC inactivity remain very unclear and certainly become extremely difficult to interpret when comparing acute laboratory animal and cell culture models to chronic aging diseases. Still, we are gathering essential data that will allow us to develop a fundamental understanding of this critical and deeply conserved regulatory biologic system. Class I HDAC expression is considered ubiquitous though we have observed significant differences in immuno-localization patterns in the mouse retina with HDAC1/2. Class II HDACs are known to display highly specific tissue-dependent expression patters leading to variable sub-cellular localization and certainly tissue-specific biological effects of enzyme inactivity and subsequent imbalances in the acetylome. Many diseases have been associated with altered global acetylation patterns including cancer, cardiovascular disease and inflammatory diseases. Hyper-acetylation via HDACi is known to be cytoprotective in models of neuronal ischemic injury (Kim and Chuang 2014; Murphy et al. 2014), Huntington's disease (Ferrante et al. 2003), and stroke (Liu et al. 2012). Yet, HDACi is nearly uniformly cytotoxic in cancer models (McConkey et al. 2012). HDACi also has opposing effects on critical immune system mediators. Toll-like receptors (TLRs) are potent cell-signaling gateways to innate immune pathways and downstream inflammatory responses. Treatment of cultured human macrophages with HDACi leads to caspase-dependent apoptosis and release of pro-inflammatory cytokines; however, this effect is reversed by pre-treatment with TLR agonists including LPS and poly I:C (Tsolmongyn et al. 2013). Data revealing the protean biology of the acetylome must be seriously addressed and rigorously studied in the laboratory prior to pharmacologically approaching HDAC/HAT manipulation for the treatment of human diseases.

A potent and well-characterized Class I/II HDACi is suberoylanilide hydroxamic acid (SAHA also known as vorinostat) which is currently in advanced phase clinical phase trials for multiple myeloma and several solid tumors. Similar to previous HDACi results, the pharmacologic effects of SAHA are highly dependent on cell-type and state coupled with a limited therapeutic window. While low concentrations of SAHA may be significantly cytoprotective, higher concentrations are pro-apoptotic in many immune cell types (Li et al. 2008). Nearly identical data exists for valproic acid (VPA), another small molecule Class I/II HDACi which is most widely used for seizure prophylaxis. VPA has been shown to reduce brain damage in an animal model of transient cerebral ischemia (Ren et al. 2004), provide acute neuro-protection in ischemic retinal injury (Alsarraf et al. 2014), and stimulate axonal regrowth after optic nerve crush (Biermann et al. 2010). These data have rapidly opened translational avenues of pharmacologic induced chromatin remodeling as a novel target for the epigenetic regulation of critical cell death and survival pathways in aging and neurodegenerative diseases.

6.3 Differential Effects of Histone Deacetylase in the Retina and Retinal Pigment Epithelium

Investigations of the *rd1* mouse demonstrated significant protection form loss of photoreceptors after broad inhibition of Class I/II HDACs with trichostatin A (TSA) (Sancho-Pelluz et al. 2010). A single report was then published suggesting the therapeutic efficacy of VPA in the treatment of retinitis pigmentosa (Clemson et al. 2011). Similar benefits were reported for VPA in *rd1* mice (Mitton et al. 2012); however, the same treatment had the contrary effect in *rd10* mice (Guzman et al. 2014). Additional studies were performed even though the original data had been hotly contested with multiple letters in the literature with severe limitations to the study design and reports of inefficacy and even loss of vision associated with the use of VPA for retinal degeneration (van Schooneveld et al. 2011; Sisk 2012). Recently, a long-term follow-up study confirmed visual decline and adverse side-effects associated with VPA therapy in patients with retinitis pigmentosa (Bhalla et al. 2013).

Four independent groups have presented varying data regarding VPA and retinal degeneration. Reports included positive (Iraha et al. 2014), variable (Guzman et al. 2014; Lai et al. 2014) or outright negative findings (Berner et al. 2014; Kumar et al. 2014). In a transgenic *Xenopus* model expressing various human rhodopsin mutations, only retinal degeneration secondary to the P23H mutation was favorably treated with VPA (Lai et al. 2014). Despite VPA's described neuro-protective and anti-inflammatory properties, in just these few studies, significant retinotoxicity was encountered in numerous animal and cell-culture models. We have demonstrated that VPA up-regulates caspase-3 activation and cell death in primary human RPE isolates, a finding which has been confirmed in other studies (Suuronen et al. 2007; Kumar et al. 2014). VPA treatment exhibits a significant pro-inflammatory response *in vitro* and *in vivo* with an array of cytokines, cytokine receptors, mediating enzymes and transcription factors (Kleinman et al. 2013; Kleinman et al. 2014). This pro-inflammatory signature is in accordance to the known immune response in AMD (Suuronen et al. 2007; Shakespear et al. 2011; Miao et al. 2012; Whitcup et al. 2013). Further investigations into this powerful epigenetic regulatory system will continue to yield important features of HDAC involvement in the pathogenesis and treatment of retinal degenerations; however, at this time we urge caution using VPA as a treatment option for these diseases given the variable treatment effect dependent on tissue-type and cellular target (Fig. 6.1).

Acknowledgments M.E.K. was supported by NEI/NIH, Career Development Awards from the Foundation Fighting Blindness and Research to Prevent Blindness, and the American Federation for Aging Research.

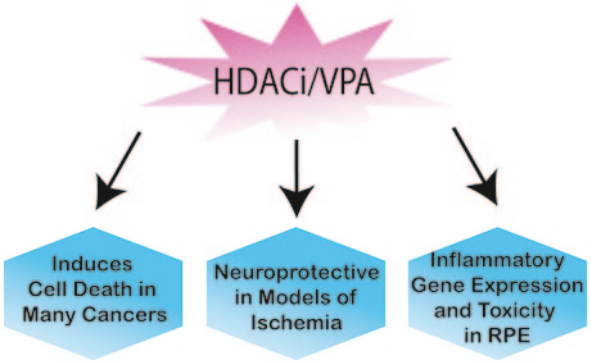

Fig. 6.1 While HDAC inhibition is cytoprotective in many models of neuronal cell death, it is also capable of inducing significant cytotoxicity in various cancers and up-regulating inflammatory gene expression and cell death in the RPE

References

Alsarraf O, Fan J, Dahrouj M et al (2014) Acetylation: A lysine modification with neuroprotective effects in ischemic retinal degeneration. Exp Eye Res 127C:124–131

Balaiya S, Khetpal V, Chalam KV (2012) Hypoxia initiates sirtuin1-mediated vascular endothelial growth factor activation in choroidal endothelial cells through hypoxia inducible factor-2alpha. Mol Vis 18:114–120

Bantscheff M, Hopf C, Savitski MM et al (2011) Chemoproteomics profiling of HDAC inhibitors reveals selective targeting of HDAC complexes. Nat Biotechnol 29:255–265

Berner A, Mohan K, Lou D-Y et al (2014) RPE Cytotoxicity and Caspase Activation after Treatment with Valproic Acid. ARVO Meeting Abstracts 55:5991

Bhalla S, Joshi D, Bhullar S et al (2013) Long-term follow-up for efficacy and safety of treatment of retinitis pigmentosa with valproic acid. Br J Ophthalmol 97:895–899

Biermann J, Grieshaber P, Goebel U et al (2010) Valproic acid-mediated neuroprotection and regeneration in injured retinal ganglion cells. Investigative ophthalmology & visual science 51:526–534

Clemson CM, Tzekov R, Krebs M et al (2011) Therapeutic potential of valproic acid for retinitis pigmentosa. Br J Ophthalmol 95:89–93

de Ruijter AJ, van Gennip AH, Caron HN et al (2003) Histone deacetylases (HDACs): characterization of the classical HDAC family. Biochem J 370:737–749

Di Marcotullio L, Canettieri G, Infante P et al (2011) Protected from the inside: endogenous histone deacetylase inhibitors and the road to cancer. Biochim Biophys Acta 1815:241–252

Dokmanovic M, Clarke C, Marks PA (2007) Histone deacetylase inhibitors: overview and perspectives. Mol Cancer Res 5:981–989

Ferrante RJ, Kubilus JK, Lee J et al (2003) Histone deacetylase inhibition by sodium butyrate chemotherapy ameliorates the neurodegenerative phenotype in Huntington's disease mice. The Journal of neuroscience: the official journal of the Society for Neuroscience 23:9418–9427

Gao L, Cueto MA, Asselbergs F et al (2002) Cloning and functional characterization of HDAC11, a novel member of the human histone deacetylase family. The Journal of biological chemistry 277:25748–25755

Glozak MA, Sengupta N, Zhang X et al (2005) Acetylation and deacetylation of non-histone proteins. Gene 363:15–23

Guzman E, Despande M, Byrd DW et al (2014) Systemic Valproic Acid can Accelerate Photoreceptor Loss in rd10 mice. Invest Ophthalmol Vis Sci 55:1281-

Imai SI, Guarente L (2014) NAD and sirtuins in aging and disease. Trends in cell biology 24:464–471

Iraha S, Hirami Y, Oota S et al (2014) The efficacy of valproic acid for retinitis pigmentosa patients. ARVO Meeting Abstracts 55:1390

Kim HJ, Chuang DM (2014) HDAC inhibitors mitigate ischemia-induced oligodendrocyte damage: potential roles of oligodendrogenesis, VEGF, and anti-inflammation. Am J Transl Res 6:206–223

Kleinman M, Berner A, Lou D et al (2013) Epigenetic Regulation of Eotaxin Expression in Human Retinal Pigment Epithelium. Invest Ophthalmol Vis Sci 54:344-

Kleinman ME, Berner A, Mohan K et al (2014) Histone Deacetylase Expression and Inhibition in Age Related Macular Degeneration. ARVO Meeting Abstracts 55:3457

Kumar A, Kothary PC, Rossi B et al (2014) Valproic Acid Induced Inhibition of Fibroblast Growth Factor 2 Synthesis in Human Retinal Pigment Epithelial Cells. Invest Ophthalmol Vis Sci 55:364-

Lai RYJ, Zong Z, Tam BM et al (2014) Opposing effects of valproic acid treatment in four animal models of retinitis pigmentosa. ARVO Meeting Abstracts 55:4370

Li N, Zhao D, Kirschbaum M et al (2008) HDAC inhibitor reduces cytokine storm and facilitates induction of chimerism that reverses lupus in anti-CD3 conditioning regimen. Proc Natl Acad Sci U S A 105:4796–4801

Liu XS, Chopp M, Kassis H et al (2012) Valproic acid increases white matter repair and neurogenesis after stroke. Neuroscience 220:313–321

Luger K, Mader AW, Richmond RK et al (1997) Crystal structure of the nucleosome core particle at 2.8 A resolution. Nature 389:251–260

McConkey DJ, White M, Yan W (2012) HDAC inhibitor modulation of proteotoxicity as a therapeutic approach in cancer. Adv Cancer Res 116:131–163

Miao H, Tao Y, Li XX (2012) Inflammatory cytokines in aqueous humor of patients with choroidal neovascularization. Mol Vis 18:574–580

Mitton KP, Guzman EE, Byrd D et al (2012) Rescue Of Photoreceptor Degeneration In Rd1 Mice By Systemic Treatment With Valproic Acid. Invest Ophthalmol Vis Sci 53:5585-

Murphy SP, Lee RJ, McClean ME et al (2014) MS-275, a class I histone deacetylase inhibitor, protects the p53-deficient mouse against ischemic injury. J Neurochem 129:509–515

Peserico A, Simone C (2011) Physical and functional HAT/HDAC interplay regulates protein acetylation balance. J Biomed Biotechnol 2011:371832

Ren M, Leng Y, Jeong M et al (2004) Valproic acid reduces brain damage induced by transient focal cerebral ischemia in rats: potential roles of histone deacetylase inhibition and heat shock protein induction. J Neurochem 89:1358–1367

Sancho-Pelluz J, Alavi MV, Sahaboglu A et al (2010) Excessive HDAC activation is critical for neurodegeneration in the rd1 mouse. Cell Death Dis 1:e24

Shakespear MR, Halili MA, Irvine KM et al (2011) Histone deacetylases as regulators of inflammation and immunity. Trends Immunol 32:335–343

Sisk RA (2012) Valproic acid treatment may be harmful in non-dominant forms of retinitis pigmentosa. Br J Ophthalmol 96:1154–1155

Suuronen T, Nuutinen T, Ryhanen T et al (2007) Epigenetic regulation of clusterin/apolipoprotein J expression in retinal pigment epithelial cells. Biochem Biophys Res Commun 357:397–401

Tsolmongyn B, Koide N, Odkhuu E et al (2013) Lipopolysaccharide prevents valproic acid-induced apoptosis via activation of nuclear factor-kappaB and inhibition of p53 activation. Cellular immunology 282:100–105

van Schooneveld MJ, van den Born LI, van Genderen M et al (2011) The conclusions of Clemson et al concerning valproic acid are premature. Br J Ophthalmol 95:153:153–154 (author reply)

Whitcup SM, Sodhi A, Atkinson JP et al (2013) The role of the immune response in age-related macular degeneration. Int J Inflam 2013:348092

Chapter 7
A Brief Discussion on Lipid Activated Nuclear Receptors and their Potential Role in Regulating Microglia in Age-Related Macular Degeneration (AMD)

Mayur Choudhary and Goldis Malek

Abstract Age-related macular degeneration (AMD) is the leading cause of legal blindness and visual impairment in individuals over 60 years of age in the Western World. A common morphological denominator in all forms of AMD is the accumulation of microglia within the sub-retinal space, which is believed to be a contributing factor to AMD progression. However, the signaling pathway and molecular players regulating microglial recruitment have not been completely identified. Multiple *in-vitro* and *in-vivo* studies, to date, have highlighted the contributions of nuclear receptor ligands in the treatment of inflammation related disorders such as atherosclerosis and Alzheimer's disease. Given that inflammation and the immune response play a vital role in the initiation and progression of AMD, in this brief review we will highlight some of these studies with a particular focus on the lipid activated "adopted orphan" nuclear receptors, the liver x receptors (LXRs) and the peroxisome proliferator-activated receptors (PPARs). The results of these studies strongly support the rationale that treatment with LXR and PPAR ligands may ameliorate microglial activation in the sub-retinal space and ultimately slow down or reverse the progression of AMD.

Keywords Nuclear receptor · Peroxisome proliferator-activated receptor · Liver x receptor · Age-related macular degeneration · Sub-retinal microglia · Inflammation · Retinal pigment epithelium · Choroidal neovascularization

G. Malek (✉)
Department of Ophthalmology, Duke University School of Medicine,
2351 Erwin Road, AERI Room 4006, Durham, NC 27710, USA
e-mail: gmalek@duke.edu

M. Choudhary
Departments of Ophthalmology and Pathology, Albert Eye Research Institute,
Duke University, 2351 Erwin Road, AERI Room 4000, Durham, NC, 27710, USA
e-mail: mayur.choudhary@dm.duke.edu

C. Bowes Rickman et al. (eds.), *Retinal Degenerative Diseases,* Advances in Experimental Medicine and Biology 854, DOI 10.1007/978-3-319-17121-0_7

7.1 Introduction

Age-related macular degeneration (AMD) is one of the leading causes of progressive blindness in the elderly (Coleman et al. 2008). Clinically, AMD progresses from early to intermediate stages of the disease and subsequently to the two major advanced forms, namely, geographic atrophy (GA) or "late dry" and neovascular or "wet" AMD. The pathogenesis of early AMD involves the accumulation of lipid- and protein-rich extracellular deposits called drusen under the retinal pigment epithelial cells (RPE). The progression to the late dry form involves RPE dystrophy with a loss of photoreceptors in the central macula and subsequent blindness. Wet AMD, which affects approximately 10 % of the AMD patients, is characterized by development of abnormal choroidal neovascularization (CNV) under the retina, which leads to scarring in the macular region. Currently there are no treatments available for dry AMD, but anti-angiogenic approaches targeting vascular endothelial growth factor (VEGF) are available for wet AMD patients with some success. Therefore there is an immediate need to identify new targets and develop alternate therapeutic approaches to help people afflicted with this disease.

7.2 Microglial Cells Accumulate Within the Retina and Subretinal Space of AMD Patients

Retinal microglia represent a population of macrophages, which constantly survey their microenvironment, responding to cellular damage by increasing their phagocytic activity (Karlstetter and Langmann 2014). Multiple reports have corroborated the role of inflammation and microglial cells in the pathogenesis of the early and late forms of AMD (Patel and Chan 2008). The sub-retinal space, the interface between the RPE and the outer segments of photoreceptors, in particular, is a region of great interest in studies of inflammation in AMD. Under normal conditions, retinal microglia are excluded from the outer retina, due to the presence of immunosuppressive factors secreted by the RPE (Zamiri et al. 2007). As such, RPE cells play an important role in immunomodulation of the outer retina, regulating RPE-microglial interactions though expression of cytokine receptors, production and secretion of inflammatory cytokines and adhesion molecules, and regulation of the tight-junction integrity (Holtkamp et al. 2001; Streilein et al. 2002). In advanced age, following light-induced photoreceptor injury, and in late AMD, an influx of microglia to outer retina has been observed, followed by, their accumulation within the sub-retinal space (Ng and Streilein 2001; Gupta et al. 2003). In support of this, evaluation of retinal samples from the *Cx3cr1*$^{-/-}$ mice [chemokine (c-x3-c motif) receptor 1, important in microglial migration], has revealed the accumulation of subretinal microglia associated with drusen-like deposits, RPE structural alterations, and CNV formation (Combadiere et al. 2007; Tuo et al. 2007). It is clear, that a better understanding of RPE-microglial cell interactions is imperative in accurately explaining the inflammatory etiology of AMD and ultimately developing new therapeutic targets.

7.3 Overview of Lipid-Activated Nuclear Receptors

Nuclear receptors are the largest superfamily of transcription factors in the human genome. There is increasing evidence of their involvement in metabolic regulation of immune cells. This mini-review will focus on the role of the liver x receptors (LXRs) and peroxisome proliferator-activated receptors (PPARs) in shaping the metabolic and immune functions of microglial cells and macrophages, since these receptors have been most extensively studied in diseases, which share common pathogenic pathways with AMD, including atherosclerosis, metabolic syndrome and Alzheimer's disease.

LXRs are critical regulators of cholesterol homeostasis, glucose homeostasis, detoxification of bile acids, immunity, and neurological functions (Apfel et al. 1994). Their activating ligands include endogenous oxidized and hydroxylated cholesterol derivatives (22(R)- hydroxycholesterol and 24(S)-hydroxycholesterol) and synthetic agonists (GW3965 and TO901317) (Lehmann et al. 1997; Viennois et al. 2011). Although the two isoforms, LXRα (NR1H3) and LXRβ (NR1H2) show significant similarities in their DNA binding domain and ligand binding domains, their tissue expression patterns are different (Jakobsson et al. 2012). LXRα is predominantly expressed in metabolically active tissues, while LXRβ is ubiquitously expressed (Laffitte et al. 2001).

PPARs were originally discovered as receptors that induce the proliferation of peroxisomes in *Xenopus* (Dreyer et al. 1992). Three isoforms have been identified (Berger and Moller 2002). PPARα (NR1C1) regulates fatty acid oxidation and is highly expressed in tissues which perform substantial mitochondrial and peroxisomal β-oxidation such as brown adipose tissue, liver, kidney and heart (Kliewer et al. 1994). PPARβ/δ (NR1C2) has a ubiquitous expression pattern and plays a more general role in the activation of oxidative metabolism (Escher et al. 2001). PPARγ (NR1C3) plays a major role in the activation of adipocyte differentiation and is expressed in adipose tissue (Tontonoz et al. 1994). A broad range of endogenous molecules can act as agonists for the PPARs. These include a variety of unsaturated fatty acids, branched chain fatty acids, oxidized fatty acids eicosanoids, phospholipids and serotonin metabolites (Schupp and Lazar 2010). A number of synthetic ligands have also been identified for the different isoforms of PPARs (Grygiel-Gorniak 2014). PPARα ligands include fenofibrate, clofibrate and gemfibrozil; PPARβ/δ ligands include GW0742, GW501516 and GW9578; PPARγ ligands include rosiglitazone, pioglitazone, troglitazone, ciglitazone, farglitazar, S26948 and INT131.

7.4 LXRs and PPARs Regulate Inflammation

In addition to their role in reverse cholesterol transport, LXRs are important regulators of inflammatory gene expression and innate immunity. Regulation of inflammation by LXRs can be highlighted by reviewing previous studies demonstrating that LXR

activation downregulates the expression of pro-inflammatory molecules, such as inducible nitric oxide synthase (iNOS), IL-6, IL-1β, cyclooxygenase-2 (COX-2), monocyte chemoattractant protein-1 (MCP-1), prostaglandin E2, and matrix metalloproteinase-9 (MMP-9) in cultured macrophages, and primary isolated microglia and astrocytes in response to lipopolysaccharide (LPS) stimulation or bacterial infection (Castrillo and Tontonoz 2004; Rigamonti et al. 2008). LXR agonists can also attenuate inflammation through suppression of NF-κB DNA-binding activity, by blocking the degradation of IκB-α in LPS-stimulated microglia (Zhang-Gandhi and Drew 2007). Similarly, GW3965 attenuates LPS-induced inflammation in primary rat Kupffer cells through repression of tumor necrosis factor-alpha (TNF-α) and prostaglandin E2 (Wang et al. 2009). Another LXR agonist, T0901317, has been shown to downregulate interferon-γ (IFN-γ), TNF-α and IL-2 secretion by Th1 lymphocytes (Liu et al. 2012). Finally, LXR agonists have been shown to attenuate inflammatory responses *in vivo,* in experimental autoimmune encephalomyelitis, and irritant and allergic contact dermatitis models (Hindinger et al. 2006; Cui et al. 2011).

PPARs, also important in maintaining lipid homeostasis through regulation of fatty acid metabolism, have been shown to be molecular mediators of inflammatory pathways. For example, PPARβ/δ-dependent repression of NF-κB/AP1 transcription represents a major mechanism of attenuating inflammation by PPARβ/δ agonists (Schnegg and Robbins 2011). PPARγ activation leads to protection against atherosclerosis through reduced expression of inflammatory markers such as TNF-α and MMP-9 in both macrophages and artery wall tissue samples (Chawla et al. 2001a). While, loss of PPARγ bone marrow expression was associated with a significant increase in atherosclerotic lesion development. It is important to note, that an alternative explanation of the anti-inflammatory and atheroprotective effects of PPARγ has been proposed and this involves its ability of PPAR to crosstalk and induce LXRα expression. This in turn can lead to induction of cholesterol efflux as well as attenuation of expression of pro-inflammatory molecules in macrophages (Chawla et al. 2001b). The ability of LXRs and PPARs to repress expression of pro-inflammatory cytokines provides us with a likely therapeutic target to attenuate inflammation and their harmful downstream effects.

7.5 Rationale for Studying the Therapeutic Potential of Nuclear Receptors in AMD

Morphological examinations of retinas from AMD patients have revealed the accumulation and retention of activated microglia within the outer nuclear layer as well as the sub-retinal space (Gupta et al. 2003). The presence of these immune cells in the outer retina may contribute to the initiation of AMD pathology. The convergence of these morphological studies of AMD tissue, and investigations of nuclear receptor regulation of inflammation in other diseases that share common pathogenic pathways with AMD, advocate the notion that reversal of age-related

accumulation and influx of activated microglia modulated by nuclear receptors is a viable path to pursue to ameliorate the progression of AMD. Cellular targets for prevention and/or reversal of microglial influx may include the RPE, since RPE cells are critical in maintaining the immunosuppressive state and are contributors to local cytokine production and secretion. While the microglial cells, which in their activated state have been shown to be associated with drusenoid deposits as well as CNV lesions, would be potential targets for reversal of immune cell influx, serving as a therapeutic avenue for the treatment of both forms of late AMD. Most recently direct evidence for the use of LXR agonists in late AMD comes from studies, which have demonstrated that treatment with LXR agonists in an eye drop formulation is effective in reducing the severity of CNV lesions in an experimental model of wet AMD (Sene et al. 2013). Though throughout this review we have focused on the potential benefit of targeting nuclear receptors in decreasing inflammation, it is not trivial to note that, additionally, these ligands may also slow down AMD progression by regulating cholesterol and lipid homeostasis.

7.6 Conclusions

In the healthy retina, microglia are excluded from the sub-retinal space. However, changes in the sub-retinal microenvironment and RPE due to aging results in invasion of the sub-retinal space by these immune cells, where they can tip the balance to a "pathological state" and contribute to the progression of AMD. Given the potential that activation of LXRs and PPARs can lead to a downregulation of pro-inflammatory signals, targeting these nuclear receptors appear to provide an important therapeutic opportunity to tip the balance back again to a homeostatic state and hopefully either delay the onset of AMD or slow down its progression.

Acknowledgements Many thanks to the funding agencies supporting our research endeavors: The International Retinal Research Foundation Loris and David Rich Post-doctoral Fellowship (MC), NEI EY02868 (GM), P30 EY05722, and a Research to Prevent Blindness, Inc. Sybil B. Harrington Scholar award (GM).

References

Apfel R, Benbrook D, Lernhardt E et al (1994) A novel orphan receptor specific for a subset of thyroid hormone-responsive elements and its interaction with the retinoid/thyroid hormone receptor subfamily. Mol Cell Biol 14:7025–7035

Berger J, Moller DE (2002) The mechanisms of action of PPARs. Ann Rev Med 53:409–435

Castrillo A, Tontonoz P (2004) Nuclear receptors in macrophage biology: at the crossroads of lipid metabolism and inflammation. Ann Rev Cell Dev Biol 20:455–480

Chawla A, Barak Y, Nagy L et al (2001a) PPAR-gamma dependent and independent effects on macrophage-gene expression in lipid metabolism and inflammation. Nature Med 7:48–52

Chawla A, Boisvert WA, Lee CH et al (2001b) A PPAR gamma-LXR-ABCA1 pathway in macrophages is involved in cholesterol efflux and atherogenesis. Mol Cell 7:161–171
Coleman HR, Chan CC, Ferris FL, 3rd et al (2008) Age-related macular degeneration. Lancet 372:1835–1845
Combadiere C, Feumi C, Raoul W et al (2007) CX3CR1-dependent subretinal microglia cell accumulation is associated with cardinal features of age-related macular degeneration. J Clin Invest 117:2920–2928
Cui G, Qin X, Wu L et al (2011) Liver X receptor (LXR) mediates negative regulation of mouse and human Th17 differentiation. J Clin Invest 121:658–670
Dreyer C, Krey G, Keller H et al (1992) Control of the peroxisomal beta-oxidation pathway by a novel family of nuclear hormone receptors. Cell 68:879–887
Escher P, Braissant O, Basu-Modak S et al (2001) Rat PPARs: quantitative analysis in adult rat tissues and regulation in fasting and refeeding. Endocrinology 142:4195–4202
Grygiel-Gorniak B (2014) Peroxisome proliferator-activated receptors and their ligands: nutritional and clinical implications-a review. Nutrition J 13:17
Gupta N, Brown KE, Milam AH (2003) Activated microglia in human retinitis pigmentosa, late-onset retinal degeneration, and age-related macular degeneration. Exp Eye Res 76:463–471
Hindinger C, Hinton DR, Kirwin SJ et al (2006) Liver X receptor activation decreases the severity of experimental autoimmune encephalomyelitis. J Neurosci Res 84:1225–1234
Holtkamp GM, Kijlstra A, Peek R et al (2001) Retinal pigment epithelium-immune system interactions: cytokine production and cytokine-induced changes. Prog Ret Eye Res 20:29–48
Jakobsson T, Treuter E, Gustafsson JA et al (2012) Liver X receptor biology and pharmacology: new pathways, challenges and opportunities. Trend Pharm Sci 33:394–404
Karlstetter M, Langmann T (2014) Microglia in the aging retina. Adv Exp Med Biol 801:207–212
Kliewer SA, Forman BM, Blumberg B et al (1994) Differential expression and activation of a family of murine peroxisome proliferator-activated receptors. Proc Natl Acad Sci USA 91:7355–7359
Laffitte BA, Repa JJ, Joseph SB et al (2001) LXRs control lipid-inducible expression of the apolipoprotein E gene in macrophages and adipocytes. Proc Natl Acad Sci USA 98:507–512
Lehmann JM, Kliewer SA, Moore LB et al (1997) Activation of the nuclear receptor LXR by oxysterols defines a new hormone response pathway. J Biol Chem 272:3137–3140
Liu Y, Qiu de K, Ma X (2012) Liver X receptors bridge hepatic lipid metabolism and inflammation. J Digest Dis 13:69–74
Ng TF, Streilein JW (2001) Light-induced migration of retinal microglia into the subretinal space. Invest Ophthalmol Vis Sci 42:3301–3310
Patel M, Chan CC (2008) Immunopathological aspects of age-related macular degeneration. Semin Immunopathol 30:97–110
Rigamonti E, Chinetti-Gbaguidi G, Staels B (2008) Regulation of macrophage functions by PPAR-alpha, PPAR-gamma, and LXRs in mice and men. Arterio Thromb Vasc Biol 28:1050–1059
Schnegg CI, Robbins ME (2011) Neuroprotective mechanisms of PPARdelta: modulation of oxidative stress and inflammatory processes. PPAR Res 2011:373560
Schupp M, Lazar MA (2010) Endogenous ligands for nuclear receptors: digging deeper. J Biol Chem 285:40409–40415
Sene A, Khan AA, Cox D et al (2013) Impaired cholesterol efflux in senescent macrophages promotes age-related macular degeneration. Cell Metab 17:549–561
Streilein JW, Ma N, Wenkel H et al (2002) Immunobiology and privilege of neuronal retina and pigment epithelium transplants. Vision Res 42:487–495
Tontonoz P, Hu E, Spiegelman BM (1994) Stimulation of adipogenesis in fibroblasts by PPAR gamma 2, a lipid-activated transcription factor. Cell 79:1147–1156
Tuo J, Bojanowski CM, Zhou M et al (2007) Murine ccl2/cx3cr1 deficiency results in retinal lesions mimicking human age-related macular degeneration. Invest Ophthalmol Vis Sci 48:3827–3836

Viennois E, Pommier AJ, Mouzat K et al (2011) Targeting liver X receptors in human health: deadlock or promising trail? Expert Opin Ther Targets 15:219–232

Wang YY, Dahle MK, Steffensen KR et al (2009) Liver X receptor agonist GW3965 dose-dependently regulates lps-mediated liver injury and modulates posttranscriptional TNF-alpha production and p38 mitogen-activated protein kinase activation in liver macrophages. Shock 32:548–553

Zamiri P, Sugita S, Streilein JW (2007) Immunosuppressive properties of the pigmented epithelial cells and the subretinal space. Chem Immunol Allergy 92:86–93

Zhang-Gandhi CX, Drew PD (2007) Liver X receptor and retinoid X receptor agonists inhibit inflammatory responses of microglia and astrocytes. J Neuroimmun 183:50–59

Chapter 8
Extracellular Matrix Alterations and Deposit Formation in AMD

Rosario Fernandez-Godino, Eric A. Pierce and Donita L. Garland

Abstract Age related macular degeneration (AMD) is the primary cause of vision loss in the western world (Friedman et al., Arch Ophthalmol 122:564–572, 2004). The first clinical indication of AMD is the presence of drusen. However, with age and prior to the formation of drusen, extracellular basal deposits accumulate between the retinal pigment epithelium (RPE) and Bruch's membrane (BrM). Many studies on the molecular composition of the basal deposits and drusen have demonstrated the presence of extracellular matrix (ECM) proteins, complement components and cellular debris. The evidence reviewed here suggests that alteration in RPE cell function might be the primary cause for the accumulation of ECM and cellular debri found in basal deposits. Further studies are obviously needed in order to unravel the specific pathways that lead to abnormal formation of ECM and complement activation.

Keywords AMD · Extracellular matrix · basal deposits · RPE · Drusen · Complement system · Inflammation · MMP

8.1 Introduction

Macular degenerations (MDs) are disorders that include both inherited forms and the more prevalent age-related forms. AMD is the most common form of MD and is the primary cause of vision loss in the western world (Friedman et al. 2004). Although it is a prevalent disease, the initiation and pathogenesis are not well understood. The success of the treatments for AMD is limited (Lotery and Trump 2007; Miller 2013).

MDs are considered disorders of the RPE/BrM/choroid complex (Hageman and Mullins 1999). BrM is a specialized ECM located between the RPE and choroid. RPE cells secrete the proteins of BrM and have a role in the regulation of their

R. Fernandez-Godino (✉) · E. A. Pierce · D. L. Garland
Ocular Genomics Institute, Massachusetts Eye and Ear Infirmary, Harvard Medical School, Boston, MA 02114, USA
e-mail: rosario_godino@meei.harvard.edu

C. Bowes Rickman et al. (eds.), *Retinal Degenerative Diseases,* Advances in Experimental Medicine and Biology 854, DOI 10.1007/978-3-319-17121-0_8

turnover (Campochiaro et al. 1986; Chen et al. 2003; Aisenbrey et al. 2006). Structure and functions of BrM have recently been reviewed (Curcio and Johnson 2013). Briefly, BrM consists of five layers: RPE basal lamina/inner collagenous layer/elastin layer/outer collagenous layer/basal lamina of choriocapillaris. The major matrix structural proteins of BrM include collagens I-VI, elastin, perlecan (heparin sulfate proteoglycan), laminin and nidogen. Also present in BrM are matricellular proteins and associated proteins. Matricellular proteins contribute to cell-matrix interactions and RPE cell responses and include thrombospondin 1, fibulins, TGF-beta (Bornstein and Sage 2002). Growth factors comprise one class of associated proteins. In addition to the structural role of BrM, it has a critical role in signaling and provides barrier and filtering functions.

8.2 Extracellular Matrix, More than a Mere Structural Scaffold

ECMs are highly organized structures of proteins that cells secrete in order to create and maintain proper tissue architecture. The ECM structures are determined largely by composition, hence any alteration in composition will likely affect function (Davis et al. 2000; Paszek and Weaver 2004; Hynes 2009). ECMs are not static structures; studies in cancer, fibrosis and myocardial diseases demonstrated that ECM undergoes continuous dynamic remodeling (Cox and Erler 2011; Iijima et al. 2011; Rienks et al. 2014). Remodeling is regulated by a group of zinc-dependent endopeptidases called matrix metalloproteinases (MMPs) and their inhibitors, tissue-inhibitor of metalloproteinases (TIMPs) (Matrisian 1992). MMPs are capable of degrading all of the structural elements of the ECM, but also can process cytokines, growth factors, chemokines, and receptors on the cell membranes (Chang and Werb 2001; Van Lint and Libert 2007). MMPs have been shown to regulate not only the ECM turnover but signaling pathways as well (Hu and Ivashkiv 2006; Dufour et al. 2008; Glasheen et al. 2009). In BrM, signalling to the RPE cells occurs through interactions of integrins with laminin in BrM (Campochiaro et al. 1986; Chen et al. 2003; Aisenbrey et al. 2006).

MMP activity is tightly regulated by specific inhibitors, TIMPs (Nagase and Woessner 1999; Bergers and Coussens 2000). Impairment of the endogenous activity of the MMP/TIMP complexes causes pathologies such as tumor progression, rheumatoid arthritis, heart diseases, blood vessel diseases and atherosclerosis (Liotta et al. 1991; Gomis-Ruth et al. 1997; Chang and Werb 2001). Ocular diseases to which impaired MMP/TIMP balance contributes include retinal dystrophy, retinitis pigmentosa, AMD, inherited MD and diabetic retinopathy (Jones et al. 1994; Fariss et al. 1998; Nita et al. 2014). In AMD, TIMP3 accumulates in BrM (Kamei and Hollyfield 1999).

8.3 Macular Degenerations: Alterations in Bruch's Membrane and Deposit Formation

With age and before the presence of clinical evidence of macular disease, histopathological studies show BrM becomes thickened and extracellular basal deposits develop between the RPE and BrM (Kliffen et al. 1995; Kliffen et al. 1997; Reale et al. 2009). Basal deposits, accumulations of extracellular material in BrM and between BrM and the RPE are called basal linear (BLinD) or basal laminar deposits (BLamD), respectively (Sarks 2007; Curcio and Millican 1999; Sarks et al. 1976). BLamD, composed of granular material with wide-spaced collagen are located between the plasma membrane and the basal lamina of the RPE (Green and Enger 1993). BLamD are also a common feature in mouse models used to study AMD (Malek et al. 2003; Espinosa-Heidmann et al. 2006; Fu et al. 2007; Fujihara et al. 2009). BLinD, characterized by coated and non-coated vesicles composed of membranous material are located in the inner collagenous layer of BrM (Loeffler and Lee 1998; Curcio and Millican 1999). BLamD and BLinD as well as drusen all contain varying amounts of ECM proteins, complement components or complement regulators and inflammatory proteins (Hageman and Mullins 1999; Crabb et al. 2002; Chong et al. 2005; Sivaprasad et al. 2005; Lommatzsch et al. 2008; Wang et al. 2010). Proteomic analysis of BLamD in a mouse model of an inherited MD confirmed the presence of ECM/BrM components (Garland et al. 2014). The mechanisms of how any of these deposits form are essentially unknown. The presence of ECM proteins in all types of sub-RPE basal deposits provides strong evidence for a role of dysregulation of ECM in MD. The presence of complement and inflammatory proteins in drusen led to the conclusion that the complement system plays a direct role in drusen biogenesis (Mullins et al. 2000; Hageman et al. 2001; Anderson et al. 2002). In fact, in a mouse model the formation of BLamD was inhibited in the absence of an active complement system (Garland et al. 2014).

8.4 RPE Dysfunction and Aberrant ECM

What needs to be revealed is whether RPE dysfunction leads to ECM alterations and basal deposit formation or whether changes in ECM/BrM lead to RPE dysfunction and formation of aberrant ECM, and how inflammation and complement become involved.

Any process that disrupts signaling pathways between BrM and RPE could induce altered RPE function, including expression and secretion of ECM, and altered expression and secretion of MMPs and TIMPs (Leu et al. 2002; Kortvely et al. 2010; Hussain et al. 2011). Altered secretion of MMPs and TIMPs would likely lead to altered ECM turnover and ultimately to altered ECM composition. While the presence of basal deposits will almost certainly disrupt signaling pathways between BrM and RPE they could also be the consequence of disrupted signaling (Leu et al. 2002; Kortvely et al. 2010; Hussain et al. 2011).

The process of degradation of the ECM by MMPs generates matrikines, some of which can provoke an inflammatory response (Davis et al. 2000; Egeblad and Werb 2002; Sorokin 2010; Iijima et al. 2011). This is supported by the observation that matrikines derived from collagen I, collagen IV, fibronectin, laminins, elastin, nidogen, and thrombospondin-1 and −2 that exhibit chemotactic activity for inflammatory cells have been found in the sub-RPE deposits (Adair-Kirk and Senior 2008). There is evidence that MMPs can degrade these proteins and may be involved in generating the matrikines (Guo et al. 1999; Zhuge and Xu 2001; Marin-Castano 2005). However, evidence has been presented for increased and decreased MMP activity (Guo et al. 1999; Hussain et al. 2011). Alternatively, an altered composition of the ECM could alter its structure exposing neo-epitopes that could engage the complement system or the accumulation of ECM proteolytic fragments and other debris along the interface of the RPE and BrM might lead to complement activation.

While changes in BrM are the earliest age-related changes observed, the role of the RPE in expression and secretion of the ECM components of BrM and in the regulation of its turnover suggest that altered RPE cell function might be the primary cause for the accumulation of ECM and cellular debri found in basal deposits. The altered RPE cell function could be caused by any of the proposed processes such as oxidative stress or mutations that are thought to lead to macular degeneration (Marin-Castano 2005).

Further studies are needed in order to unravel the specific pathways that lead to abnormal formation of ECM and complement activation and the formation of drusen. Understanding these mechanisms should be extremely helpful in identifying targets for new AMD therapies.

References

Adair-Kirk TL, Senior RM (2008) Fragments of extracellular matrix as mediators of inflammation. Int J Biochem Cell Biol 40:1101–1110

Aisenbrey S, Zhang M, Bacher D et al (2006) Retinal pigment epithelial cells synthesize laminins, including laminin 5, and adhere to them through alpha3- and alpha6-containing integrins. Invest Ophthalmol Vis Sci 47:5537–5544

Anderson DH, Mullins RF, Hageman GS et al (2002) A role for local inflammation in the formation of drusen in the aging eye. Amer J Ophthalmol 134:411–431

Bergers G, Coussens LM (2000) Extrinsic regulators of epithelial tumor progression: metalloproteinases. Curr Opin Genet Dev 10:120–127

Bornstein P, Sage EH (2002) Matricellular proteins: extracellular modulators of cell function. Curr Opin Cell Biol 14:608–616

Campochiaro PA, Jerdon JA, Glaser BM (1986) The extracellular matrix of human retinal pigment epithelial cells in vivo and its synthesis in vitro. Invest Ophthalmol Vis Sci 27:1615–1621

Chang C, Werb Z (2001) The many faces of metalloproteases: cell growth, invasion, angiogenesis and metastasis. Trends Cell Biol 11:S37–43

Chen L, Miyamura N, Ninomiya Y et al (2003) Distribution of the collagen IV isoforms in human Bruch's membrane. Br J Ophthalmol 87:212–215

Chong NH, Keonin J, Luthert PJ et al (2005) Decreased thickness and integrity of the macular elastic layer of Bruch's membrane correspond to the distribution of lesions associated with age-related macular degeneration. Am J Pathol 166:241–251

Cox TR, Erler JT (2011) Remodeling and homeostasis of the extracellular matrix: implications for fibrotic diseases and cancer. Dis Model Mech 4:165–178
Crabb JW, Miyagi M, Gu X et al (2002) Drusen proteome analysis: an approach to the etiology of age-related macular degeneration. Proc Natl Acad Sci USA 99:14682–14687
Curcio CA, Millican CL (1999) Basal linear deposit and large drusen are specific for early age-related maculopathy. Arch Ophthalmol 117:329–339
Curcio CA, Johnson M (2013) Structure, function, and pathology of Bruch's membrane. Retina 1:465–481
Davis GE, Bayless KJ, Davis MJ et al (2000) Regulation of tissue injury responses by the exposure of matricryptic sites within extracellular matrix molecules. Am J Pathol 156:1489–1498
Dufour A, Sampson NS, Zucker S et al (2008) Role of the hemopexin domain of matrix metalloproteinases in cell migration. J Cell Physiol 217:643–651
Egeblad M, Werb Z (2002) New functions for the matrix metalloproteinases in cancer progression. Nat Rev Cancer 2:161–174
Espinosa-Heidmann DG, Suner IJ, Catanuto P et al (2006) Cigarette smoke-related oxidants and the development of sub-RPE deposits in an experimental animal model of dry AMD. Invest Ophthalmol Vis Sci 47:729–737
Fariss RN, Apte SS, Luthert PJ et al (1998) Accumulation of tissue inhibitor of metalloproteinases-3 in human eyes with Sorsby's fundus dystrophy or retinitis pigmentosa. Br J Ophthalmol 82:1329–1334
Friedman DS, O'Colmain BJ, Munoz B et al (2004) Prevalence of age-related macular degeneration in the United States. Arch Ophthalmol 122:564–572
Fu L, Garland D, Yang Z et al (2007) The R345W mutation in EFEMP1 is pathogenic and causes AMD-like deposits in mice. Hum Mol Genet 16:2411–2422
Fujihara M, Bartels E, Nielsen LB et al (2009) A human apoB100 transgenic mouse expresses human apoB100 in the RPE and develops features of early AMD. Exp Eye Res 88:1115–1123
Garland DL, Fernandez-Godino R, Kaur I et al (2014) Mouse genetics and proteomic analyses demonstrate a critical role for complement in a model of DHRD/ML, an inherited macular degeneration. Hum Mol Genet 23:52–68
Glasheen BM, Kabra AT, Page-McCaw A (2009) Distinct functions for the catalytic and hemopexin domains of a Drosophila matrix metalloproteinase. Proc Natl Acad Sci USA 106:2659–2664
Gomis-Ruth FX, Maskos K, Betz M et al (1997) Mechanism of inhibition of the human matrix metalloproteinase stromelysin-1 by TIMP-1. Nature 389:77–81
Green WR, Enger C (1993) Age-related macular degeneration histopathologic studies. The 1992 Lorenz E. Zimmerman Lecture. Ophthalmol 100:1519–1535
Guo L, Hussain AA, Limb GA et al (1999) Age-dependent variation in metalloproteinase activity of isolated human Bruch's membrane and choroid. Invest Ophthalmol Vis Sci 40:2676–2682
Hageman GS, Mullins RF (1999) Molecular composition of drusen as related to substructural phenotype. Mol Vis 5:28
Hageman GS, Luthert PJ, Victor Chong NH et al (2001) An integrated hypothesis that considers drusen as biomarkers of immune-mediated processes at the RPE-Bruch's membrane interface in aging and age-related macular degeneration. Prog Retin Eye Res 20:705–732
Hu Y, Ivashkiv LB (2006) Costimulation of chemokine receptor signaling by matrix metalloproteinase-9 mediates enhanced migration of IFN-alpha dendritic cells. J Immunol 176:6022–6033
Hussain AA, Lee Y, Zhang JJ et al (2011) Disturbed matrix metalloproteinase activity of Bruch's membrane in age-related macular degeneration. Invest Ophthalmol Vis Sci 52:4459–4466
Hynes RO (2009) The extracellular matrix: not just pretty fibrils. Science 326:1216–1219
Iijima J, Konno K, Itano N (2011) Inflammatory alterations of the extracellular matrix in the tumor microenvironment. Cancers (Basel) 3:3189–3205
Jones SE, Jomary C, Neal MJ (1994) Expression of TIMP3 mRNA is elevated in retinas affected by simplex retinitis pigmentosa. FEBS Lett 352:171–174
Kamei M, Hollyfield JG (1999) TIMP-3 in Bruch's membrane: changes during aging and in age-related macular degeneration. Invest Ophthalmol Vis Sci 40:2367–2375
Kliffen M, de Jong PT, Luider TM (1995) Protein analysis of human maculae in relation to age-related maculopathy. Lab Invest 73:267–272

Kliffen M, van der Schaft TL, Mooy CM et al (1997) Morphologic changes in age-related maculopathy. Microsc Res Tech 36:106–122
Kortvely E, Hauck SM, Duetsch G et al (2010) ARMS2 is a constituent of the extracellular matrix providing a link between familial and sporadic age-related macular degenerations. Invest Ophthalmol Vis Sci 51:79–88
Leu ST, Batni S, Radeke MJ et al (2002) Drusen are cold spots for proteolysis: expression of matrix metalloproteinases and their tissue inhibitor proteins in age-related macular degeneration. Exp Eye Res 74:141–154
Liotta LA, Steeg PS, Stetler-Stevenson WG (1991) Cancer metastasis and angiogenesis: an imbalance of positive and negative regulation. Cell 64:327–336
Loeffler KU, Lee WR (1998) Terminology of sub-RPE deposits: do we all speak the same language? Br J Ophthalmol 82:1104–1105
Lommatzsch A, Hermans P, Muller KD et al (2008) Are low inflammatory reactions involved in exudative age-related macular degeneration? Morphological and immunhistochemical analysis of AMD associated with basal deposits. Graefes Arch Clin Exp Ophthalmol 246:803–810
Lotery A, Trump D (2007) Progress in defining the molecular biology of age related macular degeneration. Hum Genet 122:219–236
Malek G, Li CM, Guidry C et al (2003) Apolipoprotein B in cholesterol-containing drusen and basal deposits of human eyes with age-related maculopathy. Am J Pathol 162:413–425
Marin-Castano (2005) Nonlethal oxidant injury to human retinal pigment epithelium cells causes cell membrane blebbing but decreased MMP-2 activity. Invest Ophthalmol Vis Sci 46:3331–3340
Matrisian LM (1992) The matrix-degrading metalloproteinases. Bioessays 14:455–463
Miller JW (2013) Age-related macular degeneration revisited–piecing the puzzle: the LXIX Edward Jackson memorial lecture. Am J Ophthalmol 155:1–35 e13
Mullins RF, Russell SR, Anderson DH et al (2000) Drusen associated with aging and age-related macular degeneration contain proteins common to extracellular deposits associated with atherosclerosis, elastosis, amyloidosis, and dense deposit disease. Faseb J 14:835–846
Nagase H, Woessner JF, Jr. (1999) Matrix metalloproteinases. J Biol Chem 274:21491–21494
Nita M, Strzalka-Mrozik B, Grzybowski A et al (2014) Age-related macular degeneration and changes in the extracellular matrix. Med Sci Monit 20:1003–1016
Paszek MJ, Weaver VM (2004) The tension mounts: mechanics meets morphogenesis and malignancy. J Mammary Gland Biol Neoplasia 9:325–342
Reale E, Groos S, Eckardt U et al (2009) New components of 'basal laminar deposits' in age-related macular degeneration. Cell Tiss Organs 190:170–181
Rienks M, Papageorgiou AP, Frangogiannis NG et al (2014) Myocardial extracellular matrix: an ever-changing and diverse entity. Circ Res 114:872–888
Sarks SH (1976) Ageing and degeneration in the macular region: a clinico-pathological study. Br J Ophthalmol 60:324–341
Sarks S, Cherepanoff S, Killingsworth M et al (2007) Relationship of Basal laminar deposit and membranous debris to the clinical presentation of early age-related macular degeneration. Invest Ophthalmol Vis Sci 48:968–977
Sivaprasad S, Chong NV, Bailey TA (2005) Serum elastin-derived peptides in age-related macular degeneration. Invest Ophthalmol Vis Sci 46:3046–3051
Sorokin L (2010) The impact of the extracellular matrix on inflammation. Nat Rev Immunol 10:712–723
Van Lint P, Libert C (2007) Chemokine and cytokine processing by matrix metalloproteinases and its effect on leukocyte migration and inflammation. J Leukoc Biol 82:1375–1381
Wang L, Clark ME, Crossman DK et al (2010) Abundant lipid and protein components of drusen. PLoS ONE 5:e10329
Zhuge Y, Xu J (2001) Rac1 mediates type I collagen-dependent MMP-2 activation. role in cell invasion across collagen barrier. J Biol Chem 276:16248–16256

Chapter 9
The NLRP3 Inflammasome and its Role in Age-Related Macular Degeneration

Cristhian J. Ildefonso, Manas R. Biswal, Chulbul M. Ahmed and Alfred S. Lewin

Abstract Age related macular degeneration (AMD) is the most common cause of blindness among people of 65 years and older in developed countries (Klein and Klein, Invest Ophthalmol Vis Sci 54:7395–7401, 2013). Recent advances in dry AMD research points towards an important role of the inflammatory response in the development of the disease. The presence of inflammatory cells, antibodies, complement factors and pro-inflammatory cytokines in AMD retinas and drusen indicates that the immune system could be an important driving force in dry AMD. The NLRP3 inflammasome has been proposed as an integrator of process associated with AMD and the induction of inflammation. Herein we summarize the most recent studies that attempt to understand the role of the NLRP3 inflammasome in AMD.

Keywords Blindness · Complement system proteins · Cytokines · Immune system · Immunity · Inflammasomes · Inflammation · Macular degeneration

9.1 Introduction

Using genome wide association studies, variations in the complement factor H (CFH) have been associated with AMD (Narayanan et al. 2007; Shastry 2007). Complement proteins are also found in drusen (Mullins et al. 2000). These studies

C. J. Ildefonso (✉) · M. R. Biswal · C. M. Ahmed · A. S. Lewin
Department of Molecular Genetics and Microbiology, University of Florida College of Medicine, Gainesville, FL 32610-0001, USA
e-mail: ildefons@ufl.edu

M. R. Biswal
e-mail: biswal@ufl.edu

C. M. Ahmed
e-mail: ahmed1@ufl.edu

A. S. Lewin
e-mail: lewin@ufl.edu

C. Bowes Rickman et al. (eds.), *Retinal Degenerative Diseases,* Advances in Experimental Medicine and Biology 854, DOI 10.1007/978-3-319-17121-0_9

provided a potential link between inflammatory processes and the development of AMD. Over the years the hypothesis that sterile inflammation plays a key role in the development of AMD has taken center stage (Camelo 2014). As a result, researchers have focused on the NLRP3 inflammasome signaling pathway.

When activated, the NLRP3 inflammasome forms a large cytoplasmic complex (Stutz et al. 2009). The Nod-like receptor family, pyrin domain containing 3 (NLRP3) is an intracellular receptor that responds to wide range of pathogen associated molecular patterns (PAMPS) and danger associated molecules (DAMPS) such as extracellular ATP (Cassel et al. 2009). It has a ligand binding leucine-rich repeat domain (LRR), a nucleotide binding and oligomerization domain (NATCH), and a pyrin domain (PYD). Upon engagement by a ligand, the NLRP3 receptor associates with the adaptor protein apoptosis-associated speck-like protein containing a CARD (ASC) through a PYD-PYD interaction. The recruited ASC, in turn, recruits the pro-caspase-1 via its caspase activation and recruitment domain (CARD) (Srinivasula et al. 2002). This CARD-CARD interaction activates caspase-1, which can then process the pro-forms of the interleukins 1 beta (IL-1β) and 18 (IL-18). These proteolytically activated cytokines are then secreted to initiate a pro-inflammatory response.

The expression of NLRP3 and the transcription of both IL-1β and IL-18 are regulated by transcription factor NF-kB. Signaling pathways such as those initiated by the Toll-like Receptor 4 (TLR-4) can activate NF-κB and induce the expression of NLRP3 and its signaling components (Bauernfeind et al. 2009). A secondary signal sensed by the NLRP3 receptor is responsible for the assembly of the inflammasome multi-protein complex.

9.2 Activation of the NLRP3 Inflammasome in AMD

The NLRP3 inflammasome has been found to be present in samples from AMD patients (Kaneko et al. 2011). Several compounds associated with AMD have been shown to activate the inflammasome. The reactive aldehyde 4-hydroxynonenal (4-HNE) was demonstrated to activate the inflammasome *in vitro* (Kauppinen et al. 2012). The addition of 4-HNE to ARPE-19 cells (a human RPE like cell line) caused the secretion of IL-1β, thus suggesting a potential link between oxidative stress and activation of the inflammasome. Proteins modified by carboxyethylpyrrole (CEP), an oxidation production of docosahexanoic acid, have been discovered within drusen from patients with AMD (Crabb et al. 2002). The CEP adducts have been shown to induce the activation of the inflammasome (Doyle et al. 2012) and activate macrophages (Cruz-Guilloty et al. 2014) when delivered *in vivo*. Another molecule associated with AMD that was demonstrated to induce the activation of the inflammasome is the pyridinium bisretinoid A2E (Anderson et al. 2013). A2E is a byproduct of the condensation of all trans-retinal that accumulates within the RPE cells with aging. The internalization of A2E can induce the secretion of IL-1β

in ARPE-19 cells. Anderson et al. also demonstrated that in ABCA4 knock-out mice there are increased levels of IL-1β that correlate with increase in A2E accumulation.

Amyloid beta (Aβ) protein is seen in drusen (Johnson et al. 2002). One of the effects of Aβ in the RPE is the induction of senescence. Further more, Aβ induces the secretion of matrix metalloproteinase 9 and the destabilization of the tight junctions between the RPE cells (Cao et al. 2013), suggesting that Aβ can induce the breakdown of the retina-blood-barrier known to occur in AMD. In another report, Liu and co-workers demonstrated that intravitreal injection of Aβ in rats resulted in the induction of IL-1β, IL-18, and MIP-3α (CCL20) (Liu et al. 2013). This group also reported an increase in all the components of the NLRP3 inflammasome not only in the RPE/choroid layer but also within the neural retina. Their results suggest that cells other than microglia can be a source of inflammasome activation.

One mechanism proposed to activate the inflammasome in AMD is the destabilization of the lysosomes. Destabilization of lysosomes in ARPE-19 cells resulted in activation of caspase-1 and release of IL-1β (Tseng et al. 2013). Cell death induced by the lysosomal destabilization was abrogated by the inhibition of caspase-1, the key enzyme in the process of pyroptosis (Fernandes-Alnemri et al. 2007; Miao et al. 2011). Similarly, defects in autophagy in the RPE may stimulate inflammation (Kaarniranta et al. 2013) by activating the inflammasome.

Inflammasome activation can be stimulated in RPE cells when co-cultured with activated microglia (Ma et al. 2009). When transplanted sub-retinally, activated microglia promotes neovascularization and RPE disorganization. These results suggest that migration of microglia into the subretinal space contributes to AMD by provoking inflammation and dysplasia of the RPE.

9.3 Cytokines Induced by the NLRP3 Inflammasome and Their Role in AMD

The cytokine IL-1β is a potent pro-inflammatory cytokine. As one of the cytokines processed by the NLRP3 inflammasome, the role of IL-1β on AMD has become of great importance to AMD research. A potential role for IL-1β in AMD was highlighted by Marneros et al. who showed that VEGF-A, a molecule associated with the development of neovascular AMD, can induce the secretion of IL-1β (Marneros 2013). The knock-down of either NLRP3 or IL-1R decreased the neovascular lesions characteristically observed in mice that over-express VEGF-A. Of note, when IL-18 was knocked down in this model, a modest increase in the neovascular lesions was observed.

Once activated by caspase-1, IL-18 is secreted from the cell. Extracellular IL-18 can bind to either its cognate receptor IL-18R or to the IL-18 binding protein (IL-18BP). Upon binding to IL-18R, a signaling pathway involving the activation of the protein MyD88 leads to the expression of other cytokines such as VEGF, IL-6 and TNF-α (Dinarello et al. 2013).

The function of IL-18 in the development of AMD remains unclear. In 2012 Doyle et al. reported that deletion of the NRLP3 followed by laser injury of the retina leads to an increase in neovascularization when compared with eyes that expressed this receptor (Doyle et al. 2012). This group also reported that drusen isolated from AMD eyes increase IL-1β secretion from peripheral blood mononuclear cells obtained from healthy human donors. In a follow up study, they demonstrated that pro-IL-18 induces the swelling of RPE cells leading to cell death (Doyle et al. 2014). Injecting the active form of the IL-18 into the mouse retina did not cause damage to the tissue, however. In agreement with their original findings, they found that injection of IL-18 either alone or in combination with anti-VEGF therapy reduced neovascularization in the laser-induced CNV mouse model. Their results point towards a protective role of IL-18 in wet AMD.

Conflicting data regarding the protective role of IL-18 on AMD has emerged from different labs. Researchers reported in 2011 that there is a decreased expression of the enzyme DICER in donated eyes from patients with AMD. In the same article, Kaneko and colleagues demonstrated that decrease of this enzyme is sufficient to induce RPE damage due to the accumulation of the *Alu* RNA (Kaneko et al. 2011). In follow up studies, this group demonstrated that the *Alu* induced RPE toxicity was dependent on the expression of the NLRP3 inflammasome components such as caspase-1 and PYCARD (Tarallo et al. 2012). To test the IL-18 protective role hypothesis, this group injected IL-18 in mice lacking caspases-1 and found that it induced an RPE damage similar to the accumulation of *Alu* RNA.

9.4 Targeting the NLRP3 Signaling Pathway

The purinergic receptor P2X7 was shown to modulate the activity of the NLRP3 inflammasome in *Alu*-induced AMD model (Kerur et al. 2013). Mice lacking the expression of P2X7 or NF-κB were protected from the RPE damaged induced by the *Alu* RNA. Another proposed target for the treatment of AMD is the signaling molecule MyD88. The inhibition of MyD88 with an inhibitor peptide protected mice from the degeneration induced by *Alu* RNA (Tarallo et al. 2012). One potential advantage of targeting MyD88 is that it is important for both the induction of NLRP3 expression and as a signaling component of the IL-18 receptor.

Although conflicting evidence regarding the function of IL-18 in AMD remains to be resolved, this cytokine presents another potential target for therapy. It is likely that increased expression of IL-18 exacerbates the inflammatory response in early AMD and in geographic atrophy. While Campbell et al. (Campbell et al. 2014; Doyle et al. 2014) have suggested injecting purified IL-18 as a treatment for wet AMD, this protein is a potent inflammatory cytokine with significant potential side effects relative to current inhibitors of VEGF signaling.

The extracellular-signal-regulated kinase 1/2 (ERK1/2) has been implicated in AMD. Inhibition of ERK by the specific inhibitor PD98059 protected the RPE of mice treated with *Alu* RNA (Dridi et al. 2012). No protection was observed when

mice receive inhibitors of either p38 or JNK. Interestingly, the route of administration utilized in this study was systemic which protected their retinas without adverse side-effects. Their results suggest that ERK 1/2 could be a potential target in AMD.

The rate limiting step of the inflammasome signaling is the activation of caspase-1, which makes it a therapeutic target for the treatment of AMD. Mice lacking caspase-1 are viable and develop normally (Kuida et al. 1995). Furthermore, several CARD only proteins (COPS) have been identified as negative regulators of the inflammasome signaling suggesting that it is plausible to inhibit its activity under certain situations (Le and Harton 2013). The induction of some of these COPS, or their exogenous over expression within the retina via gene therapy is an alternative that deserves further investigation.

9.5 Conclusion

Even though patients affected by AMD do not usually succumb to complete blindness, their visual impairment significantly affects their quality of life. Current treatment for wet AMD is based on the monthly injection of biological agents like ranibizumab that block VEGF signaling thus halting the growth of new blood vessels. Unfortunately there is no treatment available for dry AMD. Being a multifactorial disease there are different animal models of the disease that recapitulate certain aspects of the disease (Fletcher et al. 2014). The consensus among experts in the field points towards an active role of NLRP3 signaling in both dry and wet AMD (Campbell and Doyle 2013). By studying different animal and cellular models of AMD and human specimens from donor patients it has been possible to identify several important molecules associated with the NLRP3 inflammasome signaling pathway that could be targeted as a therapy. With the development of novel animal models of AMD, especially those with a defined macular region, developing an effective treatment for geographic atrophy becomes more likely.

Acknowledgements This work was supported by a grant from the National Eye Institute and a research fellowship from Genentech through the Association for Research in Vision and Ophthalmology.

References

Anderson OA, Finkelstein A, Shima DT (2013) A2E induces IL-1ß production in retinal pigment epithelial cells via the NLRP3 inflammasome. PLoS ONE 8:e67263

Bauernfeind FG, Horvath G, Stutz A et al (2009) Cutting edge: NF-kB activating pattern recognition and cytokine receptors license NLRP3 inflammasome activation by regulating NLRP3 expression. J Immunol 183:787–791

Camelo S (2014) Potential sources and roles of adaptive immunity in age-related macular degeneration: shall we rename AMD into autoimmune macular disease? Autoimmune Dis 2014:e532487

Campbell M, Doyle SL (2013) An eye on the future of inflammasomes and drug development in AMD. J Mol Med 91:1059–1070
Campbell DM, Doyle SL, Ozaki E et al (2014) An overview of the involvement of Interleukin-18 in degenerative retinopathies. In: Ash JD, Grimm C, Hollyfield JG et al (eds) Retinal degenerative diseases. Springer, New York, pp 409–415. (Adv Exp Med Biol)
Cao L, Wang H, Wang F et al (2013) Aβ-induced senescent retinal pigment epithelial cells create a proinflammatory microenvironment in AMD. Invest Ophthalmol Vis Sci 54:3738–3750
Cassel SL, Joly S, Sutterwala FS (2009) The NLRP3 inflammasome: a sensor of immune danger signals. Semin Immunol 21:194–198
Crabb JW, Miyagi M, Gu X et al (2002) Drusen proteome analysis: an approach to the etiology of age-related macular degeneration. Proc Natl Acad Sci U S A 99:14682–14687
Cruz-Guilloty F, Saeed AM, Duffort S et al (2014) T cells and macrophages responding to oxidative damage cooperate in pathogenesis of a mouse model of age-related macular degeneration. PLoS ONE 9:e88201
Dinarello C, Novick D, Kim S et al (2013) Interleukin-18 and IL-18 binding protein. Inflammation 4:289
Doyle SL, Campbell M, Ozaki E et al (2012) NLRP3 has a protective role in age-related macular degeneration through the induction of IL-18 by drusen components. Nature Med 18:791–798
Doyle SL, Ozaki E, Brennan K et al (2014) IL-18 Attenuates experimental choroidal neovascularization as a potential therapy for wet age-related macular degeneration. Sci Transl Med 6:230ra44–230ra44
Dridi S, Hirano Y, Tarallo V et al (2012) ERK1/2 activation is a therapeutic target in age-related macular degeneration. Proc Natl Acad Sci U S A 109:13781–13786
Fernandes-Alnemri T, Wu J, Yu J-W et al (2007) The pyroptosome: a supramolecular assembly of ASC dimers mediating inflammatory cell death via caspase-1 activation. Cell Death Differ 14:1590–1604
Fletcher EL, Jobling AI, Greferath U et al (2014) Studying age-related macular degeneration using animal models. Optom Vis Sci 91:878–886
Johnson LV, Leitner WP, Rivest AJ et al (2002) The Alzheimer's Aβ-peptide is deposited at sites of complement activation in pathologic deposits associated with aging and age-related macular degeneration. Proc Natl Acad Sci U S A 99:11830–11835
Kaarniranta K, Sinha D, Blasiak J et al (2013) Autophagy and heterophagy dysregulation leads to retinal pigment epithelium dysfunction and development of age-related macular degeneration. Autophagy 9:973–984
Kaneko H, Dridi S, Tarallo V et al (2011) DICER1 deficit induces Alu RNA toxicity in age-related macular degeneration. Nature 471:325–330
Kauppinen A, Niskanen H, Suuronen T et al (2012) Oxidative stress activates NLRP3 inflammasomes in ARPE-19 cells–implications for age-related macular degeneration (AMD). Immunol Lett 147
Kerur N, Hirano Y, Tarallo V et al (2013) TLR-Independent and P2 × 7-dependent signaling mediate alu RNA-induced NLRP3 inflammasome activation in geographic atrophy. Invest Ophthalmol Vis Sci 54:7395–7401
Klein R, Klein BEK (2013) The prevalence of age-related eye diseases and visual impairment in aging: current estimates. Invest Ophthalmol Vis Sci 54:ORSF5–ORSF13
Kuida K, Lippke JA, Ku G et al (1995) Altered cytokine export and apoptosis in mice deficient in interleukin-1 beta converting enzyme. Science 267:2000–2003
Le HT, Harton JA (2013) Pyrin- and CARD-only proteins as regulators of NLR functions. Mol Innate Immun 4:275
Liu RT, Gao J, Cao S et al (2013) Inflammatory mediators induced by Amyloid-Beta in the Retina and RPE in vivo: implications for inflammasome activation in age-related macular degeneration. Invest Ophthalmol Vis Sci 54:2225–2237
Ma W, Zhao L, Fontainhas AM et al (2009) Microglia in the mouse retina alter the structure and function of retinal pigmented epithelial cells: a potential cellular interaction relevant to AMD. PLoS ONE 4:e7945

Marneros AG (2013) NLRP3 inflammasome blockade inhibits VEGF-A-induced age-related macular degeneration. Cell Rep 4:945–958

Miao EA, Rajan JV, Aderem A (2011) Caspase-1-induced pyroptotic cell death. Immunol Rev 243:206–214

Mullins RF, Russell SR, Anderson DH et al (2000) Drusen associated with aging and age-related macular degeneration contain proteins common to extracellular deposits associated with atherosclerosis, elastosis, amyloidosis, and dense deposit disease. FASEB J 14:835–846

Narayanan R, Butani V, Boyer DS et al (2007) Complement factor H polymorphism in age-related macular degeneration. Ophthalmol 114:1327–1331

Shastry BS (2007) Assessment of the contribution of the LOC387715 gene polymorphism in a family with exudative age-related macular degeneration and heterozygous CFH variant (Y402H). J Hum Genet 52:384–387

Srinivasula SM, Poyet J-L, Razmara M et al (2002) The PYRIN-CARD protein ASC is an activating adaptor for Caspase-1. J Biol Chem 277:21119–21122

Stutz A, Golenbock DT, Latz E (2009) Inflammasomes: too big to miss. J Clin Invest 119:3502–3511

Tarallo V, Hirano Y, Gelfand BD et al (2012) DICER1 loss and alu RNA induce age-related macular degeneration via the NLRP3 inflammasome and MyD88. Cell 149:847–859

Tseng WA, Thein T, Kinnunen K et al (2013) NLRP3 inflammasome activation in retinal pigment epithelial cells by lysosomal destabilization: implications for age-related macular degeneration. Invest Ophthalmol Vis Sci 54:110–120

Chapter 10
Oxidative Stress and the Nrf2 Anti-Oxidant Transcription Factor in Age-Related Macular Degeneration

Mandy L. Lambros and Scott M. Plafker

Abstract Age-related macular degeneration (AMD) is the leading cause of acquired and irreversible blindness among elderly Americans. Most AMD patients have the dry form of the disease (dAMD) for which reliable therapies are lacking. A major obstacle to the development of effective treatments is a deficit in our understanding of what triggers dAMD onset. This is particularly the case with respect to the events that cause retinal pigment epithelial (RPE) cells to transition from a state of health and homeostasis to one of dysfunction and atrophy. These cells provide critical support to the photoreceptors and their atrophy often precipitates photoreceptor death in dAMD. Chronic oxidative stress is a primary driver of age-dependent, RPE atrophy. Sources of this stress have been identified (e.g., cigarette smoke, photo-oxidized bisretinoids), but we still do not understand how these stressors damage RPE constituents or what age-dependent changes undermine the cytoprotective systems in the RPE. This review focuses on Nrf2, the master antioxidant transcription factor, and its role in the RPE during aging and dAMD onset.

Keywords Age-related macular degeneration · Oxidative stress · Nrf2 · Retinal pigment epithelium · Mitochondria

10.1 Introduction

By 2050, the number of US adults over the age of 50 with age-related macular degeneration (AMD) is estimated to be 5 million (http://www.nei.nih.gov/eyedata/amd.asp). Of the two forms of the disease, wet and dry, ~85 % of cases are dry yet no reliable treatments currently exist. Characteristics of dry AMD (dAMD) include:

S. M. Plafker (✉) · M. L. Lambros
Free Radical Biology and Aging Program, Oklahoma Medical Research Foundation, 825 Northeast 13th Street, Oklahoma City, OK 73104, USA
e-mail: plafkers@omrf.org

M. L. Lambros
Department of Cell Biology, University of Oklahoma Health Sciences Center, Oklahoma City, OK 73104, USA

C. Bowes Rickman et al. (eds.), *Retinal Degenerative Diseases,* Advances in Experimental Medicine and Biology 854, DOI 10.1007/978-3-319-17121-0_10

(1) photoreceptor degeneration in the macula, a cone-enriched region near the center of the retina, (2) extracellular drusen deposits containing oxidized lipids and proteins, (3) a thickening of Bruch's membrane, (4) hypo- and hyperpigmentation, and (5) geographic atrophy of the retinal pigment epithelium (RPE) (reviewed in (Ambati and Fowler 2012)). The RPE is a critical layer of cells posterior to the neuro-retina that provides trophic support to the photoreceptors and is essential for sustaining photoreceptor function and viability. It is therefore not surprising that RPE dysfunction and atrophy are common pathological hallmarks of dAMD (Ambati and Fowler 2012). Recent efforts have established mouse models of RPE debilitation that are age-dependent and mimic the cardinal features of AMD with the goal of identifying therapeutic targets that can block disease onset (e.g., (Zhao et al. 2011a; Seo et al. 2012)).

Multiple lines of evidence link chronic oxidative stress in the RPE to the etiology of AMD. The RPE is subjected to such stresses due to its elevated metabolic rhythm, exposure to photo-oxidative stress and high oxygen tension, and from the daily phagocytic ingestion of shed photoreceptor outer segments, which are enriched in light damaged, polyunsaturated fatty acids. Clinical studies of mitochondrial DNA (mtDNA) damage have been very informative within this context as mtDNA provides a "history" of oxidative stress exposure. This " history" derives from the mitochondrial genome being more susceptible to age-associated damage than its nuclear counterpart (Karunadharma et al. 2010) and because mtDNA damage tends to be cumulative due to a less efficient DNA repair capacity (Lin et al. 2011). In AMD patient eyes, mtDNA lesions increase significantly in all regions of the mitochondrial genome compared to age-matched control eyes, where the damage is largely confined to the common deletion region (Karunadharma et al. 2010). Additionally, studies have shown that mtDNA damage positively correlates with AMD severity and is enriched in the macula relative to the peripheral retina (Lin et al. 2011).

A model to account for this disease-linked increase in mtDNA damage centers on the notion that leading up to AMD initiation, the capacities of the RPE autophagy and lysosomal degradation systems decrease. As shed outer segments are continually phagocytosed but not efficiently degraded, A2E and related bisretinoid pigments accumulate, undergo photo-oxidization, aggregate, and become a chronic source of oxidative stress by reacting with and depleting pools of reduced glutathione (Yoon et al. 2011). The buildup of bisretinoid photoproducts, peroxidized lipids, and aggregated proteins leads to unchecked free radical production. These excess free radicals, and the aldehydes and ketones they produce, further damage proteins, lipids, DNA, and organelles, especially mitochondria. The damaged mitochondria accumulate due to decreased autophagy (i.e., mitophagy), and in turn produce additional reactive oxygen species (ROS), adding further "fuel to the fire." Thus, the accumulation of ROS-generating, crippled mitochondria leads to wholesale damage of mitochondrial components including the mtDNA. Oxidatively-damaged mtDNA further propagate this cycle by limiting the capacity of the RPE to produce the necessary electron transport chain components needed for oxidative phosphorylation. Proteomic studies consistent with this model have identified altered expression

levels of mitochondrial proteins in RPE cells isolated from AMD patients (Nordgaard et al. 2008). In addition, RPE mitochondrial morphology and structure in AMD patients is more extensively disrupted compared to age-matched, non-AMD controls (Feher et al. 2006). Together, these and additional studies implicate ROS-mediated mtDNA damage, mitochondrial protein dysfunction, and loss of structure as key contributors to RPE atrophy.

10.2 Nrf2, the Antioxidant Defense System

The nuclear factor E2-related factor 2 (Nrf2) pathway is a primary system employed by the RPE to neutralize oxidative stress and maintain cellular homeostasis. Nrf2 is the master antioxidant transcription factor; it induces the expression of genes encoding ROS-neutralizing enzymes, detoxifying enzymes, molecular chaperones, proteasome subunits, and enzymes essential for intermediary metabolism (Hayes and Dinkova-Kostova 2014). During homeostasis, Nrf2 is constitutively targeted for degradation by the multi-subunit, E3 ubiquitin ligase $CUL3^{KEAP1}$ (Kobayashi et al. 2004). Keap1 is the redox-sensitive substrate adaptor that recruits Nrf2 to $CUL3^{KEAP1}$ for polyubiquitylation and subsequent delivery to the 26S proteasome for degradation. Oxidative stress dissociates $CUL3^{KEAP1}$ and stabilizes Nrf2. The transcription factor then rapidly translocates to the nucleus, heterodimerizes with Maf proteins, and binds to the antioxidant response elements (AREs) in the promoters of its cognate target genes (Itoh et al. 1997).

10.3 Nrf2 Knockout Studies in Mice

Nrf2 knockout mice are relatively healthy in the absence of stress, but upon oxidative challenge, be it pharmacological, environmental, or age-induced, they manifest various phenotypes (e.g., (Cano et al. 2010; Zhao et al. 2011b)). Recently, Nrf2-deficient mice were characterized as a model for retinopathy (Zhao et al. 2011b). These mice exhibit multiple, age-dependent pathologies characteristic of human AMD including progressive RPE and Bruch's membrane degeneration, drusen deposits and lipofuscin accumulation, and decreased electroretinography responses. Together, these findings underscore that Nrf2 deficiency may contribute to AMD pathogenesis. Additional studies demonstrated that aged, wild type mice express elevated basal levels of Nrf2 but that this does not correlate with an increase in protection against acute oxidative challenge (Sachdeva et al. 2014). Furthermore, when ROS measurements in young and old mice were compared before acute oxidative challenge, both cohorts had similar levels of superoxide anion and the lipid peroxidation product, maldionaldehyde. However, following acute challenge with the RPE-specific oxidant, sodium iodate, the RPE of the aged animals showed increased staining for both stress markers, whereas the RPE cells of the younger

mice did not. RPE-specific knockout of KEAP1 in the 15-month-old mouse only partially rescued the phenotype, revealing that increased Nrf2 stability is not sufficient for a full reversal. These data indicate that aging decreases the efficacy of the cytoprotective Nrf2 machinery, and in doing so, increases the susceptibility of the RPE to oxidative damage. The authors proposed that post-translational modifications in aged RPE might alter Nrf2 activity and that other transcription factors compensate to maintain basal levels of antioxidant gene expression. An additional explanation is that, despite sufficient levels of stabilized Nrf2, the transcription factor fails to productively associate with the promoters of its target genes due to age-dependent, epigenetic modifications to the AREs. This remains to be tested, but it is noteworthy that the promoters of several Nrf2 target genes (HO-1, NQO1, GST, GCLC) are enriched in CpG islands, which are targets of epigenetic silencing by methylation (reviewed in (Newell-Price et al. 2000)). For example, the murine NQO1 promoter has 18 CpG islands and the HO-1 promoter has 300 whereas the human NQO1 promoter has 177 CpG islands and the GCLC promoter has 489. This analysis (Stothard 2000) combined with RT-PCR to monitor the induction of a panel of Nrf2 target genes in oxidatively-challenged, aged mice should prove useful for identifying candidates to pursue for deeper epigenetic evaluation.

10.4 Nrf2 and the Mitochondria

Mitochondrial dynamics maintain the morphology, integrity, and function of mitochondria in part by constituting a first line of defense against oxidative insult. These dynamics involve mitochondria physically associating with (fusion) or dissociating from (fission) the interconnected mitochondrial network. Fusion involves individual, damaged mitochondria melding with the mitochondrial network to mix and exchange contents thereby rescuing, via complementation, the damaged unit. In contrast, fission pinches off individual, irreparably damaged mitochondria from the larger network and liberates them for mitophagy (reviewed in (Youle and van der Bliek 2012)).

Interestingly, a population of Nrf2 has been identified at the mitochondrial outer membrane in a ternary complex with the atypical phosphatase PGAM5 and a dimer of KEAP1 (Lo and Hannink 2008). The function of this Nrf2 population is unknown. In recent studies, we identified a mitochondrial trafficking defect in cultured RPE cells following Nrf2 depletion by siRNA. These findings led us to the hypothesis that the mitochondrial population of Nrf2 mediates mitochondrial dynamics. We tested this in an RPE explant model using video microscopy of live RPE flatmounts from $Nrf2^{-/-}$ and $Nrf2^{+/+}$ mice expressing mito-targeted GFP. These experiments revealed two populations of mitochondria in the RPE, a static cluster of similarly-sized, ovoid mitochondria on the basal side of the RPE nuclei (Fig. 10.1, panel A), and a dynamic group of mitochondria scattered across the apical side of the RPE that vary in shape and actively interact with one another (Fig. 10.1, panel B). We hypothesize that the transient “kiss-and-run” events taking place among

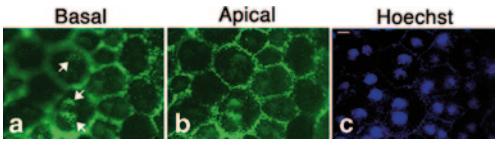

Fig. 10.1 RPE flatmounts contain two populations of mitochondria. We observed a basal population of mitochondria that were clustered in a perinuclear locale (*panel A*) and a second, more abundant population on the apical side that exhibited dynamic fusion and fission activity (*panel B*). Shown are two focal planes of the same RPE cells and Hoechst staining to demarcate the nuclei (*panel C*). Basal mitochondria denoted with *white arrows* (*panel A*). Scale bar: 10 μm

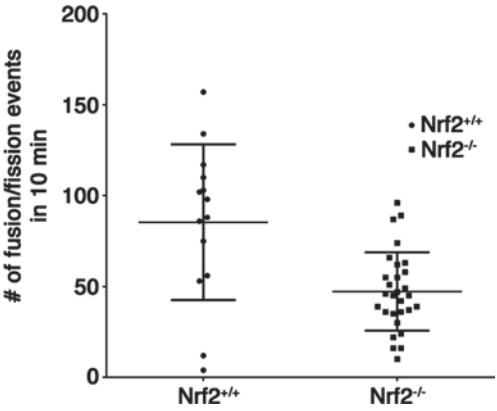

Fig. 10.2. Genetic ablation of Nrf2 reduces the frequency of mitochondrial "kiss and run" events. Graph of fusion and fission events from live RPE flatmounts ($Nrf2^{+/+}$ (wt) v. $Nrf2^{-/-}$ (knockout)) expressing a mitoGFP transgene. Movies were recorded for 10 min and each diamond represents a single RPE cell. Mice were 33–43 weeks of age. Errors bars represent standard deviation

the apically-positioned mitochondria represent fusion and fission however, experiments demonstrating the transfer of a fluorescent label between mitochondria will be needed to definitively draw this conclusion. Interestingly, time-lapse imaging of live flatmounts demonstrated that Nrf2 ablation reduced the frequency of "kiss and run" events (Fig. 10.2). These data indicate that Nrf2 may have a cytoprotective function(s) distinct from its transcriptional role. Further studies are being pursued to elucidate this novel function.

10.5 Concluding Remarks

Clinical and experimental evidence continues to mount in support of chronic oxidative stress as a central driving force in dAMD initiation. It is our contention that understanding the endogenous cellular machinery and pathways that counter oxida-

tive stress in the RPE (i.e., the Nrf2 system, mitochondria, and the autophagy and ubiquitin degradation systems) and how age impacts each of these systems and their interactions with one another, will provide a gateway to the design of much needed therapeutics for staving off dAMD onset.

References

Ambati J, Fowler BJ (2012) Mechanisms of age-related macular degeneration. Neuron 75:26–39

Cano M, Thimmalappula R, Fujihara M et al (2010) Cigarette smoking, oxidative stress, the anti-oxidant response through Nrf2 signaling, and Age-related Macular Degeneration. Vision Res 50:652–664

Feher J, Kovacs I, Artico M et al (2006) Mitochondrial alterations of retinal pigment epithelium in age-related macular degeneration. Neurobiol Aging 27:983–993

Hayes JD, Dinkova-Kostova AT (2014) The Nrf2 regulatory network provides an interface between redox and intermediary metabolism. Trends Biochem Sci 39:199–218

Itoh K, Chiba T, Takahashi S et al (1997) An Nrf2/small Maf heterodimer mediates the induction of phase II detoxifying enzyme genes through antioxidant response elements. Biochem Biophys Res Commun 236:313–322

Karunadharma PP, Nordgaard CL, Olsen TW et al (2010) Mitochondrial DNA damage as a potential mechanism for age-related macular degeneration. Invest Ophthalmol Vis Sci 51:5470–5479

Kobayashi A, Kang MI, Okawa H et al (2004) Oxidative stress sensor Keap1 functions as an adaptor for Cul3-based E3 ligase to regulate proteasomal degradation of Nrf2. Mol Cell Biol 24:7130–7139

Lin H, Xu H, Liang FQ et al (2011) Mitochondrial DNA damage and repair in RPE associated with aging and age-related macular degeneration. Invest Ophthalmol Vis Sci 52:3521–3529

Lo SC, Hannink M (2008) PGAM5 tethers a ternary complex containing Keap1 and Nrf2 to mitochondria. Exp Cell Res 314:1789–1803

Newell-Price J, Clark AJ, King P (2000) DNA methylation and silencing of gene expression. Trends Endocrinol Metab: TEM 11:142–148

Nordgaard CL, Karunadharma PP, Feng X et al (2008) Mitochondrial proteomics of the retinal pigment epithelium at progressive stages of age-related macular degeneration. Invest Ophthalmol Vis Sci 49:2848–2855

Sachdeva MM, Cano M, Handa JT (2014) Nrf2 signaling is impaired in the aging RPE given an oxidative insult. Exp Eye Res 119:111–114

Seo SJ, Krebs MP, Mao H et al (2012) Pathological consequences of long-term mitochondrial oxidative stress in the mouse retinal pigment epithelium. Exp Eye Res 101:60–71

Stothard P (2000) The sequence manipulation suite: JavaScript programs for analyzing and formatting protein and DNA sequences. Biotechniques 28:1102:1104

Yoon KD, Yamamoto K, Zhou J et al (2011) Photo-products of retinal pigment epithelial bisretinoids react with cellular thiols. Mol Vis 17:1839–1849

Youle RJ, van der Bliek AM (2012) Mitochondrial fission, fusion, and stress. Science 337:1062–1065

Zhao C, Yasumura D, Li X et al (2011a) mTOR-mediated dedifferentiation of the retinal pigment epithelium initiates photoreceptor degeneration in mice. J Clin Invest 121:369–383

Zhao Z, Chen Y, Wang J et al (2011b) Age-related retinopathy in NRF2-deficient mice. PLoS ONE 6:e19456

Chapter 11
Aging Changes in Retinal Microglia and their Relevance to Age-related Retinal Disease

Wenxin Ma and Wai T. Wong

Abstract Age-related retinal diseases, such as age-related macular degeneration (AMD) and glaucoma, contain features of chronic retinal inflammation that may promote disease progression. However, the relationship between aging and neuroinflammation is unclear. Microglia are long-lived, resident immune cells of the retina, and mediate local neuroinflammatory reactions. We hypothesize that aging changes in microglia may be causally linked to neuroinflammatory changes underlying age-dependent retinal diseases. Here, we review the evidence for (1) how the retinal microglial phenotype changes with aging, (2) the factors that drive microglial aging in the retina, and (3) aging-related changes in microglial gene expression. We examine how these aspects of microglial aging changes may relate to pathogenic mechanisms of immune dysregulation driving the progression of age-related retinal disease. These relationships can highlight microglial aging as a novel target for the prevention and treatment of retinal disease.

Keywords Microglia · Aging · Complement · Retinal pigment epithelium · Senescence

11.1 Introduction

Common retinal diseases, such as AMD and glaucoma, contribute significantly to vision loss in the US and worldwide (Congdon et al. 2003, 2004). They however have an intriguing age-dependence in their prevalence which increases markedly with aging (Friedman et al. 2004a, 2004b). The causes for their association with aging are not well-understood, but because these diseases are characterized by an

W. T. Wong (✉) · W. Ma
Unit on Neuron-Glia Interactions in Retinal Diseases, National Eye Institute, National Institutes of Health, 6 Center Drive, 6/125, Bethesda, MD 20892, USA
e-mail: wongw@nei.nih.gov

C. Bowes Rickman et al. (eds.), *Retinal Degenerative Diseases,* Advances in Experimental Medicine and Biology 854, DOI 10.1007/978-3-319-17121-0_11

early emergence of retinal neuroinflammation (Wax and Tezel 2009; Buschini et al. 2011), it has been hypothesized that an age-related dysregulation of immune response in the retina can contribute to disease pathogenesis (Xu et al. 2009; Wong 2013). As microglia are the primary resident immune cell in the retina, and are long-lived cells that persist across long periods of chronological time (Albini et al. 2005; Ajami et al. 2007), senescent changes occurring within aging microglia may be one cause of immune response "failure", conferring upon the retina an age-dependent vulnerability to disease. Here we review the evidence that retinal microglia in fact demonstrate aging-dependent physiological and molecular changes, and speculate on the drivers and consequences of microglia aging in the retina.

11.2 Aging Phenotypes of Retinal Microglia

Microglia in the young healthy retina demonstrate an orderly laminar distribution in which individual cells are evenly spread out in a regularly tiled distribution in the inner and outer plexiform layers but are intriguingly excluded from the outer retina (Santos et al. 2008). Each microglial cell possesses ramified, branching processes that exhibit rapid, constitutive motility that enables the cell to effectively survey the extracellular milieu in its vicinity (Lee et al. 2008). While microglial somata are evenly spaced and relatively stationary in the uninjured state, microglia following focal injury promptly polarize their processes and migrate in the direction of injury to cluster around the injury site. In our studies, we found that these phenotypic features of retinal microglia are not static but change progressively with aging. Compared to the young (3–4 month old) mouse retina, the aged (18–24 month old) retina contains a slightly but significantly greater density of microglia; each of these aged microglia have a significantly smaller ramified dendritic arbor on average, with fewer branches and shorter total process lengths (Damani et al. 2011). In addition, the constitutive movements of aged microglial processes were significantly slower than those in their younger counterparts. Similar observations were also found for microglia in the cortex (Hefendehl et al. 2014) and hippocampus (Mouton et al. 2002) of the brain, indicating that CNS microglia may decline in their ability to perform everyday functions of immune surveillance and synapse maintenance with aging, which may translate to an increasing vulnerability to neurodegenerative disease (Streit and Xue 2009).

In addition to microglial phenotypes in the steady state, we found that the nature and extent of microglial responses to injury become altered with aging. While young retinal microglia responded dynamically to exogenous applications of ATP, an injury-related signal, by increasing motility and the degree of branching in their processes, aged microglia demonstrated a converse response by decreasing both process motility and ramification (Damani et al. 2011). In a laser model of focal retinal injury, we found that aged microglia failed to upregulate their process motility in the immediate aftermath of focal injury (minutes to hours) in a manner observed in young microglia. Aged retinal microglia also migrated to the injury site more

slowly compared with young microglia. In the longer term, while young microglia demonstrated dispersal from the injury site 16 days after laser injury, aged microglia remained clustered at the laser burn with a reduced rate of dispersal. These data indicated while microglial injury responses in the young retina have a prompt and rapid initiation upon the onset of injury, followed by an expeditious downregulation upon injury resolution, those in the aged retina are slower to initiate but are also slower to reverse and return to the resting state. These dysregulated responses may thus contribute defects in efficient homeostasis and help contribute to a more chronically active neuroinflammatory state in the retina.

The exclusion of microglia from the young healthy outer retina is a unique feature that indicates the outer retina as a special zone of immune regulation where the spatial segregation of microglia from outer retinal cell types is required. However, with aging, this zone of exclusion is increasingly transgressed by microglia that translocate into the outer retina to accumulate in the subretinal space (Xu et al. 2008; Chinnery et al. 2012). In the young retina, physical contact and interaction between microglia and RPE cells are highly infrequent, but in the aged retina, these RPE-microglia contacts increase monotonically in prevalence as a function of aging. Microglia accumulating in the subretinal space demonstrate morphological and molecular markers of increased activation (Xu et al. 2008; Ma et al. 2013b), indicating their ability to contribute to an increased pro-inflammatory local environment. These changes were similarly observed in aged and AMD human retinas (Ma et al. 2013a). While the factors that drive this translocation are unclear, these increasing age-dependent RPE-microglia interactions result in changes in RPE cells that induce further immune dysregulation at this outer retinal interface and promote pathological changes similar to those observed in AMD (Ma et al. 2009, 2012). From observations *in vitro* and *in vivo* systems, we found that activated retinal microglia induced in RPE cells (1) changes in RPE structure and distribution, (2) increased expression and secretion of pro-inflammatory, chemotactic, and pro-angiogenic molecules, and (3) an increased ability to promote choroidal neovascularization *in vivo*. As such, we speculate that the migration of retinal microglia into the subretinal space induces significant changes in RPE cells that perpetuate further microglial accumulation, increase inflammation in the outer retina, and fosters an environment conducive for the formation of neovascular changes in wet AMD.

11.3 Potential Factors Driving the Aging Microglial Phenotype in the Retina

How do aging-related phenotypes arise in retinal microglia? Elucidation of the drivers of microglial aging can not only enable an understanding of microglial physiology but also present therapeutic opportunities for modulating of these phenotypes to inhibit or reverse vulnerabilities to aging-related retinal disease. Factors influencing microglial phenotypes may arise from the environment of the aging retina or otherwise from intrinsic age-related changes within microglial cells themselves. Genetic

expression profiling of the entire retina have shown that retinal aging involves gene sets involved in the regulation of local inflammatory responses, particularly those involved with the innate immune system (Chen et al. 2010), suggesting that modulatory influences onto microglia, possibly from neighboring retinal cells such as Müller cells (Wang et al. 2011, 2014; Wang and Wong 2014), may change with aging. On the other hand, microglia themselves demonstrate intrinsic age-dependent changes such as the accumulation of lipofuscin, which are likely built up as a function of continuing phagocytosis of byproducts of the visual cycle. We discovered that the accumulation of A2E, a primary bisretinoid of lipofuscin, has the effect of increasing microglial activation, suppressing microglial chemotactic responses, and altering complement gene expression to favor complement activation. As such, lipofuscin buildup in aging microglia may constitute one potential driver of pathogenic aging microglial phenotypes.

We found by microarray analysis of microglia isolated ex vivo from the mouse retina that patterns of gene expression in microglia demonstrate progressive change with aging (Ma et al. 2013b). In particular, molecular pathways involving immune function and regulation, angiogenesis, and neurotrophin signaling demonstrated age-related changes. Interestingly, expression levels of complement genes C3 and CFB, which have been associated with AMD, also increased with aging, indicating that microglia, which can contribute to local complement regulation (Rutar et al. 2011), may falter in their ability to limit complement activation with aging. Indeed, we also found immunohistochemical and mRNA evidence of increased C3 and CFB expression, as well as complement activation in the aging retina (Ma et al. 2013b). Therefore, intrinsic changes in complement gene expression, combined with outer retinal accumulation, may constitute a mechanism by which aging microglia alter the immune environment in ways pathologically relevant to AMD.

11.4 Conclusions and Perspectives

Microglia in the young healthy animal have a highly ordered, regular and laminar distribution in the retina, in which they conduct constitutive activities of synapse maintenance and immune surveillance via highly dynamic processes. They also express multiple inflammatory proteins, including complement and complement regulatory proteins, indicative of their role in the immune regulation of the retinal environment. With retinal aging, these phenotypes demonstrate age-related changes that result in a disordered microglial distribution in the retina, deficient constitutive microglial function, and abnormal microglial injury responses. These alterations, combined with molecular and gene expression aging changes within microglia, indicate that aged microglia may be less capable of maintaining homeostasis in the immune environment, particularly of the outer retina. Further study into the factors in the aging retinal environment influential on microglial phenotype and into the key molecular regulators of microglial function will be helpful in understanding

how microglial aging can be modulated or reversed. The ability to successfully modulate microglial aging phenotype has the promise of "rejuvenating" the immune environment of the retina in ways that may be protective against the progression of age-related retinal diseases.

References

Ajami B, Bennett JL, Krieger C et al (2007) Local self-renewal can sustain CNS microglia maintenance and function throughout adult life. Nat Neurosci 10:1538–1543

Albini TA, Wang RC, Reiser B et al (2005) Microglial stability and repopulation in the retina. Br J Ophthalmol 89:901–903

Buschini E, Piras A, Nuzzi R et al (2011) Age related macular degeneration and drusen: neuroinflammation in the retina. Prog Neurobiol 95:14–25

Chen M, Muckersie E, Forrester JV et al (2010) Immune activation in retinal aging: a gene expression study. Invest Ophthalmol Vis Sci 51:5888–5896

Chinnery HR, McLenachan S, Humphries T et al (2012) Accumulation of murine subretinal macrophages: effects of age, pigmentation and CX3CR1. Neurobiol Aging 33:1769–1776

Congdon NG, Friedman DS, Lietman T (2003) Important causes of visual impairment in the world today. JAMA 290:2057–2060

Congdon N, O'Colmain B, Klaver CC et al (2004) Causes and prevalence of visual impairment among adults in the United States. Arch Ophthalmol 122:477–485

Damani MR, Zhao L, Fontainhas AM et al (2011) Age-related alterations in the dynamic behavior of microglia. Aging Cell 10:263–276

Friedman DS, O'Colmain BJ, Munoz B et al (2004a) Prevalence of age-related macular degeneration in the United States. Arch Ophthalmol 122:564–572

Friedman DS, Wolfs RC, O'Colmain BJ et al (2004b) Prevalence of open-angle glaucoma among adults in the United States. Arch Ophthalmol 122:532–538

Hefendehl JK, Neher JJ, Suhs RB et al (2014) Homeostatic and injury-induced microglia behavior in the aging brain. Aging Cell 13:60–69

Lee JE, Liang KJ, Fariss RN et al (2008) Ex vivo dynamic imaging of retinal microglia using time-lapse confocal microscopy. Invest Ophthalmol Vis Sci 49:4169–4176

Ma W, Zhao L, Fontainhas AM et al (2009) Microglia in the mouse retina alter the structure and function of retinal pigmented epithelial cells: a potential cellular interaction relevant to AMD. PLoS ONE 4:e7945

Ma W, Zhao L, Wong WT (2012) Microglia in the outer retina and their relevance to pathogenesis of age-related macular degeneration. Adv Exp Med Biol 723:37–42

Ma W, Coon S, Zhao L et al (2013a) A2E accumulation influences retinal microglial activation and complement regulation. Neurobiol Aging 34:943–960

Ma W, Cojocaru R, Gotoh N et al (2013b) Gene expression changes in aging retinal microglia: relationship to microglial support functions and regulation of activation. Neurobiol Aging 34:2310–2321

Mouton PR, Long JM, Lei DL et al (2002) Age and gender effects on microglia and astrocyte numbers in brains of mice. Brain Res 956:30–35

Rutar M, Natoli R, Kozulin P et al (2011) Analysis of complement expression in light-induced retinal degeneration: synthesis and deposition of C3 by microglia/macrophages is associated with focal photoreceptor degeneration. Invest Ophthalmol Vis Sci 52:5347–5358

Santos AM, Calvente R, Tassi M et al (2008) Embryonic and postnatal development of microglial cells in the mouse retina. J Comp Neurol 506:224–239

Streit WJ, Xue QS (2009) Life and death of microglia. J Neuroimmune Pharmacol 4:371–379

Wang M, Wong WT (2014) Microglia-Muller cell interactions in the retina. Adv Exp Med Biol 801:333–338
Wang M, Ma W, Zhao L et al (2011) Adaptive Muller cell responses to microglial activation mediate neuroprotection and coordinate inflammation in the retina. J Neuroinflammation 8:173
Wang M, Wang X, Zhao L et al (2014) Macroglia–microglia interactions via TSPO signaling regulates microglial activation in the mouse retina. J Neurosci 34:3793–3806
Wax MB, Tezel G (2009) Immunoregulation of retinal ganglion cell fate in glaucoma. Exp Eye Res 88:825–830
Wong WT (2013) Microglial aging in the healthy CNS: phenotypes, drivers, and rejuvenation. Front Cell Neurosci 7:22
Xu H, Chen M, Manivannan A et al (2008) Age-dependent accumulation of lipofuscin in perivascular and subretinal microglia in experimental mice. Aging Cell 7:58–68
Xu H, Chen M, Forrester JV (2009) Para-inflammation in the aging retina. Prog Retin Eye Res 28:348–368

Chapter 12
VEGF-A and the NLRP3 Inflammasome in Age-Related Macular Degeneration

Alexander G. Marneros

Abstract The pathomechanisms that lead to age-related macular degeneration (AMD) are only partially understood. The NLRP3 inflammasome has been shown to be activated in the retinal pigment epithelium (RPE) in eyes with AMD. However, it is not known whether inflammasome activation is a cause or consequence of pathologic changes in AMD. A roadblock to defining the role of inflammasome activation and pathways that regulate it for AMD has been the lack of a mouse model that forms AMD-like pathologies in an age-dependent manner in which the role of the inflammasome can be investigated using genetic studies. We have recently identified such a mouse model, in which increased VEGF-A levels result in early degenerative changes of the RPE, followed by cardinal features of both nonexudative and neovascular AMD. Importantly, higher VEGF-A levels lead to increased oxidative damage and a sub-retinal inflammatory infiltrate that are associated with NLRP3 inflammasome activation in the RPE. Targeting the NLRP3 inflammasome inhibited AMD-like pathologies in these mice. These findings suggest that inhibiting the NLRP3 inflammasome or pathways that regulate it may provide novel therapeutic approaches for the treatment of both forms of AMD.

Keywords VEGF-A · NLRP3 inflammasome · Age-related macular degeneration, AMD · Macrophages · Oxidative stress

12.1 Introduction

AMD is the most common cause of irreversible blindness in the elderly, and the number of affected individuals is anticipated to increase significantly in the near future (van Leeuwen et al. 2003; Friedman et al. 2004). AMD has been classified clinically as either the neovascular ("wet") form, with excessive choroidal neovascularization (CNV) that impairs vision, or as the nonexudative ("dry") form that is characterized by atrophic degeneration of the RPE and subsequent retinal degeneration.

A. G. Marneros (✉)
Department of Dermatology, Cutaneous Biology Research Center, Massachusetts General Hospital, Harvard Medical School, Charlestown, MA 02129, USA
e-mail: amarneros@mgh.harvard.edu

C. Bowes Rickman et al. (eds.), *Retinal Degenerative Diseases,* Advances in Experimental Medicine and Biology 854, DOI 10.1007/978-3-319-17121-0_12

Importantly, nonexudative AMD may co-occur with neovascular AMD, suggesting a common pathomechanism (Sunness et al. 1999). In addition, genetic association studies in AMD patients have also suggested a common pathomechanism for both forms of AMD, and have found an association of gene loci for complement pathway components as well as the VEGF-A gene locus with both forms of AMD (Yu et al. 2011). Identifying a shared pathomechanism for both neovascular and nonexudative AMD would provide the unique opportunity to develop a comprehensive treatment approach for all forms of AMD, or even develop therapeutic strategies to prevent AMD from progressing at its early stages. A significant roadblock to the development of novel therapies and potentially comprehensive therapeutic approaches that target both forms of AMD has been the lack of a mouse model that manifests cardinal features of both forms of AMD in an age-dependent manner with complete penetrance and without external artificial experimental manipulation (such as laser injury), in which novel therapies could be tested.

Several specific pathways and cellular changes have been hypothesized to be important for human AMD pathogenesis, but the limitations in the experimental animal models used so far have limited the evidence for the *in vivo* significance of such pathways. Particularly increased reactive oxygen species (ROS) and more recently activation of the NLRP3 inflammasome have been suggested to contribute to AMD pathogenesis, in addition to increased expression of proangiogenic factors (e.g. VEGF-A) in neovascular AMD (Tarallo et al. 2012; Tseng et al. 2013).

We speculated that increased VEGF-A levels in the eye would lead to both nonexudative and neovascular AMD-like pathologies, as (1) major risk factors for AMD development (such as smoking) lead to oxidative damage or hypoxia in the RPE, which are both main inducers of VEGF-A expression in the RPE (Klettner and Roider 2009), and (2) because the VEGF-A gene locus has been linked to both forms of AMD in patients (Yu et al. 2011). Furthermore, VEGF-A has been shown to induce breakdown of the RPE barrier *in vitro* in a VEGFR2-dependent manner, and this RPE barrier breakdown is a requirement for the infiltration of choroidal neovessels into the sub-retinal space in neovascular AMD (Ablonczy and Crosson 2007; Ablonczy et al. 2011). We hypothesized that VEGF-A-induced RPE abnormalities may contribute not only to CNV through RPE barrier breakdown, but also promote photoreceptor degeneration through impaired interactions of the RPE with the photoreceptor outer segments, leading to nonexudative AMD-like pathologies. In order to test the consequences of increased VEGF-A in the eye, we have analyzed eyes in a mouse strain in which insertion of a lacZ sequence into the 3′UTR of the VEGF-A gene results in increased VEGF-A levels in the RPE, retina and serum (VEGF-A^{hyper} mice) (Miquerol et al. 1999; Marneros 2013).

12.2 Increased VEGF-A Is Sufficient to Cause Choroidal Neovascularization in a Novel Mouse Model of AMD

While increased VEGF-A has been implicated in neovascular AMD, it is not known whether an increase of VEGF-A alone is sufficient to cause CNV. We could indeed show that all VEGF-A^{hyper} mice developed CNV with complete penetrance, demonstrating that an increase in VEGF-A alone is not only associated with CNV, but moreover sufficient to induce CNV (Fig. 12.1a) (Marneros 2013; Ablonczy et al. 2014). Increased VEGF-A expression in the RPE resulted early on in a progressive age-dependent RPE barrier breakdown in VEGF-A^{hyper} mice (Fig. 12.1b), with cytoplasmic translocation of membrane-localized junctional proteins, such as ZO-1 and β-catenin (Marneros 2013). At sites of RPE barrier breakdown sub-retinal infiltration of activated macrophages was observed that was accompanied by a subsequent activation of adjacent retinal glia cells that highly express the proangiogenic factors IL-1β and VEGF-A (Marneros 2013). Multifocal CNV lesions formed subsequently at sites of RPE barrier breakdown and retinal glia cell activation. These findings suggest that infiltrating macrophages are essential for the activation of retinal glia cells and that these proangiogenic glia cells together with activated macrophages induce CNV. In support of this hypothesis, we could show that in laser-induced acute CNV, ablation of macrophages inhibited glia cell activation and subsequent CNV (Marneros 2013). Similarly as in the spontaneously forming CNV lesions in VEGF-A^{hyper} mice, activated glia cells in neovascular lesions induced by laser injury also expressed VEGF-A or IL-1β.

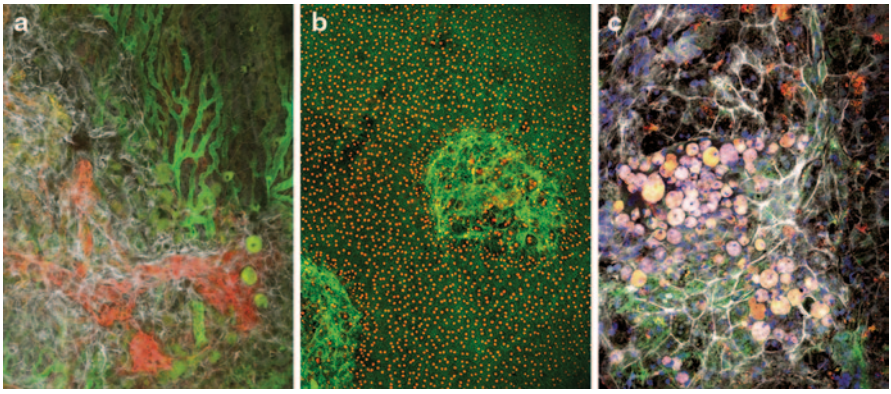

Fig. 12.1 AMD-like pathologies in VEGF-A^{hyper} mice. **a** Choroidal neovessels (*red,* CD31) originate from the underlying choroidal vasculature (*green,* FITC-tomato lectin) and displace the RPE (*white,* phalloidin) in mice with increased VEGF-A levels. **b** Phalloidin staining (*green*) shows areas of RPE barrier breakdown and CNV lesions in choroidal flatmounts of eyes from VEGF-A^{hyper} mice. Nuclear β-galactosidase staining shows expression of VEGF-A in RPE cells (*red*). **c** Lipid-like deposits (round autofluorescent structures, here in *yellow*) in the sub-RPE space in mice with increased VEGF-A levels. Phalloidin staining (*white*) shows RPE cells

Importantly, the observed neovascular lesions in VEGF-A^{hyper} mice strongly resemble human neovascular AMD with the formation of neovascular membranes (Marneros 2013). Thus, these mice allow us to investigate mechanisms that regulate not only the growth of CNV lesions, but also their spontaneous induction in an age-dependent manner without experimental injury (in contrast to the laser-injury model of CNV, which allows only to assess how factors influence growth of CNV lesions in response to acute injury and not their induction).

12.3 Targeting the NLRP3 Inflammasome Inhibits VEGF-A-induced Choroidal Neovascularization

Importantly, the NLRP3 inflammasome has recently been reported to be activated in human AMD (Tarallo et al. 2012; Tseng et al. 2013), but it is not known whether its activation contributes to AMD pathologies, and whether it acts to inhibit or promote AMD, as these questions could not be tested so far in a valid genetic mouse model of AMD where these pathologies form in an age-dependent manner.

Higher VEGF-A levels in VEGF-A^{hyper} mice were associated with increased oxidative damage to the RPE, accumulation of lipid-rich sub-RPE deposits, and subretinal accumulation of complement factors, including C1q (Marneros 2013). Both C1q and oxidative damage are known inducers of the NLRP3 inflammasome, and we could show that VEGF-A-induced AMD-like pathologies correlated with C1q accumulation and activation of the NLRP3 inflammasome in the RPE of VEGF-A^{hyper} mice, consistent with studies that suggest a pathogenic role of NLRP3 inflammasome activation in AMD (Doyle et al. 2012; Tarallo et al. 2012; Tseng et al. 2013). Importantly, genetic inactivation of NLRP3 or the inflammasome effector cytokine IL-1β in this AMD mouse model strongly reduces but does not prevent VEGF-A-induced CNV, demonstrating a direct role of the NLRP3 inflammasome in promoting CNV in these mice (Marneros 2013). These findings establish a novel link between increased VEGF-A and NLRP3 inflammasome activation for the formation of CNV.

12.4 Increased VEGF-A Results in RPE and Photoreceptor Degeneration and a Disruption of the Visual Cycle

Already prior to CNV formation RPE abnormalities are noticed that increase with progressive age and that result in RPE atrophy and sub-RPE deposits (Fig. 12.1c). These VEGF-A-induced RPE pathologies lead to progressive age-dependent focal RPE cell death and photoreceptor loss, resembling aspects of nonexudative human AMD (Marneros 2013).

We have performed a detailed analysis of RPE and retinal functions in VEGF-A^{hyper} mice and could show that these mice indeed manifest both morphological and functional abnormalities resembling important aspects of nonexudative AMD (Ablonczy et al. 2014). Similarly as in nonexudative AMD, we could show progressive dysfunction of the RPE and photoreceptors to occur due to a disruption of retinoid transport processes between the RPE and photoreceptors that worsened with progressive age (Ablonczy et al. 2014). The observed VEGF-A-induced RPE barrier breakdown in VEGF-A^{hyper} mice impaired the interdigitation between apical villi of the RPE with photoreceptor outer segments, which was associated with a disruption of the visual cycle and reduced 11-*cis* and all-*trans* retinal levels in retinas of these mice (Ablonczy et al. 2014). These retinoid transport abnormalities were associated with progressive RPE and photoreceptor degeneration and age-dependent accumulation of sub-RPE deposits (Ablonczy et al. 2014). These morphological changes correlated also with reduced retinal rhodopsin levels and abnormal ERGs (Ablonczy et al. 2014). Notably, morphological degenerative changes of the RPE already occurred prior to CNV formation and at sites in the posterior eye that had no CNV lesions, as observed in human AMD (Marneros 2013). These data provide support for the hypothesis that VEGF-A^{hyper} mice serve as a valuable tool to study mechanisms that result in the manifestation of both nonexudative and neovascular AMD-like pathologies.

12.5 Summary

VEGF-A^{hyper} mice serve as an important novel genetic mouse model for AMD, and show that what has been considered as a multifactorial pathogenesis in humans can be triggered by increased VEGF-A-signaling in mice. The observations in these mice suggest that in human AMD multiple risk factors converge to cause mainly RPE hypoxia and oxidative damage, which are main inducers of VEGF-A expression in the RPE. These findings are consistent with recent genetic association data that have provided evidence for linkage of both forms of advanced AMD with the VEGF-A gene locus (Fritsche et al. 2013;Yu et al. 2011). While increased VEGF-A has been associated with CNV and RPE barrier breakdown, these mice reveal a previously not fully appreciated role of increased VEGF-A in impairing RPE and photoreceptor function during aging. However, it is important to emphasize that these findings do not necessarily imply that both forms of AMD are caused in humans by increased VEGF-A, but they suggest that these mice serve as a valuable experimental tool to elucidate mechanisms that result in the manifestation of AMD-like pathologies and that may also play a role in human AMD.

Notably, anti-VEGF-A therapies are currently the main therapeutic approach for neovascular AMD. Recent observations suggest that chronic anti-VEGF-A therapies may promote RPE and photoreceptor degeneration as adverse effects of this treatment approach (Rofagha et al. 2013). These findings are not necessarily surprising, as anti-VEGF-A therapies are likely to deplete even baseline extracellular

VEGF-A levels, which are required for choriocapillaris maintenance, and an intact choriocapillaris in turn is essential to maintain proper RPE function (Marneros et al. 2005; Saint-Geniez et al. 2009). In addition, VEGF-A has been suggested to function as a photoreceptor survival factor, and its complete depletion may impair long-term photoreceptor function (Saint-Geniez et al. 2008). However, the potential adverse effects of chronic anti-VEGF-A therapies on RPE and photoreceptor function do not contradict the observation of RPE and photoreceptor abnormalities in mice with increased VEGF-A levels (VEGF-A^{hyper} mice). In these VEGF-A^{hyper} mice age-dependent RPE and photoreceptor abnormalities are most likely a direct consequence of increased VEGF-A-mediated signaling in the RPE, which results in RPE barrier breakdown, subsequent CNV and photoreceptor degeneration due to disruption of the visual cycle. Thus, we hypothesize that inhibition of increased VEGF-A-signaling specifically in the RPE is likely going to prevent AMD pathologies without impairing choriocapillaris function, in contrast to depleting all extracellular VEGF-A at the RPE/choroid interface through neutralizing anti-VEGF-A antibodies. We speculate that reducing factors that promote increased VEGF-A expression specifically in the RPE, such as hypoxia or oxidative damage, may thus prevent pathologic RPE barrier breakdown and subsequent AMD-like pathologies without adverse effects on the choriocapillaris or photoreceptors, which are being observed with anti-VEGF-A therapies targeting extracellular VEGF-A. This hypothesis is also consistent with observations that show a beneficial effect of diets rich in antioxidants in slowing progression of AMD (Chew et al. 2013).

References

Ablonczy Z, Crosson CE (2007) VEGF modulation of retinal pigment epithelium resistance. Exp Eye Res 85:762–771

Ablonczy Z, Dahrouj M, Tang PH et al (2011) Human retinal pigment epithelium cells as functional models for the RPE in vivo. Invest Ophthalmol Vis Sci 52:8614–8620

Ablonczy Z, Dahrouj M, Marneros AG (2014) Progressive dysfunction of the retinal pigment epithelium and retina due to increased VEGF-A levels. FASEB J 28:2369–2379

Chew EY, Clemons TE, Agron E et al (2013) Long-term effects of vitamins C and E, beta-carotene, and zinc on age-related macular degeneration: AREDS Report No. 35. Ophthalmology 120:1604–1611

Doyle SL, Campbell M, Ozaki E et al (2012) NLRP3 has a protective role in age-related macular degeneration through the induction of IL-18 by drusen components. Nat Med 18:791–798

Friedman DS, O'Colmain BJ, Munoz B et al (2004) Prevalence of age-related macular degeneration in the United States. Arch Ophthalmol 122:564–572

Fritsche LG, Chen W, Schu M et al (2013) Seven new loci associated with age-related macular degeneration. Nat Genet 45:433–439

Klettner A, Roider J (2009) Constitutive and oxidative-stress-induced expression of VEGF in the RPE are differently regulated by different Mitogen-activated protein kinases. Graefes Arch Clin Exp Ophthalmol 247:1487–1492

Marneros AG (2013) NLRP3 inflammasome blockade inhibits VEGF-A-induced age-related macular degeneration. Cell Rep 4:945–958

Marneros AG, Fan J, Yokoyama Y et al (2005) Vascular endothelial growth factor expression in the retinal pigment epithelium is essential for choriocapillaris development and visual function. Am J Pathol 167:1451–1459

Miquerol L, Gertsenstein M, Harpal K et al (1999) Multiple developmental roles of VEGF suggested by a LacZ-tagged allele. Dev Biol 212:307–322

Rofagha S, Bhisitkul RB, Boyer DS et al (2013) Seven-year outcomes in Ranibizumab-treated patients in ANCHOR, MARINA, and HORIZON: a multicenter cohort study (SEVEN-UP). Ophthalmology 120:2292–2299

Saint-Geniez M, Maharaj AS, Walshe TE et al (2008) Endogenous VEGF is required for visual function: evidence for a survival role on muller cells and photoreceptors. PLoS ONE 3:e3554

Saint-Geniez M, Kurihara T, Sekiyama E et al (2009) An essential role for RPE-derived soluble VEGF in the maintenance of the choriocapillaris. Proc Natl Acad Sci U S A 106:18751–18756

Sunness JS, Gonzalez-Baron J, Bressler NM et al (1999) The development of choroidal neovascularization in eyes with the geographic atrophy form of age-related macular degeneration. Ophthalmology 106:910–919

Tarallo V, Hirano Y, Gelfand BD et al (2012) DICER1 loss and Alu RNA induce age-related macular degeneration via the NLRP3 inflammasome and MyD88. Cell 149:847–859

Tseng WA, Thein T, Kinnunen K et al (2013) NLRP3 inflammasome activation in retinal pigment epithelial cells by lysosomal destabilization: implications for age-related macular degeneration. Investig Ophthalmol Vis Res 54:110–120

van Leeuwen R, Klaver CC, Vingerling JR et al (2003) Epidemiology of age-related maculopathy: a review. Eur J Epidemiol 18:845–854

Yu Y, Bhangale TR, Fagerness J et al (2011) Common variants near FRK/COL10A1 and VEGFA are associated with advanced age-related macular degeneration. Hum Mol Genet 20: 3699–3709

Chapter 13
Interrelation Between Oxidative Stress and Complement Activation in Models of Age-Related Macular Degeneration

Luciana M. Pujol-Lereis, Nicole Schäfer, Laura B. Kuhn, Bärbel Rohrer and Diana Pauly

Abstract Millions of individuals older than 50-years suffer from age-related macular degeneration (AMD). Associated with this multifactorial disease are polymorphisms of complement factor genes and a main environmental risk factor—oxidative stress. Until now the linkage between these risk factors for AMD has not been fully understood. Recent studies, integrating results on oxidative stress, complement activation, epidemiology and ocular pathology suggested the following sequence in AMD-etiology: initially, chronic oxidative stress results in modification of proteins and lipids in the posterior of the eye; these tissue alterations trigger chronic inflammation, involving the complement system; and finally, invasive immune cells facilitate pathology in the retina. Here, we summarize the results for animal studies which aim to elucidate this molecular interplay of oxidative events and tissue-specific complement activation in the eye.

Luciana M. Pujol-Lereis and Nicole Schäfer both have contributed equally to the study.

D. Pauly (✉) · N. Schäfer
Department of Ophthalmology, University Hospital Regensburg,
Franz-Josef-Strauss-Allee 11, 93053 Regensburg, Germany
e-mail: Diana.Pauly@klinik.uni-regensburg.de

N. Schäfer
e-mail: Nicole.schafer@klinik.uni-regensburg.de

B. Rohrer
Department of Ophthalmology, Ralph H. Johnson VA Medical Center, Medical University of South Carolina and Research Service, Charleston, SC 29401, USA
e-mail: rohrer@musc.edu

L. M. Pujol-Lereis · L. B. Kuhn
Institute of Human Genetics, University of Regensburg,
Franz-Josef-Strauss-Allee 11, 93053 Regensburg, Germany
e-mail: Luciana.pujol@klinik.uni-regensburg.de

L. B. Kuhn
e-mail: laura.kuhn@stud.uni-regensburg.de

C. Bowes Rickman et al. (eds.), *Retinal Degenerative Diseases,* Advances in Experimental Medicine and Biology 854, DOI 10.1007/978-3-319-17121-0_13

Keywords Oxidative stress · Complement system · Age-related macular degeneration · Oxidation-specific epitopes · Alternative pathway · Cigarette smoke model · Light-damage model · CEP-immunization model · Sodium iodate-treatment model · Knock-out mice models

13.1 Introduction

13.1.1 Complement System in the Eye

The complement system (CS) is a part of the immune system, which provides a host defense against foreign organisms and modified self-tissue. The local CS in the healthy eye is continuously activated at a low level, but it is kept under control by intraocular CS regulatory proteins (Sohn et al. 2000). The soluble CS proteins are mainly produced in the liver, and some of them also in the choroid and retinal pigment epithelium (RPE) (Anderson et al. 2010; Bora et al. 1993). Additionally, it is well described that stressed and injured cells locally secrete CS proteins (Pratt et al. 2002). The neuroretina and the apical border of the RPE are shielded from the systemic CS by the blood retina barrier; however, under pathological conditions that lead to the disruption of the barrier, systemically-derived CS components might contribute to pathology. Components of all three different CS activation pathways [classical (CP), lectin (LP) and alternative (AP)] have been found in the eye (Sohn et al. 2000). These pathways are typically initiated by immune complexes (CP), pathogen or non-self surfaces (LP) or spontaneous hydrolysis (AP) and result in the formation of a membrane-bound C3-convertase which cleaves C3 into its active forms C3b and C3a. C3b interacts with other CS proteins and forms the C5-convertase which is required for initiation of the terminal part of the cascade that forms the membrane attack complex (MAC). At sublytic concentrations, the MAC can either lyse the target cell or change cellular behavior. Additionally, anaphylatoxins (C3a, C5a) act as pro-inflammatory stimuli, and opsonins (iC3b, C3d, C3dg) flag altered membranes. Hence, through the production of multiple biological effector molecules, the CS can have a wide-ranging effect.

13.1.2 Oxidative Stress in the Human Retina

Oxidative stress occurs as a consequence of an imbalance between the detoxification and production of reactive oxygen species. Photoreceptor outer segments (POS) are very sensitive to oxidative stress as they contain high concentrations of polyunsaturated fatty acids (PUFA) in their membrane phospholipids (Ebrahem et al. 2006). In RPE cells, lipofuscin granules accumulate as a consequence of the ingestion of POS, and are rich in the fluorescent pigment (A2E), which generates reactive oxygen species and expands the oxidative damage (Schütt et al. 2000). Malondialdehyde (MDA) and 4-hydroxynonenal (HNE) -modified proteins, as well as advanced glycosylation end-products (AGE) were found in lipofuscin granules located in the

RPE of human eyes (Schutt et al. 2003). Oxidized PUFA, ω-(2-carboxyethyl)pyrrole (CEP) adducts, 4-hydroxyhexenal (HHE), MDA and AGE also increase with age in human Bruch's membrane as a consequence of oxidative damage (Beattie et al. 2010; Weismann et al. 2011).

Studies indicate that even mild forms of lipid peroxidation can cause changes in gene expression and alter tissue homeostasis (Weismann et al. 2011; Wang et al. 2009; Woodell et al. 2013). The immune system, including components of the CS pathway, senses and reacts to oxidative modifications, which can trigger an immune response in the affected tissues.

13.2 Interplay of the CS and Oxidative Stress in AMD Animal Models

13.2.1 Cigarette Smoke

Cigarette smoke is the only proven, modifiable risk factor for AMD (Khan et al. 2006). It contributes to oxidative load by generating free radicals and depleting the antioxidant defense system. Interestingly, it has been reported that cigarette smoke can directly activate C3 (Kew et al. 1985). Constant smoke exposure has been shown to lead to oxidative damage and CS deposition at the level of the RPE in mice (Wang et al. 2009). This resulted in dry AMD-like pathology, including thickening of Bruch's membrane and mitochondrial damage in mice, and ocular pathology was found to require AP activation since mice lacking complement factor B did not develop these alterations (Woodell et al. 2013). It will be of great interest to determine the link between different oxidant factors and CS activation in this and other models.

13.2.2 Light-Damage

Constant white light can generate free radicals and increase expression of oxidative-stress-related enzymes, as well as HNE-modifications of proteins in the retina of mice (Hadziahmetovic et al. 2012a; Rutar et al. 2012). In parallel, an up-regulated expression of complement factors C1q, C3 and others was observed in the eye without the corresponding increase in CS inhibitors such as CD59 or complement factor H (CFH) (Rohrer et al. 2007; Rutar et al. 2011; Hadziahmetovic et al. 2012a; Song et al. 2012). In addition, infiltrating microglia cells expressing C3 enhance the local inflammation (Rutar et al. 2012). The AP is required in this oxidative stress model because constant-light-exposed complement factor D-deficient mice showed more healthy photoreceptors compared to wild-type or C1q-deficient mice (Rohrer et al. 2007). Finally, long-wavelength light can reduce oxidative damage as mitochondrial respiration is improved. Lipid-peroxidation as well as the expression of CP-related genes are lower in 670 nm pretreated animals (Rutar et al. 2012).

13.2.3 CEP-Immunization

Antibodies are generated randomly or in response to foreign substances. Recent studies have suggested that antibodies against self-antigens might play a role in AMD pathogenesis (Joseph et al. 2013). To test whether oxidation-specific epitopes might trigger an inflammatory response involving the CS, Hollyfield and colleagues immunized mice with CEP-modified mouse serum albumin (Hollyfield et al. 2008). CEP-immunized mice had elevated circulating anti-CEP antibody levels, accumulated C3d in Bruch's membrane, and CS protein expressing macrophages infiltrated into the interphotoreceptor matrix (Cruz-Guilloty et al. 2013). These results suggested that the CS may be fundamentally involved in the generation of pathologic changes related to oxidation-specific neoepitopes.

13.2.4 Sodium Iodate-Treatment

Sodium iodate is a retinotoxin, which generates reactive oxygen species and selectively damages RPE as well as photoreceptors. Sodium iodate-treatment induces a fast retinal degeneration with an increased expression of the oxidative stress-related gene heme oxygenase-1 and CS component C3 in mice. While this effect can be ameliorated by the cell-permeant iron chelator deferiprone (Hadziahmetovic et al. 2012b), the involvement of the complement system has not yet been tested on protein level.

13.2.5 Knock-Out Mice

13.2.5.1 $Cfh^{-/-}$

CFH is the major negative CS regulator of the AP. The absence of CFH leads to uncontrolled activation of the AP, severe systemic depletion of C3 and AMD-like changes (Pickering et al. 2002; Coffey et al. 2007). Nevertheless, increased C3 and C3b deposition was demonstrated within the neuroretina (Coffey et al. 2007). Additional changes included increased expression of CS inhibitory factor, decay-accelerating factor (DAF) in Müller cells and a concomitant decrease in retinal CD59a (Faber et al. 2012; Williams et al. 2013). The relation between oxidative stress and CS proteins in *Cfh*$^{-/-}$ mice could be demonstrated by treating aged *Cfh*$^{-/-}$ mice with 670 nm light, which increased mitochondrial function and reduced inflammation in the retina (Begum et al. 2013).

13.2.5.2 Abca4$^{-/-}$

The ATP-binding cassette sub-family A, member 4 (ABCA4), functions as a flippase in photoreceptor disk membranes. Radu et al. (2011) showed a correlation between deposited A2E-lipofuscin in *Abca4*$^{-/-}$ mice, oxidative stress, and CS activation. Anti-oxidative stress proteins (SOD1 and CAT1) and oxidative stress markers (MDA and HNE) were increased in the RPE of aged *Abca4*$^{-/-}$ mice compared to controls. Furthermore, deposition of C3 and its degradation products were elevated in RPE cells of aged *Abca4*$^{-/-}$ mice. CS inhibitory proteins DAF, CD55, CD59, CD46, CRRY and CFH were all down-regulated in these mice when compared to the age-matched wild-type mice (Radu et al. 2011).

13.2.5.3 Ceruloplasmin/Hephaestin$^{-/-}$

Iron is a potent generator of oxidative stress. It is exported from cells by transmembrane ferroxidases such as ceruloplasmin and its homologue hephaestin. Mice deficient in these two enzymes showed age-dependent retinal iron accumulation associated with oxidative stress and pathological characteristics of AMD. In mice older than 9 months, activation products of C3 could be detected at the sub-RPE level and at Bruch's membrane (Hadziahmetovic et al. 2008).

13.2.5.4 Sod$^{-/-}$

The superoxide dismutase (SOD) family is the main antioxidant system in the retina. Depending on which of the three isoforms is deleted, this generates a model for oxidative stress either in the cytosol (SOD1), the mitochondria (SOD2), or the extracellular space (SOD3). The activity and amount of SOD1 is the highest among the three forms in the retina. The systemic *Sod1*$^{-/-}$ knockout mice exhibited oxidative damage and features of AMD, with elevated staining in RPE for drusen-markers C5, CD46 and vitronectin (Imamura et al. 2006). In humans, *Sod2* gene polymorphisms have been found to be associated with AMD. Mice carrying an RPE-specific *Sod2* knockdown exhibit features of dry AMD including oxidative stress in the RPE and C5 and CD46 deposits in the retina (Seo et al. 2012; Mao et al. 2014). There are no results describing the effect of *Sod3*-deficiency on RPE; but a conditional knockdown in smooth muscle cells suggests that it plays an important role in vascular remodeling and inflammation (Birari et al. 2012).

13.2.5.5 Nrf2$^{-/-}$

Nuclear factor erythroid 2-related factor 2 (Nrf2) is a transcription factor which is important for antioxidant responses. *Nrf2*$^{-/-}$ mice showed an AMD-like pathology. Relevant to this review, immunostaining showed an age-dependent increase in C3d

and vitronectin deposition in the subretinal space. The authors suggest that impaired lysosomal function and autophagic activity may release extracellular waste which is recognized by the immune system (Zhao et al. 2011).

13.3 Conclusion

The main conclusions that can be drawn from this mini-review are as follows: (1) oxidative stress, whether induced by chemical exposure, poor diet or genetic alteration results in the generation of neoepitopes; (2) oxidative stress alters gene and protein expression of CS components, which may contribute to the observed increase in CS activation in these stressed tissues; (3) these changes in RPE may result in impairment of photoreceptor cell integrity and functionality, which leads to AMD.

References

Anderson DH, Radeke MJ, Gallo NB et al (2010) The pivotal role of the complement system in aging and age-related macular degeneration: hypothesis re-visited. Prog Retin Eye Res 29:95–112

Beattie JR, Pawlak AM, Boulton ME et al (2010) Multiplex analysis of age-related protein and lipid modifications in human Bruch's membrane. FASEB J 24:4816–4824

Begum R, Powner MB, Hudson N et al (2013) Treatment with 670 nm light up regulates cytochrome C oxidase expression and reduces inflammation in an age-related macular degeneration model. PLoS One 8:e57828

Birari R, Villegas L, Locke J et al (2012) Conditional knock down of SOD3 in smooth muscle cells augments chronic hypoxic pulmonary vascular remodeling and inflammation. Am J Respir Crit Care Med 185.1_MeetingAbstracts.A4742

Bora NS, Gobleman CL, Atkinson JP et al (1993) Differential expression of the complement regulatory proteins in the human eye. Invest Ophthalmol Vis Sci 34:3579–3584

Coffey PJ, Gias C, McDermott CJ et al (2007) Complement factor H deficiency in aged mice causes retinal abnormalities and visual dysfunction. Proc Natl Acad Sci USA 104:16651–16656

Cruz-Guilloty F, Saeed A, Echegaray J et al (2013) Infiltration of proinflammatory m1 macrophages into the outer retina precedes damage in a mouse model of age-related macular degeneration. Int J Inflam 2013:503725

Ebrahem Q, Renganathan K, Sears J et al (2006) Carboxyethylpyrrole oxidative protein modifications stimulate neovascularization: implications for age-related macular degeneration. Proc Natl Acad Sci U S A 103:13480–13484

Faber C, Williams J, Juel HB et al (2012) Complement factor H deficiency results in decreased neuroretinal expression of Cd59a in aged mice. Invest Ophthalmol Vis Sci 53:6324–6330

Hadziahmetovic M, Dentchev T, Song Y et al (2008) Ceruloplasmin/hephaestin knockout mice model morphologic and molecular features of AMD. Invest Ophthalmol Vis Sci 49:2728–2736

Hadziahmetovic M, Kumar U, Song Y et al (2012a) Microarray analysis of murine retinal light damage reveals changes in iron regulatory, complement, and antioxidant genes in the neurosensory retina and isolated RPE. Invest Ophthalmol Vis Sci 53:5231–5241

Hadziahmetovic M, Pajic M, Grieco S et al (2012b) The oral iron chelator deferiprone protects against retinal degeneration induced through diverse mechanisms. Transl Vis Sci Technol 1:2

Hollyfield JG, Bonilha VL, Rayborn ME et al (2008) Oxidative damage-induced inflammation initiates age-related macular degeneration. Nat Med 14:194–198

Imamura Y, Noda S, Hashizume K et al (2006) Drusen, choroidal neovascularization, and retinal pigment epithelium dysfunction in SOD1-deficient mice: a model of age-related macular degeneration. Proc Natl Acad Sci U S A 103:11282–11287

Joseph K, Kulik L, Coughlin B et al (2013) Oxidative stress sensitizes retinal pigmented epithelial (RPE) cells to complement-mediated injury in a natural antibody-, lectin pathway-, and phospholipid epitope-dependent manner. J Biol Chem 288:12753–12765

Kew RR, Ghebrehiwet B, Janoff A (1985) Cigarette smoke can activate the alternative pathway of complement in vitro by modifying the third component of complement. J Clin Invest 75:1000–1007

Khan JC, Thurlby DA, Shahid H et al (2006) Smoking and age related macular degeneration: the number of pack years of cigarette smoking is a major determinant of risk for both geographic atrophy and choroidal neovascularisation. Br J Ophthalmol 90:75–80

Mao H, Seo SJ, Biswal MR et al (2014) Mitochondrial oxidative stress in the retinal pigment epithelium leads to localized retinal degeneration. Invest Ophthalmol Vis Sci 55:4613–4627

Pickering MC, Cook HT, Warren J et al (2002) Uncontrolled C3 activation causes membranoproliferative glomerulonephritis in mice deficient in complement factor H. Nat Genet 31:424–428

Pratt JR, Basheer SA, Sacks SH (2002) Local synthesis of complement component C3 regulates acute renal transplant rejection. Nat Med 8:582–587

Radu RA, Hu J, Yuan Q et al (2011) Complement system dysregulation and inflammation in the retinal pigment epithelium of a mouse model for Stargardt macular degeneration. J Biol Chem 286:18593–18601

Rohrer B, Guo Y, Kunchithapautham K et al (2007) Eliminating complement factor D reduces photoreceptor susceptibility to light-induced damage. Invest Ophthalmol Vis Sci 48:5282–5289

Rutar M, Natoli R, Kozulin P et al (2011) Analysis of complement expression in light-induced retinal degeneration: synthesis and deposition of C3 by microglia/macrophages is associated with focal photoreceptor degeneration. Invest Ophthalmol Vis Sci 52:5347–5358

Rutar M, Natoli R, Albarracin R et al (2012) 670-nm light treatment reduces complement propagation following retinal degeneration. J Neuroinflammation 9:257

Schütt F, Davies S, Kopitz J et al (2000) Photodamage to human RPE cells by A2-E, a retinoid component of lipofuscin. Invest Ophthalmol Vis Sci 41:2303–2308

Schutt F, Bergmann M, Holz FG et al (2003) Proteins modified by malondialdehyde, 4-hydroxynonenal, or advanced glycation end products in lipofuscin of human retinal pigment epithelium. Invest Ophthalmol Vis Sci 44:3663–3668

Seo S, Krebs MP, Mao H et al (2012) Pathological consequences of long-term mitochondrial oxidative stress in the mouse retinal pigment epithelium. Exp Eye Res 101:60–71

Sohn JH, Kaplan HJ, Suk HJ et al (2000) Chronic low level complement activation within the eye is controlled by intraocular complement regulatory proteins. Invest Ophthalmol Vis Sci 41:3492–3502

Song D, Song Y, Hadziahmetovic M et al (2012) Systemic administration of the iron chelator deferiprone protects against light-induced photoreceptor degeneration in the mouse retina. Free Radic Biol Med 53:64–71

Wang AL, Lukas TJ, Yuan M et al (2009) Changes in retinal pigment epithelium related to cigarette smoke: possible relevance to smoking as a risk factor for age-related macular degeneration. PLoS One 4:e5304

Weismann D, Hartvigsen K, Lauer N et al (2011) Complement factor H binds malondialdehyde epitopes and protects from oxidative stress. Nature 478:76–81

Williams JAE, Greenwood J, Moss SE (2013) Retinal changes precede visual dysfunction in the complement factor H knockout mouse. PLoS One 8:e68616

Woodell A, Coughlin B, Kunchithapautham K et al (2013) Alternative complement pathway deficiency ameliorates chronic smoke-induced functional and morphological ocular injury. PLoS One 8:e67894

Zhao Z, Chen Y, Wang J et al (2011) Age-related retinopathy in NRF2-deficient mice. PLoS One 6:e19456

Chapter 14
Gene-Diet Interactions in Age-Related Macular Degeneration

Sheldon Rowan and Allen Taylor

Abstract Age-related macular degeneration (AMD) is a prevalent blinding disease, accounting for roughly 50% of blindness in developed nations. Very significant advances have been made in terms of discovering genetic susceptibilities to AMD as well as dietary risk factors. To date, nutritional supplementation is the only available treatment option for the dry form of the disease known to slow progression of AMD. Despite an excellent understanding of genes and nutrition in AMD, there is remarkably little known about gene-diet interactions that may identify efficacious approaches to treat individuals. This review will summarize our current understanding of gene-diet interactions in AMD with a focus on animal models and human epidemiological studies.

Keywords Age-related macular degeneration · Gene-diet interaction · Knockout mice · Nutrition · Genetic susceptibility · CFH · ARMS2 · Glycemic index · High fat diet · Retinal pigmented epithelium

14.1 Introduction: Genetic and Dietary Factors in AMD

AMD was first human disease wherein gene-wide association studies were able to identify gene variants that account for a significant risk of disease. The two most common associations are for the Y402H variant of Complement factor H (*CFH, rs1061170)*) and the Age-related maculopathy susceptibility 2 (*ARMS2,*

S. Rowan (✉) · A. Taylor
USDA-JM Human Nutrition Research Center on Aging (HNRCA), Tufts University, Boston, MA 02111, USA
e-mail: Sheldon.rowan@tufts.edu

Department of Ophthalmology, Tufts University School of Medicine, Boston, MA 02111, USA

A. Taylor
Friedman School of Nutrition Science and Policy, Tufts University, Boston, MA 02111, USA
e-mail: Allen.taylor@tufts.edu

C. Bowes Rickman et al. (eds.), *Retinal Degenerative Diseases,* Advances in Experimental Medicine and Biology 854, DOI 10.1007/978-3-319-17121-0_14

rs10490924) gene. The population-attributable risk for late AMD is 53 or 43 % for *CFH* and *ARMS2* risk alleles respectively, with a lesser increased risk for developing early AMD (Klein et al. 2013). When accounting for a larger number of genes, and within an elderly population, individuals in the highest decile of AMD risk based on genotype have an almost 80 % chance of developing AMD compared to a less than 5 % chance for individuals in the lowest decile of risk (Chen et al. 2010). There was also some association between the forms of the disease related to genetic risk factors. *CFH* risk variants were more common in individuals who developed geographic atrophy relative to those with large drusen or neovascularization (Chen et al. 2010), whereas *ARMS2* risk alleles were more closely associated with neovascularization (Chen et al. 2010; Sobrin et al. 2011). These kinds of associations point to different mechanism by which genetic risk can influence disease pathophysiology.

Diet also impacts significantly on the incidence and treatment of AMD. It has long been known that individuals consuming the lowest amount of several nutrients are at increased risk for AMD relative to individuals consuming the highest amounts. This relationship holds true to ω-3 fatty acids, particularly DHA, lutein and zeaxanthin carotenoids, and to various extents for zinc intake (Weikel et al. 2012a). It should be noted that different populations, different classifications systems, and different study designs dramatically impinge on these findings. Dietary patterns also impact on risk of AMD. Individuals consuming higher glycemic index (GI) diets, that is diets that deliver glucose to the blood more rapidly, are at increased risk for AMD (Weikel et al. 2012a). Conversely, individuals consuming lower GI diets are protected from developing AMD, particularly early forms of the disease. Other dietary patterns, like a Western dietary pattern, which typically contains more red meats, high-fat dairy products, processed meats and refined grains, are associated with dramatically elevated risk for AMD relative to diets that provide more fruits, vegetables, legumes, seafood, and whole grains (Chiu et al. 2014).

14.2 Human Studies

14.2.1 Human Studies of Gene-Diet Interactions

Studies using pharmacogenetics and nutrigenetics provide improved capacity to predict individual responses to pharmacological or nutritional interventions. AMD management should benefit from such approaches because the genetic contributions are well defined (discussed above), and there are few drugs or nutritional interventions available. Because it has been shown to delay progression of AMD to advanced stages, the AREDS2 formulation of vitamin C, vitamin E, zinc, copper, ω-3 fatty acids, lutein, and zeaxanthin is now the standard of care (AREDS2 Research Group 2013). For the wet form of AMD, a variety of VEGF inhibitors are be-

ing used, and strong clinical evidence is present for additional benefit of combined VEGF/PDGF inhibition (Ratner 2014).

The first examination of gene-diet interactions in AMD centered on whether there were genotype-specific benefits for antioxidant and/or zinc supplementation on AMD progression, evaluating the two common *CFH* (Y402H, rs1061170) and *ARMS2* (A69S, rs10490924) variants. Klein et al. found a protective gene-diet interaction between the low risk *CFH* allele and supplementation with antioxidants and zinc within the AREDS study, with subgroup analysis revealing the interaction to be via the zinc component (Klein et al. 2008). No statistically significant interactions were observed for individuals with the high risk *CFH* alleles or any *ARMS2* alleles in this study. Analyzing the Blue Mountains Eye Study population, Wang et al., found a protective gene-diet interaction between the high-risk *CFH* Y402H allele and frequent fish consumption (Wang et al. 2009). This interaction only existed for late AMD and not early AMD and was not highly significant ($p = 0.04$). Nevertheless, the results of these studies suggested that individuals with early AMD may want to consider their *CFH* Y402H status when considering treatment and dietary options.

The Klein study was independently followed-up with consideration of all the *CFH* and *ARMS2* allele combination within the same study population. Awh et al. corroborated the protective interaction between zinc supplementation for individuals without the *CFH* risk allele, and suggested a negative interaction between zinc supplementation for individuals with *CFH* risk alleles (Awh et al. 2013). They further suggested different AREDS-based treatment options for individuals with different genotypes of *CFH* and *ARMS2*. In contrast, Chew et al., also evaluating *CFH* and *ARMS2* allele combinations in AREDS patients, found no significant gene-diet interactions for AMD progression (Chew et al. 2014). Although different statistical methods and subgroup analyses were used for these studies, the lack of concordance is troubling, and suggests that at the current sample size of AREDS, a consensus conclusion may not be reachable.

Two different studies evaluated food frequency questionnaire (FFQ) data in the context of genetic factors. Ho et al. analyzed the population based Rotterdam Study to evaluate the role for several nutrients in AMD development and found that individuals with risk alleles of *CFH* and *ARMS* had protective interactions with zinc or EPA + DHA (Ho et al. 2011). Individuals with *CFH* risk alleles benefitted from dietary carotenoids, but no interactions were observe for vitamins A, C, or E in any genotypes. Reynolds et al., evaluating AREDS FFQ data, reported that DHA alone showed a strong protective gene-diet interaction with the high risk allele of *ARMS2* and a weaker gene-diet interaction with the low risk allele of *CFH* for AMD progression to geographic atrophy (Reynolds et al. 2013).

14.2.2 Conclusions from Human Data

The number of studies that have methodically evaluated gene-diet interactions in AMD is small, and the conclusions have not been consistent. Discrepancies occur because of different populations, different outcomes, different study designs, and different statistical methodologies. The strongest statistical interaction has been found between *ARMS2* high risk alleles and consumption of DHA or DHA+EPA, which appears to protect against early forms of AMD, as well as progression to geographic atrophy. *CFH* non-risk alleles also tend to show protective interactions for late AMD with zinc and DHA.

Current medical practice is not to routinely genotype individuals, as the standard of care, AREDS2, appears to be effective across the major genotypes. However, other groups disagree with this conclusion, and are offering patients customized AREDS-based treatments based on their genotype (Awh et al. 2013). As new treatments are being developed to treat various forms of AMD, it will be prudent to consider gene-diet interactions in order to obtain the best possible treatment for each patient.

14.3 Mouse AMD Models

14.3.1 Mouse AMD Models to Explore Gene-Diet Interactions

The mouse has proven to be a difficult model organism to model human AMD. For a variety of reasons, including a very different lifespan and mode of aging, a different eye structure that lacks a macula, and different dietary needs, no single mouse model has recapitulated all of the key features of human AMD (Pennesi et al. 2012). Nevertheless, the mouse is a powerful experimental system for diet and aging studies, particularly with regard to early signs of disease within the RPE. Since most animal models involve genetic and dietary manipulations, the mouse should be a rich system to uncover gene-diet interactions.

14.3.2 Gene-Diet Interactions with Dietary Glycemic Index

Based on the human genetic association data, we and others have evaluated the *Cfh*-null mouse as a potential mouse model for AMD. Normally aged *Cfh*-null mice do not appear to develop AMD-like features when fed a regular diet, and we sought to explore whether there might be a specific gene-diet interaction between *Cfh*-null mice and dietary GI. Previously, we showed that wildtype mice aged on high GI diets showed increased numbers of age-related AMD-like features, including basal

laminar deposits and loss of basal infoldings (Weikel et al. 2012b). When mice were aged to 10-months on high and low GI diets, we did not find any changes in wildtype mice on either diet. *Cfh*-null mice, however, showed AMD-like features when fed a low GI diet, but not a high GI diet (Rowan et al. 2014). These features included loss of basal infoldings, increased numbers of basal laminar deposits, increased vacuolation, and increased numbers of lipofuscin granules. It remains unclear why the gene-diet interaction was observed with the low GI diet, and not the high GI index diet, as we predicted.

14.3.3 Gene-Diet Interactions with Lipids

One particular diet that appears to promote AMD-like features in mice is a high fat and high cholesterol (HFC) diet. Mice with human *ApoE* alleles knocked-in developed AMD-like features, only when fed HFC diets (Malek et al. 2005). The phenotypes were particularly marked in *ApoE4* knock-in mice, some of which went on to develop choroidal neovascularization. These phenotypes were much more severe than any aging study in wildtype mice using HFC diets, and were also more severe than studies where mice transgenically expressing a mutant *ApoE3* allele developed only minor AMD-like features on a high fat diet (Kliffen et al. 2000).

Long-term consumption of high fat diets has been linked to accumulation of basal laminar deposits and lipid deposits in the RPE and Bruch's membrane. The mouse, however, is not an ideal organism to model lipid transport and accumulation, in part because mice express a predominantly truncated form of *ApoB, ApoB-48,* which is easily cleared by non-LDL-dependent mechanisms. Young mice expressing the human version of *ApoB-100* showed accelerated RPE accumulation of basal laminar deposits, when coupled with blue light exposure and a high fat diet (Espinosa-Heidmann et al. 2004). Aged *ApoB-100* transgenic mice fed a high fat diet went on to develop more severe AMD-like phenotypes, including basal linear deposits within Bruch's membrane, a specific gene-diet interaction (Fujihara et al. 2009). *ApoB-100* transgenic mice also interact with a high cholesterol diet, where they show a thickened Bruch's membrane, accumulation of electroluscent material within the Bruch's membrane, and some deposits between the RPE and Bruch's membrane (Sallo et al. 2009).

It is worth noting that whereas gene-diet interactions in human studies of AMD primarily uncover protective interactions, in mouse studies, they are more likely to uncover synthetic interactions that reveal phenotypes not observed by gene or diet change alone. One mouse model that uncovered a protective effect is the gene-diet interaction between dietary ω-3 fatty acids, AMD, and increased inflammation. The *Ccl2/Cx3cr1* double knockout mouse develops retinal lesions that resemble those found in human AMD, as well as some associated RPE and changes (Tuo et al. 2009). Such mice fed diets with high levels of EPA, DHA, along with docosapentaenoic acid developed fewer retinal lesions, and had less dystrophic RPE, relative to mice fed diets with low levels of ω-3 fatty acids (Tuo et al. 2009).

These changes correlated with reduced levels of lipofuscin and inflammatory cytokines in mice fed a high ω-3 fatty acid diet. This work was followed by comparing double knockout mice treated with the AREDS2 formulation compared to control diet alone, once retinal lesions had developed. AREDS2 supplementation led to increased lesion regression, with improved retinal gene expression patterns (Ramkumar et al., 2013).

14.3.4 Conclusions from Animal Models and Perspective

The mouse remains a useful experimental system to study the role of genes and diet in AMD. Because of an emphasis on modeling the disease state, and not modeling nutritional treatments, most dietary studies have not been highly relevant to human translational findings. Furthermore, most mouse models rely on genetic constructs that would never exist in a human. Future models need to take into account meaningful human gene variants (e.g. *CFH* Y402H) and dietary factors known to account for disease risk in humans (e.g. Western dietary patterns). A promising intersection of these may be possible using rhesus macaques, which show some common susceptibility genes for AMD, including *ARMS2* (Francis et al. 2008), and have been reared and aged on diets lacking macular pigments and ω-3 fatty acids.

References

AREDS2 Research Group (2013) Lutein + zeaxanthin and omega-3 fatty acids for age-related macular degeneration: the age-related eye disease study 2 (AREDS2) randomized clinical trial. JAMA 309:2005–2015

Awh CC, Lane AM, Hawken S et al (2013) CFH and ARMS2 genetic polymorphisms predict response to antioxidants and zinc in patients with age-related macular degeneration. Ophthalmology 20:00679–00679

Chen W, Stambolian D, Edwards AO et al (2010) Genetic variants near TIMP3 and high-density lipoprotein-associated loci influence susceptibility to age-related macular degeneration. Proc Natl Acad Sci U S A 107:7401–7406

Chew EY, Klein ML, Clemons TE et al (2014) No clinically significant association between CFH and ARMS2 genotypes and response to nutritional supplements: AREDS report number 38. Ophthalmology 121(11):2173–2180

Chiu CJ, Chang ML, Zhang FF et al (2014) The relationship of major american dietary patterns to age-related macular degeneration. Am J Ophthalmol 158:118–127

Espinosa-Heidmann DG, Sall J, Hernandez EP et al (2004) Basal laminar deposit formation in APO B100 transgenic mice: complex interactions between dietary fat, blue light, and vitamin E. Invest Ophthalmol Vis Sci 45:260–266

Francis PJ, Appukuttan B, Simmons E et al (2008) Rhesus monkeys and humans share common susceptibility genes for age-related macular disease. Hum Mol Genet 17:2673–2680

Fujihara M, Bartels E, Nielsen LB et al (2009) A human apoB100 transgenic mouse expresses human apoB100 in the RPE and develops features of early AMD. Exp Eye Res 88:1115–1123

Ho L, van Leeuwen R, Witteman JC et al (2011) Reducing the genetic risk of age-related macular degeneration with dietary antioxidants, zinc, and {omega}-3 fatty acids: the Rotterdam Study. Arch Ophthalmol 129:758–766

Klein ML, Francis PJ, Rosner B et al (2008) CFH and LOC387715/ARMS2 genotypes and treatment with antioxidants and zinc for age-related macular degeneration. Ophthalmology 115:1019–1025

Klein R, Myers CE, Meuer SM et al (2013) Risk alleles in CFH and ARMS2 and the long-term natural history of age-related macular degeneration: the Beaver Dam Eye Study. JAMA Ophthalmol 131:383–392

Kliffen M, Lutgens E, Daemen MJ et al (2000) The APO(*)E3-Leiden mouse as an animal model for basal laminar deposit. Br J Ophthalmol 84:1415–1419

Malek G, Johnson LV, Mace BE et al (2005) Apolipoprotein E allele-dependent pathogenesis: a model for age-related retinal degeneration. Proc Natl Acad Sci U S A 102:11900–11905

Pennesi ME, Neuringer M, Courtney RJ (2012) Animal models of age related macular degeneration. Mol Aspects Med 33:487–509

Ramkumar HL, Tuo J, Shen de F et al (2013) Nutrient supplementation with n3 polyunsaturated fatty acids, lutein, and zeaxanthin decrease A2E accumulation and VEGF expression in the retinas of Ccl2/Cx3cr1-deficient mice on Crb1rd8 background. J Nutr 143:1129–1135

Ratner M (2014) Next-generation AMD drugs to wed blockbusters. Nat Biotechnol 32:701–702

Reynolds R, Rosner B, Seddon JM (2013) Dietary omega-3 fatty acids, other fat intake, genetic susceptibility, and progression to incident geographic atrophy. Ophthalmology 120:1020–1028

Rowan S, Weikel K, Chang ML et al (2014) Cfh genotype interacts with dietary glycemic index to modulate age-related macular degeneration-like features in mice. Invest Ophthalmol Vis Sci 55:492–501

Sallo FB, Bereczki E, Csont T et al (2009) Bruch's membrane changes in transgenic mice overexpressing the human biglycan and apolipoprotein b-100 genes. Exp Eye Res 89:178–186

Sobrin L, Reynolds R, Yu Y et al (2011) ARMS2/HTRA1 locus can confer differential susceptibility to the advanced subtypes of age-related macular degeneration. Am J Ophthalmol 151:345–352, e343

Tuo J, Ross RJ, Herzlich AA et al (2009) A high omega-3 fatty acid diet reduces retinal lesions in a murine model of macular degeneration. Am J Pathol 175:799–807

Wang JJ, Rochtchina E, Smith W et al (2009) Combined effects of complement factor H genotypes, fish consumption, and inflammatory markers on long-term risk for age-related macular degeneration in a cohort. Am J Epidemiol 169:633–641

Weikel KA, Chiu CJ, Taylor A (2012a) Nutritional modulation of age-related macular degeneration. Mol Aspects Med 33:318–375

Weikel KA, Fitzgerald P, Shang F et al (2012b) Natural history of age-related retinal lesions that precede AMD in mice fed high or low glycemic index diets. Invest Ophthalmol Vis Sci 53:622–632

Chapter 15
Challenges in the Development of Therapy for Dry Age-Related Macular Degeneration

Cynthia X. Wei, Aixu Sun, Ying Yu, Qianyong Liu, Yue-Qing Tan, Isamu Tachibana, Hong Zeng and Ji-Ye Wei

Abstract Dry age-related macular degeneration (AMD), a multifactorial progressive degenerative disease of the retinal photoreceptors, pigmented epithelium and Bruch's membrane/choroid in central retina, causes visual impairment in millions of elderly people worldwide. The only available therapy for this disease is the over-

J.-Y. Wei (✉) · A. Sun · Y. Yu · Q. Liu
Departments of Biological Science, Allergan Inc,
RD3–2B, 2525 Dupont Drive, Irvine, CA 92612, USA
e-mail: Jiye_wei@yahoo.com

C. X. Wei · I. Tachibana
Department of Ophthalmology,
University of Texas Southwestern Medical Center, 75390 Dallas, TX, USA

Y.-Q. Tan
Department of Community Medicine,
University of North Texas Health Science Center, Fort Worth TX 76107, USA
e-mail: Yue-Qing.Tan@unthsc.edu

H. Zeng
University of Houston College of Optometry, Houston, TX 77204, USA
e-mail: hzeng.2017@alumni.opt.uh.edu

C. X. Wei
e-mail: Cynthua.Wei@UTSouthwestern.edu

A. Sun
e-mail: Sun_Aixu@Allergan.com

Y. Yu
e-mail: Yu_Ying@Allergan.com

Q. Liu
e-mail: Liu_Qianyong@Allergan.com

I. Tachibana
e-mail: Isamu.Tachibana@UTSouthwestern.edu

C. Bowes Rickman et al. (eds.), *Retinal Degenerative Diseases,* Advances in Experimental Medicine and Biology 854, DOI 10.1007/978-3-319-17121-0_15

the-counter (OTC) multi-vitamins plus macular xanthophyll (lutein/zeaxanthin) which attempts to block the damages of oxidative stress and ionizing blue light. Therefore development of dry AMD prescribed treatment is a pressing unmet medical need. However, this effort is currently hindered by many challenges, including an incomplete understanding of the mechanism of pathogenesis that leads to uncertain targets, confounded by not yet validated preclinical models and the difficulty to deliver the drugs to the posterior segment of the eye. Additionally, with slow disease progression and a less than ideal endpoint measurement method, clinical trials are necessarily large, lengthy and expensive. Increased commitment to research and development is an essential foundation for dealing with these problems. Innovations in clinical trials with novel endpoints, nontraditional study designs and the use of surrogate diseases might shorten the study time, reduce the patient sample size and consequently lower the budget for the development of the new therapies for the dry AMD.

Keywords Dry AMD · Geographic atrophy · Drusen · Retinal pigment epithelium · Bruch'smembrane · Photoreceptor · Complement · Antioxidants · Anti-VEGF DARPin · OZURDEX

15.1 Introduction

AMD is one of the leading causes of irreversible blindness in the elderly worldwide, which is hypothesized to be a progressive disease, with the dry and wet forms likely representing different points on a spectrum of disease severity. The initial stage of AMD is characterized by the appearance of white or yellowish lipid-rich deposits in Bruch's membrane, called drusen formation (Pikuleva and Curcio 2014). Subsequently, the loss of rod photoreceptors and retinal pigmented epithelia (RPE) function occurs in advanced dry AMD patients, resulting in geographic atrophy (GA). Wet AMD is occurs in approximately 10–15% of patients and is characterized by choroidal neovascularization extending through Bruch's membrane/RPE into the subretinal space. All current AMD treatments are anti-VEGF and/or anti-angiogenic for wet form only, such as bevacizumab, (Avastin), a full-length antibody against VEGF approved for the intravenous treatment of advanced carcinomas, pegaptanib (Macugen), ranibizumab (Lucentis) and aflibercept (Eylea) that have been developed specifically for intraocular use. Notably, abicipar pegol, an anti-VEGF DARPin (**D**esigned **A**nkyrin **R**epeat **P**rotein), will enter phase III clinic trials in 2015 for intraocular use to treat wet AMD (Souied et al. 2014; Maturi et al. 2014). Although the anti-VEGF therapies are clinically proven for managing the late-stage, severe AMD patients, interventions in the early-stage of dry AMD can be more effective to control this disease and reduce the burden for the patients. Therefore, providing novel earlier diagnostic, prophylactic and therapeutic approaches against dry AMD are highly compelling medical needs.

Table 15.1 Proposed mechanisms of pathogenesis and corresponding therapeutic targets for dry AMD

Proposed mechanisms	Therapeutic targets
Trophic factors deprivation	CNTF, PEDF and their trophic factor stimulants
Local immune system and inflammation	Anti-complement inhibitors, immune modulators
	Anti-inflammatory drugs
Blue light and other oxidative stresses	Antioxidants, reactive oxygen species scavengers
	Anti-ER stress reagents/chaperone regulators
Vascular insufficiency	Vasodilators and erythropoietin
Others	Visual cycle modulator (e.g. emixustat HCL)
	Anti-cholesterol drugs, anti-apoptotic compound
	Mitochondrial agents, multiple kinase inhibitors
	Phagocytosis modulators, drusen in situ clearance
	Agents, gene therapy, stem cell therapy

15.2 Pathogenic Mechanisms of Dry AMD

Aging is the major risk factor for development of AMD. Other systemic risk factors, such as smoking, obesity, sunlight exposure and oxidative stress have also been found to play very important roles in this disease (Bowes Rickman et al. 2013). Additionally, variations in AMD-related genes, such as complement factor H (*CFH*) and *HTRA1/ARMS2/PLEKHA1*, account for as much as 50% of the genetic risk of AMD. Genes involved in regulating lipid metabolism, complement immunity and oxidative damage are considered to be vital to a healthy macula and retina (Zhang et al. 2012). Although numerous research studies have contributed to understanding how AMD develops and advances, the complete picture is still to be fully elucidated. Uncertainties in the understanding of the pathogenesis of the disease pose fundamental challenges to the development of therapy for dry AMD. Some of the hypothetical mechanisms and therapeutic targets are presented in Table 15.1.

15.3 Pre-clinical Dry AMD Animal Models

The validity of an animal model depends on the degree of its similarity to human conditions. In dry AMD studies, rodents, especially mouse models, are widely used because of their similarity to human ocular morphology, high degree of availability, relatively low cost and amenability to genetic manipulation. However, several reports indicated that pre-existing retinal abnormalities or/and retinal degenerative lesions are found in the naïve mice line (Bell et al. 2012). For example, the C57BL/6N mouse substrain, which is widely used to produce transgenic and knockout mice, exhibited typical AMD-like white-spotted degenerative fundus lesions

(Mattapallil et al. 2012). All these mice showed *rd8* mutation of *Crb1* gene regardless of the purchasing sources (e.g. Charles River, Harlan, Taconic or DCT). The mutation presents in all the US vendor lines of C57BL/6N mice and its embryonic stem cells. This confounds ocular induced mutant phenotypes and confuses retinal degeneration research. Fortunately, the Jackson labs' mice strains C57BL/6J and C57BL/10J did not show any of these retinal abnormalities. But in the mixed substrain, C57BL/6NJ line, the AMD-like retinal degenerative phenotype and *rd8* mutant appeared again. Therefore, usage of mice for AMD and/or retinal degenerative disease studies should be prescreened with the fundus examination and images of confocal scanning laser ophthalmoscopy (SLO) and spectral-domain optical coherence tomography (SD-OCT) before experiments. Genotyping the mice for the *rd8* mutation is also highly recommended.

15.4 Drug Delivery for Dry AMD

Topical ocular application is the traditional ophthalmic drug delivery method. But for AMD therapy, intravitreal injection is the only approach that currently can pass over the blood-retinal barrier (BRB) and reach to the retina (Edelhauser et al. 2010). The presence of intravitreal clearance mechanisms (posterior transretinal and anterior aqueous humor elimination pathways) causes the peak drug concentration levels to decline to nontherapeutic levels over time, unless the intraocular injections are given frequently and repeatedly. However, the repeated injections impose a significant treatment burden on the patients as well as health care providers, and a cumulative risk of adverse effects from each subsequent injection. The disadvantage caused by the short to medium duration of action of intravitreal drug solutions has been partially overcome through product formulation or sustained-release device development (e.g., free-floating or scleral-fixated, biodegradable intravitreal implants or micro- or nanoparticles), such as Allergan's FDA approved Ozurdex (dexamethasone intravitreal biodegradable implant, the proprietary and innovative NOVADUR® solid polymer delivery system), which is used for treatment of diabetic macular edema, retinal vein occlusion and uveitis.

15.5 Novel Clinical Trial Endpoints for Dry AMD Therapy

Dry AMD has extremely slow disease progression with substantial variability among patients, which makes it very challenging to find an ideal clinical endpoint measurement method. Currently, the clinical trials for dry AMD therapy, i.e. CNTF encapsulated implant, anti-complement C5 inhibitor (eculizumab, Alexion/GSK) or anti-factor D complement inhibitor (Genentech/Roche), measured growth rate of geographic atrophy (GA) areas using SD-OCT imaging and also checked patient's

visual acuities in normal and low-luminance conditions (Yehoshua et al. 2014). Recently, by using SD-OCT technology, change in drusen volume was chosen as a novel surrogate clinical trial endpoint to study complement inhibition for dry AMD (de Amorim Garcia Filho et al. 2014). It could be studied over a shorter period of time compared with previous dry AMD studies that used the progression to advanced AMD or vision loss as efficacy endpoints and required years of follow-up (Yehoshua et al. 2014). In the future, clinical trials for dry AMD should consider the use of a composite clinical trial endpoint in which efficacy is defined by the treatment's ability to prevent drusen growth, progression of geographic atrophy (GA), visual acuity changes and formation of neovascularization. In addition to these modifications, perhaps a surrogate disease approach would be useful. An alternative approach would be to assess potential drug candidates in other retinal diseases that share certain characteristics of dry AMD but that have a more rapid course of disease progression, such as Stargardt's disease, an inherited form of juvenile macular degeneration, and most of these patients experience rapid deterioration of vision during early life (once a visual acuity of 20/40 is reached, there is often rapid progression of additional vision loss until it reaches 20/200, Fishman et al. 1987).

15.6 Current Status of the Dry AMD Therapy

Currently available therapies for dry AMD are only the OTC multi-vitamins plus xanthophyll (lutein/zeaxanthin) and zinc. The Age-Related Eye Disease Study (AREDS 2001), a large randomized clinical trial that studied the effects of antioxidants (beta-carotene, vitamin C, and vitamin E) and zinc supplements on the progression to advanced AMD, showed 25% reduction of progression to advanced AMD after a follow-up period of 6 years. However, the nutrients with beta-carotene supplementation have been noted to associate with a higher incidence of lung cancer in smokers. Researchers tried substituting lutein and zeaxanthin for beta-carotene to reduce the risk of lung cancer. More than 4000 people, ages 50–85 years, who were at risk for advanced AMD participated in AREDS2 at 82 clinical sites across the USA. The study found that lutein and zeaxanthin together appeared to be a safe alternative to beta-carotene (AREDS2 Research Group 2013).

Several drug candidates are in ongoing clinical trials for dry AMD treatment, which can be found on ClinicalTrials.gov. Recently, CNTF delivered by encapsulated-cell intraocular implants for treatment of geographic atrophy in dry AMD has been initially reported with positive results (Zhang et al. 2011). However, subsequent long-term follow-up results on retinitis pigmentosa showed no positive effects on patients' visual function (Birch et al. 2013), which is consistent with the animal studies that showed CNTF can keep the retinal photoreceptor morphology intact without functional improvement (ERG depression with CNTF overexpression, Wen et al. 2012). Trials of dry AMD treatments with Alcon's 5-HT_{1A} agonist, tandospirone (Collier et al. 2011), Othera's anti-oxidative agents, OT-511 (Wong et al. 2010) and Alexion's monoclonal antibody for targeting complement C5a,

eculizumab (Yehoshua et al. 2014) either failed to meet their primary endpoints or the compounds were withdrawn from further clinical development. The only ongoing dry AMD therapy that showed some promising results is the monthly injections of Roche's lampalizumb (anti-factor D complement inhibitor, humanized monoclonal antibody antigen-binding fragment, Fab). The phase II trial data of lampalizumb met its primary efficacy endpoint in slowing the progression of geographic atrophy lesions in a subgroup of 20.4% of patients with advanced dry AMD over 18 months observation (Williams and MAHALO study, 2013). In addition, several other complement inhibitors, such as LFG316 (Novartis), an antibody against C5, ARC-1905 (Ophthotech), an anti-C5 pegylated aptamer, as well as AL-78898A (POT-4, Alcon), a cyclic peptide that binds reversibly to C3 and inhibits three major complement pathways, are all in the phase 1/2 clinical trials. The results are still inconclusive.

Human retinal stem cells/progenitor cells replacement, gene therapy as well as retinal prosthesis are other promising therapeutic strategies for dry AMD patients, but all of them are in the early stages of development. For example, most transplanted retinal tissues and cells are too difficult to integrate into the host degenerative retinal structures for repairing and restoring vision. Also, human stem cells have so far shown little ability to differentiate into retinal phenotypes when transplanted into adult retina. Although retinal prosthesis are extremely effective at converting the visual image into a series of electrical impulses, the issue of precisely reconnecting them with the human retina will be paramount.

15.7 Conclusion

In summary, although we are currently facing many challenges to find an optimal treatment for dry AMD, at least we can focus our attention on resolving the identified critical issues. Hence, more research and development for dry AMD treatment is essential for new drug innovation.

Acknowledgements We thank Drs. Wha-Bin Im and Daniel Gil for their encouragement and editing this manuscript. This work was supported by Allergan and UT Southwestern Medical Center.

References

Age-Related Eye Disease Study (AREDS) (2001) A randomized, placebo-controlled, clinical trial of high-dose supplementation with vitamins C and E, beta carotene, and zinc for age-related macular degeneration and vision loss: AREDS report no. 8. Arch Ophthalmol 119:1417–1436

AREDS2 Research Group (2013) Lutein + zeaxanthin and omega-3 fatty acids for age-related macular degeneration: the age-related eye disease study 2 (AREDS2) randomized clinical trial. JAMA 309:2005–2015

Bell BA, Kaul C, Rayborn ME et al (2012) Baseline imaging reveals preexisting retinal abnormalities in mice. Adv Exp Med Biol 723:459–469

Birch DG, Weleber RG, Duncan JL et al (2013) Randomized trial of ciliary neurotrophic factor delivered by encapsulated cell intraocular implants for retinitis pigmentosa. Am J Ophthalmol 156:283–292

Bowes Rickman C, Farsiu S, Toth CA et al (2013) Dry age-related macular degeneration: mechanisms, therapeutic targets and imaging. Invest Ophthalmol Vis Sci 54:ORSF68–80

Collier RJ, Patel Y, Martin EA et al (2011) Agonist at the serotonin receptor (5-HT1A) protect the retina from severe photo-oxidative stress. Invest Ophthalmol Vis Sci 52:2118–2126.

de Amorim Garcia Filho CA, Yehoshua Z, Gregori G et al (2014) Change in drusen volume as a novel clinical trial endpoint for the study of complement inhibition in age-related macular degeneration. Ophthalmic Surg Lasers Imaging Retina 45:18–31

Edelhauser HF, Rowe-Rendleman CL, Robinson MR et al (2010) Ophthalmic drug delivery systems for the treatment of retinal diseases: basic research to clinical applications. Invest Ophthalmol Vis Sci 51:5403–5420

Fishman GA, Farber M, Patel BS et al (1987) Visual acuity loss in patients with Stargardt's macular dystrophy. Ophthalmology 94:809–814

Mattapallil MJ, Wawrousek EF, Chan CC et al (2012) The Rd8 mutation of the *crb1* gene is present in vendor lines of C57BL/6N mice and embryonic stem cells, and confounds ocular induced mutant phenotypes. Invest Ophthalmol Vis Sci 53:2921–2927

Maturi R, Callanan D, Khan B, REACH Study Group (2014) Abicipar pegol (anti-VEGF DARPin) phase 2 study in patients with neovascular age-related macular degeneration. 32nd American Society of Retinal Specialists Annual Meeting, Aug. 9, San Diego, USA

Pikuleva IA, Curcio CA (2014) Cholesterol in the retina: the best is yet to come. Prog Ret Eye Res 41:64–89

Souied EH, Devin F, Mauget-Faysse M et al (2014) Treatment of exudative age-related macular degeneration with a designed ankyrin repeat protein that binds vascular endothelial growth factor: a phase I/II study. Am J Ophthalmol S0002–9394(14):00326

Wen R, Tao W, Li Y, Sieving PA. (2012) CNTF and retina. Prog Retin Eye Res 31:136–151

Williams D (2013) MAHALO phase II study: safety, tolerability and activity of lampalizumab (anti-factor D) in patients with geographic atrophy. 31th Annual Meeting of the American Society of Retina Specialists. Aug. 27, Toronto, Canada

Wong WT, Kam W, Cunningham D et al (2010) Treatment of geographic atrophy by the topical administration of OT-551: results of a phase II clinical trial. Invest Ophthalmol Vis Sci 51:6131–6139

Yehoshua Z, de Amorim Garcia Filho CA, Numes RP et al (2014) Systemic complement inhibition with eculizumab for geographic atrophy in age-related macular degeneration: The COMPLETE study. Ophthalmology 121:693–701

Zhang K, Hopkins JJ, Heier JS et al (2011) Ciliary neurotrophic factor delivered by encapsulated cell intraocular implants for treatment of geographic atrophy in age-related macular degeneration. Proc Natl Acad Sci U S A 108:6241–6245

Zhang K, Zhang L, Weinreb RN (2012) Ophthalmic drug discovery: novel targets and mechanisms for retinal diseases and glaucoma. Nat Rev Drug Discov 11:541–559

Chapter 16
Nanoceria: a Potential Therapeutic for Dry AMD

Xue Cai and James F. McGinnis

Abstract Age-related macular degeneration (AMD) is the leading cause of blinding diseases. The "dry" form of AMD is the most common form of AMD. In contrast to the treatable neovascular (wet) AMD, no effective treatment is available for dry AMD. In this review, we summarize the animal models and therapeutic strategies for dry AMD. The novel candidates as potential treatment targets and the potential effectiveness of nanoceria as a treatment of dry AMD are also discussed.

Keywords Dry AMD · Drusen · RPE · Animal models · Therapeutic strategies · Nanoceria

Abbreviation

AMD	Age-related macular degeneration
RPE	Retinal pigment epithelium
BM	Bruch's membrane
GA	Geographic atrophy
CEP	Carboxyethylpyrrole
DHA	Docosahexaenoic acid
AREDS	The age-related eye disease study
CNTF	Ciliary neurotrophic factor
Aβ	Amyloid-β
ER	Endoplasmic reticulum
ROS	Reactive oxygen species
Nanoceria	Cerium oxide nanoparticles

X. Cai (✉) · J. F. McGinnis
Department of Ophthalmology, Dean McGee Eye Institute, University of Oklahoma Health Sciences Center, 608 Stanton L. Young Blvd, Oklahoma City, OK 73104, USA
e-mail: xue-cai@ouhsc.edu

J. F. McGinnis
Department of Ophthalmology, Dean McGee Eye Institute, Department of Cell Biology, Oklahoma Center for Neuroscience, University of Oklahoma Health Sciences Center, Oklahoma City, OK 73104, USA
e-mail: james-mcginnis@ouhsc.edu

C. Bowes Rickman et al. (eds.), *Retinal Degenerative Diseases,* Advances in Experimental Medicine and Biology 854, DOI 10.1007/978-3-319-17121-0_16

16.1 Introduction

Dry AMD (age-related macular degeneration), is the most common form of AMD. It develops very slowly with gradual loss of vision. The initial pathological sign of dry AMD is the appearance of drusen, which presents as yellowish deposits, in the macula between the retinal pigment epithelium (RPE) and the Bruch's membrane (BM). As the size of drusen increases, the BM thickens, and RPE become atrophied. Dry AMD develops into the late (advanced) stage: geographic atrophy (GA), and the loss of central vision eventually occurs. About 10–15 % of dry AMD may develop into another advanced form of AMD, the neovascular (wet) AMD. At present, no completely curative medical treatment is available for dry AMD.

16.2 Mechanism of Dry AMD

Many risk factors are associated with the pathology of AMD including age, race, diet, genetic variants, oxidative stress, dysregulation of the immune system, the complement system and inflammation, RPE damage and dysfunction, lysosomal lipofuscin accumulation, and drusen formation, etc. (Ambati and Fowler 2012; Cai and McGinnis 2012; Bowes Rickman et al. 2013; Kanagasingam et al. 2014). It was demonstrated that oxidative stress-induced inflammation is strongly associated with dry AMD, and RPE plays a key role in triggering AMD: RPE dysfunction, being the primary cause, results in photoreceptor death as a secondary event (Ambati and Fowler 2012; Bowes Rickman et al. 2013). Recently, an innate immune complex, the NLRP3 inflammasome in the RPE cells, was defined and linked with the microRNA-processing enzyme DICER1 and oxidative stress (Kaneko et al. 2011; Dridi et al. 2012; Tarallo et al. 2012). This axis provides a new mechanism for the development of GA and further confirms the central role of RPE in the pathogenesis of AMD. Experiments showed that deficiency of DICER1 in the RPE of GA patients, or conditional knockout mice, resulted in increases of Alu RNA in RPE cells (Kaneko et al. 2011), and consequently activated NLRP3 inflammasome which in turn induced RPE cell death (Tarallo et al. 2012). Furthermore, one component of the classical complement pathways, C1Q, which was found to be present in drusen, also activated the NLRP3 inflammasome to produce IL-18 for protection (Doyle et al. 2012). Many techniques are employed for clinical diagnosis of AMD, to image, measure and evaluate drusen development, as well as imaging the abnormalities of RPE, BM, and GA. However the etiology of AMD is very difficult to determine because of the slow progression of the disease, its late onset, environmental contributions, involvement of multiple genetic factors and most importantly, the lack of suitable good animal models which exactly mimic the phenotype of dry AMD.

16.3 Animal Models

Currently only aged simian primates develop drusen and share that similarity with humans with respect to its formation, composition and cellular location (Pennesi et al. 2012; Fletcher et al. 2014). More than 30 non-primate models of AMD are available and their origination and phenotypic characteristics have been reviewed (Ramkumar et al. 2010; Pennesi et al. 2012; Fletcher et al. 2014). These models are either: (1) naturally occurring gene mutations such as *arrd2/arrd2*, *Nr2e3*^{rd7}; or (2) genetically created with mutations of genes which lead to AMD symptoms, such as *abcr*$^{-/-}$, *elovl4*$^{-/-}$; or genes associate with AMD, such as inflammation cytokines (*Cx3crl*$^{-/-}$, *cfh*$^{-/-}$), oxidative stress associated genes (*Sod1*$^{-/-}$), or metabolic activity associated genes (*ApoE*$^{-/-}$, *mcd/mcd*). Another category of animal models was induced by physical injury or chemical oxidants, such as blue light induced A2E oxidation (Wielgus et al. 2010), sodium iodate (Enzmann et al. 2006), smoking (Wang and Neufeld 2010), and immunization with CEP (carboxyethylpyrrole, an adduct of oxidized docosahexaenoic acid (DHA)) (Hollyfield et al. 2010). One distinguished difference between human and mouse retina is that the mouse does not have a macular structure. However, a few of these models display some characteristics of dry AMD phenotypes such as "drusen-like" deposits, or a thickened BM or elevation of A2E levels. Unfortunately, most of them develop the pathogenesis of dry AMD at a very late age (usually beyond 8–9 months of age) which makes development of therapeutics more difficult.

16.4 Therapeutic Strategies

Nowadays, therapeutic strategies for the treatment of dry AMD are either: (1) targeting inflammation; suppression of oxidative stress, neuroprotection, or clearance of aggregates from the RPE; or (2) cellular therapies using a variety of types of stem cells. However, although all of these therapies delayed or slowed progression of dry AMD to wet AMD, they showed little or no benefit towards curing dry AMD.

16.4.1 Inhibition of Inflammation

Elements of inflammation cytokines and inflammation associated factors provide potential targets for the treatment of dry AMD. Compstatin is a selective complement C3 inhibitor and was shown to suppress and reverse drusen formation in cynomolgus monkeys (Chi et al. 2010), and its derivative (POT-4) is now in phase III trial (Evans and Syed 2013). Several other drugs targeting C3, C5 and factor D, are currently in clinical trial phase II or phase III for dry AMD (Evans and Syed 2013).

16.4.2 Suppression of Oxidative Stress

The age-related eye disease study (AREDS) clinical trial, that included a formulation of high dose of multiple vitamins with beta-carotene and zinc, significantly slowed the progression of dry AMD to wet AMD and visual loss but did not stop or cure the disease. AREDS2, adding lutein, zeaxanthin and omega-3 fatty acids to the formulation to test the effectiveness, was completed in May 2013 (www.nei.nih.gov/amd/).

16.4.3 Neuroprotection

In a clinical trial phase II study, encapsulated ciliary neurotrophic factor (CNTF) implant for the treatment of GA patients was conducted, and results obtained at 12 months after treatment showed dose-dependent increases in the thickness of the outer nuclear layer and stable visual acuity (Zhang et al. 2011). The mechanism of CNTF action for neuroprotection was shown to require cytokine receptor gp130 in Muller glia in a mouse model of retinitis pigmentosa, *rds/P216L* (Rhee et al. 2013).

16.4.4 Increased Clearance of Cellular Aggregates

This approach is based on the fact that the deposits of drusen and lipofuscin contain the oxidized byproducts of the visual cycle. Preventing the accumulation of these byproducts or slowing the visual cycle by visual cycle modulators should inhibit the progression of dry AMD. Oral intake of Fenretinide (vitamin A competitor for binding to the retinol binding protein) decreased the lesion growth rate in GA patients (Mata et al. 2013). A phase II trial of Fenretinide is ongoing (Evans and Syed 2013). Another phase II/III trial to test the efficacy of another drug (ACU-4429) for slowing the visual cycle and preventing the accumulation of A2E by modulation of RPE65 is ongoing (Evans and Syed 2013). Systemic supplementation of an anti-Aβ (amyloid-β) antibody (6F6) to the $cfh^{-/-}$ mice was shown to reduce Aβ and activate complement C3 deposition (Catchpole et al. 2013). Two phase II trials using antibodies that binds to Aβ are now ongoing (Evans and Syed 2013).

16.4.5 Cellular Therapies Using Stem Cells

A variety of stem cell types for use as AMD therapeutics have been developed in recent years (Evans and Syed 2013; Melville et al. 2013; Heller and Martin 2014). Most recently a phase I/II clinical trial involving the transplantation of human embryonic stem cell-derived RPE stem cells into the subretinal space of

patients with dry AMD showed improvement in vision (Schwartz et al. 2012). Several other approaches using induced pluripotent stem cell-derived and adult RPE stem cell-derived RPE cells are in the earlier development stage (Bharti et al. 2014).

16.4.6 Novel Candidates for Potential Therapy

With the extensive investigation of AMD mechanisms, many genes and signaling pathways were identified to be related to dry AMD, thus providing new candidate targets for AMD treatment.

16.4.6.1 NLRP3 Inflammasome

As stated above, a decrease in DICER1 and increase in Alu RNA resulted in the activation of the NLRP3-inflammasome in dry AMD. Therefore up-regulation of DICER1 or inhibition of Alu RNA and NLRP3, or targeting their signaling mediators/effectors, should slow the progression of the pathology (Dridi et al. 2012; Campbell and Doyle 2013).

16.4.6.2 Autophagy and ER Stress Chaperone

One important function of RPE cells is phagocytosis of aged photoreceptor outer segment discs (Strauss 2005). Chaperone (Hsp70)-mediated autophagy clearance, one of the three lysosomal pathways, is responsible for the removal of protein aggregates in the RPE cells (Ryhanen et al. 2009). In AMD patients, oxidative stress-induced ER (endoplasmic reticulum) stress (protein folding stress, caused by accumulation of unfolded/misfolded proteins) regulated autophagy for the degradation of damaged proteins (Yao et al. 2014). Up-regulation of autophagy and molecular chaperones, and their associated signaling pathways, should be effective for the treatment of dry AMD (Kaarniranta et al. 2012).

16.5 Nanoceria Targeting ROS and Downstream Pathology

Drusen and lipofuscin contain damaged DNA, lipids, and proteins, which are the oxidized byproducts from visual cycle and other metabolic activities. The prevention of upstream reactive oxygen species (ROS) formation during the visual cycle, without disturbance of normal retinal activities, is a critical key for treating of AMD.

Nanoceria are cerium oxide nanoparticles which, because of the physicochemical characteristics of their surface structure, have the ability to switch between +3 and +4 valance states and thereby destroy ROS. They mimic the catalytic activities of superoxide dismutase and catalase and convert ROS into harmless products—oxygen and water (Karakoti et al 2008).

Our laboratory is the first to use nanoceria to demonstrate their therapeutic potency in several rodent models of ocular diseases. Published data from our lab demonstrated that the use of nanoceria *in vivo* is a feasible strategy to prevent light induced-retinal damage in the albino rat (Chen et al. 2006), delay photoreceptor death and preserve retinal function in *tubby* mice (Kong et al. 2011; Cai et al. 2012), inhibit/regress neovascularization in a wet AMD mouse model, the *vldlr*$^{-/-}$ mice (Zhou et al. 2011; Cai et al. 2014), and protect the structural integrity of RPE cells in albino *vldlr*$^{-/-}$ mice (unpublished data). We have also shown that nanoceria can be retained in the retina for up to one year without structural and functional changes of the retina (Wong et al. 2013). Although the mechanisms for nanoceria retention in the retina are unknown, experiments to address this are currently under way.

Nanoceria have tremendous potential as effective therapeutics for treatment of dry AMD because: (1) nanoceria in a single low dose (172 ng) is effective for months; (2) their tiny size (3–5 nm) allows passage through cell and nuclear membranes without restriction; (3) they act as direct antioxidants and target oxidative stress and its downstream pathways. By continuously scavenging ROS oxidants, nanoceria prevent the formation of oxidized and damaged molecules and thereby decrease the accumulation of these lipofuscin-drusen precursors and prevent the death of RPE and photoreceptors.

References

Ambati J, Fowler BJ (2012) Mechanisms of age-related macular degeneration. Neuron 75:26–39

Bharti K, Rao M, Hull SC et al (2014) Developing cellular therapies for retinal degenerative diseases. Invest Ophthalmol Vis Sci 55:1191–1202

Bowes Rickman C, Farsiu S, Toth CA et al (2013) Dry age-related macular degeneration: mechanisms, therapeutic targets, and imaging. Invest Ophthalmol Vis Sci 54:68–80

Cai X, McGinnis JF (2012) Oxidative stress: the Achilles' heel of neurodegenerative diseases of the retina. Front Biosci (Landmark Ed) 17:1976–1995

Cai X, Sezate SA, Seal S et al (2012) Sustained protection against photoreceptor degeneration in tubby mice by intravitreal injection of nanoceria. Biomaterials 33:8771–8781

Cai X, Seal S, McGinnis JF (2014) Sustained inhibition of neovascularization in vldlr$^{-/-}$ mice following intravitreal injection of cerium oxide nanoparticles and the role of the ASK1-P38/JNK-NF-kappaB pathway. Biomaterials 35:249–258

Campbell M, Doyle SL (2013) An eye on the future of inflammasomes and drug development in AMD. J Mol Med (Berl) 91:1059–1070

Catchpole I, Germaschewski V, Hoh Kam J et al (2013) Systemic administration of Abeta mAb reduces retinal deposition of Abeta and activated complement C3 in age-related macular degeneration mouse model. PLoS One 8:e65518

Chen J, Patil S, Seal S et al (2006) Rare earth nanoparticles prevent retinal degeneration induced by intracellular peroxides. Nat Nanotechnol 1:142–150
Chi ZL, Yoshida T, Lambris JD et al (2010) Suppression of drusen formation by compstatin, a peptide inhibitor of complement C3 activation, on cynomolgus monkey with early-onset macular degeneration. Adv Exp Med Biol 703:127–135
Doyle SL, Campbell M, Ozaki E et al (2012) NLRP3 has a protective role in age-related macular degeneration through the induction of IL-18 by drusen components. Nat Med 18:791–798
Dridi S, Hirano Y, Tarallo V et al (2012) ERK1/2 activation is a therapeutic target in age-related macular degeneration. Proc Natl Acad Sci U S A 109:13781–13786
Enzmann V, Row BW, Yamauchi Y et al (2006) Behavioral and anatomical abnormalities in a sodium iodate-induced model of retinal pigment epithelium degeneration. Exp Eye Res 82:441–448
Evans JB, Syed BA (2013) New hope for dry AMD? Nat Rev Drug Discov 12:501–502
Fletcher EL, Jobling AI, Greferath U et al (2014) Studying age-related macular degeneration using animal models. Optom Vis Sci 91:878–886
Heller JP, Martin KR (2014) Enhancing RPE cell-based therapy outcomes for AMD: the role of Bruch's membrane. Transl Vis Sci Technol 3:11
Hollyfield JG, Perez VL, Salomon RG (2010) A hapten generated from an oxidation fragment of docosahexaenoic acid is sufficient to initiate age-related macular degeneration. Mol Neurobiol 41:290–298
Kaarniranta K, Kauppinen A, Blasiak J et al (2012) Autophagy regulating kinases as potential therapeutic targets for age-related macular degeneration. Future Med Chem 4:2153–2161
Kanagasingam Y, Bhuiyan A, Abramoff MD et al (2014) Progress on retinal image analysis for age related macular degeneration. Prog Retin Eye Res 38:20–42
Kaneko H, Dridi S, Tarallo V et al (2011) DICER1 deficit induces Alu RNA toxicity in age-related macular degeneration. Nature 471:325–330
Karakoti AS, Monteiro-Riviere NA, Aggarwal R et al (2008) Nanoceria as antioxidant: Synthesis and biomedical applications. JOM 60:33–37
Kong L, Cai X, Zhou X et al (2011) Nanoceria extend photoreceptor cell lifespan in tubby mice by modulation of apoptosis/survival signaling pathways. Neurobiol Dis 42:514–523
Mata NL, Lichter JB, Vogel R et al (2013) Investigation of oral fenretinide for treatment of geographic atrophy in age-related macular degeneration. Retina 33:498–507
Melville H, Carpiniello M, Hollis K et al (2013) Stem cells: a new paradigm for disease modeling and developing therapies for age-related macular degeneration. J Transl Med 11:53
Pennesi ME, Neuringer M, Courtney RJ (2012) Animal models of age related macular degeneration. Mol Aspects Med 33:487–509
Ramkumar HL, Zhang J, Chan CC (2010) Retinal ultrastructure of murine models of dry age-related macular degeneration (AMD). Prog Retin Eye Res 29:169–190
Rhee KD, Nusinowitz S, Chao K et al (2013) CNTF-mediated protection of photoreceptors requires initial activation of the cytokine receptor gp130 in Muller glial cells. Proc Natl Acad Sci U S A 110:E4520–4529
Ryhanen T, Hyttinen JM, Kopitz J et al (2009) Crosstalk between Hsp70 molecular chaperone, lysosomes and proteasomes in autophagy-mediated proteolysis in human retinal pigment epithelial cells. J Cell Mol Med 13:3616–3631
Schwartz SD, Hubschman JP, Heilwell G et al (2012) Embryonic stem cell trials for macular degeneration: a preliminary report. Lancet 379:713–720
Strauss O (2005) The retinal pigment epithelium in visual function. Physiol Rev 85:845–881
Tarallo V, Hirano Y, Gelfand BD et al (2012) DICER1 loss and Alu RNA induce age-related macular degeneration via the NLRP3 inflammasome and MyD88. Cell 149:847–859
Wang AL, Neufeld AH (2010) Smoking mice: a potential model for studying accumulation of drusen-like material on Bruch's membrane. Vision Res 50:638–642
Wielgus AR, Collier RJ, Martin E et al (2010) Blue light induced A2E oxidation in rat eyes–experimental animal model of dry AMD. Photochem Photobiol Sci 9:1505–1512

Wong LL, Hirst SM, Pye QN et al (2013) Catalytic nanoceria are preferentially retained in the rat retina and are not cytotoxic after intravitreal injection. PLoS One 8:e58431

Yao J, Tao ZF, Li CP et al (2014) Regulation of autophagy by high glucose in human retinal pigment epithelium. Cell Physiol Biochem 33:107–116

Zhang K, Hopkins JJ, Heier JS et al (2011) Ciliary neurotrophic factor delivered by encapsulated cell intraocular implants for treatment of geographic atrophy in age-related macular degeneration. Proc Natl Acad Sci U S A 108:6241–6245

Zhou X, Wong LL, Karakoti AS et al (2011) Nanoceria inhibit the development and promote the regression of pathologic retinal neovascularization in the Vldlr knockout mouse. PLoS One 6:e16733

Chapter 17
β-amyloidopathy in the Pathogenesis of Age-Related Macular Degeneration in Correlation with Neurodegenerative Diseases

Victor V. Ermilov and Alla A. Nesterova

Abstract Involvement of new biotechnology and genetic engineering methods to the study of the aging organism allowed to select a group of neurodegenerative diseases (NDD) which have a similar mechanism of pathogenesis including pathological processes of protein aggregation and its deposition in the structures of nerve tissue. The development of eye and brain from one embryonic germ layer, community of ethiopathogenetic and morphological manifestations of age-related macular degeneration (AMD) and Alzheimer's disease (AD), a common pathway of β-amyloid precursor protein (APP) are associated with the pathological aggregation of fibrillar β-amyloid (Aβ) protein and the development of β-amyloidopathy in structural elements of the eye and the brain. The review demonstrates the keynote of AMD and AD pathogenesis is β-amyloidopathy that is a manifestation of proteinopathy leading to cytotoxicity, neurodegeneration and the development of pathological apoptosis activated by the formation of intracellular Aβ. This view on the problem predetermines the development of new strategies for the creating of ophthalmogeriatric and neuroprotective drugs affecting the pathogenesis and including all stages of Aβ formation and pathological aggregation.

Keywords β-amyloidopathy · Senile local amyloidosis · Age-related macular degeneration · Neurodegenerative diseases · Alzheimer's disease · Amyloidogenesis · Proteinopathy

V. V. Ermilov (✉)
Department of Forensic Medicine and Pathology, Volgograd State Medical University, 8 Dvinskaya, app 85, Volgograd 400087, Russia
e-mail: vladimirovich2001@hotmail.com

A. A. Nesterova
Department of Histology, Embryology, Cytology, Volgograd State Medical University, 49 Universitetskiy pr, app 149, Volgograd 400011, Russia
e-mail: alla.nesterova2013@yandex.ru

C. Bowes Rickman et al. (eds.), *Retinal Degenerative Diseases,* Advances in Experimental Medicine and Biology 854, DOI 10.1007/978-3-319-17121-0_17

17.1 Introduction

Senile local amyloidosis is closely connected with clinical medicine. The appearance of amyloid in eye is related with development of gerontoophthalmological diseases. AMD is a leading cause of severe visual impairment in the elderly and its pathogenesis remains poorly understood. Current treatments do not satisfy the demands of society and would be improved by better understanding of the molecular events causing the retina degeneration. It may be possible to gain insight into AMD pathogenesis by exploring similarities to another age-related disease of the central nervous system: AD. Recent evidence implicates Aβ in the pathogenesis of AMD and AD, involving amyloidogenesis in the development of both diseases (Kaarniranta et al. 2011; Sivak 2013). Amyloidogenesis is referred to as multifactorial process, however, molecular biological studies conducted in the past decades have shown the leading role of APP in the pathogenesis of the AMD and AD diseases. A number of neurodegenerative disorders have been recently coalesced into a group of proteinopathies because of the similarity of molecular mechanisms underlying their pathogenesis (Skovronsky et al. 2006; Shelkovnikova et al. 2012). A key step in the development of proteinopathies is a structural change that triggers aggregation of proteins which are prone to form aggregates due to their physical and chemical properties. Based on the commonality of APP processing some authors identify β-amyloidopathy as a key mechanism in the pathogenesis of AMD and AD (Perez et al. 2009; Ohno-Matsui 2011).

17.2 Senile Local Amyloidosis: Associated Degeneration in the Retina in AMD

Amyloidosis and aging are fundamental biological problems. This is mainly based on age-related metabolic disfunctioning due to the various specific fibrillar protein amyloid (Ermilov and Serov 1994; Picken et al. 2012). Amyloidosis comprises a group of diseases with a wide variety of clinical manifestations caused by systemic or local deposition of fibrillar protein mass (amyloid) in organs and tissues. Endocrine and non-endocrine forms should be distinguished among senile local amyloidosis (Ermilov and Serov 1994). Non-endocrine senile local amyloidosis includes cerebral amyloidosis and eye amyloidosis (Ermilov 1993; Serov 1994).

In recent years the interest to the study of the local senile eye amyloidosis and its relationship to NDD has increased (Ohno-Matsui 2011; Ermilov et al. 2013). Clinical manifestation of senile local amyloidosis with primary lesion of fundus of the eye is AMD (Ermilov and Serov 1994). AMD is one of the most widely spread diseases among people over sixty. This disease is a chronic degenerative process mainly in the choroid, Bruch's membrane (BM), retinal pigment epithelium (RPE) and retina (Gass 1997; Virgil Alfaro et al. 2006). The results of morphometric

studies of retinal pigment epithelial (RPE) cells in the macular region are particularly noteworthy. They have demonstrated a significant decrease in the number of RPE cells with age. Besides, the lowest number of RPE cells was found in the eyes with AMD and amyloidosis (Ermilov and Serov 1994).

It is known that normal aging retina has a high degree of plasticity that underlies the development of compensatory mechanisms of senescence (Zueva 2010; Jones et al. 2012). The role of amyloidosis in the mechanism of accelerated aging of ocular fundic tissues has not been yet investigated completely and continues to be studied using the techniques of molecular biology and genetic engineering.

17.3 Amyloidogenesis in the Neurodegenerative Diseases: Age-Related Macular Degeneration and Alzheimer's Disease

Involvement of new biotechnology and genetic engineering methods to the study of the aging organism allowed to select a group of NDD which have a similar mechanism of pathogenesis including pathological processes of protein aggregation and deposition of insoluble fibrillar structures in the form of histopathological inclusions in nerve tissue. This allowed them to combine the group of diseases with the general name proteinopathies (Skovronsky et al. 2006; Shelkovnikova et al. 2012). Recent data of molecular analysis pointing to the key role of certain proteins in the etiology and pathogenesis of a number NDD including AMD has given an impulse to the development of new concepts that allocate separate versions of proteinopaties such as tauopathy, synucleinopathy, amyloidopathy (Shelkovnikova et al. 2012; Ermilov et al. 2013). The results obtained in the study of the proteinopaties mechanisms pay attention to the similarity of the principal stages of the protein aggregates formation. Under the influence of oxidative stress, chemical modifications, mutations and other genetic factors the soluble precursor protein is converted into its pathogenic form prone to aggregation. Pathogenic form of protein becomes be organized to oligomers which subsequently generate protofibrils. At the final stage of aggregation mature fibrils formed from protofibrils generate insoluble protein deposits in the nervous tissues not only extracellularly but also intracellularly (Li et al. 2007). Analyzing the current data of the molecular basis of proteinopathy some researchers believe Aβ is a keynote in the pathogenesis of a number of NDD (Glabe 2006; Sivak 2013). In this connection the problem of amyloidosis and amyloidogenesis remains relevant. Today, there is a sufficient number of evidence according to which the primary cytotoxic agents in amyloidopathy are oligomers of Aβ protein prone to aggregation (Li et al. 2007). The neurotoxic effect of Aβ oligomers and protofibrils is associated with its damaging effect on the cell membranous structures including cell membrane, Golgi apparatus, mitochondria. This stimulates the overproduction of reactive oxygen that causes damage and death of neurons (Kayed et al. 2003; Glabe 2006; Ferreira et al. 2007; Zhang 2012).

Molecular level investigation has showed that under the influence of risk factors the transmembrane precursor protein of β-amyloid—APP (amyloid precursor protein) normally expressed in the cell membrane structures in many tissues is cleaved by a sequential activity of β-secretase and γ-secretase. This produces β-amyloid polypeptide chain with 40 (Aβ1–40) and 42 (Aβ1–42) amino acid residues. Aβ42 and Aβ40 tend to form oligomers and protofibrils have toxic effect on neurons. Oligomers and protofibrils of Aβ42 and Aβ40, in turn, form mature fibrils that produce deposits in cytoplasm of the retinal cells and extracellularly including the formation of retinal drusen (Zhang et al. 2012).

Drusen are extracellular deposits that lie between RPE and BM in the fundus of eye. The formation of drusen in the structures of blood-retinal barrier is one of the first objective clinical and morphological characters observed in AMD (Gass 1997; Virgil Alfaro et al. 2006). A number of original articles have shown the presence positive reactivity in the drusen and in the retina to Aβ by immunostaining (Luibl et al. 2006; Perez et al. 2009). Isas et al. (2010) have found both soluble and insoluble forms of Aβ in macular drusen of human eye. Biochemical and immunohistochemical studies have allowed to identify different proteins and lipids in drusen: Aβ, vitronectin, P component, apolipoprotein E, transthyretin, C3 and C5b9 complement fractions (Crabb et al. 2002). Most researchers point to the fact that Aβ, apolipoprotein E, complement proteins found in drusen are the components of senile plaques in AD (Perez et al. 2009; Isas et al. 2010).

Ophthalmic findings are common features of NDD and, in addition to being clinically important, have emerged as potentially useful biomarkers of disease progression in several conditions. Clinicians and morphologists discuss in details different morphological and functional visual system abnormalities in patients with AD (Armstrong 2009; Parnell et al. 2012). It is still not quite understand the mechanisms of visual impairment in this group of patients, however, we may not ignore the fact that the retina, developed from the same source as the brain (neuroectoderm) and included more than 20 types of neurons demonstrates synchronous processes occurring in itself and in the brain (Ning et al. 2008; Parnell et al. 2012). The results of some studies conducted in animal models of AD showed immunopositivity to Aβ in the drusen and in the retina correlated to that in senile plaques in AD (Isas et al. 2010; Parnell et al. 2012). These findings allow assume a key role of Aβ in Alzheimer's and AMD combining their pathogenesis.

17.4 Development of β-amyloidopathy in AMD

Taking the commonability of APP metabolism in AMD and AD into consideration we found it possible to assume the following mechanism of β-amyloidopathy and neurodegeneration in AMD.

In normal aging retina has a high degree of plasticity (Zueva 2010; Jones et al. 2012) that compensates for age-related loss of photoreceptors, ganglion cells and

RPE cells undergone to receptor-mediated apoptosis (Zimmermann et al. 2001). The interaction between Fas-ligand and Fas-receptor causes the conversion of inactive procaspase-8 in its active form which, in turn, activates caspase-3 and mitochondrial signaling pathways of apoptosis (Nixon and Yang 2012). APP is normally present in many cells including RPE and retinal neurons (Zhang 2012). Intracellular APP localizes in Golgi apparatus, endoplasmic reticulum, lysosomes, endosomes, nuclear envelope and cell membrane (Zhang 2012). Nonamyloidogenic pathway involves sequential influence of α-and γ-secretase on APP processing with the formation of s-APPα, P3 and AICD (APP intracellular domain) that take part in an adequate cellular metabolism. In the aging organism under risk factors the activity of the proteasome—lysosomal system, the number of phagolysosomes, endosomes, lipofuscin granules decreases in RPE cells and retinal neurons (Zhang 2012; Zhang et al. 2012). With age RPE melanin granules demonstrate their depletion and the phagolysosomes with toxic A2E (bis-retiniliden—ethanolamine) are accumulated (Ostrovskij 2005). These changes cause the development of intracellular oxidative stress and cytotoxicity. In such conditions APP pathway involves activation of β- and γ-secretases (Zhang 2012) which sequentially cleave APP to form Aβ40 or Aβ42 polypeptides prone to β-transformation and fibrillogenesis. This process leads to the formation of oligomeric, prefibrillar and ultimately insoluble fibrillar forms of Aβ deposited intracellularly and extracellularly. Amyloidogenic processing of APP is completed by the formation of Aβ deposits in the retina, in the material of drusen, blood-retinal barrier structures: Bruch's membrane, choroidal vessels (amyloid angiopathy). Intracellular Aβ stimulates autophagy and contributes to the increase of the structural components of Golgi apparatus, lysosomes and endosomes (Nixon and Yang 2012; Zhang 2012). Intracellular Aβ deposits cause swelling and degeneration of retina neurons axons, dysfunction and destruction of synapses. Intracellular cytotoxic effect of Aβ is associated with its ability to activate the main protein "dispatcher" of apoptosis—p53 which directly initiates the caspase cascade, receptor-dependent signaling pathway and mitochondrial signaling pathway of apoptotic cell death. Such a mechanism of β-amyloidopathy in AMD, in our view, is justified and considers modern concepts of intracellular protein pathology and mechanisms of cell death, based on advances in molecular biology.

Thus, the analysis of recent data obtained in the investigation of molecular and cellular processes underlying the development of NDD, suggest that the keynote of pathogenesis of AMD and AD is the aggregation of Aβ underlying cytotoxicity and neurodegeneration of neurons in the brain tissue and retina including RPE cells. In our view this allows AMD to be interpreted as a proteinopathy—β-amyloidopathy. This view on the problem provides the preconditions for the development of new strategies and the creation of new generation of neuroprotective and ophthalmogeriatric pharmaceuticals justified pathogenetically and acting directly on all stages of pathological aggregation of key protein—Aβ, its stability and metabolism.

References

Armstrong RA (2009) Alzheimer's disease and the eye. J Ophthalmol 2:103–111
Crabb JW, Miyagi M, Gu X et al (2002) Drusen proteome analysis: an approach to the etiology of age-related macular degeneration. Proc Natl Acad Sci U S A 99:14682–14687
Ermilov VV (1993) Senile amyloidosis of the eye as a manifestation of senile cerebral amyloidosis. Arkhiv Patolgii (Archive of Pathol) 55:43–45 (In Russ.)
Ermilov VV, Serov VV (1994) Position of ocular amyloidosis among various forms of amyloidosis. Arkhiv Patologii (Archive of Pathol) 56:9–14 (In Russ.)
Ermilov V, Nesterova A, Makhonina O (2013) Amyloid-b and age-related macular degeneration. 25th European Congress of Pathology, Lisbon (31 August–4 September 2013) Virchows Archiv, S 117
Ferreira ST, Vieira MN, De Felice FG (2007) Soluble protein oligomers as emerging toxins in Alzheimer's and other amyloid diseases IUBMB Life 59:332–345
Gass JD (1997) Stereoscopic atlas of macular diseases: diagnosis and treatment, 4th ed, vol 1. Mosby-Year Book Inc, St Louis, pp 1–17
Glabe CG (2006) Common mechanisms of amyloid oligomer pathogenesis in degenerative disease. Neurobiol Aging 27:570–575
Isas JM, Luibl V, Johnson LV et al (2010) Soluble and mature amyloid fibrils in drusen deposits. Invest Ophthalmol Vis Sci 51:1304–1310
Jones BW, Kondo M, Terasaki H et al (2012) Retinal remodeling. Jpn J Ophthalmol 56:289–306
Kaarniranta K, Salminen A, Haapasalo A et al (2011) Age-related macular degeneration (AMD): Alzheimer's disease in the eye? J Alzheimer's Dis 24:615–631
Kayed R, Head E, Thompson JE (2003) Common structure of soluble amyloid oligomers implies common mechanism of pathogenesis. Science 300:486–489
Li M, Chen L, Lee DHS et al (2007) The role of intracellular amyloid β in Alzheimer's disease. Progr Neurobiol 83:131–139
Luibl V, Isas JM, Kayed R et al (2006) Drusen deposits associated with aging and age-related macular degeneration contain nonfibrillar amyloid oligomers. J Clin Invest 116:378–385
Ning A, Cui J, To E et al (2008) Amyloid-beta deposits lead to retinal degeneration in a mouse model of Alzheimer disease. Invest Ophthalmol Vis Sci 49:5136–5143
Nixon RA, Yang DS (2012) Autophagy and neuronal cell death in neurological disorders. Cold Spring Harb Perspect Biol. doi:10.1101/cshperspect.a008839
Ohno-Matsui K (2011) Parallel findings in age-related macular degeneration and Alzheimer's disease. Prog Retin Eye Res 30:217–238
Ostrovskij M A (2005) Molecular mechanisms of the damaging effect of light on the structure of the eye and the system of protection against such damage. Uspehi biologicheskoj himii (Success Biol Chem) 45:173–204 (In Russ.)
Parnell M, Guo L, Abdi M et al (2012) Ocular manifestations of Alzheimer's disease in animal models. Int J Alzheimer's Dis 39:187–204
Perez SE, Lumayag S, Kovacs B et al (2009) Beta-amyloid deposition and functional impairment in the retina of the APPswe/PS1DeltaE9 transgenic mouse model of Alzheimer's disease. Invest Ophthalmol Vis Sci 50:793–800
Picken MM, Guillermo AD, Herrera A (2012) Amyloid and related disorders. Springer Science+Business Media, Berlin
Serov VV (1994) Local forms of amyloidosis as a manifestation of age-related pathology: a new look at the problem. Arkhiv Patologii (Arch Pathol) 5:39–43 (In Russ.)
Shelkovnikova TA, Kulikova AA, Tsvetkov FO et al (2012) Proteinopathies—forms of neurodegenerative disorders with protein aggregation-based pathology. Mol Biol (Mosk) 46:402–415 (In Russ.)
Sivak JM. (2013) The aging eye: common degenerative mechanisms between the Alzheimer's brain and retinal disease. Invest Ophthalmol Vis Sci 54:871–880

Skovronsky DM, Lee VM, Trojanowski JQ (2006) Neurodegenerative diseases: new concepts of pathogenesis and their therapeutic implications. Annu Rev Pathol 1:151–170
Virgil Alfaro III D, Liggett PE, Mieler WF et al (2006) Age-related macular degeneration. Lippincott, Williams & Wilkins, Philadelphia
Zhang C (2012) Alzheimer's disease-related amyloidopathy in visual impairment. J Addict Res Ther S5:005. http://dx.doi.org/10.4172/2155-6105.S5-005. Accessed 31 August
Zhang H, Ma Q, Zhang YW, Xu H (2012) Proteolytic processing of Alzheimer's β-amyloid precursor protein. J Neurochem 120:9–21
Zimmermann KC, Bonzon C, Green DR (2001) The machinery of programmed cell death. Pharmacol Ther 92:57–70
Zueva MV (2010) The aging of the retina. Rossijskij oftal'mologicheskij zhurnal (Russ Ophthalmol J) 2:53–61; 3:54–62 (In Russ.)

Part II
Macular Dystrophies/Inherited Macular Degeneration

Chapter 18
Different Mutations in ELOVL4 Affect Very Long Chain Fatty Acid Biosynthesis to Cause Variable Neurological Disorders in Humans

Martin-Paul Agbaga

Abstract All mammalian cell membranes are characterized by amphipathic lipid molecules that interact with proteins to confer structural and functional properties on the cell. The predominant lipid species are phospholipids, glycolipids, sphingolipids and cholesterol. These lipids contain fatty acids with variable hydrocarbon chain lengths between C14-C40, either saturated or unsaturated, that are derived from diet, synthesized *de novo,* or elongated from shorter chain fatty acids by fatty acid elongase enzymes. One member of the family of elongases, **ELO**ngation of **V**ery **L**ong chain fatty acids**-4** (ELOVL4), mediates the biosynthesis of both saturated and unsaturated very long chain fatty acids (VLC-FA; >C26) in the retina, meibomian gland, brain, skin, and testis. Different mutations in ELOVL4 cause tissue-specific maculopathy and/or neuro-ichthyotic disorders. The goal of this mini-review is to highlight how different mutations in *ELOVL4* can cause variable phenotypic disorder, and propose a possible mechanism, based on the role of fatty acids in membranes, which could explain the different phenotypes.

Keywords Retinal degeneration · Very long chain polyunsaturated fatty acids (VLC-PUFA) · Elongation of very long chain fatty acids-4 (ELOVL4) · Autosomal dominant Stargardt-like macular dystrophy · Spinocerebellar ataxia (SCA) · Erythrokeratodermia (EKV)

18.1 Introduction

Eight separate mutations in human *ELOVL4* have been identified (Bernstein et al. 2001; Edwards et al. 2001; Zhang et al. 2001; Maugeri et al. 2004; Aldahmesh et al. 2011; Cadieux-Dion et al. 2014; Mir et al. 2014). The *ELOVL4* gene encodes a protein that is expressed in retina, testis, skin, meibomian gland, and brain, where it mediates tissue-specific biosynthesis of very long chain saturated fatty

M.-P. Agbaga (✉)
Department of Ophthalmology, Dean McGee Eye Institute, University of Oklahoma Health Sciences Center, 608 Stanton L. Young Blvd., DMEI 429PB, Oklahoma City, OK 73104, USA
e-mail: martin-paul-agbaga@ouhsc.edu

C. Bowes Rickman et al. (eds.), *Retinal Degenerative Diseases,* Advances in Experimental Medicine and Biology 854, DOI 10.1007/978-3-319-17121-0_18

acids (VLC-SFA, >C26) and/or very long chain polyunsaturated fatty acids (VLC-PUFA; >C26), collectively referred to as VLC-FA (Agbaga et al. 2008). VLC-FA are constituents of complex lipid molecules such as phosphatidylcholine (PC) in photoreceptors cells, sphingolipids in testes and sperm, and brain, wax esters in tear film (Butovich et al. 2009), and omega-O-acylceramides essential for skin barrier function (Vasireddy et al. 2007). Two important regions of wild-type ELOVL4 are a catalytic histidine dideoxy binding motif (HVYHH) essential for fatty acid condensation and a carboxyl terminal endoplasmic reticulum (ER) retention/retrieval signal (KXKXX) necessary to direct the protein to the ER, site of fatty acid elongation. Seven of the *ELOVL4* mutations encode truncated ELOVL4 proteins lacking the ER retention motif and hence are misrouted from the ER. The eighth mutation encodes full length ELOVL4 with a point mutation located five amino acids downstream of the conserved histidine active site (Cadieux-Dion et al. 2014). How each of these mutations in ELOVL4 causes the different tissue-specific phenotypes is under investigation in our laboratory.

18.2 Distinct Mutations in ELOVL4 Cause Differential Tissue-Specific Disorders

In 2001, three independent labs identified three distinct frame-shift mutations in the *ELOVL4* gene as the cause of autosomal dominant Stargardt-like macular dystrophy (STGD3), which is characterized by early onset, progressive degeneration of retinal pigment epithelial and cone photoreceptor cells, leading to vision loss (Bernstein et al. 2001; Edwards et al. 2001; Zhang et al. 2001). The mutations, a 5 base-pair deletion (790–794_del AACTT) in five large STGD3 pedigrees and two concurrent single base-pair deletions (789delT and 794delT) in a large Utah pedigree, results in the introduction of premature stop codons (p. Asn264Thrfs*10 and p.Asn264Leufs*9, respectively) in the *ELOVL4* message. In 2004, a fourth mutation (810C>G) encoding a truncated ELOVL4 protein (p.Y270stop) was reported in a Dutch family with early onset STGD3 (Maugeri et al. 2004). All four mutations occur within exon 6 of *ELOVL4* and result in a truncated ELOVL4 lacking the C-terminal conserved ER retention signal, causing macular degeneration.

In 2011, a Saudi Arabian and two Asian Indian children were reported with recessive homozygous *ELOVL4* mutations (689delT and conversion c. 646C>T) which results in truncated ELOVL4 proteins (lle230Metfs*22 and Arg216stop, respectively) (Aldahmesh et al. 2011). The affected children had congenital ichthyosis, seizures, intellectual disability, spastic quadriplegia, and small testicles, and died within the first few years of life. They showed delayed myelination and evidence of cortical atrophy as determined by magnetic resonance imaging. Interestingly, no significant retinal phenotype was observed in these patients or their heterozygous parents. In 2014, another novel homozygous recessive *ELOVL4* mutation (c. 78C>G) encoding a Try26stop was reported in four Pakistani family members aged 16–24 years (Mir et al. 2014), who displayed neuro-ichthyotic disorders

similar to the Saudi and Asian Indian children. Much like the Asian Indian children, one of the Pakistani patients had severe intellectual disability, impaired speech and hearing, spastic quadriplegia, was constantly bed ridden, and had frequent seizures and small testicles. He died at 17 years of age, while the Asian Indian children died at 6 months and 2 years of age. The only retinal phenotype reported in these patients was tortuous blood vessels, subtle macular changes, and mild degree of myopia with subtle peripapillary changes (Aldahmesh et al. 2011; Mir et al. 2014). Of the surviving Pakistani family members, intra-familial phenotypic differences were observed, suggesting the severity of the phenotypes was age-dependent or due to the degree of activity of expressed mutant ELOVL4, or both.

Again in 2014, mapping and genetic sequencing of a French-Canadian family previously thought to have Sjögren-Larsson syndrome resulted in identification of another *ELOVL4* mutation (c.504G>C) that caused an L168F substitution in ELOVL4 (Cadieux-Dion et al. 2014). Detailed clinical examination of 19 carriers of this mutation revealed an age-dependent onset of autosomal dominant spinocerebellar ataxia (SCA) and erythrokeratodermia (EKV). Each of the affected individuals had a different age of disease onset, severity of ataxia, brain atrophy, and skin lesions. Older patients (51–87 years of age) had more pronounced cerebellar, cortical, pons, and peripheral axonal neuropathy, postural tremor, and slow pursuit. While younger patients (25–36 years of age) displayed mostly normal phenotypes, almost all the older patients were affected and displayed different levels of SCA and EKV with no reported significant macular phenotype.

18.3 ELOVL4 Is Essential for Biosynthesis of Saturated and Polyunsaturated Very Long Chain Fatty Acids

In 2008, we first identified the biological function of ELOVL4 as a fatty acid elongase essential for biosynthesis of both very long chain saturated (VLC-SFA) and polyunsaturated (VLC-PUFA) fatty acids (Agbaga et al. 2008), both of which are constituents of membrane glycero- and sphingolipids in a select group of tissues. The 5-bp deletion STGD3 mutant ELOVL4 could not synthesize VLC-PUFA and acted in a dominant negative manner on VLC-PUFA biosynthesis by the WT ELOVL4 in cultured cells (Logan et al. 2013) and in retinas of *Elovl4* knock in (KI) mice expressing the 5-bp deletion (McMahon et al. 2007a). The KI mice have an age-dependent decline in retinal function (McMahon et al. 2007b) but no other evident central nervous system phenotype. Deletion of one *Elovl4* allele in mice led to no retinal phenotype (Raz-Prag et al. 2006), suggesting that the observed phenotype in the KI mice was not due to haploinsufficiency. Global knockout or KI of the STGD3 mutant caused neonatal lethality due to loss of skin barrier function, which underscores the importance of these fatty acids in health and disease. The molecular mechanism of the dominant retinal degeneration remains unclear; it could be due to expression and mis-localization of the mutant ELOVL4 or to an age-dependent decrease in VLC-PUFA as a result of the dominant negative effect

of the mutant ELOVL4. Although both are possible, here I focus on the role of ELOVL4-biosynthesized VLC-FA in maintaining the structure and function of tissues in which ELOVL4 is expressed.

18.4 Functional Role of VLC-SFA and VLC-PUFA in ELOVL4 Expressing Tissues

We know that in mammalian tissues, the same ELOVL4 synthesizes two vastly different fatty acid products and that there is tissue specificity in their synthesis. One product is a family of C28–34 saturated fatty acids (VLC-SFA) that are found in wax esters, glucosylceramides, and other sphingolipids that are essential for skin barrier permeability function. These fatty acids are found in meibomian glands (McMahon et al. 2014) and brain as well (Brush et al. 2010). In the eye, VLC-SFA synthesized from meibomian glands contribute to stability of the lipid layer in tear film to control tear evaporation from the cornea and prevent dry eye symptoms (McMahon et al. 2014). The role of these fatty acids in the brain is not known and is a subject of investigation by our laboratory.

The other fatty acids synthesized by ELOVL4 are a family of C28–38 PUFA (VLC-PUFA) that are highly unsaturated and are incorporated into PC in retina and sphingolipids in testes and sperm, where they are essential for normal vision and male fertility, respectively. In sperm, depletion of VLC-PUFA leads to sterility (Zanetti et al. 2007; Zadravec et al. 2011).

We hypothesize that the different mutations in ELOVL4 affect the enzymatic activity in one of two ways. A specific mutation may affect the relative biosynthesis of either VLC-SFA or VLC-PUFA, so that the mutant ELOVL4 that causes SCA may not synthesize VLC-SFA in the brain, but may produce VLC-PUFA in the retina. Alternatively, since mutant ELOVL4 exerts a dominant negative effect on WT ELOVL4, different mutations may influence the types of fatty acids synthesized by WT ELOVL4. We propose a series of experiments to test this hypothesis.

18.5 Proposed Experimental Approaches

The VLC-FA produced by ELOVL4 are absolutely essential for human survival since homozygous inheritance of any known *ELOVL4* mutation leads to death. Understanding the structural and functional role of these fatty acids in tissues in which they are found is important as it will lead to development of potential therapeutic agents for treating the various disorders caused by the different mutations. It is also now clear that different mutations in *ELOVL4* can result in vastly different phenotypes. How is this possible? One plausible explanation lies in the types of fatty acids synthesized by ELOVL4 and the tissue-specific need for these products. For

example, retina has the highest levels of VLC-PUFA of any tissue, followed by the testes which make VLC-PUFA that are incorporated into ceramides and sphingolipids. Skin makes only VLC-SFA, which are incorporated into omega-O-acylceramides and provide the skin permeability barrier. Similarly, ELOVL4 expressed in the meibomian glands makes VLC-SFA that are essential for ocular cell surface integrity and function. Interestingly, although brain has large amounts of C20 and C22 PUFA, it does not contain VLC-PUFA, but rather contains VLC-SFA that are incorporated into sphingolipids.

Since the wild type ELOVL4 synthesizes both VLC-SFA and VLC-PUFA, I hypothesize that the different mutations in the ELOVL4 may affect the quality and the quantity of the fatty acids it synthesizes. This is because the substrates are vastly different, one being a C24–26 saturated fatty acid (highly viscous, linear) and the other a C24–26 polyunsaturated fatty acid (fluid, spiral folding due to 5–6 *cis* double bonds). Therefore, it is possible that the location of the mutation may alter the substrate specificity for either precursor. Alternatively, the mutant ELOVL4 could exert a dominant negative effect on the WT ELOVL4, affecting substrate specificity and thus the products that are formed. In other words, the locations of the mutations could affect the biosynthesis of either VLC-SFA or VLC-PUFA. We know that the STGD3 mutant ELOVL4 exerts a dominant negative effect on VLC-PUFA biosynthesis in the retina and in cultured cells (Logan et al. 2013). However, we do not know its effect on VLC-SFA biosynthesis. Based on the tissue-specific disorders caused by the different ELOVL4 mutations, a number of questions arise that we can address experimentally:

1. Can novel mutant ELOVL4 proteins that cause SCA and neuro-ichthyotic disorders make VLC-PUFA?
2. In the brain, what is the effect of STGD3 mutant ELOVL4 on VLC-SFA biosynthesis?
3. Do these mutant ELOVL4s affect the enzymatic activity of the WT ELOVL4 through a dominant negative effect on biosynthesis of either VLC-SFA or VLC-PUFA?

These questions can be addressed experimentally to determine if the different mutant ELOVL4 enzymes have differential fatty acid condensation and elongation properties that direct the synthesis of either VLC-SFA or VLC-PUFA. I expect that in patients where the mutant ELOVL4 causes CNS and skin disorders, the relative biosynthesis of VLC-PUFA in retina and testes may not be affected, although VLC-SFA biosynthesis will be significantly reduced. Alternatively, just as the STGD3 mutant ELOVL4 exerts a dominant negative effect on the ability of the WT ELOVL4 to synthesize VLC-PUFA, the various mutant ELOVL4s may exert a dominant negative effect on the WT ELOVL4 activity, thereby affecting the quality and quantity of VLC-FA products in a tissue-specific manner.

Lastly, it is possible that since different proteins cooperate with ELOVL4 to synthesize VLC-FA, the various ELOVL4 mutations may affect how these other proteins interact with and regulate VLC-FA biosynthesis, thereby affecting the quality and quantity of VLC-FA synthesized.

18.6 Conclusions

Increasing evidence supports the pathophysiological importance of VLC-FA in health and disease. The ELOVL4 enzyme is the only fatty acid elongase known to mediate biosynthesis of VLC-FA. Hence, mutations in *ELOVL4* result in human disorders of clinical importance. With the advent of new technology that aids identification and analysis of ELOVL4 biosynthesized products, we are at the threshold of understanding the biological importance of these unique molecules, which have been ignored for decades. An understanding of the structural and functional role of these fatty acids will pave the way for development of therapeutic agents for treating human diseases that are caused by mutations in the *ELOVL4* gene.

Acknowledgements Supported in part by grants from Hope for Vision, Knight Templar Eye Foundation Inc., and BrightFocus Foundation Inc., to MPA; NIH/NEI (EY04149 and EY21725 and the Foundation Fighting Blindness to my mentor, Robert E. Anderson, MD, PhD; and Research to Prevent Blindness, Inc. Thanks to Professor Anderson for his valuable comments and suggestions.

References

Agbaga MP, Brush RS, Mandal MN et al (2008) Role of Stargardt-3 macular dystrophy protein (ELOVL4) in the biosynthesis of very long chain fatty acids. Proc Natl Acad Sci U S A 105:12843–12848.

Aldahmesh MA, Mohamed JY, Alkuraya HS et al (2011) Recessive mutations in ELOVL4 cause ichthyosis, intellectual disability, and spastic quadriplegia. Am J Hum Genet 89:745–750.

Bernstein PS, Tammur J, Singh N et al (2001) Diverse macular dystrophy phenotype caused by a novel complex mutation in the ELOVL4 gene. Invest Ophthalmol Vis Sci 42:3331–3336.

Brush RS, Tran JT, Henry KR et al (2010) Retinal sphingolipids and their very-long-chain fatty acid-containing species. Invest Ophthalmol Vis Sci 51:4422–4431.

Butovich IA, Wojtowicz JC, Molai M (2009) Human tear film and meibum. Very long chain wax esters and (O-acyl)-omega-hydroxy fatty acids of meibum. J Lipid Res 50:2471–2485.

Cadieux-Dion M, Turcotte-Gauthier M, Noreau A et al (2014) Expanding the clinical phenotype associated with ELOVL4 mutation: study of a large French–Canadian family with autosomal dominant spinocerebellar ataxia and erythrokeratodermia. JAMA Neurol 71:470–475

Edwards AO, Donoso LA, Ritter R 3rd (2001) A novel gene for autosomal dominant Stargardt-like macular dystrophy with homology to the SUR4 protein family. Invest Ophthalmol Vis Sci 42:2652–2663.

Logan S, Agbaga MP, Chan MD et al (2013) Deciphering mutant ELOVL4 activity in autosomal-dominant Stargardt macular dystrophy. Proc Natl Acad Sci USA 110:5446-

Maugeri A, Meire F, Hoyng CB et al (2004) A novel mutation in the ELOVL4 gene causes autosomal dominant Stargardt-like macular dystrophy. Invest Ophthalmol Vis Sci 45: 4263–4267.

McMahon A, Jackson SN, Woods AS et al (2007a) A Stargardt disease-3 mutation in the mouse Elovl4 gene causes retinal deficiency of C32-C36 acyl phosphatidylcholines. FEBS Lett 581:5459–5463.

McMahon A, Butovich IA, Mata NL et al (2007b) Retinal pathology and skin barrier defect in mice carrying a Stargardt disease-3 mutation in elongase of very long chain fatty acids-4. Mol Vis 13:258–272.

McMahon A, Lu H, Butovich IA (2014) A role for ELOVL4 in the mouse meibomian gland and sebocyte cell biology. Invest Ophthalmol Vis Sci 55:2832–2840.

Mir H, Raza SI, Touseef M et al (2014) A novel recessive mutation in the gene ELOVL4 causes a neuro-ichthyotic disorder with variable expressivity. BMC Med Genet 15:25.

Raz-Prag D, Ayyagari R, Fariss RN et al (2006) Haploinsufficiency is not the key mechanism of pathogenesis in a heterozygous Elovl4 knockout mouse model of STGD3 disease. Invest Ophthalmol Vis Sci 47:3603–3611.

Vasireddy V, Uchida Y, Salem N Jr, et al (2007) Loss of functional ELOVL4 depletes very long-chain fatty acids (≧C28) and the unique omega-O-acylceramides in skin leading to neonatal death. Hum Mol Genet 16:471–482.

Zadravec D, Tvrdik P, Guillou H et al (2011) ELOVL2 controls the level of n-6 28:5 and 30:5 fatty acids in testis, a prerequisite for male fertility and sperm maturation in mice. J Lipid Res 52:245–255.

Zanetti SR, Maldonado EN, Aveldano MI (2007) Doxorubicin affects testicular lipids with long-chain (C18-C22) and very long-chain (C24-C32) polyunsaturated fatty acids. Cancer Res 67:6973–6980.

Zhang K, Kniazeva M, Han M et al (2001) A 5-bp deletion in ELOVL4 is associated with two related forms of autosomal dominant macular dystrophy. Nat Genet 27:89–93.

Chapter 19
Mouse Models of Stargardt 3 Dominant Macular Degeneration

Peter Barabas, Aruna Gorusupudi, Paul S Bernstein and David Krizaj

Abstract Stargardt type 3 macular degeneration is dependent on a dominant defect in a single gene, *ELOVL4* (elongase of very long chain fatty acids 4). The encoded enzyme, ELOVL4, is required for the synthesis of very long chain polyunsaturated fatty acids (VLC-PUFAs), a rare class of >C24 lipids. *In vitro* expression studies suggest that mutated ELOVL4^{STGD3} proteins fold improperly, resulting in ER stress and formation of cytosolic aggresomes of wild type and mutant ELOVL4. Although a number of mouse models have been developed to determine whether photoreceptor cell loss in STGD3 results from depletion of VLC-PUFAs, aggresome-dependent cell stress or a combination of these two factors, none of these models adequately recapitulates the disease phenotype in humans. Thus, the precise molecular mechanism by which *ELOVL4* mutation causes photoreceptor degeneration in mice and in human patients remains to be characterized. This mini review compares and evaluates current STGD3 mouse models and determines what conclusions can be drawn from past work.

Keywords ELOVL4 · STGD3 · Very long chain polyunsaturated fatty acids (VLC-PUFAs) · Transgenic mice · Knock-in mice · Knock-out mice · pLox · Cre · Phenotype

P. Barabas (✉) · A. Gorusupudi · P. S. Bernstein · D. Krizaj
Department of Ophthalmology and Visual Sciences, John A. Moran Eye Institute, University of Utah School of Medicine, Salt Lake City, UT 84132, USA
e-mail: peter.barabas@utah.edu

A. Gorusupudi
e-mail: aruna.gorusupudi@utah.edu

P. S. Bernstein
e-mail: paul.bernstein@hsc.utah.edu

D. Krizaj
e-mail: david.krizaj@hsc.utah.edu

C. Bowes Rickman et al. (eds.), *Retinal Degenerative Diseases,* Advances in Experimental Medicine and Biology 854, DOI 10.1007/978-3-319-17121-0_19

19.1 Introduction

Stargardt 3 is an early onset macular degeneration characterized by a progressive loss of central vision (McMahon and Kedzierski 2010; Zhang et al. 2001; Bernstein et al. 2001). Similarly to the more prevalent Stargardt 1 disease, the STGD3 phenotype has been associated with defects in a single gene (Bernstein et al. 2001; Zhang et al. 2001), the elongase of very long chain fatty acids 4 (*ELOVL4)*. Mutations found in STGD3 patients affect the C-terminal end of the ELOVL4 protein that contains a di-lysine motif thought to regulate protein retention within the endoplasmic reticulum (ER) (Vasireddy et al. 2010). This is believed to derail proper localization of the protein to the ER, where very long chain fatty acid (VLC-FA) synthesis takes place and to suppress the biosynthetic capacity of the wild type ELOVL4 enzyme by removing it as well from the ER (Agbaga et al. 2008; Guillou et al. 2010; Logan et al. 2013). Because ELOVL4 expression in adult vertebrate eyes is limited to the photoreceptor layer (Zhang et al. 2003; Agbaga et al. 2008), its VLC-PUFA products are likely to play specific but yet to be defined, functions in cones and rods (Zemski Berry et al. 2014). It has been hypothesized that these lipids provide superior fluidity and stabilizing highly curved regions of cell membranes and might therefore play a function in phototransduction, outer segment maintenance and/or formation and release of synaptic vesicles (SanGiovanni and Chew 2005; Guillou et al. 2010; McMahon and Kedzierski 2010; Bennett et al. 2014b).

19.2 Cell Culture Studies

The leading hypotheses of STGD3 pathomechanisms are based on studies of transgenic cell cultures where ELOVL4 was expressed alone and/or in combination with the STGD3-causing mutant *ELOVL4* gene (Karan et al. 2005; Logan et al. 2013). These studies showed that the mutant protein aggregates with the wild type version and translocates it from the ER to the cytoplasm, possibly forming aggresomes (Ambasudhan et al. 2004; Karan et al. 2005; Grayson and Molday 2005). The impaired trafficking hypothesis provides a plausible mechanism for the dominant inheritance of the disease in STGD3 patients. It also predicts that photoreceptor cells expressing mutated ELOVL4 face ER stress and unfolded protein response (Lin et al. 2008) in parallel to the lost ELOVL4 function and depletion of VLC-PUFAs. Thus, it would be important to determine whether STDG3 is primarily mediated by loss of function due to mutated ELOVL4 or, as observed in other degenerative diseases of photoreceptor cells (Lin and Lavail 2010), as a result of protein misfolding and ER stress.

While misrouting is sufficient to induce loss of enzyme function (Logan et al. 2014), recent studies also established that the mutant ELOVL4 protein's loss of function and dominant negative effect is not necessarily driven by insufficient ER retention (Logan et al. 2013). *In vivo* analysis in the transgenic Xenopus model showed that the mutant protein is trafficked to the photoreceptor outer segment,

but it does not impede the normal compartmentalization of wild type ELOVL4 (Agbaga et al. 2014). Thus, whether and to what extent information from *in vitro* studies can be applied to understand the human STGD3 disease process remains an open question.

19.3 Mouse Models: Knock-IN and Knock-OUT Strains

An overarching aim of STGD3 animal model development has been to unveil the causal connection between the genotype and early-onset progressive cone degeneration observed in humans. The early studies were stymied by the discovery that global homozygous *Elovl4* knockout and knock-in of the human mutation into the mouse *Elovl4* gene are perinatally lethal due to loss of skin acyl-ceramides, required to maintain the water barrier function (Vasireddy et al. 2007). Heterozygotes of both strains are viable but *Elovl4*$^{+/-}$ mice show no detectable phenotype (Raz-Prag et al. 2006; Li et al. 2007), suggesting that *Elovl4* haploinsufficiency and decreased function does not result in degeneration in the mouse. Further questions were raised by the observation that knock-in (KI) heterozygote mice, which represent the closest genetic approximation to the human condition, do not exhibit early-onset cone degeneration. Rather, late onset (8–15 months) and conflicting physiological changes were reported for KI animals: maximal scotopic ERG b-wave amplitudes were increased (Vasireddy et al. 2006) in one, decreased in a different study (McMahon et al. 2007). Consistent with other reports (McMahon et al. 2007; Mandal et al. 2014), our own analysis shows ~50% decrease of C30-C36 VLC-PUFA levels in retinas of KI mice (53.7±8.8% of control). However, this decrease in VLC-PUFA content was not sufficient to induce a behavioral phenotype. As shown in Fig. 19.1, the KI strain exhibits no visual acuity defect, as measured by their optomotor tracking behavior.

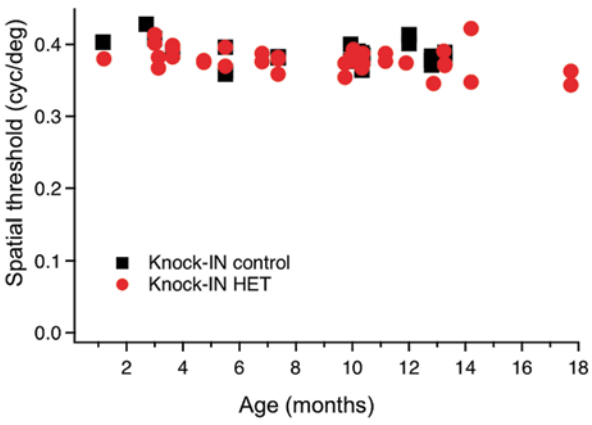

Fig. 19.1 Visual performance was measured in Knock-IN heterozygous mice and wild type strain controls using their optomotor reflex to establish a spatial frequency threshold (OptoMotry, Cerebral Mechanics). Each symbol represents the visual acuity for the test of a single mouse at the specified age. No significant difference between the groups was detected

19.4 Mouse Models: Transgenic and Cell Specific Knockout Mice

Other STGD3 mouse models include transgenic mice that express either human wild type or mutant *ELOVL4* (Karan et al. 2005; Kuny et al. 2010, 2012; Barabas et al. 2013) or cell specific knockdowns where mouse *Elovl4* was knocked out specifically from cones (Harkewicz et al. 2012; Barabas et al. 2013) or rods (Harkewicz et al. 2012; Barabas et al. 2013; Marchette et al. 2014) or the entire retina (Bennett et al. 2014a, 2014b). Unexpectedly, only the transgenic strains show early onset photoreceptor degeneration (Karan et al. 2005; Kuny et al. 2010, 2012) with onset time and severity depending on transgene expression level. A major discrepancy with regard to the human disease is that degeneration in transgenic animals starts with a massive loss of rods only secondarily followed by cone degeneration (Kuny et al. 2012; Barabas et al. 2013).

Pan-retinal *Elovl4* KOs were characterized by decreased synaptic vesicle size & number in rod terminals, formation of ectopic rod-bipolar synapses associated with sprouting of bipolar dendrites and a reduction in scotopic ERG causing late (after 12 months) degeneration of rods (Bennett et al. 2014a, 2014b). Interestingly, the phenotype was not associated with changes in the postsynaptic excitatory response (Bennett et al. 2014b).

Conditional elimination of ELOVL4 from a single photoreceptor cell class gave discrepant results. The first study indicated a reduction in VLC-PUFA content and loss of rod and cone function in rod and cone conditional knockout (cKO) animals, respectively (Harkewicz et al. 2012). However, the subsequent two studies found no effect on rod (Barabas et al. 2013; Marchette et al. 2014) or cone function and survival (Barabas et al. 2013). Differences between cre expression and knockdown efficiency do not account for these discrepancies as the same cre system with approximately 60–80% efficiency (Le et al. 2006; Barabas et al. 2013) was used in all of these studies. The latter studies (Barabas et al. 2013; Marchette et al. 2014) observed no effect on scotopic or photopic ERGs or visual behavior even when the highly efficient iCre-75 was used to cause a massive (98%) reduction in retinal VLC-PUFA content (Barabas et al. 2013). Major distinguishing factors in these studies were the use of different controls (C57B/6 mice in the Harkewicz et al. study, and congenic controls in the Barabas et al and Marchette et al studies), as well as the ages of the mice varied.

The important conclusion from knockdown studies is that deletion of *Elovl4* from photoreceptor cells does indeed deplete retinal >C30 VLC-PUFA levels (Barabas et al. 2013; Bennett et al. 2014a). Selective and highly efficacious elimination of the gene (together with near total loss of VLC-PUFAs from the mouse retina) shows a late-onset rod phenotype but no single KO or cKO strains has so far replicated the early cone loss phenotype seen in STGD3 patients.

19.5 Open Questions

Taken together, many open questions remain with respect to the pathophysiology of STGD3. Among the fundamental unresolved issues are (1) what is the function of VLC-PUFAs in photoreceptors? (2) What is the actual cause of the autosomal dominance of ELOVL4? And (3) Why does STGD3 affect cones in humans, are macular cones more sensitive to loss of VLC-PUFAs? The mild-to-none phenotypes of knock-in heterozygotes (McMahon et al. 2007; Vasireddy et al. 2006), knock-out heterozygotes (Raz-Prag et al. 2006; Li et al. 2007), and cell-specific homozygote knockout mice (Barabas et al. 2013; Marchette et al. 2014) and the late-onset rod-specific phenotype of total retinal knockdowns (Bennett et al. 2014a, 2014b) suggest that significant loss of VLC-PUFA levels is not sufficient to cause early onset cone degeneration in the mouse retina. It is possible that residual VLC-PUFAs (~2% of control) are sufficient to maintain mouse photoreceptors, especially given that normal levels of VLC-PUFAs in mice are approximately 10 times higher compared to human (*post mortem*) retinal tissue (Liu et al. 2013). This may confer resistance to mouse photoreceptors in the form of VLC-PUFA "buffering". Indeed, clinical and biochemical studies indicate that the human retina may be more sensitive to VLC-PUFA depletion. An inverse association was found between the severity of STGD3 and dietary intake of VLC-PUFA precursors (Hubbard et al. 2006) and loss of VLC-PUFAs was exacerbated in AMD patient eyes compared to age matched controls (Liu et al. 2010). The above data give an impetus to mouse studies, which will need to endow the mouse retina with at least some features of the human macula, establish the relative importance of loss of VLC-PUFAs and presence of the mutated protein and unveil the function of VLC-PUFAs in the healthy retina.

References

Agbaga MP, Brush RS, Mandal MN et al (2008) Role of Stargardt-3 macular dystrophy protein (ELOVL4) in the biosynthesis of very long chain fatty acids. Proc Natl Acad Sci U S A 105:12843–12848

Agbaga MP, Tam BM, Wong JS (2014) Mutant ELOVL4 that causes autosomal dominant stargardt-3 macular dystrophy is misrouted to rod outer segment disks. Invest Ophthalmol Vis Sci 55:3669–3680

Ambasudhan R, Wang X, Jablonski MM et al (2004) Atrophic macular degeneration mutations in ELOVL4 result in the intracellular misrouting of the protein. Genomics 83:615–625

Barabas P, Liu A, Xing W et al (2013) Role of ELOVL4 and very long-chain polyunsaturated fatty acids in mouse models of Stargardt type 3 retinal degeneration. Proc Natl Acad Sci U S A 110:5181–5186

Bennett LD, Brush RS, Chan M et al (2014a) Effect of reduced retinal VLC-PUFA on rod and cone photoreceptors. Invest Ophthalmol Vis Sci 55:3150–3157

Bennett LD, Hopiavuori BR, Brush RS et al (2014b) Examination of VLC-PUFA-deficient photoreceptor terminals. Invest Ophthalmol Vis Sci 55:4063–4072

Bernstein PS, Tammur J, Singh N et al (2001) Diverse macular dystrophy phenotype caused by a novel complex mutation in the ELOVL4 gene. Invest Ophthalmol Vis Sci 42:3331–3336

Grayson C, Molday RS (2005) Dominant negative mechanism underlies autosomal dominant Stargardt-like macular dystrophy linked to mutations in ELOVL4. J Biol Chem 280:32521–32530
Guillou H, Zadravec D, Martin PG et al (2010) The key roles of elongases and desaturases in mammalian fatty acid metabolism: insights from transgenic mice. Prog Lipid Res 49:186–199
Harkewicz R, Du H, Tong Z et al (2012) Essential role of ELOVL4 protein in very long chain fatty acid synthesis and retinal function. J Biol Chem 287:11469–11480
Hubbard AF, Askew EW, Singh N et al (2006) Association of adipose and red blood cell lipids with severity of dominant Stargardt macular dystrophy (STGD3) secondary to an ELOVL4 mutation. Arch Ophthalmol 124:257–263
Karan G, Lillo C, Yang Z et al (2005) Lipofuscin accumulation, abnormal electrophysiology, and photoreceptor degeneration in mutant ELOVL4 transgenic mice: a model for macular degeneration. Proc Natl Acad Sci U S A 102:4164–4169
Kuny S, Gaillard F, Mema SC et al (2010) Inner retina remodeling in a mouse model of stargardt-like macular dystrophy (STGD3). Invest Ophthalmol Vis Sci 51:2248–2262
Kuny S, Gaillard F, Sauvé Y (2012) Differential gene expression in eyecup and retina of a mouse model of Stargardt-like macular dystrophy (STGD3). Invest Ophthalmol Vis Sci 53:664–675
Le YZ, Zheng L, Zheng W et al (2006) Mouse opsin promoter-directed Cre recombinase expression in transgenic mice. Mol Vis 12:389–398.
Li W, Chen Y, Cameron DJ et al (2007) Elovl4 haploinsufficiency does not induce early onset retinal degeneration in mice. Vis Res 47:714–722
Lin JH, Lavail MM (2010) Misfolded proteins and retinal dystrophies. Adv Exp Med Biol. 664:115–121
Lin JH, Walter P, Yen TS (2008) Endoplasmic reticulum stress in disease pathogenesis. Annu Rev Pathol 3:399–425
Liu A, Chang J, Lin Y et al (2010) Long-chain and very long-chain polyunsaturated fatty acids in ocular aging and age-related macular degeneration. J Lipid Res 51:3217–3229
Liu A, Terry R, Lin Y et al (2013) Comprehensive and sensitive quantification of long-chain and very long-chain polyunsaturated fatty acids in small samples of human and mouse retina. J Chromatogr A 1307:191–200
Logan S, Agbaga MP, Chan MD et al (2013) Deciphering mutant ELOVL4 activity in autosomal-dominant Stargardt macular dystrophy. Proc Natl Acad Sci U S A 110:5446–5451
Logan S, Agbaga MP, Chan MD et al (2014) Endoplasmic reticulum microenvironment and conserved histidines govern ELOVL4 fatty acid elongase activity. J Lipid Res 55:698–708
Mandal NA, Tran JT, Zheng L et al (2014) In vivo effect of mutant ELOVL4 on the expression and function of wild-type ELOVL4. Invest Ophthalmol Vis Sci 55:2705–2713
Marchette LD, Sherry DM, Brush RS et al (2014) Very long chain polyunsaturated fatty acids and rod cell structure and function. Adv Exp Med Biol 801:637–645
McMahon A, Kedzierski W (2010) Polyunsaturated very-long-chain C28-C36 fatty acids and retinal physiology. Br J Ophthalmol 94:1127–1132
McMahon A, Jackson SN, Woods AS et al (2007) A Stargardt disease-3 mutation in the mouse Elovl4 gene causes retinal deficiency of C32-C36 acyl phosphatidylcholines. FEBS Lett 581:5459–5463
Raz-Prag D, Ayyagari R, Fariss RN et al (2006) Haploinsufficiency is not the key mechanism of pathogenesis in a heterozygous Elovl4 knockout mouse model of STGD3 disease. Invest Ophthalmol Vis Sci 47:3603–3611
SanGiovanni JP, Chew EY (2005) The role of omega-3 long-chain polyunsaturated fatty acids in health and disease of the retina. Prog Retin Eye Res 24:87–138
Vasireddy V, Jablonski MM, Mandal MN et al (2006) Elovl4 5-bp-deletion knock-in mice develop progressive photoreceptor degeneration. Invest Ophthalmol Vis Sci 47:4558–4568
Vasireddy V, Uchida Y, Salem N Jr. et al (2007) Loss of functional ELOVL4 depletes very long-chain fatty acids (> or = C28) and the unique omega-O-acylceramides in skin leading to neonatal death. Hum Mol Genet 16:471–482
Vasireddy V, Wong P, Ayyagari R (2010) Genetics and molecular pathology of Stargardt-like macular degeneration. Prog Retin Eye Res 29:191–207

Zemski Berry KA, Gordon WC, Murphy RC et al (2014) Spatial organization of lipids in the human retina and optic nerve by MALDI imaging mass spectrometry. J Lipid Res 55:504–515
Zhang K, Kniazeva M, Han M et al (2001) A 5-bp deletion in ELOVL4 is associated with two related forms of autosomal dominant macular dystrophy. Nat Genet 27:89–93
Zhang XM, Yang Z, Karan G et al (2003) Elovl4 mRNA distribution in the developing mouse retina and phylogenetic conservation of Elovl4 genes. Mol Vis 9:301–307

Chapter 20
Current Progress in Deciphering Importance of VLC-PUFA in the Retina

Lea D. Bennett and Robert E. Anderson

Abstract Stargardt-like macular dystrophy-3 (STGD3) is a juvenile-onset disease caused by mutations in *ELOVL4* (**elo**ngation of **v**ery **l**ong fatty acids-**4**). This gene product catalyzes the elongation of long chain saturated and polyunsaturated fatty acids (LC-FAs and LC-PUFAs) into *very* long chain FAs and PUFAs (VLC-FAs and VLC-PUFAs). These mutations cause a frame shift in the ELOVL4 transcript, introducing a premature stop codon that results in the translation of a truncated protein that has lost a C-terminus endoplasmic reticulum (ER) retention/retrieval signal. The truncated protein is not targeted to the ER, the site of very long-chain PUFA (VLC-PUFA; 28–40 carbons) synthesis. Expression of the *ELOVL4* gene is limited mainly to the brain, testis, skin, and photoreceptor cells of the retina. While the skin and brain contain very long chain saturated fatty acids (VLC-FAs), the other tissues expressing ELOVL4 contain VLC-PUFAs, with sperm and the retina having the highest levels. This review focuses on the current information available concerning the role of VLC-PUFAs in the retina.

Keywords VLC-PUFA · ELOVL4 · STGD3 · Dominant Stargardt's · Rod and cone function · Conditional KO mice · Transgenic mice · Cre · Retina

R. E. Anderson (✉)
Department of Cell Biology and Ophthalmology, University of Oklahoma Health Sciences Center, 608 Stanton L. Young Blvd., Oklahoma City, OK 73104, USA
e-mail: Robert-Anderson@ouhsc.edu

Dean A. McGee Eye Institute, Oklahoma City, OK, USA

L. D. Bennett
Retina Foundation of the Southwest, 9600 North Central Expwy, Suite 200, Dallas, TX 75231, USA
e-mail: LBennett@retinafoundation.org

C. Bowes Rickman et al. (eds.), *Retinal Degenerative Diseases,* Advances in Experimental Medicine and Biology 854, DOI 10.1007/978-3-319-17121-0_20

20.1 Introduction

Stargardt-like macular dystrophy-3 (STGD3) is an autosomal dominant disease with juvenile onset. Patients have retinal pigmented epithelium (RPE) atrophy, macular lesions with surrounding yellow flecks, and progressive loss of central vision (Edwards et al. 1999). The gene responsible for STGD3 is *ELOVL4* (elongation of very long-chain fatty acids-4) (Bernstein et al. 2001; Edwards et al. 2001; Zhang et al. 2001). Mutations in *ELOVL4* truncate the protein so that it loses the endoplasmic reticulum retention signal and is mislocalized from the site of synthesis of very long chain polyunsaturated fatty acids (VLC-PUFAs).

VLC-PUFAs comprise ~13 mol% in the fatty acids in phosphatidylcholine (PC) of bovine retina rod outer segments, with ~26% of the PC containing one of these fatty acids (Aveldaño and Sprecher 1987). These fatty acids have been shown to interact tightly with rhodopsin, suggesting a role for VLC-PUFAs in phototransduction (Aveldano 1988). It has also been suggested that these unusually long fatty acids with bulky hydrocarbon tails are anatomically suited to provide structure to highly curved membranes such as photoreceptor outer segment disks and sperm heads (Aveldano 1992; Agbaga et al. 2008). Recently, VLC-PUFAs were reported to be localized to conventional and ribbon synapses in the retina (Bennett et al. 2014a). Enrichment of VLC-PUFA in the retina is indicative of the need for these specialized molecules in this tissue, although their role has not yet been established.

20.2 Comparison of Mouse Models

The role of VLC-PUFAs in membranes is not known. Global deletion of *Elovl4* in mice is neonatal lethal (Raz-Prag et al. 2006; Vasireddy et al. 2006; Anne McMahon et al. 2007; Li et al. 2007) and all other mouse models used to study the role of these fatty acids is obscured with either at least one wild type (WT) or one mutant copy of *Elovl4* (Raz-Prag et al. 2006; Vasireddy et al. 2006; Anne McMahon et al. 2007; McMahon et al. 2011; Harkewicz et al. 2012; Barabas et al. 2013).

Removal of Elovl4 expression in rods, cones, or both rods and cones has been achieved by breeding mice expressing *Cre*-recombinase driven by different photoreceptor specific promoters to *Elovl4*$^{flox/flox}$ mice (Harkewicz et al. 2012; Barabas et al. 2013; Bennett et al. 2014b; Marchette et al. 2014). Cone-specific human red-green pigment *(HRGP)-Cre*- and rod-specific *Opsin-cre*- or *opsin-iCre75*-expressing mice were used to delete Elovl4 from cones and rods, respectively, whereas *Elovl4* was deleted from both photoreceptor types using *Chx10-cre*-expressing mice (Harkewicz et al. 2012; Barabas et al. 2013; Bennett et al. 2014b). A summary of the results from each study are provided in Table 20.1.

Harkewicz et al. (2012) reported that rod-specific *Elovl4* conditional KO (R-cKO) mice had retinal degeneration at 10 and 15 months of age, whereas Barabas et al. (2013) and Marchette et al. (2014) did not find photoreceptor degeneration in R-cKO mice at 7 and 15 months, respectively. Harkewicz et al. (2012)

found R-cKO mice had decreased rod b-wave responses, but Barabas et al. (2013) and Marchette et al. (2014) did not find rod-mediated deficits in their 6- or 7-month-old R-cKO mice, respectively. When *Elovl4* was deleted from both rods and cones (RC-cKO), retinal degeneration occurred and rod ERG responses were decreased in 12-month-old mice (Bennett et al. 2014b). One possible explanation for the contradictory results could be the mosaic expression of *Cre*-recombinase, which resulted in varying degrees of *Elovl4* ablation from rod cells. Rod *Opsin-Cre* has been previously reported to have 77% recombinase efficiency (Le et al. 2006), whereas the *Chx10-Cre* has been shown to have more than 95% recombinase efficiency (Rowan and Cepko 2004). This is obviated when the reduction of retinal VLC-PUFAs are considered (Table 20.1). These fatty acids were decreased by 36–97% of WT values in the R-cKO and RC-cKO mice (Harkewicz et al. 2012; Barabas et al. 2013; Bennett et al. 2014b; Marchette et al. 2014).

Table 20.1 Comparison of the effects of mutations in *Elovl4* on various retinal parameters

–	Age (months)	ERG	Retinal degeneration	Retina VLC-PUFA levels	RPE
R-cKO (Harkewicz et al. 2012)	10 and 15	Decreased rod b-wave and mixed response b-wave	Yes	Decreased more than half	Lipofuscin and lipid drops (TEM)
C-cKO (Harkewicz et al. 2012)	7	Decreased cone flicker response	No	Mild decrease	Lipofuscin and lipid drops (TEM)
R-cKO (Barabas et al. 2013)	6	Not affected	No	Lines 1 and 2 decreased by 58 and 97%	Putative lipid droplets (TEM)
C-cKO (Barabas et al. 2013)	6	Not affected	No	normal	No (TEM)
R-cKO (Marchette et al. 2014)	7, 9, and 15	Not at 7 months. Not tested later.	No	Decrease by 36%	Not tested
RC-cKO (Bennett et al. 2014a, 2014b)	1 and 12	Rod a- and b-waves, STR, and OPs decreased (12 mo). Cones not affected	Yes (12 mo)	Decrease by 88%	No (9 mo; A2E and derivitives; MS/MS)
Human (Edwards et al. 1999)	Diagnosed in teenage years	Variable; moderately reduced in older patients	Yes	Unknown	Lipofuscin

R-cKO rod-specific conditional KO, *C-cKO* cone-specific conditional KO, *RC-cKO* rod and Cone-specific conditional KO, *RPE* retinal pigmented epithelium, *VLC-PUFA* very long chain polyunsaturated fatty acids, *TEM* transmission electron microscopy, *MS/MS* tandem mass spectroscopy, *ERG* electroretinography

The VLC-PUFA levels in the cone-specific *Elovl4* ablated mice (C-cKO) were unaffected (Table 20.1), but this could be due to the fact that mice are rod-dominant and that these fatty acids comprise only 12% of the total fatty acids in the retina (Rotstein and Aveldano 1988). Despite the minimal decrease in VLC-PUFAs, Harkewicz et al. (2012) found that *Elovl4 C*-cKO mice had decreased cone flicker responses at 7 months of age compared to WT mice. These results are contrary to Barabas et al. (2013) and Bennett et al. (2014b), who did not find cone dysfunction at 6 and 12 months, respectively.

Differences between the published results could be attributed to the different mouse backgrounds and/or the absence of using similar mice as controls. Harkewicz et al. (2012) used generic WT mice whereas Barabas et al. (2013), Bennett et al. (2014b), and Marchette et al. (2014) used $Cre^{-/-}/Elovl4^{flox/flox}$ mice as controls. Cre expression remained in the photoreceptors of adult R-cKO and C-cKO mice, unlike the RC-cKO mice, which did not express Cre in adult photoreceptors. Since the $Elovl4^{f/f}$ mice used in all four studies were from the same founders and had intronic LoxP sites, the wild type Elovl4 protein would be expressed in the absence of Cre-recombinase. To control for potential consequences of Cre transgene expression, Bennett et al. (2014b) included control mice that expressed Cre and were heterozygous for the floxed allele ($Cre^{+}/Elovl4^{flox/WT}$; Het). Given that VLC-PUFAs were not reduced in the Het mice and other measured parameters such as ERG and histology were not different than WT, consequences of tissue-specific *Elovl4* ablation were not due to off-target effects of Cre expression.

20.3 Discussion

After reviewing the current literature on the role of VLC-PUFAs in the retina, we can certainly agree that these fatty acids are important in photoreceptor function with a secondary contribution to photoreceptor longevity. Because VLC-PUFAs were localized to the synaptic membranes and the RC-cKO retinas had smaller vesicles and fewer vesicles per ribbon than their littermates, these fatty acids are probably enriched in the retinal synaptic vesicles (Bennett et al. 2014a). This is supported by the single cell recordings on the RC-cKO retinas that showed that receptor calcium currents and the post-receptor glutamate currents were not affected by reduced VLC-PUFAs (Bennett et al. 2014a). Therefore it is likely that VLC-PUFAs are incorporated into the glutamate-containing vesicles of rod terminals, increasing vesicle size with their bulky polyunsaturated hydrocarbon tails (Fig. 20.1a), and ultimately affecting biophysical properties of the vesicles at the photoreceptor terminals. Vesicles comprised of VLC-PUFA would also be more fluid, allowing for ease of fusion with the plasma membrane (Fig. 20.1b and c). The VLC-PUFAs could be incorporated into vesicles that contain or interact with synaptic proteins that mediate endo/exocytic activity, thereby affecting vesicle recycling pathway in the rod terminal. In the same way, reduction of VLC-PUFAs could affect protein transport, especially if that protein were localized to the synaptic ribbon in

photoreceptor terminals, as this may affect vesicle tethering or glutamate release mechanisms.

The importance of these fatty acids would be solidified if VLC-PUFAs could be reconstituted in the deficient retinas. However, VLC-PUFAs cannot be chemically synthesized in large enough quantities to allow feeding studies in mice with specific Elovl4 deletions. Our current strategy is to express *Elovl4* in the RPE under the control of the bestropin promoter and use the short loop of fatty acid recycling between the retina and the RPE to provide VLC-PUFA to the retinal synapses and

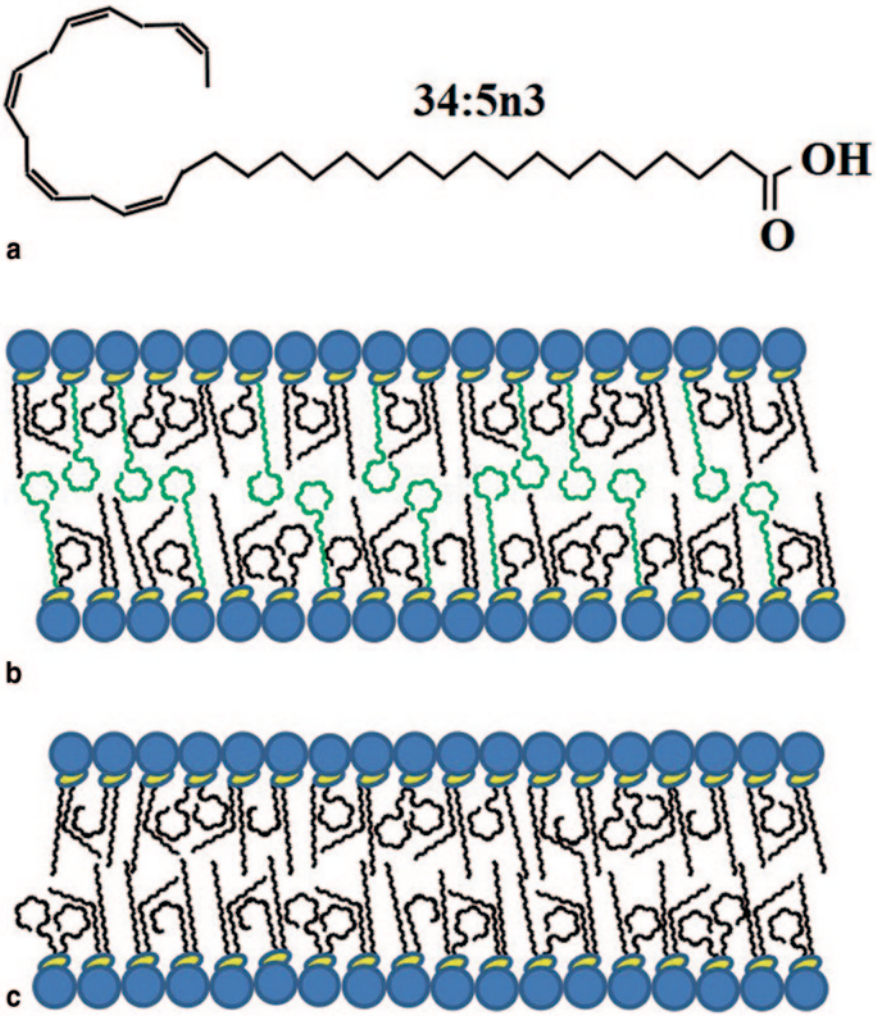

Fig. 20.1 VLC-PUFA affect vesicle biophysical properties. **a** An example of VLC-PUFA (34:5n3) that has 34 carbons and 5 omega-3 double bonds. **b** Vesicle phospholipid membrane with VLC-PUFAs (*green*) would be larger and more compliant compared to **c** A vesicle membrane without VLC-PUFA, which would be smaller and more rigid

outer segments. We are also working on ways to silence the mutant *Elovl4* with siRNA. A combined therapy of VLC-PUFA supplementation with knock down of the mutant transcript would be the ideal therapeutic to address possible effects of the mutant protein and the decrease in retinal VLC-PUFAs.

Acknowledgments This work was supported by NIH Grants EY00871, EY04149, EY12190, EY21725 and RR17703; Foundation Fighting Blindness, and Research to Prevent Blindness.

References

Agbaga M-P, Brush RS, Mandal MNA et al (2008) Role of Stargardt-3 macular dystrophy protein (ELOVL4) in the biosynthesis of very long chain fatty acids. Proc Natl Acad Sci U S A 105:12843–12848

Anne McMahon IAB, Nathan L Mata, Martin Klein, Robert Ritter III, James Richardson, David G Birch, Albert O Edwards, Wojciech Kedzierski (2007) Retinal pathology and skin barrier defect in mice carrying a Stargardt disease-3 mutation in elongase of very long chain fatty acids-4. Mol Vis 13:258–272

Aveldano MI (1988) Phospholipid species containing long and very long polyenoic fatty acids remain with rhodopsin after hexane extraction of photoreceptor membranes. Biochemistry 27:1229–1239

Aveldano MI (1992) Long and very long polyunsaturated fatty acids of retina and spermatozoa: the whole complement of polyenoic fatty acid series. Adv Exp Med Biol 318:231–242

Aveldaño MI, Sprecher H (1987) Very long chain (C24 to C36) polyenoic fatty acids of the n-3 and n-6 series in dipolyunsaturated phosphatidylcholines from bovine retina. J Biol Chem 262:1180–1186

Barabas P, Liu A, Xing W et al (2013) Role of ELOVL4 and very long-chain polyunsaturated fatty acids in mouse models of Stargardt type 3 retinal degeneration. Proc Natl Acad Sci U S A 110:5181–5186

Bennett LD, Hopiavuori BR, Brush RS et al (2014a) Examination of VLC-PUFA-deficient photoreceptor terminals. Invest Ophthalmol Vis Sci 55(7):4063–72

Bennett LD, Brush RS, Chan MD et al (2014b) Effect of reduced retinal VLC-PUFA on rod and cone photoreceptors. Invest Ophthalmol Vis Sci 55(5):3150–3157

Bernstein PS, Tammur J, Singh N et al (2001) Diverse macular dystrophy phenotype caused by a novel complex mutation in the ELOVL4 gene. Invest Ophthalmol Vis Sci 42:3331–3336

Edwards AO, Miedziak A, Vrabec T et al (1999) Autosomal dominant Stargardt-like macular dystrophy: I. Clinical characterization, longitudinal follow-up, and evidence for a common ancestry in families linked to chromosome 6q14. Am J Ophthalmol 127:426–435

Edwards AO, Donoso LA, Ritter R 3rd (2001) A novel gene for autosomal dominant Stargardt-like macular dystrophy with homology to the SUR4 protein family. Invest Ophthalmol Vis Sci 42:2652–2663

Harkewicz R, Du H, Tong Z et al (2012) Essential role of ELOVL4 protein in very long chain fatty acid synthesis and retinal function. J Biol Chem 287:11469–11480

Le YZ, Zheng L, Zheng W et al (2006) Mouse opsin promoter-directed Cre recombinase expression in transgenic mice. Mol Vis 12:389–398

Li W, Chen Y, Cameron DJ et al (2007) Elovl4 haploinsufficiency does not induce early onset retinal degeneration in mice. Vis Res 47:714–722

Marchette LD, Sherry DM, Brush RS et al (2014) Very long chain polyunsaturated fatty acids and rod cell structure and function. Adv Exp Med Biol 801:637–645

McMahon A, Butovich IA, Kedzierski W (2011) Epidermal expression of an Elovl4 transgene rescues neonatal lethality of homozygous Stargardt disease-3 mice. J Lipid Res 52:1128–1138

Raz-Prag D, Ayyagari R, Fariss RN et al (2006) Haploinsufficiency is not the key mechanism of pathogenesis in a heterozygous Elovl4 knockout mouse model of STGD3 disease. Invest Ophthalmol Vis Sci 47:3603–3611

Rotstein NP, Aveldano MI (1988) Synthesis of very long chain (up to 36 carbon) tetra, penta and hexaenoic fatty acids in retina. Biochem J 249:191–200

Rowan S, Cepko CL (2004) Genetic analysis of the homeodomain transcription factor Chx10 in the retina using a novel multifunctional BAC transgenic mouse reporter. Dev Biol 271:388–402

Vasireddy V, Jablonski MM, Mandal MNA et al (2006) Elovl4 5-bp–deletion knock-in mice develop progressive photoreceptor degeneration. Invest Ophthalmol Vis Sci 47:4558–4568

Zhang K, Kniazeva M, Han M et al (2001) A 5-bp deletion in ELOVL4 is associated with two related forms of autosomal dominant macular dystrophy. Nat Genet 27:89–93

Chapter 21
Malattia Leventinese/Doyne Honeycomb Retinal Dystrophy: Similarities to Age-Related Macular Degeneration and Potential Therapies

John D. Hulleman

Abstract Fibulin-3 (F3) is a secreted, disulfide-rich glycoprotein which is expressed in a variety of tissues within the body, including the retina. An Arg345Trp (R345W) mutation in F3 was identified as the cause of a rare retinal dystrophy, Malattia Leventinese/Doyne Honeycomb Retinal Dystrophy (ML/DHRD). ML/DHRD shares many phenotypic similarities with age-related macular degeneration (AMD). The most prominent feature of ML/DHRD is the development of radial or honeycomb patterns of drusen which can develop as early as adolescence. Two independent mouse models of ML/DHRD show evidence of complement activation as well as retinal pigment epithelium (RPE) atrophy, strengthening the phenotypic connection with AMD. Because of its similarities with AMD, ML/DHRD is receiving increasing interest as a potential surrogate disease to study the underpinnings of AMD. This mini-review summarizes the current knowledge of F3 and points toward potential therapeutic strategies which directly or indirectly target cellular dysfunction associated with R345W F3.

Keywords Fibulin-3 · Malattia leventinese/Doyne honeycomb retinal dystrophy · Protein misfolding · Age-related macular degeneration · Retinal degeneration · Drusen · Therapeutics

21.1 Introduction

F3 belongs to the fibulin protein family, which is comprised of seven other secreted disulfide-rich glycoproteins. Secreted fibulin proteins are integrated into the extracellular matrix (ECM) and are involved in basement membrane formation. While the function and expression of each fibulin protein is unique, they are generally thought to function in elastogenesis or elastic fiber maintenance. Each fibulin protein is comprised of a series of tandem calcium-binding epidermal growth factor domains followed by a C-terminal fibulin-type domain. Of the eight fibulin proteins,

J. D. Hulleman (✉)
Departments of Ophthalmology and Pharmacology, University of Texas Southwestern Medical Center, 5323 Harry Hines Blvd., Dallas, TX 75390-9057, USA

C. Bowes Rickman et al. (eds.), *Retinal Degenerative Diseases,* Advances in Experimental Medicine and Biology 854, DOI 10.1007/978-3-319-17121-0_21

mutations in two, F3 (S1–5, EFEMP1) (Stone et al. 1999), and fibulin-5 (EVEC, DANCE) (Stone et al. 2004), have been associated with retinal degeneration and AMD, respectively. A mutation in fibulin-6 (hemicentin) has also been suggested to affect AMD progression (Thompson et al. 2007), although other studies question its influence on disease (Klein et al. 1998; Schultz et al. 2005). Nonetheless, it is clear that mutations in fibulin proteins can significantly impact retinal physiology.

Inheritance of ML/DHRD occurs in an autosomal dominant fashion, suggesting that the disease is caused by a toxic gain-of-function mechanism. Consistent with this observation, mice expressing R345W F3 develop sub-RPE basal laminar membranous deposits that progress with age and gene dosage, and show signs of complement activation and RPE atrophy (Fu et al. 2007; Marmorstein et al. 2007), whereas knockout mice which do not express F3 have no observable eye-related phenotype (McLaughlin et al. 2007). Cell culture studies suggest that the R345W mutation causes the F3 protein to misfold, resulting in higher intracellular steady state levels and reduced amounts of F3 mutant secretion (Marmorstein et al. 2002; Hulleman et al. 2011). Thus, it has been speculated that the higher intracellular levels of R345W F3 in the endoplasmic reticulum (ER) activates the unfolded protein response (UPR) and triggers the ML/DHRD phenotype (Roybal et al. 2005). Even though there have been a series of cell culture/biochemical studies focused on understanding R345W F3 protein homeostasis, as well as two mouse models of ML/DHRD, it is still unknown exactly how the R345W mutation causes retinal degeneration. Does R345W F3 exert its detrimental effects from within the cell, outside of the cell, or a combination of both of these possibilities? How does the R345W mutant lead to an increase in complement activation? What is the origin of the basal deposits in ML/DHRD mice? While there are many unanswered questions regarding how the R345W mutant causes ML/DHRD, it is clear that developing a deeper understanding of the role of F3 in the retina is warranted.

21.2 Comparison between ML/DHRD and AMD

To date, no mutation in F3 has been identified and correlated with the development of AMD. The absence of such a finding has tempered enthusiasm for exploring the role F3 plays in AMD onset or progression. However, several similarities between ML/DHRD and AMD are too striking to ignore. The first histologic dissection of ML/DHRD patient eyes found that F3 accumulated between the RPE and the site of drusen formation (Marmorstein et al. 2002). AMD patients also demonstrated similar F3 immunoreactivity where drusen were found. In non-AMD eyes, however, no F3 was detected at the site of drusen. These studies have been corroborated (Sohn et al. 2014), and they imply that not only the ML/DHRD-associated R345W F3 mutant is involved in drusen formation, but that WT F3 (as would be present in AMD patients), also may be a culprit involved in pathogenic drusen formation.

A recent study has also demonstrated that drusen from ML/DHRD and AMD patients are compositionally similar. Sohn and colleagues found that drusen from

both ML/DHRD and AMD patients were eosinophilic and sudanophilic positive (Sohn et al. 2014). Additionally, drusen (or the area surrounding drusen) from AMD or ML/DHRD patients contained membrane attack complex, vitronectin, amyloid P and tissue inhibitor of matrix metalloproteinase 3 (TIMP3) (Sohn et al. 2014). However, the same study noted some differences including strong staining of collagen type IV in ML/DHRD drusen which was absent in AMD drusen. Nonetheless, the abundant similarities suggest that these diseases are phenotypically quite similar.

Much like AMD, the phenotypes associated with ML/DHRD can be variable; Michaelides and colleagues observed intrafamilial and interfamilial variability in vision loss, natural history, ophthalmoscopic observations, and retinal autofluorescence in ML/DHRD patients (Michaelides et al. 2006). Furthermore, this study identified a 62 year-old patient with the R345W F3 mutation who was asymptomatic, demonstrating a lack of full penetrance of the disease. Overall, this phenotypic variability demonstrates that ML/DHRD is likely a modifiable disease that is strongly influenced by slight differences in environmental and/or genetic composition.

21.3 Potential Approaches for Treating ML/DHRD

Since it is still unclear how the R345W F3 mutation causes ML/DHRD and the resulting AMD-like phenotypes, it is difficult to identify a priori a concrete therapeutic strategy which will address the underlying causes of ML/DHRD. While a strategy which directly and selectively targets disease-causing R345W F3 for degradation would be ideal, given the observations that F3 knockout mice do not have any eye-related phenotypes, strategies which target and affect both WT and R345W F3 may also be beneficial for disease treatment.

One potential approach to alter ML/DHRD progression would be to identify and pharmacologically or genetically manipulate unique binding partners of R345W F3. The ultimate goal of such a strategy would be to redirect the fate of mutant F3, promoting its intracellular degradation instead of allowing the protein to be secreted or to accumulate intracellularly within the RPE. However, to date, surprisingly few F3 interacting partners have been identified. Identified F3 interacting proteins include: TIMP3 (Klenotic et al. 2004), extracellular matrix protein 1 (ECM-1) (Sercu et al. 2009), complement factor H (CFH) (Wyatt et al. 2013), ER resident protein 57 (ERp57) (Jessop et al. 2007), ERdj5 (Oka et al. 2013), calnexin, calreticulin, 78 kDa glucose-regulated protein (GRP78), and 94 kDa glucose-regulated protein (GRP94) (Hulleman and Kelly 2015). This list of known interacting proteins is a good starting point for a systematic analysis of potential modifiers of R345W F3 protein homeostasis. Six of the identified binding partners, calnexin, calreticulin, ERp57, ERdj5, GRP78 and GRP94 interact with F3 in the ER where the F3 folding and secretion vs. degradation decision is made and are likely to significantly affect F3 secretion. Nonetheless, a more comprehensive characterization of the WT and R345W F3 interactome is needed.

As a secreted protein, the synthesis, folding and trafficking of F3 is likely regulated by one or more arms of the UPR, the tripartite stress-responsive signaling pathway which governs protein quality control in the ER. Indeed, overexpression of R345W F3, and to a lesser extent, WT F3, has been shown to cause activation of the UPR (specifically, the IRE1 and ATF6 pathways), but it is still unclear if this observation is due to the overexpression approach used, or if the result is actually physiologically meaningful (Roybal et al. 2005). Nonetheless, it is likely that activation of UPR signaling pathways will significantly affect F3 protein homeostasis. Since the activation of the UPR is important for upregulating ER-associated degradation (ERAD) of misfolded proteins (reviewed in Ruggiano et al. 2014), it is conceivable that selective, stress-independent regulation of one or more of the UPR pathways could manipulate R345W F3 fate. Consistent with this notion, previous studies have indicated that selective activation of the PERK arm of the UPR can modulate the amount of secreted R345W F3, partially rescuing its secretion defect (Hulleman et al. 2012). However, utilizing alternative, stress-independent approaches to selectively activating the IRE1 and ATF6 arms of the UPR is very intriguing, especially since levels of an F3 binding partner, ERp57, are regulated by both the IRE1 and ATF6 arms of the UPR (Shoulders et al. 2013).

Another approach to identifying treatments for ML/DHRD is to use unbiased phenotypic screening of chemical libraries. Such an approach has been used recently based on the assumption that altering the levels of secreted R345W F3 may alter ML/DHRD disease phenotypes. This study demonstrated, at least from a proof-of-principle perspective, that selective pharmacological manipulation of R345W F3 secretion was possible (Hulleman et al. 2013). Unfortunately, the lead compound which selectively reduced R345W F3 secretion from ARPE-19 cells (with no effect on WT F3 secretion) was the tumor-promoting and pleiotropic chemical, phorbol 12-myristate 13-acetate (PMA). Another compound, ARP-101, a matrix metalloproteinase 2 inhibitor, was found to reduce the secreted levels of both WT and R345W F3 from ARPE-19 cells. While not selective for WT vs. R345W F3 secretion, this compound could nonetheless be potentially used as a therapeutic compound in ML/DHRD mice since removal of F3 (WT or R345W) from the eye has no apparent adverse effects (McLaughlin et al. 2007). Future studies could be directed at dissection of the structure-activity relationships of PMA and ARP-101 to yield more pharmacologically attractive and potent compounds that don't bear the adverse effects of the parent compound.

Two recent studies have taken alternative therapeutic approaches which do not directly target R345W F3, but instead are directed at (i) pathways downstream of R345W F3 expression, or (ii) the consequences of mutant F3 production (i.e., drusen formation). The first approach originated from an in-depth proteomic analysis of retinas from R345W F3 mice. The proteomic signature from these mice demonstrated dysregulation of the complement system (Garland et al. 2014). These data, along with evidence from the ML/DHRD mouse model, suggested that reducing complement factor C3 could be beneficial in preventing drusen formation associated with ML/DHRD. Indeed, genetic knockout of C3 prevented basal laminar deposit formation in the R345W F3 mice (Garland et al. 2014). While these studies

are extremely promising and exciting, there still is missing information that links how R345W F3 causes complement dysfunction and whether such an approach will be beneficial in ML/DHRD patients. Given the success of this study, it would be interesting to determine whether ML/DHRD patients could benefit from treatment with the primate-specific C3 inhibitor, compstatin, or one of its analogs such as POT-4 (Ricklin and Lambris 2008).

In the second alternative approach for ML/DHRD, Lenassi and colleagues used low level laser-induced photocoagulation to promote drusen reabsorption in 11 ML/DHRD patients (Lenassi et al. 2013). A similar treatment has been used previously to successfully reduce drusen load in randomized controlled trials of AMD patients (Parodi et al. 2009). Unfortunately, this treatment had no effect on halting the development of choroid neovascularization, geographic atrophy or loss in visual acuity in AMD patients. Surprisingly, laser clearance of drusen deposits in ML/DHRD patients improved visual acuity in five patients, whereas five other patients demonstrated no change in vision and one patient experienced a significant deterioration in vision (Lenassi et al. 2013). These results are quite promising, although they highlight the notion that a single treatment for all ML/DHRD patients may be difficult to identify due to disease heterogeneity. Continuing these efforts to develop a more in-depth understanding of ML/DHRD should provide us with a deeper knowledge of ML/DHRD etiology and may identify cellular pathways to target in the phenotypically similar, yet etiologically more complex disease, AMD.

Acknowledgments This work was funded by an endowment from the Roger and Dorothy Hirl Research Fund, an NEI core grant (EY020799), a career development award from Research to Prevent Blindness (RPB), and an unrestricted grant from RPB. The author thanks Bonnie Miller and Rafael Ufret-Vincenty for their review of this manuscript.

References

Fu L, Garland D, Yang Z et al (2007) The R345W mutation in EFEMP1 is pathogenic and causes AMD-like deposits in mice. Hum Mol Genet 16:2411–2422

Garland DL, Fernandez-Godino R, Kaur I et al (2014) Mouse genetics and proteomic analyses demonstrate a critical role for complement in a model of DHRD/ML, an inherited macular degeneration. Hum Mol Genet 23:52–68

Hulleman JD, Kelly JW (2015) Genetic ablation of N-linked glycosylation reveals two key folding pathways for R345W fibulin-3, a secreted protein associated with retinal degeneration. FASEB J 29:565–575

Hulleman JD, Kaushal S, Balch WE et al (2011) Compromised mutant EFEMP1 secretion associated with macular dystrophy remedied by proteostasis network alteration. Mol Biol Cell 22:4765–4775

Hulleman JD, Balch WE, Kelly JW (2012) Translational attenuation differentially alters the fate of disease-associated fibulin proteins. FASEB J 26:4548–4560

Hulleman JD, Brown SJ, Rosen H et al (2013) A high-throughput cell-based Gaussia luciferase reporter assay for identifying modulators of fibulin-3 secretion. J Biomol Screen 18:647–658

Jessop CE, Chakravarthi S, Garbi N et al (2007) ERp57 is essential for efficient folding of glycoproteins sharing common structural domains. EMBO J 26:28–40

Klein ML, Schultz DW, Edwards A et al (1998) Age-related macular degeneration. Clinical features in a large family and linkage to chromosome 1q. Arch Ophthalmol 116:1082–1088

Klenotic PA, Munier FL, Marmorstein LY et al (2004) Tissue inhibitor of metalloproteinases-3 (TIMP-3) is a binding partner of epithelial growth factor-containing fibulin-like extracellular matrix protein 1 (EFEMP1). Implications for macular degenerations. The J Biol Chem 279:30469–30473

Lenassi E, Troeger E, Wilke R et al (2013) Laser clearance of drusen deposit in patients with autosomal dominant drusen (p.Arg345Trp in EFEMP1). Am J Ophthalmol 155:190–198

Marmorstein LY, Munier FL, Arsenijevic Y et al (2002) Aberrant accumulation of EFEMP1 underlies drusen formation in malattia leventinese and age-related macular degeneration. Proc Natl Acad Sci U S A 99:13067–13072

Marmorstein LY, McLaughlin PJ, Peachey NS et al (2007) Formation and progression of sub-retinal pigment epithelium deposits in Efemp1 mutation knock-in mice: a model for the early pathogenic course of macular degeneration. Hum Mol Genet 16:2423–2432

McLaughlin PJ, Bakall B, Choi J et al (2007) Lack of fibulin-3 causes early aging and herniation, but not macular degeneration in mice. Hum Mol Genet 16:3059–3070

Michaelides M, Jenkins SA, Brantley MA Jr et al (2006) Maculopathy due to the R345W substitution in fibulin-3: distinct clinical features, disease variability, and extent of retinal dysfunction. Invest Ophthalmol Vis Sci 47:3085–3097

Oka OB, Pringle MA, Schopp IM et al (2013) ERdj5 is the ER reductase that catalyzes the removal of non-native disulfides and correct folding of the LDL receptor. Mol Cell 50:793–804

Parodi MB, Virgili G, Evans JR (2009) Laser treatment of drusen to prevent progression to advanced age-related macular degeneration. Cochrane Database Syst Rev 8(3):CD006537

Ricklin D, Lambris JD (2008) Compstatin: a complement inhibitor on its way to clinical application. Adv Exp Med Biol 632:273–292

Roybal CN, Marmorstein LY, Vander Jagt DL et al (2005) Aberrant accumulation of fibulin-3 in the endoplasmic reticulum leads to activation of the unfolded protein response and VEGF expression. Invest Ophthalmol Vis Sci 46:3973–3979

Ruggiano A, Foresti O, Carvalho P (2014) Quality control: ER-associated degradation: protein quality control and beyond. J Cell Biol 204:869–879

Schultz DW, Weleber RG, Lawrence G et al (2005) HEMICENTIN-1 (FIBULIN-6) and the 1q31 AMD locus in the context of complex disease: review and perspective. Ophthalmic Genet 26:101–105

Sercu S, Lambeir AM, Steenackers E et al (2009) ECM1 interacts with fibulin-3 and the beta 3 chain of laminin 332 through its serum albumin subdomain-like 2 domain. Matrix Biol 28:160–169

Shoulders MD, Ryno LM, Genereux JC et al (2013) Stress-independent activation of XBP1s and/or ATF6 reveals three functionally diverse ER proteostasis environments. Cell Rep 3:1279–1292

Sohn EH, Wang K, Thompson S et al (2014) Comparison of drusen and modifying genes in autosomal dominant radial drusen and age-related macular degeneration. Retina 35(1):48-57

Stone EM, Lotery AJ, Munier FL et al (1999) A single EFEMP1 mutation associated with both malattia leventinese and Doyne honeycomb retinal dystrophy. Nat Genet 22:199–202

Stone EM, Braun TA, Russell SR et al (2004) Missense variations in the fibulin 5 gene and age-related macular degeneration. N Engl J Med 351:346–353

Thompson CL, Klein BE, Klein R et al (2007) Complement factor H and hemicentin-1 in age-related macular degeneration and renal phenotypes. Hum Mol Genet 16:2135–2148

Wyatt MK, Tsai JY, Mishra S et al (2013) Interaction of complement factor h and fibulin3 in age-related macular degeneration. PLoS ONE 8:e68088

Part III
Inherited Retinal Degenerations

Chapter 22
Hsp90 as a Potential Therapeutic Target in Retinal Disease

Mònica Aguilà and Michael E. Cheetham

Abstract The molecular chaperone heat shock protein 90 (Hsp90) is a pivotal cellular regulator involved in the folding, activation and assembly of a wide range of proteins. Hsp90 has multiple roles in the retina and the use of different Hsp90 inhibitors has been shown to prevent retinal degeneration in models of retinitis pigmentosa and age-related macular degeneration. Hsp90 is also a potential target in uveal melanoma. Mechanistically, Hsp90 inhibition can evoke a dual response in the retina; stimulating a stress response with molecular chaperone expression. Thereby leading to an improvement in visual function and photoreceptor survival; however, prolonged inhibition can also stimulate the degradation of Hsp90 client proteins potentially deleteriously affect vision. Here, we review the multiple roles of Hsp90 in the retina and the therapeutic potential of Hsp90 as a target.

Keywords Hsp90 · Retinal degeneration · Hsp90 inhibition · Molecular chaperones · RP · AMD · Uveal melanoma

22.1 Introduction

Hsp90 is an abundant molecular chaperone involved in many cellular processes. It plays a role in the folding, stability, maturation, intracellular transport, maintenance, and degradation of a number of client proteins. These clients include proteins involved in signal transduction, protein trafficking, and innate and adaptive immunity. Hsp90 is one of the most conserved heat shock proteins and is an essential component of the protective heat shock response, therefore playing a role in

M. E. Cheetham (✉) · M. Aguilà
Department of Ocular Biology and Therapeutics, UCL Institute of Ophthalmology, 11-43 Bath Street, London EC1V 9EL, UK
e-mail: m.cheetham @ucl.ac.uk; m.aguila@ucl.ac.uk

C. Bowes Rickman et al. (eds.), *Retinal Degenerative Diseases,* Advances in Experimental Medicine and Biology 854, DOI 10.1007/978-3-319-17121-0_22

regulating cell physiology under normal and stressed conditions (McClellan et al. 2007). Hsp90 is expressed in the cytosol and the nucleus and contains an N-terminal ATP-binding domain that is essential for most of its cellular functions. Hsp90 has been shown to suppress the aggregation of a wide range of client proteins and hence acts as a general protective chaperone. Certain Hsp90 inhibitors (e.g. geldanamycin, 17-AAG or HSP990) bind with a high affinity to the ATP-binding pocket and block the chaperone ATPase cycle leading to the degradation of client proteins that can no longer be folded (Li and Buchner 2013). In addition, under resting conditions Hsp90 binds the stress responsive transcription factor, heat shock factor 1 (HSF-1), to silence the transcription factor activity and forms an auto-regulatory feedback loop that couples molecular chaperone levels to the need for chaperones to bind misfolded proteins (Neueder et al. 2014). Inhibition of Hsp90 leads to the release of HSF-1 and the activation of the stress response and an increase in molecular chaperones. Therefore, Hsp90 inhibition can either lead to the proteasome-mediated degradation of Hsp90 client proteins or upregulation of molecular chaperones, such as Hsp70 and Hsp40, which results in an enhanced protective effect against protein aggregation and reduced protein toxicity (Labbadia et al. 2011).

The retina is a complex tissue with a high metabolic demand, constantly exposed to stress (Athanasiou et al. 2013). To maintain cell homeostasis and prevent damage, the retina contains high levels of heat shock proteins under normal conditions (Urbak and Vorum 2010). Hsp90 is widely distributed in all retinal layers, from the retinal ganglion cells (RGC) to the inner segment (IS), the tips of the outer segment (OS) and retinal pigment epithelium (RPE) cells (Dean and Tytell 2001). Hsp90 plays an indispensable role in homeostasis of the retina as prolonged Hsp90 inhibition leads to photoreceptor cell death (Kanamaru et al. 2014).

22.2 Manipulation of Hsp90 as a Potential Therapy for Retinal Degeneration

Pharmacological intervention with compounds that target Hsp90 function could potentially be therapeutic against several different forms of retinal degeneration and pathology.

22.2.1 Retinitis Pigmentosa (RP)

RP is the most common form of inherited photoreceptor degeneration and mutations in the rhodopsin gene are the most common cause of autosomal dominant RP. It has been previously shown that the Hsp90 inhibitor 17-*N*-allylamino-17-demethoxy-geldanamycin (17-AAG) can protect against rhodopsin aggregation and toxicity in a cell model of a class II misfolding mutation in rhodopsin, P23H, which is the most common rhodopsin mutation in the USA (Mendes and Cheetham 2008). This

protection appears to be dependent on HSF-1, as mouse embryonic fibroblasts from HSF-1 knock-out mice were not protected against P23H rhodopsin aggregation by 17-AAG, suggesting that the protective effect is dependent on induction of the stress response (Aguila et al. 2014). Systemic administration of the blood brain barrier permeable Hsp90 inhibitor, HSP990, can activate HSF-1 and stimulate molecular chaperone expression *in vivo* in the retina (Aguila et al. 2014). In a P23H rhodopsin transgenic rat model with progressive retinal degeneration, a single low dose of HSP990 was sufficient to mediate an improvement in visual function and photoreceptor survival several weeks later. Importantly, this treatment did not affect any phototransduction component, but did induce molecular chaperones and reduced rhodopsin aggregation, showing the ability of Hsp90 inhibition to stimulate the proteostasis machinery that protects against misfolded proteins (Aguila et al. 2014). Other examples of how imbalances in photoreceptor proteostasis can be targeted with Hsp90 inhibition are IMPDH misfolding mutations associated with RP10. In this instance, claudin 5 RNAi was used to transiently permeabilize the blood retinal barrier and allow 17-AAG to stimulate a protective response in photoreceptors expressing R224P mutant IMPDH, with a concomitant reduction in mutant IMPDH aggregation and protection of ONL structure (Tam et al. 2010).

Interestingly, in a disease model for a different class of rhodopsin mutation (R135L) inhibition of Hsp90 was also protective, but this was independent of HSF-1. The R135L mutation causes rhodopsin hyperphosphorylation, arrestin binding and aberrant rhodopsin endocytosis (Fig. 22.1a), which deleteriously affects vesicular traffic (Chuang et al. 2004). Hsp90 inhibition blocked the recruitment of arrestin to R135L mutant rhodopsin and thereby alleviated aberrant endocytosis (Aguila et al. 2014). This effect was still maintained in HSF-1 null cells, showing that it was independent of HSF-1. Further investigation revealed that, like many kinases, rhodopsin kinase (GRK1) is an obligate Hsp90 client protein and the effect of Hsp90 inhibition on R135L rhodopsin arrestin binding was mediated by an upstream reduction in phosphorylation of R135L because of lack of an appropriate kinase (Aguila et al. 2014). This mechanism related to the reduction of a specific client protein that is mediating an adverse effect of a genetic mutation is distinct from the enhanced production of protective factors through the activation of the stress response to combat a mutational consequence. Overall, these data suggest that Hsp90 has multiple roles in the retina and that the use of Hsp90 inhibitors can be potentially protective against different types of RP through different mechanisms.

22.2.2 Age-Related Macular Degeneration (AMD) and RPE Biology

AMD is a complex multifactorial disease involving genetic, environmental, metabolic, and functional factors. Functional abnormalities and cell death in the RPE cells contribute to the development of AMD, and are associated with increased oxidative stress (Jarrett and Boulton 2012). Hsp90 is expressed in RPE cells and its

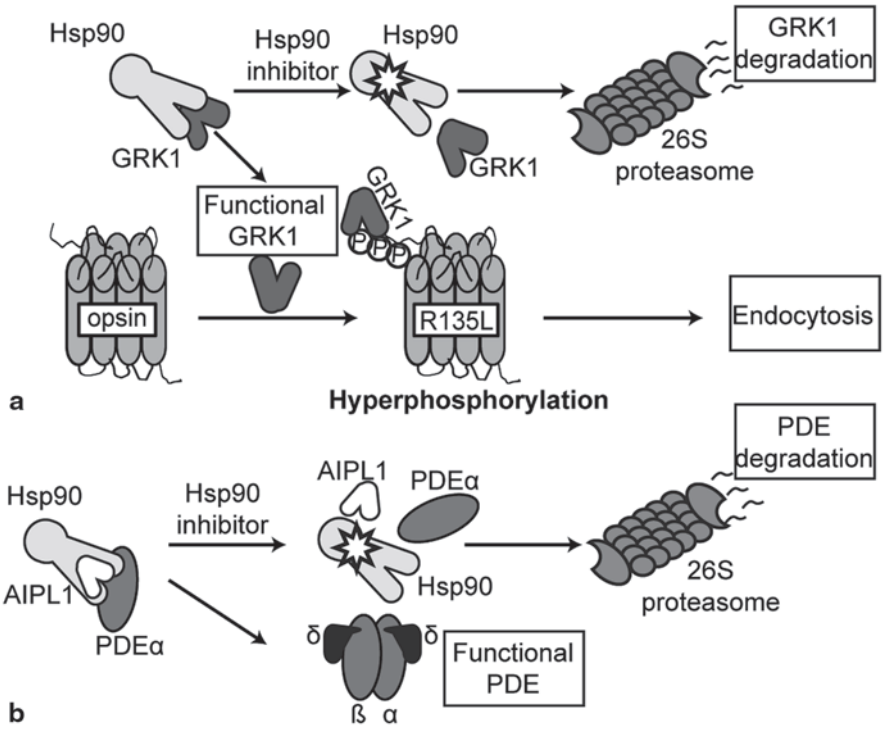

Fig. 22.1 Hsp90 is required for GRK1 and PDE function. **a** GRK1 requires Hsp90 for maturation. R135L rhodopsin mutant is hyperphosphorylated by functional GRK1 leading to arrestin binding and endocytosis. Hsp90 inhibitors prevent Hsp90 mediated GRK1 folding, leading to GRK1 degradation and loss of R135L hyperphosphrylation. **b** PDE needs Hsp90 and its co-chaperone AIPL1 for maturation. Hsp90 inhibition blocks the Hsp90-AIPL1 interaction, resulting in PDE degradation

expression increases significantly during the progression of AMD (Decanini et al. 2007). It has been suggested that Hsp90 expressed from necrotic RPE cells may function as a trigger for inflammatory responses in adjacent healthy RPE (Qin et al. 2011). Inflammatory responses in RPE cells can be blocked by Hsp90 inhibition (Wang et al. 2010). Moreover, the Hsp90 inhibitor geldanamycin inhibits VEGF expression induced by hypoxia in RPE cells (Wu et al. 2007), suggesting that Hsp90 inhibitors may be effective in blocking both inflammation and neovascularization.

22.2.3 Ocular Oncology: Uveal Melanoma

Hsp90 is a major target in oncology as several aspects of tumor cell viability are reliant on Hsp90 function. Uveal melanoma (UM) is the most common primary intraocular malignancy in adults (Egan et al. 1988) and Hsp90 is emerging as a

potentially important target in UM. Focal adhesion kinase (FAK) is a cytoplasmic tyrosine kinase that plays a central role in several cellular processes including mediation of extracellular matrix-integrin signaling, cell migration, invasion and metastasis in several cancers, including UM (Hess et al. 2005). Hsp90 is crucial for the stability and functional conformation of FAK, as inhibition of Hsp90 interferes with its phosphorylation and stimulates its proteasome-mediated degradation (Faingold et al. 2008). Hsp90 inhibition resulted in a reduction of migration and invasion of cancer cells through FAK-mediated pathways (Faingold et al. 2008). Furthermore, the protein kinase Akt also requires Hsp90 for its activity and stability (Basso et al. 2002) and high levels of phosphorylated Akt (p-Akt) have been shown to be associated with a higher risk of metastatic disease in patients with UM (Saraiva et al. 2005). Treatment of human UM cell lines with 17-AAG resulted in a decrease of Akt and activated p-Akt, possibly contributing to cell growth arrest and induction of cell death. In addition, 17-AAG and 17-DMAG inhibited cell proliferation in ^{WT}B-Raf UM cell lines by downregulating the ^{WT}B-Raf protein. This downregulation led to the inactivation of the MEK/ERK module and the decrease in cyclin D1, which is necessary for the proliferation of UM cell lines (Babchia et al. 2008). Overall, these data suggest that Hsp90 inhibition could be a possible therapy against this type of cancer.

22.2.4 Therapeutic Considerations

Recent reports from oncology clinical trials have suggested that some Hsp90 inhibitors, such as 17-DMAG and AUY922, might lead to visual disturbances (Sessa et al. 2013). In a recent clinical trial for advanced solid tumors using AUY922, 43 % of the patients reported grades 1–3 visual symptoms, including night blindness, photopsia, blurred vision and visual impairment (Rajan et al. 2011). Fortunately, all the visual symptoms were reversible when drug use was discontinued. It is therefore important to identify the molecular mechanism by which Hsp90 inhibitors affect vision. As predicted by the studies on R135L rhodopsin, prolonged systemic Hsp90 inhibition led to a reduction of GRK1 levels in the retina, confirming that Hsp90 is required for GRK1 biosynthesis (Aguila et al. 2014). Furthermore, phosphodiesterase (PDE) levels were also specifically reduced in the retina following Hsp90 inhibition (Aguila et al. 2014). The Leber congential amaurosis (LCA) gene product *AIPL1* is a cochaperone for Hsp90 and is essential for PDE biosynthesis (Hidalgo-de-Quintana et al. 2008), suggesting that Hsp90 and AIPL1 co-operate in PDE biosynthesis (Fig. 22.1b). Reduction in GRK1 and PDE could cause some of the most common visual side-effects of Hsp90 inhibitors observed in oncology patients. Therefore, the effects of Hsp90 inhibition on visual function are likely to relate to essential Hsp90 client proteins in the phototransduction pathway in the retina and potentially elsewhere in the eye.

22.3 Conclusions

A range of Hsp90 inhibitors have now been developed with different affinities and bioavailability. Importantly, several Hsp90 inhibitors have been studied in oncology clinical trials and their pharmacokinetic profile and side effects have been identified. Therefore, they could potentially be applied to RP and other neurodegenerative disease with prior knowledge of the risks and benefits. Collectively, the data show that Hsp90 has multiple roles in the retina and that the use of Hsp90 inhibitors can be potentially protective against retinal degeneration and ocular oncology, but their possible adverse effects on visual function also need to be considered.

Acknowledgments This work is supported by the Wellcome Trust and RP Fighting Blindness.

References

Aguila M, Bevilacqua D, McCulley C et al (2014) Hsp90 inhibition protects against inherited retinal degeneration. Hum Mol Genet 23:2164–2175

Athanasiou D, Aguila M, Bevilacqua D et al (2013) The cell stress machinery and retinal degeneration. FEBS Lett 587:2008–2017

Babchia N, Calipel A, Mouriaux F et al (2008) 17-AAG and 17-DMAG-induced inhibition of cell proliferation through B-Raf downregulation in WT B-Raf-expressing uveal melanoma cell lines. Invest Ophthalmol Vis Sci 49:2348–2356

Basso AD, Solit DB, Chiosis G et al (2002) Akt forms an intracellular complex with heat shock protein 90 (Hsp90) and Cdc37 and is destabilized by inhibitors of Hsp90 function. J Biol Chem 277:39858–39866

Chuang JZ, Vega C, Jun W et al (2004) Structural and functional impairment of endocytic pathways by retinitis pigmentosa mutant rhodopsin-arrestin complexes. J Clin Invest 114:131–140

Dean DO, Tytell M (2001) Hsp25 and -90 immunoreactivity in the normal rat eye. Invest Ophthalmol Vis Sci 42:3031–3040

Decanini A, Nordgaard CL, Feng X et al (2007) Changes in select redox proteins of the retinal pigment epithelium in age-related macular degeneration. Am J Ophthalmol 143:607–615

Egan KM, Seddon JM, Glynn RJ et al (1988) Epidemiologic aspects of uveal melanoma. Surv Ophthalmol 32:239–251

Faingold D, Marshall JC, Antecka E et al (2008) Immune expression and inhibition of heat shock protein 90 in uveal melanoma. Clin Cancer Res 14:847–855

Hess AR, Postovit LM, Margaryan NV et al (2005) Focal adhesion kinase promotes the aggressive melanoma phenotype. Cancer Res 65:9851–9860

Hidalgo-de-Quintana J, Evans RJ, Cheetham ME et al (2008) The Leber congenital amaurosis protein AIPL1 functions as part of a chaperone heterocomplex. Invest Ophthalmol Vis Sci 49:2878–2887

Jarrett SG, Boulton ME (2012) Consequences of oxidative stress in age-related macular degeneration. Mol Aspects Med 33:399–417

Kanamaru C, Yamada Y, Hayashi S et al (2014) Retinal toxicity induced by small-molecule Hsp90 inhibitors in beagle dogs. J Toxicol Sci 39:59–69

Labbadia J, Cunliffe H, Weiss A et al (2011) Altered chromatin architecture underlies progressive impairment of the heat shock response in mouse models of Huntington disease. J Clin Invest 121:3306–3319

Li J, Buchner J (2013) Structure, function and regulation of the hsp90 machinery. Biomed J 36:106–117

McClellan AJ, Xia Y, Deutschbauer AM et al (2007) Diverse cellular functions of the Hsp90 molecular chaperone uncovered using systems approaches. Cell 131:121–135

Mendes HF, Cheetham ME (2008) Pharmacological manipulation of gain-of-function and dominant-negative mechanisms in rhodopsin retinitis pigmentosa. Hum Mol Genet 17:3043–3054

Neueder A, Achilli F, Moussaoui S et al (2014) Novel isoforms of heat shock transcription factor 1, HSF1gammaalpha and HSF1gammabeta, regulate chaperone protein gene transcription. J Biol Chem 289:19894–19906

Qin S, Ni M, Wang X et al (2011) Inhibition of RPE cell sterile inflammatory responses and endotoxin-induced uveitis by a cell-impermeable HSP90 inhibitor. Exp Eye Res 93:889–897

Rajan A, Kelly RJ, Trepel JB et al (2011) A phase I study of PF-04929113 (SNX-5422), an orally bioavailable heat shock protein 90 inhibitor, in patients with refractory solid tumor malignancies and lymphomas. Clin Cancer Res 17:6831–6839

Saraiva VS, Caissie AL, Segal L et al (2005) Immunohistochemical expression of phospho-Akt in uveal melanoma. Melanoma Res 15:245–250

Sessa C, Shapiro GI, Bhalla KN et al (2013) First-in-human phase I dose-escalation study of the HSP90 inhibitor AUY922 in patients with advanced solid tumors. Clin Cancer Res 19:3671–3680

Tam LC, Kiang AS, Campbell M et al (2010) Prevention of autosomal dominant retinitis pigmentosa by systemic drug therapy targeting heat shock protein 90 (Hsp90). Hum Mol Genet 19:4421–4436

Urbak L, Vorum H (2010) Heat shock proteins in the human eye. International journal of proteomics 2010:479571

Wang YQ, Zhang XM, Wang XD et al (2010) 17-AAG, a Hsp90 inhibitor, attenuates the hypoxia-induced expression of SDF-1alpha and ILK in mouse RPE cells. Mol Biol Rep 37:1203–1209

Wu WC, Kao YH, Hu PS et al (2007) Geldanamycin, a HSP90 inhibitor, attenuates the hypoxia-induced vascular endothelial growth factor expression in retinal pigment epithelium cells in vitro. Exp Eye Res 85:721–731

Chapter 23
Leber Congenital Amaurosis: Genotypes and Retinal Structure Phenotypes

Samuel G. Jacobson, Artur V. Cideciyan, Wei Chieh Huang, Alexander Sumaroka, Hyun Ju Nam, Rebecca Sheplock and Sharon B. Schwartz

Abstract Leber congenital amaurosis (LCA) patients of 10 known genotypes ($n=24$; age range, 3–25 years) were studied clinically and by optical coherence tomography (OCT). Comparisons were made between OCT results across the horizontal meridian (central 60°) of the patients. Three patterns were identified. First, there were LCA genotypes with unusual and readily identifiable patterns, such as near normal outer nuclear layer (ONL) across the central retina or severely dysplastic retina. Second, there were genotypes with well-formed foveal architecture but only residual central islands of normal or reduced ONL thickness. Third, some genotypes showed central ONL losses or dysmorphology suggesting early macular disease or foveal maldevelopment. Objective *in vivo* morphological features could complement other phenotypic characteristics and help guide genetic testing of LCA patients or at least permit a differential diagnosis of genotypes to be made in the clinic.

S. G. Jacobson (✉) · A. V. Cideciyan · W. C. Huang · A. Sumaroka · H. J. Nam · R. Sheplock · S. B. Schwartz
Scheie Eye Institute, Department of Ophthalmology, Perelman School of Medicine, University of Pennsylvania, 51 N. 39th Street, Philadelphia, PA 19104, USA
e-mail: jacobsos@mail.med.upenn.edu

A. V. Cideciyan
e-mail: cideciya@mail.med.upenn.edu

W. C. Huang
e-mail: weichieh.huang@gmail.com

A. Sumaroka
e-mail: asumarok@mail.med.upenn.edu

H. J. Nam
e-mail: HyunJu.Nam@uphs.upenn.edu

R. Sheplock
e-mail: Rebecca.Sheplock@uphs.upenn.edu

S. B. Schwartz
e-mail: Sharon.Wolfe@uphs.upenn.edu

C. Bowes Rickman et al. (eds.), *Retinal Degenerative Diseases,* Advances in Experimental Medicine and Biology 854, DOI 10.1007/978-3-319-17121-0_23

Keywords Optical coherence tomography · Retinal dysplasia · Leber congenital amaurosis · Outer nuclear layer · Macular disease · Fovea development

23.1 Introduction

LCA is a genetically heterogeneous group of mainly autosomal recessive retinopathies beginning in infancy and childhood with at least 19 different molecular causes (OMIM; www.omim.org). Once the clinical diagnosis is made, there is now an opportunity to make a molecular diagnosis. As in other medical disciplines involving genetic diagnosis, the field has advanced from discovery to research-based exploration to commercially-available genetic tests, recently including whole exome and whole genome testing.

Is there anything to do in the retina clinic to guide gene identification? Sorting LCA phenotypes has occurred. One scheme uses patient behavior in response to light, refractive error, and other visual parameters (Kaplan 2008). LCA genes have been tabulated and fundus photographs or clinical descriptions provided for each genotype (den Hollander et al. 2008; Chung and Traboulsi 2009). OCT was used to examine laminar architecture of 4 LCA genotypes and differences demonstrated (Pasadhika et al. 2010). An attempt to combine genotyping with phenotyping to make genetic testing more efficient has been proposed for small outbred families (Hebrard et al. 2011).

In the current work, we study OCT imaging from young LCA patients representing 10 different genotypes. We categorize the retinal structural changes and conclude that some are associated with a specific genotype while others are indistinguishable.

23.2 Materials and Methods

23.2.1 Subjects

There were 24 LCA patients, representing 10 genotypes (Table 23.1). Informed consent was obtained; procedures were approved by the institutional review board.

23.2.2 Imaging Studies: Optical Coherence Tomography

Retinal cross-sections with OCT were collected at the earliest-age visit of patients using mainly spectral-domain systems. Our methods are published (e.g. Jacobson et al. 2005).

Table 23.1 Clinical and molecular characteristics of the patients

Gene (LCA type) Patient/Age(year)/sex	Allele 1/Allele 2	Visual acuity[a, b]	Refraction[c]
GUCY2D (LCA1)			
P1/11/M	p.H980L/p.H980L	LP	+3.50
P2/11/F	p.R768W/p.R822P	20/125–20/100	+4.00
P3/14/F	p.T280R/p.T280R	CF at 6″-20/300	+0.75
RPE65 (LCA2)			
P4/7/M	p.R44Q/p.R44Q	20/160	−10.25
P5/9/M	p.A500fs/ p.A500fs	20/160–20/200	−2.00
P6/13/F	p.V287F/p.V287F	20/125–20/200	−3.75
AIPL1 (LCA4)			
P7/16/F	p.W278Ter/p.V33fs	HM	+2.00
P8/23/F	p.C89R/p.W72R	LP	+4.00
Lebercilin (LCA5)			
P9/6/M	p.Q279Ter/p.Q279Ter	LP	+6.50
RPGRIP1 (LCA6)			
P10/21/M	p.V1211E/p.V1211E	20/100	+3.25
P11/24/F	c.630del/c.2796dup	20/400	+0.75
CRB1 (LCA8)			
P12/13/F	p.C948Y/p.C948Y	20/63	+4.75
P13/19/M	p.C948Y/p.C948Y	HM	+7.50
P14/21/M	p.C948Y/p.C948Y	20/100–2/200	+3.25
NMNAT1 (LCA9)			
P15/3/F	p.E257K/p.I197T	FF	+8.50
CEP290 (LCA10)			
P16/8/M	IVS26+1655A>G/p.E97Ter	NLP	+7.00
P17/9/F	IVS26+1655A>G/IVS13+1G>C	NLP	+4.00
P18/10/F	IVS26+1655A>G/p.L517Ter	LP	+7.75
RDH12 (LCA13)			
P19/7/M	p.R259Ter/p.A270fs	20/50–20/63	+0.75
P20/13/F	p.Y194Ter/p.A206D	HM-20/500 at 1M	+6.00
P21/15/F	p.A47T/p.L99I	20/63–20/125	+4.00
TULP1 (LCA15)			
P22/15/F	p.Q301Ter/p.Q301Ter	20/160–20/125	−3.00
P23/19/M	p.Q301Ter/p.Q301Ter	20/640–20/400	+6.75
P24/25/F	p.G368W/p.D355V	20/80	+0.25

LP light perception; *HM* hand motions; *FF* fix and follow; *NLP* no light perception

[a] Best corrected visual acuity

[b] Similar in the two eyes; otherwise, specified individually, as RE-LE

[c] Spherical equivalent; average of the two eyes

23.3 Results

23.3.1 Cross Sectional Retinal Imaging

Distinctive Structural Phenotypes in Two Genotypes Retinal lamination of a normal subject and two LCA patients representing genotypes with a characteristic OCT are shown. The scan from a *GUCY2D*-LCA1 patient is remarkable for its relatively normal appearance; retinal and ONL thicknesses across the retina are within normal limits. Young *GUCY2D*-LCA1 patients (ages 11–14) have normal or subnormal retinal and ONL thickness in the central few degrees, but normal thickness across the rest of the scan. This pattern was typical of *GUCY2D*-LCA1 patients (Pasadhika et al. 2010; Jacobson et al. 2013a) (Fig. 23.1).

Another recognizable structural phenotype is associated with *CRB1*-LCA8. There is reduced foveal ONL, limited extracentral ONL and thickened dysplastic-appearing retina across the remainder of the section (Fig. 23.1). Retained central ONL and better acuity in some patients may lead to a diagnosis of *CRB1*-RP (Jacobson et al. 2013b). Whether LCA or RP, patients show extracentral coarse and abnormal lamination with thickening (Jacobson et al. 2003; Aleman et al. 2011; Jacobson et al. 2013b).

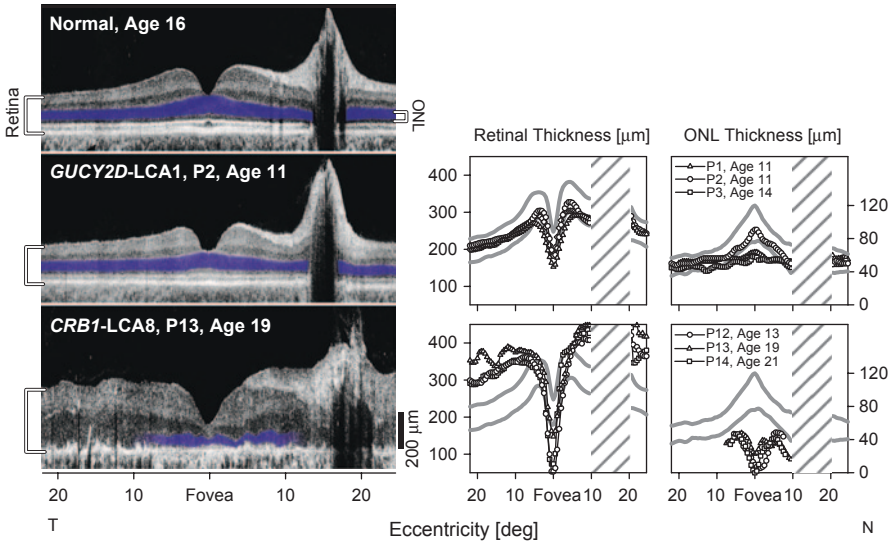

Fig. 23.1 Two LCA genotypes with unique structural phenotypes. *Top* Normal OCT along the horizontal meridian through the fovea. *Middle GUCY2D*-LCA1 patient with normal retinal and ONL thickness. *Lower CRB1*-LCA8 patient with thick dysplastic-appearing retina and limited ONL. Quantitative analyses of retinal and ONL thicknesses in other patients with these genotypes (*right*). Normal limits (*gray lines*, mean ± 2SD); *P* numbers refer to Table 23.1

Preserved Central Island in Five Genotypes Five genotypes showed a preserved central island of ONL, but a decrease with eccentricity. The foveal ONL peak could be normal or reduced. A common gene mechanism in the group was ciliopathy, which includes *Lebercilin*-LCA5, *RPGRIP1*-LCA6, *CEP290*-LCA10, and *TULP1*-LCA15, although the latter disorder may have a more complex mechanism (Jacobson et al. 2014). *RPE65*-LCA2 could show a similar pattern. Retinal thickness in these genotypes was at the lower limit of normal or subnormal, in contrast, for example, to *CRB1*-LCA8 (Fig. 23.2).

Severe Maculopathy in Three Genotypes This group includes two with macular disease (*AIPL1*-LCA4 and *RDH12*-LCA13) and one that appears to be a developmental abnormality with lack of foveal formation and inner retinal laminae crossing the central retina (*NMNAT1*-LCA9). ONL thickness in all three is detectable,

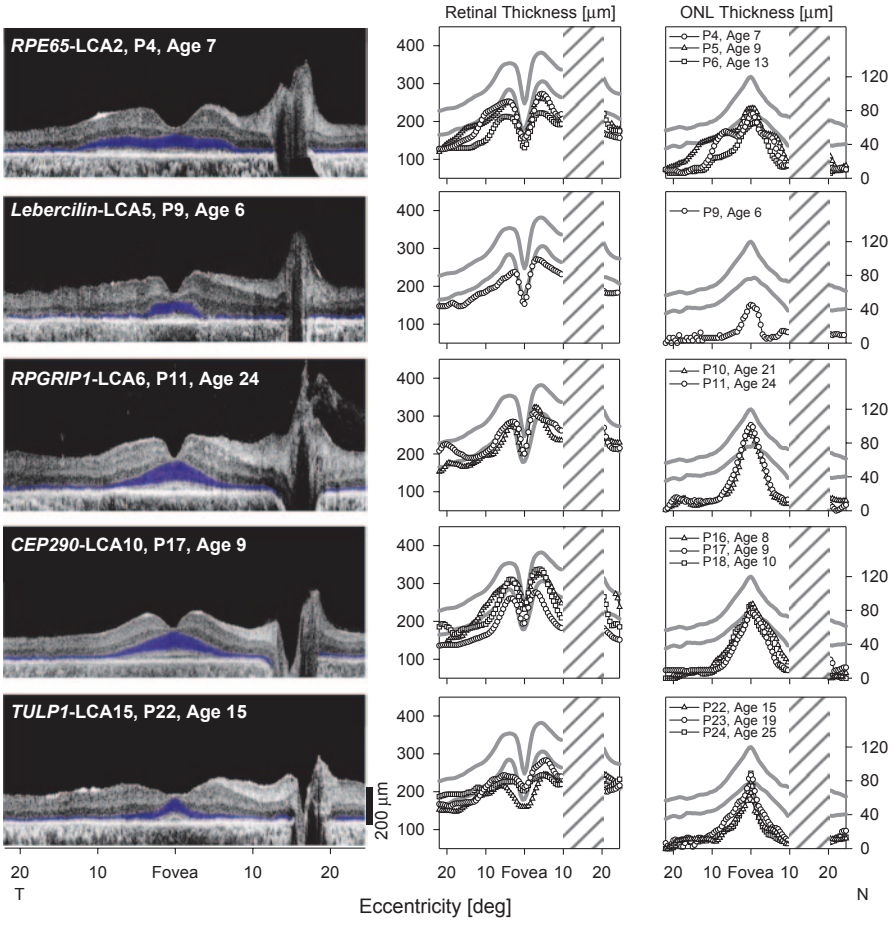

Fig. 23.2 Five LCA genotypes with preserved foveal architecture but mainly central ONL. OCTs and quantitative analyses of retinal and ONL thicknesses

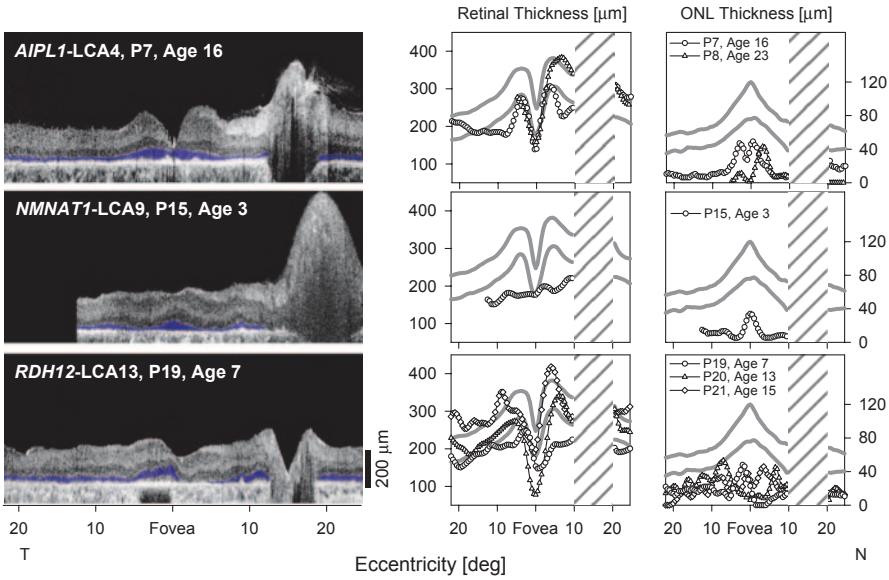

Fig. 23.3 Three LCA genotypes with macular disease or maldevelopment. OCTs and quantitative analyses of retinal and ONL thicknesses

but reduced centrally and across most of the scan. Retinal thickness varied in *AIPL1*-LCA4 and *RDH12*-LCA13; the *NMNAT1*-LCA15 patient had thinned retina (Fig. 23.3).

23.4 Discussion

Despite the advent of molecular diagnostics, there remains a need to understand disease expression (function and structure) in individual patients and within genotypes as treatment strategies emerge for retinal degenerations (Jacobson and Cideciyan 2010). Function is quantified with ERG and psychophysics. Retinal structure, beyond ophthalmoscopy and fundus photography, was understood from post-mortem retina donor studies (Milam et al. 1998). Optical imaging of the human retina can offer microscopic-level observations, and serial quantitation.

Our survey of 10 LCA genotypes indicates that there can be similarly severe visual deficits, but *in vivo* microscopic differences. Recognizable are *GUCY2D*-LCA1 patients with reduced vision but normal ONL thickness across a relatively wide expanse of retina (Jacobson et al. 2013a), and *CRB1*-LCA8 with thickened and coarsely laminated retinas.

Many LCA genotypes showed a foveal pit, suggesting normal central retinal development; foveal ONL was relatively preserved but ONL thickness declined with eccentricity. This implies early and profound loss of rods with less disease impact on central cones. Most of these genotypes are considered photoreceptor

ciliopathies. *RPE65*-LCA2 is a secondary photoreceptor loss due to visual cycle abnormality (Cideciyan 2010).

The third LCA group shares abnormalities in foveal-macular structure. The foveal pit in *AIPL1*-LCA4 suggests foveal development but early cone (and rod) loss. *NMNAT1*-LCA15 and maculopathy are associated; lack of a foveal pit and persistent inner retinal laminae suggest abnormal central retinal development. The exact mechanism causing *RDH12*-LCA13 is unclear; RDH12, localized to inner segments of rods and cones, may detoxify stray retinal (Chen et al. 2012).

Acknowledgements This study was supported by National Eye Institute Grant U10 EY 017290, Foundation Fighting Blindness, Hope for Vision, Macula Vision Research Foundation, the Chatlos Foundation, Inc. and the NU Foundation. AVC is an RPB Senior Scientific Scholar.

References

Aleman TS, Cideciyan AV, Aguirre GK et al (2011) Human CRB1-associated retinal degeneration: comparison with the rd8 Crb1-mutant mouse model. Invest Ophthalmol Vis Sci 52:6898–6910

Chen C, Thompson DA, Koutalos Y (2012) Reduction of all-trans-retinal in vertebrate rod photoreceptors requires the combined action of RDH8 and RDH12. J Biol Chem 287:24662–24670

Chung DC, Traboulsi EI (2009) Leber congenital amaurosis: clinical correlations with genotypes, gene therapy trials update, and future directions. J AAPOS 6:587–592

Cideciyan AV (2010) Leber congenital amaurosis due to RPE65 mutations and its treatment with gene therapy. Prog Retin Eye Res 29:398–427

den Hollander AI, Roepman R, Koenekoop RK et al (2008) Leber congenital amaurosis: genes, proteins and disease mechanisms. Prog Retin Eye Res 27:391–419.

Hebrard M, Manes G, Bocquet B et al (2011) Combining gene mapping and phenotype assessment for fast mutation finding in non-consanguineous autosomal recessive retinitis pigmentosa families. Eur J Hum Genet 19:1256–1263

Jacobson SG, Cideciyan AV (2010) Treatment possibilities for retinitis pigmentosa. N Engl J Med 363:1669–1671

Jacobson SG, Cideciyan AV, Aleman TS et al (2003) Crumbs homolog 1 (CRB1) mutations result in a thick human retina with abnormal lamination. Hum Mol Genet 12:1073–1078

Jacobson SG, Aleman TS, Cideciyan AV (2005) Identifying photoreceptors in blind eyes caused by RPE65 mutations: prerequisite for human gene therapy success. Proc Natl Acad Sci U S A 102:6177–6182

Jacobson SG, Cideciyan AV, Peshenko IV et al (2013a) Determining consequences of retinal membrane guanylyl cyclase (RetGC1) deficiency in human Leber congenital amaurosis en route to therapy. Hum Mol Genet 22:168–183

Jacobson SG, Sumaroka A, Luo X et al (2013b) Retinal optogenetic therapies: clinical criteria for candidacy. Clin Genet 84:175–182

Jacobson SG, Cideciyan AV, Huang WC et al (2014) TULP1 mutations causing early-onset retinal degeneration: preserved but insensitive macular cones. Invest Ophthalmol Vis Sci 55(8)5354–5364

Kaplan J (2008) Leber congenital amaurosis: from darkness to spotlight. Ophthalmic Genet 29:92–98

Milam AH, Li ZY, Fariss RN (1998) Histopathology of the human retina in retinitis pigmentosa. Prog Retin Eye Res 17:175–205

Pasadhika S, Fishman GA, Stone EM et al (2010) Differential macular morphology in patients with RPE65-, CEP290-, GUCY2D-, and AIPL1-related Leber congenital amaurosis. Invest Ophthalmol Vis Sci 51:2608–2614

Chapter 24
A Chemical Mutagenesis Screen Identifies Mouse Models with ERG Defects

Jeremy R. Charette, Ivy S. Samuels, Minzhong Yu, Lisa Stone, Wanda Hicks, Lan Ying Shi, Mark P. Krebs, Jürgen K. Naggert, Patsy M. Nishina and Neal S. Peachey

Abstract Mouse models provide important resources for many areas of vision research, pertaining to retinal development, retinal function and retinal disease. The Translational Vision Research Models (TVRM) program uses chemical mutagenesis to generate new mouse models for vision research. In this chapter, we report the identification of mouse models for *Grm1, Grk1* and *Lrit3*. Each of these is characterized by a primary defect in the electroretinogram. All are available without restriction to the research community.

Keywords Mutagenesis · Electroretinogram · Photoreceptor · Mice · Retina

N. S. Peachey (✉) · I. S. Samuels
Louis Stokes Cleveland VA Medical Center, Cleveland, OH 44106, USA
e-mail: peachen@ccf.org

I. S. Samuels
e-mail: Ivy.Samuels@va.gov

J. R. Charette · L. Stone · W. Hicks · L. Y. Shi · M. P. Krebs · J. K. Naggert · P. M. Nishina
The Jackson Laboratory, Bar Harbor, ME 04609, USA
e-mail: Jeremy.Charette@jax.org

L. Stone
e-mail: Lisa.Stone@jax.org

W. Hicks
e-mail: Wanda.jordan@jax.org

L. Y. Shi
e-mail: lanying_shi1234@163.com

M. P. Krebs
e-mail: Mark.Krebs@jax.org

J. K. Naggert
e-mail: Juergen.Naggert@jax.org

C. Bowes Rickman et al. (eds.), *Retinal Degenerative Diseases,* Advances in Experimental Medicine and Biology 854, DOI 10.1007/978-3-319-17121-0_24

24.1 Introduction

Mouse models of retinal diseases are an important genetic resource for furthering our understanding of molecules necessary for vision. This reflects, in part, our ability to develop and discover mouse models that bear disruption in genes implicated in human conditions and that replicate key features of human disease. The Translational Vision Research Models (TVRM) program, sited at The Jackson Laboratory (JAX), uses chemical mutagenesis followed by high throughput eye-specific screens to identify mouse models bearing mutations that lead to ocular phenotypes (Won et al. 2011, 2012). The purpose of this report is to describe three new models that extend allelic series for genes known to play important roles in the outer retina.

24.2 Materials and Methods

24.2.1 Mouse Mutagenesis, Husbandry, and Ocular Screening

As described in detail (Won et al. 2011), N-ethyl-N-nitrosourea (ENU) was administered to male C57BL/6J mice. G3 offspring generated using a three-generation backcross mating scheme (Won et al. 2011) were examined at 12 weeks of age. All mice underwent screening by indirect ophthalmoscopy (Hawes et al. 1999). A subset of mice were also screened by ERG, using a previously described system and protocol (Hawes et al. 2000). In brief, after a minimum of 2 h of dark adaptation, mice were anesthetized with ketamine (16 mg/kg) and xylazine (80 mg/kg) diluted in normal saline. Strobe stimuli were presented in darkness and again after 10 min of light adaption. In depth ERG studies were conducted at the Cleveland Clinic, using published protocols (Yu et al. 2012).

P. M. Nishina
e-mail: Nishina@jax.org

M. Yu · I. S. Samuels · N. S. Peachey
Cole Eye Institute, Cleveland Clinic, Cleveland, OH 44195, USA
e-mail: YUM@ccf.org

N. S. Peachey
Department of Ophthalmology, Cleveland Clinic Lerner College of Medicine of Case Western Reserve University, Cleveland, OH, USA

24.2.2 Genetic Mapping and Mutational Analysis

We mated *tvrm207* and *tvrm257* mutants with abnormal ERGs with DBA/2J mice. Resulting F1 offspring were intercrossed to generate a segregating F2 population. Each F2 progeny underwent ERG testing and genome wide scans using a DNA pooling strategy, and genotyping with simple sequence length polymorphism markers was carried out. We found *tvrm207* to map to Chr. 8 proximal to marker D8Mit124 while *tvrm257* mapped to Chr. 3 between markers D3Mit348 and D3Mit14. The mapping was based on 154 and 704 meioses, respectively.

Exome capture libraries prepared from *tvrm84* and *tvrm207* mutant DNAs were subject to high throughput sequencing. Mutations within candidate genes were identified by comparison of mutant and WT sequences and verified in 10 affected and 10 unaffected mice from the inbred *tvrm84* and *tvrm207* colonies. Without exception, affected mice were homozygous for the mutation while unaffected mice were either heterozygous or WT for the mutations.

In the case of *tvrm257,* primers within introns flanking exons in candidate genes were generated to amplify each exon from genomic DNA. DNA of mice from the mapping population (10 affected and 10 unaffected) and inbred *tvrm257* (5 affected and 5 unaffected) colonies were amplified, sequenced and compared using published procedures (Won et al. 2011). Without exception, affected mice were homozygous for the mutation while unaffected mice were either heterozygous or WT for the mutation.

24.2.3 Histological Analysis

Mice were euthanized by CO_2 inhalation and eyes were enucleated. Eyes were fixed overnight in cold methanol/acetic acid solution (3:1, v/v). Paraffin embedded eyes were cut into 6 µm sections, stained by hematoxylin and eosin (H&E), and examined by light microscopy.

24.3 Results

24.3.1 A New Allele of *Grm1*^{tvrm84}

The glutamate receptor, metabotropic 1 (GRM1) is widely expressed in the central nervous system (CNS). *GRM1* mutations or copy number variations may predispose to a variety of conditions including schizophrenia (Ayoub et al. 2012) or depression (Menke et al. 2012). Previously described *Grm1* mouse mutants include the recoil wobbler (*Grm1*^{rcw}) (Sachs et al. 2007), *Grm1*^{nmf373} (Sachs et al. 2007), *Grm1*^{crv4} (Conti et al. 2006) and *Grm1*$^{-/-}$ (Conquet et al. 1994) models. All have

reduced body size, a neurological phenotype including ataxic gait, tremor, skeletal defects, and learning abnormalities in the absence of gross structural defects of the CNS.

Affected *tvrm84* mice were identified based on their ataxic phenotype. Subsequent ERG testing showed the presence of a normal ERG waveform of reduced amplitude. Affected mice present with a normal fundus appearance and retinal histology. Comparison of high throughout sequencing data between mutant and WT mice indicated a c.1607T>A mutation in *Grm1*. The *Grm1*^{tvrm84} mutation is predicted to lead to a point mutation: p.Iso536Lys.

Figure 24.1 summarizes the ERG analysis. The upper panels present representative ERGs obtained under dark-adapted (Fig. 24.1a) or light-adapted (Fig. 24.1b) conditions. The overall ERG waveform is maintained in *Grm1*^{tvrm84} mice, but is reduced under dark-adapted conditions. The lower panels present average (±sem) measures of the major ERG components. The reduction of the dark-adapted ERG is seen across the stimulus range used (Fig. 24.1c), while the light-adapted data superimpose (Fig. 24.1d). No gross morphological abnormalities were observed in homozygous *Grm1*^{tvrm84} mice (data not shown).

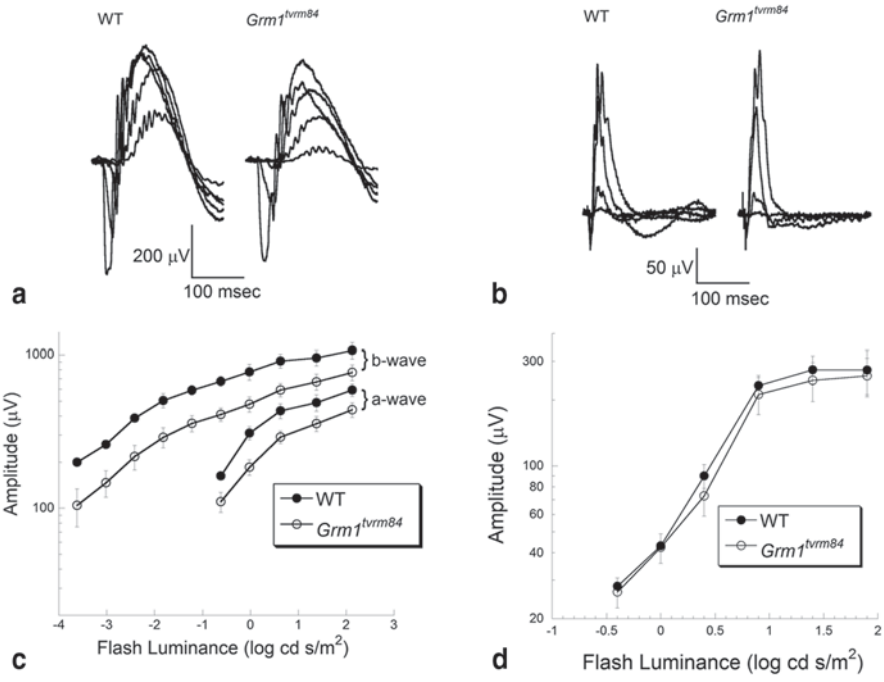

Fig. 24.1 ERG characteristics of *Grm1*^{tvrm84} mutant. Representative ERGs obtained from 1 month old mice under dark-adapted **a** and light-adapted **b** stimulus conditions. Summary response functions for the major components of the dark-adapted **c** and light-adapted **d** ERG. Symbols indicate average±sem of 8–9 mice

24.3.2 A New Allele for *Grk1*^{tvrm207}

Rhodopsin kinase, encoded by *GRK1/Grk1*, is responsible for the initial steps by which light-activated rhodopsin is returned to an inactive state. Rhodopsin kinase accomplishes this through phosphorylation of a series of serine residues on the C-terminus of rhodopsin (Mendez et al. 2000). In humans, *GRK1* mutations cause Oguchi's Disease (Yamamoto et al. 1997; Cideciyan et al. 1998). In mice, single cell studies of *Grk1*$^{-/-}$ rods reveal abnormal phototransduction deactivation kinetics (Chen et al. 1999). *Grk1*$^{-/-}$ mice have a modest loss of cells in the outer nuclear layer, but a more rapid loss of outer segment length (Fan et al. 2010).

The *tvrm207* line was identified by a reduced amplitude ERG and this feature was used to map *tvrm207* to Chr. 8. Comparison of exome sequences of *Grk1* identified a nucleotide transition: c.1088T>C. The *Grk1*^{tvrm207} mutation is predicted to lead to an amino acid change: p.Leu363Pro. As shown in Fig. 24.2a, ERG amplitudes are significantly reduced in *Grk1*^{tvrm207} mice. The amplitude reduction is present as early as P19, and there is relatively little progression up to 4 months of age (Fig. 24.2b). Consistent with the ERG data, the outer nuclear layer of *Grk1*^{tvrm207} mice changes little in overall thickness over the first 3 months. Photoreceptors are absent, however, by 1 year of age (Fig. 24.2d). The loss of photoreceptors may be due to the extended exposure to vivarium lighting over the lifetime of the animals, as *Grk1*$^{-/-}$ mice are sensitive to light induced damage (Chen et al. 1999).

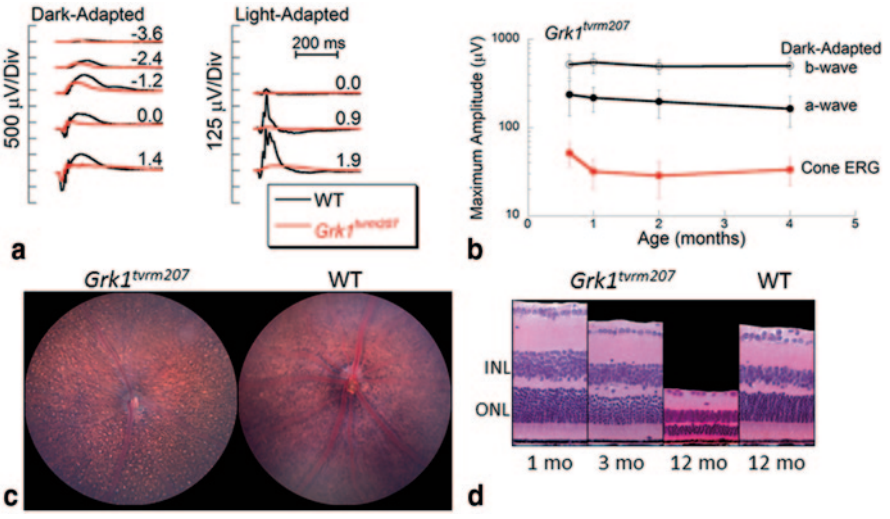

Fig. 24.2 Characteristics of *Grk1*^{tvrm207} mutant. **a** ERGs obtained from 1-month-old mice under dark-adapted (*left*) and light-adapted (*right*) stimulus conditions. **b** The reduction in ERG amplitude is present at an early age and remains stable across the age-range examined. **c** Fundus photo of a 12-old-mutant indicate retinal spotting and granular appearance in comparison to a 3-month-old C57BL/6J mouse. **d** Representative retinal cross-sections obtained from 1-, 3-, and 12-month-old mutant and 12-month-old control mice

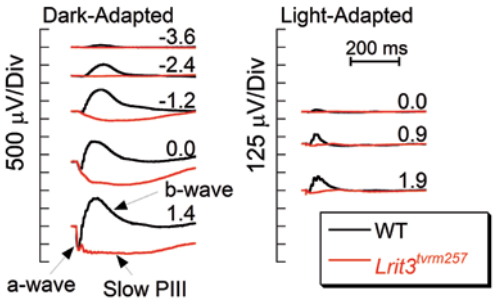

Fig. 24.3 ERG Characteristics of *Lrit3*^{tvrm257} mutant. ERGs obtained from 1 month old mice under dark-adapted (*left*) and light-adapted (*right*) stimulus conditions

24.3.3 A New Allele for Lrit3^{tvrm257}

Leucine-rich repeat, immunoglobulin-like and transmembrane domains 3 (*LRIT3*) is the most recently identified gene in which mutations cause complete congenital stationary night blindness (cCSNB) (Zeitz et al. 2013). This discovery was followed by the description of a null mutant for *Lrit3,* which has a preserved ERG a-wave, an absent ERG b-wave, and normal retinal morphology (Neuillé et al. 2014). The *tvrm257* line was identified based on an absent ERG b-wave, and this feature was mapped to the *Lrit3* locus. Direct sequencing of amplified exons of *Lrit3* from *tvrm257* mice identified a nucleotide transition: c.401T>C. The *Lrit3*^{tvrm257} mutation is predicted to lead to a point mutation: p.Leu134Pro.

ERG studies document the presence of a normal a-wave without a subsequent b-wave in *Lrit3*^{tvrm257} mice (Fig. 24.3). The cone ERG is also abnormal. Gross morphological abnormalities are not observed in *Lrit3*^{tvrm257} mutants up to 7 months of age, the oldest age examined (data not shown). Overall this phenotype matches that of the *Lrit3*$^{-/-}$ mouse (Neuillé et al. 2014) and other mouse models involving proteins expressed in depolarizing bipolar cells (Pardue and Peachey 2014).

24.4 Discussion

We report the identification of three new mouse strains with disruption in *Grm1*, *Grk1* or *Lrit3*. The main retinal abnormality is an abnormal ERG, although the nature of this abnormality differs across the three mouse models. Unlike the knockout models that are currently available, these mouse lines all involve missense mutations which are not expected to abrogate protein translation, and all mutations are coisogenic on the C57BL/6J background. Overall, such point mutants are rare, as knockout targeting vectors are designed to ensure total loss of expression and absence of the encoded protein. Point mutants can provide information about domain functions and may exhibit different phenotypes compared to their knock-out counterparts (e.g., Peachey et al. 2012). These mice, therefore, provide or expand the allelic series for the genes involved. As is the case for other TVRM models, these mice are available without restriction to the research community.

Acknowledgments This work was supported by NIH grants (R01EY16501; P30CA34196), Foundation Fighting Blindness, VA Medical Research Service, and Research to Prevent Blindness.

References

Ayoub MA, Angelicheva D, Vile D et al (2012) Deleterious GRM1 mutations in schizophrenia. PLoS ONE 7:e32849

Chen CK, Burns ME, Spencer M et al (1999) Abnormal photoresponses and light-induced apoptosis in rods lacking rhodopsin kinase. Proc Natl Acad Sci U S A 96:3718–3722

Cideciyan AV, Zhao X, Nielsen L et al (1998) Null mutation in the rhodopsin kinase gene slows recovery kinetics of rod and cone phototransduction in man. Proc Natl Acad Sci U S A 95:328–333

Conquet F, Bashir ZI, Davies CH et al (1994) Motor deficit and impairment of synaptic plasticity in mice lacking mGluR1. Nature 372:237–243

Conti V, Aghaie A, Cilli M et al (2006) crv4, a mouse model for human ataxia associated with kyphoscoliosis caused by an mRNA splicing mutation of the metabotropic glutamate receptor 1 (Grm1). Int J Mol Med 18:593–600

Fan J, Sakurai K, Chen CK et al (2010) Deletion of GRK1 causes retina degeneration through a transducin-independent mechanism. J Neurosci 30:2496–2503

Hawes NL, Smith RW, Chang B et al (1999) Mouse fundus photography and angiography: a catalogue of normal and mutant phenotypes. Mol Vis 5:22

Hawes NL, Chang B, Hageman GS et al (2000) Retinal degeneration 6 (rd6): a new mouse model for human retinitis punctata albescens. Invest Ophthalmol Vis Sci 41:3149–3157

Mendez A, Burns ME, Roca A et al (2000) Rapid and reproducible deactivation of rhodopsin requires multiple phosphorylation sites. Neuron 28:153–164

Menke A, Sämann P, Kloiber S et al (2012) Polymorphisms within the metabotropic glutamate receptor 1 gene are associated with depression phenotypes. Psychoneuroendocrinol 37:565–575

Neuillé M, El Shamieh S, Orhan E et al (2014) Lrit3 deficient mouse (nob6): a novel model of complete congenital stationary night blindness (cCSNB). PLoS ONE 9:e90342

Pardue MT, Peachey NS (2014) Mouse b-wave mutants. Doc Ophthalmol 128:77–89

Peachey NS, Pearring JN, Bojang P Jr et al (2012) Depolarizing bipolar cell dysfunction due to a *Trpm1* point mutation. J Neurophysiol 108:2442–2451

Sachs AJ, Schwendinger JK, Yang AW et al (2007) The mouse mutants *recoil wobbler* and *nmf373* represent a series of *Grm1* mutations. Mamm Genome 18:749–756

Won J, Shi LY, Hicks W et al (2011) Mouse models for vision research. J Ophthalmol 2011:391384

Won J, Shi LY, Hicks W et al (2012) Translational vision research models program. Adv Exp Med Biol 723:391–397

Yamamoto S, Sippel KC, Berson EL, Dryja TP (1997) Defects in the rhodopsin kinase gene in the Oguchi form of stationary night blindness. Nat Genet 15:175–178

Yu M, Sturgill-Short G, Ganapathy P et al (2012) Age-related changes in visual function in *cystathionine-beta-synthase* mutant mice, a model of hyperhomocysteinemia. Exp Eye Res 96:124–131

Zeitz C, Jacobson SG, Hamel CP et al (2013) Whole-exome sequencing identifies LRIT3 mutations as a cause of autosomal-recessive complete congenital stationary night blindness. Am J Hum Genet 92:67–75

Chapter 25
Ablation of *Chop* Transiently Enhances Photoreceptor Survival but Does Not Prevent Retinal Degeneration in Transgenic Mice Expressing Human P23H Rhodopsin

Wei-Chieh Chiang, Victory Joseph, Douglas Yasumura, Michael T. Matthes, Alfred S. Lewin, Marina S. Gorbatyuk, Kelly Ahern, Matthew M. LaVail and Jonathan H. Lin

Abstract *RHO* (Rod opsin) encodes a G-protein coupled receptor that is expressed exclusively by rod photoreceptors of the retina and forms the essential photopigment, rhodopsin, when coupled with 11-cis-retinal. Many rod opsin disease mutations cause rod opsin protein misfolding and trigger endoplasmic reticulum (ER) stress, leading to activation of the Unfolded Protein Response (UPR) signal transduction network. *Chop* is a transcriptional activator that is induced by ER stress and promotes cell death in response to chronic ER stress. Here, we examined the role of *Chop* in transgenic mice expressing human P23H rhodopsin (hP23H Rho Tg) that undergo retinal degeneration. With the exception of one time point, we found no significant induction of *Chop* in these animals and no significant change in retinal degeneration by histology and electrophysiology when hP23H Rho Tg animals were bred into a $Chop^{-/-}$ background. Our results indicate that *Chop* does not play a significant causal role during retinal degeneration in these animals. We suggest that other modules of the ER stress-induced UPR signaling network may be involved photoreceptor disease induced by P23H rhodopsin.

Keywords Rhodopsin · P23H · Unfolded protein response · UPR · ER stress · Photoreceptor cell death · Chop · Retinal degeneration · Transgenic mice

D. Yasumura is deceased.

J. H. Lin (✉) · W.-C. Chiang · V. Joseph
Department of Pathology, University of California, La Jolla, San Diego, CA 92093, USA
e-mail: JLIN@ucsd.edu

J. H. Lin
VA San Diego Healthcare System, San Diego, CA 92161, USA

W.-C. Chiang
e-mail: wcchiang@ucsd.edu

V. Joseph
e-mail: vtj2101@gmail.com

C. Bowes Rickman et al. (eds.), *Retinal Degenerative Diseases,* Advances in Experimental Medicine and Biology 854, DOI 10.1007/978-3-319-17121-0_25

25.1 Introduction

Rhodopsin protein folding begins when *RHO* mRNA is translated into protein at the endoplasmic reticulum (ER) in the photoreceptor (PR) inner segment (IS) ellipsoid region. Many rhodopsin mutations associated with retinal degeneration introduce amino acid substitutions that impair rod opsin's ability to fold properly in the ER (Sung et al. 1991; Kaushal and Khorana 1994). Accumulation of unfolded proteins in the ER triggers ER stress. The Unfolded Protein Response (UPR) is an intracellular signal transduction network that is activated by ER stress and, in turn, activates transcriptional, translational, and post-translational programs that help cells correct the protein misfolding problem that caused ER stress (Walter and Ron 2011). However, if misfolded proteins persist, UPR signaling can activate pro-apoptotic programs leading to cell death (Walter and Ron 2011).

Chop (C/EBP homologous protein) is one genetic component of the UPR and encodes a transcription factor whose mRNA and protein levels are upregulated by the UPR in response to ER stress (Oyadomari and Mori 2004). $Chop^{-/-}$ mouse embryonic fibroblasts are resistant to cell death induced by thapsigargin, an inhibitor of the Ca^{2+} ATPase of the ER, and tunicamycin, which blocks N-linked glycosylation (Zinszner et al. 1998). Akita mice expressing mutant insulin 2 undergo pancreatic β-cell death that was delayed in a $Chop^{-/-}$ background (Oyadomari et al. 2002). Mice expressing mutant myelin protein zero undergo increased Schwann cell death that was delayed by loss of *Chop* (Pennuto 2008). These findings indicate that CHOP contributes to cell death and injury in response to certain types of ER stress. Here, we examined whether *Chop* was induced in transgenic mice expressing

D. Yasumura · M. T. Matthes · K. Ahern
Department of Ophthalmology, University of California, San Francisco, CA 94143, USA

M. T. Matthes
e-mail: Michael.Matthes@ucsf.edu

A. S. Lewin
Department of Molecular Genetics and Microbiology, University of Florida,
Gainesville, FL 32610, USA
e-mail: lewin@UFL.EDU

M. S. Gorbatyuk
Department of Vision Sciences, University of Alabama at Birmingham,
Birmingham, AL 35294, USA
e-mail: mgortk@uab.edu

K. Ahern
e-mail: kcahern@gmail.com

M. M. LaVail
Departments of Anatomy and Ophthalmology, University of California,
San Francisco, CA 94143, USA
e-mail: Matthew.LaVail@ucsf.edu

human P23H rhodopsin, and how retinal degeneration was affected when these animals were bred into a $Chop^{-/-}$ background.

25.2 Materials and Methods

$Chop^{-/-}$ mice were obtained from Jackson Laboratory. Human P23H rhodopsin transgenic (hP23H Rho Tg) mice were generated as previously described (White et al. 2007) and maintained in wild-type rhodopsin ($Rho^{+/+}$) background (C57Bl/6J) for these studies. Histologic studies were performed as previously described (Chiang et al. 2014)

Quantitative PCR analysis of murine *Chop* mRNA levels was performed as previously described (Hiramatsu et al. 2011). Electroretinographic studies were performed on dark-adapted mice as previously described (Gorbatyuk et al. 2010). Studies were conducted in accordance with the ARVO Statement for the Use of Animals in Ophthalmic and Vision Research and IACUC guidelines at the University of California, San Francisco and the University of California, San Diego.

25.3 Results

25.3.1 Retinal Degeneration of Human P23H Rhodopsin Transgenic Mice in $Chop^{-/-}$ Background

The outer nuclear layer (ONL) thickness of $Chop^{-/-}$ mice did not differ from wild-type over the first ~9 months of life (Fig. 25.1a). hP23H Rho Tg mice in a $Rho^{+/+}$ background underwent relatively mild retinal degeneration compared to P23H rhodopsin transgenic rats (Pennesi et al. 2008) and P23H rhodopsin knock-in mice (Sakami et al. 2011). At postnatal day (P) 90, the ONL thickness of the hP23H Rho Tg mice was ~25% thinner than the ONL of age-matched wild-type mice (Fig. 25.1b). To investigate the role of *Chop* in photoreceptor cell death induced by P23H rhodopsin, we crossed $Chop^{-/-}$ mice with hP23H Rho Tg mice and measured ONL from P30 to P210. At P60, we found a small, but significant increase in the ONL thickness of retinas from $Chop^{-/-}$ hP23H Rho Tg mice (39.9 ± 0.36 μm) compared to hP23H Rho Tg mice (36.5 ± 0.42 μm) ($P = 0.00124$) (Fig. 25.1b). However, we saw no other improvement of ONL thicknesses in $Chop^{-/-}$ hP23H Rho Tg mice compared to $Chop^{+/-}$ hP23H Rho Tg mice or hP23H Rho Tg mice at any other time points studied (Fig. 25.1b). These data indicated that loss of *Chop* provided a small transient protective effect at P60 but did not significantly alter the eventual loss of photoreceptors in hP23H Rho Tg mice.

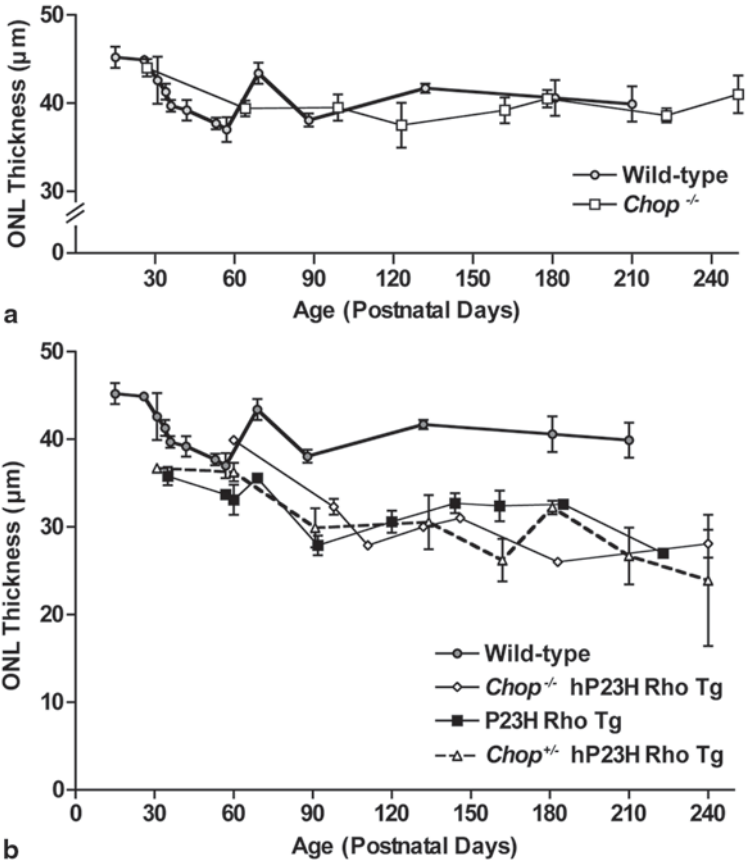

Fig. 25.1 Retinal degeneration in wild-type, hP23H Rho Tg, *Chop*$^{-/-}$, *Chop*$^{-/-}$ hP23H Rho Tg, and *Chop*$^{+/-}$ hP23H Rho Tg mice. **a** Mean ONL thickness of wild-type, and *Chop*$^{-/-}$ mice at the indicated ages. **b** Mean ONL thickness of wild-type, hP23H Rho Tg, *Chop*$^{-/-}$ hP23H Rho Tg, and *Chop*$^{+/-}$ hP23H Rho Tg at the indicated ages. Each value is the mean ± SEM of 2–7 retinas

25.3.2 Expression of Chop in Human P23H Rhodopsin Transgenic Mice

In parallel with our histologic analysis, we measured *Chop* mRNA levels in the retinas of hP23H Rho Tg mice by quantitative RT-PCR from P13 to P118 (Fig. 25.2). *Chop* mRNA levels in hP23H Rho Tg retinas did not differ from age-matched wild-type mice, except at P56 when we observed a modest, but significant, increase of *Chop* expression (1.21 fold increase in *Chop* mRNA levels compared to age-matched wild-types, $P = 0.018$) (Fig. 25.2a and 25.2b). This age of increased *Chop* expression roughly coincided with the rescue in ONL thickness we observed in P60 *Chop*$^{-/-}$ hP23H Rho Tg mice (Fig. 25.1b).

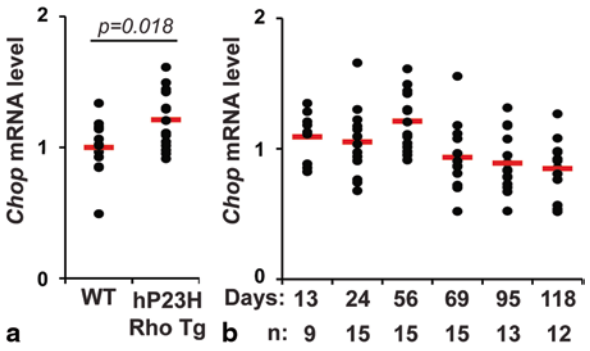

Fig. 25.2 Induction of *Chop* mRNA in retinas of human P23H rhodopsin transgenic mice. **a** Analysis of *Chop* mRNA levels by quantitative PCR using wild-type or hP23H Rho Tg mouse retina samples at postnatal day age 56. Student's two-tailed t-tests were performed to determine *P* values. **b** Analysis of *Chop* mRNA levels in the retinas of hP23H Rho Tg mice by quantitative PCR using mouse retina samples at indicated postnatal day ages. Samples were plotted relative to the average *Chop* mRNA levels at the same age in wild-type control mice. **a**–**b** The mean value at each time point is plotted as a *horizontal line*

25.3.3 Chop Knock-out Did Not Rescue the Function of Retinas of Human P23H Rhodopsin Transgenic Mice

We performed electroretinogram (ERG)) analysis in wild-type and $Chop^{-/-}$ hP23H Rho Tg mice at P95, an age with clear ONL differences between hP23H Rho Tg and wild-type mice. Under scotopic settings, we observed decreased a-wave and b-wave responses in hP23H Rho Tg mice compared to that of the wild-type mice (Fig. 25.3). $Chop^{-/-}$ hP23H Rho Tg mice showed no significant difference in ERG responses compared to hP23H Rho Tg mice or $Chop^{+/-}$ hP23H Rho Tg mice (Fig. 25.3). Together with our ONL measurements (Fig. 25.1), these results show that loss of *Chop* did not significantly alter photoreceptor cell death or retinal function during retinal degeneration in the hP23H Rho Tg mice.

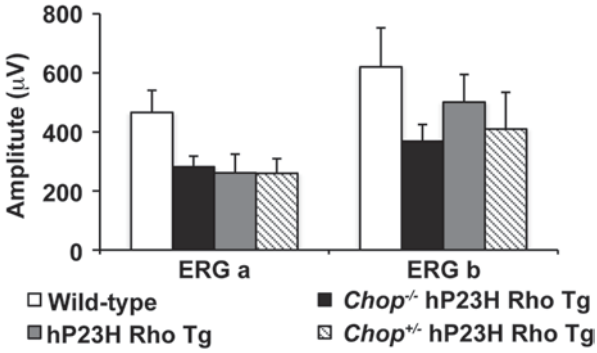

Fig. 25.3 *Chop* deficiency did not rescue the function of photoreceptors in human P23H rhodopsin transgenic mice. ERG a- and b-wave amplitudes were measured with wild-type, hP23H Rho Tg, $Chop^{-/-}$ hP23H Rho Tg, and $Chop^{+/-}$ hP23H Rho Tg mice at postnatal day 95

25.4 Discussion

Many mutations in the human *RHO* causing autosomal dominant retinitis pigmentosa lead to rhodopsin misfolding and activate the UPR signaling network (Mendes et al. 2005; Lin et al. 2007; Gorbatyuk 2010; Chiang et al. 2012). CHOP is one component of the UPR that is potently induced by ER toxins *in vitro* and in some animal models of diabetes and neuropathy; and loss of *Chop* partially prevents cell death in response to these types of ER stress (Zinszner et al. 1998; Oyadomari et al. 2002; Pennuto 2008). Here, we found that transgenic mice expressing human P23H rhodopsin did not induce the expression of *Chop* during retinal degeneration, nor did loss of *Chop* significantly alter retinal degeneration by histology or ERG during the time period we studied, with the exception of an early time point at ~P60, when we saw a mild improvement that did not persist in older animals.

Our findings are similar to prior studies of transgenic mice expressing T17M rhodopsin, transgenic "*GHL*" mice expressing triply mutated V20G, P23H, and P27L rhodopsin, and heterozygous P23H rhodopsin knock-in mice ($Rho^{P23H/+}$) (Nashine et al. 2013; Adekeye et al. 2014; Chiang et al. 2014), where the loss of *Chop* also did not confer significant protection from retinal degeneration in T17M Rho, $Rho^{P23H/+}$, or "*GHL*" mice, except in older *GHL* animals with severe retinal degeneration and then, only in their central retinas. As we did not study hP23H Rho Tg mice beyond 9 months of age, we cannot exclude that *Chop* may play additional roles at more advanced stages of retinal degeneration in older hP23H Rho Tg mice. In summary, our results provide additional evidence that CHOP does not significantly contribute to the photoreceptor cell death associated with rhodopsin mutations. We suggest that photoreceptors expressing mutant rhodopsins may preferentially activate components of the UPR other than CHOP. Given the complexity and diversity of signaling programs activated by ER stress, future studies will determine which components of the UPR signaling network are most important in photoreceptors undergoing misfolded rhodopsin-induced ER stress.

Acknowledgments These studies were supported by NIH grants EY001919, P30EY002162, and EY020846, VA Merit award BX002284, and the Foundation Fighting Blindness. W.-C. Chiang received postdoctoral support from the Fight-for-Sight Foundation.

References

Adekeye A, Haeri M, Solessio E et al (2014) Ablation of the proapoptotic genes chop or Ask1 does not prevent or delay loss of visual function in a P23H transgenic mouse model of retinitis pigmentosa. PLoS One 9:e83871

Chiang WC, Messah C, Lin JH (2012) IRE1 directs proteasomal and lysosomal degradation of misfolded rhodopsin. Mol Biol Cell 23:758–770

Chiang WC, Kroeger H, Sakami S et al (2014) Robust endoplasmic reticulum-associated degradation of rhodopsin precedes retinal degeneration. Mol Neurobiol

Gorbatyuk MS (2010) Restoration of visual function in P23H rhodopsin transgenic rats by gene delivery of BiP/Grp78. Proc Natl Acad Sci U S A 107:5961–5966
Gorbatyuk MS, Knox T, LaVail MM et al (2010) Restoration of visual function in P23H rhodopsin transgenic rats by gene delivery of BiP/Grp78. Proc Natl Acad Sci U S A 107:5961–5966
Hiramatsu N, Joseph VT, Lin JH (2011) Monitoring and manipulating mammalian unfolded protein response. Methods Enzymol 491:183–198
Kaushal S, Khorana HG (1994) Structure and function in rhodopsin. 7. Point mutations associated with autosomal dominant retinitis pigmentosa. Biochemistry 33:6121–6128
Lin JH, Li H, Yasumura D et al (2007) IRE1 signaling affects cell fate during the unfolded protein response. Science 318:944–949
Mendes HF, van der Spuy J, Chapple JP et al (2005) Mechanisms of cell death in rhodopsin retinitis pigmentosa: implications for therapy. Trends Mol Med 11:177–185
Nashine S, Bhootada Y, Lewin AS et al (2013) Ablation of C/EBP homologous protein does not protect T17M RHO mice from retinal degeneration. PLoS One 8:e63205
Oyadomari S, Mori M (2004) Roles of CHOP/GADD153 in endoplasmic reticulum stress. Cell Death Differ 11:381–389
Oyadomari S, Koizumi A, Takeda K et al (2002) Targeted disruption of the Chop gene delays endoplasmic reticulum stress-mediated diabetes. J Clin Invest 109:525–532
Pennesi ME, Nishikawa S, Matthes MT et al (2008) The relationship of photoreceptor degeneration to retinal vascular development and loss in mutant rhodopsin transgenic and RCS rats. Exp Eye Res 87:561–570
Pennuto M (2008) Ablation of the UPR-mediator CHOP restores motor function and reduces demyelination in Charcot-Marie-Tooth 1B mice. Neuron 57:393–405
Sakami S, Maeda T, Bereta G et al (2011) Probing mechanisms of photoreceptor degeneration in a new mouse model of the common form of autosomal dominant retinitis pigmentosa due to P23H opsin mutations. J Biol Chem 286:10551–10567
Sung CH, Schneider BG, Agarwal N et al (1991) Functional heterogeneity of mutant rhodopsins responsible for autosomal dominant retinitis pigmentosa. Proc Natl Acad Sci U S A 88:8840–8844
Walter P, Ron D (2011) The unfolded protein response: from stress pathway to homeostatic regulation. Science 334:1081–1086
White DA, Fritz JJ, Hauswirth WW et al (2007) Increased sensitivity to light-induced damage in a mouse model of autosomal dominant retinal disease. Invest Ophthalmol Vis Sci 48:1942–1951
Zinszner H, Kuroda M, Wang X et al (1998) CHOP is implicated in programmed cell death in response to impaired function of the endoplasmic reticulum. Genes Dev 12:982–995

Chapter 26
Identification of a Novel Gene on 10q22.1 Causing Autosomal Dominant Retinitis Pigmentosa (adRP)

Stephen P. Daiger, Lori S. Sullivan, Sara J. Bowne, Daniel C. Koboldt, Susan H. Blanton, Dianna K. Wheaton, Cheryl E. Avery, Elizabeth D. Cadena, Robert K. Koenekoop, Robert S. Fulton, Richard K. Wilson, George M. Weinstock, Richard A. Lewis and David G. Birch

Abstract Whole-genome linkage mapping identified a region on chromosome 10q21.3-q22.1 with a maximum LOD score of 3.0 at 0% recombination in a six-generation family with autosomal dominant retinitis pigmentosa (adRP). All known adRP genes and X-linked RP genes were excluded in the family by a combination of methods. Whole-exome next-generation sequencing revealed a missense

S. P. Daiger (✉) · L. S. Sullivan · S. J. Bowne · C. E. Avery · E. D. Cadena
Human Genetics Center, School of Public Health, The University of Texas HSC, 1200 Pressler St., Houston, TX 77030, USA
e-mail: Stephen.P.Daiger@uth.tmc.edu

S. P. Daiger
Ruiz Department of Ophthalmology and Visual Science, Medical School, The University of Texas Health Science Center, Houston, TX 77030, USA

D. C. Koboldt · R. S. Fulton · R. K. Wilson
The Genome Institute, Washington University School of Medicine, St. Louis, MO 63108, USA
e-mail: dkoboldt@genome.wustl.edu

S. H. Blanton
John P. Hussman Institute for Human Genomics, University of Miami Miller School of Medicine, Miami, FL 33136, USA
e-mail: sblanton@med.miami.edu

Dr. John T. Macdonald Foundation Department of Human Genetics, University of Miami Miller School of Medicine, Miami, FL 33136, USA

D. K. Wheaton · D. G. Birch
The Retina Foundation of the Southwest, Dallas, TX 75231, USA
e-mail: dwheaton@retinafoundation.org

R. K. Koenekoop
McGill Ocular Genetics Laboratory, Departments of Paediatric Surgery, Human Genetics and Ophthalmology, Montreal Children's Hospital, McGill University Health Center, Montreal, QC H3H 1P3, Canada
e-mail: robkoenekoop@hotmail.com

C. Bowes Rickman et al. (eds.), *Retinal Degenerative Diseases,* Advances in Experimental Medicine and Biology 854, DOI 10.1007/978-3-319-17121-0_26

mutation in hexokinase 1, HK1 c.2539G>A, p.Glu847Lys, tracking with disease in all affected family members. One severely-affected male is homozygous for this region by linkage analysis and has two copies of the mutation. No other potential mutations were detected in the linkage region nor were any candidates identified elsewhere in the genome. Subsequent testing detected the same mutation in four additional, unrelated adRP families, for a total of five mutations in 404 probands tested (1.2%). Of the five families, three are from the Acadian population in Louisiana, one is French Canadian and one is Sicilian. Haplotype analysis of the affected chromosome in each family and the homozygous individual revealed a rare, shared haplotype of 450 kb, suggesting an ancient founder mutation. HK1 is a widely-expressed gene, with multiple, abundant retinal transcripts, coding for hexokinase 1. Hexokinase catalyzes phosphorylation of glucose to glusose-6-phospate, the first step in glycolysis. The Glu847Lys mutation is in a highly-conserved site, outside of the active site or known functional sites.

Keywords Hexokinase · Founder effect · Retinitis pigmentosa · Autosomal dominant retinitis pigmentosa · Next-generation sequencing · Linkage mapping

R. A. Lewis
Departments of Ophthalmology, Medicine, Pediatrics and Molecular and Human Genetics, Baylor College of Medicine, Houston, TX 77030, USA
e-mail: rlewis@bcm.tmc.edu

G. M. Weinstock
Microbial Genomics, The Jackson Laboratory for Genomic Medicine, Farmington, CT 06032, USA
e-mail: george.weinstock@jax.org

L. S. Sullivan
e-mail: lori.s.sullivan@uth.tmc.edu

S. J. Bowne
e-mail: sara.j.bowne@uth.tmc.edu

D. C. Koboldt
e-mail: dkoboldt@genome.wustl.edu

D. K. Wheaton
e-mail: dwheaton@retinafoundation.org

C. E. Avery
e-mail: cheryl.e.avery@uth.tmc.edu

E. D. Cadena
e-mail: elizabeth.d.cadena@uth.tmc.edu

R. S. Fulton
e-mail: rfulton22@wustl.edu

R. K. Wilson
e-mail: rwilson@wustl.edu

D. G. Birch
e-mail: dbirch@retinafoundation.org

26.1 Introduction

Retinitis pigmentosa (RP) has a prevalence of approximately 1 in 4000 and affects more than 1.5 million individuals world-wide (Haim 2002; Daiger et al. 2007). RP is extremely heterogeneous: mutations in more than 60 genes cause syndromic and non-syndromic forms of RP, more than 3100 mutations have been described in these genes, and disease symptoms and progression are highly variable (Daiger et al. 2007; Berger et al. 2010; Wright et al. 2010; RetNet 2014). Our research focuses on finding genes and mutations causing autosomal dominant RP (adRP). To date mutations in more than 20 genes are known to cause adRP and these genes and mutations are themselves highly heterogeneous (Daiger et al. 2014a).

In research over the past 25 years we have assembled a cohort of adRP families and applied a wide range of methods to detect the disease-causing mutation in each family, most recently using several next-generation sequencing (NGS) approaches (Sohocki et al. 2001; Sullivan et al. 2006; Daiger et al. 2014a; Daiger et al. 2014b). In one large, six-generation Louisiana family, UTAD003, linkage mapping identified a novel adRP locus on chromosome 10q22. Here we report identification of the disease-causing gene and mutation in this family and evidence of a founder-effect in the gene, hexokinase 1 (HK1), accounting for approximately 1% of adRP in Americans of European origin and Europeans (Sullivan et al. 2014).

26.2 Materials and Methods

26.2.1 Family Ascertainment and Clinical Characterization

Families in the Houston AdRP Cohort are ascertained and examined by clinical collaborators in Houston, at the Retina Foundation of the Southwest, and in other retinal genetics centers. Clinical examinations include best-corrected visual acuity, visual fields, dark adaptometry, dark-adapted full-field electroretinograms, spectral-domain optical coherence tomography, anterior and indirect ophthalmoscopy, and retinal imaging (Churchill et al. 2013; Sullivan et al. 2014). Genetic testing is conducted in the Laboratory for Molecular Diagnosis of Inherited Eye Diseases, a CLIA-Certified research facility in the Human Genetics Center, School of Public Health, at the University of Texas Health Science Center, Houston. Families in the Cohort have an initial diagnosis of adRP and three or more affected generations with affected females, or two or more generations with male-to-male transmission. Currently, there are 270 families in the Cohort (Daiger et al. 2014a).

The research adhered to the tenets of the Declaration of Helsinki and the study was approved by the Committee for the Protection of Human Subjects at UTHealth, Houston, and by human subjects review boards at participating institutions.

26.2.2 Next-Generation Sequencing (NGS)

Whole-exome NGS of 4 affected and 4 unaffected members of UTAD003 was done at The Genome Institute, Washington Univ., St. Louis (Bowne et al. 2011). Exome capture was done using a customized Agilent SureSelect All Exome Kit v.2.0 or the Nimblegen SeqCap EZ Human Exome Library v.2.0. Illumina paired-end sequencing, alignment, and variant calling were performed using the VarScan and MendelScan software packages developed for this project (Koboldt et al. 2014). Variants were ranked based on segregation, rareness in human populations, predicted functional impact, and expression level in human retinal tissue.

26.2.3 Linkage Mapping and Haplotype Analysis

DNA samples from nine affected and six unaffected, at-risk, members of the UTAD003 family, and an additional parent, were genotyped at the UCLA Sequencing and Genotyping Center with an ABI High Density 5 cM STR marker set. Data from the 811 STR markers were analyzed with the LINKAGE package. For haplotyping, STR markers were selected from the ABI linkage mapping set and haplotypes were determined by inspection and confirmed by segregation analysis (Sullivan et al. 2014).

26.3 Results

26.3.1 Linkage Mapping in UTAD003

UTAD003 is a large Louisiana adRP family with over six known, affected generations (Fig. 26.1). It is one of the 270 AdRP Cohort families in our studies. Probands of families in the cohort have been tested for mutations causing adRP by Sanger sequencing and retinal-capture NGS and, in the absence of male-to-male transmission, for mutations in RPGR and RP2 (Sullivan et al. 2006; Churchill et al. 2013; Wang et al. 2013). No disease-causing mutations were detected in UTAD003 by these methods.

Samples from 19 family members were tested for linkage. Multipoint linkage analysis with affected family members produced a single chromosomal region with a LOD score of 3.0, on chromosome 10q21.3–10q22.1. This region spans approximately 9 Mb and includes 96 putative genes. Subsequently, intragenic and flanking STR markers from the ABI linkage set were tested to refine the linkage region (Sullivan et al. 2014).

Whole-exome NGS revealed a missense mutation in the HK1 gene, c.2539G>A, p.Glu847Lys, tracking with disease in all available, affected members of UTAD003, with two homozygous copies in one severely-affected family member. No other potentially-pathogenic mutations were identified in the linkage region or elsewhere in the genome.

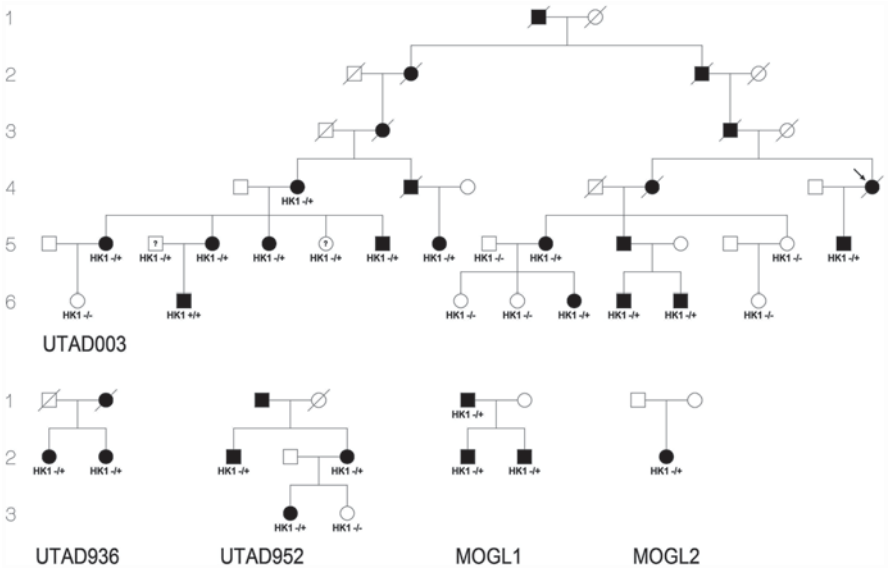

Fig. 26.1 Pedigrees of five adRP families with the HK1 Glu847Lys missense mutation. *Squares* males; *circles* females; *blackened symbols* affected. All individuals with an HK1 genotype indicated were tested. $HK1^{-/+}$, heterozygous for the mutation; $HK1^{+/+}$, homozygous for the mutation; $HK1^{-/-}$, no mutation

26.3.2 Linkage Mapping in Additional Families

The entire HK1 gene was sequenced in 346 additional, unrelated probands with a diagnosis of adRP (Sullivan et al. 2014). The HK1 Glu847Lys mutation was found in all affected members of two additional families from the AdRP Cohort, UTAD936 and UTAD952, both from Louisiana (Fig. 26.1). No other potential disease-causing mutations were observed in HK1. The exon containing the HK1 mutation was then sequenced in 64 more adRP families, from Canada and Europe, provided by the McGill Ocular Genetics Laboratory, McGill Univ. Health Center, Montreal. The Glu847Lys mutation was observed in all affected members of two of these families, MOGL1 and MOGL2, from Canada and Sicily, respectively (Fig. 26.1). The smallest shared linkage region, including one informative, unaffected, at-risk member of UTAD952, is 55 kb (Fig. 26.2).

26.3.3 Disease Chromosome Haplotypes

Haplotypes defined by SNP markers flanking the HK1 mutation were tested in the five families, including the homozygous member of UTAD003, to determine the degree of sharing identical-by-descent between families (Fig. 26.2—excluding the unaffected individual in UTAD952). Since UTAD003, UTAD936 and UTAD952 derive from Louisiana we expected a common ancestor. In confirmation, the shared

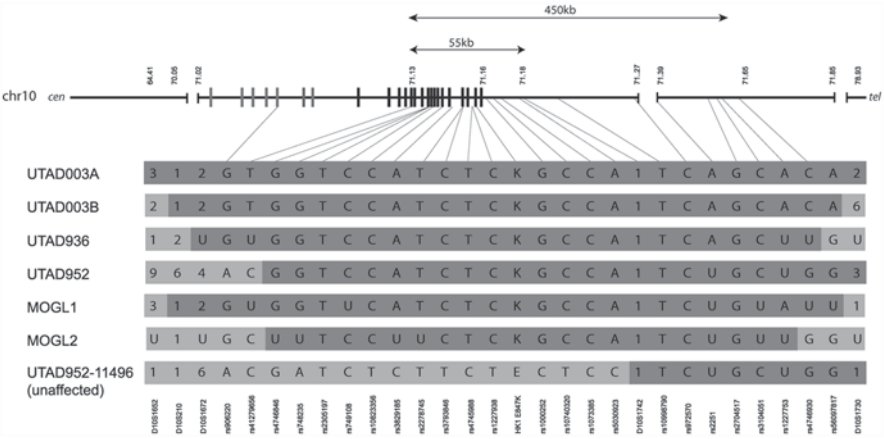

Fig. 26.2 Chromosomal haplotypes in *cis* to the HK1 Glu847Lys mutation, including two distinct haplotypes in the homozygous individual in UTAD003, and an unaffected, at-risk individual in UTAD952. Exons of HK1 and distances (in kb) of chromosome 10q21.1 are shown at the top of the figure. SNP and markers defining the haplotype are listed at *bottom*. Observed SNP alleles are listed in each bar. *Dark gray* region of bars, shared SNP alleles; *light gray* region of bars, alleles not shared. The shared haplotype across all families is 450 kb (*top arrows*), whereas the shortest region of linkage overlap, including the unaffected member of UTAD952, is 55 kb (*second arrows*)

region in these families is approximately 500 kb centered on the HK1 mutation. (The homozygous male has distinct but overlapping haplotypes.) The Canadian and Sicilian families also share this haplotype with a total overlap of 450 kb. This is consistent with the mutation arising from a common ancestor living 100s of years ago (Sullivan et al. 2014).

26.3.4 Functional Evaluation

At least five alternate transcripts of HK1 are expressed in humans, encoding multiple alternate protein isoforms. Two isoforms predominate in the human retina; both contain the Glu847Lys mutation. Analysis of pathogenicity, e.g., PolyPhen 2, was inconclusive because of the multiple transcripts and several close-related hexokinase genes in vertebrate species. Hexokinase 1 catalyzes the first step in phosphorylation of glucose to glucose-6-phosphate and may play a role in mitochondrial activity. However, the Glu847Lys mutation, though in a highly-conserved site, lies outside of known active sites in the protein, so the pathogenic mechanism of the mutation is not established at present (Sullivan et al. 2014).

26.3.5 Clinical Findings

Affected members of the families display a highly-variable RP phenotype including pericentral RP, an arcuate band of pigmentary degeneration, and/or central areolar

choroidal dystrophy. Symptoms by mid-life are mild to moderate. The homozygous male showed symptoms of RP at age 4 and when examined at age 33 had count-finger acuity, severe retinal vascular attenuation, extensive bone spicule accumulation, and macular atrophy in both eyes (Sullivan et al. 2014).

26.4 Discussion and Conclusion

The Glu847Lys missense mutation in the HK1 gene on 10q22.1 causes retinal dystrophy in five independently-ascertained families with adRP, including a homozygous patient. The five families share a 450 kb haplotype suggesting the variant arose as an ancient founder mutation. The mutation has a frequency of 1 % in American, Canadian and European adRP families. The HK1 transcript is abundant in mammalian retina, with at least five alternate transcripts. All of the transcripts are predicted to contain the mutation, at a highly conserved site. The hexokinase gene family (HK1–HK4) encodes proteins involved in the phosphorylation of glucose, an essential step in glycolysis. The glycolytic pathway plays a central role in photoreceptor and retinal cell metabolism. In addition, the hexokinase 1 protein is known to interact with mitochondrial membranes, as a modulator of apoptosis. The HK1 mutation may cause retinal disease as a result of perturbations in glycolysis and/or mitochondrial activity. Rare recessive, null, mutations in HK1 cause early-onset, non-spherocytic hemolytic anemia, which was not observed in these patients, and the Glu847Lys missense mutation is outside of any known active site. Thus the HK1 adRP mutation may act through a unique biological mechanism.

Acknowledgements We dedicate this report to the memory of Dr. Mary Kay Pelias who worked closely with the Louisiana families throughout her career. This work was supported by NIH grant EY007142, by grant HG003079 from the NHGRI, by a Wynn-Gund TRAP Award, and by the Foundation Fighting Blindness.

References

Berger W, Kloeckener-Gruissem B, Neidhardt J (2010) The molecular basis of human retinal and vitreoretinal diseases. Prog Ret Eye Res 29:335–375

Bowne SJ, Humphries MM, Sullivan LS et al (2011) A dominant mutation in RPE65 identified by whole-exome sequencing causes retinitis pigmentosa with choroidal involvement. Euro J Hum Genet 19:1074–1081

Churchill JD, Bowne SJ, Sullivan LS et al (2013) Mutations in the X-linked retinitis pigmentosa genes RPGR and RP2 found in 8.5 % of families with a provisional diagnosis of autosomal dominant retinitis pigmentosa. Invest Ophthalmol Vis Sci 54:1411–1416

Daiger SP, Bowne SJ, Sullivan LS (2007) Perspective on genes and mutations causing retinitis pigmentosa. Arch Ophthalmol 125:151–158

Daiger SP, Bowne SJ, Sullivan LS (2014a) Genes and mutations causing autosomal dominant retinitis pigmentosa. Cold Spring Harb Perspect Med. pii: a017129. doi: 10.1101/cshperspect.a017129. [Epub ahead of print]

Daiger SP, Bowne SJ, Sullivan LS et al (2014b) Application of next-generation sequencing to identify genes and mutations causing autosomal dominant retinitis pigmentosa (adRP). Adv Exp Med Biol 801:123–129

Haim M (2002) Epidemiology of retinitis pigmentosa in Denmark. Acta Ophthalmol Scand Suppl 233:1–34

Koboldt DC, Larson DE, Sullivan LS et al (2014) Exome-based mapping and variant prioritization for inherited Mendelian disorders. Am J Hum Genet 94:373–384

RetNet (2014) The Retinal Information Network, http://www.sph.uth.tmc.edu/RetNet/. In: Stephen P. Daiger, PhD, Administrator, The University of Texas Health Science Center at Houston

Sohocki MM, Daiger SP, Bowne SJ et al (2001) Prevalence of mutations causing retinitis pigmentosa and other inherited retinopathies. Hum Mutat 17:42–51

Sullivan LS, Bowne SJ, Birch DG et al (2006) Prevalence of disease-causing mutations in families with autosomal dominant retinitis pigmentosa: a screen of known genes in 200 families. Invest Ophthalmol Vis Sci 47:3052–3064

Sullivan LS, Koboldt DC, Bowne SJ, Lang S, Blanton SH, Cadena E, Avery CE, Lewis RA, Webb-Jones K, Wheaton DH, Birch DG, Coussa R, Ren H, Lopez I, Chakarova C, Koenekoop RK, Garcia CA, Fulton RS, Wilson RK, Weinstock GM, Daiger SP (2014). A dominant mutation in hexokinase 1 (HK1) causes retinitis pigmentosa. Invest Ophthalmol Vis Sci 55:7147–7158.

Wang F, Wang H, Tuan HF et al (2013) Next generation sequencing-based molecular diagnosis of retinitis pigmentosa: identification of a novel genotype-phenotype correlation and clinical refinements. Hum Genet 133:331–345

Wright AF, Chakarova CF, Abd El-Aziz MM et al (2010) Photoreceptor degeneration: genetic and mechanistic dissection of a complex trait. Nat Rev Genet 11:273–284

Chapter 27
FAM161A and *TTC8* are Differentially Expressed in Non-Allelelic Early Onset Retinal Degeneration

Louise M Downs and Gustavo D Aguirre

Abstract Ciliary genes *FAM161A* and *TTC8* have been implicated in retinal degeneration (RD) in humans and in dogs. The identification of *FAM161A* and *TTC8* mutations in canine RD is exciting as there is the potential to develop novel large animal models for RD. However, the disease phenotypes in the dog and the roles of abnormal genes in disease pathology have yet to be fully characterized. The present study evaluated the expression patterns of *FAM161A* and *TTC8* during normal retinal development in dogs, and in three non-allelic, early onset canine RD models at critical time points of the disease: RCD1, XLPRA2 and ERD. Both genes were differentially expressed in RCD1 and ERD, but not in XLPRA2. These results add evidence to the hypothesis that (a) mutations in many retinal genes have a cascade effect on the expression of multiple, possibly unrelated genes and (b) a large number and wide range of genes probably contribute to RD in general.

Keywords Retinal degeneration · Dog model · Expression study · Photoreceptor · Microtubules · FAM161A · TTC8

27.1 Introduction

Progressive Retinal Atrophy (PRA) is the term used for a group of inherited retinal diseases that is characterized by degeneration of the retina, ultimately resulting in loss of vision. Rod photoreceptor (PR) responses are typically lost first, followed by cone PR responses (Parry 1953). Bilateral and symmetrical changes are

The online version of this chapter 10.1007/978-3-319-17121-0_27 contains supplementary material, which can be downloaded from: http://extra.springer.com.

L. M. Downs (✉) · G. D. Aguirre
Section of Ophthalmology, Department of Clinical Studies, School of Veterinary Medicine, University of Pennsylvania, Ryan-VHUP, Room 2050, 3900 Delancey St., Philadelphia, PA 19104-6010, USA
e-mail: loudowns@vet.upenn.edu

G. D. Aguirre
e-mail: gda@vet.upenn.edu

C. Bowes Rickman et al. (eds.), *Retinal Degenerative Diseases,* Advances in Experimental Medicine and Biology 854, DOI 10.1007/978-3-319-17121-0_27

observed in the fundus, including a hyper-reflective tapetum in the early stages, followed by attenuation of blood vessels, pigmentary changes and atrophy of the optic nerve head (Miyadera et al. 2012). PRA is considered the canine homologue of the retinitis pigmentosa (RP) group of diseases in man, and most of the genes that have been implicated in PRA to date have also been implicated in human retinal degeneration (RD).

Recently the ciliary genes *FAM161A* (family with sequence similarity 161, member A) and *TTC8* (tetratricopeptide repeat domain 8) have been reported to be causally associated with two distinct forms of PRA in the Tibetan Spaniel and Golden Retriever breeds, respectively (Downs and Mellersh 2014; Downs et al. 2014). Both genes have also been implicated in human RD: *FAM161A* in RP (Bandah-Rozenfeld et al. 2010; Langmann et al. 2010), and *TTC8* in RP and Bardet-Biedl Syndrome (Ansley et al. 2003; Riazuddin et al. 2010). While these discoveries may enable the study of new canine models for human RD, the models have yet to be established and adequately characterized.

While retinal tissues from dogs homozygous for *FAM161A* or *TTC8* mutations was not available for study, retinas were available from three non-allelic canine models: RCD1 (Suber et al. 1993; Ray et al. 1994), XLPRA2 (Zhang et al. 2002) and ERD (Goldstein et al. 2010). To this end, we evaluated the expression of *FAM161A* and *TTC8* throughout normal retinal development, and in the three disease models, and compared the expression with that of PR-specific genes.

27.2 Materials and Methods

27.2.1 Tissue Samples

Retinal tissue was obtained from age-matched normal and mutant dogs as described previously (Genini et al. 2013). Mutant dogs comprised three canine models for early onset RD: rod cone dysplasia 1 (RCD1), X-linked progressive retinal atrophy 2 (XLPRA2) and early retinal degeneration (ERD). In all three models retinal development begins normally, but abnormalities soon develop, and there is progressive and relatively fast PR degeneration (Supplementary Fig. 27.S1, reproduced from Genini et al. 2013). PR loss and the decrease in outer nuclear layer thickness is more rapid and aggressive in RCD1, and slightly delayed in XLPRA2 (Acland and Aguirre 1987; Farber et al. 1992; Beltran et al. 2006). ERD is characterized by abnormal development and degeneration of PR cells, as well as concurrent photoreceptor mitosis that generated new hybrid rod/S-cone cells (Berta et al. 2011). Tissues were obtained from normal, RCD1 and XLPRA2 animals at 3, 5, 7 and 16 weeks of age (3 biological replicates/time-point/group) and from two ERD mutants at 6.4 weeks, three at 8.3/9.9 weeks and two at 11.9/14.1 weeks of age (labelled 6, 9 and 13 weeks, respectively, for analysis).

27.2.2 qRT-PCR

Unlabeled primers were used to detect all isoforms of *FAM161A* (Fwd: GCTGAAAGCTGCCCACTTGGAAAC and Rev: TCAAGGAGGAAGACGGCCCTAAATC) and *TTC8* (Fwd: ACTCATGTGGAAGCCATTGCATGC and Rev: AGCTGCCTCTTCTTCGTTTTCAGC). Primers and fluorescently labelled probes described previously (Komaromy et al. 2010) were used to detect *RHO* and *OPN1LW*. TaqMan assays (Applied Biosystems) were used to detect *ARR3* (Cf03460116_m1), *SAG* (Cf02628845_m1) and *GAPDH* (Hs02786624_g1). The preparation of cDNA and qRT-PCR reactions were conducted as described previously (Genini et al. 2013), using the 7500 real-time PCR machine and detection software (v2.0.1, Applied Biosystems).

27.2.3 qRT-PCR Analysis

The C_T values of the genes were normalized against those of *GAPDH*. The ratios and fold change (FC) were calculated using the $\Delta\Delta C_T$ method (Livak and Schmittgen 2001) for 3, 5 and 7 week normal versus 16 week normal; RCD1 and XLPRA2 versus age-matched normal; and ERD at 6, 9 and 13 weeks versus normal at 5, 7 and 16 weeks. An unpaired t-test was applied, and *p*-values were controlled using the Benjamini & Hochberg (BH) step-up false discovery rate (FDR) procedure to determine whether any differences observed were statistically significant ($p < 0.05$). Samples with $p < 0.05$ and FC $> \pm 2$ were considered differentially expressed (DE).

27.3 Results

27.3.1 Expression in Normal Retina

Expression levels of all six genes in normal retinal development (3, 5 and 7 weeks) was compared with normal adult retina at 16 weeks (Acland and Aguirre 1987). The expression levels of cone genes, Arrestin (*ARR3*) and L/M-Opsin (*OPN1LW*) and rod gene S-Antigen (*SAG*), did not change significantly throughout development (Fig. 27.1). However, the other rod gene analyzed, rhodopsin (*RHO*), was DE (−2.3 fold) at 3 weeks, and then increased from 5 weeks to levels that were not significantly different than at 16 weeks. Expression of *FAM161A* and *TTC8* was highest at 3 and 5 weeks of age, followed by decreased expression to the levels in the 16 week retina; only *TTC8* was DE (+2.6 fold) at 3 weeks compared with 16 weeks.

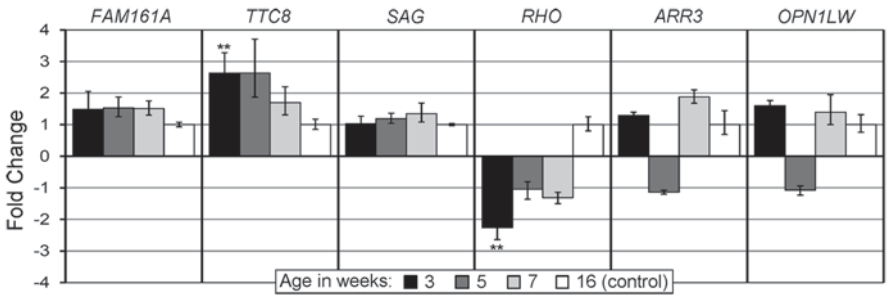

Fig. 27.1 RNA expression changes in developing normal retina at 3, 5 and 7 weeks compared to young adult (16 weeks). A double asterisk indicates significant differential expression and error bars represent standard deviation of biological triplicates

27.3.2 Expression in Disease Models

Expression levels of all six genes in mutant retina at all ages was compared with age-matched normals (Fig. 27.2 and Supplementary Fig. 27.S2), and DE genes/models/time-points identified. In all models *RHO, ARR3* and *SAG* showed a general trend of down-regulation compared with age-matched normal. *RHO* was DE in one or more stages of all three models, *ARR3* in RCD1 and ERD, and *SAG* in RCD1 only. Conversely, *OPN1LW* was not DE in any disease. *FAM161A* and *TTC8* have similar expression patterns to one another in each model (Fig. 27.2 and Table 27.1). In RCD1 both genes are down-regulated throughout, with *FAM161A* DE at 7 and 16 weeks (−2.1 and −2.5 fold, respectively), and *TTC8* at 3 weeks (−2.1 fold). In XLPRA2, neither gene is DE. In ERD, only *TTC8* is DE at 13 weeks (+4.1 fold), although the up-regulation of FAM161A is also statistically significant (+1.6 fold).

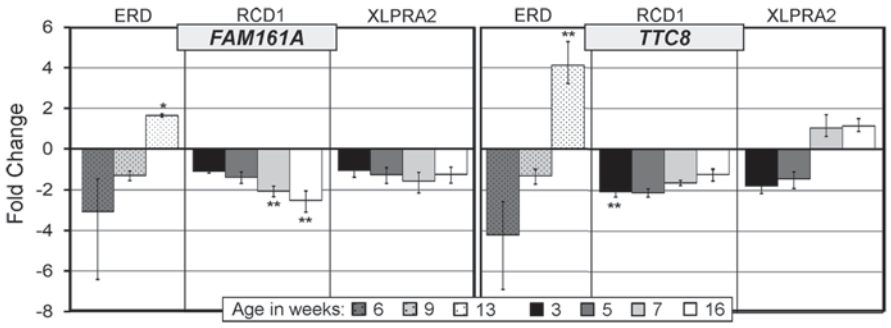

Fig. 27.2 RNA expression changes in RCD1 and XLPRA2 at 3, 5, 7 and 16 weeks versus age-matched normal, and in ERD at 6, 9 and 13 weeks versus normal at 5, 7 and 16 weeks, respectively. An asterisk indicates statistical significance, a double asterisk differential expression and error bars represent standard deviation of biological triplicates/duplicates

Table 27.1 Fold change of *TTC8* and *FAM161A*. Differentially expressed genes (FC > ±2, $p < 0.05$) are in **bold**

		ERD	RCD1	XLPRA2
3 weeks	*FAM161A*	–	−1.1	−1.0
	TTC8	–	**−2.1**	−1.8
5/6 weeks	*FAM161A*	−3.1	−1.4	−1.2
	TTC8	−4.2	−2.1	−1.4
7/9 weeks	*FAM161A*	−1.3	**−2.1**	−1.6
	TTC8	−1.3	−1.6	+1.0
16/13 weeks	*FAM161A*	+1.6	−2.5	−1.2
	TTC8	**+4.1**	−1.2	+1.1

27.4 Discussion

In this study we examined the expression of *FAM161A* and *TTC8,* along with selected rod- and cone-specific genes throughout normal retinal development, and in three canine RD models, RCD1, XLPRA2 and ERD.

FAM161A exists in two isoforms formed by alternative splicing of exon 4, and is expressed in multiple tissues, including the retina (Langmann et al. 2010). It localizes to the basal body, connecting cilium and centriole, and associates with the microtubule network during mitosis (Di Gioia et al. 2012; Zach et al. 2012). *TTC8* also exists in two main isoforms. One isoform, containing exon 2A, is expressed exclusively in the retina (Riazuddin et al. 2010), while the isoform lacking exon 2A is expressed in multiple ciliated tissues. Both isoforms localize to ciliated structures such as connecting cilium, centrosomes and basal bodies (Ansley et al. 2003). Our finding that maximum expression of *TTC8* and *FAM161A* occurs at 3 and 5 weeks in normal retina, and is followed by reduced expression at 7 and 16 weeks suggests that both of these genes are required for both the development and maintenance of the retina. This is similar to previously reported results for *FAM161A* expression in mice (Langmann et al. 2010).

Similar expression patterns, for the most part, were reported for *RHO, SAG, ARR3* and *OPN1LW* using the same models and time-points in a previous study (Genini et al. 2013). The main difference was observed with *SAG,* which was DE in the late stages of ERD and XLPRA2 in the Genini study, but not here. Two factors may account for these differences: (1) this study was conducted and cDNA generated separately from that of Genini et al. resulting in probable variations in template concentration; (2) the small number of tests in this study will have impacted the BH-controlled *p*-value. *FAM161A* and *TTC8* are DE at one or more time-points in the RCD1 retina, while neither are DE in XLPRA2. The difference in expression between RCD1 and XLPRA2 could be due to the comparatively greater severity of the former. Interestingly, we observed that *FAM161A* and *TTC8* are significantly upregulated at 13 weeks in ERD, compared with 16 weeks normal. *FAM161A* binds to microtubules and undergoes redistribution during mitosis (Zach et al. 2012) and is thought to play a role in the structural composition, maintenance and function of the connecting cilium (Karlstetter et al. 2014). *TTC8* is thought to be associated with ciliary biogenesis or function (Ansley et al. 2003). Characteristic of ERD is

concurrent PR apoptosis and mitosis (Berta et al. 2011). It is therefore not entirely unexpected to observe the up-regulation of *FAM161A* and *TTC8* in this disease, especially given the pivotal role of the microtubule network in mitosis.

We have characterized *FAM161A* and *TTC8* expression throughout the development of the normal retina, as well as in three non-allelic RD models. Both genes are DE in two of these models, providing further evidence that degeneration of the retina is likely caused by aberrant expression of multiple genes, not only by the mutant gene.

Acknowledgments We thank K. Carlisle and the staff of the Retinal Disease Studies Facility for animal care. This study was supported by Foundation Fighting Blindness (FFB), NIH Grants EY06855, EY017549, and 5P30EY001583–38, and the Van Sloun Fund for Canine Genetic Research.

References

Acland GM, Aguirre GD (1987) Retinal degenerations in the dog: IV. Early retinal degeneration (erd) in Norwegian elkhounds. Exp Eye Res 44:491–521

Ansley SJ, Badano JL, Blacque OE et al (2003) Basal body dysfunction is a likely cause of pleiotropic Bardet–Biedl syndrome. Nature 425:628–633

Bandah-Rozenfeld D, Mizrahi-Meissonnier L, Farhy C et al (2010) Homozygosity mapping reveals null mutations in FAM161A as a cause of autosomal-recessive retinitis pigmentosa. Am J Hum Genet 87:382–391

Beltran WA, Hammond P, Acland GM et al (2006) A frameshift mutation in RPGR exon ORF15 causes photoreceptor degeneration and inner retina remodeling in a model of X-linked retinitis pigmentosa. Invest Ophthalmol Vis Sci 47:1669–1681

Berta AI, Boesze-Battaglia K, Genini S et al (2011) Photoreceptor cell death, proliferation and formation of hybrid rod/S-cone photoreceptors in the degenerating STK38L mutant retina. PLoS ONE 6:e24074

Di Gioia SA, Letteboer SJ, Kostic C et al (2012) FAM161A, associated with retinitis pigmentosa, is a component of the cilia-basal body complex and interacts with proteins involved in ciliopathies. Hum Mol Genet 21:5174–5184

Downs LM, Mellersh CS (2014) An Intronic SINE insertion in FAM161A that causes exon-skipping is associated with progressive retinal atrophy in Tibetan Spaniels and Tibetan Terriers. PLoS ONE 9:e93990

Downs LM, Wallin-Hakansson B, Bergstrom T et al (2014) A novel mutation in TTC8 is associated with progressive retinal atrophy in the golden retriever. Canine Genet Epidemiol 1:e21452

Farber DB, Danciger JS, Aguirre G (1992) The beta subunit of cyclic GMP phosphodiesterase mRNA is deficient in canine rod-cone dysplasia 1. Neuron 9:349–356

Genini S, Beltran WA, Aguirre GD (2013) Up-regulation of tumor necrosis factor superfamily genes in early phases of photoreceptor degeneration. PLoS ONE 8:e85408

Goldstein O, Kukekova AV, Aguirre GD et al (2010) Exonic SINE insertion in STK38L causes canine early retinal degeneration (erd). Genomics 96:362–368

Karlstetter M, Sorusch N, Caramoy A et al (2014) Disruption of the retinitis pigmentosa 28 gene Fam161a in mice affects photoreceptor ciliary structure and leads to progressive retinal degeneration. Hum Mol Genet 23(19):5197–5210

Komaromy AM, Alexander JJ, Rowlan JS et al (2010) Gene therapy rescues cone function in congenital achromatopsia. Hum Mol Genet 19:2581–2593

Langmann T, Di Gioia SA, Rau I et al (2010) Nonsense mutations in FAM161A cause RP28-associated recessive retinitis pigmentosa. Am J Hum Genet 87:376–381

Livak KJ, Schmittgen TD (2001) Analysis of relative gene expression data using real-time quantitative PCR and the 2(-Delta Delta C(T)) method. Methods 25:402–408

Miyadera K, Acland GM, Aguirre GD (2012) Genetic and phenotypic variations of inherited retinal diseases in dogs: the power of within- and across-breed studies. Mamm Genome 23:40–61

Parry HB (1953) Degenerations of the dog retina. II. Generalized progressive atrophy of hereditary origin. Br J Ophthalmol 37:487–502

Ray K, Baldwin VJ, Acland GM et al (1994) Cosegregation of codon 807 mutation of the canine rod cGMP phosphodiesterase beta gene and rcd1. Invest Ophthalmol Vis Sci 35:4291–4299

Riazuddin SA, Iqbal M, Wang Y et al (2010) A splice-site mutation in a retina-specific exon of BBS8 causes nonsyndromic retinitis pigmentosa. Am J Hum Genet 86:805–812

Suber ML, Pittler SJ, Qin N et al (1993) Irish setter dogs affected with rod/cone dysplasia contain a nonsense mutation in the rod cGMP phosphodiesterase beta-subunit gene. Proc Natl Acad Sci U S A 90:3968–3972

Zach F, Grassmann F, Langmann T et al (2012) The retinitis pigmentosa 28 protein FAM161A is a novel ciliary protein involved in intermolecular protein interaction and microtubule association. Hum Mol Genet 21: 4573–4586

Zhang Q, Acland GM, Wu WX et al (2002) Different RPGR exon ORF15 mutations in Canids provide insights into photoreceptor cell degeneration. Hum Mol Genet 11:993–1003

Chapter 28
Mutations in the Dynein1 Complex are Permissible for Basal Body Migration in Photoreceptors but Alter Rab6 Localization

Joseph Fogerty, Kristin Denton and Brian D. Perkins

Abstract The photoreceptor outer segment is a specialized primary cilium, and anchoring of the basal body at the apical membrane is required for outer segment formation. We hypothesized that basal body localization and outer segment formation would require the microtubule motor dynein 1 and analyzed the zebrafish *cannonball* and *mike oko* mutants, which carry mutations in the heavy chain subunit of cytoplasmic dynein 1 (*dync1h1*) and the p150^{Glued} subunit of Dynactin (*dctn1a*). The distribution of Rab6, a player in the post-Golgi trafficking of rhodopsin, was also examined. Basal body docking was unaffected in both mutants, but Rab6 expression was reduced. The results suggest that dynein 1 is dispensable for basal body docking but that outer segment defects may be due to defects in post-Golgi trafficking.

Keywords Zebrafish · Retinal development · Dynein · Basal body · Rab

28.1 Introduction

The formation of cilia, including photoreceptor outer segments, requires the migration of a mature centriole to the apical cell surface, where it docks and forms the basal body. Basal body docking requires an intact apical actin network and elements of the planar cell polarity pathway (Boisvieux-Ulrich et al. 1990; Park et al. 2006).

B. D. Perkins (✉) · J. Fogerty
Department of Ophthalmic Research, Cole Eye Institute,
Cleveland Clinic, Cleveland, OH 44195, USA
e-mail: perkinb2@ccf.org

K. Denton · B. D. Perkins
Department of Biology, Texas A&M University, College Station, TX 77843, USA

J. Fogerty
e-mail: fogertj@ccf.org

K. Denton
e-mail: denton.kristin@gmail.com

C. Bowes Rickman et al. (eds.), *Retinal Degenerative Diseases,* Advances in Experimental Medicine and Biology 854, DOI 10.1007/978-3-319-17121-0_28

Further, disruption of the microtubule network by nocodazole did not prevent basal body migration, but did block cilia growth, suggesting microtubule-based motors may function in vesicle-mediated trafficking (Boisvieux-Ulrich et al. 1989). Nevertheless, the identity of the molecular motors and the precise cellular mechanism(s) governing basal body migration remain unclear. As cilia defects cause disorders termed "ciliopathies," of which retinal degeneration is often a symptom (Kim et al. 2004), it is critical to understand the mechanisms directing basal body localization.

Cytoplasmic dyneins are multisubunit, minus end-directed microtubule motors (Kardon and Vale 2009). Cytoplasmic dynein 1 (Dynein1) controls all minus-end directed microtubule transport within the cytoplasm, while cytoplasmic dynein 2 (Dynein2) transports cargo along the ciliary axoneme. We and others have shown that photoreceptor outer segment formation requires both Dynein1 and Dynein2, but the precise mechanisms remain poorly defined (Tai et al. 1999; Krock et al. 2009; Insinna et al. 2010). We hypothesized that Dynein1 contributes to outer segment development by promoting apical migration of the centriole and tested this hypothesis in zebrafish lacking components of the Dynein1 complex. The zebrafish *cannonball* (*cnb*) mutant contains a null mutation in the heavy chain of Dynein1 (*dync1h1*) (Insinna et al. 2010) while the zebrafish mutant *mikre oko* (*mok*) disrupts the $p150^{Glued}$ subunit of the dynactin complex. Both mutants show outer segment and nuclear positioning defects (Tsujikawa et al. 2007). We investigated basal body localization in the zebrafish Dynein1 mutant *cnb* and the dynactin mutant *mikre oko*. We also explored the alternate hypothesis that outer segment disruption is due to impaired post-Golgi trafficking by examining the distribution of Rab6 in photoreceptors.

28.2 Materials and Methods

28.2.1 Animal Husbandry

Adult zebrafish were maintained at 28.5 °C in recirculating water systems (Pentair, Apopka, FL). The *cannonball* mutant *dync1h1*^{mw20} and the *Tg(-5actb2:cetn4-GFP)* line (Randlett et al. 2011) were gifts from Dr. Brian Link (Medical College of Wisconsin), while the *mikre oko* mutant, *dctn1a*^{m632} was obtained from the Zebrafish International Resource Center (Eugene, OR). All experiments were approved by the IACUC at the Cleveland Clinic and conformed to the ARVO policy on animal care.

28.2.2 Basal Body Localization in Dynein Mutants

Larvae were fixed in 4% paraformaldehyde in PBS, followed by infiltration with 30% sucrose and embedding in Tissue Freezing Medium. Cryosections (10 μm) were stained with Alexa-568 phalloidin (Life Technologies, 1:100) and DAPI. Im-

aging was performed on a Zeiss AxioImager Z.2 fluorescence microscope with ApoTome.2 attachment and AxioCam MRm camera. Images were exported to ImageJ, and basal bodies in single Z slices were categorized as being present in the ONL or apical to it. The ONL was defined as the region of DAPI staining between phalloidin reactivity at the outer limiting membrane and outer plexiform layer. Samples for electron microcopy were prepared as described (Sukumaran and Perkins 2009), although wash and dehydration steps were carried out in a BioWave Pro (Pelco).

28.2.3 Genetic Mosaics and Immunohistochemistry

In vitro transcribed RNA encoding mCherry with a nuclear localization signal (nls-mCherry) was prepared using the Message Machine kit (Ambion) and 50 pg of RNA was injected into *cnb;Tg(-5actb2:cetn4-GFP)* and *mok;Tg(-5actb2:cetn4-GFP*) embryos at the 1-cell stage. Embryos were grown to the 1000 cell stage and cells were transplanted to age-matched wild-type embryos. Donor embryos were genotyped by high-resolution melt curve analysis on a BioRad CFX96 real-time PCR machine. Retinal cryosections of mosaic fish were stained with a polyclonal mCherry antibody (BioVision, 1:500) and imaged as described above. For Rab6 immunostaining, sections were stained with rabbit polyclonal Rab6 antibodies (Santa Cruz, 1:1000), followed by Alexa conjugated secondary antibodies and imaged as described above.

28.3 Results

We examined basal body localization in *cnb* and *mok* larvae harboring the *Tg(-5actb2:cetn4-GFP*) transgene, which expresses a centrin-GFP fusion protein from the actin promoter and labels centrioles and basal bodies. At 2.5 days post fertilization (dpf) phalloidin staining was disorganized and photoreceptor nuclei failed to form an orderly layer in the mutants. By 4 dpf both mutants exhibited a significant degree of retinal degeneration, with rounded nuclei and disorganized lamination (Fig. 28.1a–c). Despite this phenotype, both mutants contained areas of well-preserved apical actin network, in which basal bodies were localized near the OLM. Outside of these areas, basal bodies could be occasionally observed among photoreceptor nuclei in the ONL. Mislocalized basal bodies usually colocalized with ectopic actin staining (Fig. 28.1c, arrow). Semi-quantitative analysis of mutant retinas showed significant mislocalization of basal bodies in 3 dpf *cnb* fish (Fig. 28.1d). Transmission electron microscopy (TEM) revealed properly formed basal bodies and cilia near the apical membrane, but we were unable to locate any mislocalized basal bodies by TEM (Fig. 28.1e–g).

Closer examination of the mislocalized basal bodies revealed that they were apical and adjacent to nuclei that were similarly displaced (Fig. 28.2a–c), sug-

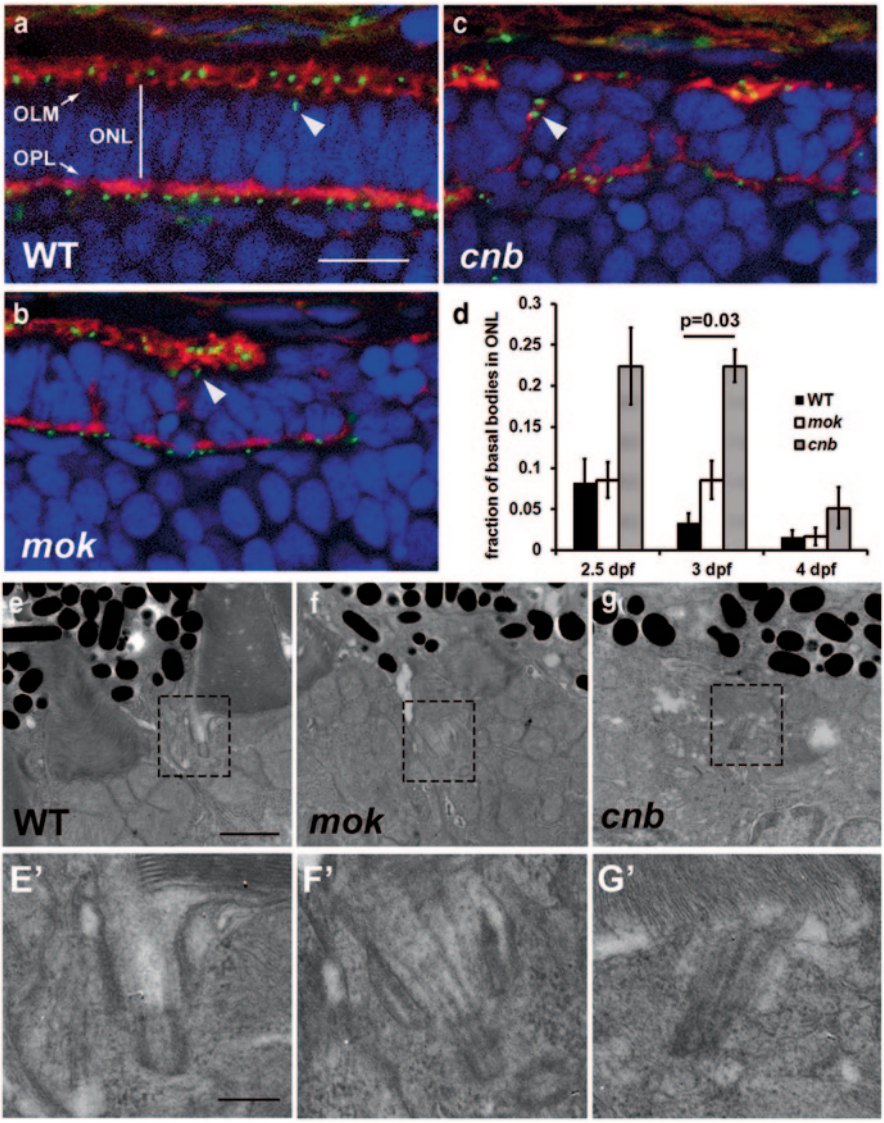

Fig. 28.1 **a**–**c** Representative images of basal body positioning in 3 dpf larvae. *Green*=centrin-GFP, *red*=phalloidin, *blue*=DAPI. *OLM* outer limiting membrane, *ONL* outer nuclear layer, *OPL* outer plexiform layer. Bar=10 μm. **d** Quantification of basal bodies in the ONL. **e**–**g** Electron microscopy images of 3 dpf larvae. Bar=1 μm. Boxed areas are magnified in **e**′–**g**′ to show basal bodies (bar=250 nm)

gesting that basal bodies were properly positioned in the displaced cells. To test this hypothesis, mosaic animals were generated by blastula transplantation to assign individual basal bodies to their nuclei. *cnb;Tg(-5actb2:cetn4-GFP)* and *mok;Tg(-5actb2:cetn4-GFP)* embryos were injected with RNA encoding NLS-mCherry

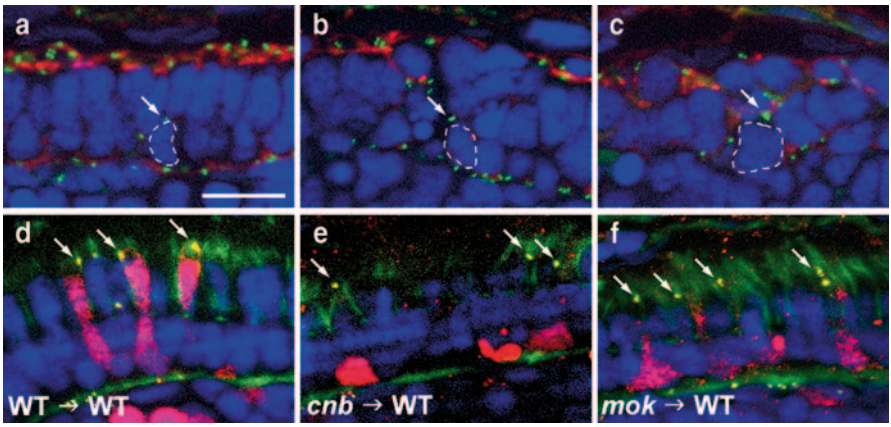

Fig. 28.2 **a–c** Basally displaced nuclei (*blue, outlined*) are adjacent to mislocalized basal bodies (*green, arrows*). Phalloidin staining (*red*). **d–f** Genetically mosaic 5 dpf fish expressing centrin-GFP (*yellow*) and nuclear mCherry (*red*) in donor cells. Basally displaced photoreceptor nuclei (*asterisks*) are associated with properly localized basal bodies (*arrows*). Sections are stained with phalloidin (*green*) and DAPI (*blue*). Bar = 10 μm

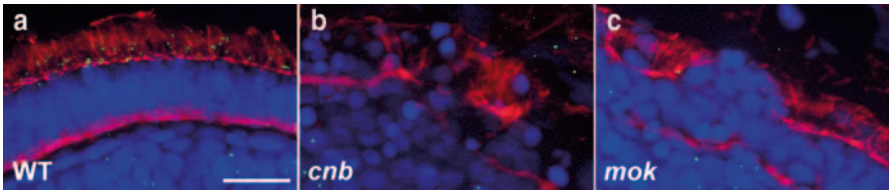

Fig. 28.3. Rab6 immunostaining (*green*) is reduced in *cnb* and *mok* larvae at 4 dpf. *Red* = phalloidin, *blue* = DAPI. Bar = 10 μm

to label nuclei. Transplanted donor cells from these embryos had mCherry-labeled nuclei and GFP-labeled basal bodies in an unlabeled wild-type host. While the nuclei of mutant donor cells were frequently positioned at the basal extent of the ONL, consistent with previous observations (Insinna et al. 2010), the basal bodies of these cells were not only apical relative to the cell body but also properly positioned near the OLM (Fig. 28.2d–f). This indicated that the apical domain remained intact despite the majority of the cell's volume being displaced, and suggested that *dync1h1* and *dctn1a* are dispensable for basal body migration in retinal photoreceptors.

An alternative hypothesis for the disruption of outer segment formation in *cnb* and *mok* larvae is that loss of Dynein1 activity blocks ciliary transport of post-Golgi vesicles. Rab6 is present in the trans-Golgi and in rhodopsin transport carriers, and interacts with the dynactin complex and the dynein light chain DYNLRB1. Staining with Rab6 antibodies revealed fewer Rab6-positive foci in *cnb* and *mok* retinas at 4 dpf, suggesting that post-Golgi trafficking is disrupted in mutant cells (Fig. 28.3).

28.4 Discussion

Our finding that basal body positioning at the apical membrane during ciliogenesis is independent of Dynein1 function is somewhat surprising, especially given the role of dynein in other centriole functions such as spindle positioning (Kiyomitsu and Cheeseman 2013). However, evidence from multiciliated epithelial cells suggests that basal body positioning depends on an intact actin network, suggesting a myosin motor (Boisvieux-Ulrich et al. 1990). In the developing retinal epithelium, basal bodies remain apically polarized except during M phase, after which they quickly return to the apical membrane. This phenomenon is conserved even after centrin2 knockdown, which destabilizes tubulin (Norden et al. 2009). These observations, when combined with the results from genetic mosaic animals presented here, argue against a role for microtubule-based motors in basal body migration.

We evaluated a role for dynein-based motility on post-Golgi trafficking in zebrafish photoreceptors. The dynein light chain Tctex-1 binds rhodopsin (Tai et al. 1999), and minus-end directed motors are thought to transport rhodopsin from the Golgi (Troutt and Burnside 1988). Moreover, Rab6 and Rab11 label rhodopsin-containing vesicles and interact with components of the dynein-dynactin complex (Short et al. 2002; Wanschers et al. 2008; Mazelova et al. 2009). Our finding that Rab6 immunoreactivity is decreased in *cnb* and *mok* photoreceptors indicates that interactions between the dynein complex and post-Golgi trafficking machinery are critical for outer segment development, and may explain why mutant outer segments fail to elongate.

References

Boisvieux-Ulrich E, Laine MC, Sandoz D (1989) In vitro effects of colchicine and nocodazole on ciliogenesis in quail oviduct. Biol Cell/Under Auspices Europ Cell Biol Org 67:67–79

Boisvieux-Ulrich E, Laine MC, Sandoz D (1990) Cytochalasin D inhibits basal body migration and ciliary elongation in quail oviduct epithelium. Cell Tiss Res 259:443–454

Insinna C, Baye LM, Amsterdam A et al (2010) Analysis of a zebrafish dync1h1 mutant reveals multiple functions for cytoplasmic dynein 1 during retinal photoreceptor development. Neural Dev 5:12

Kardon JR, Vale RD (2009) Regulators of the cytoplasmic dynein motor. Nat Rev: Mol Cell Biol 10:854–865

Kim JC, Badano JL, Sibold S et al (2004) The Bardet-Biedl protein BBS4 targets cargo to the pericentriolar region and is required for microtubule anchoring and cell cycle progression. Nat Genet 36:462–470

Kiyomitsu T, Cheeseman IM (2013) Cortical dynein and asymmetric membrane elongation coordinately position the spindle in anaphase. Cell 154:391–402

Krock BL, Mills-Henry I, Perkins BD (2009) Retrograde intraflagellar transport by cytoplasmic dynein-2 is required for outer segment extension in vertebrate photoreceptors but not arrestin translocation. Invest Ophthalmal Vis Sci 50:5463–5471

Mazelova J, Astuto-Gribble L, Inoue H et al (2009) Ciliary targeting motif VxPx directs assembly of a trafficking module through Arf4. EMBO J 28:183–192

Norden C, Young S, Link BA et al (2009) Actomyosin is the main driver of interkinetic nuclear migration in the retina. Cell 138:1195–1208

Park TJ, Haigo SL, Wallingford JB (2006) Ciliogenesis defects in embryos lacking inturned or fuzzy function are associated with failure of planar cell polarity and Hedgehog signaling. Nat Genet 38:303–311

Randlett O, Poggi L, Zolessi FR et al (2011) The oriented emergence of axons from retinal ganglion cells is directed by laminin contact in vivo. Neuron 70:266–280

Short B, Preisinger C, Schaletzky J et al (2002) The Rab6 GTPase regulates recruitment of the dynactin complex to golgi membranes. Curr Biol 12:1792–1795

Sukumaran S, Perkins BD (2009) Early defects in photoreceptor outer segment morphogenesis in zebrafish ift57, ift88 and ift172 intraflagellar transport mutants. Vis Res 49:479–489

Tai AW, Chuang JZ, Bode C et al (1999) Rhodopsin's carboxy-terminal cytoplasmic tail acts as a membrane receptor for cytoplasmic dynein by binding to the dynein light chain Tctex-1. Cell 97:877–887

Troutt LL, Burnside B (1988) Microtubule polarity and distribution in teleost photoreceptors. J Neurosci 8:2371–2380

Tsujikawa M, Omori Y, Biyanwila J et al (2007) Mechanism of positioning the cell nucleus in vertebrate photoreceptors. Proc Natl Acad Sci U S A 104:14819–14824

Wanschers B, van de Vorstenbosch R, Wijers M et al (2008) Rab6 family proteins interact with the dynein light chain protein DYNLRB1. Cell Motil Cytoskeleton 65:183–196

Chapter 29
RDS Functional Domains and Dysfunction in Disease

Michael W. Stuck, Shannon M. Conley and Muna I. Naash

Abstract The photoreceptor specific tetraspanin protein retina degeneration slow (RDS) is a critical component of the machinery necessary for the formation of rod and cone outer segments. Over 80 individual pathogenic mutations in RDS have been identified in human patients that lead to a wide variety of retinal degenerative diseases including retinitis pigmentosa, cone-rod dystrophy, and various forms of macular dystrophy. RDS-associated disease is characterized by a high degree of variability in phenotype and penetrance, making analysis of the underlying molecular mechanisms of interest difficult. Here we summarize our modern understanding of RDS functional domains and oligomerization and how disruption of these domains and complexes could contribute to the variety of disease pathologies seen in human patients with RDS mutations.

Keywords RDS · Retinal degeneration slow · Retinal degeneration · Pattern dystrophy · Outer segment · Retinitis pigmentosa · Macular degeneration

29.1 Introduction

Mutations in the photoreceptor specific gene RDS (also known as peripherin-2) lead to a variety of dominantly inherited retinal diseases such as cone-rod dystrophies, retinitis pigmentosa and various forms of macular degeneration including various pattern dystrophies (for review see Boon et al. 2008). RDS mutations are

M. I. Naash (✉) · M. W. Stuck · S. M. Conley
Department of Cell Biology, University of Oklahoma Health Sciences Center, 940 Stanton L. Young Blvd., BMSB 781, Oklahoma City, OK 73104, USA
e-mail: muna-naash@ouhsc.edu

M. W. Stuck
e-mail: mstuck@ouhsc.edu

S. M. Conley
e-mail: Shannon-conley@ouhsc.edu

C. Bowes Rickman et al. (eds.), *Retinal Degenerative Diseases,* Advances in Experimental Medicine and Biology 854, DOI 10.1007/978-3-319-17121-0_29

characterized by a high degree of inter- and intra- familial phenotypic heterogeneity, with differences in age-of-onset, severity, and penetrance all of which complicate scientific examination of underlying molecular mechanisms (Boon et al. 2008). To date no effective treatment has been developed that allows for the targeted treatment of RDS associated pathologies.

RDS is a tetraspanin transmembrane glycoprotein that specifically localizes to the disc/lamellar rim region of rod and cone photoreceptor outer segments (OSs). It is important for the initial formation of OSs during development and the proper maintenance and organization of these structures over the life of the animal (Goldberg 2006). While both rods and cones require RDS for the proper formation of their OSs, it is clear that the two cell-types have differences in their utilization of RDS as shown by the cell-type specificity of many disease causing mutations as well as animal studies (Farjo et al. 2006; Boon et al. 2008).

29.2 RDS Functional Domains

RDS function and importance to OS development and maintenance can be viewed through two critically important functional domains, the C-terminus and the second intradiscal (D2) loop. The C-terminal domain of RDS is characterized by multiple critical regions: the OS targeting sequence, an amphipathic helix, and sites that mediate non-covalent protein-protein interactions. The OS targeting sequence necessary for the proper delivery of RDS from its site of synthesis in the inner segment to the OS resides within residues 317–336 with a critical valine residue at position 332 (Tam et al. 2004; Salinas et al. 2013). Once in the OS, the C-terminal amphipathic helix (residues 310–328) is thought to act as a membrane curvature sensor, encourage membrane fusion events, or directly promote rim curvature through insertion of the amphipathic helix into the outer leaflet of disc membranes (Boesze-Battaglia et al. 1998; Khattree et al. 2013). While it is clear that this domain plays a role in the membrane dynamics of the OS, it is not clear to what extent this domain regulates membrane curvature *in vivo*. The C-terminal domain also interacts with melanoregulin, calmodulin, glutamic acid rich protein (GARP), and the GARP domain on the cyclic nucleotide gated channel (CNGB1) (Poetsch et al. 2001; Boesze-Battaglia et al. 2007b; Edrington et al. 2007). GARP interactions are thought to help organize the rod OS by linking the disc rim to the plasma membrane through the CNG channel. Both melanoregulin and calmodulin are proposed to regulate the fusogenic/membrane curvature activity of the RDS C-terminus and have been proposed to play a role in the addition of discs at the base of the OS and the shedding of discs to the retinal pigment epithelium (RPE) (Boesze-Battaglia et al. 2007b; Edrington et al. 2007).

The second critical domain of RDS is the D2 loop. The RDS D2 loop mediates the assembly of RDS and its non-glycosylated homologue rod outer segment membrane protein-1 (ROM-1) into covalent and non-covalent homo- and hetero-oligomers (Goldberg and Molday 1996; Ding et al. 2005). ROM-1 is thought

to primarily play an ancillary role in RDS function possibly through regulating membrane curvature/fusion and disc size (Clarke et al. 2000; Boesze-Battaglia et al. 2007a). Following synthesis, RDS and ROM-1 assemble into non-covalent heterotetramers (Goldberg et al. 1995; Goldberg and Molday 1996). These tetramer "building blocks" further assemble into large stable complexes through the formation of a covalent disulfide bond mediated by a cysteine residue at position 150 (Goldberg et al. 1998; Chakraborty et al. 2009). Importantly although the C-terminus is the region involved in sensing and mediating membrane curvature, formation of the large covalently linked RDS complexes is necessary for RDS to curve membranes (Wrigley et al. 2000), highlighting the importance of oligomerization for RDS function. Interestingly, while both RDS and ROM-1 form intermolecular disulfide bonds, ROM-1 is excluded from the largest RDS oligomers, being found only in intermediate and tetrameric complexes (Loewen and Molday 2000). In summary, the RDS D2 loop regulates the formation of large RDS arrays, as well as smaller RDS/ROM-1 oligomers which are necessary for proper OS formation.

29.3 RDS and Disease

Of the diseases associated with RDS mutations, retinitis pigmentosa remains the most clearly understood. As demonstrated by the $rds^{+/-}$ mouse, RDS haploinsufficiency leads to a significant disruption of OS morphogenesis and slow degeneration within the retina (Hawkins et al. 1985). In the $rds^{+/-}$, rods are impacted preferentially with the cones remaining largely spared from degeneration until around 6 months of age (Cheng et al. 1997). Rod degeneration occurs first in this model followed by cone death, similar to what has been seen in patients. While it is unclear why rod photoreceptors are more sensitive to RDS haploinsufficiency than cones, this line of reasoning is well supported by studies both *in vitro* and *in vivo* examining disease causing mutations of RDS. For example, the retinitis pigmentosa linked mutation C214S results in a misfolded protein which is degraded and results in haploinsufficiency *in vivo* (Saga et al. 1993; Stricker et al. 2005). The loss of RDS protein as a molecular mechanism for retinitis pigmentosa has made RDS an attractive target for gene replacement therapies although significant difficulties remain in terms of generating sufficient expression to mediate good rescue (Cai et al. 2009).

While the molecular mechanisms that underlie RDS' role in diseases such as cone-rod dystrophies and macular dystrophy are less well understood, recent studies have begun to shed light on these important classes of RDS associated diseases. In patients, the disease progression associated with this class of RDS mutation often involves significant defects in the neighboring RPE cells and can lead to retinal or choroidal neovascularization, although phenotypes vary significantly (Wroblewski et al. 1994; Khani et al. 2003; Yang et al. 2004; Boon et al. 2008). In models we have studied, macular or pattern dystrophy mutations produce an RDS protein which is able to fold sufficiently well to avoid misfolded protein-mediated degradation and retains the ability to traffic to the OS but exhibits defects in RDS/ROM-1

oligomerization. This results in defects in OS morphogenesis, maintenance, and function (Ding et al. 2004; Conley et al. 2014; Stuck et al. 2014). For example, we have studied mouse models carrying either of two D2 loop mutations (R172W and Y141C) which lead to macular or pattern dystrophy in patients. Both R172W-RDS and Y141C-RDS form different types of abnormal disulfide linked RDS/ROM-1 complexes in the OS even in the presence of wild-type RDS (Conley et al. 2014; Stuck et al. 2014). In the case of R172W, ROM-1 is incorporated into abnormal intermediate sized RDS/ROM-1 disulfide linked complexes and the total pool of RDS is more susceptible to tryptic digestion than wild-type RDS (Ding et al. 2004; Conley et al. 2014). In contrast, Y141C forms abnormally large covalently linked complexes which also incorporate ROM-1. In keeping with the differences in oligomerization defects in the R172W vs. Y141C, other phenotypes were also distinct. R172W expression led to dramatic vascular defects and cone-specific functional deficits, while the Y141C mice displayed abnormal yellowish fundus flecking and defects in both rod and cone function.

Although the pathways that link biochemical defects in RDS oligomerization to changes in retinal health (like vascular/fundus abnormalities or ERG changes) remain under investigation, multiple types of downstream effects are known. First is a direct effect of the abnormal RDS on photoreceptors. Because oligomerization is a prerequisite for RDS function, and properly functioning RDS is required for OS morphogenesis, it makes sense that mutants with altered oligomerization would not be able to support normal OS development. This manifests as shortened and or swirly/malformed OSs, which logically do not function properly. Of particular remaining interest is how abnormal RDS/ROM-1 oligomerization could lead to alterations in the ability of RDS to mediate membrane curvature/fusion or OS scaffolding; both properties that are involved in OS development.

However, direct photoreceptor effects do not account for the many variable phenotypes seen in patients, thus the second level on which biochemical alterations in RDS complexes impact retinal health lies in their ability to disrupt the RPE. It has been shown that in the *rds*$^{+/-}$ mouse significant changes occur in both the size of RPE OS phagosomes as well as the temporal regulation of their uptake (Hawkins et al. 1985). We have hypothesized that in the case of macular dystrophy mutations, there is additional stress since the phagosomes will also be packed with abnormal RDS complexes which could have a negative impact on RPE health. The idea that RPE phenotypes in patients occur due to RPE stress from abnormal RDS complexes and degenerating photoreceptors is useful because it can help explain the phenotypic heterogeneity associated with RDS mutations. While many individual mutations affect RDS oligomerization, we observe that the changes are not uniform from mutation to mutation and would thus be predicted to result in phenotypic variability in patients. Furthermore, a wide variety of non-genetic factors can also influence long-term RPE health which could contribute to phenotypic variability within patients carrying the same mutation. While this model provides a powerful explanation for how individual mutations can lead to the complex phenotypes observed in different human patients, it also implies that many mutations do have toxic gain-of-function effects and thus simple gene replacement therapies alone may not be

effective in treating RDS-associated diseases. Further exploration of mechanisms connecting defects in the photoreceptor protein RDS and abnormalities in adjacent tissues (such as the RPE and vasculature) are ongoing.

Many questions remain in regards to how the different types of RDS complexes (tetramers, intermediate complexes, large oligomers) function in the OS under both normal and pathological conditions. It is unclear why rods and cones have differential requirements for RDS and how these differences are affected by disease-causing-mutations. A better understanding of how RDS fulfills its normal function during OS morphogenesis will play an important role in enabling us to elucidate disease mechanisms and develop rational therapeutics.

Acknowledgements This work was supported by the National Institutes of Health (EY010609-MIN, T32EY023202-MWS), the Foundation Fighting Blindness, and the Oklahoma Center for the Advancement of Science and Technology.

References

Boesze-Battaglia K, Lamba OP, Napoli AA Jr et al (1998) Fusion between retinal rod outer segment membranes and model membranes: a role for photoreceptor peripherin/rds. Biochemistry (Mosc) 37:9477–9487

Boesze-Battaglia K, Stefano FP, Fitzgerald C et al (2007a) ROM-1 potentiates photoreceptor specific membrane fusion processes. Exp Eye Res 84:22–31

Boesze-Battaglia K, Song H, Sokolov M et al (2007b) The tetraspanin protein peripherin-2 forms a complex with melanoregulin, a putative membrane fusion regulator. Biochemistry (Mosc) 46:1256–1272

Boon CJ, den Hollander AI, Hoyng CB et al (2008) The spectrum of retinal dystrophies caused by mutations in the peripherin/RDS gene. Prog Retin Eye Res 27:213–235

Cai X, Nash Z, Conley SM et al (2009) A partial structural and functional rescue of a retinitis pigmentosa model with compacted DNA nanoparticles. PLoS ONE 4:e5290

Chakraborty D, Ding XQ, Conley SM et al (2009) Differential requirements for retinal degeneration slow intermolecular disulfide-linked oligomerization in rods versus cones. Hum Mol Genet 18:797–808

Cheng T, Peachey NS, Li S et al (1997) The effect of peripherin/rds haploinsufficiency on rod and cone photoreceptors. J Neurosci 17:8118–8128

Clarke G, Goldberg AF, Vidgen D et al (2000) Rom-1 is required for rod photoreceptor viability and the regulation of disk morphogenesis. Nat Genet 25:67–73

Conley SM, Stuck MW, Burnett JL et al (2014) Insights into the mechanisms of macular degeneration associated with the R172W mutation in RDS. Hum Mol Genet 23:3102–3114

Ding XQ, Nour M, Ritter LM et al (2004) The R172W mutation in peripherin/rds causes a cone-rod dystrophy in transgenic mice. Hum Mol Genet 13:2075–2087

Ding XQ, Stricker HM, Naash MI (2005) Role of the second intradiscal loop of peripherin/rds in homo and hetero associations. Biochemistry (Mosc) 44:4897–4904

Edrington TCt, Yeagle PL, Gretzula CL et al (2007) Calcium-dependent association of calmodulin with the C-terminal domain of the tetraspanin protein peripherin/rds. Biochemistry (Mosc) 46:3862–3871

Farjo R, Skaggs JS, Nagel BA et al (2006) Retention of function without normal disc morphogenesis occurs in cone but not rod photoreceptors. J Cell Biol 173:59–68

Goldberg AF (2006) Role of peripherin/rds in vertebrate photoreceptor architecture and inherited retinal degenerations. Int Rev Cytol 253:131–175

Goldberg AF, Molday RS (1996) Subunit composition of the peripherin/rds-rom-1 disk rim complex from rod photoreceptors: hydrodynamic evidence for a tetrameric quaternary structure. Biochemistry (Mosc) 35:6144–6149

Goldberg AF, Moritz OL, Molday RS (1995) Heterologous expression of photoreceptor peripherin/rds and Rom-1 in COS-1 cells: assembly, interactions, and localization of multisubunit complexes. Biochemistry (Mosc) 34:14213–14219

Goldberg AF, Loewen CJ, Molday RS (1998) Cysteine residues of photoreceptor peripherin/rds: role in subunit assembly and autosomal dominant retinitis pigmentosa. Biochemistry (Mosc) 37:680–685

Hawkins RK, Jansen HG, Sanyal S (1985) Development and degeneration of retina in rds mutant mice: photoreceptor abnormalities in the heterozygotes. Exp Eye Res 41:701–720

Khani SC, Karoukis AJ, Young JE et al (2003) Late-onset autosomal dominant macular dystrophy with choroidal neovascularization and nonexudative maculopathy associated with mutation in the RDS gene. Invest Ophthalmol Vis Sci 44:3570–3577

Khattree N, Ritter LM, Goldberg AF (2013) Membrane curvature generation by a C-terminal amphipathic helix in peripherin-2/rds, a tetraspanin required for photoreceptor sensory cilium morphogenesis. J Cell Sci 126(Pt 20):4659–4670

Loewen CJ, Molday RS (2000) Disulfide-mediated oligomerization of Peripherin/Rds and Rom-1 in photoreceptor disk membranes. Implications for photoreceptor outer segment morphogenesis and degeneration. J Biol Chem 275:5370–5378

Poetsch A, Molday LL, Molday RS (2001) The cGMP-gated channel and related glutamic acid-rich proteins interact with peripherin-2 at the rim region of rod photoreceptor disc membranes. J Biol Chem 276:48009–48016

Saga M, Mashima Y, Akeo K et al (1993) A novel Cys-214-Ser mutation in the peripherin/RDS gene in a Japanese family with autosomal dominant retinitis pigmentosa. Hum Genet 92: 519–521

Salinas RY, Baker SA, Gospe SM 3rd et al (2013) A single valine residue plays an essential role in peripherin/rds targeting to photoreceptor outer segments. PLoS ONE 8:e54292

Stricker HM, Ding XQ, Quiambao A et al (2005) The Cys214– > Ser mutation in peripherin/rds causes a loss-of-function phenotype in transgenic mice. Biochem J 388:605–613

Stuck MW, Conley SM, Naash MI (2014) The Y141C knockin mutation in RDS leads to complex phenotypes in the mouse. Hum Mol Genet 23(23):6260–6274

Tam BM, Moritz OL, Papermaster DS (2004) The C terminus of peripherin/rds participates in rod outer segment targeting and alignment of disk incisures. Mol Biol Cell 15:2027–2037

Wrigley JD, Ahmed T, Nevett CL et al (2000) Peripherin/rds influences membrane vesicle morphology. Implications for retinopathies. J Biol Chem 275:13191–13194

Wroblewski JJ, Wells JA 3rd, Eckstein A et al (1994) Macular dystrophy associated with mutations at codon 172 in the human retinal degeneration slow gene. Ophthalmology 101:12–22

Yang Z, Li Y, Jiang L et al (2004) A novel RDS/peripherin gene mutation associated with diverse macular phenotypes. Ophthalmic Genet 25:133–145

Chapter 30
TULP1 Missense Mutations Induces the Endoplasmic Reticulum Unfolded Protein Response Stress Complex (ER-UPR)

Glenn P. Lobo, Lindsey A. Ebke, Adrian Au and Stephanie A. Hagstrom

Abstract Mutations in the *TULP1* gene are associated with early-onset retinitis pigmentosa (RP); however, the molecular mechanisms related to the deleterious effects of *TULP1* mutations remains unknown. Several studies have shown that misfolded proteins secondary to genetic mutations can accumulate within the endoplasmic reticulum (ER), causing activation of the unfolded protein response (UPR) complex followed by cellular apoptosis. We hypothesize that *TULP1* mutations produce misfolded protein products that accumulate in the ER and induce cellular apoptosis via the UPR. To test our hypothesis, we first performed three *in-silico* analyses of *TULP1* missense mutations (I459K, R420P and F491L), which predicted misfolded protein products. Subsequently, the three mutant TULP1-GFP constructs and wild-type (wt) TULP1-GFP were transiently transfected into hTERT-RPE-1 cells. Staining of cells using ER tracker followed by confocal microscopy showed wt-TULP1 localized predominantly to the cytoplasm and plasma membrane. In contrast, all three mutant TULP1 proteins revealed cytoplasmic punctate staining which co-localized with the ER. Furthermore, western blot analysis of cells expressing mutant TULP1 proteins revealed induction of downstream targets of the ER-UPR complex, including BiP/GPR-78, phosphorylated-PERK (Thr980) and CHOP. Our *in-vitro* analyses suggest that mutant TULP1 proteins are misfolded and accumulate within the ER leading to induction of the UPR stress response complex.

S. A. Hagstrom (✉) · G. P. Lobo · L. A. Ebke · A. Au
Department of Ophthalmic Research-i31, Cole Eye Institute, Cleveland Clinic, 9500 Euclid Avenue, Cleveland, OH 44195, USA
e-mail: hagstrs@ccf.org

G. P. Lobo
e-mail: lobog@ccf.org

L. A. Ebke
e-mail: ebkel@ccf.org

A. Au
e-mail: aca14@case.edu

S. A. Hagstrom
Department of Ophthalmology, Cleveland Clinic Lerner College of Medicine of Case Western Reserve University, Cleveland, OH 44195, USA

C. Bowes Rickman et al. (eds.), *Retinal Degenerative Diseases,* Advances in Experimental Medicine and Biology 854, DOI 10.1007/978-3-319-17121-0_30

Keywords Endoplasmic reticulum · Unfolded protein response · Photoreceptor · Retinal degeneration · Tulp1

Abbreviations

TULP1	Tubby like protein 1
PERK	Double-stranded RNA activated protein kinase (PKR)-like endoplasmic reticulum kinase
pPERK	Phosphorylated PERK on amino acid position Thr980
UPR	Unfolded protein response
ER	Endoplasmic reticulum
wt	Wild-type
RP	Retinitis pigmentosa
BiP/ GRP-78	Binding of immunoglobulin protein or 78 kDa glucose-regulated protein
CHOP	CCAAT-enhancer-binding protein homologous protein

30.1 Introduction

Retinitis pigmentosa (RP) is an inherited retinal disease estimated to affect approximately 1 in 4000 individuals in the US and Europe. The disease is typically diagnosed in young adults and the progression of retinal degeneration is insidious, which can ultimately lead to blindness (Hartong et al. 2006). This devastating disease causes functional impairment and significant decline in quality of life. Unfortunately, no current therapies cure or prevent the onset of symptoms. Through elucidating molecular pathogenesis of disease, therapeutic interventions can be targeted towards preventing or delaying photoreceptor cell death and subsequent vision loss.

Mutations in the gene Tubby-like protein-1 (*TULP1*) have been shown to be the underlying cause of an early-onset form of autosomal recessive RP (Hagstrom et al. 1998). TULP1 is a photoreceptor-specific protein that is involved in protein transportation between the inner and outer segments (IS and OS, respectively) (Hagstrom et al. 1999). It has been suggested that misfolded proteins, secondary to genetic mutations, induce activation of the unfolded protein response (UPR) mediated by the ER. As a result, an intracellular signal transduction pathway initiates a cascade of events that ultimately leads to photoreceptor cell death (Chakrabarti et al. 2011; Noorwez et al. 2008; Jing et al. 2012; Ryoo et al. 2007). This study investigates whether *TULP1* missense mutations produce misfolded proteins that accumulate within the ER and induce the UPR complex. Although this *in-vitro* study provides the foundation for understanding the pathogenesis of *TULP1*-induced RP, *in- vivo* or *ex-vivo* models are required to further validate this pathway and allow for investigation of therapeutics to aid in the attenuation of photoreceptor cell death.

30.2 Materials and Methods

30.2.1 Cell Culture

Human hTERT-RPE-1 cells (human pigmented retinal pigment epithelial cells) were maintained in F12:DMEM medium containing high-glucose supplemented with 10 % fetal bovine serum (FBS).

30.2.2 In Silico Analyses of TULP1 Mutations

Protein stability of three missense *TULP1* mutations were evaluated using the programs PolyPhen 2.0 (http://genetics.bwh.harvard.edu/pph2/), SIFT (http://sift.jcvi.org/) and I-Mutant 3.0 (http://gpcr.biocomp.unibo.it/cgi/predictors/I-Mutant3.0/I-Mutant3.0.cgi) (Adzhubei et al. 2010; Kumar et al. 2009; Capriotti et al. 2005, 2008). SIFT predicts whether an amino acid substitution affects protein function. Mutations with a SIFT score of <-2.5 are predicted to be deleterious. PolyPhen 2.0 predicts the damaging effects of missense mutations on protein folding. I-Mutant 3.0 predicts the thermostability changes created by a single point mutation on a native protein sequence. Values of <-0.5 predict decreased protein stability with the potential for aggregation.

30.2.3 TULP1 Plasmid Construction

The full-length TULP1 (ENST00000229771) open-reading frame was amplified from human retina RNA by RT-PCR using the primers Tulp1-Fwd (5′-GGAA-GATCTCATGCCTCTGCGGATGAA-3′) and Tulp1-Rev (5′-GTAGAATTC-GCTCGCAAGCCAGCTTCCC-3′). The TULP1 fragment was cloned into the mammalian expression vector pEGFP-N1 (Clontech) containing a GFP tag. The pTULP1-wt-GFP plasmid was used as a template to engineer (*in-vitro* site directed mutagenesis system: Stratagene) each of the *TULP1* mutations (I459K, R420P and F491L) previously identified in patients with RP (Hagstrom et al. 1999). Appropriate construction of the GFP-tagged wt and mutant TULP1 plasmids were verified by sequence analysis using pEGFP-N1 vector primers.

30.2.4 Cell Culture and Transient Transfection

hTERT-RPE-1 cells were grown on glass coverslips in six-well plates (for subcellular localization assays) or cultured in 100 cm^2 dishes (for western blot analysis). At 60 % confluence, cells were transfected with 3 µg of purified plasmid DNA (pTULP1-wt-GFP or individual mutant pTULP1-GFP) using FuGENE6 (Roche) as previously described (Lobo et al. 2012).

30.2.5 Immunofluorescence

Six days after transfection, cells on coverslips were washed once with PBS and stained using the ER tracker-red dye for 30 min (Invitrogen) and processed as described before (Lobo et al. 2010, 2012). Subcellular localization patterns of the GFP tagged TULP1 proteins and the ER in hTERT-RPE-1 cells was achieved by imaging at 488 nm (TULP1 expression-green fluorescence) and 587 nm (ER tracker-red fluorescence) wavelengths respectively. All experiments were carried out in triplicate. Approximately 100 cells from 10–15 fields were counted per experiment.

30.2.6 Western Blot Analysis

Total protein from transfected hTERT-RPE-1 cells was isolated using lysis buffer as previously described (Lobo et al. 2010, 2012). Primary antibodies included anti-α-tubulin (Cell Signaling; at 1:10,000 dilution) as the loading control, anti-Tulp1 (Hagstrom et al. 1999), anti-BiP, anti-phosphorylated PERK (Thr980) and anti-CHOP (Cell Signaling; all at 1:1000 dilution).

30.3 Results

30.3.1 In-Silico Analyses Predict Mutant TULP1 Protein to be Misfolded

We first evaluated the protein stability of three missense *TULP1* mutations predicted by the programs PolyPhen 2.0, SIFT and I-Mutant 3.0. All three bioinformatic programs predict that the three mutant TULP1 proteins would be unstable and misfolded under physiological conditions and therefore pathological (Table 30.1).

Table 30.1 *In-silico* analysis of *TULP1* mutations on protein stability

TULP1 mutation	SIFT score and predictions	Predicted protein tertiary structure by PolyPhen 2.0	I-Mutant 3.0 (kcal/mol) Thermostability
R420P	−4.436, deleterious	Misfolded	−0.94, unstable
I459K	−6.027, deleterious	Misfolded	−1.80, unstable
F491L	−5.576, deleterious	Misfolded	−1.55, unstable

30.3.2 Mutant TULP1 Protein Localizes to the ER

To confirm *in-silico* predictions, we expressed recombinant wt-TULP1 and mutant TULP1 constructs in hTERT-RPE-1 cells, comparing the expression and localization patterns of resultant proteins. Using immunostaining and confocal microscopy, we observed wt-TULP1 to be distributed predominantly in the cytoplasm and plasma membrane (Fig. 30.1a). In contrast, all three mutant TULP1 proteins showed punctate localization staining within the cytoplasm in a pattern resembling the ER. To confirm this observation, we performed immunostaining for the ER using an ER tracker. Merged images showed that the three mutant TULP1 proteins, but not wt-TULP1, co-localized with ER tracker, confirming ER localization for the mutant TULP1 proteins (Fig. 30.1b–d). These results provide evidence that, in hTERT-RPE-1 cells, mutant TULP1 protein can exist in an improperly folded state, the majority of which resides within the ER.

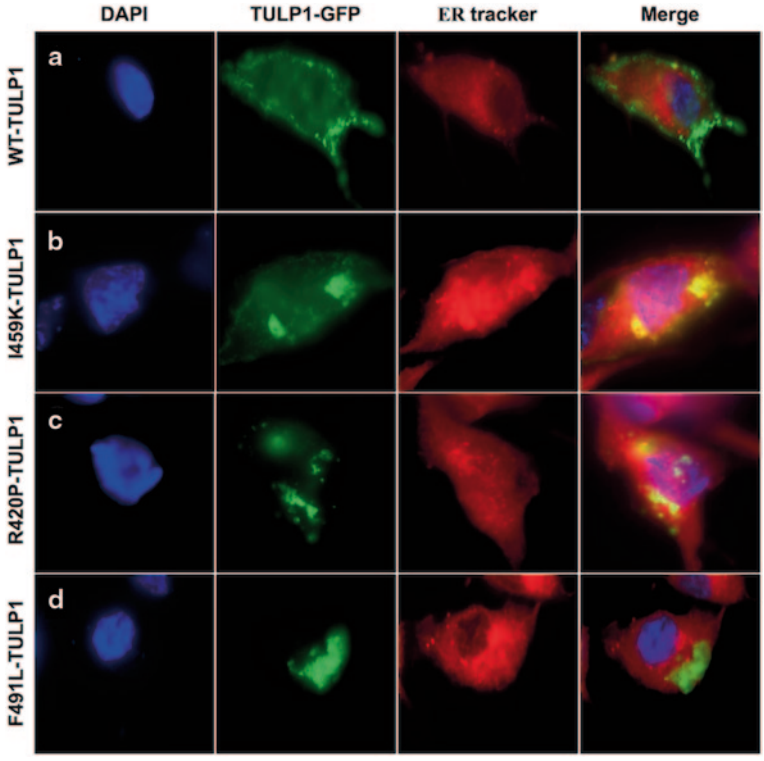

Fig. 30.1 Mutant TULP1 protein is retained within the ER. Subcellular localization of wild-type (*wt*) and mutant TULP1 proteins in hTERT-RPE1 cells. GFP tagged wt and mutant TULP1 constructs were transfected into hTERT-RPE1 cells. GFP-TULP1 proteins (*green*) and the ER (*red*) were visualized using a confocal microscope. Wt TULP1 protein (**a**) displayed predominantly cytoplasmic and plasma membrane localization patterns. In contrast, all three TULP1 mutants (**b, c** and **d**) showed punctate staining and co-localization with the ER tracker

30.3.3 Mutant TULP1 Protein Causes Induction of the UPR Stress Complex

The retention of misfolded protein within the ER can trigger the induction of the UPR complex (Chakrabarti et al. 2011). To determine if retained mutant TULP1 protein is indeed misfolded we first examined TULP1 protein expression levels in hTERT-RPE-1 cells. Immunoblotting for TULP1 in cells expressing mutant TULP1 showed that protein levels were markedly reduced compared to cells expressing wt TULP1 (Fig. 30.2). Furthermore, mutant TULP1 protein displayed slower gel migration patterns compared to wt TULP1, indicating that mutant TULP1 proteins have reduced electrophoretic mobility and are likely misfolded (Fig. 30.2). We then examined if retained mutant TULP1 proteins can activate the UPR complex. In hTERT-RPE-1 cells expressing mutant TULP1 protein, we observed significantly elevated levels of the ER resident protein BiP/GRP-78 as compared to cells expressing the wt TULP1 protein (Fig. 30.2). Reduced levels of mutant TULP1 protein expression is an indication of translational attenuation in response to UPR. This observation prompted us to investigate PERK, which is known to mediate this response (Jing et al. 2012; Ryoo et al. 2007). In fact, expression levels of phosphorylated PERK and its downstream target, CHOP, were markedly induced in cells expressing mutant TULP1 as compared to wt TULP1 expressing cells.

30.4 Discussion

Retinitis pigmentosa (RP) represents a group of inherited diseases that results in blindness through destruction of rod and cone photoreceptors. Mutations in *TULP1* are associated with early-onset RP. However, molecular mechanisms related to the deleterious effects of *TULP1* mutations remain unknown. Using *in- silico* analysis,

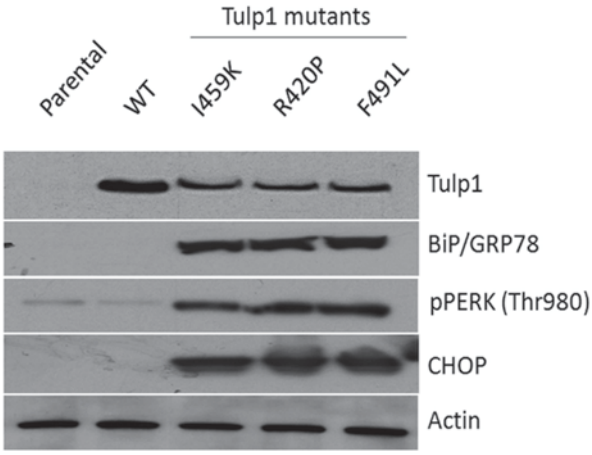

Fig. 30.2 Mutant TULP1 protein retention within the ER induces the UPR complex. hTERT-RPE-1 cells were transfected with wild-type and individual mutant *TULP1* constructs. Six days post transfection, total protein was isolated from cells and approximately 25 µg was electrophoresed on 4–20% SDS-PAGE gels. Blots were probed for TULP1 and specific stress markers of the UPR complex as indicated

our investigations determined that *TULP1* mutations alter protein conformation and stability. In an *in-vitro* cell based assay, we established that mutant TULP1 proteins are misfolded as they displayed reduced gel electrophoretic mobility patterns compared to wt TULP1. The misfolded mutant proteins were predominantly retained within the ER, as evidenced by co-localization with ER tracker. Retention of mutant TULP1 within these protein-processing organelles caused a significant induction of BiP/GPR-78, indicating retention of misfolded mutant TULP1 within the ER and activation of the UPR complex to eliminate these toxic proteins. Reduced protein expression levels of TULP1 displayed by all mutants suggest that the UPR initiated translational attenuation in an effort to prevent toxic protein production and accumulation. Indeed, we observed activation of phosphorylated PERK, a UPR protein which functions to stop translation in response to ER stress. Finally, induction of CHOP, a pro-apoptotic protein, in cells expressing mutant TULP1 protein indicated that sustained retention of misfolded mutant TULP1 within the ER causes a downstream apoptotic response. Therefore, based on our *in-silico* and *in-vitro* analysis, we propose that misfolding and retention of mutant TULP1 in the human retina could induce the ER-UPR stress complex, ultimately impacting cone and rod viability and should be considered a potential mechanism for pathogenicity associated with photoreceptor death. Future studies should be aimed at evaluating this mechanism *in-vivo* or *ex-vivo* and developing therapeutic approaches to alleviate retinal degeneration targeted protein folding by using pharmacological chaperones (Noorwez et al. 2008; Calamini et al. 2010; Stevens et al. 2010).

Acknowledgments This study was supported by NIH Grant EY15638 (SAH), Research to Prevent Blindness Center Grant, Knights Templar Eye Foundation Career-Starter Grant (GPL) and Howard Hughes Medical Institute-Foundation Fighting Blindness Medical Research Fellowship (AA).

References

Adzhubei IA, Schmidt SL, Peshkin L et al (2010) A method and server for predicting damaging missense mutations. Nat Methods 7:248–249

Calamini B, Silva MC, Madoux F et al (2010) Small molecule proteostasis regulators for protein conformational diseases. Nat Chem Biol 8:185–196

Capriotti E, Fariselli P, Casadio R (2005) I-Mutant2.0: predicting stability changes upon mutation from the protein sequence or structure. Nuc Acid Res 33:W306–310

Capriotti E, Fariselli P, Rossi I et al (2008) A three-state prediction of single point mutations on protein stability changes. BMC Bioinformat 9(Suppl 2):S6

Chakrabarti A, Chen AW, Varner JD (2011) A review of the mammalian unfolded protein response. Biotechnol Bioeng 108:2777–2793

Hagstrom SA, North M, Nishina P (1998). Recessive mutations in the gene encoding the tubby-like protein TULP1 in patients with retinitis pigmentosa. Nat Genet 18:174–176

Hagstrom SA, Duyao M, North MA et al (1999) Retinal degeneration in tulp1-/- mice: vesicular accumulation in the interphotoreceptor matrix. Invest Ophthalmol Vis Sci 40:2795–2802

Hartong DT, Berson EL, Dryja TP (2006). Retinitis Pigmentosa. Lancet 368:1795–1809.

Jing G, Wang JJ, Zhang SX (2012) ER stress and apoptosis: a new mechanism for retinal cell death. Exp Diabetes Res 2012:589589

Kumar P, Henikoff S, Ng PC (2009) Predicting the effects of coding non-synonymous variants on protein function using the SIFT algorithm. Nat Protocols 4:1073–1082

Lobo GP, Hessel S, Eichinger A et al (2010) ISX is a retinoic acid-sensitive gatekeeper that controls intestinal beta, beta-carotene absorption and vitamin A production. FASEB J 24:1656–1666

Lobo GP, Isken A, Hoff S et al (2012) BCDO2 acts as a carotenoid scavenger and gatekeeper for the mitochondrial apoptotic pathway. Development 139:2966–2977

Noorwez SM, Ostrov DA, McDowell JH et al (2008) A high-throughput screening method for small-molecule pharmacologic chaperones of misfolded rhodopsin. Invest Ophthalmol Vis Sci 49:3224–3230

Ryoo HD, Domingos PM, Kang MJ et al (2007) Unfolded protein response in a Drosophila model for retinal degeneration. EMBO J 26:242–252

Stevens RC, Sancho J, Martinez A et al (2010) Rescue of misfolded proteins and stabilization by small molecules. Methods Mol Biol 648:313–324

Chapter 31
Understanding Cone Photoreceptor Cell Death in Achromatopsia

Livia S. Carvalho and Luk H. Vandenberghe

Abstract Colour vision is only achieved in the presence of healthy and functional cone photoreceptors found in the retina. It is an essential component of human vision and usually the first complaint patients undergoing vision degeneration have is the loss of daylight colour vision. Therefore, an understanding of the biology and basic mechanisms behind cone death under the degenerative state of retinal dystrophies and how the activation of the apoptotic pathway is triggered will provide valuable knowledge. It will also have broader applications for a spectrum of visual disorders and will be critical for future advances in translational research.

Keywords Achromatopsia · Cone dystrophies · Cone photoreceptors · Cell death · Cone degeneration · Apoptosis

31.1 Introduction

Amongst the different neuronal cell types in the retina, photoreceptor cells are critically important as they are responsible for light detection. They form two classes, the rods and cones, with the cone cells responsible for daylight colour vision, photopic light detection and high visual acuity. In patients undergoing retinal degeneration, loss of acuity and colour vision is usually their main complaint and in some cases, vision deterioration is only reported once the degeneration has actually spread to the cones, even though the peripheral rods have been non-functional for months or even years. It is clear therefore that the quality of life of patients diagnosed with inherited retinal dystrophies would have a huge improvement if we were able to somehow preserve, or at least slow down, cone photoreceptors degeneration. However trying to understand the mechanisms behind cone cell death has turned out to be a complex web of up- and down-regulation of different cellular pathways. Several research

L. S. Carvalho (✉) · L. H. Vandenberghe
Department of Ophthalmology, Ocular Genomics Institute, Schepens Eye Research Institute, Massachusetts Eye and Ear Infirmary, Harvard Medical School, Harvard University, 20 Staniford Street, Boston, MA 02114, USA
e-mail: livia_carvalho@meei.harvard.edu

C. Bowes Rickman et al. (eds.), *Retinal Degenerative Diseases*, Advances in Experimental Medicine and Biology 854, DOI 10.1007/978-3-319-17121-0_31

groups have now made a considerable effort towards identifying and elucidating these pathways and their role in triggering cone death using different models of retinal degeneration. The aim of this review is to offer a succinct overview of some of these efforts using cone-specific degeneration models.

31.2 Primary Cone Loss in Achromatopsia

Complete achromatopsia (ACHM) is an autossomal recessive congenital disorder where only the cone photoreceptors are non-functional and/or undergo degeneration, while scotopic rod-mediated vision usually remains unaffected. It is mostly caused by mutations in cone-specific phototransduction genes, can affect 1:30,000 people in the US and has debilitating symptoms like severe photophobia, reduced or complete loss of colour discrimination, pedular nystagmus and severely reduced visual acuity (Michaelides et al. 2004). So far mutations in four genes have been reported to cause ACHM: cone-specific alpha transducin (*GNAT2*), the alpha and beta subunit of the cone-specific cyclic nucleotide-gated (CNG) channel (*CNGA3* and *CNGB3*) and the cone-specific phosphodiesterase alpha' subunit (*PDE6C*—reviewed in (Berger et al. 2010). All these are key players in the phototransduction cascade and essential for cone function.

The historical classification of ACHM as a stationary disorder has been due to the fact that patients usually present with either absent cone function from birth or it remaines stationary with age (Sundaram et al. 2014). This led to the belief that the cone photoreceptors in these patients did not undergo active degeneration throughout their lifetime. However, recent studies using high resolution optical coherence tomography (OCT) and adaptive optics (AO) to look at the progression of degeneration in ACHM patients showed that they can present mild to moderate morphological changes in the inner/outer segment region, substantial loss of foveal and macular cones, and, in extreme cases, hypoplasia of the retinal pigment epithelium (Thiadens et al. 2010; Genead et al. 2011; Scoles et al. 2014). Despite the controversy surrounding cone fate in human patients, in the last few years several ACHM animal models have been described and shown to have active cone degeneration: the *Cnga3* naturally-occurring mutant (Pang et al. 2010) and knockout mouse models (*Cnga3*$^{-/-}$) (Biel et al. 1999), the *Pde6c*-deficient *cpfl1* mouse and zebrafish models (Stearns et al. 2007; Chang et al. 2009) and the dog and mouse model of *Cngb3* deficiency (Sidjanin et al. 2002; Ding et al. 2009). Even though the progressive loss of cone photoreceptors was established in several of these models (Michalakis et al. 2005; Ding et al. 2009; Fischer et al. 2010; Trifunovic et al. 2010; Xu et al. 2011), the precise kinetics of the degeneration has not yet been fully elucidated.

31.3 PDE6 Deficiency and Cone Cell Death Mechanisms

Comparative analysis of three ACHM mouse models shows that they have a similar progression of cone death, with a sharp peak at roughly the same time around postnatal day 24 (P24) (Michalakis et al. 2005; Ding et al. 2009; Trifunovic et al. 2010), but a continual degeneration was also reported in both the *cpfl1* (Fischer et al. 2010) and *Cnga3*$^{-/-}$ models (Michalakis et al. 2005). The *cpfl1* mouse has presented itself as an ideal model for understanding the mechanisms behind cone cell death since a fast degeneration rate is coupled with the existence of the analogous, and extensively studied, rod-specific *Pde6b*-deficient *rd1* mouse.

Seminal work in this field has been published by the Paquet-Durand group at the University of Tübingen where initial studies on the *cpfl1* mouse indicated that the classical caspase-3-dependent apoptotic pathway is not activated in the degenerating cones (Trifunovic et al. 2010), mimicking previous results found in the *rd1* mouse (Paquet-Durand et al. 2009; Sancho-Pelluz et al. 2010). Not surprisingly, this suggests that the lack of a functional phosphodiesterase (PDE) might trigger similar cell death mechanism in both rods and cones. Indeed Trifunovic and colleagues were able to demonstrate that cyclic guanosine monophosphate (cGMP) accumulation, excessive activation of calcium-dependent calpains and cGMP-dependent protein kinase G (PKG) seen in the *rd1* retina (Paquet-Durand et al. 2006, 2009) was also observed in the degenerating *cpfl1* cones. They suggest that cone loss might be mediated by the phosphorylation of vasodilator-stimulated protein (VASP), a PKG substrate that has been linked to cell death: accumulation of cGMP leads to excessive activation of PKG which in turn phosphorylates VASP. However the role of intracellular calcium ($[Ca^{2+}]_i$) in the cell death mechanisms of *Pde6*-deficient photoreceptors remains unclear. A recent study using the transgenic *Pde6c*-deficient zebrafish (*Pde6c*^{w59}) and *rd1* mouse showed that $[Ca^{2+}]_i$ levels in mutant *Pde6c*^{w59}cones and *rd1* rods was not increased compared to wild-type (Ma et al. 2013a). These results challenge the prevailing view that photoreceptor degeneration due to *Pde6* mutation is driven by a global increase in $[Ca^{2+}]_i$ levels although there is strong evidence that ablating Ca^{2+}influx through knockout of the CNG ion channel leads to preservation of rods in the *rd1* mouse (Paquet-Durand et al. 2011). Furthermore, studies have shown that the degeneration process in *rd1* rods involves a much more complex network of interlinked players including histone deacetylases and poly-ADP-ribose-polymerase (Paquet-Durand et al. 2007; Sancho-Pelluz et al. 2010) which have not yet been investigated in the *cpfl1* retina.

An alternative mechanism for cone cell death in the *cpfl1* mouse was proposed by (Schaeferhoff et al. 2010) after showing upregulation of gene expression in cone and Müller glia cells of signal transducer and activator of transcription 3 (*Stat3*) and different components of its signaling cascade like *Cebpd*, *Socs3*, *Cntf* and *Lif*. They suggest that activation of STAT3 signaling pathways is achieved via a 28-fold upregulation of endothelin 2 (*Edn2*) which is secreted in response to photoreceptor stress. Once again there are parallels between these findings and studies in the *rd1* mouse which have shown retinal upregulation of STAT3 (Samardzija et al. 2006) and *Edn2* (Bramall et al. 2013). This suggests that *Stat3* signaling and *Edn2*

activation act as a potent cell survival response but do not however explain by which step of the active degeneration process they are triggered by. They also fail to provide evidence that *Edn2* is actually expressed in photoreceptors cells, as opposed to activated Muller glia cells found in the outer nuclear layer (ONL).

31.4 The Role of CNG Channels in Cone Cell Death

The extremely small number of cone photoreceptors (around 2–3 %) and lack of a macula/foveal region in the mouse retina has been a challenging and restrictive step towards studying the cone system independently. An interesting approach to overcome this has been developed by the Ding group at the University of Oklahoma where they have generated double knockout mouse lines of the *Cngb3*$^{-/-}$ and *Cnga3*$^{-/-}$ on the cone dominant *Nrl*$^{-/-}$ background (Thapa et al. 2012). These double knockout mice show equivalent impaired cone function and degeneration to their respective single CNG subunit knockouts: reduced or absent eletroretinogram (ERG) responses, reduced expression of phototransduction proteins and increased TUNEL-positive apoptotic cells in the ONL. They have used these models to show a positive correlation between cone photoreceptors CNG channel deficiency and endoplasmic reticulum (ER) stress-associated apoptosis (Thapa et al. 2012). Both models show a significant increase in ER-stress marker proteins like Grp78/Bip, CHOP, phosphor-eIF2α and phosphor-IP_3R; calpain II and enhanced processing of its substrate caspase-12, and the ER-stress suppressors Bcl-2 and Bcl-x proteins. The increased activation of ER stress canonical pathways in CNG deficient retinas was also shown to occur on a gene expression level (Ma et al. 2013b) and in *in vitro* testing of mutated CNGA3 subunits (Duricka et al. 2012). Interestingly, they also report nuclear translocation of mitochondria-related proteins like apoptosis-inducing factor (AIF) and endonuclease G (Endo G) (Thapa et al. 2012). This is suggestive that mitochondrial insult might have a role in the ER stress-mediated cell death process. However the fact that the levels of cytochrome *c*, caspase-3 and caspase-9 are not altered indicates that mitochondria-mediated caspase-dependent apoptotic pathways are not active in these degenerating cones. Instead, based on their results, they suggest that the ER stress observed in these degenerating cones will activate the apoptotic response by at least three separate pathways mediated by CHOP, caspase-12 and AIF/Endo G, respectively. What still remains unclear is how the ER stress is triggered in the first place. While Thapa et al. (2012) suggest three options, impaired Ca^{2+}homeostasis, opsin mis-localization and cGMP accumulation, their direct causality in this complex network of events requires further investigation.

Recently the role of cGMP cytotoxicity in CNG deficiency-related cell death has taken a step further as one of its major contributors (Xu et al. 2013). This recent study shows that increased levels of cGMP in *Cnga3*$^{-/-}$/*Nrl*$^{-/-}$ retinas strongly correlate with increased PKG activity and expression and coincided with apoptotic cone cell death. Further support for cGMP involvement comes from improved cone survival seen in the double *Cnga3*$^{-/-}$/*Gucy2e*$^{-/-}$ knockout mouse. *Gucy2e* encodes

retinal guanylate cyclase 1 (retGC1) and is responsible for cGMP production in cones, therefore knocking it out in *Cnga3*$^{-/-}$ retinas should lower cGMP levels counterbalance its cytotoxic effects and promoting cone survival.

31.5 Concluding Remarks

Recent years have seen an incredible amount of data emerge from several different studies trying to elucidate who are the key players behind cone degeneration. The studies outlined above have used a variety of different approaches both technologically and in their choice of biological system. It is reassuring however that common pathways have been reported in different models. The increased cGMP and PKG activity seen in both *Pde6c*$^{-/-}$ and *Cnga3*$^{-/-}$ retinas suggests a number of shared factors that could be involved in activating cone cell death response and therefore offers the promise of therapeutic interventions independent of the genetic lesion causing the degeneration. The role of cGMP cytotoxicity in photoreceptor cell death has already been recognized in other models of retinal degeneration like the *rd1* and GCAP1 mutants where it is clearly linked to a rise in intracellular Ca^{2+} (Paquet-Durand et al. 2009). It is interesting to note however that the increased cGMP levels observed in the *Pde6c*$^{-/-}$ and *Cnga3*$^{-/-}$ models are explained by a high and low level of intracellular Ca^{2+}, respectively. These differences between models are supported by the fact that the separate knockout of each of the CNG channel subunits generates around 70 % of unshared genes being differentially expressed between the two models (Ma et al. 2013b). Therefore, comparisons between PDE6C- and CNG-deficiency mediated cone cell death needs to take into consideration their different roles within the phototransduction cascade and what are the functional consequences of their demise.

References

Berger W, Kloeckener-Gruissem B, Neidhardt J (2010) The molecular basis of human retinal and vitreoretinal diseases. Prog Retin Eye Res 29:335–375

Biel M, Seeliger M, Pfeifer A et al (1999) Selective loss of cone function in mice lacking the cyclic nucleotide-gated channel CNG3. Proc Natl Acad Sci U S A 96:7553–7557

Bramall AN, Szego MJ, Pacione LR et al (2013) Endothelin-2-mediated protection of mutant photoreceptors in inherited photoreceptor degeneration. PLoS ONE 8:e58023

Chang B, Grau T, Dangel S et al (2009) A homologous genetic basis of the murine cpfl1 mutant and human achromatopsia linked to mutations in the PDE6C gene. Proc Natl Acad Sci U S A 106:19581–19586

Ding XQ, Harry CS, Umino Y et al (2009) Impaired cone function and cone degeneration resulting from CNGB3 deficiency: down-regulation of CNGA3 biosynthesis as a potential mechanism. Hum Mol Genet 18:4770–4780

Duricka DL, Brown RL, Varnum MD (2012) Defective trafficking of cone photoreceptor CNG channels induces the unfolded protein response and ER-stress-associated cell death. Biochem J 441:685–696

Fischer MD, Tanimoto N, Beck SC et al (2010) Structural and functional phenotyping in the cone-specific photoreceptor function loss 1 (cpfl1) mouse mutant – a model of cone dystrophies. Adv Exp Med Biol 664:593–599

Genead MA, Fishman GA, Rha J et al (2011) Photoreceptor structure and function in patients with congenital achromatopsia. Invest Ophthalmol Vis Sci 52:7298–7308

Ma EY, Lewis A, Barabas P et al (2013a) Loss of Pde6 reduces cell body Ca(2+) transients within photoreceptors. Cell Death Dis 4:e797

Ma H, Thapa A, Morris LM et al (2013b) Loss of cone cyclic nucleotide-gated channel leads to alterations in light response modulating system and cellular stress response pathways: a gene expression profiling study. Hum Mol Genet 22:3906–3919

Michaelides M, Hunt DM, Moore AT (2004) The cone dysfunction syndromes. Br J Ophthalmol 88:291–297

Michalakis S, Geiger H, Haverkamp S et al (2005) Impaired opsin targeting and cone photoreceptor migration in the retina of mice lacking the cyclic nucleotide-gated channel CNGA3. Invest Ophthalmol Vis Sci 46:1516–1524

Pang JJ, Alexander J, Lei B et al (2010) Achromatopsia as a potential candidate for gene therapy. Adv Exp Med Biol 664:639–646

Paquet-Durand F, Azadi S, Hauck SM et al (2006) Calpain is activated in degenerating photoreceptors in the rd1 mouse. J Neurochem 96:802–814

Paquet-Durand F, Silva J, Talukdar T et al (2007) Excessive activation of poly(ADP-ribose) polymerase contributes to inherited photoreceptor degeneration in the retinal degeneration 1 mouse. J Neurosci 27:10311–10319

Paquet-Durand F, Hauck SM, van Veen T et al (2009) PKG activity causes photoreceptor cell death in two retinitis pigmentosa models. J Neurochem 108:796–810

Paquet-Durand F, Beck S, Michalakis S et al (2011) A key role for cyclic nucleotide gated (CNG) channels in cGMP-related retinitis pigmentosa. Hum Mol Genet 20:941–947

Samardzija M, Wenzel A, Aufenberg S et al (2006) Differential role of Jak-STAT signaling in retinal degenerations. Faseb J 20:2411–2413

Sancho-Pelluz J, Alavi MV, Sahaboglu A et al (2010) Excessive HDAC activation is critical for neurodegeneration in the rd1 mouse. Cell Death Dis 1:e24

Schaeferhoff K, Michalakis S, Tanimoto N et al (2010) Induction of STAT3-related genes in fast degenerating cone photoreceptors of cpfl1 mice. Cell Mol Life Sci 67:3173–3186

Scoles D, Sulai YN, Langlo CS et al (2014) *In vivo* imaging of human cone photoreceptor inner segments. Invest Ophthalmol Vis Sci 55:4244–4251

Sidjanin DJ, Lowe JK, McElwee JL et al (2002) Canine CNGB3 mutations establish cone degeneration as orthologous to the human achromatopsia locus ACHM3. Hum Mol Genet 11:1823–1833

Stearns G, Evangelista M, Fadool JM et al (2007) A mutation in the cone-specific pde6 gene causes rapid cone photoreceptor degeneration in zebrafish. J Neurosci 27:13866–13874

Sundaram V, Wilde C, Aboshiha J et al (2014) Retinal structure and function in achromatopsia: implications for gene therapy. Ophthalmology 121:234–245

Thapa A, Morris L, Xu J et al (2012) Endoplasmic reticulum stress-associated cone photoreceptor degeneration in cyclic nucleotide-gated channel deficiency. J Biol Chem 287:18018–18029

Thiadens AA, Somervuo V, van den Born LI et al (2010) Progressive loss of cones in achromatopsia: an imaging study using spectral-domain optical coherence tomography. Invest Ophthalmol Vis Sci 51:5952–5957

Trifunovic D, Dengler K, Michalakis S et al (2010) cGMP-dependent cone photoreceptor degeneration in the cpfl1 mouse retina. J Comp Neurol 518:3604–3617

Xu J, Morris L, Fliesler SJ et al (2011) Early-onset, slow progression of cone photoreceptor dysfunction and degeneration in CNG channel subunit CNGB3 deficiency. Invest Ophthalmol Vis Sci 52:3557–3566

Xu J, Morris L, Thapa A et al (2013) cGMP accumulation causes photoreceptor degeneration in CNG channel deficiency: evidence of cGMP cytotoxicity independently of enhanced CNG channel function. J Neurosci 33:14939–14948

Chapter 32
Geranylgeranylacetone Suppresses *N*-Methyl-*N*-nitrosourea-Induced Photoreceptor Cell Loss in Mice

Yoshiki Koriyama, Kazuhiro Ogai, Kayo Sugitani, Suguru Hisano and Satoru Kato

Abstract Retinitis pigmentosa is a disease characterized by the loss of photoreceptor cells. The *N*-methyl-*N*-nitrosourea (MNU)-induced retinal degeneration model is widely used to study the mechanism of these retinal degenerative disorders because of its selective photoreceptor cell death. As for the cell death mechanism of MNU, calcium-calpain activation and lipid peroxidation processes are involved in the initiation of this cell death. Although such molecular mechanisms of the MNU-induced cell death have been described, the total image of the cell death is still obscure. Heat shock protein 70 (HSP70) has been shown to function as a chaperon molecule to protect cells against environmental and physiological stresses. In this study, we investigated the effect of geranylgeranylacetone (GGA), an accylic polyisoprenoid,

Y. Koriyama (✉)
Graduate School and Faculty of Pharmaceutical Sciences,
Suzuka University of Medical Science, 3500-3 Minamitamagaki,
Suzuka 513-8670, Japan
e-mail: koriyama@suzuka-u.ac.jp

K. Ogai
Wellness Promotion Science Center, Institute of Medical, Pharmaceutical and Health Sciences,
Kanazawa University, 5-11-80 Kodatsuno, Kanazawa 920-0942, Japan
e-mail: kazuhiro@staff.kanazawa-u.ac.jp

K. Sugitani
Department of Clinical Laboratory Sciences, Graduate School of Medical Science,
Kanazawa University, 5-11-80 Kodatsuno, Kanazawa, 920-0942, Japan
e-mail: sugitani@staff.kanazawa-u.ac.jp

S. Hisano
Department of Clinical Laboratory Sciences, Department of Molecular Neurobiology,
Graduate School of Medical Science, Kanazawa University, 5-11-80 Kodatsuno,
Kanazawa 920-0942, Japan
e-mail: ef.ef.soylatte.ts@gmail.com

S. Kato
Department of Molecular Neurobiology, Graduate School of Medical Science,
Kanazawa University, 13-1 Takaramachi, Kanazawa 920-8640, Japan
e-mail: satoru@med.kanazawa-u.ac.jp

C. Bowes Rickman et al. (eds.), *Retinal Degenerative Diseases,* Advances in Experimental Medicine and Biology 854, DOI 10.1007/978-3-319-17121-0_32

on MNU-induced photoreceptor cell loss. HSP70 induction by GGA was effective against MNU-induced photoreceptor cell loss as a result of its ability to prevent HSP70 degradation. The data indicate that GGA may help to suppress the onset and progression of retinitis pigmentosa.

Keywords Retinitis pigmentosa · Heat shock protein 70 · *N*-methyl-*N*-nitrosourea · Photoreceptor cell death · Geranylgeranylacetone

32.1 Introduction

Retinal degenerative diseases such as retinitis pigmentosa are major causes of blindness. There are no effective drugs, although it is estimated that at least 50 million people have these diseases. *N*-methyl-*N*-nitrosourea (MNU), an alkylating agent, causes selective photoreceptor cell death through an antiapoptotic mechanism (Yoshizawa et al. 2000). Oka et al. (2007) reported that MNU induces accumulation of intracellular calcium ions in the retina and induces calpain-dependent photoreceptor cell loss after intraperitoneal MNU injection. It has been also reported that calpain activation promotes photoreceptor cell loss via a caspase-dependent pathway (Tsubura et al. 2010). However, the mechanism of MNU-induced photoreceptor cell loss is not fully understood.

Geranylgeranylacetone (GGA), an acylic polyisoprenoid developed and used clinically in Japan, is a unique anti-ulcer drug that protects gastric mucosa through heat shock protein 70 induction (Caprioli et al. 2003). HSP70 decreases photoreceptor apoptosis after retinal detachment (Kayama et al. 2011) and MNU treatment (Koriyama et al. 2014). However, the effects of GGA on MNU-induced photoreceptor cell death have not yet been reported. Therefore, we tested the potential role of GGA through HSP70 induction on MNU-induced photoreceptor cell death.

32.2 Materials and Methods

32.2.1 Experiment with Animals

All animals were maintained and handled in accordance with the ARVO Statement for the Use of Animals in Opthalmic and Vision Research, the guidelines of the Declaration of Helsinki, and the Guiding Principles in the Care and Use of Animals. Male C57BL/6 mice (8–9 weeks old; Japan SLC, Inc., Shizuoka, Japan) were anesthetized by intraperitoneal (i.p.) injection of sodium pentobarbital (30–40 mg/kg body weight). GGA (200 mg/ml, i.p.) was injected at 1 day before MNU injection (60 mg/kg, i.p.).

32.2.2 Morphological Observation

Fixation and cryosection of retinal samples have been reported elsewhere (Koriyama et al. 2013a). Mouse eyes were enucleated and fixed overnight in a 0.1 M phosphate buffer containing 4% paraformaldehyde and 5% sucrose. They were then incubated in 30% sucrose overnight at 4 °C. Retinal sections were cut at a 12 μm thickness and mounted onto silane-coated slides. Hematoxylin and eosin staining of transverse sections was used to evaluate the retinal thickness.

32.2.3 Immunohistochemistry

After blocking with Block One (Nacalai Tesque, Kyoto, Japan), retinal sections were incubated with a primary antibody for rabbit anti-recoverin, a photoreceptor marker protein (Nagar et al. 2009; Chemicon, Millipore Corporation, CA, USA). The sections were then incubated with Alexa Fluor anti-IgG (Molecular Probes, Eugene, OR, USA) at 23 °C.

32.2.4 Western Blotting

Retinal extracts from mice were prepared under the indicated conditions after treatment. Western blot analysis was carried out on the retina as described previously (Koriyama et al. 2013b). The primary antibodies used were anti-recoverin and anti-HSP70 (Cell Signaling Technology, Tokyo, Japan).

32.3 Results

32.3.1 MNU Induces Selective and Progressive Loss of Photoreceptor

Hematoxylin and eosin staining in MNU-treated (60 mg/kg) mouse retinal sections showed that the ONL and outer plexiform layer became significantly thinner by day 3 when compared with control retinas. These changes in thickness became more severe by day 7 (Fig. 32.1a, b) (Koriyama et al. 2014). Western blot analysis of recoverin, a photoreceptor marker protein, showed that levels were significantly decreased from 3 days after MNU treatment (Fig. 32.1c). Terminal transferase-mediated dUTP nick-end labeling (TUNEL)-positive cells were observed in the ONL from 1 day after MNU treatment, but not in any other layers. The percentage of TUNEL-positive cells dramatically increased in the ONL at 1–3 days after MNU treatment (Koriyama et al. 2014).

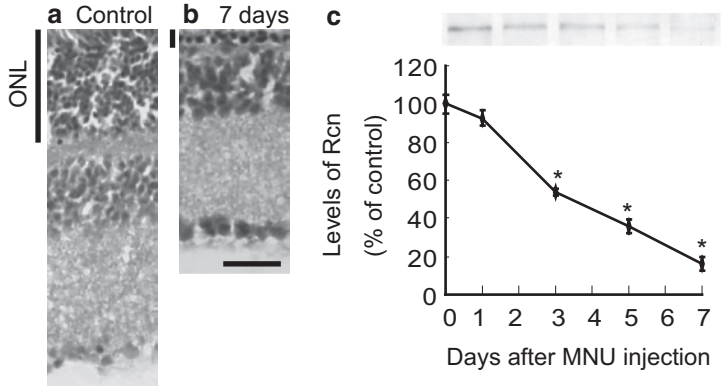

Fig. 32.1 Selective and progressive loss of photoreceptor cells by MNU. **a**, **b** Microscopy image of retinas following injection of MNU (60 mg/kg) at day 0 (**a**), day 7 (**b**). Scale bar = 50 μm, **c** Recoverin (Rcn) protein expression after MNU treatment was quantified by Western blot analysis. $^{*}p < 0.05$ vs. day 0 ($n = 3$)

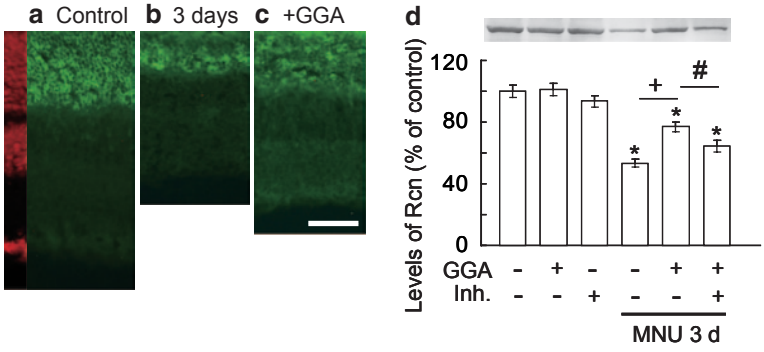

Fig. 32.2 GGA attenuated retinal degeneration by MNU in mice. **a**–**c** Immunohistochemistry for recoverin in vehicle control (**a**), 3 days of MNU (**b**), and 3 days of MNU + GGA (**c**). Scale bar = 50 μm. **d** GGA canceled the decrease of recoverin protein levels by MNU. Recoverin protein expression quantified by Western blot analysis. (Inh: HSP inhibitor.) $^{*}p < 0.01$ vs. vehicle control, $+p < 0.01$ vs. MNU, $\#p < 0.01$ vs. MNU + GGA ($n = 3$)

32.3.2 HSP70 Induced by GGA Protects Photoreceptor Cell Loss by MNU

Next, we evaluated the effect of GGA on the MNU-induced change in ONL thickness. At 3 days, the ONL was thinner in MNU-treated retinas (Fig. 32.2a, b). Pretreatment of GGA strongly reduced this MNU-induced thinning of the ONL (Fig. 32.2c). To confirm the recovery effect of GGA on MNU-induced photoreceptor cell loss, we performed a Western blot analysis for recoverin. Recoverin levels

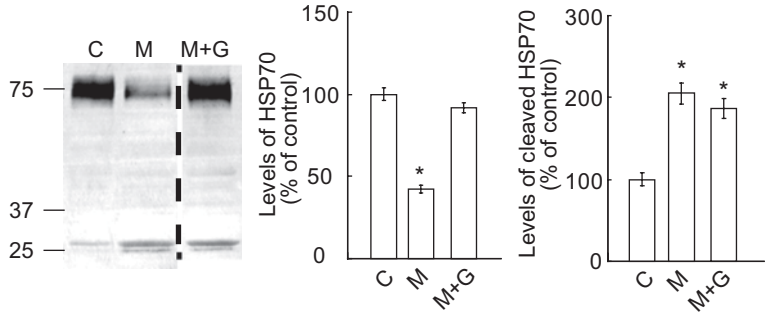

Fig. 32.3 GGA induced cleavage of HSP70 by MNU. Density of HSP70 and cleaved HSP70 in the blot were analyzed. *C*: vehicle control, *M*: MNU, *G*: GGA, $^{*}p < 0.01$ vs. vehicle control

were significantly reduced at 3 days after MNU treatment (Fig. 32.2d). Pretreatment of GGA significantly increased the levels of recoverin in the MNU-treated retina. Furthermore, the HSP inhibitor (HSP inh., Calbiochem, Darmstadt, Germany) completely canceled the rescue effect of GGA on the MNU-induced reduction in recoverin protein levels induced by MNU.

32.3.3 MNU-Induced 4-hydroxy-2-nonenal (4HNE) Production and HSP70 Cleavage Before Photoreceptor Cell Loss

Tsuruma et al. (2012) reported that oxidative stress is involved in photoreceptor cell loss by MNU. 4HNE is generated by a free radical attack on omega polysaturated fatty acids and is largely responsible for pathogenesis during oxidative stress. We recently reported that levels of 4HNE clearly increased after MNU treatment in a time-dependent manner from day 1 (Koriyama et al. 2014). After 1 day of MNU treatment, the intact bands (~70 kDa) decreased, and the cleaved bands (~30 kDa) of HSP dramatically increased (Fig. 32.3). GGA dramatically returned intact HSP70 to control levels.

32.4 Discussion

In this study, we provide compelling evidence that HSP70 induction by GGA protects photoreceptors against MNU-induced cell death. It has been reported that HSP70 has multiple antiapoptotic effects both upstream and downstream of caspase cascades (Garrido et al. 2003). In addition, we indicated that MNU cleaved HSP70 before inducing photoreceptor cell loss. There are several reports on the mechanism of photoreceptor cell loss caused by MNU (Tsubura et al. 2011). The eye requires

more oxygen than the brain and, consequently, produces more reactive oxygen species. Moreover, as retinal neurons are highly enriched in lipids containing polyunsaturated fatty acids (Fliesler et al. 1983), they can easily produce 4HNE from polyunsaturated fatty acids during oxidation from aging. Tsuruma et al. (2012) reported that MNU induced oxidative radicals and production of 4HNE within a half day of treatment. Oka et al. (2007) further reported that the total number of calcium ion in MNU-treated retinas is strongly increased, and calpain activity is dramatically increased, from 1 day after MNU administration. Furthermore, we recently reported that the calpain inhibitor prevented photoreceptor cell loss by MNU (Koriyama et al. 2014). Recently, Yamashima et al. (2012) reported that the key event in cell death by the calpain-cathepsin hypothesis is HSP70 cleavage through carbonylation of HSP70 by 4HNE. Calpain-mediated cleavage of HSP70 after 4HNE production may be possible in MNU-induced photoreceptor cell loss. In our recent study, the calpain inhibitor suppressed HSP70 cleavage and subsequent photoreceptor cell loss by MNU (Koriyama et al. 2014). In addition, induction of HSP70 by GGA prevented both HSP70 cleavage and MNU-induced photoreceptor cell loss. Taken together, we believe that GGA could be a new target for the treatment of retinal degenerative diseases, such as retinitis pigmentosa.

References

Caprioli J, Ishii Y, Kwong JM (2003) Retinal ganglion cell protection with geranylgeranylacetone, a heat shock protein inducer, in a rat glaucoma model. Trans Am Ophthalmol Soc 101:39–50

Fliesler SJ et al (1983) Chemistry and metabolism of lipids in the vertebrate retina. Prog Lipid Res 22:79–131

Garrido C, Schmitt E, Candé C et al (2003) HSP27 and HSP70: potentially oncogenic apoptosis inhibitors. Cell Cycle 2:579–584

Kayama M, Nakazawa T, Thanos A et al (2011) Heat shock protein 70 (HSP70) is critical for the photoreceptor stress response after retinal detachment via modulating anti-apoptotic Akt kinase. Am J Pathol 178:1080–1091

Koriyama Y, Nakayama Y, Matsugo S et al (2013a) Protective effect of lipoic acid against oxidative stress is mediated by Keap1/Nrf2-dependent heme oxygenase-1 induction in the RGC-5 cell line. Brain Res 1499:145–157

Koriyama Y, Takagi Y, Chiba K et al (2013b) Requirement of retinoic acid receptor β for genipin derivative-induced optic nerve regeneration in adult rat retina. PLoS One 8:e71252

Koriyama Y, Sugitani K, Ogai K et al (2014) Heat shock protein 70 induction by valproic acid delays photoreceptor cell death by N-methyl-N-nitrosourea in mice. J Neurochem 130:707–719

Nagar S, Krishnamoorthy V, Cherukuri P et al (2009) Early remodeling in an inducible animal model of retinal degeneration. Neuroscience 160:517–529

Oka T, Nakajima T, Tamada Y et al (2007) Contribution of calpains to photoreceptor cell death in N-methyl-N-nitrosourea-treated rats. Exp Neurol 204:39–48

Tsubura A, Yoshizawa K, Kuwata M et al (2010) Animal models for retinitis pigmentosa induced by MNU; disease progression, mechanisms and therapeutic trials. Histol Histopathol 25:933–944

Tsubura A, Lai YC, Miki H et al (2011) Animal models of N-Methyl-N-nitrosourea-induced mammary cancer and retinal degeneration with special emphasis on therapeutic trials. *In Vivo* 25:11–22

Tsuruma K, Yamauchi M, Inokuchi Y et al (2012) Role of oxidative stress in retinal photoreceptor cell death in N-methyl-N-nitrosourea-treated mice. J Pharmacol Sci 118:51–62

Yamashima T (2012) Hsp70.1 and related lysosomal factors for necrotic neuronal death. J Neurochem 120:477–494

Yoshizawa K, Yang J, Senzaki H et al (2000) Caspase-3 inhibitor rescues N-methyl-N-nitrosourea-induced retinal degeneration in Sprague-Dawley rats. Exp Eye Res 71:629–635

Chapter 33
My Retina Tracker™: An On-line International Registry for People Affected with Inherited Orphan Retinal Degenerative Diseases and their Genetic Relatives - A New Resource

Joan K. Fisher, Russell L. Bromley and Brian C. Mansfield

Abstract My Retina Tracker™ is a new on-line registry for people affected with inherited orphan retinal degenerative diseases, and their unaffected, genetic relatives. Created and supported by the Foundation Fighting Blindness, it is an international resource designed to capture the disease from the perspective of the registry participant and their retinal health care providers. The registry operates under an Institutional Review Board (IRB)-approved protocol and allows sharing of de-identified data with participants, researchers and clinicians. All participants sign an informed consent that includes selecting which data they wish to share. There is no minimum age of participation. Guardians must sign on behalf of minors, and children between the ages of 12 to 17 also sign an informed assent. Participants may compare their disease to others in the registry using graphical interpretations of the aggregate registry data. Researchers and clinicians have two levels of access. The first provides an interface to interrogate all data fields registrants have agreed to share based on their answers in the IRB informed consent. The second provides a route to contact people in the registry who may be eligible for studies or trials, through the Foundation.

Keywords Registry · Database · Clinical data · Natural history · Prevalence · Retinal degeneration · Retinitis pigmentosa · Longitudinal data · Usher syndrome · Stargardt disease

B. C. Mansfield (✉) · J. K. Fisher
Foundation Fighting Blindness, 7168 Columbia Gateway Drive,
Suite 100, Columbia, MD 21046-3256, USA
e-mail: bmansfield@fightblindness.org

J. K. Fisher
e-mail: jfisher@fightblindness.org

R. L. Bromley
Translational Research Acceleration Consulting, Templeton, CA 93465, USA
e-mail: russellbromley@gmail.com

C. Bowes Rickman et al. (eds.), *Retinal Degenerative Diseases,* Advances in Experimental Medicine and Biology 854, DOI 10.1007/978-3-319-17121-0_33

33.1 Introduction

While many clinicians and researchers have their own private databases for patients and families affected by an inherited orphan retinal degenerations (IRD) there are no comprehensive shared resources available to the wider community. As a result it is difficult to understand the prevalence of the diseases, especially at a genetic level. There is not a lot of publically available natural history information for specific gene mutations, and there is little to no knowledge available that correlates clinical measures to the subjective measures of disease reported by affected people on a personal level. Enrolment for research or clinical studies can be challenging in the orphan disease space, dependent on being able to identify who has patients with a particular disease in their practice, and finding sufficient collaborators to meet the desired study size. To address these challenges the Foundation Fighting Blindness has established a new on-line resource for the community; a participant-friendly patient registry. While the Foundation has maintained a patient registry with over 11,000 names for many years, it was little more than a contact list with limited disease information (Table 33.1).

To improve the value of the previous registry, the Foundation has developed an on-line patient registry that aims to collect longitudinal data provided both by affected people and their relatives, and their retinal healthcare providers. This will create a longitudinal set of data that reflects the subjective experience of the disease

Table 33.1 A snapshot of the registry composition in July 2014. The entries in the previous registry of the Foundation were rolled in to the new registry, My Retina Tracker™. While participants in the previous registry are being invited to update their entries, new profiles are also being created. My Retina Tracker has only been enrolling online publicly since June 2014. Significantly more detail on the diseases, including genotype, subtype of disease and mode of inheritance is available in My Retina Tracker. Currently 20% of new profiles have a genotype associated with them. The current combined entries are 54% female, 46% male. The focus of My Retina Tracker is the inherited orphan retinal degenerative diseases and enrolment of people with age-related macular degeneration is not being actively sought

Composition of the registries		
Disease	Previous registry	My Retina Tracker New/updated profiles
Age-related macular degeneration	1,554	54
Retinitis pigmentosa-atypical	183	38
Retinitis pigmentosa-typical	6,941	501
Usher syndrome	879	114
Stargardt disease	631	53
Bardet-Biedl syndrome	168	12
Leber's congenital amaurosis	145	43
Cone, cone-rod dystrophy	144	79
Choroideremia	110	110
Other	1,020	296
Total	11,775	1300

in parallel with a clinical record of disease. The registry software platform is provided and supported by PatientCrossroads™, who also host and maintain the site www.MyRetinaTracker.org. The registry was established using protocols approved by the Western Institutional Review Board (WIRB) and the US Army Medical Research and Materiel Command (USAMRMC) Human Research Protection Office (HRPO). The host site security meets HIPAA requirements to comply with the Health Information Technology for Economic and Clinical Health Act (HITECH Act) (78 FR 5565, January 25, 2013). Initially established as one of the registries contributing to the National Institutes of Health (NIH) Office of Rare Diseases, Global Rare Disease Registry (GRDR) initiative (Rubinstein et al. 2010), My Retina Tracker™ conforms to the use of the Global Unique Identifier (GUID) (Johnson et al. 2010), a universal subject identifier initially developed by the Simons Foundation Autism Research and National Database for Autism Research. This allows researchers to both share data specific to a study participant without exposing personally identifiable information, and to link those patients across independent databases that conform to the GUID standard. My Retina Tracker also conforms to the use of the NIH-supported Common Data Elements (CDE) for standardized terminology, which also facilitates the sharing of de-identified data across databases and enhances the accuracy of database searches.

The design of the registry was developed in collaboration with a team of 19 advisors from within the US, Europe and Canada, that included leading retinal researchers and clinical experts, three genetic counselors, and two patient advocates. The site is compatible with multiple operating systems and devices, and is compatible with all major assistive reading technology software including Window-Eyes (GW Micro, Fort Wayne, IN), Apple assistive technologies (Cupertino, CA), and JAWS (Freedom Scientific, St. Petersburg, FL).

My Retina Tracker consists of three different portals into the registry database-one for the registry participants, one for healthcare providers, and one for research access. Participation is open to anyone internationally. While the current interface is in English only, future plans include a multi-lingual interface. For people lacking internet access, or those who prefer a non-electronic submission, paper copies of the website are available that are then entered electronically by registry staff, trained in human research protection procedures. There is a complete firewall between the registry data and other activities of the Foundation, such as fundraising, to ensure the privacy of registry participants and to prevent unsolicited contact. A dedicated registry coordinator, who is certified in human subject research protection, provides active daily curation to ensure the accuracy and consistency of entered data.

33.2 Participant Portal

The participant portal is the access point for participants to create a registry account, establishing a username and password. After entering personal identification and contact information, which is not visible to users other than the registry coordina-

tor, the participant is led through an on-line informed consent process and asked to make selections on how their data is shared, their willingness to be contacted if identified as a potential candidate for a research or clinical study, their willingness to share de-identified data with other registries such as the GRDR, and their preferences for being contacted by registry staff. While there is no age restriction for participants, minors are registered by guardians, who file an informed consent on their behalf, and minors between the ages of 12 and 17 years old are requested to fill out their own informed assent form also. At the age of maturity, minors are contacted and asked to re-consent. Informed consent choices can be changed, on-line at any time by participants. Any participant can request removal from the registry at any time using an on-line option, or by contacting the registry coordinator by phone, email or regular mail. While participants cannot enter data for other members of their family, they can create a family ID and then invite other members of their family to join using an "invite" function. Exposing the family ID allows participants to show their family relationships if they wish. Genetic counselors may provide a family tree which can also be entered into the registry profile using the "attachment" function described below.

Having established an account, a series of questions, developed with the registry advisory team, guide the participant to build a retinal health profile. Most entries use drop-down menus to select answers with standardized terminology. The questions cover the participant's understanding of their disease and diagnosis, family history, general health, vision self-evaluation and visual functioning, incorporates the content covered by the National Eye Institute (NEI) VFQ25 (Mangione et al. 2001) questions, impact on life such as driving and night time activities, measures they take for eye care including medications, vitamins and over the counter products, any clinical trials they have participated in and the dates of participation, their willingness to be considered for clinical trials, and similar lifestyle questions. While there are a total of 85 structured questions in the profile, some are contextual and seen only if relevant to previous question responses. Participants not completing their profiles when registering are guided back to the remaining questions at their next log-in. Using the registry data view, participants can then view graphs that show how their response to any particular question compares with the aggregated responses in the registry for that question. A limited number of free text boxes are provided for additional comments and a variety of file types including scanned images and pdf can be attached to the participant's record. Importantly, the attachments cannot be viewed by other users since they may contain personal identifiers, but the registry acts as a convenient place to store clinical notes, test results, or other documents the participants can have ready access to at any time. A communications initiative is being developed to encourage patients to actively engage with the registry and update their records at least once annually to create a longitudinal record of the disease from their perspective.

All participants in the previous Foundation registry were rolled in to My Retina Tracker and are being contacted to re-consent and update their profiles.

33.3 Clinical Portal

The clinical portal was designed with the registry advisory team, to provide a way for the patient to accumulate their clinical data in their registry profile, while making the process quick and easy for their healthcare provider. Access to the clinical portal does not require the clinician to remember a username and password. The clinician navigates to the registry site, selects the "For Clinicians" tab and then enters the name, postal/zip code of the patient, along with the clinician's information. A data matching program determines if the patient is in the registry, and if there is a match puts the clinical data into a holding database, awaiting final acceptance by the registry curator. The portal is one-way and the clinician can not see any data in the registry. A clinician wanting access to their patient's registry profile needs to request access from the patient. To see the universe of entries in the registry, the clinician must apply for access through the research portal. A downloadable form on the registry site allows the patient to formalize a written request, to their healthcare provider, for data entry, for the providers' records. Clinical data is split into 11 categories, and the clinician selects to display only those categories relevant to the exam they have performed: Diagnosis and Co-morbidities; Genetic Diagnosis (genes and specific mutations); Visual Acuity; Ocular Assessment; EZ Width; Static Visual Field; Kinetic Visual Field; ERG (Full Field); mfERG; Light/Dark Adaptation; and Biosamples. Each category consists of a small set of essential questions, with drop-down menus used wherever possible to standardize and speed data entry. It is anticipated that data from most routine clinical exams will take no longer than 5–10 min to enter.

33.4 Research Portal

The research portal provides researchers and clinicians with access to all de-identified data in the registry that the participants agreed to share in their informed consent. A user-friendly on-line interface enables complex Boolean searches of all data fields available and returns the results along with the registry ID, which is a registry-specific ID, not the GUID. Using this interface, researchers can mine the data, visualize the results graphically, and carry out real-time inclusion/exclusion analysis to determine the numbers of participant who might be eligible for clinical studies. The de-identified data can be exported into an Excel file for further manipulation.

33.5 Access to Data in the Registry

To ensure registry participants are not being approached inappropriately, the Foundation provides two levels of access to the registry data for researchers and healthcare providers. Level One access, which requires a username and password, allows these users to view and search the de-identified registry data. Level One access is applied for using a simple on-line request through the "For Researcher" tab on the My Retina Tracker website. The credentials of the person applying for access are verified before a username and password are activated. No reasonable request will be denied. Level Two access is provided for credentialed users seeking to make contact with registry participants. A Registry Scientific Review Board receives and reviews written applications. An application form is provided on-line, but requires a scientific outline and justification for the request, and evidence that the study is approved by an Institutional Review Board and an appropriate institution. If approved, applicants provide their contact information, a lay statement of why they wish to contact registry participants, a list of the registry IDs for the participants they wish to contact and an IRB-approved announcement or recruitment letter, if applicable. The registry coordinator then contacts each selected participant, provides the approved announcement, and invites the participant to contact the investigator using the information provided. Any further interaction occurs outside of the registry and its coordinator. It is in the hands of the participant who may choose whether or not to contact the investigator. When appropriate, the investigator may request a broadcast email to all registry participants, or a subset based on specific criteria, using a registry Newsletter functionality that enables all registrants to be contacted through the registry by the registry coordinator.

My Retina Tracker is free for participants and there are no charges for access to the clinical portal or for academic/non-profit researchers using the research portal. A charge will be made for commercial access to the research portal. As the registry grows and acquires longitudinal data this new resource should become a valuable tool for participants, researchers and clinicians.

Acknowledgments The establishment of My Retina Tracker was supported in part by the Department of Defense Telemedicine and Advanced Technology Research Center (TATRC) under the Inherited Retinal Degenerative Disease Clinical Trial Network award number W81XHW-09–2-0189 to the Foundation Fighting Blindness Clinical Research Institute. Views and opinions of, and endorsements by the author(s) do not reflect those of the US Army or the Department of Defense. Other funding was provided by the Foundation Fighting Blindness.

We thank the registry advisory team for their invaluable input; the American Foundation for the Blind (AFB) Technical Evaluation Services for software testing and guidance to ensure compatibility with the assistive reading software products; and Russell Bromley of TRA Consulting for assistance in development and implementation.

We thank Stephen Rose, Amy Laster, Annette Hinkle, and Patricia Zilliox for critical reading of the manuscript.

JKF and BCM are employees of the Foundation Fighting Blindness, a 501(c)(3) organization that established and supports My Retina Tracker.

References

FR 5565 (25 Jan 2013) Modifications to the HIPAA Privacy, Security, Enforcement, and Breach Notification Rules Under the Health Information Technology for Economic and Clinical Health Act and the Genetic Information Nondiscrimination Act; Other Modifications to the HIPAA Rules; Final Rule

Johnson SB, Whitney G, McAuliffe M et al (2010) Using global unique identifiers to link autism collections. J Am Med Informatics Assn 17:689–695

Mangione CM, Lee PP, Gutierrez PR et al (2001) Development of the 25-item National Eye Institute Visual Function Questionnaire. Arch Ophthalmol 119:1050–1058

Rubinstein YR, Groft SC, Bartek R et al (2010) Creating a global rare disease patient registry linked to a rare diseases biorepository database: Rare Disease-HUB (RD-HUB). Contemp Clin Trials 31:394–404

Chapter 34
A Mini-review: Animal Models of *GUCY2D* Leber Congenital Amaurosis (LCA1)

Shannon E. Boye

Abstract *GUCY2D* encodes retinal guanylate cylase-1 (retGC1), a protein that plays a pivotal role in the recovery phase of phototransduction. Mutations in *GUCY2D* are associated with a leading cause of recessive Leber congenital amaurosis (LCA1). Patients present within the first year of life with aberrant or unrecordable electroretinogram (ERG), nystagmus and a relatively normal fundus. Aside from abnormalities in the outer segments of foveal cones and, in some patients, foveal cone loss, LCA1 patients retain normal retinal laminar architecture suggesting they may be good candidates for gene replacement therapy. Several animal models of LCA1, both naturally occurring and engineered, have been characterized and provide valuable tools for translational studies. This mini-review will summarize the phenotypes of these models and describe how each has been instrumental in proof of concept studies to develop a gene replacement therapy for *GUCY2D*-LCA1.

Keywords Leber congenital amaurosis · LCA1 · Retinal guanylate cyclase · RetGC1 · GC1 · GUCY2D · AAV · Gene therapy

34.1 Introduction

Retinal guanylate cyclase-1 (*GUCY2D*) encodes retGC1, a protein expressed in the outer segments of rods and cones (Dizhoor et al. 1994; Liu et al. 1994) which plays a pivotal role in the ability of photoreceptors to respond to light. In the dark, intracellular levels of Ca^{2+} and cGMP are high and the continuous flow of Na^{+} and Ca^{2+} ions through cGMP-gated channels and Na^{+}/Ca^{2+} exchangers keep photoreceptors in a depolarized state. Absorption of photons results in hydrolysis of cGMP by cGMP phosphodiesterase (PDE), closure of the cGMP-gated channels, reduced influx of Na^{+}/Ca^{2+} and ultimately hyperpolarization of the cell (Pugh et al. 1997). Recovery from light stimulation is owed, in part, to this change in intracellular

S. E. Boye (✉)
Departments of Ophthalmology and Molecular Genetics and Microbiology, University of Florida, 1600 SW Archer Rd, Academic Research Building Rm R2–236, Gainesville, FL 32621, USA
email: Shannon.Boye@eye.ufl.edu

C. Bowes Rickman et al. (eds.), *Retinal Degenerative Diseases,* Advances in Experimental Medicine and Biology 854, DOI 10.1007/978-3-319-17121-0_34

Ca^{2+}. Vertebrate species possess two forms of retinal guanylate cyclases (retGC1 and retGC2) and two guanlyate cyclase activating proteins (GCAP1 and GCAP2) (Dizhoor et al. 1995). GCAPs act as Ca^{2+} sensors that regulate the activity of retGCs. In the dark, high levels of intracellular Ca^{2+} promote its binding to GCAPs thereby inhibiting retGC activity. Upon light stimulation, Ca^{2+}-dissociates from GCAPs, activating retGCs which then produce cGMP, reopen cGMP-gated channels and return the photoreceptor to the depolarized, dark-state (Arshavsky and Burns 2012). Mutations which reduce or abolish the ability of retGC1 to replenish intracellular Ca^{2+} are thought to lead to the biochemical equivalent of chronic light exposure.

34.2 LCA1 and Available Animal Models

Recessive mutations in *GUCY2D* are associated with Leber congenital amourosis (LCA1), accounting for between 10–20% of cases (Perrault et al. 2000). LCA1-causing mutations are distributed throughout *GUCY2D* and are predicted to alter enzyme structure/stability, impact transport of other peripheral membrane-associated proteins and/or result in a null allele (Karan et al. 2010). Patients present within the first year of life with reduced visual acuity, aberrant or unrecordable ERG, nystagmus, oculo-digital sign and apparently normal fundus (Perrault et al. 1999). Only two examples of post mortem, histopathological anaylsis from patients with confirmed *GUCY2D* mutations have been reported, each of which showed that LCA1 was associated with degeneration of both rods and cones (Milam et al. 2003; Porto et al. 2003). However, more recent studies employing optical coherence tomography (OCT) to visualize patient retinas in-life report hallmark retinal preservation, even into the fifth decade (Pasadhika et al. 2010; Simonelli et al. 2007). The most thorough clinical characterization to date finds that LCA1 patients retain normal photoreceptor laminar architecture aside from foveal cone outer segment abnormalities and, in a few patients, foveal cone loss (Jacobson et al. 2013). Rod outer segment lengths were preserved and, in many patients, ERG, psychophysical and visually-guided behavior testing revealed that some rod function was retained. On the contrary, cone function was severely impaired. Cone ERGs were undetectable in all LCA1 patients evaluated. Psychophysical and behavior tests revealed the majority of patients lacked cone-mediated vision. This correlated with severely reduced visual acuity and a lack of color perception. It is now apparent that LCA1 is a disease of profound cone dysfunction and hallmark retinal preservation suggesting that these patients may be good candidates for gene replacement therapy. As a means to this end, several animal models of LCA1 have been characterized and used to establish proof of concept.

34.2.1 GUCY1*B Chicken

The naturally occurring *retinal degeneration (rd),* or GUCY1*B chicken carries a null mutation in the gene encoding retGC1 (Cheng et al. 1980; Semple-Rowland et al. 1998). Affected chickens are blind at hatch and have an unrecordable ERG. cGMP levels in post-hatch day 1 (P1) chickens are ~10% of normal and photoreceptors in this cone-dominant species begin degenerating at 1 week. Cones are lost by ~3.5 months followed by rods at ~8 months (Ulshafer and Allen 1985). With the goal of providing therapy as soon as possible, and because subretinal injections are difficult to perform in developed chickens, an *in ovo* treatment paradigm was developed. HIV1-based lentivirus (LV) carrying a cDNA encoding bovine GC1 (bGC1) was delivered to the neural tube of embryonic day 2 (E2) chickens. Within days of hatch, optokinetic reflex (OKN) and volitional visual behavior were evident in the majority of treated chickens. ERG analysis revealed modest increases (~6%) in a- and b-wave amplitudes under both dark- and light-adapted conditions. LV-bGC1 treatment slowed, but did not prevent retinal degeneration (Williams et al. 2006). Results of these studies established that gene replacement could be effective for the treatment of LCA1. However, results were transient (behavioral and ERG responses disappeared after ~5 weeks post hatch, retinal degeneration was not prevented), an *in ovo* treatment paradigm was used (currently not translatable to the patient population) and studies were conducted in a non-mammalian model. Taken together, this highlighted the need for a more translatable animal model and gene replacement strategy.

34.2.2 GC1KO Mouse

In 1999, Yang et al. described the first mammalian model of LCA1- the guanylate cyclase 1 knockout (GC1KO) mouse (Yang et al. 1999). This null model was engineered by insertion of a neomycin resistance cassette into exon 5 of *Gucy2e* (the murine homologue). Loss of cone function in this mouse precedes their degeneration (photopic ERGs are barely detectably by 1 month and cone degeneration begins between 4–5 weeks of age). Rods, on the other hand, maintain variable levels of function (30–50% of WT) and do not degenerate, a finding owed to the presence of retGC2 in these cells (Baehr et al. 2007). GCAP1 and GCAP2 transcripts and GCAP1 expression are downregulated and light-induced cone arrestin translocation is disrupted in this model (Coleman et al. 2004; Coleman and Semple-Rowland 2005). While it was not appreciated at the time, the profound cone dysfunction, variably retained rod function and rod preservation highlights how well the GC1KO mouse models the human condition (Jacobson et al. 2013).

For its ability to transduce postmitotic photoreceptors (Yang et al. 2002), Adeno associated virus (AAV5) was used to deliver bovine cDNA (same sequence used in the GUCY1*B chicken studies) to the subretinal space of GC1KO mice (Haire et al. 2006). Due to the species non-specific nature of the cDNA used, treatment failed to improve ERG or prevent cone degeneration. A later study by Boye et al. revealed that P14-P25 treatment with AAV5 carrying species-specific *Gucy2e* cDNA led to robust improvements in cone function (~45% of WT), restoration of cone-mediated vision (OKN) and prevented cone degeneration (Boye et al. 2010). Follow up studies asked whether long term therapy was possible (Boye et al. 2011; Mihelec et al. 2011). Mihelec et al. showed that P10 treatment with AAV8 containing human *GUCY2D* restored cone ERGs (65% of normal), cone-mediated behavior (OKN), preserved cones and also significantly improved rod responses for at least 6 months. Proof of concept using human *GUCY2D* is relevant for future preclinical studies. In the longest follow up to date, Boye et al. demonstrated that P14-P25 treatment with AAV5 or AAV8(Y733F) vectors containing *Gucy2e* restored cone function, cone-mediated behavior (OKN) and preserved cones for at least 1 year post treatment. Differences in cone ERG improvements between these studies (65% vs. 45% of WT) is likely attributed to the treatment age (prior to eye opening in Mihelec et al. study vs. P14-P25 in Boye et al. study)/the onset of therapeutic gene expression. Taken together, the stable therapeutic effects observed in AAV-treated GC1KO mice laid the groundwork for the development of an AAV-based treatment for LCA1.

34.2.3 GCDKO Mouse

The retGC1/retGC2 double knockout (GCDKO) mouse lacks both rod and cone function (ERG) (Baehr et al. 2007). Photoreceptor outer segments shorten by 2 months and, by 4 months there is appreciable outer nuclear layer thinning. Creation of this model occurred at a time when rod degeneration was thought to be a feature of LCA1 (Milam et al. 2003; Porto et al. 2003). Thus, it was valuable in the sense that it was the only model in which to evaluate the effects of GC1 expression on rod photoreceptors. It also provided an opportunity to examine the functional efficiency of AAV-delivered retGC1 (biochemical assays of guanylate cyclase activity do not discriminate between retGC1 and retGC2) (Olshevskaya et al. 2004).

P18-P108 treatment of GCDKO mice with AAV8(Y733F)-*Gucy2e* led to robust and stable restoration of both cone and rod ERGs, cone- and rod-mediated visual behavior (cortically and subcortically-driven) and preservation of photoreceptors over the long term (at least 1 year post-treatment) (Boye et al. 2013). As in the GC1KO study, WT-like visual behavior was observed in GCDKO mice that exhibited only partial ERG recovery (~45% of WT). retGC activity assays suggested complete restoration of enzyme activity in the area exposed to vector.

34.3 Conclusions

Proof of concept now exists in three different models of LCA1- the GUCY1*B chicken, the GC1KO and the GCDKO mouse. Work is also underway to evaluate therapy in a cone-only mouse model of LCA1, the *Nrl*$^{-/-}$*Gucy2e*$^{-/-}$ mouse. Taken together, these studies have paved the way for clinical application of an AAV-based gene therapy for treatment of this severe, early onset disease.

Acknowledgements I would like to thank Sue Semple Rowland, Ph.D., Wolfgang Baehr, Ph.D., Samuel G. Jacobson M.D., Ph.D., William W. Hauswirth, Ph.D., Alex Dizhoor, Ph.D., and Sanford L. Boye for their contributions to this research over the years.

References

Arshavsky VY, Burns ME (2012) Photoreceptor signaling: supporting vision across a wide range of light intensities. J Biol Chem 287:1620–1626.

Baehr W, Karan S, Maeda T et al (2007) The function of guanylate cyclase 1 (GC1) and guanylate cyclase 2 (GC2) in rod and cone photoreceptors. J Biol Chem 282:8837–8847

Boye SE, Boye SL, Pang J et al (2010) Functional and behavioral restoration of vision by gene therapy in the guanylate cyclase-1 (GC1) knockout mouse. PLoS One 5:e11306

Boye SL, Conlon T, Erger K et al (2011) Long-term preservation of cone photoreceptors and restoration of cone function by gene therapy in the guanylate cyclase-1 knockout (GC1KO) mouse. Invest Ophthalmol Vis Sci 52:7098–7108

Boye SL, Peshenko IV, Huang WC et al (2013) AAV-mediated gene therapy in the guanylate cyclase (RetGC1/RetGC2) double knockout mouse model of Leber congenital amaurosis. Hum Gene Ther 24:189–202

Cheng KM, Shoffner RN, Gelatt KN, Gum GG, Otis JS, Bitgood JJ (1980) An autosomal recessive blind mutant in the chicken. Poult Sci 59:2179–2181

Cideciyan AV, Aleman TS, Boye SL et al (2008) Human gene therapy for RPE65 isomerase deficiency activates the retinoid cycle of vision but with slow rod kinetics. Proc Natl Acad Sci U S A 105:15112–15117

Coleman JE, Semple-Rowland SL (2005) GC1 deletion prevents light-dependent arrestin translocation in mouse cone photoreceptor cells. Invest Ophthalmol Vis Sci 46:12–16

Coleman JE, Zhang Y, Brown GA et al (2004) Cone cell survival and downregulation of GCAP1 protein in the retinas of GC1 knockout mice. Invest Ophthalmol Vis Sci 45:3397–3403

Dizhoor AM, Lowe DG, Olshevskaya EV et al (1994) The human photoreceptor membrane guanylyl cyclase, RetGC, is present in outer segments and is regulated by calcium and a soluble activator. Neuron 12:1345–1352

Dizhoor AM, Olshevskaya EV, Henzel WJ et al (1995) Cloning, sequencing, and expression of a 24-kDa Ca(2+)-binding protein activating photoreceptor guanylyl cyclase. J Biol Chem 270:25200–25206

Haire SE, Pang J, Boye SL et al (2006) Light-driven cone arrestin translocation in cones of postnatal guanylate cyclase-1 knockout mouse retina treated with AAV-GC1. Invest Ophthalmol Vis Sci 47:3745–3753

Jacobson SG, Cideciyan AV, Peshenko IV et al (2013) Determining consequences of retinal membrane guanylyl cyclase (RetGC1) deficiency in human Leber congenital amaurosis en route to therapy: residual cone-photoreceptor vision correlates with biochemical properties of the mutants. Hum Mol Genet 22:168–183

Karan S, Frederick JM, Baehr W (2010) Novel functions of photoreceptor guanylate cyclases revealed by targeted deletion. Mol Cell Biochem 334:141–155
Liu X, Seno K, Nishizawa Y et al (1994) Ultrastructural localization of retinal guanylate cyclase in human and monkey retinas. Exp Eye Res 59:761–768
Mihelec M, Pearson RA, Robbie SJ et al (2011) Long-term preservation of cones and improvement in visual function following gene therapy in a mouse model of leber congenital amaurosis caused by guanylate cyclase-1 deficiency. Hum Gene Ther 22:1179–1190
Milam AH, Barakat MR, Gupta N et al (2003) Clinicopathologic effects of mutant GUCY2D in Leber congenital amaurosis. Ophthalmology 110:549–558
Olshevskaya EV, Calvert PD, Woodruff ML et al (2004) The Y99C mutation in guanylyl cyclase-activating protein 1 increases intracellular Ca^{2+} and causes photoreceptor degeneration in transgenic mice. J Neurosci 24:6078–6085
Pasadhika S, Fishman GA, Stone EM et al (2010) Differential macular morphology in patients with RPE65-, CEP290-, GUCY2D-, and AIPL1-related Leber congenital amaurosis. Invest Ophthalmol Vis Sci 51:2608–2614
Perrault I, Rozet JM, Gerber S et al (1999) Leber congenital amaurosis. Mol Genet Metab 68: 200–208
Perrault I, Rozet JM, Gerber S et al (2000) Spectrum of retGC1 mutations in Leber's congenital amaurosis. Eur J Hum Genet 8:578–582
Peshenko IV, Olshevskaya EV, Savchenko AB et al (2011) Enzymatic properties and regulation of the native isozymes of retinal membrane guanylyl cyclase (RetGC) from mouse photoreceptors. Biochemistry 50:5590–5600
Porto FB, Perrault I, Hicks D et al (2003) Prenatal human ocular degeneration occurs in Leber's congenital amaurosis (LCA1 and 2). Adv Exp Med Biol 533:59–68
Pugh EN Jr, Duda T, Sitaramayya A et al (1997) Photoreceptor guanylate cyclases: a review. Biosci Rep 17:429–473
Semple-Rowland SL, Lee NR, Van Hooser JP et al (1998) A null mutation in the photoreceptor guanylate cyclase gene causes the retinal degeneration chicken phenotype. Proc Natl Acad Sci U S A 95:1271–1276
Simonelli F, Ziviello C, Testa F et al (2007) Clinical and molecular genetics of Leber's congenital amaurosis: a multicenter study of Italian patients. Invest Ophthalmol Vis Sci 48:4284–4290
Ulshafer RJ, Allen CB (1985) Ultrastructural changes in the retinal pigment epithelium of congenitally blind chickens. Curr Eye Res 4:1009–1021
Williams ML, Coleman JE, Haire SE et al (2006) Lentiviral expression of retinal guanylate cyclase-1 (RetGC1) restores vision in an avian model of childhood blindness. PLoS Med 3:e201
Yang RB, Garbers DL (1997) Two eye guanylyl cyclases are expressed in the same photoreceptor cells and form homomers in preference to heteromers. J Biol Chem 272:13738–13742
Yang RB, Robinson SW, Xiong WH et al (1999) Disruption of a retinal guanylyl cyclase gene leads to cone-specific dystrophy and paradoxical rod behavior. J Neurosci 19:5889–5897
Yang GS, Schmidt M, Yan Z et al (2002) Virus-mediated transduction of murine retina with adeno-associated virus: effects of viral capsid and genome size. J Virol 76:7651–7660

Chapter 35
A Comprehensive Review of Mutations in the *MERTK* Proto-Oncogene

Célia Parinot and Emeline F. Nandrot

Abstract Phagocytosis and elimination of shed aged photoreceptor outer segments (POS) by retinal pigment epithelial cells is crucial for photoreceptor function and survival. Genetic studies on a natural animal model of recessive retinal degeneration allowed the identification of *MerTK*, the gene encoding the surface receptor required for POS internalization. Following this discovery, screenings of DNA samples from patients have revealed that *MERTK* mutations cause retinal degenerations in humans. *MERTK* patients present some of the classical symptoms of retinitis pigmentosa, but it is atypical in that the disease develops very early during childhood and the macula is also involved early on. Therefore, the phenotype ought to be qualified as a rod-cone dystrophy. Recently, *MERTK* has been implicated in various types of cancers and sclerosis. This review identifies the different *MERTK* mutations known so far and describes associated pathologies.

Keywords MerTK · Phagocytosis · Retinal pigment epithelium · RCS rat · Mutations · Rod-cone dystrophies · Retinitis pigmentosa · Photoreceptor death · Proto-oncogene · Cancer

35.1 Introduction

Photoreceptors (PRs) constantly renew them the photosensitive disks contained in their outer segments (POS) to counteract the permanent light stress affecting them. POS aged extremities are daily shed and phagocytosed by cells from the retinal pigment epithelium (RPE) (Young and Bok 1969). With a maximum activity 2 h after light onset (LaVail 1976), this process is mainly achieved by two membrane receptors: αvβ5 integrin allows POS binding (Finnemann et al. 1997) and initiates the rhythm of POS clearance (Nandrot et al. 2004) while MerTK is necessary for POS

E. F. Nandrot (✉) · C. Parinot
Institut de la Vision, INSERM, U968, Sorbonne Universités, UPMC Univ Paris 06, UMR_S968, CNRS, UMR_7210, 17 rue Moreau, 75012 Paris, France
e-mail: emeline.nandrot@inserm.fr

C. Bowes Rickman et al. (eds.), *Retinal Degenerative Diseases,* Advances in Experimental Medicine and Biology 854, DOI 10.1007/978-3-319-17121-0_35

engulfment (D'Cruz et al. 2000; Nandrot et al. 2000; Feng et al. 2003) and controls the amounts of POS bound to RPE cells (Nandrot et al. 2012). This review focuses on the *MERTK* pathological implications in various tissues.

35.2 The MerTK Receptor

35.2.1 A Tyrosine Kinase Receptor

MERTK, located on chromosome 2q14.1 (Weier et al. 1999), is expressed in several hematopoietic (macrophages), epithelial (RPE) and reproductive tissues (Linger et al. 2008). Its 19 exons encode a 999-amino acid transmembrane receptor (Graham et al. 1994) ranging from 160–205 kDa depending on glycosylation levels. MerTK is constituted of two immunoglobulin (Ig)-like 1 and 2 fibronectin type III (FnIII) extracellular domains, and of an intracellular tyrosine kinase domain including the KWIAIES sequence specific to the TAM family of receptors. MerTK binds two main extracellular ligands, Gas6 (Nagata et al. 1996) and Protein S (Hall et al. 2005), leading to MerTK dimerization, tyrosine autophosphorylations and intracellular signaling (Ling et al. 1996). In macrophages, MerTK mediates the phagocytic clearance of apoptotic cells (Scott et al. 2001).

35.2.2 Role in RPE Cells

The Royal College of Surgeons (RCS) rat is a natural animal model which RPE cells are unable to phagocytose shed POS (Bok and Hall 1971). Consequently, debris accumulate causing complete vision loss and PR cell death by 3 months of age (Dowling and Sidman 1962). In 2000, two groups characterized a large genomic deletion in the second exon of *MerTK* leading to a missing protein (D'Cruz et al. 2000; Nandrot et al. 2000).

In vivo, the alphavbeta5 integrin–Mfg-E8 couple rhythmically signals for MerTK phosphorylation at peak phagocytosis time (Nandrot et al. 2004, 2007). In addition, both MerTK ligands are required as double knockout mice present a phenotype similar to RCS rats (Burstyn-Cohen et al. 2012).

35.3 *MerTK* Mutations and Associated Diseases

35.3.1 Retinal Degenerations

With an autosomal recessive transmission, *MERTK* mutations (Table 35.1) have been mostly identified in consanguineous families native from Spain (Brea-Fernández

Table 35.1 *MERTK* mutations listed in order respective to their protein domain location. Nucleotide/protein changes and corresponding references are detailed (*Italics* reference = cancer-related)

Protein domain	Mutation	Protein defect	References
Signal peptide	*c.61 + 1G>A intron 1 splicing*	*aberrant protein*	Mackay et al. (2010)
Ig-like1 #1–FnIII #1	*exons 1–7 deletion*	*aberrant protein*	Ostergaard et al. (2011)
Ig-like1 #2	*c.718G>T exon 4*	*p.Glu240X*	Shahzadi et al. (2010)
FnIII #2	*exon 8 deletion*	*aberrant protein*	Mackay et al. (2010)
Intracellular—below membrane	*IVS10–2A>G intron 10 splicing*	*aberrant protein*	Gal et al. (2000)
Tyrosine kinase	*c.1951C>T exon 14*	*p.Arg651X*	Gal et al. (2000) Mackay et al. (2010)
	c.2070delAGGAC exon 15	*aberrant protein*	Gal et al. (2000)
	exon 15 deletion	*p.Gly654AlafsX41*	Siemiatkowska et al. (2011)
	c.2164C>T exon 16	*p.Arg722X*	McHenry et al. (2004)
	c.2180G>A exon 16	p.Arg727Gln	Coppieters et al. (2014)
	c.2189 + 1G>T exon 16 splicing	*p.His694ValfsX4*	Ebermann et al. (2007) Charbel Issa et al. (2009)
	IVS16 + 1G>T intron 16 splicing	*aberrant protein*	(Brea-Fernandez et al. 2008)
	c.2214delT exon 17	*p.Cys738TrpfsX31*	Tschernutter et al. (2006)
	c.2323C>T exon 17	*p.Arg775X*	Ksantini et al. (2012)
	c.2487–2A>G exon 19 splicing	*aberrant protein*	Siemiatkowska et al. (2011)
C-terminal	c.2530C>T exon 19	p.Arg844Cys	McHenry et al. (2004)
	c.2593C>T exon 19	p.Arg865Trp	McHenry et al. (2004) *Hucthagowder et al.* (2012)

et al. 2008), Morocco (Charbel Issa et al. 2009; Ksantini et al. 2012), the Middle East (Tschernutter et al. 2006; Mackay et al. 2010; Coppieters et al. 2014), Pakistan (Tschernutter et al. 2006; Shahzadi et al. 2010), Asia (Tada et al. 2006; Siemiatkowska et al. 2011) and the Faroe Islands (Ostergaard et al. 2011).

Primarily described as retinitis pigmentosa (RP) (Gal et al. 2000), patient phenotypes are atypical. RP, a slow degeneration targeting rods, manifests progressively as night blindness, reduced visual fields, retinal vasculature attenuation, optic disc pallor, and bone spicule pigments and apparition. *MERTK* patient symptoms are

severe, often arise during the first decade of life and worsen quickly with an early macular atrophy. Moreover, some patients show an autofluorescent macula, sign of imperfect POS elimination (Tschernutter et al. 2006). Thus it seems more appropriate to designate *MERTK*-related pathologies as rod-cone dystrophies.

35.3.2 Other pathologies

First identified as a proto-oncogene (Graham et al. 1994), MerTK carries a transforming potential on cultured cells (Lierman et al. 2009). Logically, *MERTK* is involved in various types of cancer: upregulated in a large spectrum of malignant cells including leukemia, lymphoma (Linger et al. 2008) and colorectal cancer (Watanabe et al. 2011), its expression is associated with poor prognosis in gastric cancer (Linger et al. 2008). Somatic variants exist in melanoma (p.Pro802Ser) (Tworkoski et al. 2013), multiple myeloma (p.Thr690Ile, p.Glu823Gln; Table 35.1) (Hucthagowder et al. 2012), renal cancer and carcinoma (p.Ala446Gly, p.Ala708Ser) (Greenman et al. 2007). In addition, MerTK expression increases in various sclerotic lesions (Weinger et al. 2009; Hurtado et al. 2011).

35.3.3 Other Variants

Non-pathogenic *MERTK* variants p.Arg20Ser, p.Asp118Ser, p.Ala282Thr, p.Arg293His, p.Arg466Lys, p.Asp498Ser, p.Ile518Val and p.Val870Ile have been described (Gal et al. 2000; McHenry et al. 2004; Tada et al. 2006; Tschernutter et al. 2006). Present at similar frequencies in retinal dystrophy and unaffected individuals they are enriched as somatic mutations in cancers (Greenman et al. 2007; Hucthagowder et al. 2012). The pathological implication of some heterozygous missense substitutions present in both patients and their unaffected parents is not clear (p.Glu540Lys, p.Ser661Cys, p.Ile871Thr) (Gal et al. 2000). Yet, heterozygous mutations in Leber Congenital Amaurosis cases seem to co-segregate with other gene defects (p.Phe214Val, p.Pro958Leu) (Li et al. 2011). Taken together, these data suggest that some variants might be pathogenic in combination with other factors.

35.4 Perspectives

MERTK is now considered as a good target for the treatment of certain cancers (Linger et al. 2013a, 2013b; Schlegel et al. 2013). Various gene therapy approaches have been tested in rodent retinae using adenoviruses (Vollrath et al. 2001), AAVs (Smith et al. 2003; Deng et al. 2012; Conlon et al., 2013) or lentiviruses (Tschernutter et al. 2005). Preservation of PRs and retinal function can persist up to 12 months post-injection (Tschernutter et al. 2005; Deng et al. 2012). In August 2011, the first

phase I clinical trial has been launched in Saudi Arabia on 6 *MERTK* patients (clinicaltrials.gov; NCT01482195) after validation of the vector (Conlon et al. 2013).

References

Bok D, Hall MO (1971) The role of the pigment epithelium in the etiology of inherited retinal dystrophy in the rat. J Cell Biol 49:664–682

Brea-Fernández AJ, Pomares E, Brión MJ et al (2008) Novel splice donor site mutation in MERTK gene associated with retinitis pigmentosa. Br J Ophthalmol 92:1419–1423

Burstyn-Cohen T, Lew ED, Través PG et al (2012) Genetic dissection of TAM receptor-ligand interaction in retinal pigment epithelial cell phagocytosis. Neuron 76:1123–1132

Charbel Issa P, Bolz HJ, Ebermann I et al (2009) Characterisation of severe rod-cone dystrophy in a consanguineous family with a splice site mutation in the MERTK gene. Br J Ophthalmol 93:920–925

Conlon TJ, Deng W-T, Erger K et al (2013) Preclinical potency and safety studies of an AAV2-mediated gene therapy vector for the treatment of MERTK associated retinitis pigmentosa. Hum Gene Ther Clin Dev 24:23–28

Coppieters F, Van Schil K, Bauwens M et al (2014) Identity-by-descent-guided mutation analysis and exome sequencing in consanguineous families reveals unusual clinical and molecular findings in retinal dystrophy. Genet Med. doi:10.1038/gim.2014.24

D'Cruz PM, Yasumura D, Weir J et al (2000) Mutation of the receptor tyrosine kinase gene Mertk in the retinal dystrophic RCS rat. Hum Mol Genet 9:645–651

Deng W-T, Dinculescu A, Li Q et al (2012) Tyrosine-mutant AAV8 delivery of human MERTK provides long-term retinal preservation in RCS rats. Invest Ophthalmol Vis Sci 53:1895–1904

Dowling JE, Sidman RL (1962) Inherited retinal dystrophy in the rat. J Cell Biol 14:73–109

Ebermann I, Walger M, Scholl HP et al (2007) Truncating mutation of the DFNB59 gene causes cochlear hearing impairment and central vestibular dysfunction. Hum Mutat 28:571–577

Feng W, Yasumura D, Matthes MT et al (2003) Mertk triggers uptake of photoreceptor outer segments during phagocytosis by cultured retinal pigment epithelial cells. J Biol Chem 277:17016–17022

Finnemann SC, Bonilha VL, Marmorstein AD et al (1997) Phagocytosis of rod outer segments by retinal pigment epithelial cells requires alpha(v)beta5 integrin for binding but not for internalization. Proc Natl Acad Sci U S A 94:12932–12937

Gal A, Li Y, Thompson DA et al (2000) Mutations in MERTK, the human orthologue of the RCS rat retinal dystrophy gene, cause retinitis pigmentosa. Nat Genet 26:270–271

Graham DK, Dawson TL, Mullaney DL et al (1994) Cloning and mRNA expression analysis of a novel human protooncogene, c-mer. Cell Growth Differ 5:647–657

Greenman C, Stephens P, Smith R et al (2007) Patterns of somatic mutation in human cancer genomes. Nature 446:153–158

Hall MO, Obin MS, Heeb MJ et al (2005) Both protein S and Gas6 stimulate outer segment phagocytosis by cultured rat retinal pigment epithelial cells. Exp Eye Res 81:581–591

Hucthagowder V, Meyer R, Mullins C et al (2012) Resequencing analysis of the candidate tyrosine kinase and RAS pathway gene families in multiple myeloma. Cancer Genet 205:474–478

Hurtado B, Muñoz X, Recarte-Pelz P et al (2011) Expression of the vitamin K-dependent proteins GAS6 and protein S and the TAM receptor tyrosine kinases in human atherosclerotic carotid plaques. Thromb Haemost 105:873–882

Ksantini M, Lafont E, Bocquet B et al (2012) Homozygous mutation in MERTK causes severe autosomal recessive retinitis pigmentosa. Eur J Ophthalmol 22:647–653

LaVail MM (1976) Rod outer segment disk shedding in rat retina: relationship to cyclic lighting. Science 194:1071–1074

Lierman E, Van Miegroet H, Beullens E et al (2009) Identification of protein tyrosine kinases with oncogenic potential using a retroviral insertion mutagenesis screen. Haematologica 94:1440–1444

Li L, Xiao X, Li S (2011) Detection of variants in 15 genes in 87 unrelated Chinese patients with Leber congenital amaurosis. PLoS One 6:e19458

Ling L, Templeton D, Kung HJ (1996) Identification of the major autophosphorylation sites of Nyk/Mer, an NCAM-related receptor tyrosine kinase. J Biol Chem 271:18355–18362

Linger RMA, Keating AK, Earp HS et al (2008) TAM receptor tyrosine kinases: biologic functions, signaling, and potential therapeutic targeting in human cancer. Adv Cancer Res 100:35–83

Linger RMA, Cohen RA, Cummings CT et al (2013a) Mer or Axl receptor tyrosine kinase inhibition promotes apoptosis, blocks growth and enhances chemosensitivity of human non-small cell lung cancer. Oncogene 32:3420–3431

Linger RMA, Lee-Sherick AB, DeRyckere D et al (2013b) Mer receptor tyrosine kinase is a therapeutic target in pre-B-cell acute lymphoblastic leukemia. Blood 122:1599–1609

Mackay DS, Henderson RH, Sergouniotis PI et al (2010) Novel mutations in MERTK associated with childhood onset rod-cone dystrophy. Mol Vis 16:369–377

McHenry CL, Liu Y, Feng W et al (2004) MERTK arginine-844-cysteine in a patient with severe rod-cone dystrophy: loss of mutant protein function in transfected cells. Invest Ophthalmol Vis Sci 45:1456–1463

Nagata K, Ohashi K, Nakano T et al (1996) Identification of the product of growth arrest-specific gene 6 as a common ligand for Axl, Sky, and Mer receptor tyrosine kinases. J Biol Chem 271:30022–30027

Nandrot E, Dufour EM, Provost AC et al (2000) Homozygous deletion in the coding sequence of the c-mer gene in RCS rats unravels general mechanisms of physiological cell adhesion and apoptosis. Neurobiol Dis 7:586–599

Nandrot EF, Kim Y, Brodie SE et al (2004) Loss of synchronized retinal phagocytosis and age-related blindness in mice lacking alphavbeta5 integrin. J Exp Med 200:1539–1545

Nandrot EF, Anand M, Almeida D et al (2007) Essential role for MFG-E8 as ligand for alphavbeta5 integrin in diurnal retinal phagocytosis. Proc Natl Acad Sci U S A 104:12005–12010

Nandrot EF, Silva KE, Scelfo C et al (2012) RPE cells use a MerTK-dependent mechanism to limit alphavbeta5 integrin binding activity. Biol Cell 104:326–341

Ostergaard E, Duno M, Batbayli M et al (2011) A novel MERTK deletion is a common founder mutation in the Faroe Islands and is responsible for a high proportion of retinitis pigmentosa cases. Mol Vis 17:1485–1492

Schlegel J, Sambade MJ, Sather S et al (2013) MERTK receptor tyrosine kinase is a therapeutic target in melanoma. J Clin Invest 123:2257–2267

Scott RS, McMahon EJ, Pop SM et al (2001) Phagocytosis and clearance of apoptotic cells is mediated by MER. Nature 411:207–211

Shahzadi A, Riazuddin SA, Ali S et al (2010) Nonsense mutation in MERTK causes autosomal recessive retinitis pigmentosa in a consanguineous Pakistani family. Br J Ophthalmol 94:1094–1099

Siemiatkowska AM, Arimadyo K, Moruz LM et al (2011) Molecular genetic analysis of retinitis pigmentosa in Indonesia using genome-wide homozygosity mapping. Mol Vis 17:3013–3024

Smith AJ, Schlichtenbrede FC, Tschernutter M et al (2003) AAV-Mediated gene transfer slows photoreceptor loss in the RCS rat model of retinitis pigmentosa. Mol Ther 8:188–195

Tada A, Wada Y, Sato H et al (2006) Screening of the MERTK gene for mutations in Japanese patients with autosomal recessive retinitis pigmentosa. Mol Vis 12:441–444

Tschernutter M, Schlichtenbrede FC, Howe S et al (2005) Long-term preservation of retinal function in the RCS rat model of retinitis pigmentosa following lentivirus-mediated gene therapy. Gene Ther 12:694–701

Tschernutter M, Jenkins SA, Waseem NH et al (2006) Clinical characterisation of a family with retinal dystrophy caused by mutation in the Mertk gene. Br J Ophthalmol 90:718–723

Tworkoski KA, Platt JT, Bacchiocchi A et al (2013) MERTK controls melanoma cell migration and survival and differentially regulates cell behavior relative to AXL. Pigment Cell Melanoma Res 26:527–541

Vollrath D, Feng W, Duncan JL et al (2001) Correction of the retinal dystrophy phenotype of the RCS rat by viral gene transfer of Mertk. Proc Natl Acad Sci U S A 98:12584–12589

Watanabe T, Kobunai T, Yamamoto Y et al (2011) Differential gene expression signatures between colorectal cancers with and without KRAS mutations: crosstalk between the KRAS pathway and other signalling pathways. Eur J Cancer 47:1946–1954

Weier HU, Fung J, Lersch RA (1999) Assignment of protooncogene MERTK (a.k.a. c-mer) to human chromosome 2q14.1 by in situ hybridization. Cytogenet Cell Genet 84:91–92

Weinger JG, Omari KM, Marsden K et al (2009) Up-regulation of soluble Axl and Mer receptor tyrosine kinases negatively correlates with Gas6 in established multiple sclerosis lesions. Am J Pathol 175:283–293

Young RW, Bok D (1969) Participation of the retinal pigment epithelium in the rod outer segment renewal process. J Cell Biol 42:392–403

Part IV
In Vivo Imaging and Other Diagnostic Advances

Chapter 36
New Developments in Murine Imaging for Assessing Photoreceptor Degeneration *In Vivo*

Marie E. Burns, Emily S. Levine, Eric B. Miller, Azhar Zam, Pengfei Zhang, Robert J. Zawadzki and Edward N. Pugh, Jr.

Abstract Optical Coherence Tomography (OCT) is a powerful clinical tool that measures near infrared light backscattered from the eye and other tissues. OCT is used for assessing changes in retinal structure, including layer thicknesses, detachments and the presence of drusen in patient populations. Our custom-built OCT system for the mouse eye quantitatively images all layers of the neural retinal, the RPE, Bruchs' membrane and the choroid. Longitudinal assessment of the same retinal region reveals that the relative intensities of retinal layers are highly stable in healthy tissue, but show progressive increases in intensity in a model of retinal degeneration. The observed changes in OCT signal have been correlated with ultrastructural disruptions that were most dramatic in the inner segments and nuclei of the rods. These early changes in photoreceptor structure coincided with activation

M. E. Burns (✉) · R. J. Zawadzki · E. N. Pugh
Department of Ophthalmology and Vision Science,
University of California Davis, 3301B Tupper Hall, Davis, CA 95616, USA
e-mail: meburns@ucdavis.edu

M. E. Burns · E. B. Miller
Center for Neuroscience, University of California Davis,
1544 Newton Court, Davis, CA 95618, USA
e-mail: ebmiller@ucdavis.edu

M. E. Burns · E. S. Levine · A. Zam · P. Zhang · R. J. Zawadzki · E. N. Pugh
Cell Biology and Human Anatomy, University of California Davis,
3307 Tupper Hall, Davis, CA 95616, USA

E. S. Levine
e-mail: elevine@ucdavis.edu

A. Zam
e-mail: azam@ucdavis.edu

P. Zhang
e-mail: pfzhang@ucdavis.edu

R. J. Zawadzki
e-mail: rjzawadzki@ucdavis.edu

E. N. Pugh
e-mail: enpugh@ucdavis.edu

C. Bowes Rickman et al. (eds.), *Retinal Degenerative Diseases,* Advances in Experimental Medicine and Biology 854, DOI 10.1007/978-3-319-17121-0_36

of retinal microglia, which migrated vertically from the inner to the outer retina to phagocytose photoreceptor cell bodies (Levine et al., Vis Res 102:71–79, 2014). We conclude that quantitative analysis of OCT light scattering signals may be a useful tool for early detection and subcellular localization of cell stress prior to cell death, and for assessing the progression of degenerative disease over time. Future efforts to develop sensitive approaches for monitoring microglial dynamics *in vivo* may likewise elucidate earlier signs of cellular stress during retinal degeneration.

Keywords Photoreceptor · Rod · Phototransduction · Arrestin-1 · Optical coherence tomography (OCT) · Scanning laser ophthalmoscopy (SLO) · Imaging · Mouse · Microglia

36.1 Phototransduction Signaling and Photoreceptor Degeneration

Despite the prevalence of photoreceptor degeneration in the general population, we know little about how photoreceptors die. In contrast, we know more about the biochemistry, physiology and cell biology of rod photoreceptors than of any other retinal cell type. Mutations in proteins that help to transduce light into electrical signals (phototransduction proteins) often cause prolonged electrical signaling but only degeneration in certain instances. For example, prolonged rod signaling that arises from defects in rhodopsin deactivation causes Oguchi disease and can lead to light-dependent degeneration (Paskowitz et al. 2006). In contrast, loss of the protein complex responsible for G protein deactivation (RGS9–1, Gβ5-L, and R9AP) also greatly prolongs signaling and causes visual impairment, but does not lead to photoreceptor damage (Nishiguchi et al. 2004). Other RP-related mutations in phototransduction proteins do not cause defective signaling per se, but rather cause protein misfolding (Tzekov et al. 2011). Although the unfolded protein response (UPR) itself causes apoptosis, degeneration resulting from these mutations can be exacerbated by visible light (Paskowitz et al. 2006). To better understand the interplay between electrical signaling and the cell biology of degenerating photoreceptors, it is first essential to monitor photoreceptors longitudinally *in vivo* without exposure to the high intensity visible light typically used during fundus imaging (Cideciyan et al. 2005).

OCT, which uses the backscattering of near-infrared light to visualize retinal structure, allows longitudinal assessment of the same retinal region over time without exposure to visible light that would activate phototransduction and bleach visual pigment. When OCT images are not subject to auto-gain adjustments and are aligned with landmarks like retinal vessels, the backscattered light increases within photoreceptor-specific layers during light-dependent degeneration (Cideciyan et al. 2005; Zam et al. 2013). In mice, such changes in light scattering can precede typical measures of photoreceptor cell loss like outer nuclear layer thickness,

and have been correlated with ultrastructural disruptions in the inner segments and cell bodies (Levine et al. 2014). Further development of quantitative OCT methods may prove to be a useful tool for early detection of cell stress prior to cell death.

36.2 Quantitative OCT Light Scattering Measurements and Their Ultrastructural Correlates

We have recently constructed a Fourier-Domain OCT (Fd-OCT) system for imaging the mouse eye (Zam et al. 2013). Like most OCT systems, ours uses a broad bandwidth near-infrared light source for a reference beam and a highly sensitive CMOS camera as the detector of the spectrometer. The detector captures the spectral power density of the reference beam, which is modulated by the interference arising from the light backscattered with varying delays from reflecting elements in the retina. To derive an A-scan, which is the retinal scattering profile as a function of depth (z), the Fd-OCT system computes the inverse Fourier transform of the measured spectral density function, yielding an intensity profile $I(z)$ proportional to the square root of the intensity $I_{sample}(z)$ of the light backscattered from the sample at each depth (z) in the retina: thus, $I(z) \propto \sqrt{I_{ref}}\sqrt{I_{sample}(z)}$, where I_{ref} is the (constant) average intensity of the reference beam (Wojtkowski 2010; Oldenburg et al. 2013). B-scans, $I(x,z)$, are compounded of successive A-scans, where x is the lateral position in the retina. Commercial OCT systems typically display OCT B-scan data on a logarithmic (decibel) scale:

$$S(x,z) = 20\ log_{10}[I(x,z)/I_{ref}] \propto 20\log_{10}\left(\sqrt{I_{sample}(x,z)/I_{ref}}\right)$$

where $S(x, z)$ is proportional to the display pixel value. In contrast, all analysis of our images was performed on 16-bit linear intensity B-scan data.

The average B-scan intensity value $I(x,z)$ was measured from each retinal layer at precisely same eccentricity (x) over time in the same animal (Fig. 36.1a). In a mouse model of dim light damage (Arr1$^{-/-}$ mice; (Xu et al. 1997; Chen et al. 1999)) a profound increase in the intensity of the reflectance of the inner segment/outer segment border was apparent after 12 h of light exposure. By 36 h, a 2-fold increase in intensity had spread to the outer nuclear layer, which corresponds to a 4-fold light scattering change within the retina itself (Fig. 36.1b). While these changes were consistently apparent in the B-scans across all animals examined, there were also small variations in absolute intensity across imaging sessions that arose from differences in alignment and other factors affecting image quality. The intensity of the INL reflectance, which was unaffected by light exposure, was used to normalize the light scattering changes in the photoreceptor layers, reducing the baseline intensity values for both WT and Arr1$^{-/-}$ strains (Levine et al. 2014).

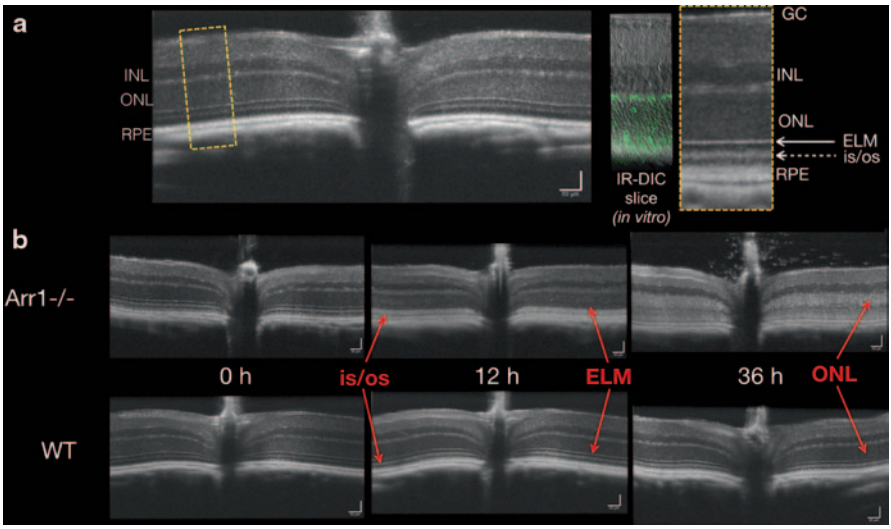

Fig. 36.1 Increased OCT light scattering during light-induced photoreceptor degeneration. **a** B-scan of a WT (c57Bl/6J) mouse. *Yellow dashed box* is shown expanded on the *right* and compared to a retinal slice in which the cones express GFP (7m8-hLM-GFP) to help demark the photoreceptor layers (*GC* ganglion cell layer, *INL* inner nuclear layer, *ONL* outer nuclear layer, *ELM* external limiting membrane, *is/os* inner segment/outer segment border, *RPE* retinal pigment epithelium). **b** *Dark-reared* $Arr1^{-/-}$ (Xu et al. 1997) and WT (c57Bl/6J) mice were imaged sequentially before and after the onset of 200 lx constant light. By 12 h, the ELM had disappeared and the is/os border showed increased scattering in the $Arr1^{-/-}$ mouse. By 36 h, the increased scattering had spread to the ONL and was correlated with increased chromatin condensation and related ultrastructural changes (Levine et al. 2014)

Rhodopsin mutant dogs have also shown acute increases in OCT light scattering with photoreceptor degeneration, which is dramatically accelerated by bright light (Cideciyan et al. 2005). The observed changes in light scattering were restricted to illuminated retinal regions and did not progressively enlarge over time, though the extent and time course of degeneration depended on light intensity. In this model, the changes in light scattering were evident within 1 h and seemed to initiate at the inner segment/outer segment border and spread over time to the outer nuclear layer and beyond. A similar trend but different time scale was observed in the $Arr1^{-/-}$ OCT images and was correlated with ultrastructural changes within the photoreceptors themselves (Fig. 36.1b and Levine et al. 2014).

It is not known whether the slower progression of degeneration common in most human retinal degenerations can likewise be detected with longitudinal OCT intensity comparisons. One challenge for the future will be to test the limits of OCT imaging sensitivity in other animal models of degeneration that proceed with different rates and from different retinal loci. In adapting this approach to the clinic, it will also be important to further develop and distribute computational tools for image analysis that allow post-hoc image registration without intensity normalization, which most commercial platforms currently hard-wire into their imaging systems.

36.3 Monitoring Microglial Dynamics during Photoreceptor Degeneration *In Vivo*

In all forms of retinal damage and degeneration, activated phagocytic monocytes like microglia (resident in CNS tissue) and macrophages (infiltrated from the circulation) can exacerbate the loss of neural tissue (Streit et al. 2004). Microglia are the first responders to disease and injury in the retina, transforming from a highly dynamic, branched resting state to an amoeboid, activated state along a continuum of stages that may or may not be reversible and memoryless, depending on the severity and duration of the insult (Block et al. 2007; Langmann 2007). In $Arr1^{-/-}$ (Walter and Neumann 2009) mice, microglia vertically migrate to the ONL and begin to engulf photoreceptor somata within 12 h of light exposure (Levine et al. 2014). Thus, visualizing microglial dynamics in intact retinal tissue could be a sensitive biological indicator for early signs of cell stress.

A common tool for imaging living microglia is a commercially available strain in which GFP has been knocked into the fractalkine receptor locus ($Cx3cr1^{GFP/GFP}$; Jackson Labs 005582). However, the loss of CX_3CR1 expression in the knock-in mutant does reduce microglial dynamics (Liang et al. 2009). Moreover, homozygous *Cx3cr1* knockout mice show photoreceptor degeneration and the accumulation of phagocytic monocytes in the subretinal space (Combadière et al. 2007). While heterozygous ($Cx3cr1^{GFP/+}$) mice appear to have normal microglial behavior and are thus may be a convenient tool for answering certain questions about neuroinflammation in the retina, developing acute means for labeling microglia *in vivo* offers advantages for live tissue imaging in all species.

Viral transduction of microglia is a well-suited alternative for retinal studies because full access to the posterior eye can now be achieved by a single intravitreal injection (Dalkara et al. 2013). Microglial cells in the brain have been successfully infected with AAV2 or 5 using the promoters of F4/80 and CD11b, resulting in varying levels of expression (Cucchiarini et al. 2003). Low efficiency viral transductions would facilitate *in vivo* microglia imaging by making it more likely that a single microglia could be individually followed over an extended period (Cucchiarini et al. 2003). Indeed, using SLO and AO-SLO imaging methods in the mouse, it is now possible to follow the activation and migration of a microglial cells *in vivo* (Fig. 36.2a–c; Alt et al. 2014).

Quantum dots, which are readily phagocytosed by microglia and macrophages, are another adaptable means for achieving cell-specific labeling (Jackson et al. 2007; Minami et al. 2012). In *ex vivo* retinal flatmounts, wheat germ agglutinin (WGA) conjugated quantum dots label rods, and can be become concentrated within the lysosomes of dynamic microglia (Fig. 36.2d). Thus, quantum dots tagged with specific cell-surface ligands may be a way to preferentially label active phagocytes targeting a specific cell type, providing a way to specifically detect regions of active phagocytosis, both *ex vivo* or *in vivo*.

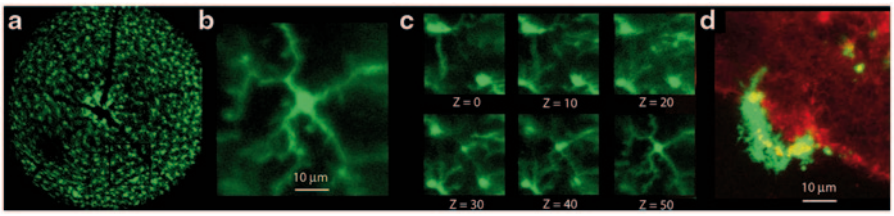

Fig. 36.2 Imaging retinal microglia. **a** Wide-field SLO image of the retina of a live *Cx3cr1*$^{GFP/+}$ mouse. **b** AO-SLO of a single microglia cell from a. **c** Six images of the AO-SLO z-stack from which b ($Z=50$) was taken, spanning 50 µm of the IPL (~0.5 mm per Z-step). **d** *Ex vivo* confocal image of an *Arr1*$^{-/-}$ *Cx3cr1*$^{GFP/+}$ retinal explant: the microglia cell engulfed WGA-conjugated quantum dots (*red*), which accumulated within highly motile intracellular lysosomes (*yellow*)

36.4 Conclusion

Applying ocular imaging approaches like OCT and AO-SLO to the mouse retina presents exciting opportunities for further developing methods like quantitative light scatter and microglial imaging, which could lead to earlier detection of cell stress and degeneration. Combined with the power of mouse genetics, viral transfection methods, and numerous available models of retinal degeneration, the mouse provides new avenues for studying the interplay between degeneration and inflammation, as well as the basic biology of normal retinal physiology and homeostasis across an individual's lifetime.

References

Alt C, Runnels JM, Mortensen LJ et al (2014) *In vivo* imaging of microglia turnover in the mouse retina after ionizing radiation and dexamethasone treatment. Invest Ophthalmol Vis Sci 55:5314–5319

Block ML, Zecca L, Hong J-S (2007) Microglia-mediated neurotoxicity: uncovering the molecular mechanisms. Nat Rev Neurosci 8:57–69

Chen J, Simon MI, Matthes MT et al (1999) Increased susceptibility to light damage in an arrestin knockout mouse model of Oguchi disease (stationary night blindness). Invest Ophthalmol Vis Sci 40:2978–2982

Cideciyan AV, Jacobson SG, Aleman TS et al (2005) *In vivo* dynamics of retinal injury and repair in the rhodopsin mutant dog model of human retinitis pigmentosa. Proc Natl Acad Sci U S A 102:5233–5238

Combadière C, Feumi C, Raoul W et al (2007) CX3CR1-dependent subretinal microglia cell accumulation is associated with cardinal features of age-related macular degeneration. J Clin Invest 117:2920–2928

Cucchiarini M, Ren X, Perides G et al (2003) Selective gene expression in brain microglia mediated via adeno-associated virus type 2 and type 5 vectors. Gene Ther 10:657–667

Dalkara D, Byrne LC, Klimczak RR et al (2013) *In vivo*-directed evolution of a new adeno-associated virus for therapeutic outer retinal gene delivery from the vitreous. Sci Transl Med 5:189ra76

Jackson H, Muhammad O, Daneshvar H et al (2007) Quantum dots are phagocytized by macrophages and colocalize with experimental gliomas. Neurosurgery 60:524–530
Langmann T (2007) Microglia activation in retinal degeneration. J Leukoc Biol 81:1345–1351
Levine ES, Zam A, Zhang P et al (2014) Rapid light-induced activation of retinal microglia in mice lacking Arrestin-1. Vis Res 102:71–79
Liang KJ, Lee JE, Wang YD et al (2009) Regulation of dynamic behavior of retinal microglia by CX3CR1 signaling. Invest Ophthalmol Vis Sci 50:4444–4451
Minami SS, Sun B, Popat K et al (2012) Selective targeting of microglia by quantum dots. J Neuroinflammation 9:22
Nishiguchi KM, Sandberg MA, Kooijman AC et al (2004) Defects in RGS9 or its anchor protein R9AP in patients with slow photoreceptor deactivation. Nature 427:75–78
Oldenburg AL, Chherti RK, Cooper JM et al (2013) Motility-, autocorrelation-, and polarized-sensitive optical coherence tomography discriminates cells and gold nanorods within 3D tissue cultures. Opt Lett 38:2923–2926
Paskowitz DM, LaVail MM, Duncan JL (2006) Light and inherited retinal degeneration. Br J Ophthalmol 90:1060–1066
Streit WJ, Mrak RE, Griffin WST (2004) Microglia and neuroinflammation: a pathological perspective. J Neuroinflammation 1:14
Tzekov R, Stein L, Kaushal S (2011) Protein misfolding and retinal degeneration. Cold Spring Harb Perspect Biol 3:a007492
Walter L, Neumann H (2009) Role of microglia in neuronal degeneration and regeneration. Semin Immunopathol 31:513–525
Wojtkowski M (2010) High-speed optical coherence tomography: basics and applications. Appl Opt 49:D30–D61
Xu J, Dodd RL, Makino CL et al (1997) Prolonged photoresponses in transgenic mouse rods lacking arrestin. Nature 389:505–509
Zam A, Dsouza R, Subhash HM et al (2013) Feasibility of correlation mapping optical coherence tomography (cmOCT) for anti-spoof sub-surface fingerprinting. J Biophotonics 6:663–667

Chapter 37
Reliability and Repeatability of Cone Density Measurements in Patients with Congenital Achromatopsia

Mortada A. Abozaid, Christopher S. Langlo, Adam M. Dubis, Michel Michaelides, Sergey Tarima and Joseph Carroll

Abstract Adaptive optics scanning light ophthalmoscopy (AOSLO) allows non-invasive assessment of the cone photoreceptor mosaic. Confocal AOSLO imaging of patients with achromatopsia (ACHM) reveals an altered reflectivity of the remaining cone structure, making identification of the cells more challenging than in normal retinas. Recently, a "split-detector" AOSLO imaging method was shown to enable direct visualization of cone inner segments in patients with ACHM. Several studies have demonstrated gene replacement therapy effective in restoring cone function in animal models of ACHM and human trials have on the horizon, making

Mortada A. Abozaid and Christopher S. Langlo are contributed equally to the study.

J. Carroll (✉) · M. A. Abozaid
Department of Ophthalmology, The Eye Institute, Medical College of Wisconsin, 925 N. 87th Street, Milwaukee, WI 53226, USA
e-mail: jcarroll@mcw.edu

M. A. Abozaid
Department of Ophthalmology, Sohag University, Sohag, Egypt
e-mail: mabdelaal@mcw.edu

C. S. Langlo · J. Carroll
Department of Cell Biology, Neurobiology and Anatomy, Medical College of Wisconsin, Milwaukee, WI, USA
e-mail: clanglo@mcw.edu

A. M. Dubis · M. Michaelides
UCL Institute of Ophthalmology, University College London, London, UK

Moorfields Eye Hospital, London, UK
e-mail: a.dubis@ucl.ac.uk
e-mail: michel.michaelides@ucl.ac.uk

S. Tarima
Division of Biostatistics, Institute for Health and Society, Medical College of Wisconsin, Milwaukee, WI, USA
e-mail: starima@mcw.edu

J. Carroll
Department of Biophysics, Medical College of Wisconsin, Milwaukee, WI, USA

C. Bowes Rickman et al. (eds.), *Retinal Degenerative Diseases,* Advances in Experimental Medicine and Biology 854, DOI 10.1007/978-3-319-17121-0_37

the ability to reliably assess cone structure increasingly important. Here we sought to examine whether absolute estimates of cone density obtained from split-detector and confocal AOSLO images differed from one another and whether the inter- and intra-observer reliability is significantly different between these modes. These findings provide an important foundation for evaluating the role of these images as tools to assess the efficacy of future gene therapy trials.

Keywords Achromatopsia · Adaptive optics · Repeatability · Reliability · Cone photoreceptor

37.1 Introduction

AOSLO enables visualization of the cone photoreceptor mosaic in the living human eye (Dubra et al. 2011; Rossi et al. 2011). Quantitative measurements from such images include cone density (Chui et al. 2008), cone spacing (Duncan et al. 2007; Rossi and Roorda 2010; Cooper et al. 2013) and Voronoi geometry (Baraas et al. 2007). These methods typically rely on identification of individual cones in the image and thus whether this is done manually or via an automated (or semi-automated) process, there is a need to assess the inherent reliability and repeatability of each approach.

Previously we assessed the repeatability of cone density measurements in a population of young healthy individuals using a semi-automated method and found that if repeated images of the same retinal location were precisely aligned, the repeatability was 2.7% (Garrioch et al. 2012). Chiu et al. (2013) demonstrated similar repeatability using the same data set and a fully automatic algorithm based on graph theory and dynamic programming. Most recently, we examined the inter-observer and inter-instrument reliability of cone density measurements and found that the inter-observer study's largest contribution to variability was the subject (95.72%) while the observer's contribution was only 1.03% (Liu et al. 2014). For the inter-instrument study, we reported an average cone density ICC of between 0.931 and 0.975 (Liu et al. 2014).

These studies are only relevant for individuals with intact cone mosaics and do not apply in conditions such as ACHM, where cone appearance can be greatly altered (Genead et al. 2011; Merino et al. 2011). This makes it difficult to disambiguate cones from other reflective material in the outer retina. Scoles et al. (2014) developed a split-detector AOSLO method to directly visualize cone inner segments in a manner independent of the cone's waveguide properties (from which the reflective confocal AOSLO signal arises) allowing for easier and more complete visualization of residual cone structure in patients with ACHM. In patients with ACHM, we sought to (1) assess whether estimates of cone density obtained with split-detector AOSLO images differed from those obtained from confocal AOSLO images and (2) determine whether the inter- and intra-observer reliability is significantly different between the two imaging modes. The findings presented here serve

as a foundation for subsequent studies aimed at monitoring residual cone structure over time in patients with ACHM.

37.2 Materials and Methods

37.2.1 Subjects

All research followed the tenets of the Declaration of Helsinki and study protocols were approved by IRBs at the Medical College of Wisconsin and Moorfields Eye Hospital. Subjects provided written informed consent after the nature and possible consequences of the study were explained. Images from seven subjects with molecularly confirmed ACHM (five with *CNGB3* mutations, two with *CNGA3* mutations) were used in this study (five males and two females, aged 11–64 years). Axial length measurements were obtained from all of the subjects using an IOL Master (Carl Zeiss Meditec, Dublin, CA) in order to calculate the lateral scale of each retinal image.

37.2.2 AOSLO Imaging of the Photoreceptor Mosaic

Each patient's head was stabilized using a dental impression on a bite bar and both eyes were dilated and cyclopleged using a combination of phenylephrine hydrochloride 2.5 % and tropicamide 1 %. Images of the photoreceptor mosaic were obtained using 790-nm light with two previously described AOSLOs that allow simultaneous acquisition of confocal and split-detector images as in Fig. 37.1 (Scoles et al. 2014). Image sequences (100–200 frames) subtending either $1 \times 1°$ or $1.5 \times 1.5°$ were collected between the foveal center and 20° temporal to fixation. Each confocal image sequence was registered to produce a single image with improved signal-to-noise ratio (Dubra and Harvey 2010), with the same transforms applied to the corresponding split-detector image sequence, yielding a second image of the exact same retinal location. From these images, a total of 80 100×100 μm areas were cropped for analysis.

37.2.3 Analyzing the Cone Mosaic

The data set consisted of 960 images (80 images, 2 modalities, 3 observers, 2 trials/observer). Three observers with varying familiarity in analyzing AOSLO images reviewed each image and manually identified cones after adjusting the brightness and contrast of the image to assist in determining cone presence. Images were displayed in random order, with the identity and retinal location of the images masked

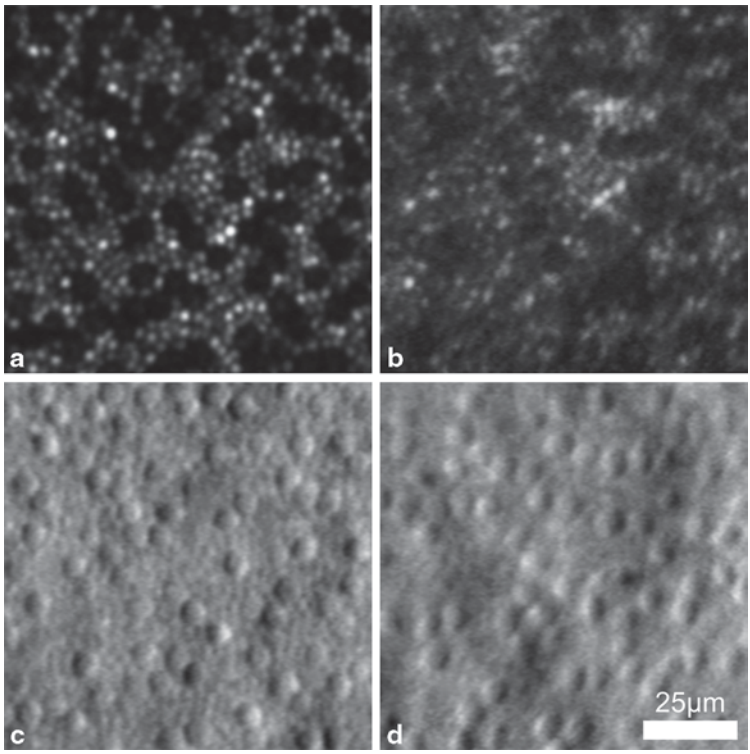

Fig. 37.1 Confocal (**a**, **b**) and split-detector (**c**, **d**) AOSLO images from two subjects with ACHM—JC_10069 (**a**, **c**) and MM_0005 (**b**, **d**)

(ensuring any effect of fatigue is captured by the observer's variance component). The number of cones in the cropped 100 × 100 μm region was divided by its area to derive an estimate of the cone density for that image.

37.2.4 Statistical Methods

The sample size and other characteristics of this study were chosen using a Monte Carlo simulation with preliminary estimates of unknown quantities estimated on a pilot data set. The objective was to secure the half-width of the 90 % CI for the relative contribution to the total variance, such that it is bounded by 1 % for observer, trial and image and the half-width of the 90 % CI for subjects' relative contribution to the total variance is not higher than 2.5 %. In this simulation study, 1000 repetitions were performed for a variance components model to assess the contribution of subject, mode, observer and trial to overall variability.

Highly significant biases prevented further analysis of the variance components model. Table 37.2 reports the fixed effects (regression coefficients) of the parsimo-

Table 37.1 Fixed effects for all observers

Variable	Estimate	Std.Err.	t
(Intercept)	8.35	0.060	138.53[a]
Mode=Split	−0.083	0.035	−2.34[a]
Trial=2	0.061	0.016	3.78[a]
Obs=2	−0.030	0.020	−1.47
Obs=3	−0.119	0.029	−4.04[a]
Trial=2:Obs=2	−0.068	0.022	−3.08[a]
Trial=2:Obs=3	0.035	0.022	1.59
Mode=Split:Obs=2	−0.074	0.022	−3.34[a]
Mode=Split:Obs=3	0.025	0.022	1.12

The model intercept corresponds to the expected LN (cone density) for the confocal mode, observer=1 and trial=1

[a] Statistically significant

nious linear mixed regression model, including both random and fixed effects for predicting cone density values on a natural logarithmic (LN) scale. As each image was assessed 12 times (2 modes, 3 observers, 2 trials) we needed to account for possible correlation between measurements. To do so, our model used three random effects: mode, observer and trial. In addition to the three random effects accounting for within image correlation, we investigated three fixed effects of mode, observer and trial, as well as the two-way interactions and the three-way interaction. Statistical significance was declared at 5%. We found that the three-way interaction between mode, observer and trial was not significant ($P=0.194$). The two-way interaction between mode and trial was also not significant ($P=0.479$). The interactions between observer and trial and between observer and mode were highly significant ($P<0.0001$).

The linear mixed model used to build Table 37.2 absorbed information from all 960 observations. The presence of significant interactions with the observer prevents easily explaining the content of Table 37.1. To simplify the explanation of the regression modeling we fitted separate models for each observer, allowing us to interpret findings separately for each observer. Table 37.2 reports the estimates of mean LN (cone density) separately for each observer. Observer 1 had a significantly different interaction between trial and mode ($P=0.006$), precluding investigation of further interactions for this observer. The interactions between mode and trial ($P=0.951$) and the main effect of trial ($P=0.447$) were not significant for observer 2. Only the effect of mode was significant for observer 2 ($P<0.0001$). The interac-

Table 37.2 Cone density measurements for each observer

–	Observer 1		Observer 2		Observer 3	
Mode (trial)	Estimate	Std. Err.	Estimate	Std. Err.	Estimate	Std. Err.
Confocal (1)	8.34	0.062	8.32	0.058	8.24	0.056
Confocal (2)	8.43	0.057	8.31	0.058	8.32	0.050
Split (1)	8.28	0.071	8.16	0.068	8.17	0.064
Split (2)	8.31	0.067	8.16	0.068	8.27	0.060

tion between mode and trial was not significant for observer 3 ($P=0.632$), nor was the main effect of mode ($P=0.160$). Surprisingly, we observed a strong effect of trial ($P<0.0001$).

This result indicates that the observers' counts differ for different trials and modes, such that one observer may have different responses between modes and another observer may show no difference. Likewise, one observer may have different responses between trials with another observer showing no difference.

37.3 Discussion

The results of the linear mixed regression model analysis demonstrated a strong effect of observer in cone counting in images from patients with ACHM using two different imaging modalities. This strong observer effect prevents further analysis of the reliability and repeatability of cone measurements in these retinas. Upon further analysis two of three observers showed a strong effect of trial (independent effect for one and interacting with mode for another), indicating that they were not able to consistently identify the same number of cells in the image set between two trials, with observer 1 showing an effect in the interaction between trial and mode. Observer 2, however, showed no effect of trial and the effect of mode indicates a difference between the confocal and split-detector measurements for this observer. Varying experience working with ACHM images (observer 2 had the most and observer 3 the least) may partially explain these results—thus analysis of diseased retinas may require a more experienced observer than analysis of cone structure in normal retinas. This result demonstrates the need for more experienced observers to analyze images of diseased retinas and development of automated methods for split-detector analysis.

Acknowledgements The work was supported by grants from the The Wellcome Trust [099173/Z/12/Z], National Institute for Health Research Biomedical Research Centre at Moorfields Eye Hospital National Health Service Foundation Trust and UCL Institute of Ophthalmology, NIH grants R01EY017607, R24EY022023, P30EY001931, C06RR016511, & UL1TR000055, Fight For Sight (UK), Moorfields Eye Hospital Special Trustees, the Foundation Fighting Blindness (USA), RP Fighting Blindness, an unrestricted departmental grant from Research to Prevent Blindness (RPB). Dr. Michaelides is supported by an FFB Career Development Award.

References

Baraas RC, Carroll J, Gunther KL et al (2007) Adaptive optics retinal imaging reveals S-cone dystrophy in tritan color-vision deficiency. J Opt Soc Am A 24:1438–1446

Chiu SJ, Lokhnygina Y, Dubis AM et al (2013) Automatic cone photoreceptor segmentation using graph theory and dynamic programming. Biomed Opt Express 4:924–937

Chui TYP, Song HX, Burns SA (2008) Individual variations in human cone photoreceptor packing density: variations with refractive error. Invest Ophthamol Vis Sci 49:4679–4687

Cooper RF, Langlo CS, Dubra A et al (2013) Automatic detection of modal spacing (Yellott's ring) in adaptive optics scanning light ophthalmoscope images. Ophthal Physl Opt 33:540–549

Dubra A, Harvey Z (2010) Registration of 2D Images from fast scanning ophthalmic instruments. In: The 4th International Workshop on Biomedical Image Registration Lübeck, Germany

Dubra A, Sulai Y, Norris JL et al (2011) Noninvasive imaging of the human rod photoreceptor mosaic using a confocal adaptive optics scanning ophthalmoscope. Biomed Opt Express 2:1864–1876

Duncan JL, Zhang Y, Gandhi J et al (2007) High-resolution imaging with adaptive optics in patients with inherited retinal degeneration. Invest Ophthamol Vis Sci 48:3283–3291

Garrioch R, Langlo C, Dubis AM et al (2012) Repeatability of *in vivo* parafoveal cone density and spacing measurements. Optom Vis Sci 89:632–643

Genead MA, Fishman GA, Rha J et al (2011) Photoreceptor structure and function in patients with congenital achromatopsia. Invest Ophthamol Vis Sci 52:7298–7308

Liu BS, Tarima S, Visotcky A et al (2014) The reliability of parafoveal cone density measurements. Br J Ophthalmol 98:1126–1131

Merino D, Duncan JL, Tiruveedhula P et al (2011) Observation of cone and rod photoreceptors in normal subjects and patients using a new generation adaptive optics scanning laser ophthalmoscope. Biomed Opt Express 2:2189–2201

Rossi EA, Roorda A (2010) The relationship between visual resolution and cone spacing in the human fovea. Nat Neurosci 13:156–157

Rossi EA, Chung M, Dubra A et al (2011) Imaging retinal mosaics in the living eye. Eye 25:301–308

Scoles D, Sulai YN, Langlo CS et al (2014) *In vivo* imaging of human cone photoreceptor inner segments. Invest Ophthamol Vis Sci 55:4244–4251

Chapter 38
Quantitative Fundus Autofluorescence in Best Vitelliform Macular Dystrophy: RPE Lipofuscin is not Increased in Non-Lesion Areas of Retina

Janet R. Sparrow, Tobias Duncker, Russell Woods and François C. Delori

Abstract Since the lipofuscin of retinal pigment epithelial (RPE) cells has been implicated in the pathogenesis of Best vitelliform macular dystrophy, we quantified fundus autofluorescence (quantitative fundus autofluorescence, qAF) as an indirect measure of RPE lipofuscin levels. Mean non-lesion qAF was found to be within normal limits for age. By spectral domain optical coherence tomography (SD-OCT) vitelliform lesions presented as fluid-filled subretinal detachments containing reflective material. We discuss photoreceptor outer segment debris as the source of the intense fluorescence of these lesions and loss of anion channel functioning as an explanation for the bullous photoreceptor-RPE detachment. Unexplained is the propensity of the disease for central retina.

Keywords Best vitelliform macular dystrophy · *BEST1* · Fundus autofluorescence · Quantitative autofluorescence · SD-OCT

J. R. Sparrow (✉) · T. Duncker
Department of Ophthalmology, Harkness Eye Institute,
Columbia University Medical Center, 635 W. 165th Street, New York, NY 10032, USA
e-mail: jrs88@cumc.columbia.edu

J. R. Sparrow
Department of Pathology and Cell Biology, Columbia University Medical Center,
635 W. 165th Street, New York, NY 10032, USA

T. Duncker
e-mail: tobias.duncker@gmail.com

R. Woods · F. C. Delori
Department of Ophthalmology, Harvard Medical School,
Schepens Eye Research Institute, Boston, MA 02114, USA
e-mail: russell_woods@meei.harvard.edu

F. C. Delori
e-mail: Francois_delori@meei.harvard.edu

C. Bowes Rickman et al. (eds.), *Retinal Degenerative Diseases,* Advances in Experimental Medicine and Biology 854, DOI 10.1007/978-3-319-17121-0_38

38.1 Introduction

The inherent fluorescence of retina originates primarily from the lipofuscin of retinal pigment epithelial (RPE) cells and is commonly imaged as fundus autofluorescence (AF) by confocal laser scanning ophthalmoscopy (cSLO). The lipofuscin fluorophores that have been described are vitamin A aldehyde adducts with excitation maxima from ~430–510 nm and peak emission of ~600 nm. Topographic patterns of fundus AF are well known to be altered in age-related macular degeneration, retinitis pigmentosa, acute macular disease, pattern dystrophies and Bull's eye maculopathy (von Ruckmann et al. 1997b; Robson et al. 2006; Boon et al. 2007; Kellner et al. 2009; Michaelides et al. 2010; Gelman et al. 2012). Fundus autofluorescence intensity is particularly elevated in recessive Stargardt disease (STGD1) (Delori et al. 1995a; Lois et al. 2004; Cideciyan et al. 2005). Emission spectra recorded at the fundus in healthy eyes and in patients with STGD1 and age-related macular degeneration all exhibit emission maxima at 580–620 nm (Delori et al. 1995b; Delori et al. 1995a).

38.2 Best Vitelliform Macular Dystrophy: Clinical Findings

Best vitelliform macular dystrophy (BVMD) is an autosomal dominant disease associated with mutations in *BEST1*, the gene encoding the bestrophin-1 protein located on the basolateral membrane and within intracellular compartments of RPE cells (Petrukhin et al. 1998; Marmorstein et al. 2000). Ophthalmoscopic features of BVMD typically present in juveniles, and overt disease is most often limited to the macula (Boon et al. 2009). Aberrant responses recorded by electrooculography (EOG) can be diagnostic (Deutman 1969). The onset of the disorder is usually characterized by a central oval lesion (vitelliform lesion) that exhibits intense fluorescence in fundus AF images (Spaide et al. 2006) (Fig. 38.1a) and that is visible as a dome shaped separation between photoreceptor cells and RPE in images acquired by spectral domain optical coherence tomography (SD-OCT) (Querques et al. 2008; Ferrara et al. 2010) (Fig. 38.1c).

38.3 RPE Lipofuscin and BVMD

There have been numerous reports indicating that RPE lipofuscin is increased in BVMD. Some of these human studies have been based on non-quantitative analysis (Frangieh et al. 1982; Weingeist et al. 1982) while others acquired measurements from electron micrographs (O'Gorman et al. 1988) or biochemical analysis (Bakall

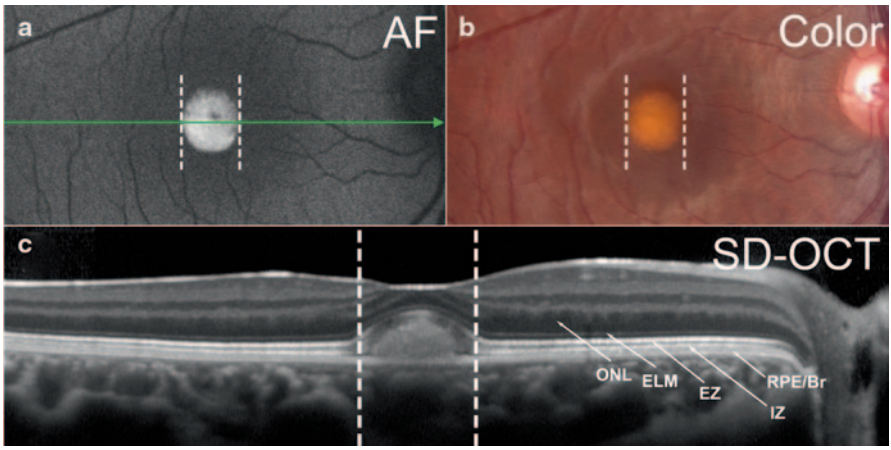

Fig. 38.1 Multimodal imaging of a BVMD patient (age 14 years) in the vitelliform stage. Fundus autofluorescence (**a**), color fundus photograph (**b**) and horizontal SD-OCT scan (**c**). Corresponding positions in **a**, **b** and **c** are shown as *dashed vertical lines*. The position and horizontal extent of the SD-OCT scan (**c**) is indicated by the *green arrow* in (**a**). **a**. By fundus autofluorescence the foveal lesion exhibits an increased signal. In the SD-OCT image, a *dome-shaped* foveal lesion that includes a hyperreflective component is revealed. The retina appears qualitatively normal outside the lesion. Reflectivity bands in outer retina are attributed to outer nuclear layer (*ONL*); external limiting membrane (*ELM*); ellipsoid region of inner segment (*EZ*); interdigitation zone (*IZ*) and RPE/Bruch's membrane complex (*RPE/Br*) (Staurenghi et al. 2014). The area of separation is between bands attributable to EZ and RPE/Br

et al. 2007). In some BVMD patients non-lesion posterior fundus exhibited AF levels within 2 standard deviations of age-matched controls while in most cases the entire fundus was reported to display abnormally intense AF (von Ruckmann et al. 1997a).

38.4 Quantitative Fundus Autofluorescence in Best Vitelliform Macular Dystrophy

Underlying disease processes in BVMD are poorly understood and a pathway leading to increased RPE lipofuscin formation is not obvious. Thus, we undertook a disciplined approach to measuring the intensity of fundus AF outside the lesion area. To this end, short-wavelength AF images (488 nm excitation) were acquired with a cSLO (Heidelberg Spectralis, HRA+OCT; Heidelberg Engineering, Heidelberg, Germany). To enable comparisons amongst patients, image grey levels (GLs) were normalized to the GLs in an internal fluorescent reference (Fig. 38.2b) installed in the instrument and the sensitivity used was within the linear range of the detector ($GL < 175$). Additional protocol details are described in Fig. 38.2 and in published work (Delori et al. 2011).

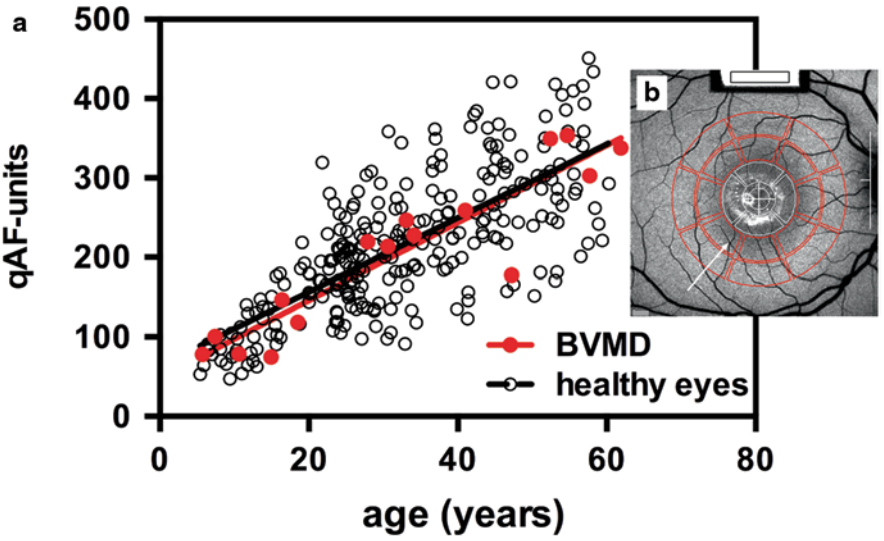

Fig. 38.2 Quantitative fundus autofluorescence (qAF)**.** qAF was calculated from images (488 nm excitation) obtained from 27 eyes of 16 BVMD patients (*red circles*) and 277 healthy subjects reported previously (Greenberg et al. 2013) (*black circles*) and plotted as function of age (**a**). qAF was measured in pre-determined circularly arranged segments (*red*; 8 segments/ring). (**b**) Mean non-lesion qAF plotted (**a**) are based on values obtained from outer ring (**b**). Mean non-lesion qAF (*solid black line* in **a**) of healthy subjects is also shown. The segments were scaled to the distance between the temporal edge of the optic disc (*white vertical line*) and the center of the fovea (*white cross*) (**b**). Details of image acquisition and analysis are published (Delori et al. 2011)

As shown in Fig. 38.2a, qAF increased with age in both healthy eyes and in non-lesion areas of BVMD retina. Importantly, in all BVMD eyes, qAF values outside the lesion were within normal limits for age. qAF values within the lesion were elevated and the emission spectra were consistent with that of lipofuscin (Duncker et al. 2014).

38.5 What Have We Learned?

By applying the qAF approach to BVMD patients, we found that in fundus areas outside the central lesion, RPE lipofuscin levels are not increased. Thus a generalized increase in RPE lipofuscin is unlikely to contribute to the pathogenesis of BVMD. Except for the area of the lesion and an adjacent transition zone, retinal lamina appeared normal in SD-OCT scans.

The precise role of the BEST1 protein has been difficult to elucidate. Multiple anion channel functions have been attributed to BEST1 including an outward calcium-dependent chloride conductance and bicarbonate efflux (Sun et al. 2002; Rosenthal et al. 2006; Qu and Hartzell 2008; Marmorstein et al. 2009). Due to

osmotic forces, the outward flux of chloride and bicarbonate across the basolateral membrane of RPE is followed by fluid transport. Mutations in *BEST1* leading to the loss of anion channel activity and insufficient fluid transport could be the cause of the fluid-filled detachment between photoreceptor cells and RPE that is detected by SD-OCT. Reduced fluid flux is a feature of an induced pluripotent stem cell model of BVMD (Singh et al. 2013). Since RPE lipofuscin is well known to originate from photoreceptor outer segments (Sparrow et al. 2012), the intensely autofluorescent reflective material in the vitelliform lesion likely originates from accumulating outer segment debris within the lesion. Otherwise, increased RPE lipofuscin is unlikely to be a feature of the primary disease process.

Acknowledgements Supported by National Eye Institute EY024091 and a grant from Research to Prevent Blindness to the Department of Ophthalmology, Columbia University.

References

Bakall B, Radu RA, Stanton JB et al (2007) Enhanced accumulation of A2E in individuals homozygous or heterozygous for mutations in BEST1 (VMD2). Exp Eye Res 85:34–43

Boon CJ, van Schooneveld MJ, den Hollander AI et al (2007) Mutations in the peripherin/RDS gene are an important cause of multifocal pattern dystrophy simulating STGD1/fundus flavimaculatus. Br J Ophthalmol 91:1504–1511

Boon CJ, Klevering BJ, Leroy BP et al (2009) The spectrum of ocular phenotypes caused by mutations in the BEST1 gene. Prog Retin Eye Res 28:187–205

Cideciyan AV, Swider M, Aleman TS et al (2005) ABCA4-associated retinal degenerations spare structure and function of the human parapapillary retina. Invest Ophthalmol Vis Sci 46:4739–4746

Delori FC, Staurenghi G, Arend O et al (1995a) *In vivo* measurement of lipofuscin in Stargardt's disease—fundus flavimaculatus. Invest Ophthalmol Vis Sci 36:2327–2331

Delori FC, Dorey CK, Staurenghi G et al (1995b) *In vivo* fluorescence of the ocular fundus exhibits retinal pigment epithelium lipofuscin characteristics. Invest Ophthalmol Vis Sci 36:718–729

Delori F, Greenberg JP, Woods RL et al (2011) Quantitative measurements of autofluorescence with the scanning laser ophthalmoscope. Invest Ophthalmol Vis Sci 52:9379–9390

Deutman AF (1969) Electro-oculography in families with vitelliform dystrophy of the fovea. Detection of the carrier state. Arch Ophthalmol 81:305–316

Duncker T, Greenberg JP, Ramachandran R et al (2014) Quantitative fundus autofluorescence and optical coherence tomography in best vitelliform macular dystrophy. Invest Ophthalmol Vis Sci 55:1471–1482

Ferrara DC, Costa RA, Tsang SH et al (2010) Multimodal fundus imaging in best vitelliform macular dystrophy. Graefes Arch Clin Exp Ophthalmol 248:1377–1386

Frangieh GT, Green R, Fine SL (1982) A histopatholgic study of best's macular dystrophy. Arch Ophthalmol 100:1115–1121

Gelman R, Chen R, Blonska A et al (2012) Fundus autofluorescence imaging in a patient with rapidly developing scotoma. Retinal Cases Brief Reports 6:345–348

Greenberg JP, Duncker T, Woods RL et al (2013) Quantitative fundus autofluorescence in healthy eyes. Invest Ophthalmol Vis Sci 54:6820–6826

Kellner U, Kellner S, Weber BH et al (2009) Lipofuscin- and melanin-related fundus autofluorescence visualize different retinal pigment epithelial alterations in patients with retinitis pigmentosa. Eye (Lond) 23:1349–1359

Lois N, Halfyard AS, Bird AC et al (2004) Fundus autofluorescence in stargardt macular dystrophy-fundus flavimaculatus. Am J Ophthalmol 138:55–63

Marmorstein AD, Marmorstein LY, Rayborn M et al (2000) Bestrophin, the product of the best vitelliform macular dystrophy gene (VMD2), localizes to the basolateral plasma membrane of the retinal pigment epithelium. Proc Natl Acad Sci U S A 97:12758–12763

Marmorstein A, Cross HE, Peachey NS (2009) Functional roles of bestrophins in ocular epithelia. Prog Retin Eye Res 28:206–226

Michaelides M, Gaillard MC, Escher P et al (2010) The PROM1 mutation p.R373C causes an autosomal dominant bull's eye maculopathy associated with rod, rod-cone, and macular dystrophy. Invest Ophthalmol Vis Sci 51:4771–4780

O'Gorman S, Flaherty WA, Fishman GA et al (1988) Histopathological findings in best's vitelliform macular dystrophy. Arch Ophthalmol 106:1261–1268

Petrukhin K, Koisti MJ, Bakall B et al (1998) Identification of the gene responsible for best macular dystrophy. Nat Genet 19:241–247

Qu Z, Hartzell HC (2008) Bestrophin Cl- channels are highly permeable to HCO3-. Am J Physiol Cell Physiol 294:C1371–C1377

Querques G, Regenbogen M, Quijano C et al (2008) High-definition optical coherence tomography features in vitelliform macular dystrophy. Am J Ophthalmol 146:501–507

Robson AG, Saihan Z, Jenkins SA et al (2006) Functional characterisation and serial imaging of abnormal fundus autofluorescence in patients with retinitis pigmentosa and normal visual acuity. Br J Ophthalmol 90:472–479

Rosenthal R, Bakall B, Kinnick T et al (2006) Expression of bestrophin-1, the product of the VMD2 gene, modulates voltage-dependent Ca2+ channels in retinal pigment epithelial cells. FASEB J 20:178–180

von Ruckmann A, Fitzke FW, Bird AC (1997a) *In vivo* fundus autofluorescence in macular dystrophies. Arch Ophthalmol 115:609–615

von Ruckmann A, Fitzke FW, Bird AC (1997b) Fundus autofluorescence in age-related macular disease imaged with a laser scanning ophthalmoscope. Invest Ophthalmol Vis Sci 38:478–486

Singh R, Shen W, Kuai D et al (2013) iPS cell modeling of best disease: insights into the pathophysiology of an inherited macular degeneration. Hum Mol Genet 22:593–607

Spaide RF, Noble K, Morgan A et al (2006) Vitelliform macular dystrophy. Ophthalmol 113:1392–1400

Sparrow JR, Gregory-Roberts E, Yamamoto K et al (2012) The bisretinoids of retinal pigment epithelium. Prog Retin Eye Res 31:121–135

Staurenghi G, Sadda S, Chakravarthy U et al (2014) Proposed lexicon for atomic landmarks in normal posterior segment spectral-domain optical coherence tomography: the IN*OCT consensus. Ophthalmology 121:1572–1578

Sun H, Tsunenari T, Yau KW et al (2002) The vitelliform macular dystrophy protein defines a new family of chloride channels. Proc Natl Acad Sci U S A 99:4008–4013

Weingeist TA, Kobrin JL, Watzke RC (1982) Histopathology of best's macular dystrophy. Arch Ophthalmol 100:1108–1114

Chapter 39
Interpretation of Flood-Illuminated Adaptive Optics Images in Subjects with *Retinitis Pigmentosa*

Michael J. Gale, Shu Feng, Hope E. Titus, Travis B. Smith and Mark E. Pennesi

Abstract The purpose of this study was to correlate features on flood-illuminated adaptive optics (AO) images with color fundus, fundus autofluorescence (FAF) and spectral domain optical coherence tomography (SD-OCT) images in patients with retinitis pigmentosa (RP). We imaged 39 subjects diagnosed with RP using the rtx1™ flood-illuminated AO camera from Imagine Eyes (Orsay, France). We observed a correlation between hyper-autofluoresence changes on FAF, disruption of the interdigitation zone (IZ) on SD-OCT and loss of reflective cone profiles on AO. Four main patterns of cone-reflectivity were seen on AO: presumed healthy cone mosaics, hypo-reflective blurred cone-like structures, higher frequency disorganized hyper-reflective spots, and lower frequency hypo-reflective spots. These regions were correlated to progressive phases of cone photoreceptor degeneration observed using SD-OCT and FAF. These results help provide interpretation of en face images obtained by flood-illuminated AO in subjects with RP. However, significant ambiguity remains as to what truly constitutes a cone, especially in areas of degeneration. With further refinements in technology, flood illuminated AO imaging has the potential to provide rapid, standardized, longitudinal and lower cost imaging in patients with retinal degeneration.

M. E. Pennesi (✉) · M. J. Gale · S. Feng · H. E. Titus · T. B. Smith
Department of Ophthalmology, Casey Eye Institute, Oregon Health & Science University, Portland, OR 97239, USA
e-mail: pennesim@ohsu.edu

M. J. Gale
e-mail: galem@ohsu.edu

S. Feng
e-mail: feng@ohsu.edu

H. E. Titus
e-mail: hopeetitus@gmail.com

T. B. Smith
e-mail: smittrav@ohsu.edu

C. Bowes Rickman et al. (eds.), *Retinal Degenerative Diseases,* Advances in Experimental Medicine and Biology 854, DOI 10.1007/978-3-319-17121-0_39

Keywords Flood · Illuminated adaptive optics · Retinal degeneration · Retinitis pigmentosa · Cone photoreceptors · Multimodal imaging

39.1 Introduction

Adaptive optics (AO) imaging technology has revolutionized our understanding of structural changes in retinal disease(Choi et al. 2006; Duncan et al. 2007; Carroll et al. 2008; Gocho et al. 2013; Tojo et al. 2013a; Tojo et al. 2013b). AO scanning laser ophthalmoscopy (AOSLO) provides high-resolution images sufficient to resolve single cone and rod photoreceptors. Although commercially available flood-illuminated AO cameras do not achieve the same resolution as custom built AOSLO systems, they are less expensive, easier to maintain and operate, and offer standardization from site to site, making them potentially useful in the clinical setting or as part of multi-center trials. The rtx1™ flood-illuminated AO camera has been used previously to study both healthy subjects(Lombardo et al. 2012) and those with retinal disease(Gocho et al. 2013; Tojo et al. 2013a; Tojo et al. 2013b). Although cone-like structures are easily identifiable in healthy regions of the macula, it is often difficult to distinguish a cone from debris in areas of retinal atrophy. We observed common patterns in RP patients including: normal cone mosaics, hypo-reflective blurred cone-like structures, higher frequency disorganized hyper-reflective spots, and lower frequency hypo-reflective spots. In order to elucidate what these different regions represented on a microstructural level, we compared and correlated the AO images to registered color fundus, fundus autofluorescence (FAF) and spectral domain optical coherence tomography (SD-OCT) images.

39.2 Materials and Methods

This research adhered to the tenets of the Declaration of Helsinki and was approved by the OHSU IRB. We used the rtx1™ flood-illuminated adaptive optics camera to image 39 subjects with RP ranging in age from 17 to 77 years old. For each subject, a series of 4° × 4° retinal images with 50% overlap between adjacent images was obtained in one or both eyes. Using i2k Retina (DualAlign LLC, Clifton Park, NY, USA), these images were combined to create a retinal montage spanning a 12° × 12° field of the central macula. Cone counting was performed automatically by applying background subtraction and thresholding of local maxima in Matlab (MathWorks, Natick, MA, USA). The central fovea was excluded from cone counting due to the camera's inability to resolve cones in this region. Retinal magnification factors for each eye were calculated with the model of the eye developed by Bennett et al.(Bennett et al. 1994) from the axial length as measured by an IOLMaster 500 (Carl Zeiss Meditec AG, Jena, Germany). The imaging success rate was also calculated; if the 9 central tiles and at least 20 of the 25 total images could be used to

form a montage, then the imaging session was considered successful. Montaged AO images and Voronoi cone density plots were compared to registered areas from other imaging modalities including color fundus, FAF (Optos 200 Tx ultra-widefield camera, Scotland, UK) and SD-OCT (Spectralis HRA-OCT, Heidelberg Engineering, Germany).

39.3 Results

39.3.1 AO Imaging Success Rate and Trends

To determine the ability to image a spectrum of RP patients, we acquired images in both mild and severe cases and only initially excluded patients if visually acuity was less than 20/200. From these patients with RP and based on our imaging success parameters, 45 out of 60 eyes (75%) were successfully imaged. The majority of eyes in which we could not obtain high-quality images had at least one of the following issues: cataracts, corneal scarring, cloudy optical media, nystagmus, poor central vision or a severely degenerated outer retina. Imaging success rates also tended to decrease with age, with the ability to obtain useful AO images particularly difficult in patients over 60 years old.

39.3.2 Correlating FAF and SD-OCT to AO Images

In the subjects with RP that we imaged, a relationship was often seen between hyper-autofluorescent regions on FAF, disruption or loss of the IZ or ellipsoid zone (EZ) on SD-OCT and blurred or hypo-reflective cone-like structures on AO. For example, FAF imaging in the left eye of subject 1 showed a hyper-autofluorescent ring in the central macula with the inferior nasal portion of the border located nearest to the fovea (Fig. 39.1a). Near the border of this ring and peripheral to it, AO density plots revealed a decreased number of cone-like profiles (Fig. 39.1b and c), while SD-OCT demonstrated disruption of the IZ and loss of the EZ (Fig. 39.1d and e). Within the hyper-autofluorescent ring, a healthy cone photoreceptor mosaic was observed (Fig. 39.1g) while blurred cones and non-uniform hyper-reflective spots were seen in the hyper-autofluorescent area or outside of the ring (Fig. 39.1f).

39.3.3 Stages of Cone Degeneration on AO Imaging

Four distinct types of AO images were observed and correlated to progressive phases of cone photoreceptor degeneration noted by SD-OCT and FAF. The right eye of subject 2 showed peripheral retinal atrophy (Fig. 39.2a) and concentric advancing

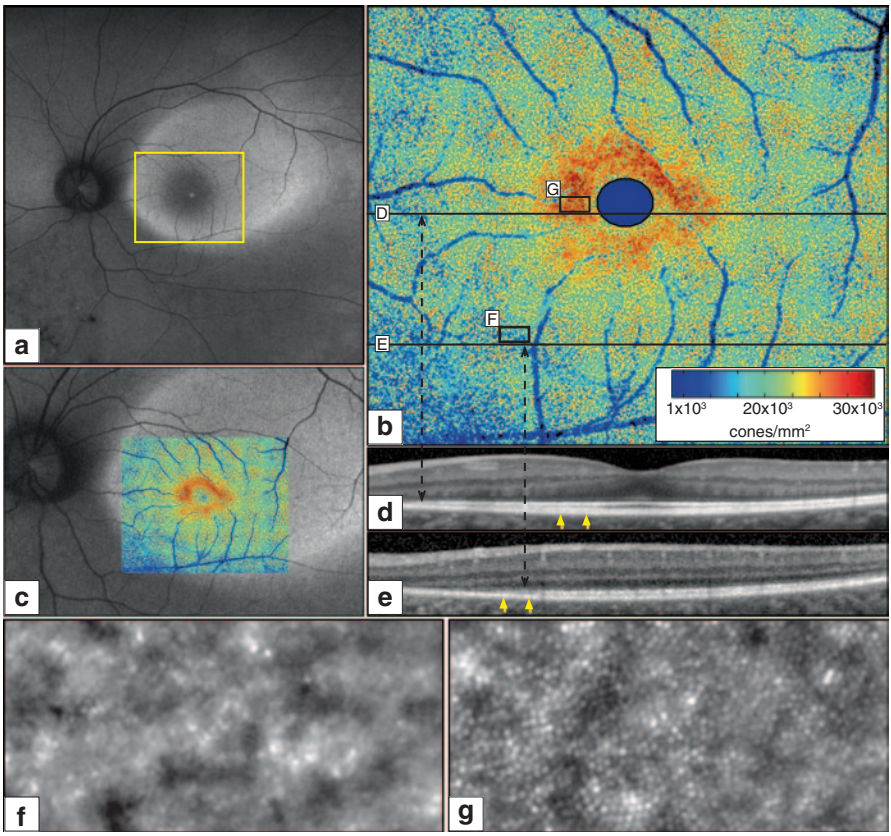

Fig. 39.1 Multiple imaging modalities showing the OS macula of subject 1. **a** FAF image (*yellow box* indicates region of AO imaging), **b** Voronoi cone density plot with SD-OCT line scan locations (**d, e**), indicated by *solid black lines*, and magnified AO image areas (**f, g**), indicated by *black rectangles*, **c** Voronoi cone density plot registered on the FAF image. *Yellow arrowheads* on **d** and **e** indicate the magnified AO image locations. *Dashed black lines* show the correlation between cone density change and alteration of outer retinal structure on SD-OCT

stages of cone degeneration (Fig. 39.2b). A normal mosaic of presumptive cones was seen just outside of the fovea (Fig. 39.2d) and SD-OCT revealed an intact outer retina, especially on the temporal side of the fovea where both the IZ and EZ could be visualized (Fig. 39.2h). At a slightly wider eccentricity, hypo-reflective blurred cones were noted (Fig. 39.2e) and loss of the EZ with a thinned outer nuclear layer were seen on SD-OCT (Fig. 39.2h). The next concentric area revealed a mixture of hypo and hyper-reflective spots that were more irregularly spaced than a typical cone mosaic (Fig. 39.2f) and further loss of the outer nuclear layer (ONL) was observed on SD-OCT (Fig. 39.2h). The perifovea showed sparse hypo-reflective spots with no discernable cones (Fig. 39.2g) while SD-OCT demonstrated complete loss of the ONL (Fig. 39.2h).

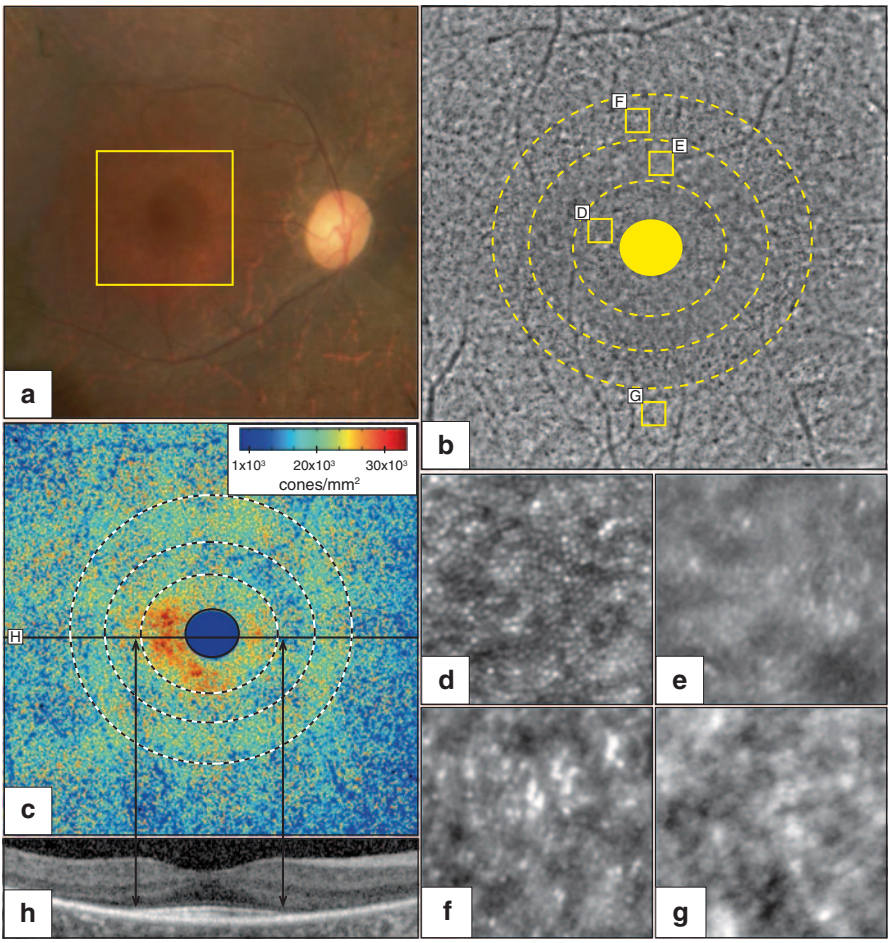

Fig. 39.2 Multiple imaging modalities showing the OD macula of subject 2 **a** Color fundus image (*yellow box* indicates region of AO imaging), **b** AO montage. *Dashed yellow lines* demarcate concentric stages of cone degeneration and *yellow boxes* indicate the location of magnified AO image areas (**d** healthy cones, **e** stressed cones, **f** photoreceptor cellular debris, **g** RPE pigmentation), **c** Voronoi cone density plot with the SD-OCT line scan location **h** indicated by a *horizontal black line*. *Vertical black lines* show the correlation between cone density change and alteration of outer retinal structure on SD-OCT

39.4 Discussion

Due to the fact that imaging success and image quality in subjects with RP was influenced by factors other than outer retinal structure, caution must be used when interpreting flood-illuminated AO images. Interpretation was made difficult by the fact that what appeared to be highly reflective cone-like structures were frequently dispersed throughout areas of poorly reflective dying cone-like structures. It is very

important to correlate the AO images with other imaging modalities in order to acquire a complete understanding of the structural state of the retina. Pockets of edema, cloudy media, nystagmus and poor central vision are all issues that detracted from image quality.

Even though imaging patients with RP was difficult due to the previously mentioned factors, in many cases we managed to obtain high quality images. A correlation was observed between hyper-autofluorescence on FAF, IZ disruption on SD-OCT and hypo-reflective blurred cone-like structures on AO. A previous study demonstrated an association between hyper-autofluorescence and blurred cones on flood-illuminated AO in patients with retinal degeneration (Tojo et al. 2013a). We observed the same correlation between AO and FAF, as well as noting the beginning of IZ disruption on SD-OCT in these same regions. These findings suggest that cones found in the hyper-autofluorescent regions on FAF are still potentially structurally viable and could be rescued by future therapeutic treatments.

We also noted four distinct types of AO imaging patterns and correlated them to various stages of cone photoreceptor degeneration using SD-OCT and FAF. These four general types of AO images were healthy cones (Fig. 39.2d), a blurred area that we believe might be stressed or dying cones (Fig. 39.2e), photoreceptor and cellular debris (Fig. 39.2f) and RPE cell patterning and pigmentation (Fig. 39.2g). Other studies have shown that AOSLO images can be correlated to other imaging modalities and tests of visual function to elucidate cone structure in patients with retinal disease (Choi et al. 2006; Duncan et al. 2007; Carroll et al. 2008). Our findings agree with these studies and illustrate that when compared with other imaging techniques, flood-illuminated AO can also be used to obtain detailed information about outer retinal structure.

In summary, we have found SD-OCT and autofluorescence to be the most useful clinical imaging techniques for comparison with AO. SD-OCT is particularly helpful because it allows for the precise visualization of outer retinal layers. When correlated with AO images, SD-OCT allows us to be more confident that identified cones are actually cones rather than just cellular debris or RPE cells. While it is possible to acquire images from a wide variety of subjects, AO is most successful when imaging subjects with good central vision and at least partial photoreceptor preservation, such as individuals with RP. AO also appears to be most useful in cases of subtle or subclinical photoreceptor changes that are difficult to track on traditional fundus or OCT imaging modalities. Even minor changes in outer retinal structure can make it difficult to successfully visualize cones, which can provide highly sensitive information about photoreceptor health. Due to all of these factors, AO imaging could become an invaluable tool in tracking the longitudinal progression of a variety of photoreceptor-related diseases.

Acknowledgements This study was supported by grants from Research to Prevent Blindness (Unrestricted, CEI and CDA, MEP), the Foundation Fighting Blindness (CD-CL-0808-0469-OHSU, MEP), an NIH/NEI grant (K08EY02118601, MEP) and Fight for Sight Summer Student Fellowships (Gale and Titus).

References

Bennett AG, Rudnicka AR, Edgar DF (1994) Improvements on Littmann's method of determining the size of retinal features by fundus photography. Graefes Arch Clin Exp Ophthalmol 232:361–367

Carroll J, Choi SS, Williams DR (2008) *In vivo* imaging of the photoreceptor mosaic of a rod monochromat. Vision Res 48:2564–2568

Choi SS, Doble N, Hardy JL et al (2006) *In vivo* imaging of the photoreceptor mosaic in retinal dystrophies and correlations with visual function. Invest Ophthalmol Vis Sci 47:2080–2092

Duncan JL, Zhang Y, Gandhi J et al (2007) High-resolution imaging with adaptive optics in patients with inherited retinal degeneration. Invest Ophthalmol Vis Sci 48:3283–3291

Gocho K, Sarda V, Falah S et al (2013) Adaptive optics imaging of geographic atrophy. Invest Ophthalmol Vis Sci 54:3673–3680

Lombardo M, Serrao S, Ducoli P et al (2012) Variations in image optical quality of the eye and the sampling limit of resolution of the cone mosaic with axial length in young adults. J Cataract Refract Surg 38:1147–1155

Tojo N, Nakamura T, Fuchizawa C et al (2013a) Adaptive optics fundus images of cone photoreceptors in the macula of patients with retinitis pigmentosa. Clin Ophthalmol 7:203–210

Tojo N, Nakamura T, Ozaki H et al (2013b) Analysis of macular cone photoreceptors in a case of occult macular dystrophy. Clin Ophthalmol 7:859–864

Chapter 40
Intra-familial Similarity of Wide-Field Fundus Autofluorescence in Inherited Retinal Dystrophy

Yuka Furutani, Ken Ogino, Akio Oishi, Norimoto Gotoh, Yukiko Makiyama, Maho Oishi, Masafumi Kurimoto and Nagahisa Yoshimura

Abstract To examine the similarity of wide-field fundus autofluorescence (FAF) imaging in inherited retinal dystrophy between siblings and between parents and their children. The subjects included 17 siblings (12 with retinitis pigmentosa and 5 with cone rod dystrophy) and 10 parent-child pairs (8 with retinitis pigmentosa and 2 with cone rod dystrophy). We quantified the similarity of wide-field FAF using image processing techniques of cropping, binarization, superimposition, and subtraction. The estimated similarity of the siblings was compared with that of the parent-child pairs and that of the age-matched unrelated patients. The similarity between siblings was significantly higher that of parent-child pairs or that of age-matched unrelated patients ($P=0.004$ and $P=0.049$, respectively). Wide-field FAF images were similar between siblings with inherited retinal dystrophy but different

K. Ogino (✉) · Y. Furutani · A. Oishi · N. Gotoh · Y. Makiyama · M. Oishi · N. Yoshimura
Department of Ophthalmology and Visual Sciences, Kyoto University Graduate School of Medicine, 54 Shogoin-Kawaharacho, Sakyo, Kyoto 606-8507, Japan
e-mail: kenboo@kuhp.kyoto-u.ac.jp

M. Kurimoto
Department of Ophthalmology, Kyoto Katsura Hospital, Kyoto, Japan
e-mail: mkurimoto@dream.com

Y. Furutani
e-mail: yukaf@kuhp.kyoto-u.ac.jp

A. Oishi
e-mail: aquio@kuhp.kyoto-u.ac.jp

N. Gotoh
e-mail: eyegotoh@kuhp.kyoto-u.ac.jp

Y. Makiyama
e-mail: yukimaki@kuhp.kyoto-u.ac.jp

M. Oishi
e-mail: mah0ham@kuhp.kyoto-u.ac.jp

N. Yoshimura
e-mail: nagaeye@kuhp.kyoto-u.ac.jp

C. Bowes Rickman et al. (eds.), *Retinal Degenerative Diseases,* Advances in Experimental Medicine and Biology 854, DOI 10.1007/978-3-319-17121-0_40

between parent-child pairs. This suggests that aging is a confounding factor in genotype-phenotype correlation studies.

Keywords Cone rod dystrophy · Inherited retinal dystrophy · Retinitis pigmentosa · Similarity · Wide-field fundus autofluorescence

40.1 Introduction

Fundus autofluorescence (FAF) has enabled the evaluation of photoreceptor cells and retinal pigment epithelium (RPE) status. Increased FAF is thought to occur because of abnormal accumulations of lipofuscin or other fluorophores, whereas reduced FAF seems to result from the presence of retinal pigment epithelium atrophy or fibrotic tissue. In retinitis pigmentosa (RP) patients, a hypo-FAF area that corresponds to outer retinal atrophy and a hyper-FAF area in the surviving peripheral retina have been reported (von Ruckmann et al. 1999; Meyerle et al. 2006). We used a recently developed wide-field scanning laser ophthalmoscope that allows non-mydriatic FAF imaging of the fundus of up to 200° and showed the usefulness of wide-field FAF related to visual function in RP (Oishi et al. 2013).

Theoretically, affected siblings or affected parents and their children with inherited retinal dystrophy (IRD) have common causative mutations and an intra-familial comparison of phenotypes minimizes genetic and environmental background differences. Thus, intra-familial comparison of phenotype helps our understanding of the disease with a mutation.

In the present study, we evaluated the intra-familial similarity of wide-field FAF in patients with RP and con-rod dystrophy (CRD), particularly between siblings, to determine the genetic and environmental impacts on clinical phenotype.

40.2 Material and Methods

All procedures conformed to the tenets of the Declaration of Helsinki. Approval from the Institutional Review Board (IRB)/Ethics Committee of the Kyoto University Graduate School of Medicine was obtained.

40.2.1 Inclusion of Patients

We reviewed the clinical records of 545 consecutive patients with retinal dystrophy who underwent wide-field FAF imaging from March 2012 through August 2013 in a retinal dystrophy clinic at Kyoto University Hospital. There were 17 siblings and 10 parent-child pairs with RP or CRD among the 545 patients. The siblings were

from 12 families with typical RP and 5 families with CRD. The parent-child pairs were from 8 families with typical RP and 2 families with CRD. Additionally, we recruited 2 unrelated controls from the 545 patients for each sibling. The 2 controls were selected as phenotype-matched (with RP or CRD) and had the nearest and the second nearest birthday to the elder individual of the sibling pairs in the cohort. A clinical diagnosis of typical RP and CRD were based on detailed hearing of history and comprehensive ophthalmic examinations including fundus scope, electroretinography, and perimetry. Genotype screening was performed previously based on arrayed primer extension (Asper Biotech, Tartu, Estonia), (Ogino et al. 2013) Sanger sequencing and next generation sequencing of candidate genes.

40.2.2 Quantification of Similarity

Wide-field FAF images were obtained with an Optos 200 Tx imaging system (Optos PLC, Dunefermline, United Kingdom) as previously reported (Oishi et al. 2013). Left eye images were selected for the analysis, except in cases in which image quality was poor.

First, as described previously (Oishi et al. 2013), we cropped an elliptically shaped area of 3000 × 2100 pixels centered on the fovea from the original 3900 × 3072 pixel image by using ImageJ 1.46r (National Institutes of Health, Bethesda, MD) (Fig. 40.1a and b). This cropping removed the peripheral area containing greater errors resulting from the use of an ellipsoidal mirror and the creation of a planar image from a spherical globe, cilia, and eyelid. Second, the cropped image was converted to a binary image by thresholding on a value from the optic disc area, which was automatically calculated using a histogram tool after manually delineating the optic disc area with a polygonal selection tool (Fig. 40.1c). The purpose of binarization was to quantitatively estimate the similarity of the images. The grey value of the optic disc area was adopted to adjust the background values of the 2 different FAF images. Third, 2 cropped binary images were superimposed using Photoshop CS5.1 (Adobe Systems Inc. San Jose, CA) and a new image was created using a subtraction tool in which black and white pixels represented equivalent and differing values between the 2 images, respectively (Fig. 40.1d). We defined the number of black pixels as the similarity of 2 wide-field FAF images in this study.

40.2.3 Statistical Analysis

The statistical program SPSS version 20 (IBM Japan, Tokyo, Japan) was used for the analysis. The descriptive analyses are reported as the mean ± standard deviation, unless otherwise specified. The averaged similarity of the 17 siblings was compared to that of the 10 parent-child pairs using an unpaired *t*-test and to that between the elder sibling and 1 of the 2 age-matched controls whose birthday was closer to the subject's by using a paired *t*-test. *P*-values less than 0.05 were considered statistically significant.

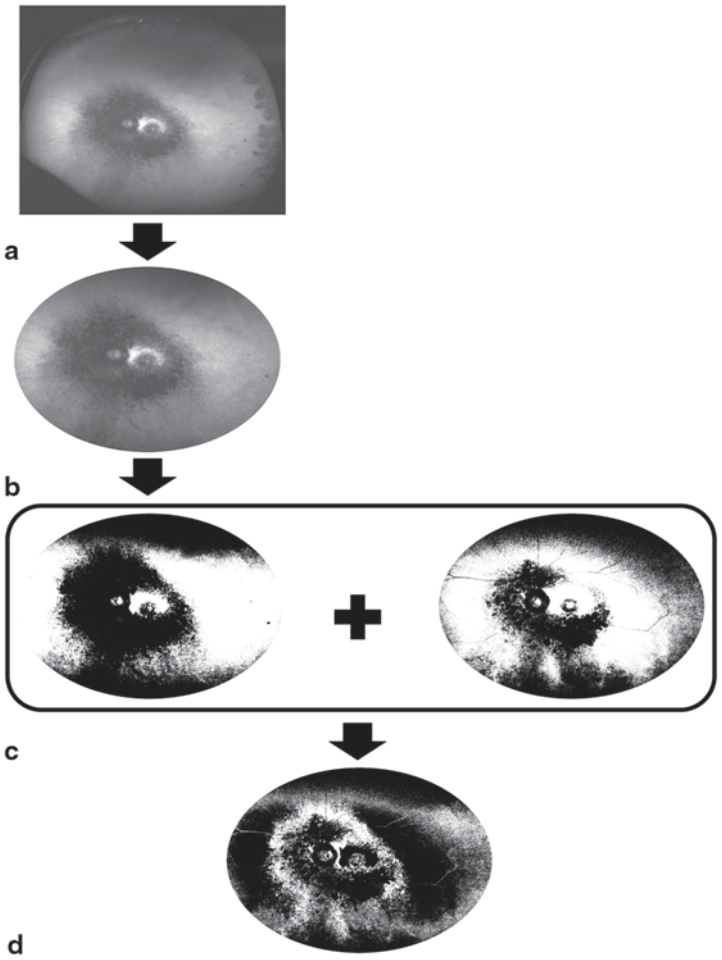

Fig. 40.1 Image processing for similarity quantification. Original image (**a**) cropped image with an elliptically shaped area of 3000 × 2100 pixels (**b**) and a binary image thresholded on the value of the optic disc area (**c**)**.** Two cropped binary images were superimposed, and a new image was created using a subtraction tool, in which the *black* and *white* pixels represent similar and differing values, respectively, in the 2 images

40.3 Results

The characteristics of the families are shown in the figure caption (Figs. 40.2 and 40.3). The mean difference in age between the siblings was 4.4 ± 2.3 years. The difference among the parent-child pairs was 29.6 ± 5.0 years. These values were significantly different ($P = 0.000016$).

The similarity between the siblings was 3,716,285 ± 743,807 pixels (range, 2,039,191–4,898,368 pixels). The similarity between unrelated patients was 3,109,154 ± 823,150 pixels (range, 1,815,265–4,313,255 pixels). The similarity

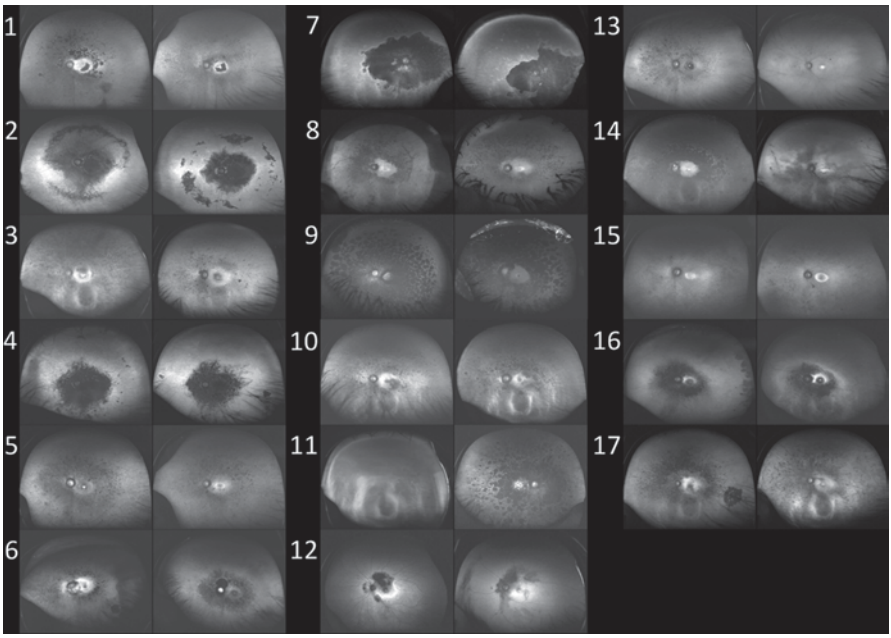

Fig. 40.2 Wide-field fundus autofluorescence findings of siblings with inherited retinal dystrophy. *Left* and *right* rows show images of older and younger individuals, respectively. The Arabic numeral indicates each family. Family *1*: RP with PRCD mutation (p.M1T/p.M1T). Family *2*: AR-CRD. Family *3*: AR-RP. Family *4*: CRD with ABCA4 mutation (p.Y865fs/c.1760+2T>G). Family *5*: AD-RP. Family *6*: RP with EYS mutation (p.S1653Kfs/deletion of exon 33). Family *7*: AD-CRD. Family *8*: RP with EYS mutation (p.S1653Kfs/p.S1653Kfs). Family *9*: AR-RP. Family *10*: RP with EYS mutation (p.S1653Kfs/p.Y2935X). Family *11*: AR-RP. Family *12*: AR-CRD. Family *13*: RP with MERTK mutation (p.T75fs/p.Q124X). Family *14*: RP with RPGR mutation (p.A308P). Family *15*: RP with RHO mutation (p.R135W). Family *16*: AD-CRD. Family *17*: RP with EYS mutation (p.1734_1735del/p.E2794fs). *AD*: autosomal dominant, *AR*: autosomal recessive, *RP*: retinitis pigmentosa, and *CRD*: cone-rod dystrophy

between parent-child pairs was 2,582,853 ± 1,124,619 pixels (range, 1,017,018–3,993,698 pixels). The original wide-field FAF images of the siblings and the parent-child pairs used for estimation are shown in Figs. 40.2 and 40.3, respectively. The similarity of the siblings with IRD was higher than that of unrelated patients and that of parent-child pairs ($P = 0.049$ and $P = 0.004$, respectively).

40.4 Discussion

In the present study, we investigated the similarity of wide-field FAF images of IRD within families using image processing. The estimated similarity measure we defined showed significantly higher intra-sibling values than those for parent-child pairs or between unrelated patients.

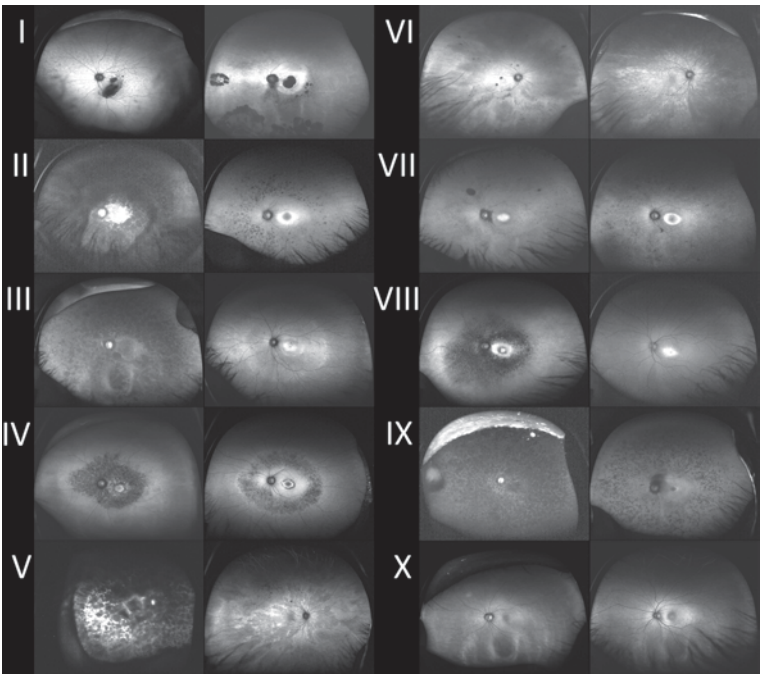

Fig. 40.3 Wide-field fundus autofluorescence findings of parent-child pairs with inherited retinal dystrophy. *Left* and *right* rows show images obtained from parents and children, respectively. A Roman numeral indicates each family. Family *I*: RP with PRPH2 mutation (p.G167S). Family *II*: AD-RP. Family *III*: AD-RP. Family *IV*: AD-RP. Family *V*: AD-RP. Family *VI*: RPGR mutation (p.A308P). Family *VII*: RP with RHO mutation (p.R135W). Family *VIII*: AD-CRD. Family *IX*: RP with RHO mutation (p.Y60X). Family *X*; AD-CRD. *AD* autosomal dominant, *AR* autosomal recessive, *RP* retinitis pigmentosa, and *CRD* cone-rod dystrophy

Hypo-FAF areas in RP where the RPE and photoreceptors were severely damaged showed a loss of retinal sensitivity on Goldmann perimetry and were clinically meaningful (Oishi et al. 2013). Therefore, to reduce dimensionality and to detect hypo-FAF areas, we simply attempted a binarization of wide-field FAF images and used the reflectivity of the optic disc area as a threshold, which seemed to be relatively appropriate for adjusting the background FAF of each image. We considered that the number of black pixels in the final images after the superimposition and subtraction of the 2 binary images represented some Euclidian distance between the 2 wide-field FAF images.

As we expected, the similarity between siblings was significantly higher than that of unrelated patients with the same disease. This was very acceptable and consistent with the hypothesis of phenotype-genotype correlation. Grover et al. previously described that there were no intra-familial variations in the pattern of the Goldmann visual field in RP patients and speculated that these visual field patterns were correlated with different genetic mutations (Grover et al. 1998). Considering our previous report (Oishi et al. 2013), which found that the hypo-FAF area

in wide-field FAF was correlated with the V-4e isopter measured by Goldmann perimetry, our results support Grover's speculation. Interestingly, the similarity between siblings was higher than that of parent-child pairs. Patients with IRD must have the same causative gene within a family. In terms of the possibility of epistasis (Zernant et al. 2005; Khanna et al. 2009), a parent-child pair or siblings share 50% of all genes with each other, and there tend to be similar lifestyles within a family. The biggest difference between siblings and parent-child pairs was thought to be age. Our results indicated that aging had a great impact on the phenotypic variety of wide-field FAF.

There are 2 major limitations to this study. First, the small number of IRD cases did not allow for a statistical analysis separating typical RP and CRD in this study. Second, we defined the similarity between 2 wide-field FAF images. To our knowledge, this was the first challenge for quantifying similarity, and we used minimal image processing. It is thought that our method evaluated hypo-FAF areas and distributions well, but it may have underestimated the shape. Further modifications using updated image processing techniques would provide better and less biased quantification.

We conclude that wide-field FAF images were generally similar between siblings with IRD and were possibly influenced by aging. Intra-familial varieties previously reported in retinal dystrophies might derive from comparison among different generations. This should be the basis of further genotype-phenotype correlation studies.

References

Grover S, Fishman GA, Brown J Jr (1998) Patterns of visual field progression in patients with retinitis pigmentosa. Ophthalmology 105:1069–1075

Khanna H, Davis EE, Murga-Zamalloa CA et al (2009) A common allele in RPGRIP1L is a modifier of retinal degeneration in ciliopathies. Nat Genet 41:739–745

Meyerle CB, Fisher YL, Spaide RF (2006) Autofluorescence and visual field loss in sector retinitis pigmentosa. Retina 26:248–250

Ogino K, Oishi A, Makiyama Y et al (2013) [Genotype screening of retinal dystrophies in the Japanese population using a microarray]. Nihon Ganka Gakkai Zasshi 117:12–18

Oishi A, Ogino K, Makiyama Y et al (2013) Wide-field fundus autofluorescence imaging of retinitis pigmentosa. Ophthalmology 120:1827–1834

von Ruckmann A, Fitzke FW, Bird AC (1999) Distribution of pigment epithelium autofluorescence in retinal disease state recorded *in vivo* and its change over time. Graefes Arch Clin Exp Ophthalmol 237:1–9

Zernant J, Kulm M, Dharmaraj S et al (2005) Genotyping microarray (disease chip) for Leber congenital amaurosis: detection of modifier alleles. Invest Ophthalmol Vis Sci 46:3052–3059

Chapter 41
Wide-Field Fundus Autofluorescence for Retinitis Pigmentosa and Cone/Cone-Rod Dystrophy

Akio Oishi, Maho Oishi, Ken Ogino, Satoshi Morooka and Nagahisa Yoshimura

Abstract Retinitis pigmentosa and cone/cone-rod dystrophy are inherited retinal diseases characterized by the progressive loss of rod and/or cone photoreceptors. To evaluate the status of rod/cone photoreceptors and visual function, visual acuity and visual field tests, electroretinogram, and optical coherence tomography are typically used. In addition to these examinations, fundus autofluorescence (FAF) has recently garnered attention. FAF visualizes the intrinsic fluorescent material in the retina, which is mainly lipofuscin contained within the retinal pigment epithelium. While conventional devices offer limited viewing angles in FAF, the recently developed Optos machine enables recording of wide-field FAF. With wide-field analysis, an association between abnormal FAF areas and visual function was demonstrated in retinitis pigmentosa and cone-rod dystrophy. In addition, the presence of "patchy" hypoautofluorescent areas was found to be correlated with symptom duration. Although physicians should be cautious when interpreting wide-field FAF results because the peripheral parts of the image are magnified significantly, this examination method provides previously unavailable information.

Keywords Fundus autofluorescence · Ultra-widefield scanning laser ophthalmoscope · Retinitis pigmentosa · Cone rod dystrophy · Stargardt disease

A. Oishi (✉) · M. Oishi · K. Ogino · S. Morooka · N. Yoshimura
Departments of Ophthalmology and Visual Sciences, Kyoto University Graduate School of Medicine, 54 Kawahara, Shogoin, Sakyo, Kyoto 606-8507, Japan
e-mail: aquio@kuhp.kyoto-u.ac.jp

M. Oishi
e-mail: mah0ham@kuhp.kyoto-u.ac.jp

K. Ogino
e-mail: kenboo@kuhp.kyoto-u.ac.jp

S. Morooka
e-mail: moro@kuhp.kyoto-u.ac.jp

N. Yoshimura
e-mail: nagaeye@kuhp.kyoto-u.ac.jp

C. Bowes Rickman et al. (eds.), *Retinal Degenerative Diseases,* Advances in Experimental Medicine and Biology 854, DOI 10.1007/978-3-319-17121-0_41

41.1 Introduction

Inherited retinal dystrophy (IRD) is a clinical term that describes a heterogeneous group of diseases that affect photoreceptors. IRD is a major cause of blindness, especially in developed countries (Hartong et al. 2006). IRD can be categorized into four major groups: rod-dominant diseases, cone-dominant diseases, generalized retinal degenerations, and vitreoretinal disorders (Berger et al. 2010). Retinitis pigmentosa (RP) and cone/cone-rod dystrophy (CD/CRD) are relatively common IRD phenotypes, and they represent rod-dominant and cone-dominant diseases, respectively.

IRD disease severity can be evaluated using various examinations, including visual acuity and visual field tests, optical coherence tomography (OCT), and electroretinogram (ERG). Among these, visual field tests and ERG provide information regarding whole retinal function; however, this examination are rather time- and labor-consuming.

Fundus autofluorescence (FAF) is another method to evaluate retinal integrity. Standard FAF imaging uses short wave-length light to excite the fluorescent material in the retina, which mainly reveals the distribution of lipofuscin. Based on the observation that the number of photoreceptor cells reduces with increasing amounts of lipofuscin in the retinal pigment epithelium (RPE), it is hypothesized that the accumulation of lipofuscin precedes cell death (Dorey et al. 1989; von Ruckmann et al. 1997). In fact, abnormal accumulation of lipofuscin is evident in histopathologic IRD studies, (Eagle et al. 1980) and increased FAF is clinically observed in these cases. In addition, loss of RPE results in decreased FAF. Thus, FAF is suitable for IRD evaluation. Although there is an inherent limitation to FAF examination in that the angle of view is limited to the central 30–55° using a conventional fundus camera or scanning laser ophthalmoscope (SLO), recent technological advancements have enabled recording of the peripheral retina. Wide-field SLO Optos or Optomap (Optos, Scotland, United Kingdom) is a device that can record an extensive retinal field of view in a single image (Manivannan et al. 2005). Since photoreceptors are distributed throughout the retina, wide-field imaging should be considered the optimal method for evaluating the entire retina. In fact, several studies have reported the utility of Optos wide-field FAF imaging for evaluating retinal diseases such as chorioretinitis, (Seidensticker et al. 2011) retinal detachment, (Witmer et al. 2012) RP, (Oishi et al. 2013) and CD/CRD (Oishi et al. 2014b).

In this article, we will review the clinical significance of wide-field FAF as well as conventional FAF in RP and CD/CRD.

41.2 FAF Findings Using Conventional Fundus Camera/SLO

41.2.1 Retinitis Pigmentosa

Among IRDs, RP is the most common phenotype that starts with night blindness and concentric visual field defects. As the disease progresses, cone photoreceptors

are also affected and some patients experience total blindness (Hartong et al. 2006). FAF abnormalities in RP have been rigorously investigated. The most studied feature is a ring of increased FAF around the fovea. The hyperautofluorescent ring demarcates the preserved and damaged areas of the retina (Robson et al. 2004, 2006; Murakami et al. 2008; Fleckenstein et al. 2009; Lima et al. 2009, 2012). Retinal sensitivity decreases and outer retinal structures depicted on OCT become disrupted outside the ring. Moreover, longitudinal observations have shown that the ring constricts as the disease progresses (Robson et al. 2006, 2011). In advanced cases, the ring disappears and increased FAF is observed in the fovea. In these cases, visual acuity is further impaired relative to the visual acuity in cases with a ring of increased FAF (Iriyama and Yanagi 2012). Taken together, the presence or the size of the hyperautofluorescent ring is associated with macular functions, including visual acuity in RP.

41.2.2 Cone/Cone-Rod Dystrophy

Cone photoreceptors are primarily affected in CD/CRD. CD and CRD were differentiated based on the extent of rod impairment; however, the two conditions show both symptomatic and causative gene overlap, and this differentiation is now blurred (Traboulsi 2012).

The characteristics of FAF in CD/CRD are less investigated compared to those in RP. However, a hyperautofluorescent ring is also observed in CD/CRD (Michaelides et al. 2005; Wang et al. 2009). In contrast to RP, the retina is impaired inside the ring and generally preserved outside the ring. Moreover, the size of the ring is associated with rod and cone function and the ring enlarges longitudinally (Robson et al. 2008). The longitudinal enlargement of the atrophic lesions, depicted as decreased FAF, and the association between this area and ERG amplitude were also observed in Stargardt's disease (Chen et al. 2010). Evaluation of hypoautofluorescent lesions and the circumscribing hyperautofluorescent ring can be an indicator of visual function in these predominantly macular affecting diseases.

41.3 FAF Findings in Wide-Field SLO

41.3.1 Principle of Wide-Field Imaging

Optos uses an ellipsoid mirror, which has two foci (Fig. 41.1, F1 and F2), to create images. The laser source/detector is placed at F1 with a scanning mirror and the laser emitted from F1 always passes through F2. Setting the patient's pupil at F2 allows the laser emitted from F1 to reach wide angles of the fundus (Fig. 41.1).

Optos employs red (633 nm wavelength), green (532 nm wavelength), and blue (488 nm) laser sources, and a pseudocolor image is created by compositing the red

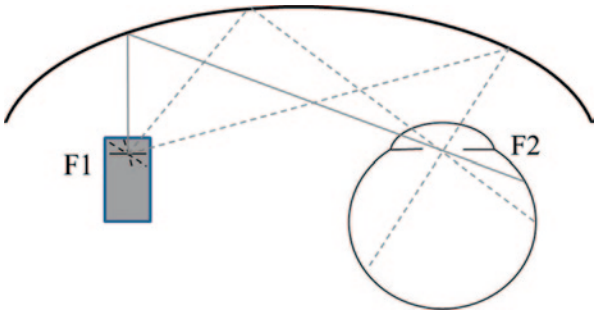

Fig. 41.1 Schematic drawing of the principle of the wide-field SLO device. As a property of the ellipse, the laser emitted from one focus (*F1*) is reflected and meets the other focus (*F2*) and returns to the original focus *F1*, where the detector is also located. Thus, the laser can cover a wide range of the fundus without being disrupted by the pupil

and green laser images; angiography is performed with the blue laser and FAF is performed with the green laser.

41.3.2 Retinitis Pigmentosa

The above mentioned hyperautofluorescent ring in RP is also observed in Optos images. The presence of the ring is associated with worse visual acuity or retinal sensitivity as measured by Humphrey visual field analyzer. In addition, characteristic findings are identified in more peripheral regions of the retina with this device. The damaged retina generally shows granular or patchy hypoautofluorescent lesions and the area of these hypoautofluorescent lesions is associated with the size of the visual field defect (Oishi et al. 2013). Other studies also reported the association between the hypoautofluorescent area and visual field defect using conventional devices (Meyerle et al. 2006) or Optos (Ogura et al. 2014). In addition, it has been shown that the more patchy the autofluorescent lesion, the longer the duration of the disease. Thus, the presence of patchy autofluorescent lesions can be an indicator of chronic disease processes (Oishi et al. 2013). We currently use Optos findings to differentiate RP from autoimmune or cancer-associated retinopathies, which show more rapid progression.

41.3.3 Cone-Rod Dystrophy

Although most abnormalities appear in the macular area in CD/CRD, rod photoreceptors and visual fields can be impaired in the late stages. The remaining peripheral visual field is important for patients with central scotoma, and Optos images provide information pertaining to remaining photoreceptor/RPE integrity in the periphery. Atrophic lesions in the fovea are depicted as decreased FAF with Optos

as well as with conventional devices. Lesions are often accompanied by hyperautofluorescent margins. The abnormal FAF areas, including hyper- and hypo- autofluorescence, correlate well with the area of the visual field defect and ERG amplitude (Oishi et al. 2014b). In CD/CRD, the extent of abnormal FAF findings can be a good indicator of whole retina function as well as in RP.

41.3.4 Caution When Interpreting Optos Images

As previously mentioned, Optos is useful for evaluating IRD. However, there are some specific issues to be cognizant of when interpreting findings or attempting quantification. First, Optos creates planar images from the fundus sphere, which involves some distortion, especially in the periphery. Recently, we used a model eye and investigated how much distortion exists depending on the position on the image. Our results showed that overall image is stretched 1.12-fold in the horizontal direction with respect to the vertical direction and the peripheral part of the image is magnified by factors up to 2.0×1.5 (Oishi et al. 2014a). Thus, the features on these images cannot be measured as is. To quantify the image, specific correction has to be employed, but such a methodology has yet to be established. Strategies to avoid or decrease the consequences of this warping include performing qualitative measurements, comparing baseline and follow-up data, or creating composite images with pictures taken at different angles (Spaide 2011). Second, clinicians should ensure that the excitation wavelength and detection range are not the same on different devices. For example, Heidelberg retinal angiography 2 (HRA2) uses a 488-nm wavelength blue light for excitation and detects signals with wavelengths >500 nm. Meanwhile, Optos uses a green light with a wavelength of 532 nm for excitation and detects the signal within a wavelength of 570–780 nm. Although the difference seems to be inconsequential to date, further comparisons are needed to fully elucidate potential complications.

41.4 Conclusions

FAF is useful for evaluating retina integrity in IRD. Wide-field FAF images obtained with Optos provide previously unavailable information and the Optos FAF image findings correlate well with visual field measurements or ERG in IRD. Although physicians should be cognizant of peripheral image magnification, the device will increase our understanding of these diseases. Investigations using wide-field FAF are in their infancy; thus, we expect detailed investigations of structure-function and phenotype-genotype correlations in the near future. Studies using this device will undoubtedly increase our understanding of IRD.

Acknowledgment This study was supported in part by the Japan Ministry of Health, Labor and Welfare (No. 12103069).

References

Berger W, Kloeckener-Gruissem B, Neidhardt J (2010) The molecular basis of human retinal and vitreoretinal diseases. Prog Retin Eye Res 29:335–375

Chen B, Tosha C, Gorin MB et al (2010) Analysis of autofluorescent retinal images and measurement of atrophic lesion growth in Stargardt disease. Exp Eye Res 91:143–152

Dorey CK, Wu G, Ebenstein D et al (1989) Cell loss in the aging retina. Relationship to lipofuscin accumulation and macular degeneration. Invest Ophthalmol Vis Sci 30:1691–1699

Eagle RC Jr, Lucier AC, Bernardino VB Jr et al (1980) Retinal pigment epithelial abnormalities in fundus flavimaculatus: a light and electron microscopic study. Ophthalmology 87:1189–1200

Fleckenstein M, Charbel Issa P, Fuchs HA et al (2009) Discrete arcs of increased fundus autofluorescence in retinal dystrophies and functional correlate on microperimetry. Eye (Lond) 23:567–575

Hartong DT, Berson EL, Dryja TP (2006) Retinitis pigmentosa. Lancet 368:1795–1809

Iriyama A, Yanagi Y (2012) Fundus autofluorescence and retinal structure as determined by spectral domain optical coherence tomography, and retinal function in retinitis pigmentosa. Graefes Arch Clin Exp Ophthalmol 250:333–339

Lima LH, Cella W, Greenstein VC et al (2009) Structural assessment of hyperautofluorescent ring in patients with retinitis pigmentosa. Retina 29:1025–1031

Lima LH, Burke T, Greenstein VC et al (2012) Progressive constriction of the hyperautofluorescent ring in retinitis pigmentosa. Am J Ophthalmol 153:718–727, 727. e711–e712

Manivannan A, Plskova J, Farrow A et al (2005) Ultra-wide-field fluorescein angiography of the ocular fundus. Am J Ophthalmol 140:525–527

Meyerle CB, Fisher YL, Spaide RF (2006) Autofluorescence and visual field loss in sector retinitis pigmentosa. Retina 26:248–250

Michaelides M, Holder GE, Webster AR et al (2005) A detailed phenotypic study of "cone dystrophy with supernormal rod ERG". Br J Ophthalmol 89:332–339

Murakami T, Akimoto M, Ooto S et al (2008) Association between abnormal autofluorescence and photoreceptor disorganization in retinitis pigmentosa. Am J Ophthalmol 145:687–694

Ogura S, Yasukawa T, Kato A et al (2014) Wide-field fundus autofluorescence imaging to evaluate retinal function in patients with retinitis pigmentosa. Am J Ophthalmol 158(5):1093–1098

Oishi A, Ogino K, Makiyama Y et al (2013) Wide-field fundus autofluorescence imaging of retinitis pigmentosa. Ophthalmology 120:1827–1834

Oishi A, Hidaka J, Yoshimura N (2014a) Quantification of the image obtained with a wide-field scanning ophthalmoscope. Invest Ophthalmol Vis Sci 55:2424–2431

Oishi M, Oishi A, Ogino K et al (2014b) Wide-field fundus autofluorescence abnormalities and visual function in patients with cone and cone-rod dystrophies. Invest Ophthalmol Vis Sci 55:3572–3577

Robson AG, Egan CA, Luong VA et al (2004) Comparison of fundus autofluorescence with photopic and scotopic fine-matrix mapping in patients with retinitis pigmentosa and normal visual acuity. Invest Ophthalmol Vis Sci 45:4119–4125

Robson AG, Saihan Z, Jenkins SA et al (2006) Functional characterisation and serial imaging of abnormal fundus autofluorescence in patients with retinitis pigmentosa and normal visual acuity. Br J Ophthalmol 90:472–479

Robson AG, Michaelides M, Luong VA et al (2008) Functional correlates of fundus autofluorescence abnormalities in patients with RPGR or RIMS1 mutations causing cone or cone rod dystrophy. Br J Ophthalmol 92:95–102

Robson AG, Tufail A, Fitzke F et al (2011) Serial imaging and structure-function correlates of high-density rings of fundus autofluorescence in retinitis pigmentosa. Retina 31:1670–1679

Seidensticker F, Neubauer AS, Wasfy T et al (2011) Wide-field fundus autofluorescence corresponds to visual fields in chorioretinitis patients. Clin Ophthalmol 5:1667–1671

Spaide RF (2011) Peripheral areas of nonperfusion in treated central retinal vein occlusion as imaged by wide-field fluorescein angiography. Retina 31:829–837

Traboulsi EI (2012) Cone dysfunction syndromes, cone dystrophies, and cone-rod degenerations. In: Traboulsi EI (ed) Genetic diseases of the eye. Oxford University Press, New York

von Ruckmann A, Fitzke FW, Bird AC (1997) Fundus autofluorescence in age-related macular disease imaged with a laser scanning ophthalmoscope. Invest Ophthalmol Vis Sci 38:478–486

Wang NK, Chou CL, Lima LH et al (2009) Fundus autofluorescence in cone dystrophy. Doc Ophthalmol 119:141–144

Witmer MT, Cho M, Favarone G et al (2012) Ultra-wide-field autofluorescence imaging in non-traumatic rhegmatogenous retinal detachment. Eye (Lond) 26:1209–1216

Chapter 42
The Development of a Cat Model of Retinal Detachment and Re-attachment

Sarah Wassmer, Brian C. Leonard, Stuart G. Coupland, Adam Baker, John Hamilton, Renée Torlone, David N. Zacks and Catherine Tsilfidis

Abstract We present an optimized surgical technique for feline retinal detachment which allows for natural re-attachment, reduces retinal scarring and vitreal bands, and allows central placement of the detachment in close proximity to the optic nerve. This enables imaging via Optical Coherence Tomography (OCT) and multifocal electroretinography (mfERG) analysis. Ideal detachment conditions involve a lensectomy followed by a three-port pars plana vitrectomy. A 16–20 % retinal

Sarah Wassmer and Brian C. Leonard contributed equally to the study.

C. Tsilfidis (✉) · S. Wassmer · B. C. Leonard · S. G. Coupland · A. Baker · J. Hamilton
Ottawa Hospital Research Institute, Regenerative Medicine, Ottawa, ON K1H 8L6, Canada
e-mail: ctsilfidis@ohri.ca

S. Wassmer
e-mail: swassmer@ohri.ca

B. C. Leonard
e-mail: bleonard@ottawahospital.on.ca

S. G. Coupland
e-mail: scoupland@ohri.ca

A. Baker
e-mail: adbaker@ohri.ca

J. Hamilton
e-mail: johhamilton@toh.on.ca

S. Wassmer · S. G. Coupland · C. Tsilfidis
Department of Cellular and Molecular Medicine, University of Ottawa, Ottawa, ON K1H 8M5, Canada

B. C. Leonard · S. G. Coupland · C. Tsilfidis
Department of Ophthalmology, University of Ottawa, Ottawa, ON K1H 8M5, Canada

R. Torlone
Ottawa Hospital General Division, Eye Institute, Ottawa, ON K1H 8L6, Canada
e-mail: rtorlone@toh.on.ca

D. N. Zacks
Department of Ophthalmology and Visual Sciences, Kellogg Eye Center, University of Michigan Medical School, Ann Arbor, MI 48105, USA
e-mail: davzacks@med.umich.edu

C. Bowes Rickman et al. (eds.), *Retinal Degenerative Diseases,* Advances in Experimental Medicine and Biology 854, DOI 10.1007/978-3-319-17121-0_42

detachment is induced by injecting 8% C_3F_8 gas into the subretinal space in the central retina with a 42G cannula. The retinal detachment resolves approximately 6 weeks post-surgery. Imaging is enhanced by using a 7.5 and 20 diopter lens for OCT and mfERG fundus imaging, respectively, to compensate for the removed lens.

Keywords Retinal detachment · Feline · Lensectomy · Vitrectomy · C3F8 gas (Octafluoropropane) · Subretinal space · Photoreceptor · Hemorrhage

42.1 Introduction

Retinal detachment is a common form of injury. Treatment typically involves surgical re-attachment of the retina, but recovery of vision depends on the nature and duration of the detachment. Retinal detachments often lead to changes in the retina that can have permanent effects on visual function. Loss of vision is further increased if the macula is involved in the detachment (Erickson et al. 1983).

Animal studies have shown histological and molecular evidence that retinal degeneration ensues as early as 1 h post detachment (Erickson et al. 1983; Zacks et al. 2003). A major cause for vision loss is photoreceptor apoptosis (Zacks et al. 2003). Oxidative stress has also been implicated in photoreceptor apoptosis and disease pathology (Cederlund et al. 2013; Huang et al. 2013).

We have shown that the X-linked Inhibitor of Apoptosis (XIAP) is effective in protecting photoreceptor structure in a rat model of retinal detachment (Zadro-Lamoureux et al. 2009). However, due to the small size of the rodent eye, surgical re-attachment is technically very challenging. Thus, while the effects of XIAP on the structure of photoreceptors can be determined, the function of the photoreceptors is difficult to assess. Consequently, for our studies, and for those of others interested in studying therapeutic strategies for retinal detachment, there is still a critical need to develop a larger animal model of detachment and re-attachment of the retina. We present here a feline model of detachment and re-attachment which allows central placement of the detachment so that structural and functional recovery of photoreceptors can be assessed using OCT and multifocal ERG.

42.2 Materials and Methods

42.2.1 Animals

Three wild type (domestic) cats (Liberty Research, Waverly, NY) aged 12 months were studied. Animal procedures were conducted in accordance with the University of Ottawa Animal Care Committee rules and regulations and adhered to the ARVO statement for the Use of Animals in Ophthalmic and Vision Research.

42.2.2 Pre- and Post-Operative Treatments

Felines were given propofol (1 mL/min) intravenously or 5 % isoflurane by aerosol mask before surgery and during the anesthetic regime (see below). Throughout the surgery animals were kept on 2–3 % isoflurane. After the surgery, the eyes were treated with 5–10 drops of 1.0 % w/v atropine sulphate (Chauvin Pharmaceuticals) and covered with Tobradex Ophthalmic Ointment (tobramycin 0.3 %, dexamethasone 0.1 %) (Alcon). The animals were treated 4 times daily with Tobradex for 10 days.

42.2.3 Animal Anesthetic Regimes

Animals were treated with one of five anesthetic regimes in order to optimize the drug cocktail and concentrations. Regime 1: hydromorphone (Sandoz) 0.1 mg/kg (2 mg/mL), acepromazine (Boerhinger) 0.1 mg/kg (10 mg/mL), glycopyrrolate (American Regent) 0.01 mg/mL (0.2 mg/mL) and propofol (1 mL/min); Regime 2: medetomidine hydrochloride (Modern Veterinary Therapeutics) 0.015 mg/kg (1 mg/kg) and hydromorphone 0.1 mg/kg (2 mg/mL) and isoflurane; Regime 3: medetomidine hydrochloride 0.04 mg/kg (1 mg/kg) and isoflurane; Regime 4: medetomidine hydrochloride 0.015 mg/kg (1 mg/mL), hydromorphone 0.1 mg/kg (2 mg/mL), Cerenia (Pfizer) 0.5 mg/kg (10 mg/kg), buprenorphine (Champion Alstoe) 0.02 mg/kg and isoflurane; Regime 5: medetomidine 0.015 mg/kg (1 mg/mL), hydromorphone 0.1 mg/kg (2 mg/mL), Cerenia 0.5 mg/kg (10 mg/kg) and isoflurane. Animals were administered normosol fluids under all regimes, and given Mydriacyl (Alcon) (1 %), Mydfrin (Alcon) (2.5 %) and Alcaine (Alcon) (0.5 %) drop-wise to the surgical eye.

42.2.4 Retinal Detachment Procedure

Animals were administered one of the anesthetic regimes discussed above by intramuscular injection, in addition to pre-operative treatment and held on 2–3 % isoflurane during the procedure. All techniques were performed under sterile operating room conditions. The head was elevated to ensure the eye was directly under the Zeiss ophthalmic operating microscope. The operative field was swabbed with 10 % providone iodine (3M). Supplemental oxygen (2 L/min) was administered via intubation (Engler Engineering Corporation), and vital signs (oxygen saturation, heartrate, blood pressure) were monitored throughout the procedure (Surgivet Smith Medicals).

A generous lateral canthotomy was performed to enhance exposure of the surgical site. A fornix-based conjunctival and Tenon's capsule flap was dissected temporally. A Barraquer wire eye speculum was placed incorporating the eyelid margins, the nictitating membrane and the conjunctival and Tenon's capsule flap. Bipolar cautery of the scleral surface with a 25 gauge (G) straight disposable bipolar pencil (Kirwan Surgical Products) minimized bleeding from the rich ciliary vascular complex. Three sclerotomies were then fashioned 4 mm from the limbus within this tight temporal area of exposure. One 20 G equatorial incision was placed centrally with a 20 G 1.3 mm V-lance knife (Alcon) to accommodate a 20 G Alcon Accurus Fragmatome handpiece, flanked by two 25 G cannula ports used interchangeably for a 25 G Accurus vitrectomy handpiece, an intraocular infusion cannula and an endoilluminator probe. Placement of all three sclerotomies into the lateral temporal quadrant was necessary due to the limited exposure imposed by the large feline eye, deeply set within a small tight socket.

A pars plana lensectomy was performed with linear phacofragmentation using a 20 G Accurus Fragmatome handpiece. A vitrectomy was performed with a 25 G Accurus vitrectomy handpiece with visualization from an Oculus BIOM posterior segment panoramic imaging system with image inverter. A 16–20 % retinal detachment was placed in the posterior central pole by subretinal injection of 8 % C_3F_8 gas via an angled 42 G subretinal cannula using a disposable vitrectomy flat lens (Dutch Ophthalmic). Coaxial illumination from the microscope through the contact lens system, without an endoilluminator probe, provided a sufficient magnified view of the posterior segment to allow precise two-handed placement of the subretinal cannnula.

At the completion of the surgery, the posterior chamber was filled with automated air-fluid exchange to promote internal sclerotomy wound integrity. The sclerotomies, conjunctiva and Tenon's capsule were closed with 7-0 Vicryl suture (Ethicon).

42.2.5 Functional Testing

Multifocal electroretinograms (mfERGs) were recorded with the VERIS™ Multifocal System (Electro-Diagnostic Imaging, Inc), using an unscaled stimulus containing 7 hexagonal elements projected on the central 45 ° of retina through a dilated pupil. Multifocal ERGs were recorded with OcuScience ERG-jet contact lens electrodes and ERG signals were amplified 50,000 times using Grass P511J amplifiers (Grass Technologies) with a 10–100 Hz bandpass. The first order kernel of the M-13 sequence was extracted and displayed. Spectral-domain Optical Coherence Tomography (sd-OCT) (OPKO SLO/OCT) was used to image the area of the retinal detachment. Accessory lenses (Eschenbach Optik GmbH) were used for mfERGs and sd-OCT imaging to compensate for the aphakia and provide focused conditions. Line scans, raster scanning and 3-D retinal topographic scanning modes were used.

42.3 Results

In order to optimize the retinal detachment model, three parameters were evaluated: type of surgery required (lens/vitreous removal or sparing), method of detachment (percentage of the C_3F_8 gas), and the optimal anesthetic regime to be administered.

A total of three cats were studied to determine the proper parameters for a retinal detachment and re-attachment. The detachment surgery for the first animals was a "direct" approach in which the lens and vitreous were spared. We used a 42 G cannula to inject C_3F_8 gas into the subretinal space. In an attempt to place the detachment as centrally as possible, the lens was slightly nicked, and this later presented as a mild, stable cataract. The detachment surgery caused a small retro-vitreal hemorrhage (which later resolved) and the appearance of vitreal bands that extended from the pars plana sclerotomy sites to the posterior retinotomy. However, the fiber tracts did not progress to full tractional bands, as one would expect in a non-vitrectomised eye. Overall, we found that the large size of the feline lens discouraged lens and vitrectomy-sparing procedures because it made it virtually impossible to place the detachment site in the central retina. Consequently, imaging of the detached retina via sd-OCT and functional assessment with mfERG were impossible since the instruments can only monitor the central 29 and 45°, respectively, of the retina. As a result, removal of the lens and vitreous was necessary to allow central placement of the detachment and to remove hemorrhages or vitreal bands from the posterior chamber.

In the second cat, a mechanical suction cutter (cutter speed of 800 and vacuum up to 175) was used to remove the lens. However, the size and viscosity of the lens posed challenges that interfered with the timely and complete removal of the lens, and created post-operative complications in the eye. Therefore, the ideal technique for rapid and efficient removal of the lens involved phacofragmentation of the lens, with 100% power, 2500 cut rate and 600 mmHg with an Alcon Accuris Vitrector & Fragmatome. This was followed by a vitrectomy to clean the vitreous cavity and to prevent retinal scarring and vitreal bands.

A 42 G needle was used to deliver C_3F_8 gas into the subretinal space to induce the retinal detachment. We tested several different concentrations of the C_3F_8 gas (100, 16 and 8%) and monitored the detachment over time for spread and speed of reabsorption. The 100 and 16% C_3F_8 gas expanded in the subretinal space, allowing less control over the size of the detachment. The 8% gas did not expand. In all cases, the gas was slowly reabsorbed (within 6 weeks), allowing the retina to re-attach on its own without surgical intervention. A 6-week detachment is ideal for neuroprotection studies as it creates a significant amount of permanent damage, allowing the testing of therapeutic interventions to prevent photoreceptor death.

Notably, we found that the anesthetic protocol can drastically affect the multifocal ERG waveform. Animals administered drug regimen 3, 4 or 5 (see Materials and Methods) displayed flat-lined mfERGs. These results were not due to a malfunction of the equipment, as a similar set up yielded healthy waveforms in rats (under 2% isoflurane administration) and human volunteers. Using the same equipment, and anesthetic regimens 1 and 2 in the cats (ie. no Cerenia and a low

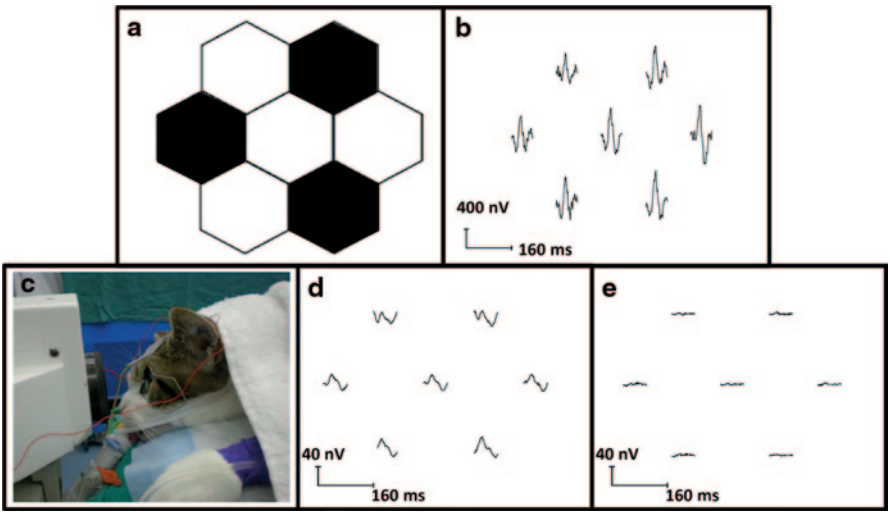

Fig. 42.1 Multifocal ERG set up and results. **a** A 7 hexagon array was projected onto the central 45° of the retina. **b** Control image of a human subject. **c** Experimental cat set-up with contact lens electrode on the cornea, and reference and ground electrodes in the forehead and ear, respectively. **d** Healthy mfERG in a cat. **e** Flat-lined ERG with the same experimental setup as **d**, but with the anesthetic cocktail containing Cerenia and a higher dose of medetomidine hydrochloride

dose of medetomidine [0.015 mg/mL]), the mfERG waveforms obtained were typical of a healthy cat (Fig. 42.1).

42.4 Discussion

In this study, we determined the ideal experimental conditions for the creation of a cat model of retinal detachment and re-attachment. We found that a 3-port pars plana phacofragmentation lensectomy followed by a full vitrectomy allows unfettered access to the central retina where a controlled retinal detachment can be induced by the injection of 8% C_3F_8 gas into the subretinal space through a 42 G cannula. The detachment slowly resolves over 6 weeks, allowing the retina to re-attach without surgical intervention. We also determined that an anesthetic regimen that contains low dose medetomidine and no Cerenia is critical for obtaining mfERGs. The effects of the anesthetic on the amplitude of the ERG may not be surprising since it has been shown that mild to moderate sedation in dogs using medetomidine significantly lowers flash electroretinogram a- and b-wave values (Norman et al. 2008; Lin et al. 2009). Furthermore, the antiemetic, Cerenia, is a substance-P inhibitor. Substance-P is an important signaling neuropeptide in two subpopulations of amacrine cells in the feline (Pourcho and Goebel 1988). Inhibiting this neuropeptide may have contributed to the flat-line mfERG responses.

It has previously been reported that vitreous or sclerotomy hemorrhage is quite prevalent in cat models of stem cell or allograft transplantation (Bragadottir and

Narfstrom 2003). This is due to the large vascular plexus in the pars plana region. Cauterization of the episcleral venous plexus and the use of topical vasoconstriction drugs to reduce intraocular hemorrhage have been proposed as a solution. In our hands, intraoperative hemorrhage did not present a significant problem. Small haemorrhages, when they presented, were treated by cauterizing the vessels.

The feline model that we have developed offers advantages over small rodent models of retinal detachment for testing therapeutic compounds. In rodent models, retinal detachment is most often induced by injection of hyaluronic acid into the subretinal space. The viscosity of the hyaluronic acid, and the small size of the rodent eye makes surgical reattachment and functional assessment of photoreceptors technically challenging. The size of the cat eye allows re- attachment of the retina and subsequent analysis of retinal structure and function by OCT and mfERG. Moreover, a number of studies have previously been conducted on retinal detachment in cats (Lewis and Fisher 2000; Sakai et al. 2014), although as far as we are aware, none of these studies have subsequently re-attached the retina after long-term detachment. Thus, a good body of literature exists on the structural alterations (remodeling) in the retina following retinal detachment, and this information is very useful for assessing the therapeutic efficacy of experimental compounds.

Acknowledgment We would like to thank the members of the University of Ottawa Animal Care and Veterinary Services for their help with animals and surgeries.

References

Bragadottir R, Narfstrom K (2003) Lens sparing pars plana vitrectomy and retinal transplantation in cats. Vet Ophthalmol 6:135–139

Cederlund M, Ghosh F, Arner K et al (2013) Vitreous levels of oxidative stress biomarkers and the radical-scavenger alpha1-microglobulin/A1M in human rhegmatogenous retinal detachment. Graefes Arch Clin Exp Ophthalmol 251:725–732

Erickson PA, Fisher SK, Anderson DH et al (1983) Retinal detachment in the cat: the outer nuclear and outer plexiform layers. Invest Ophthalmol Vis Sci 24:927–942

Huang W, Li G, Qiu J et al (2013) Protective effects of resveratrol in experimental retinal detachment. PLoS One 8:e75735

Lewis GP, Fisher SK (2000) Muller cell outgrowth after retinal detachment: association with cone photoreceptors. Invest Ophthalmol Vis Sci 41:1542–1545

Lin SL, Shiu WC, Liu PC et al (2009) The effects of different anesthetic agents on short electroretinography protocol in dogs. J Vet Med Sci 71:763–768

Norman JC, Narfstrom K, Barrett PM (2008) The effects of medetomidine hydrochloride on the electroretinogram of normal dogs. Vet Ophthalmol 11:299–305

Pourcho RG, Goebel DJ (1988) Substance P-like immunoreactive amacrine cells in the cat retina. J Comp Neurol 275:542–552

Sakai T, Tsuneoka H, Lewis GP et al (2014) Remodelling of retinal on- and off-bipolar cells following experimental retinal detachment. Clin Experiment Ophthalmol 42:480–485

Zacks DN, Hanninen V, Pantcheva M et al (2003) Caspase activation in an experimental model of retinal detachment. Invest Ophthalmol Vis Sci 44:1262–1267

Zadro-Lamoureux LA, Zacks DN, Baker AN et al (2009) XIAP effects on retinal detachment-induced photoreceptor apoptosis [corrected]. Invest Ophthalmol Vis Sci 50:1448–1453

Part V
Mechanisms of Degeneration

Chapter 43
The Role of X-Chromosome Inactivation in Retinal Development and Disease

Abigail T. Fahim and Stephen P. Daiger

Abstract The expression of X-linked genes is equalized between males and females in mammalian species through X-Chromosome inactivation (XCI). Every cell in a female mammalian embryo randomly chooses one X Chromosome for epigenetic silencing at the 8–16 cell stage, resulting in a Gaussian distribution of XCI ratios with a peak at 50:50. At the tail extremes of this distribution, X-linked recessive mutations can manifest in disease in female carriers if the mutant allele is disproportionately active. The role of XCI skewing, if any, in X-linked retinal disease is still unknown, although many have speculated that such skewing accounts for phenotypic variation in female carriers of X-linked retinitis pigmentosa (XlRP). Some investigators have used clinical findings such as tapetal-like reflex, pigmentary changes, and multifocal ERG parameters to approximate XCI patches in the retina. These studies are limited by small cohorts and the relative inaccessibility of retinal tissue for genetic and epigenetic analysis. Although blood has been used as a proxy for other tissues in determining XCI ratios, blood XCI skews with age out of proportion to other tissues and may not accurately reflect retinal XCI ratios. Future investigations in determining retinal XCI ratios and the contribution of XCI to phenotype could potentially impact prognosis for female carriers of X-linked retinal disease.

Keywords X-Chromosome inactivation · Dosage compensation · Skewed inactivation · Escape genes · Retinal dystrophies · X-linked retinitis pigmentosa · X-linked retinoschisis · Choroideremia

A. T. Fahim (✉)
Department of Ophthalmology and Visual Sciences, University of Michigan, Kellogg Eye Center, 1000 Wall Street, Ann Arbor, MI 48105, USA
e-mail: ahteich@med.umich.edu

S. P. Daiger
School of Public Health, University of Texas Health Science Center, 1200 Herman Pressler Drive, RAS W-522, Houston, TX 77030, USA
e-mail: stephen.p.daiger@uth.tmc.edu

C. Bowes Rickman et al. (eds.), *Retinal Degenerative Diseases,* Advances in Experimental Medicine and Biology 854, DOI 10.1007/978-3-319-17121-0_43

43.1 Introduction

X-Chromosome Inactivation (XCI) is a dosage compensation mechanism used in mammals to equilibrate the expression of X-linked genes across genders (Lyon 2002). Every cell in the female embryo inactivates either the maternal or the paternal X chromosome, and the inactivation choice is passed down to subsequent daughter cells. This choice is typically made at random, although there are exceptions, and the XCI ratio in newborn females follows a normal distribution with a peak at 50:50. Inactivation of the X chromosome is facilitated by expression of *XIST* RNA, which binds to the chromosome of choice and mediates downstream methylation and inactivation (Brown et al. 1991).

XCI is determined at the 8–16 cell stage. This was demonstrated in human embryo studies that showed accumulation of *XIST* RNA starting at the 8-cell stage (van den Berg et al. 2009). Another study modeled distribution curves for XCI ratios based on theoretical numbers of stem cells present at the time of XCI choice. The predictions for 8- and 16-cell embryos most closely fit the empirically determined distribution curve, suggesting that XCI occurs within this window (Amos-Landgraf et al. 2006).

43.2 Escape Genes and Retinal Disease

A subgroup of X-linked genes escapes inactivation and is expressed from both X chromosomes. In a comprehensive study looking at inactivation status of 612 X-linked genes in human-rodent hybrid cells, 15% of genes escaped inactivation, and an additional 10% showed variable inactivation between individuals (Carrel and Willard 2005). Escape genes were often expressed at lower levels from the inactivated chromosome compared to the active chromosome. Both Retinitis Pigmentosa GTPase Regulator (*RPGR*) and *RP2*, which are together responsible for >90% of X-linked retinitis pigmentosa (XLRP), were found to be completely silenced. See Table 43.1 for a complete list of X-linked genes associated with retinal disease and their inactivation status in the hybrid cell lines (Carrel and Willard 2005; Daiger 2014).

43.3 XCI Skewing

Skewing of the XCI ratio from the expected 50:50 ratio can occur at the time of XCI choice in the early embryo (primary), or during embryonic development or later in life (secondary). In mice, XCI choice is greatly biased by variation at the X Controlling Element locus (*XCE)* on the X chromosome (Courtier et al. 1995; Chadwick and Willard 2005). In humans, nonrandom XCI choice occurs due to mutations in X-linked genes, including the *XIST* gene (Plenge et al. 1997).

Table 43.1 Retinal disease genes and inactivation status. (Carrel and Willard 2005; Daiger 2014)

Gene or locus (alias)	Disease	Inactivation
OFD1 (RP23, CXORF5)	Joubert syndrome, orofaciodigital syndrome 1, Simpson-Golabi, Behmel syndrome 2, retinitis pigmentosa	Escapes inactivation
RS1 (XLRS1)	Retinoschisis	Variable escape
RP6	Retinitis pigmentosa	Not determined
DMD	Oregon eye disease	Variable escape
OPA2	Optic atrophy	Not determined
NYX (CSNB1, CSNB1A, CSNB4)	Congenital stationary night blindness	Not determined
COD1	Cone dystrophy	Not determined
RPGR (CORDX1, RP3)	Retinitis pigmentosa, cone dystrophy	Inactivated
PRD	Primary retinal dysplasia	Not determined
NDP (EVR2)	Norrie disease, familial exudative vitreoretinopathy, Coats disease	Not determined
AIED (OA2)	Åland island eye disease	Not determined
CACNA1F (CORDX3, CSNB2, CSNB2A, CSNBX2)	Congenital stationary night blindness, ÅIED-like disease, cone-rod dystrophy	Inactivated
RP2	Retinitis pigmentosa	Inactivated
PGK1	Retinitis pigmentosa with myopathy	Inactivated
CHM	Choroideremia	Variable escape
TIMM8A (DDP, DDP2, DFN1)	Optic atrophy with deafness-dystonia syndrome	Variable escape
RP24	Retinitis pigmentosa	Not determined
COD2 (CORDX2)	Cone dystrophy	Not determined
RP34	Retinitis pigmentosa	Not determined
OPN1LW (BCM, CBP, COD5, RCP)	Deuteranopia, macular dystrophy in blue cone monochromacy with loss of locus control element	Not determined
OPN1MW (CBD, GCP)	Protanopia, macular dystrophy in blue cone monochromacy with loss of locus control element	Not determined

The table includes a comprehensive list of X-linked genes and loci known to be associated with retinal phenotypes and their inactivation status on the inactivated X chromosome in human-rodent hybrid cell lines

Disease-causing X-linked mutations often bias cell survival and replication during development and cause secondary XCI skewing (Orstavik 2009). For example, in Lesch-Nyhan Syndrome and Menkes disease, cells with a normal active X chromosome have a growth advantage over cells with a mutant active

X (Migeon 2007; Desai et al. 2011). In contrast, some female carriers of Duchenne Muscular Dystrophy and Hemophilia A demonstrate preferential inactivation of the wild-type allele and can manifest disease (Pegoraro et al. 1994; Di Michele et al. 2014). This pattern appears to be heritable in some cases (Renault et al. 2007; Esquilin et al. 2012), indicating that either the disease locus or another genetic modifier is biasing XCI in these families.

Even in the absence of a pathologic mutation XCI ratios skew with age, in some tissues more than others (Hatakeyama et al. 2004; Amos-Landgraf et al. 2006). Blood is particularly prone to XCI skewing with time, and blood has shown increased XCI skewing compared to buccal mucosa, skin, muscle, and urinary epithelium (Sharp et al. 2000; Knudsen et al. 2007; Bolduc et al. 2008). Only 4.9% of newborns show skewing >80:20 in blood compared to 14.2% of adults (Amos-Landgraf et al. 2006). This is particularly relevant because blood is the most frequently sampled tissue in the literature for determining XCI ratios and may not always be a good proxy for the tissue of interest. For example, in severely affected female carriers of X-linked ornithine transcarbamylase deficiency, skewed XCI was found in the liver, but not in the blood (Yorifuji et al. 1998).

There is very little data on correlation of XCI in the retina compared to blood. In one study that examined multiple tissues at autopsy from a female affected with Leber's Hereditary Optic Neuropathy, the XCI ratio in retina was 43:57, compared to 65:35 in blood and 56:44 in optic nerve (Pegoraro et al. 2003). Not only was the ratio more skewed in blood than in retina, but it was also skewed in the opposite direction.

43.4 XCI Patches in the Retina

Due to the relative inaccessibility of human retina tissue for investigation, XCI patches in the retina have largely been studied in animal models. The mouse retina displays clonal patches of XCI in a radial pattern. XCI occurs between E5.5 and E8.5 in mice, and at day E10.5 female mice heterozygous for an X-linked *lacZ* transgene showed random intermingling of *lacZ* active and inactive cells, indicating free migration of neuroepithelial cells. At birth, the mouse retinas showed alternating columns of *lacZ* active and inactive cells, indicating that the progenitor cells became fixed in location at some point (Reese and Tan 1998; Smallwood et al. 2003). Cone, horizontal, amacrine, and ganglion cells were interspersed into non-matching columns, suggesting tangential migration of these cells (Reese and Galli-Resta 2002).

In XLPRA2, a canine model of XLRP, carrier female dogs displayed patches of mislocalization of rod opsin at 3.9 weeks, followed by outer segment disruption and rod loss in these patches, which the authors attributed to patches of inactivation of the wild-type allele (Beltran et al. 2009). Older dogs by 39 weeks of age had a more uniform, although thinner, outer nuclear layer, which the authors speculated may result from early migration of healthy rods into diseased areas.

Adaptive optics was used to examine the cone mosaic in a human female carrier of protan color-blindness (deficiency of L-opsin on one X-chromosome) (Hofer et al. 2005). If cones were organized into XCI patches, one would see patches of M-cones devoid of L-cones. Instead, the L, M, and S cones were randomly dispersed in the fovea. The ratio of L:M cones was 0.37:1 (or 27% L cones), suggesting an XCI ratio of approximately 54:46. This interspersion of cones is consistent with prior studies demonstrating migration of cones into the fovea during fetal development (Yuodelis and Hendrickson 1986; Diaz-Araya and Provis 1992). It is unknown whether rods are distributed in XCI patches in the adult human retina.

43.5 XCI Patches and Skewing in Retinal Disease

XCI has been investigated in several X-linked retinal diseases, including XLRP, choroideremia, and retinoschisis. XLRP in particular is known for variable manifestation in female carriers, and differences in XCI ratios have been proposed as a chief mechanism for this variation. To date, investigations have been performed in small groups of patients using blood to determine XCI ratios. In one study involving three families with the same *RPGR* mutation, XCI ratios in blood were not associated with carrier phenotype (Banin et al. 2007). Of note, two families had unaffected carriers and shared a common haplotype, while the third family had severely affected carriers with a different surrounding haplotype, suggesting a linked genetic modifier affecting phenotype. Others have reported patchy disease in female carriers of XLRP (Szamier and Berson 1985; Cideciyan and Jacobson 1994; Banin et al. 2007). In one study of multifocal electroretinography (mfERG) in five clinically unaffected female carriers of XLRP, two carriers demonstrated patches of reduced amplitude, and three carriers demonstrated patches of implicit time delay. However, these patches did not correlate with each other and did not correlate with patches of tapetal-like reflex (Vajaranant et al. 2002).

In a study of seven obligate carriers of X-linked choroideremia, one carrier showed visual field abnormalities, six carriers showed patches of significant implicit time delays on mfERG, and four of these six also showed overlapping patches of significantly reduced amplitude (Vajaranant et al. 2008). All carriers had patches of pigmentary retina changes on fundoscopic exam, although these patches did not always correlate with areas of reduced function on mfERG. In two families with X-linked choroideremia, no link was found between female carrier phenotype and XCI skewing in peripheral blood (Perez-Cano et al. 2009).

Carriers of X-linked retinoschisis (XLRS) are generally not affected. There are rare reports of fundoscopic and psychophysical abnormalities (Ali et al. 2003; Rodriguez et al. 2005). In a study of mfERG in nine obligate carriers of XLRS, two carriers showed patches of significant implicit time delay that overlapped almost perfectly with patches of significantly reduced amplitude (Kim et al. 2007).

43.6 Conclusion

The studies described above have yielded variable results, and the extent to which XCI ratios contribute to X-linked retinal diseases remains controversial. Of note, these studies have all included very small numbers of patients, and those that looked at XCI ratios did so in blood samples. Given the notoriety of blood for instability of XCI populations and increased XCI skewing with age, this tissue may be a particularly poor proxy for retina tissue despite the advantage of accessibility. Future studies would benefit from larger cohorts and exploration of XCI ratios in other accessible tissues with potentially more stable XCI. Determining the contribution of XCI ratios to phenotype could have prognostic utility for carriers of X-linked retinal diseases. In particular, female carriers of XLRP vary in phenotype from unaffected to severely affected and may benefit from prognostic information, which is currently lacking. In addition, with gene therapy on the horizon for XLRP, prognostic factors may play an important role in selecting appropriate female candidates for intervention.

References

Ali A, Feroze AH, Rizvi ZH et al (2003) Consanguineous marriage resulting in homozygous occurrence of X-linked retinoschisis in girls. Am J Ophthalmol 136:767–769

Amos-Landgraf JM, Cottle A, Plenge RM et al (2006) X chromosome-inactivation patterns of 1,005 phenotypically unaffected females. Am J Hum Genet 79:493–499

Banin E, Mizrahi-Meissonnier L, Neis R et al (2007) A non-ancestral RPGR missense mutation in families with either recessive or semi-dominant X-linked retinitis pigmentosa. Am J Med Genet A 143A:1150–1158

Beltran WA, Acland GM, Aguirre GD (2009) Age-dependent disease expression determines remodeling of the retinal mosaic in carriers of RPGR exon ORF15 mutations. Invest Ophthalmol Vis Sci 50:3985–3995

Bolduc V, Chagnon P, Provost S et al (2008) No evidence that skewing of X chromosome inactivation patterns is transmitted to offspring in humans. J Clin Invest 118:333–341

Brown CJ, Ballabio A, Rupert JL et al (1991) A gene from the region of the human X inactivation centre is expressed exclusively from the inactive X chromosome. Nature 349:38–44

Carrel L, Willard HF (2005) X-inactivation profile reveals extensive variability in X-linked gene expression in females. Nature 434:400–404

Chadwick LH, Willard HF (2005) Genetic and parent-of-origin influences on X chromosome choice in Xce heterozygous mice. Mamm Genome 16:691–699

Cideciyan AV, Jacobson SG (1994) Image analysis of the tapetal-like reflex in carriers of X-linked retinitis pigmentosa. Invest Ophthalmol Vis Sci 35:3812–3824

Courtier B, Heard E, Avner P (1995) Xce haplotypes show modified methylation in a region of the active X chromosome lying 3' to Xist. Proc Natl Acad Sci U S A 92:3531–3535

Daiger SP (2014) https://sph.uth.edu/retnet. Accessed 29 Aug 2014

Desai V, Donsante A, Swoboda KJ et al (2011) Favorably skewed X-inactivation accounts for neurological sparing in female carriers of Menkes disease. Clin Genet 79:176–182

Di Michele DM, Gibb C, Lefkowitz JM et al (2014) Severe and moderate haemophilia A and B in US females. Haemophilia 20:e136–e143

Diaz-Araya C, Provis JM (1992) Evidence of photoreceptor migration during early foveal development: a quantitative analysis of human fetal retinae. Vis Neurosci 8:505–514

Esquilin JM, Takemoto CM, Green NS (2012) Female factor IX deficiency due to maternally inherited X-inactivation. Clin Genet 82:583–586
Hatakeyama C, Anderson CL, Beever CL et al (2004) The dynamics of X-inactivation skewing as women age. Clin Genet 66:327–332
Hofer H, Carroll J, Neitz J et al (2005) Organization of the human trichromatic cone mosaic. J Neurosci 25:9669–9679
Kim LS, Seiple W, Fishman GA et al (2007) Multifocal ERG findings in carriers of X-linked retinoschisis. Doc Ophthalmol 114:21–26
Knudsen GP, Pedersen J, Klingenberg O et al (2007) Increased skewing of X chromosome inactivation with age in both blood and buccal cells. Cytogenet Genome Res 116:24–28
Lyon MF (2002) X-chromosome inactivation and human genetic disease. Acta Paediatr Suppl 91:107–112
Migeon BR (2007) Why females are mosaics, X-chromosome inactivation, and sex differences in disease. Gend Med 4:97–105
Orstavik KH (2009) X chromosome inactivation in clinical practice. Hum Genet 126:363–373
Pegoraro E, Schimke RN, Arahata K et al (1994) Detection of new paternal dystrophin gene mutations in isolated cases of dystrophinopathy in females. Am J Hum Genet A 54:989–1003
Pegoraro E, Vettori A, Valentino ML et al (2003) X-inactivation pattern in multiple tissues from two Leber's hereditary optic neuropathy (LHON) patients. Am J Med Genet A 119A:37–40
Perez-Cano HJ, Garnica-Hayashi RE, Zenteno JC (2009) CHM gene molecular analysis and X-chromosome inactivation pattern determination in two families with choroideremia. Am J Med Genet A 149A:2134–2140
Plenge RM, Hendrich BD, Schwartz C et al (1997) A promoter mutation in the XIST gene in two unrelated families with skewed X-chromosome inactivation. Nat Genet 17:353–356
Reese BE, Galli-Resta L (2002) The role of tangential dispersion in retinal mosaic formation. Prog Retin Eye Res 21:153–168
Reese BE, Tan SS (1998) Clonal boundary analysis in the developing retina using X-inactivation transgenic mosaic mice. Semin Cell Dev Biol 9:285–292
Renault NK, Dyack S, Dobson MJ et al (2007) Heritable skewed X-chromosome inactivation leads to haemophilia A expression in heterozygous females. Eur J Hum Genet 15:628–637
Rodriguez FJ, Rodriguez A, Mendoza-Londono R et al (2005) X-linked retinoschisis in three females from the same family: a phenotype-genotype correlation. Retina 25:69–74
Sharp A, Robinson D, Jacobs P (2000) Age- and tissue-specific variation of X chromosome inactivation ratios in normal women. Hum Genet 107:343–349
Smallwood PM, Olveczky BP, Williams GL et al (2003) Genetically engineered mice with an additional class of cone photoreceptors: implications for the evolution of color vision. Proc Natl Acad Sci U S A 100:11706–11711
Szamier RB, Berson EL (1985) Retinal histopathology of a carrier of X-chromosome-linked retinitis pigmentosa. Ophthalmology 92:271–278
Vajaranant TS, Seiple W, Szlyk JP et al (2002) Detection using the multifocal electroretinogram of mosaic retinal dysfunction in carriers of X-linked retinitis pigmentosa. Ophthalmology 109:560–568
Vajaranant TS, Fishman GA, Szlyk JP et al (2008) Detection of mosaic retinal dysfunction in choroideremia carriers electroretinographic and psychophysical testing. Ophthalmology 115:723–729
van den Berg IM, Laven JS, Stevens M et al (2009) X chromosome inactivation is initiated in human preimplantation embryos. Am J Hum Genet 84:771–779
Yorifuji T, Muroi J, Uematsu A et al (1998) X-inactivation pattern in the liver of a manifesting female with ornithine transcarbamylase (OTC) deficiency. Clin Genet 54:349–353
Yuodelis C, Hendrickson A (1986) A qualitative and quantitative analysis of the human fovea during development. Vis Res 26:847–855

Chapter 44
A Non-Canonical Role for β-Secretase in the Retina

Qingwen Qian, Sayak K. Mitter, S. Louise Pay, Xiaoping Qi, Catherine Bowes Rickman, Maria B. Grant and Michael E Boulton

Abstract It has long been established that β-Secretase (BACE) plays a critical role in the formation of amyloid plaques in Alzheimer's Disease patients, but it is only recently that the importance of β-secretases in retinal pathophysiology has been recognized. BACE expression is elevated in response to stress, and downregulation results in lysosomal abnormalities and mitochondrial changes. Inhibition of BACE can lead to reduced retinal function, retinal thinning, lipofuscin accumulation and vascular dysfunction in mice. Furthermore, BACE inhibition accelerates choroidal neovascularization (CNV) in mice. We propose that BACE plays an important role in retinal homeostasis and that BACE upregulation in response to stress is a protective measure.

Keywords β-secretase · Retinal degeneration · Choroidal neovascularisation · Retinal pigment epithelium · Lysosomes · Mitochondria · Angiogenesis · Age-related macular degeneration

44.1 Introduction

There are two β-secretase enzymes, BACE1 and BACE2. BACE1 is a 501 amino acid type 1 transmembrane aspartic protease with levels reportedly highest in the brain and pancreas (De Strooper et al. 2010; Zhao et al. 2011). BACE1 catalyzes the rate limiting step in the production of the β-amyloid (Aβ) protein. Amyloid precursor protein (APP) undergoes sequential proteolytic cleavage by BACE1 and γ-secretase to liberate Aβ, which is a consistent feature of amyloid plaques associated with Alzheimer's

M. E. Boulton (✉) · Q. Qian · S. K. Mitter · S. L. Pay · X. Qi · M. B. Grant
Department of Ophthalmology, Indiana University, 980 Walnut Street, R3-426A, Indianapolis, IN 46202, USA
e-mail: mboulton@iupui.edu

S. L. Pay
Department of Medical and Molecular Genetics, Indiana University School of Medicine, Indianapolis, IN 46202, USA
e-mail: slpay@iupui.edu

C. Bowes Rickman et al. (eds.), *Retinal Degenerative Diseases,* Advances in Experimental Medicine and Biology 854, DOI 10.1007/978-3-319-17121-0_44

disease (AD) (Vassar et al. 2009). BACE2 shares approximately 68 % homology with BACE1, but is expressed at low levels in neurons of the brain and does not have the same cleavage activity on APP as BACE1. Studies in animals demonstrate the critical importance of BACE1. Crossing BACE1$^{-/-}$ mice with APP transgenic Tg2576 mice markedly reduces Aβ deposition (Ohno et al. 2004), and BACE RNA interference reduces amyloid Aβ production and neurodegeneration in an APP transgenic mouse model (Singer et al. 2005). BACE1 has therefore emerged as a promising therapeutic target for AD, resulting in the design of numerous BACE1 inhibitors (Vassar et al. 2009; De Strooper et al. 2010). In addition to cleavage of APP, BACE1 also cleaves a growing number of other substrates including vascular endothelial growth factor receptor-1 (VEGFR1), voltage-gated sodium (Na_v) channel β2-subunit ($Na_v\beta_2$) and potassium (K_v) channel subunits KCNE1, KCNE2, neuregulin, interleukin-1 receptor 2 and LDL receptor-related protein (Vassar et al. 2009; Klaver et al. 2010; Cai et al. 2012). Thus, it is likely that BACE has an important physiological role in a number of tissues including the retina. In this review, we summarize the physiological roles of BACE1 and BACE2 in the retina, the implications for BACE1 in retinal degeneration and consider the off target effect of BACE1 inhibitors in the retina.

44.2 Retinal Localization of BACE1 and 2

Although it is widely known that BACE1 is highly expressed in the brain there has been surprisingly little investigation into BACE expression in other tissues even though, for example, BACE 1 appears to be more highly expressed in the pancreas than in the brain (Yan et al. 1999). In the eye, BACE1 and 2 have been detected in the lens, neural retina, retinal pigment epithelium (RPE) and choroid of mice, rats and humans (Li et al. 2003; Cai et al. 2012; Wang et al. 2012). BACE1 expression is observed in all layers of the retina, however, it is strongest in the inner and outer plexiform layers and the retinal vasculature in both mouse and human retinas. Levels of BACE1 in the neural retina are approximately half that observed in the brain. BACE1

C. Bowes Rickman
Departments of Ophthalmology and of Cell Biology, Duke University Medical Center, Durham, NC 27710, USA
e-mail: bowes007@duke.edu

Q. Qian
e-mail: qiank@iupui.edu

S. K. Mitter
e-mail: skmitter@iupui.edu

X. Qi
e-mail: qixi@iupui.edu

M. B. Grant
e-mail: mabgrant@iupui.edu

is weakly expressed in both RPE and the choroid. In contrast, BACE2 is highly expressed in the RPE and choroid where it is over 30 times higher than BACE1, but it is only weakly expressed in the neural retina (Cai et al. 2012; Wang et al. 2012).

The intracellular localization of BACE within retinal cells has also received limited attention. In the brain, BACE primarily localizes to endosomes to facilitate cellular translocation and the necessary acidic pKa for optimal enzyme activity. BACE expression has also been reported in lysosomes but this has been assumed to be part of the degradation pathway. However, studies in retinal cells indicate that BACE1, in addition to localization in endosomes, also associates with mitochondria and lysosomes where it plays a functional role (Qian and Boulton, unpublished).

44.3 The Role of BACE in Retinal Homeostasis and Dysfunction

It is reasonable to infer that since both BACE1 and BACE2 are expressed at high levels in normal retina and choroid, these enzymes play an important functional role in the physiology of the posterior segment. This is supported by studies involving BACE1 knock-down in RPE cell cultures with either pharmacological agents or siRNA which have demonstrated: (a) an increase in lysosomal pH, (b) a decrease in lysosomal enzyme activity, (c) the formation of lipofuscin-like material (Cai et al. 2012) and (d) regulation of mitochondrial integrity (Qian and Boulton, unpublished data). Interestingly, mitochondrial respiratory function has been reported to increase BACE expression in the rat retina (Xiong et al. 2007). BACE1 also plays a critical role in maintaining retinal vascular endothelial cell quiescence by cleaving the ectodomain of VEGFR1 and facilitating negative regulation of angiogenesis (Cai et al. 2012). BACE2 is expressed in pigmented cells, cleaving pigment-cell-specific melanocyte protein (PMEL) to produce amyloid fibrils required for production of melanin by melanocytes (Rochin et al. 2013). However, although highly expressed in the RPE choroid, the physiological importance of BACE2 remains largely unknown.

Elucidation of the role for BACE in retinal dysfunction has come from BACE inhibition studies. BACE1$^{-/-}$ mice exhibit reduced, visual function thinning of the neural retina, atrophic retinal ganglion cells (RGCs), decreased retinal capillary density in both the superficial and deep retinal plexus, a marked increase in lipofuscin and areas of RPE atrophy with thinning of underlying Bruch's membrane compared to age-matched wild type controls (Cai et al. 2012). In support of these findings, Drosophila BACE ortholog knockdown in photoreceptor neurons leads to degeneration of glia (Bolkan et al. 2012). A different, much milder retinal phenotype was observed in BACE2$^{-/-}$ mice in which the overall neural retina appeared normal apart from occasional foci of hyperplasia. However, the choroid was highly disrupted in BACE2$^{-/-}$ mice, which was not observed in BACE1$^{-/-}$ mice. Abnormal melanosome morphology in the RPE was also observed in BACE2$^{-/-}$ mice consistent with the role of BACE2 in melanogenesis (Rochin et al. 2013) and altered melanophore migration is observed in BACE2$^{-/-}$ zebrafish (van Bebber et al. 2013).

BACE1$^{-/-}$BACE2$^{-/-}$ double knockout mice exhibited a retinal phenotype similar to BACE1$^{-/-}$ mice. Since knockout mice can compensate and may not truly represent loss of BACE activity in adult animals, we and others undertook studies in which BACE1 activity was reduced by either siRNA knockdown or chemical inhibitors (May et al. 2011; Cai et al. 2012). This resulted in photoreceptor loss, increased lipofuscin accumulation in the RPE and an acceleration of laser-induced CNV in rodents. These studies strongly support the hypothesis that BACE1 plays a critical role in normal retinal function, and that its inhibition is detrimental. The mechanism remains largely uninvestigated, but may be context-dependent since BACE inhibition has been reported to be neuroprotective to retinal ganglion cells *in vitro* (Yamamoto et al. 2004) while the opposite has been reported *in vivo* (Cai et al. 2012).

44.4 Implications for BACE in AMD and Diabetic Retinopathy

A number of studies over the last decade have suggested that AD shares several clinical and pathological features with age-related macular degeneration (AMD), including the deposition of Aβ (Anderson et al. 2004; Ding et al. 2011). As described earlier BACE1 performs the first of two sequential cleavages of APP in the formation of Aβ. Elevated Aβ levels are associated with aging and senescence of retinal cells (Wang et al. 2012) and anti-amyloid therapy protects against RPE damage and vision loss in a mouse model of AMD (Ding et al. 2011). Interestingly, BACE cleavage of APP is required for glial survival in Drosophila (Bolkan et al. 2012). BACE2 is known to be important to preserve RPE morphology and function (Rochin et al. 2013). However, the increase of Aβ, the product of BACE1 cleavage, also results in an increase in the paracellular permeability of RPE cells in AD patients (Kim et al. 2012; Cao et al. 2013), suggesting that reduced RPE barrier function may result in accumulation of BACE inhibitors in the inner retina, augmenting their effects on BACE1.

Oxidative stress, a risk factor in both AMD and diabetic retinopathy (DR), is associated with increased BACE levels in a variety of retinal and non-retinal cells types (Xiong et al. 2007; Zhu et al. 2009; Parada et al. 2013; Qian and Boulton unpublished). A significant feature of retinal disease is cell death, with acellular capillaries a feature of DR and RPE cell loss a hallmark of geographic atrophy in AMD. The contribution of BACE to apoptosis is controversial. Some studies show that an increase of BACE1 and Aβ leads to apoptosis, whereas other studies have suggested that Aβ increase has no effect on apoptosis. BACE1 activity and protein levels have been shown to be increased 31 and 67 %, respectively, in ischemic cortical extracts, compared with contralateral cortical extracts and elevated BACE colocalizes with TUNEL-positive cells in ischemic regions (Wen et al. 2004). Caspase 3 levels increase with Aβ level in rats with optic nerve transection (Zhao et al. 2011) and BACE2 can protect against caspase 3-dependent apoptosis in other cell types (Li et al. 2001). A balance between BACE1 and BACE2 may be required to protect against apoptosis in response to oxidative stress in normal cellular function. Confirmation of the role of BACE in retinal cell death requires further investigation.

BACE1 also has a potential role in the regulation of aberrant neovascularization such as occurs in wet AMD and proliferative DR. Pigment epithelium derived factor (PEDF) is a potent anti-angiogenic factor, capable of inhibiting the pro-angiogenic effect of vascular endothelial growth factor (VEGF) (Cai et al. 2011). Interestingly, PEDF induces a time-dependent, six-fold increase in the levels of BACE1 in cultured retinal endothelial cells, but has no effect on BACE1 expression in RPE cells. Inhibition of BACE1 blocks the inhibitory effect of PEDF on VEGF-induced angiogenesis, both *in vitro* and in a laser-induced CNV mouse model. It appears that BACE1 plays a critical role in the PEDF-induced ectodomain cleavage of VEGFR1, which is required for the regulation of angiogenesis (Cai et al. 2012). Therefore, it appears likely that BACE plays a critical role in maintaining vascular quiescence.

44.5 Conclusions and Future Directions

Given the significant expression of BACE in the retina and choroid it is surprising that so little research has been undertaken to determine the role that BACE1 and 2 play in pathophysiology. This is, however, now beginning to be addressed and it is evident that BACE is associated with maintaining retinal pathophysiology and that its upregulation in response to stress may reflect a protective mechanism. The observation that BACE plays an important role in retinal health strongly advises caution in the development of BACE inhibitors for AD patients. Further research is required to delineate the role of BACE in retinal maintenance and the mechanisms by which it can regulate lysosomal and mitochondrial function. Furthermore, it is important to determine the role BACE plays in retinal pathologies such as AMD and DR and whether BACE expression changes are cause or consequence of these diseases (Fig. 44.1).

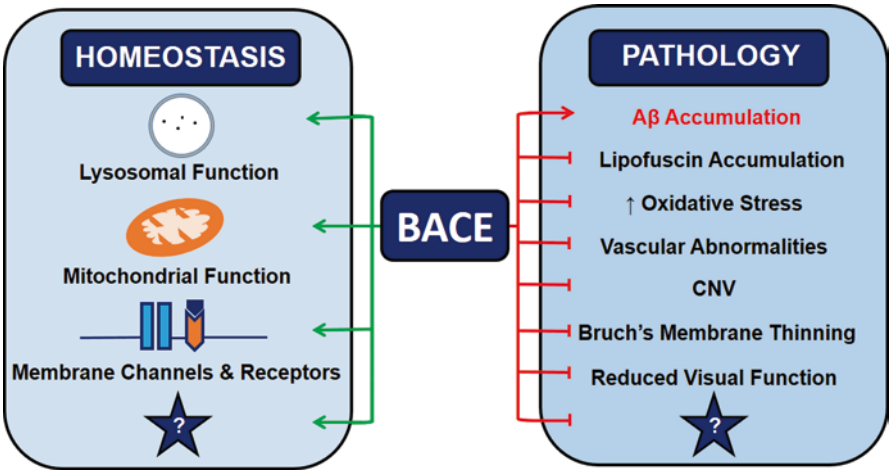

Fig. 44.1 The diagram summarizing the role of BACE in retinal homeostasis and pathology. *Arrows* indicate functional targets of BACE. *Blind ending lines* indicate pathological response following BACE inhibition

Acknowledgements MEB is supported by NIH EY018358; NIH EY019688; AHAF M2009024, BIMR 1309; RPB Unrestricted Award and CBR by EY019038.

References

Anderson DH, Talaga KC, Rivest AJ et al (2004) Characterization of beta amyloid assemblies in drusen: the deposits associated with aging and age-related macular degeneration. Exp Eye Res 78:243–256

Bolkan BJ, Triphan T, Kretzschmar D (2012) β-secretase cleavage of the fly amyloid precursor protein is required for glial survival. J Neurosci 32:16181–16192

Cai J, Wu L, Qi X et al (2011) PEDF regulates vascular permeability by a γ-secretase-mediated pathway. PloS ONE 6:e21164

Cai J, Qi X, Kociok N et al (2012) β-Secretase (BACE1) inhibition causes retinal pathology by vascular dysregulation and accumulation of age pigment. EMBO Mol Med 4:980–991

Cao L, Wang H, Wang F et al (2013) Aβ-induced senescent retinal pigment epithelial cells create a proinflammatory microenvironment in AMD. Invest Ophthalmol Vis Sci 54:3738–3750

De Strooper B, Vassar R, Golde T (2010) The secretases: enzymes with therapeutic potential in Alzheimer disease. Nat Rev Neurol 6:99–107

Ding JD, Johnson LV, Herrmann R et al (2011) Anti-amyloid therapy protects against retinal pigmented epithelium damage and vision loss in a model of age-related macular degeneration. Proc Natl Acad Sci U S A 108:E279–E287

Kim JH, Lee SJ, Kim KW et al (2012) Oxidized low density lipoprotein-induced senescence of retinal pigment epithelial cells is followed by outer blood-retinal barrier dysfunction. Int J Biochem Cell Biol 44:808–814

Klaver DW, Wilce MC, Cui H et al (2010) Is BACE1 a suitable therapeutic target for the treatment of Alzheimer's disease? Current strategies and future directions. Biol Chem 391:849–859

Li Y, Liu YW, Cordell B (2001) Novel functional assay for proteases and modulators. Application in beta-secretase studies. Mol Biotechnol 18:1–10

Li G, Percontino L, Sun Q et al (2003) Beta-amyloid secretases and beta-amloid degrading enzyme expression in lens. Mol Vis 9:179–183

May PC, Dean RA, Lowe SL et al (2011) Robust central reduction of amyloid-β in humans with an orally available, non-peptidic β-secretase inhibitor. J Neurosci 31:16507–16516

Ohno M, Sametsky EA, Younkin LH et al (2004) BACE1 deficiency rescues memory deficits and cholinergic dysfunction in a mouse model of Alzheimer's disease. Neuron 41:27–33

Parada E, Egea J, Buendia I et al (2013) The microglial α7-acetylcholine nicotinic receptor is a key element in promoting neuroprotection by inducing heme oxygenase-1 via nuclear factor erythroid-2-related factor 2. Antioxid Redox Signal 19:1135–1148

Rochin L, Hurbain I, Serneels L et al (2013) BACE2 processes PMEL to form the melanosome amyloid matrix in pigment cells. Proc Natl Acad Sci U S A 110:10658–10663

Singer O, Marr RA, Rockenstein E et al (2005) Targeting BACE1 with siRNAs ameliorates Alzheimer disease neuropathology in a transgenic model. Nat Neurosci 8:1343–1349

van Bebber F, Hruscha A, Willem M et al (2013) Loss of Bace2 in zebrafish affects melanocyte migration and is distinct from Bace1 knock out phenotypes. J Neurochem 127:471–481

Vassar R, Kovacs DM, Yan R et al (2009) The beta-secretase enzyme BACE in health and Alzheimer's disease: regulation, cell biology, function, and therapeutic potential. J Neurosci 29:12787–12794

Wang J, Ohno-Matsui K, Morita I (2012) Elevated amyloid β production in senescent retinal pigment epithelium, a possible mechanism of subretinal deposition of amyloid β in age-related macular degeneration. Biochem Biophys Res Commun 423:73–78

Wen Y, Onyewuchi O, Yang S et al (2004) Increased beta-secretase activity and expression in rats following transient cerebral ischemia. Brain Res 1009:1–8

Xiong K, Cai H, Luo XG et al (2007) Mitochondrial respiratory inhibition and oxidative stress elevate beta-secretase (BACE1) proteins and activity *in vivo* in the rat retina. Exp Brain Res 181:435–446

Yamamoto R, Yoneda S, Hara H (2004) Neuroprotective effects of beta-secretase inhibitors against rat retinal ganglion cell death. Neurosci Lett 370:61–64

Yan R, Bienkowski MJ, Shuck ME et al (1999) Membrane-anchored aspartyl protease with Alzheimer's disease beta-secretase activity. Nature 402:533–537

Zhao TT, Li YQ, Tang LS et al (2011) Effect of Bak Foong Pills on the expression of β-amyloid in rat retina with optic nerve transection. Int J Ophthalmol 4:58–61

Zhu X, Zhou W, Cui Y et al (2009) Muscarinic activation attenuates abnormal processing of beta-amyloid precursor protein induced by cobalt chloride-mimetic hypoxia in retinal ganglion cells. Biochem Biophys Res Commun 384:110–113

Chapter 45
The Consequences of Hypomorphic RPE65 for Rod and Cone Photoreceptors

Marijana Samardzija, Maya Barben, Philipp Geiger and Christian Grimm

Abstract RPE65 is essential for both rod- and cone-mediated vision. So far, more than 120 disease-associated mutations have been identified in the human *RPE65* gene. Differential clinical manifestations suggested that some patients suffer from null mutations while others retain residual RPE65 activity and some useful vision. To understand the mechanism of retinal degeneration or dysfunction caused by such hypomorphic RPE65 alleles, we generated an $Rpe65^{R91W}$ knock-in mouse (*R91W*) that expresses a mutant RPE65 protein with reduced function. Data obtained suggested that the *R91W* mouse is highly suitable to study the impact of RPE65 insufficiency on rod pathophysiology. To study the impact on cones, we combined the *R91W* with the $Nrl^{-/-}$ mouse that develops an all-cone retina. Here we summarize the consequences of hypomorphic RPE65 function (reduced 11-*cis*-retinal synthesis) for rod and cone pathophysiology.

Keywords RPE65 · Retina · Photoreceptors · Cones · Nrl · Dystrophy · Blindness · Degeneration · Mouse model · R91W

45.1 Introduction

Retinal pigment epithelial protein RPE65 is essential for the regeneration of 11-*cis*-retinal—the chromophore of both cone and rod visual pigments. Photoisomerisation of 11-*cis*-retinal results in the dissociation of all-*trans*-retinal from the opsin molecule. The restoration of light sensitivity of the bleached opsin requires regeneration

M. Samardzija (✉) · M. Barben · P. Geiger · C. Grimm
Laboratory for Retinal Cell Biology, Department of Ophthalmology, University of Zurich, Wagistr. 14, 8952 Schlieren, Switzerland
e-mail: marijana.samardzija@usz.uzh.ch

M. Barben
e-mail: maya.barben@uzh.ch

P. Geiger
e-mail: philipp.geiger@bluewin.ch

C. Grimm
e-mail: cgrimm@opht.uzh.ch

C. Bowes Rickman et al. (eds.), *Retinal Degenerative Diseases,* Advances in Experimental Medicine and Biology 854, DOI 10.1007/978-3-319-17121-0_45

of 11-*cis*-retinal through an enzymatic pathway termed the visual cycle. RPE65 acts in this cycle as an isomerohydrolase catalyzing the hydrolysis of all-*trans*-retinol and subsequently the isomerization into 11-*cis*-retinol (Jin et al. 2005; Moiseyev et al. 2005; Redmond et al. 2005). Mutations in *RPE65* lead to autosomal recessive dystrophies ranging from Leber congenital amaurosis to Retinitis Pigmentosa (Marlhens et al. 1997; Morimura et al. 1998). Recently, however, a dominant-acting mutation was also reported in RPE65 patients (Bowne et al. 2011). Based on the clinical picture some mutations are null, while some are hypomorphic and allow partial RPE65 activity leading to reduced but detectable vision in affected patients. Mouse models exist to mimic both situations in patients, with *Rpe65*$^{-/-}$ (Redmond et al. 1998) and *rd12* (Pang et al. 2005) mice being null mutants, and *R91W* (Samardzija et al. 2008) mice (see below) representing a group of patients with a milder phenotype and remnant visual function. Here we discuss the consequences of the hypomorphic RPE65^{R91W} protein for rod and cone function, and retinal pathology in general.

45.2 R91W

Patients with an amino acid substitution at position 91 (R91W) in the *RPE65* gene have useful cone-mediated vision in the first decade of life (El Matri et al. 2006) suggesting partial activity of the mutant RPE65^{R91W} protein. To understand the retinal pathophysiology caused by the mutant RPE65 protein, we generated and analyzed the *R91W* knock-in mouse (Samardzija et al. 2008). Consistent to the assumed diminished enzymatic activity of mutant RPE65^{R91W} in patients, the *R91W* mice exhibit very low chromophore levels—accounting for less than 10% of wild-type levels. The low chromophore content is a direct result of the mutant RPE65^{R91W} protein which (a) has severely reduced enzymatic activity, (b) is mislocalized and (c) is expressed at much lower levels than *wt* (Takahashi et al. 2006; Samardzija et al. 2008). It was previously shown that reduction of RPE65 protein levels directly influences rhodopsin regeneration kinetics; i.e. less RPE65 means that less 11-*cis*-retinal can be synthetized in a given period (Wenzel et al. 2003). All of these factors lead to the severely impaired synthesis of 11-*cis*-retinol resulting in minute amounts of 11-*cis*-retinal chromophore and accumulation of retinyl ester substrate in the retinal pigment epithelium of *R91W* mice (Samardzija et al. 2008). Maximal 11-*cis*-retinal amount recovered after 24 h dark-adaptation in *R91W* mice corresponded to 6% of *wt* levels (Samardzija et al. 2008). Even after prolonged dark-adaptation—adult mice were placed for days in darkness—rhodopsin levels were still below 10% of normal. Only mice that were born and kept for 24 weeks in complete darkness had rhodopsin levels 94.2 ± 11.8 pmol per eye, which is 20% of normal levels (unpublished data).

Figure 45.1a, b shows retinal morphology of wild-type and *R91W* mice. The *R91W* mutation causes slow but progressive retinal degeneration, which is characterized by the initial rapid loss of cones that is followed by a slow rod photo-

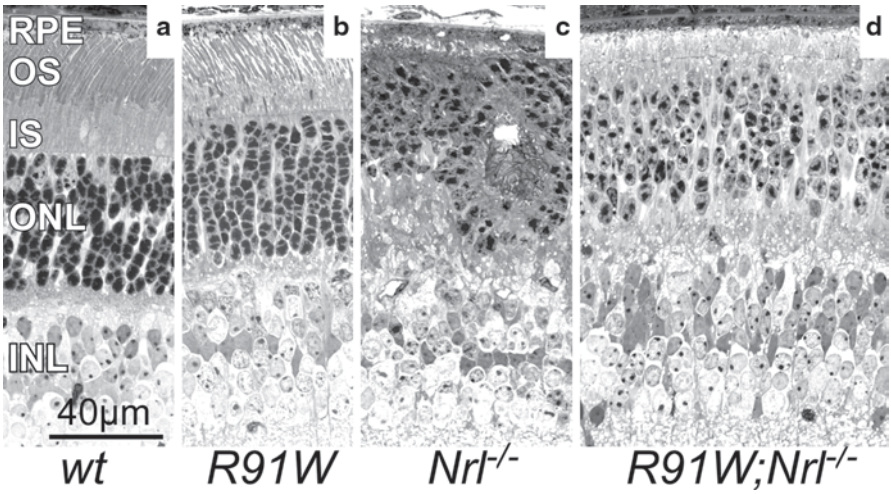

Fig. 45.1 Morphological consequences of hypomorphic RPE65 on rods and cones. *R91W* mice show reduced numbers of cone photoreceptor nuclei and a pronounced disorganization of rod outer segments already at 4 weeks of age. The functional all-cone retinas of 6 week-old *R91W;Nrl*$^{-/-}$ mice have a normal layering and better preserved cone outer segments than age-matched single mutant *Nrl*$^{-/-}$ mice

receptor death (Samardzija et al. 2008, 2009). Dark-adapted electroretinography (ERG) responses were almost undetectable but strong light-adapted responses initially suggested better preservation of the cone function in *R91W* mice (Samardzija et al. 2008). This would have been in line with the human pathology caused by the R91W mutation: night blindness and retention of useful color vision in younger patients. However, upon closer inspection of crossbreeds between *R91W*, *Rho*$^{-/-}$ and *Gnat1*$^{-/-}$ mice, generated to specifically segregate rod- from cone-mediated function, it became evident that *R91W* mice cannot generate significant cone-driven responses (Samardzija et al. 2009). Namely, the small amount of chromophore found in the rod-dominated retina of *R91W* mice is utilized almost exclusively by rods and not by cones. Since rods outnumber cones roughly by 20:1 (Carter-Dawson and LaVail 1979) and maximal levels of chromophore regenerated never exceeds 10%, rod photoreceptors in *R91W* mice may simply have a higher chance to acquire the scarce chromophore. Rods may thus act as 'chromophore trap' preventing 11-*cis*-retinal delivery to cones. Cone opsin mislocalization in *R91W*, a known consequence of chromophore insufficiency (Rohrer et al. 2005), further supports such conclusion (Samardzija et al. 2009). The final proof that under limiting conditions the chromophore ends up in rods rather than in cones came from *R91W;Gnat1*$^{-/-}$ double mutant mice. *Gnat1*$^{-/-}$ mice have a morphologically normal retina but lack rod transducin alpha and therefore have non-functional rods (Calvert et al. 2000). The lack of any photopic and scotopic responses in *R91W*;*Gnat1*$^{-/-}$ mice suggests that their cones have no access to the chromophore and that the function detected in single mutant *R91W* mice indeed originated from rods. This was further confirmed

in *R91W*;*Gnat1*$^{-/-}$;*Rho*$^{-/-}$ triple mutant mice in which a clear ERG response was recorded that could only have been generated by cones. Obviously, physical removal of the rod opsin eliminated the chromophore trap allowing 11-*cis*-retinal to reach cones and restore cone function in *R91W*;*Gnat1*$^{-/-}$;*Rho*$^{-/-}$ mice.

Considering that the rod-cone ratio in the human macula is distinctive from the rest of the retina, the results obtained in *R91W* mice most likely phenocopy the situation in the peripheral retina of patients suffering from hypomorphic RPE65. As the mice lack a cone-rich macular region we decided to analyze the consequences of the *R91W* mutation by using the all-cone *Nrl*$^{-/-}$ mouse (Mears et al. 2001).

45.3 R91W;Nrl$^{-/-}$

The lack of neural retina leucine zipper (NRL) transcription factor during mouse retinal development drives all photoreceptor progenitors towards a cone cell fate (Mears et al. 2001). Functionally, rod-like behavior is suppressed and a super-normal light-adapted ERG is detected in *Nrl*$^{-/-}$ mice. The *Nrl*$^{-/-}$ retina is populated by a surplus of S-cones while M-cones seem to retain normal number. However, retinal morphology of *Nrl*$^{-/-}$ mice is dysmorphic and characterized by formation of rosette-like structures within the cone photoreceptor layer (Fig. 45.1c). Cone photoreceptors in *Nrl*$^{-/-}$ mice degenerate with time and rosettes are lost in older mice. We and others reported normal photoreceptor layering in *Rpe65*$^{-/-}$;*Nrl*$^{-/-}$, which, along with other evidence, suggested that rosettes may arise from normal levels of chromophore supplied by wild-type RPE65 (Wenzel et al. 2007; Feathers et al. 2008; Kunchithapautham et al. 2009). As *Rpe65*$^{-/-}$;*Nrl*$^{-/-}$ mice lack cone function, they cannot be used to test treatment options to prevent cone loss on a functional level. To reduce chromophore supply to the cones and to generate a mouse model to study the effects of the hypomorphic R91W mutation in an all-cone environment, which should represent the situation found in the macular region of patients suffering from this mutation, we crossbred *R91W* and *Nrl*$^{-/-}$ mice. Owing to reduced (3 % of wt) but detectable levels of chromophore, the resulting *R91W;Nrl*$^{-/-}$ double mutant mouse had a normally layered retinal structure without rosettes (Fig. 45.1d) and preserved retinal function (Samardzija et al. 2014). It is interesting to note that the all-cone retina of *R91W;Nrl*$^{-/-}$ mice is relatively stable with only very slow degeneration despite the severely reduced chromophore levels (Samardzija et al. 2014). Under similar—low chromophore—conditions, cone opsin is mislocalized and cones degenerate rapidly in the rod-dominated retina of *R91W* and even faster in retinas of *Rpe65*$^{-/-}$ mice that lack the chromophore (Samardzija et al. 2009). Previous studies suggested the importance of the chromophore for proper cone opsin trafficking and that cone opsin mislocalization detected in synaptic terminals in both *R91W* and *Rpe65*$^{-/-}$ mice can be corrected by different means of chromophore supplemetation (Rohrer et al. 2005; Znoiko et al. 2005; Fan et al. 2006; Zhang et al. 2008; Kunchithapautham et al. 2009; Samardzija et al. 2009; Kostic et al. 2011). The lack of cone opsin mislocalization in *R91W;Nrl*$^{-/-}$ suggested that the minute

amounts of chromophore in *R91W;Nrl*$^{-/-}$ are sufficient for proper cone opsin trafficking thereby stabilizing cone cells. Indeed, qualitative comparison of retinal degeneration in *Rpe65*$^{-/-}$*;Nrl*$^{-/-}$ (Wenzel et al. 2007; Kunchithapautham et al. 2009) and *R91W;Nrl*$^{-/-}$ (Samardzija et al. 2014) suggests better preservation of the all-cone retina in the latter. Yet, it is unclear why in the absence of chromophore cones die rapidly in rod-dominant retinas (*Rpe65*$^{-/-}$) but survive much longer in all-cone retinas (*Rpe65*$^{-/-}$;*Nrl*$^{-/-}$).

45.4 Concluding Remarks

Human vision largely depends on cones and the incidence of cone degenerative diseases such as age-related macular degeneration is expected to rise in the near future. The understanding of cone physiology and pathophysiology is urgently needed to develop therapeutic approaches for the preservation of cone-mediated vision in patients. *R91W* knock-in mice mimic many aspects of the human pathology caused by RPE65 insufficiency, complementing the *Rpe65* knock-out mouse model. While *R91W* mice are representative for the situation in the retinal periphery, *R91W;Nrl*$^{-/-}$ mice mimic more closely the situation in the central, cone-rich retina of human patients suffering from hypomorphic RPE65 function. *R91W;Nrl*$^{-/-}$ mice not only allow the investigation of the consequences of disease causing cone-specific mutations in an organized all-cone environment, but their preserved retinal function and retinal morphology should also improve the qualitative and quantitative outcomes of experiments aiming at rescuing cones on a functional level. The mice might especially be suited for neuroprotective studies, gene therapy approaches and above all, for cone cell transplantation experiments to rescue cone vision.

References

Bowne SJ, Humphries MM, Sullivan LS et al (2011) A dominant mutation in RPE65 identified by whole-exome sequencing causes retinitis pigmentosa with choroidal involvement. Eur J Hum Genet 19:1074–1081

Calvert PD, Krasnoperova NV, Lyubarsky AL et al (2000) Phototransduction in transgenic mice after targeted deletion of the rod transducin alpha -subunit. Proc Natl Acad Sci U S A 97:13913–13918

Carter-Dawson LD, LaVail MM (1979) Rods and cones in the mouse retina. I. Structural analysis using light and electron microscopy. J Comp Neurol 188:245–262

El Matri L, Ambresin A, Schorderet DF et al (2006) Phenotype of three consanguineous Tunisian families with early-onset retinal degeneration caused by an R91W homozygous mutation in the RPE65 gene. Graefes Arch Clin Exp Ophthalmol 244:1104–1112

Fan J, Wu BX, Sarna T et al (2006) 9-cis Retinal increased in retina of RPE65 knockout mice with decrease in coat pigmentationt. Photochem Photobiol 82:1461–1467

Feathers KL, Lyubarsky AL, Khan NW et al (2008) Nrl-knockout mice deficient in Rpe65 fail to synthesize 11-cis retinal and cone outer segments. Invest Ophthalmol Vis Sci 49:1126–1135

Jin M, Li S, Moghrabi WN et al (2005) Rpe65 is the retinoid isomerase in bovine retinal pigment epithelium. Cell 122:449–459

Kostic C, Crippa SV, Pignat V et al (2011) Gene therapy regenerates protein expression in cone photoreceptors in Rpe65(R91W/R91W) mice. PLoS ONE 6:e16588

Kunchithapautham K, Coughlin B, Crouch RK et al (2009) Cone outer segment morphology and cone function in the Rpe65-/- Nrl-/- mouse retina are amenable to retinoid replacement. Invest Ophthalmol Vis Sci 50:4858–4864

Marlhens F, Bareil C, Griffoin JM et al (1997) Mutations in RPE65 cause Leber's congenital amaurosis. Nat Genet 17:139–141

Mears AJ, Kondo M, Swain PK et al (2001) Nrl is required for rod photoreceptor development. Nat Genet 29:447–452

Moiseyev G, Chen Y, Takahashi Y et al (2005) RPE65 is the isomerohydrolase in the retinoid visual cycle. Proc Natl Acad Sci U S A 102:12413–12418

Morimura H, Fishman GA, Grover SA et al (1998) Mutations in the RPE65 gene in patients with autosomal recessive retinitis pigmentosa or leber congenital amaurosis. Proc Natl Acad Sci U S A 95:3088–3093

Pang JJ, Chang B, Hawes NL et al (2005) Retinal degeneration 12 (rd12): a new, spontaneously arising mouse model for human Leber congenital amaurosis (LCA). Mol Vis 11:152–162

Redmond TM, Yu S, Lee E et al (1998) Rpe65 is necessary for production of 11-cis-vitamin A in the retinal visual cycle. Nat Genet 20:344–351

Redmond TM, Poliakov E, Yu S et al (2005) Mutation of key residues of RPE65 abolishes its enzymatic role as isomerohydrolase in the visual cycle. Proc Natl Acad Sci U S A 102:13658–13663

Rohrer B, Lohr HR, Humphries P et al (2005) Cone opsin mislocalization in Rpe65-/- Mice: a defect that can be corrected by 11-cis retinal. Invest Ophthalmol Vis Sci 46:3876–3882

Samardzija M, von Lintig J, Tanimoto N et al (2008) R91W mutation in Rpe65 leads to milder early-onset retinal dystrophy due to the generation of low levels of 11-cis-retinal. Hum Mol Genet 17:281–292

Samardzija M, Tanimoto N, Kostic C et al (2009) In conditions of limited chromophore supply rods entrap 11-cis-retinal leading to loss of cone function and cell death. Hum Mol Genet 18:1266–1275

Samardzija M, Caprara C, Heynen SR et al (2014) A mouse model for studying cone photoreceptor pathologies. Invest Ophthalmol Vis Sci

Takahashi Y, Chen Y, Moiseyev G et al (2006) Two point mutations of RPE65 from patients with retinal dystrophies decrease the stability of RPE65 protein and abolish its isomerohydrolase activity. J Biol Chem 281:21820–21826

Wenzel A, Grimm C, Samardzija M et al (2003) The genetic modifier Rpe65Leu(450): effect on light damage susceptibility in c-Fos-deficient mice. Invest Ophthalmol Vis Sci 44:2798–2802

Wenzel A, von Lintig J, Oberhauser V et al (2007) RPE65 is essential for the function of cone photoreceptors in NRL-deficient mice. Invest Ophthalmol Vis Sci 48:534–542

Zhang H, Fan J, Li S et al (2008) Trafficking of membrane-associated proteins to cone photoreceptor outer segments requires the chromophore 11-cis-retinal. J Neurosci 28:4008–4014

Znoiko SL, Rohrer B, Lu K et al (2005) Downregulation of cone-specific gene expression and degeneration of cone photoreceptors in the Rpe65-/- mouse at early ages. Invest Ophthalmol Vis Sci 46:1473–1479

Chapter 46
The Rate of Vitamin A Dimerization in Lipofuscinogenesis, Fundus Autofluorescence, Retinal Senescence and Degeneration

Ilyas Washington and Leonide Saad

Abstract One of the earliest events preceding several forms of retinal degeneration is the formation and accumulation of vitamin A dimers in the retinal pigment epithelium (RPE) and underlying Bruch's membrane (BM). Such degenerations include Stargardt disease, Best disease, forms of retinitis pigmentosa, and age-related macular degeneration (AMD). Since their discovery in the 1990's, dimers of vitamin A, have been postulated as chemical triggers driving retinal senescence and degeneration. There is evidence to suggest that the rate at which vitamin A dimerizes and the eye's response to the dimerization products may dictate the retina's lifespan. Here, we present outstanding questions, finding the answers to which may help to elucidate the role of vitamin A dimerization in retinal degeneration.

Keywords Stargardt · Age-related macular degeneration · AMD · ABCA4 · RPE · Vitamin A · Retinaldehyde · Bisretinoids · Vitamin A dimer · A2E · Lipofuscin · Fundus autofluorescence · Visual cycle

46.1 Introduction: How and where does vitamin A dimerize in the eye?

Vitamin A as retinaldehyde (RAL) (Fig. 46.1-**1**; Note: All numbers in bold, below, refer to Fig. 46.1) (**1**) can dimerize on any primary amine (**2**). The first step involves condensation of RAL on the amine to form a Schiff base (**3**). The second step is the

I. Washington (✉)
Department of Ophthalmology, Columbia University Medical Center,
160 Fort Washington Ave, Eye Research, New York, NY 10032, USA
e-mail: iw2101@columbia.edu

L. Saad
Alkeus Pharmaceuticals, Inc., Boston, MA 02210, USA
e-mail: leonide@alkeus.com

C. Bowes Rickman et al. (eds.), *Retinal Degenerative Diseases,* Advances in Experimental Medicine and Biology 854, DOI 10.1007/978-3-319-17121-0_46

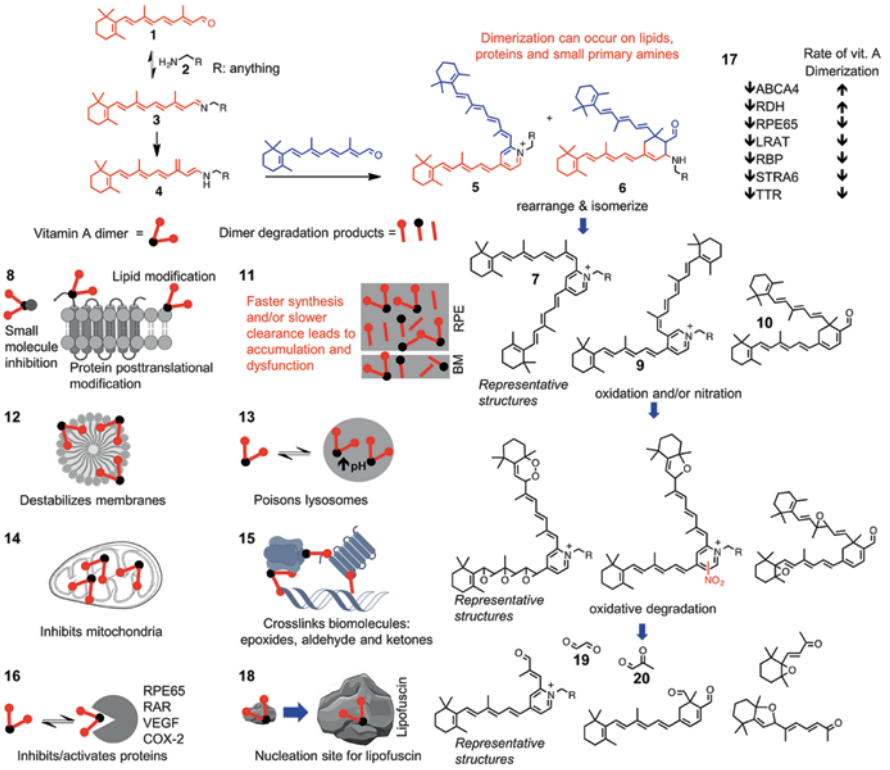

Fig. 46.1 Vitamin A dimers: formation and proposed roles in retinal degeneration. For further description, see the *bolded numbers* in the main text

rate-limiting step and involves rearrangement of the Schiff base to a nucleophilic reactive intermediate (**4**) (Kaufman et al. 2011; Ma et al. 2011). In the third step, the intermediate (**4**) attacks another RAL, leading to two major products: an ambiphilic pyridinium (**5**) and a neutral dimer (**6**). The dimer's name depends on the terminal group (**R**). In addition, the dimers exist as isomers, with different chemical properties. For example, **5** can exist in as many as 15 isomers reflecting the possible configurations of the shorter polyene arm (all-*trans*, 9- or 11-*cis*) and the longer arm (all-*trans*-, 9-, 11-, 13-*cis* and 9,13-di-*cis*). Compound **7** is an example of such an isomer.

Dimerization is more likely to occur where relatively high concentrations of RAL and primary amines exist. In the eye, these two requirements can be met in the retinal disc membranes, where RAL is concentrated due to its binding to densely packed opsin proteins. Dimerization may occur when RAL enters or exits opsin binding sites for any number of reasons. The most abundant primary amine in the disc is phosphatidylethanolamine (PE). As a result, a large proportion of dimers might form on the surface of these lipids (**8**). Dimerization can also occur on primary amines such as lysine residues, on proteins such as opsin (**8**) and on exogenous and endogenous primary amines (such as histamine, amphetamines, dopamines, thyronamines, small molecule therapeutics, etc.) (**8**).

46.2 How Many Vitamin A Dimers are There and What is A2E?

Subsequent to dimerization, dimers **5** and **6** can undergo transformations yielding dozens of dimers with potentially unique chemical and biological properties. After dimerization on PE, hydrolysis of the phosphate ester yields A2E. A2E has been studied the most because it is relatively easy to make, extract and quantify (Penn et al. 2014). This has made A2E an exemplar dimer to study the effects of dimerized vitamin A in retinal health. Although A2E is often used as an indication of dimerization, A2E might not be the most abundant nor toxic dimer.

There are potentially dozens of other dimers, about which less is known. Some of the dimers are *de novo* synthesized on other primary amines, and some result from subsequent chemical transformations such as re-arrangements, deamination, oxidation, isomerization, degradation and nitration of the dimers (Murdaugh et al. 2010). For example, A2E has been suggested to rearrange to form **9**. Deamination of **6**, yields what has been called the ATR-dimer (all-trans retinal dimer, **10**). Polyene chains of the dimers are held in a spatial orientation making them more susceptible to light-induced and/or auto-oxidation (Washington et al. 2005, 2006). For example, one to nine oxygen atoms can be added to any geometric isomer of A2E, resulting in dozens of oxidative derivatives of A2E. Further, dimers may oxidatively degrade giving rise to multiple products. Combining the number of primary amines that vitamin A can dimerize on and the above transformations, countless dimers can be formed and deposited in the RPE and BM (**11**).

46.3 How Might Dimerized Vitamin A be Bad for the Retina?

Several mechanisms have been proposed by which the dimers, mainly A2E, may dysregulate cellular homeostasis (Eldred 1993; Sparrow et al. 2003; Sparrow and Boulton 2005; Sparrow et al. 2012). Mechanisms include: solubilizing lipid membranes (**12**), inactivating lysosomes by increasing lysosomal pH (**13**), and inhibiting the mitochondria (**14**), properties all shared by most cationic detergents. Once dimerized, oxidation of the dimers leads to reactive ketone, aldehyde and epoxide toxicants (**15**) (Yoon et al. 2012). Others mechanisms include, inhibiting RPE65 (Moiseyev et al. 2010), binding to retinoic acid receptors, increasing VEGF (Iriyama et al. 2008) and cyclooxygenase-2 (Lukiw et al. 2006) and covalently modifying biomolecules (Fishkin et al. 2003; Thao et al. 2014) (**8** and **16**). More recent data suggest that dimerized vitamin A act as immunogens triggering chronic inflammation via activation of the complement cascade (Issa et al. 2015; Radu et al. 2014; Zhou et al. 2006).

46.4 If Everyone Accumulates Vitamin A Dimers with Age, Why Doesn't Everyone Develop Retinal Degeneration?

The concentration of dimers is thought to increase with age in the RPE and BM (**11**). This accumulation can result from faster synthesis and/or slower clearance, with age or from an accumulation over a lifetime. The rates of appearance and disappearance of the dimers most likely vary with the retina's milieu, e.g. peripheral vs. central retina, or with the amine the dimer forms on (i.e. lipid, protein, small molecule), however, current knowledge is limited.

Two major factors seemingly influence one's susceptibility to dimer-induced toxicity: (1) the rate of dimerization; and (2) an individual's response to dimers potential insult. Genetics can influence the dimerization rate. For example, genetic mutations that lead to decreased activity of proteins such as ABCA4 and retinaldehyde dehydrogenases (RDH), can increase the rate of dimerization. Severe mutations in *ABCA4* result in accelerated dimerization leading to Stargardt disease. In contrast, decreased activity in RPE65, LRAT, retinol binding protein (RBP), transthyretin (TTR) or the stimulated by retinoic acid 6 (STRA6) protein can all reduce concentrations of RAL and thus its chances of dimerizing (**17**). Subtle differences in the activities of all the above genes can potentially affect dimerization rates. Additional factors that influence the flux of RAL in and out of the disc, such as phagocytosis, daily photon catch, retinal detachments, retinal degeneration, nicotine exposure (Brogan et al. 2005) and certain drugs, may also influence the dimerization rate of vitamin A.

Out of the many potential mechanisms for toxicity, the actual mechanism of dimer-induced retinal death may differ based on genetics and environment. For example, RPE cells with the AMD-predisposing *CFH* haplotype are attacked by complement following exposure to dimers more so than RPE cells with the AMD-protective *CFH* haplotype (Radu et al. 2014). Environmental factors such as dietary carotenoids may protect against dimer toxicity (Bhosale et al. 2009). Retinal degenerations remain multifactorial, and so are the factors that dictate the formation of and response to vitamin A dimerization.

46.5 What is the Relationship Between Dimerized Vitamin A and Lipofuscin?

Lipofuscin is approximately 1000 nm in diameter and thought to be end-stage lysosomes, and accumulate with age in the RPE and other tissues. Vitamin A dimers are small molecules about 2.5 nm in size. In the eye, the dimers can be found as components of lipofuscin (**18**).

Defects in ABCA4 result in increased dimerization and RPE lipofuscin, which can be quantified by electron microscopy. Conversely, defects in RPE65 or LRAT result in decreased dimerization and lipofuscin. Further, restricting dietary intake

of vitamin A in rodents, results in a decrease in lipofuscin. Finally, inhibiting the ability of vitamin A to dimerize, without modifying its concentration or movement through the visual cycle, causes a decrease in lipofuscin (Kaufman et al. 2011; Ma et al. 2011).

Although evidence suggest that dimerization is involved in RPE lipofuscinogenesis, how dimers contribute to lipofuscin formation is not clear. For example, lipofuscin may be formed when dimers act as a lysosomal poison (**13**). Alternatively, oxidative metabolites of dimers may crosslink tissue (**15**), which is also known to increase lipofuscin. These mechanisms of dimer-induced lipofuscinogenesis predict respectively a positive or negative correlation between dimers and lipofuscin granules. Both mechanisms may be at play, making the overall relationship unclear. However, they both predict a positive correlation between the *rate* of dimerization and the volume occupied by lipofuscin granules, as observed in animal models and humans.

46.6 How is Fundus Autofluorescence Related to Lipofuscin and Dimerized Vitamin A?

Historically, tissue autofluorescence (AF) has been used as a measure of lipofuscin granules and as an indicator of aging. However, in the eye, fundus AF is complicated by overlapping fluorescence of dimers. Although the dimers, in particularly A2E, can be incorporated into lipofuscin granules, they do not necessarily reflect the amount of lipofuscin granules. The *rate* of dimerization seems to be positively correlated with abnormal fundus AF but the *concentration* of A2E dimer, typically used to quantify dimerization, might not be correlated with fundus AF or dimerization rate. For example, dimers on protein surfaces might be expected to exhibit stronger AF due to decreased vibrational relaxation of the excited state. Further, dimer-induced tissue cross-linking (**15**) might be a major contributor to fundus AF. Thus, while patterns and intensity of AF may be used to monitor and predict the progression of retinal degenerations, the exact contribution of each molecular entity to AF signals is not understood.

46.7 What Might Cause Toxicity, Lipofuscin Granules or Dimerized Vitamin A?

The majority of proposed mechanisms by which dimers, such as A2E, might induce toxicity, involve the free molecule. It is unclear whether the dimers are confined to lipofuscin granules or if they sample the cytoplasmic space. As A2E is slightly water-soluble—its oxidative adducts and metabolites ever more so—the dimers are probably not confined because of the entropic cost of confinement. Lipofuscin granules are thought to disrupt cell functioning mainly by taking up cytoplasmic space thereby physically inhibiting phagocytosis and by acting as a photosensitizer.

However, free A2E has also been shown to inhibit phagocytosis (Finnemann et al. 2002) and is thought to confer lipofuscin its phototoxic properties.

The observation of dimers in lipofuscin granules could be the result of the dimers acting as a nucleation site for granule formation or that of dimer sequestration into formed granules. Sequestrated dimers would be expected to have reduced toxicity. They would not for example, be as available to display surfactant-like properties (**12**), inhibit lysosomes (**13**), bind to RPE65 or RAR proteins, or modulate Cox-2 expression (**16**). Sequestration would also be expected to protect the polyene chains from degrading into toxic small molecules such as methylglyoxal and glyoxal (**19** and **20**) (Yoon et al. 2012). Recently, Dontsov concluded that "A2E excess in the RPE could be bound by melanosome melanin and lose its [photo-] toxicity" (Dontsov et al. 2013). Taken together, sequestration of dimers into lipofuscin granules might serve to mute their toxicity.

46.8 Is There Any Benefit to Vitamin A Dimerization?

Based on an observation that A2E's precursor, RAL, was more toxic towards a RPE cell line, it was suggested that dimerization might be protective by decreasing the overall amount of free RAL (Maeda et al. 2009). However, upon closer investigation, A2E was found to be more toxic than RAL (Mihai and Washington 2014). As a small fraction of RAL is thought to dimerize at a given time, dimerization is not expected to significantly reduce the flux of RAL and thus is unlikely a mechanism to reduce the concentrations of RAL. Dimerization is not an enzymetically-catalyzed process, suggesting that it has not been directly selected for and is a byproduct of vision. In mice, reduction of the rate of dimerization by 5-fold for 9 months was shown to be safe, demonstrating that the dimerization of vitamin A does not confer any benefit (Issa et al. 2015). To date, vitamin A dimers have only been shown to be detrimental.

Acknowledgements We thank the U.S. National Institutes of Health (1R01EY021207 and 5P30EY019007) and Research to Prevent Blindness (RPB) Inc., New York.

References

Bhosale P, Serban B, Bernstein PS (2009) Retinal carotenoids can attenuate formation of A2E in the retinal pigment epithelium. Arch Biochem Biophys 483:175–181

Brogan AP, Dickerson TJ, Boldt GE et al (2005) Altered retinoid homeostasis catalyzed by a nicotine metabolite: implications in macular degeneration and normal development. Proc Natl Acad Sci U S A 102:10433–10438

Charbel Issa P, Barnard A, Herrmann P et al (2015) Rescue of the Stargardt phenotype in Abca4 knockout mice through inhibition of vitamin A dimerization. Proc Natl Acad Sci doi: 10.1073/pnas.1506960112

Dontsov AE, Koromyslova AD, Sakina NL (2013) Lipofuscin component A2E does not reduce antioxidant activity of DOPA-melanin. Bull Exp Biol Med 154:624–627

Eldred GE (1993) Retinoid reaction products in age related retinal degeneration. In: Hollyfield JG, Anderson RE, LaVail MM (eds) Retinal degeneration: clinical and laboratory applications. Plenum, New York, pp 15–24

Finnemann S, Leung LW, Rodriguez-Boulan E (2002) The lipofuscin component A2E selectively inhibits phagolysosomal degradation of photoreceptor phospholipid by the retinal pigment epithelium. Proc Natl Acad Sci U S A 99:3842–3847

Fishkin N, Jang YP, Itagaki Y et al (2003) A2-rhodopsin: a new fluorophore isolated from photoreceptor outer segments. Org Biomol Chem 1:1101–1105

Iriyama A, Fujiki R, Inoue Y et al (2008) A2E, a pigment of the lipofuscin of retinal pigment epithelial cells, is an endogenous ligand for retinoic acid receptor. J Biol Chem 283:11947–11953

Kaufman Y, Ma L, Washington I (2011) Deuterium enrichment of vitamin A at the C20 position slows the formation of detrimental vitamin A dimers in wild-type rodents. J Biol Chem 286:7958–7965

Lukiw WJ, Mukherjee PK, Cui JG et al (2006) A2E selectively induces cox-2 in ARPE-19 and human neural cells. Curr Eye Res 31:259–263

Ma L, Kaufman Y, Zhang J et al (2011) C20-D3-vitamin A slows lipofuscin accumulation and electrophysiological retinal degeneration in a mouse model of Stargardt disease. J Biol Chem 286:7966–7974

Maeda A, Maeda T, Golczak M et al (2009) Involvement of all-trans-retinal in acute light-induced retinopathy of mice. J Biol Chem 284:15173–15183

Mihai DM, Washington I (2014) Vitamin A dimers trigger the protracted death of retinal pigment epithelium cells. Cell Death Dis 5:e1348

Moiseyev G, Nikolaeva O, Chen Y et al (2010) Inhibition of the visual cycle by A2E through direct interaction with RPE65 and implications in Stargardt disease. Proc Natl Acad Sci U S A 107:17551–17556

Murdaugh LS, Wang Z, Del Priore LV et al (2010) Age-related accumulation of 3-nitrotyrosine and nitro-A2E in human Bruch's membrane. Exp Eye Res 90:564–571

Penn J, Mihai DM, Washington I (2014) Morphologic and physiologic retinal degeneration induced by intravenous delivery of vitamin A dimers in the leporid retina. Dis Model Mech 8:131–8

Radu RA, Hu J, Jiang Z et al (2014) Bisretinoid-mediated complement activation on retinal pigment epithelial cells is dependent on complement factor H haplotype. J Biol Chem 289:9113–9120

Sparrow JR, Boulton M (2005) RPE lipofuscin and its role in retinal pathobiology. Exp Eye Res 80:595–606

Sparrow JR, Gregory-Roberts E, Yamamoto K et al (2012) The bisretinoids of retinal pigment epithelium. Prog Retin Eye Res 31:121–135

Sparrow JR, Fishkin N, Zhou J et al (2003) A2E, a byproduct of the visual cycle. Vision Res 43:2983–2990

Thao MT, Renfus DJ, Dillon J et al (2014) A2E-mediated photochemical modification to fibronectin and its implications to age-related changes in Bruch's membrane. Photochem Photobiol 90:329–334

Washington I, Jockusch S, Itagaki Y et al (2005) Superoxidation of bisretinoids. Angew Chem Int Ed Engl 44:7097–7100

Washington I, Turro NJ, Nakanishi K (2006) Superoxidation of retinoic acid. Photochem Photobiol 82:1394–1397

Yoon KD, Yamamoto K, Ueda K et al (2012) A novel source of methylglyoxal and glyoxal in retina: implications for age-related macular degeneration. PLoS One 7:e41309

Zhou J, Jang YP, Kim SR et al (2006) Complement activation by photooxidation products of A2E, a lipofuscin constituent of the retinal pigment epithelium. Proc Natl Acad Sci 103:16182–7

Chapter 47
Can Vitamin A be Improved to Prevent Blindness due to Age-Related Macular Degeneration, Stargardt Disease and Other Retinal Dystrophies?

Leonide Saad and Ilyas Washington

Abstract We discuss how an imperfect visual cycle results in the formation of vitamin A dimers, thought to be involved in the pathogenesis of various retinal diseases, and summarize how slowing vitamin A dimerization has been a therapeutic target of interest to prevent blindness. To elucidate the molecular mechanism of vitamin A dimerization, an alternative form of vitamin A, one that forms dimers more slowly yet maneuvers effortlessly through the visual cycle, was developed. Such a vitamin A, reinforced with deuterium (C20-D_3-vitamin A), can be used as a non-disruptive tool to understand the contribution of vitamin A dimers to vision loss. Eventually, C20-D_3-vitamin A could become a disease-modifying therapy to slow or stop vision loss associated with dry age-related macular degeneration (AMD), Stargardt disease and retinal diseases marked by such vitamin A dimers. Human clinical trials of C20-D_3-vitamin A (ALK-001) are underway.

Keywords Stargardt · Age-related macular degeneration · AMD · Retinal dystrophies · ABCA4 · Vitamin A · Retinaldehyde · ALK-001 · C20-D_3-vitamin A · Bisretinoids · Vitamin A dimer · A2E · Lipofuscin · Visual cycle

47.1 Introduction

Age-related macular degeneration (AMD) is currently the leading cause of unpreventable blindness and principally affects the elderly with a prevalence of 12 % for those over 80 years of age. Macular dystrophies such as Stargardt disease, Best

L. Saad (✉)
Alkeus Pharmaceuticals, Inc., 21 Drydock Ave, 6th Floor, Boston, MA 02210, USA
e-mail: leonide@alkeus.com

I. Washington
Department of Ophthalmology, Columbia University Medical Center, Eye Research, New York, NY 10032, USA
e-mail: iw2101@columbia.edu

C. Bowes Rickman et al. (eds.), *Retinal Degenerative Diseases,* Advances in Experimental Medicine and Biology 854, DOI 10.1007/978-3-319-17121-0_47

disease and cone-rod dystrophy result in comparable vision loss but are rarer and affect younger individuals. Except for a minority of people—those with neovascular AMD—there are no treatments for any of these conditions.

47.2 Vitamin A, Lipofuscin & Eye Disease

One of mankind's earliest recorded medical treatments, documented on Egyptian papyrus (Kahun ~ 1825 B.C), describes applying ox liver, a source of vitamin A, directly to the eye as a treatment for night blindness. Four thousand years later, vitamin A has been evaluated as a potential therapy for eye diseases such as retinitis pigmentosa, dry eye, Stargardt disease and AMD. The National Eye Institute (NEI) currently recommends oral vitamin A for some forms of retinitis pigmentosa. Conversely, vitamin A, once recommended for Stargardt, is now more widely discouraged. Vitamin A is also less commonly advised for AMD. Despite attempts, vitamin A-based interventions have shown inconsistent results for the prevention of vision loss.

Nevertheless, there is continued interest in the role played by vitamin A to enable or steal vision. For example, genetic impairments that result in mishandling of vitamin A in the retina can lead to accelerated (*ABCA4* defects) or reduced (*RPE65* or *LRAT* defects) amounts of ocular lipofuscin, yet both lead to retinal degeneration. Although lipofuscin's age-dependent increase is a feature consistent with aging and diseased eyes, how and why lipofuscin forms is not understood (See Chap. 46 in this book). Data however seem to indicate the involvement of vitamin A, in particular its ability to dimerize (Issa et al. 2015).

With toxicity demonstrated in models, it is believed that dimerized vitamin A plays an active role in triggering and sustaining retinal degeneration. Decreasing the formation of vitamin A dimers may therefore slow or prevent vision loss in diseases characterized by increased rates of vitamin A dimerization.

47.3 Preventing Vitamin A Dimers Through Alterations of the Visual Cycle

Because dimers are thought to be formed as byproducts of the "visual cycle", the process used by the eye to enable vision (Radu et al. 2003; Maiti et al. 2006; Golczak et al. 2008), molecules designed to slow the cycle, known as visual cycle modulators, could potentially retard the formation of these dimers. Among such molecules, emixustat hydrochloride, a RPE65 inhibitor, which slows the regeneration of rhodopsin, is in Phase 2b clinical trials in geographic atrophy (Dugel et al. 2015). Another approach developed to retard dimerization is to reduce the delivery of vitamin A to the eye, thereby lowering its likelihood to dimerize (Radu et al. 2005). For example, fenretinide, a retinol binding protein (RBP) antagonist, has

been tested in a 246 patient trial in geographic atrophy (Mata et al. 2013). Further, molecules known as "retinal traps" are being researched in hopes of trapping vitamin A to prevent it from dimerizing (Maeda et al. 2012). As the proper function and survival of the retina is contingent upon an adequate supply of vitamin A and upon its unhindered processing by the visual cycle, short-term interference with the cycle can result in visual side effects such as night blindness and impaired dark adaptation, while long term interference might lead to constitutive opsin signaling, photoreceptor death and vision loss as seen in those with genetically impaired visual cycles due to *LRAT, RPE65 or RBP4* defects.

47.4 Can Deuterium Prevent Vitamin A Dimerization?

Vitamin A dimers are formed via a non-enzymatic reaction when two molecules of vitamin A react with an amine (Fig. 47.1a). Although the most abundant amine in the photoreceptors is the lipid phosphatidylethanolamine, dimerization also occurs on other amines of the visual cycle proteins, such as opsin, and potentially on other endogenous and/or exogenous amines (Vollmer-Snarr et al. 2006). To dimerize, a

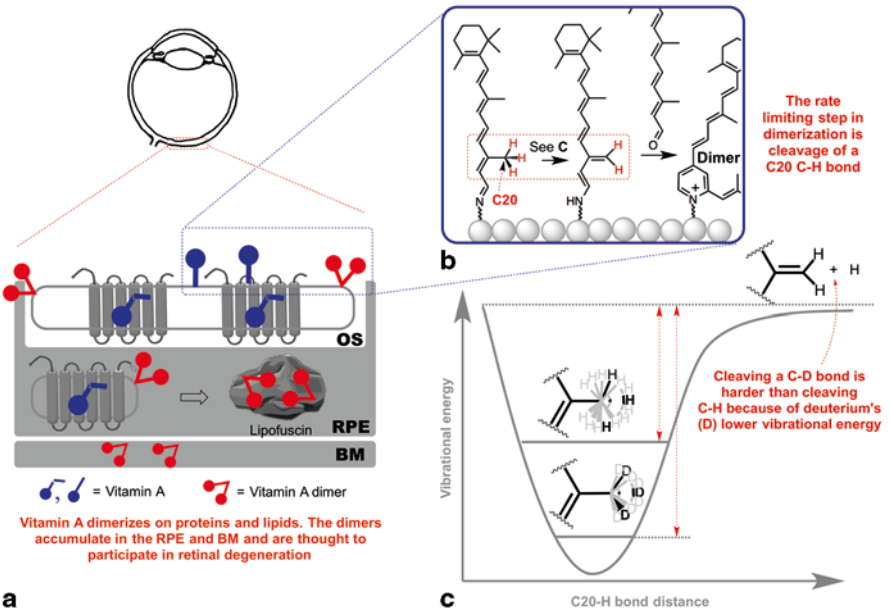

Fig. 47.1 Several forms of retinal degeneration can be characterized by the accumulation of dimerized vitamin A in the RPE and BM followed by the death of the photoreceptors and supporting cells, leading to loss of vision. **a** Vitamin A dimers are formed in the disc membranes of the retina on the surface of lipid membranes and proteins. **b** To dimerize, a carbon-hydrogen at carbon 20 of retinaldehyde must be cleaved. **c** By enriching the C20 hydrogens with deuterium atoms, the vitamin's vibrational energy is lowered. Thus, more energy is required to cleave the bond, impeding dimerization

carbon-hydrogen bond must be broken at the carbon twenty (C20) position of vitamin A (Fig. 47.1b). By substituting hydrogen atoms on C20 with deuteriums, the energy required to break that bond is raised, slowing dimerization (Fig. 47.1c). The potential of this approach has been demonstrated in test tube, wild-type rodents and in a mouse model of Stargardt. In Abca4 knock-out mice given C20-D_3-vitamin A, the amount of vitamin A dimers was reduced to approximately that of wild-type animals raised on non-deuterated vitamin A. Impeding dimerization resulted in reductions in both lipofuscin and fundus autofluoresence, along with a preservation of visual function as measured by electroretinography (Kaufman et al. 2011; Ma et al. 2011; Issa et al. 2015). Notably, the amount of dimerized vitamin A, lipofuscin granules and fundus autofluoresence all decreased the longer animals were given C20-D_3-vitamin A, regardless of whether they were treated from birth or from adulthood. In addition, complement status was found to be dysregulated due to the *Abca4* defect, and administration of C20-D_3-vitamin A prevented this dysregulation. When the animals were returned to their normal vitamin A diet, dimerized vitamin A and fundus autofluoresence increased (Issa et al. 2015). Since vitamin A dimerizes through a non-enzymatic and therefore species-independent process, it is likely that the dimerization will also be slowed in humans by replacing dietary vitamin A with its C20-D_3-vitamin A counterpart.

Deuterium is a stable, non-radioactive, and naturally-occurring isotope of hydrogen. The properties of a carbon-deuterium bond are close to identical to that of a carbon-protonium (the more abundant isotope of hydrogen) bond. However, deuterium contains an extra neutron doubling the mass of protonium. As a result, carbon-deuterium bonds require more energy to break compared to carbon-protonium bonds, therefore chemical reactions involving the breaking of a carbon-deuterium bond will proceed more slowly compared to the same reactions in which a carbon-protonium is broken (Fig. 47.1c). This process is known as “kinetic isotope effect”.

47.5 C20-D_3-vitamin A as a Drug for Macular Degenerations

To effectively reduce vitamin A dimerization, a “sufficiently high” percentage of C20-D_3-vitamin A relative to total vitamin A would need to be reached and maintained in the retina. The higher this percentage, the more dimerization will be impeded. In mice, a diet containing 80 or 95% deuterated vitamin A reduced the concentration of the A2E vitamin A dimer four- (Kaufman et al. 2011; Ma et al. 2011) or fivefold (Issa et al. 2015), respectively, compared to mice fed normal vitamin A.

While direct delivery to the retina could be considered, for example with eyedrops, intravitreal injections, or drug-eluting implants, oral delivery as a pill could improve compliance and convenience. This is particularly true when chronic administration is required in children and the elderly. Oral delivery is also appropriate for vitamin A, absorbed and stored by the body then rapidly taken up by the eye (Mihai et al. 2013).

Swine given oral daily doses of 95% deuterated C20-D_3-vitamin A attained a steady state of 95% deuterated retinaldehyde in the retina after 4 weeks despite consuming dietary beta-carotene (Mihai et al. 2013). These preclinical findings indicate that swapping the retina's vitamin A with C20-D_3-vitamin A is fast relative to the rate of disease progression, and confirm that dietary pro-vitamin A carotenoids do not significantly contribute to the retinol pool when consuming an adequate amount of vitamin A. Nonetheless, how high a percentage of deuterated vitamin A can be achieved in humans remains to be shown.

To prevent vitamin A toxicity (hypervitaminosis A), the total consumption of vitamin A should be kept within known tolerable limits. Adverse events linked to chronic hypervitaminosis A (Myhre et al. 2003) are usually reversible upon discontinuation of vitamin A. While the adult Recommended Dietary Allowance is about 3000 IU per day, vitamin A has been administered for over a year in clinical trials at doses up to 300,000 IU/day with reasonable tolerability (Infante et al. 1991; Alberts et al. 2004). Such 300,000 IU/day doses would however not be suitable for children, pregnant or lactating women, and other populations that might be sensitive or intolerant to vitamin A (Allen and Haskell 2002). Because the deuteriums at the C20 position on vitamin A are non-exchangeable, they are not expected to exchange with hydrogens in the body during deuterated vitamin A metabolism. Finally, a daily dose of 10,000 IU of C20-D_3-vitamin A, a dose commonly found in drug stores, would contain approximately 500 times less deuterium than deuterium naturally present in the average volume of drinking water consumed daily.

Administration of deuterated vitamin A in humans is common when studying vitamin A's pharmacokinetics and metabolism (Reinersdorff et al. 1996). Because none of the known metabolites of vitamin A involve cleavage of the C20 carbon-hydrogen bonds (NCI 1996), the only reaction potentially slowed by C20-D_3-vitamin A should be its aberrant dimerization.

As C20-D_3-vitamin A should have the same biological activity as vitamin A, swapping vitamin A with C20-D_3-vitamin A is not expected to result in a side effect or toxicity profile any different from that of vitamin A. The visual cycle, using the substituted C20-D_3-vitamin A should work seamlessly, as demonstrated in animals, differentiating C20-D_3-vitamin A from alternative approaches aimed at preventing the formation of vitamin A dimers

Hence, C20-D_3-vitamin A could be used as a precise clinical tool to determine the extent to which the dimerization of vitamin A triggers or participates in the progression of retinal degenerations such as Stargardt disease or dry-AMD. If the molecule is capable of modifying the course of such diseases, C20-D_3-vitamin A could also become an intervention to treat these unpreventable currently causes of blindness.

47.6 Conclusion

Retinal degenerations and dystrophies make up a phenotypically and genetically (over 200 associated genes) complex group. A common thread among these degenerative conditions is the enhanced autofluorescence thought to be caused by increased rates of vitamin A dimerization. Evidence gathered over three decades suggest that the dimers are toxic (See Chapter 46) and that reducing their formation may impede the progression of retinal degeneration. A 2-year clinical trial provided human evidence that preventing vitamin A dimerization could slow the progression of late stage dry-AMD (Mata et al. 2013). Nevertheless, establishing a cause-effect relationship between dimers, lipofuscin and vision loss remains an active topic of research. Such a relationship may however only be confirmed through human clinical testing.

Stargardt disease is a rare and seriously debilitating genetic disease marked by the rapid dimerization of vitamin A followed by irreversible vision loss. As the disease is diagnosed early during childhood, an oral prophylactic that could slow disease progression would be of significant benefit. C20-D_3-vitamin A acts as a substitute for vitamin A and prevents its non-enzymatic dimerization. If tolerability of C20-D_3-vitamin A is clinically confirmed and sufficient levels of C20-D_3-vitamin A can be achieved in the blood, there would be reasonable likelihood that the dimerization of vitamin A would be slowed in the human eye. At the time of this writing, Phase 2 clinical trials assessing C20-D_3-vitamin A (ALK-001) are on-going.

Acknowledgements We thank the U.S. National Institutes of Health (1R01EY021207 and 5P30EY019007) and Research to Prevent Blindness (RPB) Inc., New York.

References

Alberts D, Ranger-Moore J, Einspahr J et al (2004) Safety and efficacy of dose-intensive oral vitamin A in subjects with sun-damaged skin. Clin Cancer Res 10:1875–1880

Allen LH, Haskell M (2002) Estimating the potential for vitamin A toxicity in women and young children. J Nutr 132:2907S–2919S

Charbel Issa P, Barnard A, Herrmann P et al (2015) Rescue of the Stargardt phenotype in Abca4 knockout mice through inhibition of vitamin A dimerization. Proc Natl Acad Sci doi: 10.1073/pnas.1506960112

Dugel PU, Novack RL, Csaky KG et al (2015) Phase II, randomized, placebo-controlled, 90-day study of emixustat hydrochloride in geographic atrophy associated with dry age-related macular degeneration. Retina 35:1173–83

Golczak M, Maeda A, Bereta G et al (2008) Metabolic basis of visual cycle inhibition by retinoid and nonretinoid compounds in the vertebrate retina. J Biol Chem 283:9543–9554

Infante M, Pastorino U, Chiesa G et al (1991) Laboratory evaluation during high-dose vitamin A administration: a randomized study on lung cancer patients after surgical resection. J Cancer Res Clin Oncol 117:156–162

Kahun (~ 1825 B.C) Kahun Gynecological Papyrus

Kaufman Y, Ma L, Washington I (2011) Deuterium enrichment of vitamin A at the C20 position slows the formation of detrimental vitamin A dimers in wild-type rodents. J Biol Chem 286:7958–7965

Ma L, Kaufman Y, Zhang J et al (2011) C20-D3-vitamin A slows lipofuscin accumulation and electrophysiological retinal degeneration in a mouse model of stargardt disease. J Biol Chem 286:7966–7974

Maeda A, Golczak M, Chen Y et al (2012) Primary amines protect against retinal degeneration in mouse models of retinopathies. Nature Chem Biol 8:170–178

Maiti P, Kong J, Kim SR et al (2006) Small molecule RPE65 antagonists limit the visual cycle and prevent lipofuscin formation. Biochemistry 45:852–860

Mata NL, Lichter JB, Vogel R et al (2013) Investigation of oral fenretinide for treatment of geographic atrophy in age-related macular degeneration. Retina 33:498–507

Mihai DM, Jiang H, Blaner WS et al (2013) The retina rapidly incorporates ingested C20-D(3)-vitamin A in a swine model. Mol Vis 19:1677–1683

Myhre AM, Carlsen MH, Bohn SK et al (2003) Water-miscible, emulsified, and solid forms of retinol supplements are more toxic than oil-based preparations. Am J Clin Nutri 78:1152–1159

NCI (1996) Clinical development plan: vitamin A. J Cell Biochem Suppl 26:269–307

Radu RA, Mata NL, Nusinowitz S et al (2003) Treatment with isotretinion inhibits lipuscin accumulationin a mouse model of recessive stargardt macular degeneration. Proc Natl Acad Sci U S A 100:4742–4747

Radu RA, Han Y, Bui TV et al (2005) Reductions in serum vitamin A arrest accumulation of toxic retinal fluorophores: a potential therapy for treatment of lipofuscin-based retinal diseases. Invest Ophthalmol Vis Sci 46:4393–4401

Reinersdorff DV, Bush E, Liberato DJ (1996) Plasma kinetics of vitamin A in humans after a single oral dose of [8,9,19-13C]retinyl palmitate. J Lipid Res 37:1875–1885

Vollmer-Snarr HR, Pew MR, Alvarez ML et al (2006) Amino-retinoid compounds in the human retinal pigment epithelium. Adv Exp Med Biol 572:69–74

Chapter 48
Class I Phosphoinositide 3-Kinase Exerts a Differential Role on Cell Survival and Cell Trafficking in Retina

Seifollah Azadi, Richard S. Brush, Robert E. Anderson and Raju V.S. Rajala

Abstract Phosphoinositide 3-kinases (PI3Ks) are a family of lipid kinases that phosphorylates the 3'OH of the inositol ring of phosphoinositides. They are responsible for coordinating a diverse range of cell functions including proliferation, cell survival, degranulation, vesicular trafficking, and cell migration. The PI 3-kinases are grouped into three distinct classes: I, II, and III. Class III PI3K has been shown to be involved in intracellular protein trafficking, whereas class I PI3K is known to regulate cell survival following activation of cell surface receptors. However, studies from our laboratory and others have shown that class I PI3K may also be involved in photoreceptor protein trafficking. Therefore, to learn more about the role of class I and class III P13K in trafficking and to understand the impact of the lipid content of trafficking cargo vesicles, we developed a methodology to isolate trafficking vesicles from retinal tissue. PI3K class I and III proteins were enriched in our extracted trafficking vesicle fraction. Moreover, levels of ether phosphatidylethanolamine (PE) and ether phosphatidylcholine (PC) were significantly higher in the trafficking vesicle fraction than in total retina. These two lipid classes have been suggested to be involved with fusion/targeting of trafficking vesicles.

S. Azadi (✉) · R. S. Brush
Departments of Ophthalmology, Dean McGee Eye Institute, University of Oklahoma Health Sciences Center, 608 Stanton L. Young Blvd, 73104 Oklahoma City, OK, USA
e-mail: Seifollah-azadi@ouhsc.edu

R. S. Brush
e-mail: Richard-Brush@ouhsc.edu

R. E. Anderson
Departments of Ophthalmology and Cell Biology, Dean McGee Eye Institute, University of Oklahoma Health Sciences Center, 608 Stanton L. Young Blvd, 73104 Oklahoma City, OK, USA
e-mail: robert-anderson@ouhsc.edu

R. V.S. Rajala
Departments of Cell Biology, Physiology and Ophthalmology, Dean McGee Eye Institute, University of Oklahoma Health Sciences Center, 608 Stanton L. Young Blvd, 73104, Oklahoma City, OK, USA
e-mail: raju-rajala@ouhsc.edu

C. Bowes Rickman et al. (eds.), *Retinal Degenerative Diseases,* Advances in Experimental Medicine and Biology 854, DOI 10.1007/978-3-319-17121-0_48

Keywords Retina · Photoreceptors · Phosphoinositide 3-Kinase · Trafficking · Lipid · Degeneration

48.1 Introduction

Phosphoinositide 3-kinases (PI3Ks) are a family of lipid kinases that catalyze the phosphorylation of D3-hydroxyls in the inositol head group and generate several phosphorylated phosphoinositides (Fruman et al. 1998). These lipid second messengers regulate a diverse range of cell functions including proliferation, cell survival, degranulation, vesicular trafficking, and cell migration. The PI 3-kinases are grouped into three distinct classes: I, II, and III (Leevers et al. 1999). Class III PI3K-generated PI-3P has been previously reported to be involved in the vesicular trafficking of rhodopsin (Chuang et al. 2007), whereas class I PI3K is known to regulate cell survival (Gross and Bassell 2014). However, in *Drosophila,* arrestin binds to class I PI3K-generated PI-3,4,5-P_3, which appears to regulate its movement their photoreceptor cells (Lee et al. 2003). Studies from our laboratory on the conditional deletion of class I PI3K (deletion of regulatory p85α-subunit of PI3K) in rods resulted in the delay of light-dependent arrestin trafficking from the inner segment to the outer segment of rod photoreceptors (Ivanovic et al. 2011a). Interestingly, conditional deletion of class I PI3K in cones resulted in age-related cone degeneration (Ivanovic et al. 2011b). These studies suggest that class I PI3K may be involved in both cell survival and protein trafficking in retinal photoreceptor cells. However, the detailed mechanism of PI3K trafficking and the role of this protein family in the targeting of other retinal proteins are poorly understood.

In this chapter, we describe a novel methodology for purifying trafficking vesicles from bovine retinal tissue. We provide evidence that both class I and III PI3K are present in trafficking vesicles. Moreover, we report the results of our analysis of the lipid contents of the trafficking vesicle-enriched fraction, which show an increase in ether lipids in the major phospholipid classes.

48.2 Materials and Methods

48.2.1 Fractionation of Bovine Retina Followed by Sedimentation Using a Continuous 30–50 % Sucrose Gradient

One bovine retina was lysed in 2 ml hypotonic buffer (HB) containing 20 mM Hepes (pH 7.4) and a protease inhibitor (Roche). Retinal lysate was then centrifuged for 10 min at 1000 g. The pellet contained nuclei and unbroken cells (P1K). The supernatant (S1K) was centrifuged one more time to ensure removal of large particles and the S1K was centrifuged at 11,000 g, which pelleted all the heavy

membranes, including rough ER, rough Golgi, and ribosomes (P11K). This fraction also contained the photoreceptor outer segments. The supernatant (S11K) was further centrifuged for 20 min at 50,000 g. The pellet containing light membranes such as smooth ER, newly synthesized outer segment discs, and trafficking vesicles, was washed twice with the same HB. Using a gradient maker (Bio-Rad), we generated a continuous 30–50 % sucrose gradient, and the homogenized P50K pellet was placed on the top of this gradient and centrifuged for 15 h at 25,000 g. The gradient was fractionated into 26 samples using an Econo Gradient Pump kit (Bio-Rad) and each was examined by acrylamide SDS gel electrophoresis. Western blotting was performed using specific antibodies against p85α-subunit of class I PI3K (Upstate Biotechnology, Lake Placid, NY, 1/2000), catalytic subunit of class III PI3K (Cell Signaling, Beverly, MA, 1/2000), rab11 (Sigma, St. Louis, MO,1/1000), VAMP2 (Gottingen, Germany, 1/1000), syntaxin3 (Synaptic System, Gottingen, Germany, 1/1000), calretinin (Sigma, St. Louis, MO, 1/2000), and GM130 (Sigma, St. Louis, MO, 1/2000). An aliquot of the P50K pellet was fixed and cross-linked to a glass slide for immunohistochemistry (IHC). Antibodies against class I PI3K and Rab11 (a trafficking marker) were applied to show that the fraction was enriched in trafficking markers. Tandem mass spectrometry analysis of the lipid content of the trafficking vesicle fraction was performed as described previously (Bennett et al. 2014).

48.3 Results

48.3.1 Protein and Lipid Characterization of Trafficking Vesicles from Bovine Retina: Enrichment and Further Purification of Trafficking Vesicles from Bovine Retina

Our methodology successfully enabled us to enrich the trafficking vesicles from whole bovine retina lysates. Figure 48.1 illustrates the different fractions obtained in this procedure. We hypotonically lysed bovine retina using a hypotonic buffer, followed by several centrifugations to isolate different fractions (see Materials and Methods). The P50K contained light membranes, but also contained particles of other organelles, which were impossible to avoid at this stage. Therefore, we further purified the P50K fraction using a 30–50 % continuous sucrose gradient. As illustrated in Fig. 48.2, a peak of trafficking markers, vesicle-associated membrane protein 2 (VAMP2) and rab11, were enriched in fraction 20 (F20). Syntaxin3 was also strongly enriched in this fraction (not shown). Both Class I and Class III PI3K were detected in P50K (Fig. 48.2). The Class III antibody also detected two other proteins with lower molecular weights (Fig. 48.2a), which may be nonspecific. The P50K was fixed and cross-linked to a glass slide for IHC. We applied antibodies against PI3K class I as well as a known trafficking marker, Rab11, to show that the fraction was enriched in trafficking markers (Fig. 48.2b). We found a co-localization of class I PI3K with Rab11, suggesting the presence of class I PI3K in trafficking vesicles (Fig. 48.2).

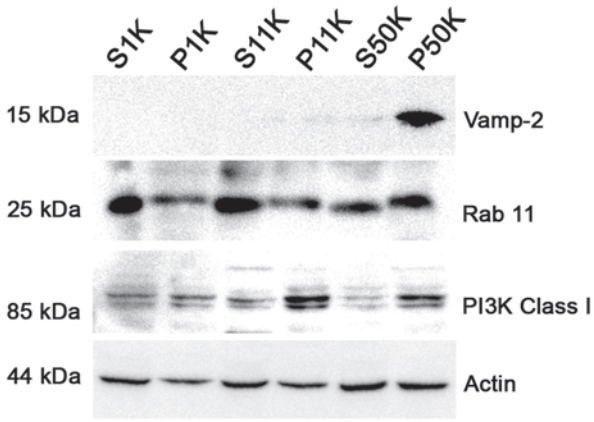

Fig. 48.1 Fractionation of bovine retina using differential centrifugation. Hypotonically lysed retina was subjected to subsequent rounds of centrifugation. P50K contains the putative particles of trafficking cargo vesicles

48.3.2 Ether-PC or Ether-PE in the Enriched Trafficking Vesicle Fraction

The importance of ether lipids in the structure and function of trafficking cargo vesicles has frequently been proposed (Thai et al. 2001; Kuerschner et al. 2012). We therefore performed a detailed analysis on the lipid content of purified trafficking vesicles. Tandem mass spectrometry analysis showed higher levels of PE- and PC-ether species in the trafficking vesicle fraction than in the bovine total control retinas (32 %, $p < 0.001$; Fig. 48.3). Individual species of ether–PE, including 34:01, 36:01, 36:02, 36:04, and 38:03 showed a greater increase in our trafficking vesicle fraction. Although we could not differentiate between alkyl and vinyl ethers by MS, based on a large literature, we predict that the PC ethers are alkyl and the PE ethers are vinyl. The total amount of ether-PC was 21 % higher in P50K than in total retina ($p < 0.01$). Individual ether-PC showed significant increases, including 34:02, 36:00, 36:01, and 38:02, and were more abundant in P50K than in total retina.

48.4 Discussion

The lack of proper protein targeting in the retina is known to cause several degenerative diseases (Hunt et al. 2010). However, the molecular mechanisms executing the trafficking pathways are still ambiguous and need to be thoroughly evaluated. This ambiguity is in large part due to the structural differences between photoreceptor and other cell types (Sung and Chuang 2010). VAMP2 is the main component of a protein complex involved in the active, ATP-required docking and/or fusion of vesicles with the target membranes. VAMP2, SNAPs (Synaptosome-Associated Proteins), and syntaxin are the three main components of this protein complex, the assembly of which results in active exocytosis (Caceres et al. 2014). We found

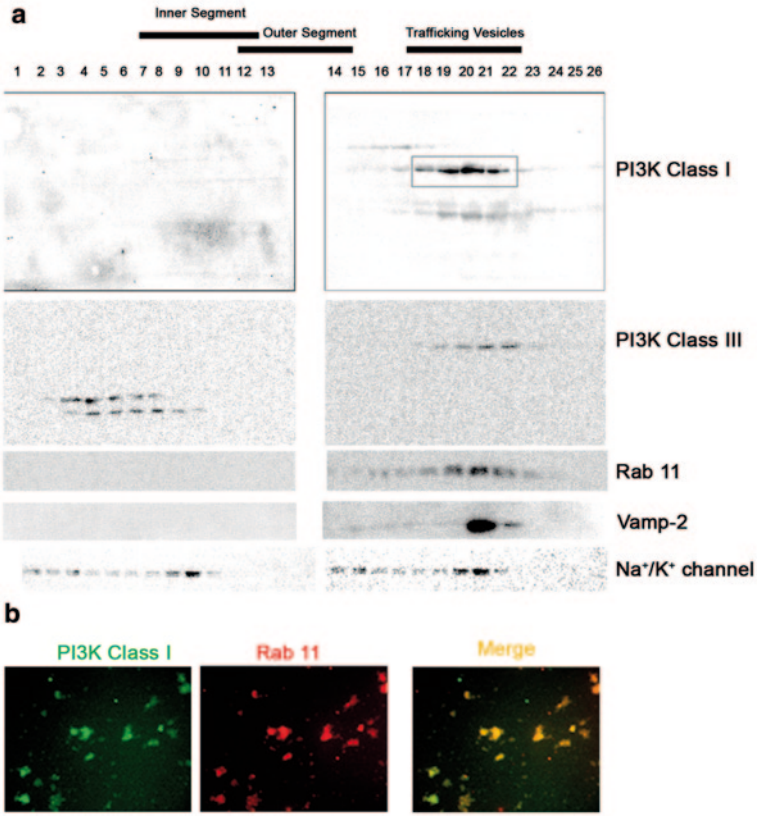

Fig. 48.2 Purification of P50K using 30–50 % continuous sucrose gradient. Following the cellular fractionation, P50K was placed on top of a continuous sucrose gradient. The fractions were then equally distributed to 26 tubes using an automatic pump and a sample collector (see Materials and Methods). The resultant fractions were then separated by an acrylamide SDS gel, transferred to PVDF membrane, and finally subjected to Western blotting

that both VAMP2 and syntaxin 3 were enriched in fraction 20 (Fig. 48.2), which strongly suggests that we were successful in isolating the active trafficking vesicles.

We found that Class I and Class III PI3K were present in the same peak as the trafficking markers (Fig. 48.2). Therefore, we suggest that these play a role in protein trafficking in the retina. Moreover, this is likely the first report of the biochemical detection of any components of Class I PI3K in association with trafficking membranes. This finding provides an opportunity to explore the detailed mechanism of targeting of these proteins or lipid products (PIPs) by detecting the interacting partners in fraction 20. This will certainly help to define the role of PI3K in targeting of other proteins.

Analysis of the lipid content of the trafficking vesicle fraction shows several changes in ether lipids species. An involvement of these lipids in membrane organi-

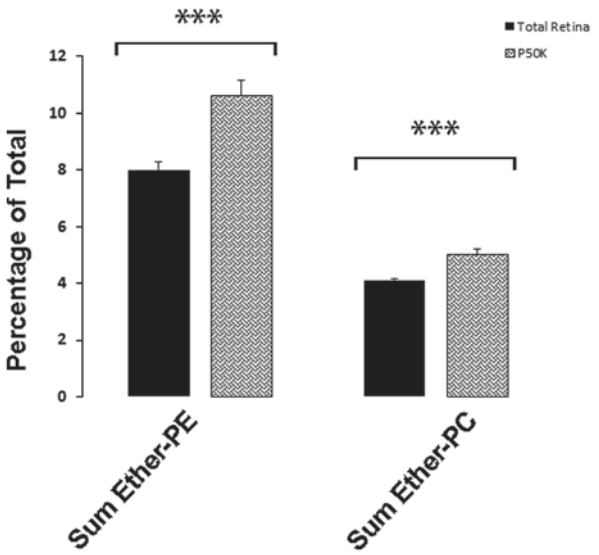

Fig. 48.3 Tandem mass spectrometry analysis of the lipid content of the trafficking vesicle fraction. Ether PE and PC lipids in the trafficking vesicle fraction showed a 32 and 21% increase, respectively, compared with total retina. The values represent the relative percent of the total PE and PC detected, respectively. One-way ANOVA with post-hoc Scheffe was used for statistical analyses. Data are displayed as means ± SD ($n > 3$; ***$p < 0.001$)

zation, fusion, and targeting has been suggested and the lack of these lipids has been shown to cause impaired trafficking and neurological dysfunction and degeneration (Thai et al. 2001). Therefore, it is important to perform further analyses to understand how these lipids may regulate the process of trafficking in the retina.

In conclusion, isolation of trafficking vesicles facilitates the identification of the protein/lipid key molecules that are involved in this process, and allows a deeper understanding of the trafficking of membrane proteins in the retina.

Acknowledgments This study was supported by NIH/NEI grant (EY000871) and NEI core grant (EY021725), Research to Prevent Blindness, and the Knights Templar Eye Foundation (KTEF) grants C5067001 and C5067002.

References

Bennett LD, Hopiavuori BR, Brush RS et al (2014) Examination of VLC-PUFA-deficient photoreceptor terminals. Invest Ophthalmol Vis Sci 55:4063–4072

Caceres PS, Mendez M, Ortiz PA (2014) Vesicle-associated membrane protein 2 (VAMP2) but Not VAMP3 mediates cAMP-stimulated trafficking of the renal Na+-K+-2Cl- co-transporter NKCC2 in thick ascending limbs. J Biol Chem 289:23951–23962

Chuang JZ, Zhao Y, Sung CH (2007) SARA-regulated vesicular targeting underlies formation of the light-sensing organelle in mammalian rods. Cell 130:535–547

Fruman DA, Meyers RE, Cantley LC (1998) Phosphoinositide kinases. Annu Rev Biochem 67:481–507

Gross C, Bassell GJ (2014) Neuron-specific regulation of class I PI3K catalytic subunits and their dysfunction in brain disorders. Front Mol Neurosci 7:12

Hunt DM, Buch P, Michaelides M (2010) Guanylate cyclases and associated activator proteins in retinal disease. Mol Cell Biochem 334:157–168

Ivanovic I, Allen DT, Dighe R et al (2011a) Phosphoinositide 3-kinase signaling in retinal rod photoreceptors. Invest Ophthalmol Vis Sci 52:6355–6362

Ivanovic I, Anderson RE, Le YZ et al (2011b) Deletion of the p85alpha regulatory subunit of phosphoinositide 3-kinase in cone photoreceptor cells results in cone photoreceptor degeneration. Invest Ophthalmol Vis Sci 52:3775–3783

Kuerschner L, Richter D, Hannibal-Bach HK et al (2012) Exogenous ether lipids predominantly target mitochondria. PLoS ONE 7(2):e31342

Lee SJ, Xu H, Kang LW et al (2003) Light adaptation through phosphoinositide-regulated translocation of drosophila visual arrestin. Neuron 39:121–132

Leevers SJ, Vanhaesebroeck B, Waterfield MD (1999) Signalling through phosphoinositide 3-kinases: the lipids take centre stage. Curr Opin Cell Biol 11:219–225

Sung CH, Chuang JZ (2010) The cell biology of vision. J Cell Biol 190:953–963

Thai TP, Rodemer C, Jauch A et al (2001) Impaired membrane traffic in defective ether lipid biosynthesis. Hum Mol Genet 10:127–136

Chapter 49
Cell Cycle Proteins and Retinal Degeneration: Evidences of New Potential Therapeutic Targets

Yvan Arsenijevic

Abstract During different forms of neurodegenerative diseases, including the retinal degeneration, several cell cycle proteins are expressed in the dying neurons from Drosophila to human revealing that these proteins are a hallmark of neuronal degeneration. This is true for animal models of Alzheimer's, and Parkinson's diseases, Amyotrophic Lateral Sclerosis and for Retinitis Pigmentosa as well as for acute injuries such as stroke and light damage. Longitudinal investigation and loss-of-function studies attest that cell cycle proteins participate to the process of cell death although with different impacts, depending on the disease. In the retina, inhibition of cell cycle protein action can result to massive protection. Nonetheless, the dissection of the molecular mechanisms of neuronal cell death is necessary to develop adapted therapeutic tools to efficiently protect photoreceptors as well as other neuron types.

Keywords Retinal degeneration · Alzheimer's disease · Parkinson's disease · CDK5 · BMI1 · Cell cycle · Neuroprotection · Stroke · CDK4

49.1 Introduction

Cell cycle protein expression is a hallmark of neuronal degeneration. During development, the proliferation of stem cells, progenitors and finally precursors is tightly controlled by several cell cycle proteins that define different steps of the cell cycle to harmonize the DNA duplication with the final mitosis. When the differentiation

Y. Arsenijevic (✉)
Unit of Gene Therapy and Stem Cell Biology, Department of Ophthalmology, University of Lausanne, 15, av. De France, 1004 Lausanne, Switzerland
e-mail: yvan.arsenijevic@fa2.ch

C. Bowes Rickman et al. (eds.), *Retinal Degenerative Diseases,* Advances in Experimental Medicine and Biology 854, DOI 10.1007/978-3-319-17121-0_49

occurs, the cells are arrested at Go phase in a postmitotic state. The strict regulation of cell proliferation is required for organs to reach their correct size and content of the different cell populations composing the organ. In the CNS, after development neurons are in consequence frozen in their final phenotype and cannot further proliferate in physiological conditions.

In a quiescent cell (G_0), E2F1 activity is inhibited by the binding of the retinoblastoma protein (Rb). The transition to G_1 consists in phosphorylating Rb to release E2F1 which will activate the different genes necessary for DNA replication and cell mitosis. At least 4 phosphorylated sites are necessary to inactivate Rb. CDK4 and CDK2 are involved in this process when they are activated by Cyclin-D and Cyclin-E respectively. The S-phase then occurs with DNA and centrosome duplications, followed by the G_2 phase which prepares the mitosis process (M phase). The coordination of each phases is in part controlled by the gene expression regulation and by specific tumor suppressors that inhibit the CDK actions at defined stages of the cell cycle progression (for review (Hindley and Philpott 2012)).

Several independent studies reported that during neurodegenerative processes, neurons express some proteins of the cell cycle. Indeed, the expression of certain CDKs such as CDK4 and CDK2 is found in the motoneurons of the SOD1(G37R) mouse model of the Amyotrophic Lateral Sclerosis (Nguyen et al. 2003), of Cyclins in the dopaminergic neurons of the substantia nigra of mouse models of Parkinson's disease (PD) and PD patients (Hoglinger et al. 2007), and of Cyclins and CDKs in the brain of patients affected by Alzheimer's disease (Vincent et al. 1997). Interestingly these neurons also expressed CDK4 and CDK2 when cell death was studied *in vitro* facilitating the molecular dissection of their actions. In the retina of the *Rd1* mouse, bearing a mutation in the *Pde6b* gene coding for a protein of the phototransduction pathway, the number of photoreceptors expressing CDK4 is 4–5 times more elevated than the number of photoreceptors containing CDK2 (Zencak et al. 2013). Moreover, transgenic rats affected by a dominant mutation in the rhodopsin gene also express CDK4 during the time course of photoreceptor cell death process. Acute injury similarly induces CDK4 expression in the retina and the brain consecutively to high light exposure and stroke respectively (Zencak et al. 2013; Osuga et al. 2000), suggesting that these kinases may have an important role in the process of cell death for both inherited diseases and acute injury. In all these different disease cases, the expression of the CDKs was observed in correct location, the nucleus, suggesting that other proteins of the cell cycle regulation may also be expressed during this degenerative stage.

The downstream target of CDK4 and CDK2 is the phosphorylation of Rb which provokes the release of the E2F1 transcription factor. Phospho-Rb was detected in degenerating dopaminergic and motoneurons as well as in photoreceptors (Nguyen et al. 2003; Hoglinger et al. 2007; Zencak et al. 2013). Injection of the BrdU or EdU thymidine analogues during neuron loss revealed that certain neuron types duplicate or attempt to duplicate their DNA. Dopaminergic neurons undergo DNA synthesis, whereas only very few photoreceptors incorporated BrdU or EdU during the retina degeneration process of the *Rd1* mouse (Menu dit Huart et al. 2004; Hoglinger et al. 2007; Zencak et al. 2013). In contrast, in an animal model of polyglutamine expansion, the Spinocerebellar ataxia 7 (SCA7) mouse, several photoreceptors

incorporated BrdU and were positive for phospho-Histone-3 during the course of the disease, indicating that markers of the late phase of the cell cycle can also be present during the course of cell death (Yefimova et al. 2010). So far however it is unclear whether the mutation provokes an abnormal development of the rods due to a deregulation of the cell cycle control, and/or whether the features related to the cell cycle are the consequence of the degenerative process. The fact that such events occur during 7–9 weeks suggest that the appearance of cell cycle markers is probably more related to the process of cell death.

Other proteins involved in the cell cycle regulation were also observed during the process of neuronal cell death. Ki-67 is present during all phases of the cell cycle and allows in consequence to identify the cell fraction in proliferation (for review (Scholzen and Gerdes 2000)). Ectopic Ki-67 expression has been detected in the retina of *Rd1* mice (unpublished data). PCNA (proliferation cell nuclear antigen) which favors DNA polymerase action and coordinates the action of other proteins (review (Moldovan et al. 2007)) was also documented to be present in the dopaminergic neurons of rodent models of Parkinson's disease (Hoglinger et al. 2007). Interestingly, in dogs affected by mutations in STK38L, a kinase controlling the cell cycle, many photoreceptor cells express cell cycle markers during the early stage of the disease, when the animals are aged from 7 to 14 weeks, then the photoreceptor number decreases dramatically (Berta et al. 2011). Indeed, PCNA and phospho-H3 are present in the ONL and not in the microglia (CD18) of the STK38L mutant dogs. RT-PCR analysis confirms the expression of cell cycle proteins such as Cyclin A1 and LATS1, which are related to STK38L. LATS1, acts as a tumor suppressor. In this case, it is seems that the deregulation of the cell cycle during photoreceptor generation affects their survival.

The expression of cell cycle protein during neuronal degeneration including photoreceptors appears to be a hallmark of all the neurodegenerative diseases studied so far. Interestingly, such phenomenon seems to be conserved through evolution over a long period. Indeed, Drosophila expressing a mutated form of the filament tau also present a degenerating retina together with an expression of diverse cell cycle proteins revealing the importance of such proteins for the control of neuronal cell death (Khurana et al. 2006).

49.2 Cell Cycle Proteins Intervene at a Late Phase of the Neuron Death Process

Several molecular pathways are involved in the process of retinal degeneration implicating numerous actors (for review (Sancho-Pelluz et al. 2008)). Studies of the cell cycle protein expression at different stages of the degenerative process have revealed that certain cell cycle proteins are expressed in TUNEL-positive neurons. For instance in a rat stroke model, cortical neurons expressing pRb are also positive for TUNEL (Osuga et al. 2000). In the retina a co-localization analysis of photoreceptors expressing both CDK4 and TUNEL revealed that a large percentage of

CDK4-positive cells undergo DNA fragmentation (Zencak et al. 2013). In contrast, the accumulation of cGMP known to be a marker of the photoreceptor degenerative process does not co-localize with TUNEL-positive cells (Sahaboglu et al. 2013) showing that distinct processes occur at different time points of the photoreceptor death induction. Interestingly by revealing different events occurring during retinal degeneration Sahaboglu et al. (Sahaboglu et al. 2013) estimated the duration of the process of photoreceptor death to be around 83 h, including cell clearance, and that DNA fragmentation happens during the last 7–8 h. These data reveal that the cell cycle proteins are expressed at a late stage of the cell death process suggesting that either they attempt to save the cell or they participate to cell execution.

49.3 Cell Cycle Proteins are Involved in the Process of Cell Death

Different approaches were used *in vitro* and *in vivo* to repress the action of the different cell cycle proteins to reveal their contribution to the process of neuron death. The overexpression of a dominant-negative form of CDK4, but not of CDK2 protects CA1 hippocampal neurons against ischemia produced by middle artery occlusion (Rashidian et al. 2005). Around 40% of CA1 neurons survived in this group compared to 15% in the control GFP group. The genetic ablation of *E2f1* in mice injected with MPTP which is neurotoxic for nigral dopaminergic neurons, protects these dopaminergic neurons. In absence of E2F1, 50% of the neurons survived whereas only 30% remained in the control group (Hoglinger et al. 2007). In *Rd1* retina explants, the inhibition of CDK activity by the roscovitin inhibitor rescued around 40% of the photoreceptors (Zencak et al. 2013). A similar protection was also observed at P18 when *E2f1* is deleted, but the rescue is only transient. Interestingly looking upstream of CDK actions, BMI1, a master actor of the cell cycle regulation, has an important role in the process of photoreceptor death. BMI1 is a polycomb protein which has a permissive role in the cell cycle by preventing the p16 and p19 tumour suppressor actions, by inhibiting their locus (Jacobs et al. 1999; Meng et al. 2010). The deletion of *Bmi1* in the *Rd1* mouse protects around 70% of rods at P30, when almost no rods remained at this age in the *Rd1* control animal (Zencak et al. 2013). This rescue is the most effective to protect *Rd1* photoreceptors and is not related to interference with components of the transduction pathway. Interestingly, cones, which are not affected by the *Pde6b* mutation and which die due to the loss of rods, survive well in the *Rd1;Bmi1*$^{-/-}$ genetic background and are functional showing that the rescue of rods allows the survival of functional cones. Nonetheless, whether cone degeneration is also mediated by cell cycle proteins and whether function inhibition of these proteins directly protects cones are two questions that remain to be solved.

49.4 Are Cell Cycle Proteins Involved in the Reinitiation of the Cell Division or Do They Play Another Role?

Few studies have attempted to verify whether the neurons undertake division during the process of neurodegeneration. Analyses of dopaminergic neurons of PD patients revealed that some of these neurons duplicate their DNA. Indeed, FISH staining for specific chromosome markers confirmed that some dopaminergic neurons contain 4 chromosomes 18 and 2 chromosomes X in a male patient (Hoglinger et al. 2007). In this case, the neurons duplicate the DNA, but there is no data indicating that they actually can divide or whether DNA synthesis is an attempt to repair the DNA. In the retina, no strong evidence of cell division was documented during the course of retinal degeneration with the exception of the STK38L dog (Berta et al. 2011), but this mutation affects the function of a gene involved in the regulation of the cell cycle, and in this case we probably face a development problem. Beside cell cycle regulation, cell cycle proteins may have other targets.

For instance, CDK5 is involved in the cell cycle regulation by recruiting p27 in the nucleus to maintain neurons in a postmitotic state (Zhang et al. 2010). During neuronal degeneration CDK5 is also expressed in various neurons of animal models of neurodegenerative diseases (for review (Herrup and Yang 2007)). Interestingly in an animal model of PD, CDK5 was shown to act as a kinase on different targets depending on the isoform of the p35 protein which activates it (like Cyclin). When p35 binds CDK5, the kinase has multiple functions during development including cell cycle regulation, whereas when p35 is cleaved into p25, p25 modifies the activity of CDK5 which in turn phosphorylates the Peroxidase-2 thus decreasing its activity and increasing reactive oxygen species leading to neuronal death (Qu et al. 2007). These results show that during the disease process the cell cycle proteins may be diverted from their original target and participate to a “pathological” pathway.

The most common target of BMI1 is the INK4a/ARF locus which codes for the two tumor suppressors $p16^{Ink4a}$ and $p19^{Arf}$. In the *Rd1;Bmi1*$^{-/-}$ retina, the ablation of this locus does not restore retinal degeneration indicating that BMI1 acts on other genes (Zencak et al. 2013). Different works have shown that BMI1 is involved, but dispensable, in the DNA repair initiation, as well as in the control of the oxidative stress or mitochondria function (Chatoo et al. 2009; Liu et al. 2009) confirming that BMI1 has different actions. In consequence, it would be interesting to also investigate whether the cell cycle proteins in the retina may be involved in other mechanisms than the cell cycle regulation.

49.5 Conclusions

Cell cycle protein re-expression appears to be a hallmark of a wide range of neurodegenerative processes, including retinal degeneration. In this case, the interference with the cell cycle protein function leads to a massive neuroprotection opening

new targets for therapy. However, the function and the action mechanisms of these proteins have to be unraveled to better translate this knowledge to the clinic using adapted therapeutic tools to efficiently protect the photoreceptors. Such development can be beneficial for other neuron types.

Ackowledgements I thank Martial K. Mbefo for fruitful discussions. This work was supported by the Swiss National Foundation.

References

Berta AI, Boesze-Battaglia K, Genini S et al (2011) Photoreceptor cell death, proliferation and formation of hybrid rod/S-cone photoreceptors in the degenerating STK38L mutant retina. PloS ONE 6:e24074

Chatoo W, Abdouh M, David J et al (2009) The polycomb group gene Bmi1 regulates antioxidant defenses in neurons by repressing p53 pro-oxidant activity. J Neurosci 29:529–542

Herrup K, Yang Y (2007) Cell cycle regulation in the postmitotic neuron: oxymoron or new biology? Nat Rev Neurosci 8:368–378

Hindley C, Philpott A (2012) Co-ordination of cell cycle and differentiation in the developing nervous system. Biochem J 444:375–382

Hoglinger GU, Breunig JJ, Depboylu C et al (2007) The pRb/E2F cell-cycle pathway mediates cell death in Parkinson's disease. Proc Natl Acad Sci U S A 104:3585–3590

Jacobs JJ, Kieboom K, Marino S et al (1999) The oncogene and Polycomb-group gene bmi-1 regulates cell proliferation and senescence through the ink4a locus. Nature 397:164–168

Khurana V, Lu Y, Steinhilb ML et al (2006) TOR-mediated cell-cycle activation causes neurodegeneration in a drosophila tauopathy model. Curr Biol 16:230–241

Liu J, Cao L, Chen J et al (2009) Bmi1 regulates mitochondrial function and the DNA damage response pathway. Nature 459:387–392

Meng S, Luo M, Sun H et al (2010) Identification and characterization of Bmi-1-responding element within the human p16 promoter. J Biol Chemistry 285:33219–33229

Menu dit Huart L, Lorentz O, Goureau O et al (2004) DNA repair in the degenerating mouse retina. Mol Cell Neurosci 26:441–449

Moldovan GL, Pfander B, Jentsch S (2007) PCNA, the maestro of the replication fork. Cell 129:665–679

Nguyen MD, Boudreau M, Kriz J et al (2003) Cell cycle regulators in the neuronal death pathway of amyotrophic lateral sclerosis caused by mutant superoxide dismutase 1. J Neurosci 23:2131–2140

Osuga H, Osuga S, Wang F et al (2000) Cyclin-dependent kinases as a therapeutic target for stroke. Proc Natl Acad Sci U S A 97:10254–10259

Qu D, Rashidian J, Mount MP et al (2007) Role of Cdk5-mediated phosphorylation of Prx2 in MPTP toxicity and Parkinson's disease. Neuron 55:37–52

Rashidian J, Iyirhiaro G, Aleyasin H et al (2005) Multiple cyclin-dependent kinases signals are critical mediators of ischemia/hypoxic neuronal death *in vitro* and *in vivo*. Proc Natl Acad Sci U S A 102:14080–14085

Sahaboglu A, Paquet-Durand O, Dietter J et al (2013) Retinitis pigmentosa: rapid neurodegeneration is governed by slow cell death mechanisms. Cell Death Dis 4:e488

Sancho-Pelluz J, Arango-Gonzalez B, Kustermann S et al (2008) Photoreceptor cell death mechanisms in inherited retinal degeneration. Mol Neurobiol 38:253–269

Scholzen T, Gerdes J (2000) The Ki-67 protein: from the known and the unknown. J Cell Physiol 182:311–322

Vincent I, Jicha G,Rosado M et al (1997) Aberrant expression of mitotic cdc2/cyclin B1 kinase in degenerating neurons of Alzheimer's disease brain. J Neurosci 17:3588–3598

Yefimova MG, Messaddeq N, Karam A et al (2010) Polyglutamine toxicity induces rod photoreceptor division, morphological transformation or death in spinocerebellar ataxia 7 mouse retina. Neurobiol Dis 40:311–324

Zencak D, Schouwey K, Chen D et al (2013) Retinal degeneration depends on Bmi1 function and reactivation of cell cycle proteins. Proc Natl Acad Sci U S A 110:E593–E601

Zhang J, Li H, Herrup K (2010) Cdk5 nuclear localization is p27-dependent in nerve cells: implications for cell cycle suppression and caspase-3 activation. J Biol Chem 285:14052–14061

Chapter 50
Nitric Oxide Synthase Activation as a Trigger of *N*-methyl-*N*-nitrosourea-Induced Photoreceptor Cell Death

Suguru Hisano, Yoshiki Koriyama, Kazuhiro Ogai, Kayo Sugitani and Satoru Kato

Abstract Retinal degeneration (RD) such as retinitis pigmentosa and age-related macular degeneration are major causes of blindness in adulthood. As one of the model for RD, intraperitoneal injection of *N*-methyl-*N*-nitrosourea (MNU) is widely used because of its selective photoreceptor cell death. It has been reported that MNU increases intracellular calcium ions in the retina and induces photoreceptor cell death. Although calcium ion influx triggers the neuronal nitric oxide synthase (nNOS) activation, the role of nNOS on photoreceptor cell death by MNU has not been reported yet. In this study, we investigated the contribution of nNOS on photoreceptor cell death induced by MNU in mice. MNU significantly increased NOS activation at 3 day after treatment. Then, we evaluated the effect of nNOS specific inhibitor, ethyl[4-(trifluoromethyl) phenyl]carbamimidothioate (ETPI) on the MNU-induced photoreceptor cell death. At 3 days, ETPI clearly inhibited the MNU-induced cell death in the ONL. These data indicate that nNOS is a key molecule for pathogenesis of MNU-induced photoreceptor cell death.

Keywords Oxidative stress · *N*-methyl-*N*-mitrosourea · Photoreceptor cell death · Neural nitric oxide synthease

Y. Koriyama (✉)
Graduate School and Faculty of Pharmaceutical Sciences, Suzuka University of Medical Science, 3500-3 Minamitamagaki, Suzuka 513-8670, Japan
e-mail: koriyama@suzuka-u.ac.jp

S. Hisano
Department of Clinical Laboratory Science, Department of Molecular Neurobiology, Graduate School of Medical Science, Kanazawa University, 5-11-80 Kodatsuno, Kanazawa 920-0942, Japan
e-mail: ef.ef.soylatte.ts@gmail.com

K. Ogai
Wellness Promotion Science Center, Institute of Medical, Pharmaceutical and Health Sciences, Kanazawa University, 5-11-80 Kodatsuno, Kanazawa 920-0942 Japan
e-mail: kazuhiro@staff.kanazawa-u.ac.jp

C. Bowes Rickman et al. (eds.), *Retinal Degenerative Diseases,* Advances in Experimental Medicine and Biology 854, DOI 10.1007/978-3-319-17121-0_50

50.1 Introduction

Retinal degeneration (RD) such as retinitis pigmentosa and age-related macular degeneration is one of the major causes of blindness (Margalit and Sadda 2003; Hartong et al. 2006). To understand the mechanisms and potential treatments for RD, there are a number of retinal degeneration animal models that mimic human pathology. *N*-methyl-*N*-nitrosourea (MNU), a DNA alkylating agent has been widely used to produce retinal degeneration models in various animals (Tsubura et al. 2011). MNU can induce selective photoreceptor cell death through an apoptotic mechanism (Yoshizawa et al. 2000), and results in retinal thinning (Koriyama et al. 2014). However, the mechanism of MNU-induced photoreceptor cell death is only partially understood. For example, MNU increases retinal calcium concentration (Oka et al. 2007). Given that neuronal nitric oxide synthase (nNOS) is activated by calcium through calmodulin activation (Koch et al. 1994), it is possible that nNOS may play a central role in MNU-induced photoreceptor cell death. Therefore, in this study we investigated the relationship between nNOS and photoreceptor cell death induced by MNU.

50.2 Materials and Methods

50.2.1 Animals and Retinal Section Preparation

The Animal Care and Use Committee of Kanazawa University approved all animal care and handling procedures. Male C57BL/6 mice (8–9 weeks old) were used throughout this study. Mice were anesthetized by intraperitoneal injection of sodium pentobarbital (30–40 mg/kg body weight). MNU (60 mg/kg body weight) treatment was performed by intraperitoneal injection. Under anesthesia, an nNOS inhibitor, ethyl [4-(trifluoromethyl)phenyl] carbamimidothioate (ETPI) (400 nM/eye, Cayman Chemical, Ann Arbor, Michigan, USA), was intraocularly injected immediately after MNU treatment. Enucleated eyes were fixed overnight in 4% paraformaldehyde at 4 °C. After fixation, the eyes were incubated in 30% su-

K. Sugitani
Department of Clinical Laboratory Sciences, Graduate School of Medical Science, Institute of Medical, Pharmaceutical and Health Sciences, Kanazawa University, 5-11-80 Kodatsuno, Kanazawa 920-0942, Japan
e-mail: sugitani@staff.kanazawa-u.ac.jp

S. Kato
Department of Molecular Neurobiology, Graduate School of Medicine, Kanazawa University, 13-1 Takaramachi, Kanazawa 920-8640, Japan
e-mail: satoru@med.kanazawa-u.ac.jp

crose overnight at 4 °C followed by embedding in optimal cutting temperature compound (Sakura finetek, Tokyo, Japan). Cryosections were prepared at 12 µm thickness.

50.2.2 NADPH Diaphorase Staining

The retinal cryosections were incubated in 0.1 M Tris-HCl (pH 8.0) containing 0.3 % Triton X-100 overnight at 23 °C. They were then stained in buffer including NADPH and 4-nitroblue tetrazolium chloride (Roche Diagnostics Corporation, Indianapolis, IN, USA) for 2–3 h at 37 °C.

50.2.3 Immunohistochemistry

The retinal sections were microwaved in 0.1 M citrate buffer followed by incubation with primary antibody of anti-nNOS (Sigma Aldrich, St. Louis, MO, USA). The sections were then incubated with appropriate Alexa Fluor-conjugated secondary antibody (Molecular Probe, Eugene, OR, USA).

50.2.4 Terminal Transferase-Mediated dUTP Nick-End Labeling (TUNEL) Staining

Apoptotic cells were detected using *In Situ* Cell Death Detection Kit, Fluorescein (Roche Applied Science, Mannheim, Germany) according to the procedure described by the manufacturer. In brief, the retinal cryosections were microwaved in 0.1 M citrate buffer (pH 6.0), washed, blocked and incubated with terminal transferase and fluorescein-conjugated dUTP. To count the number of TUNEL-positive cells in ONL, we randomly selected one area (400 × 100 µm, covering whole layer) of retina in each image of section (× 200 magnification). The number of TUNEL-positive cells in ONL of the area was counted using ImageJ software (Wayne Rasband, NIH, Bethesda, MD, USA).

50.3 Results

50.3.1 MNU Induces nNOS Activation in Inner Segment (IS)

To examine NOS activity in retina after MNU treatment, we assessed retinal NADPH diaphorase activity which reflects NOS activity (Koriyama et al. 2009;

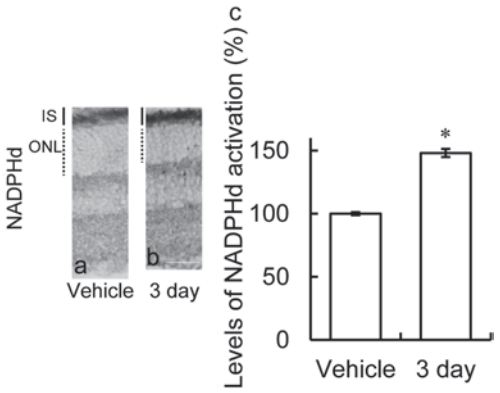

Fig. 50.1 MNU induced nNOS activation in IS. **a**, **b**: NADPH diaphorase staining in the retina increased at 3 day after MNU treatment (**b**) compared to vehicle control retina (**a**). (**c**) NADPH diaphorase activity in IS. $^{*}P<0.05$ versus vehicle control ($n=4$). Scale bar = 50 μm

Dauson et al. 1991), by NADPH diaphorase staining. In vehicle control retina, NADPH diaphorase activity was observed in IS (Fig. 50.1a). MNU treatment significantly increased NADPH diaphorase activity in IS at 3 days after treatment compared to control retina (Fig. 50.1). Next, we examined nNOS localization by immunohistochemistry. In retinal section, the immunoreactivity of nNOS was localized in IS (Y. Koriyama unpublished data).

50.3.2 nNOS Inhibition Reduces Photoreceptor Cell Death by MNU Treatment

In ONL, TUNEL-positive cells dramatically increased by 3 days after MNU treatment (Koriyama et al. 2014, Table 50.1). We evaluated the effects of nNOS inhibition on the number of TUNEL-positive cells in ONL after MNU treatment. At 3 days post MNU treatment, ETPI significantly decreased the number of TUNEL-positive cells compared to MNU alone (Table 50.1).

Table 50.1 ETPI inhibited photoreceptor cell death induced by MNU. The numbers of TUNEL-positive cells in the ONL per visual field (×200 magnification) are shown

The number of TUNEL-positive cell in ONL	
–	$TUNEL^{+}$ cells (mean ± SEM)
Vehicle control	1.15 ± 0.33
3 days post MNU alone	53.15 ± 7.92[a]
3 days post MNU and ETPI	31.80 ± 6.57[a,b]

[a] $P<0.05$ versus vehicle control ($n=20$)
[b] $P<0.05$ versus MNU alone ($n=20$)

50.4 Discussion

In animal models and human cases of retinitis pigmentosa, photoreceptor cell loss is led by apoptosis via common final pathway (Chang et al. 1993). A number of studies have described MNU toxicity to retina, and proposed various possible therapies for MNU-induced photoreceptor cell death (Tezel 2006; Kindzelskii et al. 2004; Doonan et al. 2003). In the present study, we showed evidence that the NOS were activated in IS after MNU intraperitoneal injection, and nNOS immunoreactivity was observed in the same area. Although IS of photoreceptors were weak of reduction product of NADPH diaphorase (Darius et al. 1995), nNOS is abundantly present in the OS (Neufeld et al. 2000). Oka et al. reported that total calcium ion in MNU-treated retinas is significantly increased before induction of photoreceptor cell death (Oka et al. 2007). Koch et al. further reported that NOS activity is strongly enhanced by elevated free calcium ion in photoreceptor cells (Koch et al. 1994). In the light-induced photoreceptor cell death model, elevation of intracellular calcium levels took place in an early and rapid event in light-induced cell death (Donovan et al. 2001). In this study, we clearly showed that ETPI, a selective inhibitor of nNOS, significantly decreased the number of apoptotic cells in ONL, suggesting a possibility that MNU-induced photoreceptor cell death was caused dominantly by nNOS activation (e.g., Fig. 50.2). These findings in turn will propose the possibility that nNOS inhibitors can be one of the new candidates of the therapy for RD such as retinitis pigmentosa.

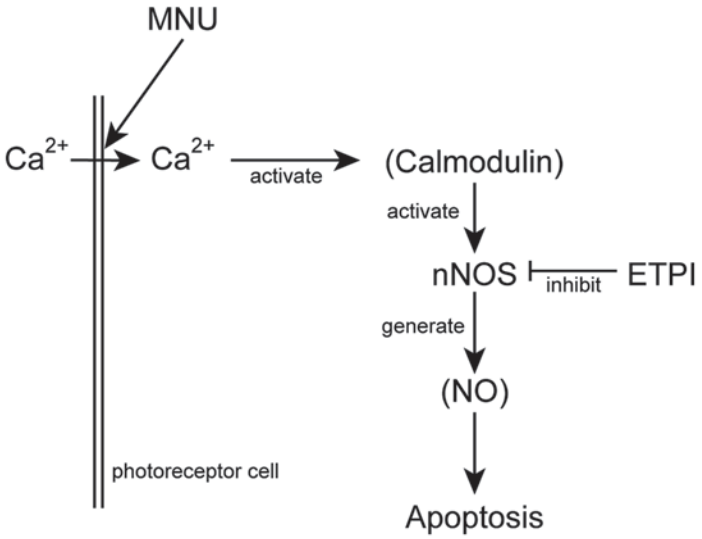

Fig. 50.2 Proposed pathway of MNU-induced photoreceptor cell death in this study. MNU might induce the influx of calcium ions, which in turn activates nNOS via calmodulin activation. Activated nNOS might be a key factor for induction of photoreceptor cell death as nNOS inhibitor (ETPI) could prevent cell loss

References

Chang GQ, Hao Y, Wong F (1993) Apoptosis: final common pathway of photoreceptor death in rd, rds, and rhodopsin mutant mice. Neuron 11:595–605

Darius S, Wolf G, Huang PL et al (1995) Localization of NADPH-diaphorase/nitric oxide synthase in the rat retina: an electron microscopic study. Brain Res 690:231–235

Dauson TM, Bredt DS, Fotuhi M et al (1991) Nitric oxide synthase and neuronal NADPH diaphorase are identical in brain and peripheral tissues. Proc Natl Acad Sci U S A 88:7797–7801

Donovan M, Carmody RJ, Cotter TG (2001) Light-induced photoreceptor apoptosis *in vivo* requires neuronal nitric-oxide synthase and guanylate cyclase activity and is caspase-3 independent. J Biol Chem 276:23000–23008

Doonan F, Donovan M, Cotter TG (2003) Caspase-independent photoreceptor apoptosis is mouse models of retinal degeneration. J Neurosci 23:5723–5731

Hartong DT, Berson EL, Dryja TP (2006) Retinitis pigmentosa. Lancet 368:1795–1809

Kindzelskii AL, Elner VM, Elner SG et al (2004) Human, but not bovine, photoreceptor outer segments prime human retinal pigment epithelial cells for metabolic activation and massive oxidant release in response to lipopolysaccharide and interferon-gamma. Exp Eye Res 79:431–435

Koch KW, Lambrecht HG, Haberecht M et al (1994) Functional coupling of a Ca^{2+}/calmodulin-dependant nitric oxide synthase and a soluble guanylyl cyclase in vertebrate photoreceptor cells. EMBO J 13:3312–3320

Koriyama Y, Yasuda R, Homma K et al (2009) Nitric oxide-cGMP signaling regulates axonal elongation during optic nerve regeneration in the goldfish *in vitro* and *in vivo*. J Neurochem 110:890–901

Koriyama Y, Sugitani K, Ogai K et al (2014) Heat shock protein 70 induction by valproic acid delays photoreceptor cell death by N-methyl-N-nitrosourea in mice. J Neurochem 130:707–719

Margalit E, Sadda SR (2003) Retinal and optic nerve diseases. Artif Organs 27:963–974

Neufeld AH, Shareef S, Pena J (2000) Cellular localization of neuronal nitric oxide synthase (NOS-1) in the human and rat retina. J Comp Neurol 416:269–275

Oka T, Nakajima T, Tamada Y et al (2007) Contribution of calpains to photoreceptor cell death in N-methyl-N-nitrosourea-treated rats. Exp Neurol 204:39–48

Tezel G (2006) Oxidative stress in glaucomatous neurodegeneration: mechanisms and consequences. Prog Retin Eye Res 25:490–513

Tsubura A, Lai YC, Miki H et al (2011) Animal models of N-Methyl-N-nitrosourea-induced mammary cancer and retinal degeneration with special emphasis on therapeutic trials. *In Vivo* 25:11–22

Yoshizawa K, Yang J, Senzaki H et al (2000) Caspase-3 inhibitor rescues N-Methyl-N-nitrosourea-induced retinal degeneration in sprague-dawlay rats. Exp Eye Res 71:629–635

Chapter 51
Molecular Principles for Decoding Homeostasis Disruptions in the Retinal Pigment Epithelium: Significance of Lipid Mediators to Retinal Degenerative Diseases

Nicolas G. Bazan

Abstract Dysregulated neuroinflammatory signaling during impending disruption of homeostasis in retinal pigment epithelium (RPE) and photoreceptor cells (PRC) takes place in early stages of retinal degeneration. PRCs avidly retain and display the highest content in the human body of docosahexaenoic acid (DHA; an omega-3 essential fatty acid). Docosanoids are DHA-derived mediators, such as neuroprotectin D1 (NPD1), made on-demand that promote repair, phagocytic clearance, cell survival, and are active participants of effective, well-concerted homeostasis restoration. Here we develop the concept that there is a molecular logic that sustains PRC survival and that transcriptional signatures governed by NPD1 in the RPE may be engaged.

Keywords Docosahexaenoic acid · Neuroprotectin D1 · Retinal pigment epithelium · 661W · Pigment epithelial-derived factor

51.1 Introduction

A consequence of increased life expectancy is a rise in the occurrence of PRC survival failure, as reflected by age-related macular degeneration (AMD) and other neurodegenerative diseases. Retinal development, as is the case with the rest of the central nervous system, is driven by neuronal apoptotic cell death, and thereafter neurons, including PRC, are post-mitotic cells. In retinal degenerative diseases, apoptosis and other forms of cell death are set in motion, leading to PRC loss. AMD is a disease of failed aging and not of developmental failure (Sharma et al. 2014).

N. G. Bazan (✉)
Neuroscience Center of Excellence, School of Medicine, Louisiana State University Health Sciences Center, 2020 Gravier Street, Suite D, New Orleans, LA 70112, USA
e-mail: nbazan@lsuhsc.edu

C. Bowes Rickman et al. (eds.), *Retinal Degenerative Diseases,* Advances in Experimental Medicine and Biology 854, DOI 10.1007/978-3-319-17121-0_51

There is a marvelous interdependent relationship between PRC and RPE whereby key molecules are recycled (Bazan 2007; Lehmann et al. 2014) by the daily shedding of PRC tips and RPE phagocytosis (Strauss 2005; Mukherjee et al. 2007b; Mazzoni et al. 2014). These include the tightly-regulated recycling of retinoids of the visual cycle in rod PRC. The cone PRC retinoid recycling also involves the Müller cell. DHA, attains its highest concentrations in the human body in the PRC (Fliesler and Anderson 1983), and it is remarkable that this fatty acid is retained and conserved between PRC and RPE cells (Bazan et al. 2011; Gordon and Bazan 1990). The outer and disks membranes of PRC features phospholipids richly endowed with DHA acyl chains. In contrast, the other essential fatty acid family, the omega-6, is present in all tissues in similar amounts, and its major member, arachidonic acid (AA), is the precursor of eicosanoids that includes prostaglandins and related mediators.

Although age is the main risk factor for AMD, not everyone develops this disease during aging. Despite decades of important findings about signaling that sustains functional integrity of PRC and RPE cells, the decisive mechanisms that sustain the survival of these cells remain incompletely understood. Here we discuss the notion that there is a molecular logic that sustains PRC survival and the potential significance of transcriptional signatures in the RPE directed by DHA-derived lipid mediators.

51.2 Photoreceptor Cell Survival

It is becoming apparent that consequences of dysregulated networks of neuroinflammatory signaling responses to impending homeostasis disruptions underlie RPE demise. Since these cells are necessary for PRC functional integrity and survival, it is important to understand and unravel key signaling engaged under these conditions. We are learning that DHA is related to pivotal events for vision, which include the following: (a) DHA is the precursor of very long chain polyunsaturated fatty acids (VLC-PUFAs), which are intimately associated with rhodopsin (Aveldaño et al. 1988) and remarkably decrease in content in Stargardt syndrome and in AMD (these fatty acids are made by an ELOV4-mediated elongation pathway) (Harkewicz et al. 2012; Liu et al. 2010; Logan et al. 2013); (b) DHA is the precursor of cytoprotective, homeostasis modulator neuroprotectin D1 (NPD1; 10R,17S-dihydroxy-docosa-4Z,7Z,11E,13E,15Z,19Z-hexaenoic acid) and of other bioactive docosanoids; and (c) DHA peroxidation protein adducts evolve and accumulates in Drusen in AMD, exerting enhancing actions on its pathology (Hollyfield et al. 2008).

NPD1 is a mediator made on demand; thus, a question to ask is “what is the ‘signal/s’ for turning on the synthesis of this lipid mediator?” Using primary human RPE cells in monolayer cultures, the neurotrophin pigment epithelium-derived factor (PEDF), and others to a smaller extent, were found to be agonists for the synthesis and, apical release of NPD1 (Mukherjee et al. 2007a). Thus even though the significance of phospholipid signaling in PRCs is becoming clearer,

we still have major gaps in our understanding of the molecular principles that underlie these critical events decisive for cell integrity. Docosanoids include mediators that promote repair, phagocytic clearance and homeostasis, and that are active participants of an effective, active, well-concerted process of homeostasis restoration; they comprise NPD1, resolvins D1 and D2 (RvD1, RvD2), and maresins (Bazan et al. 2011).

51.3 What are the Molecular Principles that Decode Homeostasis Disruptions in the Retinal Pigment Epithelium to Sustain PRC Functional Integrity?

This question highlights our quest based on the following: (a) in inheritable retinal degenerative diseases (and in other familial forms of neurodegeneration), why doesn't the disease manifest during latency?; (b) does a cell-specific initial response/s counteract the consequences of mutation expression?; and (c) why can the latency period last for decades? Because early responses to retinal degenerative diseases engage uncompensated oxidative stress and neuroinflammation, corollaries to these questions are whether a neuroadaptation failure response is involved, and also whether there is an impediment to membrane encoding of information for retention and/or release of specific mediators (Bazan 2014). There are a multitude of factors involved, including developmentally-expressed genes, since most of the inherited retinal degenerative diseases remain asymptomatic during development and maturation of the retina. Our lab began deciphering aspects of the molecular logic that sustain RPE survival by uncovering molecular principles (transcriptional signatures) governed by the docosanoid NPD1. In other neural cells, bioactivity of NPD1, in addition, modulates amyloid precursor protein processing, inducing cell survival (Zhao et al. 2011).

51.4 How Does the PRC Counter Early Disruptions of Homeostasis?

The cellular molecular protective responses of the RPE/PRC to potential homeostatic disturbances are only partly understood. For example, oxidative stress is needed for cell functions, however uncompensated oxidative stress is a central disruptor of homeostasis. There are several offsetting signals that respond to set in motion neuroprotection, that, in turn, might influence RPE/PRC integrity. While searching for early mechanisms set in motion in RPE cells in response to survival threats, we have discovered and named NPD1 (Mukherjee et al. 2004). This finding has provided initial validation to the concept that signaling mechanisms are activated early to sustain homeostasis.

Hinting at an inability to further allow pathways to form the bioactive products, and further supporting the notion of a perturbation in docosanoid synthesis, a corollary of these predictions is that administered DHA will make the precursor of docosanoids accessible to cells. As a consequence, the synthesis of lipid mediators would be increased and nurture a resolving inflammatory response; this, in turn, would counteract sustained inflammation.

Recently, using mouse-derived transformed cone 661W cells, it was shown that NPD1 is also made in PRC (Kanan et al. 2014). NPD1 exerts protective bioactivity on these cells upon incubation with 9-*cis* retin*al* in the presence of bright light that triggers cell damage and death. Viability assays of 9-*cis* retin*al*-treated cells demonstrated DHA protection after bright light exposure, and that NPD1 further increased protection. The bioactivity of DHA is supported by the observation that d4-DHA added to the media synthesized 4–9 times as much d4-NPD1 under bright light exposure compared to cells in darkness (Kanan et al. 2014). Thus RPE and at least a transform cone PRC are able to synthesize NPD1. The implications are that DHA in both cells can become the NPD1 precursor to counter disruptions of homeostasis.

51.5 Lipid-Mediated RPE-Specific Transcriptional Modulation Necessary to Withstand Cell Survival: cREL, an Intracellular Messenger of NPD1

Omega-3 fatty acids from the diet, linolenic and DHA are taken up by the liver. The liver is endowed with active enzymes to elongate and introduce double bonds in linolenic acid, leading to the formation of DHA. This fatty acid is then shuttled to the nervous system, where it becomes acylated in phospholipids that, in turn, is used for membrane biogenesis of PRC and synapses, as shown during postnatal development (Scott and Bazan 1989). Figure 51.1 illustrates the routes followed by DHA. Box a indicates the presence of a molecule for the retention of the fatty acid in the RPE cell. Very recently, adiponectin receptor 1 was shown to be this molecule (Rice et al. 2015). Box b is the high affinity binding site for NPD1 (Marcheselli et al. 2010). NPD1 induces RPE transcriptional upregulation of cREL followed by BIRC3 (baculoviral IAP-inhibitor of apoptosis protein-repeat containing 3) expression, which in turn leads to cell survival. NPD1-mediated c-Rel transcription nuclear translocation occurs, as was recently identified in human RPE cells (Calandria et al. 2015). Based on these results, it is tempting to postulate that the selective upregulation of BIRC3 by DHA, using cREL as an intracellular messenger, reveals a transcriptional signature that might underlie a key molecular principle fostering RPE/PRC survival. Figure 51.1 outlines the route of DHA as a precursor of NPD1 to elicit transcriptional activation of cREL after its release from the RPE cell. cREL acts as an intracellular messenger of NPD1 that regulates BIRC3 and, in turn, upregulates RPE cell survival (Calandria et al. 2015).

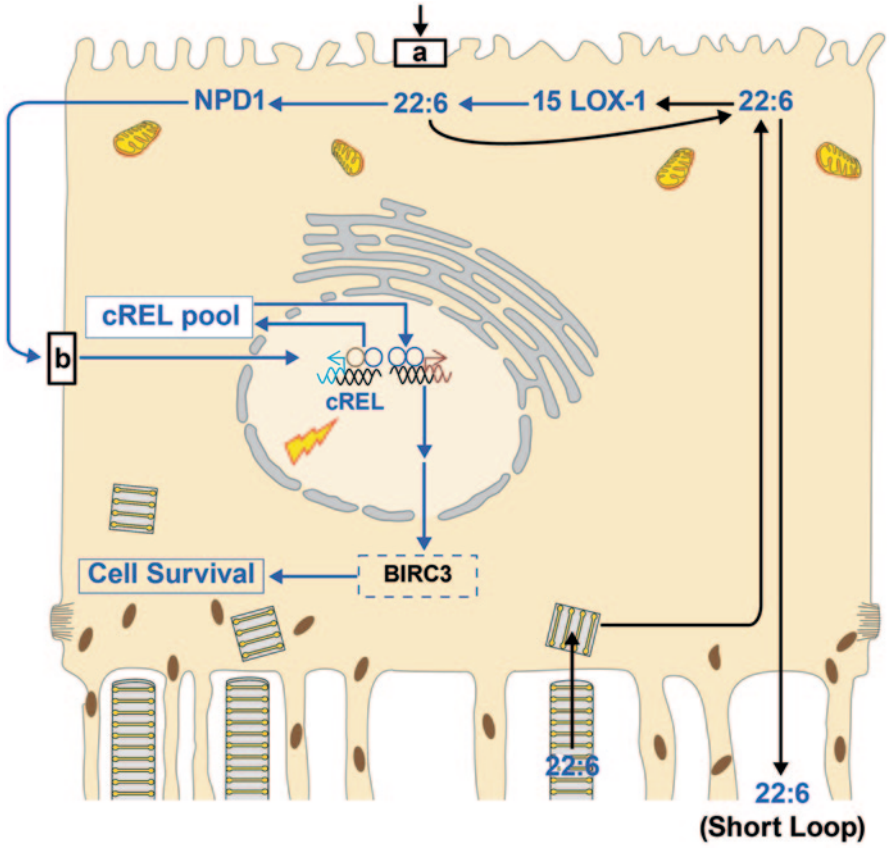

Fig. 51.1 Cartoon of the RPE cell. DHA is depicted being recycled from PRC outer segment renewal (*short loop*) and being used as the precursor for NPD1 synthesis. In the top, Box **a** indicates a putative mechanism for DHA uptake. The high affinity binding site for the lipid mediator is depicted in **b**. cREL transcription is induced by NPD1, and then it becomes an intracellular messenger to induce BIRC3 transcription that executes RPE cell survival

51.6 Perspective Outlooks

Phospholipid signaling stemming from RPE or PRC DHA reservoirs leads to the synthesis of docosanoids that promote cell survival. NPD1 mediates transcriptional signatures in the RPE, highlighting cREL as an intracellular messenger that activates BIRC3 transcription and, in turn, cell survival. These findings open an avenue to ascertain mechanistic details that counteract unresolved inflammation, retinal microglial activation (Sheets et al. 2013) and uncompensated oxidative stress to foster homeostasis restoration. The homeostatic responses mediated by DHA/NPD1 could be mimicked in preventive and therapeutic approaches. Thus identification of the molecular principles that control the molecular logic for supporting PRC survival

will bring a paradigm shift to the understanding, prevention and treatment of retinal degenerative diseases.

Acknowledgements This works was supported by National Institutes of Health grants GM103340, NS046741 and EY005121 (NGB).

References

Aveldaño MI (1988) Phospholipid species containing long and very long polyenoic fatty acids remain with rhodopsin after hexane extraction of photoreceptor membranes. Biochemistry 27:1229–1239

Bazan NG (2007) Homeostatic regulation of photoreceptor cell integrity: significance of the potent mediator neuroprotectin D1 biosynthesized from docosahexaenoic acid: the Proctor Lecture. Invest Ophthalmol Vis Sci 48:4866–4881

Bazan NG, Molina MF, Gordon WC (2011) Docosahexaenoic acid signalolipidomics in nutrition: significance in aging, neuroinflammation, macular degeneration, Alzheimer's, and other neurodegenerative diseases. Annu Rev Nutr 31:321–351

Bazan NG (2014) Is there a molecular logic that sustains neuronal functional integrity and survival? Lipid signaling is necessary for neuroprotective neuronal transcriptional programs 50:1–5

Calandria JM, Asatryan A, Balaszczuk V, Knott E, Jun BK, Mukherjee PK, Belayev L, Bazan NG (2015) NPD1-mediated stereoselective regulation of BIRC3 expression through cREL is decisive for neural cell survival. Cell Death Dis. doi 10.1038/cdd.2014.233

Fliesler SJ, Anderson RE (1983) Chemistry and metabolism of lipids in the vertebrate retina. Prog Lipid Res 22:79–131

Gordon WC, Bazan NG (1990) Docosahexaenoic acid utilization during rod photoreceptor cell renewal. J Neurosci 10:2190–202.

Harkewicz R, Du H, Tong Z, Alkuraya H, Bedell M, Sun W, Wang X, Hsu YH, Esteve-Rudd J, Hughes G, Su Z, Zhang M, Lopes VS, Molday RS, Williams DS, Dennis EA, Zhang K (2012) Essential role of ELOVL4 protein in very long chain fatty acid synthesis and retinal function. J Biol Chem 287:11469–11480

Hollyfield JG, Bonilha VL, Rayborn ME, Yang X, Shadrach KG, Lu L, Ufret RL, Salomon RG, Perez VL (2008) Oxidative damage-induced inflammation initiates age-related macular degeneration. Nat Med 14:194–198

Kanan Y, Gordon WC, Mukherjee PK, Bazan NG, Al-Ubaidi MR (2014) Neuroprotectin D1 is synthesized in the cone photoreceptor cell line 661W and elicits protection against light-induced stress. Cell Mol Neurobiol 35:197–204

Lehmann GL, Benedicto I, Philp NJ, Rodriguez-Boulan E (2014) Plasma membrane protein polarity and trafficking in RPE cells: past, present and future. Exp Eye Res 126C:5–15

Liu A, Chang J, Lin Y, Shen Z, Bernstein PS (2010) Long-chain and very long-chain polyunsaturated fatty acids in ocular aging and age-related macular degeneration. J Lipid Res 51:3217–3229

Logan S, Agbaga MP, Chan MD, Kabir N, Mandal NA, Brush RS, Anderson RE (2013) Deciphering mutant ELOVL4 activity in autosomal-dominant Stargardt macular dystrophy. Proc Natl Acad Sci U S A 110:5446–5451

Marcheselli VL, Mukherjee PK, Arita M, Hong S, Antony R, Sheets K, Winkler JW, Petasis NA, Serhan CN, Bazan NG (2010) Neuroprotectin D1/protectin D1 stereoselective and specific binding with human retinal pigment epithelial cells and neutrophils. Prostaglandins Leukot Essent Fatty Acids 82:27–34

Mazzoni F, Safa H, Finnemann SC (2014) Understanding photoreceptor outer segment phagocytosis: use and utility of RPE cells in culture. Exp Eye Res 126C:51–60

Mukherjee PK, Marcheselli VL, Serhan CN, Bazan NG (2004) Neuroprotectin D1: a docosahexaenoic acid-derived docosatriene protects human retinal pigment epithelial cells from oxidative stress. Proc Natl Acad Sci U S A 101:8491–8496

Mukherjee PK, Marcheselli VL, Barreiro S, Hu J, Bok D, Bazan NG (2007a) Neurotrophins enhance retinal pigment epithelial cell survival through neuroprotectin D1 signaling. Proc Natl Acad Sci U S A 104:13152–13157

Mukherjee PK, Marcheselli VL, de Rivero Vaccari JC, Gordon WC, Jackson FE, Bazan NG (2007b) Photoreceptor outer segment phagocytosis attenuates oxidative stress-induced apoptosis with concomitant neuroprotectin D1 synthesis. Proc Natl Acad Sci U S A 104:13158–13163

Rice DS, Calandria JM, Gordon WC, Jun B, Zhou Y, Gelfman CM, Li S, Jin M, Knott EJ, Chang B, Abuin A, Issa T, Potter D, Platt KA, Bazan NG (2015) Adiponectin receptor 1 conserves docosahexaenoic acid and promotes photoreceptor cell survival. Nat Commun 6:6228

Scott BL, Bazan NG (1989) Membrane docosahexaenoate is supplied to the developing brain and retina by the liver. Proc Natl Acad Sci U S A 86:2903–2907

Sharma K, Sharma NK, Anand A (2014) Why AMD is a disease of ageing and not of development: mechanisms and insights. Front Aging Neurosci 6:151

Sheets KG, Jun B, Zhou Y, Zhu M, Petasis NA, Gordon WC, Bazan NG (2013) Microglial ramification and redistribution concomitant with the attenuation of choroidal neovascularization by neuroprotectin D1. Mol Vis 19:1747–1759

Strauss O (2005) The retinal pigment epithelium in visual function. Physiol Rev 85:845–881

Zhao Y, Calon F, Julien C, Winkler JW, Petasis NA, Lukiw WJ, Bazan NG (2011) Docosahexaenoic acid-derived neuroprotectin D1 induces neuronal survival via secretase- and PPARγ-mediated mechanisms in Alzheimer's disease models. PLoS ONE 6:e15816

Chapter 52
Aging and Vision

Marcel V. Alavi

Abstract Aging involves defined genetic, biochemical and cellular pathways that regulate lifespan. These pathways are called longevity pathways and they have relevance for many age-related diseases. In the eye, longevity pathways are involved in the major blinding diseases, cataract, glaucoma, age-related macular degeneration (AMD) and diabetic retinopathy. Pharmaceutical targeting of longevity pathways can extend healthy lifespan in laboratory model systems. This offers the possibility of therapeutic interventions to also delay onset or slow the progression of age-related eye diseases. I suggest that retinal degeneration may be viewed as accelerated aging of photoreceptors and that interventions extending healthy lifespan may also slow the pace of photoreceptor loss.

Keywords Lens · Cataract · Retinal ganglion cells · Glaucoma · Retina · Age-related macular degeneration (AMD) · Insulin Diabetic retinopathy · Longevity pathways · Aging · Vision impairments

52.1 Aging and Longevity

Aging is the time-dependent accumulation of cellular insults or damage accompanied by subsequent functional decline that increase organisms' vulnerability to death (Lopez-Otin et al. 2013). This involves typical diseases associated with advanced age. The World Health Organization classifies these age-related diseases as noncommunicable diseases, the leading cause of death worldwide (Hunter and Reddy 2013). Age-related diseases of the eye are the major blinding diseases, cataract, glaucoma, age-related macular degeneration (AMD) and diabetic retinopathy, amongst others.

Many extrinsic factors in parallel influence the time-dependent accumulation of cellular insults or damage. Hence, there is no single aging process, and this is also

M. V. Alavi (✉)
Department of Ophthalmology, University of California, San Francisco, 10 Koret Way, San Francisco, CA 94143, USA
e-mail: marcel.alavi@gmail.com

C. Bowes Rickman et al. (eds.), *Retinal Degenerative Diseases,* Advances in Experimental Medicine and Biology 854, DOI 10.1007/978-3-319-17121-0_52

the case for the aging eye. On the other hand, mutations in single genes can extend lifespan of laboratory model organism suggesting that there are defined genetic, biochemical and cellular pathways that regulate lifespan (Kenyon et al. 1993; Partridge 2010; Kenyon 2011). How evolution selected for these pathways is beyond the scope of this review and I would like to refer the interested reader to the literature (e.g. Gavrilov and Gavrilova 2002; Pletcher et al. 2007; Partridge 2010). Pathways that (1) manifest over time, (2) whose experimental aggravation accelerates, and (3) whose amelioration retards the normal aging process are called longevity pathways, or hallmarks of aging (Lopez-Otin et al. 2013). To date, nine different hallmarks of aging have been identified, all of which more or less fulfill these three criteria. These longevity pathways are: genomic instability, telomere attrition, epigenetic alterations, loss of protein homeostasis (proteostasis), deregulated nutrient sensing, mitochondrial dysfunction, cellular senescence, stem cell exhaustion, and altered intercellular communication (Lopez-Otin et al. 2013).

A classical paradigm for a longevity pathway, and the first discovered (Kenyon et al. 1993; Kenyon 2011), is the nutrient sensing insulin- and insulin-like growth factor 1 (IGF-1)-signaling pathway, because IGF-1 levels decline during aging, anabolic signaling accelerates aging, and decreased nutrient signaling extends longevity (Alic and Partridge 2011; Barzilai et al. 2012). Another paradigm for a longevity pathway is loss of proteostasis, with profound alterations in the elderly. These alterations involve decline of quality control mechanisms that either degrade unfolded, misfolded, or aggregated proteins by the proteasome or the lysosomal system, or preserve the stability and functionality of the proteome by chaperones (Hartl et al. 2011). In various model systems proteostasis also can be experimentally manipulated in both directions, shortening and increasing lifespan (Hartl et al. 2011; Lopez-Otin et al. 2013). Age-related proteotoxicity thus contributes to development of age-related pathologies emphasizing how interwoven longevity pathways and age-related diseases are (Koga et al. 2011; Lopez-Otin et al. 2013). This is also the case for age-related eye diseases as discussed below.

52.2 Age-Related Diseases of the Eye

Age-related diseases are clinically heterogeneous and multifactorial with environmental and complex genetic contributions. As discussed above, the complex genetic contribution to age-related diseases involve longevity pathways. The eye is a terminally differentiated organ, which forms during development and is maintained throughout life. Advanced age is widely recognized as one of the biggest risk factors for many of the leading causes of vision loss, such as cataract, glaucoma, AMD and diabetic retinopathy (Klein and Klein 2013). Longevity pathways also play a pivotal role in the pathophysiology of these blinding diseases.

52.2.1 Cataracts—Loss of Proteostasis

Cataracts are very common in older people; in fact they are the leading cause of blindness worldwide. The prevalence for cataract was estimated at 17.2%, and this increased with ethnicity, sex, and age, with a maximum prevalence of 77% for caucasian woman above 80 years of age (Klein and Klein 2013). A cataract is clouding of the lens that affects vision. The lens is a key refractive element of the visual apparatus and its high protein content accounts for the high refractive index. Crystallins make up 30% of these proteins. With age, a continuous series of biochemical and biophysical changes caused by loss of proteostasis and mainly involving post-translational modifications of crystallins and other lens proteins lead to clouding, stiffness and increased light-scattering of the lens. To date, the best available treatment still is removing the cloudy lens and replacing it with an artificial lens (Michael and Bron 2011).

52.2.2 Glaucoma— Mitochondrial Dysfunction

Glaucoma is the leading cause of incurable worldwide blindness. It is a non-syndromic optic neuropathy clinically characterized by visual impairments and pathological changes of the optic nerve, which is caused by loss of retinal ganglion cells (Quigley 2011). Retinal ganglion cells project their axons via the optic nerve from the eye to the brain and are key for visual perception. What is more, there seems to be something special about retinal ganglion cells making them more vulnerable to age-related changes than other neurons. Hence, retinal ganglion cell impairments are associated with—and even precede—neurological changes in major age-related neurodegenerative diseases, including Parkinson's disease (Garcia-Martin et al. 2014; Satue et al. 2014), multiple sclerosis (Petzold et al. 2010), and Alzheimer's disease (Hinton et al. 1986). Glaucoma—as do many neurodegenerative diseases—involves mitochondrial dysfunction (Osborne 2010; Maresca et al. 2013). Mitochondrial quality control plays a pivotal role in containing mitochondrial dysfunction. Therefore, it is not surprising that sequence variants in mitochondrial quality control genes are associated with neurodegenerative diseases (Cho et al. 2010), in particular familial Parkinsonism (Pilsl and Winklhofer 2012). Remarkably, sequence variants in one mitochondrial quality control gene (*OPA1*), however, are associated with dominant optic atrophy, a juvenile non-syndromic optic neuropathy. For this, one may say that the relation of dominant optic atrophy to glaucoma is the same relation as of familial Parkinsonism to Parkinson's disease (Alavi and Fuhrmann 2013). To date, glaucoma is treated by intra-ocular pressure lowering drugs, because of a correlation of intra-ocular pressure and retinal ganglion cell loss (Quigley 2011). Drugs that prevent retinal ganglion cell loss still are not available.

52.2.3 Age-Related Macular Degeneration (AMD)—Altered Intercellular Communication

Not surprisingly, there is a correlation between patients showing signs of Alzheimer's disease and yet another devastating eye disease, AMD, as the risk for both diseases strongly increases with age (Williams et al. 2014). AMD is the leading cause of blindness in persons over the age of 50 and it affects 1.8 million Americans, who suffer from progressive central vision loss through photoreceptor degeneration (Swaroop et al. 2009). The majority of patients present with the dry forms of AMD, characterized by lipid deposits (drusen) beneath the retina and geographic atrophy (Curcio et al. 2011). Dry forms may progress to wet or neovascular forms of AMD, associated with sudden, acute and irreversible vision loss, because nascent vessels are leaky and prone to hemorrhages, which cause severe photoreceptor degeneration (Swaroop et al. 2009; Curcio et al. 2011). Immune processes play an essential role in the development and progression of AMD as lipid deposits provoke activation of the complement pathway, which leads to inflammation and aggravation of the disease (Ambati et al. 2013). AMD involves several longevity pathways, amongst others altered intercellular communication, because of the strong immune component of this disease (Ambati et al. 2013). The currently available therapies for AMD mainly target neovascularization, and there are no effective therapies for the majority of patients presenting with dry AMD.

52.2.4 Diabetic Retinopathy—Deregulated Nutrient Sensing

Another blinding disease, characterized by microaneurysms and small hemorrhages apparent on ophthalmoscopic examination, is diabetic retinopathy, the leading cause of blindness in working age adults. Diabetes is a multifactorial chronic disease that gives rise to many symptoms, such as cardiovascular impairments, stroke and neuropathy, and every third patient with diabetes develops diabetic retinopathy. Diabetes is a metabolic disorder with deregulated nutrient sensing, which involves the Insulin- and IGF-1-signaling pathway, among others. Insulin resistance increases with age leading to adult-onset or type 2 diabetes (Barzilai et al. 2012). Duration of diabetes and level of metabolic control are major risk factors for diabetic retinopathy, because hyperglycemia appears to drive development of the disease (Cunha-Vaz et al. 2014). Hyperglycemia affects different components of the retinal neurovascular unit giving rise to individual variation in the presentation and course of diabetic retinopathy (Cunha-Vaz et al. 2014). Therapeutic options for diabetic retinopathy to date are limited to governing these different symptoms.

52.3 Significance and Outlook

Gradual decline in mortality rates and fertility steadily increase the length of life and the proportion of older people. Consequently age-related diseases are becoming a growing burden for society. One way to alleviate society's burden is to increase healthy and disease-free lifespan. Manipulations of longevity pathways extends lifespan, and these interventions often keep laboratory models healthy and pathology-free to later ages by protecting them against age-related diseases, including neurodegenerative diseases and cancer (Lopez-Otin et al. 2013). If this holds true in a broader and more general context, then longevity pathways are promising targets for pharmacological interventions for age-related eye diseases, as well. Preserving proteostasis may help maintain the refractive properties of the lens and therefore delay onset of cataracts. More stringent mitochondrial quality control, on the other hand, counteracts age-related decline of mitochondrial integrity, and pharmaceuticals able to manipulate the mitochondrial quality control machinery may be neuroprotective in many neurodegenerative diseases, including glaucoma. Understanding the complex aspects of immune regulation in the eye will lead to new immune-based therapies for patients with AMD. Diabetic retinopathy involves deregulated nutrient sensing, and maintaining well regulated blood glucose levels also protects the eyes.

52.4 Concluding Remarks

Loss of proteostasis is a hallmark of aging with relevance for many age-related diseases. Roughly one-third of all cellular proteins reside in or pass through the endoplasmatic reticulum (ER), and a complex set of efficient signaling pathways, collectively referred to as the unfolded protein response (UPR) of the ER, carefully regulate proteostasis within the ER (van Anken and Braakman 2005). The UPR also triggers cellular responses that lead to apoptosis upon persistent ER stress (Lin et al. 2007). Interestingly, deletions of *xbp1,* a critical signaling molecule in the UPR, shortens lifespan in the worm *C. elegans* (Henis-Korenblit et al. 2010), while overexpression of a spliced *xbp1* isoform is able to alleviate ER stress and extend the healthy lifespan (Taylor and Dillin 2013), emphasizing the relation of proteostasis and aging. Rhodopsin mutations that cause ER stress lead to retinal degeneration in patients with autosomal dominant retinitis pigmentosa, as well as different laboratory models (Lin et al. 2007), and proteins of the UPR are promising targets for the treatment of this complex disease (Gorbatyuk et al. 2010; Ghosh et al. 2014). Given the fundamental significance of proteostasis for cell maintenance and survival, one may view retinal degeneration as accelerated aging of photoreceptor cells. Therapies that can extend healthy lifespan of organisms hence should also have the potential to slow photoreceptor cell loss in retinal degeneration.

Acknowledgements The cited literature refers mainly to overview articles that I believe provide a good entry point for the discussed topics. I apologize to those whose work was not discussed or referenced. I am very grateful to Drs. Matthew M. LaVail, Douglas B. Gould and Nico Fuhrmann for their insightful discussions and helpful comments.

References

Alavi MV, Fuhrmann N (2013) Dominant optic atrophy, OPA1, and mitochondrial quality control: understanding mitochondrial network dynamics. Mol Neurodegener 8:32

Alic N, Partridge L (2011) Death and dessert: nutrient signalling pathways and ageing. Curr Opin Cell Biol 23:738–743

Ambati J, Atkinson JP, Gelfand BD (2013) Immunology of age-related macular degeneration. Nat Rev Immunol 13:438–451

Barzilai N, Huffman DM, Muzumdar RH et al (2012) The critical role of metabolic pathways in aging. Diabetes 61:1315–1322

Cho DH, Nakamura T, Lipton SA (2010) Mitochondrial dynamics in cell death and neurodegeneration. Cell Mol Life Sci 67:3435–3447

Cunha-Vaz J, Ribeiro L, Lobo C (2014) Phenotypes and biomarkers of diabetic retinopathy. Prog Retin Eye Res 41C:90–111

Curcio CA, Johnson M, Rudolf M et al (2011) The oil spill in ageing Bruch membrane. Br J Ophthalmol 95:1638–1645

Garcia-Martin E, Larrosa JM, Polo V et al (2014) Distribution of retinal layer atrophy in patients with Parkinson disease and association with disease severity and duration. Am J Ophthalmol 157:470–478

Gavrilov LA, Gavrilova NS (2002) Evolutionary theories of aging and longevity. Sci World J 2:339–356

Ghosh R, Wang L, Wang ES et al (2014) Allosteric inhibition of the IRE1alpha RNase preserves cell viability and function during endoplasmic reticulum stress. Cell 158:534–548

Gorbatyuk MS, Knox T, LaVail MM et al (2010) Restoration of visual function in P23H rhodopsin transgenic rats by gene delivery of BiP/Grp78. Proc Natl Acad Sci U S A 107:5961–5966

Hartl FU, Bracher A, Hayer-Hartl M (2011) Molecular chaperones in protein folding and proteostasis. Nature 475:324–332

Henis-Korenblit S, Zhang P, Hansen M et al (2010) Insulin/IGF-1 signaling mutants reprogram ER stress response regulators to promote longevity. Proc Natl Acad Sci U S A 107:9730–9735

Hinton DR, Sadun AA, Blanks JC et al (1986) Optic-nerve degeneration in Alzheimer's disease. N Engl J Med 315:485–487

Hunter DJ, Reddy KS (2013) Noncommunicable diseases. N Engl J Med 369:1336–1343

Kenyon C (2011) The first long-lived mutants: discovery of the insulin/IGF-1 pathway for ageing. Philos Trans R Soc Lond B Biol Sci 366:9–16

Kenyon C, Chang J, Gensch E et al (1993) A *C. elegans* mutant that lives twice as long as wild type. Nature 366:461–464

Klein R, Klein BE (2013) The prevalence of age-related eye diseases and visual impairment in aging: current estimates. Invest Ophthalmol Vis Sci 54:ORSF5–ORSF13

Koga H, Kaushik S, Cuervo AM (2011) Protein homeostasis and aging: the importance of exquisite quality control. Ageing Res Rev 10:205–215

Lin JH, Li H, Yasumura D et al (2007) IRE1 signaling affects cell fate during the unfolded protein response. Science 318:944–949

Lopez-Otin C, Blasco MA, Partridge L et al (2013) The hallmarks of aging. Cell 153:1194–1217

Maresca A, la Morgia C, Caporali L et al (2013) The optic nerve: a "mito-window" on mitochondrial neurodegeneration. Mol Cell Neurosci 55:62–76

Michael R, Bron AJ (2011) The ageing lens and cataract: a model of normal and pathological ageing. Philos Trans R Soc Lond B Biol Sci 366:1278–1292
Osborne NN (2010) Mitochondria: their role in ganglion cell death and survival in primary open angle glaucoma. Exp Eye Res 90:750–757
Partridge L (2010) The new biology of ageing. Philos Trans R Soc Lond B Biol Sci 365:147–154
Petzold A, de Boer JF, Schippling S et al (2010) Optical coherence tomography in multiple sclerosis: a systematic review and meta-analysis. Lancet Neurol 9:921–932
Pilsl A, Winklhofer KF (2012) Parkin, PINK1 and mitochondrial integrity: emerging concepts of mitochondrial dysfunction in Parkinson's disease. Acta Neuropathol 123:173–188
Pletcher SD, Kabil H, Partridge L (2007) Chemical complexity and the genetics of aging. Annu Rev Ecol Evol Syst 38:299–326
Quigley HA (2011) Glaucoma. Lancet 377:1367–1377
Satue M, Seral M, Otin S et al (2014) Retinal thinning and correlation with functional disability in patients with Parkinson's disease. Br J Ophthalmol 98:350–355
Swaroop A, Chew EY, Rickman CB et al (2009) Unraveling a multifactorial late-onset disease: from genetic susceptibility to disease mechanisms for age-related macular degeneration. Annu Rev Genomics Hum Genet 10:19–43
Taylor RC, Dillin A (2013) XBP-1 is a cell-nonautonomous regulator of stress resistance and longevity. Cell 153:1435–1447
van Anken E, Braakman I (2005) Versatility of the endoplasmic reticulum protein folding factory. Crit Rev Biochem Mol Biol 40:191–228
Williams MA, Silvestri V, Craig D et al (2014) The prevalence of age-related macular degeneration in Alzheimer's disease. J Alzheimers Dis 42:909–914

Part VI
Neuroprotection, Small Molecules and Related Therapeutic Approaches

Chapter 53
The Potential Use of PGC-1α and PGC-1β to Protect the Retina by Stimulating Mitochondrial Repair

Carolina Abrahan and John D. Ash

Abstract Damage to mitochondria is a common mechanism of cell death in inherited neurodegenerative disorders. Therefore, mitochondrial protection and mitochondrial repair are promising strategies to induce retinal neuroprotection. Peroxisome proliferator-activated receptor γ coactivator-α (PGC-1α) and β (PGC-1β) are transcriptional coactivators that are the main regulators of mitochondrial biogenesis. We propose that PGC-1α and PGC-1β could play a role in regulating retina cell survival, and may be important therapeutic targets to prevent retinal degeneration.

Keywords Neuroprotection · Retina · PGC-1alpha · PGC-1beta · Mitochondrial biogenesis

Abbreviations

PGC-1α	Peroxisome proliferator-activated receptor γ coactivator-α
PGC-1β	Peroxisome proliferator-activated receptor γ coactivator-β
ROS	Reactive oxygen species
mtDNA	Mitochondrial DNA
NRF-1 and NRF-2	Nuclear respiratory factors -1 and 2
PPAR	Peroxisome proliferator-activated receptor
AMPK	Adenosine mono-phoshpate-dependent Kinase
UCP	Uncoupling protein

The original version of this chapter was revised. An erratum to this chapter can be found at DOI 10.1007/978-3-319-17121-0_107

J. D. Ash (✉)
Department of Ophthalmology, University of Florida, ARB-RG232, 1600 SW Archer Rd, Gainesville, FL 32610, USA
e-mail: jash@ufl.edu

C. Abrahan
Department of Environmental Horticulture Research, University of Florida, Gainesville, FL 32611-0670, USA
e-mail: cabrahan@ufl.edu

C. Bowes Rickman et al. (eds.), *Retinal Degenerative Diseases,* Advances in Experimental Medicine and Biology 854, DOI 10.1007/978-3-319-17121-0_53

53.1 Introduction

Retinal neurodegenerative disorders are associated with aging and inherited mutations. As with other neurodegenerative diseases, retinal degeneration has been associated with mitochondrial dysfunction and toxic oxidative damage. The mitochondrial free-radical theory of aging proposes that cumulative oxidative damage to cellular macromolecules is a consequence of reactive oxygen species (ROS) produced by a leaky mitochondrial respiratory chain. Therefore, one of the first approaches to revert or stop the mitochondrial decline was the development of antioxidant therapies, or therapies designed to stimulate antioxidant self-defense systems. Despite promising results in cell culture and animal studies, antioxidant therapies in humans have not been highly beneficial (Stuart et al. 2014). These disappointing setbacks have led to realization that prevention of oxidative stress is not sufficient and that treatment of mitochondrial dysfunction is likely to require a more multifaceted approach. This has been supported by studies showing that ROS production is not necessarily a cause for disease, but may in fact by a signaling mechanism to induce protective pathways (Bratic and Larsson 2013). Oxidative stress may be a sign of mitochondrial damage, but other factors may be responsible for cell damage. Recent studies suggest that somatic mutations in mitochondrial DNA could be involved in degeneration (Srivastava et al. 2009). Repairing or replacing damaged mitochondria is therefore a promising new approach to slow or prevent retinal degeneration.

53.2 PGC-1α and β as Regulators of Mitochondrial Biogenesis

Multiple transcription factors have been shown to be essential regulators of mitochondrial biogenesis and nuclear encoded gene expression. Most mitochondrial proteins are encoded by nuclear genes. Therefore, nuclear transcription factors are essential for regulating mitochondrial biogenesis and function. Two key factors are nuclear respiratory factors-1 and 2 (NRF-1 and NRF-2). These factors activate the synthesis of nuclear proteins that are involved in transport of proteins through mitochondrial membranes as well as protein in the respiratory chain and Krebs cycle (Ventura-Clapier et al. 2008). In addition, NRF-1 and -2 promote mitochondrial biogenesis by activating the expression of mitochondrial transcription factor A (Tfam), transcription factor B1 and B2 (TFB1M and TFB2M), which increase mtDNA transcription and mitochondrial RNA polymerase activity, and DNA replication (Chen et al. 2009). While NRFs are essential factors for mitochondrial gene expression, they require co-factors for activity. Peroxisome proliferator-activated receptor γ coactivator (PGC-1) is a family of co-activators that are important for NRF activity. To date there are three related genes in the family including PGC-1α, PGC-1β, and PRC-1. The three proteins share a do-

main (LXXLL), through which they interact with nuclear hormone receptors. PGC-1α and β have an NH2-terminal activation domain as well as RNA recognition motifs. In addition, PGC-1α has a COOH-terminal arginine/serine rich (R/S) domain through which PGC-1α activates transcription and RNA processing. This (R/S) domain is absent in PGC-1β (Scarpulla 2008). Both PGC-1α and PGC-1β have prominent roles in mitochondrial biogenesis and gene expression, but little is known about PRC-1. PGC-1α has been shown to induce expression of NRF-1 and NRF-2, and bind both factors to enhance their transcriptional activity (Gleyzer et al. 2005). In addition to NRF-1and NRF-2, PGC-1α and PGC-1β have been shown to be binding partners and co-activators of additional transcription factors required for mitochondrial gene expression including PPARs (Peroxisome proliferator-activated receptor), ERR (estrogen-related receptor), RXR (retinoid X receptor), PXR (pregnane X receptor), FOXO1 (forkhead box O1), MEF-2 (myocyte enhancer factor-2), and SREBP1 (Sterol regulatory element-binding transcription factor 1) (Finck and Kelly 2006). Thus, PGC-1s play a prominent role in mitochondrial biogenesis.

53.3 Regulation of PGC-1α Expression and Activity

PGC-1 expression and activity is highly regulated. Most studies have focused on the regulation of PGC-1α. Depending of the tissue, PGC-1α expression can be up-regulated by several pathways including activation of Ca^{2+}/calmodulin-dependent protein kinase IV (CaMKIV), calcineurin A, the p38 mitogen-activated protein kinase (p38 MAPK), adenosine mono-phosphate-dependent Kinase (AMPK) and protein kinase A (PKA). However, PGC-1α is normally maintained in an inactive state by acetylation at multiple sites on the protein. The activity of PGC-1α can be modified by post-translational modifications such as phosphorylation, ubiquitination, methylation and acetylation. A review of how PGC-1α expression and activity is regulated can be found in (Fernandez-Marcos and Auwerx 2011). To become fully active, PGC-1 must be deacetylated by NAD-dependent-protein de-acetylaces such as Sirtuin 1 (Sirt-1) and phosphorylated by serine/threonine kinases such as AMPK (Canto and Auwerx 2009). Because of the requirement for de-acetylation and phosphorylation, PGC-1 activity is highly regulated by mitochondrial output and oxidative stress. Under conditions of mitochondrial dysfunction, cells have elevated ratios of adenosine mono-phosphate (AMP) to adenosine tri-phosphate (ATP), and increased levels of NAD^+, which will activate both AMPK and Sirt-1 respectively. Then, AMPK and Sirt-1 cooperate to activate PGC-1s by phosphorylation and de-acetylation. Once activated, PGC-1s increase mitochondrial gene expression to increase energy production and reduce oxidative stress and thus rescue the cell. PGC-1s are therefore a target to induce protection by regulating mitochondrial biogenesis and repair.

53.4 PGC-1s as Regulators of Mitochondrial Editing and Repair

Mitochondria can have multiple copies of their genome, so that it is possible that damaged or mutated mtDNA coexists with normal mtDNA (heteroplasmy). MtDNA mutations can cause respiratory chain dysfunction, and this will lead to catastrophic oxidative stress and cell death. It is know that mitochondria within a cell exist as a dynamic network capable of exchanging proteins and DNA. These processes are regulated by cycles of fusion and fission (Seo et al. 2010). Through a process of fusion, smaller mitochondria fuse together as a way to equilibrate the concentration of all nuclear-encoded mitochondria proteins in the mitochondria network, exchange and mix mitochondrial DNA as a mechanism to dilute damaged DNA, and to improve efficiency of ATP production. On the other hand, fission is thought to be a mechanism of mitochondrial editing. Under stress states, mitochondria are fragmented into smaller segments, and segments that cannot maintain a membrane potential are removed by mitophagy (Kowald and Kirkwood 2011). Once oxidative stress is reduced, mitochondria undergo a biogenic repair by inducing mtDNA replication and increased gene expression, and reinitiate fusion. Promoting cycles of fission, followed by editing, biogenesis, and fusion can be a therapeutic target to prevent cell death. This process of biogenesis and fusion can be regulated by PGC-1α. In a mouse model of accelerated mitochondrial damage, overexpression of PGC-1α in the muscle improved skeletal muscle function by increasing mitochondrial biogenesis. Although the overexpression of PGC-1α did not reduce the proportion of mutated mtDNA (Dillon et al. 2012), the coactivation of the orphan nuclear receptor ERRα by PGC-1α could stimulate the transcription of Mitofusin 1 and 2, two proteins involved in the mitochondrial fusion as part of the neuroprotective program activated by PGC-1α (Martin et al. 2014; Cartoni et al. 2005). By these mechanisms, PGC-1α can promote mitochondrial activity by increasing the synthesis of nuclear encoded mitochondrial proteins, and their distribution by fusion through the mitochondria network. It is interesting to note that the process of fission, mitophagy, fusion and biogenesis is coordinated by the activation of AMPK. AMPK is thought to promote mitophagy of defective mitochondria, but also activates PGC-1α to initiate a program of biogenesis and replacement with new, more functional mitochondria (Mihaylova and Shaw 2011)).

53.5 Regulation of Uncoupling Proteins as a Mechanism of Protection

Functionally, PGC-1α and β have some similarities as well as differences. For example, both PGC-1α and β are capable of inducing mitochondrial biogenesis, however, it is know that PGC-1α activates thermogenesis in brown fat and gluco-

neogenesis in hepatocytes and PGC-1β does not (Lin et al. 2003). PGC-1s were first described as cofactors of nuclear receptor PPARγ (Peroxisome proliferator-activated receptor γ) and the thyroid hormone receptor. Through these interactions PGC-1 was shown to be responsible for promoting the expression of uncoupling protein-1 (UCP-1) and promoting an increase in mitochondrial DNA as part of adaptive thermogenesis (Puigserver et al. 1998). Later, PGC-1α and β were shown to be activators of UCP-2 and UCP-3 transcription (Rigoulet et al. 2011). As with UCP-1, these two proteins are anion carriers, however, they are not associated with adaptive thermogenesis (Brand and Esteves 2005). Instead, it has been proposed that these two uncoupling proteins could have neuroprotective properties by reducing mitochondrial ROS production (Mattiasson et al. 2003; Mailloux and Harper 2011). Experiments *in vitro* have shown that isolated mitochondria have a higher rate of ROS production when the electrochemiosmotic potential is higher. Proton leak through UCPs or protonophores across the mitochondrial inner membrane leads to a reduced production of ROS with minimal respiration rate but still sufficient ATP production (Brand and Esteves 2005). It is know that UCP-2 protein is expressed in ganglionar cells but it is not clear if UCPs are expressed in photoreceptors (Barnstable and Tombran-Tink 2006). Whether or not these proteins have neuroprotective properties after activation by PGC-1α or β in the retina is not known yet.

53.6 PGC-1α and β in the Retina

Despite numerous studies on the role of PGC-1s in muscle and adipose tissue, little is known about their roles in the neural retina and RPE. In ARPE-19 human retinal pigment epithelial cells, hydroxytyrosol, an antioxidant polyphenol, protects cells from oxidative stress by activating PGC-1α (Zhu et al. 2010). As was found in skeletal muscle, PGC-1α induces the expression of vascular endothelial growth factor (VEGFA) in retinal cells. Since PGC-1α is highly expressed in the inner nuclear layer of the retina in a mouse model of oxygen-induced retinopathy, it therefore suggests a role for PGC-1α during neovascularization (Saint-Geniez et al. 2013). Moreover, there are other studies that suggest a role of PGC-1α and β in the neural retina, as their expression would be important in preventing light damage (Egger et al. 2012).

53.7 Future Approaches

The number of studies to develop therapeutic tools based on induction of mitochondrial biogenesis are growing. This strategy could have an impact on diseases caused by mitochondrial disorders, but may also be beneficial in aging and neurodegenerative diseases.

More work is needed to establish the function of PGC-1α and β in the retina. Retina specific knockouts for PGC-1α and β can now be used to determine if these factors play and important role in rod and cone function under normal conditions, and in aging or during oxidative stress. PGC-1α and β have partially redundant functions and therefore simple knockouts might not show an alteration in retina function. The development of double knockouts may be required to clarify the importance of PGC-1α and/or β in the retina in normal and stressed conditions. Furthermore, as metabolic activity in the retina is different depending on the cell type, cell-type specific PGC-1α/β knockouts are necessary.

Overexpression of PGC-1α and β appears to be a promising approach to promote cell survival (Srivastava et al. 2009). Adeno-associated virus gene therapy vectors could be used. However, it is necessary to deliver the proper isoforms of PGC-1α and/or PGC-1β to photoreceptors or RPE to induce cell survival. In addition to the overexpression of the PGC-1s, it may also be necessary to induce a physiological state to activate these coactivators.

It is clear that more research is needed to determine the role of the different isoforms of PGC-1s in the retina, and the mechanisms of activation. This knowledge is necessary to develop drug or gene therapies to promote retinal protection through induced mitochondrial biogenesis.

References

Barnstable CJ, Tombran-Tink J (2006) Molecular mechanisms of neuroprotection in the eye. Adv Exp Med Biol 572:291–295

Brand MD, Esteves TC (2005) Physiological functions of the mitochondrial uncoupling proteins UCP2 and UCP3. Cell Metab 2:85–93

Bratic A, Larsson NG (2013) The role of mitochondria in aging. J Clin Invest 123:951–957

Canto C, Auwerx J (2009) PGC-1alpha, SIRT1 and AMPK, an energy sensing network that controls energy expenditure. Curr Opin Lipidol 20:98–105

Cartoni R, Léger B, Hock MB, Praz M, Crettenand A, Pich S, Ziltener JL, Luthi F, Dériaz O, Zorzano A, Gobelet C, Kralli A, Russell AP et al (2005) Mitofusins 1/2 and ERRalpha expression are increased in human skeletal muscle after physical exercise.J Physiol.15;567(Pt 1):349-58. Accessed 16 June 2005. PMID: 15961417

Chen JQ, Cammarata PR, Baines CP, Yager JD (2009) Regulation of mitochondrial respiratory chain biogenesis by estrogens/estrogen receptors and physiological, pathological and pharmacological implications. Biochim Biophys Acta 1793:1540–1570

Dillon LM, Williams SL, Hida A, Peacock JD, Prolla TA, Lincoln J et al (2012) Increased mitochondrial biogenesis in muscle improves aging phenotypes in the mtDNA mutator mouse. Hum Mol Genet 21:2288–2297

Egger A, Samardzija M, Sothilingam V, Tanimoto N, Lange C, Salatino S, Fang L, Garcia-Garrido M, Beck S, Okoniewski MJ, Neutzner A, Seeliger MW, Grimm C, Handschin C et al (2012) PGC-1α determines light damage susceptibility of the murine retina. PLoS One.7(2):e31272. doi: 10.1371/journal.pone.0031272. PMID: 22348062

Fernandez-Marcos PJ, Auwerx J (2011) Regulation of PGC-1alpha, a nodal regulator of mitochondrial biogenesis. Am J Clin Nutr 93:884S–890S

Finck BN, Kelly DP (2006) PGC-1 coactivators: inducible regulators of energy metabolism in health and disease. J Clin Invest 116:615–622

Gleyzer N, Vercauteren K, Scarpulla RC (2005) Control of mitochondrial transcription specificity factors (TFB1M and TFB2M) by nuclear respiratory factors (NRF-1 and NRF-2) and PGC-1 family coactivators. Mol Cell Biol 25:1354–1366

Kowald A, Kirkwood TB (2011) Evolution of the mitochondrial fusion-fission cycle and its role in aging. Proc Natl Acad Sci U S A 108:10237–10242

Lin J, Tarr PT, Yang R, Rhee J, Puigserver P, Newgard CB et al (2003) PGC-1 beta in the regulation of hepatic glucose and energy metabolism. J Biol Chem 278:30843–30848

Mailloux RJ, Harper ME (2011) Uncoupling proteins and the control of mitochondrial reactive oxygen species production. Free Radic Biol Med 51:1106–1115

Martin OJ, Lai L, Soundarapandian MM, Leone TC, Zorzano A, Keller MP et al (2014) A role for peroxisome proliferator-activated receptor gamma coactivator-1 in the control of mitochondrial dynamics during postnatal cardiac growth. Circ Res 114:626–636

Mattiasson G, Shamloo M, Gido G, Mathi K, Tomasevic G, Yi S et al (2003) Uncoupling protein-2 prevents neuronal death and diminishes brain dysfunction after stroke and brain trauma. Nat Med 9:1062–1068

Mihaylova MM, Shaw RJ (2011) The AMPK signalling pathway coordinates cell growth, autophagy and metabolism. Nat Cell Biol 13:1016–1023

Puigserver P, Wu Z, Park CW, Graves R, Wright M, Spiegelman BM (1998) A cold-inducible coactivator of nuclear receptors linked to adaptive thermogenesis. Cell 92:829–839

Rigoulet M, Yoboue ED, Devin A (2011) Mitochondrial ROS generation and its regulation: mechanisms involved in H(2)O(2) signaling. Antioxid Redox Signal 14:459–468

Saint-Geniez M, Jiang A, Abend S, Liu L, Sweigard H, Connor KM et al (2013) PGC-1alpha regulates normal and pathological angiogenesis in the retina. Am J Pathol 182:255–265

Scarpulla RC (2008) Transcriptional paradigms in mammalian mitochondrial biogenesis and function. Physiol Rev 88:611–638

Seo AY, Joseph AM, Dutta D, Hwang JC, Aris JP, Leeuwenburgh C (2010) New insights into the role of mitochondria in aging: mitochondrial dynamics and more. J Cell Sci 123(Pt 15):2533–2542

Srivastava S, Diaz F, Iommarini L, Aure K, Lombes A, Moraes CT (2009) PGC-1alpha/beta induced expression partially compensates for respiratory chain defects in cells from patients with mitochondrial disorders. Hum Mol Genet 18:1805–1812

Stuart JA, Maddalena LA, Merilovich M, Robb EL (2014) A midlife crisis for the mitochondrial free radical theory of aging. Longev Healthspan 3:4

Ventura-Clapier R, Garnier A, Veksler V (2008) Transcriptional control of mitochondrial biogenesis: the central role of PGC-1alpha. Cardiovasc Res 79:208–217

Zhu L, Liu Z, Feng Z, Hao J, Shen W, Li X et al (2010) Hydroxytyrosol protects against oxidative damage by simultaneous activation of mitochondrial biogenesis and phase II detoxifying enzyme systems in retinal pigment epithelial cells. J Nutr Biochem 21:1089–1098

Chapter 54
Retinal Caveolin-1 Modulates Neuroprotective Signaling

Alaina Reagan, Xiaowu Gu, Stefanie M. Hauck, John D. Ash, Guangwen Cao, Timothy C. Thompson and Michael H. Elliott

Abstract Caveolin-1 (Cav-1), the scaffolding protein of caveolae, is expressed in several retinal cell types and is associated with ocular pathologies. Cav-1 modulates neuroinflammatory/neuroprotective responses to central nervous system injury. We have shown that loss of Cav-1 results in a blunted cytokine response in retinas challenged with inflammatory stimuli. As neuroinflammatory and neuroprotective signaling overlap in their cytokine production and downstream signaling pathways, we hypothesized that loss of Cav-1 may also suppress neuroprotective signaling in the retina. To test this, we subjected mice in which Cav-1 was deleted specifically in the retina to a neurodegenerative insult induced by sodium iodate ($NaIO_3$) and measured STAT3 activation, a measure of neuroprotective signaling. Our results show that Cav-1 ablation blunts STAT3 activation induced by $NaIO_3$. STAT3 activation in response to intravitreal administration of the IL-6 family cytokine, leukemia inhibitory factor (LIF), was not affected by Cav-1 deletion indicating a competent gp130 receptor response. Thus, Cav-1 modulates neuroprotective signaling by regulating the endogenous production of neuroprotective factors.

Keywords Caveolin-1 · Cre/lox · Conditional knockout · Neuroprotection · Cytokines · Sodium Iodate · STAT3

M. H. Elliott (✉) · A. Reagan · X. Gu
Department of Ophthalmology, University of Oklahoma Health Sciences Center, Oklahoma City, OK 73104, USA
e-mail: Michael-Elliott@ouhsc.edu

Oklahoma Center for Neuroscience, University of Oklahoma Health Sciences Center, Oklahoma City, OK 73104, USA

Dean A. McGee Eye Institute, University of Oklahoma Health Sciences Center, 608 Stanton L. Young Boulevard Rm. 423, Oklahoma City, OK 73104, USA

A. Reagan
e-mail: alaina-reagan@ouhsc.edu

C. Bowes Rickman et al. (eds.), *Retinal Degenerative Diseases,* Advances in Experimental Medicine and Biology 854, DOI 10.1007/978-3-319-17121-0_54

54.1 Introduction

Cav-1 is the principal protein of caveolae and is involved in cellular functions including endocytosis, mechanotransduction, and cell signaling (Parton and Simons 2007). Cav-1 is expressed in several retinal cell types including retinal vasculature, retinal pigment epithelium (RPE) and Müller glia (Gu et al. 2014a, b; Li et al. 2014). Cav-1 is linked to diseases with significant retinal pathologies including diabetic retinopathy and glaucoma (Klaassen et al. 2013; Thorleifsson et al. 2010) but its role in retinal neuroprotection is unknown. Retinal cells express several toll-like receptors (TLRs) that recognize and respond to pathogenic stimuli and initiate pro-inflammatory cytokine responses. Cav-1 associates with TLRs and regulates TLR signaling (Jiao et al. 2013). In addition to recruiting circulating leukocytes during inflammation, cytokines also act as ligands for neuroprotective signaling. In particular, IL-6 family cytokines including ciliary neurotrophic factor (CNTF) and LIF activate the JAK/STAT pathway, which upregulates anti-apoptotic factors to prevent retinal neuronal death (Chucair-Elliott et al. 2012; Lavail et al. 1992).

The purpose of this study was to determine if retina-specific ablation of Cav-1 alters expression of downstream neuroprotective signaling after insult. We subjected retina-specific Cav-1 knockout and littermate control mice to $NaIO_3$ treatment, which induces RPE damage and secondary retinal degeneration (Carido et al. 2014). We show that loss of Cav-1 dampens injury-induced STAT3 activation in the retina.

X. Gu
e-mail: xgu12@jhmi.edu

M. H. Elliott
Department of Physiology, University of Oklahoma Health Sciences Center, Oklahoma City, OK 73104, USA

S. M. Hauck
Research Unit Protein Science, Helmoltz Zentrum München, 85764 Neuherberg, Germany
e-mail: hauck@helmholtz-muenchen.de

J. D. Ash
Department of Ophthalmology Research, University of Florida, Gainesville, FL 32610, USA
e-mail: jash@ufl.edu

G. Cao
Department of Epidemiology, Second Military Medical University, Shanghai 200433, China
e-mail: gcao@smmu.edu.cn

T. C. Thompson
Department of Genitourinary Medical Oncology-Research, MD Anderson Cancer Center, The University of Texas, Houston, TX 77030, USA
e-mail: timthomp@mdanderson.org

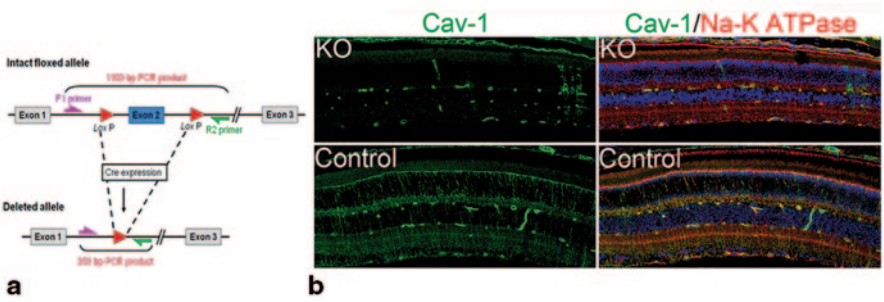

Fig. 54.1 **a** Cartoon illustrating deletion of exon 2 of Cav-1 by tissue-specific Cre recombinase expression. **b** Cav-1 localization in retinal sections of conditional KO and the control retinas. Cav-1 (*green*), Na-K ATPase (*red*) and DAPI (*blue*)

54.2 Materials and Methods

54.2.1 Mice

All procedures were carried out according to the Association for Research in Vision and Ophthalmology Statement for the Use of Animals in Ophthalmic and Vision Research and were approved by Institutional Animal Care and Use Committee of the University of Oklahoma Health Sciences Center. Retina specific Cav-1 KO mice (Retina-Cav-1-KO) were generated by crossing floxed Cav-1 mice carrying loxP sites inserted in intronic regions flanking exon 2 of the *Cav1* gene (Cao et al. 2003) with mice carrying Cre recombinase driven by the Chx10 promoter (Rowan and Cepko 2004). Mice were backcrossed to generate littermate mice homozygous for the *Cav1* floxed allele that carried either Chx10-Cre (Retina-Cav-1-KO) or did not (littermate controls wild type for Cav-1 expression). Recombined retinal cells in Retina-Cav-1-KO mice were null for Cav-1 protein (Fig. 54.1b) as previously described for global Cav-1 KO mice generated using the same floxed construct (Cao et al. 2003).

54.2.2 Sodium Iodate and LIF Injection

Adult male and female retina-Cav-1-KO mice and littermate controls were systemically injected with 25 mg/kg $NaIO_3$ (Sigma-Aldrich, St. Louis, MO). In other experiments, 0.5 μg LIF in 1 μL PBS (Millipore, Billerica, MA) was injected intravitreally. Seven days after $NaIO_3$ treatment or 24 h after LIF injection mice were euthanized by CO_2 inhalation, eyes were prepared for eyecup flatmounts, histology, immunohistochemistry, and Western blot analysis.

54.2.3 Retinal Flatmount Preparation, Immunohistochemistry

For eyecup flatmounts, enucleated eyes were fixed in 4% paraformaldahyde (PFA; Electron Microscopy Sciences, Hattfield, PA) in PBS for 10 min after a small incision was made at the limbus. Anterior segments, lens and vitreous were removed and eyecups were fixed for an additional 40 min. Retinas were then removed and resulting eyecups with RPE intact were permeabilized in PBS containing 1% Triton X-100. Immunohistochemistry was performed as previously described for retinas (Gu et al. 2014a). Eyecups were stained with FITC-Phalloidin (Life Technologies, Grand Island, NY) to label the actin cytoskeleton at RPE cell borders. Immunohistochemistry of retinal paraffin sections fixed with Prefer fixative (Anatech, Ltd., Battlefield, MI) was performed as described (Gu et al. 2014b) using rabbit polyclonal rabbit anti-Cav-1 (1:400, BD Biosciences, San Jose, CA) and monoclonal anti-α1-Na/K-ATPase (clone a6f; 1:100, DSHB, University of Iowa, Iowa City, IA). Imaging was performed on an FV1200 (Olympus, Tokyo, Japan) confocal microscope.

54.2.4 Western Blotting

Retinas were lysed in buffer containing 60 mM octylglucoside, 10 mM Tris-HCl, pH 7.4, 100 mM NaCl, 0.5 mM EDTA and 1 mM orthovanadate and Western blots were probed with: mouse monoclonal antibodies against β-actin (Sigma, 1:7500) and α-tubulin (Sigma, 1:500) and rabbit polyclonal antibodies against Cav-1 (BD Biosciences, 1:3000) and pSTAT3 (Cell Signaling, 1:1000). Imaging and densitometry were performed on an *In Vivo* F-Pro Image System (Carestream Health, Inc., Rochester, NY).

54.3 Results

54.3.1 Efficient Cav-1 Deletion in Retina-Cav-1-KO Mice

The Chx10 promoter is expressed in neuroretinal progenitor cells during development (Rowan and Cepko 2004) and Chx10-driven Cre expression promotes efficient recombination in retinal neurons and Müller glia (Chucair-Elliott et al. 2012). Recombination of floxed Cav-1 (Fig. 54.1a) resulted in loss of Cav-1 protein in the neural retina except for a small number of cells with Müller glial morphology (Fig. 54.1b). Cav-1 expression is retained in retinal vasculature and RPE as these cells are not targeted by Chx10-driven Cre. By quantitative mass spectrometry and Western blot densitometric analysis (not shown), Cav-1 protein was reduced by 70%. As the non-targeted retinal vasculature contributes to the remaining 30% of Cav-1 protein in whole retinal lysates, we estimate the deletion in targeted cells to be even more efficient.

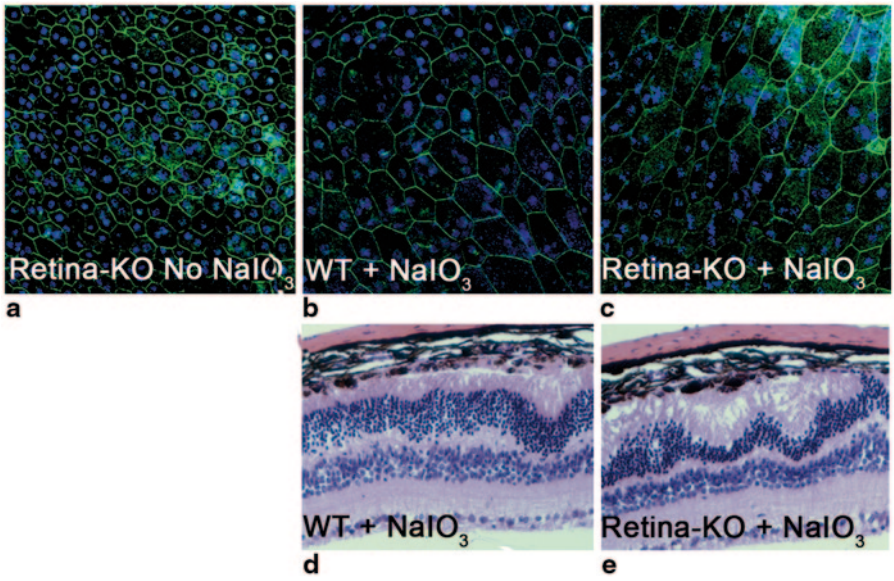

Fig. 54.2 **a–c** RPE damage is similar between genotypes at 7 day post-$NaIO_3$ treatment. Eyecups were stained with Phalloidin (*green*) and DAPI (*blue*). **d**, **e** Hematoxylin/eosin stained sections from Retina-Cav-1-KO and littermate controls after $NaIO_3$ treatment

54.3.2 Sodium Iodate Induces Similar Damage to the RPE of Both Genotypes

Intraperitoneal injection of $NaIO_3$ specifically destroys the RPE resulting in secondary retinal injury resembling that observed in macular degenerations. As the RPE is not targeted by Chx10-Cre, Cav-1 expression in the RPE is retained similarly in both genotypes. Thus, RPE damage from $NaIO_3$ should not differ between genotypes and any effects on the retina should be derived only from deletion of Cav-1 in the neural retina. In undamaged eyes, the hexagonal RPE cells are consistent in size and shape and are, in many cases, binucleated. Figure 54.2a shows a typical WT RPE monolayer from an untreated Retina-Cav-1-KO mouse stained with Phalloidin and DAPI. As expected, 7 days after $NaIO_3$ treatment, RPE damage was not different between genotypes (Fig. 54.2b and c). Figure 54.2d and e show representative retinal sections from $n=4$ eyes per genotype that also display similar damage. Quantitative assessment of retinal neuronal loss is difficult at this relatively early post-$NaIO_3$ time, so we are not yet certain if loss of Cav-1 specifically in the neural retina/Müller glia results in enhanced neurodegeneration. Of note, retinal function as assessed by electroretinography was also virtually lost in both genotypes treated with $NaIO_3$ (data not shown). As $NaIO_3$ induced similar insults to the RPE in both genotypes, we next assessed whether Cav-1 deletion specifically in the retina resulted in altered endogenous neuroprotective signaling.

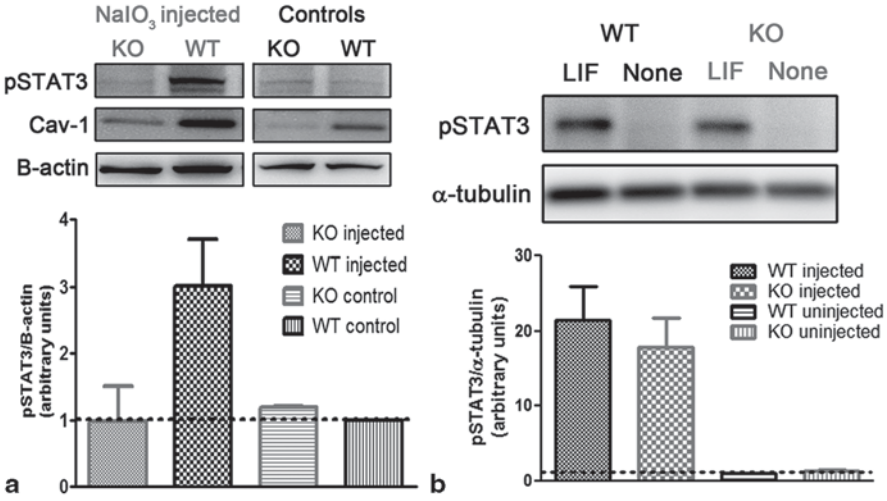

Fig. 54.3 **a** Blunted STAT3 activation in Retina-Cav-1 KO mice after $NaIO_3$ treatment. **b** Activation of STAT3 pathway by exogenous administration of LIF is not affected by retina-specific Cav-1 ablation

54.3.3 STAT3 Activation is Suppressed in $NaIO_3$-Treated Retina-Cav-1-KO Retinas

The typical retinal damage response results in local production of endogenous neuroprotective molecules including IL-6 family cytokines (Lavail et al. 1992; Chucair-Elliott et al. 2012). This results in activation of the IL-6 family signaling receptor, gp130, and a downstream STAT3 response. Thus, we assessed STAT3 activation in $NaIO_3$-treated Retina-Cav-1-KO and control retinas by Western blot analysis for phosphorylated STAT3 as previously described (Chucair-Elliott et al. 2012). Sodium iodate treatment resulted in characteristic STAT3 activation in littermate controls which was dramatically suppressed in Retina-Cav-1-KO retinas (Fig. 54.3a). These results suggest that retinal Cav-1 modulates either the production of neuroprotective cytokines and/or the downstream activation of the gp130 receptor pathway.

To directly determine whether the gp130/STAT3 pathway is competent in Retina-Cav-1-KO retinas, we intravitreally injected LIF and assessed STAT3 activation. As shown in Fig. 54.3b, LIF induced equivalent STAT3 activation in both genotypes suggesting that the blunted neuroprotective response to $NaIO_3$ is upstream of gp130.

54.4 Discussion

Here we demonstrate the first successful generation of a conditional knockout mouse with efficient retina-specific Cav-1 deletion. Because Cav-1 has previously been linked to ocular pathologies (Klaassen et al. 2013; Thorleifsson et al. 2010),

this mouse model allows us to test the retina-intrinsic roles of Cav-1 in retinal neuroprotection in a variety of disease-relevant insults. Using this unique mouse model we show here that retinal Cav-1 plays a critical role in modulating stress-induced neuroprotective signaling. As inducers of retinal STAT3 activation (e.g., CNTF) are currently in clinical trials for retinal degenerative diseases, understanding the endogenous signaling cascades that mediate retinal neuroprotection is essential. Our results provide evidence that retina-intrinsic Cav-1 promotes neuroprotective signaling upstream of the gp130 receptor. We have recently shown that Cav-1 supports the production of inflammatory cytokines such as IL-6 in response to inflammatory challenge (Li et al. 2014). In the context of these published results, the findings presented herein suggest that Cav-1 may also promote the damage-associated induction of neuroprotective cytokines but this remains to be determined directly. Intriguingly, Cav-1 regulates TLR4 activity (Jiao et al. 2013) outside of the eye and our results suggest that similar Cav-1-modulated innate immune receptors may also initiate damage responses in the retina. Because retinal pathology so often results in functional and/or morphological neuronal loss, the identification of Cav-1 as a potential neuroprotective modulator may be significant.

Acknowledgements This research is supported in part by NIH grants EY019494, NEI core grant P30EY021725, M.D. Anderson's Cancer Center Support Grant P30 CA016672, a Sybil B. Harrington Special Scholar Award for Macular Degeneration Research and an unrestricted grant from Research to Prevent Blindness, Inc.

References

Cao G, Yang G, Timme TL, Saika T, Truong LD, Satoh T, Goltsov A, Park SH, Men T, Kusaka N, Tian W, Ren C, Wang H, Kadmon D, Cai WW, Chinault AC, Boone TB, Bradley A, Thompson TC (2003) Disruption of the caveolin-1 gene impairs renal calcium reabsorption and leads to hypercalciuria and urolithiasis. Am J Pathol 162:1241–1248

Carido M, Zhu Y, Postel K, Benkner B, Cimalla P, Karl MO, Kurth T, Paquet-Durand F, Koch E, Munch T, Tanaka EM, Ader M (2014) Characterization of a mouse model with complete RPE loss and its use for RPE cell transplantation. Invest Ophthalmol Vis Sci 55:5431–5444

Chucair-Elliott AJ, Elliott MH, Wang J, Moiseyev GP, Ma JX, Politi LE, Rotstein NP, Akira S, Uematsu S, Ash JD (2012) Leukemia inhibitory factor coordinates the down-regulation of the visual cycle in the retina and retinal-pigmented epithelium. J Biol Chem 287:24092–24102

Gu X, Fliesler SJ, Zhao YY, Stallcup WB, Cohen AW, Elliott MH (2014a) Loss of caveolin-1 causes blood-retinal barrier breakdown, venous enlargement, and mural cell alteration. Am J Pathol 184:541–555

Gu X, Reagan A, Yen A, Bhatti F, Cohen AW, Elliott MH (2014b) Spatial and temporal localization of caveolin-1 protein in the developing retina. Adv Exp Med Biol 801:15–21

Jiao H, Zhang Y, Yan Z, Wang ZG, Liu G, Minshall RD, Malik AB, Hu G (2013) Caveolin-1 Tyr14 phosphorylation induces interaction with TLR4 in endothelial cells and mediates MyD88-dependent signaling and sepsis-induced lung inflammation. J Immunol 191:6191–6199

Klaassen I, Van Noorden CJ, Schlingemann RO (2013) Molecular basis of the inner blood-retinal barrier and its breakdown in diabetic macular edema and other pathological conditions. Prog Retin Eye Res 34:19–48

Lavail MM, Unoki K, Yasumura D, Matthes MT, Yancopoulos GD, Steinberg RH (1992) Multiple growth factors, cytokines, and neurotrophins rescue photoreceptors from the damaging effects of constant light. Proc Natl Acad Sci U S A 89:11249–11253

Li X, Gu X, Boyce TM, Zheng M, Reagan AM, Qi H, Mandal N, Cohen AW, Callegan MC, Carr DJ, Elliott MH (2014) Caveolin-1 increases pro-inflammatory chemoattractants and blood-retinal barrier breakdown but decreases leukocyte recruitment in inflammation. Invest Ophthalmol Vis Sci 55:6224–6234

Parton RG, Simons K (2007) The multiple faces of caveolae. Nat Rev Mol Cell Biol 8:185–194

Rowan S, Cepko CL (2004) Genetic analysis of the homeodomain transcription factor Chx10 in the retina using a novel multifunctional BAC transgenic mouse reporter. Dev Biol 271:388–402

Thorleifsson G et al (2010) Common variants near CAV1 and CAV2 are associated with primary open-angle glaucoma. Nat Genet 42:906–909

Chapter 55
Photoreceptor Neuroprotection: Regulation of Akt Activation Through Serine/Threonine Phosphatases, PHLPP and PHLPPL

Raju V.S. Rajala, Yogita Kanan and Robert E. Anderson

Abstract Serine/threonine kinase Akt is a downstream effector of insulin receptor/PI3K pathway that is involved in many processes, including providing neuroprotection to stressed rod photoreceptor cells. Akt signaling is known to be regulated by the serine/threonine phosphatases, PHLPP (PH domain and leucine rich repeat protein phosphatase) and PHLPPL (PH domain and leucine rich repeat protein phosphatase-like). We previously reported that both phosphatases are expressed in the retina, as well as in photoreceptor cells. In this study, we examined the PHLPP and PHLPPL phosphatase activities towards non-physiological and physiological substrates. Our results suggest that PHLPP was more active than PHLPPL towards non-physiological substrates, whereas both PHLPP and PHLPP dephosphorylated the physiological substrates of Akt1 and Akt3 with similar efficiencies. Our results also suggest that knockdown of PHLPPL alone does not increase Akt phosphorylation, due to a compensatory increase of PHLPP, which results in the dephosphorylation of Akt. Therefore, PHLPP and PHLPPL regulate Akt activation together when both phosphatases are expressed.

R. V.S. Rajala (✉) · R. E. Anderson
Department of Ophthalmology, University of Oklahoma Health Sciences Center, Oklahoma City, OK 73104, USA
e-mail: raju-rajala@ouhsc.edu

Dean McGee Eye Institute, University of Oklahoma Health Sciences Center, 608 Stanton L. Young Blvd., Oklahoma City, OK 73104, USA

R. E. Anderson
e-mail: Robert-Anderson@ouhsc.edu

R. V.S. Rajala
Department of Physiology, University of Oklahoma Health Sciences Center, Oklahoma City, OK 73104, USA

R. V.S. Rajala · Y. Kanan · R. E. Anderson
Department of Cell Biology, University of Oklahoma Health Sciences Center, Oklahoma City, OK 73104, USA

Y. Kanan
e-mail: ykanan1@jhmi.edu

C. Bowes Rickman et al. (eds.), *Retinal Degenerative Diseases,* Advances in Experimental Medicine and Biology 854, DOI 10.1007/978-3-319-17121-0_55

Keywords PHLPP · PHLPPL · Akt · Neuroprotection · Photoreceptors · Phosphatases · Activation

55.1 Introduction

Akt (serine/threonine protein kinase B) is an important kinase that is activated by a variety of growth factors and insulin (Galetic et al. 1999; Lawlor and Alessi 2001; Marte and Downward 1997). These factors activate phosphoinositide-3-kinase (PI3K), which in turn leads to the generation of the lipid second messengers phosphoinositide-3,4,5-trisphosphate (PI-3,4,5-P_3) and phosphoinositide-3,4-bisphosphate (PI-3,4-P_2). These lipid second messengers recruit Akt to the membrane by engaging its PH domain and facilitate its activation. Activated Akt dissociates from the membrane and phosphorylates many substrates in the cytoplasm and nucleus. Thus, activated Akt plays an important role in the regulation of metabolism, apoptosis, cell cycle, and transcription of various genes (New et al. 2007; Parcellier et al. 2008).

Two serine/threonine protein phosphatases, PHLPP (PH domain and leucine rich repeat protein phosphatase) and PHLPPL (PH domain and leucine rich repeat protein phosphatase-like) have been discovered that can directly dephosphorylate Akt at the serine 473 residue and terminate downstream Akt signaling (Brognard et al. 2007; Gao et al. 2005). We have previously reported that these two phosphatases are expressed in the retina (Kanan et al. 2010). Akt activation is an essential component of retinal neuroprotection (Li et al. 2007, 2008). The major remaining question is how Akt overcomes the effect of these two phosphatases. In this study, we characterized how PHLPP and PHLPPL activate Akt and how they affect each other.

55.2 Materials and Methods

55.2.1 Cloning, Construction, and Expression of PHLPP and PHLPPL Phosphatase Domains

Phosphatase domains were amplified from PHLPP and PHLPPL cDNA (Open Biosystems, Rockford, IL) using primers: PHLPP—sense: CGGAATTCACCATGTCAATAACATTCGCTGCTTCA, antisense: GCGTCGACTCATCCTTGATGACCATGTTGACG; PHLPPL—sense: CGGAATTCACCATGCAGAAGCCTTTGCCAGCCACAGAC, antisense: GCGTCGACTCACAAATAAACCACCATTGCCCCCACGTT. The transcripts were cloned into the EcoR1 and Sal1 sites in pGEX-4T-1 vector. The protein expression and purification was carried out as described (Rajala et al. 2013). Activity of the phosphatase domains of PHLPP or PHLPPL was determined by incubating the GST-phosphatase domains of PHLPP

or PHLPPL with 0, 10, 15, 20, 25, 30, 35, 40, and 45 mM p-nitrophenylphosphate (pNPP) substrate for 1 h at 30 °C (Brognard et al. 2007).

55.2.2 Knockdown of PHLPPL with siRNA

Silencer® select Pre-designed siRNA directed against PHLPPL were purchased from Ambion Biosystems (Austin, TX). The targeting sequences were siRNA-1 sense- GCAUCUAUAAUGUACGCAAtt, antisense-UUGCGUACAUUAUAGAUGCca. siRNA-2 sense-CUGUCAAUGCUGUACGUCAtt, antisense-UGACGUACAGCAUUGACAGct. The PHLPPL-directed siRNAs and Silencer® select negative control (scrambled siRNA) were transfected under serum-free conditions using siPORT™ Neo*FX*™ transfection agent. After transfection overnight in serum-free media, media containing serum was added to the cells and the cells were allowed to grow for 72 h before the cells were harvested for analysis of PHLPPL knockdown. An untransfected control was also included as a control.

55.3 Results

55.3.1 Phosphatase Domains of PHLPP and PHLPPL are Catalytically Active In Vitro

The phosphate domains of PHLPP and PHLPPL share more than 58 % homology in their primary structure (data not shown). We found that both phosphatase domains were catalytically active by their ability to dephosphorylate pNPP substrate. However, PHLPP was more active than PHLPPL in our *in vitro* experiments (Fig. 55.1a). To verify if the phosphatase domains of PHLPP and PHLPPL were active against their physiological substrate, recombinant HA-tagged Akt1 and Akt3 were immunoprecipitated from HEK-293T transfected cells (gown in 10 % serum) with anti-HA-antibody, followed by incubation with bacterially-expressed phosphatase domains of PHLPP or PHLPPL. Control experiments were carried out in the absence of enzyme. After incubation at 30 °C for 1 h, reactions were stopped by addition of SDS sample buffer. The reaction products were subjected to Western blot analysis with anti-pAkt antibody. To ensure an equal amount of Akt pull-down in each immunoprecipitate, the blot was stripped and reprobed with anti-Akt antibody. Densitometric analysis of immunoblots was performed in the linear range of detection and absolute values were normalized against total Akt. Both PHLPP and PHLPP dephosphorylated Akt 1 (Fig. 55.1b and c) and Akt3 (Fig. 55.1d and e). These results suggest that retinal PHLPP and PHLPPL phosphatase domains are functionally active and could dephosphorylate the physiological substrates.

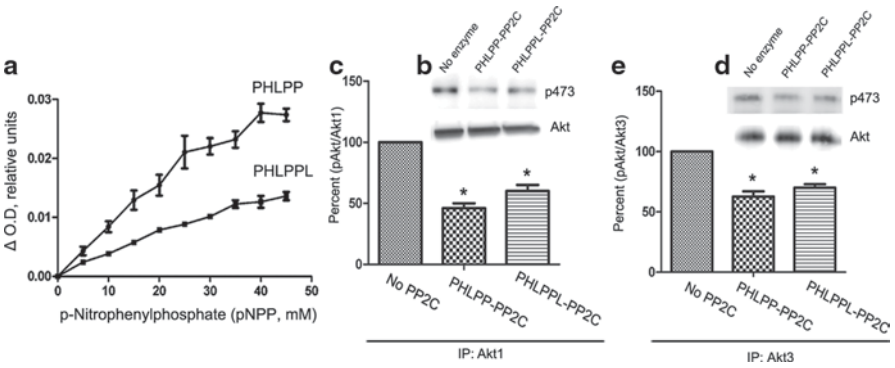

Fig. 55.1 Activity of PHLPP and PHLPPL phosphatase domains (PP2C) towards non-physiological (pNPP) and physiological substrates (Akt1 and Akt3). PHLPP and PHLPPL phosphatase domains were incubated in the presence of varying concentrations of pNPP (0–45 mM) and measured the phosphatase activity (**a**). Western blot of pAkt (ser 473) levels in Akt1 (**b**) or Akt3 (**d**) immunoprecipitated from HEK-293T cells incubated with no enzyme or phosphatase domains of PHLPP or PHLPPL for 1 h at 30 °C. Quantification of data expressed as pAkt/Akt for Akt1 (**c**) and Akt3 (**e**). Samples treated in the absence of enzyme were considered to be 100 %. Data are expressed as mean ± SD, $n = 3$. Student's t test was used to calculate the significance between the groups. *$p < 0.05$

55.3.2 Knockdown of PHLPPL by siRNA Activates PHLPP

Since PHLPPL is the principal phosphatase that regulates Akt in the photoreceptors, we studied the effects of PHLPPL knockdown on PHLPP levels and phosphorylation of Akt (p473) in HEK-293T cells that express both PHLPP and PHLPPL. HEK-293T cells were transfected with 2 siRNAs against PHLPPL and a negative or scrambled control siRNA. We were able to successfully knock down PHLPPL to 80 % with siRNA-1 and 98 % with siRNA-2. Transfection with the negative control did not change levels of PHLPPL in HEK-293T cells compared with non-transfected controls (Fig. 55.2b). Under these conditions, we found that the levels of pAkt (p473) surprisingly decreased to 40 % of non-transfected controls in siRNA-1 to complete absence of p473 in siRNA-2 transfected HEK samples (Fig. 55.2c). The levels of p473 in the negative controls were similar to non-transfected controls (Fig. 55.2c). The total Akt and actin levels in the cells transfected with siRNA-1 and siRNA-2 were similar to the negative controls and non-transfected controls (Fig. 55.2d and e). To account for low levels of p473, we looked at the levels of PHLPP in the siRNA-1 and siRNA-2 transfected controls, and found increased levels of PHLPP in siRNA-1 and siRNA-2 transfected HEK-293T cell lysates, which may account for decreased levels of p473 in the siRNA transfected samples (Fig. 55.2a). HEK-293T lysates transfected with negative control had similar levels of PHLPP levels compared with non-transfected controls (Fig. 55.2a). Therefore, inhibiting PHLPPL alone does not increase pAKT levels in the cells because PHLPLL activates PHLPP, which results in dephosphorylation of p473. Therefore, PHLPP and PHLPPL together regulate pAKT levels in cells where both phosphatases are expressed.

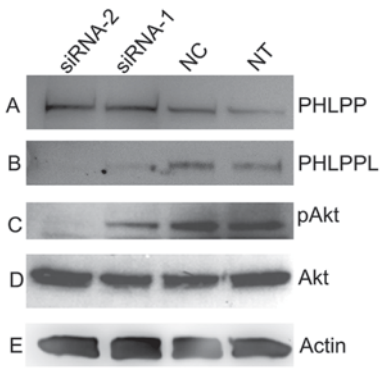

Fig. 55.2 Effect of siRNA knockdown of PHLPPL in HEK cells. HEK-293T cells were transfected with two siRNAs directed against PHLPPL (*siRNA-1* and *siRNA-2*), a negative control (*NC*, scrambled siRNA), and compared for expression against a non-transfected control (NT). HEK-293T cell proteins were subjected to Western blot analysis with anti-PHLPP (**a**), anti-PHLPPL (**b**), anti-pAkt (**c**), anti-Akt (**d**) and anti-actin (**e**) antibodies

55.4 Discussion

The Akt pathway is active in the retina and protects the photoreceptors from oxidative stress (Yu et al. 2006), light stress (Li et al. 2007, 2008), and apoptotic stimulus (Mackey et al. 2008). Inactivating the Akt pathway using PI3K inhibitors results in photoreceptor death (Mackey et al. 2008; Yu et al. 2004, 2006). The retina expresses all three Akt isoforms: Akt1, Akt2, and Akt3 (Li et al. 2007; Reiter et al. 2003). However, the isoform-specific regulation of Akt was a mystery until the discovery of the PHLPP family of protein phosphatases.

The PHLPP family of proteins comprises 2 members, PHLPP and PHLPPL, which belong to the PP2C subfamily of phosphatases and selectively dephosphorylate Akt isoforms (Brognard et al. 2007; Gao et al. 2005). We have previously reported their expression in rod and cone photoreceptors (Kanan et al. 2010). In addition, we have previously described light-induced Akt1 and Akt3 phosphorylation, but not Akt2, in rod photoreceptors in the presence of both PHLPP and PHLPPL (Li et al. 2008). These observations suggest that these two phosphatases may not be functional in the intact retina. In order to address this possibility, we expressed the phosphatase domains of PHLPP and PHLPPL and examined their activity towards preferred substrates. We found phosphatase activities associated with both PHLPP and PHLPPL.

It is interesting to note that knockdown of PHLPPL alone did not increase Akt phosphorylation, but increased the expression of PHLPP, which results in the dephosphorylation of Akt. This result suggests that PHLPP and PHLPPL together regulate pAKT levels in cells in which both phosphatases are expressed. In photoreceptors, Akt overcomes inactivation by PHLPP and PHLPPL through inhibition of their activities via insulin receptor activation of phosphoinositide 3-kinase (Kanan

et al. 2010). Further studies are required to understand the interaction of these phosphatases on Akt isoforms in the retina.

Acknowledgments This study was supported by grants from the National Institutes of Health (EY016507, EY00871, and NEI Core grant EY021725) and an unrestricted grant from Research to Prevent Blindness, Inc. to the Department of Ophthalmology.

References

Brognard J, Sierecki E, Gao T et al (2007) PHLPP and a second isoform, PHLPP2, differentially attenuate the amplitude of Akt signaling by regulating distinct Akt isoforms. Mol Cell 25:917–931

Galetic I, Andjelkovic M, Meier R et al (1999) Mechanism of protein kinase B activation by insulin/insulin-like growth factor-1 revealed by specific inhibitors of phosphoinositide 3-kinase–significance for diabetes and cancer. Pharmacol Ther 82:409–425

Gao T, Furnari F, Newton AC (2005) PHLPP: a phosphatase that directly dephosphorylates Akt, promotes apoptosis, and suppresses tumor growth. Mol Cell 18:13–24

Kanan Y, Matsumoto H, Song H et al (2010) Serine/threonine kinase akt activation regulates the activity of retinal serine/threonine phosphatases, PHLPP and PHLPPL. J Neurochem 113:477–488

Lawlor MA, Alessi DR (2001) PKB/Akt: a key mediator of cell proliferation, survival and insulin responses? J Cell Sci 114:2903–2910

Li G, Anderson RE, Tomita H et al (2007) Nonredundant role of Akt2 for neuroprotection of rod photoreceptor cells from light-induced cell death. J Neurosci 27:203–211

Li G, Rajala A, Wiechmann AF et al (2008) Activation and membrane binding of retinal protein kinase Balpha/Akt1 is regulated through light-dependent generation of phosphoinositides. J Neurochem 107:1382–1397

Mackey AM, Sanvicens N, Groeger G et al (2008) Redox survival signalling in retina-derived 661W cells. Cell Death Differ 15:1291–1303

Marte BM, Downward J (1997) PKB/Akt: connecting phosphoinositide 3-kinase to cell survival and beyond. Trends Biochem Sci 22:355–358

New DC, Wu K, Kwok AW et al (2007) G protein-coupled receptor-induced Akt activity in cellular proliferation and apoptosis. FEBS J 274:6025–6036

Parcellier A, Tintignac LA, Zhuravleva E et al (2008) PKB and the mitochondria: AKTing on apoptosis. Cell Signal 20:21–30

Rajala A, Dilly AK, Rajala RV (2013) Protein tyrosine phosphatase-1B regulates the tyrosine phosphorylation of the adapter Grb2-associated binder 1 (Gab1) in the retina. Cell Commun Signal 11:20

Reiter CE, Sandirasegarane L, Wolpert EB et al (2003) Characterization of insulin signaling in rat retina *in vivo* and ex vivo. Am J Physiol Endocrinol Metab 285:E763–E774

Yu X, Rajala RV, McGinnis JF et al (2004) Involvement of insulin/phosphoinositide 3-kinase/Akt signal pathway in 17 beta-estradiol-mediated neuroprotection. J Biol Chem 279:13086–13094

Yu XR, Jia GR, Gao GD et al (2006) Neuroprotection of insulin against oxidative stress-induced apoptosis in cultured retinal neurons: involvement of phosphoinositide 3-kinase/Akt signal pathway. Acta Biochim Biophys Sin (Shanghai) 38:241–248

Chapter 56
The Role of AMPK Pathway in Neuroprotection

Lei Xu and John D. Ash

Abstract Adenosine monophosphate-activated kinase (AMPK) is a highly conserved protein kinase found in all eukaryotic genomes. It exists as heterotrimeric protein consisting of α, β, and γ subunits. AMPK is activated by elevated levels of adenosine mono-phosphate (AMP), which is produced during conditions of low ATP production and perhaps mitochondrial dysfunction. Activation of AMPK has been shown to regulate a large number of downstream pathways. These will either increase energy production such as increase oxidation of fatty acids and glucose, or decrease energy utilization such as inhibiting synthesis of glycogen, fatty acid synthesis, and protein synthesis. In addition, being a key regulator of physiological energy dynamics, AMPK has been demonstrated to play roles in regulating various cellular processes such as mitochondrial biogenesis (Jager et al. Proc Natl Acad Sci U S A 104:12017–12022, 2007), autophagy (Hyttinen et al. Rejuven Res 14:651–660, 2011) and inflammation and immune responses (Giri et al. 2004). Retinal neurons have a high energy demand but have a poor energy storage capacity. Because of this, it is likely that the AMPK signaling pathway plays an important role in maintaining energy balance, and therefore may be a therapeutic target to prevent or delay retinal degeneration.

Keywords Neuroprotection · AMPK · Mitochondrial biogenesis · Autophagy · Inflammation response

Abbreviations

AMPK	Adenosine monophosphate protein activated kinase
CaMKK IIβ	Calmodulin-dependent protein kinase kinase IIβ
TAK1	Mammalian transforming growth factor β-activated kinase

J. D. Ash (✉) · L. Xu
Department of Ophthalmology, University of Florida, 1600 SW Archer Road, Gainesville, FL 32610, USA
e-mail: jash@ufl.edu

L. Xu
e-mail: leixu@ufl.edu

C. Bowes Rickman et al. (eds.), *Retinal Degenerative Diseases,* Advances in Experimental Medicine and Biology 854, DOI 10.1007/978-3-319-17121-0_56

AMP	Adenosine monophosphate
ADP	Adenosine diphosphate
PGC-1	Peroxisome proliferator-activated receptor-γ co-activator
AICAR	5-aminoimidazole-4-carboxamide ribonucleoside
mTOR	Mammalian target of rapamycin
ICAM1	Intercellular adhesion molecule 1
4E-BP1	Eukaryotic translation initiation factor 4E-binding protein 1.

56.1 Introduction

Adenosine monophosphate-activated kinase (AMPK) is an evolutionally conserved serine/threonine kinase. Homologs for AMPK subunits have been found in all eukaryotic species including Snf1 kinase in yeast. AMPK has been considered to function as energy sensor to maintain energy homeostasis at the cellular level. AMPK functions as a heterotrimeric protein comprising of catalytic α-subunit (α1, α2), β-regulatory subunit (β1, β2) and the AMP-binding subunit (γ1, γ2 and γ3). Each of these three subunits has a specific role in regulating the activity and stability of AMPK. Because there are multiple isoforms for each subunit in mammals, there are 12 possible combinations of subunits and therefore 12 unique AMPK complexes. However, isotypes have different tissue distributions, suggesting that not all AMPK complex's exist in anyone cell type. For example α1 and α2 are both present in liver; while in adipose tissue, AMPK complexes containing the α1 catalytic subunit (Viollet et al. 2009). In addition, different isotypes may have different cellular distributions. For example AMPKα2 containing complexes are found in both the nucleus and the cytoplasm, which raises the possibility that α2 complexes may phosphorylate transcription co-activators and transcription factors in the nucleus to regulate gene expression (Viollet et al. 2006; Jager et al. 2007). In contrast, AMPKα1 containing complexes are localized only in the cytoplasm. These unique tissue and sub-cellular distributions suggest that complex types may have different substrates and therefore have unique functions. Consistent with this possibility, AMPK α2 but not α1 mediates oxidative stress-induced inhibition of RPE cell phagocytosis of photoreceptor outer segment (Qin and De Vries 2008). In addition, *in vitro* data have suggested AMPKα1 and α2 play distinct roles in regulating 4-HNE effects on RPE function and viability (Qin and Rodrigues 2010). The role of each isoform and their distribution in the retina is not yet known. This review will introduce the various pathways regulated by AMPK, and how these may function in neuroprotection.

56.2 AMPK as an Energy Sensor

AMPK is allosterically activated by elevated AMP, and the mechanisms of activation have been reviewed in (Hardie et al. 2012). In brief, binding of AMP to the γ-subunit promotes a conformational change that either enables the phosphorylation

of Thr172 in the activation domain of the α-subunit or prevents it dephosphorylation by protein phosphatases. Several kinases have been proposed to phosphorylate AMPK including LKB1 (a tumor suppressor gene whose germ line mutations in humans are the cause of Peutz-Jeghers syndrome), CaMKK IIβ (calmodulin-dependent protein kinase kinase IIβ), and TAK1 (mammalian transforming growth factor β-activated kinase) (Herrero-Martin et al. 2009; Viollet et al. 2009). Because AMPK is activated by elevated AMP levels, it has been proposed that AMPK functions as a cellular energy sensor and plays a central role in regulating energy homeostasis. Normal functioning cells have very little AMP, and AMPK is maintained in the inactive, dephosphorylated state. When cells undergo an energy crisis, and ATP levels decline, adenylate kinase is activated, which uses two molecules of adenosine diphosphate (ADP) to produce ATP and the byproduct AMP. As AMP levels rise, AMPK is phosphorylated making it an activated kinase. AMPK functions to restore energy balance by turning down ATP-consuming pathways such as protein synthesis, RNA synthesis, and fatty acid synthesis, while at the same time turning on pathways that generate ATP such as glycolysis, β-oxidation, and mitochondrial biogenesis (Hardie et al. 2012).

56.3 Regulation of Mitochondrial Biogenesis by AMPK

The mitochondrion is a critical organelle for cell function and survival. It is not only the major source of energy production, but also is a major source of reactive oxygen species (ROS). However, mitochondria are also the major source of ROS detoxifying enzymes, and produce ATP among many other activities, including steroid synthesis, and calcium regulation. Mitochondrial dysfunction has been proposed as a mechanism of cell death in retinal degenerative diseases, such as age related macular degeneration, diabetic retinopathy, inherited retinal degenerations, and glaucoma (Barot et al. 2011). Regulation of mitochondrial biogenesis has been proposed as a neuroprotection target in retinal degeneration models and diseases (Lee et al. 2011) since mitochondrial biogenesis is likely an adaptation to compromised bioenergetics (Wu et al. 2014).

Mitochondrial biogenesis is regulated by nuclear transcription factors NRF-1 and NRF-2, EER, thyroid hormone receptors, and retinoic acid receptors. These however, all require a co-activator peroxisome proliferator-activated receptor-λ co-activator (PGC-1α) (Lin et al. 2005). AMPK has been shown to directly phosphorylate and activate PGC-1α in muscle to induce mitochondrial biogenesis (Jager et al. 2007). PGC-1α and β are expressed in mouse retina, and have been shown to determine susceptibility to light damage (Egger et al. 2012). Retinal mitochondrial biogenesis is impaired in diabetic retinopathy, possibly due to decreased transport of TRAM to the mitochondria (Santos et al. 2011). These studies suggest that PGC-1α activation is important for photoreceptor survival under conditions of oxidative stress. This suggests that AMPK is also important for mitochondrial function and resistance to oxidative stress. In support of this hypothesis, mice lacking both AMPK α1 and α2 subunits in the muscle had greatly reduced muscle mitochondrial

DNA content (O'Neill et al. 2011). A small molecular agonist of AMPK, Metformin, has been used to promote mitochondrial biogenesis and conferring neuroprotection against apoptotic cell death in primary cortical neurons *in vitro* (El-Mir et al. 2008). In *in vivo* studies, daily subcutaneous injections of metformin in Balbc/j mice for 7 days results in activation of AMPK in the retina, increased mitochondrial DNA content, and protected photoreceptors from light damage (unpublished data from L. Xu and J. Ash).

56.4 Regulation of mTOR Pathway by AMPK

A potential mechanism by which AMPK activation can protect neurons is through activation of autophagy or inhibition of protein synthesis. These processes are regulated by AMPK substrates mTORC1 and mTORC2 respectively. Activated AMPK kinase will inhibit mammalian target of rapamycin (mTOR). The mTOR pathway is a serine/ threonine protein kinase that regulates multiple cellular processors such as cell growth, cell cycle and autophagy. mTOR forms two protein complexes: mTOR complex 1 (mTORC1) and mTOR complex 2 (mTORC2). AMPK directly phosphorylates multiple components in the mTORC1 pathway including TSC2 and Raptor (Hyttinen et al. 2011; Inoki et al. 2012). Activation of ULK1 and ULK2 are essential to form autophagosomes. It has been shown that AMPK and mTOR regulate autophagy through direct phosphorylation of ULK1 (Kim et al. 2011). Experimental evidence has suggested that pre-activation of AMPK-dependent autophagy pathway with metformin treatment confers neuroprotection against focal cerebral ischemia (Jiang et al. 2014), also induction of AMPK dependent autophagy by ischemic preconditioning can also protect from ischemic stroke (Jiang et al. 2015). In retinal RPE cells, autophagy regulating kinases have been proposed as potential therapeutic targets for age-related macular degeneration through activation of AMPK pathway (Kaarniranta et al. 2012). In support of this hypothesis, another agonist of AMPK, AICAR, was found to protect RPE cells in response to oxidative stress (Qin and De Vries 2008). Moreover, AMPK-induced autophagy protected RPE cells from TRAIL-induced cell death (Herrero-Martin et al. 2009).

Activation of AMPK inhibits mTORC2 signaling pathway, thus regulating translation and protein synthesis through inhibiting eukaryotic translation initiation factor 4E-binding protein 1 (4E-BP1) and S6 kinase 1 (S6K1). Pharmacological inhibition of mTOR with rapamycin has been proposed to applied in neurodegenerative diseases, such as Parkinson's disease, Huntington's disease and Alzheimer's disease and retinal degeneration such as age-related retinal degeneration (Bove et al. 2011). In the eye, treatment with rapamycin blunted RPE dedifferentiation and hypertrophy as well as preserved photoreceptor numbers and function for both metabolic and oxidative stress models (Zhao et al. 2011). In addition, treatment with rapamycin dramatically promotes retinal ganglion cells survival in a rat chronic ocular hypertension model (Ai et al. 2014). AMPK linage to mediator of protein synthesis and cell growth through regulation of mTOR pathway could be a potential target for preventing retinal degeneration.

56.5 Regulation of Inflammation Response by AMPK

Multiple inflammatory signaling pathways are involved in the pathogenesis of retinal degeneration. Although AMPK is well known for its role in cellular energy homeostasis, it may also regulate inflammatory signals (O'Neill and Hardie 2013). In a lipopolysaccharide (LPS) induced mouse model of retina inflammation, AICAR injections preserved photoreceptor function and rhodopsin protein levels. This protection was associated with inhibition of NF-κB signaling (Kamoshita et al. 2014). In diabetic retinopathy, the role of AMPK has also been examined. Inflammation in diabetes was found to down regulate the AMPK pathway which lead to NF-κB activation and increased inflammation as shown by elevated ICAM1 (Intercellular adhesion molecule 1) and VEGF expression (Kubota et al. 2011). In addition, resveratrol also prevents the development of choroid neovascularization by restoring AMPK activity and inhibiting macrophage migration (Nagai et al. 2014).

56.6 Conclusion and Perspectives

Many approaches has been proposed and applied to induce neuroprotection. AMPK is a major energy sensor of energy and redox status. Once activated, AMPK can restore energy balance to promote cell health and function. The ability of AMPK to stimulate mitochondrial biogenesis, autophagy, inhibit inflammation, and prevent cell death suggest that AMPK should be considered as a key target for new therapies to slow or prevent retinal degeneration.

Reference

Ai D, Jiang H, Westerterp M et al (2014) Disruption of mammalian target of rapamycin complex 1 in macrophages decreases chemokine gene expression and atherosclerosis. Circ Res 114:1576–1584

Barot M, Gokulgandhi MR, Mitra AK (2011) Mitochondrial dysfunction in retinal diseases. Curr Eye Res 36:1069–1077

Bove J, Martinez-Vicente M, Vila M (2011) Fighting neurodegeneration with rapamycin: mechanistic insights. Nat Rev Neurosci 12:437–452

Egger A, Samardzija M, Sothilingam V et al (2012) PGC-1alpha determines light damage susceptibility of the murine retina. PLoS One 7:e31272

El-Mir MY, Detaille D, G RV et al (2008) Neuroprotective role of antidiabetic drug metformin against apoptotic cell death in primary cortical neurons. J Mol Neurosci 34:77–87

Giri S, Nath N, Smith B et al (2004) 5-aminoimidazole-4-carboxamide-1-beta-4-ribofuranoside inhibits proinflammatory response in glial cells: a possible role of AMP-activated protein kinase. J Neurosci 24:479–487

Hardie DG, Ross FA, Hawley SA (2012) AMPK: a nutrient and energy sensor that maintains energy homeostasis. Nat Rev Mol Cell Biol 13:251–262

Herrero-Martin G, Hoyer-Hansen M, Garcia-Garcia C et al (2009) TAK1 activates AMPK-dependent cytoprotective autophagy in TRAIL-treated epithelial cells. EMBO J 28:677–685

Hyttinen JM, Petrovski G, Salminen A et al (2011) 5′-Adenosine monophosphate-activated protein kinase—mammalian target of rapamycin axis as therapeutic target for age-related macular degeneration. Rejuven Res 14:651–660

Inoki K, Kim J, Guan KL (2012) AMPK and mTOR in cellular energy homeostasis and drug targets. Ann Rev Pharm Toxicol 52:381–400

Jager S, Handschin C, St-Pierre J et al (2007) AMP-activated protein kinase (AMPK) action in skeletal muscle via direct phosphorylation of PGC-1alpha. Proc Natl Acad Sci U S A 104:12017–12022

Jiang T, Yu JT, Zhu XC et al (2014) Acute metformin preconditioning confers neuroprotection against focal cerebral ischaemia by pre-activation of AMPK-dependent autophagy. Br J Pharmacol 171:3146–3157

Jiang T, Yu JT, Zhu XC et al (2015) Ischemic preconditioning provides neuroprotection by induction of AMP-activated protein kinase-dependent autophagy in a rat model of ischemic stroke. Mol Neurobiol. 51(1):220–229

Kaarniranta K, Kauppinen A, Blasiak J et al (2012) Autophagy regulating kinases as potential therapeutic targets for age-related macular degeneration. Future Med Chem 4:2153–2161

Kamoshita M, Ozawa Y, Kubota S et al (2014) AMPK-NF-kappaB axis in the photoreceptor disorder during retinal inflammation. PLoS One 9:e103013

Kim J, Kundu M, Viollet B et al (2011) AMPK and mTOR regulate autophagy through direct phosphorylation of Ulk1. Nat Cell Biol 13:132–141

Kubota S, Ozawa Y, Kurihara T et al (2011) Roles of AMP-activated protein kinase in diabetes-induced retinal inflammation. Invest Ophthalmol Vis Sci 52:9142–9148

Lee S, Van Bergen NJ, Kong GY et al (2011) Mitochondrial dysfunction in glaucoma and emerging bioenergetic therapies. Exp Eye Res 93:204–212

Lin J, Handschin C, Spiegelman BM (2005) Metabolic control through the PGC-1 family of transcription coactivators. Cell Metab 1:361–370

Nagai N, Kubota S, Tsubota K et al (2014) Resveratrol prevents the development of choroidal neovascularization by modulating AMP-activated protein kinase in macrophages and other cell types. J Nutr Biochem 25:1218–1225

O'Neill LA, Hardie DG (2013) Metabolism of inflammation limited by AMPK and pseudo-starvation. Nature 493:346–355

O'Neill HM, Maarbjerg SJ, Crane JD et al (2011) AMP-activated protein kinase (AMPK) beta1beta2 muscle null mice reveal an essential role for AMPK in maintaining mitochondrial content and glucose uptake during exercise. Proc Natl Acad Sci U S A 108:16092–16097

Qin S, De Vries GW (2008) alpha2 but not alpha1 AMP-activated protein kinase mediates oxidative stress-induced inhibition of retinal pigment epithelium cell phagocytosis of photoreceptor outer segments. J Biol Chem 283:6744–6751

Qin S, Rodrigues GA (2010) Differential roles of AMPKalpha1 and AMPKalpha2 in regulating 4-HNE-induced RPE cell death and permeability. Exp Eye Res 91:818–824

Santos JM, Tewari S, Goldberg AF et al (2011) Mitochondrial biogenesis and the development of diabetic retinopathy. Free Rad Biol Med 51:1849–1860

Viollet B, Foretz M, Guigas B et al (2006) Activation of AMP-activated protein kinase in the liver: a new strategy for the management of metabolic hepatic disorders. J Phys 574:41–53

Viollet B, Athea Y, Mounier R et al (2009) AMPK: lessons from transgenic and knockout animals. Front Biosci (Landmark Ed) 14:19–44

Wu SB, Wu YT, Wu TP et al (2014) Role of AMPK-mediated adaptive responses in human cells with mitochondrial dysfunction to oxidative stress. Biochim Biophys Acta 1840:1331–1344

Zhao C, Yasumura D, Li X et al (2011) mTOR-mediated dedifferentiation of the retinal pigment epithelium initiates photoreceptor degeneration in mice. J Clin Invest 121:369–383

Chapter 57
Tauroursodeoxycholic Acid Protects Retinal Function and Structure in *rd1* Mice

Eric C. Lawson, Shagun K. Bhatia, Moon K. Han, Moe H. Aung, Vincent Ciavatta, Jeffrey H. Boatright and Machelle T. Pardue

Abstract We explored the potential protective effects of tauroursodeoxycholic acid (TUDCA) on cone photoreceptor survival in a model of rapid retinal degeneration, the ß-Pde6^{rd1} (*rd1*) mouse model. We injected two strains of *rd1* mice (B6.C3-Pde6b^{rd1}Hps4^{le}/J and C57BL/6J-Pde6b^{rd1-2}/J mice) daily from postnatal day (P) 6 to P21 with TUDCA or vehicle. At P21, retinal function was evaluated with light-adapted electroretinography (ERG) and retinal structure was observed with plastic or frozen sections. TUDCA treatment partially preserved function and structure in B6.C3-Pde6b^{rd1}Hps4^{le}/J mice but only partially preserved structure in C57BL/6J-Pde6b^{rd1-2}/J mice. Our results suggest a possible intervention for patients undergoing rapid retinal degeneration.

Keywords Tauroursodeoxycholic acid · Bile acids · TUDCA · rd1 mice · Retinal degeneration · Retinitis pigmentosa.

M. T. Pardue (✉) · E. C. Lawson · S. K. Bhatia · M. H. Aung · V. Ciavatta · J. H. Boatright
Department of Ophthalmology, Emory University School of Medicine,
Atlanta, GA 30322, USA
e-mail: mpardue@emory.edu

M. T. Pardue · E. C. Lawson · S. K. Bhatia · M. K. Han · M. H. Aung · V. Ciavatta
Rehab R&D Center, Research Service (151Oph), Atlanta VA Medical Center,
1670 Clairmont Rd., Decatur, GA 30033, USA

E. C. Lawson
e-mail: eric.lawson90@gmail.com

S. K. Bhatia
e-mail: shagun88@gmail.com

M. H. Aung
e-mail: mhaung@emory.edu

V. Ciavatta
e-mail: vciavat@emory.edu

J. H. Boatright
e-mail: jboatri@emory.edu

M. K. Han
e-mail: moonkwon.han@gmail.com

C. Bowes Rickman et al. (eds.), *Retinal Degenerative Diseases,* Advances in Experimental Medicine and Biology 854, DOI 10.1007/978-3-319-17121-0_57

57.1 Introduction

Tauroursodeoxycholic acid (TUDCA) is neuroprotective in several rodent models of neurodegeneration (reviewed in Boatright et al. 2009) and retinal degeneration (Boatright et al. 2006; Phillips et al. 2008). In this study we explored the possible neuroprotective effects of daily injections of TUDCA on two strains of *rd1* mice. The *rd1* mouse, considered a model of retinitis pigmentosa, has a nonsense mutation in the ß-subunit of the rod cGMP phosphodiesterase, resulting in loss of rod photoreceptors beginning at postnatal day P10 and finishing by about P21 (Sancho-Pelluz et al. 2008). Despite the rapid degeneration of rod photoreceptors, cone photoreceptors degenerate at a slower rate, providing potential therapeutic opportunities. In this study, we sought to examine whether TUDCA could preserve cone function. We were able to replicate that no functional protection was observed in C57BL-*rd1* mice with TUDCA (Drack et al. 2012), even though we found partial structural preservation. More importantly, we show functional and structural protection with daily injections of TUDCA from P6 to P21 in B6.C3-*rd1* mice.

57.2 Material and Methods

57.2.1 Animals

All animal procedures were approved by the Institutional Animal Care and Use Committee at the Atlanta VA Medical Center and conform to the standards of the Association for Research in Vision and Ophthalmology Statement for the Use of Animals in Ophthalmic and Vision Research. Two strains of ß-Pde6^{rd1} mice were obtained from Jackson Laboratories (Bar Harbor, ME): B6.C3-Pde6b^{rd1}Hps4^{le}/J mice (B6.C3-*rd1*; Stock #: 000002) and C57BL/6J-Pde6b^{rd1-2}/J mice (C57BL-*rd1*; Stock #: 004766). All mice were housed under controlled lighting conditions on a 12 h light/12 h dark cycle.

57.2.2 TUDCA Treatments

rd1 litters were randomly divided at P6 to receive TUDCA (500 mg/kg, Calbiochem, San Diego, CA) or vehicle (0.15 M $NaHCO_3$ 1 ml/kg) treatment. TUDCA solution was made fresh daily and pH was adjusted to 7.4 using 0.1 M HCl. Daily intraperitoneal injections began at P6 as it has been previously shown that injections every 3 days have no protective effects on the *rd1* retina, most likely due to the increased degeneration rate compared to other models (Boatright et al. 2009). Treatments ended at P21 for each animal. Mice were weighed daily prior to injection to determine proper dosing of TUDCA and vehicle.

57.2.3 Electroretinography

Electroretinography was performed at P21, as previously detailed (Mocko et al. 2011). Briefly, mice were anesthetized with ketamine (80 mg/kg) and xylazine (16 mg/kg), the cornea was anesthetized (1% tetracaine), and the pupils dilated (1% tropicamide) in both eyes. The body temperature was maintained at 37 °C via a heating pad while the recording electrode, a nylon-silver thread, contacted the cornea using 1% methylcellulose. The responses were referenced and grounded to needle electrodes placed in the cheek and tail, respectively. A series of full-field flash stimuli (− 0.82 to 1.9 log cd-s/m^2) were presented by a Ganzfeld dome under light-adapted conditions (30 cd/m^2) to isolate cone responses. Acquired responses were stored on a commercial ERG system (UTAS 3000, LKC Technologies, Gaithersburg, MD).

57.2.4 Histology

Retinal morphology was assessed as previously reported (Mocko et al. 2011). Briefly, mice were euthanized and eyes enucleated, injected with 4% paraformaldehyde, and immersion fixed in the same fixative for 45 min. Eyecups of B6.C3-*rd1* mice were rinsed with 0.1 M phosphate buffer, processed through a graded alcohol series, and embedded in plastic resin (Embed 812/DER 736, Electron Microscopy Science, Inc, Hatfield, PA). Sections (0.5 μm) bisecting the optic disc at the superior-inferior axis were cut using an ultramicrotome (Reichert Ultracut, Leica Inc., Buffalo Grove, IL) with a histo-diamond knife. Eyecups of C57BL-*rd1* mice were frozen in OCT and cryosectioned (10 μm thickness) onto glass slides. Both plastic and cryosections sections were stained with 1% aqueous toluidine blue (Sigma; St. Louis MO) and imaged using a phase contrast microscope (Leica DM LB, Leica Inc., Buffalo Grove, IL) at 20× power. Photoreceptor nuclei cells were counted using an image analysis program (Image-Pro Plus 5.0; MediaCybernetics; Rockville, MD). For each retinal section, we quantified photoreceptor nuclei across the retina moving outwards superiorly and inferiorly from the optic nerve. The number of photoreceptor nuclei were averaged across three retinal sections for each eye.

57.2.5 Statistical Analyses

We performed two-way repeated measures ANOVAs with Holm-Sidak post-hoc comparisons and Student's *t*-tests using commercial statistical analysis software (SigmaStat 3.5; Systat Software; Chicago, IL). Significance was set at $p < 0.05$ for all analyses and values are expressed as mean ± standard error of the mean (sem).

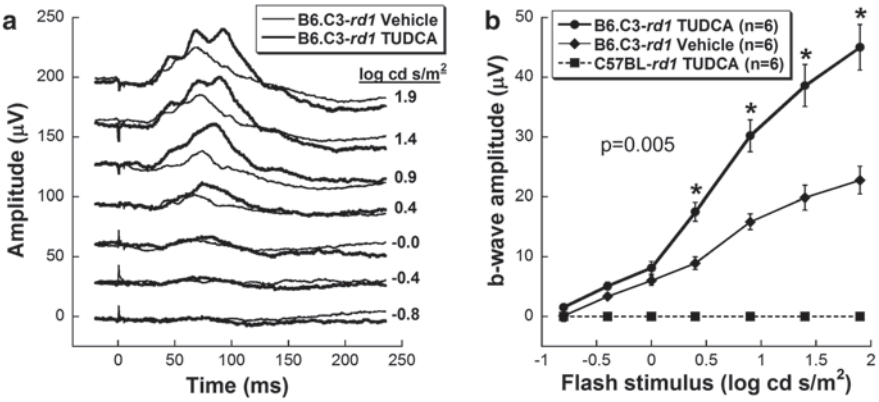

Fig. 57.1 TUDCA protects cone photoreceptor function in B6.C3-*rd1* mice at P21. **a** Representative light-adapted ERG waveforms from B6.C3-*rd1* mice across flash stimuli (− 0.81 to 1.9 log cd s/m^2). **b** B6.C3-*rd1* TUDCA-treated mice have significantly larger b-wave amplitudes responses at the brightest flash stimuli compared to vehicle-treated mice (two-way repeated measures ANOVA; F(1, 41) = 16.986, $p = 0.005$). C57BL-*rd1* mice did not exhibit measurable b-wave responses at any flash stimulus

57.3 Results

57.3.1 TUDCA Injections Preserved Retinal Function to P21 in B6.C3-rd1 Mice

Light-adapted ERG waveforms from representative mice in each group showed larger amplitudes with TUDCA treatment for B6.C3-*rd1* mice compared to B6.C3-*rd1* vehicle treated (Fig. 57.1a). Within the B6.C3-*rd1* mice, those injected with TUDCA had significantly preserved light adapted b-wave amplitudes compared to vehicle treated mice at the brightest flash stimuli (Fig. 57.1b; 0.4, 0.9, 1.4, and 1.9 log cd s/m^2; two-way repeated measures ANOVA; F(1, 41) = 16.986, $p = 0.005$). C57BL-*rd1* mice exhibited no measurable a-or b-waveforms at P21, regardless of treatment.

57.3.2 TUDCA Injections Preserved Photoreceptor Cell Counts in Both rd1 Strains

After TUDCA injections, the retinas of B6.C3-*rd1* and C57BL-*rd1* mice maintained a thicker outer nuclear layer (ONL) of about 2 rows of photoreceptor nuclei (Fig. 57.2b and 57.3b) compared to vehicle treated mice, which degenerated to a sparse single row of photoreceptor nuclei (Fig. 57.2a and 57.3a). The summed photoreceptor nuclei across the retina in TUDCA-treated B6.C3-*rd1* mice was significantly greater compared to vehicle-treated littermates (Student's *t*-test; $p = 0.005$;

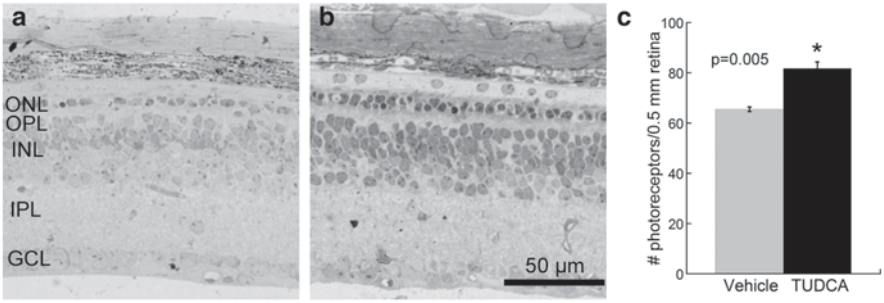

Fig. 57.2 TUDCA protects cone photoreceptor structure in B6.C3-*rd1* mice. Retinal micrographs of plastic sections taken 1.0 mm from the optic nerve from B6.C3-*rd1* mice shows that mice injected with TUDCA had a thicker ONL (**b**) compared to those injected with vehicle (**a**). **c** TUDCA-treated B6.C3-*rd1* mice had significantly more photoreceptor nuclei compared to vehicle-treated mice (Student's *t*-test; $p = 0.005$)

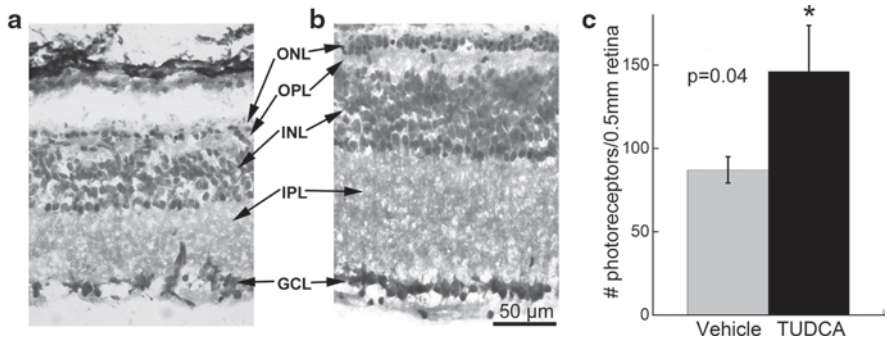

Fig. 57.3 TUDCA protects cone photoreceptor structure in C57BL-*rd1* mice. Retinal micrographs of cryosections taken 1.0 mm from the optic nerve in C57BL-*rd1* mice injected with TUDCA had a thicker ONL (**b**) compared to those injected with vehicle (**a**). **c** TUDCA-treated C57BL-*rd1* mice had significantly more photoreceptor nuclei compared to vehicle-treated mice (Student's *t*-test; $p = 0.038$)

Fig. 57.2c). C57BL-*rd1* mice also showed significantly more photoreceptor nuclei with TUDCA treatment (Student's *t*-test; $p = 0.038$; Fig. 57.3c).

57.4 Discussion

Here we demonstrate that significant cone protection in *rd1* mice is possible with TUDCA injections. Daily injections of TUDCA were sufficient to protect both retinal function (specifically light-adapted ERGs) and structure in B6.C3-*rd1* mice. However, in C57BL-*rd1* mice, photoreceptor nuclei were preserved, but not retinal function. A previous report also observed no functional preservation in C57BL-*rd1*

mice (Dr. Val Sheffield, personal communication) with TUDCA injections at P21 (Drack et al. 2012), however, structural preservation was not explored. The differences in efficacy of TUDCA between the two strains of *rd1* mice may be due to the different rates of degeneration. It is possible that C57BL-*rd1* have a more aggressive degeneration compared to B6.C3-*rd1* mice, as C57BL-*rd1* mice have no measurable ERG response at any age (Chang et al. 2007), while B6.C3-*rd1* mice treated with vehicle still have residual ERG responses at P21 (Fig. 57.1). Nonetheless, our findings illustrate the protective effects of TUDCA on cone photoreceptors in a model of rapid retinal degeneration, and suggest a possible intervention for aggressive forms of retinitis pigmentosa.

Acknowledgments Grant support provided by NIH P30 EY006360, NIH R01 EY014026 and a grant from the Abraham J. & Phyllis Katz Foundation (to J.H.B.), Rehabilitation Research and Development Service Veterans Affairs Research Career Scientist Award (to M.T.P.), Atlanta VA Center of Excellence in Vision and Neurocognitive Rehabilitation, and Departmental Award from Research to Prevent Blindness.

References

Boatright JH, Moring AG, McElroy C et al (2006) Tool from ancient pharmacopoeia prevents vision loss. Mol Vis 12:1706–1714

Boatright JH, Nickerson JM, Moring AG et al (2009) Bile acids in treatment of ocular disease. J Ocul Biol Dis Inform 2:149–159

Chang B, Hawes NL, Pardue MT et al (2007) Two mouse retinal degenerations caused by missense mutations in the beta-subunit of rod cGMP phosphodiesterase gene. Vis Res 47:624–633

Drack AV, Dumitrescu AV, Bhattarai S et al (2012) TUDCA slows retinal degeneration in two different mouse models of retinitis pigmentosa and prevents obesity in Bardet-Biedl syndrome type 1 mice. Invest Ophthalmol Vis Sci 53:100–106

Mocko JA, Kim M, Faulkner AE et al (2011) Effects of subretinal electrical stimulation in mer-KO mice. Invest Ophthalmol Vis Sci 52:4223–4230

Phillips MJ, Walker TA, Choi HY et al (2008) Tauroursodeoxycholic acid preservation of photoreceptor structure and function in the rd10 mouse through postnatal day 30. Invest Ophthalmol Vis Sci 49:2148–2155

Sancho-Pelluz J, Arango-Gonzalez B, Kustermann S et al (2008) Photoreceptor cell death mechanisms in inherited retinal degeneration. Mol Neurobiol 38:253–269

Chapter 58
Near-Infrared Photobiomodulation in Retinal Injury and Disease

Janis T. Eells, Sandeep Gopalakrishnan and Krisztina Valter

Abstract Evidence is growing that exposure of tissue to low energy photon irradiation in the far-red (FR) to near-infrared (NIR) range of the spectrum, collectively termed "photobiomodulation" (PBM) can restore the function of damaged mitochondria, upregulate the production of cytoprotective factors and prevent apoptotic cell death. PBM has been applied clinically in the treatment of soft tissue injuries and acceleration of wound healing for more than 40 years. Recent studies have demonstrated that FR/NIR photons penetrate diseased tissues including the retina. The therapeutic effects of PBM have been hypothesized to result from intracellular signaling pathways triggered when FR/NIR photons are absorbed by the mitochondrial photoacceptor molecule, cytochrome c oxidase, culminating in improved mitochondrial energy metabolism, increased cytoprotective factor production and cell survival. Investigations in rodent models of methanol-induced ocular toxicity, light damage, retinitis pigmentosa and age-related macular degeneration have demonstrated the PBM attenuates photoreceptor cell death, protects retinal function and exerts anti-inflammatory actions.

Keywords Photobiomodulation (PBM) · Methanol intoxication · Light damage (LD) · Macular degeneration · Retinitis pigmentosa.

J. T. Eells (✉)
Department of Biomedical Sciences, University of Wisconsin-Milwaukee, 2400 E. Hartford Ave., Milwaukee, WI 53201, USA
e-mail: jeells@uwm.edu

S. Gopalakrishnan
College of Nursing, University of Wisconsin-Milwaukee, Milwaukee, WI 53201, USA
e-mail: sandeep@uwm.edu

K. Valter
Divsion of Biomedical Sciences, Research School of Biology, Australian National University, Acton 0200, Australia
e-mail: krisztina.valter-kocsi@anu.edu.au

C. Bowes Rickman et al. (eds.), *Retinal Degenerative Diseases,* Advances in Experimental Medicine and Biology 854, DOI 10.1007/978-3-319-17121-0_58

58.1 Introduction

Mitochondrial dysfunction and oxidative damage to the retina have been implicated in many forms of retinal injury and degeneration including methanol intoxication, light-induced retinal damage, age-related macular degeneration (AMD) and retinitis pigmentosa (Shen et al. 2005; Stone et al. 1999; Jarrett and Boulton 2012). Mitochondrial repair and attenuation of oxidative stress are critical to the long-term survival of the retina.

Therapeutic strategies directed towards improving mitochondrial integrity and function and reducing oxidative stress have considerable potential for the treatment of retinal disease. Low-intensity far-red to near-infrared (FR/NIR) light has been shown to act on mitochondria-mediated signaling pathways to preserve mitochondrial function, attenuate oxidative stress, stimulate the production of cytoprotective factors and prevent neuronal death in cultured neurons and in animal models of neuronal injury and disease (Karu, 1999 Eells et al. 2004; Wong-Riley et al. 2005; Huang et al. 2011; Chung et al. 2012). FR/NIR photons penetrate the brain, retina and optic nerve and this treatment, commonly known as photobiomodulation (PBM) has documented efficacy in the prevention and treatment of neurodegenerative diseases in experimental and clinical studies (Fitzgerald et al. 2013). Numerous studies have documented the therapeutic potential and mechanism(s) of action of PBM in the treatment and pathogenesis of retinal injury and disease.

58.2 Methanol Intoxication

Methanol intoxication produces toxic injury to the retina and optic nerve, resulting in blindness. Both acute and chronic exposure to methanol has been shown to produce retinal dysfunction and optic nerve damage clinically and in experimental animal models (Seme et al 1999). A toxic acute exposure to methanol results in formic acidemia, metabolic acidosis and visual toxicity within 72 h of ingestion (Seme et al. 1999). The toxic metabolite is formic acid, a mitochondrial toxin known to inhibit the essential mitochondrial enzyme, cytochrome c oxidase (Eells et al. 2003). Eells et al. (2003) reported the first direct link between the actions of far-red to NIR light on mitochondrial oxidative metabolism *in vitro* and retinoprotection *in vivo* in a well-established rodent model of methanol toxicity (Seme et al. 1999). Using the electroretinogram as a sensitive indicator of retinal function, these studies demonstrated that three brief 670-nm LED treatments (160 s at 25 mW/cm^2 producing a fluence 4 J/cm^2 at the surface of the eye) delivered at 5, 25, and 50 h of methanol intoxication, attenuated the retinotoxic effects of methanol-derived formate. There was a significant recovery of rod- and cone-mediated function in PBM-treated, methanol-intoxicated rats. 670 nm PBM also protected the retina from the histopathologic changes induced by methanol-derived formate.

58.3 Light-Induced Retinal Damage

Oxidative damage produced by photo-oxidation of the photoreceptor outer segments is widely accepted as the initiating event in light-induced retinal damage (LD) (Hollyfield et al. 2008). Lesions produced by LD are characterized by photoreceptor cell death, RPE cell damage, Müller cell gliosis and disruption of the outer limiting membrane (OLM). In addition to these structural changes, there is the induction of an inflammatory state characterized by an invasion of the outer retina by activated microglia (Albarracin et al. 2011; Albarracin and Valter, 2012.). This progressive degeneration has been used to model many of the factors contributing to the expansion of the degenerative area, similar to the changes observed in AMD (Rutar et al. 2010, 2011, 2012).

Several studies have shown that 670 nm PBM is protective against light-induced retinal degeneration (Albarracin et al. 2011; Qu et al. 2010; Natoli et al. 2010). 670 nm PBM (9 J/cm^2) administered before, during or after exposure to LD protected photoreceptor function as measured by ERG responses and morphology. This protection involved a reduction in photoreceptor cell death and inflammatory stress biomarkers in the retina, and reduction in microglial and macrophage invasion (Albarracin et al. 2011). Pretreatment with PBM proved to be most effective against LD compared to treatment during or after LD. However, animals treated with PBM post-LD also recovered photoreceptor function by 1 month post-exposure (Albarracin et al. 2011).

Complement activation is associated with the pathogenesis of AMD, and also occurs following LD (Rutar et al. 2012). 670 nm PBM pretreatment (9 J/cm^2) reduced the expression of complement components and receptors in the retina following LD (Rutar et al. 2010). Moreover, there was a reduction in the recruitment of C-3 expressing microglia/macrophages in the retina following 670 nm PBM, and a concomitant reduction in the biomarker of oxidative damage 4-hydroxynonenal (4-HNE). These findings indicate the 670 nm PBM pretreatment attenuates oxidative damage to photoreceptors and reduces inflammation, which may reduce the stimulation of the complement cascade, thus further protecting photoreceptors.

58.4 Retinitis Pigmentosa

The therapeutic efficacy and mechanism of action of 670 nm PBM was investigated in a rodent model of retinitis pigmentosa, the P23H rat (Kirk et al. 2013). In this model, the transgene is a rhodopsin gene engineered to mimic a mutation that causes an autosomal dominant form of human RP common in North America. P23H rat pups were treated once per day during the critical period of photoreceptor development with a 670 nm LED array (180 s treatments at 50 mW/cm^2; fluence 9 J/cm^2). Sham-treated rats were restrained, but not exposed to NIR light. In the first series of studies, rats were treated from postnatal day (p) 16 to p20. The status of

the retina was determined at p22 by assessment of mitochondrial function, oxidative stress and cell death. In a second series of studies, rat pups were treated from p10–p25. Retinal status was assessed at p30 by measuring photoreceptor function by ERG and retinal morphology by Spectral Domain Optical Coherence Tomography (SD-OCT). 670 nm PBM increased retinal mitochondrial cytochrome c oxidase activity and upregulated the retina's production of the key mitochondrial antioxidant enzyme, manganese superoxide reductase (MnSOD). PBM also attenuated photoreceptor cell loss and improved photoreceptor function. PBM thus protects photoreceptors in the developing P23H retina, by augmenting mitochondrial function and stimulating antioxidant protective pathways.

58.5 Aging and Age Related Macular Degeneration

Inflammation is a common feature in the aged retina, and in many retinal diseases including AMD. In addition, mitochondrial function has been shown to decline in aging and AMD (Jarrett and Boulton 2012). Brief exposure to 670 nm PBM in the aged retina has been shown to increase mitochondrial membrane potential and reduce inflammation (Kokkinopoulos et al. 2012). Using an aged mouse model of AMD, the complement factor H knockout ($CFH^{-/-}$) in which inflammation is a key feature. Begum et al. (2013) investigated the effects of 670 nm PBM delivered briefly in environmental lighting rather than directly focused on the retina. Mice were exposed to 670 nm for 6 min twice a day for 14 days in the form of supplemented environmental light. Exposed animals exhibited a significant increase in cytochrome c oxidase. Complement component C3, an inflammatory marker in the outer retina was downregulated, as were vimentin and glial fibrillary acidic protein (GFAP) expression, which reflect retinal stress in Müller glia. Hence, 670 nm PBM is effective in reducing retinal inflammation likely by cytochrome c oxidase activation in mice with a genotype similar to that in 50% of AMD patients, even when brief exposures are delivered via environmental lighting. The efficacy revealed here supports current early stage clinical trials of 670 nm in AMD patients.

58.6 Conclusions

Taken as a whole, these studies in experimental models of retinal and optic nerve injury and disease show that far-red (FR) and NIR PBM improves mitochondrial function, reduces oxidative stress, and modulates inflammatory mediators, leading to decreased apoptosis and retinoprotection. Further studies are necessary to characterize the effect of PBM on the human retina and to define safe protocols for the application of this novel therapy to mechanistically complex diseases.

References

Albarracin RS, Valter K (2012) Treatment with 670-nm light protects the cone photoreceptors from white light-induced degeneration. Adv Exp Med Biol 723:121–128

Albarracin R, Eells J, Valter K (2011) Photobiomodulation protects the retina from light-induced photoreceptor degeneration. Invest Ophthalmol Vis Sci 52:3582–3592

Begum R, Powner MB, Hudson N et al (2013) Treatment with 670 nm light upregulates cytochome c oxidase expression and reduces inflammation in an age-related macular degeneration model. PLoS One 8:e57828

Chung H, Dai T, Sharma SK et al (2012) The nuts and bolts of low-level laser (light) therapy. Ann Biomed Eng 40:516–533

Eells JT, Henry MM, Summerfelt P et al (2003) Therapeutic photobiomodulation for methanol-induced retinal toxicity. Proc Natl Acad Sci U S A 100:3439–3444

Eells JT, Wong-Riley MT, VerHoeve J et al (2004) Mitochondrial signal transduction in accelerated wound and retinal healing by near-infrared light therapy. Mitochondrion 4:559–567

Fitzgerald M, Hodgetts S, Van den Heuvel C et al (2013) Red/near-infrared irradiation therapy for treatment of central nervous system injuries and disorders. Rev Neurosci 24:205–226

Hollyfield JG, Bonilha VL, Rayborn ME et al (2008) Oxidative damage-induced inflammation initiates age-related macular degeneration. Nat Med 14:194–198

Huang YY, Sharma SK, Carroll J et al (2011) Biphasic dose response in low level light therapy-an update. Dose Response 9:602–618

Jarrett SG, Boulton ME (2012) Consequences of oxidative stress in age-related macular degeneration. Mol Aspects Med 33:399–417

Karu T (1999) Primary and secondary mechanisms of action of visible to near-IR radiation on cells. J Photochem Photobiol B 49:1–17

Kirk DK, Gopalakrishnan S, Schmitt H et al (2013) Photobiomodulation reduces photoreceptor death and regulates cytoprotection in early states of P23H retinal dystrophy. Proceedings of SPIE BIOS, San Francisco, January 2013

Kokkinopoulos I, Colman A, Hogg Cet al (2012) Age-related retinal inflammation is reduced by 670 nm light via increased mitochondrial membrane potential. Neurobiol Aging 34:602–609

Natoli R, Zhu Y, Valter K et al (2010) Gene and noncoding RNA regulation underlying photoreceptor protection: microarray study of dietary antioxidant saffron and photobiomodulation in rat retina. Mol Vis 16:1801–1822

Qu C, Cao W, Fan Y, Lin Y (2010) Near-infrared light protects the photoreceptor from light-induced damage in rats. Adv Exp Med Biol 664:365–374

Rutar M, Provis JM, Valter K (2010) Brief exposure to damaging light causes focal recruitment of macrophages and long-term destabilization of photoreceptors in the albino rat retina. Curr Eye Res 35:631–643

Rutar M, Natoli R, Valter K et al (2011) Early focal expression of the chemokine Ccl2 by Muller cells during exposure to damage-inducing bright continuous light. Invest Ophthalmol Vis Sci 52:2379–2388

Rutar M, Natoli R, Albarracin R et al (2012) 670 nm light treatment reduces complement propagation following retinal degeneration. J Neuroinflamm 9:257–263

Seme MT, Summerfelt P, Henry MM et al (1999) Formate-induced inhibition of photoreceptor function in methanol intoxication. J Pharmacol Exp Ther 289:361–370

Shen J, Yang X, Dong A et al (2005) Oxidative damage is a potential cause of cone cell death in retinitis pigmentosa. J Cell Physiol 203:457–464

Stone J, Maslim J, Valter-Kocsi K et al (1999) Mechanisms of photoreceptor death and survival in mammalian retina. Prog Retin Eye Res 18:689–735

Wong-Riley MT, Liang HL, Eells JT et al (2005) Photobiomodulation directly benefits primary neurons functionally inactivated by toxins: role of cytochrome c oxidase. J Biol Chem 280:4761–4771

Chapter 59
Exercise and Cyclic Light Preconditioning Protect Against Light-Induced Retinal Degeneration and Evoke Similar Gene Expression Patterns

Micah A. Chrenek, Jana T. Sellers, Eric C. Lawson, Priscila P. Cunha, Jessica L. Johnson, Preston E. Girardot, Cristina Kendall, Moon K. Han, Adam Hanif, Vincent T. Ciavatta, Marissa A. Gogniat, John M. Nickerson, Machelle T. Pardue and Jeffrey H. Boatright

Abstract To compare patterns of gene expression following preconditioning cyclic light rearing versus preconditioning aerobic exercise. BALB/C mice were preconditioned either by rearing in 800 lx 12:12 h cyclic light for 8 days or by running on treadmills for 9 days, exposed to toxic levels of light to cause light-induced retinal degeneration (LIRD), then sacrificed and retinal tissue harvested. Subsets of mice were maintained for an additional 2 weeks and for assessment of retinal function by electroretinogram (ERG). Both preconditioning protocols partially but significantly

J. H. Boatright (✉) · M. A. Chrenek · J. T. Sellers · E. C. Lawson · P. P. Cunha · J. L. Johnson · P. E. Girardot · C. Kendall · M. K. Han · A. Hanif · V. T. Ciavatta · M. A. Gogniat · J. M. Nickerson · M. T. Pardue
Department of Ophthalmology, Emory University School of Medicine, Room B5500, Emory Eye Center, 1365B, Clifton Road, N.E., Atlanta, GA 30322, USA
e-mail: jboatri@emory.edu

J. H. Boatright · E. C. Lawson · M. K. Han · A. Hanif · V. T. Ciavatta · M. A. Gogniat · M. T. Pardue
Atlanta VA Center of Excellence for Visual and Neurocognitive Rehabilitation, Atlanta VA Medical Center, Decatur, GA 30033, USA

M. A. Chrenek
e-mail: mchrene@emory.edu

J. T. Sellers
e-mail: jana.t.sellers@emory.edu

E. C. Lawson
e-mail: eric.lawson90@gmail.com

P. P. Cunha
e-mail: priscila.cunha@emory.edu

C. Bowes Rickman et al. (eds.), *Retinal Degenerative Diseases,* Advances in Experimental Medicine and Biology 854, DOI 10.1007/978-3-319-17121-0_59

preserved retinal function and morphology and induced similar leukemia inhibitory factor (LIF) gene expression pattern. The data demonstrate that exercise preconditioning and cyclic light preconditioning protect photoreceptors against LIRD and evoke a similar pattern of retinal LIF gene expression. It may be that similar stress response pathways mediate the protection provided by the two preconditioning modalities.

Keywords Aerobic exercise · Retinal degeneration · Preconditioning · Light-induced retinal degeneration · Cyclic light rearing

59.1 Introduction

Preconditioning of neural tissue produces local and systemic responses that protect the tissue from toxic levels of stress. For instance mild hypoxia/ischemia (Roth et al. 1998; Grimm et al. 2005, 2006; Gidday 2006; Li et al. 2006; Zhu et al. 2007; Thiersch et al. 2009; Grimm and Willmann 2012; Wacker et al. 2012), moderate-intensity cyclic light (Li et al. 2001, 2003; Chollangi et al. 2009; Ueki et al. 2009), and even whole body exercise (Zhang et al. 2011) are preconditioning stressors that protect several neuronal structures from the effects of exposure to toxic levels of stress. These reports and others further suggest that the mechanisms of preconditioning stressors may be common across preconditioning and toxic modalities. We recently demonstrated that modest treadmill exercise protects photoreceptor morphology and function against light-induced retinal degeneration (LIRD; reported elsewhere

J. L. Johnson
e-mail: Jessica.johnson@emory.edu

P. E. Girardot
e-mail: preston.girardot@emory.edu

C. Kendall
e-mail: cristina.kendall@gmail.com

M. K. Han
e-mail: zlalunar@hotmail.com

A. Hanif
e-mail: ahanif@emory.edu

V. T. Ciavatta
e-mail: vciavat@emory.edu

M. A. Gogniat
e-mail: mgognia@emory.edu

J. M. Nickerson
e-mail: litjn@emory.edu

M. T. Pardue
e-mail: mpardue@emory.edu

at this meeting and in (Lawson et al. 2014)). We hypothesized that preconditioning cyclic light rearing and preconditioning exercise will be protective against LIRD and that the two forms of preconditioning elicit similar patterns of gene expression.

59.2 Methods

Adult male albino BALB/C mice were used in all experiments; $n = 3–6$ per experimental condition. For cyclic light preconditioning, mice were reared on 12:12 h light:dark cycles. Half the mice were exposed to light at ~50 lx (i.e., normal maintenance level) and for the other half to 800 lx. After 8 days, half of each light-rearing group was exposed to 5000 lx white light for 4 h (i.e., toxic light) and the other half were exposed to 50 lx of light. Immediately following light exposure, subsets of mice were sacrificed and retinas harvested for RNA extraction for use in real-time reverse-transcriptase PCR. In some cases, retinal extracts were pooled from individual eyes prior to PCR. To confirm the putative protective effect, another subset of mice was returned to maintenance housing and after 2 weeks were assessed for visual function by electroretinogram (ERG), after which they were sacrificed and ocular paraffin sections prepared for morphological assessment (data not shown).

For exercise preconditioning, mice were exercised on a treadmill running at 10 m/min for 1 h for 9 consecutive days. Controls were mice placed on a stationary treadmill at the same time. Immediately following the last exercise period, mice were exposed to either maintenance levels or toxic levels of light as above. At the end of exposure, mice were sacrificed and retinas harvested for RNA extraction. To confirm the putative protective effect, in other experiments, mice were exercised for 2 weeks, exposed to maintenance or toxic light, then exercised 2 more weeks, after which their ERGs were obtained, they were sacrificed, and ocular paraffin sections prepared for morphological assessment.

59.3 Results

Both forms of preconditioning protected against LIRD to remarkably similar extents, with cyclic light and exercise preconditioned mice showing significantly preserved retinal function (Fig. 59.1) and photoreceptor nuclei (2x greater total counts) and thicker outer nuclear layers than non-preconditioned mice exposed to toxic light (data not shown). Real-time polymerase chain reaction assays using retina RNA revealed that preconditioning by cyclic light rearing and aerobic exercise similarly increased the expression of LIF (Fig. 59.2). Increases were also seen in expression of other preconditioning or stress response genes (e.g., HMOX1, IL-6, PPARgamma, STAT3, HIF1alpha, etc.), but not in expression of CLU and citrate synthetase (data not shown).

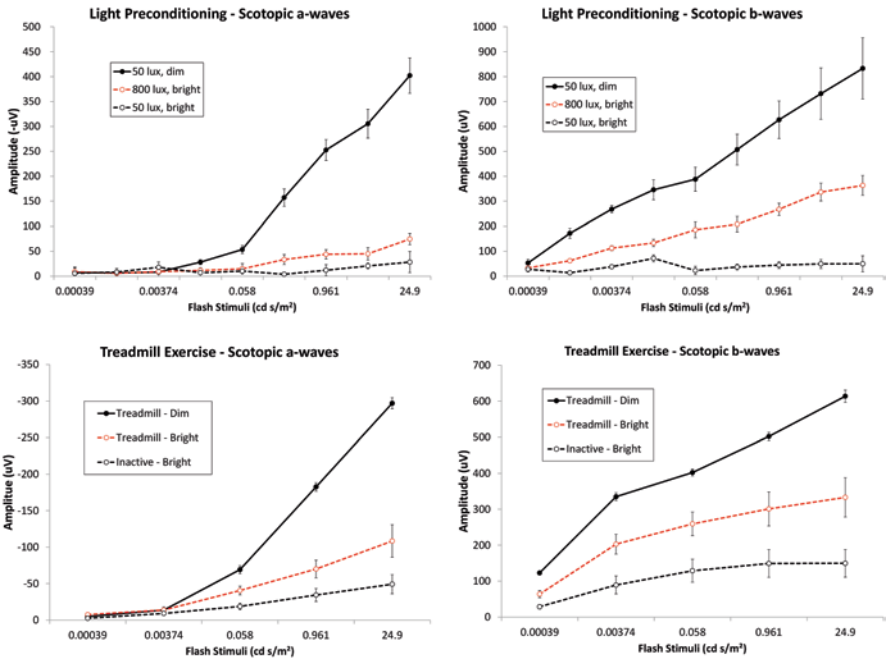

Fig. 59.1 Preconditioning protects retinal function. Panels show ERG stimulus response curves 2 weeks after light exposure for dark-adapted a-wave (*left panels*) and b-wave (*right panels*) amplitudes. Exposure to "bright" light (5000 lx for 4 h; *dashed black lines*) suppressed ERG amplitudes compared to exposure to "dim" (50 lx) light (*solid black lines*). Rearing in 800 lx cyclic light (*top panels*) or treadmill running (*bottom panels*) preserved ERG amplitudes (*dashed red lines*)

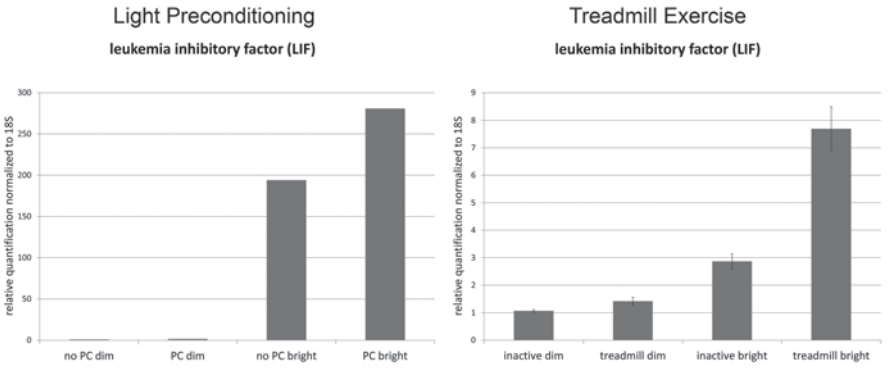

Fig. 59.2 Preconditioning by cyclic light rearing or by treadmill running increases expression of LIF. Rearing in 800 lx cyclic light ("PC") or treadmill running ("treadmill") similarly increased expression of the preconditioning gene LIF immediately following exposure toxic light (5000 lx for 4 h)

59.4 Discussion

The data suggest that exercise preconditioning and cyclic light preconditioning protect photoreceptors against LIRD and evoke similar patterns of retinal gene expression. Models of protective preconditioning have been used well to increase our understanding of innate protective stress responses in retina (Roth et al. 1998; Li et al. 2001; Grimm et al. 2002, 2004, 2005, 2006; Li et al. 2003; Zhu et al. 2006, 2007, 2008; Chollangi et al. 2009; Thiersch et al. 2009; Ueki et al. 2009; Gidday 2010; Grimm and Willmann 2012; Zhu et al. 2012; McLaughlin and Gidday 2013); such approaches are revealing several exciting potential therapeutic targets. In the case of exercise, though, it may be that this form of preconditioning, which is accessible to the majority of the population, is itself a therapeutic intervention. To that end, additional studies on the mechanisms underlying this neuroprotection, the optimal exercise regimen, and effects in humans are being pursued.

Acknowledgments Supported by NIH P30 EY006360, NIH R01 EY014026 and a grant from the Abraham J. & Phyllis Katz Foundation (to J.H.B.), Rehabilitation Research and Development Service Veterans Affairs Research Career Scientist Award (to M.T.P.), Atlanta VA Center of Excellence in Vision and Neurocognitive Rehabilitation, and Departmental Award from Research to Prevent Blindness.

References

Chollangi S, Wang J, Martin A et al (2009) Preconditioning-induced protection from oxidative injury is mediated by leukemia inhibitory factor receptor (LIFR) and its ligands in the retina. Neurobiol Dis 34:535–544

Gidday JM (2006) Cerebral preconditioning and ischaemic tolerance. Nat Rev Neurosci 7:437–448

Gidday JM (2010) Pharmacologic preconditioning: translating the promise. Transl Stroke Res 1:19–30

Grimm C, Willmann G (2012) Hypoxia in the eye: a two-sided coin. High Alt Med Biol 13:169–175

Grimm C, Wenzel A, Groszer M et al (2002) HIF-1-induced erythropoietin in the hypoxic retina protects against light-induced retinal degeneration. Nat Med 8:718–724

Grimm C, Wenzel A, Stanescu D et al (2004) Constitutive overexpression of human erythropoietin protects the mouse retina against induced but not inherited retinal degeneration. J Neurosci 24:5651–5658

Grimm C, Hermann DM, Bogdanova A et al (2005) Neuroprotection by hypoxic preconditioning: HIF-1 and erythropoietin protect from retinal degeneration. Semin Cell Dev Biol 16:531–538

Grimm C, Wenzel A, Acar N et al (2006) Hypoxic preconditioning and erythropoietin protect retinal neurons from degeneration. Adv Exp Med Biol 588:119–131

Lawson EC, Han MK, Sellers JT et al (2014) Aerobic exercise protects retinal function and structure from light-induced retinal degeneration. J Neurosci 34:2406–2412

Li F, Cao W, Anderson RE (2001) Protection of photoreceptor cells in adult rats from light-induced degeneration by adaptation to bright cyclic light. Exp Eye Res 73:569–577

Li F, Cao W, Anderson RE (2003) Alleviation of constant-light-induced photoreceptor degeneration by adaptation of adult albino rat to bright cyclic light. Invest Ophthalmol Vis Sci 44:4968–4975

Li W, Luo Y, Zhang F et al (2006) Ischemic preconditioning in the rat brain enhances the repair of endogenous oxidative DNA damage by activating the base-excision repair pathway. J Cereb Blood Flow Metab 26:181–198

McLaughlin B, Gidday JM (2013) Poised for success: implementation of sound conditioning strategies to promote endogenous protective responses to stroke in patients. Transl Stroke Res 4:104–113

Roth S, Li B, Rosenbaum PS et al (1998) Preconditioning provides complete protection against retinal ischemic injury in rats. Invest Ophthalmol Vis Sci 39:777–785

Thiersch M, Lange C, Joly S et al (2009) Retinal neuroprotection by hypoxic preconditioning is independent of hypoxia-inducible factor-1 alpha expression in photoreceptors. Eur J Neurosci 29:2291–2302

Ueki Y, Le YZ, Chollangi S et al (2009) Preconditioning-induced protection of photoreceptors requires activation of the signal-transducing receptor gp130 in photoreceptors. Proc Natl Acad Sci U S A 106:21389–21394

Wacker BK, Perfater JL, Gidday JM (2012) Hypoxic preconditioning induces stroke tolerance in mice via a cascading HIF, sphingosine kinase, and CCL2 signaling pathway. J Neurochem 123:954–962

Zhang F, Wu Y, Jia J (2011) Exercise preconditioning and brain ischemic tolerance. Neuroscience 177:170–176

Zhu Y, Ohlemiller KK, McMahan BK et al (2006) Constitutive nitric oxide synthase activity is required to trigger ischemic tolerance in mouse retina. Exp Eye Res 82:153–163

Zhu Y, Zhang Y, Ojwang BA et al (2007) Long-term tolerance to retinal ischemia by repetitive hypoxic preconditioning: role of HIF-1alpha and heme oxygenase-1. Invest Ophthalmol Vis Sci 48:1735–1743

Zhu Y, Zhang L, Gidday JM (2008) Deferroxamine preconditioning promotes long-lasting retinal ischemic tolerance. J Ocul Pharmacol Ther 24:527–535

Zhu Y, Zhang L, Schmidt JF et al (2012) Glaucoma-induced degeneration of retinal ganglion cells prevented by hypoxic preconditioning: a model of glaucoma tolerance. Mol Med 18:697–706

Chapter 60
Small Molecules that Protect Mitochondrial Function from Metabolic Stress Decelerate Loss of Photoreceptor Cells in Murine Retinal Degeneration Models

Craig Beeson, Chris Lindsey, Cecile Nasarre, Mausumi Bandyopadhyay, Nathan Perron and Bärbel Rohrer

Abstract One feature common to many of the pathways implicated in retinal degeneration is increased metabolic stress leading to impaired mitochondrial function. We found that exposure of cells to calcium ionophores or oxidants as metabolic stressors diminish maximal mitochondrial capacity. A library of 50,000 structurally diverse "drug-like" molecules was screened for protection against loss of calcium-induced loss of mitochondrial capacity in 661W rod-derived cells and C6 glioblastomas. Initial protective hits were then tested for protection against IBMX-induced loss

C. Beeson (✉) · C. Lindsey
MitoChem Therapeutics Inc, 280 Calhoun Street, MSC140,
Charleston, SC 29403, USA
e-mail: beesonc@musc.edu

Departments of Drug Discovery and Biomedical Sciences, Medical University of South Carolina, Charleston, SC 29425, USA

C. Nasarre · M. Bandyopadhyay · N. Perron · B. Rohrer
Departments of Ophthalmology, Medical University of South Carolina,
Charleston, SC 29425, USA
e-mail: nassarre@musc.edu

B. Rohrer
Division of Research, Ralph H. Johnson VA Medical Center,
Charleston, SC 29401, USA
e-mail: rohrer@musc.edu

C. Lindsey
e-mail: lindseyc@musc.edu

M. Bandyopadhyay
e-mail: bandyom@musc.edu

N. Perron
e-mail: perron@musc.edu

C. Bowes Rickman et al. (eds.), *Retinal Degenerative Diseases,* Advances in Experimental Medicine and Biology 854, DOI 10.1007/978-3-319-17121-0_60

of mitochondrial capacity as measured via respirometry. Molecules that protected mitochondria were then evaluated for protection of rod photoreceptor cells in retinal explants from *rd1* mice. Two of the molecules attenuated loss of photoreceptor cells in the *rd1* model. In the 661W cells, exposure to calcium ionophore or tert-butylhydroperoxide caused mitochondrial fragmentation that was blocked with the both compounds. Our studies have identified molecules that protect mitochondria and attenuate loss of photoreceptors in models of retinal degeneration suggesting that they could be good leads for development of therapeutic drugs for treatment of a wide variety of retinal dystrophies.

Keywords Mitochondria · Respirometry · Glycolysis · Neuroprotectant · ATP

60.1 Introduction

Photoreceptors are specialized to convert light to neurochemical signals, a process that has high energy requirements, calcium ion transients, and oxidative stress (Stone et al. 1999; Linton et al. 2010). Thus, photoreceptor degeneration can result from changes in energy metabolism, calcium ion concentrations, or oxygen tension (Lohr et al. 2006). It is thus perhaps not surprising to find that alterations in metabolic pathways that produce ATP, whether they be glycolysis or oxidative phosphorylation, underlie a number of retinal pathologies. For example, our group has shown that in three different mouse models of retinal degeneration, the *rd1* and the *rds* mouse, two models for retinitis pigmentosa (RP), as well as the constant light damage model in Balb/c mice, gene expression for metabolic genes such as phosphofructokinase-1, the rate limiting enzyme for glycolysis, is increased prior to the onset of degeneration, but drops as degeneration commences (Lohr et al. 2006). Acosta and colleagues made similar observations in the *rd1* mouse retina as well as in the P23H rhodopsin rat (line 3) in which they reported increased lactate dehydrogenase activities prior to degeneration, followed by a drop in activity with the onset of photoreceptor cell loss (Acosta et al. 2010). On the other hand, reduced retinal complex I activity (oxidative phosphorylation) concomitant with oxidative stress was reported at stages prior to cell death in four mouse RP models, including the *rd1* and *rds* mouse (Vlachantoni et al. 2011). In contrast, in the RCS rat, Graymore (Graymore 1964) demonstrated a reduction in LDH activity prior to degeneration. These observations in animal models were strengthened by reports in patients. Vingolo and colleagues (Vingolo et al. 1999) demonstrated that RP patients showed significant improvements in their maximum electroretinogram responses when treated with hyperbaric oxygen therapy. Finally, mitochondrial structure and function appears to be altered in general aging, retinal dysfunction associated with Parkinson's disease, retinal diseases including diabetic retinopathy and glaucoma, age-related diseases such as age-related macular, as well as in neurodegeneration (Soane et al. 2007). Thus, it is reasonable to hypothesize that early changes in energy metabolism underlie a, number of photoreceptor dystrophies; and that agents that ameliorate the

dysregulation of energy metabolism could be developed into therapeutic strategies for treatment of retinal degeneration.

In previous publications we have shown that we can utilize 661W cells (Kunchithapautham and Rohrer 2007) treated with the Ca^{2+} -ionophore A23187, non-hydrolyzable cGMP (8-Bromo-cGMP), or IBMX (phosphodiesterase inhibitor and adenosine receptor antagonist), to mimic the pathological increased Ca^{2+} influx seen in the *rd1* photoreceptors. Likewise, 661W cells challenged with hydroperoxides recapitulate many of the steps in cell death observed in the light-damaged albino mouse retina, a model for oxidative stress in AMD (Kunchithapautham and Rohrer 2007). Both the light-damage and the *rd1* mouse retina have been used to investigate neuroprotective therapies, focusing predominantly on neurotrophins and antioxidants. Although the effects of excess calcium or oxidative stress on mitochondrial function have not been measured directly in the mouse retina, we found that *rd1* retina expressed high levels of stress and metabolic genes at onset of damage but expression of metabolic genes dropped in parallel with the loss of cells.

60.2 Results

60.2.1 Screening with Metabolic Assays

Recently, novel assay methods have become available to monitor energy metabolism using high throughput assay platforms. In particular, the technology developed by Seahorse Biosciences, based on the original work using the Cytosensor® microphysiometer to measure extracellular fluxes linked to energy metabolism (Wiley and Beeson 2002; Ferrick et al. 2008), demonstrated the feasibility of a multi-well plate assay (XF24 or XF96) for measuring extracellular fluxes of metabolic acid extrusion, a measure of glycolysis, and oxygen uptake, a measure of oxidative phosphorylation (Ferrick et al. 2008). Using the XF assay, we made a similar observation regarding increased glycolytic rates prior to the onset of cell death that we observed in retinas of RP models, when analyzing the metabolic responses of the 661W cells to the calcium or oxidant stress before succumbing to cell death (Perron et al. 2013).

Thus, it is reasonable to hypothesize that these early metabolic perturbations are the phenotypic measures of losses of mitochondrial integrity that underlie retinal pathology leading to loss of photoreceptor structure and function. Based on this assumption, we first used a high throughput MTT assay to screen the ChemBridge DiverSET 50,000 chemical diversity small molecule library for protection against the A23187 calcium stress known to cause loss of metabolic function in many cells (Perron et al. 2013). The hits identified in this screen were confirmed using rat C6 glioblastoma cells using the same calcium stress, to show that protective effects translate to other cell types of neuroectodermal lineage. The 12 hits identified in the

initial assay were used to test for protection of maximal oxygen capacity, estimated from FCCP uncoupled rates, to identify leads that protect against loss of mitochondrial function. The respirometric assay identified four compounds that protect mitochondria from 24 h exposure to IBMX.

60.2.2 Photoreceptor Protection in rd1 Organ Cultures

The combined data thus far suggested that we had identified unique compounds with mostly unknown activities that protect mitochondrial metabolism in cells treated with calcium or oxidant stress. As a translational bridge we utilized mouse retina organ cultures. These retinal explants are a powerful ex vivo screening tool that allow the testing of photoreceptor cell survival within the retinal network without systemic interference. Here we utilized the *rd1* mouse. The genotype of the *rd1* mouse is a mutation in the β-subunit of the phosphodiesterase gene that results in high levels of cGMP, leaving an increased number of the cGMP-gated channels in the open state, allowing intracellular calcium to rise to toxic levels and rapid rod degeneration ensues (Sharma and Rohrer 2007). The genetic deficit and the retinal pathology is very similar to that observed in the patients with βPDE-dependent RP. In these mice, rod photoreceptor degeneration starts after postnatal day 10 (P10), progressing rapidly, such that at P21, only 1–2 rows of photoreceptor remains, mainly representing cones. Finally, the *rd1* mouse retina is amenable to culturing, replicating both retinal development and degeneration, following the same time course as *in vivo* (Ogilvie et al. 1999; Bandyopadhyay and Rohrer 2010). The retinal explants were cultured for 11 days ex vivo. Explants were treated with CB3, CB10, CB11 or CB12 (5 μM). Additives were replaced with fresh medium every alternate day. At the end of the experiments, tissues were fixed, sectioned and stained with 0.1% toluidine and numbers of rows of photoreceptors remaining in the outer nuclear layer (ONL) were counted. *Rd1* explants treated with vehicle only were found to contain 1.2 ± 0.19 cells in the ONL. This is in contrast to cultures treated with CB10 (2.9 ± 0.32), CB11 (3.2 ± 0.36) and CB12 (3.9 ± 0.10) that all contained significantly ($P < 0.001$) more rows of photoreceptors. CB3, was found to cytotoxic in the *rd1* explants.

60.2.3 Effects of CB11 and CB12 on Mitochondrial Morphology

Mitochondria play an essential role in mediating cell health and death. The mitochondrial network is constantly being remodeled via fission/fusion, autophagy and biogenesis, with dysfunctional mitochondria being removed and replaced via biogenesis. Since some of the hits increase mitochondrial respiration, it would stand to reason that the mitochondrial network is more structurally intact in compound-treated as opposed to vehicle-treated cells under toxicant stress. Live 661W cells were imaged using nonyl-acridine orange (NAO, 50 nM), a dye that is partly selective for

cardiolipin-containing membranes such as the mitochondrial inner membrane. The mitochondrial network in control cells exhibited a complex morphology, consisting of mainly fused mitochondria, whereas in 661W cells treated with 600 μM IBMX, the network consisted of mostly small, punctate mitochondria. A pro-fission state of mitochondria is often an implication of mitochondrial damage and disease. CB11 and CB12 were found to both protect against mitochondrial fission, promoting a more healthy balance between mitochondrial fusion and fission in IBMX-treated cells. CB11 and or CB12 did not alter mitochondrial morphology in non-stressed cells. Mitochondrial fission and fusion are controlled by Drp1, a GTPase that is a member of the dynamin superfamily of proteins, and Mfn1/2, which are GTPases embedded in the mitochondrial outer membrane. Treatment of naïve 661W cells with CB11 or CB12 induced an increase in the protein level of Mfn2 and a concomitant decrease in Drp1 that are consistent with the morphology measurements in stressed cells.

60.3 Discussion

The genesis of the program to identify metabolic neuroprotectants was our previously published observation that calcium or oxidative stress causes a rapid loss in maximal mitochondrial ATP-producing capacity in 661W cells as measured by respirometry, and that the degree of loss in maximal capacity was predictive of subsequent cell death measured (Perron et al. 2013). Our rationale was that a primary screen focused on metabolic capacity (MTT assay) would rapidly identify potential cytoprotective agents that we could follow up with secondary and tertiary screens focused on separating out those agents that specifically target the metabolic phenotype related to photoreceptor cell degeneration.

Following this strategy, the main results of the current study are that 12 compounds out of the 50,000 compound ChemBridge library were identified that reversed dysregulation of energy metabolism triggered by calcium stress, the respirometry assay confirmed that 4/12 compounds protected against calcium stress by increasing maximum respiratory capacity, and three of the lead compounds were found to attenuate loss of photoreceptor cells in the *rd1* mouse organ culture.

In our perspective, the regulatory pathways determining a givens cell's response to metabolic load and its ability to deal with dysfunction is likely related to the pathways that emerged during metazoan development. Prior to that evolutionary stage, nascent eukaryotes were tuning their regulatory pathways that involved a somewhat related "metazoan-like" existence in which endosymbiotic bacterial particles now called mitochondria were becoming part of the whole unicellular organism. As the pre-mitochondria evolved into committed intracellular organelles, they shed much of their own genome and adopted proteins encoded by the nuclear genome. The best evidence to date suggests that eukaryote divergence during early mega-evolution coincided with expansion of the myosin domain and motor structural heterogeneity and these proteins were also involved in structural assemblies found in

mitochondria (*i.e.*, the mitochondrial ATP synthase) and regulatory pathways seen in the mitochondria intersect with cellular life/death decisions. For example, oxidative stress will damage biomolecules but cells have evolved efficient mechanisms of dealing with oxidants. The deactivation of oxidants, and repair of oxidative damage is part of the metabolic load that a tissue bears. While dysfunctions in either the endogenous antioxidant or repair mechanisms are certainly deleterious, in the long run, the primary effect of oxidative stress is the increased metabolic load and, thus, they are not fundamentally different than other stressors that cause metabolic load. For example, many RP mutations cause protein misfolding and a subsequent unfolded protein response (UPR) leading to endoplasmic reticulum (ER) stress with increased metabolic load. We would predict that UPR and ER stress are not significantly different than oxidative stress and the molecules identified here could be more generally protective in many forms of RP.

References

Acosta ML, Shin YS, Ready S, et al (2010) Retinal metabolic state of the proline-23-histidine rat model of retinitis pigmentosa. Am J Physiol Cell Physiol 298:C764–C774

Bandyopadhyay M, Rohrer B (2010) Photoreceptor structure and function is maintained in organotypic cultures of mouse retinas. Mol Vis 16:1178–1185

Ferrick DA, Neilson A, Beeson C (2008) Advances in measuring cellular bioenergetics using extracellular flux. Drug Discov Today 13:268–274

Graymore C (1964) Metabolism of the developing retina. 7. Lactic dehydrogenase isoenzyme in the normal and degenerating retina. A preliminary communication. Exp Eye Res 89:5–8

Kunchithapautham K, Rohrer B (2007) Apoptosis and autophagy in photoreceptors exposed to oxidative stress. Autophagy 3:433–441

Linton JD, Holzhausen LC, BaBai N et al (2010) Flow of energy in the outer retina in darkness and in light. Proc Natl Acad Sci U S A 107:8599–8604

Lohr HR, Kuntchithapautham K, Sharma AK et al (2006) Multiple, parallel cellular suicide mechanisms participate in photoreceptor cell death. Exp Eye Res 83:380–389

Ogilvie JM, Speck JD, Lett JM et al (1999) A reliable method for organ culture of neonatal mouse retina with long- term survival. J Neurosci Methods 87:57–65

Perron NR, Beeson C, Rohrer B (2013) Early alterations in mitochondrial reserve capacity; a means to predict subsequent photoreceptor cell death. J Bioenerg Biomembr 45:101–109

Sharma AK, Rohrer B (2007) Sustained elevation of intracellular cGMP causes oxidative stress triggering calpain-mediated apoptosis in photoreceptor degeneration. Curr Eye Res 32:259–269

Soane L, Kahraman S, Kristian T et al (2007) Mechanisms of impaired mitochondrial energy metabolism in acute and chronic neurodegenerative disorders. J Neurosci Res 85:3407–3415

Stone J et al (1999) Mechanisms of photoreceptor death and survival in mammalian retina. Prog Retin Eye Res 18:689–735

Vingolo EM, Pelaia P, Forte R et al (1999) Does hyperbaric oxygen (HBO) delivery rescue retinal photoreceptors in retinitis pigmentosa? Doc Ophthalmol 97:33–39

Vlachantoni D, Bramall AN, Murphy MP et al (2011) Evidence of severe mitochondrial oxidative stress and a protective effect of low oxygen in mouse models of inherited photoreceptor degeneration. Hum Mol Genet 20:322–335

Wiley C, Beeson C (2002) Continuous measurement of glucose utilization in heart myoblasts. Anal Biochem 304:139–146

Chapter 61
Histone Deacetylase: Therapeutic Targets in Retinal Degeneration

Conor Daly, Jun Yin and Breandán N. Kennedy

Abstract Previous studies report that retinitis pigmentosa (RP) patients treated with the histone deacetylase inhibitor (HDACi) valproic acid (VPA) present with improved visual fields and delayed vision loss. However, other studies report poor efficacy and safety of HDACi in other cohorts of retinal degeneration patients. Furthermore, the molecular mechanisms by which HDACi can improve visual function is unknown, albeit HDACi can attenuate pro-apoptotic stimuli and induce expression of neuroprotective factors. Thus, further analysis of HDACi is warranted in pre-clinical models of retinal degeneration including zebrafish. Analysis of HDAC expression in developing zebrafish reveals diverse temporal expression patterns during development and maturation of visual function.

Keywords Histone deacetylase · Histone deacetylase inhibtors · Retinal degeneration · Retinitis pigmentosa · Zebrafish

Abbreviations

BDNF	Brain derived neurotrophic factor
CNTF	Ciliary neurotrophic factor
DPF	Days post fertilisation
HAT	Histone acetyltransferase
HDAC	Histone deacetylase
HDACi	Histone deacetylase inhibitor
HPF	Hours post fertilization
rd1	Retinal degeneration 1

B. N. Kennedy (✉) · C. Daly
School of Biomolecular and Biomedical Science, Conway Institute,
University College Dublin, Belfield, Dublin 4, Ireland
e-mail: brendan.kennedy@ucd.ie

C. Daly
e-mail: conor.daly@ucdconnect.ie

J. Yin
Department of Genetics, Yale University School of Medicine,
New Haven, CT 06520, USA
e-mail: jun.yin@yale.edu

C. Bowes Rickman et al. (eds.), *Retinal Degenerative Diseases,* Advances in Experimental Medicine and Biology 854, DOI 10.1007/978-3-319-17121-0_61

RP Retinitis pigmentosa
TSA Trichostatin A
VA Visual acuity
VF Visual field

61.1 Introduction

The 18 HDAC proteins are divided into two families, "classical" HDACs and SIR2 HDACs which are further subdivided into four classes based on homology to yeast HDAC orthologues and functional activity. In general, Class I members (HDAC1, 2, 3, 8) are localized to the nucleus while Class II members (HDAC4, 5, 6, 7, 9, 10) can be either localised in the nucleus or cytoplasm. Class III are a family of 7 NAD+ dependent proteins, known as sirtuins (SIRT1–7), similar to yeast Sir2 proteins. Class IV HDACs show structural similarity to both Class I and II HDACs (Yang and Seto 2008). These proteins can control gene transcription via epigenetic alteration of chromatin or modulate the activity of non-histone proteins by altering their acetylation (Choudhary et al. 2009). Consequently, HDACs regulate cell cycle progression, differentiation and survival.

61.2 HDACi as Potential Therapeutics for Treatment of Retinal Degeneration

A retrospective study of 7 RP patients reported improved visual field (VF) and visual acuity (VA) scores and delayed vision loss in five patients following treatment for 4 months with a mean dose of 643(+/− 133) mg/day valproic acid (VPA) (Clemson et al. 2011). Only mild side-effects, such as fatigue and stomach irritation were reported and liver function and blood chemistry remained normal. However, in a similar study of pigmentary dystrophy patients treated with 500–1000 mg/day VPA for 10 months; the five patients for which VF field tracings were available before and after treatment presented with a decline in VF, 22 patients had a decline in VA and 12 patients reported severe negative side effects inclding high alanine aminotransferase, aspartate aminotransferase and ammonia levels (Bhalla et al. 2013). The Clemson study has been criticised regarding study design, patient numbers (van Schooneveld 2011), and statistical analyses (Sandberg et al. 2011). Indeed, VPA may compromise photoreceptor function due to antagonistic effects on sodium and calcium channels in the retina (Sisk 2012). Despite these concerns, a randomized, placebo-controlled trial of oral VPA for treatment of autosomal dominant RP (NCT01233609), and a non-randomized trial (NCT01399515) are in progress.

61.3 HDAC Inhibition in a Pre-Clinical Rodent Model of Retinal Degeneration

In the *rd1* (retinal degeneration 1) mouse model of RP, histone acetylation is dramatically reduced in retinal cells. Retinal degeneration in *rd1* mice is mediated by phosphodiesterase-6 (PDE6) dysfunction resulting in high cyclic guanosine-monophosphate (cGMP) levels and increased oxidative stress (Sahaboglu et al. 2013). Increased expression of cell proliferation and oxidative stress genes is observed during *rd1* photoreceptor degeneration (Hackam et al. 2004) as is increased HDAC activity, with class I/II HDACs contributing the majority of total HDAC activity (Sancho-Pelluz et al. 2010). TUNEL positive cells in the degenerating *rd1* mouse eye also have reduced histone acetylation. Overall, reduced histone acetylation due to aberrant HDAC activity appears to be a major contributing factor to retinal degeneration in the *rd1* model. Notably, treatment of *rd1* retinal explants with Class I/II HDAC inhibitors, 1 μM Trichostatin A (TSA) or 6 μM Scriptaid, reduced photoreceptor cell death and restored photoreceptor outer segments (Sancho-Pelluz et al. 2010). These results suggest a major contribution of class I/II HDACs, to mutation-induced *rd1* photoreceptor cell death.

61.4 Mechanism of Action

A number of mechanisms by which HDACi produce their therapeutic effects have been suggested. HDACi diminish the activity of the Hsp90 chaperone, by increased acetylation (Scroggins et al. 2007; Kekatpure et al. 2009). Hsp90 inhibition increases expression of the neuroprotective chaperone Hsp70, which promotes neuronal survival (Wen et al. 2008). TNF-α is lowly expressed in wildtype retina but increased in models of ischemic injury (Genini et al. 2013). Pharmacological inhibition of Class I/II HDACs with 2.5 mg/kg TSA blocks increases in TNF-α levels in the rat eye post ischemic injury (Crosson et al. 2010). HDACi also modulate expression of brain derived neurotrophic factor (BDNF) via repression of its promoter. Selective pharmacological inhibition of class II HDACs with 5 μM MC1568 leads to rapid induction of BDNF expression while inhibition of class I HDACs with 5 μM MS-275 leads to a comparatively slower induction (Koppel and Timmusk 2013). In agreement, treatment of *rd1* retinal explants with BDNF and ciliary neurotrophic factor (CNTF) provides a neuroprotective effect (Azadi et al. 2007).

61.5 HDAC Expression in The Zebrafish Model

Zebrafish eye development is rapid. At 11 hpf the optic vesicle is visible (Kimmel et al. 1995). At 3 days post fertilisation (dpf) all cell types of the retina have differentiated and measurable cone mediated visual responses develop (Easter and

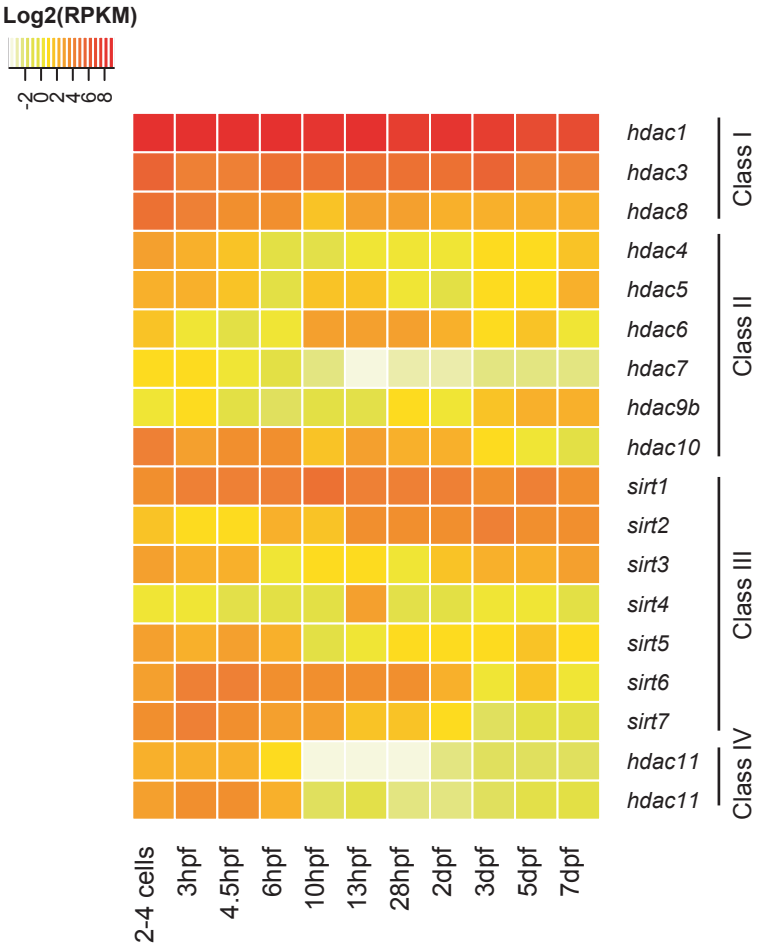

Fig. 61.1 Heatmap overview of gene expression profiles of HDACs using RNA-sEq. RNA-seq data sets on whole embryos were used. Genes expression levels were depicted using Log2 transformed Reads per kilobase per million (*RPKM*)

Nicola 1996). The zebrafish eye has a similar structure to other vertebrates, sharing the cell types and laminate structure present in humans. In early stages of development (2–16 hpf) *hdac1* is ubiquitously expressed. At later stages (36–48 hpf), expression is partially restricted to the branchial arches, fin bud mesenchyme and hindbrain. Pharmacological inhibition of HDACs by TSA results in a failure of craniofacial cartilage to develop from these tissues (Pillai et al. 2004). Similarly, in the hindbrain of *hdac1* mutants there is reduced cell proliferation marked by defects in axial extension of hindbrain branchiomotor neurons caused by reduced activation of non-canonical Wnt/PCP pathway regulators (Cunliffe 2004). In addition, inhibition of class I/II HDACs affects migration of the posterior lateral line primordium. Treatment disrupted neuromast deposition in a dose dependent

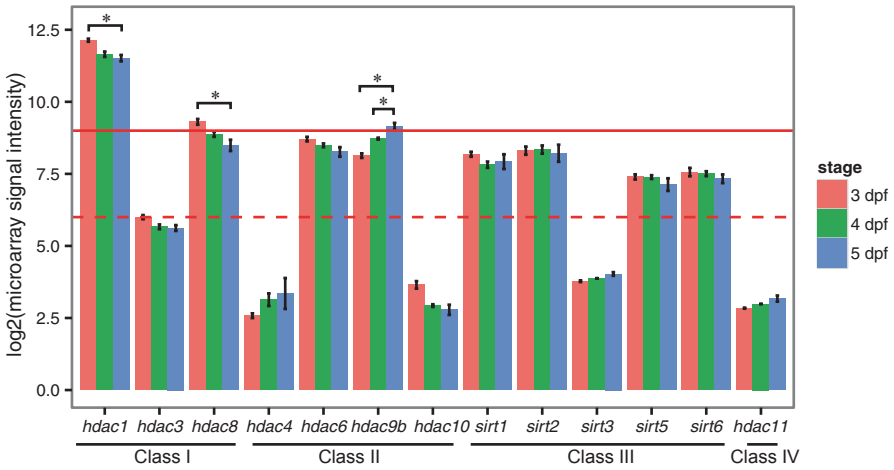

Fig. 61.2 Gene expression profiles of HDACs on microarray. Log2 transformed signal intensities of embryonic eyes on 3, 4 and 5 days post fertilization (*dpf*). The *solid red line* indicates high gene expression (log2 signal intensity of 9). The *dashed red line* indicates medium gene expression (log2 signal intensity of 6). **p*-value < 0.05

manner (He et al. 2014). Treatment with VPA also reduces proliferation of neural stem cells in the adult zebrafish optic tectum via inhibition of Notch signaling (Dozawa et al. 2014).These reports underline the importance of HDAC activity for cell proliferation and migration.

An analysis of publically available RNA-seq data (Fig. 61.1) depicts the expression of zebrafish HDACs during development in whole larvae (Aanes et al. 2011; Collins et al. 2012). *Hdac* genes show diverse expression patterns during development. *Hdac1* and *hdac3* (Class I) are highly expressed from 2–4 cells until 7 dpf, when visual function is matured. *Sirt7*, *hdac7* and *hdac11* (Class III, II and IV respectively) show higher expression at earlier stages, while *sirt2* and *hdac9b* (Class II) show increased gene expression after 6 hpf or at later developmental stages.

To begin to explore the importance of HDACs in the zebrafish eye, we profiled HDAC gene expression in eyes from 3, 4 and 5 dpf larvae (Yin et al. 2012). As shown in Fig. 61.2, *hdac1* and *hdac3* show similar decreasing expression from 3–5 dpf. In contrast expression of *hdac9b* significantly increased from 3–5 dpf. The differential expression of *hdac*s during the development of visual function indicates a temporal importance of HDAC expression during eye development. Other *hdac* genes did not exhibit any significant difference in gene expression from 3 to 5 dpf.

With the notable exception of *hdac1*, the role of most HDAC genes in the zebrafish eye is poorly understood. The absence of *hdac1* in the zebrafish retina results in increased cell proliferation, the optic stalk fails to terminally differentiate resulting in a reduced plexiform layer and number of retinal ganglion cells, photoreceptors are also absent (Stadler et al. 2005). *hdac1* is necessary for controlling

transcription of the key cell cycle regulators cyclin D1 and E2. *hdac1* appears to be required for the switch from proliferation to differentiation in the zebrafish retina mediated by the Wnt and Notch pathways (Yamaguchi et al. 2005).

61.6 Conclusion

Clinical and pre-clinical studies suggest that HDACi may be effective therapeutics in certain models of retinal degeneration. Zebrafish are an excellent model to gain further insight into the requirement of HDACs for eye development and function. Aditionally, zebrafish models of inherited blindness can be utilised to determine the efficacy and safety of HDACi in genetically diverse models of retinal degeneration and to understand the neuroprotective mechanisms of HDACi.

References

Aanes H, Winata CL, Lin CH et al (2011) Zebrafish mRNA sequencing deciphers novelties in transcriptome dynamics during maternal to zygotic transition. Genome Res 21:1328–1338

Azadi S, Johnson LE, Paquet-Durand F et al (2007) CNTF+ BDNF treatment and neuroprotective pathways in the rd1 mouse retina. Brain Res 1129:116–129

Bhalla S, Joshi D, Bhullar S et al (2013) Long-term follow-up for efficacy and safety of treatment of retinitis pigmentosa with valproic acid. Br J Ophthalmol 97:895–899

Choudhary C, Kuman C, Gnad F et al (2009) Lysine acetylation targets protein complexes and co-regulates major cellular functions. Science 325:834–840

Clemson CM, Tzekov R, Krebs M et al (2011) Therapeutic potential of valproic acid for retinitis pigmentosa. Br J Ophthalmol 95:89–93

Collins JE, White S, Searle SM et al (2012) Incorporating RNA-seq data into the zebrafish Ensembl genebuild. Genome Res 22:2067–2078

Crosson CE, Mani SK, Husain S et al (2010) Inhibition of histone deacetylase protects the retina from ischemic injury. Invest Ophthalmol Vis Sci 51:3639–3645

Cunliffe VT (2004) Histone deacetylase 1 is required to repress Notch target gene expression during zebrafish neurogenesis and to maintain the production of motoneurones in response to hedgehog signalling. Development 131:2983–2995

Dozawa M, Kono H, Sato Y et al (2014) Valproic acid, a histone deacetylase inhibitor, regulates cell proliferation in the adult zebrafish optic tectum. Dev Dyn 243(11):1401–1415

Easter SS, Nicola GN (1996) The development of vision in the zebrafish (Danio rerio). Dev Biol 180:646–663

Genini S, Beltran WA, Aguirre GD (2013) Up-regulation of tumor necrosis factor superfamily genes in early phases of photoreceptor degeneration. PLoS One 8:e85408

Hackam A, Strom R, Liu D et al (2004) Identification of gene expression changes associated with the progression of retinal degeneration in the rd1 mouse. Invest Opthalmol Vis Sci 45:2929–2942

He Y, Wu J, Mei H et al (2014) Histone deacetylase activity is required for embryonic posterior lateral line development. Cell Prolif 47:91–104

Kekatpure VD, Dannenberg AJ, Subbaramaiah K (2009) HDAC6 modulates Hsp90 chaperone activity and regulates activation of aryl hydrocarbon receptor signaling. J Biol Chem 284:7436–7445

Kimmel CB, Ballard WW, Kimmel SR et al (1995) Stages of embryonic development of the zebrafish. Dev Dyn 203:253–310

Koppel I, Timmusk T (2013) Differential regulation of Bdnf expression in cortical neurons by class-selective histone deacetylase inhibitors. Neuropharm 75:106–115

Pillai R, Coverdale LE, Dubey G et al (2004) Histone deacetylase 1 (HDAC-1) required for the normal formation of craniofacial cartilage and pectoral fins of the zebrafish. Dev Dyn 231:647–654

Sahaboglu A, Paquet-Durand O, Dietter J et al (2013) Retinitis pigmentosa: rapid neurodegeneration is governed by slow cell death mechanisms. Cell Death Dis 4:e488

Sancho-Pelluz J, Alavi MV, Sahaboglu A et al (2010) Excessive HDAC activation is critical for neurodegeneration in the rd1 mouse. Cell Death Dis 1:e24

Sandberg MA, Rosner B, Weigel-DiFranco C et al (2011) Lack of scientific rationale for use of valproic acid for retinitis pigmentosa. Br J Ophthalmol 95:744

Scroggins BT, Robzyk K, Wang D et al (2007) An acetylation site in the middle domain of Hsp90 regulates chaperone function. Mol Cell 25:151–159

Sisk RA (2012) Valproic acid treatment may be harmful in non-dominant forms of retinitis pigmentosa. Br J Ophthalmol 96:1154–1155

Stadler JA, Shkumatava A, Norton WH et al (2005) Histone deacetylase 1 is required for cell cycle exit and differentiation in the zebrafish retina. Dev Dyn 233:883–889

van Schooneveld, MJ et al (2011) The conclusions of Clemson et al concerning valproic acid are premature. Br J Ophthalmol 95(1):153-154

Wen XR, Li C, Zong Y et al (2008) Dual inhibitory roles of geldanamycin on the c-Jun NH2-terminal kinase 3 signal pathway through suppressing the expression of mixed-lineage kinase 3 and attenuating the activation of apoptosis signal-regulating kinase 1 via facilitating the activation of Akt in ischemic brain injury. Neuroscience 156:483–497

Yamaguchi M, Tonou-Fujimori N, Komori A et al (2005). Histone deacetylase 1 regulates retinal neurogenesis in zebrafish by suppressing Wnt and Notch signaling pathways. Development 132:3027–3043

Yang XJ, Seto E (2008) The Rpd3/Hda1 family of lysine deacetylases: from bacteria and yeast to mice and men. Nat Rev Mol Cell Biol 9:206–218

Yin J, Shine L, Raycroft F et al (2012) Inhibition of the pim1 oncogene results in diminished visual function. PLoS One 7:e52177

Chapter 62
Therapeutic Approach of Nanotechnology for Oxidative Stress Induced Ocular Neurodegenerative Diseases

Rajendra N. Mitra, Shannon M. Conley and Muna I. Naash

Abstract Oxidative stress plays a role in many different forms of neurodegenerative ocular disease. The imbalance between the generation of endogenous reactive oxygen species (ROS) and their corresponding neutralization by endogenous antioxidant defense systems leads to cellular oxidative stress, oxidation of different bio-macromolecules, and eventually retinal disease. As a result, the administration of supplemental endogenous antioxidant materials or exogenous ROS scavengers is an interesting therapeutic approach for the treatment of forms of ocular disease associated with oxidative stress. Thus far, different dietary antioxidant supplements have been proven to be clinically reliable and effective, and different antioxidant gene therapy approaches are under investigation. In addition, various metal oxide nanoparticles were shown to be effective in defending against oxidative stress-associated injury. These benefits are due to free radical scavenging properties of the materials arising from non-stoichiometric crystal defects and oxygen deficiencies. Here we discuss the application of this approach to the protection of the retina.

Keywords Nanoparticle · Antioxidant · Oxidative stress · ROS · Rescue · Light damage · Retinitis pigmentosa · Glaucoma · Diabetic retinopathy · Age-related macular degeneration · Enzymes · Vitamins · Mice · Rat

M. I. Naash (✉) · R. N. Mitra · S. M. Conley
Department of Cell Biology, University of Oklahoma Health Sciences Center,
940 Stanton L. Young Blvd., BMSB 781, Oklahoma City, OK 73104, USA
e-mail: muna-naash@ouhsc.edu

R. N. Mitra
e-mail: rajendra-mitra@ouhsc.edu

S. M. Conley
e-mail: shannon-Conley@ouhsc.edu

C. Bowes Rickman et al. (eds.), *Retinal Degenerative Diseases,* Advances in Experimental Medicine and Biology 854, DOI 10.1007/978-3-319-17121-0_62

62.1 Introduction

Accumulation of ROS including oxygen free radicals, hydrogen peroxide, superoxide, and hydroxyl free radicals can be induced by physiological overproduction and/or poor endogenous antioxidant defense systems. Importantly, oxidative stress plays a crucial role in the progression of widely varying diseases ranging from cancer and diabetes to different neurodegenerative conditions (Uttara et al. 2009). Retinal photoreceptor cells are susceptible to oxidative stress since they have a large number of mitochondria, high exposure to intense light, and a high rate of metabolism. Imbalance between the production and neutralization of ROS leads to oxidation to DNA, RNA, lipids and protein molecules and eventually to dysfunction and degeneration of retinal tissues (Kowluru and Chan 2007; Cabrera and Chihuailaf 2011). Oxidative stress worsens with age and becomes a key contributor to age related cellular degeneration by increasing the amount of dysfunctional cellular entities. Hence, neutralizing ROS has been proposed as a logical therapeutic approach in dealing with oxidative stress associated retinal disorders.

62.2 Oxidative Stress in Ocular Diseases

Several ocular diseases have been linked to oxidative stress and accumulation of ROS, including retinitis pigmentosa, macular dystrophy, diabetic retinopathy, glaucoma, retinopathy of prematurity, cataract etc. (Chen et al. 2006; Kowluru and Chan 2007; Martinez-Fernandez de la Camara et al. 2013). For example, it was long thought that oxidative stress played a role in the pathology of age-related macular degeneration (AMD), a leading cause of blindness in the United States associated with progressive loss of central vision. This hypothesis was confirmed when mass spectroscopy revealed multiple oxidized proteins in analyses of druse that were collected from human AMD patients (Crabb et al. 2002). The pathobiology of diabetic retinopathy also involves oxidative stress (Kowluru and Kanwar 2009). For example, it has been shown that levels of superoxide and hydrogen peroxide are increased in the retinas of diabetic rats (Kowluru and Chan 2007). In addition, complications in diabetic retinopathy can arise when oxidative stress causes disruption in the tight-junction complex, vascular permeability, the blood–retinal barrier (BRB) and mitochondrial DNA (mtDNA) (Frey and Antonetti 2011).

Oxidative stress has also been associated with other ocular disorders. Ascorbic acid and glutathione (GSH) are two important antioxidant components of aqueous humor that protect from photo-oxidation. It was observed that ascorbic acid levels were reduced in animals with cataracts suggesting that oxidative stress may play a role in the development of cataracts in elderly patients (Cabrera and Chihuailaf 2011). Oxidative stress is also thought to be involved in glaucoma. For example, it has been shown that oxidative stress in retinal ganglion cells may be an early response to increased intraocular pressure, a key risk factor for glaucoma (Liu et al.

2007), and other studies have suggested that glaucoma patients may have reduced levels of some antioxidants (Lopez-Riquelme et al. 2014).

62.3 Approaches for Antioxidant Therapy

Oxidative stress is generated by radical and non-radical medicated mechanisms. Both of these components can induce chemical modifications to different biological molecules like lipids, protein, DNA or RNA. Ocular tissues are under the protection of endogenous enzymatic and non-enzymatic antioxidants. Superoxide dismutase (SOD), catalase (CAT), and glutathione peroxidase (GPx) are key enzymatic antioxidant systems, while vitamin A, vitamin C, vitamin E, and GSH are the most important non-enzymatic antioxidant systems that protect the eye from oxidative stress (Cabrera and Chihuailaf 2011). Therefore radical scavenging by supplemental enzymatic or non-enzymatic antioxidants is a logical approach to defend against oxidative stress induced degeneration of retinal cells and thus prevent or delay the development of ocular diseases.

Delivery of different exogenous antioxidants can be beneficial for a variety of retinal diseases. Alpha-lipoic acid is a well-known biological antioxidant which showed reduced oxidative stress and improved survival of retinal ganglion cells in the DBA/2J mouse model of glaucomatous optic neuropathy (Inman et al. 2013). Similarly, lithospermic acid B (LAB), an isolated antioxidant compound from *Salvia miltiorrhiza radix* (a traditional Chinese herbal medicine), provided partial protection from the development of diabetic retinopathy in a rat model of type 2 diabetes (Jin et al. 2014).

Several models which share phenotypes with AMD also benefit from a variety of exogenous antioxidants. The antioxidant rich dietary components grapes or marigold extract (which contain macular pigments lutein/zeaxanthin) prevented loss of retinal function in a mouse model with age related retinal pigment epithelium damage (Yu et al. 2012). Curcumin, an important antioxidant component of turmeric, protected retinal neurons in a rat model of light-induced retinal degeneration (LIRD) which exhibits a significant amount of oxidative stress and has been characterized as an AMD model (Mandal et al. 2009). It was observed that N-acetyl cysteine (NAC), a thiol antioxidant, was able to protect bovine retinal RPE cells from hypoxia induced degeneration (Castillo et al. 2002) and has thus been suggested to slow the development of AMD. Lutein, an antioxidant located in the lens and macula that can scavenge free radicals and filter toxic blue light, showed neuroprotection of retinal cells against retinal oxidative injury (Koushan et al. 2013).

Several groups have also tried to combat oxidative stress by modulating endogenous antioxidant pathways. For example, the delivery of antioxidant enzymes like SOD and catalase via adenoviral vectors was able to decrease oxidative injury and delay retinal degeneration in some mouse models characterized by ROS elevation (Rex et al. 2004; Qi et al. 2007). Similarly, low dose irradiation was observed to protect photoreceptor cells by up regulating the endogenous antioxidant gene per-

oxiredoxin-2 (Prdx2) which has been shown to play a role in RP and other oxidative stress related neurodegenerative diseases (Otani et al. 2012).

62.4 Alternative Therapeutic Approach: Use of Nanotechnology

The availability of wide ranging forms of nanotechnology have significantly enhanced the development of advanced ocular therapeutics. Nanoparticles come in two main categories, those that are intended as packaging/delivery vehicles for other drugs or genes, and those which have intrinsic therapeutic properties. Often, nanoparticles are easy to synthesize and manipulate at the atomic level, and their small size facilitates direct interaction at the cellular level. Over the past few years, the antioxidant nanoparticle field has emerged as an exciting and promising research area and has progressed quickly. Searching PubMed for "antioxidant nanoparticle" from 2003 to 2013 highlights the rapid growth of interest and development in this new field of nanotherapy, particularly in comparison to hits for "antioxidant and retina" which have held constant over that same time period (Fig. 62.1).

Several different types of nanoparticles fall into the group of particles that have intrinsic beneficial properties. For example, gold nanoparticles were well-tolerated and able to protect pancreatic cells against hyperglycemia induced degeneration in diabetic mice (Barathmanikanth et al. 2010). However, lanthanide- and lanthanide-like nanoparticles have been more thoroughly explored. They often have high redox scavenging capability due to non-stoichiometric crystal defects (Schubert et al. 2006) and they have shown little or no toxicity after delivery to the eye (Mitra et al. 2014). Nanoceria (nanoparticulate cerium oxide), a well-known redox active lanthanide nanoparticle (Karakoti et al. 2010), was able to prevent the peroxide induced accumulation of ROS in primary cultures of retinal cells (Chen et al. 2006). Consistent with this benefit, intravitreal injection of these nanoparticles in a light-

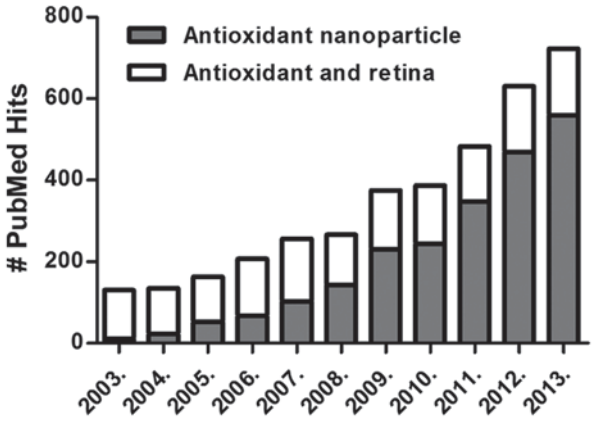

Fig. 62.1 Graph of antioxidant nanoparticle research from 2003 to 2013. (Data were obtained from PubMed searches)

induced rat model of retinal degeneration showed a rescue of photoreceptor cells (Chen et al. 2006; Karakoti et al. 2010). More recent work has shown that nanoceria can also be effective in inherited models of retinal degeneration (Kong et al. 2011). Nanoceria have both direct scavenging activity enabling neutralization of ROS, and also showed the ability to up-regulate cell-survival genes (Kong et al. 2011). Nanoceria also decreased retinal angiomatous proliferation by scavenging radicals and down regulating vascular endothelial growth factor (VEGF) in very low density lipoprotein receptor (Vldlr) knockout mice, a model which mimics some AMD phenotypes (Zhou et al. 2011). Nanoceria and nanoyttria (another rare earth substance, nanoparticulate yttrium oxide) also showed free radical scavenging activity and protection of neuronal cell line (HT22) from exogenous oxidants (Schubert et al. 2006). Our group recently demonstrated that nanoyttria could also prevent photoreceptor degeneration and loss of retinal function in a murine light damage model (Mitra et al. 2014). Interestingly, we observed therapeutic benefits when the nanoparticles were delivered either before or after light damage suggesting they may be useful in practical applications (i.e. where treatment before insult is not possible) (Mitra et al. 2014). These encouraging results suggest that safe lanthanide oxide nanoparticles may be an excellent option for ocular antioxidant therapy.

On the gene therapy side, human serum albumin nanoparticles were used to encapsulate and deliver a plasmid containing the Cu/Zn superoxide dismutase (SOD1) gene both in the ARPE-19 cell line and in the retina of mice (Mo et al. 2007). Though these were not tested for therapeutic efficacy, they may be beneficial in future. In addition, poly (lactic co-glycolic acid) nanoparticles were used to encapsulate catalase, an endogenous antioxidant enzyme. Importantly, the authors showed that encapsulation in the nanoparticles did not adversely affect the catalase activity, and were able to protect cultured neurons from hydrogen peroxide-induced oxidative damage (Singhal et al. 2013).

62.5 Conclusion

Here we have demonstrated the promising potential of antioxidant nanotechnology for the prevention and retardation of degenerative ocular diseases associated with oxidative stress. Lanthanide and lanthanide-like nanoparticle antioxidant systems have shown efficient protection of retinal cells against oxidative damages in light stress animal models. Future testing may include assessment in other chronic degenerative models. In addition, the promising protective effect of this nanoparticle approach can also be extended to other neurodegenerative diseases such as Parkinson disease, Alzheimer disease, Huntington disease, and amyotrophic lateral sclerosis in which oxidative stress has also been implicated.

Acknowledgements This work was supported by the Foundation Fighting Blindness, the National Eye Institute (EY022778, EY018656), the Oklahoma Center for the Advancement of Science and Technology, and Fight for Sight (RNM).

References

Barathmanikanth S, Kalishwaralal K, Sriram M et al (2010) Anti-oxidant effect of gold nanoparticles restrains hyperglycemic conditions in diabetic mice. J Nanobiotechnology 8:16

Cabrera MP, Chihuailaf RH (2011) Antioxidants and the integrity of ocular tissues. Vet Med Int 2011:905153

Castillo M, Bellot JL, Garcia-Cabanes C et al (2002) Effects of hypoxia on retinal pigmented epithelium cells: protection by antioxidants. Ophthalmic Res 34:338–342

Chen J, Patil S, Seal S et al (2006) Rare earth nanoparticles prevent retinal degeneration induced by intracellular peroxides. Nat Nanotechnol 1:142–150

Crabb JW, Miyagi M, Gu XR et al (2002) Drusen proteome analysis: an approach to the etiology of age-related macular degeneration. Proc Natl Acad Sci U S A 99:14682–14687

Frey T, Antonetti DA (2011) Alterations to the blood-retinal barrier in diabetes: cytokines and reactive oxygen species. Antioxid Redox Signal 15:1271–1284

Inman DM, Lambert WS, Calkins DJ et al (2013) Alpha-lipoic acid antioxidant treatment limits glaucoma-related retinal ganglion cell death and dysfunction. PLoS ONE 8:e65389

Jin CJ, Yu SH, Wang XM et al (2014) The effect of lithospermic acid, an antioxidant, on development of diabetic retinopathy in spontaneously obese diabetic rats. PLoS ONE 9:e98232

Karakoti A, Singh S, Dowding JM et al (2010) Redox-active radical scavenging nanomaterials. Chem Soc Rev 39:4422–4432

Kong L, Cai X, Zhou X et al (2011) Nanoceria extend photoreceptor cell lifespan in tubby mice by modulation of apoptosis/survival signaling pathways. Neurobiol Dis 42:514–523

Koushan K, Rusovici R, Li W et al (2013) The role of lutein in eye-related disease. Nutrients 5:1823–1839

Kowluru RA, Chan PS (2007) Oxidative stress and diabetic retinopathy. Exp Diabetes Res 2007:43603

Kowluru RA, Kanwar M (2009) Oxidative stress and the development of diabetic retinopathy: contributory role of matrix metalloproteinase-2. Free Radic Biol Med 46:1677–1685

Liu Q, Ju WK, Crowston JG et al (2007) Oxidative stress is an early event in hydrostatic pressure-induced retinal ganglion cell damage. Invest Ophthalmol Vis Sci 48:4580–4589

Lopez-Riquelme N, Villalba C, Tormo C et al (2014) Endothelin-1 levels and biomarkers of oxidative stress in glaucoma patients. Int Ophthalmol (ePub ahead of print)

Mandal MN, Patlolla JM, Zheng L et al (2009) Curcumin protects retinal cells from light-and oxidant stress-induced cell death. Free Radic Biol Med 46:672–679

Martinez-Fernandez de la Camara C, Salom D, Sequedo MD et al (2013) Altered antioxidant-oxidant status in the aqueous humor and peripheral blood of patients with retinitis pigmentosa. PLoS ONE 8:e74223

Mitra RN, Merwin MJ, Han Z et al (2014) Yttrium oxide nanoparticles prevent photoreceptor death in a light-damage model of retinal degeneration. Free Radic Biol Med 75C:140–148

Mo Y, Barnett ME, Takemoto D et al (2007) Human serum albumin nanoparticles for efficient delivery of Cu, Zn superoxide dismutase gene. Mol Vis 13:746–757

Otani A, Kojima H, Guo CR et al (2012) Low-dose-rate, low-dose irradiation delays neurodegeneration in a model of retinitis pigmentosa. Am J Pathol 180:328–336

Qi XP, Sun L, Lewin AS et al (2007) Long-term suppression of neurodegeneration in chronic experimental optic neuritis: antioxidant gene therapy. Invest Ophthalmol Vis Sci 48:5360–5370

Rex TS, Tsui I, Hahn P et al (2004) Adenovirus-mediated delivery of catalase to retinal pigment epithelial cells protects neighboring photoreceptors from photo-oxidative stress. Hum Gene Ther 15:960–967

Schubert D, Dargusch R, Raitano J et al (2006) Cerium and yttrium oxide nanoparticles are neuroprotective. Biochem Biophys Res Commun 342:86–91

Singhal A, Morris VB, Labhasetwar V et al (2013) Nanoparticle-mediated catalase delivery protects human neurons from oxidative stress. Cell Death Dis 4:e903

Uttara B, Singh AV, Zamboni P et al (2009) Oxidative stress and neurodegenerative diseases: a review of upstream and downstream antioxidant therapeutic options. Curr Neuropharmacol 7:65–74

Yu CC, Nandrot EF, Dun Y et al (2012) Dietary antioxidants prevent age-related retinal pigment epithelium actin damage and blindness in mice lacking alphavbeta5 integrin. Free Radic Biol Med 52:660–670

Zhou X, Wong LL, Karakoti AS et al (2011) Nanoceria inhibit the development and promote the regression of pathologic retinal neovascularization in the Vldlr knockout mouse. PLoS ONE 6:e16733

Chapter 63
Transscleral Controlled Delivery of Geranylgeranylaceton Using a Polymeric Device Protects Rat Retina Against Light Injury

Nobuhiro Nagai, Hirokazu Kaji, Matsuhiko Nishizawa, Toru Nakazawa and Toshiaki Abe

Abstract We evaluated the effects of a transscleral drug delivery device, consisting of a reservoir and controlled-release cover, which were made of photopolymerized polyethylene glycol dimethacrylate and triethylene glycol dimethacrylate, combined at different ratios. Geranylgeranylacetone (GGA), a heat-shock protein (HSP) inducer, was loaded into the device. The GGA was released from the device under zero-order kinetics. At both 1 week and 4 weeks after device implantation on rat sclera, HSP70 gene and protein expression were up-regulated in the sclera-choroid-retinal pigment epithelium fraction of rat eyes treated with the GGA-loaded device compared with rat eyes treated with saline-loaded devices or eyes of non-treated rats. Flash electroretinograms were recorded 4 days after white light exposure (8000 lx for 18 h). Electroretinographic amplitudes of the a- and b-waves were preserved significantly in rats treated with GGA-loaded devices compared with rats treated with saline-loaded devices. Histological examination showed that the outer nuclear layer thickness was preserved in rats that had the GGA-loaded device.

T. Abe (✉) · N. Nagai
Division of Clinical Cell Therapy, Center for Advanced Medical Research and Development (ART), Tohoku University Graduate School of Medicine, 2-1 Seiryo-machi, Aoba-ku, Sendai 980-8575, Japan
e-mail: toshi@oph.med.tohoku.ac.jp

N. Nagai
e-mail: nagai@med.tohoku.ac.jp

H. Kaji · M. Nishizawa
Department of Bioengineering and Robotics, Tohoku University Graduate School of Engineering, 6-6-01 Aramaki-Aoba, Aoba-ku, Sendai 980-8579, Japan
e-mail: kaji@biomems.mech.tohoku.ac.jp

M. Nishizawa
e-mail: nishizawa@biomems.mech.tohoku.ac.jp

T. Nakazawa
Department of Ophthalmology, Tohoku University Graduate School of Medicine, 1-1 Seiryo-machi, Aoba-ku, Sendai 980-8574, Japan
e-mail: ntoru@oph.med.tohoku.ac.jp

C. Bowes Rickman et al. (eds.), *Retinal Degenerative Diseases,* Advances in Experimental Medicine and Biology 854, DOI 10.1007/978-3-319-17121-0_63

These results may show that transscleral GGA delivery using our device may offer an alternative method to treat retinal diseases.

Keywords Drug delivery · Geranylgeranylacetone · Heat shock protein (HSP) · Poly(ethyleneglycol) dimethacrylate (PEG) · Tri(ethyleneglycol) dimethacrylate (TEG) · Phototoxicity · Transsclera

63.1 Introduction

Recent studies have shown that administration of geranylgeranylacetone (GGA), an acyclic polyisoprenoid, up-regulates heat-shock protein (HSP) expression and exerts protective effects on a variety of organs, such as the eye (Suemasu et al. 2009; Tanito et al. 2005; Kayama et al. 2011), the brain (Yasuda et al. 2005), neurons (Katsuno et al. 2005), and the heart (Ooie et al. 2001). In the retina, GGA induced both HSP72 and thioredoxin (Trx) predominantly in the retinal pigment epithelium layer (RPE) and protected photoreceptors from light damage (Tanito et al. 2005). We found that administration of GGA decreased photoreceptor apoptosis after retinal detachment, through prolonged activation of the Akt pathway (Kayama et al. 2011).

Drug delivery to intraocular tissue by topical application may be limited by the significant barrier of corneal epithelium and the process of tear drainage. Systemic drug administration is not a viable alternative, due to the blood-retina barrier that limits the drug access to the posterior tissues of the eye with possible side effects (Choonara et al. 2010). Although intravitreal injections and implants deliver drugs effectively to the retina, this approach is invasive and may cause severe adverse effects such as endophthalmitis and retinal detachment. The periocular or transscleral routes are less invasive than intravitreal administration and provide higher retinal and vitreal drug bioavailability (0.01–0.1 %) compared to eye drops ($\leq$0.001 %). Due to a high degree of hydration and a low cell population, soluble substrates pass easily through the sclera (Kim et al. 2007). Thus, the transscleral route is a promising method for intraocular drug delivery that is more effective and less invasive.

We recently developed a polymeric delivery system that consists of a drug reservoir sealed with a controlled-release cover (Kawashima et al. 2011). This episcleral implantable device offers localized drug delivery via a less invasive method compared to intravitreous drug administration. In this study, we made a GGA-releasing device with photopolymerized polyethylene glycol dimethacrylate (PEGDM) and triethylene glycol dimethacrylate (TEGDM) and evaluated the drug effects in a rat model of phototoxicity.

63.2 Materials and Methods

63.2.1 Device Fabrication, GGA Loading, and Release

The GGA-releasing device was made from PEGDM and TEGDM, as reported previously (Kawashima et al. 2011). GGA was obtained from Eisai Co., Ltd. (Tokyo, Japan) and was suspended in P60 prepolymer (60% PEGDM + 40% TEGDM) at a concentration of 250 mg/mL. The GGA mixture (1.2 μL) was poured into the reservoir and photopolymerized for 90 s. A reservoir cover was prepared by applying a prepolymer mixture of the required concentrations of PEGDM and TEGDM of P0 (0% PEGDM + 100% TEGDM), P40 (40% PEGDM + 60% TEGDM), or P80 (80% PEGDM + 20% TEGDM) to the reservoir, followed by ultraviolet light (UV) curing for 3 min. A device with no cover (pellet) was prepared as the control. The devices were incubated in 1 mL of phosphate-buffered saline (PBS) at 37 °C, and GGA amounts were then measured by high-performance liquid chromatography. The results are reported as the mean ± standard deviation (SD) of six evaluated samples of each device (GGA, saline, or pellets alone).

63.2.2 Animals, Device Implantation, and Light Exposure

Male Sprague-Dawley rats (Japan SLC; Hamamatsu, Japan) were used in this study. All animals were handled in accordance with the ARVO Statement for the Use of Animals in Ophthalmic and Vision Research, after receiving approval from the Institutional Animal Care and Use Committee of the Tohoku University Environmental & Safety Committee (No. 22MdA-457). The rats were anesthetized and the devices were placed onto the left eyes at the sclerae, then the conjunctiva was sutured in place. The right eye of each animal served as the control. The pupils were dilated and exposed to 8000 lx of white fluorescent light (Toshiba Corp.; Tokyo, Japan) for 18 h, kept in the dark for 4 days, and then electroretinograms (ERGs) were recorded.

63.2.3 RNA Extraction and RT-PCR

To explore the GGA effects on the retina, HSP70 and Trx1 expression in the retina and RPE/choroid were examined by real-time polymerase chain reaction (RT-PCR). The entire retina and RPE-choroid-sclera tissues ($n = 6$ eyes/group) were homogenized, followed cDNA generation, and RT-PCR was performed. The sequences of the PCR primer pairs were: HSP70, 5′- CCA AGA ATG CGC TCG AGT CCT ATG—3′ (forward) and 5′- CCT CTT TCT CAG CCA GCG TGT TAG A—3′ (reverse); Trx1, 5′- ATG GTG AAG CTG ATC GAG AGC—3′ (forward) and 5′- TTA GGC AAA CTC CGT AAT AGT GG—3′ (reverse); GAPDH, 5′- AAG GTG AAG

GTC GGA GTC AA—3′ (forward) and 5′- TTG AGG TCA ATG AAG GGG TC—3′ (reverse).

63.2.4 Western Blotting

The retinas were lysed, electrophoresed, and transferred to polyvinylidene fluoride membranes (Nagai et al. 2014). A primary antibody against HSP70 (1:1000; Cell Signaling Technology; Danvers, MA, USA) and GAPDH (1:1000; Cell Signaling) were used.

63.2.5 ERG

At 1 and 4 weeks after light exposure, flash ERGs were recorded (Mayo Corp.; Aichi, Japan) according to the methods we reported previously (Nagai et al. 2014).

63.2.6 Histological Analysis

At 1 and 4 weeks after light exposure, the eyes were enucleated and kept immersed for 24 h at 4 °C in a fixative solution containing 4% paraformaldehyde, and stained with hematoxylin and eosin.

63.2.7 Statistical Analysis

Experimental data are presented as means ± SD. Statistical significance was calculated with Ekuseru-Toukei 2012 (Social Survey Research Information Co., Ltd.; Tokyo, Japan), using unpaired t-tests. Differences were considered significant if $P < 0.05$.

63.3 Results

63.3.1 ControlledRrelease of GGA, RT-PCR, Western Blotting

The GGA was loaded in the polymeric device with capsule dimensions of 2.5 mm (length) × 2 mm (width) × 1 mm (height). The GGA was released according to the PEGDM/TEGDM ratio. Namely, increasing the PEGDM ratio increased the release

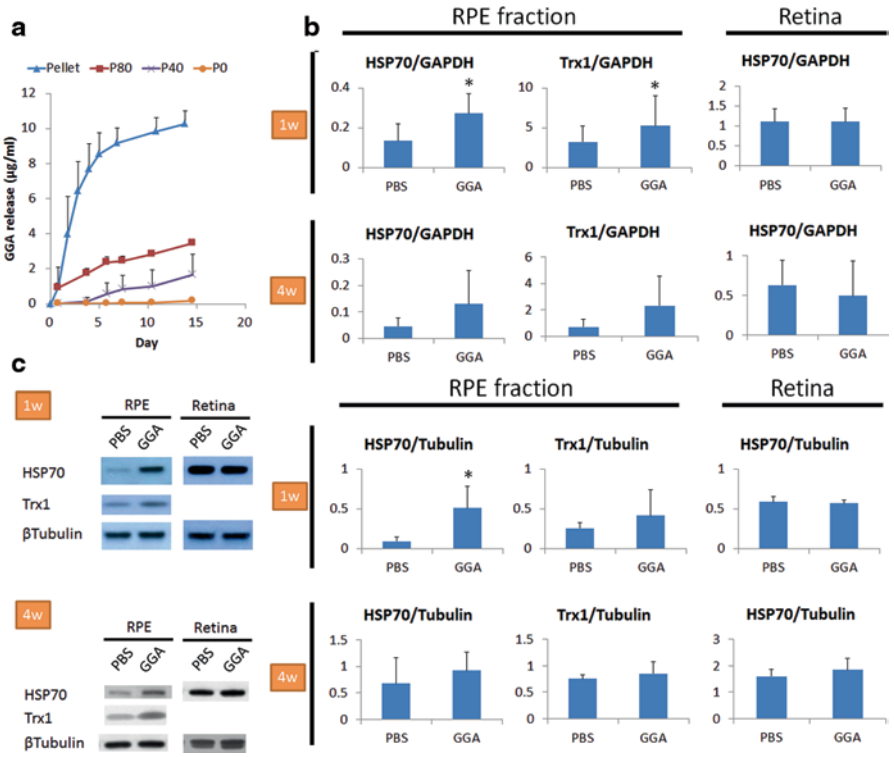

Fig. 63.1 **a** GGA was released depending on the ratio of PEGDM/TEGDM. P0, 40, and 80 show the PEGDM ratio against TEGDM. Pellet shows no reservoir. HSP70 and Trx1 expression were examined in the sclera/choroid/RPE (*RPE fraction*) and retina at 1 or 4 weeks after device implantation using RT-PCR (**b**) or western blotting (**c**). Statistically significant HSP70 gene expression was observed in the GGA-loaded device-treated RPE fraction at 1 week after implantation

of GGA. If we applied no PEGDM (P0), no GGA was released; conversely, a burst was observed if we used no capsule and cover (pellets alone) (Fig. 63.1a). Gene expression analysis showed significant upregulation of HSP70 and Trx1 in the sclera/choroid/RPE of rats treated with the GGA-loaded device (at 1 week post-implantation) compared with those rats treated with PBS-loaded device (Fig. 63.1b). In the neural retina, HSP70 and Trx1 were slightly up-regulated at 4 weeks post-implantation. Western blotting also showed induction of HSP70 and Trx1 in sclera/choroid/RPE fraction (Fig. 63.1c). HSP70 and Trx1 expression were not affected in the retina.

63.3.2 ERG and Histology

The ERG b-wave amplitudes in rats receiving the GGA-loaded devices were significantly preserved at 1 week (Fig. 63.2a) and 4 weeks (Fig. 63.2b) after device

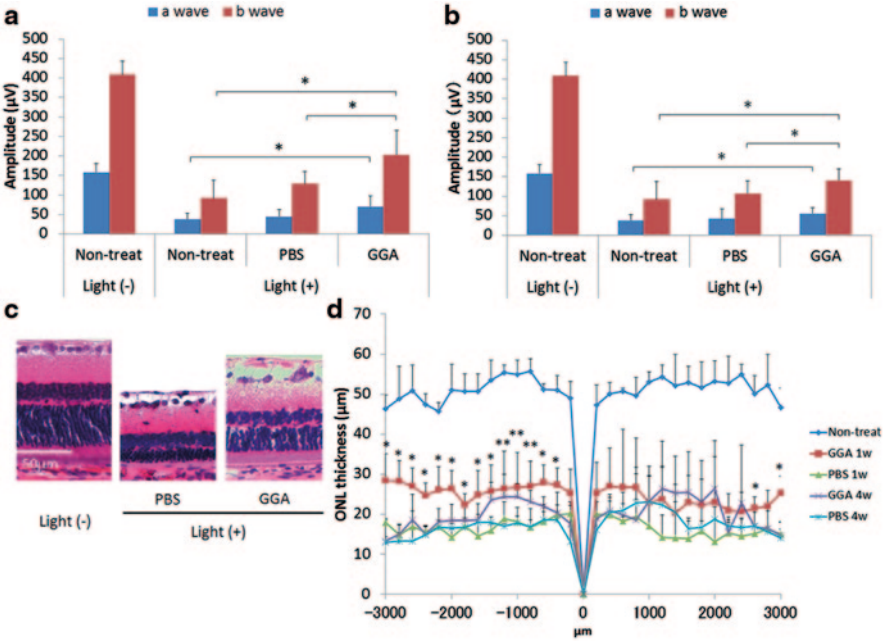

Fig. 63.2 The ERG b-wave amplitudes were significantly preserved in rats at 1 week (**a**) and 4 weeks (**b**) after GGA-loaded device implantation when compared to those receiving the PBS-loaded devices or the non-treated controls. **c** shows representative results of histological examination. **d** represents the results of each thickness of outer nuclear layer (*ONL*). Statistically significant preservation of the *ONL* thickness was observed in the GGA-loaded device treated rats when compared to those of PBS-loaded device group. * and ** show significant difference at 1 week and 4 weeks, respectively

implantation when compared to those rats receiving the PBS-loaded device or the non-treated control rats. Histological evaluations showed that the outer nuclear layer (ONL) thickness was remarkably thinned in the PBS-loaded device group or the non-treated group; the group receiving the GGA-loaded device significantly suppressed light damage when compared with the PBS-loaded device group at both 1 and 4 weeks (Fig. 63.2c, d).

63.4 Discussion

The design of drug-delivery systems targeting the retina is a challenging ophthalmological task. Transscleral delivery has emerged as a more attractive method for treating retinal disorders, because it can deliver a drug locally and is less invasive compared with intravitreal injections. In the present study, we demonstrated retinal neuroprotection using a polymeric device that can release GGA transsclerally.

The challenges of transscleral delivery are the reduction of drug elimination by conjunctival lymphatic/blood clearance and a device design that can release drugs in a zero-order controlled-release manner while being implantable onto the sclera. Lee et al. (2010) reported that conjunctival blood and lymphatic vessel elimination considerably limit transscleral drug delivery to the retina. Ranta et al. (2010) noted that local clearance by blood flow and lymphatics removes most of a drug dose. The loss from the sub-conjunctival depot to the blood and lymphatic vessels is 83 to 95 % (Ranta et al. 2010). Our device released drug mainly to the sclera-facing side, but not to the conjunctiva. Although the devices were loosely covered with connective tissue by the end of our experiments, the amount released after implantation was almost the same as before implantation (data not shown). This may indicate that the release performance would be maintained after transplantation.

In conclusion, transscleral GGA delivery using our device protected rats against light-induced retinal damage. This device may offer a less-invasive drug delivery method to treat retinal diseases.

Acknowledgements This study was supported by a Health Labour Sciences Research Grant from the Ministry of Health Labour and Welfare (H23-kankaku-ippan-004, H24-nanchitoh-ippan-067). The GGA was provided by Eisai Co., Ltd. (Tokyo, Japan).

References

Choonara YE, Pillay V, Danckwerts MP et al (2010) A review of implantable intravitreal drug delivery technologies for the treatment of posterior segment eye diseases. J Pharm Sci 99:2219–2239

Katsuno M, Sang C, Adachi H et al (2005) Pharmacological induction of heat-shock proteins alleviates polyglutamine-mediated motor neuron disease. Proc Natl Acad Sci U S A 102:16801–16806

Kayama M, Nakazawa T, Thanos A et al (2011) Heat shock protein 70 (HSP70) is critical for the photoreceptor stress response after retinal detachment via modulating anti-apoptotic Akt kinase. Am J Pathol 178:1080–1091

Kawashima T, Nagai N, Kaji H et al (2011) A scalable controlled-release device for transscleral drug delivery to the retina. Biomaterials 32:1950–1956

Kim SH, Lutz RJ, Wang NS et al (2007) Transport barriers in transscleral drug delivery for retinal diseases. Ophthalmic Res 39:244–254

Lee SJ, He W, Robinson SB et al (2010) Evaluation of clearance mechanisms with transscleral drug delivery. Invest Ophthalmol Vis Sci 51:5205–5212

Nagai N, Kaji H, Onami H et al (2014) A platform for controlled dual-drug delivery to the retina: protective effects against light-induced retinal damage in rats. Adv Health Mater 3:1555–1560

Ooie T, Takahashi N, Saikawa T et al (2001) Single oral dose of geranylgeranylacetone induces heat-shock protein 72 and renders protection against ischemia/reperfusion injury in rat heart. Circulation 104:1837–1843

Ranta VP, Mannermaa E, Lummepuro K et al (2010) Barrier analysis of periocular drug delivery to the posterior segment. J Control Release 148:42–48

Suemasu S, Tanaka K, Namba T et al (2009) A role for HSP70 in protecting against indomethacin-induced gastric lesions. J Biol Chem 284:19705–19715

Tanito M, Kwon YW, Kondo N et al (2005) Cytoprotective effects of geranylgeranylacetone against retinal photooxidative damage. J Neurosci 25:2396–2404

Yasuda H, Shichinohe H, Kuroda S et al (2005) Neuroprotective effect of a heat shock protein inducer, geranylgeranylacetone in permanent focal cerebral ischemia. Brain Res 1032:176–182

Chapter 64
Targeting the Proteostasis Network in Rhodopsin Retinitis Pigmentosa

David A. Parfitt and Michael E. Cheetham

Abstract Mutations in rhodopsin are one of the most common causes of retinitis pigmentosa (RP). Misfolding of rhodopsin can result in disruptions in cellular protein homeostasis, or proteostasis. There is currently no available treatment for RP. In this review, we discuss the different approaches currently being investigated for treatment of rhodopsin RP, focusing on the potential of manipulation of the proteostasis network as a therapeutic approach to combat retinal degeneration.

Keywords Retinal degeneration · Retinitis pigmentosa · Rhodopsin · P23H · Proteostasis · Molecular chaperones · Heat shock proteins · ERAD

64.1 Introduction

Retinitis pigmentosa is a group of inherited disorders that cause retinal degeneration via progressive loss of the rod and cone photoreceptors (Hartong et al. 2006). The first RP gene identified was rhodopsin (Dryja et al. 1990). Rhodopsin is the prototypical G-protein coupled receptor (GPCR), responsible for detecting light in the rod photoreceptors, comprised of the protein rod opsin with its chromophore 11-*cis*-retinal. Rod opsin is produced in the endoplasmic reticulum (ER), where it undergoes multiple post-translational modifications, such as glycosylation and disulfide bond formation (Kosmaoglou et al. 2008). Correctly folded rhodopsin is then transported and packed into the disks in the outer segment (OS) of the photoreceptor (Pearring et al. 2013). Over 200 point mutations in rhodopsin have been identified so far (RetNet https://sph.uth.edu/retnet/), which can be classified according to their biochemical and cellular properties (Mendes et al. 2005). The majority of rhodopsin mutations are class II mutations, including P23H the most common

M. E. Cheetham (✉) · D. A. Parfitt
Ocular Biology and Therapeutics, UCL Institute of Ophthalmology,
11-43 Bath Street, London EC1V 9EL, UK
e-mail: michael.cheetham@ucl.ac.uk

D. A. Parfitt
e-mail: d.parfitt@ucl.ac.uk

C. Bowes Rickman et al. (eds.), *Retinal Degenerative Diseases,* Advances in Experimental Medicine and Biology 854, DOI 10.1007/978-3-319-17121-0_64

mutation in North America, that cause protein misfolding, retention in the ER and degradation. Rhodopsin is the major protein of the rod OS, so there is a high demand on the photoreceptor ER to produce rhodopsin. Photoreceptors have multiple mechanisms to cope with high protein turnover and maintain protein homeostasis, or proteostasis, including the heat shock response (HSR), the unfolded protein response (UPR), ER-associated degradation (ERAD) and autophagy systems (Balch et al. 2008; Athanasiou et al. 2013). Misfolded proteins, such as P23H rhodopsin, can induce these adaptive networks to reduce protein production, enhance folding facilitators and stimulate degradation. Targeting these networks may, therefore, be beneficial in rhodopsin RP.

64.2 Potential Treatments for Rhodopsin RP

Pharmacological agents may be used to directly target the folding of misfolded proteins, as in the case of pharmacological and chemical chaperones, or by inducing the cell's molecular chaperone machinery.

64.2.1 Pharmacological and Chemical Chaperones

Pharmacological chaperones are compounds that specifically bind and stabilize near-native states to improve the folding of misfolded proteins. For example, the retinoids 9-*cis*- and 11-*cis*-retinal have been shown to stabilize P23H rod opsin in the ER allowing it to traffic through the secretory pathway and improve the yield of folded rhodopsin (Saliba et al. 2002; Noorwez et al. 2004). Importantly, toxic gain-of-function effects, cell death and protein aggregation, of misfolded P23H rod opsin were reduced by retinoids in a cell model. Retinoids also counteracted the dominant-negative effect of misfolded rod opsin on wild-type rod opsin (Mendes and Cheetham 2008). Furthermore, transgenic mice with another rhodopsin misfolding mutation, T17M, had improved electroretinogram (ERG) responses and preservation of photoreceptor survival when treated with 11-*cis*-retinal (Li et al. 1998). Recent work suggests that 11-*cis*-retinal treatment can partially rescue the traffic and folding of a range of rhodopsin misfolding mutants *in vitro* (Krebs et al. 2010); however, the rescued mutant rhodopsin is still inherently unstable (Opefi et al. 2013; Chen et al. 2014) and is likely to misfold after leaving the ER, especially if the retinoid leaves the binding pocket following light exposure.

In contrast, chemical chaperones or kosmotropes are small molecules (e.g. 4-phenylbutyric acid (4-PBA)) that stabilize proteins in a non-specific manner. Kosmotropes have been shown to reduce P23H-mediated cell death and insoluble protein load in cells (Mendes and Cheetham 2008). Tauroursodeoxycholic acid (TUDCA) is another chemical chaperone with anti-apoptotic properties. P23H

transgenic rats treated with TUDCA had improved ERG responses and preserved retinal architecture (Fernandez-Sanchez et al. 2011).

64.2.2 HSR Inducers

The HSR is a transcriptional response to a wide variety of cell stress and induces the expression of many proteins, in particular heat shock proteins (Hsps). Many Hsps function as molecular chaperones to help proteins attain their correct conformation, regulate protein quality control and the degradation of misfolded client proteins. Therefore, this network is a potential target to treat protein-misfolding diseases, and upregulation of the HSR can protect against several models of neurodegeneration. One method of upregulating molecular chaperone expression is to inhibit Hsp90. Hsp90 is in a feedback loop with the HSR transcription factor, heat shock factor 1 (HSF-1), and Hsp90 inhibition results in the post-translational modification and traffic of HSF-1 to nucleus where it induces other heat shock proteins that act on misfolded proteins (Fig. 64.1; Morimoto 1998). Treatment with Hsp90 inhibitors reduced aggregation of P23H rod opsin and associated cell death in a cell model (Mendes and Cheetham 2008). Furthermore, the Hsp90 inhibitor HSP990

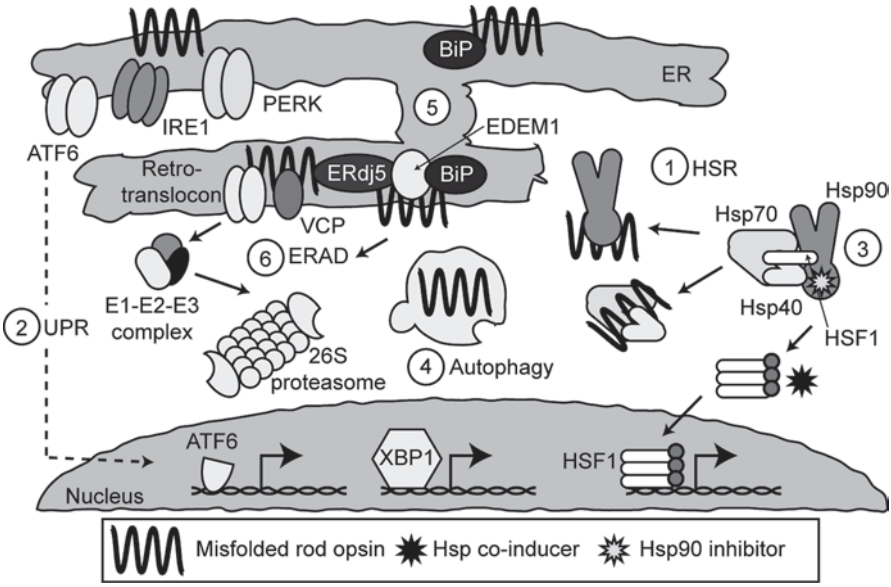

Fig. 64.1 Pharmacological manipulation of proteostasis networks in rhodopsin RP. Inducing molecular chaperone expression by manipulating (1) the HSR, (2) the UPR or (3) inhibiting Hsp90 can alleviate the effects of misfolded rhodopsin. (4) Inducing autophagy helps remove aggregated misfolded protein. (5) ER chaperones such as BiP, EDEM1 and ERdj5 can be directly manipulated to maintain solubility in the ER and promote ERAD (6) for the removal of misfolded rhodopsin

can improve retinal function and architecture *in vivo* in models of rhodopsin RP (Aguila et al. 2014).

Another method to induce the HSR is with hydroxylamine derivatives (HADs), such as bimoclomol and arimoclomol (Vigh et al. 1997). These compounds potentiate the induction of the HSR but rely upon a boosting a pre-existing stress; as such they are HSR co-inducers. We recently used arimoclomol in cell and animal models of P23H rhodopsin RP (Parfitt et al. 2014). Arimoclomol potentiated the HSR in the presence of P23H rhodopsin in cells, leading to enhanced Hsp expression. Interestingly, the HSR was already activated by the mutant rhodopsin expression in the retinae of P23H transgenic rats and this HSR was further enhanced by arimoclomol treatment. Furthermore, arimoclomol led to improved ERG responses and photoreceptor survival in lines of transgenic rats with fast (P23H-1) and medium (P23H-3) rates of degeneration. Arimoclomol treatment caused a reduction of rhodopsin immunoreactivity in the cell bodies of the ONL and decreased the amount of insoluble rhodopsin, but there was no change in the normalized levels of soluble rhodopsin, suggesting that arimoclomol was stimulating the degradation of aggregation-prone rhodopsin, rather than rescuing the folding of the mutant protein. These changes correlated with a preservation of the photoreceptor OS structure implying that the defects in OS structure seen in these models is due, at least in part, to a dominant gain of function potentially related to unstable rhodopsin, which can be suppressed by arimoclomol. Interestingly, in addition to the enhanced HSR, arimoclomol potentiated the UPR in the retina, suggesting that these two proteostasis pathways might co-operate in photoreceptors (Parfitt et al. 2014).

64.3 The UPR in Rhodopsin RP

The UPR is activated in P23H and T17M animal models (Lin et al. 2007; Kunte et al. 2012). Chronic activation of the UPR is associated with cell death; however, arimoclomol treatment enhanced the activation of all three branches of the UPR, whilst still protecting against mutant rhodopsin (Parfitt et al. 2014). Furthermore, the ablation of CHOP, which is a downstream pro-apoptotic effector of PERK, in P23H or T17M rhodopsin mouse models did not alter retinal degeneration (Nashine et al. 2013; Adekeye et al. 2014). Collectively these data suggest that activation of the UPR by mutant rhodopsin *per se* is not toxic to photoreceptors and might be a protective adaptive response that stimulates factors that can help deal with the mutant rhodopsin.

64.4 ER Chaperones and ERAD of Rhodopsin.

The ER-resident chaperones that interact with WT and mutant rhodopsin in the ER to facilitate rhodopsin folding or quality control and degradation are starting to be identified. BiP (HSPA5) has an important role in rod opsin biogenesis, as wild type

rod opsin aggregates in the absence of BiP, whereas BiP overexpression improves P23H rhodopsin mobility and loss of BiP increases P23H rhodopsin aggregation (Athanasiou et al. 2012). BiP expression is increased in P23H transgenic rats (Lin et al. 2007; Parfitt et al. 2014), and overexpression of BiP in P23H rats improves ERG responses and ONL thickness (Gorbatyuk et al. 2010).

In ERAD, misfolded proteins are transported out of the ER where they are degraded by the ubiquitin-proteasome system (UPS) in the cytosol (Fig. 64.1). The ERAD effector EDEM1 can stimulate the degradation of P23H mutant rhodopsin and promote the traffic of the remaining P23H protein by improving folding, although this is only transient as the protein is unstable once it leaves the ER (Kosmaoglou et al. 2009). The ER-resident reductase, ERdj5 (DNAJC10), forms a chaperone network with EDEM1 and BiP and also plays a role regulating the biogenesis of rhodopsin, maintaining solubility of mutant rhodopsin within the ER and stimulating ERAD (Athanasiou et al. 2014). The identity of the complex involved in translocation of P23H rhodopsin is unknown; however, the AAA-ATPase VCP/p97 promotes the retrotranslocation and degradation of P23H rhodopsin (Griciuc et al. 2010).

An alternative method for removing misfolded protein is autophagy, where substrates are enclosed in double-membrane autophagosomes before degradation by lysozymes. Rapamycin is an inhibitor of mTOR, which is a negative regulator of autophagy. Rapamycin treatment reduced inclusion formation in cells expressing P23H rod opsin (Mendes and Cheetham 2008). Recent work showed that rapamycin treatment in P23H-3 rats improved ERG responses (Sizova et al. 2014).

64.5 Conclusions

The proteostasis networks have varied roles in protecting cells against misfolded proteins, which is particularly important in photoreceptors. Manipulation of these pathways, through chemical or genetic means, has provided insights into the mechanisms behind this protection. The identification of compounds with low toxicity, like arimoclomol, that can restore proteostasis could be potentially beneficial for rhodopsin RP.

References

Adekeye A, Haeri M, Solessio E et al (2014) Ablation of the proapoptotic genes chop or ask1 does not prevent or delay loss of visual function in a P23H transgenic mouse model of retinitis pigmentosa. PloS One 9:e83871

Aguila M, Bevilacqua D, McCulley C et al (2014) Hsp90 inhibition protects against inherited retinal degeneration. Hum Mol Genet 23:2164–2175

Athanasiou D, Kosmaoglou M, Kanuga N et al (2012) BiP prevents rod opsin aggregation. Mol Biol Cell 23:3522–3531

Athanasiou D, Aguila M, Bevilacqua D et al (2013) The cell stress machinery and retinal degeneration. FEBS Lett 587:2008–2017
Athanasiou D, Bevilacqua D, Aguila M et al (2014) The co-chaperone and reductase ERdj5 facilitates rod opsin biogenesis and quality control. Hum Mol Genet 23:6594–6606
Balch WE, Morimoto RI, Dillin A et al (2008) Adapting proteostasis for disease intervention. Science 319:916–919
Chen Y, Jastrzebska B, Cao P et al (2014) Inherent instability of the retinitis pigmentosa P23H mutant opsin. J Biol Chem 289:9288–9303
Dryja TP, McGee TL, Hahn LB et al (1990) Mutations within the rhodopsin gene in patients with autosomal dominant retinitis pigmentosa. N Engl J Med 323:1302–1307
Fernandez-Sanchez L, Lax P, Pinilla I et al (2011) Tauroursodeoxycholic acid prevents retinal degeneration in transgenic P23H rats. Invest Ophthalmol Vis Sci 52:4998–5008
Gorbatyuk MS, Knox T, LaVail MM et al (2010) Restoration of visual function in P23H rhodopsin transgenic rats by gene delivery of BiP/Grp78. Proc Natl Acad Sci U S A 107:5961–5966
Griciuc A, Aron L, Piccoli G et al (2010) Clearance of Rhodopsin(P23H) aggregates requires the ERAD effector VCP. Biochim Biophys Acta 1803:424–434
Hartong DT, Berson EL, Dryja TP (2006) Retinitis pigmentosa. Lancet 368:1795–1809
Kosmaoglou M, Schwarz N, Bett JS et al (2008) Molecular chaperones and photoreceptor function. Prog Ret Eye Res 27:434–449
Kosmaoglou M, Kanuga N, Aguila M et al (2009) A dual role for EDEM1 in the processing of rod opsin. J Cell Sci 122:4465–4472
Krebs MP, Holden DC, Joshi P et al (2010) Molecular mechanisms of rhodopsin retinitis pigmentosa and the efficacy of pharmacological rescue. J Mol Biol 395:1063–1078
Kunte MM, Choudhury S, Manheim JF et al (2012) ER stress is involved in T17M rhodopsin-induced retinal degeneration. Invest Ophthalmol Vis Sci 53:3792–3800
Li T, Sandberg MA, Pawlyk BS et al (1998) Effect of vitamin A supplementation on rhodopsin mutants threonine-17 – > methionine and proline-347 – > serine in transgenic mice and in cell cultures. Proc Natl Acad Sci U S A 95:11933–11938
Lin JH, Li H, Yasumura D et al (2007) IRE1 signaling affects cell fate during the unfolded protein response. Science 318:944–949
Mendes HF, Cheetham ME (2008) Pharmacological manipulation of gain-of-function and dominant-negative mechanisms in rhodopsin retinitis pigmentosa. Hum Mol Genet 17:3043–3054
Mendes HF, van der Spuy J, Chapple JP et al (2005) Mechanisms of cell death in rhodopsin retinitis pigmentosa: implications for therapy. Trend Mol Med 11:177–185
Morimoto RI (1998) Regulation of the heat shock transcriptional response: cross talk between a family of heat shock factors, molecular chaperones, and negative regulators. Genes Dev 12:3788–3796
Nashine S, Bhootada Y, Lewin AS et al (2013) Ablation of C/EBP homologous protein does not protect T17M RHO mice from retinal degeneration. PloS One 8:e63205
Noorwez SM, Malhotra R, McDowell JH et al (2004) Retinoids assist the cellular folding of the autosomal dominant retinitis pigmentosa opsin mutant P23H. J Biol Chem 279:16278–16284
Opefi CA, South K, Reynolds CA et al (2013) Retinitis pigmentosa mutants provide insight into the role of the N-terminal cap in rhodopsin folding, structure, and function. J Biol Chem 288:33912–33926
Parfitt DA, Aguila M, McCulley CH et al (2014) The heat-shock response co-inducer arimoclomol protects against retinal degeneration in rhodopsin retinitis pigmentosa. Cell Death Dis 5:e1236
Pearring JN, Salinas RY, Baker SA et al (2013) Protein sorting, targeting and trafficking in photoreceptor cells. Prog Ret Eye Res 36:24–51
Saliba RS, Munro PM, Luthert PJ et al (2002) The cellular fate of mutant rhodopsin: quality control, degradation and aggresome formation. J Cell Sci 115:2907–2918
Sizova OS, Shinde VM, Lenox AR et al (2014) Modulation of cellular signaling pathways in P23H rhodopsin photoreceptors. Cell Signal 26:665–672
Vigh L, Literati PN, Horvath I et al (1997) Bimoclomol: a nontoxic, hydroxylamine derivative with stress protein-inducing activity and cytoprotective effects. Nat Med 3:1150–1154

Part VII
Gene Therapy and Antisense

Chapter 65
Gene Therapy for *MERTK*-Associated Retinal Degenerations

Matthew M. LaVail, Douglas Yasumura, Michael T. Matthes, Haidong Yang, William W. Hauswirth, Wen-Tao Deng and Douglas Vollrath

Abstract *MERTK*-associated retinal degenerations are thought to have defects in phagocytosis of shed outer segment membranes by the retinal pigment epithelium (RPE), as do the rodent models of these diseases. We have subretinally injected an RPE-specific AAV2 vector, AAV2-VMD2-h*MERTK*, to determine whether this would provide long-term photoreceptor rescue in the RCS rat, which it did for up to 6.5 months, the longest time point examined. Moreover, we found phagosomes in the RPE in the rescued regions of RCS retinas soon after the onset of light. The same vector also had a major protective effect in *Mertk*-null mice, with a concomitant increase in ERG response amplitudes in the vector-injected eyes. These findings suggest that planned clinical trials with this vector will have a favorable outcome.

Keywords Gene therapy · Retinal degeneration · MERTK · Phagocytosis · Treatment

M. M. LaVail (✉) · D. Yasumura · M. T. Matthes · H. Yang
Beckman Vision Center, UCSF School of Medicine, 10 Koret Way,
San Francisco, CA 94143-0730, USA
e-mail: matthew.lavail@ucsf.edu

D. Yasumura (Deceased)
e-mail: matthew.lavail@ucsf.edu

M. T. Matthes
e-mail: Michael.Matthes@ucsf.edu

H. Yang
e-mail: yang.harvey@gmail.com

W. W. Hauswirth · W.-T. Deng
Department of Ophthalmology, College of Medicine, University of Florida,
Gainesville, FL 32610-0284, USA
e-mail: hauswrth@ufl.edu

D. Vollrath
Department of Genetics, Stanford University School of Medicine, Stanford, CA 94305, USA
e-mail: Vollrath@stanford.edu

C. Bowes Rickman et al. (eds.), *Retinal Degenerative Diseases,* Advances in
Experimental Medicine and Biology 854, DOI 10.1007/978-3-319-17121-0_65

65.1 Introduction

Retinitis pigmentosa is a family of diseases that affects approximately one in 3500 people worldwide and is a major cause of inherited blindness in the Western world. More than 50 genes have been identified in which mutations lead to retinitis pigmentosa (http://www.sph.uth.tmc.edu/ retnet/). Vision loss results from the degeneration of rod and cone photoreceptors due to mutation of genes expressed either in these cells, or in the closely interacting retinal pigment epithelial (RPE) cells.

The RCS rat is a widely studied retinal degeneration (RD) model in which photoreceptor cells begin to degenerate at postnatal day (P) 20, with most disappearing by about P60 (Dowling and Sidman 1962). It has been known since the 1970s that this degeneration has a defect in the ability of the RPE to phagocytize rod outer segment tips, leading to an accumulation of outer segment debris in the subretinal space (Bok and Hall 1971; Mullen and LaVail 1976). The gene responsible for the defect in RCS rats was identified as the mer proto-oncogene tyrosine kinase (*Mertk*) (D'Cruz et al. 2000), which encodes a transmembrane receptor tyrosine kinase (Strick and Vollrath 2010).

Once the mutated gene was identified, proof of concept of gene replacement therapy was obtained in RCS rats using an adenovirus vector by Vollrath et al. (2001). Subsequently, a number of studies using different vectors, including adeno-associated virus (AAV) (Smith et al. 2003; Deng et al. 2012) and lentivirus (Tschernutter et al. 2005) were effective to different degrees, each showing improvement in photoreceptor survival, electroretinographic responses and RPE phagocytic function.

Numerous studies have described individuals with inherited RD due to *MERTK* mutations (Gal et al. 2000; Thompson et al. 2002; Tschernutter et al. 2006; Charbel Issa et al. 2009; Mackay et al. 2010; Shahzadi et al. 2010; Ostergaard et al. 2011), emphasizing the critical need for appropriate vectors for gene replacement therapy. Recombinant AAV (rAAV) in particular has gained prominence in the treatment of inherited retinal disorders in recent years (Boye et al. 2013). Three separate Phase I clinical trials for Leber congenital amaurosis type 2 have demonstrated the safety of AAV2 in human patients (Jacobson et al. 2006; Bainbridge et al. 2008; Cideciyan et al. 2008; Maguire et al. 2008).

A series of preclinical potency and safety evaluations of an AAV2 vector expressing human *MERTK* cDNA driven by an RPE-specific VMD2 (Bestrophin) promoter that was planned for human patients was recently carried out (Conlon et al. 2013). The −585/+38 bp version of the human VMD2 promoter had previously been shown to drive efficient and exclusive transgene expression in the RPE (Alexander and Hauswirth 2008). The effectiveness of the vector in RCS rats was demonstrated by electroretinogram (ERG) analysis done 60 days after injection at P9. The potential toxicity of the vector was assessed in Sprague–Dawley (SD) rats by electrophysiology, retinal morphology, and GLP-compliant experiments based on clinical observations and histopathology.

For the assessment of this RPE-specific vector on RDs for clinical trial application, it would be useful to know whether the vector is effective in long-term reversal of the defect in RPE phagocytosis and in rescue of photoreceptors in RCS rats. In addition, it would be important to demonstrate that the vector can rescue photoreceptors in a *MERTK*-associated RD in a different species with a different gene mutation. In this study, we have addressed both of these issues.

65.2 Materials and Methods

65.2.1 Animals

All studies were conducted in accordance with the ARVO Statement for the Use of Animals and the IACUC at UCSF. Inbred, pink-eyed RCS rats with inherited retinal dystrophy due to a deletion in the *Mertk* gene (D'Cruz et al. 2000) were characterized previously (Dowling and Sidman 1962; LaVail and Battelle 1975). *Mertk* knockout mice with an RCS-like retinal dystrophy phenotype were described earlier (Duncan et al. 2003).

65.2.2 Vector Injections, ERG Procedure and Histological Analysis

Subretinal injections of the AAV2-VMD2-h*MERTK* vector were made at P10 for RCS rats and at P4 for *Mertk* knockout mice using a previously described method (Lewin et al. 1998).

ERG analysis was carried out as previously described (Lewin et al. 1998).

For histologic studies to quantify the outer nuclear layer (ONL) thickness, methods previously described were used (LaVail and Battelle 1975; LaVail et al. 1987; Faktorovich et al. 1992).

65.3 Results

65.3.1 Long-Term Photoreceptor Rescue and Reversal of Phagocytosis Defect in RCS Rats

Comparison at P196 of the retinal structure of eyes of RCS rats injected subretinally with AAV2-VMD2-h*MERTK* and uninjected contralateral control eyes revealed a remarkable difference, equal to that seen by Conlon et al. (2013) for younger rats. In the uninjected eyes, most of the photoreceptor nuclei in the ONL had degenerated

and disappeared, and an outer segment debris layer characteristic of retinal dystrophy in RCS rats was evident (Fig. 65.1a). By contrast, the vector-injected eyes appeared virtually normal in the areas of maximal rescue (Fig. 65.1b). The extent of photoreceptor rescue was typically about half of the full retinal length as shown in a retinal spidergram (Fig. 65.1c). When the RCS retinas were taken soon after the onset of light in the morning, large packets of outer segment disc membranes (phagosomes) were abundant in the RPE cell processes and internally within the RPE cell bodies (Fig. 65.1d).

65.3.2 Photoreceptor Rescue in the MERTK-null Mouse

The differences at P52 in retinal structure between eyes of *Mertk* knockout mice injected subretinally with AAV2-VMD2-h*MERTK* at P4 and uninjected contralateral

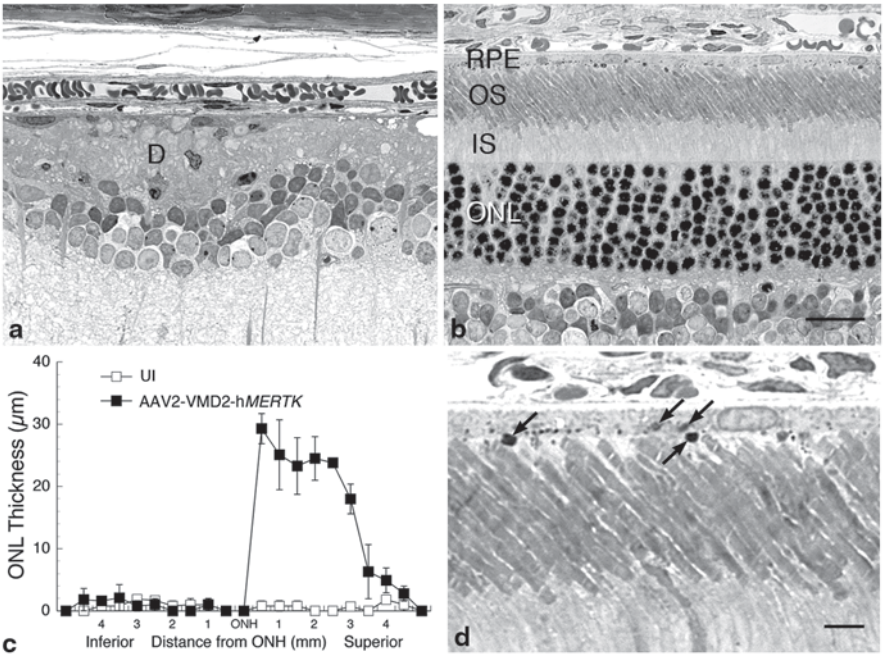

Fig. 65.1 Structural analysis of RCS rats injected subretinally into one eye with AAV2-VMD2-h*MERTK* compared with uninjected (UI) contralateral eyes of the same rats. **a, b** Light micrographs of 1-μm plastic sections of the posterior retina of the UI eye (**a**), where most photoreceptor nuclei in the ONL have degenerated and disappeared, and an outer segment debris (**d**) zone is present. The retina of the opposite eye from the eye injected with vector is shown (**b**), which is comparable in appearance to that of normal rat retinas. **c** Retinal spidergram showing the ONL thickness along the vertical meridian of UI and vector-injected eyes (each data point is the mean ± SD from 2 rats). **d** Higher magnification of a vector-injected eye showing phagosomes (*arrows*) at the apical surface and intracellularly in the RPE. *IS* inner segments. Scale bars: **b** = 20 μm; **d** = 5 μm

eyes were also remarkable. In the uninjected eyes, the ONL had been reduced to less than one complete row (Fig. 65.2a). By contrast, the vector-injected eyes appeared virtually normal in the areas of maximal rescue (Fig. 65.2b). The extent of photoreceptor rescue typically was most of the full retinal length, as viewed in a retinal spidergram of ONL thickness (Fig. 65.2c). The ERG responses were dramatically different for each of the waveforms; the uninjected eyes showed no scotopic a- or b-waves, and only minimal photopic b-waves, but the vector-injected eyes had responses that were 40–60 % of normal (Fig. 65.2d).

65.4 Discussion

In this study, we found that when the RPE-specific AAV2-VMD2-h*MERTK* vector was injected subretinally, it protected photoreceptors from degeneration in the RCS rat for up to 6.5 months of age, the oldest examined. Moreover, the absence

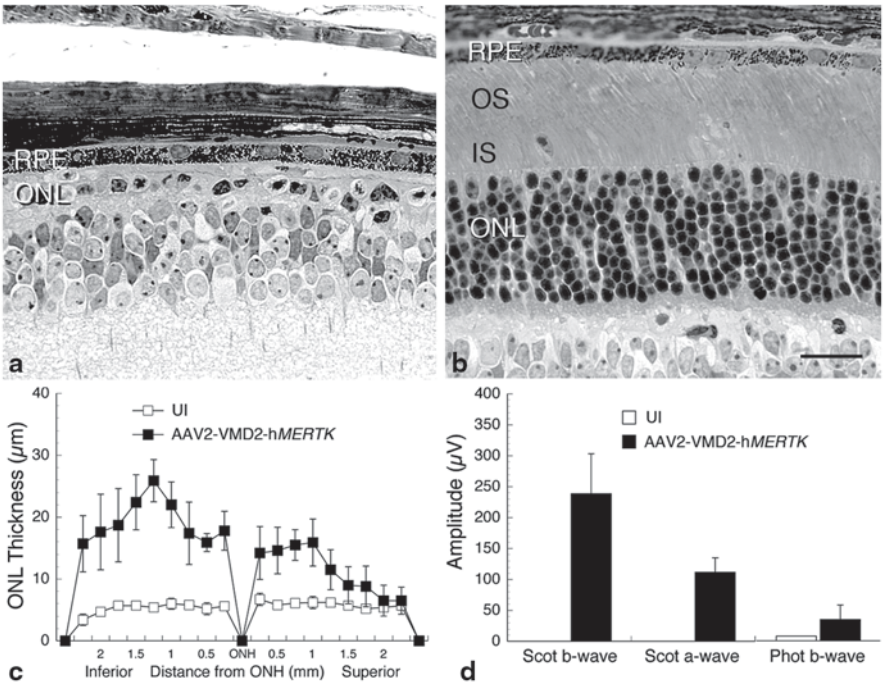

Fig. 65.2 Structural and functional analysis of *Mertk* knockout mice injected subretinally into one eye with AAV2-VMD2-h*MERTK* (**b**) compared with uninjected (UI) contralateral eyes of the same mice (**a**). Labeling as described in Fig. 65.1 and in the text. **c** Retinal spidergram showing the ONL thickness along the vertical meridian of UI and vector-injected eyes (each data point is the mean ± SD from 5 mice). **d** Electroretinographic response amplitudes from the same mice as in **c**. Scale bar = 20 μm

in phagocytosis imparted by the *Mertk* gene defect in the RCS rats (Bok and Hall 1971) was clearly reversed, as large phagosomes were abundant when the eyes were taken soon after the onset of light, typical of circadian outer segment disc shedding in the rat (LaVail 1976, 1980).

We also found that in the *Mertk* knockout mouse, which exhibits rapid loss of most photoreceptors (Duncan et al. 2003), subretinal injection of the AAV2-VMD2-h*MERTK* vector protected a majority of photoreceptor cells from degenerating. As a consequence, the electrical activity of the photoreceptors in response to light was significantly increased over that in the uninjected control eyes, where the responses were almost abolished.

These findings strongly suggest that the RPE-specific AAV2-VMD2-h*MERTK* vector that is being used in a clinical trial of different forms of *MERTK*-associated RDs (FS Alkuraya, personal communation) will prove to be effective.

Acknowledgements This study was supported by NIH grants EY001919, EY006842 and EY002162 (MML), The Foundation Fighting Blindness (MML, DV, WWH) and Unrestricted Awards to UCSF and the University of Florida from Research to Prevent Blindness.

References

Alexander JJ, Hauswirth WW (2008) Adeno-associated viral vectors and the retina. Adv Exp Med Biol 613:121–128

Bainbridge JW, Smith AJ, Barker SS et al (2008) Effect of gene therapy on visual function in Leber' congenital amaurosis. N Engl J Med 358:2231–2239

Bok D, Hall MO (1971) The role of the pigment epithelium in the etiology of inherited retinal dystrophy in the rat. J Cell Biol 49:664–682

Boye SE, Boye SL, Lewin AS et al (2013) A comprehensive review of retinal gene therapy. Mol Ther 21:509–519

Charbel Issa P, Bolz HJ, Ebermann I et al (2009) Characterisation of severe rod-cone dystrophy in a consanguineous family with a splice site mutation in the MERTK gene. Br J Ophthalmol 93:920–925

Cideciyan AV, Aleman TS, Boye SL et al (2008) Human gene therapy for RPE65 isomerase deficiency activates the retinoid cycle of vision but with slow rod kinetics. Proc Natl Acad Sci U S A 105:15112–15117

Conlon TJ, Deng WT, Erger K et al (2013) Preclinical potency and safety studies of an AAV2-mediated gene therapy vector for the treatment of MERTK associated retinitis pigmentosa. Hum Gene Ther Clin Devt 24:23–28

D'Cruz PM, Yasumura D, Weir J et al (2000) Mutation of the receptor tyrosine kinase gene *Mertk* in the retinal dystrophic RCS rat. Hum Mol Genet 9:645–651

Deng WT, Dinculescu A, Li Q et al (2012) Tyrosine-mutant AAV8 delivery of human MERTK provides long-term retinal preservation in RCS rats. Invest Ophthalmol Vis Sci 53:1895–1904

Dowling JE, Sidman RL (1962) Inherited retinal dystrophy in the rat. J Cell Biol 14:73–109

Duncan JL, LaVail MM, Yasumura D et al (2003) An RCS-like retinal dystrophy phenotype in *Mer* knockout mice. Invest Ophthalmol Vis Sci 44:826–838

Faktorovich EG, Steinberg RH, Yasumura D et al (1992) Basic fibroblast growth factor and local injury protect photoreceptors from light damage in the rat. J Neurosci 12:3554–3567

Gal A, Li Y, Thompson DA et al (2000) Mutations in *MERTK*, the human orthologue of the RCS rat retinal dystrophy gene, cause retinitis pigmentosa. Nat Genet 26:270–271

Jacobson SG, Boye SL, Aleman TS et al (2006) Safety in nonhuman primates of ocular AAV2-RPE65, a candidate treatment for blindness in Leber congenital amaurosis. Hum Gene Ther 17:845–858

LaVail MM (1976) Rod outer segment disc shedding in rat retina: relationship to cyclic lighting. Science 194:1071–1074

LaVail MM (1980) Circadian nature of rod outer segment disc shedding in the rat. Invest Ophthalmol Vis Sci 19:407–411

LaVail MM, Battelle BA (1975) Influence of eye pigmentation and light deprivation on inherited retinal dystrophy in the rat. Exp Eye Res 21:167–192

LaVail MM, Gorrin GM, Repaci MA et al (1987) Genetic regulation of light damage to photoreceptors. Invest Ophthalmol Vis Sci 28:1043–1048

Lewin AS, Drenser KA, Hauswirth WW et al (1998) Ribozyme rescue of photoreceptor cells in a transgenic rat model of autosomal dominant retinitis pigmentosa. Nat Med 4:967–971

Mackay DS, Henderson RH, Sergouniotis PI et al (2010) Novel mutations in MERTK associated with childhood onset rod-cone dystrophy. Mol Vis 16:369–377

Maguire AM, Simonelli F, Pierce EA et al (2008) Safety and efficacy of gene transfer for Leber's congenital amaurosis. N Engl J Med 358:2240–2248

Mullen RJ, LaVail MM (1976) Inherited retinal dystrophy: primary defect in pigment epithelium determined with experimental rat chimeras. Science 192:799–801

Ostergaard E, Duno M, Batbayli M et al (2011) A novel MERTK deletion is a common founder mutation in the Faroe Islands and is responsible for a high proportion of retinitis pigmentosa cases. Mol Vis 17:1485–1492

Shahzadi A, Riazuddin SA, Ali S et al (2010) Nonsense mutation in MERTK causes autosomal recessive retinitis pigmentosa in a consanguineous Pakistani family. Br J Ophthalmol 94:1094–1099

Smith AJ, Schlichtenbrede FC, Tschernutter M et al (2003) AAV-mediated gene transfer slows photoreceptor loss in the RCS rat model of retinitis pigmentosa. Mol Ther 8:188–195

Strick DJ, Vollrath D (2010) Focus on molecules: MERTK. Exp Eye Res 91:786–787

Thompson DA, McHenry CL, Li Y et al (2002) Retinal dystrophy due to paternal isodisomy for chromosome 1 or chromosome 2, with homoallelism for mutations in RPE65 or MERTK, respectively. Am J Hum Genet 70:224–229

Tschernutter M, Schlichtenbrede FC, Howe S et al (2005) Long-term preservation of retinal function in the RCS rat model of retinitis pigmentosa following lentivirus-mediated gene therapy. Gene Ther 12:694–701

Tschernutter M, Jenkins SA, Waseem NH et al (2006) Clinical characterisation of a family with retinal dystrophy caused by mutation in the Mertk gene. Br J Ophthalmol 90:718–723

Vollrath D, Feng W, Duncan JL et al (2001) Correction of the retinal dystrophy phenotype of the RCS rat by viral gene transfer of Mertk. Proc Natl Acad Sci U S A 98:12584–12589

Chapter 66
Tamoxifen-Containing Eye Drops Successfully Trigger *Cre*-Mediated Recombination in the Entire Eye

Anja Schlecht, Sarah V Leimbeck, Ernst R Tamm and Barbara M Braunger

Abstract Embryonic lethality in mice with targeted gene deletion is a major issue that can be circumvented by using Cre-loxP-based animal models. Various inducible *Cre* systems are available, e.g. such that are activated following tamoxifen treatment, and allow deletion of a specific target gene at any desired time point during the life span of the animal. In this study, we describe the efficiency of topical tamoxifen administration by eye drops using a *Cre*- reporter mouse strain (*R26R*). We report that tamoxifen-responsive *CAGGCre-ER*^{TM} mice show a robust *Cre*-mediated recombination throughout the entire eye.

Keywords Cre · Cre-loxP · Tamoxifen · Eye drops · Eye · Retina

66.1 Introduction

When working with genes associated with germline null alleles that are required for major developmental or cell maintenance pathways, scientists frequently face the problem of embryonic lethality after constitutional targeted deletion of their gene of interest (Branda and Dymecki 2004; Maddison and Clarke 2005). The use of Cre-loxP-based animal models has greatly expanded the possibilities for scientists to delete essential genes in the mouse and thus circumvent the embryonic lethality, as this approach allows the generation of tissue- or cell-specific conditional deletions

Anja Schlecht and Sarah V Leimbeck contributed equally to the study.

B. M. Braunger (✉) · A. Schlecht · S. V. Leimbeck · E. R. Tamm
Institute of Human Anatomy and Embryology, University of Regensburg, Universitätsstr. 31, D-93053 Regensburg, Germany
e-mail: Barbara.Braunger@vkl.uni-regensburg.de

A. Schlecht
e-mail: Anja.Schlecht@vkl.uni-regensburg.de

S. V. Leimbeck
e-mail: Sarah.Leimbeck@gmx.de

E. R. Tamm
e-mail: Ernst.Tamm@vkl.uni-regensburg.de

C. Bowes Rickman et al. (eds.), *Retinal Degenerative Diseases,* Advances in Experimental Medicine and Biology 854, DOI 10.1007/978-3-319-17121-0_66

(Kühn and Torres 2002). Moreover, different inducible *Cre* systems are availabe, like such that are tamoxifen-responsive, and allow gene deletion at any desired time point. In this study, we used *CAGGCre-ER*^{TM} mice (Hayashi and McMahon 2002) that carry the *Cre-ER*^{TM} fusion protein, which is comprised of the *Cre*-recombinase fused to a mutant form of the mouse estrogen receptor (Hayashi and McMahon 2002). The fusion protein is restricted to the cytoplasm and *Cre- ER*^{TM} will only access the nucleus after exposure to tamoxifen. Thus, exposure to tamoxifen in a spatially-defined manner allows tissue-specific targeted gene deletion. In this article, we describe a protocol that efficiently causes *Cre*-mediated recombination following topical tamoxifen treatment by applying tamoxifen-containing eye drops. Using a *Cre*- reporter mouse strain (*R26R*), we show a robust *Cre*-mediated recombination throughout the entire eye.

66.2 Material and Methods

Mice All procedures conformed to the tenets of the National Institutes of Health Guidelines on the Care and Use of Animals in Research, the EU Directive 2010/63/E, and institutional guidelines. Mice that were heterozygous for *CAGGCre-ER*^{TM} were crossed with homozygous *Cre*-reporter (*R26R*) (Soriano 1999) mice. *R26R* mice carry a loxP-flanked DNA segment that prevents the expression of the downstream lacZ gene. However, when *R26R* mice are crossed with a *Cre* transgenic strain, the *Cre* expression results in the removal of the loxP-flanked DNA segment and lacZ is expressed in all cells or tissues where *Cre* is expressed. In this study, *CAG-Cre-ER*^{TM}*/R26R* mice were used as experimental mice, and *R26R* littermates as control mice. Genetic backgrounds were 129SV (*R26R*) or C57Bl6 (*CAGGCre-ER*^{TM}).

66.2.1 Tamoxifen Treatment

To induce the nuclear trans-localization of the *Cre* recombinase and its activation, *CAG-CreER*^{TM}*/R26R* mice and *R26R* littermates were treated with tamoxifen-containing eye drops. To this end, tamoxifen (Sigma) was diluted in corn oil (Sigma) to a final concentration of 5 mg/ml and the solution was pipetted as eye drops (10 µl/drop) onto the closed eyelids of mouse pups three times per day in 4 h intervals. Our treatment started at p8 and lasted to p12, which obviously can be adjusted for other time points depending on the gene and molecular processes of interest.

66.2.2 PCR Analysis

Genotypes were screened by isolating genomic DNA from tail biopsies and testing for transgenic sequences by PCR as described previously (Braunger et al. 2013b). The following PCR primers were used: Cre genotyping (5′-CAC CCT GTT ACG

TAT AGC-3′ and 5′-CTA ATC GCC ATC TTC CAG-3′) and LacZ genotyping (5′-ATC CTC TGC ATG GTC AGG TC-3′ and 5′-CGT GGC CTG ATT CAT TCC-3′). The thermal cycle profile was denaturation at 96 °C for 30 s, annealing at 57 °C (Cre), or 60 °C (LacZ) for 30 s, and extension at 72 °C for 1 min for 35 cycles.

66.2.3 β-galactosidase Staining

Lac-Z-staining was performed in mixed *CAGGCre-ER^{TM}/R26R* and *R26R* mice following a previously published protocol (Baulmann et al. 2002). Briefly, after enucleation, eyes were fixed in LacZ fixative solution (2 mM $MgCl_2$, 5 mM EGTA (pH 7.3), 0.2 % glutaraldehyde in 0.1 M phosphate buffer (pH 7.3) at 4 °C for 30 min. After three 10 min rinses in LacZ wash buffer (0.01 % sodium deoxycholate, 0.02 % NP-40, 2 mM $MgCl_2$ in 0.1 M phosphate buffer (pH 7.3)), β-galactosidase activity was visualized in X-Gal staining solution (500 mM K_4 $Fe(CN)_6 \times 3$ H_20, 500 mM $K_3Fe(CN)_6$, 1 mg/ml X-gal in LacZ wash buffer). The eyes were stained in X-Gal solution at 37 °C for 24 h, rinsed in LacZ wash buffer (3 × 10 min) followed by one 10 min rinse in phosphate buffer and then processed to paraffin embedding. Paraffin sections (6 µm thick) were analyzed as mentioned previously (Braunger et al. 2013a).

66.3 Results- Localization of Cre-mediated Recombination in Ocular Tissues

After topical tamoxifen treatment with eye drops, we used β-galactosidase staining to localize *Cre*-mediated recombination in the eye. Eyes of *CAGGCre-ER^{TM}/R26R* mice (Fig. 66.1b) showed an intense β-galactosidase reaction throughout the entire organ while control eyes (*R26R*) were essentially negative (Figs. 66.1a and Fig. 66.2a, c, e, and g). The detailed analysis of *CAGGCre-ER^{TM}/R26R* eyes showed an intense β-galactosidase reaction in the anterior eye segment. We observed in particular a strong β-galactosidase staining in the structures of the chamber angle outflow pathway, in the ciliary body (Fig. 66.2b) and in the cornea, as well as in the epithelium of the lens (Fig. 66.2d). In the posterior eye segment of *CAGGCre-ER^{TM}/R26R* eyes, the sensory retina, the retinal pigment epithelium (RPE) and the choroid (Fig. 66.2f) stained positive for β-galactosidase indicating a successful *Cre*-mediated recombination in basically every ocular cell type. In addition, in sections where the optic nerve was cut, we observed positive staining along the sheaths surrounding the nerve indicating that tamoxifen had been distributed outside the eye (Fig. 66.2h).

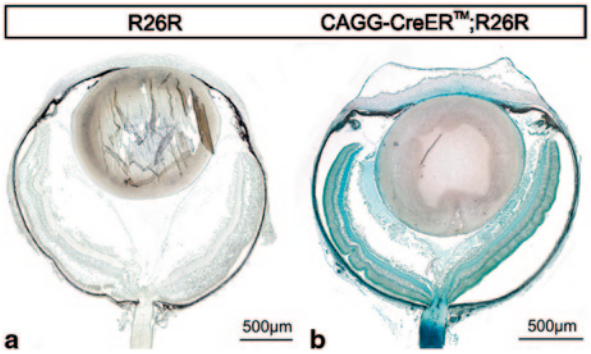

Fig. 66.1 Localization and activation of *Cre* recombinase in the eye following tamoxifen containing eye drops. An intense β-galactosidase staining throughout the entire eye in 14 days old *CAGGCre-ER*^{TM}*/R26R* mouse (**b**) indicates a successful activation of the *Cre* recombinase in ocular tissue following treatment with tamoxifen eye drops. Control littermates (*R26R*) (**a**) did not show a positive reaction

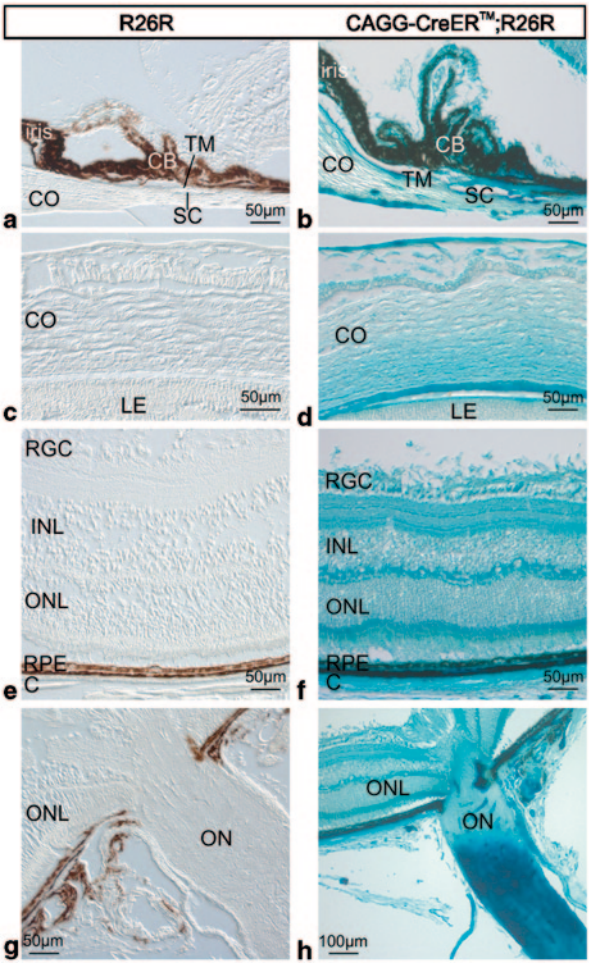

Fig. 66.2 Detailed localization and activation of *Cre* recombinase in the eye. Detailed magnification of the β-galactosidase staining in the structures of the chamber angle outflow pathway (**b**), the cornea and the lens epithelium (**d**), the retina and choroid (**f**) and the optic nerve (**h**) of a 14 days old *CAGGCre-ER*^{TM}*/R26R* mouse. The control littermate did not show a positive reaction for β-galactosidase (**a, c, e** and **g**). *RGC* retinal ganglion cells, *INL* inner nuclear layer, *ONL* outer nuclear layer, *RPE* retinal pigment epithelium, *C* choroid, *ON* optic nerve, *CB* ciliary body, *CO* cornea, *TM* Trabecular meshwork, *SC* Schlemm's canal, *LE* lens

66.4 Discussion

Our results show that induction of *Cre* recombinase by using tamoxifen-containing eye drops is a suitable method to induce a tamoxifen-dependent *Cre*-mediated recombination in ocular tissues.

The topical application of tamoxifen-containing eye drops provides several advantages. As a non-invasive method it greatly reduces or even avoids the potential risk of infections, which might eventually result from intra-peritoneal injections (Leenaars et al. 1998; Leenaars and Hendriksen 2005), which is a common method to administer tamoxifen. Intravitreal tamoxifen injections harbor the same risks of infection. Furthermore this route might influence the expression level of potential genes of interests because intravitreal injection of the vehicle alone already results in the activation of microglia and/or an elevated expression of neuroprotective molecules (Braunger 2014; Seitz and Tamm 2014).

In our study, we noticed staining along the optic nerve outside the eye, a finding that appears to indicate that tamoxifen is distributed to tissues outside the eye. One could avoid this and achieve even greater spatial control of Cre expression by reducing the duration of tamoxifen treatment, e.g. from 5 days, to 3 days or maybe even less. Of course, this approach could in turn result in a *Cre*-mediated recombination gradient in the eye itself. This scenario might be of great interest for scientist focusing on the anterior segment of the eye like the cornea or the chamber angle outflow pathway. Here, a reduced exposure time might reduce the tamoxifen- induced Cre- mediated recombination in other parts of the eye or the body to an even greater extend. As a side note, our system also allows the usage of strong promoters like CMV or β- actin that would drive *Cre*- expression in every cell. The expression of Cre, however, can be spatially controlled, as the tamoxifen is applied topical.

Finally, considering tamoxifen induced toxicity, which may influence cell viability or even promote cell death (Kim et al. 2014), the topical administration of tamoxifen using eye drops could obviously reduce this risk, too.

In summary, our approach may be of great interest for scientists in the field of experimental eye research.

References

Baulmann DC, Ohlmann A, Flügel-Koch C et al (2002) Pax6 heterozygous eyes show defects in chamber angle differentiation that are associated with a wide spectrum of other anterior eye segment abnormalities. Mech Dev 118:3–17

Branda CS, Dymecki SM (2004) Talking about a revolution: the impact of site-specific recombinases on genetic analyses in mice. Dev Cell 6:7–28

Braunger BM (2014) Molecular analysis of the neuroprotective role of Norrin for photoreceptors in the mammalian retina. http://epub.uni-regensburg.de/29296. Accessed 15 Jan 2014

Braunger BM, Ohlmann A, Koch M et al (2013a) Constitutive overexpression of Norrin activates Wnt/β-catenin and endothelin-2 signaling to protect photoreceptors from light damage. Neurobiol Dis 50:1–12

Braunger BM, Pielmeier S, Demmer C et al (2013b) TGF-β signaling protects retinal neurons from programmed cell death during the development of the mammalian eye. J Neurosci Off J Soc Neurosci 33:14246–14258

Hayashi S, McMahon AP (2002) Efficient recombination in diverse tissues by a tamoxifen-inducible form of Cre: a tool for temporally regulated gene activation/inactivation in the mouse. Dev Biol 244:305–318

Kim LA, Amarnani D, Gnanaguru G et al (2014) Tamoxifen toxicity in cultured retinal pigment epithelial cells is mediated by concurrent regulated cell death mechanisms. Invest Ophthalmol Vis Sci 55:4747–4758

Kühn R, Torres RM (2002) Cre/loxP recombination system and gene targeting. Methods Mol Biol Clifton NJ 180:175–204

Leenaars M, Hendriksen CFM (2005) Critical steps in the production of polyclonal and monoclonal antibodies: evaluation and recommendations. ILAR J Natl Res Counc Inst Lab Anim Resour 46:269–279

Leenaars M, Koedam MA, Hendriksen CFM et al (1998) Immune responses and side effects of five different oil-based adjuvants in mice. Vet Immunol Immunopathol 61:291–304

Maddison K, Clarke AR (2005) New approaches for modelling cancer mechanisms in the mouse. J Pathol 205:181–193

Seitz R, Tamm ER (2014) Müller cells and microglia of the mouse eye react throughout the entire retina in response to the procedure of an intravitreal injection. Adv Exp Med Biol 801:347–353

Soriano P (1999) Generalized lacZ expression with the ROSA26 Cre reporter strain. Nat Genet 21:70–71

Chapter 67
Distinct Expression Patterns of AAV8 Vectors with Broadly Active Promoters from Subretinal Injections of Neonatal Mouse Eyes at Two Different Ages

Wenjun Xiong and Constance Cepko

Abstract The retinal expression patterns were analyzed following the injection of serotype 8 adeno-associated virus (AAV8) vectors that utilize two broadly active and commonly used sets of transcription regulatory sequences. These include the human cytomegalovirus (CMV) immediate early (IE) enhancer/promoter and the hybrid CAG element (also known as CAGGS or CBA) composed of a partial human CMV IE enhancer and the chicken β-actin promoter and intron. Subretinal delivery to postnatal day 0 (P0) or 6 (P6) mouse eyes resulted in efficient labeling of retinal cells, but with very distinct patterns. With P0 delivery, AAV8-CMV-GFP selectively labelled photoreceptors, while AAV8-CAG-GFP efficiently labeled both outer and inner retinal neurons, including photoreceptors, horizontal cells, amacrine cells and retinal ganglion cells. With P6 delivery, both vectors led to efficient labeling of photoreceptors and Müller glia cells, but not of inner retinal neurons. Our results suggest that the cell types that express the genes encoded by subretinally delivered AAV8 vectors are determined by both the timing of the injection and the regulatory sequences.

Keywords AAV8 · Subretinal injection · Neonatal mouse eye · Cellular tropism · Transgene expression · Human cytomegalovirus (CMV) immediate early (IE) enhancer/promoter · Chicken β-actin promoter/enhancer/intron

C. Cepko (✉)
Departments of Genetics and Ophthalmology, Howard Hughes Medical Institute, Harvard Medical School, 77 Avenue Louis Pasteur, NRB 360, Boston, MA 02115, USA
e-mail: cepko@genetics.med.harvard.edu

W. Xiong
Departments of Genetics and Ophthalmology, Howard Hughes Medical Institute, Harvard Medical School, 77 Avenue Louis Pasteur, NRB 360, Boston, MA 02115, USA
e-mail: wjxiong@genetics.med.harvard.edu

C. Bowes Rickman et al. (eds.), *Retinal Degenerative Diseases,* Advances in Experimental Medicine and Biology 854, DOI 10.1007/978-3-319-17121-0_67

67.1 Introduction

In recent years, adeno-associated virus (AAV) vectors have been widely used for ocular gene transfer. It has been shown that the labeling pattern of retinal cell types is determined by several factors, including the AAV serotype, administration route (intravitreal vs. subretinal) and timing (neonatal vs. adult), as well as the regulatory sequences used. Although cell type-specific regulatory elements of human origin are ideal for clinical applications, composite elements, such as CMV (human CMV IE enhancer/promoter/human β-globin intron) and CAG (human CMV IE enhancer/chicken β-actin promoter/intron with rabbit β-globin 3' splice site, also called the CBA or CAGGS promoter) (Boshart et al. 1985; Niwa et al. 1991), are useful for robust and long-term transgene expression in a broad range of cell types in preclinical animal studies. Here we report on the labeling patterns from these two broadly active sets of elements in AAV8 vectors following subretinal delivery at two different ages. The expression patterns from these vectors changed dramatically when they were delivered at P0 vs. P6, demonstrating that the timing of injection during neonatal eye development is an important determinant of the expression patterns within retinal cell types. These changes in expression patterns may reflect the fate of AAV genomes when delivered to mitotic vs. postmitotic cells.

67.2 Materials and Methods

67.2.1 AAV Vector Construction and Production

AAV-CMV-GFP was constructed by cloning GFP cDNA from a pCAG-GFP vector (Addgene plasmid 11150 (Matsuda and Cepko 2004)) via EcoR1/Not1 sites into an AAV-MCS8 vector, which was obtained from HMS DF/HCC DNA resource core. The AAV-CMV-GFP construct contains a human CMV enhancer/promoter, human β-globin intron, GFP cDNA, SV40 polyA signal. AAV-CAG-GFP was constructed by replacing the CMV promoter with the CAG promoter from pCAG-GFP via Spe1/EcoR1. The AAV-CAG-GFP construct contains partial human CMV IE enhancer, chicken β-actin promoter, a hybrid intron composed of a chicken β-actin 5' splice site and rabbit β-globin 3' splice site with the majority of the intron deriving from the chicken β-actin intron 1, GFP cDNA, woodchuck hepatitis virus posttranscriptional regulatory element, and SV40 polyA. AAV8 vectors were produced by triple transfection of 293T cells (AAV vector, Rep2/Cap8, and pHGTI-adeno1 helper plasmids), purified based on published method (Vandenberghe et al. 2010), titered by RT-PCR, and diluted to 5×10^{12} genome copies (gc)/ml in PBS.

67.2.2 Animals and AAV Injection

Timed pregnant E18 *CD1* animals were ordered from Charles River Laboratory. Subretinal injection of P0 and P6 eyes was performed as described (Matsuda and Cepko 2004; Wang et al. 2014). A preset volume of virus (~0.3 µl) was delivered by the Femtojet (Eppendorf).

67.2.3 Histology and Imaging

At 15 days post injection, retinas were processed for immunohistochemistry as described (Matsuda and Cepko 2004; Wang et al. 2014). Antibodies used in this study included goat anti-ChAT (Millipore, 1:100) and Cy3 anti-goat (Jackson Immuno, 1:1000).

67.3 Results

67.3.1 Distinct Patterns of GFP Expression from AAV8-CMV-GFP and AAV8-CAG-GFP Following Subretinal Injection into P0 Mouse Eyes

CMV and CAG are two commonly used broadly active sets of regulatory elements that drive robust gene expression in a broad spectrum of cell types. Although these elements have been evaluated in the past for their expression in the retina in the context of AAV vectors (Allocca et al. 2007; Watanabe et al. 2013), a comparison of the patterns following injection at P0 has not been reported. P0 subretinal injections allow for fairly uniform spread of an inoculum throughout the entire retina, presumably as the photoreceptor outer segments have not yet developed, and thus their interactions with the retinal pigment epithelium (RPE) have not created a barrier to the spread of the inoculum. We evaluated the activities of these promoters in AAV8 vectors for retina transduction (Fig. 67.1a). AAV8-CMV-GFP or AAV8-CAG-GFP vectors at a dose of $\sim 1.5 \times 10^9$ gc/eye were injected subretinally into P0 *CD1* mouse eyes, and retinas were harvested 15 days after virus injection. Bright GFP signal was observed from nearly all retinas under a dissecting fluorescent microscope, demonstrating that the early mouse retina is quite susceptible to infection and expression from these vectors (Fig. 67.1b). About 90% of the eyes examined appeared to have nearly the entire retina expressing GFP, at least some cells throughout indicating that the inoculum can indeed spread readily throughout the subretinal space when delivered at P0.

Retinal sections were processed and imaged for direct GFP fluorescence. We found that AAV8-CMV-GFP and AAV8-CAG-GFP resulted in distinct patterns of GFP expression. AAV8-CMV-GFP mainly resulted in labelled photoreceptor cells

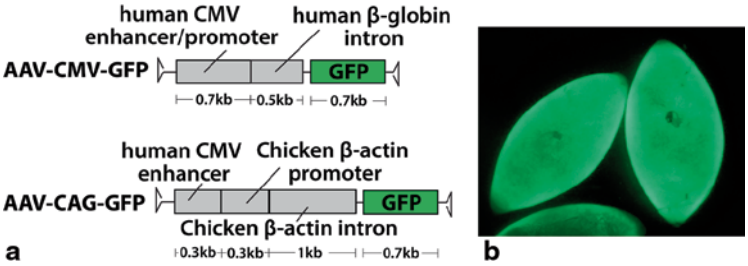

Fig. 67.1 **a** Illustrations of AAV-CMV-GFP and AAV-CAG-GFP constructs. **b** The native GFP fluorescence of the retinas transduced by AAV8-CMV-GFP with P0 subretinal injection. Retinas were harvested 15 days post infection

in the outer nuclear layer (ONL), with very few cells expressing GFP in the inner nuclear layer (INL) and ganglion cell layer (GCL) (Fig. 67.2a). In contrast, AAV8-CAG-GFP led to expression in many retinal cells in the ONL, INL, and GCL (Fig. 67.2b). In AAV8-CMV-GFP infected retinas, cones were the most efficiently and brightly labelled, while rods expressed a modest level of GFP (Fig. 67.2c). The inner, more vitreal, rods were more obviously labeled than the outer rods. In AAV8-CAG-GFP infected retinas, the cell types that expressed GFP included rods, cones, horizontal cells, amacrine cells, and ganglion cells (Fig. 67.2d). ChAT antibody staining showed that most cholinergic amacrine cells were transduced by AAV8-CAG-GFP (data not shown). As RPE cells were not included in the analysis, we cannot compare the labeling efficiency by these two vectors in the RPE. In summary, AAV8-CMV-GFP resulted in efficient labeling of photoreceptors, while AAV8-CAG-GFP provided a broader labeling pattern.

67.3.2 The Timing of Subretinal Injections in Neonatal Animals Yields Different Labelling Patterns

Next we examined the expression patterns following subretinal injection of the same AAV8 vectors at P6. At 15 days post infection, retinas were harvested and analyzed. Both vectors resulted in efficient transduction of photoreceptors and Müller glia cells, a pattern that is different from those following P0 injections (Fig. 67.2e, f).

67.4 Discussion

We found that the CMV and CAG elements drive different expression patterns of a GFP reporter in retinal cells when used in AAV8 vectors and delivered subretinally at P0. Because AAV8-CMV-GFP and AAV8-CAG-GFP vectors were packaged using the same AAV8 capsids, the different expression patterns are due to the activities of the regulatory elements. The fact that AAV8-CAG-GFP results in efficient expression of cells in the ONL, INL, and GCL demonstrates that AAV8 virions can

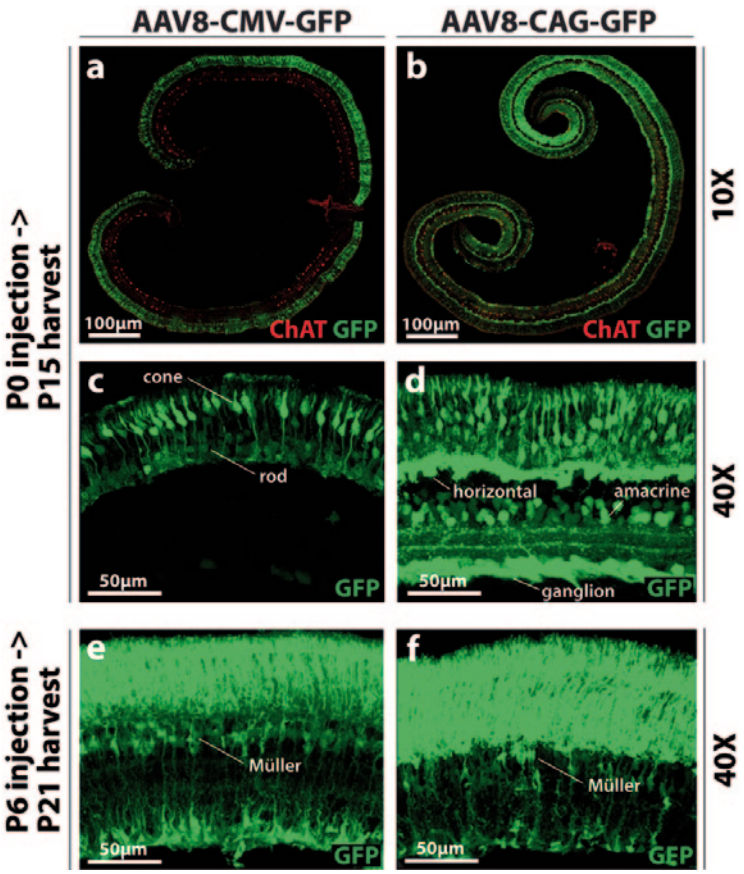

Fig 67.2 The entire cross sections of AAV8-CMV-GFP **(a)** and AAV8-CAG-GFP (**b**) P0 infected eyes. Retinal sections were imaged for native GFP signal (*green*) and Cy3 for ChAT staining (*red*), which highlighted laminae 2&4 in the INL. **c–d** Higher magnification images of the retinas shown in **a–b**. Representative cell types that were efficiently infected and expressed GFP are labeled. **e–f** Higher magnification images of retinal sections from P6 infected and P21 harvested retinas. In both groups of retinas, photoreceptors and Müller glia were efficiently transduced

diffuse across the retina to infect the innermost cells. The fact that no GFP signal was observed in these cell types following AAV8-CMV-GFP P0 subretinal infection must be a reflection of the regulatory elements in this vector. This is consistent with the previous reports that the CMV element has more variability in expression than other broadly active elements and that it is silenced in some cell types (Qin et al. 2010). Although the term "promoter" is often used to describe these elements, it is worth noting that not only the promoter sequence, but also the intron and splice sequences, differ among these vectors. In the CAG vector, the majority of the intron is from the chicken β-actin intron 1, which is thought to include enhancer activity (Niwa et al. 1991). In the CMV vector, the intron and splice sites were taken from human β-globin intron b region. Furthermore, the human CMV IE enhancer in the CAG vector is a short version (~360 bp) of the one used in the CMV vector

(~700 bp). Any or all of these differences might contribute to the different expression patterns noted between these two vectors.

In addition to the differences in the patterns seen using the two sets of regulatory sequences, the timing of the subretinal injection resulted in a fairly dramatic difference in the final expression patterns. One developmental difference that may, at least in part, be responsible for these observations concerns the access of the virions to the inner retina. P6 subretinal injections of either AAV8-CMV-GFP or AAV8-CAG-GFP resulted in efficient GFP expression in photoreceptors and Müller glial cells, but not in inner retinal neurons. Müller glia are born postnatally, and form the outer limiting membrane (OLM). Although the timing of formation of the OLM has not been specifically tracked in mice, it may be at least partially in place by P5 (Uga and Smelser 1973). The OLM may restrict the diffusion of AAV to the inner retina, but allow access of AAV to photoreceptors, which have their developing inner/outer segments protruding beyond the OLM. Similarly, Müller glia may be infected through their OLM processes. Higher titer inoculations, or viruses with other capsids, may produce more infection of the INL, but were not tested here.

AAV injection relative to a cell's last cell cycle may also be important in determining the expression pattern. Transgene expression may be different following introduction into mitotic vs. postmitotic cells. Given that AAV does not replicate, and the vector form integrates with a very low efficiency into the host cell's genome (McCarty et al. 2004), an AAV genome will be passed on to only one daughter cell in each cell cycle. It might be the case that an initially infected postmitotic cell retains many or all of the AAV genomes delivered by the inoculum, but the daughters of mitotic cells receive a diluted number of AAV genomes. This may explain why cones, horizontal, and retinal ganglion cells have the highest GFP expression level in AAV8-CAG-GFP P0 infected retinas, as these cells are postmitotic by P0. This is also in keeping with the curious finding that inner rods, relative to outer rods, express GFP more highly following infection at P0. Birthdating studies have shown that the inner rods are born before or at P0-P1, while the majority of the outer rods are born after P0 (Young 1985). Both inner and outer rods express GFP equally well following P6 infection, so there is no intrinsic difference between them regarding their use of the viral regulatory sequences. The fate of the AAV genome in mitotic may also differ from its fate in postmitotic cells. Silencing, or destruction of the genome, are additional possibilities for the lack of GFP expression in the descendants of infected mitotic cells.

One additional aspect of the expression patterns to be considered is the absence of expression in bipolar cells using either vector and infection time. This could be due to a lack of diffusion of virions to bipolar cells at P6, and/or a lack of a receptor on bipolar cells for AAV8, and/or lack of activity of the regulatory elements in bipolar cells. We have noted that CMV-based plasmids do not express as highly in bipolar cells as they do in Müller glia when plasmids are delivered by electroporation into retinal progenitor cells, suggesting a limitation in the strength of these elements in bipolar cells (Matsuda and Cepko 2004). Moreover, AAV8 vectors with a Grm6 promoter, which is active in ON-bipolar cells, can express in bipolar cells when delivered to adult murine retinas from intravitreal injections, when the capsid

has a tyrosine mutation in the capsid (Doroudchi et al. 2011). This mutation presumably reduces proteosomal degradation of the capsid in bipolar cells and thus may result in a higher copy number of AAV genomes in bipolar cells. Recent reports have shown improved expression of AAV-encoded genes in bipolar cells following intravitreal injection in adults. These vectors had changes in the capsid (Cronin et al. 2014; Macé et al. 2014) and improvements in the regulatory elements that were more active in bipolar cells (Cronin et al. 2014). These findings indicate that both infection and expression in bipolar cells need to be addressed for efficient expression, at least from intravitreal injections, and this may well be true for successful expression in bipolar cells following subretinal injections as well.

References

Allocca M, Mussolino C, Garcia-Hoyos M et al (2007) Novel adeno-associated virus serotypes efficiently transduce murine photoreceptors. J Virol 81:11372–11380

Boshart M, Weber F, Jahn G et al (1985) A very strong enhancer is located upstream of an immediate early gene of human cytomegalovirus. Cell 41:521–530

Cronin T, Vandenberghe LH, Hantz P et al (2014) Efficient transduction and optogenetic stimulation of retinal bipolar cells by a synthetic adeno-associated virus capsid and promoter. EMBO Mol Med 6(9):1175–1190

Doroudchi MM, Greenberg KP, Liu J et al (2011) Virally delivered channelrhodopsin-2 safely and effectively restores visual function in multiple mouse models of blindness. Mol Ther 19:1220–1229

Macé E, Caplette R, Marre O et al (2015) Targeting channelrhodopsin-2 to ON-bipolar cells with vitreally administered AAV restores ON and OFF visual responses in blind mice. Mol Ther 23(1):7–16

Matsuda T, Cepko CL (2004) Electroporation and RNA interference in the rodent retina in vivo and in vitro. Proc Natl Acad Sci USA 101:16–22

McCarty DM, Young SM, Samulski RJ (2004) Integration of adeno-associated virus (AAV) and recombinant AAV vectors. Annu Rev Genet 38:819–845

Niwa H, Yamamura K, Miyazaki J (1991) Efficient selection for high-expression transfectants with a novel eukaryotic vector. Gene 108:193–199

Qin JY, Zhang L, Clift KL et al (2010) Systematic comparison of constitutive promoters and the doxycycline-inducible promoter. PLoS One 5:e10611

Uga S, Smelser GK (1973) Electron microscopic study of the development of retinal Müllerian cells. Invest Ophthalmol 12:295–307

Vandenberghe LH, Xiao R, Lock M et al (2010) Efficient serotype-dependent release of functional vector into the culture medium during adeno-associated virus manufacturing. Hum Gene Ther 21:1251–1257

Wang S, Sengel C, Emerson M et al (2014) The binary decision of rod and bipolar fate in the vertebrate retina is controlled by a gene regulatory network. Dev Cell 30:513–527

Watanabe S, Sanuki R, Ueno S et al (2013) Tropisms of AAV for subretinal delivery to the neonatal mouse retina and its application for in vivo rescue of developmental photoreceptor disorders. PLoS One 8:e54146

Young RW (1985) Cell differentiation in the retina of the mouse. Anat Rec 212:199–205

Chapter 68
Characterization of Ribozymes Targeting a Congenital Night Blindness Mutation in Rhodopsin Mutation

Shannon M. Conley, Patrick Whalen, Alfred S. Lewin and Muna I. Naash

Abstract The G90D mutation in the rhodopsin gene leads to autosomal dominant congenital stationary night blindness (CSNB) in patients. This occurs because the G90D mutant protein cannot efficiently bind chromophore and is constitutively active. To combat this mutation, we designed and characterized two different hammerhead ribozymes to cleave G90D transcript. *In vitro* testing showed that the G90D1 ribozyme efficiently and specifically cleaved the mutant transcript while G90D2 cleaved both WT and mutant transcript. AAV-mediated delivery of G90D1 under the control of the mouse opsin promoter (MOP500) to G90D transgenic eyes showed that the ribozyme partially retarded the functional degeneration (as measured by electroretinography [ERG]) associated with this mutation. These results suggest that with additional optimization, ribozymes may be a useful part of the gene therapy knockdown strategy for dominant retinal disease.

Keywords Rhodopsin · G90D · Gene therapy · Ribozyme · Retinal degeneration · Congenital stationary night blindness

M. I. Naash (✉) · S. M. Conley
Department of Cell Biology, University of Oklahoma Health Sciences Center, 940 Stanton L. Young Blvd. BMSB 781, Oklahoma City, OK 73104, USA
e-mail: muna-naash@ouhsc.edu

S. M. Conley
e-mail: Shannon-conley@ouhsc.edu

Patrick Whalen · Alfred S. Lewin
Department of Molecular Genetics and Microbiology, University of Florida, Gainesville, FL 32611, USA

Alfred S. Lewin
e-mail: lewin@ufl.edu

C. Bowes Rickman et al. (eds.), *Retinal Degenerative Diseases,* Advances in Experimental Medicine and Biology 854, DOI 10.1007/978-3-319-17121-0_68

68.1 Introduction

Mutations in the rhodopsin gene cause both retinitis pigmentosa and CSNB. The dominant nature of these diseases means that gene therapy is likely to require knockdown of the mutant allele in addition to supplementation with the wild-type (WT) allele. One knockdown approach employs ribozymes which cleave RNAs in a site-specific manner (e.g. (Lewin et al. 1998; Shaw et al. 2006)). Hammerhead ribozymes recognize the substrate sequence on either side of an NUX cleavage site by means of two flanking arms that hybridize to the substrate RNA. Cleavage occurs with variable efficiency at the 3′ end of the NUX site, where N = any nucleotide, and X = any nucleotide except G (Shimayama et al. 1995).

Our goal was to develop an effective ribozyme targeted to the G90D CSNB mutation. This mutation results in a constitutively active rhodopsin protein and suppresses rod sensitivity (Rao et al. 1994; Naash et al. 2004). Patients with the G90D mutation experience largely stationary night blindness with retinal degeneration occurring only late in life (Sieving et al. 1995). To study G90D-associated disease we generated transgenic mice carrying the G90D mutation (Naash et al. 2004). Because overexpression of rhodopsin protein is toxic to photoreceptors (Tan et al. 2001), we identified a transgenic line which expresses normal amounts of total rhodopsin protein. These mice exhibit reduction of scotopic a- and b-wave amplitudes by 4 weeks of age. However, as in patients, retinal degeneration is not present in transgenic mice until later ages: progressive thinning of the photoreceptor layer is first detectable at ~4 months of age (Naash et al. 2004). Here we generate and characterize hammerhead ribozymes targeting the G90D mutant opsin transcript and assess their ability to retard functional losses in G90D transgenic animals.

68.2 Materials and Methods

68.2.1 Generation of Ribozyme Constructs and Target Oligonucleotide

Ribozymes and target oligonucleotides were generated as described previously (Partono and Lewin 1991; Fritz et al. 2004). Sequences were as follows: *G90D1 ribozyme:* sense strand-5′CCG GGA TCC GTC GTA ACT GAT GAG CCG CTT CGG C, and antisense strand-5′GCC ACG CGT CGG AGA TTT CGC CGC CGA AGC GG, *G90D2 ribozyme:* sense strand-5′CGG GAA TTC ATC TCC CTG ATG ACG GCG AAA GCC GGA AAA GAC CAC GCG TCG G, antisense strand-5′CCG ACG CGT GGT CTT TTC CGG CTT TCG CCG TCA TCA GGG AGA TGA ATT CCC G, *mutant G90D1 RNA oligonucleotide*: 5′GGA GAU UUU ACG AC, *wild-type (WT) G90D1*: 5′GGA GGA UUC ACC AC, *mutant G90D2*: 5′UGG UCU UCG GAG AUU, *WT G90D2*: 5′UGG UCU UCG GAG GAU.

68.2.2 In Vitro Cleavage Reactions

Ribozyme cleavage reactions were performed as described previously (Drenser et al. 1998; Fritz et al. 2004). For time course experiments, ribozyme was diluted to 20 nM and a volume of 40 µL, while the substrate was diluted to 400 nM and a volume of 50 µL. Aliquots of 5 µL were taken at various intervals. In order to determine kinetic parameters, the final concentration of ribozyme was kept constant at 10 nM while the concentration of target RNA ranged from 40 to 180 nM.

68.2.3 Total Retinal RNA Extraction and Cleavage

RNA was prepared from mouse retinas according to manufacturer's instructions using Trizol (Life Technologies, Grandview, NY). Briefly, ~6 µg of total RNA was incubated with 600 nM ribozyme and RNase inhibitor at 37 °C. Reverse transcription was performed with β-actin primer or a mouse opsin primer. The product was amplified by PCR with β-actin/opsin primers. When the PCR reaction finished, 10 µCi of [α-^{32}P] ATP was added and an additional cycle was carried out followed by digest with NcoI which enables differentiation of WT vs. mutant transcript.

68.2.4 Recombinant AAV Ribozyme Constructs

G90D1 was cloned into a recombinant AAV construct based on the pTR-UF2 vector. The ribozyme was expressed from the MOP500 promoter (Flannery et al. 1997). In control AAVs the ribozyme was replaced by GFP, allowing transduction efficiency to be determined. DNA constructs were packaged into AAV particles as in (Lewin et al. 1998).

68.2.5 Animals Experiments

All animal procedures were approved by the Institutional Care and Use Committee, and conformed to guidelines set forth by the Association for Research in Vision and Ophthalmology. G90D transgenic animals (line $G_{0.5/86}$ (Naash et al. 2004)) on the rhodopsin heterozygous background (*rho*$^{+/-}$) or WT (*rho*$^{+/+}$) were used. Mice were maintained under a 14L:10D cycle (~7 foot-candles). Mice were anesthetized with ketamine (60 mg/kg) and xylazine (8 mg/kg) and dilated with phenylephrine and tropicamide. A 30G needle was guided through sclera and choroid until the needle tip was seen in the intravitreal space. 2–3 µl of AAV-G90D ribozyme or AAV-GFP were given (10^{12} vector particles/mL). For ERG, animals were dark-adapted overnight and anesthetized/dilated as above. Full-field ERG responses were measured at flash intensities ranging from −3.01 to 1.02 log-cd/s m^2.

68.3 Results

68.3.1 *In Vitro Characterization of Catalytic Activity of G90D Ribozymes*

Two ribozymes targeting the G90D transcript were designed. G90D1 targeted an AUU cleavage triplet created by the G90D mutation (Fig. 68.1a). G90D2 targeted a UUC cleavage triplet (known to be more efficiently cleaved than AUU) just upstream of the mutation which should cleave mutant but not WT mRNA due to mismatched base pairs disrupting the hybridization of the ribozyme arm to the substrate (Joseph et al. 1993). The rates of cleavage and specificity were measured by incubating ribozymes with radiolabeled RNA oligonucleotides corresponding to either the G90D mutant or WT RNA. For G90D1, the amount of cleaved product (bottom band Fig. 68.1b) increased linearly for the duration of the experiment with 10 % of the substrate cleaved by 12 h, and cleavage was specific to the mutant RNA. Although G90D2 cleaved the mutant RNA substrate more efficiently than G90D1 (10 % cleavage in 4 h, not shown), it also cleaved the WT substrate. Due to this lack of specificity, G90D2 was not examined further.

To ensure cleavage of RNA substrates *in vivo*, it is important to design ribozymes with the highest possible catalytic activity. This requires the determination

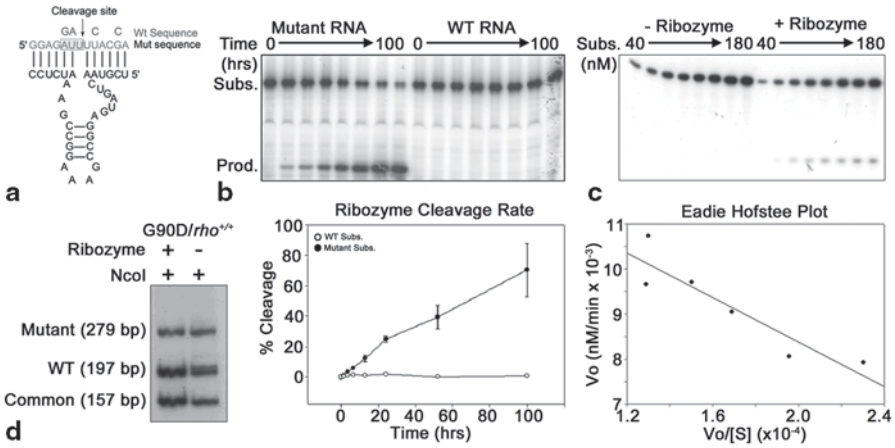

Fig. 68.1 Characterization of G90D1 ribozyme. **a** The sequence of the G90D1 ribozyme. **b** Representative autoradiogram showing that the G90D1 hammerhead ribozyme cleaves [32P]-labled mutant but not *WT RNA* oligonucleotide. The substrate (Subs.) is 13 nucleotides and the product (Prod.) is 7 nucleotides. *Bottom* panel quantifies the time courses of the cleavage reaction. **c** Kinetic analysis was performed after 12 h with constant ribozyme and varying concentrations of substrate. *Bottom* panel shows the Eadiee-Hofstee plot used to calculate the kinetic coefficients. **d** *RNA* prepared from G90D/rho$^{+/+}$ retinas underwent treatment with ribozyme for 48 h followed by RT-PCR using opsin primers and digestion with NcoI. All experiments were repeated at least three times

of the turnover number (k_{cat}) and Michaelis constant (K_M) of the ribozymes. Here we measured cleavage at 12 h using 10 nM ribozyme and substrate concentrations ranging from 40 to 180 nM (Fig. 68.1c). Product was first detected when ribozyme was incubated with 80 nM substrate, and the ribozyme was saturated at a substrate concentration of approximately 160 nM. Eadie-Hofstee analysis showed that the G90D1 ribozyme had a K_M of 24 nM, **a** k_{cat} of 1.33×10^{-3}/min, and an efficiency (k_{cat}/K_M) of 5.5×10^4 min^{-1} M^{-1}.

68.3.2 *In Vivo Cleavage of G90D Substrate in the Presence of WT Rhodopsin*

Next we determined whether G90D1 ribozyme cleaved G90D mutant transcript in the presence of the WT. We prepared RNA from G90D/*rho*$^{+/-}$ retinas (in which the ratio of transgene:WT opsin message is 1:1). After incubation of retinal RNA with G90D1 ribozyme, RT-PCR was used to amplify from the rhodopsin gene (or β-actin as a control). The WT opsin amplicon contains two NcoI sites, one of which is ablated in the transgene. As a result, digest with NcoI results in the formation of 279 bp and 157 bp bands from the transgenic transcript, and 197, 157, and 80 bp (not shown on the gel) bands arising from the WT transcript. Examination of the ratio of the 279:197 bands in ribozyme treated vs. untreated samples showed that ~66% of the mutant transgene was specifically degraded (Fig. 68.1d) in 48 h with no ribozyme-mediated degradation of the WT.

68.3.3 *Phenotypic Benefit of G90D Ribozymes In Vivo*

We next asked whether the G90D1 ribozyme provided therapeutic benefit when delivered to the G90D mouse model of CNB. Photoreceptor-specific MOP500-G90D1 and MOP500-GFP (as a control) constructs were formulated into rAAVs. G90D/*rho*$^{+/-}$ animals were intravitreally injected at 4 weeks of age. We observed GFP-positive cells distributed diffusely throughout the retina after confirming transduction of retinal cells. GFP-positive cells were first detected at PI-6 weeks and remained evident up to 10 months.

Animals next underwent scotopic ERG. At PI-6 weeks, there was no difference between the AAV-G90D1 and AAV-GFP eyes after intravitreal injection (Fig. 68.2a). However, at both 3 and 8 months after injection, mean scotopic b-waves in AAV-G90D1-treated eyes were increased by ~25 and ~66% (respectively) at the highest light intensity compared to AAV-GFP controls (Fig. 68.2b, c). The sample size was too small to detect statistically significant differences between individual pairs of data points, however, regression analysis of log light intensity vs. mean b-wave amplitude indicated that the slopes were significantly different between AAV-GFP and AAV-G90D1 at PI-3 and PI-8 months ($P = 0.018$, and $P = 0.00024$, respectively) suggesting that the G90D1 ribozyme is capable of preserving ERG function in G90D mice.

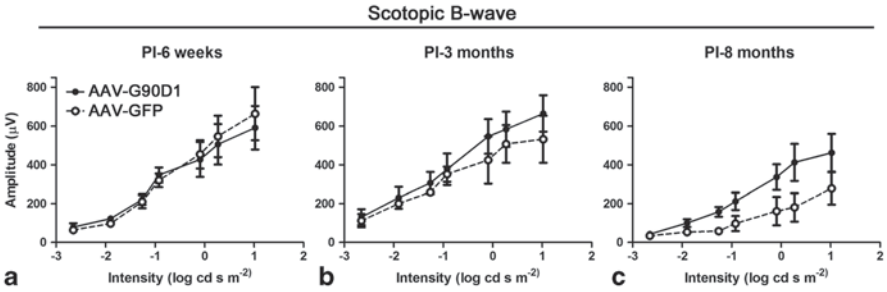

Fig. 68.2 Functional improvements after *in vivo* delivery of *G90D1* ribozyme. *G90D1* ribozyme was packaged in r*AAV* and delivered via intravitreal injection. **a–c.** Shown are mean scotopic b-wave amplitudes after full-field ERG at the indicated timepoints. $N = 2–5$/group

68.4 Discussion

Here we identified a ribozyme that specifically cleaved the mutant G90D allele. We used two different strategies during the design process: the G90D1 ribozyme targets a cleavage triplet (AUU) found only in the mutant allele, while the G90D2 ribozyme targets a cleavage triplet found in both the mutant and WT alleles (UUC) but which is close enough to the mutation that the two most distal nucleotides in one of the hybridizing arms were specific to the mutant allele. Two noteworthy observations arose from comparison of these two ribozymes. The first is that in spite of the mismatches in the hybridizing arm between G90D2 and the WT substrate, the WT was cleaved as efficiently as the mutant. This is consistent with previous work showing that mismatches in the regions of the hybridizing arms closer to the cleavage site are more effective for preventing binding between the ribozyme and the substrate (Joseph et al. 1993). Secondly, the UUC triplet is cleaved 9.4 times more efficiently than the AUU triplet (Shimayama et al. 1995). However, comparison of the time it took each ribozyme to cleave 10% of its substrate under similar conditions showed that the G90D2 ribozyme was only three times more efficient than the G90D1 ribozyme suggesting that more factors than the cleavage triplet affect ribozyme efficiency.

Although our goal here was specific knockdown of the G90D transcript, allele-independent knockdown is a popular strategy for dominant disease genes, including rhodopsin. This approach involves the development of a knockdown vector which targets both the mutant and WT allele and is usually coupled with concurrent supplementation of a knockdown-resistant WT gene. This approach has been tested with multiple knockdown strategies (e.g. (Gorbatyuk et al. 2007a, b)). It has the dual benefits of enabling design of an optimal ribozyme without reference to the location of the mutation and of targeting multiple different disease causing mutations with the same therapeutic. For a gene with as many disease causing mutations as rhodopsin, this is a striking benefit, so testing of this therapeutic approach is ongoing.

We showed that the G90D1 ribozyme effectively slowed the long-term loss of ERG function associated with the G90D transgene. Interestingly, although ERGs in this model are reduced (compared to WT) as early as 4 weeks of age, we did not see benefits of G90D1 until 3 and 9 months post-injection. The time course of this outcome suggests that the ribozyme-mediated knockdown may slow photoreceptor cell loss; however confirmation of this must await histological study. In conclusion these results suggest that ribozymes can be used to knockdown mutant alleles and provide some therapeutic benefit. With additional optimization, they may be a useful addition to our repertoire of knockdown technologies for dominant genetic diseases.

Acknowledgments The authors thank Dr. Bienvenido Castillo for his technical assistance and Dr. William Hauswirth for assistance preparing the AAVs. This work was supported by the NIH (EY022778 and EY018656-MIN), the Foundation Fighting Blindness (MIN) the Oklahoma Center for the Advancement of Science and Technology (SMC) and the Knights Templar Eye Foundation (SMC).

References

Drenser KA, Timmers AM, Hauswirth WW et al (1998) Ribozyme-targeted destruction of RNA associated with autosomal-dominant retinitis pigmentosa. Invest Ophthalmol Vis Sci 39:681–689

Flannery JG, Zolotukhin S, Vaquero MI et al (1997) Efficient photoreceptor-targeted gene expression in vivo by recombinant adeno-associated virus. Proc Natl Acad Sci U S A 94:6916–6921

Fritz JJ, Gorbatyuk M, Lewin AS et al (2004) Design and validation of therapeutic hammerhead ribozymes for autosomal dominant diseases. Methods Mol Biol 252:221–236

Gorbatyuk M, Justilien V, Liu J et al (2007a) Suppression of mouse rhodopsin expression in vivo by AAV mediated siRNA delivery. Vis Res 47:1202–1208

Gorbatyuk M, Justilien V, Liu J et al (2007b) Preservation of photoreceptor morphology and function in P23H rats using an allele independent ribozyme. Exp Eye Res 84:44–52

Joseph S, Berzal-Herranz A, Chowrira BM et al (1993) Substrate selection rules for the hairpin ribozyme determined by in vitro selection, mutation, and analysis of mismatched substrates. Genes Dev 7:130–138

Lewin AS, Drenser KA, Hauswirth WW et al (1998) Ribozyme rescue of photoreceptor cells in a transgenic rat model of autosomal dominant retinitis pigmentosa. Nat Med 4:967–971

Naash MI, Wu TH, Chakraborty D et al (2004) Retinal abnormalities associated with the G90D mutation in opsin. J Comp Neurol 478:149–163

Partono S, Lewin AS (1991) The rate and specificity of a group I ribozyme are inversely affected by choice of monovalent salt. Nucleic Acids Res 19:605–609

Rao VR, Cohen GB, Oprian DD (1994) Rhodopsin mutation G90D and a molecular mechanism for congenital night blindness. Nature 367:639–642

Shaw LC, Pan H, Afzal A et al (2006) Proliferating endothelial cell-specific expression of IGF-I receptor ribozyme inhibits retinal neovascularization. Gene Ther 13:752–760

Shimayama T, Nishikawa S, Taira K (1995) Generality of the NUX rule: kinetic analysis of the results of systematic mutations in the trinucleotide at the cleavage site of hammerhead ribozymes. Biochemistry 34:3649–3654

Sieving PA, Richards JE, Naarendorp F et al (1995) Dark-light: model for nightblindness from the human rhodopsin Gly-90→Asp mutation. Proc Natl Acad Sci U S A 92:880–884

Tan E, Wang Q, Quiambao AB et al (2001) The relationship between opsin overexpression and photoreceptor degeneration. Invest Ophthalmol Vis Sci 42:589–600

Chapter 69
Antisense Oligonucleotide Therapy for Inherited Retinal Dystrophies

Xavier Gerard, Alejandro Garanto, Jean-Michel Rozet and Rob W. J. Collin

Abstract Inherited retinal dystrophies (IRDs) are an extremely heterogeneous group of genetic diseases for which currently no effective treatment strategies exist. Over the last decade, significant progress has been made utilizing gene augmentation therapy for a few genetic subtypes of IRD, although several technical challenges so far prevent a broad clinical application of this approach for other forms of IRD. Many of the mutations leading to these retinal diseases affect pre-mRNA splicing of the mutated genes. Antisense oligonucleotide (AON)-mediated splice modulation appears to be a powerful approach to correct the consequences of such mutations at the pre-mRNA level, as demonstrated by promising results in clinical trials for several inherited disorders like Duchenne muscular dystrophy, hypercholesterolemia and various types of cancer. In this mini-review, we summarize ongoing pre-clinical research on AON-based therapy for a few genetic subtypes of IRD, speculate on other potential therapeutic targets, and discuss the opportunities and challenges that lie ahead to translate splice modulation therapy for retinal disorders to the clinic.

Keywords Antisense oligonucleotides · AON · CEP290 · Genetic therapy · Inherited retinal dystrophy · Splice correction · Splicing

R. W. J. Collin (✉)
Department of Human Genetics (855), Radboud Institute for Molecular Life Sciences, Radboud University Medical Center, Geert Grooteplein 10, Nijmegen, 6525 GA, The Netherlands
e-mail: rob.collin@radboudumc.nl

X. Gerard · J.-M. Rozet
Laboratory of Genetics in Ophthalmology, INSERM UMR1163-Imagine Institute, Paris Descartes - Sorbonne Paris Cité University 24 boulevard du Montparnasse, Paris, France
e-mail: xavier.gerard@inserm.fr

J.-M. Rozet
e-mail: jean-michel.rozet@inserm.fr

A. Garanto
Department of Human Genetics, Radboud Institute for Molecular Life Sciences, Radboud University Medical Center, Geert Grooteplein 10, Nijmegen, The Netherlands
e-mail: alex.garantoiglesias@radboudumc.nl

C. Bowes Rickman et al. (eds.), *Retinal Degenerative Diseases,* Advances in Experimental Medicine and Biology 854, DOI 10.1007/978-3-319-17121-0_69

69.1 Therapeutic Possibilities for Inherited Retinal Dystrophies

Inherited retinal dystrophies (IRDs) are a large and heterogeneous group of disorders, that, based on the age of onset, rate of progression, and the primary involvement of either rod or cone photoreceptor cells, can be subdivided into different subtypes (den Hollander et al. 2010). Mutations in more than 200 different genes have been reported to underlie one or more of the clinical subtypes of IRD, and this number is still growing (https://sph.uth.edu/retnet/). Although IRDs for a long time have been considered incurable diseases, recent progress in different areas now offers a number of therapeutic possibilities. As IRDs in general are progressive diseases due to the concomitant death of retinal cells, the most effective therapeutic strategy to a large extent will depend on the stage of the disease. With the primary genetic defect often affecting a gene expressed in the photoreceptor or retinal pigment epithelium (RPE) cells, directly correcting the consequences of these mutations, e.g. with gene therapy, only makes sense if there are sufficient photoreceptor or RPE cells left to treat (Boye et al. 2013; Sahel and Roska 2013). If not, other strategies can be applied, such as cell transplantation therapy (Stern and Temple 2014), optogenetics (Sahel and Roska 2013) or epi-/subretinal electronic implants (Stingl and Zrenner 2013). Each of these strategies has made tremendous progress over the last few years, and may ultimately be suitable for specific groups of IRD patients. On the short term however, the best improvement in visual function is expected in the field of genetic therapy, as here, the naturally existing photoreceptor or RPE cells are targeted.

The safety and efficacy reported in phase I/II clinical trials of a *RPE65* gene augmentation therapy, by subretinal delivery of adeno-associated viruses (AAVs) carrying the wild-type *RPE65* cDNA, have enormously boosted the field of ocular gene therapies (Bainbridge et al. 2008; Hauswirth et al. 2008; Maguire et al. 2008), and resulted in the development of similar approaches for other subtypes of IRD, with promising results (MacLaren et al. 2014). A severe limitation of this approach however is the limited packaging capacity (~4.9 Kb) of AAV-vectors. Several of the most frequently mutated IRD genes (e.g. *ABCA4, CEP290, EYS* and *USH2A*) have a cDNA size way exceeding this limit and hence are not amenable for AAV-based gene therapy. Other vectors (e.g. lentiviruses, adenoviruses) with a larger cargo capacity have a limited tropism for photoreceptor cells, and may produce insertional mutagenesis by integration into the host genome.

An alternative therapeutic strategy that can bypass these impediments, focuses on rescuing aberrant pre-mRNA processing rather than supplementing a healthy cDNA copy of a gene that is mutated. Antisense oligonucleotides (AONs) are small and versatile molecules that are complementary to their target mRNA, and as such can modulate pre-mRNA splicing or stability. Since a substantial amount of IRD-causing mutations also affects pre-mRNA splicing of the corresponding genes, AON-based therapy may be an attractive treatment strategy for IRDs.

69.2 Antisense Oligonucleotides: Structure, Function and Clinical Applications

Pre-mRNA splicing is an essential step in the production of a correct template for protein synthesis. This process is carried out by the spliceosome, and involves multiple interactions mediated by splicing factors that recognize regulatory elements in the target pre-mRNA molecules (Hastings and Krainer 2001). It is estimated that up to 50 % of disease-causing mutations affect pre-mRNA splicing (Disterer et al. 2014), with obvious consequences at the protein level. Thus, altering splicing offers an interesting therapeutic strategy for many genetic disorders (Hammond and Wood 2011).

Initially, AONs were used to inhibit gene expression by degrading the target mRNA through RNase-H mediated cleavage (Zamecnik and Stephenson 1978; Kurreck 2003). Subsequently, different generations of oligonucleotides have been developed, with chemical modifications to make them resistant to the RNase-H activity, increase their half-life and improve their binding affinity (Chan et al. 2006). A major class of AONs are those with a phosphorothioate backbone, and based on the chemistry 2′-O-methyl or 2′-O-methoxyethyl, or the phosphoramidate morpholino oligonucleotides (Chan et al. 2006; Disterer et al. 2014). These molecules have a high ability to interfere with splicing, either by masking splice sites, or by targeting regulatory sequences to promote or block splicing (Hammond and Wood 2011). A great advantage of this strategy is that the endogenous transcriptional regulation of the target gene is preserved.

Examples of AON-based therapies that have reached the clinic mainly focus on inducing exon skipping or insertion. The most advanced studies are several phase II clinical trials for Duchenne muscular dystrophy, where AONs are used to skip exons in order to restore the reading-frame of the *DMD* mRNA that is disrupted as a result of recurrent deletions (van Deutekom et al. 2007; Kinali et al. 2009; Cirak et al. 2011; Goemans et al. 2011; Koo and Wood 2013). Another phase I/II clinical trial utilizes AONs to induce the insertion of exon 7 of the *SMN2* gene in patients with spinal muscular atrophy (Zanetta et al. 2014), and for the treatment of patients with familial hypercholesterolemia, an AON targeting *APOB* has recently been approved as a drug in the US (Raal et al. 2010).

Besides monogenic disorders, AON-based therapies have also been developed to treat several cancer and inflammation disorders, such as chronic lymphocytic leukemia (Durig et al. 2011), acute myeloid leukemia (Erba et al. 2013), or psoriasis (Colin et al. 2014). All these studies denote the potential of AONs as a treatment strategy for a wide range of disorders, by showing beneficial effects in the patients with low toxicity and little inflammatory responses.

69.3 AON-based Therapy for Inherited Retinal Degenerations

Given the high therapeutic potential of AONs, plus the advantages of the eye as a therapeutic target organ, using AONs to treat certain genetic subtypes of IRD seems logical. An ideal candidate for AON-based therapy is a recurrent intronic mutation in *CEP290* (c.2991+1655A>G) that is causative for up to 15% of all LCA cases in the US and several European countries (den Hollander et al. 2006; Perrault et al. 2007; Stone 2007; Coppieters et al. 2010). This mutation activates a cryptic splice donor site that results in the insertion of a pseudo-exon with a premature termination codon to approximately 50–75 % of the *CEP290* transcripts (den Hollander et al. 2006; Gerard et al. 2012). We have shown that, in lymphoblastoid and fibroblast cells from LCA patients with a homozygous intronic *CEP290* mutation, administration of AONs targeting the pseudo-exon fully restores normal *CEP290* pre-mRNA splicing (Collin et al. 2012; Gerard et al. 2012) (Fig. 69.1a). In addition, AON treatment resulted in an increase in wild-type CEP290 protein levels and fully rescued a ciliary defect present in the patient fibroblast cell lines (Gerard et al. 2012), demonstrating the enormous potential of AON-based therapy for *CEP290*-associated LCA.

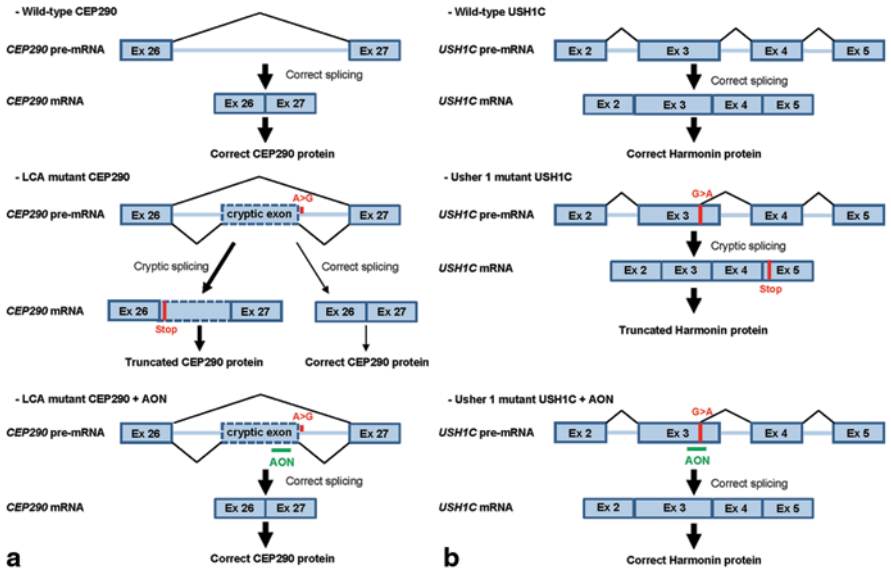

Fig. 69.1 AON-therapy for *CEP290*-associated LCA or *USH1C*-associated Usher syndrome. **a** A deep-intronic mutation in *CEP290* (c.2991+1655A>G, in *red*) results in the insertion of a pseudo-exon with a premature termination codon to part of *CEP290* mRNA. Administration of AONs (in *green*) blocks the recognition of the pseudo-exon and restores normal *CEP290* splicing (Collin et al. 2012; Gerard et al. 2012). **b** An exonic mutation in *USH1C* (c.216G>A) activates a new cryptic splice donor site that results in the insertion of a shorter fragment of exon 3 to *USH1C* mRNA, causing a frame-shift and premature termination of the harmonin protein encoded by *USH1C*. Administration of AONs (in *green*) blocks the cryptic splice donor site and restores normal *USH1C* splicing (Lentz et al. 2013)

Other deep-intronic mutations underlying IRD and that could be treated in a similar way include those in *ABCA4* (Braun et al. 2013; Zernant et al. 2014), *CHM* (van den Hurk et al. 2003), *OFD1* (Webb et al. 2012) and *USH2A* (Vache et al. 2012). Alternatively, AONs can be employed to skip (combinations of) exons that contain nonsense or frame-shift mutations, taking into account to leave the reading-frame intact, or to restore the reading-frame in case this is disrupted by large deletions encompassing one or more exons. This may particularly be beneficial for larger genes, as the shortened protein that results from exon skipping should still have some residual function as recently shown in CEP290-associated LCA (Drivas et al. 2015; Rozet and Gerard 2015). A third therapeutic approach involves restoring normal splicing in case exonic mutations activate cryptic splice sites within the exon. An illustrative example of this is a recurrent mutation in *USH1C* (c.216G>A), underlying Usher syndrome type 1C, a disease characterized by hearing impairment, vestibular dysfunction and retinal dystrophy. This mutation activates a cryptic splice donor site, resulting in a shortened mRNA and premature termination of the harmonin protein (Lentz et al. 2005). In a humanized mouse model carrying part of the human *USH1C* gene, including the c.216G>A mutation, systemic delivery of AONs targeting the exonic region with the mutation, resulted in an increase of correctly spliced *USH1C* transcripts and the rescue of the auditory and vestibular phenotype (Lentz et al. 2013) (Fig. 69.1b).

It is to be expected that several other exonic variants for which the potential pathogenicity is currently not well understood, may also affect pre-mRNA splicing of the corresponding gene. In addition, with transcriptome and whole genome sequencing emerging as widely-used tools to discover the remaining genetic causes of IRD, many other mutations that are amenable to AON therapy are likely identified in the coming years.

69.4 Future Perspective: Translating AON-based Therapies for IRD into the Clinic

An important question that remains is how to translate AON-based therapy for IRDs to the clinic. One crucial step entails identifying the right *in vitro* and *in vivo* models to assess the therapeutic efficacy. Many of the genes underlying IRD are predominantly or exclusively expressed in the retina, and hence it is often not possible to study these genes in easily accessible patient cells such as lymphoblasts or fibroblasts. The ability to generate photoreceptor-like cells *in vitro* via induced pluripotent stem cell technology offers opportunities in this area (Tucker et al. 2013). An alternative approach involves animal studies, aiming to show proof-of-principle in the retina *in vivo*. Since AON-therapy in general is considered to be a mutation-specific therapy, tailor-made models, e.g. mice need to be generated in order to mimic the exact human genotype and phenotype. Whereas in some cases, this works well (Lentz et al. 2013), in other cases the mouse splicing machinery fails to recognize cryptic splice sites or pseudo-exons, as was shown in a mouse model for the recurrent LCA-causing intronic *CEP290* mutation (Garanto et al. 2013). The

generation of other animal models more closely resembling humans is also challenging, although with novel gene editing strategies like CRISPR/Cas9 emerging, this will likely get easier in the near future (Hsu et al. 2014).

For the actual therapeutic intervention in patients, AONs have to be able to efficiently reach their target cells (e.g photoreceptors), without causing undesired side effects. Approaches of topically delivered oligonucleotides have not been successful so far to reach intraocular tissues, probably due to the impermeable nature of the cornea (Janoria et al. 2007). As mentioned earlier, a single intraperitoneal injection of AONs could rescue an auditory and vestibular phenotype in a mouse model for *USH1C* (Lentz et al. 2013), although no rescue of the retinal degeneration was mentioned in that model. Indeed, upon systemic drug delivery, it is hard to reach the desired effective concentration in the eye because of the blood-retina barrier (Lalezari et al. 1997), and obviously, this also increases the chances of side effects. Intraocular administration of AONs seems to be the best way to bypass these anatomical and physical obstacles. In humans, intravitreal injections of naked AONs have proven safety and efficacy to treat cytomegalovirus-induced retinitis in immunocompromized individuals (Tawse and Baumal 2014). Although these injections are common practice in the eye clinic to treat some chronic diseases, long-term therapeutic effects of AONs need to be improved in order to facilitate their clinical development. In this view, a virus-based delivery of AONs to retinal cells sounds appealing. Strategies using modified U7snRNA constructs containing AON sequences packaged into AAV vectors have been shown to be effective in cellular and animal models for Duchenne muscular dystrophy (Goyenvalle et al. 2004). With the increasing availability of multiple AAV serotypes that efficiently transduce the various cell types in the retina (Vandenberghe and Auricchio 2012), this strategy can become a powerful tool to modulate splicing in photoreceptor cells.

In conclusion, the applications of AON-based therapy for IRDs are just starting to emerge and show great promise, although some locks must be lifted to ensure their success. The private nature of many IRD-causing mutations poses a significant challenge on a broad implementation of splicing therapy, as safety and efficacy data need to be generated for each individual mutation. Identifying ways to deliver AONs to the retina in a safe and effective manner will be a major step forward in the pre-clinical development of AON-based therapies for IRD, and will reveal the true potential of this approach for restoring vision, or at least halting or slowing down disease progression.

References

Bainbridge JW, Smith AJ, Barker SS et al (2008) Effect of gene therapy on visual function in Leber's congenital amaurosis. N Engl J Med 358:2231–2239

Boye SE, Boye SL, Lewin AS et al (2013) A comprehensive review of retinal gene therapy. Mol Ther 21:509–519

Braun TA, Mullins RF, Wagner AH et al (2013) Non-exomic and synonymous variants in ABCA4 are an important cause of Stargardt disease. Hum Mol Genet 22:5136–5145

Chan JH, Lim S, Wong WS (2006) Antisense oligonucleotides: from design to therapeutic application. Clin Exp Pharmacol Physiol 33:533–540

Cirak S, Arechavala-Gomeza V, Guglieri M et al (2011) Exon skipping and dystrophin restoration in patients with Duchenne muscular dystrophy after systemic phosphorodiamidate morpholino oligomer treatment: an open-label, phase 2, dose-escalation study. Lancet 378:595–605

Colin S, Darne B, Kadi A et al (2014) The antiangiogenic insulin receptor substrate-1 antisense oligonucleotide aganirsen impairs AU-rich mRNA stability by reducing 14-3-3beta-tristetraprolin protein complex, reducing inflammation and psoriatic lesion size in patients. J Pharmacol Exp Ther 349:107–117

Collin RWJ, den Hollander AI, van der Velde-Visser S et al (2012) Antisense oligonucleotide (AON)-based therapy for leber congenital amaurosis caused by a frequent mutation in CEP290. Mol Ther Nucleic Acids 1:e14

Coppieters F, Lefever S, Leroy BP et al (2010) CEP290, a gene with many faces: mutation overview and presentation of CEP290base. Hum Mutat 31:1097–1108

den Hollander AI, Koenekoop RK, Yzer S et al (2006) Mutations in the CEP290 (NPHP6) gene are a frequent cause of Leber congenital amaurosis. Am J Hum Genet 79:556–561

den Hollander AI, Black A, Bennett J et al (2010) Lighting a candle in the dark: advances in genetics and gene therapy of recessive retinal dystrophies. J Clin Invest 120:3042–3053

van Deutekom JC, Janson AA, Ginjaar IB et al (2007) Local dystrophin restoration with antisense oligonucleotide PRO051. N Engl J Med 357:2677–2686

Disterer P, Kryczka A, Liu Y et al (2014) Development of therapeutic splice-switching oligonucleotides. Hum Gene Ther 25:587–598

Drivas TG, Wojno AP, Tucker BA et al (2015) Basal exon skipping and genetic pleiotropy: A predictive model of disease pathogenesis. Sci Transl Med 7:291ra97

Durig J, Duhrsen U, Klein-Hitpass L et al (2011) The novel antisense Bcl-2 inhibitor SPC2996 causes rapid leukemic cell clearance and immune activation in chronic lymphocytic leukemia. Leukemia 25:638–647

Erba HP, Sayar H, Juckett M et al (2013) Safety and pharmacokinetics of the antisense oligonucleotide (ASO) LY2181308 as a single-agent or in combination with idarubicin and cytarabine in patients with refractory or relapsed acute myeloid leukemia (AML). Invest New Drugs 31:1023–1034

Garanto A, van Beersum SE, Peters TA et al (2013) Unexpected CEP290 mRNA splicing in a humanized knock-in mouse model for Leber congenital amaurosis. PLoS One 8:e79369

Gerard X, Perrault I, Hanein S et al (2012) AON-mediated exon skipping restores ciliation in fibroblasts harboring the common leber congenital amaurosis CEP290 mutation. Mol Ther Nucleic Acids 1:e29

Goemans NM, Tulinius M, van den Akker JT et al (2011) Systemic administration of PRO051 in Duchenne's muscular dystrophy. N Engl J Med 364:1513–1522

Goyenvalle A, Vulin A, Fougerousse F et al (2004) Rescue of dystrophic muscle through U7 snRNA-mediated exon skipping. Science 306:1796–1799

Hammond SM, Wood MJ (2011) Genetic therapies for RNA mis-splicing diseases. Trends Genet 27:196–205

Hastings ML, Krainer AR (2001) Pre-mRNA splicing in the new millennium. Curr Opin Cell Biol 13:302–309

Hauswirth WW, Aleman TS, Kaushal S et al (2008) Treatment of leber congenital amaurosis due to RPE65 mutations by ocular subretinal injection of adeno-associated virus gene vector: short-term results of a phase I trial. Hum Gene Ther 19:979–990

Hsu PD, Lander ES, Zhang F (2014) Development and applications of CRISPR-Cas9 for genome engineering. Cell 157:1262–1278

Janoria KG, Gunda S, Boddu SH et al (2007) Novel approaches to retinal drug delivery. Expert Opin Drug Deliv 4:371–388

Kinali M, Arechavala-Gomeza V, Feng L et al (2009) Local restoration of dystrophin expression with the morpholino oligomer AVI-4658 in Duchenne muscular dystrophy: a single-blind, placebo-controlled, dose-escalation, proof-of-concept study. Lancet Neurol 8:918–928

Koo T, Wood MJ (2013) Clinical trials using antisense oligonucleotides in duchenne muscular dystrophy. Hum Gene Ther 24:479–488
Kurreck J (2003) Antisense technologies. Improvement through novel chemical modifications. Eur J Biochem 270:1628–1644
Lalezari JP, Stagg RJ, Kuppermann BD et al (1997) Intravenous cidofovir for peripheral cytomegalovirus retinitis in patients with AIDS. A randomized, controlled trial. Ann Intern Med 126:257–263
Lentz JJ, Savas S, Ng SS et al (2005) The USH1C 216G→a splice-site mutation results in a 35-base-pair deletion. Hum Genet 116:225–227
Lentz JJ, Jodelka FM, Hinrich AJ et al (2013) Rescue of hearing and vestibular function by antisense oligonucleotides in a mouse model of human deafness. Nat Med 19:345–350
MacLaren RE, Groppe M, Barnard AR et al (2014) Retinal gene therapy in patients with choroideremia: initial findings from a phase 1/2 clinical trial. Lancet 383:1129–1137
Maguire AM, Simonelli F, Pierce EA et al (2008) Safety and efficacy of gene transfer for Leber's congenital amaurosis. N Engl J Med 358:2240–2248
Perrault I, Delphin N, Hanein S et al (2007) Spectrum of NPHP6/CEP290 mutations in Leber congenital amaurosis and delineation of the associated phenotype. Hum Mutat 28:416
Raal FJ, Santos RD, Blom DJ et al (2010) Mipomersen, an apolipoprotein B synthesis inhibitor, for lowering of LDL cholesterol concentrations in patients with homozygous familial hypercholesterolaemia: a randomised, double-blind, placebo-controlled trial. Lancet 375:998–1006
Rozet JM, Gérard X (2015) Understanding disease pleiotropy: From puzzle to solution. Sci Transl Med 7:291fs24.
Sahel JA, Roska B (2013) Gene therapy for blindness. Annu Rev Neurosci 36:467–488
Stern J, Temple S (2014) Stem cells for retinal repair. Dev Ophthalmol 53:70–80
Stingl K, Zrenner E (2013) Electronic approaches to restitute vision in patients with neurodegenerative diseases of the retina. Ophthalmic Res 50:215–220
Stone EM (2007) Leber congenital amaurosis - a model for efficient genetic testing of heterogeneous disorders: LXIV Edward Jackson Memorial Lecture. Am J Ophthalmol 144:791–811
Tawse KL, Baumal CR (2014) Intravitreal foscarnet for recurring CMV retinitis in a congenitally infected premature infant. J AAPOS Off Publ Am Assoc Pediat Ophthalmol Strabismus/Am Assoc Pediatr Ophthalmol Strabismus 18:78–80
Tucker BA, Mullins RF, Streb LM et al (2013) Patient-specific iPSC-derived photoreceptor precursor cells as a means to investigate retinitis pigmentosa. Elife 2:e00824
Vache C, Besnard T, le Berre P et al (2012) Usher syndrome type 2 caused by activation of an USH2A pseudoexon: implications for diagnosis and therapy. Hum Mutat 33:104–108
van den Hurk JAJM, van de Pol DJ, Wissinger B et al (2003) Novel types of mutation in the choroideremia (CHM) gene: a full-length L1 insertion and an intronic mutation activating a cryptic exon. Hum Genet 113:268–275
Vandenberghe LH, Auricchio A (2012) Novel adeno-associated viral vectors for retinal gene therapy. Gene Ther 19:162–168
Webb TR, Parfitt DA, Gardner JC et al (2012) Deep intronic mutation in OFD1, identified by targeted genomic next-generation sequencing, causes a severe form of X-linked retinitis pigmentosa (RP23). Hum Mol Genet 21:3647–3654
Zamecnik PC, Stephenson ML (1978) Inhibition of Rous sarcoma virus replication and cell transformation by a specific oligodeoxynucleotide. Proc Natl Acad Sci U S A 75:280–284
Zanetta C, Nizzardo M, Simone C et al (2014) Molecular therapeutic strategies for spinal muscular atrophies: current and future clinical trials. Clin Ther 36:128–140
Zernant J, Xie YA, Ayuso C et al (2014) Analysis of the ABCA4 genomic locus in Stargardt disease. Hum Mol Genet 23:6797–6806

Chapter 70
Functional Rescue of Retinal Degeneration-Associated Mutant RPE65 Proteins

Minghao Jin, Songhua Li, Jane Hu, Heather H. Jin, Samuel G. Jacobson and Dean Bok

Abstract More than 100 different mutations in the *RPE65* gene are associated with inherited retinal degeneration. Although some missense mutations have been shown to abolish isomerase activity of RPE65, the molecular bases leading to loss of function and retinal degeneration remain incompletely understood. Here we show that several missense mutations resulted in significant decrease in expression level of RPE65 in the human retinal pigment epithelium cells. The 26S proteasome non-ATPase regulatory subunit 13, a newly identified negative regulator of RPE65, mediated degradation of mutant RPE65s, which were misfolded and formed aggregates in the cells. Many mutations, including L22P, T101I, and L408P, were mapped on nonactive sites of RPE65. Enzyme activities of these mutant RPE65s were significantly rescued at low temperature, whereas mutant RPE65s with a distinct active site mutation could not be rescued under the same conditions. 4-phenylbutyrate (PBA) displayed a significant synergistic effect on the low temperature-mediated rescue of the mutant RPE65s. Our results suggest that a low temperature eye mask and PBA, a FDA-approved oral medicine, may provide a promising "protein repair

M. Jin (✉) · S. Li
Department of Ophthalmology and Neuroscience Center, Louisiana State University Health Sciences Center, 2020 Gravier St. Suite D, New Orleans, LA 70112, USA
e-mail: mjin@lsuhsc.edu

S. Li
e-mail: sli@lsuhsc.edu

J. Hu · D. Bok
Jules Stein Eye Institute, University of California, Los Angeles, CA 90095, USA
e-mail: hu@jsei.ucla.edu

D. Bok
e-mail: bok@jsei.ucla.edu

H. H. Jin
Department of Biology, Washington University, St. Louis, MO 63130, USA
e-mail: jin.hui@wustl.edu

S. G. Jacobson
Scheie Eye Institute, Department of Ophthalmology, Perelman School of Medicine, University of Pennsylvania, Philadelphia, PA 19104, USA
e-mail: jacobsos@mail.med.upenn.edu

C. Bowes Rickman et al. (eds.), *Retinal Degenerative Diseases,* Advances in Experimental Medicine and Biology 854, DOI 10.1007/978-3-319-17121-0_70

therapy" that can enhance the efficacy of gene therapy for delaying retinal degeneration caused by RPE65 mutations.

Keywords RPE65 · Retinoid · Visual cycle · Leber congenital amaurosis · Retinitis pigmentosa · PSMD13 · Proteasome · Low temperature · Chemical chaperone · Gene therapy · Retina

70.1 Introduction

RPE65 is a key retinoid isomerase (Jin et al. 2005; Moiseyev et al. 2005) necessary for regenerating 11-*cis* retinal, which functions as a molecular switch for activating opsins in response to light stimulation. The significance of RPE65 in retinal health is reflected by the effect of its mutations, over 100 of which are associated with retinal degenerative diseases. Among these mutations, more than 70 are missense mutations. Although most of these mutations have not been studied for their pathogenicity, some mutations have been shown to severely eliminate isomerase activity of RPE65 (Redmond et al. 2005). The activities of mutant RPE65s measured in the laboratory were related to whether or not they were disease-causing in the patients (Philp et al. 2009). Several missense mutations resulted in rapid degradation of RPE65 in HEK cell lines with unknown mechanisms (Chen et al. 2006; Takahashi et al. 2006).

Recent gene therapy trials showed improvement in vision in some patients with RPE65 mutations (Cideciyan et al. 2008; Hauswirth et al. 2008; Maguire et al. 2008). However, a subsequent study showed that gene therapy could not stop the progressive retinal degeneration (Cideciyan et al. 2013). In general, gene therapy can confer enzyme activity to retinal pigment epithelium (RPE) of patients by expressing wild-type (WT) RPE65, but it cannot stop the degenerative component of the disease process. Recently, a dominant mutation in the *RPE65* gene has been found in patients with retinitis pigmentosa (Bowne et al. 2011). Misfolding, mislocalization, and aggregation of mutant RPE65 (Chen et al. 2006; Takahashi et al. 2006; Li et al. 2014) may cause cytotoxic effects. To enhance the gene therapy effect, it is important to develop a strategy that can rescue the enzyme activity but also reduce cytotoxic effects of mutant RPE65s. In this study, we investigated the common properties of several disease-causing RPE65s with regard to their pathogenic mechanism and rescue of their function.

70.2 Materials and Methods

70.2.1 Immunohistochemistry and Immunoblot Analysis

All animal experiments were approved by the Institutional Animal Care and Use Committee for the Louisiana State University Health Sciences Center and performed according to guidelines established by the Association for Research in Vi-

sion and Ophthalmology Statement for the Use of Animals in Ophthalmic and Vision Research. Retinal and cellular immunostaining as well as immunoblot analysis were performed as described previously (Sato et al. 2013; Li et al. 2014).

70.2.2 Cell Culture, Transfection and Knockdown of PSMD13

Primary human RPE (Hu and Bok 2001), ARPE-19 (Dunn et al. 1996), and 293 T-LC (Jin et al. 2005) cells were maintained as described previously. PolyJet (SignaGen) was used for transfection. To reduce the expression level of endogenous RPE65 in the human RPE cells, transfected RPE was maintained in plastic culture plates instead of Millicell-HA chambers (Hu and Bok 2001). Knockdown of the 26S proteasome non-ATPase regulatory subunit 13 (PSMD13) in ARPE-19 cells was performed by transfecting PSMD13 siRNA (OriGene).

70.2.3 Retinoid Isomerase Assay

The 293 T-LC cells transfected with wild-type (WT) or mutant RPE65 constructs (Philp et al. 2009; Li et al. 2014) were incubated with 5 μM all-*trans*-retinol (a*t*ROL) for 16 h at 30 or 37 °C. Retinoids extracted from the cells were saponified and analyzed by HPLC (Jin et al. 2007).

70.3 Results

70.3.1 PSMD13 Promoted Degradation of Disease-Associated RPE65 Proteins

To analyze the impact of disease-causing mutations on expression of RPE65 in RPE, we transfected WT and mutant RPE65 constructs into primary human RPE cells. As shown in Fig. 70.1a, protein levels of all tested mutant RPE65s were significantly lower than that of WT RPE65. Coexpression of PSMD13 exacerbated the decrease in protein levels of some mutant RPE65s, whereas knockdown of PSMD13 increased proteins of these mutant RPE65s (Fig. 70.1b). Immunohistochemistry revealed that PSMD13 expresses in mouse RPE (Fig. 70.1c).

70.3.2 Rescue of Enzyme Activity of Disease-Causing RPE65s with Nonactive Site Mutations

By mapping disease-causing mutation sites onto the crystal structure of RPE65 (Kiser et al. 2009), we found that many mutations are nonactive site mutations

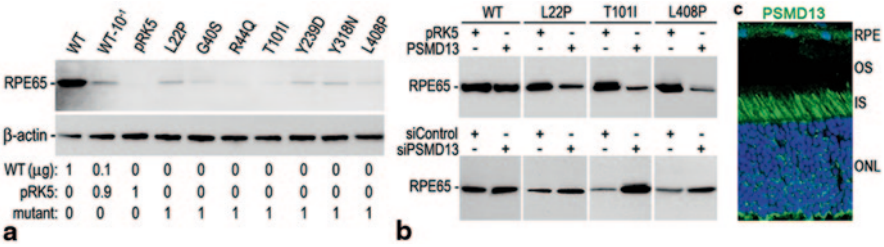

Fig. 70.1 *PSMD13* mediates degradation of mutant *RPE65*s. **a** Immunoblot analysis of human *RPE* cells transfected with the indicated amount of *pRK5* mock vector and constructs for *WT* or disease-causing *RPE65*. Beta actin was used as a loading control. **b** Immunoblot analysis of *WT* and mutant *RPE65*s in ARPE-19 cells cotransfected with the indicated vector or siRNA. **c** Mouse retinal immunohistochemistry for *PSMD13*. Nuclei were stained with DAPI

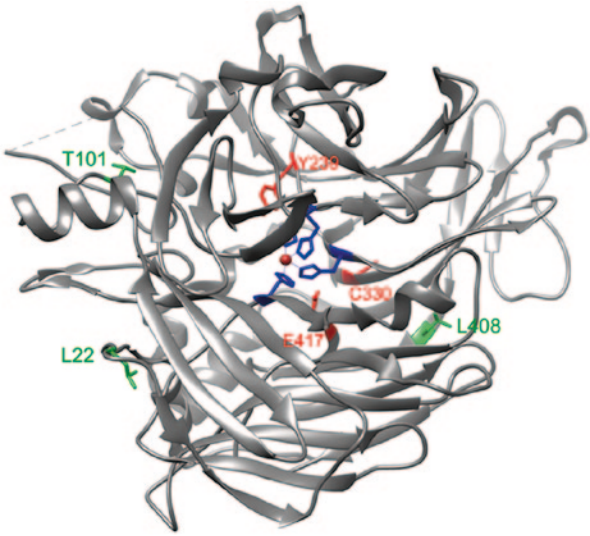

Fig. 70.2 Mapping of disease-causing mutation sites on the crystal structure of bovine RPE65. The catalytic site containing Fe2+ (*brown* sphere) is in the *center* of RPE65. The three mutation sites (*L22, T101*, & *L408*) shown in *green* are mapped in the nonactive sites, whereas the other three mutation sites (*Y239, C330*, & *E417*) shown in *red* are close to the active site cavity. The four iron-binding histidines (H180, H241, H313, & H527) are shown in *blue*

(Fig. 70.2). This observation prompted us to test whether low temperature can rescue enzyme activity of mutant RPE65s. Isomerase activities of three mutant RPE65s with nonactive site mutations (L22P, T101I, and L408P) are significantly increased at 30 °C, whereas mutant RPE65s with active site (H180R and H313R) or near active site (Y239D, C330Y, and E417Q) mutations could not be rescued under the same conditions (Table 70.1).

Table 70.1 Retinoid isomerase activities of WT and the indicated mutant RPE65s were determined by measuring synthesis of 11-*cis* retinol (11*c*ROL) at 30 or 37 °C. Numbers indicate 11*c*ROL content (pmol ± SD, $n = 3$) in 1 mg of cellular protein (*middle columns*) or ratio of the isomerase activities at 30 °C to those at 37 °C (*right column*). *NA* no activity

Synthesis of 11cROL (pmol/mg protein)			
Mutation	Activity at 30° C	Activity at 37° C	Ratio 30/37 ° C
L22P	22 ± 3	4 ± 1	5.5
T101I	12 ± 2	2 ± 1	6.0
L408P	26 ± 3	5 ± 1	5.2
H180R	NA	NA	–
H313R	NA	NA	–
Y239D	1.3 ± 0.3	1.3 ± 0.5	1.0
C330Y	1.8 ± 0.3	1.6 ± 0.3	1.1
E417Q	1.2 ± 0.4	1.1 ± 0.4	1.1
WT	124 ± 10	138 ± 10	0.9

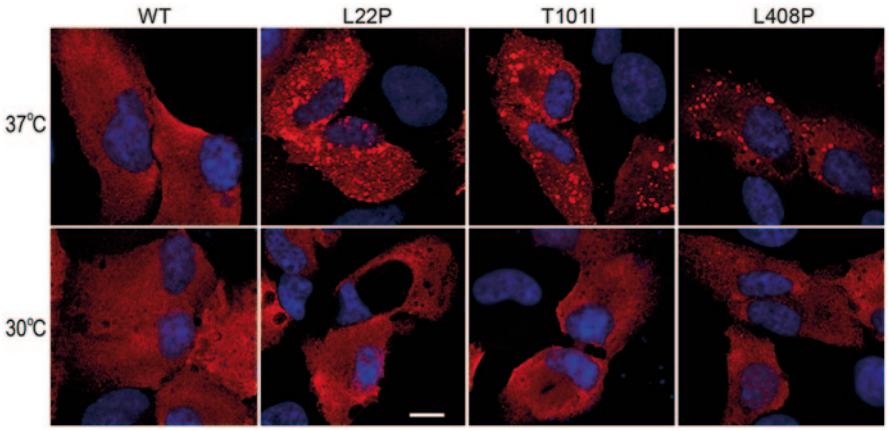

Fig. 70.3 *Low* temperature reduced aggregation of mutant RPE65s. ARPE-19 cells expressing *WT* or the indicated mutant RPE65 were incubated at 37 or 30 °C, stained with RPE65 antibody, and observed using a confocal microscope. Scale bar denotes 10 m

70.3.3 Low Temperature Inhibited Aggregate Formation of Mutant RPE65s

Results described above suggest that misfolding is the main molecular basis for loss of function of the nonactive site mutant RPE65s. We tested this possibility by immunocytochemistry. As shown in Fig. 70.3, the mutant RPE65s formed numerous aggregates in ARPE-19 cells grown at 37 °C. These aggregates were significantly reduced in the cells incubated at 30 °C (Fig. 70.3).

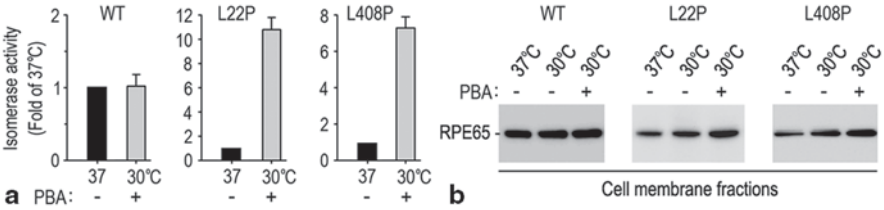

Fig. 70.4 **a** *PBA* enhanced *low* temperature-mediated rescue of mutant *RPE65*s. Relative retinoid isomerase activities of the indicated mutant *RPE65*s at 30 °C in the presence of *PBA* are shown as fold of their activities at 37 °C. Error bars show SD ($n=3$). **b** Association of the mutant *RPE65* with membrane was also significantly increased in the cells incubated with *PBA* at 30 °C

70.3.4 PBA Enhanced Low Temperature Rescue of the Nonactive Site Mutant RPE65s

4-phenylbutyrate (PBA) has been shown to help proper folding of other mutant proteins (Bonapace et al. 2004; Li et al. 2013a). We therefore tested whether PBA and low-temperature display synergistic effects on rescue of mutant RPE65s. As shown in Fig. 70.4a, activity of L22P RPE65 was increased approximately 10-fold at 30 °C in the presence of PBA compared to its activity at 37 °C. Association of the mutant RPE65 with membrane was also significantly increased in the cells incubated with PBA at 30 °C (Fig. 70.4b).

70.4 Discussion

The role of PSMD13 in vision and retinal health remains poorly understood. In our previous study, we identified PSMD13 as a negative regulator of RPE65 (Li et al. 2013b). The RPE65-mediated synthesis of 11-*cis* retinol (11*c*ROL) was reduced PSMD13-cotransfected cells (Li et al. 2013b). This might be due to the slight promotion of RPE65 degradation by PSMD13 (Fig. 70.1b). Abundant expression of PSMD13 in RPE (Fig. 70.1c) suggests that PSMD13 could regulate synthesis of 11*c*ROL by controlling degradation of RPE65. Importantly, PSMD13 strongly promoted degradation of disease-causing RPE65s (Fig. 70.1b). Knockdown of PSMD13 significantly increased expression levels of mutant RPE65s (Fig. 70.1b), indicating that PSMD13 mediates degradation of mutant RPE65s in the proteasome. The results also suggest that PSMD13 may play a critical role in regulation of pathogenicity of mutant RPE65s.

Low temperature has been shown to restore functions to mutated proteins and reduce cellular damage by promoting proper folding of many mutated proteins (Denning et al. 1992; Li et al. 2013a). In this study, we observed that low temperature significantly reduced formation of aggregates of mutant RPE65s (Fig. 70.3), and rescued enzyme activity of disease-causing RPE65s with different mutations in

nonactive sites (Fig. 70.2 and Table 70.1). Under the same experimental conditions, RPE65s with mutations in the active or near the active sites could not be rescued (Fig. 70.2 and Table 70.1). Although the biochemical attributes of amino acid residue mutated are important in determining the enzyme activity of a mutant RPE65 (Nikolaeva et al. 2010), our results also suggest that the relative spatial distance between a mutation site and the catalytic site is a critical factor in determining whether the mutant RPE65 can be rescued. Importantly, many disease-causing missense mutations are nonactive site mutations. Further studies are needed to test whether these mutations can also be rescued at low temperature.

PBA, a FDA-approved safe oral medication, has also been shown to reverse cellular mislocalization and rescue function of many mutant proteins (Rubenstein and Zeitlin 1998; Bonapace et al. 2004; Li et al. 2013a). We observed that PBA and low temperature exhibited a significant synergistic effect on rescue of the nonactive site mutant RPE65s (Fig. 70.4a). Since low temperature inhibited aggregate formation of mutant RPE65s (Fig. 70.3), our results suggest that low temperature and PBA not only can restore enzymatic function to nonactive site mutant RPE65s but also can reduce the cytotoxic effect of misfolded RPE65s. Continuing retinal degeneration in patients who received gene therapy (Cideciyan et al. 2013) indicates that a combinatorial therapy is needed to improve vision and to prevent or delay progressive retinal degeneration in patients with RPE65 mutations. A low temperature eye mask and PBA functioning as a "protein repair therapy" may be a promising option for combinatorial therapy.

Acknowledgments This work was supported by NIH grants (EY021208 to M. J., EY017280 to S. G. J., and GM103340 to LSU Neuroscience COBRE facility), Macula Vision Research Foundation grants (to D. B. and to S.G.J.), and a Research to Prevent Blindness grant (to LSU Ophthalmology).

References

Bonapace G, Waheed A, Shah GN et al (2004) Chemical chaperones protect from effects of apoptosis-inducing mutation in carbonic anhydrase IV identified in retinitis pigmentosa 17. Proc Natl Acad Sci U S A 101:12300–12305

Bowne SJ, Humphries MM, Sullivan LS et al (2011) A dominant mutation in RPE65 identified by whole-exome sequencing causes retinitis pigmentosa with choroidal involvement. Eur J Hum Genet 19:1074–1081

Chen Y, Moiseyev G, Takahashi Y et al (2006) Impacts of two point mutations of RPE65 from Leber's congenital amaurosis on the stability, subcellular localization and isomerohydrolase activity of RPE65. FEBS Lett 580:4200–4204

Cideciyan AV, Aleman TS, Boye SL et al (2008) Human gene therapy for RPE65 isomerase deficiency activates the retinoid cycle of vision but with slow rod kinetics. Proc Natl Acad Sci U S A 105:15112–15117

Cideciyan AV, Jacobson SG, Beltran WA et al (2013) Human retinal gene therapy for Leber congenital amaurosis shows advancing retinal degeneration despite enduring visual improvement. Proc Natl Acad Sci U S A 110:E517–E525

Denning GM, Anderson MP, Amara JF et al (1992) Processing of mutant cystic fibrosis transmembrane conductance regulator is temperature-sensitive. Nature 358:761–764

Dunn KC, Aotaki-Keen AE, Putkey FR et al (1996) ARPE-19, a human retinal pigment epithelial cell line with differentiated properties. Exp Eye Res 62:155–169

Hauswirth WW, Aleman TS, Kaushal S et al (2008) Treatment of leber congenital amaurosis due to RPE65 mutations by ocular subretinal injection of adeno-associated virus gene vector: short-term results of a phase I trial. Hum Gene Ther 19:979–990

Hu J, Bok D (2001) A cell culture medium that supports the differentiation of human retinal pigment epithelium into functionally polarized monolayers. Mol Vis 7:14–19

Jin M, Li S, Moghrabi WN et al (2005) Rpe65 is the retinoid isomerase in bovine retinal pigment epithelium. Cell 122:449–459

Jin M, Yuan Q, Li S et al (2007) Role of LRAT on the retinoid isomerase activity and membrane association of Rpe65. J Biol Chem 282:20915–20924

Kiser PD, Golczak M, Lodowski DT et al (2009) Crystal structure of native RPE65, the retinoid isomerase of the visual cycle. Proc Natl Acad Sci U S A 106:17325–17330

Li S, Yang Z, Hu J et al (2013a) Secretory defect and cytotoxicity: the potential disease mechanisms for the retinitis pigmentosa (RP)-associated interphotoreceptor retinoid-binding protein (IRBP). J Biol Chem 288:11395–11406

Li S, Lee J, Zhou Y et al (2013b) Fatty acid transport protein 4 (FATP4) prevents light-induced degeneration of cone and rod photoreceptors by inhibiting RPE65 isomerase. J Neurosci 33:3178–3189

Li S, Izumi T, Hu J et al (2014) Rescue of enzymatic function for disease-associated RPE65 proteins containing various missense mutations in non-active sites. J Biol Chem 289:18943–18956

Maguire AM, Simonelli F, Pierce EA et al (2008) Safety and efficacy of gene transfer for Leber's congenital amaurosis. N Engl J Med 358:2240–2248

Moiseyev G, Chen Y, Takahashi Y et al (2005) RPE65 is the isomerohydrolase in the retinoid visual cycle. Proc Natl Acad Sci U S A 106:12413–12418

Nikolaeva O, Takahashi Y, Moiseyev G et al (2010) Negative charge of the glutamic acid 417 residue is crucial for isomerohydrolase activity of RPE65. Biochem Biophys Res Commun 391:1757–1761

Philp AR, Jin M, Li S et al (2009) Predicting the pathogenicity of RPE65 mutations. Hum Mutat 30:1183–1188

Redmond TM, Poliakov E, Yu S et al (2005) Mutation of key residues of RPE65 abolishes its enzymatic role as isomerohydrolase in the visual cycle. Proc Natl Acad Sci U S A 102:13658–13663

Rubenstein RC, Zeitlin PL (1998) Use of protein repair therapy in the treatment of cystic fibrosis. Curr Opin Pediatr 10:250–255

Sato K, Li S, Gordon WC et al (2013) Receptor interacting protein kinase-mediated necrosis contributes to cone and rod photoreceptor degeneration in the retina lacking interphotoreceptor retinoid-binding protein. J Neurosci 33:17458–17468

Takahashi Y, Chen Y, Moiseyev G et al (2006) Two point mutations of RPE65 from patients with retinal dystrophies decrease the stability of RPE65 protein and abolish its isomerohydrolase activity. J Biol Chem 281:21820–21826

Chapter 71
Evaluation of Ocular Gene Therapy in an Italian Patient Affected by Congenital Leber Amaurosis Type 2 Treated in Both Eyes

Francesco Testa, Albert M Maguire, Settimio Rossi, Kathleen Marshall, Alberto Auricchio, Paolo Melillo, Jean Bennett and Francesca Simonelli

Abstract Gene therapy clinical trials with gene augmentation therapy for Leber Congenital Amaurosis have shown partial reversal of retinal dysfunction. Most studies described the effect of treatment in a single eye and limited evidence is reported in literature about patients treated in both eyes. In this chapter, we present the findings of a young patient treated in both eyes. Efficacy of the treatment was assessed with Best Corrected Visual Acuity, Goldman Visual Field testing, Esterman computerized binocular visual field and Microperimetric testing. Post-treatment results showed improvement of visual function in both eyes, in particular,

F. Simonelli (✉) · F. Testa · S. Rossi · P. Melillo
Eye Clinic, Multidisciplinary Department of Medical, Surgical and Dental Sciences, Second University of Naples, Naples, Italy
e-mail: francesco.testa@unina2.it

A. M. Maguire · J. Bennett
Scheie Eye Institute, F.M. Kirby Center for Molecular Ophthalmology, University of Pennsylvania, Philadelphia, PA, USA
e-mail: amaguire@mail.med.upenn.edu

S. Rossi
e-mail: settimio.rossi@unina2.it

K. Marshall
Center for Cellular and Molecular Therapeutics, The Children's Hospital of Philadelphia, Philadelphia, PA, USA
e-mail: marshallk1@email.chop.edu

A. Auricchio
Telethon Institute of Genetics and Medicine (TIGEM), Naples, Italy
e-mail: auricchio@tigem.it

P. Melillo
e-mail: paolo.melillo@unina2.it

J. Bennett
e-mail: jebennet@mail.med.upenn.edu

F. Simonelli
Via Pansini, 5, 80131 Napoli, Italy
e-mail: francesca.simonelli@unina2.it

C. Bowes Rickman et al. (eds.), *Retinal Degenerative Diseases,* Advances in Experimental Medicine and Biology 854, DOI 10.1007/978-3-319-17121-0_71

a strong amelioration was observed after the first injection, by using conventional monocular tests. Moreover, the treatment in the second eye resulted in a further improvement of binocular visual functionality, as easily detected by computerized binocular visual field. In conclusion, our data suggest that gene therapy can inhibit retinal degeneration and can be safe and effective in restoring visual functionality in young subjects treated in both eyes. Finally, new outcome measurements, in particular binocular computerized visual field parameters, can therefore be useful to quantify overall visual gain in patients undergoing gene therapy in both eyes.

Keywords Gene therapy · Leber's Congenital Amaurosis · Optical coherence tomography · Microperimetry · Binocular computerized visual field

71.1 Introduction

In the last decade, gene therapy was explored for the treatment of incurable inherited retinal diseases both in animal models and in human subjects. Particularly, 3 independent clinical trials that began almost contemporaneously in 2007–NCT00481546 (Cideciyan et al. 2009), NCT00516477 (Maguire et al. 2008), NCT00643747 (Bainbridge et al. 2008) - were performed to evaluate safety and efficacy of gene therapy for Leber Congenital Amaurosis type 2 (LCA2), a retinal degeneration resulting from mutations in the RPE65 gene.

In the three initial clinical trials, the patients were treated with a single unilateral subretinal injection of adeno-associated virus 2 (AAV2) carrying the RPE65 gene in the eye with worse vision. A safety assessment showed the presence of minimal systemic immunological response in two trials (Hauswirth et al. 2008; Maguire et al. 2008) and the absence of serious adverse events in all three trials. In particular, in the clinical trial NCT00516477, performed at the Children's Hospital of Philadelphia (CHOP) in conjunction with the Second University of Naples (SUN), 12 patients were treated by subretinal AAV2-hRPE65v2 injection in the worse eye (Maguire et al. 2009). The findings of this clinical trial showed an improvement of visual functionality and a stability over long-term follow-up in most patients (Simonelli et al. 2010; Testa et al. 2013). The promising results obtained motivated a new clinical trial for the re-injection of previously treated patients in the contralateral eye (NCT01208389). Since there is limited evidence in literature about LCA patients treated in both eyes, in this chapter we present our clinical findings in the youngest subject of our cohort of patients treated in both eyes.

71.2 Materials and Methods

All details on design, consent, and vector administration in this clinical trial have previously been reported (Maguire et al. 2009). Briefly, the LCA subject NP15, aged 8 years old was first evaluated at the Second University of Napoli (Napoli,

Italy) and received the diagnosis based on visual and retinal function studies (Simonelli et al. 2007). All patients underwent mutation screening for LCA genes and received molecular diagnosis of LCA2 by the Telethon Institute of Genetics and Medicine. After informed consent and confirmation of trial eligibility criteria, including independent evaluation of the likelihood that the mutations were disease-causing (Carver Lab, Iowa City, IA), the eye with worse visual function was selected for delivery of AAV2-hRPE65v2. The study subject (NP15) underwent an initial AAV2-hRPE65v2 injection in the right eye (at the age of 11 years) and after 3 years in the left eye (at the age of 14 years). NP15 received the same dose/volume (1.5×1011 vg/300 μl) in both eyes. Baseline tests and follow-up visits up to day 30 were performed at both the Children's Hospital of Philadelphia and Second University of Napoli while the follow-up visits were performed at the Second University of Napoli. Follow-up data are available up to 4 years after the initial treatment and 1 year after the treatment in the contralateral eye. In the current study, efficacy of the treatment was assessed with Best Corrected Visual Acuity (BCVA), Goldman Visual Field testing (VF), Esterman computerized binocular visual field and Microperimetric testing (MP).

BCVA was measured by trained vision examiners using a standard protocol involving Early Treatment Diabetic Retinopathy Study (ETDRS) charts and letter counts. Letter scores were converted to the log of the Minimum Angle of Resolution (logMAR), on a scale ranging from 0.00 to 2.00, with higher values indicating poorer vision. Eyes that could detect hand motion were assigned a score that was one line worse than the largest printed line on the chart tested at a standardized distance of 4 m (<20/1600) to provide the most conservative evaluation in terms of underestimating the actual extent of visual impairment.

VF was measured using Goldman perimetry (Haag Streit Perimeter 940; Haag Streit, Mason, OH).(Ross et al. 1984) The visual field isopters were obtained using the V4e test object.

The Esterman binocular visual field test on the field analyzer perimeter uses a grid of 120 test points to examine more than 130° of visual field. It was originally developed for manual perimeters and, similar to its monocular predecessor, gives more weight to the functionally more important parts of the visual field (i.e., central and inferior).(Esterman 1982)

Microperimetry was performed by an automatic fundus-related perimeter (MP1 Microperimeter, Nidek Technologies, Padova, Italy). For the purpose of this study, the following parameters were used: a fixation target of 2° in diameter consisting of a red ring; a white monochromatic background with a luminance of 4 abs; and a Goldman III–size stimulus with a projection time of 200 ms.(Sohn et al. 2010) The stimulus was randomly projected according to a customized radial grid of 61 points covering the central portion of the retina (108 centered onto the fovea; points aligned on the 08, 308, 608, 908, 1208, and 1508 radial axes, 18 apart), and a 4-2-1 double staircase strategy was used with an automatic eye tracker that compensated for eye movements.(Midena et al. 2007)

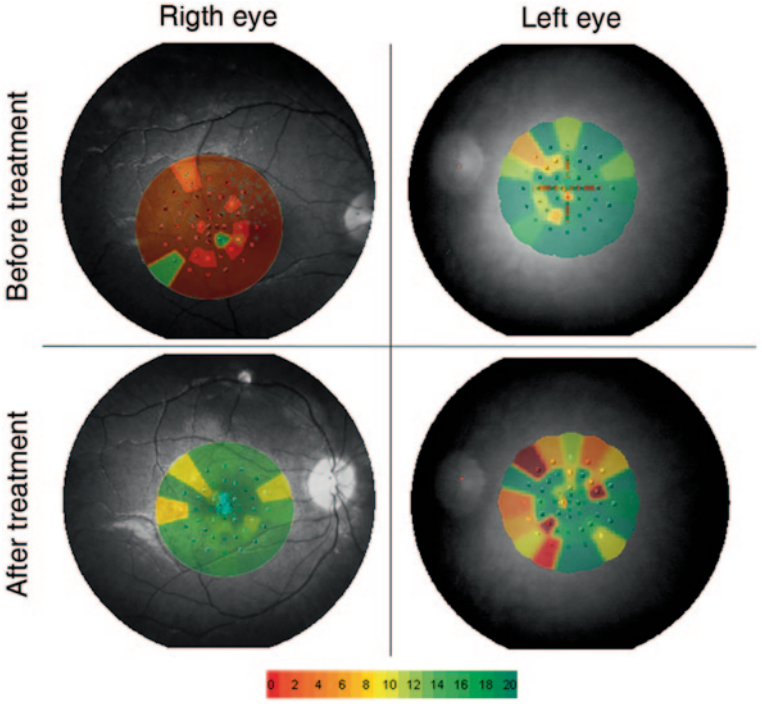

Fig. 71.1 Microperimetry macular sensitivity maps before and after treatment

71.3 Results

Both eyes showed improvement in visual functionality, as evaluated 1 year after treatment.

In particular, in the first treated eye (right eye), BCVA improved from 0.85 to 0.42 logMAR, Mean macular sensitivity increased from 0.8 dB (with unstable fixation) to 17.9 dB (with stable fixation), and central VF radius increased from 44° (area: 6197°^{2}) to 52° (area: 8549°^{2}; $p<0.001$). Figure 71.1 shows the microperimetry macular sensitivity maps before and after treatment.

One year after treatment in the second eye (left eye) BCVA improved from 0.42 to 0.34 logMAR; Mean macular sensitivity remained stable (16.6 vs 14.2 dB with stable fixation); and central VF radius increased from 46° (area: 6659°^{2}) to 50° (area: 7,762°^{2}; $p=0.02$). Moreover, binocular computerized visual field, performed before and after the injection in the contralateral left eye and reported in Fig. 71.2, showed an improvement of Esterman score from 59 to 74%, associated with an increase of mean sensitivity from 2.9 to 8.4 dB.

Comparing the 1 year post-injection time-points, we observed a BCVA improvement of 51% (RE) and 19% (LE), a fixation stability increase of 10 (RE) and 0.02 times (LE), and a VF enlargement of 38% in the right eye and 17% in the left eye.

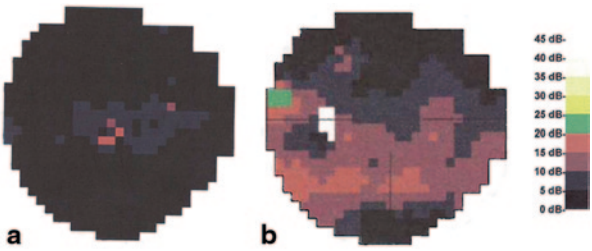

Fig. 71.2 Binocular visual field performed before (**a**), and after (**b**), treatment in the *left* eye

As regards the 4-year follow-up, the right eye showed an improved visual functionality compared to baseline, i.e., improved BCVA (0.56 vs 0.82 logMAR), increased mean macular sensitivity (10.3 vs 0.8 dB), enlarged VF area (8211 vs 6197°^{2}). Moreover, mean Macular Thickness evaluated by Spectral Domain OCT remained stable over the follow-up in both eyes (239±3 μm in the right eye, 239±8 μm in the left eye, see Fig. 71.3).

71.4 Discussion

The results of previous studies on gene therapy for LCA patients with RPE65 mutations support the hypothesis that the greatest improvement in visual function with subretinal gene therapy will occur in young individuals (Simonelli et al. 2010). Although young patients had better visual function at baseline than did older individuals, they also had the greatest overall improvement in vision. However, most previous studies focused on treatment of the first eye, while only one study reported the results of re-injections in the contralateral (untreated) eye in three patients, showing that the gains in retinal and visual function that had resulted from the initial injection were maintained after the second eye was injected (Bennett et al. 2012). In addition, the results of retreatment may reflect an age effect whereby the individuals who were younger (and thus whose retinas had not undergone as much degeneration) showed larger gains than older individuals. Here we reported

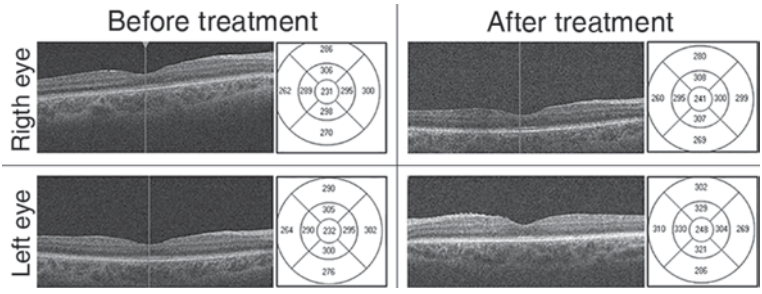

Fig. 71.3 OCT scans performed before and after treatment

the preliminary findings related to a teenager treated in both eyes, who represents the youngest subject among those treated in both eyes and described in literature. The post-treatment results showed improvement of visual function in both eyes, in particular, a strong amelioration was observed after the first injection, by using conventional monocular tests (i.e., BCVA, microperimetry and Goldman visual field). Moreover, the treatment in the second eye did not alter the gain achieved in the first eye and resulted in a further improvement of binocular visual functionality, as easily detected by computerized binocular visual field.

In literature, data on retinal degeneration revealed by OCT scan in patients treated in another clinical trial showed that therapy did not slow retinal degeneration, since a thinning of the outer nuclear layer (ONL) was detected by an ad hoc segmentation algorithm (Cideciyan et al. 2013). Although the comparison was limited by differences in methods (ad hoc developed versus commercial software), in demographic characteristics (i.e. age), and in the vector preparation and surgical approach, our observations showed that the overall macular thickness, including ONL, measured in OCT scans, remained stable over the whole follow-up (4 years), suggesting that gene therapy can slow retinal degeneration. However, further analysis on the overall treated cohort with a similar technique could be useful to confirm this hypothesis.

In conclusion, our data suggest that gene therapy can inhibit retinal degeneration and can be safe and effective in restoring visual functionality in young subjects treated in both eyes. In particular, the treatment in the second eye resulted in a further improvement of binocular visual functionality. Finally, new outcome measurements, in particular binocular computerized visual field parameters, can therefore be useful to quantify overall visual gain in patients undergoing gene therapy in both eyes.

Acknowledgments We thank Carmela Acerra for technical assistance. This work was supported by Italian Telethon Foundation (grant GGP10199 to Francesca Simonelli) and The Children's Hospital of Philadelphia. The outcome measures were approved by the Italian Ethics Committee. The surgical delivery of AAV2-.hRPE65v2 was carried out at The Children's Hospital of Philadelphia as approved by IRB protocol #10-007752.

References

Bainbridge JW, Smith AJ, Barker SS et al (2008) Effect of gene therapy on visual function in Leber's congenital amaurosis. N Engl J Med 358:2231–2239

Bennett J, Ashtari M, Wellman J et al (2012) AAV2 gene therapy readministration in three adults with congenital blindness. Sci Transl Med 4:120ra115

Cideciyan AV, Hauswirth WW, Aleman TS et al (2009) Human RPE65 gene therapy for Leber congenital amaurosis: persistence of early visual improvements and safety at 1 year. Hum Gene Ther 20:999–1004

Cideciyan AV, Jacobson SG, Beltran WA et al (2013) Human retinal gene therapy for Leber congenital amaurosis shows advancing retinal degeneration despite enduring visual improvement. Proc Natl Acad Sci U S A. 110:E517–E525

Esterman B (1982) Functional scoring of the binocular field. Ophthalmology 89:1226–1234

Hauswirth WW, Aleman TS, Kaushal S et al (2008) Treatment of leber congenital amaurosis due to RPE65 mutations by ocular subretinal injection of adeno-associated virus gene vector: short-term results of a phase I trial. Hum Gene Ther 19:979–990

Maguire AM, Simonelli F, Pierce EA et al (2008) Safety and efficacy of gene transfer for Leber's congenital amaurosis. N Engl J Med 358:2240–2248

Maguire AM, High KA, Auricchio A et al (2009) Age-dependent effects of RPE65 gene therapy for Leber's congenital amaurosis: a phase 1 dose-escalation trial. Lancet 374:1597–1605

Midena E, Vujosevic S, Convento E et al (2007) Microperimetry and fundus autofluorescence in patients with early age-related macular degeneration. Br J Ophthalmol 91:1499–1503

Ross DF, Fishman GA, Gilbert LD et al (1984) Variability of visual field measurements in normal subjects and patients with retinitis pigmentosa. Arch Ophthalmol 102:1004–1010

Simonelli F, Ziviello C, Testa F et al (2007) Clinical and molecular genetics of Leber's congenital amaurosis: a multicenter study of Italian patients. Invest Ophthalmol Vis Sci 48:4284–4290

Simonelli F, Maguire AM, Testa F et al (2010) Gene therapy for Leber's congenital amaurosis is safe and effective through 1.5 years after vector administration. Mol Ther 18:643–650

Sohn EH, Chen FK, Rubin GS et al (2010) Macular Function Assessed by Microperimetry in Patients with Enhanced S-Cone Syndrome. Ophthalmology 117:1199–1206.e1191

Testa F, Maguire AM, Rossi S et al (2013) Three-year follow-up after unilateral subretinal delivery of adeno-associated virus in patients with leber congenital amaurosis type 2. Ophthalmology 120:1283–1291

Part VIII
Stem Cells and Cell-Based Therapies

Chapter 72
Regenerative Medicine: Solution in Sight

Qingjie Wang, Jeffrey H. Stern and Sally Temple

Abstract The retina, like other central nervous system tissues, has poor regenerative properties in humans. Therefore, diseases that cause retinal cell loss, such as Age-related macular degeneration (AMD), retinitis pigmentosa (RP), Leber congenital amaurosis, Usher syndrome, glaucoma, and diabetic retinopathy, typically result in permanent visual impairment. Stem cell technologies have revolutionized our ability to produce neural cells in abundant supply. Much stem cell research effort is focused on producing the required cell types for cell replacement, or to generate disease-in-a-dish models to elucidate novel disease mechanisms for therapeutic development. Here we review the recent advances in stem cell studies relevant to producing RPE and retinal cells, and highlight future directions.

Keywords Stem cells · Retina · RPE · hESC · iPSC · Progenitor · Direct cellular reprogramming · Disease modeling

72.1 Induction of RPE and Neural Retinal lineages from Embryonic Stem Cells

Since the derivation of embryonic stem cells (ESCs), first in mouse and later in human (Evans and Kaufman 1981; Martin 1981; Thomson et al. 1998), several protocols have been developed to direct ESC differentiation towards RPE and neural retinal progeny. A combination of environmental factors known to stimulate retinal

S. Temple (✉) · Q. Wang · J. H. Stern
Neural Stem Cell Institute, Regenerative Research Foundation, Rensselaer, NY, 12144, USA
e-mail: sallytemple@neuralsci.org

Q. Wang
e-mail: qingjiewang@neuralsci.org

J. H. Stern
e-mail: jeffreystern@neuralsci.org

C. Bowes Rickman et al. (eds.), *Retinal Degenerative Diseases,* Advances in Experimental Medicine and Biology 854, DOI 10.1007/978-3-319-17121-0_72

development in animal models, including Lefty-A, Dkk1 and Activin A, were used to induce retinal progenitor cells from mouse ESCs, which resulted in 25–30 % Rx^+/$Pax6^+$ retina progenitor cells (Ikeda et al. 2005). Pioneering studies using human embryonic stem cells (hESCs) demonstrated that treatment with a combination of BMP inhibitor, Wnt inhibitor and IGF-1 efficiently generated (~80 %) human neural retinal progenitor cells (Lamba et al. 2006). A combination of Wnt and BMP/Nodal antagonists was also found effective in neural retina induction from hESCs (Osakada et al. 2008). Functional RPE cells have been derived from hESCs, first via spontaneous differentiation (Klimanskaya et al. 2004; Lund et al. 2006) and then by more rapid and efficient protocols assisted by Nicotinamide and Activin A (Idelson et al. 2009). These RPE cells can be purified by manual picking, which is effective but laborious, or by a simpler enzymatic process (Maruotti et al. 2013).

Recent technological advances have created three dimensional organoid cultures resembling the optic cup or the neural retina. In modified serum-free and growth-factor-reduced medium (SFEBq culture), mESCs spontaneously form a hollow vesicle of neuroepithelium. The suspension organoid cultures then can form a cup-like structure resembling the embryonic optic cup, a process driven by self-organization (Eiraku et al. 2011). Similar self-forming optic cup structures have been observed when using human pluripotent stem cells (Nakano et al. 2012; Zhong et al. 2014). The 3-D organoid cultures result in more robust and efficient retinal cell differentiation and are better models to recapitulate eye development. Still, production of functional photoreceptors with fully developed outer segments *in vitro* remains a key goal.

72.2 Using iPSCs to Model Retinal Degenerative Diseases

The regenerative medicine field witnessed another unprecedented discovery when Takahashi and Yamanaka reported the first study on turning somatic cells into an embryonic stem cell-like state: induced pluripotent stem cells (iPSCs) (Takahashi and Yamanaka 2006). Like ESCs, iPSCs can give rise to the full repertoire of somatic cell types. Most importantly, iPSCs match the patient from which they are derived in genetic background, and therefore are invaluable to model diseases, especially those with a strong genetic component. The RPE cells derived from human iPSC lines show similar properties to the ones derived from hESCs: they have similar gene expression profiles and phenotypic features, e.g. they maintain ZO-1 positive tight junctions, express functional visual cycle enzymes and are capable of photoreceptor outer segment (POS) phagocytosis (Buchholz et al. 2009; Meyer et al. 2009; Osakada et al. 2009; Maeda et al. 2013). In addition, neural retinal progenitor cells and their progeny including photoreceptor cells were also successfully derived from human iPSCs (Meyer et al. 2009; Osakada et al. 2009; Lamba et al. 2010; Mellough et al. 2012; Zhong et al. 2014).

Most retinal degenerative diseases are complex, and their underlying mechanisms remain unclear. Disease modeling using patient-specific iPSCs is a promising approach to elucidate the mechanisms of degenerative disorders. Patient-specific iPSC lines derived from RP patients with distinct mutations in the *RP1, RP9, PRPH2* or *RHO* genes have been generated, and rod photoreceptors derived from such lines expressed markers of cellular stress and underwent degeneration, recapitulating key aspects of the disease (Jin et al. 2011). In a separate study, iPSCs derived from RP patients with mutations in the *USH2A* gene were used to generate the multi-layer eyecup-like organoid cultures (Tucker et al. 2013). Analysis of the photoreceptor precursor cells revealed that the USH2A variant Arg4192His causes photoreceptor degeneration through protein mis-folding and ER stress (Tucker et al. 2013). Best disease (BD) is another inherited retinal degenerative disease; it is caused by mutations in the *BESTROPHIN1 (BEST1)* gene. RPE cells derived from BD patient-specific iPSCs are less effective in conducting POS phagocytosis (Singh et al. 2013). These studies demonstrate the potential of using patient-specific iPSCs to model and study retinal degenerative diseases. More such retinal disease models are anticipated, and further studies are eagerly awaited to identity disease pathways and drug candidates.

72.3 Direct Cellular Reprogramming

Several cellular reprogramming strategies have been developed: (1) cell fusion; (2) nuclear transfer (3) forced expression of cell fate specific transcription factors; (4) stimulation with small molecules and environmental factors. The iPSC reprogramming technology indicates that surprising plasticity is present in many types of cells. However, it takes multiple steps and a long time to reprogram somatic cells back to a pluripotent state then differentiate them towards the targeted cell types. An alternative is direct reprogramming, which aims to switch cells from one type to another directly. To date, there are just a few studies focused on generating induced retinal cells or induced RPE cells via direct cellular reprogramming.

Cell fusion mediated somatic cell reprogramming is a classic strategy to push cells towards different fates (Ambrosi and Rasmussen 2005). Retinal cells including Müller glia, amacrine and retinal ganglion neurons can fuse with transplanted hematopoietic stem and progenitor cells (HSPCs), ESCs or retinal stem and progenitor cells (RSPCs) *in vivo* upon retinal damage (Sanges et al. 2013). Activation of the Wnt/β-catenin signaling pathway in the transplanted cells is critical for cell fusion and reprogramming to occur. The fused cells can proliferate and differentiate *in vivo*, to partially regenerate the damaged retinal tissue (Sanges et al. 2013).

Müller glial cells are an endogenous resource for regeneration and repair of retinal injuries in fish and amniotes, and several studies have examined the plasticity of mammalian Müller glia. Müller glia harvested from both adult human vitreoretinal explants and the adult mouse retina are able to produce cells similar to other retinal

cell types, including bipolar, amacrine, horizontal cells and photoreceptors, under a defined differentiation environment (Giannelli et al. 2011). Forced-expressing of *Ascl1* (*Mash1*) in mouse Müller glia cells resulted in retinal progenitor-like cells that could proliferate *in vitro* and showed neuron-like response to neurotransmitters (Pollak et al. 2013).

Other cell types also show potential for direct reprogramming into retinal progeny. By forcing expression of the photoreceptor specific homeobox gene *Crx*, primary cells derived from adult rat iris tissue could produce photoreceptor-like cells that expressed rhodopsin and recoverin (Haruta et al. 2001). Combinations of (1) *Crx* and *Otx2*, (2) *Crx, Nrl* and *NeuroD* or (3) *Crx, Rx* and *NeuroD* produced similar results, and generated photoreceptor-like cells that express photoreceptor-specific markers and exhibited rod photoreceptor-specific electrophysiological responses to light stimuli (Akagi et al. 2004, 2005; Seko et al. 2012). A related strategy has been applied to generate RPE-like cells from human fibroblast cells. A combination of *cMYC, Mitf, Otx2, Rax, Crx, Kif4, Nrl* and *Pax6* was found to reprogram human fibroblast cells into RPE-like cells (Zhang et al. 2014). The induced RPE-like cells form a typical cobblestone morphology and express key RPE markers including *Bestrophin1, ZO-1* and *Cralbp* but have low expression of *RPE65* and *Tyr*. It will be useful to perform additional characterization of these RPE-like cells, including examination of cell polarity, physiology and phagocytosis, to understand how similar they are to native RPE.

Specific combinations of intrinsic factors and environmental cues are critical for successful direct reprogramming. Additional work to optimize conditions such as the mixture of transcription factors, the growth factors used, and the sequence of their application, is needed to determine the optimal protocols for deriving specific retinal and RPE cells that function well. Nevertheless, work to date indicates that direct cellular reprogramming is a viable and potentially more efficient strategy to generate specific retinal cell types from various sources of cells.

72.4 Future Perspectives

Through these pioneering stem cell studies we have learned that key factors that generate neural retinal and RPE cells are evolutionarily conserved, and that the retinal cells emerging in the dish have remarkable powers of self-assembly to create structures with appropriately organized layers. Still, there is the need for improvements in technologies that will include (a) even more efficient and consistent differentiation protocols, especially for the neural retinal lineages (b) more rapid differentiation, (c) production of purified retinal populations. Using the variety of culture methods being developed, from 2D to organoid cultures, we look forward to gaining a better understanding of human retinal cell development. We predict that iPSC-based modeling will profoundly improve study of disease mechanism and therapeutic development. An exciting future strategy deserving exploration is regeneration of retinal

cells via endogenous sources such as RPE cells and Müller glia. This will require strategies to safely activate the target cells, and possibly direct reprogramming by introducing genes, taking advantage of strides made in viral gene delivery to the retina (Day et al. 2014). In summary, stem cell research provides the opportunity to advance basic research relevant to human retinal development and function. We look forward to translational research progress from bench to bedside, and ultimately, to a new era of regenerative medicine for preserving and improving vision.

Acknowledgments We are grateful for support from the Macula Vision Research Foundation.

References

Akagi T, Mandai M, Ooto S et al (2004) Otx2 homeobox gene induces photoreceptor-specific phenotypes in cells derived from adult iris and ciliary tissue. Investig Ophthalmol Vis Sci 45:4570–4575

Akagi T, Akita J, Haruta M et al (2005) Iris-derived cells from adult rodents and primates adopt photoreceptor-specific phenotypes. Investig Ophthalmol Vis Sci 46:3411–3419

Ambrosi DJ, Rasmussen TP (2005) Reprogramming mediated by stem cell fusion. J Cell Mol Med 9:320–330

Buchholz DE, Hikita ST, Rowland TJ et al (2009) Derivation of functional retinal pigmented epithelium from induced pluripotent stem cells. Stem Cells 27:2427–2434

Day TP, Byrne LC, Schaffer DV et al (2014) Advances in AAV vector development for gene therapy in the retina. Adv Exp Med Biol 801:687–693

Eiraku M, Takata N, Ishibashi H et al (2011) Self-organizing optic-cup morphogenesis in three-dimensional culture. Nature 472:51–56

Evans MJ, Kaufman MH (1981) Establishment in culture of pluripotential cells from mouse embryos. Nature 292:154–156

Giannelli SG, Demontis GC, Pertile G et al (2011) Adult human Muller glia cells are a highly efficient source of rod photoreceptors. Stem Cells 29:344–356

Haruta M, Kosaka M, Kanegae Y et al (2001) Induction of photoreceptor-specific phenotypes in adult mammalian iris tissue. Nature Neurosci 4:1163–1164

Idelson M, Alper R, Obolensky A et al (2009) Directed differentiation of human embryonic stem cells into functional retinal pigment epithelium cells. Cell Stem Cell 5:396–408

Ikeda H, Osakada F, Watanabe K et al (2005) Generation of Rx+/Pax6+ neural retinal precursors from embryonic stem cells. Proc Natl Acad Sci U S A 102:11331–11336

Jin ZB, Okamoto S, Osakada F et al (2011) Modeling retinal degeneration using patient-specific induced pluripotent stem cells. PLoS One 6:e17084

Klimanskaya I, Hipp J, Rezai KA et al (2004) Derivation and comparative assessment of retinal pigment epithelium from human embryonic stem cells using transcriptomics. Clon Stem Cells 6:217–245

Lamba DA, Karl MO, Ware CB et al (2006) Efficient generation of retinal progenitor cells from human embryonic stem cells. Proc Natl Acad Sci U S A 103:12769–12774

Lamba DA, McUsic A, Hirata RK et al (2010) Generation, purification and transplantation of photoreceptors derived from human induced pluripotent stem cells. PLoS One 5:e8763

Lund RD, Wang S, Klimanskaya I et al (2006) Human embryonic stem cell-derived cells rescue visual function in dystrophic RCS rats. Clon Stem Cells 8:189–199

Maeda T, Lee MJ, Palczewska G et al (2013) Retinal pigmented epithelial cells obtained from human induced pluripotent stem cells possess functional visual cycle enzymes in vitro and in vivo. J Biol Chem 288:34484–34493

Martin GR (1981) Isolation of a pluripotent cell line from early mouse embryos cultured in medium conditioned by teratocarcinoma stem cells. Proc Natl Acad Sci U S A 78:7634–7638
Maruotti J, Wahlin K, Gorrell D et al (2013) A simple and scalable process for the differentiation of retinal pigment epithelium from human pluripotent stem cells. Stem Cells Transl Med 2:341–354
Mellough CB, Sernagor E, Moreno-Gimeno I et al (2012) Efficient stage-specific differentiation of human pluripotent stem cells toward retinal photoreceptor cells. Stem Cells 30:673–686
Meyer JS, Shearer RL, Capowski EE et al (2009) Modeling early retinal development with human embryonic and induced pluripotent stem cells. Proc Natl Acad Sci U S A 106:16698–16703
Nakano T, Ando S, Takata N et al (2012) Self-formation of optic cups and storable stratified neural retina from human ESCs. Cell Stem Cell 10:771–785
Osakada F, Ikeda H, Mandai M et al (2008) Toward the generation of rod and cone photoreceptors from mouse, monkey and human embryonic stem cells. Nature Biotech 26:215–224
Osakada F, Jin Z-B, Hirami Y et al (2009) In vitro differentiation of retinal cells from human pluripotent stem cells by small-molecule induction. J Cell Sci 122:3169–3179
Pollak J, Wilken MS, Ueki Y et al (2013) ASCL1 reprograms mouse Muller glia into neurogenic retinal progenitors. Development 140:2619–2631
Sanges D, Romo N, Simonte G et al (2013) Wnt/beta-catenin signaling triggers neuron reprogramming and regeneration in the mouse retina. Cell Reports 4:271–286
Seko Y, Azuma N, Kaneda M et al (2012) Derivation of human differential photoreceptor-like cells from the iris by defined combinations of CRX, RX and NEUROD. PLoS One 7:e35611
Singh R, Shen W, Kuai D et al (2013) iPS cell modeling of best disease: insights into the pathophysiology of an inherited macular degeneration. Hum Mol Genet 22:593–607
Takahashi K, Yamanaka S (2006) Induction of pluripotent stem cells from mouse embryonic and adult fibroblast cultures by defined factors. Cell 126:663–676
Thomson JA, Itskovitz-Eldor J, Shapiro SS et al (1998) Embryonic stem cell lines derived from human blastocysts. Science 282:1145–1147
Tucker BA, Mullins RF, Streb LM et al (2013) Patient-specific iPSC-derived photoreceptor precursor cells as a means to investigate retinitis pigmentosa. eLife 2:e00824
Zhang K, Liu G-H, Yi F et al (2014) Direct conversion of human fibroblasts into retinal pigment epithelium-like cells by defined factors. Protein Cell 5(1):48–58
Zhong X, Gutierrez C, Xue T et al (2014) Generation of three-dimensional retinal tissue with functional photoreceptors from human iPSCs. Nat Commun 5:4047

Chapter 73
Personalized Medicine: Cell and Gene Therapy Based on Patient-Specific iPSC-Derived Retinal Pigment Epithelium Cells

Yao Li, Lawrence Chan, Huy V Nguyen and Stephen H Tsang

Abstract Interest in generating human induced pluripotent stem (iPS) cells for stem cell modeling of diseases has overtaken that of patient-specific human embryonic stem cells due to the ethical, technical, and political concerns associated with the latter. In ophthalmology, researchers are currently using iPS cells to explore various applications, including: (1) modeling of retinal diseases using patient-specific iPS cells; (2) autologous transplantation of differentiated retinal cells that undergo gene correction at the iPS cell stage via gene editing tools (e.g., CRISPR/Cas9, TALENs and ZFNs); and (3) autologous transplantation of patient-specific iPS-derived retinal cells treated with gene therapy. In this review, we will discuss the uses of patient-specific iPS cells for differentiating into retinal pigment epithelium (RPE) cells, uncovering disease pathophysiology, and developing new treatments such as gene therapy and cell replacement therapy via autologous transplantation.

Keywords iPS · RPE · Gene therapy · Cell therapy · Disease modeling · Sub-retinal transplantation · Gene correction

S. H. Tsang (✉)
New York Presbyterian Hospital/Columbia University Medical Center,
New York, NY 10032, USA
e-mail: sht2@columbia.edu

Department of Pathology and Cell Biology, Department of Ophthalmology, Edward Harkness Eye Institute, Columbia University, 160 Fort Washington Avenue, Research Annex, Room 509B, New York, NY 10032 USA

Y. Li · L. Chan
Department of Ophthalmology, Columbia University Medical Center, Columbia University,
160 Fort Washington Ave, Research Annex, Room 513, New York, NY 10032, USA
e-mail: yl2635@columbia.edu

L. Chan
e-mail: lc2988@columbia.edu

H. V. Nguyen
Columbia University College of Physicians and Surgeons, 100 Haven Ave,
Apt 14B, New York, NY 10032, USA
e-mail: hvn2102@columbia.edu

C. Bowes Rickman et al. (eds.), *Retinal Degenerative Diseases,* Advances in Experimental Medicine and Biology 854, DOI 10.1007/978-3-319-17121-0_73

73.1 Introduction

As a platform to study patient-specific targeted disease cells, iPS cells have exciting potential in regenerative medicine and human disease modeling. The *in vitro* phenotypes of disease-specific iPS-derived cells can be used to bridge the gap between the clinical phenotype and molecular/cellular mechanisms, creating new strategies for drug screening, and developing novel therapeutic agents for clinical trials without the use of more expensive animal models (Tsuji et al. 2010; Jin et al. 2011; Lustremant et al. 2013; Singh et al. 2013).

iPS-based therapies hold great promise for treating retinal degenerative diseases. Among these diseases, retinitis pigmentosa (RP) is one of the most devastating and prevalent, affecting 1.5 million people worldwide. Cell transplantation into the human retina has the potential to restore vision and provide treatment in diseases like RP with significant retinal pigment epithelium (RPE) loss. Replacement of damaged RPE in patients with age-related macular degeneration (AMD), another leading cause of blindness, is now being offered (Wang et al. 2010). In 2011, the U.S. Food and Drug Administration advanced the treatment of macular degenerations by approving clinical trials using embryonic stem (ES) cell-derived RPE transplants (Schwartz et al. 2012). In addition to the prospect of transplantations, human iPS cell technology provides a platform for investigating the pathophysiological mechanisms of genetic mutations and testing of gene therapy vectors on RPE-based disease models. iPS-derived RPE (iPS-RPE) can be reproducibly isolated and closely monitored both morphologically and functionally before experiments.

73.2 RPE Loss and Retinal Disease

Dysfunction and death of RPE has been observed in various blinding diseases, including AMD and RP, two of the leading causes of blindness in the developed world. AMD alone affects approximately 8 million Americans, and its incidence is expected to double by 2020. The RPE, a monolayer of cells located at the back of the eye between the retina and Bruch's membrane, is essential for photoreceptor function and survival. Hence, RPE loss accounts for a significant number of neurodegenerative diseases that severely impair activities of daily living. Anti-VEGF therapy has been shown to slow the rate of vision loss, but it has no more than a 10% rate of effectiveness in all AMD cases (Rosenfeld et al. 2006). No other treatments are currently available to restore the vision of patients who suffer from RPE loss.

Researchers have generated animal models to develop treatments such as stem cell replacement therapy for retinal disease caused by RPE loss. One model is the *Rpe65*^{rd12}/*Rpe65*^{rd12} (rd12) mouse for studying Leber congenital amaurosis (LCA) (Pang et al. 2005). LCA Type 2 is caused by mutations in the gene encoding RPE-specific protein 65 kDa (RPE65), an isomerase that is involved in the conversion of the chromophore necessary for rhodopsin to detect light (Jin et al. 2005). Successful stem cell replacement therapy resulting in functional improvements with this model

has been previously reported (Wang et al. 2010; Li et al. 2012). Another model that has been widely tested with gene therapy is the *Mfrp*^{rd6}/*Mfrp*^{rd6} mouse, which has a deletion in the Membrane Frizzled-Related Protein (*Mfrp)* gene. These mice have abnormal expressions of MFRP protein, an RPE-specific membrane receptor, and exhibit progressive retinal degeneration beginning at 1 month of age, with photoreceptor function completely extinguished by 70 weeks (Kameya et al. 2002). Due to their slow rates of degeneration, these mice are ideal recipients for testing *in vivo* treatments for RP caused by MFRP deficiency.

73.3 iPSC and Eye Disease

73.3.1 Cell Therapy: Retinal Pigment Epithelium Sub-retinal Transplantation

The eye is an ideal testing ground for stem cell therapies for numerous reasons: its relative immune privilege, its accessibility for monitoring and imaging, and the presence of a contralateral control eye. iPS cells offer a compelling alternative approach for stem cell therapy, given its potentially unlimited capacity for generating cells for functional testing and optimization studies. When derived from the transplant recipient, autologous iPS-derived cells obviate the need for immunosuppression after transplantation.

RPE transplantation poses fewer challenges than other kinds of cell transplantation since routine culture of RPE cells has been well described (Idelson et al. 2009; Sonoda et al. 2009). Pigmented RPE monolayers have an easily identifiable hexagonal structure and can be isolated and transferred to a variety of substrates without the need for synaptic integration. Much information regarding pluripotent cell-derived RPE transplantation has come from a multicenter trial, run by Advanced Cell Technologies, for the treatment of dry macular degeneration and Stargardt macular dystrophy (Schwartz et al. 2012). In these studies, a near pure population of RPE was obtained from human ES cells maintained under good manufacturing practice (GMP) conditions and injected subretinally into the patients with good results. Similarly, iPS-RPE autologous cell transplantations have recently been approved in Japan for AMD clinical trials (Cyranoski 2013).

At present, human iPS-derived RPE cell transplantation data are limited to animal models. In one experiment, Li et al. injected dissociated suspensions of human iPS-RPE into the subretinal space of the *Rpe65* mutant mouse model and showed integration of the transplant with the host RPE, as well as a modest improvement of visual function as measured by electroretinogram (ERG) (Li et al. 2012). Carr et al. (2009) also showed that subretinal injections of dissociated human iPS-RPE into Royal College of Surgeons (RCS) rats resulted in long-term preservation of visual function. Intracellular RHO staining suggested that these transplanted cells behaved normally by phagocytosing photoreceptor outer segments *in vivo* (Carr et al. 2009).

73.3.2 Progress of Retinal Disease Modeling

The first retinal disease to be modeled via patient-specific iPS cells is Best vitelliform macular dystrophy (BVMD) (Singh et al. 2013). BVMD is caused by a defect in the RPE gene *BEST1*, which results in the subretinal accumulation of photoreceptor waste products (e.g., lipofuscin) and fluid, leading to secondary photoreceptor death and central vision loss. Singh et al. observed clinically relevant disease phenotypes for BVMD, such as disrupted fluid flux and increased accrual of autofluorescent material, in iPS-RPE from affected patients compared to those obtained from unaffected siblings. On a molecular level, rhodopsin degradation after photoreceptor outer segment (POS) feeding was delayed in BVMD iPS-RPE, directly implicating impaired POS handling in the pathophysiology of the disease.

iPS cells have also been used to study the pathophysiology of AMD. Although the closely linked *ARMS2*/*HTRA1* genes were found to be strongly associated with the risk of AMD, their downstream targets are unknown. Further complicating the study of this age-related disease is the lack of appropriate models; mice do not have maculae and human autopsy samples are from the end, not early, stages of disease. To circumvent these obstacles, Yang et al. created AMD patient-specific iPS-derived RPE that were pharmacologically aged with bisretinoid N-retinylidine-N-ethanolamine (A2E) and blue light (Yang et al. 2014). With this novel AMD model, the researchers showed that impaired superoxide dismutase 2 (SOD2) response was related to a high risk of AMD. SOD2 and reactive oxygen species (ROS) assays confirmed that the AMD-associated genetic risk factors impair the ability of RPE to defend against aging-related oxidative stress, thereby contributing to AMD pathogenesis.

In a recently published report (Li et al. 2014), the authors showed that the phenotypes of patient-specific cells differed from that of a mouse model, underscoring the necessity for multiple models of disease. Compared to wild-type control iPS-RPE cells, patient iPS-RPE containing a mutation in the *Mfrp* gene exhibited the loss of apical microvilli as observed by electron microscopy. This result was in stark contrast to the phenotype $Mfrp^{rd6}/Mfrp^{rd6}$ mice RPE, which showed higher densities of apical microvilli (Fogerty and Besharse 2011). Because differences in phenotypic expression can be observed among species with the same genetic mutation, it is important to study patient-specific cell lines as a complement to mouse models.

73.4 Personalized Medicine: Patient-Specific iPSC-based Therapy

73.4.1 Development of Gene Correction on Patient-Specific iPSCs

Gene-corrected patient-specific iPS cells offer a unique approach to autologous therapies, with the potential to treat a wide range of acquired and inherited diseases.

Genome editing tools, such as zinc finger nucleases (ZFNs), transcription activator-like effector nucleases (TALENs), and the clustered regularly interspaced short palindromic repeats (CRISPR)/Cas9 system, are able to correct the mutations that lead to genetic diseases. By editing the mutations in the patients' genomic DNA through double strand break induction and subsequent homology-directed repair, the corrected gene will remain under the normal endogenous expression control elements (Tucker et al. 2014).

Among the three technologies, the CRISPR/Cas9 system is particularly attractive because its guide RNAs can be more readily generated, unlike the protein-based DNA targeting motifs of ZFNs and TALENs. Mali et al. reported success in targeting the endogenous AAVS1 locus in human iPSCs via the CRISPR/Cas9 system and achieved homology-directed repair of fibroblast-derived iPSCs (Cho et al. 2013; Mali et al. 2013). Despite the ease of use, there are concerns of possible mispairings between the guides and genomic DNA, as well as induction of double strain breaks in undesired locations (Fu et al. 2013). Accordingly, strategies to decrease these risks of off-targeting are being developed. Ran et al. recently demonstrated that by mutating a single amino acid in the catalytic domain of the Cas9 nuclease, they could generate a "nicking" enzyme that only cleaves a single strand of DNA in DNA repair (Ran et al. 2013). The researchers were able to achieve efficient modification of three distinct genetic loci with a 200 to 1500-fold increase in specificity (Ran et al. 2013). In short, these experiments demonstrate the potential of employing nickases to increase the specificity and safety of the CRISPR/Cas9 genome editing technology.

73.4.2 Gene Therapy on Patient-Specific iPSC-Derived RPE Cells.

There are also reports of using patient-specific iPS-derived RPE cells as the recipient for gene therapy. In 2013, researchers at the University of Pennsylvania used adeno-associated virus (AAV)-mediated gene therapy to restore Rab Escort Protein 1 (REP1) function in iPSC from choroideremia (CHM) patients (Vasireddy et al. 2013). Less than 1 year later, Cereso et al. applied AAV2/5-mediated gene therapy to the differentiated RPE cells from CHM patient-specific iPSCs (Cereso et al. 2014). With this CHM model, they assayed a panel of AAV vector serotypes and showed that AAV2/5 is the most efficient at transducing iPSC-derived RPE.

Meanwhile, Li et al. showed successful correction of the overall phenotype using human iPS-RPE cells as gene therapy recipients (Li et al. 2014). They created two patient-specific iPS-derived RPE cell lines with MFRP defects and applied the AAV8 vector expressing human MFRP. As a result, AAV-treated *Mfrp* mutant iPS-RPE cells recovered wildtype pigmentation and transepithelial resistance. The AAV-mediated gene therapy was also evaluated in $Mfrp^{rd6}/Mfrp^{rd6}$ mice, yielding long-term improvement in visual function as observed via ERG.

73.5 Future Directions

iPS technology has the promise to make significant contributions to our understanding of the most pressing blinding diseases of our time. Patient-specific iPS cells have been shown to not only complement animal models of human disease but also be an excellent model in their own right. These cells provide a window for testing the efficacy of gene- or drug-based therapies, elucidate new mechanisms and pathways of disease, and enable researchers to experiment with the parameters for successful cell replacement therapy *in vitro*. The efforts of the biotechnology industry to make large-scale stem cell production feasible will only make stem cell technology more widely accessible (Borooah et al. 2013). Major progress has also been made in developing Good Manufacturing Practice (GMP) laboratories and bringing iPS applications to clinical trials. The future direction of iPS development offers the hope of slowing progression or perhaps improving visual function for patients with currently untreatable retinal diseases.

References

Borooah S, Phillips MJ, Bilican B et al (2013) Using human induced pluripotent stem cells to treat retinal disease. Prog Ret Eye Res 37:163–181

Carr AJ, Vugler AA, Hikita ST et al (2009) Protective effects of human iPS-derived retinal pigment epithelium cell transplantation in the retinal dystrophic rat. PLoS One 4:e8152

Cereso N, Pequignot MO, Robert L et al (2014) Proof of concept for AAV2/5-mediated gene therapy in iPSC-derived retinal pigment epithelium of a choroideremia patient. Mol Ther Methods Clin Dev 1:14011. doi:10.1038/mtm.2014.11

Cho SW, Kim S, Kim JM et al (2013) Targeted genome engineering in human cells with the Cas9 RNA-guided endonuclease. Nat Biotech 31:230–232

Cyranoski D (2013) Stem cells cruise to clinic. Nature 494:413

Fogerty J, Besharse JC (2011) 174delG mutation in mouse MFRP causes photoreceptor degeneration and RPE atrophy. Invest Ophthalmol Vis Sci 52:7256–7266

Fu Y, Foden JA, Khayter C et al (2013) High-frequency off-target mutagenesis induced by CRISPR-Cas nucleases in human cells. Nat biotech 31:822–826

Idelson M, Alper R, Obolensky A et al (2009) Directed differentiation of human embryonic stem cells into functional retinal pigment epithelium cells. Cell Stem Cell 5:396–408

Jin M, Li S, Moghrabi WN et al (2005) Rpe65 is the retinoid isomerase in bovine retinal pigment epithelium. Cell 122:449–459

Jin ZB, Okamoto S, Osakada F et al (2011) Modeling retinal degeneration using patient-specific induced pluripotent stem cells. PLoS one 6:e17084

Kameya S, Hawes NL, Chang B et al (2002) Mfrp, a gene encoding a frizzled related protein, is mutated in the mouse retinal degeneration 6. Hum Mol Genet 11:1879–1886

Li Y, Tsai YT, Hsu CW et al (2012) Long-term safety and efficacy of human-induced pluripotent stem cell (iPS) grafts in a preclinical model of retinitis pigmentosa. Mol Med 18:1312–1319

Li Y, Wu WH, Hsu CW et al (2014) Gene therapy in patient-specific stem cell lines and a preclinical model of retinitis pigmentosa with membrane frizzled-related protein defects. Mol Ther 22(9):1688–1697. doi:10.1038/mt.2014.100

Lustremant C, Habeler W, Plancheron A et al (2013) Human induced pluripotent stem cells as a tool to model a form of Leber congenital amaurosis. Cell Reprogram 15:233–246

Mali P, Yang L, Esvelt KM et al (2013) RNA-guided human genome engineering via Cas9. Science 339:823–826

Pang JJ, Chang B, Hawes NL et al (2005) Retinal degeneration 12 (rd12): a new, spontaneously arising mouse model for human Leber congenital amaurosis (LCA). Mol Vis 11:152–162

Ran FA, Hsu PD, Lin CY et al (2013) Double nicking by RNA-guided CRISPR Cas9 for enhanced genome editing specificity. Cell 154:1380–1389

Rosenfeld PJ, Brown DM, Heier JS et al (2006) Ranibizumab for neovascular age-related macular degeneration. N Engl J Med 355:1419–1431

Schwartz SD, Hubschman JP, Heilwell G et al (2012) Embryonic stem cell trials for macular degeneration: a preliminary report. Lancet 379(9817):713–720. doi:10.1016/S0140-6736(12)60028-2

Singh R, Shen W, Kuai D et al (2013) iPS cell modeling of best disease: insights into the pathophysiology of an inherited macular degeneration. Hum Mol Genet 22:593–607

Sonoda S, Spee C, Barron E et al (2009) A protocol for the culture and differentiation of highly polarized human retinal pigment epithelial cells. Nat Protoc 4:662–673

Tsuji O, Miura K, Okada Y et al (2010) Therapeutic potential of appropriately evaluated safe-induced pluripotent stem cells for spinal cord injury. Proc Natl Acad Sci U S A 107:12704–12709

Tucker BA, Mullins RF, Stone EM (2014) Stem cells for investigation and treatment of inherited retinal disease. Hum Mol Genet 23(R1):R9–R16. doi:10.1093/hmg/ddu124

Vasireddy V, Mills JA, Gaddameedi R et al (2013) AAV-mediated gene therapy for choroideremia: preclinical studies in personalized models. PLoS One 8:e61396

Wang NK, Tosi J, Kasanuki JM et al (2010) Transplantation of reprogrammed embryonic stem cells improves visual function in a mouse model for retinitis pigmentosa. Transplantation 89:911–919

Yang J, Li Y, Chan L et al (2014) Validation of genome-wide association study (GWAS)-identified disease risk alleles with patient-specific stem cell lines. Hum Mol Genet 23:3445–3455

Chapter 74
Human Retinal Pigment Epithelium Stem Cell (RPESC)

Janmeet S. Saini, Sally Temple and Jeffrey H. Stern

Abstract The retinal pigment epithelium (RPE) is a pigmented cellular monolayer that supports photoreceptor cells located in the overlying neural retina. The RPE is critical for vision and its dysfunction results in numerous pathologies, several with limited available disease-altering strategies. Regeneration of the retina from RPE is robust in lower vertebrates, but is not normally exhibited in mammals. We recently found that a subpopulation of human RPE cells can be stimulated in culture to generate multipotent self-renewing cells—the RPE stem cell (RPESC). RPESC can be expanded to generate RPE progeny that are a potential source for cell replacement therapy. Alternatively, RPESC can produce mesenchymal progeny which serve as a disease model of epiretinal membrane formation. Yet another potential application of RPESCs is activation within the eye to awaken dormant endogenous repair.

Keywords Retina · Stem cells · Tissue specific stem cells · Retinal pigment epithelium (RPE) · Retinal pigment epithelium stem cells (RPESC) · Regeneration · Disease modeling · Epiretinal membrane · Transplantation · Endogenous repair

74.1 Introduction

The sense of sight is critical, and our quality of life deteriorates with vision loss, for example due to retinal disease. Vision loss associated with the dysfunction and death of retinal pigment epithelial (RPE) cells occurs in several types of retinal

J. H. Stern (✉) · J. S. Saini · S. Temple
Neural Stem Cell Institute, Regenerative Research Foundation,
One Discovery Drive, Rensselaer, NY 12144, USA
e-mail: jeffreystern@neuralsci.org

S. Temple
e-mail: sallytemple@neuralsci.org

J. S. Saini
Department of Biomedical Sciences, University at Albany, 12201 Albany, NY, USA
e-mail: janmeetsaini@neuralsci.org

C. Bowes Rickman et al. (eds.), *Retinal Degenerative Diseases,* Advances in Experimental Medicine and Biology 854, DOI 10.1007/978-3-319-17121-0_74

degenerative disease, including age-related macular degeneration and forms of retinitis pigmentosa. Disease-altering strategies are lacking for many of these RPE degenerative diseases. We recently discovered that a sub-population of multipotent, self-renewing RPE stem cells (RPESC) are present in the human RPE layer (Salero et al. 2012). In this chapter we review the unique RPESC and its use to (1) generate RPE progeny for RPE replacement therapy, (2) produce disease-in-a-dish models for drug discovery and (3) promote endogenous RPE layer self-repair.

74.2 The RPE Layer

The eye derives from the neuroepithelium during embryonic development. Early in this process, the neuroepithelium invaginates to give rise to the optic cup with two distinct layers: an inner layer that forms the neural retina, including the light-sensitive photoreceptor cells, and an outer layer that forms the RPE layer. Subsequent maturation of neural retina and RPE occurs in concert and is driven by interaction between the layers and the surrounding tissues, including the mesenchyme and overlying ectoderm (Strauss 2005). Initially, the cells of the optic vesicle are all competent to make RPE and neural retina and are morphologically and molecularly similar. Specification and differentiation of the different retinal cell types is regulated by signaling molecules over time (Chow et al. 1999; Zuber et al. 2003) resulting in differentiated progenitor cells that produce the specialized cells of the fully mature eye (Zaghloul et al. 2005).

The differentiated RPE layer has many functions, including providing nutrition to the inner retina, visual pigment recycling, fluid and electrolyte homeostasis, cytokine release, photoreceptor phagocytosis and protecting the photoreceptors from light damage (Bok 1993; Strauss 2005). Most types of epithelium undergo constant replacement of damaged cells via tissue homeostasis (Blanpain et al. 2007); in contrast, the RPE, like other central nervous system tissues, shows limited renewal. Thus progressive damage due to aging and disease results in permanent loss of RPE cells.

74.3 Regeneration of the Retina

The vertebrate eye structure and its development are highly conserved evolutionarily (Wawersik and Maas 2000; Vopalensky and Kozmik 2009). However, in lower vertebrates, the retina retains the ability to regenerate and in several species, RPE cells have a critical role in this process (Keefe 1973; Mitashov 1997; Raymond and Hitchcock 2000; Fischer and Reh 2001). Retinal injury in amphibians, for example, can activate RPE cells to revert to a proliferative neuroepithelial fate and then reconstitute the entire retina (Klein et al. 1990; Mitashov 1997). Unknown factors prevent such RPE cell activation in adult mammals, and thus prevent the regeneration of the retina (Mitashov 1997).

74.4 Tissue-Specific Stem Cells

Stem cells are defined by their ability to self-renew and differentiate into specialized cells. While embryonic stem cells are pluripotent, having the ability to differentiate into all the derivatives of the three germ layers, tissue-specific stem cells primarily generate cell types of their parent tissue (Young and Black 2004; Blanpain et al. 2007). During development, the cells of the three germ layers undergo rounds of proliferation giving rise to progenitor cells and subsequently to differentiated cells; a fraction of cells leave this continuum and become reserve somatic stem or progenitor cells. Such cells may mediate continuous repair and maintenance of tissues (Young and Black 2004). Tissue specific stem cells or somatic stem cells have been identified in the hematopoietic system (Mikkola and Orkin 2006; Moore and Lemischka 2006), skin (Ghazizadeh and Taichman 2001), and intestinal epithelia (Bjerknes and Cheng 2002) where a rapid rate of cellular turnover is required. More recently, somatic stem cells have been found in tissues with lower self-renewal demand such as prostate (Lawson et al. 2007) and nervous system (Reynolds and Weiss 1992; Clarke et al. 2000). Typically, somatic stem cells are dormant or slowly dividing, but upon activation generate a rapidly dividing cellular pool of transit amplifying cells that will differentiate into a particular cell lineage and thus repair tissue (Moore and Lemischka 2006; Blanpain et al. 2007).

74.5 RPE Stem Cells (RPESC)

Pioneering studies have demonstrated that human RPE from fetal through adult stages can proliferate in culture and produce monolayers valuable for studying RPE cell function and polarity (Hu and Bok 2001; Maminishkis et al. 2006; Blenkinsop et al. 2013). We recently determined that although RPE cells appear morphologically similar, only a subpopulation of them have the ability to proliferate extensively. Therefore, monolayers of RPE are typically produced from a minor subpopulation of cells. We recently characterized this process and described a sub-population of tissue-specific adult human RPESC that can be stimulated in culture to self-renew and produce multipotent proliferating cells (Salero et al. 2012).

In order to establish the existence of stem cell characteristics in adult human RPE, we extracted the cells from donated globes and performed well-established tests of stem cell activity: clonal non-adherent sphere formation assays (Reynolds and Rietze 2005) and clonal adherent growth assays (Davis and Temple 1994). We found that a minor subset of RPE cells can form spheres in non-adherent cultures, and just 3–10 % of isolated RPE cells are highly proliferative in clonal adherent cultures. Time-lapse movies of acutely isolated RPE cells also demonstrate that most RPE cells divide occasionally, but a subpopulation of RPE cells has a much more substantial capacity to proliferate, migrate and contribute to a confluent monolayer of cells. Combined, these observations demonstrate that the adult RPE contains a subset of cells that can be activated to a stem cell state (RPESC), extensively self-renewing to produce new RPE cells *in vitro*.

RPESCs divide robustly and can be induced to differentiate into a highly polarized cobblestone monolayer accompanied by expression of RPE markers such as RPE-65, CRALBP, Bestrophin and MITF (Blenkinsop et al. 2013). We have expanded RPESC to produce $>5 \times 10^8$ progeny after 2 passages which then differentiate into polarized RPE, suggesting that this is a useful candidate cell source for RPE replacement therapy. When grown on transwell polyester membranes, these RPESC-derived RPE can be transplanted into animal models such as the rabbit and remain as a stabilized, polarized monolayer for at least a month (Stanzel et al. 2014).

We also found that RPESCs are multipotent and can differentiate into neural and mesenchymal progeny when grown in culture conditions known to promote these fates. RPE cells grown in media that stimulates the production of neural progeny from human pluripotent stem cells can up-regulate neural progenitor cell markers, including Nestin and TuJ1 (von Bohlen Und Halbach 2007), however to date, these progeny do not acquire the morphology of mature neurons or glia. In contrast, the generation of differentiated mesenchymal progeny from RPESC cultures is robust when RPESC are exposed to mesenchymal differentiation media. Importantly, we have observed differentiation in clonal RPE lines split into different growth conditions- the same RPESC-derived clonal line that in control conditions produces RPE progeny, when exposed to osteogenic, adipogenic or chondrogenic media can produce differentiated cells of these mesenchymal lineages.

Mesenchymal progeny are found in retinal diseases such as epiretinal membrane formation that are known to involve RPE cells (Newsome et al. 1981; Heidenkummer and Kampik 1991). The disease process has been suggested to involve an epithelial to mesenchymal transition and differentiation of the cells into mesenchymal fates. Our findings that this can be reproduced in the culture dish strengthens the concept that RPE is an important cell of origin in epiretinal membranes. In addition, RPESC cultures can be used as a model of epiretinal membrane formation, useful to understand the disease process and for drug discovery. We found that RPE cells generated from pluripotent sources, including human embryonic stem cells and induced pluripotent stem cells, or from fetal eyes can also generate mesenchymal progeny, hence this is not a unique feature of the adult RPESC. It is important to understand the mechanisms underlying this plasticity not only because it has implications for retinal pathologies, but also because pluripotent stem cell-derived RPE are already approved for clinical trials (DR1-01444; Schwartz et al. 2012), and this is a potential adverse event that must be avoided.

RPESC cultures also provide a model to study the factors that stabilize RPE to prevent RPE and retinal regeneration in higher organisms. We have observed that appropriate culture conditions switch off repressive factors to activate RPESC proliferation. Doing so within a patient's eye to activate the intrinsic surviving RPE is a strategy to replenish the RPE layer and may also benefit the neural retina by producing beneficial growth factors or improving RPE support of neural retinal cell function. A number of challenges remain to selectively activate the RPESC to differentiate along appropriate RPE lineages without affecting other eye progenitor cell types. We are currently exploring RPESC activation both *in vitro* and *in vivo* to define conditions that safely increase RPE cell number by activating endogenous RPESCs as a therapeutic avenue for retinal degenerative disease.

Our ongoing work aims to uncover the factors and pathways promoting stem cell like behavior in mature human RPE. FGF (Spence et al. 2007), Shh (Spence et al. 2004; Spence et al. 2007), Activin (Sakami et al. 2008), ERK (Mizuno et al. 2012) and other signaling factors have been implicated in the regulation of RPE in regenerating retina of lower vertebrates. Prior studies of intraocular growth factors have shown benefit in degenerative disease models (Unoki and LaVail 1994; Kimizuka et al. 1997), and combinations of exogenous factors may selectively activate the RPESC *in vivo*.

In the future, we hope that discovery of the RPESC and further characterization of this cell will enable us to control endogenous RPE regeneration *in vivo*. This approach may be preferable to increasing the RPE cell number by surgical implantation of cells because endogenous activation has the potential to avoid surgical injury and immunosuppression. Overcoming the barriers to endogenous regeneration and enabling RPE cell repair *in vivo* could, in the future, lead to further regenerative abilities of the RPESCs, to benefit patients suffering from retinal degenerations.

Acknowledgments This research was supported in part by the National Eye Institute award, EY022079, and the NYS Empire State Stem Cell Fund award, C028504. Opinions expressed here are solely those of the authors.

References

Bjerknes M, Cheng H (2002) Multipotential stem cells in adult mouse gastric epithelium. Am J Physil Gastro Liver Physiol 283:G767–G777

Blanpain C, Horsley V, Fuchs E (2007) Epithelial stem cells: turning over new leaves. Cell 128:445–458

Blenkinsop TA, Salero E, Stern JH et al (2013) The culture and maintenance of functional retinal pigment epithelial monolayers from adult human eye. Method Mol Biol 945:45–65

Bok D (1993) The retinal pigment epithelium: a versatile partner in vision. J Cell Sci Suppl 17:189–195

Chow RL, Altmann CR, Lang RA et al (1999) Pax6 induces ectopic eyes in a vertebrate. Development 126:4213–4222

Clarke DL, Johansson CB, Wilbertz J et al (2000) Generalized potential of adult neural stem cells. Science 288:1660–1663

Davis AA, Temple S (1994) A self-renewing multipotential stem cell in embryonic rat cerebral cortex. Nature 372:263–266

Fischer AJ, Reh TA (2001) Transdifferentiation of pigmented epithelial cells: a source of retinal stem cells? Dev Neurosci 23:268–276

Ghazizadeh S, Taichman LB (2001) Multiple classes of stem cells in cutaneous epithelium: a lineage analysis of adult mouse skin. EMBO J 20:1215–1222

Heidenkummer HP, Kampik A (1991) [Comparative immunohistochemical studies of epiretinal membranes in proliferative vitreoretinal diseases]. Fortschr Ophthalmol 88:219–224

Hu J, Bok D (2001) A cell culture medium that supports the differentiation of human retinal pigment epithelium into functionally polarized monolayers. Mol Vis 7:14–19

Keefe JR (1973) An analysis of urodelian retinal regeneration. I. Studies of the cellular source of retinal regeneration in Notophthalmus viridescens utilizing 3 H-thymidine and colchicine. J Exp Zool 184:185–206

Kimizuka Y, Yamada T, Tamai M (1997) Quantitative study on regenerated retinal pigment epithelium and the effects of growth factor. Curr Eye Res 16:1081–1087

Klein LR, MacLeish PR, Wiesel TN (1990) Immunolabelling by a newt retinal pigment epithelium antibody during retinal development and regeneration. J Comp Neurol 293:331–339
Lawson DA, Xin L, Lukacs RU et al (2007) Isolation and functional characterization of murine prostate stem cells. Proc Natl Acad Sci U S A 104:181–186
Maminishkis A, Chen S, Jalickee S et al (2006) Confluent monolayers of cultured human fetal retinal pigment epithelium exhibit morphology and physiology of native tissue. Investig Ophthalmol Vis Sci 47:3612–3624
Mikkola HK, Orkin SH (2006) The journey of developing hematopoietic stem cells. Development 133:3733–3744
Mitashov VI (1997) Retinal regeneration in amphibians. Internat J Dev Biol 41:893–905
Mizuno A, Yasumuro H, Yoshikawa T et al (2012) MEK-ERK signaling in adult newt retinal pigment epithelium cells is strengthened immediately after surgical induction of retinal regeneration. Neurosci Lett 523:39–44
Moore KA, Lemischka IR (2006) Stem cells and their niches. Science 311:1880–1885
Newsome DA, Rodrigues MM, Machemer R (1981) Human massive periretinal proliferation. In vitro characteristics of cellular components. Arch Ophthalmol 99:873–880
Raymond PA, Hitchcock PF (2000) How the neural retina regenerates. Results Prob Cell Diff 31:197–218
Reynolds BA, Rietze RL (2005) Neural stem cells and neurospheres–re-evaluating the relationship. Nat Methods 2:333–336
Reynolds BA, Weiss S (1992) Generation of neurons and astrocytes from isolated cells of the adult mammalian central nervous system. Science 255:1707–1710
Sakami S, Etter P, Reh TA (2008) Activin signaling limits the competence for retinal regeneration from the pigmented epithelium. Mech Dev 125:106–116
Salero E, Blenkinsop TA, Corneo B et al (2012) Adult human RPE can be activated into a multipotent stem cell that produces mesenchymal derivatives. Cell Stem Cell 10:88–95
Schwartz SD, Hubschman JP, Heilwell G et al (2012) Embryonic stem cell trials for macular degeneration: a preliminary report. Lancet 379:713–720
Spence JR, Madhavan M, Ewing JD et al (2004) The hedgehog pathway is a modulator of retina regeneration. Development 131:4607–4621
Spence JR, Aycinena JC, Del Rio-Tsonis K (2007) Fibroblast growth factor-hedgehog interdependence during retina regeneration. Dev Dyn 236:1161–1174
Stanzel BV, Liu Z, Somboonthanakij S et al (2014) Human RPE stem cells grown into polarized rpe monolayers on a polyester matrix are maintained after grafting into rabbit subretinal space. Stem Cell Rep 2:64–77
Strauss O (2005) The retinal pigment epithelium in visual function. Physiol Rev 85:845–881
Unoki K, LaVail MM (1994) Protection of the rat retina from ischemic injury by brain-derived neurotrophic factor, ciliary neurotrophic factor, and basic fibroblast growth factor. Invest Ophthalmol Vis Sci 35:907–915
von Bohlen Und Halbach O (2007) Immunohistological markers for staging neurogenesis in adult hippocampus. Cell Tiss Res 329:409–420
Vopalensky P, Kozmik Z (2009) Eye evolution: common use and independent recruitment of genetic components. Phil Trans Roy Soc Lond B 364:2819–2832
Wawersik S, Maas RL (2000) Vertebrate eye development as modeled in Drosophila. Hum Mol Genet 9:917–925
Young HE, Black AC Jr (2004) Adult stem cells. Anat Rec Part A 276:75–102
Zaghloul NA, Yan B, Moody SA (2005) Step-wise specification of retinal stem cells during normal embryogenesis. Biol Cell 97:321–337
Zuber ME, Gestri G, Viczian AS et al (2003) Specification of the vertebrate eye by a network of eye field transcription factors. Development 130:5155–5167

Chapter 75
Embryonic Stem Cell-Derived Microvesicles: Could They be Used for Retinal Regeneration?

Debora B. Farber and Diana Katsman

Abstract Mouse embryonic stem cells (mESCs) release into the medium in which they are cultured heterogeneous populations of microvesicles (mESMVs), important components of cell-cell communication, that transfer their contents not only to other stem cells but also to cells of other origins. The purpose of these studies was to demonstrate that ESMVs could be the signals that lead the retinal progenitor Müller cells to de-differentiate and re-entry the cell cycle, followed by differentiation along retinal lineages. Indeed, we found that ESMVs induce these processes and change Müller cells' microenvironment towards a more permissive state for tissue regeneration.

Keywords Embryonic stem cells · Stem cells · Stem cell microvesicles · Retina · Retina regeneration · Müller progenitor cells · Müller cell cultures · De-differentiation · Differentiation · Retinal cell lineages

75.1 Introduction

mESMVs released by mESCs into the intercellular environment are heterogeneous in size (from ~ 30 nm to 1 um) and contain mRNA, miRNA and proteins (Yuan et al. 2009). They can transfer their contents to cells of other origins, acting as

D. B. Farber (✉) · D. Katsman
Stein Eye Institute, David Geffen School of Medicine, University of California Los Angeles, Los Angeles, CA 90095-7000, USA
e-mail: farber@jsei.ucla.edu

Department of Ophthalmology, David Geffen School of Medicine, University of California Los Angeles, Los Angeles, CA 90095-7000, USA

D. B. Farber
Molecular Biology Institute, Paul Boyer Hall, University of California Los Angeles, Los Angeles, CA 90095, USA

Brain Research Institute, University of California Los Angeles, Los Angeles, CA 90095, USA

D. Katsman
e-mail: katsman@jsei.ucla.edu

C. Bowes Rickman et al. (eds.), *Retinal Degenerative Diseases,* Advances in Experimental Medicine and Biology 854, DOI 10.1007/978-3-319-17121-0_75

"physiologic liposomes". ESMVs have been shown to reprogram and enhance the proliferation of hematopoietic progenitors (Ratajczak et al. 2006) and to induce the regenerative capacity of several tissues, likely by activating endogenous progenitor cells. As a result, ESMVs have helped to repopulate and repair injured liver (Herrera et al. 2010), lung (Tetta et al. 2011) and kidneys (Bruno et al. 2012). Moreover, ESMVs may be responsible for the paracrine effect ESCs demonstrate on adjacent and distant tissues.

Müller cells meet several of the requirements to be considered progenitor cells, including the ability to differentiate along multiple retinal lineages such as photoreceptors and inner retina neurons (Jadhav 2009; Bernardos et al. 2007). Moreover, it has been shown that Müller cells are activated in injured retinas with some regenerative success (Karl et al. 2008), but functional retinal recovery has not yet been achieved. Identification of factors that induce Müller cells to de-differentiate, enter the cell cycle, and differentiate along retinal neural lineages may lead to novel therapy development for retinal degenerative diseases. We explored the possibility of employing mESMVs as agents that activate the regeneration program in Müller cells.

75.2 mESMVs from mESCs Containing a GFP Transgene Transfer GFP mRNA/protein to Unlabeled mESCs

To determine if mESMVs can transfer transgenes expressed in ESCs (i.e., GFP), we incubated Vybrant DiD-labeled ESCs with ESMVs from ESCs containing GFP, and imaged the cells by confocal microscopy, using the appropriate DiD or GFP filter sets (Figs. 75.1a and b, respectively). Figure 75.1b shows many green vesicles docked on the ESCs and several patches of diffuse GFP signal inside the cells near the plasma membrane and in the cytoplasm, confirming that mESMVs transfer GFP mRNA/protein to other ESCs (Yuan et al. 2009). Figure 75.1c shows the merged images of Figs. 75.1a and 75.1b.

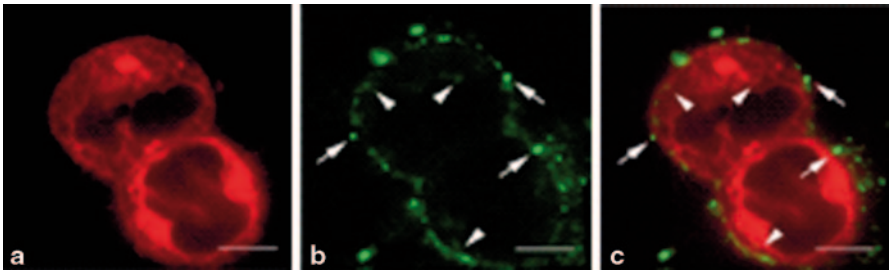

Fig. 75.1 ESMVs transfer GFP. **a** DiD signal from ESCs incubated with ESMVs containing the GFP transgene. **b** GFP signal from the same cells. *Arrows* indicate signal representing docked vesicles. *Arrowheads* indicate signal likely from the diffusion of GFP inside the cell or from the production of newly translated GFP. **c** Merged (**a**) and (**b**). (Modified from Yuan et al. 2009)

75.3 mESMVs Transfer to Human Müller Cells mRNAs and miRNAs that Induce Pluripotency and Expression of Early Retinal Genes

Using qRT-PCR and species-specific primers, we were able to distinguish the mESMV transfer to human Müller cells of mRNAs from the induction by mESMVs of the endogenous human Müller cell transcripts. Mouse *Oct4* mRNA level was 27-fold higher than in control cells 8 h after transfer and decreased to 1.7-fold above control in 2 days. Human *Oct4* mRNA was increased above control 3-fold 8 h post-mESMV exposure and remained elevated 1.8 fold for the next 40 h, indicating that its induction by ESMVs may persist for days (Katsman et al. 2012). Similar induction (5- and 180-fold increases above control, respectively) of the human early retinal genes *Pax6* and *Rax,* which encode transcription factors expressed throughout retinogenesis (Mathers 2000), was detected post mESMV exposure. miRNAs 292 and 295 also transferred efficiently and at very high levels (~200–400-fold) from mESMVs to Müller cells and persisted for at least 48 h post treatment, possibly playing a role in gene expression alterations of Müller cells. The lack of *nanog* mRNA transfer, despite its abundance in mESMVs, suggests that there exists a selection mechanism to direct the genetic transfer, or that only a subset of mRNAs transferred are retained by the recipient cells, while the rest are rapidly degraded.

75.4 mESMV Exposure Induces Morphological Changes in Müller Cells

Differences in the morphology of mESMV-treated and control Müller cells became evident after the first mESMV exposure. With continued treatments every 48 h, the mESMV- exposed cells showed decreased cell-cell adhesion than the sheets of homogeneous, spindle-like control Müller cells, and many grew as heterogeneous individual cells with multiple processes or unilateral boutons, stellar shapes and often enlarged nuclei. However, the number of cells in treated and control cultures remained very similar (Katsman et al. 2012). A couple of times we were able to visualize ESC-like colonies among the regular looking Müller cells. Moreover, we found that these colonies expressed Oct4 (Fig. 75.2).

To further characterize the heterogeneous Müller cell population resulting from the mESMV treatment, we analyzed their immunocytochemical expression of retinal cell lineage markers. In addition to GS, we observed immunoreactivity to syntaxin 1a, an amacrine cell marker, Brn3a, a ganglion cell marker and rhodopsin, a rod photoreceptor marker (Fig. 75.3). Gad67, an amacrine and horizontal cell marker and NeuN, an amacrine and ganglion cell marker, were also found in small populations of ESMV-treated Müller cells. None of these markers were present in untreated cultures. Our data suggest that mESMV treatment induces human Müller cells to de-differentiate, turn on an early retinogenic program, and transdifferentiate towards cells of amacrine, ganglion cell, and rod photoreceptor lineage *in vitro*.

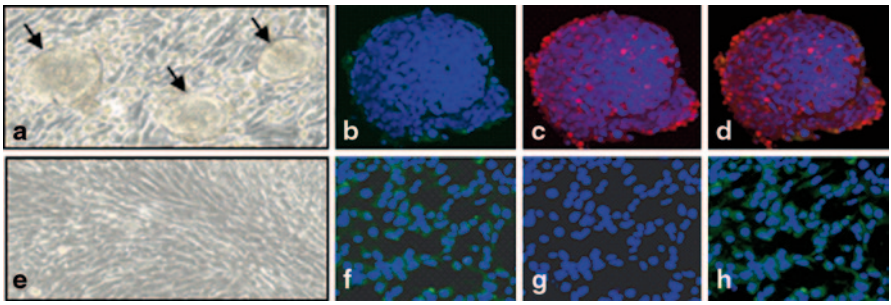

Fig. 75.2 Appearance of ESC-like colonies in cultured Müller cells after several mESMV treatments administered every 48 h. **a** Phase contrast microscopy image (10X) of live ESC-like colonies (*arrows*) growing among Müller cells that exhibit typical post-ESMV treatment morphology, with larger individual cells and increased heterogeneity than the untreated control culture (**e**), which grows as an adherent cellular sheet of tightly packed spindle-like cells. The ESC-like colonies have a rounded shape and a dense mass of cells. **b-c** Confocal image of one of the ESC-like colonies and (**f-g**) untreated Müller cells, doubly labeled with the pluripotency marker Oct-4 (*red*) and Müller cell marker glutamine synthase (GS, *green*). Panels (**d**) and (**h**) are merged images of (**b**) and (**c**) and (**f**) and (**g**), respectively. While GS staining is scant within the ESC-like colony and mostly seen in its borders (**b**), some of the Oct4 positive cells retained GS staining (*yellowish* in (**d**)), indicative of their Müller cell origin. Cell nuclei were counterstained with DAPI (*blue*). No Oct-4 staining is seen in control Müller cells

75.5 mESMV Exposure of Müller Cells Activates in them a Transcriptome Markedly Different from that of Untreated Müller Cells

We used microarrays of cDNAs and stringent statistical parameters to compare the transcriptional response of mESMV-treated and untreated Müller cells (Katsman et al. 2012). mESMV exposure caused enrichment in pro-pluripotency genes, early retinal genes, retinoprotective genes, and genes known to induce regeneration, and depletion of pro-differentiation genes, consistent with our observations of Müller cells' morphological changes towards a more de-differentiated phenotype. Among the differentially regulated genes were also those coding for ECM components and modifying molecules, their changes reflecting a shift to a tissue remodeling profile. Interestingly, *c-Myc*, a pluripotency-inducing factor detected in Müller cells (Takahashi 2006), remained unchanged during the course of ESMV treatments. Following are examples of mRNAs up- and down-regulated in Müller cells by mESMV exposure:

Up-Regulated

- Pluripotency genes: *Oct4, Lin28, Klf4, Lif*
- Early retinal genes that direct retinal cell differentiation during embryogenesis: *Bmp7, Olig2, FoxN4, Prox1, Dll1, Pax6, Rax, Neurog2*
- Notch Pathway genes that activate progenitor phenotype in Müller cells regulating cell cycle re-entry and de-differentiation: *Hes1, Notch1, Notch2, NeuroD1, Cyclin D2, Bmp7*
- Genes with retinal protective properties: *Il6, Csf2, Igf2*

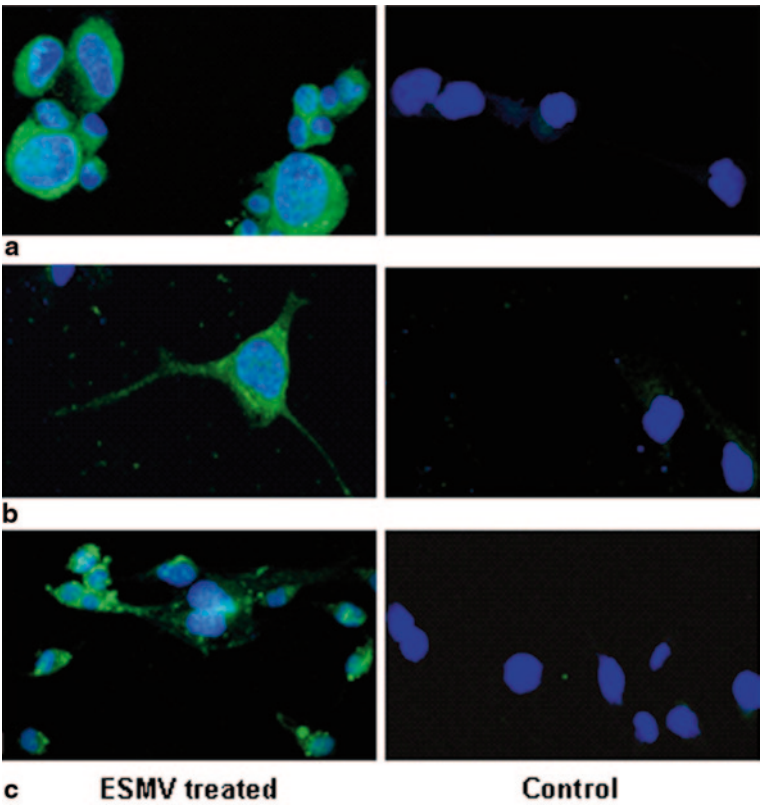

Fig. 75.3 Confocal photomicrographs of mESMV-treated and control Müller cells immunostained for markers of various retinal lineages. **a** Syntaxin 1a. **b** Brn3a. **c** rhodopsin. All secondary antibodies were conjugated to Alexa 488 (*green*). Cell nuclei were labeled with DAPI (*blue*). No green staining is observed in control cells. (Modified from Katsman et al. 2012)

- Genes that are inducers of retinal regeneration: *Fgf2, Igf2, GDNF, Ascl1*
- Extracellular matrix (ECM) modifying genes that create permissive environment for tissue remodeling: *Mmp3, Mmp9*
- Genes encoding markers of retinal lineages: glutamine synthase, clusterin, aquaporin 4, S100 calcium binding protein A16, Vimentin, and *Gfap* (Müller cells), calbindin 1 (horizontal and amacrine cells), syntaxin 1a (amacrine cells) and rhodopsin (rod photoreceptors)

Down-Regulated

- Genes that promote differentiation: *Dnmt3a, Gata4*
- Genes encoding ECM components that inhibit retinal regeneration: Aggrecan, Versican, heparan sulfate, Tenascin C, Décor
- Genes encoding inhibitory scar tissue components: *Gfap* and chondroitin sulfate proteoglycans
- Genes driving retinal progenitors towards Müller glial fate during retinogenesis: *Egfr*

We also used microRNA arrays to study the miRNA transcriptional changes in human Müller cells post-mESMV treatments and found that, as with mRNAs, mESMV exposure profoundly altered the miRNA expression profile of the retinal progenitor cells. For example:

Up-Regulated miRNAs

- The 290 cluster (miRNAs 291b-5p, 292, 294 and 295) and miRNAs 133a and 146a, involved in the maintenance of pluripotency
- miRNAs 1, 96, 182 and 183, the appearance of which marks progression of early retinal development

75.5.1 Down-Regulated miRNAs

- The let-7 cluster (miRNAs let-7b and let-7c), known to promote differentiation in most cells
- miRNA 125-2b, abundant in adult retina
- miRNA 7, which promotes photoreceptor differentiation and miRNAs 199b-5p, 214 and 143, promoting differentiation in ESCs, neuroblasts and smooth muscle progenitors, respectively

We validated the results of all microarrays with qRT-PCR of mESMV-treated and untreated RNA from Müller cells (Katsman et al. 2012). It is possible that the mESMV transfer of miRNAs changes both the mRNA and miRNA expression profiles of Müller cells.

Overall, our studies suggest that mESMVs induce cultured Müller cells to de-differentiate, turn on an early retinogenic program, and differentiate towards cells of retinal lineage. In retina, ESMVs may induce these effects on the quiescent Müller cells causing changes in their cellular microenvironment towards a more permisive state for tissue regeneration.

We tested this hypothesis in preliminary studies, injecting mESMVs + BrdU into the left eyes of mice with NMDA-damaged retinas while the right damaged eyes served as controls and received PBS + BrdU. Most cells proliferating in response to the mESMV treatment expressed the Müller cell marker, CRALBP, and some proliferating cells examined 30 days post-ESMV expressed Syntaxin 1a, GAD67 and Brn3a, suggesting that they had differentiated along the amacrine and ganglion cell neural lineages. A striking improvement in the ERG b-waves after 14 and 30 days post-ESMV injection (amplitude ~ 65 % higher than after NMDA damage) reflected recovery of retinal function. Our ongoing studies are investigating the efficiency of the mESMV *in vivo* induction of retinal regeneration and the mechanisms involved in this process.

References

Bernardos RL, Barthel LK, Meyers JR et al (2007) Late-stage neuronal progenitors in the retina are radial Müller glia that function as retinal stem cells. J Neurosci 27:7028–7040

Bruno S, Grange C, Collino F et al (2012) Microvesicles derived from mesenchymal stem cells enhance survival in a lethal model of acute kidney injury. PLoS One 7:e33115

Herrera MB, Fonsato V, Gatti S et al (2010) Human liver stem cell-derived microvesicles accelerate hepatic regeneration in hepatectomized rats. J Cell Mol Med 14:1605–1618

Jadhav AP, Roesch K, Cepko CL (2009) Development and neurogenic potential of Müller glial cells in the vertebrate retina. Prog Retin Eye Res 28:249–262

Karl MO, Hayes S, Nelson BR, Tan K, Buckingham B et al (2008) Stimulation of neural regeneration in the mouse retina. Proc Natl Acad Sci U S A 105:19508–19513

Katsman D, Stackpole EJ, Domin DR et al (2012) Embryonic stem cell-derived microvesicles induce gene expression changes in Müller cells of the retina. PLoS ONE 7(11):e50417

Mathers PH, Jamrich M (2000) Regulation of eye formation by the Rx and Pax6 homeobox genes. Cell Mol Life Sci 57:186–194

Ratajczak J, Miekus K, Kucia M et al (2006) Embryonic stem cell-derived microvesicles reprogram hematopoietic progenitors: evidence for horizontal transfer of mRNA and protein delivery. Leukemia 20:847–856

Takahashi K, Yamanaka S (2006) Induction of pluripotent stem cells from mouse embryonic and adult fibroblast cultures by defined factors. Cell 126:663–676

Tetta C, Bruno S, Fonsato V et al (2011) The role of microvesicles in tissue repair. Organogenesis 7:105–115

Yuan A, Farber EL, Rapoport AL et al (2009) Transfer of microRNAs by embryonic stem cell microvesicles. PLoS One 4:e4722

Chapter 76
Intravitreal Implantation of Genetically Modified Autologous Bone Marrow-Derived Stem Cells for Treating Retinal Disorders

Christopher J. Tracy, Douglas N. Sanders, Jeffrey N. Bryan, Cheryl A. Jensen, Leilani J. Castaner, Mark D. Kirk and Martin L. Katz

Abstract A number of retinal degenerative diseases may be amenable to treatment with continuous intraocular delivery of therapeutic agents that cannot be delivered effectively to the retina via systemic or topical administration. Among these disorders are lysosomal storage diseases resulting from deficiencies in soluble lysosomal enzymes. Most cells, including those of the retina, are able to take up these enzymes and incorporate them in active form into their lysosomes. In theory, therefore, continuous intraocular administration of a normal form of a soluble lysosomal enzyme should be able to cure the molecular defect in the retinas of subjects lacking this enzyme. Experiments were conducted to determine whether genetically modified bone marrow-derived stem cells implanted into the vitreous could be used as vehicles for continuous delivery of such enzymes to the retina. Bone marrow-derived mesenchymal stem cells (MSCs) from normal mice were implanted into the vitreous of mice undergoing retinal degeneration as a result of a mutation in the *PPT1* gene. The implanted cells appeared to survive indefinitely in the vitreous without proliferating or invading the retina. This indicates that intravitreal implantation of MSCs is likely a safe means of long-term delivery of proteins synthesized by the implanted cells. Experiments have been initiated to test the efficacy of using genetically modified autologous MSCs to inhibit retinal degeneration in a canine model of neuronal ceroid lipofuscinosis.

M. L. Katz (✉) · C. J. Tracy · D. N. Sanders · C. A. Jensen · L. J. Castaner
Department of Ophthalmology, University of Missouri School of Medicine, Mason Eye Institute, One Hospital Drive, Columbia, MO 65212, USA
e-mail: katzm@health.missouri.edu

C. A. Jensen
e-mail: jensenc@health.missouri.edu

L. J. Castaner
e-mail: castanerl@missouri.edu

C. J. Tracy
Genetics Area Program, University of Missouri, Columbia, MO 65211 USA
e-mail: cjtrvd@mail.missouri.edu

C. Bowes Rickman et al. (eds.), *Retinal Degenerative Diseases,* Advances in Experimental Medicine and Biology 854, DOI 10.1007/978-3-319-17121-0_76

Keywords Mesenchymal stem cells · Retinal degeneration · Intravitreal implantation · Trophic effects · Autologous, therapy · Lysosomal storage disease

76.1 Introduction

In recent years substantial research has been conducted to assess potential therapeutic applications of stem cells. The focus of much of this work has been on utilizing stem cells to regenerate tissues, including the retina, that have been damaged as a result of injury or disease (Ramsden et al. 2013). We implanted embryonic stem cell-derived neural precursors from normal mice into the vitreous of mice undergoing progressive retinal degeneration due to a mutation in *CLN8* (Meyer et al. 2006). The implanted cells migrated to and associated closely with the inner retinal surface. A fraction of the cells also migrated into the retina where they appeared to differentiate into specific types of retinal neurons appropriate to the retinal layers in which they were located. The proportion of the retinal neurons replaced by the donor cells was quite small. However, a profound preservation of host retinal photoreceptor cells occurred in areas of the retina with which the donor cells had closely associated. This suggested that the donor cells exerted a trophic effect that inhibited degeneration of the surrounding retina. The trophic factors involved in this protective effect were not identified, but the observed effect suggested that therapeutic compounds produced by donor cells may be effective in preventing retinal degeneration resulting from many causes. We are undertaking studies to further investigate this possibility.

In particular, we are studying the possibility that retinal degeneration resulting from lack of soluble lysosomal enzymes can be inhibited by secretion of these enzymes by cells implanted into the vitreous. To avoid potential problems associated with using embryonic stem cell derivatives as donor cells, we are evaluating the use of genetically modified autologous mesenchymal stem cells (MSCs) as the source of replacement enzymes. Initial experiments have been conducted to assess the behavior of such cells after implantation into the vitreous of eyes in animals undergoing progressive retinal degeneration.

J. N. Bryan
Department of Veterinary Medicine and Surgery, University of Missouri College of Veterinary Medicine, Columbia, MO 65211, USA
e-mail: bryanjn@missouri.edu

M. D. Kirk
Division of Biological Sciences, University of Missouri, Columbia, MO, 65211 USA
e-mail: KirkM@missouri.edu

D. N. Sanders
Department of Diagnostics Division, Novartis Pharmaceutical Inc., Cambridge, MA 02139, USA
e-mail: douglas.n.sanders@gmail.com

76.2 Materials and Methods

76.2.1 Bone Marrow-Derived Mesenchymal Stem Cells

For the mouse studies, bone marrow-derived MSCs were isolated from the femurs of 4–8 week old male C57BL/6-Tg(ACTB-EGFP)1Osb/J mice (Jackson Labs). These mice constitutively express eGFP in most cells, including the MSCs. Marrow was flushed from the isolated femurs with MSC culture medium (Gibco ά-MEM (Invitrogen)+20% FBS, 2 mM L-Glutamine, 1% Penicillin/Streptomycin), plated in culture flasks and grown in the MSC medium. After 24 h, non-adherent cells were removed and the adherent cells were defined as MSCs (Williams and Hare 2011). These cells could be maintained in culture for over 60 passages, confirming that they were stem cells. They could be induced to differentiate into adipocytes and osteocytes, confirming their identity as mesenchymal progenitors.

For the dog studies, MSCs were obtained from Dachshunds homozygous for a null mutation in *TPP1* that encodes the soluble lysosomal enzyme tripeptidyl peptidase-1 (Awano et al. 2006). When the dogs were 2.5–3 months of age, bone marrow was aspirated from the humerus using a modification of a technique described previously (Frimberger et al. 2006). The marrow was mixed with MSC culture medium and grown in culture in the same manner as the mouse MSCs. At passage 3 when the cells were near confluency, they were transduced with either AAV2-CAG-GFP or AAV2-CAG-TPP1 (SignaGen Laboratories, Gaithersburg, MD) at multiplicities of infection of 10,000–50,000. After transduction, the cells were maintained in culture for multiple passages.

76.2.2 Intravitreal Implantation of Mouse MSCs

Mice used as recipients for intravitreal MSC implantation had a null mutation in *PPT1* that encodes the soluble lysosomal enzyme palmitoyl protein thioesterase-1 (Gupta et al. 2001) . Via multiple backcrosses, the mutation was placed on a pure C57BL/6 J strain background. The retina in these mice appears to develop normally and then undergoes a progressive degeneration (Lei et al. 2006).

For intravitreal implantation into the mutant mice, the eGFP-expressing normal C57BL/6 J mouse MSCs were harvested after 4–12 passages and suspended in minimal essential medium at a concentration of 40,000 cells/μl. The recipient mice were anesthetized and approximately 2 μl of the cell suspension was injected into the vitreous. At various times up to 16 weeks after implantation, the recipient mice were euthanized. The eyes were enucleated immediately after death and prepared for and examined with either fluorescence or light microscopy (Meyer et al. 2006).

76.2.3 Characterization of Canine MSCs

Canine MSC cultures were established and maintained as described for the mouse cells. Expression of GFP in the transduced cells was monitored with fluorescence microscopy. Expression of TPP1 by the cells transduced with AAV2-CAG-TPP1 was monitored by measuring TPP1 enzyme activity in the medium in which the cells were maintained using an established protocol (Tian et al. 2006).

All studies were performed in compliance with the ARVO Statement for the "Use of Animals in Ophthalmic and Vision Research" and were approved by the University of Missouri Animal Care and Use Committee.

76.3 Results

76.3.1 Mouse MSCs After Intravitreal Implantation

The mice tolerated the intravitreal injections with no apparent adverse effects, except in rare cases where the injection needle penetrated the lens capsule. In the latter cases, the mice developed cataracts within a few days of the injection. If the lens capsule was not ruptured the implanted cells formed net-like sheets within the vitreous (Fig. 76.1). The numbers of cells within these sheets remained stable over the 16 week evaluation period, with no evidence of donor cell proliferation or loss. Unlike neural precursor cells (Meyer et al. 2006), there was no evidence of donor cell migration toward or into the retina; the sheets of donor cells remained suspended in the vitreous. The presence of the donor cells in the vitreous did not appear to have a significant effect on the rate of retinal degeneration.

In cases where the lens capsule was damaged during the injection, many donor cells migrated to the lens. Some of these cells formed a layer that tightly adhered to the posterior side of the intact portions of the lens capsule. The majority of the donor cells migrated into the lens itself.

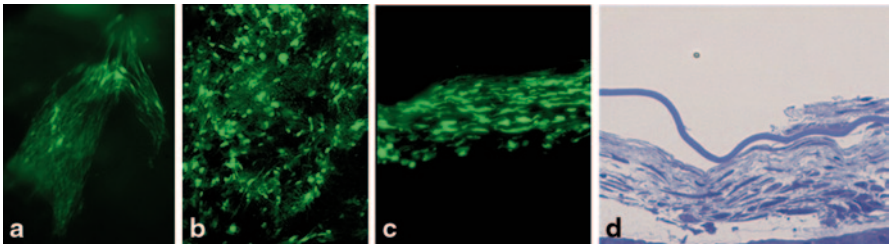

Fig. 76.1 Fluorescence micrographs of a sheet of GFP donor cells in the vitreous in the intact eye (**a**). in a retinal flat mount (**b**). and in a cryostat section of the eye (**c**). Light micrograph of a cross-section sheet of donor cells in the vitreous after fixation and embedding the eye in epoxy resin (**d**). All images were from eyes collected 16 weeks after MSC implantation

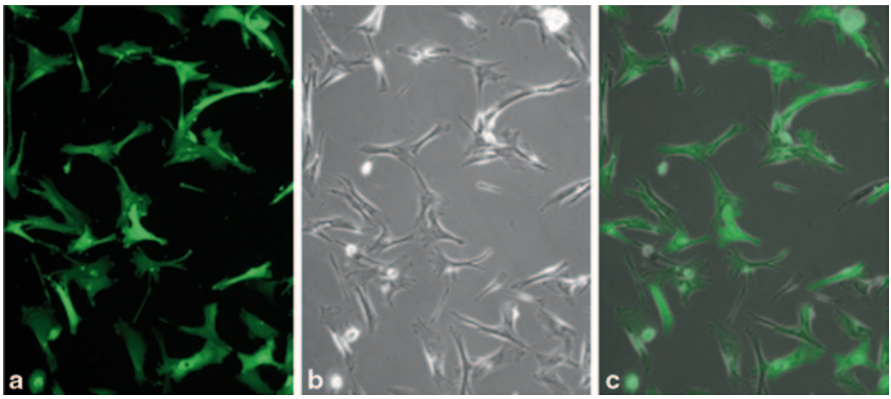

Fig. 76.2 Fluorescence (**a**). phase contrast (**b**). micrographs of rAAV2-CAG-GFP transduced passage 4 canine MSCs *in vitro*. Image in (**c**). is an overlay of images from (a) and (b)

76.3.2 In Vitro Characterization of Canine MSCs

Cells from the bone marrow aspirates were allowed to attach to culture plates for a period of 24 h, after which the plates were washed repeatedly to remove non-adherent cells. Those cells remaining were identified as MSCs by their morphology and adherence to plastic (Williams and Hare 2011). The cells typically reached confluency by 96 h after plating, at which time the cells were passaged. Subsequently the cells typically reached confluency by 48–72 h after passaging. Cell morphology remained indicative of an MSC lineage through multiple passages (Fig. 76.1).

Canine MSCs were transduced with AAV2-CAG vectors at passage 4 by adding the vector to the culture media. The inoculated media was left on the plates for 96 h, after which it was replaced with fresh media. GFP expression was detectable at 96 h post-transduction and increased in intensity over time, reaching a stable high level of intensity approximately 5 days after transduction (Fig. 76.2). GFP expression remained stable for at least two passages post-transduction. P4 and P5 transduced cells kept at confluency without additional passaging maintained high levels of fluorescence for at least 70 days *in vitro*.

To gauge TPP1 expression *in vitro*, the culture medium was collected once every 24 h starting 24 h after transduction for up to 72 h and each sample was analyzed for TPP1 enzyme activity. Based on the TPP1 activity in the conditioned media the estimated release of enzyme by the MSCs *in vitro* was approximately 3 to 5 pg per cell per 24 h.

76.4 Discussion

The mouse studies suggest that intravitreal implantation of MSCs may be a safe means of long-term intraocular delivery of therapeutic agents. As long as there was no damage to the lens the donor cells appeared to survive indefinitely in the vitreous

without proliferating or damaging the retina or lens. As the studies with the canine MSCs demonstrated, these cells can be genetically modified to produce and release therapeutic proteins, which are then likely to reach the target eye tissues adjacent to the vitreous.

In vitro the mouse MSCs proliferate indefinitely, yet after implantation into the vitreous, no proliferation was observed. This suggests that the vitreous contains factors that inhibit proliferation. These factors are present not only in eyes in which the retina is undergoing active degeneration, as the behavior of the MSCs was essentially the same when they were implanted into the eyes of normal C57BL/6 J mice. Although the vitreous is not vascularized, the donor cells apparently received enough oxygen and nutrients from the adjacent retina to support their long-term survival. In the mouse eye, the vitreous is confined to a thin layer close to the retina due to the fact that the lens occupies most of the internal volume of the eye. The consequent close proximity of the donor cells to the retina may have aided in their long-term survival. However, preliminary studies of implantation of autologous bone marrow derived MSCs into the eyes of dogs indicate that such close proximity may not be necessary for donor cell survival. MSCs implanted into the vitreous of a dog far from the retina were still present several months after implantation. This will be important in developing implantation of these cells for human therapies as the anatomy of the dog eye is more similar to that of the human eye than is the mouse eye.

The migration of the donor cells toward and into the lens when the lens capsule was damaged suggests that the lens contains trophic factors to which the donor cells respond strongly. Potential donor cell responses to endogenous trophic factors is an important consideration when considering using intravitreal implantation of such cells for treating retinal degenerative diseases. Tissues undergoing degeneration release a variety of trophic factors to which the donor cells may respond, and different donor cell types may respond differently to such trophic factors. Indeed, we found that mouse neural precursors derived from embryonic stem cells migrate toward and into the degenerating mouse retina (Meyer et al. 2006), whereas no such migration is observed with the MSCs.

These studies indicate that intravitreal implantation of genetically modified MSCs is promising as a means of long-term delivery of therapeutic agents to the retina. While the mouse and preliminary dog studies support the safety of this approach, efficacy in treating retinal degenerative disease remains to be demonstrated. Such efficacy studies are currently under way using a canine model of neuronal ceroid lipofuscinosis which exhibits a slowly progressive retinal degeneration (Katz et al. 2008).

Acknowledgments This work was supported in part by grants 1R01EY018815 and 1R01EY023968 from the U.S. National Institutes of Health. We thank Lauren E. Gillespie for technical assistance and Dr. Mark Sands for the founder *PPT1*−/− mice.

References

Awano T, Katz ML, Sohar I, Lobel P, Coates JR, Khan S, Johnson GC, Giger U, Johnson GS (2006) A frame shift mutation in the canine ortholog of human *CLN2* in a juvenile dachshund with neuronal ceroid lipofuscinosis. Mol Genet Matabol 89:254–260

Frimberger AE, Moore AS, Rassnick KM, Cotter SM, O'Sullivan JL, Quesenberry PJ (2006) A combination chemotherapy protocol with dose intensification and autologous bone marrow transplant (VELCAP-HDC) for canine lymphoma. J Vet Intern Med 20:355–364

Gupta P, Soyombo AA, Atasgband A, Wysniewski KE, Shelton JM, Richardson JA, Hammer RE, Hofmann SL (2001) Disruption of PPT1 or PPT2 causes neuronal ceroid lipofuscinosis in knockout mice. Proc Nat Acad Sci U S A 98:13566–13571

Katz ML, Coates JR, Cooper JJ, O'Brien DP, Jeong M, Narfström K (2008) Retinal pathology in a canine model of late infantile neuronal ceroid lipofuscinosis. Invest Ophthalmol Vis Sci 49:2686–2695

Lei B, Tullis GE, Kirk MD, Zhang K, Katz ML (2006) Ocular phenotype in a mouse gene knockout model for infantile neuronal ceroid-lipofuscinosis. J Neurosci Res 84:1139–1149

Meyer JS, Katz ML, Maruniak JA, Kirk MD (2006) Embryonic stem cell derived neural precursors incorporate into the degenerating retina and enhance survival of host photoreceptors. Stem Cells 24:274–283

Ramsden CM, Powner MB, Carr AJ, Smart MJ, da Cruz L, Coffey PJ (2013) Stem cells in retinal regeneration: past, present and future. Development 140:2576–2585

Tian Y, Sohar I, Taylor JW, Lobel P (2006) Determination of the substrate specificity of tripeptidyl-peptidase I using combinatorial peptide libraries and development of improved fluorogenic substrates. J Biol Chem 281:6559–6572

Williams AR, Hare JM (2011) Mesenchymal stem cells: biology, pathophysiology, translational findings, and therapeutic implications for cardiac disease. Circ Res 109:923–940

Chapter 77
Gliosis Can Impede Integration Following Photoreceptor Transplantation into the Diseased Retina

Claire Hippert, Anna B. Graca and Rachael A. Pearson

Abstract Retinal degenerations leading to the loss of photoreceptor (PR) cells are a major cause of vision impairment and untreatable blindness. There are few clinical treatments and none can reverse the loss of vision. With the rapid advances in stem cell biology and techniques in cell transplantation, PR replacement by transplantation represents a broad treatment strategy applicable to many types of degeneration. The number of donor cells that integrate into the recipient retina determines transplantation success, yet the degenerating retinae presents a number of barriers that can impede effective integration. Here, we briefly review recent advances in the field of PR transplantation. We then describe how different aspects of gliosis may impact on cell integration efficiency.

Keywords Gliosis · Müller glia · Intermediate filament · GFAP · CSPG · Photoreceptor transplantation · Barrier modulation

77.1 Introduction

Despite very different aetiologies and pathogenesis, retinal neurodegenerative diseases like age-related macular degeneration, retinitis pigmentosa (RP), glaucoma and diabetic retinopathy culminate in the loss of light-sensing PR cells and the

C. Hippert (✉) · A. B. Graca · R. A. Pearson
F. Hoffman La Roche, 124 Grenzacherstrasse, 4070 Basel, Switzerland
e-mail: claire.hippert@roche.com

A. B. Graca
e-mail: anna.graca.11@ucl.ac.uk

R. A. Pearson
e-mail: rachael.pearson@ucl.ac.uk

C. Bowes Rickman et al. (eds.), *Retinal Degenerative Diseases,* Advances in Experimental Medicine and Biology 854, DOI 10.1007/978-3-319-17121-0_77

subsequent loss of vision. Currently, there are few effective therapeutic approaches to treat PR loss, and none of them can reverse the loss of vision. Innovative medical therapies such as electronic retinal implants (Stingl and Zrenner 2013), or gene and cell therapy (Cuenca et al. 2014) are attractive approaches for the treatment of retinal disease. Gene therapy for the treatment of inherited retinal disorders has yielded very exciting and promising results (Smith et al. 2012), however this therapeutic strategy can only be applied in the early stages of retinal degeneration as it relies on the presence of the endogenous PR cells, offering limited help for advanced disease. Cell replacement therapy is of particular interest in this particular circumstance as it offers a direct replacement of the lost tissue and can potentially restore visual function. Over the past decade, we have seen a considerable progress in using this approach to repair the degenerating retina (Cuenca et al. 2014). However, it has been shown that although it is possible to treat some forms of end stage (Kwan et al. 1999; Singh et al. 2013), the precise nature and characteristics of the degeneration arising from a given disease-causing defect is important in determining transplantation outcome. As degeneration progresses the retinal microenvironment undergoes a number of significant changes that are potentially hostile to therapeutic interventions. A number of studies have indicated that a major determinant of successful retinal transplantation is the extent of reactive gliosis within the recipient retina, which acts as both a physical and chemical barrier to migrating cells (Pearson et al. 2014).

77.2 Advances in the Field of PR Transplantation

In recent years, one of the most extensively studied therapeutic strategies has been the transplantation of dissociated PRs and their precursor cells. MacLaren et al. demonstrated that integration and appropriate differentiation of donor PR cells is achievable if the transplanted cells are at an appropriate developmental stage at the time of transplantation (MacLaren et al. 2006). The use of a genetic marker, *Nrl*, a transcription factor first expressed in immature rods shortly after terminal mitosis (Akimoto et al. 2006), demonstrated that post-mitotic rod precursor cells taken from postnatal retinae were optimal for transplant and led to better integration than donor cells from earlier or later stages in development. These transplanted PR precursors were able to migrate from the site of transplantation, the subretinal space, into the recipient outer nuclear layer (ONL), where they settled in an appropriate place. The new PRs continue to mature and form inner and outer segments and synaptic connections with the remaining neurons within the retina (Warre-Cornish et al. 2013). Moreover, these new PRs are light sensitive and can transmit visual information to the brain, leading to restoration of visual function in a murine model of stationary night blindness (Pearson et al. 2012). Recent advances in stem cell technology have demonstrated the potential to generate renewable sources of donor cells from embryonic (ES) and induced pluripotent stem cells. Gonzalez-Cordero et al. have shown that ES-derived rod precursors can migrate and integrate into the recipient

retina in a manner very similar to precursors derived from the developing retina (Eiraku et al. 2011; Gonzalez-Cordero et al. 2013).

Much of the research into PR transplantation has been performed in wild-type or isolated models of RP. This raises the fundamental question as whether PR transplantation is equally able to treat a wide spectrum of inherited retinopathies. It is well known that during disease progression the retina undergoes structural remodeling, including changes in neuronal connections, gliosis and changes in outer limiting membrane integrity (OLM). These changes may then have a positive or negative influence on the outcome of PR precursor cell transplantation. Barber et al. performed the first comprehensive study of rod PR transplantation in murine models of slow, moderate and fast PR degeneration. Importantly, they found that PR transplantation was feasible in all examined animals; however disease type had a significant impact on both the number of integrated cells and their morphology. This study identified two key determinants of transplant success; the extent of glial scarring and the integrity of OLM. Both factors can impede the migration of donor cells from the subretinal space and their successful integration within the recipient retina. Below, we focus on gliosis and its impact on cell transplantation.

77.3 Gliosis a Potential Barrier to Photoreceptor Transplantation

Gliosis is the term given to the process in which the glial cells become activated. When these cells are activated, they upregulate the glial intermediate filament (IF) proteins vimentin and glial fibrillary acidic protein (GFAP), their apical terminal processes may undergo hypertrophy and a concomitant increase in the deposition of inhibitory extracellular matrix (ECM) molecules, such as chondroitin sulphate proteoglycans (CSPGs) can be observed. These changes represent physical and biochemical barriers, respectively, which may prevent transplanted PRs from reaching the recipient retina.

77.3.1 Glial Cell Hypertrophy May Act as a Physical Barrier

In the retina, Müller glia (MG) span the entire thickness of the vertebrate retina and represent the major type of glial cells. They are responsible for the structural stabilization of the retina, support the functioning and metabolism of retinal neurons and are active players in normal retinal function as well as in virtually all types of retinal degeneration where they undergo reactive gliosis (Bringmann et al. 2006). Gliosis in the retina can be induced by mechanical insult (Lewis et al. 2010), retinal degeneration (Zhang et al. 2003), inflammation (Dinet et al. 2012) and/or ageing (Kim et al. 2004). It includes morphological, biochemical and physiological changes, which can vary with the type and severity of the insult. One of the readily detectable

responses to retinal diseases and injuries, which is often used as a universal early cellular marker for retinal injury, is the upregulation of the IF protein, GFAP (Dahl 1979). In a healthy retina expression of GFAP^{+ve} IF is largely restricted to astrocytes with only a few GFAP^{+ve} Müller glial processes detected in the inner retina. In the diseased retina, GFAP is increased in both activated cell types. The level and localisation of GFAP IF expression in the MG processes is disease specific (Hippert et al., unpublished data). The increased expression of IFs is thought to help stabilize the newly formed terminal processes of MG and provide resistance to mechanical stress (Verardo et al. 2008). At first, gliosis seems to represent a cellular attempt to protect the tissue from further damage to promote repair and to limit neuronal remodeling. However, MG activation can also be exacerbated and lead to the hypertrophy of the MG end-feet processes, which fill in the gaps where PRs die (Bringmann et al. 2006). This contributes to the formation of a glial scar in the subretinal space which may impair neurite outgrowth and act as a barrier to regenerating and/or transplanted cells. Supporting this view are the findings that transgenic animals lacking both GFAP and vimentin in MG shown a more permissive environment for the grafted cells as shown by better integration and differentiation of transplanted cells as well as a higher neurite outgrowth than in wild-type recipients (Kinouchi et al. 2003). In line with this, Barber et al. (2013) reported that transplantation outcome of rod precursor cells in different models of inherited blindness is broadly inversely correlated with the extent of GFAP expression.

77.3.2 The Extracellular Matrix Changes May Act as a Chemical Barrier

The retinal environment, like elsewhere in the CNS, is enriched in CSPGs. These include a variety of core proteins each carrying chondroitin sulphate glycosaminoglycans (GAG) chains. CSPGs bind many different ECM proteins and growth factors making them important players in a variety of regulatory processes including cell adhesion, migration and differentiation (Ichijo 2004). In the CNS, CSPGs are upregulated after injury and participate in the inhibition of axon regeneration mainly through their GAG side chains. Application of the bacterial enzyme chondroitinase ABC (ChABC), which degrades GAG chains into disaccharides, promotes functional recovery in the injured CNS (Bradbury et al. 2002). In retinal degeneration our understanding of the role of CSPGs is surprisingly limited. In the healthy retina, CSPGs are found in several regions including the optic nerve, inner and outer plexiform layer, the interphotoreceptor matrix and in the ganglion cell layer (Inatani and Tanihara 2002). When using a broad spectrum CSPG antibody in murine models of RP, we have observed marked variations in the level of expression of CSPGs (Hippert et al., unpublished data). Numerous studies with both stem cell and PR precursor transplants demonstrated that treatment with ChABC prior the transplantation increased the number and survival of integrated donor cells (Singhal et al. 2008; Ma et al. 2011; Barber et al. 2013). An improvement of viral vector diffusion

and transduction has also been described when applying this enzyme in conjunction with lentiviral vector to the sub-retinal space (Grüter et al. 2005).

77.4 Conclusion; Importance of Characterizing Retinal Environment Changes

Dependent on the ocular disease type, different changes occur in the retina which lead to altered retinal microenvironments. A better understanding and characterization of these changes is essential for the development of new therapeutic approaches. To our knowledge no drugs have been able to show an efficient removal of IF proteins to overcome the glial scar barrier. We are using RNA interference to modulate the expression of GFAP in conjunction with PR precursor transplantation, to establish the precise role of GFAP in impeding donor cell integration (unpublished data). Currently, local treatment with ChABC is the major strategy to override the inhibitory effect of CSPGs on cell-based therapies. However, ChABC presents some disadvantages in using it as a therapeutic treatment in patients, including the potential for inflammatory reaction due to its bacterial origin (Lee et al. 2010). A more detailed characterization of the major changes in ECM composition may enable the identification of specific CSPGs that undergo potentially disease-specific changes. This may enable targeted breakdown of specific CSPGs and enhance cell transplantation efficiency. Our focus here has been gliosis as a barrier to cell transplantation, however other barriers exist. Different studies reported that the OLM may also act as a physical barrier to cell transplantation (West et al. 2008; Pearson et al. 2010). Finally, combining cell transplantation with the manipulation of two or more barriers will be another interesting approach to investigate. We recently combined OLM disruption and CSPG degradation with encouraging results (Barber et al. 2013), while others have combined ChABC with growth factors (IGF-1)(Ma et al. 2011).

In summary, significant progress has been made in the field of PR transplantation therapy but achieving high numbers of new integrated PRs in the diseased retina remains a major challenge. A better understanding of the microenvironmental changes in the degenerating retina should help to overcome this.]

References

Akimoto M, Cheng H, Zhu D et al (2006) Targeting of GFP to newborn rods by Nrl promoter and temporal expression profiling of flow-sorted photoreceptors. Proc Natl Acad Sci U S A 103:3890–3895

Barber AC, Hippert C, Duran Y et al (2013) Repair of the degenerate retina by photoreceptor transplantation. Proc Natl Acad Sci U S A 110:354–359

Bradbury EJ, Moon LD, Popat RJ et al (2002) Chondroitinase ABC promotes functional recovery after spinal cord injury. Nature 416:636–640

Bringmann A, Pannicke T, Grosche J et al (2006) Müller cells in the healthy and diseased retina. Prog Ret Eye Res 25:397–424

Cuenca N, Fernández-Sánchez L, Campello L et al (2014) Cellular responses following retinal injuries and therapeutic approaches for neurodegenerative diseases. Prog Ret Eye Res 43:17–75

Dahl D (1979) The radial glia of Müller in the rat retina and their response to injury. An immunofluorescence study with antibodies to the glial fibrillary acidic (GFA) protein. Exp Eye Res 28:63–69

Dinet V, Bruban J, Chalour N et al (2012) Distinct effects of inflammation on gliosis, osmohomeostasis, and vascular integrity during amyloid beta-induced retinal degeneration. Aging Cell 11:683–693

Eiraku M, Takata N, Ishibashi H et al (2011) Self-organizing optic-cup morphogenesis in three-dimensional culture. Nature 472:51–56

Gonzalez-Cordero A, West EL, Pearson RA et al (2013) Photoreceptor precursors derived from three-dimensional embryonic stem cell cultures integrate and mature within adult degenerate retina. Nat Biotech 31:741–747

Grüter O, Kostic C, Crippa S et al (2005) Lentiviral vector-mediated gene transfer in adult mouse photoreceptors is impaired by the presence of a physical barrier. Gene Ther 12:942–947

Ichijo H (2004) Proteoglycans as cues for axonal guidance in formation of retinotectal or retinocollicular projections. Mol Neurobiol 30:23–33

Inatani M, Tanihara H (2002) Proteoglycans in retina. Prog Ret Eye Res 21:429–447

Kim K-Y, Ju W-K, Neufeld AH (2004) Neuronal susceptibility to damage: comparison of the retinas of young, old and old/caloric restricted rats before and after transient ischemia. Neurobiol Aging 25:491–500

Kinouchi R, Takeda M, Yang L et al (2003) Robust neural integration from retinal transplants in mice deficient in GFAP and vimentin. Nat Neurosci 6:863–868

Kwan AS, Wang S, Lund RD (1999) Photoreceptor layer reconstruction in a rodent model of retinal degeneration. Exp Neurolo 159:21–33

Lee H, McKeon RJ, Bellamkonda RV (2010) Sustained delivery of thermostabilized chABC enhances axonal sprouting and functional recovery after spinal cord injury. Proc Natl Acad Sci U S A 107:3340–3345

Lewis GP, Chapin EA, Luna G et al (2010) The fate of Müller's glia following experimental retinal detachment: nuclear migration, cell division, and subretinal glial scar formation. Mol Vis 16:1361–1372

Ma J, Kabiel M, Tucker BA et al (2011) Combining chondroitinase ABC and growth factors promotes the integration of murine retinal progenitor cells transplanted into Rho–/– mice. Mol Vis 17:1759–1770

MacLaren RE, Pearson R, MacNeil A et al (2006) Retinal repair by transplantation of photoreceptor precursors. Nature 444:203–207

Pearson R, Barber A, West E et al (2010) Targeted disruption of outer limiting membrane junctional proteins (Crb1 and ZO-1) increases integration of transplanted photoreceptor precursors into the adult wild-type and degenerating retina. Cell Transpl 19:487–503

Pearson RA, Barber AC, Rizzi M et al (2012) Restoration of vision after transplantation of photoreceptors. Nature 485:99–103

Pearson RA, Hippert C, Graca AB et al (2014) Photoreceptor replacement therapy: challenges presented by the diseased recipient retinal environment. Vis Neurosci 31:1–12

Singh MS, Charbel Issa P, Butler R et al (2013) Reversal of end-stage retinal degeneration and restoration of visual function by photoreceptor transplantation. Proc Natl Acad Sci U S A 110:1101–1106

Singhal S, Lawrence JM, Bhatia B et al (2008) Chondroitin sulfate proteoglycans and microglia prevent migration and integration of grafted Müller stem cells into degenerating retina. Stem Cells 26:1074–1082

Smith AJ, Bainbridge JW, Ali RR (2012) Gene supplementation therapy for recessive forms of inherited retinal dystrophies. Gene Ther 19:154–161

Stingl K, Zrenner E (2013) Electronic approaches to restitute vision in patients with neurodegenerative diseases of the retina. Ophthal Res 50:215–220
Verardo MR, Lewis GP, Takeda M et al (2008) Abnormal reactivity of Müller cells after retinal detachment in mice deficient in GFAP and vimentin. Investig Ophthalmol Vis Sci 49:3659–3665
Warre-Cornish K, Barber AC, Sowden JC et al (2013) Migration, integration and maturation of photoreceptor precursors following transplantation in the mouse retina. Stem Cell Dev 23:941–954
West E, Pearson R, Tschernutter M et al (2008) Pharmacological disruption of the outer limiting membrane leads to increased retinal integration of transplanted photoreceptor precursors. Exp Eye Res 86:601–611
Zhang Y, Caffé AR, Azadi S et al (2003) Neuronal integration in an abutting-retinas culture system. Investig Ophthalmol Vis Sci 44:4936–4946

Chapter 78
Interkinetic Nuclear Migration in the Regenerating Retina

Manuela Lahne and David R. Hyde

Abstract In the adult zebrafish, death of retinal neurons stimulates Müller glia to re-enter the cell cycle to produce neuronal progenitor cells (NPCs) that undergo further cell divisions and differentiate to replace lost neurons in the correct spatial locations. Understanding the mechanisms regulating retinal regeneration will ultimately provide avenues to overcome vision loss in human. Recently, the observation of interkinetic nuclear migration (INM) of Müller glia in the regenerating zebrafish retina resulted in the inclusion of an additional complex step to the regeneration process. The pathways regulating INM and its function in the regenerating retina have not been well studied. Here, we summarize the evidence for INM in the regenerating retina and review mechanisms that control INM during neuro-epithelial development in the context of pathways known to be critical during retinal regeneration.

Keywords Retinal regeneration · Retinal damage · Müller glia · Neuronal progenitor cell · Interkinetic nuclear migration · Cytoskeleton · Signaling

Abbreviations

INL	Inner nuclear layer
INM	Interkinetic nuclear migration
MLC	Myosin light chain
NPC	Neuronal progenitor cell
ONL	Outer nuclear layer
pH3	Phospho-histone-3
PCNA	Proliferating cellular and nuclear antigen
Rock	Rho-associated coiled-coil kinase

D. R. Hyde (✉)
Department of Biological Sciences and the Center for Zebrafish Research, University of Notre Dame, 027 Galvin Life Sciences Building, Notre Dame, IN 46556, USA
e-mail: dhyde@nd.edu

M. Lahne
Department of Biological Sciences and the Center for Zebrafish Research, University of Notre Dame, Galvin Life Sciences Building, Notre Dame, IN 46556, USA
e-mail: Manuela.Lahne.1@nd.edu

C. Bowes Rickman et al. (eds.), *Retinal Degenerative Diseases,* Advances in Experimental Medicine and Biology 854, DOI 10.1007/978-3-319-17121-0_78

78.1 Introduction

In the human retina, loss/death of photoreceptors or their secondary neurons that integrate and transmit visual information results in irreversible vision loss. Currently, cures to restore vision have not been identified. In contrast to mammals, zebrafish have emerged as an organism that robustly regenerates retinal neurons following damaging insults (Vihtelic and Hyde 2000; Fausett and Goldman 2006; Bernardos et al. 2007; Kassen et al. 2007) and offer the unique opportunity to unravel an intrinsic regeneration program with the aim to develop strategies to stimulate retinal regeneration in humans.

A variety of techniques are used to damage specific retinal subtypes (Vihtelic and Hyde 2000; Fausett and Goldman 2006; Bernardos et al. 2007; Fimbel et al. 2007; Kassen et al. 2007; Montgomery et al. 2010). Regardless of the mechanism of damage or the cell types lost, the residing Müller glia dedifferentiate and re-enter the cell cycle to produce neuronal progenitor cells (NPCs, Fig. 78.1, (Bernardos et al. 2007; Kassen et al. 2007)). These NPCs divide further before migrating to the site where neurons are absent and differentiate into the lost cells (Vihtelic and Hyde 2000). Recently, an additional event, interkinetic nuclear migration (INM) of Müller glia nuclei, was observed in the regenerating light-damaged retina (Fig. 78.1, (Nagashima et al. 2013)). INM is the movement of nuclei between the apical and basal limits of epithelia in phase with the cell cycle and has been studied in the developing retina, brain and neural tube (Pearson et al. 2005; Baye and Link 2007; Del Bene et al. 2008; Norden et al. 2009; Lee and Norden 2013). Though progress

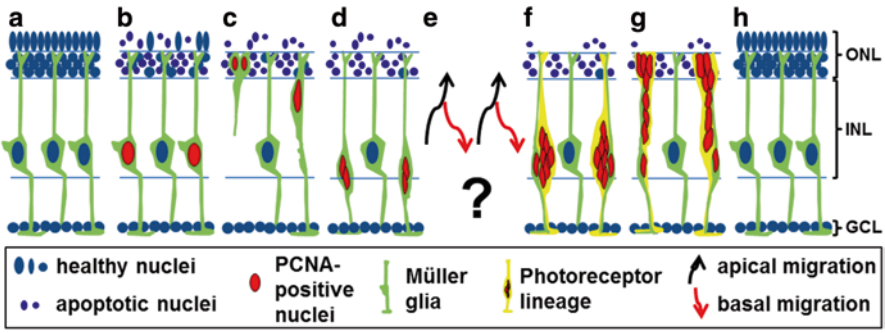

Fig. 78.1 Diagram of the light-damage-induced regeneration timecourse (**a**) A subset of healthy Müller glia (*green* with *blue* nuclei) upregulate *PCNA* (**b**, *red* nuclei) in response to photoreceptor death (**b**, smaller *dark blue* nuclei). Subsequently, Müller glia nuclei migrate to the *ONL* where they divide (**c**), producing NPCs that return to the basal *INL* (**d**) to undergo S-phase. NPC nuclei also migrate between the *ONL* and the basal *INL* in phase with the cell cycle, represented by *black* and *red arrows*, respectively (**e**). The question mark indicates discrepancies between different light-damage models in regard to NPC INM. NPCs upregulate genes that induce photoreceptor lineage commitment (*yellow*, **f**) before they migrate to the *ONL* (**g**) to differentiate into photoreceptors and regenerate a functional retina (**h**). *GCL*, ganglion cell layer; *INL*, inner nuclear layer; NPC, neuronal progenitor cell; *ONL*, outer nuclear layer; *PCNA*, proliferating cellular and nuclear antigen

has been made in identifying signaling events that induce Müller glia-mediated regeneration, the mechanisms that govern INM and its role in the regenerating retina are largely unknown (Gorsuch and Hyde 2013). Here, evidence for INM in the regenerating zebrafish retina and mechanisms regulating it in development will be reviewed.

78.2 Müller Glia INM

During development, NPC nuclei migrate along the apico-basal axis of the neuroepithelium in phase with the cell cycle, i.e. they replicate their DNA in S-phase in basal regions before migrating to the apical limit during G2-phase where they undergo mitosis (Lee and Norden 2013). In the adult retina, the outer nuclear layer (ONL) that houses rod and cone photoreceptors corresponds to the apical region. Previously, Müller glia/NPC migration to the ONL was observed during retinal regeneration; however, it either did not receive further attention or was investigated in the context of differentiation (Vihtelic and Hyde 2000; Fausett and Goldman 2006; Bernardos et al. 2007; Karl et al. 2008). Recently, Müller glia nuclei were observed to translocate from their typical basal inner nuclear layer (INL) position to the ONL, where they colabel with the mitotic marker phospho-histone-3 (pH3). The subsequent return of the arising NPCs to the basal INL gave the first evidence that INM also occurs in the light-damaged zebrafish retina (Lahne & Hyde, unpublished data; Nagashima et al. 2013). Interestingly, ablation of ganglion cells and INL neurons by ouabain, also induced Müller glia nuclei to migrate apically; however, most of these Müller glia remained in the apical INL and those that passed into the ONL did not attach to the outer limiting membrane (Nagashima et al. 2013). This raises the question as to the signal(s) that impose(s) the directionality of this nuclear migration specifically towards the apical site of the retina. During development, the position of the centrosome near the apical limit of the neuroepithelium was suggested to dictate the direction of nuclear migration during G2 and thus determined the location of mitosis (Taverna and Huttner 2010). The position of centrosomes in Müller glia is currently unknown; though presumably they are located at the apical limit of Müller glial processes in the ONL, recapitulating development. It is likely that other unidentified factors such as signaling gradients also act as driving forces of INM.

Although INM is observed in both light- and ouabain-damaged retinas, the apical migration potential is clearly reduced in the latter (Nagashima et al. 2013). Spatial restrictions due to the maintained presence of intact photoreceptors following inner retinal cell death by ouabain exposure could explain the relatively lower migration potential of Müller glia nuclei into the ONL compared to the light-damaged retina lacking photoreceptors. Similarly, NPC divisions in the developing retina change from apical to non-apical at the onset of ONL formation (Weber et al. 2014), supporting that cell density restrictions at least partially determine the position of mitosis.

78.3 Do Müller Glia-derived NPCs Undergo INM?

While Müller glia undergo INM, NPCs were suggested to divide non-apically based on pH3-positive cells only being present in the ONL early during the regeneration response in retinas acutely damaged by brief exposure to high intensity light (Nagashima et al. 2013). It is quite surprising that in the regenerating retina, Müller glia and not the Müller glia-derived NPCs behave more similar to NPCs during retinal development. Using a different light-damage paradigm that exposes zebrafish to constant intense light, the majority of mitotic nuclei were observed in the ONL at timepoints when NPCs divide. Subsequently, NPC clusters of four or more cells are present in the INL indicating that both Müller glia and NPCs undergo INM (Lahne & Hyde, unpublished data). Live cell imaging using transgenic lines that distinguish between Müller glia and NPCs would clarify whether INM is a process limited to Müller glia. In ouabain-damaged retinas neither the migration pattern nor the positon of pH3-positive NPC nuclei was investigated. However, the presence of PCNA-positive proliferating nuclei in the ONL hints that NPCs gain the capacity to undergo INM to the ONL following inner retinal cell death (Fimbel et al. 2007; Nagashima et al. 2013).

78.4 Motor Proteins Driving INM

The mechanisms mediating INM in the regenerating retina are currently unknown. During retinal development the velocity and mean squared displacement indicate that apical movement of NPC nuclei in the G2-phase of the cell cycle is an actively driven process (Baye and Link 2007; Norden et al. 2009; Leung et al. 2011). Although microtubules play a role, actin myosin-mediated contraction is the main driving force of nuclear migration during G2 in the developing retina. (Murciano et al. 2002; Del Bene et al. 2008; Norden et al. 2009; Yu et al. 2011). Both, filamentous actin and phosphorylated myosin light chain (MLC) accumulate basally to G2-phase nuclei (Norden et al. 2009; Leung et al. 2011). Various kinases, including myosin light-chain kinase and Rho-associated coiled-coil kinase (Rock) mediate MLC phosphorylation (Vicente-Manzanares et al. 2009); however, the specific kinase that phosphorylates MLC during INM has not been identified. Interestingly, disruption of Rock signaling by expressing a dominant-negative version of either Rock2a or its activator RhoA causes mislocalization of pH3-positive nuclei in basal regions of the developing retina, indicative of a defect in INM (Herder et al. 2013). Hence, Rock2 could be the MLC phosphorylating kinase.

In the regenerating retina, we also observed actin filaments at the rear of migrating Müller glia nuclei at the onset of INM (Lahne & Hyde, unpublished data). Moreover, disrupting actin filament formation by the actin polymerization inhibitior, cytochalasin D resulted in a significantly greater number of pH3-positive Müller glia in the basal INL, where quiescent Müller glia typically reside (Lahne & Hyde, unpublished data). Inhibition of Rocks caused a similar mislocalization defect alongside reduced phosphorylation of MLC, suggesting that actin-myosin-

mediated forces facilitate apical migration of Müller glia nuclei, potentially recapitulating retinal development.

In contrast to the actively driven apical migration, basal movement in G1 occurs in a stochastic passive manner (Baye and Link 2007; Norden et al. 2009; Kosodo et al. 2011; Leung et al. 2011). Blocking S-phase progression not only halts apical nuclear migration, but significantly reduced the speed of basally moving G1-phase nuclei, indicating that actively migrating G2-phase nuclei displace those that have already divided from the apical neuroepithelium to more basal positions (Kosodo et al. 2011). In contrast, disrupting both microtubule-mediated transport and the actin cytoskeleton were also shown to affect basalward nuclear migration (Del Bene et al. 2008; Norden et al. 2009; Schenk et al. 2009; Tsai et al. 2010). In the regenerating light-damaged retina, only a subset of Müller glia proliferate. Thus, the ONL unlikely becomes overcrowded during Müller glia INM, raising the question whether both apical and basal migration are mediated by active mechanisms.

78.5 Function of INM

The function of INM is difficult to determine as disruption of signaling pathways or cellular components not only affect INM but also other cellular events. It was suggested that the physical separation of S-phase and mitosis acts as a regulatory mechanism that exposes cells to distinct gradients of signaling factors which in turn control the decision of cell cycle exit/differentiation versus continued proliferation (Murciano et al. 2002; Del Bene et al. 2008). In the developing retina, Notch receptors, its ligands, and downstream targets, are expressed in an apico-basal manner (Murciano et al. 2002; Del Bene et al. 2008; Clark et al. 2012). Overexpression of the Notch intracellular domain in the INM defective dynactin mutants rescues the observed differentiation defect that is characterized by the overproduction of ganglion cells at the expense of late-born retinal neurons due to early cell cycle exit. These data, suggest that INM exposes cells to specific Notch gradients that regulate cell fate choices. In the adult zebrafish retina, Notch-signaling regulates the number of Müller glia that are recruited into the cell cycle upon retinal damage (Conner et al. 2014; Wan et al. 2012). While the role of Notch signaling in INM and in the regulation of cell cycle exit decisions of Müller glia and NPCs has not been examined in the regenerating retina, it is possible that its function is similar to that in the developing retina.

78.6 Concluding Remarks

The recent observation of INM in the regenerating zebrafish retina raises many questions regarding the regulatory mechanisms and its function. Knowledge gained studying INM during neuroepithelial development can provide candidate signaling

pathways. Long-term, establishing the function of INM in influencing neurogenic/proliferative cell fate decisions in the regenerating zebrafish retina might help reveal why the injured mammalian retina exhibits a low proliferation response (Karl et al. 2008). Thus, identifying means that can stimulate and control INM in the damaged mammalian retina could result in effective Müller glia proliferation and neuronal regeneration.

References

Baye LM, Link BA (2007) Interkinetic nuclear migration and the selection of neurogenic cell divisions during vertebrate retinogenesis. J Neurosci 27:10143–10152

Bernardos RL, Barthel LK, Meyers JR et al (2007) Late-stage neuronal progenitors in the retina are radial Muller glia that function as retinal stem cells. J Neurosci 27:7028–7040

Clark BS, Cui S, Miesfeld JB et al (2012) Loss of Llgl1 in retinal neuroepithelia reveals links between apical domain size, Notch activity and neurogenesis. Development 139:1599–1610

Conner C, Ackerman KM, Lahne M et al (2014) Repressing Notch signaling and expressing TNFalpha are sufficient to mimic retinal regeneration by inducing Muller Glial proliferation to generate committed progenitor cells. J Neurosci 34:14403–14419

Del Bene F, Wehman AM, Link BA et al (2008) Regulation of neurogenesis by interkinetic nuclear migration through an apical-basal notch gradient. Cell 134:1055–1065

Fausett BV, Goldman D (2006) A role for alpha1 tubulin-expressing Muller glia in regeneration of the injured zebrafish retina. J Neurosci 26:6303–6313

Fimbel SM, Montgomery JE, Burket CT et al (2007) Regeneration of inner retinal neurons after intravitreal injection of ouabain in zebrafish. J Neurosci 27:1712–1724

Gorsuch RA, Hyde DR (2013) Regulation of Muller glial dependent neuronal regeneration in the damaged adult zebrafish retina. Exp Eye Res 123:131–140

Herder C, Swiercz JM, Muller C et al (2013) ArhGEF18 regulates RhoA-Rock2 signaling to maintain neuro-epithelial apico-basal polarity and proliferation. Development 140:2787–2797

Karl MO, Hayes S, Nelson BR et al (2008) Stimulation of neural regeneration in the mouse retina. Proc Natl Acad Sci U S A 105:19508–19513

Kassen SC, Ramanan V, Montgomery JE et al (2007) Time course analysis of gene expression during light-induced photoreceptor cell death and regeneration in albino zebrafish. Dev Neurobiol 67:1009–1031

Kosodo Y, Suetsugu T, Suda M et al (2011) Regulation of interkinetic nuclear migration by cell cycle-coupled active and passive mechanisms in the developing brain. Embo J 30:1690–1704

Lee HO, Norden C (2013) Mechanisms controlling arrangements and movements of nuclei in pseudostratified epithelia. Trends Cell Biol 23:141–150

Leung L, Klopper AV, Grill SW et al (2011) Apical migration of nuclei during G2 is a prerequisite for all nuclear motion in zebrafish neuroepithelia. Development 138:5003–5013

Montgomery JE, Parsons MJ, Hyde DR (2010) A novel model of retinal ablation demonstrates that the extent of rod cell death regulates the origin of the regenerated zebrafish rod photoreceptors. J Comp Neurol 518:800–814

Murciano A, Zamora J, Lopez-Sanchez J et al (2002) Interkinetic nuclear movement may provide spatial clues to the regulation of neurogenesis. Mol Cell Neurosci 21:285–300

Nagashima M, Barthel LK, Raymond PA (2013) A self-renewing division of zebrafish Muller glial cells generates neuronal progenitors that require N-cadherin to regenerate retinal neurons. Development 140:4510–4521

Norden C, Young S, Link BA et al (2009) Actomyosin is the main driver of interkinetic nuclear migration in the retina. Cell 138:1195–1208

Pearson RA, Luneborg NL, Becker DL et al (2005) Gap junctions modulate interkinetic nuclear movement in retinal progenitor cells. J Neurosci 25:10803–10814
Schenk J, Wilsch-Brauninger M, Calegari F et al (2009) Myosin II is required for interkinetic nuclear migration of neural progenitors. Proc Natl Acad Sci U S A 106:16487–16492
Taverna E, Huttner WB (2010) Neural progenitor nuclei IN motion. Neuron 67:906–914
Tsai JW, Lian WN, Kemal S et al (2010) Kinesin 3 and cytoplasmic dynein mediate interkinetic nuclear migration in neural stem cells. Nat Neurosci 13:1463–1471
Vicente-Manzanares M, Ma X, Adelstein RS et al (2009) Non-muscle myosin II takes centre stage in cell adhesion and migration. Nat Rev Mol Cell Biol 10:778–790
Vihtelic TS, Hyde DR (2000) Light-induced rod and cone cell death and regeneration in the adult albino zebrafish (Danio rerio) retina. J Neurobiol 44:289–307
Wan J, Ramachandran R, Goldman D (2012) HB-EGF is necessary and sufficient for Muller glia dedifferentiation and retina regeneration. Dev Cell 22:334–347
Weber IP, Ramos AP, Strzyz PJ et al (2014) Mitotic position and morphology of committed precursor cells in the zebrafish retina adapt to architectural changes upon tissue maturation. Cell Rep 7:386–397
Yu J, Lei K, Zhou M et al (2011) KASH protein Syne-2/Nesprin-2 and SUN proteins SUN1/2 mediate nuclear migration during mammalian retinal development. Hum Mol Genet 20: 1061–1073

Part IX
Photoreceptors and Inner Retina

Chapter 79
Use of a Machine Learning-Based High Content Analysis Approach to Identify Photoreceptor Neurite Promoting Molecules

John A. Fuller, Cynthia A. Berlinicke, James Inglese and Donald J. Zack

Abstract High content analysis (HCA) has become a leading methodology in phenotypic drug discovery efforts. Typical HCA workflows include imaging cells using an automated microscope and analyzing the data using algorithms designed to quantify one or more specific phenotypes of interest. Due to the richness of high content data, unappreciated phenotypic changes may be discovered in existing image sets using interactive machine-learning based software systems. Primary postnatal day four retinal cells from the photoreceptor (PR) labeled QRX-EGFP reporter mice were isolated, seeded, treated with a set of 234 profiled kinase inhibitors and then cultured for 1 week. The cells were imaged with an Acumen plate-based laser cytometer to determine the number and intensity of GFP-expressing, i.e. PR, cells. Wells displaying intensities and counts above threshold values of interest were re-imaged at a higher resolution with an INCell2000 automated microscope. The images were analyzed with an open source HCA analysis tool, PhenoRipper (Rajaram et al., Nat Methods 9:635–637, 2012), to identify the high GFP-inducing treatments that additionally resulted in diverse phenotypes compared to the vehicle control samples. The pyrimidinopyrimidone kinase inhibitor CHEMBL-1766490, a pan kinase inhibitor whose major known targets are p38α and the Src family member lck, was identified as an inducer of photoreceptor neuritogenesis by using the open-source HCA program PhenoRipper. This finding was corroborated using a cell-based method of image analysis that measures quantitative differences in the

J. A. Fuller (✉) · C. A. Berlinicke · D. J. Zack
Ophthalmology, Molecular Biology & Genetics, Neuroscience, and Institute of Genetic Medicine, Wilmer Eye Institute, Johns Hopkins University School of Medicine, 400 N Broadway, Smith 3001, Baltimore, MD 21231, USA
e-mail: jfulle19@jhmi.edu

C. A. Berlinicke
e-mail: cdoughe1@jhmi.edu

J. Inglese
NCATS, NHGRI, National Institutes of Health, 9800 Medical Center Drive, MSC 3370, Rockville, MD 20850, USA
e-mail: jinglese@mail.nih.gov

D. J. Zack
e-mail: donzack@gmail.com

C. Bowes Rickman et al. (eds.), *Retinal Degenerative Diseases,* Advances in Experimental Medicine and Biology 854, DOI 10.1007/978-3-319-17121-0_79

mean neurite length in GFP expressing cells. Interacting with data using machine learning algorithms may complement traditional HCA approaches by leading to the discovery of small molecule-induced cellular phenotypes in addition to those upon which the investigator is initially focusing.

Keywords Photoreceptor · Neuritogenesis · Imaging · qHTS · High content analysis · Machine learning · Phenotypic screening · Protein kinase · Inhibitor

79.1 Introduction

A common challenge in HCA phenotypic screening is utilizing the image data to its fullest capacity. Generally, images are analyzed using investigator devised analysis algorithms that measure a certain set of defined features. Although this approach is powerful, it limits the assay to combinations of the stated parameters. A growing trend in the field is the use of supervised and unsupervised machine learning-based approaches that can both accelerate analysis of HCA data sets as well as facilitate discovery of novel induced phenotypes. Several open-source platforms containing machine-learning based methods have been developed and are available either as stand-alone applications such as PhenoRipper and CellCognition (Rajaram et al. 2012; Held et al. 2010) or as modules within popular HCA packages such as CellProfiler Analyst (Sommer et al. 2011; Carpenter et al. 2006).

We have been using phenotypic screening combined with primary and stem cell-derived retinal cell-based assays to identify molecules that promote differentiation and survival of PRs and retinal ganglion cells (Fuller et al. 2014; Welsbie et al. 2013). In this study, we explored the added value of the machine learning approach to analyze images from a PR differentiation and survival screen. We used the publicly available open-source program PhenoRipper (Rajaram et al. 2012) to profile cells treated with a small molecule library. PhenoRipper uses a bag-of-features classification approach to characterize images (Csurka et al. 2004). The method consists of reducing image features to a quantized color state (q-color), characterizing blocks of pixels demonstrating different q-color states, and characterizing and classifying contiguous block (superblock) types across an image (Rajaram et al. 2012; Csurka et al. 2004). A significant advantage to this approach is that it does not require cell segmentation, and can identify unique features in clumped cells. Using this software helped us identify a molecule that promotes PR neuritogenesis *in vitro*.

79.2 Materials and Methods

79.2.1 Primary Cell Dissociation

All animal procedures were performed in accordance with the ARVO statement on the “Use of Animals in Ophthalmic and Vision Research” and were approved

by the Institutional Animal Care and Use Committees at the Johns Hopkins University School of Medicine. Retinal cells were isolated and prepared for culture as previously described (Fuller et al. 2014). Briefly, retinas from the 114 strain of QRX-IRES-EGFP mice (Wang et al. 2004) are isolated at postnatal day 4. Animals are sacrificed by isoflurane overdose followed by decapitation. Eyes were enucleated, and retinas dissected and dissociated into single cell suspensions by incubation with activated papain in Hibernate-E without Ca^{2+} (BrainBits) for 15 min at 37 °C.

79.2.2 1536 well Cell Plating and Compound Library Treatment

1536 well plates were filled with 4 µL of neuronal culture medium consisting of Neurobasal-E, 2% B-27, 0.5 mM L-Glutamine, and 1X final penicillin/streptomycin (all Life Technologies). 23 nL of a stock compound solution with concentrations ranging from 10 mM to 170 nM in DMSO was transferred to each well in the culture plate from a library plate using a robotic pintool transfer tool (Wako) resulting in final concentrations ranging from 25 µM to 420 pM. Cells were resuspended at a concentration of 1.25×10^5 cells/mL, filtered, then dispensed into plates at a final well culture volume of 8 µL (1000 cells/well). Plates were then incubated for 7 days in 95% humidity at 37 °C.

79.2.3 Fixation and Imaging

Fixation and imaging of the cells were performed as described previously (Fuller et al. 2014). The cells were fixed with (4% final) paraformaldehyde, washed, stained with Hoechst 33,342, and imaged with an Acumen Explorer (TTP Labtech) plate cytometer. PRs are defined as GFP positive objects with size and GFP fluorescence intensity above defined threshold values. "On the fly" analysis identified "hit" wells, defined as wells that display a fraction of GFP positive cells greater than 2*SD relative to the vehicle (DMSO) controls or wells with the mean total GFP intensity/object greater than 8877 RFU, a threshold found to be significant in previous screens. Brightfield, nuclei and GFP images of the hit wells were then acquired with a microscope-based INCell2000 HCA platform (GE) using a 20X objective lens.

79.2.4 Analysis

The INCell images from the Hoechst (nuclei) and GFP (QRX promoter reporter) channels of the control and hit wells were loaded into PhenoRipper (Rajaram et al. 2012). All default parameters for threshold values as well as block size (15 pixels per block) for PhenoRipper were used for analysis. Representative vehicle (DMSO) control wells were used as a replicate image subsampling group. All points that are found on the periphery of the multidimensional scaling (MDS) plot (apparent

outliers) were examined and excluded from analysis if deemed to contain artifacts. The putative positive hit and control images were also analyzed using a custom algorithm developed using Neuronal Profiling 4.1 (ThermoFisher).

79.3 Results

79.3.1 Photoreceptor Neuritogenesis Uncovered by Machine Learning

In order to screen for small molecules that promote photoreceptor differentiation, we developed a high-throughput assay utilizing dissociated retinal cells from a QRX-GFP transgenic mouse that we previously reported (Wang et al. 2004). Our intended readout of the assay was number of cells expressing GFP and expression level per cell. As expected, using this assay we detected a number of molecules that modulated GFP expression, and further characterization of these molecules is underway (Fuller et al. unpublished results).

To complement the GFP intensity measurement algorithm, we also analyzed the cell image data sets using a PhenoRipper-derived MDS plot (Fig. 79.1a). This analysis revealed a superblock (common cell morphology) that appeared to be enriched in wells containing QRX positive neurites (Fig. 79.1b arrow). Cells treated with 6-(2-chlorophenyl)-8-methyl-2-(oxan-4-ylamino)pyrido[2,3-d]pyrimidin-7-one/CHEMBL-1766490/Pubchem CID 23551786, herein referred to by the CHEMBL identifier, were identified as having higher neurite counts as compared to vehicle treated cells (Fig. 79.1d, e). Analysis of the same images using an algorithm developed with the Cellomics Neuronal Profiling package measured an increased neurite length over multiple compound concentrations compared to control (Fig. 79.1c). It should be noted that the images analyzed were taken from a well-based preselection of images; therefore the neurites/well clusters may not necessarily be reflective of the dataset of kinase inhibitors as a whole.

79.4 Discussion

High content analysis is typically undertaken by acquiring images of interest and performing feature-specific (e.g. fluorescent marker intensity) analysis. Although current HCA software algorithms are capable of discerning many patterns with high precision, the algorithms are generally selected and optimized to measure specific image features and phenotypes that are already of interest to the investigator. It is generally difficult to discern a ‘global’ treatment-specific phenotype (e.g. finding *every* different morphological parameter compared to control). Although it is possible to run an image set through every possible feature algorithm to maximize the treatment specific response, this can be labor and time intensive and is not typically

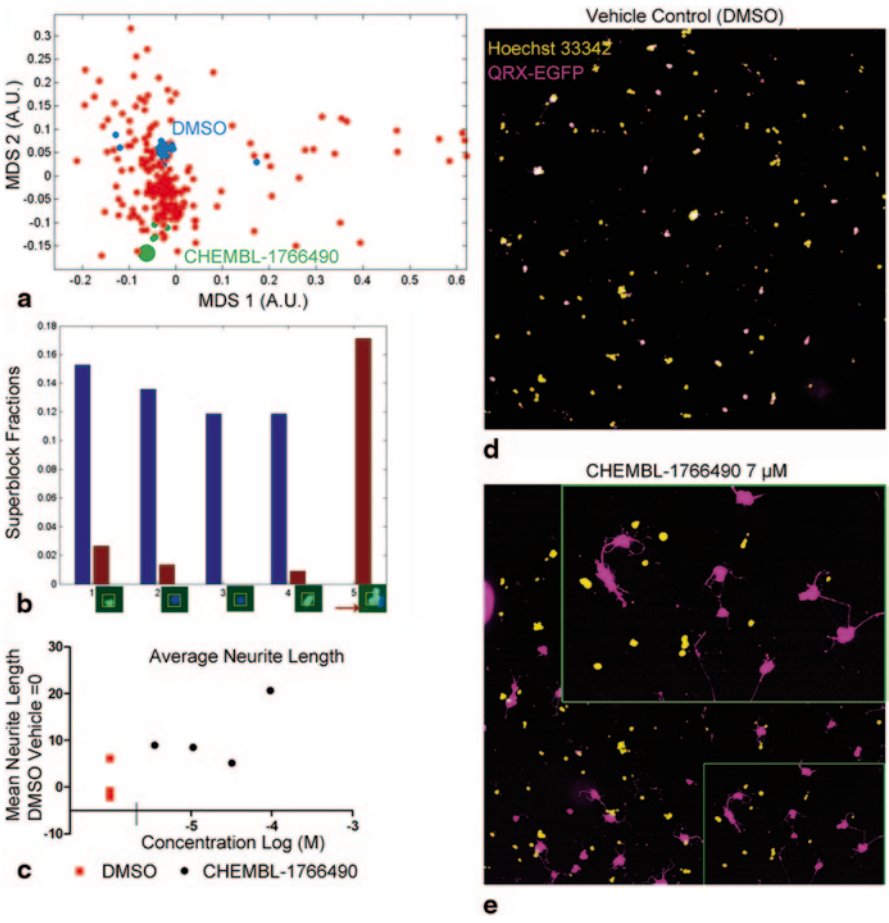

Fig. 79.1 Enhanced photoreceptor neurites following treatment with CHEMBL-1766490. **a** 2D MDS plot of PhenoRipper derived image profiles for QRX-GFP retinal cells cultured 1 week. **b** Histogram of representative superblocks that best distinguish vehicle control from CHEMBL-1766490 treated wells. *Red arrow*: superblock containing neurites. **c** Quantification of average neurite length using Cellomics Neuronal Profiling following treatment with DMSO vehicle or CHEMBL-1766490. **d**, **e** Representative images from control (**d**) and CHEMBL-1766490 (**e**) treated wells

done. Additionally, cellular heterogeneity within a cell population can make subtle (though possibly important) changes difficult to identify, and is a common phenomenon that has been widely reported in HCA data. (Gough et al. 2014; Burrell et al. 2013; Huang 2009; Altschuler and Wu 2010).

Advanced informatics methods are also being used in conjunction with traditional HCA algorithms to identify novel morphological changes within an image set. Software packages such as PhenoRipper does not rely on cell segmentation, and instead focuses on clustering similar and dissimilar morphological features within a particular experiment (Rajaram et al. 2012). It is then incumbent on the

user to determine whether a discovered feature is of biological interest. We used PhenoRipper as an agnostic way to visualize dissimilar cell morphologies within an experiment, and discovered that a particular small molecule (CHEMBL-1766490) enhanced neurite outgrowth. This finding was then validated with a more "classical" algorithm specifically designed to quantify neurite outgrowth.

Although defining the mechanism of action for this small molecule is outside the scope of this discussion, this serves as a case in point for one of the main challenges of phenotypic screening, which is elucidating the molecular mechanism of action. CHEMBL-1766490 is reported to have p38α MAPK inhibitory activity (Goldstein et al. 2011). It has been reported that p38α inhibition induces neuronal differentiation, whereas other reports suggest that neurite outgrowth is inhibited following p38α knockdown in PC12 and P19 committed neuronal cell lines (Morooka and Nishida 1998; Iwasaki et al. 1999; Aouadi et al. 2006). Although inhibiting p38MAPK to enhance neuritogenesis may be a postnatal photoreceptor-specific phenomenon, it is possible that this is an "off-target" mechanism of the molecule, perhaps due to inhibition of one or more other kinases. Indeed, the kinase selectivity profile of the pyrimidinopyridone family from which this molecule was found demonstrates submicromolar inhibition of 10 out of the 300 kinases tested (Goldstein et al. 2011). Future studies performed in a photoreceptor-specific systems pharmacology context may uncover currently unknown effects of similar small molecules on cellular phenotypes.

In this study, we started with an image data set that was derived from a screen that was originally designed to assess GFP reporter expression as a marker for photoreceptor differentiation. Then, using a machine learning-based analytical approach, we uncovered a small molecule that increased neurite outgrowth of developing photoreceptors. As many laboratories performing image-based analyses typically have extensive archives of data from previous studies, they could potentially benefit from a similar approach. By integrating machine-learning based approaches with established analysis algorithms, it should be possible to uncover previously unknown phenotypic features, and to identify molecules that modulate and regulate the pathways controlling these morphologies and phenotypes.

References

Altschuler SJ, Wu LF (2010) Cellular heterogeneity: do differences make a difference? Cell 141:559–563

Aouadi M, Bost F, Caron L et al (2006) p38 mitogen-activated protein kinase activity commits embryonic stem cells to either neurogenesis or cardiomyogenesis. Stem Cells 24:1399–1406

Burrell RA, McGranahan N, Bartek J et al (2013) The causes and consequences of genetic heterogeneity in cancer evolution. Nature 501:338–345

Carpenter AE, Jones TR, Lamprecht MR et al (2006) CellProfiler: image analysis software for identifying and quantifying cell phenotypes. Genome Biol 7:R100

Csurka G, Dance C, Fan L et al (2004) Visual categorization with bags of keypoints. Proc Workshop Statistical Learning Comput Vis 1:22

Fuller JA, Shaw GC, Bonnet-Wersinger D et al (2014) A high content screening approach to identify molecules neuroprotective for photoreceptor cells. Adv Exp Med Biol 801:773–781

Goldstein DM et al (2011) Discovery of 6-(2,4-difluorophenoxy)-2-[3-hydroxy-1-(2-hydroxyethyl)propylamino]– 8-methyl-8H-p yrido[2,3-d]pyrimidin-7-one (pamapimod) and 6-(2,4-difluorophenoxy)-8-methyl-2-(tetrahydro-2H-pyran-4-ylamino)pyrido[2,3-d]py rimidin-7(8H)-one (R1487) as orally bioavailable and highly selective inhibitors of p38alpha mitogen-activated protein kinase. J Med Chem 54:2255–2265

Gough AH, Chen N, Shun TY et al (2014) Identifying and quantifying heterogeneity in high content analysis: application of heterogeneity indices to drug discovery. PLoS One 9:e102678

Held M, Schmitz MH, Fischer B et al (2010) CellCognition: time-resolved phenotype annotation in high-throughput live cell imaging. Nat Methods 7:747–754

Huang S (2009) Non-genetic heterogeneity of cells in development: more than just noise. Development 136:3853–3862

Iwasaki S, Iguchi M, Watanabe K et al (1999) Specific activation of the p38 mitogen-activated protein kinase signaling pathway and induction of neurite outgrowth in PC12 cells by bone morphogenetic protein-2. J Biol Chem 274:26503–26510

Morooka T, Nishida E (1998) Requirement of p38 mitogen-activated protein kinase for neuronal differentiation in PC12 cells. J Biol Chem 273:24285–24288

Rajaram S, Pavie B, Wu LF et al (2012) PhenoRipper: software for rapidly profiling microscopy images. Nat Methods 9:635–637

Sommer C, Strähle C, Köthe U, Hamprecht FA (2011) in: Eighth IEEE International Symposium on Biomedical Imaging (ISBI). Proceedings, 230–233

Wang QL, Chen S, Esumi N et al (2004) QRX, a novel homeobox gene, modulates photoreceptor gene expression. Hum Mol Genet 13:1025–1040

Welsbie DS et al (2013) Functional genomic screening identifies dual leucine zipper kinase as a key mediator of retinal ganglion cell death. Proc Natl Acad Sci U S A 110:4045–4050

Chapter 80
A Novel Approach to Identify Photoreceptor Compartment-Specific Tulp1 Binding Partners

Lindsey A. Ebke, Gayle J.T. Pauer, Belinda Willard and Stephanie A. Hagstrom

Abstract Photoreceptors (PRs) are highly polarized and compartmentalized cells with large amounts of proteins synthesized in the inner segment (IS) and transported to the outer segment (OS) and synaptic terminal. The PR-specific protein, Tulp1, is localized to the IS and synapse and is hypothesized to be involved in protein trafficking. To better understand the molecular processes that regulate protein trafficking in PRs, we aimed to identify compartment-specific Tulp1 binding partners. Serial tangential sectioning of Long Evans rat retinas was utilized to isolate the IS and synaptic PR compartments. Tulp1 binding partners in each of these layers were identified using co-immunoprecipitation (co-IP) with Tulp1 antibodies. The co-IP eluates were separated by SDS-PAGE, trypsinized into peptide fragments, and proteins were identified by liquid chromatography tandem mass spectrometry. In the IS, potential Tulp1-binding partners included cytoskeletal scaffold proteins, protein trafficking molecules, as well as members of the phototransduction cascade. In the synaptic region, the majority of interacting proteins identified were cytoskeletal. A separate subset of proteins were identified in both the IS and synapse including

S. A. Hagstrom (✉) · L. A. Ebke · G. J. T. Pauer
Department of Ophthalmic Research, Cole Eye Institute, Cleveland Clinic, Cleveland, OH 44195, USA
e-mail: hagstrs@ccf.org

S. A. Hagstrom
Department of Ophthalmology, Cleveland Clinic Lerner College of Medicine of Case Western Reserve University, Cleveland, OH 44195, USA

L. A. Ebke
e-mail: ebkel@ccf.org

G. J. Pauer
e-mail: pauerg@ccf.org

B. Willard
Proteomics Core Services, Lerner Research Institute, Cleveland Clinic, Cleveland, OH 44195, USA
e-mail: willarb@ccf.org

C. Bowes Rickman et al. (eds.), *Retinal Degenerative Diseases,* Advances in Experimental Medicine and Biology 854, DOI 10.1007/978-3-319-17121-0_80

chaperones and family members of the GTPase activating proteins. Tulp1 has two distinct PR compartment-specific interactomes. Our results support the hypothesis that Tulp1 is involved in the trafficking of proteins from the IS to the OS and the continuous membrane remodeling and vesicle cycling at the synaptic terminal.

80.1 Introduction

Retinitis Pigmentosa (RP) is the most common subtype of hereditary retinal degeneration affecting one in 4000 people worldwide (Hartong et al. 2006). The disease progresses from night blindness to peripheral visual field loss, and eventual total blindness. Mutations in the gene *TULP1* cause autosomal recessive RP and Leber Congenital Amarosis (Hagstrom et al. 1998; Hanein et al. 2004; Mataftsi et al. 2007). In these patients, the disease phenotype consists of night vision disturbances, nystagmus, central vision impairment, and pigmentary retinopathy (Jacobson et al. 2014).

Extensive phenotyping of the *tulp1-/-* mouse has provided evidence that Tulp1 plays an important role in protein trafficking in PR cells (Hagstrom et al. 1999, 2001, 2012; Grossman et al. 2011). Tulp1 is expressed in PR regions in which massive amounts of protein trafficking occurs; the IS and the synaptic terminal (Hagstrom et al. 1999). At an early age in *tulp1-/-* mice prior to PR degeneration, rhodopsin and other OS-specific proteins are mislocalized (Hagstrom et al. 1999, 2001; Grossman et al. 2011). In addition, synapses of *tulp1-/-* PRs lack the tight spatial relationship between specific ribbon-associated proteins, and few intact synaptic ribbons are present (Grossman et al. 2009). These defects initiated our hypothesis that Tulp1 is involved in protein transport and raise the question of whether Tulp1 plays unique roles at opposite ends of the cell. We aimed to determine the unique binding partners of Tulp1 in the PR IS and synaptic terminal.

80.2 Materials and Methods

80.2.1 Animals

The generation of *tulp1-/-* mice has been described previously (Hagstrom et al. 1999). Wild-type C57Bl6/J mice were purchased from the Jackson Laboratory and Long Evans rats were purchased from Charles River Laboratory. All animal experiments were approved by the IACUC of the Cleveland Clinic and performed in compliance with the ARVO Statement for the Use of Animals in Ophthalmic and Visual Research.

80.2.2 Serial Tangential Sectioning

Tangential sectioning of rat retinas were carried out as previously described (Song and Sokolov 2009) with several optimizations. Long Evans rat retinas were dissected in DMEM/F12 media supplemented with complete protease inhibitors (Roche) and positioned on a disc of nitrocellulose paper photoreceptor-side down. Each retina was cut into halves or quarters and flattened individually in a custom-made flattening chamber (Fig. 80.1) by positioning the retina above a glass capillary array (BURLE Electro-Optics) and slowly removing the media from the lower chamber. The flattened retina was secured onto a 2 × 2 cm glass slide using superglue and clamped with a top slide wrapped in non-stick optically-clear tape separated by 0.5 mm plastic spacers. This sandwich assembly was placed on dry ice to freeze for 1 h. A mound of OCT compound (Sakura Finetek) was frozen on the cryostat chuck and sectioned to create a flat surface large enough to accommodate the bottom glass slide. The clamps and top slide were removed and the base slide was pressed against the OCT surface and frozen in place by the addition of water drops around the back of the glass base. The peripheral edges of each retina piece were trimmed with a scalpel blade to remove uneven parts and finally serial sectioned at a thickness of 10 µm, collecting each section in 50 µl of 2x Tris-Glycine SDS sample

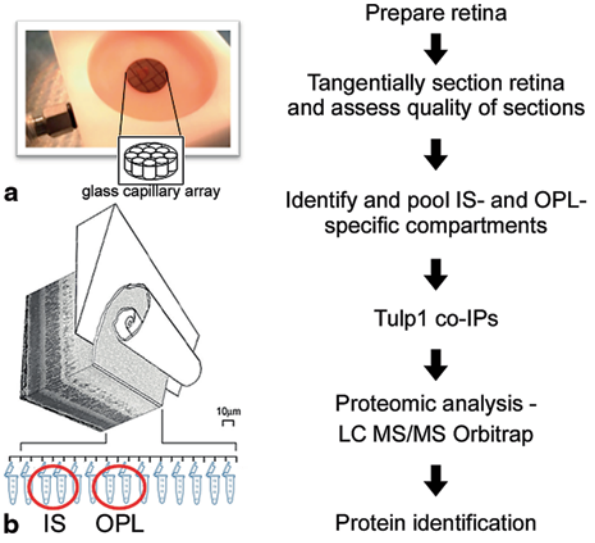

Fig. 80.1 Flowchart overview of experimental approach. **a** Flattening chamber with a quartered retina laying atop a quartered nitrocellulose disc; inset: a depiction of the glass capillary array. **b** A depiction of serial tangential sectioning through the retina; each 10 µm slice is collected into an individual microcentrifuge tube of sample buffer. The IS- and OPL-containing samples are identified and pooled across multiple retinas prior to co-IP. (Schematic illustration of retina reprinted with permission from Song and Sokolov (2009). (Copyright 2014 American Chemical Society)

buffer (Life Technologies) or Pierce IP lysis buffer (Thermo Scientific) depending upon downstream analysis. Verification of tangential sectioning was analyzed by rhodopsin dot blot as described previously (Song and Sokolov 2009). Only the tangentially sectioned retinas which contain rhodopsin in the outermost 3–6 sections corresponding to the OS were selected for proteomic analysis.

80.2.3 Tulp1 co-Immunoprecipitation

Tangentially sectioned samples containing IS, outer plexiform layer (OPL), and inner plexiform layer (IPL) regions were identified based on Western blot analysis of representative tangential sectioned retinas with compartment-specific antibodies (data not shown). The IPL lacks Tulp1 and was used as a negative control. Whole retinal lysate from *tulp1-/-* mice was also used as a negative control. In order to obtain sufficient protein for downstream proteomic analysis, region-specific samples across multiple retinas were pooled (Fig. 80.1). Co-IP of pooled IS, OPL, and negative control layers were performed as previously described (Grossman et al. 2013).

80.2.4 Liquid Chromatography Tandem Mass Spectrometry (LC-MS/MS)

Eluted co-IP products were run onto SDS-PAGE gels. For in-gel digestions, the lanes were excised and divided into a number of smaller areas for trypsin digestion according to a previously published method (Kinter and Sherman 2005). Trypsinized peptides were extracted from the polyacrylamide and resuspended in 1 % acetic acid for analysis by LC-MS/MS on a LTQ-Obitrap Elite hybrid mass spectrometer system coupled to a Dionex Ultimate 3000 HPLC. Five μL aliquots of the digests were loaded onto a 75 μm Acclaim Pepmap C18 reverse phase column and eluted by an acetonitrile/0.1 % formic acid gradient. The digest was analyzed using a data dependent acquisition and the proteins were identified by searching the LC-MS/MS data with the programs Mascot and Sequest against the rat Reference Sequence Databases. These search results were uploaded into the program Scaffold for relative quantitation using normalized spectral counts for each protein across these samples. Identified interacting partners were analyzed through the use of QIAGEN's Ingenuity® Pathway Analysis (IPA®, QIAGEN) and UniProt online protein knowledgebase.

80.3 Results

80.3.1 Tulp1 Interacting Proteins in the IS and Synapse

Our experimental approach to identify compartment-specific Tulp1 binding partners was to physically isolate PR IS and synaptic regions using serial tangential

sectioning of flat-mounted rat retinas, followed by co-IP and a proteomics-based approach (Fig. 80.1). Tangentially sectioned IPL and whole retinal lysate from *tulp1-/-* mice were used as Tulp1-negative tissues. Our inclusion criteria required each protein to be present at least two fold higher than in negative controls, and identified by a minimum of two unique peptides and at least five spectral counts. Proteomic analysis of the co-IP products identified 275 potential Tulp1-binding partners; 110 proteins were identified in the IS region, 15 proteins were identified in the synapse, and an additional 150 proteins were identified in both compartments. Tulp1 was identified in the IS co-IP product by 27 peptides covering 53 % of the protein sequence and in the synaptic co-IP product by 14 peptides covering 31 % of the protein sequence.

Next, we classified the proteins from each PR compartment into functional categories using bioinformatics methods. Two of the most abundant functional categories in the IS were protein transport molecules and cytoskeletal proteins. Examples of potential Tulp1-binding partners in this region include C2 domain-containing protein 2-like, coatomer protein complex subunit alpha, elongator complex protein 1, G kinase-anchoring protein 1, interphotoreceptor matrix proteoglycan 1 precursor, kinectin 1, kinesin family members 3a and 3b, microtubule-associated protein 9, oxygen-regulated protein 1, and both tubulin alpha-1A and -4B chains. Surprisingly, results also identified 11 known phototransduction cascade proteins which may bind Tulp1 during their transport from the IS to the OS.

The most abundant category in the synaptic region was cytoskeletal proteins. Examples of potential Tulp1-binding partners in this region include alpha-adducin, cytoskeleton-associated protein 4, desmoglein-4 precursor, and syntrophin beta 2.

A subset of proteins were present in both the IS and synaptic regions. The most abundant categories include protein synthesis and mRNA processing, examples include many ribosomal and mitochondrial proteins. However, some of the most interesting potential Tulp1-binding partners identified in both compartments included chaperone proteins such as heat shock proteins, several GTP-ase activating proteins, and the cytoskeletal proteins ensconsin isoform 1 and microtubule-associated protein 1B.

80.4 Discussion

In this study, we demonstrated a novel experimental method to isolate PR IS and synaptic regions followed by co-IP and identification of potential Tulp1 binding partners from each compartment. Our goal was to identify Tulp1 IS-specific and synaptic-specific interactions. Previous research from our lab has shown that Tulp1 is a cytoplasmic protein that associates with membranes through binding phospholipids and the cytoskeletal components F-actin, dynamin-1, and MAP1B (Xi et al. 2005, 2007; Grossman et al. 2013, 2014). Our current results support this finding, as many of the possible Tulp1 binding partners identified only in the IS and only in the synapse were components of the cytoskeleton and members of the protein transport system. To our surprise, we also identified multiple phototransduction cascade proteins that possibly interact with Tulp1 in the IS. Further experiments are required to confirm these interactions.

Potential Tulp1 interacting proteins that were identified in both the IS and synaptic regions included many involved in protein synthesis, such as ribosomal and mitochondrial proteins. This is not entirely surprising since proteins are synthesized in the PR IS and the IS also contains the vast majority of PR-specific mitochondria. This finding may be indicative of one of the limitations of co-IP, i.e. the identification of many nonspecific interactors that may be copurified with bait proteins. In fact, many of the identified proteins in this functional category are known members of the "CRAPome", or Contaminant Repository for Affinity Purification. This online resource (www.crapome.org) contains negative control data from hundreds of studies (Mellacheruvu et al. 2013).

Overall, our results indicate that Tulp1 could function at the IS in several capacities. First, it may serve as an adapter protein involved in selecting cargo for inclusion into transport vesicles. Second, it may be part of a dynamic microtubule scaffold connecting transport vesicles with the cytoskeleton. Third, it may regulate vesicle trafficking from the Golgi to the basal body for further transport to the OS. Tulp1 in the OPL is likely involved in the assembly of the ribbon synapses at the active zone, or compensatory vesicle cycling at the periactive zone. Confirmation of potential Tulp1 interacting partners identified in this study requires further investigation.

Acknowledgments This study was supported by NIH Grant EY15638 (SAH). The Orbitrap Elite instrument was purchased via a NIH shared instrument grant (1S10RR031537-01). The authors would like to thank Dr. Maxim Sokolov for his assistance in training the tangential sectioning method.

References

Grossman GH, Pauer GJT, Narendra U et al (2009) Early synaptic defects in *tulp1–/–* mice. Invest Ophthalmol Vis Sci 50:3074–3083

Grossman GH, Watson RF, Pauer GJT et al (2011) Immunocytochemical evidence of Tulp1-dependent outer segment protein transport pathways in photoreceptor cells. Exp Eye Res 93:658–668

Grossman G, Ebke L, Beight C et al (2013) Protein partners of dynamin-1 in the retina. Vis Neurosci 30:1–11

Grossman GH, Beight CD, Ebke LA et al (2014) Interaction of Tubby-like protein-1 (Tulp1) and microtubule-associated protein (MAP) 1A and MAP1B in the mouse retina. Adv Exp Med Biol 801:511–518

Hagstrom SA, North MA, Nishina PM et al (1998) Recessive mutations in the gene encoding the tubby-like protein TULP1 in patients with retinitis pigmentosa. Nat Genet 18:174–176

Hagstrom SA, Duyao M, North MA et al (1999) Retinal degeneration in *tulp1–/–* mice: vesicular accumulation in the interphotoreceptor matrix. Invest Ophthalmol Vis Sci 40:2795–2802

Hagstrom SA, Adamian M, Scimeca M et al (2001) A role for the Tubby-like protein 1 in rhodopsin transport. Invest Ophthalmol Vis Sci 42:1955–1962

Hagstrom SA, Watson RF, Pauer GJ et al (2012) Tulp1 is involved in specific photoreceptor protein transport pathways. Adv Exp Med Biol 723:783–789

Hanein S, Perrault I, Gerber S et al (2004) Leber congenital amaurosis: comprehensive survey of the genetic heterogeneity, refinement of the clinical definition, and genotype–phenotype correlations as a strategy for molecular diagnosis. Hum Mutat 23:306–317

Hartong DT, Berson EL, Dryja TP (2006) Retinitis pigmentosa. Lancet 368:1795–1809
Jacobson SG, Cideciyan AV, Huang WC et al (2014) TULP1 mutations causing early-onset retinal degeneration: preserved but insensitive macular cones. Invest Ophthalmol Vis Sci 55:5354–5364
Kinter M, Sherman NE (2005) Protein sequencing and identification using tandem mass spectrometry. In: Desiderio D, Nibbering N (Eds). John Wiley & Sons, New York
Mataftsi A, Schorderet DF, Chachoua L et al (2007) Novel *TULP1* mutation causing Leber congenital amaurosis or early onset retinal degeneration. Invest Ophthalmol Vis Sci 48:5160–5167
Mellacheruvu D, Wright Z, Couzens AL, et al (2013) The CRAPome: a contaminant repository for affinity purification-mass spectrometry data. Nat Methods 10(8):730–736
Song H, Sokolov M (2009) Analysis of protein expression and compartmentalization in retinal neurons using serial tangential sectioning of the retina. J Proteome Res 8:346–351
Xi Q, Pauer GJT, Marmorstein AD et al (2005) Tubby-like protein 1 (TULP1) interacts with F-actin in photoreceptor cells. Invest Ophthalmol Vis Sci 46:4754–4761
Xi Q, Pauer GJT, Ball SL et al (2007) Interaction between the photoreceptor-specific Tubby-like protein 1 and the neuronal-specific GTPase dynamin-1. Invest Ophthalmol Vis Sci 48:2837–2844

Chapter 81
Thyroid Hormone Signaling and Cone Photoreceptor Viability

Hongwei Ma and Xi-Qin Ding

Abstract Thyroid hormone (TH) signaling regulates cell proliferation, differentiation, and apoptosis. In the retina, TH signaling plays a central role in cone opsin expression. TH signaling inhibits S opsin expression, stimulates M opsin expression, and promotes dorsal-ventral opsin patterning. TH signaling has also been associated with cone photoreceptor viability. Treatment with thyroid hormone triiodothyronine (T3) or induction of high T3 by deleting the hormone-inactivating enzyme type 3 iodothyronine deiodinase (DIO3) causes cone death in mice. This effect is reversed by deletion of the TH receptor (TR) gene. Consistent with the T3 treatment effect, suppressing TH signaling preserves cones in mouse models of retinal degeneration. The regulation of cone survival by TH signaling appears to be independent of its regulatory role in cone opsin expression. The mechanism by which TH signaling regulates cone viability remains to be identified. The current understanding of TH signaling regulation in photoreceptor viability suggests that suppressing TH signaling locally in the retina may represent a novel strategy for retinal degeneration management.

Keywords Thyroid hormone · Thyroid hormone receptor · Cone · Cone opsin · Retinal degeneration

81.1 Introduction

Thyroid hormone (TH) signaling regulates numerous physiological functions, including cell growth, differentiation, and metabolic homeostasis. In healthy humans, the thyroid gland produces predominantly the prohormone thyroxine (T4) along with a small amount of the bioactive hormone triiodothyronine (T3). In the peripheral tissues, T4 and T3 are transported to cells where T4 is converted to T3

X.-Q. Ding (✉) · H. Ma
The Department of Cell Biology, University of Oklahoma Health Sciences Center, Oklahoma City, OK 73104, USA
e-mail: xi-qin-ding@ouhsc.edu

H. Ma
e-mail: Hongwei-ma@ouhsc.edu

C. Bowes Rickman et al. (eds.), *Retinal Degenerative Diseases,* Advances in Experimental Medicine and Biology 854, DOI 10.1007/978-3-319-17121-0_81

by the type 1 and type 2 iodothyronine deiondinases (DIO1 and DIO2). T3 is then transferred to the nucleus and binds to the TH receptors (TRs), initiating the downstream responses. The type 3 iodothyronine deiondinase (DIO3) deactivates T4 and T3 by converting T4 and T3 to reverse T3 (rT3) and 3,5-diiodo-l-thyronine (T2), respectively (Fig. 81.1). Though the TH level in the circulation is essential for normal TH signaling, increasing evidence suggests that the local control of TH signaling activity via TRs and the enzymes that regulate cellular T3 levels plays a critical role in cellular functional regulation (Cheng et al. 2010; Dentice and Salvatore 2011).

TRs belong to the nuclear hormone receptor superfamily and function as ligand-dependent transcription factors. In the absence of T3, TRs are bound to a co-repressor, as monomers, homo-dimers, or heterodimers with the retinoid X receptor (RXR). Upon T3 binding, TRs are dissociated from the co-repressor and bind to a co-activator, which initiates transcriptional responses (Fig. 81.1). Two genes encode related TRα and TRβ across vertebrate species (Flamant et al. 2006; Brent 2012). There are three TRα splice variants: TRα1 is expressed predominantly in brain, heart, and skeletal muscle while TRα2 and TRα3 are non-T3-binding splice products. TRβ has three major T3-binding splice products: TRβ1 is expressed widely; TRβ2 is expressed primarily in the brain, retina, and inner ear; and TRβ3 is expressed in kidney, liver, and lung (Brent 2012). In the retina, TRβ2 is expressed in the developmental cones (Applebury et al. 2007; Ng et al. 2009a). TH has also been shown to exert its action through non-genomic (non-TR) actions which do not include initial nuclear actions of TR or gene transcription, but involve the cell surface receptor and signal transduction pathway (Hiroi et al. 2006; Cheng et al. 2010).

TH signaling plays a central role in cone opsin expression both in developmental and adult retinas. TH signaling has also been associated with cone viability. Treatment with T3 or induction of high T3 by deleting DIO3 causes cone death in mice. Consistent with the T3 treatment effect, suppressing TH signaling preserves cones

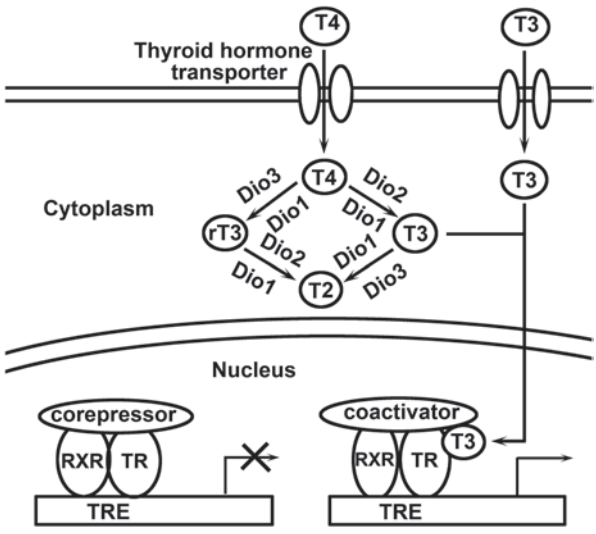

Fig. 81.1 The action of thyroid hormones at the cell level. T4 and T3 are transported into target cells where T4 is converted to T3. In the absence of T3, TR homodimerizes or heterodimerizes with RXR, and then binds to a TRE and a corepressor. T3 binding to the ligand-binding domain results in disruption of corepressor binding and promotion of coactivator binding, which then leads to initiation of gene transcription. Adapted from Brent 2012

in mouse models of retinal degeneration. In this review, we summarize the regulatory roles of TH signaling in cone opsin expression and cone viability.

81.2 Regulation of TH Signaling in Cone Opsin Expression

The regulation of TH signaling in cone opsin expression and patterning distribution is well documented in mouse models with TH signaling inhibition at the receptor or hormone levels. During retinal development and in the adult postmitotic retina, TH signaling via TRβ2 suppresses expression of S opsin, induces expression of M opsin, and promotes the dorsal-ventral opsin patterning distribution (Ng et al. 2001; Glaschke et al. 2011). *Thrβ2*$^{-/-}$ mice display loss of M opsin, universal expression of S opsin in all cones, and loss of dorsal-ventral expression patterning (Ng et al. 2001). A similar phenotype was observed in *RXR*$^{-/-}$ mice (Roberts et al. 2005) and in mice with a deficiency in NeuroD1, a transcription factor essential for TRβ2 expression (Liu et al. 2008). Consistent with the observations in models with TR defects, studies using hypothyroid mice, including *Tshr*$^{-/-}$ and *Pax8*$^{-/-}$mice and mice treated with antithyroid drugs, further demonstrated the essential role of TH signaling in cone opsin expression and patterning (Lu et al. 2009; Glaschke et al. 2010; Glaschke et al. 2011).

At the transcriptional level, TRβ2 signaling controls M opsin expression through the 5'-UTR and intron 3–4 region (Iwagawa et al. 2013). In the mouse retina, TRβ2-positive cells first appear between embryonic day 10, and 12, and continue to increase until near birth, correlating with generation of the cone population. At birth, TRβ2-expressing cells decrease until postnatal day 10, and then decline to very low levels in adulthood (Ng et al. 2009a). It has been shown that TRβ2 is expressed in human foveal cones by fetal week 12, during the period of cone genesis (Lee et al. 2006).

Mutations in the TRβ gene have been identified in humans. These mutations are primarily located in the ligand binding domain of the receptor. TRβ mutations are clinically characterized by generalized TH resistant syndrome (GTHR) with elevated T3 and T4 levels and normal or elevated thyrotropin levels (Rivolta et al. 2009; Ferrara et al. 2012). Patients with TRβ mutations have reduced vision acuity, pendular nystagmus, and a bull's-eye type of macular atrophy (Newell and Diddie 1977). Spectral electroretinogram (ERG) examinations demonstrated reduced L/M cone response, increased S cone function, and severely reduced photopic response (Weiss et al. 2012).

81.3 Regulation of TH Signaling in Cone Viability

TH signaling regulates cone viability. The typical evidence is obtained from studies using *Dio3*$^{-/-}$ mice. These mice show a dramatically reduced cone number and enhanced cone apoptosis, similar to mice receiving a high dose of T3 treatment (Ng et al. 2010). Deletion of TRβ2 abolished the cone degeneration phenotype in

Dio3$^{-/-}$ mice and in mice treated with T3, indicating a TRβ2-mediated death mechanism. Studies using *Cngb3*$^{-/-}$ and *Gucy2e*$^{-/-}$ mice, models of retinal degeneration, also demonstrated that stimulating TH signaling by T3 treatment deteriorates cones (Ma et al. 2014).

TH signaling regulation of cone viability is further demonstrated by studies showing that suppressing TH signaling promotes cone survival in mouse models of retinal degeneration. *Rpe65*$^{-/-}$ and *cpfl1* mice show rapid and severe cone death. Suppressing TH signaling with anti-thyroid drugs significantly improved cone survival in these mice (Ma et al. 2014). It is worth mentioning that anti-thyroid treatment does not cause rod degeneration, although T3 treatment or deletion of DIO3 has been shown to reduce rod numbers (Ng et al. 2010; Ma et al. 2014).

TH signaling regulation of cell viability has been demonstrated in other tissues and cell lines. Excessive TH signaling induces auditory defects (Ng et al. 2009b), causes cerebellar abnormalities (Peeters et al. 2013), and is associated with apoptosis of a variety of human cell lines, including lymphocytes (Mihara et al. 1999), breast cancer cells (Sar et al. 2011), and pituitary tumor cells (Chiloeches et al. 2008). In addition, TR signaling has been well documented in apoptotic tissue remodeling during anuran metamorphosis (Shi et al. 2001; Buchholz et al. 2004).

It appears that TH signaling-mediated regulation of cone viability is likely independent of TH regulation of cone opsin expression. Suppressing TH signaling in *Rpe65*$^{-/-}$ and *cpfl1* mice greatly reduced cone death, which was accompanied by increased expression of S-opsin, increased S cones, and decreased M cones (Ma et al. 2014). Stimulating TH signaling in *Cngb3*$^{-/-}$ and *Gucy2e*$^{-/-}$ mice increased cone death, which was accompanied by reduced levels of S-opsin expression (Ma et al. 2014). Stimulating TH signaling induces degeneration of rods (Ng et al. 2010; Ma et al. 2014) and cochlear hair cells (Ng et al. 2009b), which do not express cone opsin. Moreover, TH signaling induces death in numerous cancer cell lines (Yamada-Okabe et al. 2003; Chiloeches et al. 2008; Sar et al. 2011).

The mechanism(s) by which TH signaling regulates cone viability remains unclear, though it appears to involve apoptotic death processes (Ng et al. 2010). TH signaling-induced cancer cell death has been shown to involve several signaling pathways. The activation of TRβ by T3 binding was revealed to induce senescence and DNA damage in cultured cells and in tissues of young hyperthyroid mice (Zambrano et al. 2014). In the MCF-7 human breast cancer cell line, expression of TRβ in the presence of T3 was shown to promote apoptosis via down-regulation of the JAK-STAT-cyclin D pathways (Park et al. 2013).

81.4 Future Perspectives

The current understanding of TH signaling regulation in cone photoreceptor viability suggests that suppressing TH signaling locally in the retina may represent a novel strategy for retinal degeneration management. The first step in testing this potential is to determine whether local suppression of TH signaling in the retina protects

cones. It would be valuable to test whether ocular administration of TR antagonists, photoreceptor-specific TRβ2 deletion, and photoreceptor-specific DIO3 overexpression/activation reduces cone death in animal models of retinal degeneration. It is also important to understand how TH signaling prompts cell death. The resulting knowledge will help to identify new target(s) to manipulate this powerful signaling pathway for photoreceptor protection.

Acknowledgements This work was supported by grants from the National Center for Research Resources (P20RR017703), the National Eye Institute (P30EY12190, R01EY019490, and T32EY023202), and the Foundation Fighting Blindness.

References

Applebury ML, Farhangfar F, Glosmann M et al (2007) Transient expression of thyroid hormone nuclear receptor TRβ2 sets S opsin patterning during cone photoreceptor genesis. Dev Dyn 236:1203–1212

Brent GA (2012) Mechanisms of thyroid hormone action. J Clin Invest 122:3035–3043

Buchholz DR, Tomita A, Fu L et al (2004) Transgenic analysis reveals that thyroid hormone receptor is sufficient to mediate the thyroid hormone signal in frog metamorphosis. Mol Cell Biol 24:9026–9037

Cheng SY, Leonard JL, Davis PJ (2010) Molecular aspects of thyroid hormone actions. Endocr Rev 31:139–170

Chiloeches A, Sanchez-Pacheco A, Gil-Araujo B et al (2008) Thyroid hormone-mediated activation of the ERK/dual specificity phosphatase 1 pathway augments the apoptosis of GH4C1 cells by down-regulating nuclear factor-κB activity. Mol Endocrinol 22:2466–2480

Dentice M, Salvatore D (2011) Deiodinases: the balance of thyroid hormone: local impact of thyroid hormone inactivation. J Endocrinol 209:273–282

Ferrara AM, Onigata K, Ercan O et al (2012) Homozygous thyroid hormone receptor β-gene mutations in resistance to thyroid hormone: three new cases and review of the literature. J Clin Endocrinol Metab 97:1328–1336

Flamant F, Baxter JD, Forrest D et al (2006) International union of pharmacology. LIX. The pharmacology and classification of the nuclear receptor superfamily: thyroid hormone receptors. Pharmacol Rev 58:705–711

Glaschke A, Glosmann M, Peichl L (2010) Developmental changes of cone opsin expression but not retinal morphology in the hypothyroid Pax8 knockout mouse. Invest Ophthalmol Vis Sci 51:1719–1727

Glaschke A, Weiland J, Del Turco D et al (2011) Thyroid hormone controls cone opsin expression in the retina of adult rodents. J Neurosci 31:4844–4851

Hiroi Y, Kim HH, Ying H et al (2006) Rapid nongenomic actions of thyroid hormone. Proc Natl Acad Sci U S A 103:14104–14109

Iwagawa T, Tanaka Y, Iida A et al (2013) Enhancer/promoter activities of the long/middle wavelength-sensitive opsins of vertebrates mediated by thyroid hormone receptor β2 and COUP-TFII. PLoS One 8:e72065

Lee TC, Almeida D, Claros N et al (2006) Cell cycle-specific and cell type-specific expression of Rb in the developing human retina. Invest Ophthalmol Vis Sci 47:5590–5598

Liu H, Etter P, Hayes S et al (2008) NeuroD1 regulates expression of thyroid hormone receptor 2 and cone opsins in the developing mouse retina. J Neurosci 28:749–756

Lu A, Ng L, Ma M et al (2009) Retarded developmental expression and patterning of retinal cone opsins in hypothyroid mice. Endocrinology 150:1536–1544

Ma H, Thapa A, Morris L et al (2014) Suppressing thyroid hormone signaling preserves cone photoreceptors in mouse models of retinal degeneration. Proc Natl Acad Sci U S A 111: 3602–3607

Mihara S, Suzuki N, Wakisaka S et al (1999) Effects of thyroid hormones on apoptotic cell death of human lymphocytes. J Clin Endocrinol Metab 84:1378–1385

Newell FW, Diddie KR (1977) Typical monochromacy, congenital deafness, and resistance to intracellular action of thyroid hormone (author's transl). Klin Monbl Augenheilkd 171:731–734

Ng L, Hurley LB, Dierks B et al (2001) A thyroid hormone receptor that is required for the development of green cone photoreceptors. Nat Genet 27:94–98

Ng L, Ma M, Curran T et al (2009a) Developmental expression of thyroid hormone receptor β2 protein in cone photoreceptors in the mouse. Neuroreport 20:627–631

Ng L, Hernandez A, He W et al (2009b) A protective role for type 3 deiodinase, a thyroid hormone-inactivating enzyme, in cochlear development and auditory function. Endocrinology 150:1952–1960

Ng L, Lyubarsky A, Nikonov SS et al (2010) Type 3 deiodinase, a thyroid-hormone-inactivating enzyme, controls survival and maturation of cone photoreceptors. J Neurosci 30:3347–3357

Park JW, Zhao L, Cheng SY (2013) Inhibition of estrogen-dependent tumorigenesis by the thyroid hormone receptor β in xenograft models. Am J Cancer Res 3:302–311

Peeters RP, Hernandez A, Ng L et al (2013) Cerebellar abnormalities in mice lacking type 3 deiodinase and partial reversal of phenotype by deletion of thyroid hormone receptor α1. Endocrinology 154:550–561

Rivolta CM, Olcese MC, Belforte FS et al (2009) Genotyping of resistance to thyroid hormone in South American population. Identification of seven novel missense mutations in the human thyroid hormone receptor β gene. Mol Cell Probes 23:148–153

Roberts MR, Hendrickson A, McGuire CR et al (2005) Retinoid X receptor (γ) is necessary to establish the S-opsin gradient in cone photoreceptors of the developing mouse retina. Invest Ophthalmol Vis Sci 46:2897–2904

Sar P, Peter R, Rath B et al (2011) 3, 3’5 Triiodo L thyronine induces apoptosis in human breast cancer MCF-7 cells, repressing SMP30 expression through negative thyroid response elements. PLoS One 6:e20861

Shi YB, Fu L, Hsia SC et al (2001) Thyroid hormone regulation of apoptotic tissue remodeling during anuran metamorphosis. Cell Res 11:245–252

Weiss AH, Kelly JP, Bisset D et al (2012) Reduced L- and M- and increased S-cone functions in an infant with thyroid hormone resistance due to mutations in the THRβ2 gene. Ophthalmic Genet 33:187–195

Yamada-Okabe T, Satoh Y, Yamada-Okabe H (2003) Thyroid hormone induces the expression of 4–1BB and activation of caspases in a thyroid hormone receptor-dependent manner. Eur J Biochem 270:3064–3073

Zambrano A, García-Carpizo V, Gallardo ME et al (2014) The thyroid hormone receptor β induces DNA damage and premature senescence. J Cell Biol 204:129–146

Chapter 82
In-Depth Functional Diagnostics of Mouse Models by Single-Flash and Flicker Electroretinograms without Adapting Background Illumination

Naoyuki Tanimoto, Stylianos Michalakis, Bernhard H. F. Weber, Christian A. Wahl-Schott, Hans-Peter Hammes and Mathias W. Seeliger

Abstract Electroretinograms (ERGs) are commonly recorded at the cornea for an assessment of the functional status of the retina in mouse models. Full-field ERGs can be elicited by single-flash as well as flicker light stimulation although in most laboratories flicker ERGs are recorded much less frequently than single-flash ERGs. Whereas conventional single-flash ERGs contain information about layers, i.e., outer and inner retina, flicker ERGs permit functional assessment of the vertical pathways of the retina, i.e., rod system, cone ON-pathway, and cone OFF-pathway, when the responses are evoked at a relatively high luminance (0.5 log *cd* s/m^2) with varying frequency (from 0.5 to 30 Hz) without any adapting background illumination. Therefore, both types of ERGs complement an in-depth functional characterization of the mouse retina, allowing for a discrimination of an underlying functional pathology. Here, we introduce the systematic interpretation of the single-flash and flicker ERGs by demonstrating several different patterns

N. Tanimoto (✉) · M. W. Seeliger
Division of Ocular Neurodegeneration, Institute for Ophthalmic Research, Centre for Ophthalmology, Eberhard Karls University, Tübingen, Germany
e-mail: naoyuki.tanimoto@med.uni-tuebingen.de

M. W. Seeliger
e-mail: see@uni-tuebingen.de

S. Michalakis · C. A. Wahl-Schott
Center for Integrated Protein Science Munich, CIPSM and Department of Pharmacy–Center for Drug Research, Ludwig-Maximilians-Universität München, Munich, Germany
e-mail: michalakis@lmu.de

C. A. Wahl-Schott
e-mail: christian.wahl@cup.uni-muenchen.de

H. P. Hammes
5th Medical Clinic, Medical Faculty Mannheim, University of Heidelberg, Mannheim, Germany
e-mail: hp.hammes@umm.de

B. H. F. Weber
Institute of Human Genetics, University of Regensburg, Regensburg, Germany
e-mail: bweb@klinik.uni-regensburg.de

C. Bowes Rickman et al. (eds.), *Retinal Degenerative Diseases,* Advances in Experimental Medicine and Biology 854, DOI 10.1007/978-3-319-17121-0_82

of functional phenotype in genetic mouse models, in which photoreceptors and/or bipolar cells are primarily or secondarily affected.

Keywords Functional diagnostics · Electroretinogram · Single-flash · Flicker · Mouse model · Photoreceptor · Retinal bipolar cell · Congenital stationary night blindness · Retinal ischemia · X-linked juvenile retinoschisis

82.1 Introduction

Full-field electroretinogram (ERG) recordings at the cornea have been useful to characterize retinal functional properties of rodent models of human disease. Whereas single-flash ERGs are commonly analyzed in many laboratories, flicker ERGs are less frequently recorded, in part likely due to the variety of recording parameters and analytical methods. In our laboratory, we have used a practical flicker ERG protocol for functional phenotyping of mouse models, which is short (less than 4 min) and can be used directly after the conventional dark-adapted single-flash luminance series. The flicker ERG data partly confirm light-adapted ERG data and also contain certain types of information that cannot be assessable by single-flash ERGs only, enabling comprehensive *in vivo* functional diagnostics. In this chapter we will first give a brief description of the ERG protocols, followed by examples of differential diagnosis in genetic mouse models in terms of single-flash and flicker ERGs.

82.2 Electroretinography

Full-field ERG is a mass response of transient electrical activity of the entire retina to light stimulation, but importantly, the functionality of certain neuronal components, systems, and pathways can be assessed by varying stimulus luminances, frequencies, or additional background illumination.

82.2.1 Dark-Adapted Single-Flash ERG Luminance Series

In this series, no background illumination is used, and responses are recorded by using single white-flash stimuli in a wide luminance range (5.5 log units, in our laboratory). Under these conditions, only the rod system contributes to the waveform up to −2 log *cd* s/m^2 (scotopic), whereas both rod and cone photoreceptors are activated above −2 log *cd* s/m^2 (mesopic) (Tanimoto et al. 2013, 2015). The initial negative-going a-wave that appears at middle and high luminance is initiated by photoreceptors, whereas the following positive-going b-wave is mainly generated by ON-bipolar cells (for further details on the origin of ERG components, see Frishman and Wang 2011).

82.2.2 Flicker ERG Frequency Series

This series is started approximately 30 s after the end of the preceding single-flash protocol. Responses to trains of brief flashes for a fixed luminance (0.5 log *cd* s/m^2) with varying frequency (12 steps from 0.5 to 30 Hz) are obtained without any background illumination (0 *cd*/m^2) which are averaged over time (Tanimoto et al. 2013, 2015). This series is divided into three frequency ranges that are dominated by activity in the rod pathways (below 5 Hz, range A), cone ON-pathway (between 5 and 15 Hz, range B), and cone OFF-pathway (above 15 Hz, range C) (Tanimoto et al. 2015).

82.3 Mouse Models with Photoreceptor Dysfunction

Figure 82.1 shows representative single-flash and flicker ERGs in two photoreceptor dysfunction models. In *Gnat1* knockout (KO) mice, rods are dysfunctional due to a lack of the rod transducin α-subunit (Calvert et al. 2000), whereas cones are not affected in these mice due to the fact that cone transducin is formed by other isoforms. *cpfl1* mice are naturally occurring mutants that have two mutations in the cone specific phosphodiesterase gene, *Pde6c*; thus, only cones reveal a dysfunction (Chang et al. 2009). Due to the absence of rod signaling in *Gnat1* KO mice, no response is evoked in the scotopic luminance range up to −2.0 log *cd* s/m^2, and there is no substantial single-flash ERG a-wave (Fig. 82.1a). In contrast, these rod-driven ERG components are comparable between *cpfl1* and corresponding wild-type mice (Fig. 82.1c), as rods in *cpfl1* mice function normally. The cone photoreceptor function loss in *cpfl1* mice is demonstrated by flicker ERG, lacking any flicker responses at 5 Hz and above (Fig. 82.1d). In contrast, *Gnat1* KO mice generate normal flicker responses in ranges B and C (Fig. 82.1b), as the cone system is normal in *Gnat1* KO mice.

82.4 “No b-wave” Models

There are a number of mouse mutants that have a “no b-wave” ERG phenotype (with a preservation of the a-wave) (Pardue and Peachey 2014), which indicates a pre- or postsynaptic involvement of the photoreceptor to ON-bipolar synapse. A dysfunction of Cav1.4 L-type Ca^{2+} channels at photoreceptor synaptic terminals in *Cav1.4* KO mice (Specht et al. 2009) features presynaptic disruption of glutamate release from rod and cone photoreceptors affecting both ON- and OFF-bipolar cells, whereas in naturally occurring *nob* mutants (Pardue et al. 1998) only ON-bipolar cells are postsynaptically disturbed due to an impairment of the signaling cascade in ON-bipolar cells. In Fig. 82.2, ERGs in these pre- and postsynaptic “no b-wave” models are compared. The single-flash ERG a-wave is not reduced in the two models

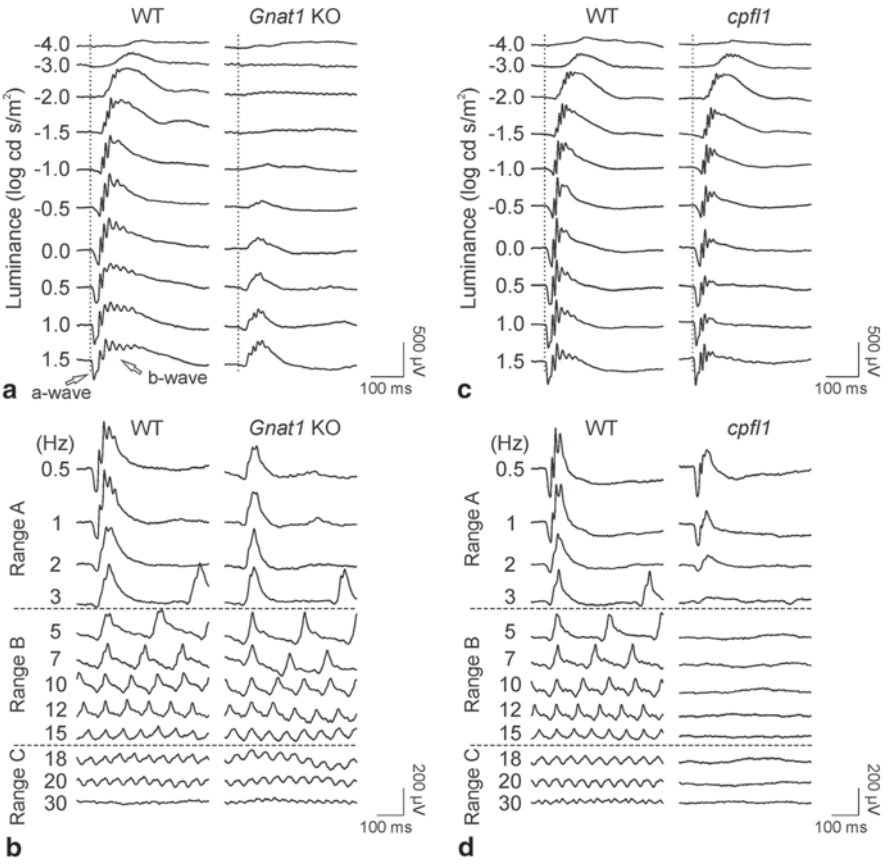

Fig. 82.1 Comparison of *Gnat1* knockout (KO) and *cpfl1* ERGs. **a, c** Representative dark-adapted single-flash ERG luminance series and **b, d** flicker ERG frequency series at 0.5 log *cd* s/m² in **a, b** *Gnat1* KO (*right*) and corresponding wild-type (WT, *left*) mice, and **c, d** *cpfl1* (*right*) and corresponding WT (*left*) mice. The a-wave and the b-wave are indicated by *open arrows* in **a**. See section 82.2.2 for details of the frequency ranges A, B, and C in **b, d**

(Fig. 82.2a, c), as the function of photoreceptor outer segments (phototransduction cascade and associated ion channels) is not affected. In contrast, the single-flash ERG b-wave is completely missing owing to a lack of light-evoked responses from ON-bipolar cells in both models. Therefore, the dark-adapted single-flash ERG cannot discriminate the two mouse models (Fig. 82.2a, c). In flicker ERG, both models display similar responses in range A, revealing the unchanged negative-going deflection and a lack of the positive-going signals. However, in range C where the responses are dominated by activity in the cone OFF-pathway, *nob* flicker ERGs are normal in size (Fig. 82.2b), reflecting the intact cone OFF-pathway in *nob* mice. In contrast, responses in range C are very strongly reduced in *Cav1.4* KO mice (Fig. 82.2d), as the cone OFF-pathway is also affected.

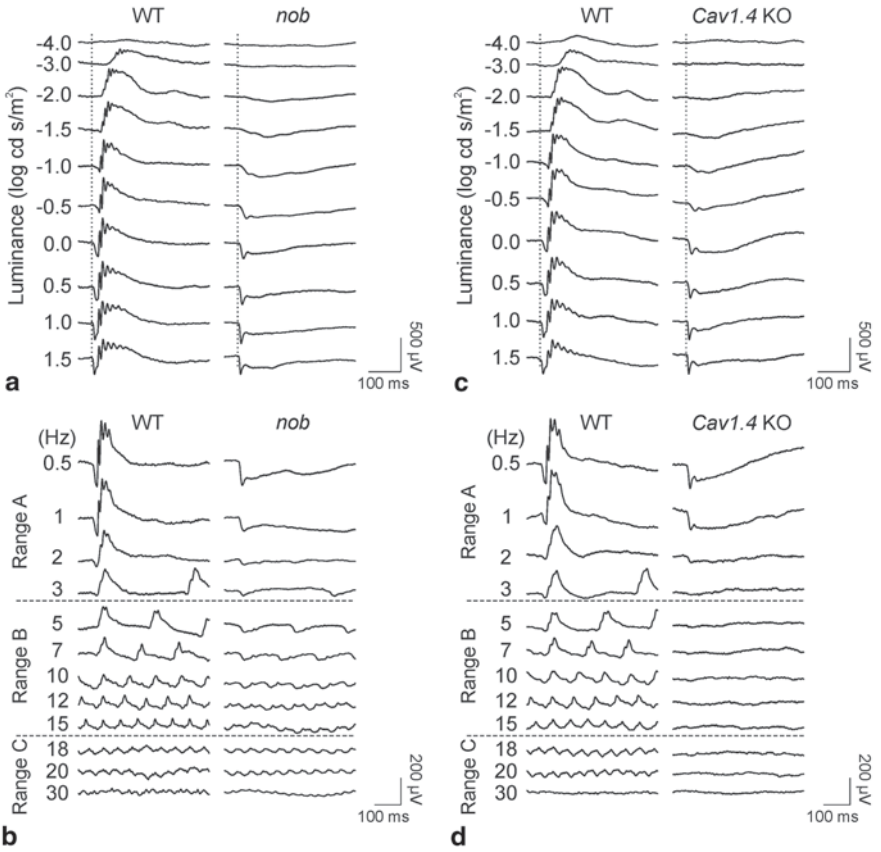

Fig. 82.2 Comparison of *nob* and *Cav1.4* knockout (KO) ERGs. **a, c** Representative dark-adapted single-flash ERG intensity series and **b, d** flicker ERG frequency series at 0.5 log *cd* s/m^2 in **a, b** *nob* (*right*) and corresponding wild-type (WT, *left*) mice, and **c, d** *Cav1.4* KO (*right*) and corresponding WT (*left*) mice.

82.5 Other "b-Wave Mutants"

The strong attenuation of the b-wave is caused not only by synaptic disturbances but also by inner retinal ischemia, e.g., in Angiopoietin-2 (*Ang2*) KO mice in which a proper formation of retinal vascular network is disturbed (Fig. 82.3a) (Feng et al. 2009). The b-wave reduction is also characteristic for the mouse model of X-linked juvenile retinoschisis (*Rs1h* KO) (Weber et al. 2002). Retinoschisin plays a critical role in the maintenance of the retinal architecture; thus, *Rs1h* KO mice demonstrate a highly disorganized retina including displacement of bipolar cells and abnormalities at the photoreceptor-bipolar synapse, leading to a reduction in the b-wave (Fig. 82.3c) (Molday et al. 2012; Weber et al. 2002). In both *Ang2* KO and *Rs1h* KO mice, all types of bipolar cells are affected, i.e., in the absence of any vertical pathway-/system-specificity the inner retina is affected. Therefore, flicker responses are

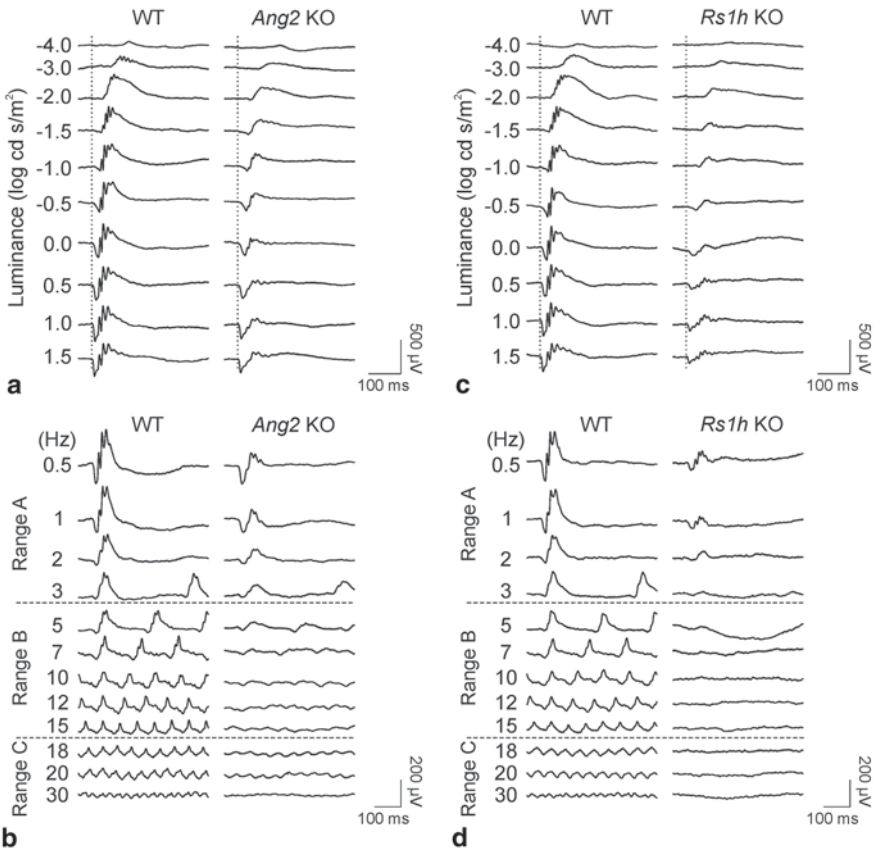

Fig. 82.3 Comparison of *Ang2* knockout (KO) and *Rs1h* KO ERGs. **a, c** Representative dark-adapted single-flash ERG luminance series and **b, d** flicker ERG frequency series at 0.5 log *cd* s/m^2 in **a, b** *Ang2* KO (*right*) and corresponding wild-type (WT, *left*) mice, and **c, d** *Rs1h* KO (*right*) and corresponding WT (*left*) mice

reduced in all ranges A, B, and C (Fig. 82.3b, d). These models can be discriminated in the single-flash ERG a-wave: The a-wave is reduced in *Rs1h* KO mice owing to the progressive outer retinal alterations with age (Fig. 82.3c) (Janssen et al. 2008). In contrast, the a-wave is unchanged in *Ang2* KO mice likely due to photoreceptors being supplied normally by the choroid (Fig. 82.3a).

82.6 Summary

In this chapter, our diagnostic strategies on the basis of the conventional dark-adapted single-flash and a novel flicker ERG protocol were presented in different genetic mouse models. All of these mouse mutants showed qualitatively different patterns of alteration in the ERGs, i.e., the flicker responses in the ranges A–C together with

the single-flash a- and b-waves, allowing for a discrimination of the underlying functional pathology. Therefore, differential diagnosis of retinal disorders in these animal models could greatly benefit by both the single-flash and the flicker ERGs.

Acknowledgment We thank Anne Kurtenbach for critical reading of the manuscript.

References

Calvert PD, Krasnoperova NV, Lyubarsky AL et al (2000) Phototransduction in transgenic mice after targeted deletion of the rod transducin alpha-subunit. Proc Natl Acad Sci U S A 97:13913–13918

Chang B, Grau T, Dangel S et al (2009) A homologous genetic basis of the murine cpfl1 mutant and human achromatopsia linked to mutations in the PDE6C gene. Proc Natl Acad Sci U S A 106:19581–19586

Feng Y, vom Hagen F, Wang Y et al (2009) The absence of angiopoietin-2 leads to abnormal vascular maturation and persistent proliferative retinopathy. Thromb Haemost 102:120–130

Frishman LJ, Wang MH (2011) Electroretinogram of human, monkey and mouse. In: Levin LA, Nilsson SFE, Ver HJ, Wu SM, Kaufman PL, Alm A (eds) Adler's physiology of the eye, 11th edn. Saunders Elsevier, New York, pp 480–501

Janssen A, Min SH, Molday LL et al (2008) Effect of late-stage therapy on disease progression in AAV-mediated rescue of photoreceptor cells in the retinoschisin-deficient mouse. Mol Ther 16:1010–1017

Molday RS, Kellner U, Weber BH (2012) X-linked juvenile retinoschisis: clinical diagnosis, genetic analysis, and molecular mechanisms. Prog Retin Eye Res 31:195–212

Pardue MT, Peachey NS (2014) Mouse b-wave mutants. Doc Ophthalmol 128:77–89

Pardue MT, McCall MA, LaVail MM et al (1998) A naturally occurring mouse model of X-linked congenital stationary night blindness. Invest Ophthalmol Vis Sci 39:2443–2449

Specht D, Wu SB, Turner P et al (2009) Effects of presynaptic mutations on a postsynaptic Cacna1s calcium channel colocalized with mGluR6 at mouse photoreceptor ribbon synapses. Invest Ophthalmol Vis Sci 50:505–515

Tanimoto N, Sothilingam V, Kondo M et al (2015) Electroretinographic assessment of rod- and cone-mediated bipolar cell pathways using flicker stimuli in mice. Sci Rep 5:10731

Tanimoto N, Sothilingam V, Seeliger MW (2013) Functional phenotyping of mouse models with ERG. Methods Mol Biol 935:69–78

Weber BH, Schrewe H, Molday LL et al (2002) Inactivation of the murine X-linked juvenile retinoschisis gene, Rs1h, suggests a role of retinoschisin in retinal cell layer organization and synaptic structure. Proc Natl Acad Sci U S A 99:6222–6227

Chapter 83
The Role of Intraflagellar Transport in the Photoreceptor Sensory Cilium

Daniel G. Taub and Qin Liu

Abstract The photoreceptor is a complex specialized cell in which a major component responsible for visual transduction is the photoreceptor sensory cilium (PSC). Building and maintenance of the PSC requires the transport of large proteins along microtubules that extend from the inner segments to the outer segments. A key process, termed intraflagellar transport (IFT), has been recognized as an essential phenomenon for photoreceptor development and maintenance, and exciting new studies have highlighted its importance in retinal and cilia related diseases. This review focuses on the important roles of IFT players, including motor proteins, IFT proteins, and photoreceptor-specific cargos in photoreceptor sensory cilium. In addition, specific IFT components that are involved in inherited human diseases are discussed.

Keywords Inherited retinal degeneration · Intraflagellar transport (IFT) · Cilia · Photoreceptor · Protein transport

83.1 Introduction

Intraflagellar Transport (IFT) is the process by which large polypeptides are transported along microtubules facilitated by motor proteins and IFT proteins in ciliated cells. In the past decade, a large number of studies have demonstrated that IFT is essential for ciliogenesis, signaling, and ciliary maintenance (Cole et al. 1998; Davis and Katsanis 2012). Consistent with the importance of IFT in cilia biology, mutations in genes that encode IFT related proteins are increasingly recognized as the underlying cause of a number of inherited cilia disorders that affect multiple

Q. Liu (✉) · D. G. Taub
Ocular Genomics Institute, and Berman-Gund Laboratory for the Study of Retinal Degenerations, Department of Ophthalmology, Massachusetts Eye and Ear Infirmary, Harvard Medical School, 243 Charles St., 5th Floor, 563C, Boston, MA 02114, USA
e-mail: qin_liu@meei.harvard.edu

D. G. Taub
e-mail: dtaub1230@gmail.com

C. Bowes Rickman et al. (eds.), *Retinal Degenerative Diseases,* Advances in Experimental Medicine and Biology 854, DOI 10.1007/978-3-319-17121-0_83

organ systems (Davis and Katsanis 2012). The photoreceptor sensory cilium (PSC) elaborated by rod and cone photoreceptors in the retina is among the largest of mammalian cilia (Besharse 1985). As in other primary cilia, IFT is essential for the development, function and maintenance of the photoreceptor sensory cilium, an organelle responsible for the transduction of light into neural signals. In this chapter, we briefly summarize the common features and the important roles of IFT players, including motor proteins, IFT complex proteins, and IFT cargos in primary cilia, with particular emphasis on photoreceptor sensory cilium. In addition, specific IFT components that are involved in inherited retinal diseases are discussed.

83.2 A Brief History of IFT

IFT was originally described by Keith Kozminski in the lab of Joel Rosenbaum at Yale University in 1993 (Kozminski et al. 1993). Using a paralyzed flagellar mutant of *Chlamydomonas*, they observed particles continuously moving along the cilium in both an anterograde and retrograde fashion (Kozminski et al. 1993). Later research identified that these IFT particles themselves are composed of more than 20 individual proteins organized into two subcomplexes, termed A- and B-complexes (Cole et al. 1998). The movement of IFT particles in the anterograde direction to the cilia tip is attributed to the molecular motor kinesin-2, while dynein-2 was attributed as the motor powering the retrograde IFT transport (Pazour et al. 1998). The studies took the primary cilium, a previously ignored organelle, into the spotlight as it became clear that primary cilium is an integral structure of the cell that coordinates the development and function of many tissues and organs throughout the body.

83.3 Mutations in IFT Components Cause Ciliopathies in Human

Since the discovery of IFT more than 20 years ago, considerable effort has gone into the discovery of the association between the IFT process and human diseases. Mutations that alter a component of IFT complex A or B, or mutations in the protein components of either one of the motor complexes, result in defective formation, elongation, or function of cilia in all organisms investigated (Cole et al. 1998; Pazour et al. 2002). Thus, IFT is absolutely required for ciliogenesis and maintenance. In the past few years, all six IFT-A components and their motor protein, DYNC2H1, have been linked to human ciliopathies, including Jeune asphyxiating thoracic dystrophy (JATD), Nephronophthisis (NPHP), Meckel Syndrome (MS), Joubert Syndrome, Bardet-Biedl Syndrome (BBS), Senior Loken Syndrome, Sensenbrenner syndrome, and Mainzer-Saldino syndrome (MSS) (Arts et al. 2011; Walczak-Sztulpa et al. 2010; Gilissen et al. 2010; Bredrup et al. 2011; Davis et al. 2011; Perrault et al. 2012; Dagoneau et al. 2009). However, despite the strong evidence showing

that disruption of IFT complex B proteins results in various of ciliary phenotypes in animal models, the majority of the 14 IFT complex B proteins have unknown roles in human disease, except IFT80 (Beales et al. 2007), IFT172 (Halbritter et al. 2013) and IFT27 (Aldahmesh et al. 2014). Cilia-related syndromic disorders can manifest as a large phenotypic and severity spectrum that include primarily retinal degeneration, renal disease, cerebral anomalies, skeletal dysplasias, congenital fibrocystic diseases of the liver and pancreas, diabetes and obesity. For example, the same missense mutation p. Leu710Ser in *WDR19/IFT144* can cause a phenotypic severity spectrum ranging from very severe manifestations such as those in Sensenbrenner syndrome and JATD to less severe isolated cases of NPHP, autosome recessive retinitis pigmentosa (arRP) and polycystic kidney with arRP (Coussa et al. 2013). In addition to *IFT144*, we have recently shown that mutations in *IFT172* can cause non-syndromic inherited retinal degeneration in humans as well (Bujakowska et al. 2014). These findings strongly suggest the presence of modifying genes and/or mutations, genetic or micro environment variations (Davis et al. 2011; Badano et al. 2006).

83.4 The Photoreceptor Outer Segment as a Specialized Sensory Cilium

The outer segment (OS) of rod and cone photoreceptor cells in the vertebrate retina is highly modified sensory cilium that is responsible for the first step of phototransduction cascade. Like all other cilia, the photoreceptor sensory cilium (PSC) is comprised of a membrane domain and its cytoskeleton backbone. During development, the microtubule based structural backbone of PSC arises from the basal body in the inner segments with the plasma membrane forming the cilia membrane. At the same time, ciliary transport mechanisms move large amount of lipids and membrane proteins synthesized in the inner segment into the cilium, initially in a form of disorganized vesicular and tubular structures, which later assembled into highly specialized discs stacking along the axoneme (Besharse et al. 1985). This transport process continues throughout the lifetime of the PSC as ~10% of the OS are shed from the distal tip each day and new discs are formed at the base of the OS (Young 1967). The molecular mechanisms underlying the transport of membrane proteins from the cell body to the PSC is largely unknown but current evidence strongly supports IFT systems as an important player (Insinna and Besharse 2008; Bhowmick et al. 2009).

83.5 IFT Particles and PSC Transport

In photoreceptor sensory cilia, IFT occurs along with the axonemal backbone between the inner segment and the outer segment. Of the 20 IFT particles originally identified in *Chlamydomonas*, all but one have been found to have mammalian

homologues within the PSC proteome (Liu et al. 2007). A few IFT proteins, including IFT88, IFT57, and IFT52, have previously been localized in the transition zone of photoreceptor cells (Baker et al. 2003). We have recently studied the localization of another six additional IFT proteins in PSC, including IFT20, IFT46, IFT54, IFT27, IFT22, IFT144, and one putative IFT protein, CLUAP1/DYF3. We observed that the IFT46 and IFT54 were localized at the transition zone and base of the axoneme, similar to the location of TTC21B/IFT139 (Davis et al. 2011). The remaining five IFT proteins were localized to multiple compartments, but predominantly to the inner segment and axoneme/transition zone region. In addition to IFT complex proteins, there are a number of IFT-associated proteins including motor proteins, BBSome proteins, and putative IFT proteins that are also present in the PSC proteome (Liu et al. 2007). All three subunits of the kinesin-2 motor co-immunoprecipitate with IFT proteins in retinal extract (Baker et al. 2003). Both heavy chain and light intermediate chain of the dynein 2 are also present in bovine photoreceptor cilia (Mikami et al. 2002). This demonstrates the large number of components involved in IFT as well as the comparability of model organisms in studying ciliogenesis and cilia maintenance.

The IFT system is required for the assembly of most types of eukaryotic cilia including the outer segments of rod and cone photoreceptors (Marszalek et al. 2000; Pazour et al. 2002). This has been further demonstrated in IFT deficient animal models. A well-characterized example of this is mutations in *Tg737*, the mouse homolog to IFT88, a Complex-B particle. Mutations in *Tg737* gene result in abnormal OS morphology, disorganized disc formation, and photoreceptor death between postnatal day 45 and 77 (Pazour et al. 2002). Furthermore, while rhodopsin is found in the OS of mutants, it is also mislocalized within the inner segments. This indicates that reduced transport is occurring either by a compromise of the structural integrity of the PSC or reduced active transport (Pazour et al. 2002). In contrast to the example of IFT complex-B dysfunction, alterations in IFT complex-A present a different etiology and phenotype. The *alien* mouse, a knockout of the *Ttc21b/Ift139* gene, presents embryonic lethality at E18.5 (Herron et al. 2002). We have recently generated a rod-specific conditional *Ttc21b/Ift139* knockout mouse line. Homozygous Ttc21b mice demonstrated an early-onset retinal degeneration with disrupted stability of OS and mislocalization of rhodopsin. We are currently using Ttc21b/Ift139 conditional knockout mice as a model to better understand the retrograde IFT transport in the PSC and other cilia.

83.6 Cargo of IFTs in the PSC

The development and maintenance of photoreceptor sensory cilium requires the transport of both cilium-specific and photoreceptor-specific proteins from inner segment to outer segment. Although it has been confirmed that the IFT system provides a mechanism for the transport of cilium-specific proteins in PSC and other cilia, the

molecular mechanisms on how IFT proteins bind to putative photoreceptor-specific cargo remains to be determined. Given the limited number of IFT particles known, it is likely that a number of options exist including conserved transport domains among cargo proteins, a large and heterogeneous number of binding sites present on the IFT particle, a certain order of IFT assembly to bind select cargo, or other external cofactors that aid in binding. One of the first studies examining the role of IFT in the photoreceptor utilized a conditional knockout mouse model of the anterograde motor kinesin-2 subunit, *Kif3A* (Marszalek et al. 2000). Loss of KIF3A, and therefore antereograde IFT, resulted in accrual of opsin and arrestin within the inner segments while α-transducin expression was unaffected. This suggests that structural defects in transport pathways were not causal for opsin and arrestin mislocalization (Marszalek et al. 2000). Given the influence of antereograde transport on arrestin trafficking, it was expected that retrograde transport might help facilitate the removal of arrestin from the OS. Surprisingly, disruption of the dynein-2 motor does not alter arrestin translocation and this process is most likely accomplished by passive diffusion (Krock et al. 2009). In 2009, Bhowmick et al. identified anterograde IFT-cargo complexes containing IFT proteins, kinesin 2 family proteins, two photoreceptor specific membrane proteins, guanylyl cyclase 1 and rhodopsin, and the chaperones MRJ and HSC70 by using a yeast two hybrid and a pull-down assay (Bhowmick et al. 2009). The role of retrograde IFT and which cargo it is transporting has been a complicated question to answer. Based on studies in other tissues and organisms, it is reasonable to predict that retrograde IFT could play a role in support of PSC dynamics at the distal tip by returning the anterograde IFT components and the soluble phototransduction proteins to the inner segment (Signor et al. 1999; Calvert et al. 2006).

83.7 Perspectives

The PSC is a tantalizing model to undertake the study of the IFT system. Genetic manipulations of the photoreceptors can be easily achieved and the effects of these manipulations can be readily measured via functional and histologic testing. The photoreceptor-specific features and the level of accessibility make the PSC an important system that can provide new insights into the function of IFT in trafficking of cell-specific cargo. While many questions have been answered, many are still puzzling. These include how the IFT particles are assembled at the base of cilia, how the specific cargos are recognized by, bound to, and released from the IFT particles, and how the IFT rafts are moved bi-directionally. Since function of each IFT protein must be essential and there is little to no overlap functionally, as knockout of anyone of the IFT particle can destroy the cilia formation or function, the study of these particles will have to take place both independently and within their native complexes. More research on the structure of these IFT particles will be crucial to ascertaining their functional role in PSC and retinal disease.

References

Aldahmesh MA, Li Y, Alhashem A et al (2014) IFT27, encoding a small GTPase component of IFT particles, is mutated in a consanguineous family with Bardet-Biedl syndrome. Hum Mol Genet 23:3307–3315

Arts HH, Bongers EM, Mans DA et al (2011) C14ORF179 encoding IFT43 is mutated in Sensenbrenner syndrome. J Med Genet 48:390–395

Badano JL, Leitch CC, Ansley SJ et al (2006) Dissection of epistasis in oligogenic Bardet-Biedl syndrome. Nature 439:326–330

Baker SA, Freeman K, Luby-Phelps K et al (2003) IFT20 links kinesin II with a mammalian intraflagellar transport complex that is conserved in motile flagella and sensory cilia. J Biol Chem 278:34211–34218

Beales PL, Bland E, Tobin JL et al (2007) IFT80, which encodes a conserved intraflagellar transport protein, is mutated in Jeune asphyxiating thoracic dystrophy. Nat Genet 39:727–729

Besharse JC, Forestner DM, Defoe DM (1985) Membrane assembly in retinal photoreceptors. III. Distinct membrane domains of the connecting cilium of developing rods. J Neurosci 5: 1035–1048

Bhowmick R, Li M, Sun J et al (2009) Photoreceptor IFT complexes containing chaperones, guanylyl cyclase 1 and rhodopsin. Traffic 10:648–663

Bredrup C, Saunier S, Oud MM et al (2011) Ciliopathies with skeletal anomalies and renal insufficiency due to mutations in the IFT-A gene WDR19. Am J Hum Genet 89:634–643

Bujakowska KM, Zhang Q, Liu Q et al (2014) Mutations in IFT172 cause isolated and syndromic retinal degeneration. Invest Ophthalmol Vis Sci 55: E-Abstract 1278

Calvert PD, Strissel KJ, Schiesser WE et al (2006) Lightdriven translocation of signaling proteins in vertebrate photoreceptors. Trends Cell Biol 16:560–568

Cole DG, Diener DR, Himelblau AL et al (1998) Chlamydomonas kinesin-II-dependent intraflagellar transport (IFT): IFT particles contain proteins required for ciliary assembly in Caenorhabditis elegans sensory neurons. J Cell Biol 141:993–1008

Coussa RG, Otto EA, Gee HY et al (2013) WDR19: an ancient, retrograde, intraflagellar ciliary protein is mutated in autosomal recessive retinitis pigmentosa and in Senior-Loken syndrome. Clin Genet 84:150–159

Dagoneau N, Goulet M, Geneviève D et al (2009) DYNC2H1 mutations cause asphyxiating thoracic dystrophy and short rib-polydactyly syndrome, type III. Am J Hum Genet 84:706–711

Davis EE, Katsanis N (2012) The ciliopathies: a transitional model into systems biology of human genetic disease. Curr Opin Genet Dev 22:290–303

Davis EE, Zhang Q, Liu Q et al (2011) TTC21B contributes both causal and modifying alleles across the ciliopathy spectrum. Nat Genet 43:189–196

Gilissen C, Arts HH, Hoischen A et al (2010) Exome sequencing identifies WDR35 variants involved in Sensenbrenner syndrome. Am J Hum Genet 87:418–423

Halbritter J, Bizet AA, Schmidts M et al (2013) Defects in the IFT-B component IFT172 cause Jeune and Mainzer-Saldino syndromes in humans. Am J Hum Genet 93:915–925

Herron BJ, Lu W, Rao C, Liu S et al (2002) Efficient generation and mapping of recessive developmental mutations using ENU mutagenesis. Nat Genet 30:185–189

Insinna C, Besharse JC (2008) Intraflagellar transport and the sensory outer segment of vertebrate photoreceptors. Dev Dyn 237:1982–1992

Kozminski KG, Johnson KA, Forscher P et al (1993) A motility in the eukaryotic flagellum unrelated to flagellar beating. Proc Natl Acad Sci U S A 90:5519–5523

Krock BL, Mills-Henry I, Perkins BD (2009) Retrograde intraflagellar transport by cytoplasmic dynein-2 is required for outer segment extension in vertebrate photoreceptors but not arrestin translocation. Invest Ophthalmol Vis Sci 50:5463–5471

Liu Q, Tan G, Levenkova N et al (2007) The proteome of the mouse photoreceptor sensory cilium complex. Mol Cell Proteomics 6:1299–1317

Marszalek JR, Liu X, Roberts EA et al (2000) Genetic evidence for selective transport of opsin and arrestin by kinesin-II in mammalian photoreceptors. Cell 102:175–187

Mikami A, Tynan SH, Hama T et al (2002) Molecular structure of cytoplasmic dynein 2 and its distribution in neuronal and ciliated cells. J Cell Sci 115(Pt 24):4801–4808

Pazour GJ, Wilkerson CG, Witman GB (1998) A dynein light chain is essential for the retrograde particle movement of intraflagellar transport (IFT). J Cell Biol 141:979–992

Pazour GJ, Baker SA, Deane JA et al (2002) The intraflagellar transport protein, IFT88, is essential for vertebrate photoreceptor assembly and maintenance. J Cell Biol 157:103–113

Perrault I, Saunier S, Hanein S et al (2012) Mainzer-Saldino syndrome is a ciliopathy caused by IFT140 mutations. Am J Hum Genet 90:864–870

Signor D, Wedaman KP, Orozco JT et al (1999) Role of a class DHC1b dynein in retrograde transport of IFT motors and IFT raft particles along cilia, but not dendrites, in chemosensory neurons of living Caenorhabditis elegans. J Cell Biol 147:519–530

Walczak-Sztulpa J, Eggenschwiler J, Osborn D et al (2010) Cranioectodermal Dysplasia, Sensenbrenner syndrome, is a ciliopathy caused by mutations in the IFT122 gene. Am J Hum Genet 86:949–956

Young RW (1967) The renewal of photoreceptor cell outer segments. J Cell Biol 33:61–72

Chapter 84
Regulation of Retinal Development via the Epigenetic Modification of Histone H3

Sumiko Watanabe and Akira Murakami

Abstract We are interested in the roles of epigenetic mechanisms in retinal development. By ChIP-qPCR using whole retinal extracts at various developmental stages, we found that the levels of methylation of histones H3K27 and H3K4 and acetylation of histone H3 at specific loci in various genes, which play critical roles in retinal proliferation and differentiation, changed dramatically during retinal development. We next focused on the roles of H3K27 trimethylation in retinal development. Ezh1 and Ezh2 are methyltransferases that act on H3K27, while Jmjd3 and Utx are demethylases. We found that Ezh2 and Jmjd3 were mainly expressed during retinal development, and a loss-of-function of these genes revealed a role for H3K27me3 in the maturation of subsets of bipolar cells. Furthermore, Ezh2 and Jmjd3 regulate H3K27 trimethylation at specific loci within Bhlhb4 and Vsx1, which play critical roles in the differentiation of subsets of bipolar cells. Utx is expressed weakly in retina, and the down-regulation of Utx by sh-RNA in retinal explants suggested that Utx also participates in the maturation of bipolar cells. Ezh1 is expressed weakly in postnatal retina, and the phenotype of Ezh2-knockout retina suggested that Ezh1 plays a role in the methylation of H3K27 in the late phase of retinal differentiation. Taken together, we found that these four genes, which exhibit temporally and spatially unique expression patterns during retinal development, play critical roles in the differentiation of retinal subsets through the regulation of histone H3K27 methylation at critical genetic loci.

Keywords Retinal development · Epigenetics modification · Histone H3 methylation · Histone H3 acetylation · ChIP-qPCR · Bipolar cells · Rod photoreceptors

S. Watanabe (✉)
Division of Molecular and Developmental Biology, Institute of Medical Science, University of Tokyo, 4-6-1 Shirokanedai, Minato-ku, Tokyo 108-8639, Japan
e-mail: sumiko@ims.u-tokyo.ac.jp

A. Murakami
Department of Ophthalmology, Graduate School of Medicine, Juntendo University, Tokyo, Japan

C. Bowes Rickman et al. (eds.), *Retinal Degenerative Diseases,* Advances in Experimental Medicine and Biology 854, DOI 10.1007/978-3-319-17121-0_84

84.1 Introduction

The methylation and acetylation of basic amino acid residues in histone proteins are crucial epigenetic modifications that positively and negatively regulate gene expression. Particular patterns of methylation and acetylation regulate the accessibility of target loci by transcription factors and RNA polymerase II, and the remodeling of heterochromatin to euchromatin (Greer and Shi 2012). The importance of histone methylation to retinal development has been highlighted in several papers (Kizilyaprak et al. 2010; Rao et al. 2010). The role of epigenetic modifications in diabetic retinopathy is emerging (Wegner et al. 2014); together, these findings indicate the potential utility of epigenetic modifications as therapeutic targets. We are interested in the epigenetic regulation of retinal development through histone modification at critical genetic loci. For that purpose, we examined changes in histone modification and employed a loss-of-function analysis to reveal the roles of histone H3 methylases and demethylases during retinal development. This article summarizes the main findings presented in Poster 149 at the RD2014 meeting and published in 2014 (Iida et al. 2014). Additional data related to this issue are presented and discussed.

84.2 Materials and Methods

84.2.1 Experiment with Animals

ICR mice were obtained from Japan SLC Co. All animal experiments were approved by the Animal Care Committee of the Institute of Medical Science, University of Tokyo and conducted in accordance with the ARVO (Association for Research in Vision and Ophthalmology) statement for the use of animals in ophthalmic and vision research. Mice used in our work are free of retinal degeneration mutations.

84.2.2 Chromatin Immunoprecipitation (ChIP) Assay, RT-qPCR and Immunostaining

ChIP assay was done as described previously (Iida et al. 2014). Control IgG experiments gave only negligible values. Quantitative PCR (qPCR) was done by the SYBR Green-based method using the Roche Light Cycler 1.5 apparatus. Antibodies used are anti-acetyl Histone H3 (acetylH3, Millipore 06-599177), -Histone H3 tri-methyl Lys27 (H3K27me3, Abcam6002205), and -Histone H3 tri-methyl Lys27 (H3K4me3, active motif 39159178) antibodies. Immunostaining of frozen sections was done as described previously (Iida et al. 2014).

84.3 Results

84.3.1 Examination of the Epigenetic Modification of Histone H3 at Retinal Development-Related Genetic Loci during Retinal Development

We first examined the changing levels of three major epigenetic modifications of histone H3 at retina-related genetic loci during retinal development. ChIP-qPCR analysis using whole retinal extracts at several different developmental stages was done for histone H3K4 trimethylation (H3K4me3), acetylation of histone H3 (acetyl H3), and histone H3K27 trimethylation (H3K27me3). H3K4me3 modification is known to positively affect transcription (Greer and Shi 2012). A number of genes that are strongly expressed in early retinal progenitors, including Math5, Ngn2, Foxn4, and Sox11, showed relatively high levels of H3K4me3 at these loci, but the level was low in adult retina (Fig. 84.1a). Rod cells are present in postnatal retina, and the transcription of rod-related genes such as Nrl, PNR, and Rhodopsin (Rho) are induced mainly during the postnatal stage of development. H3K4me3 modification at these genetic loci was strongly induced after birth. The pattern of H3K4me3 modification at other loci, which play pivotal roles in the differentiation of retinal subsets, showed a variety of patterns. The acetylation of histone H3, which occurs at several lysine residues, is generally understood to correlate with transcriptional activation via the modulation of chromatin structure (Wegner et al. 2014). Changes in the level of acetyl H3 at retina-related genetic loci are similar to those observed for H3K4me3 by ChIP analysis—especially at progenitor-enriched and rod-related genetic loci (Fig. 84.1b). H3K27me3 is generally recognized as a suppressive modification for transcription (Greer and Shi 2012), and the H3K27me3 level of genes expressed in retinal progenitor cells was mostly constantly increased, but in rod cells the level was very low and did not change during retinal development (Fig. 84.1c). In contrast, the H3K27me3 level at differentiation-related loci was relatively high, and that at Cdkn2a3 was consistently high (Fig. 84.1c).

84.3.2 Roles of H3K27me3 in Retinal Development

We next focused on H3K27me3 and analyzed the expression pattern of enzymes related to H3K27me3 during retinal development. There are two major methyltransferases, Ezh1 and Ezh2; two major demethylases, Jmjd3 (Kdm6b) and Utx (Kdm6a); and a Y chromosome-specific demethylase, Uty (Kdm6c). We analyzed expression levels of these genes at E14, P7, and P14 whole retina by RNA-seq data (Iida et al. 2014b) and found that *Ezh1* and *Jmjd3* were expressed much stronger than *Ezh2* and *Utx*, respectively in embryonic retina (Fig. 84.2a). We analyzed more detailed temporal changes in the expression of these genes during retinal development by RT-qPCR (Fig. 84.2). *Ezh2* was strongly expressed in embryonic retina,

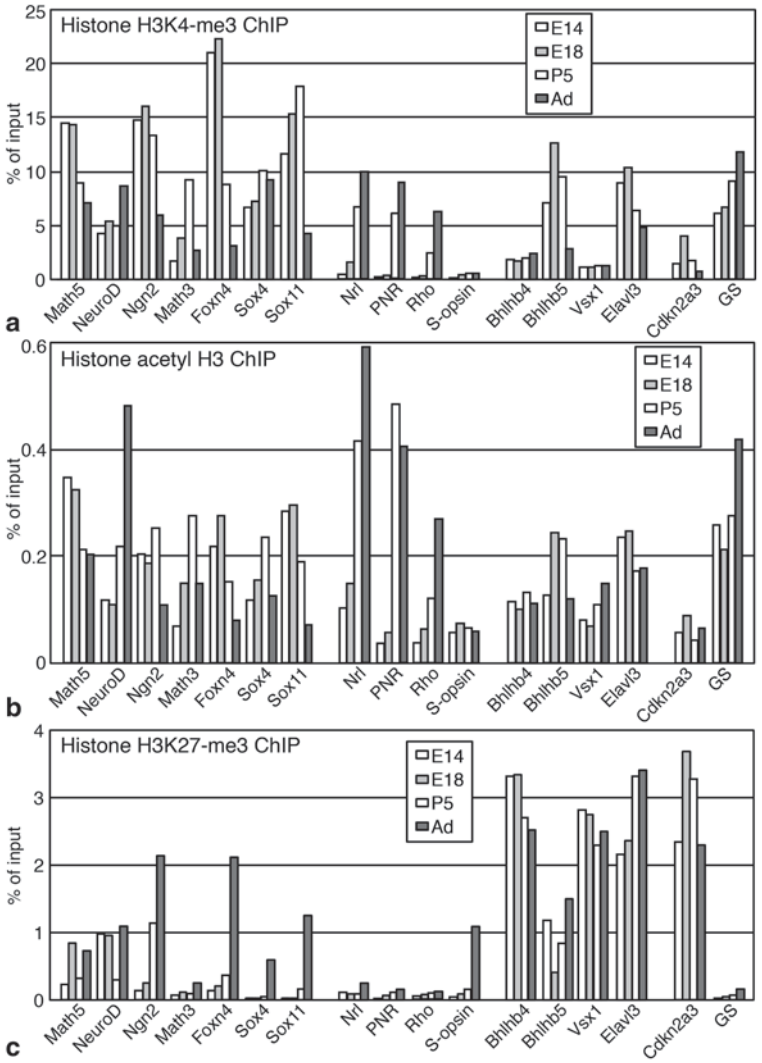

Fig. 84.1 Histone modifications in loci of genes related to retinal development. ChIP-qPCR of antibodies anti-Histone H3K4me3 (**a**), -acetyl-Histone H3 (**b**), and -Histone H3K27me3 (**c**) was done using whole retinal extract prepared from mice at E14, E18, P5, and adult. Values are indicated as % of input

but its expression deceased during the postnatal period. *Ezh1* expression was very low during the embryonic period, and significant expression was observed after birth (Fig. 84.2a). Jmjd3 showed low-level expression in embryonic retina, but it increased after birth and peaked at around P5. Utx showed relatively weak expression with a slightly higher level during the postnatal stage (Fig. 84.2b). We next examined the roles of H3K27me3 in retinal development.

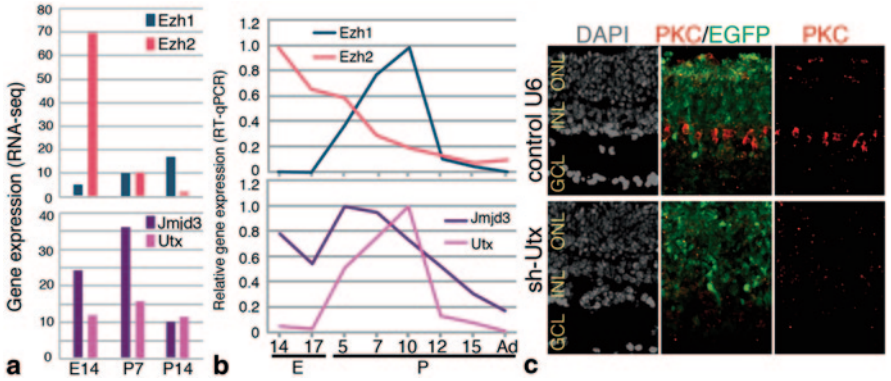

Fig. 84.2 Roles of H3K27me3 in retinal development. **a**, **b** Transition of expression of Ezh1, Ezh2, Jmjd3, and Utx during retinal development was examined by RNA-sequence (**a**), and RT-qPCR (**b**). In **b**, Gapdh was used as an internal control, and the time point with maximum values in each gene are expressed as 1, and others are expressed as relative values to the maximum value. **c** sh-Utx or control vector was electroporated into retinal explant prepared from E17 mouse, and cultured for 2 weeks. Differentiation was examined by immunostaining of frozen sections

We created an sh-RNA-mediated loss-of-function of Jmjd3 using retinal explants (Iida et al. 2014). The down-regulation of Jmjd3 in developing retina resulted in a failure of progenitor cells to differentiate to protein kinase C (PKC)-positive bipolar cell subsets (rod-ON-BP), and it reduced the expression of *Bhlhb4*, which is critical for the differentiation of rod-ON-BP cells (Iida et al. 2014). Furthermore, the H3K-27me3 level at the *Bhlhb4* locus was specifically lower in a bipolar cell-enriched fraction. Since Jmjd3 was expressed in the inner nuclear layer during late retinal development (Iida et al. 2014), we propose that the lineage-specific H3K27me3 demethylation of critical loci by spatio-temporal-specific Jmjd3 expression allows the appropriate maturation of certain subsets of retinal cells (Fig. 84.2c). We next assessed the roles of Utx using the same strategy as for Jmjd3. sh-Utx was introduced into retinal explants at E17, and retinal differentiation was examined after 2 weeks of culture by immunostaining of frozen sections. We detected a loss of PKC positive rod-ON-BP cells (Fig. 84.2c), but not other retinal cell subtypes, similar to the phenotype caused by the down-regulation of Jmjd3 (Iida et al. 2014). Thus, Jmjd3 and Utx may play cooperative roles in the maturation of certain subsets of retinal cells.

We next examined the roles of Ezh2 during retinal development using Ezh2 retina-specific knockout mice ($Ezh2^{fl/fl}$:Dkk3-cre, Ezh2-CKO). Retinas of Ezh2-CKO showed microphthalmia, and proliferation at the postnatal stage was ablated (Iida et al. 2014b). All of the examined retinal subtypes differentiated and were localized to the appropriate sub-retinal layer, but the population of PKCα-positive rod-ON-BP cells was larger in Ezh2-CKO than in control mice (Iida et al. 2014b). Interestingly, a ChIP analysis of the H3K27me3 level showed that while H3K27me3 modification of the examined genetic loci was ablated in embryonic retina of Ezh2-CKO, significant residual H3K27me3 modification was present in P8 retina at several

loci, suggesting that Ezh1 plays a role in the methylation of these loci in postnatal retina. Taking these data together, we propose that H3K27me3 plays major roles in the maturation and proliferation of subsets of bipolar cells in postnatal retina, and that the H3K27 methylation of four related enzymes, which have different spatio-temporal expression patterns, has distinct as well as redundant roles in retinal development.

84.4 Discussion

By examining temporal changes in the level of H3K4me3 at various genetic loci in developing retina, we found that the H3K4me3 level at rod photoreceptor-related loci increased constantly during retinal development. Previous work showed that H3K4me2 occupancy at the transcription start site of a group of genes, whose expression increased in parallel with rod cell maturation, was lost in rd1/rd1 retinas that lacked rods (Popova et al. 2012). Therefore, H3K4me2/3 modification plays critical roles in the up-regulation of rod photoreceptor-related genes in postnatal rod lineage cells. A remaining question is how such cell lineage-specific modification occurs during the commitment of retinal progenitor cells to a rod photoreceptor fate. Many enzymes are reported to methylate or demethylate H3K4 residues, and we examined the expression patterns of these enzymes using RNAseq data from CD73-positive and -negative retinal fractions at various developmental stages, but none of the enzymes showed specific expression in rod photoreceptor lineage or other cells (data not shown). Therefore, we propose the involvement of adaptor proteins or other modifications leading to H3K4 methylation of a specific group of genetic loci.

The level of H3K4me3 at several retinal progenitor-specific loci was decreased in adult retina, while the H3K27me3 level at the loci was strongly increased. These results indicate that attenuation of the expression of progenitor-specific genes is achieved, at least in part, by low H3K4me3 and high H3K27me3 levels, suggesting that we must consider controlling epigenetic status when attempting to reprogram differentiated retinal cells into naïve cells. Taken together, these data suggest that histone modifications, especially H3K27me3, temporally and spatially regulate retinal cell subset differentiation during retinal development.

Acknowledgements This work is supported by a grant-in-aid from the Ministry of Education, Culture, Sports, Science, and Technology of Japan.

References

Greer EL, Shi Y (2012) Molecular mechanisms and potential functions of histone demethylases. Nat Rev Mol Cell Biol 13:297–311

Iida A, Iwagawa T, Kuribayashi H et al (2014) Histone demethylase Jmjd3 is required for the development of subsets of retinal bipolar cells. Proc Natl Acad Sci U S A 111:3751–3756

Iida A, Iwagawa T, Baba Y et al (2015) Roles of histone H3K27 trimethylase Ezh2 in retinal proliferation and differentiation. Dev Neurobiolo Dec 30 (in press)

Kizilyaprak C, Spehner D, Devys D et al (2010) In vivo chromatin organization of mouse rod photoreceptors correlates with histone modifications. PLoS ONE 5:e11039

Popova EY, Xu X, DeWan AT et al (2012) Stage and gene specific signatures defined by histones H3K4me2 and H3K27me3 accompany mammalian retina maturation in vivo. PLoS ONE 7:e46867

Rao RC, Tchedre T, Malik MTA et al (2010) Dynamic patterns of histone lysine methylation in the developing retina. Invest Ophthalmol Vis Sci 51:6784–6792

Wegner M, Neddermann D, Piorunska-Stolzmann M et al (2014) Role of epigenetic mechanisms in the development of chronic complications of diabetes. Diabetes Res Clin Pract 105:164–175

Chapter 85
The Potential Role of Flavins and Retbindin in Retinal Function and Homeostasis

Ryan A. Kelley, Muayyad R. Al-Ubaidi and Muna I. Naash

Abstract Flavins are highly concentrated in the retina; likely because they are involved as cofactors in energy metabolism and photoreceptors have an extremely high metabolic rate. How this concentration is established is currently unknown, but photoreceptor specific proteins may exist that shuttle flavins to flavoproteins, which may also function in retinal neuron specific processes. It has been suggested due to sequence homology to folate receptors that retbindin could be binding flavins in the retina. Here we present a brief overview of flavins in the retina and initial findings that suggest retbindin may be located in the photoreceptor layer where flavin acquisition from the RPE would occur.

Keywords Retbindin · Flavin · Flavoprotein · Retina · Photoreceptor

85.1 Introduction

Flavins are essential cofactors involved in a wide range of biological processes where they function as electron carriers in oxidation-reduction reactions (Fraaije and Mattevi 2000). This process is carried out by the addition of one or two electrons and subsequent addition of hydrogen atoms to the isoalloxazine ring of riboflavin (Horwitt 1967). It is this ability that allows FAD to mediate steps in oxidative phosphorylation and fatty acid oxidation (Pollard et al. 2003; Ghisla and Thorpe 2004). These functional roles make this group of molecules integral to energy metabolism in the cell.

M. I. Naash (✉) · R. A. Kelley · M. R. Al-Ubaidi
Department of Cell Biology, University of Oklahoma Health Sciences Center,
940 Stanton L. Young Blvd., Oklahoma city, OK 73104, USA
e-mail: Muna-Naash@ouhsc.edu

R. A. Kelley
e-mail: Ryan-Kelley@ouhsc.edu

M. R. Al-Ubaidi
e-mail: Muayyad-Al-ubaidi@ouhsc.edu

C. Bowes Rickman et al. (eds.), *Retinal Degenerative Diseases,* Advances in Experimental Medicine and Biology 854, DOI 10.1007/978-3-319-17121-0_85

Given the high energy metabolism and the demand for poly unsaturated fatty acids in the photoreceptor cells (Stone et al. 1979; Alder et al. 1990) it is no surprise that the retina concentrates flavins. Batey et al. observed in the rabbit retina that flavins were present at a concentration of 51.9 ± 4.3 pmol/mg, while the blood contained only 2.55 ± 0.32 pmol/mg (Batey and Eckhert 1991). This finding was further confirmed by the same authors in rat retina and blood with values of 48 ± 1.7 and 2.57 ± 0.31 pmol/mg, respectively (Batey et al. 1992). Interestingly when the dietary intake of riboflavin was increased from the normal 3 mg/kg body weight to 30 mg/kg the concentration present in the retina did not significantly increase (Batey and Eckhert 1991). Furthermore, this phenomenon also occurred when the animals were fed 300 mg/kg riboflavin diet. When the mice were fed riboflavin-free diets, the flavin concentration fell drastically to 28.3 ± 2.2 pmol/mg (Batey et al. 1992). Taken together these data suggest that there is a mechanism for flavin acquisition and concentration in the retina. The high levels of polyunsaturated fatty acids present in the outer segments, the high metabolic rate of the photoreceptor cells, and their positioning adjacent to the dietary source (the retinal pigment epithelium) make photoreceptors a prime candidate for the acquisition and utilization of flavins.

The importance of proper flavin concentration in the neural retina is exemplified by the detrimental effects of abnormal flavin levels on the photoreceptors. When dietary intake of riboflavin is significantly decreased (ariboflavinosis), affected individuals first experience an increased sensitivity to light and poor dim light vision (Kruse 1940; Goldsmith 1975). On the other hand, when dietary intake of riboflavin is increased, unbound flavins are photo-reduced and cause lipid peroxidation of outer segments, which subsequently causes photoreceptor degeneration (Eckhert et al. 1993). These results are not surprising when we consider the role that the citric acid cycle and fatty acid oxidation play in the photoreceptor cells. If these two processes are perturbed the photoreceptor cells could have improper energy stores and an aberrant set of fatty acids, both of which are important for proper phototransduction and maintenance of the outer segment.

However, the high concentration of flavins in the retina and the detrimental effect of aberrant dietary riboflavin intake cannot be explained solely by metabolism and fatty acid oxidation. The neural retina must utilize flavins and/or flavoproteins in other ways that would account for the high concentration. In the neural retina a few different processes outside of metabolism could be utilizing this class of molecules. Flavins are utilized as cofactors in many isomerization reactions: such reactions are very important for retinoid and carotenoid metabolism and recycling (Olson 1964; Fraaije and Mattevi 2000; von Lintig et al. 2010). As an example, xanthine oxidase is a flavoprotein which contains two FAD molecules at its catalytic site (Fridovich and Handler 1958). Xanthine oxidase is responsible for the conversion of retinol to retinoic acid, and is localized to the cone outer segments (Fox and van Kuijk 1998; Taibi et al. 2001; Taibi and Nicotra 2007). While retinoic acid is mainly involved in the development of the eye, research has shown that it could be used as a transcription activation signal in the adult mammalian retina (Wagner et al. 1997; Luo et al. 2006). It has also been shown that cryptochromes are flavin associated proteins,

which are sensitive to blue light and have been implicated in the regulation of circadian rhythm in mammals (Thompson et al. 2003; Ozturk et al. 2008).

Not much is known about how the retina acquires and concentrates flavins. In 2002 Wistow et al. proposed the existence of a novel member of the folate receptor superfamily that is present exclusively in the neural retina (Wistow et al. 2002). This protein is now known as retbindin as it has 27% sequence identity (over 135 residues) to chicken riboflavin binding protein and belongs to the folate receptor superfamily (Wistow et al. 2002; Finn et al. 2014). Guo et al. further characterized the gene and protein to determine its localization in the retina (Guo et al. 2004). They presented that human and monkey retbindin message was expressed throughout their respective retinas. Using immunoblots they found the protein to be highly expressed in the peripheral retina, while immunohistochemistry found the protein to be localized predominantly to cones (Guo et al. 2004). However, Bhattacharya et al. did not identify the human retbindin locus as a disease-causing gene in their patient cohort (Bhattacharya et al. 2003). Here we further explore the properties of retbindin and its role in the retina.

85.2 Materials and Methods

85.2.1 Animals

All experiments involving mice were approved by the local Institutional Animal Care and Use Committees and adhered to the recommendations in the Guide for the Care and Use of Laboratory Animals of the National Institute of Health and the Association for Research in Vision and Ophthalmology Resolution on the Use of Animals in Research. C57BL/6 J mice were purchased from the Jackson Laboratories (Bar Harbor, ME, USA).

85.3 Immunoblots

Immunoblots were conducted as previously described (Ding et al. 2004). The following primary antibodies were used: Anti-retbindin antibody (1:500), Rds (1:1000) (Ding et al. 2004), and Na/K ATPase (1:5000) (mouse monoclonal, a5, developed by D.M. Fambrough was obtained from the Developmental Studies Hybridoma Bank, created by the NICHD of the NIH and maintained at The University of Iowa, Department of Biology, Iowa City, IA 52242.). Goat-anti rabbit conjugated to horseradish peroxidase (1:25000) (KPL, Gaithersburg, MD, USA) was used as a secondary antibody. Blots were probed with an anti-actin HRP conjugated antibody as a loading control. Developmental immunoblots were completed in triplicate using three separate animals for each time point.

85.3.1 Outer Segment Enrichment

Outer segment enriched preparations were prepared as previously described (Liu et al. 1997). Briefly, samples on a discontinuous sucrose gradient were centrifuged at 60,000 g for 15 min at 4 °C in a Sorvall M150 ultracentrifuge (Thermo Scientific, Waltham, MA, USA) equipped with a fixed angle rotor (Sorvall no. S55S-1009). The interface was collected and the pellet was resuspended in homogenization buffer and centrifuged at 80,000 g for 30 min. The supernatant was layered onto the discontinuous gradient and centrifuged at 60,000 g for 15 min at 4 °C. The interface was collected and added to the previous sample. This process was completed two more times and finally the pellet was resuspended in homogenization buffer. Samples were analyzed via immunoblot as described in the above section. Three separate preparations were made and analyzed in triplicate via immunoblot.

85.4 Retbindin as a Possible Flavin Binding Protein in the Neural Retina

Using an anti-peptide antibody against retbindin amino acids 115–131, we performed a developmental immunoblot. This sample set was comprised of neural retinal extracts from post-natal day (P) 3, P11, P21, P30, P45, and P60 wild-type mice. Retbindin protein begins to appear at P3 (Fig. 85.1a) right after the peak of rod photoreceptor proliferation (Young 1984, 1985). Levels rise significantly at P11 and peak at P21 (Fig. 85.1a), which is concomitant with photoreceptor outer segment development and elongation, respectively (LaVail 1973). This developmental expression seems to suggest that retbindin is associated with the rod outer segments (Kelley 2015). Indeed when we perform an outer segment preparation we find that retbindin is present predominantly within the outer segment enriched fraction (Fig. 85.1b). However, retbindin is still present at a significant amount in the outer segment depleted fraction confirming our earlier observation that it is a that it is a photoreceptor-specific protein (Kelly 2015).

85.5 Conclusions

If retbindin is indeed functioning as some sort of riboflavin binding protein it would need to be positioned at the rod outer segments where metabolite exchange with the RPE occurs. However, it could be that other currently unidentified proteins are also responsible for this binding and retbindin functions as a carrier within the retina. Further examination of the retbindin protein needs to be conducted to determine if and how this protein is involved in flavin binding and/or transport. Understanding how flavins are concentrated and used in the retina is of high importance given

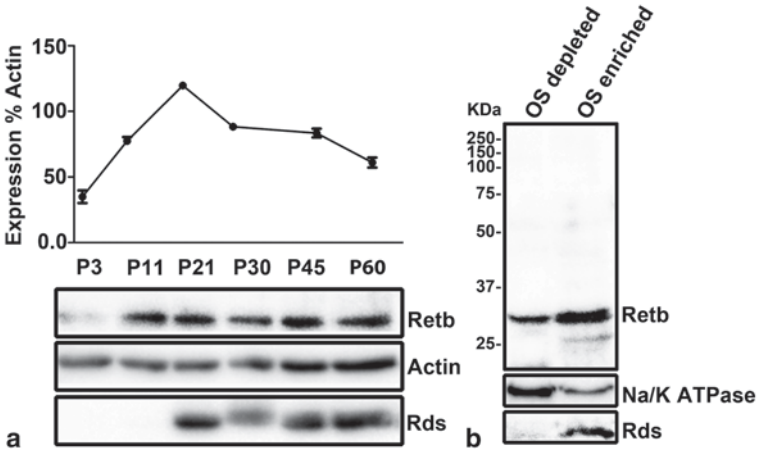

Fig. 85.1 Developmental pattern of expression of retbindin in mouse neural retina **a** *Top*. Graph depicting levels of retbindin during retinal development obtained from immunoblots as percent of actin. *Bottom*. Representative image of developmental immunoblots probed with anti-retbindin, Rds, or actin antibodies. Enrichment of retbindin in photoreceptor outer segments, **b** Immunoblot of outer segment enrichment preparation probed with anti-retbindin, Rds, or Na^+/K^+ ATPase antibodies. Retb-retbindin, Rds-retinal degeneration slow, P-postnatal, Na^+/K^+ ATPase-sodium/potassium ATPase

the active role of metabolism and lipid peroxidation during retinal development, homeostasis, and disease progression. Further understanding of flavin/flavoprotein mediated processes could lead us to exciting new understandings of retinal function and the treatment of retinal diseases.

Acknowledgments This research was partially supported by Foundation Fighting Blindness (MIN and MRA) and the National Eye Institute EY018137 (MRA), EY10609 (MIN), and P30EY021725. The funders had no role in study design, data collection and analysis, decision to publish, or preparation of the manuscript. The content is solely the responsibility of the authors and does not necessarily represent the official views of NIH or any of its institutes.

References

Alder VA, Ben-Nun J, Cringle SJ (1990) PO2 profiles and oxygen consumption in cat retina with an occluded retinal circulation. Investig Ophthalmol Vis Sci 31:1029–1034

Batey DW, Eckhert CD (1991) Analysis of flavins in ocular tissues of the rabbit. Investig Ophthalmol Vis Sci 32:1981–1985

Batey DW, Daneshgar KK, Eckhert CD (1992) Flavin levels in the rat retina. Exp Eye Res 54: 605–609

Bhattacharya SS, Patel RJ, AbuSafieh L et al (2003) Evaluation of the Retbindin Gene as a Candidate for Retinal Diseases. Invest Ophthalmol Vis Sci 44:2322

Ding XQ, Nour M, Ritter LM et al (2004) The R172W mutation in peripherin/rds causes a cone-rod dystrophy in transgenic mice. Hum Mol Genet 13:2075–2087

Eckhert CD, Hsu MH, Pang N (1993) Photoreceptor damage following exposure to excess riboflavin. Experientia 49:1084–1087
Finn RD, Bateman A, Clements J et al (2014) Pfam: the protein families database. Nucleic Acids Res 42:D222–230
Fox NE, van Kuijk FJ (1998) Immunohistochemical localization of xanthine oxidase in human retina. Free Rad Biol Med 24:900–905
Fraaije MW, Mattevi A (2000) Flavoenzymes: diverse catalysts with recurrent features. Trend Biol Sci 25:126–132
Fridovich I, Handler P (1958) Xanthine oxidase. II. Studies of the active site. J Biol Chem 231:899–911
Ghisla S, Thorpe C (2004) Acyl-CoA dehydrogenases. A mechanistic overview. Europ J Biochem/FEBS 271:494–508
Goldsmith GA (1975) Riboflavin deficiency. New York: Plenum Press
Guo Y, Wyatt K, Wistow G et al (2004) Retbindin expression in human and monkey retina. Invest Ophthalmol Vis Sci 45:662
Horwitt MKaW, L.A. (1967) Riboflavin: biochemical systems. New York: Academic Press
Kelley RA, Al-Ubaidi MR, Naash MI (2015) Retbindin is an extracellular riboflavin-binding protein found at the photoreceptor/retinal pigment epithelium interface. J Bio Chem 290:5041-5052
Kruse HDS, V. P.; Sebrell, W. H.; Cleckley, H. M. (1940) Ocular manifestations of ariboflavinosis. Public Health Reports 55:157–169
LaVail MM (1973) Kinetics of rod outer segment renewal in the developing mouse retina. J Cell Biol 58:650–661
Liu X, Wu T, et al (1997) Defective phototransduction disk membrane morphogenesis in transgenic mice expressing opsin with a mutated N-terminal domain. Hum Mol Genet 110:2589-2597
Luo T, Sakai Y, Wagner E et al (2006) Retinoids, eye development, and maturation of visual function. J Neurobiol 66:677–686
Olson JA (1964) The biosynthesis and metabolism of carotenoids and retinol (vitamin A). J Lipid Res 5:281–299
Ozturk N, Song SH, Selby CP et al (2008) Animal type 1 cryptochromes. Analysis of the redox state of the flavin cofactor by site-directed mutagenesis. J Biol Chem 283:3256–3263
Pollard PJ, Wortham NC, Tomlinson IP (2003) The TCA cycle and tumorigenesis: the examples of fumarate hydratase and succinate dehydrogenase. Ann Med 35:632–639
Stone WL, Farnsworth CC, Dratz EA (1979) A reinvestigation of the fatty acid content of bovine, rat and frog retinal rod outer segments. Exp Eye Res 28:387–397
Taibi G, Nicotra CM (2007) Xanthine oxidase catalyzes the oxidation of retinol. J Enz Inhib Med Chem 22:471–476
Taibi G, Paganini A, Gueli MC et al (2001) Xanthine oxidase catalyzes the synthesis of retinoic acid. J Enzyme Inhib 16:275–285
Thompson CL, Bowes Rickman C, Shaw SJ et al (2003) Expression of the blue-light receptor cryptochrome in the human retina. Investig Ophthalmol Vis Sci 44:4515–4521
von Lintig J, Kiser PD, Golczak M et al (2010) The biochemical and structural basis for trans-to-cis isomerization of retinoids in the chemistry of vision. Trend Biochem Sci 35:400–410
Wagner E, McCaffery P, Mey J et al (1997) Retinoic aid increases arrestin mRNA levels in the mouse retina. FASEB J 11:271–275
Wistow G, Bernstein SL, Wyatt MK et al (2002) Expressed sequence tag analysis of human retina for the NEI Bank Project: retbindin, an abundant, novel retinal cDNA and alternative splicing of other retina-preferred gene transcripts. Mol Vis 8:196–204
Young RW (1984) Cell death during differentiation of the retina in the mouse. J Comp Neurol 229:362–373
Young RW (1985) Cell differentiation in the retina of the mouse. Anat Rec 212:199–205

Chapter 86
Identification of Tyrosine *O* Sulfated Proteins in Cow Retina and the 661W Cell Line

Yogita Kanan and Muayyad R. Al-Ubaidi

Abstract Lack of tyrosine *O* Sulfation compromises both rod and cone electroretinographic responses emphasizing the importance of this post-translational modification for vision. To identify tyrosine sulfated proteins in retina, cow retinal lysates were subjected to immunoaffinity purification using an anti-sulfotyrosine antibody. The tyrosine sulfated proteins were eluted from the column using a sulfotyrosine pentapeptide and identified using mass spectrometry. Similarly, tyrosine sulfated proteins secreted by the 661W cell line were identified. Proteins identified were vitronectin, fibronectin, fibulin 2, nidogen, collagen V alpha 2, complement component 3 and C4 and fibrinogen beta. All proteins were subjected to analysis by 'Sulfinator' to determine potential sulfated tyrosines.

Keywords Tyrosine sulfation · 661W · Retina · PSG2 · Posttranslational modification

86.1 Introduction

Tyrosine sulfation is a post-translational modification of proteins that is utilized in all ocular tissues (Kanan et al. 2009, 2012) and plays a very important role in vision (Sherry et al. 2010, 2012). Eliminating tyrosine sulfation reduces scotopic electroretinographic responses to 25% of normal and photopic responses to 15% of normal (Sherry et al. 2010). Besides these functional deficits, ultrastructural examination reveals rod outer segments abnormalities (Sherry et al. 2010). To

M. R. Al-Ubaidi (✉) · Y. Kanan
Departments of Cell Biology, University of Oklahoma Health Sciences Center, Oklahoma City, OK 73104, USA
e-mail: muayyad-al-ubaidi@ouhsc.edu

Y. Kanan
e-mail: ykanan1@jhmi.edu

C. Bowes Rickman et al. (eds.), *Retinal Degenerative Diseases,* Advances in Experimental Medicine and Biology 854, DOI 10.1007/978-3-319-17121-0_86

identify the tyrosine sulfated proteins that may be responsible for these effects, we immunoaffinity purified tyrosine sulfated proteins from neural retina using the anti-sulfotyrosine antibody PSG2 (Hoffhines et al. 2006). Column elution using a sulfated pentapeptide was followed by mass spectrometry. Since all sulfated proteins are secreted, some of the tyrosine sulfated proteins produced by the cell line 661W (Tan et al. 2004) were identified by fractionating conditioned media followed by western blotting with PSG2. Proteins that immuno-reacted were identified by in-gel digestion of excised bands followed by mass spectrometry.

86.2 Materials and Methods

86.2.1 Preparation of Bovine Retinal Lysates

Bovine eyes were obtained from Country Home Meat Slaughter House (Edmond, OK). Neural retinas were isolated and lysates were prepared in buffer A (25 mM MOPS, 100 mM NaCl, pH 7.5). Bradford assay was performed and lysate concentrations were adjusted to 4 mg/ml in buffer A prior to loading onto the column.

86.2.2 PSG2 Affinity Purification of Tyrosine O Sulfated Proteins

Ten mg of extracts were filtered using a 0.45 μm syringe filter (Millipore, Billerica, MA) and loaded onto the PSG2-Affi-Gel-10 HPLC column (Hoffhines et al. 2009). Column was washed with buffer A, wash buffer 1 (25 mM MOPS, 200 mM NaCl), wash buffer 2 (25 mM MOPS, 400 mM NaCl) and eluted with elution buffer (25 mM MOPS, 400 mM NaCl, 4 mM sulfated pentapeptide). Eluted samples were concentrated with acetone precipitation. The tyrosine-sulfated pentapeptide LDYSDF was synthesized by Bio-Synthesis Inc. (Lewisville, TX).

86.2.3 Mass Spectrometry

Column fractions were separated by SDS-PAGE to remove the sulfated pentapeptide and gel lane was cut into 1 mm slices and subjected to in-gel trypsin digestion, reduction and alkylation followed by LC MS/MS analysis (ABI MDS Sciex Qstar Elite, (Life Technologies, Grand Island, NY). MS/MS data were collected using ABI Analyst QS 2.0 software and submitted to MASCOT (Matrix Science) server for protein identification against the NCBInr protein database.

86.3 Results

86.3.1 Tyrosine O Sulfated Proteins Identified by Immunoaffinity Purification

About 10% of eluted proteins were run on a gel and immunoblotted with PSG2 (Hoffhines et al. 2006). Identified proteins ranged from 250 kD to 37 kDa in size (Fig. 86.1a). The remaining eluate was acetone precipitated, fractionated by SDS-PAGE and subjected to mass spectrometry. Since tyrosine sulfated proteins transit the secretory pathway (Moore et al. 2003), only membrane or secreted proteins were included in Table 86.1. Identified targets belonged to multiple protein families such as serpins, extracellular matrix proteins and complement proteins. Since the major function of tyrosine sulfation is protein-protein interaction (Zhu et al. 2011; Costagliola et al. 2002; Ramachandran et al. 1999), immunoaffinity may have pulled down non-tyrosine sulfated proteins that co-purified due to their direct or indirect interaction with tyrosine-sulfated proteins. Therefore, each of the identified proteins was subjected to prediction of sulfated tyrosines using the software 'Sulfinator' (Monigatti et al. 2002). Seven of the proteins were predicted to be tyrosine sulfated (Table 86.2). Fibronectin and fibrinogen have previously been shown to be tyrosine sulfated (Liu and Suiko 1987; Hortin et al. 1986) and we have recently shown fibulin 2 and vitronectin to be tyrosine sulfated (Kanan et al. 2014a, 2014b). Complement component 3 and fibrinogen beta have not been previously shown to be tyrosine sulfated. Sulfinator did not predict tyrosine sulfated sites on retinol binding protein 3 (IRBP), pigment epithelium-derived factor (PEDF) precursor, collagen (type I, alpha 1), neuronal membrane glycoprotein M6-b, isoform 2 and fibrinogen alpha. The presence of these proteins suggests that they may be interacting partners to some of the identified tyrosine sulfated proteins.

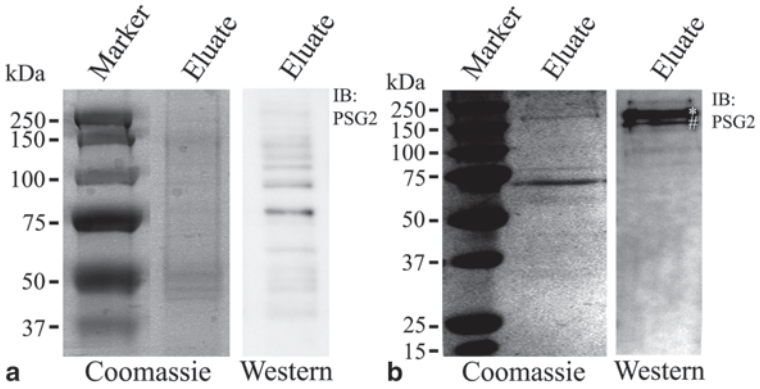

Fig. 86.1 Tyrosine sulfated proteins in cow retinal extracts and 661W cells. **a** Immunoaffinity column purification of tyrosine *O* sulfated proteins from cow retinal lysates. SDS-PAGE and coomassie blue staining of cow retinal lysates eluted from the column and western blotted with PSG2. **b** Tyrosine *O* sulfated proteins from cone derived cell line 661W. SDS-PAGE and coomassie blue staining of 661W conditioned media and western blotting with PSG2

Table 86.1 List of proteins identified in cow retinal lysates after immunoaffinity purification and mass spectrometric analysis. Eleven proteins were identified in cow retinal lysates by MALDI-MS/MS analysis of PSG2 immunoaffinity column eluent

	Protein	Mascot score	%Coverage
1	Retinol binding protein 3 (IRBP)	1500	35
2	Fibulin 2	1281	24
3	Pigment epithelium-derived factor precursor	1002	39
4	Complement component 3	925	22
5	Vitronectin	766	35
6	Fibrinogen beta	692	17
7	Collagen, type I, alpha 1	563	35
8	Fibronectin	472	7
9	Complement C4	407	14
10	Neuronal membrane glycoprotein M6-b, isoform 2	318	16
11	Fibrinogen alpha	92	4

Table 86.2 List of potential sulfated tyrosines residues in cow retina as identified by Sulfinator. Citations are provided for the tyrosine sulfation sites that were experimentally identified

Protein	Site	Sequence	Reference
Vitronectin	75	LPEDE**Y**GFHDY	Novel
Vitronectin	80	YGFHD**Y**SDAQT	Novel
Fibulin 2	197	DPERH**Y**EDPYS	Kanan et al. (2014a)
Fibulin 2	201	HYEDP**Y**SYDQE	Kanan et al. (2014a)
Fibulin 2	203	EDPYS**Y**DQEVA	
Complement component 3	1559	DDFDE**Y**IMVIE	Novel
Vitronectin	75	LPEDE**Y**GFHDY	Kanan et al. (2014b)
Vitronectin	80	YGFHD**Y**SDAQT	Kanan et al. (2014b)
Vitronectin	275	FKGNH**Y**WEYVF	Kanan et al. (2014b)
Vitronectin	278	NHYWE**Y**VFQQQ	Kanan et al. (2014b)
Fibrinogen beta	33	QFPTD**Y**DEGQD	Novel
Fibrinogen beta	259	ETSEM**Y**LIQPE	Novel
Fibrinogen beta	273	KPYRV**Y**CDMK	Novel
Fibronectin	877	QPGVQ**Y**NITIY	Liu and Suiko (1987)
Fibronectin	882	YNITI**Y**AVEEN	Liu and Suiko (1987)
Complement C4	944	REEMV**Y**ELNPL	Hortin et al. (1986)
Complement C4	1414	EAEED**Y**EDYEY	Hortin et al. (1986)
Complement C4	1417	EDYED**Y**EYEDL	Hortin et al. (1986)
Complement C4	1419	YEDYE**Y**EDLLA	Hortin et al. (1986)

86.3.2 Tyrosine Sulfated Proteins in 661W-Conditioned Media

661W-conditioned media was SDS-PAGE fractionated and immunoblotted with PSG2 revealing two major proteins between 150–250 kDa (Fig. 86.1b). These proteins were excised and subjected to MALDI MS/MS analysis. The top band (marked by an asterisk, Table 86.3) was a mixture of three proteins and the bottom

Table 86.3 List of proteins identified in 661W-conditioned media. Four proteins were identified from conditioned media of 661W cells following SDS-PAGE and MALDI-MS/MS analysis

	Protein	Mascot score	% Coverage
1.*	Fibronectin	1019	11
2.*	Fibulin 2	643	14
3.*	Nidogen-2	408	7
4.#	Collagen, type V, alpha 2	524	15

Table 86.4 List of sulfated tyrosines residues in cone derived cell line, 661W. All four proteins have been experimentally proven to contain sulfated tyrosines and citations provided

Protein	Site	Sequence	Reference
*Fibronectin	875	QPGVQ**Y**NITIY	Liu and Suiko (1987)
*Fibronectin	880	YNITIYAVEEN	Liu and Suiko (1987)
*Fibulin 2	192	DSERQ**Y**EDPYS	Kanan et al. (2014a)
*Fibulin 2	196	YEDP**Y**SYDQEV	Kanan et al. (2014a)
*Fibulin 2	198	EDPYS**Y**DQEVA	Kanan Y et al. (2014a)
#Nidogen 2	94	PRETQ**Y**VDDDF	Paulsson et al. (1985)
#Nidogen 2	317	EDSFH**Y**YDENE	Paulsson et al. (1985)
#Nidogen 2	318	DSFHY**Y**DENEE	Paulsson et al. (1985)
#Nidogen 2	327	EEDVE**Y**PPVEP	Paulsson et al. (1985)
#Collagen, type V, alpha 2	34	QENDE**Y**DEEIA	Fessler et al. (1986)
#Collagen, type V, alpha 2	1238	DIMGH**Y**DENMP	Fessler et al. (1986)

band (denoted by #, Table 86.3) was identified as collagen, type V, alpha 2. Sulfinator predicted all the four proteins to be tyrosine sulfated (Table 86.4), which has been experimentally confirmed (Liu and Suiko 1987; Kanan et al. 2014a; Paulsson et al. 1985; Fessler et al. 1986).

86.4 Discussion

We have previously shown the importance of tyrosine sulfation for vision (Sherry et al. 2010; Sherry et al. 2012) and here we identify some of the tyrosine sulfated proteins in ocular tissues. We subjected cow retinal extracts to immunoaffinity purification with PSG2. Eleven proteins were identified and seven of those were predicted to be tyrosine sulfated. The rest of the proteins may have been co-purified with their tyrosine sulfated interacting partners since tyrosine sulfation enhances protein-protein interactions (Zhu et al. 2011; Costagliola et al. 2002; Ramachandran et al. 1999). Of the identified proteins, fibulin 2 and vitronectin were also detected in cow RPE to be tyrosine *O* sulfated (Kanan et al. 2014a, b).

Since the retina is composed of six different classes of cells, identified proteins may belong to any and/or all cell types. Therefore, we used the cone derived cell line 661W to identify tyrosine sulfated proteins that may be cone specific. We identified fibronectin, fibulin 2, nidogen 2 and collagen V proteins from this cell line. These proteins were experimentally shown to be tyrosine sulfated (Liu and Suiko 1987; Kanan et al. 2014a; Paulsson et al. 1985; Fessler et al. 1986).

This is the first report of the identification of tyrosine sulfated protein in the retina and in 661W cells. Further experiments will identify the cell type that produces these proteins in the retina. The function of tyrosine sulfation in these proteins and how it affects vision will only be revealed using '*In-Vivo* knock-in' mutants that will have the tyrosine sulfated residues mutated to phenylalanines.

Acknowledgments This study was supported by grants from Oklahoma Center for Advancement of Science and Technology (OCAST to YK), Foundation Fighting Blindness (MRA), the National Eye Institute EY018137 (MRA) and a P30EY021725. The funders had no role in design, collection and analysis of data, decision to publish, or manuscript preparation.

References

Costagliola S, Panneels V, Bonomi M et al (2002) Tyrosine sulfation is required for agonist recognition by glycoprotein hormone receptors. EMBO J 21: 504–513

Fessler LI, Brosh S, Chapin S et al (1986) Tyrosine sulfation in precursors of collagen V. J Biol Chem 261:5034–5040

Hoffhines AJ, Damoc E, Bridges KG et al (2006) Detection and purification of tyrosine-sulfated proteins using a novel anti-sulfotyrosine monoclonal antibody. J Biol Chem 281:37877–37887

Hoffhines AJ, Jen CH, Leary JA et al (2009) Tyrosylprotein sulfotransferase-2 expression is required for sulfation of RNase 9 and Mfge8 in vivo. J Biol Chem 284:3096–3105

Hortin G, Sims H, Strauss AW (1986) Identification of the site of sulfation of the fourth component of human complement. J Biol Chem 261:1786–1793

Kanan Y, Hoffhines A, Rauhauser A et al (2009) Protein tyrosine-O-sulfation in the retina. Exp Eye Res 89:559–567

Kanan Y, Hamilton RA, Moore KL et al (2012) Protein tyrosine-O-sulfation in bovine ocular tissues. Adv Exp Med Biol 723:835–841

Kanan Y, Brobst D, Han Z et al (2014a) Fibulin 2, a tyrosine O-sulfated protein, is up-regulated following retinal detachment. J Biol Chem 289:13419–13433

Kanan, Y, Siefert JC, Kinter M (2014b) Complement factor H, Vitronectin and Opticin are tyrosine sulfated proteins of the retinal pigmented epithelium. PLoS One e105409

Liu MC, Suiko M (1987) Tyrosine sulfation site is located in the C-terminal fibrin-binding domain in secreted fibronectin from rat embryo fibroblasts, line 3Y1. Arch Biochem Biophys 255:162–167

Monigatti F, Gasteiger E, Bairoch A, Jung E (2002) The Sulfinator: predicting tyrosine sulfation sites in protein sequences. Bioinformatics 18:769–70

Moore KL (2003) The biology and enzymology of protein tyrosine O-sulfation. J Biol Chem 278:24243–24246

Paulsson M, Dziadek M, Suchanek C et al (1985) Nature of sulphated macromolecules in mouse Reichert's membrane. Evidence for tyrosine O-sulphate in basement-membrane proteins. Biochem J 231:571–579

Ramachandran V, Nollert MU, Qiu H et al (1999) Tyrosine replacement in P-selectin glycoprotein ligand-1 affects distinct kinetic and mechanical properties of bonds with P- and L-selectin. Proc Natl Acad Sci U S A 96:13771–13776

Sherry DM, Murray AR, Kanan Y et al (2010) Lack of protein-tyrosine sulfation disrupts photoreceptor outer segment morphogenesis, retinal function and retinal anatomy. Eur J Neurosci 32:1461–1472

Sherry DM, Kanan Y, Hamilton R et al (2012) Differential developmental deficits in retinal function in the absence of either protein tyrosine sulfotransferase-1 or -2. PLoS ONE 7:e39702

Tan E, Ding XQ, Saadi A et al (2004) Expression of cone-photoreceptor-specific antigens in a cell line derived from retinal tumors in transgenic mice. Investig Ophthalmol Vis Sci 45:764–768

Zhu JZ, Millard CJ, Ludeman JP et al (2011) Tyrosine sulfation influences the chemokine binding selectivity of peptides derived from chemokine receptor CCR3. Biochemistry 50:1524–1534

Chapter 87
The Function of Arf-like Proteins ARL2 and ARL3 in Photoreceptors

Christin Hanke-Gogokhia, Houbin Zhang, Jeanne M. Frederick and Wolfgang Baehr

Abstract Arf-like proteins (ARLs) are ubiquitously expressed small G proteins of the RAS superfamily. In photoreceptors, ARL2 and ARL3 participate in the trafficking of lipidated membrane-associated proteins and colocalize in the inner segment with UNC119A and PDEδ. UNC119A and PDEδ are acyl- and prenyl-binding proteins, respectively, involved in trafficking of acylated (transducin-α subunit, nephrocystin NPHP3) and prenylated proteins (GRK1, PDE6). Germline *Arl3* knockout mice do not survive beyond postnatal day 21 and display ciliary defects in multiple organs (kidney, liver and pancreas) as well as retinal degeneration. Conditional knockouts will be necessary to delineate mechanisms of protein transport in retina disease.

Keywords Arf-like protein 3 (ARL3) · Arf-like protein 2 (ARL2) · Phosphodiesterase δ-subunit (PDEδ) · unc-119 homolog (C. elegans) (UNC119A) · Retinitis pigmentosa protein 2 (RP2) · Rod photoreceptor

W. Baehr (✉) · C. Hanke-Gogokhia · J. M. Frederick
Department of Ophthalmology, John A. Moran Eye Center, University of Utah Health Science Center, 65 Mario Capecchi Drive, Salt Lake City, UT 84132, USA
e-mail: wbaehr@hsc.utah.edu

J. M. Frederick
e-mail: Jeanne.frederick@hsc.utah.edu

C. Hanke-Gogokhia
Department of Physical Biochemistry, University of Potsdam, Karl-Liebknecht-Strasse 24-25, 14476 Potsdam, Germany
e-mail: christin.hanke@hsc.utah.edu

H. Zhang
Sichuan Academy of Medical Sciences & Sichuan Provincial People's Hospital, Chengdu, Sichuan, China

W. Baehr
Department of Biology, University of Utah, 257 South 1400 East, Salt Lake City, UT 84112, USA

Department of Neurobiology and Anatomy, University of Utah Health Science Center, 20 North 1900 East, Room 401 MREB, Salt Lake City, UT 84132, USA

C. Bowes Rickman et al. (eds.), *Retinal Degenerative Diseases,* Advances in Experimental Medicine and Biology 854, DOI 10.1007/978-3-319-17121-0_87

87.1 Introduction

Arf-like (ARL) proteins were discovered in *Drosophila* more than 20 years ago. To date, 16 genes encoding ARL proteins (ARL1–16) have been identified in the mammalian genome. ARL proteins are 20 kDa protein with 40–60 % sequence similarity and function as key molecular switches by exchanging GDP with GTP catalyzed by a **G**uanine nucleotide **E**xchange **F**actor (GEF). Importantly, ARL proteins function in various membrane- and cytoskeleton-associated cellular processes, which are critical for cell homeostasis. ARL proteins contribute to the localization and activity of other cellular proteins and downstream signaling pathways. Those interactants include posttranslational modifiers, guanine nucleotide exchange factors (GEFs), GTPase-activating proteins (GAPs) and effectors (PDEδ, UNC119A and UNC119B) that bind specifically to the GTP-bound conformation.

87.2 ARL1-ARL3

ARL proteins, discovered in *Drosophila* more than 20 years ago (Tamkun et al. 1991), are 20 kDa protein with 40–60 % sequence similarity (reviewed in Burd et al. 2004; Gillingham and Munro 2007). ARL1-3 (Fig. 87.1) are the best-characterized of the 16 ARL genes (ARL1-16) discovered to date in the mammalian genome.

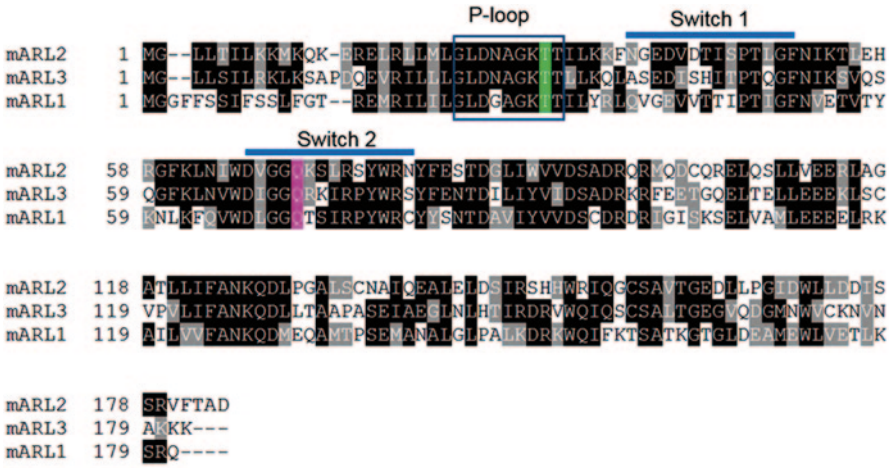

Fig. 87.1 Sequence alignment of ARL1-ARL3. Sequences of ARL1, ARL2 and ARL3 share ~78 % similarity. The P-loop involved in GDP/GTP binding is boxed. *Blue bars* denote switch 1 and switch 2 (areas of conformational change upon GDP/GTP exchange). The region between switches 1 and 2 (interswitch) of ARL2 and ARL3 is involved in binding of lipidated proteins (PDEδ, RP2, and UNC119 paralogs). Sites for dominant-inactive (T30, highlighted in *green*) and dominant-active (Q71, *magenta*) are conserved among ARL proteins 1-3

Upon exchange of GDP by GTP, like other GTPases, ARLs change conformation affecting N-terminal regions termed Switch 1 and Switch 2. ARL1 is closely related to Arf1 (the human protein shares 76% similarity) and shows some residual Arf activity (ADP-ribosylation of stimulatory G-proteins in the presence of cholera toxin) (Hong et al. 1998). Yeast and human ARL1 are N-myristoylated (Boman et al. 1999). In *Drosophila*, deletion of ARL1 was embryonically lethal demonstrating an essential function (Tamkun et al. 1991). ARL1 is found at the Golgi complex and its active conformation recruits various effectors to the Golgi, especially GRIP-domain-containing coiled-coil proteins. Depletion of mammalian ARL1 results in defective protein transport between endosomes and the Golgi complex, but its precise role is unknown (Lu et al. 2005; Graham 2013).

Mammalian ARL2 and ARL3 were cloned by PCR with degenerate primers (Clark et al. 1993; Cavenagh et al. 1994). In contrast to ARL1, ARL2 and ARL3 have no Arf activity and are not substrates for N-myristoyl transferase, most likely due to interruption of the N-myristoylation motif (Fig. 87.1) (Cavenagh et al. 1994; Ismail et al. 2012). ARL3 localizes predominantly to connecting cilia and inner segments of human (Grayson et al. 2002) and mouse photoreceptors where it colocalizes with its effectors, UNC119A and PDEδ. ARL2 has nucleotide affinities in the sub-μM range, while ARL3 has only a weak affinity for GTP (48 μM). ARL3 has very slow intrinsic GTPase-activity of 0.000012/sec, and RP2 was identified as a GAP for ARL3-GTP (Veltel et al. 2008). The active conformation of ARL3 is found to be both soluble and membrane-associated due to weak affinity to membrane (Wright et al. 2011). The ARL3-specific GEF stimulating GDP-GTP exchange is unknown.

87.3 ARL2/ARL3 Interacting Proteins

ARL2 interacts with the tubulin-specific chaperone, cofactor D, which is involved in αβ-tubulin heterodimer assembly (Bhamidipati et al. 2000). Other interactants are the ubiquitously expressed Binder of ARL2 (BART), also called ARL2BP (Davidson et al. 2013) forming a soluble complex (Sharer and Kahn 1999), PDEδ (see below), protein phosphatase 2A (PP2A) (Shern et al. 2003) and UNC119 isoforms. *ARL2BP* mutations have been linked to recessive *retinitis pigmentosa* (Davidson et al. 2013). *PDE6D* (encoding PDEδ) null mutations in human cause a severe syndromic ciliopathy (Joubert syndrome) (Thomas et al. 2014) and in mouse, a recessive cone-rod dystrophy (Zhang et al. 2007). A heterozygous stop codon (K57ter) associated with dominant cone-rod dystrophy was identified in the human *UNC119A* gene (Kobayashi et al. 2000). Mutant ARL2 or ARL3 genes have not been linked to human disease so far.

87.4 ARL2-PDEδ Interactions

ARL2 and ARL3 interact with PDEδ and the complex ARL2/PDEδ was cocrystallized (Hanzal-Bayer et al. 2002). Structure of the PDEδ and ARL2-GTP complex was determined at 2.3 Å resolution. The PDEδ structure exhibits an immunoglobulin-like β-sandwich fold with two β-sheets forming a hydrophobic pocket to accommodate lipids. The interface between ARL2-GTP and PDEδ derives from the interaction of β-sheets involving the interswitch region of ARL2 and β7 of PDEδ. The β-sandwich structure can accommodate farnesyl (C15) and geranylgeranyl (C20) lipids, but not fatty acids. The β-sheet structure of PDEδ is closely related to RhoGDI (Hoffman et al. 2000) and UNC119A (Zhang et al. 2011) although the sequence similarities among these polypeptides are relatively low. Photoreceptor PDEδ interacts with prenyl side chains of GRK1, PDE6 catalytic subunits and transducin-γ to form soluble complexes. ARL3-GTP is thought to function as a **G**DI **D**isplacement **F**actor (GDF) to unload prenylated cargo to the destination membrane (Ismail et al. 2012). Binding of ARL2- or ARL3-GTP to the soluble complex of PDEδ-GRK1 constricts the hydrophobic pocket, thereby expelling the prenyl side chain and delivering cargo (GRK1) to its target membrane. This mechanism is supported by deletion of the *Pde6d* gene in mouse in which trafficking of rhodopsin kinase (GRK1), and rod and cone PDE6 subunits, from the inner to the outer segment is impeded (Zhang et al. 2007).

87.5 The ARL3-RP2 Complex

A truncated (residues 17-177) version of ARL3 with GMPPNP bound was cocrystallized with RP2 (Kuhnel et al. 2006). ARL3 forms an interface with RP2 through the P-loop, and switch regions. RP2 structure shows an N-terminal, right-handed β-helix consisting of three stacked β-sheets (Veltel et al. 2008); the β-helix interacts with ARL3 providing the GTPase active site. Interaction with RP2 accelerates GTPase activity more 90,000-fold under saturating conditions and 1,400-fold with catalytic amounts of RP2 (Veltel et al. 2008).

87.6 The ARL3-UNC119 Complex

Truncated (residues 17-178) ARL2 and full-length ARL3-GMPPNP were co-crystallized with UNC119A (Ismail et al. 2012). The structures show that switch 1, interswitch and switch 2 regions of both ARLs interact with UNC119A β-strands. Both ARL3-GTP and ARL2-GTP bind to UNC119A with similar affinities, but only ARL3-GTP releases myristoylated cargo (nephrocystin NPHP3 or transducin-α)

from UNC119A (Ismail et al. 2012). The mechanism of cargo release from UNC119A differs from that of the ARL2/PDEδ/Rheb ternary complex. Binding of ARL-GTP to PDEδ alters the open conformation of PDEδ to a closed conformation, thereby squeezing the prenyl side chain and extruding the prenylated protein to the target membrane. Binding of ARL3-GTP to UNC119A, by contrast, widens the binding pocket to release the myristoyl side chain.

Release of myristoylated transducin-α from its binding partner UNC119A is relevant *In-Vivo*. Transducin-α translocates to the rod inner segment in constant daylight, a mechanism regulating light adaptation. During dark adaptation, UNC119A serves as a chaperone that mediates return of transducin-α to the rod outer segment (Zhang et al. 2011). Release of transducin-α to target membranes is likely mediated by the GDF ARL3-GTP. Taken together, UNC119, PDEδ and RP2 may cooperate in a network as effectors of ARL3-GTP in regulating the assembly and targeting of a subset of lipidated proteins.

87.7 ARL3 Knockout

Germline *Arl3* knockout mice were generated to study the function ARL3 *In-Vivo* (Schrick et al. 2006). Absence of ARL3 caused a syndromic ciliopathy with multiple organ defects and knockout mice survived no longer than 3 weeks. Germline *Arl3* knockout mice were born at a sub-Mendelian ratio and showed ciliary dysfunction in the kidney, liver and pancreas as well as photoreceptor degeneration. Rod outer segments were absent in the $Arl3^{-/-}$ mouse retinas reflecting defects in the trafficking of phototransduction proteins. ARL3 is also essential for spermiogenesis in mouse where ARL3 functions as a manchette-associated protein (Qi et al. 2013). Although the *Arl3* gene is not yet associated with human ciliopathy, other ARL family members (ARL6 and ARL13B) are known to be mutated in Bardet-Biedl and Joubert Syndromes (Wiens et al. 2010; Humbert et al. 2012; Cantagrel et al. 2008).

87.8 Future Directions

To further study photoreceptor protein trafficking, we generated ARL3 conditional knockout mice. We have generated $Arl3^{f/f}$;*iCre75*$^{+}$and $Arl3^{f/f}$;Six3*Cre*$^{+}$ mice in which ARL3 is depleted in rod photoreceptors and the entire retina, respectively, with the expectation of observing prenylated protein mislocalization, rapid photoreceptor degeneration and blindness. Embryonic deletion of ARL3 in the retina is predicted to produce more serious effects, including degeneration of inner retina neurons.

References

Bhamidipati A, Lewis SA, Cowan NJ (2000) ADP ribosylation factor-like protein 2 (Arl2) regulates the interaction of tubulin-folding cofactor D with native tubulin. J Cell Biol 149:1087–1096

Boman AL, Kuai J, Zhu X et al (1999) Arf proteins bind to mitotic kinesin-like protein 1 (MKLP1) in a GTP-dependent fashion. Cell Motil Cytoskeleton 44:119–132

Burd CG, Strochlic TI, Gangi Setty SR (2004) Arf-like GTPases: not so Arf-like after all. Trends Cell Biol 14:687–694

Cantagrel V, Silhavy JL, Bielas SL et al (2008) Mutations in the cilia gene ARL13B lead to the classical form of Joubert syndrome. Am J Hum Genet 83:170–179

Cavenagh MM, Breiner M, Schurmann A et al (1994) ADP-ribosylation factor (ARF)-like 3, a new member of the ARF family of GTP-binding proteins cloned from human and rat tissues. J Biol Chem 269:18937–18942

Clark J, Moore L, Krasinskas A et al (1993) Selective amplification of additional members of the ADP-ribosylation factor (ARF) family: cloning of additional human and Drosophila ARF-like genes. Proc Natl Acad Sci U S A 90:8952–8956

Davidson AE, Schwarz N, Zelinger L et al (2013) Mutations in ARL2BP, encoding ADP-ribosylation-factor-like 2 binding protein, cause autosomal-recessive retinitis pigmentosa. Am J Hum Genet 93:321–329

Gillingham AK, Munro S (2007) The small G proteins of the Arf family and their regulators. Annu Rev Cell Dev Biol 23:579–611

Graham TR (2013) Arl1 gets into the membrane remodeling business with a flippase and ArfGEF. Proc Natl Acad Sci U S A 110:2691–2692

Grayson C, Bartolini F, Chapple JP et al (2002) Localization in the human retina of the X-linked retinitis pigmentosa protein RP2, its homologue cofactor C and the RP2 interacting protein Arl3. Hum Mol Genet 11:3065–3074

Hanzal-Bayer M, Renault L, Roversi P et al (2002) The complex of Arl2-GTP and PDE delta: from structure to function. EMBO J 21:2095–2106

Hoffman GR, Nassar N, Cerione RA (2000) Structure of the Rho family GTP-binding protein Cdc42 in complex with the multifunctional regulator RhoGDI. Cell 100:345–356

Hong JX, Lee FJ, Patton WA et al (1998) Phospholipid- and GTP-dependent activation of cholera toxin and phospholipase D by human ADP-ribosylation factor-like protein 1 (HARL1). J Biol Chem 273:15872–15876

Humbert MC, Weihbrecht K, Searby CC et al (2012) ARL13B, PDE6D, and CEP164 form a functional network for INPP5E ciliary targeting. Proc Natl Acad Sci U S A 109:19691–19696

Ismail SA, Chen YX, Miertzschke M et al (2012) Structural basis for Arl3-specific release of myristoylated ciliary cargo from UNC119. EMBO J 31:4085–4094

Kobayashi A, Higashide T, Hamasaki D et al (2000) HRG4 (UNC119) mutation found in cone-rod dystrophy causes retinal degeneration in a transgenic model. Invest Ophthalmol Vis Sci 41:3268–3277

Kuhnel K, Veltel S, Schlichting I, Wittinghofer A (2006) Crystal structure of the human retinitis pigmentosa 2 protein and its interaction with Arl3. Structure 14:367–378

Lu L, Tai G, Hong W (2005) Interaction of Arl1 GTPase with the GRIP domain of Golgin-245 as assessed by GST (glutathione-S-transferase) pull-down experiments. Methods Enzymol 404:432–441

Qi Y, Jiang M, Yuan Y et al (2013) ADP-ribosylation factor-like 3, a manchette-associated protein, is essential for mouse spermiogenesis. Mol Hum Reprod 19:327–335

Schrick JJ, Vogel P, Abuin A et al (2006) ADP-ribosylation factor-like 3 is involved in kidney and photoreceptor development. Am J Pathol 168:1288–1298

Sharer JD, Kahn RA (1999) The ARF-like 2 (ARL2)-binding protein, BART. Purification, cloning, and initial characterization. J Biol Chem 274:27553–27561

Shern JF, Sharer JD, Pallas DC et al (2003) Cytosolic Arl2 is complexed with cofactor D and protein phosphatase 2A. J Biol Chem 278:40829–40836

Tamkun JW, Kahn RA, Kissinger M et al (1991) The arflike gene encodes an essential GTP-binding protein in Drosophila. Proc Natl Acad Sci U S A 88:3120–3124

Thomas S, Wright KJ, Le CS et al (2014) A homozygous PDE6D mutation in Joubert syndrome impairs targeting of farnesylated INPP5E protein to the primary cilium. Hum Mutat 35:137–146

Veltel S, Gasper R, Eisenacher E, Wittinghofer A (2008) The retinitis pigmentosa 2 gene product is a GTPase-activating protein for Arf-like 3. Nat Struct Mol Biol 15:373–380

Wiens CJ, Tong Y, Esmail MA et al (2010) Bardet-Biedl syndrome-associated small GTPase ARL6 (BBS3) functions at or near the ciliary gate and modulates Wnt signaling. J Biol Chem 285:16218–16230

Wright KJ, Baye LM, Olivier-Mason A et al (2011) An ARL3-UNC119-RP2 GTPase cycle targets myristoylated NPHP3 to the primary cilium. Genes Dev 25:2347–2360

Zhang H, Li S, Doan T et al (2007) Deletion of PrBP/{delta} impedes transport of GRK1 and PDE6 catalytic subunits to photoreceptor outer segments. Proc Natl Acad Sci U S A 104:8857–8862

Zhang H, Constantine R, Vorobiev V et al (2011) UNC119 regulates G protein trafficking in sensory neurons. Nature Neuroscience 14:874–880

Chapter 88
Characterization of Antibodies to Identify Cellular Expression of Dopamine Receptor 4

Janise D. Deming, Kathleen Van Craenenbroeck, Yun Sung Eom, Eun-Jin Lee and Cheryl Mae Craft

Abstract The dopamine receptor D4 (DRD4) plays an important role in vision. In order to study the DRD4 expression *in vivo*, it is important to have antibodies that are specific for DRD4 for both immunoblot and immunohistochemical (IHC) applications. In this study, six antibodies raised against DRD4 peptides were tested *in vitro*, using transfected mammalian cells, and *in vivo*, using mouse retinas. Three Santa Cruz (SC) antibodies, D-16, N-20, and R-20, were successful in IHC of transfected DRD4; however, N-20 was the only one effective on immunoblot analysis in DRD4 transfected cells and IHC of mouse retinal sections, while R-20, 2B9, and Antibody Verify AAS63631C were non-specific or below detection.

Keywords Dopamine receptor D4 · Dopamine · Antibody · Transfection · HEK · Immunoblot · Retina · Immunohistochemistry

C. M. Craft (✉)
Departments of Ophthalmology and Cell & Neurobiology, USC Eye Institute, Keck School of Medicine of the University of Southern California, Institute for Genetic Medicine, 2250 Alcazar Street, CSC 135H, Los Angeles, CA 90089-9075, USA
e-mail: eyesightresearch@hotmail.com

J. D. Deming
Departments of Ophthalmology, USC Eye Institute, Keck School of Medicine of the University of Southern California, Institute for Genetic Medicine, 2250 Alcazar St CSC 215, Los Angeles, CA 90033, USA
e-mail: jddeming@usc.edu

K. Van Craenenbroeck
University of Ghent, Proeftuinstraat 86, Gent 9000, Belgium
e-mail: kathleen.vancraenenbroeck@ugent.be

Y. S. Eom · E.-J. Lee
Biomedical Engineering, Viterbi School of Engineering, University of Southern California, 1042 Downey way, DRB 140, Los Angeles, CA 90007, USA
e-mail: yuneom@usc.edu

E.-J. Lee
e-mail: eunjinl@usc.edu

C. Bowes Rickman et al. (eds.), *Retinal Degenerative Diseases,* Advances in Experimental Medicine and Biology 854, DOI 10.1007/978-3-319-17121-0_88

Abbreviations

DRD4	Dopamine receptor D4
DRD1	Dopamine receptor D1
IHC	Immunohistochemistry
SC	Santa cruz biotechnologies
GPCR	G-protein-coupled receptor
GFP	Green fluorescent protein
MW	Molecular weight
CT	Circadian time
SDS	Sodium dodecyl sulfate
PAGE	Polyacrylamide gel electrophoresis
HRP	Horseradish peroxidase
OCT	Optimal cutting temperature
PFA	Paraformaldehyde
PBS	Phosphate–buffered solution
GCL	Ganglion cell layer
IS	Inner segment
OS	Outer segment
ONL	Outer nuclear layer
OPL	Outer plexiform layer
INL	Inner nuclear layer
IPL	Inner plexiform layer
EC	Extracellular
IC	Intracellular
TM	Transmembrane

88.1 Introduction

Dopamine plays an important but complex role in regulating vertebrate vision. It is synthesized in a subpopulation of amacrine cells and diffuses throughout the retinal layers to activate five types of dopaminergic G-protein-coupled receptors (GPCRs) (reviewed in Missale et al. 1998). In mice and zebrafish, the dopamine receptors DRD1 and DRD4 contribute to normal vision. In genetically engineered DRD1 and DRD2 null mice, physiological and behavioral responses were tested with electroretinography and optokinetic tracking, and these studies concluded that DRD1 and DRD2 play an important role in contrast sensitivity and visual acuity (Nir et al. 2002; Jackson et al. 2012). Other studies revealed these GPCRs regulate retinal clock genes (Hwang et al. 2013), phosphorylation levels in photoreceptors (Pozdeyev et al. 2008), and the opening and closing of gap junctions between retinal neurons (Hu et al. 2010; Li et al. 2013).

Tools to study DRD1 and DRD4 have been developed including GPCR-specific agonists and antagonists and even a transgenic mouse expressing green fluorescent protein (GFP)-tagged DRD4 (Gong et al. 2003), which are helpful but limited in elucidating receptor function. In addition, in situ hybridization studies have clearly

localized Drd4 mRNA in photoreceptors, the inner nuclear layer, and a subpopulation of ganglion cells (Klitten et al. 2008; Li et al. 2013); however, the cellular localization and amount of endogenous DRD4 protein are still unclear because of a lack of specific antibodies.

Although many DRD4 antibodies are commercially available, only limited published data are available on these reagents. It is difficult to produce good antibodies against GPCRs, which are 7-transmembrane pass cell surface receptors. With five unique, but closely related, dopamine receptors, the development is even more challenging. Previous characterizations of these antibodies have yielded confusing results, including varying molecular weights (MW) of DRD4 protein on denaturing acrylamide gels followed by immunoblot (Gomez et al. 2002; Bavithra et al. 2012), and some with no MW listed (Chu et al. 2004; Li et al. 2007; Strell et al. 2009; Gonzalez et al. 2012). Doubt has been cast on whether any of these DRD4 antibodies should be trusted (Bodei et al. 2009).

A reliable, specific antibody recognizing DRD4 to study the localization of the receptor, both in the retina and in the brain, is essential. Furthermore, it is a waste of time and resources to test multiple commercially available antibodies only to discover that they are not DRD4 specific. In this study, we characterized six anti-DRD4 antibodies using immunoblot analysis and IHC, both with human DRD4 overexpressed in transfected HEK cells and with mouse retinas from C57Bl/6J and *Drd4*$^{-/-}$.

88.2 Materials and Methods

88.2.1 Mice

All animals were treated and protocols were approved by USC IACUC. Breeders for C57BL/6J and *Drd4*$^{-/-}$ (strain B6.129P2-Drd4tm1Dkg/J) mice were obtained from Jackson Laboratory (Bar Harbor, MN). They were bred and their offspring were reared in 12 h light/12 h dark cycling light conditions. Mice were sacrificed in the dark at circadian time (CT) 0, before lights were turned on. Eyes were enucleated and eyecups were processed for IHC or retinas were stored at −80 °C for immunoblot analysis.

88.2.2 HEK293 Cell Culture and Transfection

HEK293T/17 (HEK293T) cells were purchased from ATCC (Manassas, VA) and maintained at 37 °C, 5% CO2 and used for experiments below 15 passages. For transient transfection, HEK293T were transfected with FuGENE 6 transfection reagent (Promega) for 48 h before being harvested for analysis.

88.2.3 DRD4 Expression Plasmids

Each mammalian expression plasmids encodes a common variant of human DRD4, along with an HA- or FLAG-tag for labeling and verification and were previously characterized (pcDNA3-HA-DRD4.4, and pFLAG-DRD4.4) (Oak et al. 2000; Van Craenenbroeck et al. 2005).

88.2.4 Anti-DRD4 Antibodies

Six anti-DRD4 antibodies raised against slightly different regions of rat or human DRD4 protein were tested: five from Santa Cruz Biotechnologies (2B9, D-16, H-50, N-20, R-20) and one from Antibody Verify (AAS63631C).

88.2.5 Immunoblot Analysis

Retinas or frozen cell pellets were homogenized in 50 mM Tris, pH 7.6 plus cOmplete protease inhibitor cocktail (Roche), sonicated to break apart DNA and denatured with SDS, then subjected to 10% SDS-polyacrylamide gel electrophoresis (PAGE) and transferred to PVDF membranes (Millipore). Anti-DRD4 (1:100 dilution) or anti-HA (1:1000 dilution, Cell Signaling) primary antibodies were used in conjunction with HRP-conjugated secondary antibodies (1:10,000 dilution, Bio-Rad or Santa Cruz). Hi-Blot Chemiluminescence kit (Denville) was used for detection with film.

88.2.6 Immunohistochemistry (IHC)

Mouse retinas: Mouse eyes were enucleated and immediately fixed using published methods (Zhu et al. 2002). They were fixed in 4% paraformaldehyde (PFA) for 10 min. Eyes were cut into 20 μm sections. Retina sections were blocked with normal donkey serum in PBS, and antibodies were diluted in PBS.

HEK 293: Cells were seeded onto glass slides in multi-well plates and given 24 h to adhere. Cells were transfected (see above) and 48 h later rinsed with PBS and fixed in 4% PFA. After fixation, cells were either blocked with Blotto (3% Milk, 1 mM CaCl2 in TBS), or permeabilized with Blotto plus 0.01% Triton-X. Antibodies were diluted in Blotto.

Retinas and transfected cells were labeled with anti-DRD4 primary antibodies (1:50 dilution, SC antibodies; 1:100, Antibody Verify; 1:500 dilution anti-HA or anti-FLAG for transfected cells). After rinsing with PBS, cells were labeled with fluorescent secondary antibodies (1:500, anti-goat, anti-rabbit, or anti-mouse AlexaFluor 488 and anti-rabbit or anti-mouse AlexaFluor 568), mounted with Vectashield

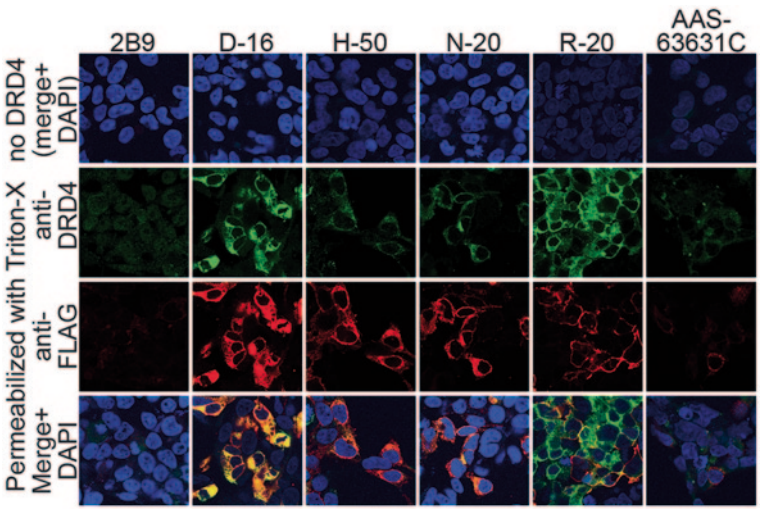

Fig. 88.1 IHC of HEK 293T with or without FLAG-DRD4 transfection. N-20, D-16, and H-50 show bright DRD4 staining that overlaps with anti-FLAG staining. No detectable signal was observed in the DRD4 untransfected cells or with 2B9 or AAS-63631C

mounting medium with DAPI (Vector Labs), and visualized using confocal fluorescent microscopy. (Zeiss Laser Scanning Microscope 710)

88.3 Results

88.3.1 Immunohistochemistry: Transfected Cells

Three SC antibodies, D-16, N-20, and H-50, labeled the DRD4-transfected cells brightly and did not label non-transfected cells (Fig. 88.1). The anti-DRD4 signal was identical to the anti-FLAG signal and the cells were labeled both with and without permeabilization, indicating an extracellular binding site (data not shown). The other three antibodies, R-20, 2B9, and AAS63631C, had little overlap with FLAG signal, indicating that the anti-DRD4 signal was not specific to the tagged protein. Interestingly, there was no signal in non-transfected cells for these antibodies.

88.3.2 Immunoblots

To test specificity of each anti-DRD4 antibody on immunoblot analysis, C57BL/6J and Drd4-/- total retinal proteins were electrophoresed simultaneously on 10% SDS-PAGE, along with HEK293T (untransfected) and HEK239T transfected with

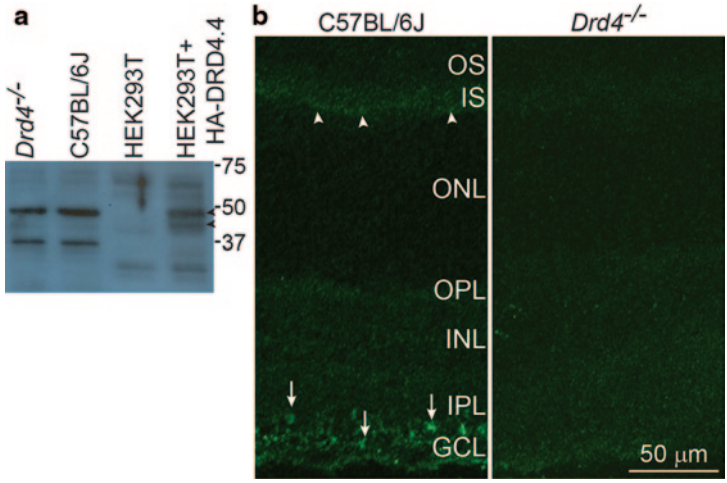

Fig. 88.2 **a** Immunoblot analysis of N-20 anti-DRD4 antibody labels DRD4 in transfected cells (45 and 48 kDa), as evidenced by the two missing immunoreactive proteins (*arrowheads*) in untransfected lane, which overlaps with the anti-HA antibody bands (data not shown). No proteins were observed in control retina that are not present in *Drd4*$^{-/-}$, indicating that N-20 does not recognize mouse retina DRD4 on immunoblot. **b** IHC of control versus *Drd4*$^{-/-}$ retina sections using N-20 (*green*) control retina compared to *Drd4*$^{-/-}$ displays specific labeling in ganglion cell layer (*GCL*) (*arrows*) and in photoreceptor inner segment layer (*IS*) (*arrowheads*)

HA-DRD4.4. The MW of human DRD4.4 is calculated to be 43.1 kiloDaltons (kDa), while mouse DRD4 is 41.5 kDa. Out of six antibodies, only N-20 recognized human DRD4, evidenced by two bands in the lane with transfected HEK293T that were not in the lane with untransfected HEK293T although their MW was higher than expected (45 and 48 kDa) (Fig. 88.2a). The bands were verified to be HA-DRD4 by their consistency with the bands identified by the anti-HA antibody (data not shown). In contrast, no distinct bands were observed in the control retina lane that were not in the *Drd4*$^{-/-}$ samples. There were multiple non-specific bands for all of the antibodies (data not shown).

88.3.3 Immunohistochemistry: Mouse Retinas

All antibodies were tested on frozen sections of control and *Drd4*$^{-/-}$ mouse retinas collected at CT0, when DRD4 mRNA expression is highest (Klitten et al., 2008; Kim et al., 2010). For all but the N-20 antibody, there was no difference between the signal intensity of control versus knockout samples (data not shown). The N-20 antibody showed a significant signal in the ganglion cell layer of the control retina that was not present in the *Drd4*$^{-/-}$ mouse retina (Fig. 88.2a). A small increase in the inner segments of the photoreceptor layer in control compared to *Drd4*$^{-/-}$ was seen; however, no differences in the outer segment layer (OS), outer nuclear layer (ONL), outer plexiform layer (OPL), inner nuclear layer (INL), or inner plexiform layer (IPL) were observed.

88.4 Discussion

These data collectively demonstrate that only one antibody candidate, N-20, tested for both mouse and human DRD4, was effective in specific labeling of control retina compared to *Drd4*$^{-/-}$ and immunoblot labeling of human DRD4 in HEK293T cells. The three antibodies D-16, H-50, and N-20 all show immunological labeling of DRD4-transfected cells using IHC.

It is unclear why these antibodies do not reveal an obvious retinal difference between control mice and *Drd4*$^{-/-}$. This may be because, as a previous study suggested, anti-DRD4 antibodies may recognize other dopamine receptors as well (Bodei et al. 2009). If this is the case, DRD4 expression in the retina is not high enough, even at its mRNA observed peak at CT0, to show significant signal above the other four dopamine receptors. Based on non-specific bands in immunoblot analysis, the anti-DRD4 antibodies may also recognize unrelated proteins of various sizes, additionally clouding the signal of DRD4.

The differences between the *in vitro* and *in vivo* studies may also be due to sequence differences. Most of the antibodies were raised against peptides based on the sequence of human DRD4, not mouse. Since the transfected cells were overexpressing human DRD4, small differences in the peptide sequence may make the antibodies specific for human, and not mouse, DRD4. The only exception is R-20, which was raised against a rat DRD4 peptide. Rat DRD4 is similar to the mouse sequence with 94 % identity between mouse DRD4 and rat DRD4, compared to 73 % for mouse and human. This may explain why R-20 did not recognize the human DRD4 in transfected cells.

Overall, no antibody was able to give clear results in all applications, but N-20 is the best choice for future studies of DRD4 in mouse retinas and transfected human cells (Deming et al. 2015).

Acknowledgments Dr. Craft is the Mary D. Allen Chair in Vision Research, Doheny Eye Institute. This work was supported, in part, from NEI/NIH EY015851 (CMC), EY03040 (DEI), Mary D. Allen foundation (CMC), Research to Prevent Blindness, Dorie Miller, Tony Gray Found., Retina Research Found./Joseph M. & Eula C. Lawrence Travel Grant (JDD), RD 2014 travel award (JDD), and William Hansen Sandberg Memorial Found. (JDD). The authors thank Kayleen Lim, Isabel Shen, and Joseph Pak for technical assistance.

References

Bavithra S, Selvakumar K, Pratheepa KR et al (2012) Polychlorinated biphenyl (PCBs)-induced oxidative stress plays a critical role on cerebellar dopaminergic receptor expression: ameliorative role of quercetin. Neurotox Res 21:149–159

Bodei S, Arrighi N, Spano P et al (2009) Should we be cautious on the use of commercially available antibodies to dopamine receptors? Naunyn Schmiedebergs Arch Pharmacol 379:413–415

Chu E, Chu J, Socci RR et al (2004) 7-OH-DPAT-induced inhibition of norepinephrine release in PC12 cells. Pharmacology 70:130–139

Deming JD, Shin J-a, Lim K et al (2015) Dopamine receptor D4 internalization requires a beta- arrestin and a visual arrestin. Cellular Signalling 27:2002–2013
Gomez MJ, Rousseau G, Nadeau R et al (2002) Functional and autoradiographic characterization of dopamine D2-like receptors in the guinea pig heart. Can J Physiol Pharmacol 80:578–587
Gong S, Zheng C, Doughty ML et al (2003) A gene expression atlas of the central nervous system based on bacterial artificial chromosomes. Nature 425:917–925
Gonzalez S, Moreno-Delgado D, Moreno E et al (2012) Circadian-related heteromerization of adrenergic and dopamine D(4) receptors modulates melatonin synthesis and release in the pineal gland. PLoS Biol 10:e1001347
Hu EH, Pan F, Volgyi B et al (2010) Light increases the gap junctional coupling of retinal ganglion cells. J Physiol 588:4145–4163
Hwang CK, Chaurasia SS, Jackson CR et al (2013) Circadian rhythm of contrast sensitivity is regulated by a dopamine-neuronal PAS-domain protein 2-adenylyl cyclase 1 signaling pathway in retinal ganglion cells. J Neurosci 33:14989–14997
Jackson CR, Ruan GX, Aseem F et al (2012) Retinal dopamine mediates multiple dimensions of light-adapted vision. J Neurosci 32:9359–9368
Kim JS, Bailey MJ, Weller JL et al (2010) Thyroid hormone and adrenergic signaling interact to control pineal expression of the dopamine receptor D4 gene (Drd4). Mol Cell Endocrinol 314:128–135
Klitten LL, Rath MF, Coon SL et al (2008) Localization and regulation of dopamine receptor D4 expression in the adult and developing rat retina. Exp Eye Res 87:471–477
Li Q, Lu G, Antonio GE et al (2007) The usefulness of the spontaneously hypertensive rat to model attention-deficit/hyperactivity disorder (ADHD) may be explained by the differential expression of dopamine-related genes in the brain. Neurochem Int 50:848–857
Li H, Zhang Z, Blackburn MR et al (2013) Adenosine and dopamine receptors coregulate photoreceptor coupling via gap junction phosphorylation in mouse retina. J Neurosci 33:3135–3150
Missale C, Nash SR, Robinson SW et al (1998) Dopamine receptors: from structure to function. Physiol Rev 78:189–225
Nir I, Harrison JM, Haque R et al (2002) Dysfunctional light-evoked regulation of cAMP in photoreceptors and abnormal retinal adaptation in mice lacking dopamine D4 receptors. J Neurosci 22:2063–2073
Oak JN, Oldenhof J, Van Tol HH (2000) The dopamine D(4) receptor: one decade of research. Eur J Pharmacol 405:303–327
Pozdeyev N, Tosini G, Li L et al (2008) Dopamine modulates diurnal and circadian rhythms of protein phosphorylation in photoreceptor cells of mouse retina. Eur J Neurosci 27:2691–2700
Strell C, Sievers A, Bastian P et al (2009) Divergent effects of norepinephrine, dopamine and substance P on the activation, differentiation and effector functions of human cytotoxic T lymphocytes. BMC Immunol 10:62
Van Craenenbroeck K, Clark SD, Cox MJ et al (2005) Folding efficiency is rate-limiting in dopamine D4 receptor biogenesis. J Biol Chem 280:19350–19357
Zhu X, Li A, Brown B et al (2002) Mouse cone arrestin expression pattern: light induced translocation in cone photoreceptors. Mol Vis 8:462–471

Chapter 89
A Possible Role of Neuroglobin in the Retina After Optic Nerve Injury: A Comparative Study of Zebrafish and Mouse Retina

Kayo Sugitani, Yoshiki Koriyama, Kazuhiro Ogai, Keisuke Wakasugi and Satoru Kato

Abstract Neuroglobin (Ngb) is a new member of the family of heme proteins and is specifically expressed in neurons of the central and peripheral nervous systems in all vertebrates. In particular, the retina has a 100-fold higher concentration of Ngb than do other nervous tissues. The role of Ngb in the retina is yet to be clarified. Therefore, to understand the functional role of Ngb in the retina after optic nerve injury (ONI), we used two types of retina, from zebrafish and mice, which have permissible and non-permissible capacity for nerve regeneration after ONI, respectively. After ONI, the Ngb protein in zebrafish was upregulated in the amacrine cells within 3 days, whereas in the mouse retina, Ngb was downregulated in the retinal ganglion cells (RGCs) within 3 days. Zebrafish Ngb (z-Ngb) significantly enhanced neurite outgrowth in retinal explant culture. According to these results, we designed an overexpression experiment with the mouse Ngb (m-Ngb) gene in RGC-5 cells (retinal precursor cells). The excess of m-Ngb actually rescued RGC-5

K. Sugitani (✉)
Department of Clinical Laboratory Science, Graduate School of Medical Science, Kanazawa University, 5-11-80 Kodatsuno, Kanazawa 920-0942, Japan
e-mail: sugitani@staff.kanazawa-u.ac.jp

Y. Koriyama
Graduate School and Faculty of Pharmaceutical Sciences, Suzuka University of Medical Sciences, 3500-3 Minamitamagaki, Suzuka, Mie 513-8670, Japan
e-mail: koriyama@suzuka-u.ac.jp

K. Ogai
Wellness Promotion Science Center, Institute of Medical, Pharmaceutical and Health Sciences, Kanazawa University, 5-11-80 Kodatsuno, Kanazawa 920-0942, Japan
e-mail: kazuhiro@staff.kanazawa-u.ac.jp

K. Wakasugi
Department of Life Sciences, Graduate School of Arts and Sciences, The University of Tokyo, 3-8-1 Komaba, Meguro-ku 153-8902, Japan
e-mail: wakasugi@bio.c.u-tokyo.ac.jp

S. Kato
Department of Molecular Neurobiology, Graduate School of Medicine, Kanazawa University, 13-1 Takara-machi, Kanazawa 920-8640, Japan
e-mail: satoru@med.kanazawa-u.ac.jp

C. Bowes Rickman et al. (eds.), *Retinal Degenerative Diseases,* Advances in Experimental Medicine and Biology 854, DOI 10.1007/978-3-319-17121-0_89

cells under hypoxic conditions and significantly enhanced neurite outgrowth in cell culture. These data suggest that mammalian Ngb has positive neuroprotective and neuritogenic effects that induce nerve regeneration after ONI.

Keywords Neuroglobin · Optic nerve regeneration · Neurite outgrowth · Neurite sprouting · Neuroprotection · Retina · Cell viability · Hypoxic damage · Zebrafish · Mouse

89.1 Introduction

In 2000, neuroglobin (Ngb) was discovered as a new member of the globin superfamily predominantly expressed in neurons (Burmester et al. 2000) and it contains hexacoordinated heme Fe atoms. Mammalian Ngb has shown high affinity for O_2 and might be involved in the alleviation of various types of oxidative stresses, elimination of reactive oxygen species (Li et al. 2008, 2011), and in preservation of mitochondrial function via prevention of apoptosis (Brittain et al. 2010; Raychaudhuri et al. 2010). Furthermore, Wakasugi et al. (2005) proposed a new function of Ngb as a regulator protein in signal transduction where it inhibits the dissociation of GDP with the α-subunit of a G protein. It is well known that retina contains the highest concentration of Ngb among various nervous tissues (Schmidt et al. 2003; Burmester and Hankeln 2009). Fish retinal ganglion cells (RGCs) can survive and regenerate their axon after optic nerve injury (ONI), whereas mouse RGCs cannot survive and fail to regenerate after ONI (Kato et al. 2013). In the present study, we examined in detail the changes of Ngb expression in zebrafish and mice after ONI. After ONI, opposite responses in retinal Ngb levels could be seen: upregulation of Ngb in the fish retina and downregulation of Ngb in the mouse retina. On the basis of these results, we tried to achieve overexpression of mouse Ngb in RGC-5 cells, a retinal precursor cell line, to induce nerve regeneration in the mammalian retina after ONI.

89.2 Stimulation of Neurite Sprouting by z-Ngb in the Zebrafish Retina after ONI

In a previous study (Kamioka et al. 2013), we reported that the level of z-Ngb mRNA in the zebrafish retina increased 3 days after ONI and returned to the control levels by 20 days after ONI. The cellular localization of z-Ngb mRNA was in amacrine cells. Immunohistochemical analysis further supported this finding regarding z-Ngb: immunoreactivity of z-Ngb in the control retina could be barely seen in the inner retina (Fig. 89.1, zebrafish 0 d). The immunoreactivity of z-Ngb increased in the amacrine cells in the inner nuclear layer and inner plexiform layer 3 days after ONI (Fig. 89.1, zebrafish 3 d). In particular, immunoreactivity of amacrine cells became conspicuously stronger than that of control retinas. Addition of z-Ngb into

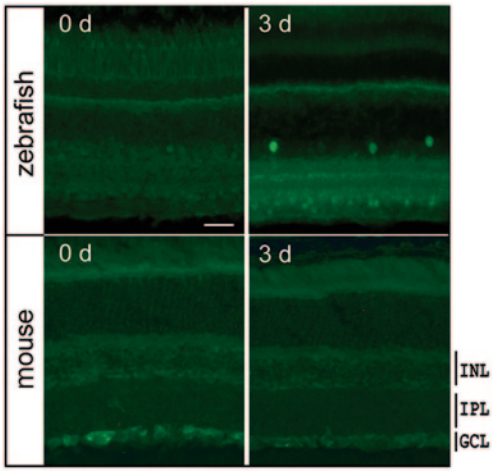

Fig. 89.1 Immunohistochemical staining of zebrafish and mouse retina with an anti-neuroglobin (anti-Ngb) antibody. The panel (zebrafish) 0 d: very weak zebrafish Ngb (z-Ngb) signals can be seen in the control (intact) retina. 3 d: z-Ngb expression clearly increased in the amacrine cells in the inner nuclear layer and the inner plexiform layer 3 days after optic nerve injury. The panel (mouse) 0 d: m-Ngb signals can be seen in the control (intact) retina. 3 d: m-Ngb expression clearly decreased in the ganglion cell layer 3 days after optic nerve injury. The scale bar is 20 μm. *INL* inner nuclear layer; *IPL* inner plexiform layer; *GCL* ganglion cell layer

the zebrafish retinal explant cultures induced a significant neurite outgrowth in a naïve (intact) retina (Sugitani, unpublished data). On the other hand, the z-Ngb protein did not protect zebrafish ZF4 cells from cell death caused by hydrogen peroxide exposure (Kamioka et al. 2013). The reason being that z-Ngb has a cell membrane-penetrating domain but not a cell-protecting domain (Wakasugi et al. 2005). Thus, the z-Ngb protein that is upregulated in the amacrine cells after ONI is easily secreted and translocated into the damaged ganglion cells to induce neurite sprouting at such an early stage (3 days) of optic nerve regeneration (Kato et al. 2013).

89.3 Neuroprotective and Neurite Sprouting Effects of Mouse Ngb in the Retina After ONI

The structure of m-Ngb comprises a monomer of 151 amino acid residues with a molecular mass of 17 kDa. The m-Ngb exhibited a very high homology with human Ngb (94% identity). Although m-Ngb has no cell membrane-penetrating activity, it exerts a cell-protecting effect through its GDP anchor protein (Wakasugi et al. 2005). Immunohistochemical analysis revealed that strong signals of the m-Ngb protein can be seen in the control retina: the tissue localization is limited to the ganglion cells (Fig. 89.1, mouse 0 d). Lechauve et al. (2013) recently showed this kind of strong immunoreactivity in rat RGCs. After ONI, m-Ngb signals disappeared

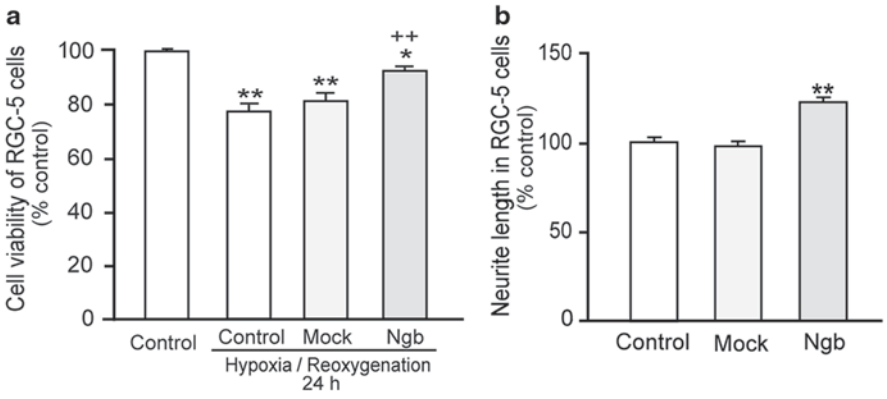

Fig. 89.2 Effects of Ngb overexpression on **a** cell viability and **b** neurite outgrowth in RGC-5 cells. **a** Overexpression of mouse Ngb (m-Ngb) increased cell viability under oxidative stress (hypoxic conditions for 24 h) compared with the control cells and mock-transfected cells (**$P<0.01$: decreased relative to the control without oxidative stress, *$P<0.05$: decreased relative to the control without oxidative stress, $^{++}P<0.01$: increased relative to the control with oxidative stress). **b** Overexpression of m-Ngb increased the length of neurite outgrowth compared with the control or mock-transfected cells (**$P<0.01$ increased relative to the control or mock). Differences between the groups were analyzed using one-way analysis of variance (ANOVA), followed by Dunnett's multiple-comparison test

from the mouse retina after 3 days (Fig. 89.1, mouse 3 d). To further explore the role of m-Ngb in mouse retina, we performed an overexpression experiment with the m-Ngb gene using murine retinal precursor cells, RGC-5 cells (Krishnamoorthy et al. 2001). The m-Ngb overexpression certainly enhanced cell viability of RGC-5 cells under hypoxia-reperfusion conditions compared to mock or control cells (Fig. 89.2a). Furthermore, the overexpressed m-Ngb induced the growth of significantly long neurites in RGC-5 cells in culture (Fig. 89.2b). These data suggest that m-Ngb is involved in dual neuroprotective and neuritogenic mechanisms. In the case of lens injury and advanced glaucoma, Ngb protein is certainly upregulated in the Müller cells and inner nuclear cells (Lechauve et al. 2013; Rajendram and Rao 2007). In the case of acute ONI, production of m-Ngb cannot catch up to the excess amount of oxygen radicals. If we overcome this disadvantage, Ngb might become a key molecule for therapeutic regeneration of mammalian central neurons, for example, in the form of a chimeric Ngb protein with a cell membrane-penetrating module from z-Ngb (Kamioka et al. 2013).

89.4 Conclusions

In this study, we compared Ngb expression in the retina before and after ONI (Table 89.1). Fish Ngb, upregulated in amacrine cells after ONI, might be released from amacrine cells followed by translocation into neighboring RGCs, and

Table 89.1 Comparison of Ngb expression in mouse and zebrafish retina after optic nerve injury (ONI)

	Ngb expression after ONI	Localization in retina	Function
Mouse Ngb	Decreases	Retinal ganglion cells	Enhances cell viability
			Neurite outgrowth
Zebrafish Ngb	Increases (~20 days)	Amacrine cells	Neurite outgrowth

may induce nerite sprouting in damaged RGCs at the early stage of optic nerve regeneration. In contrast, mammalian Ngb downregulated immediately after ONI. Mammalian Ngb has been known to have beneficial effects: neuroprotective and neuritogenic. Thus, a successful method for the maintenance of high levels of Ngb expression in the retina after ONI may protect neural cells from cell death and might induce neurite outgrowth in damaged RGCs.

Acknowledgements This work was supported by Grants-in-Aid for Scientific Research to K.S. (No. 23618006) from the Ministry of Education, Culture, Sports, Science and Technology, Japan.

References

Brittain T, Skommer J, Raychaudhuri S et al (2010) An antiapoptotic neuroprotective role for neuroglobin. Int J Mol Sci 11:2306–2321

Burmester T, Hankeln T (2009) What is the function of neuroglobin? J Exp Biol 212:1423–1428

Burmester T, Weich B, Reinhardt S et al (2000) A vertebrate globin expressed in the brain. Nature 407:520–523

Kamioka Y, Fujikawa C, Ogai K et al (2013) Functional characterization of fish neuroglobin: zebrafish neuroglobin is highly expressed in amacrine cells after optic nerve injury and can translocate into ZF4 cells. Biochim Biophys Acta 1834:1779–1788

Kato S, Matsukawa T, Koriyama Y et al (2013) A molecular mechanism of optic nerve regeneration in fish: the retinoid signaling pathway. Prog Retin Eye Res 37:13–30

Krishnamoorthy RR, Agarwal P, Prasanna G et al (2001) Characterization of a transformed rat retinal ganglion cell line. Brain Res Mol Brain Res 86:1–12

Lechauve C, Augustin S, Roussel D et al (2013) Neuroglobin involvement in visual pathways through the optic nerve. Biochim Biophys Acta 1834:1772–1778

Li RC, Morris MW, Lee SK et al (2008) Neuroglobin protects PC12 cells against oxidative stress. Brain Res 1190:159–166

Li W, Wu Y, Ren C et al (2011) The activity of recombinant human neuroglobin as an antioxidant and free radical scavenger. Proteins 79:115–125

Rajendram R, Rao NA (2007) Neuroglobin in normal retina and retina from eyes with advanced glaucoma. Br J Ophthalmol 91:663–666

Raychaudhuri S, Skommer J, Henty K et al (2010) Neuroglobin protects nerve cells from apoptosis by inhibiting the intrinsic pathway of cell death. Apoptosis 15:401–411

Schmidt M, Giessl A, Laufs T et al (2003) How does the eye breathe? Evidence for neuroglobin-mediated oxygen supply in the mammalian retina. J Biol Chem 278:1932–1935

Wakasugi K, Kitatsuji C, Morishima I (2005) Possible neuroprotective mechanism of human neuroglobin. Ann N Y Acad Sci 1053:220–230

Chapter 90
JNK Inhibition Reduced Retinal Ganglion Cell Death after Ischemia/Reperfusion *In Vivo* and after Hypoxia *In Vitro*

Nathalie Produit-Zengaffinen, Tatiana Favez, Constantin J. Pournaras and Daniel F. Schorderet

Abstract Mitogen-activated protein kinases (MAPKs) are key regulators that have been linked to cell survival and death. Among the main classes of MAPKs, c-jun N-terminal kinase (JNK) has been shown to mediate cell stress responses associated with apoptosis.

In Vitro, hypoxia induced a significant increase in 661W cell death that paralleled increased activity of JNK and c-jun. 661W cells cultured in presence of the inhibitor of JNK (D-JNKi) were less sensitive to hypoxia-induced cell death.

In vivo, elevation in intraocular pressure (IOP) in the rat promoted cell death that correlated with modulation of JNK activation. *In vivo* inhibition of JNK activation with D-JNKi resulted in a significant and sustained decrease in apoptosis in the ganglion cell layer, the inner nuclear layer and the photoreceptor layer. These results highlight the protective effect of D-JNKi in ischemia/reperfusion induced cell death of the retina.

Keywords *In vivo* · Ischemia · Hypoxia · MAPK · JNK · Therapy

D. F. Schorderet (✉) · N. Produit-Zengaffinen · T. Favez
Faculty of Life Sciences, Swiss Federal Institute of Technology, Lausanne, Switzerland
e-mail: daniel.schorderet@irovision.ch

IRO—Institute for Research in Ophthalmology, Av du Grand-Champsec 64, Sion, Switzerland

Department of Ophthalmology, University of Lausanne, Lausanne, Switzerland

C. J. Pournaras
Department of Ophthalmology, Geneva University Hospitals, Geneva, Switzerland
e-mail: constantin.pournaras@lacolline.ch

N. Produit-Zengaffinen
e-mail: nathalie.produit-zengaffinen@irovision.ch

T. Favez
e-mail: tatiana.favez@irovision.ch

C. Bowes Rickman et al. (eds.), *Retinal Degenerative Diseases,* Advances in Experimental Medicine and Biology 854, DOI 10.1007/978-3-319-17121-0_90

90.1 Introduction

Neuronal cell death following excitotoxicity is a common feature of neurodegenerative and ischemic diseases of the central nervous system and of a variety of ocular diseases, such as glaucoma. Glaucoma is characterized by a slowly progressive loss of retinal ganglion cells (RGC) and their axons and is often associated with elevated intraocular pressure (IOP). Retinal ischemia/reperfusion (I/R) induced by experimental elevation of IOP leads to damage and cell death in the different layers of the retina.

Among the signaling events downstream of the excitotoxic cascade, the three main classes of mitogen-activated protein kinases (MAPKs), extracellular signal-regulated kinase (ERK), p38 and the c-Jun N-terminal kinase (JNK) were reported to be increased after cerebral ischemia (Sugino et al. 2000; Wu et al. 2000) as well as in the retina (Peterson et al. 2000; Roth et al. 2003). The observation that JNK was activated in ischemic neurons highlighted its potential involvement in the apoptotic process following cerebral ischemia (Borsello et al. 2003).MAPKs activation has also been investigated in retinas after ischemia. Zhang et al. first made the observation that both JNK and p38 activation could be attenuated by ischemic preconditioning, suggesting that these two MAPKs were implicated in the deleterious effects induced by ischemia in the retina (Zhang et al. 2002).The use of D-JNKi provided a significant protection against neuronal loss after optic nerve crush in mice and in a model of retinopathy of prematurity (Tezel et al. 2004; Guma et al. 2009).

Here, we investigated the functional consequence of JNK activation *in Vitro* and *In vivo* and showed that JNK activity is a critical contributor to ischemic-induced retinal damages and that its inhibition resulted in the reduction of cell death.

90.2 Materials and Methods

90.2.1 Animal Handling and Surgery

All animal experiments were approved by the Veterinary Office of the State of Valais. The procedure to induce transient ischemia followed by reperfusion has previously been described (Produit-Zengaffinen et al. 2009). Animals were divided into a control and an I/R group. In the control group, rats were sham-operated by inserting a needle into in the anterior chamber of the left eye without elevation of the IOP. In the I/R group, the needle was introduced in the left eye and the pressure was increased. Animals were divided into a control and an I/R group. In the control group, rats were sham-operated by inserting a needle into in the anterior chamber of the l after reperfusion, rats were euthanized as described previously (Produit-Zengaffinen et al. 2009).

90.2.2 Cell Culture

In order to evaluate the consequences of hypoxia on 661W survival, cells were cultured in DMEM, 1 % FBS, 1 mM glucose and incubated for 48 h in normoxic (21 % O_2) or hypoxic (3 % O_2) incubators (Hypoxic Workstation Whitley H35).

90.2.3 ATPlite, LDH Assay, Western Blot Analysis

Cell survival, cell death and western blot analyses were performed as previously described. Anti-phospho JNK, anti-phospho cjun and anti-cjun were obtained from Cell Signaling Technology, anti-JNK was purchased from Santa Cruz Biotechnology.

90.2.4 Immunohistology

Eyes were fixed as previously described. Detection of apoptosis was performed using an in situ cell death detection kit (Roche Diagnostics). TUNEL staining was performed according to the manufacturer's instructions and images were viewed under a fluorescence microscope equipped with a digital camera using appropriate filters.

90.2.5 Statistic

Results are presented as mean ± standard error of the mean (SEM) of the indicated number of independent experiments. Statistical analysis was performed using Student's *t*-test. Differences were considered significant at p values of 0.05 or less.

90.3 Results

90.3.1 Hypoxia Decreased 661W Viability in vitro

We first examined the effect of hypoxia on cell viability. 661W cells cultured in hypoxia for 48 h were compared to cells cultured in normoxic conditions for the same period of time. After 48 h, 661W cells cultured in hypoxia showed a 50 % decrease in cell viability as demonstrated by ATPlite measurements: 1 vs. 0.5 ± 0.04, $p < 0.001$. This reduced viability could be attributed to an elevation in cell death induced by hypoxia as shown by LDH release measurements: 1 vs. 4.94 ± 1.3, $p < 0.05$.

90.3.2 661 W Cultured in Hypoxia Showed Increased JNK Activation

The effect of hypoxia on JNK activation was measured at the protein level by western blot. 661W cells cultured in hypoxic conditions for 48 h underwent a 2.5 fold increase in JNK activity (1 ± 0.2 vs. 2.59 ± 0.32, $p < 0.005$). The efficiency of JNK activity could be further visualized on c-jun phosphorylation, where hypoxia induced a similar increase in c-jun activity (1 vs. 1.8 ± 0.33, $p < 0.05$).

90.3.3 D-JNKi Prevented Hypoxia Induced Cell Death

We assessed the physiological relevance of JNK activation in the initiation of damages induced by the hypoxic stress. As ATPlite assay was not sensitive enough to measure D-JNKi effect on cell viability, we quantified hypoxia induced cell death in presence or absence of D-JNKi in living cells nuclei stained with propidium iodie (PI) and Hoechst. Cell death was increased about 8 folds after 48 h in hypoxia (1 vs. 7.7 ± 1.7, $p < 0.05$). A significant protective effect against cell death was obtained when cells were incubated in the presence of D-JNKi, ($p < 0.05$) (2.67 ± 0.73 vs. 7.7 ± 1.7 cell death in non-treated cells).

90.3.4 Retinal Ischemia Enhanced Apoptosis 24 h after Reperfusion

To evaluate whether this *in vitro* action was also effective *In vivo*, we analyzed the effect of I/R on retinal cell survival. In order to exclude any variation induced by the experimental method, we compared each measure to values obtained from anesthetized sham-operated rats. Twenty-four hours after reperfusion, TUNEL staining revealed a robust increase in the number of apoptotic cells in the innermost retinal layers, mainly in GCL and INL, and to a lower level, in the outer nuclear layer (ONL) (Fig. 90.1). Cells from the INL were the most sensitive to I/R (14.7% in apoptosis ± 1.3), whereas $3.8\% \pm 0.4$ of GCL and $3.7\% \pm 1.3$ of the cells within the ONL were in apoptosis. No TUNEL positive cells could be observed in the sham-operated retina. Increased apoptosis was paralleled with increased JNK phosphorylation (2.39 ± 0.18 vs. 1 ± 0.16, $p < 0.05$). This was confirmed by an increase activity of cjun visible by immunohistochemistry on retinal sections.

90.3.5 D-JNKi Reduced JNK Activation in Vivo

As increased apoptotic cells correlated with elevated pJNK, we further examined the significance of JNK activity on cell death induced by I/R. We injected serial concentrations of D-JNKi in the vitreous cavity of the eye, immediately after the

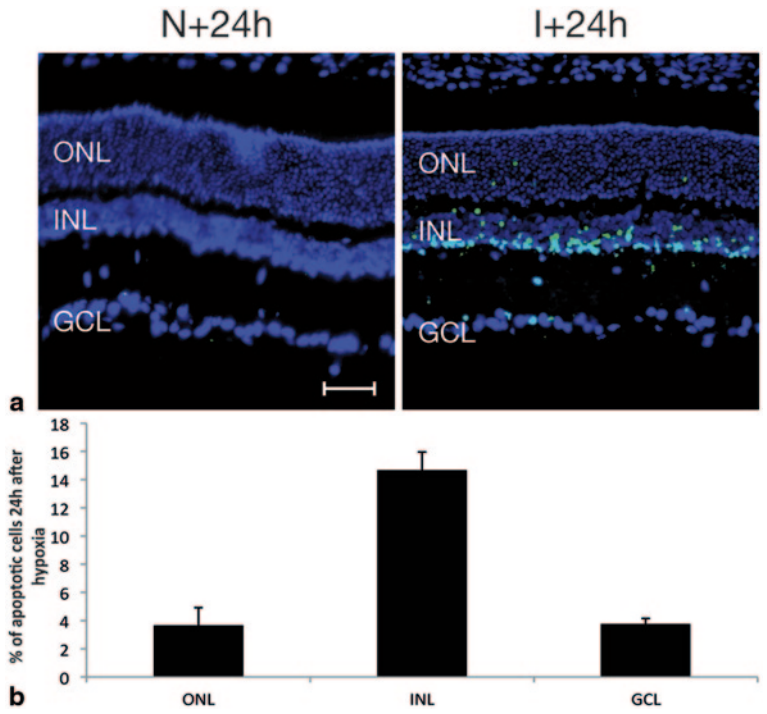

Fig. 90.1 Cell death after retinal ischemia. Retinal ischemia enhanced apoptosis 24 h after I/R. **a** TUNEL staining from sham-operated retina on the left and from I/R retina on the right, showed a robust increase in apoptosis in the GCL and INL from ischemic retina. **b** Quantification of TUNEL positive cells in the different layers of the retina. Scale bar 100 μM

1-h ischemic stress. D-JNKi was able to reduce JNK phosphorylation *In vivo* in a dose-dependent ability (1 ± 0.07 vs. 0.75 ± 0.18; 0.51 ± 0.15 and 0.52 ± 0.04 in non treated vs. D-JNKi 20 μdose-dependent ability (1 ± 0.07 vs. 0.75 ± 0.18; 0.51 ± 0.15 andificant at 500 μ dose-dependent 20 μM, 100 μM and 500 μM, respectively).

90.3.6 D-JNKi Prevented Retinal Ischemia-Induced Apoptosis 24 h after Reperfusion by Reducing the Activity of JNK

As shown in Fig. 90.2, the number of apoptotic cells within the INL was reduced by 33 % ($p < 0.05$) independently of the concentration of D-JNKi used (14.7 ± 1.3 vs. 7.9 ± 2.1; 10.1 ± 1.0 and 9.0 ± 1.1 in non treated eyes vs. D-JNKi 20 μ4.7 ± 1.3 vs. 7.9 ± 2.1; 10.1). In GCL, the number of apoptotic cells was also reduced by almost 30 %, probably in a dose-dependent manner, but was only statistically significant ($p < 0.05$) at the highest concentration of D-JNKi used (3.8 ± 0.4 vs. 2.3 ± 0.5; 2.1 ± 0.7 and 1.3 ± 0.7 in non treated vs. D-JNKi 20 μM, 100 μM and 500 μM treated eyes, respectively).

90.4 Discussion

In the present study, D-JNKi, a specific inhibitor of JNK activation, was evaluated for its ability to reduce hypoxic cell death and neuronal degeneration induced by I/R in the retina. In these two models, induction of cell death was mediated through the activation of JNK. Our results indicated that treatment with D-JNKi significantly protected hypoxic 661W cells from apoptosis. This protection was also observed *In vivo* in rat retina when D-JNKi was injected intravitreoulsy at the end of a 1-h I/R stress.

We and others previously showed that cell death programs are induced after I/R (Buchi 1992; Zhang et al. 2002; Produit-Zengaffinen et al. 2009). Recent studies have shown that cell death induced by I/R in the retina occurs through apoptosis (Rosenbaum et al. 1998; Zheng et al. 2007), necrosis (Buchi 1992; Dvoriantchikova et al. 2010) and, more recently, through necroptosis, a caspase-independent form of apoptosis (Rosenbaum et al. 2010).

Our results showed that 661W cells cultured in hypoxia have a significantly reduced cell viability, that was, at least in part, the result of JNK activation. Inhibition of JNK activation with D-JNKi significantly improved cell viability in response to hypoxia *in vitro*. We also established that D-JNKi was effective in a model of retinal

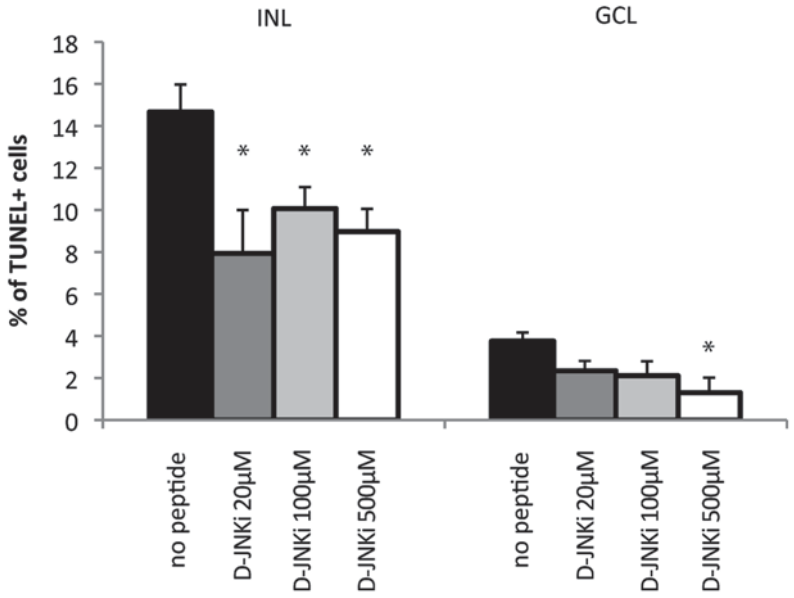

Fig. 90.2 D-JNKi effect on ischemia-induced cells death. The functional effect of D-JNKi was assessed by TUNEL staining on retinal section. Quantification of TUNEL positive cells vs. DAPI was performed in each retinal cell layer separately. Statistically significant neuroprotective effect of the inhibition of JNK activation was obtained in the INL ($p<0.05$) at each D-JNKi concentration tested and in the GCL ($p<0.05$) at 500 µM

ischemia *In vivo*, decreasing apoptosis within GCL, INL. We also demonstrated that the mechanisms induced *in vitro* by hypoxia were similar to that observed *In vivo*, which bestow new perspectives to study the molecular mechanisms induced by retinal ischemia.

Acknowledgments The authors wish to thank Nicole Gilodi for expert technical help and Dr Al-Ubaidi, Univ. of Oklahoma, for providing the 661W cells. This work was supported by a grant from the ProVisu Foundation.

References

Borsello T, Clarke PG, Hirt L et al (2003) A peptide inhibitor of c-Jun N-terminal kinase protects against excitotoxicity and cerebral ischemia. Nature Med 9:1180–1186

Buchi ER (1992) Cell death in the rat retina after a pressure-induced ischaemia-reperfusion insult: an electron microscopic study. I. Ganglion cell layer and inner nuclear layer. Exp Eye Res 55:605–613

Dvoriantchikova G, Barakat DJ, Hernandez E et al (2010) Liposome-delivered ATP effectively protects the retina against ischemia-reperfusion injury. Mol Vis 16:2882–2890

Guma M, Rius J, Duong-Polk KX et al (2009) Genetic and pharmacological inhibition of JNK ameliorates hypoxia-induced retinopathy through interference with VEGF expression. Proc Natl Acad Sci U S A 106:8760–8765

Peterson WM, Wang Q, Tzekova R et al (2000) Ciliary neurotrophic factor and stress stimuli activate the Jak-STAT pathway in retinal neurons and glia. J Neurosci 20:4081–4090

Produit-Zengaffinen N, Pournaras CJ, Schorderet DF (2009) Retinal ischemia-induced apoptosis is associated with alteration in Bax and Bcl-x(L) expression rather than modifications in Bak and Bcl-2. Mol Vis 15:2101–2110

Rosenbaum DM, Rosenbaum PS, Gupta H et al (1998) The role of the p53 protein in the selective vulnerability of the inner retina to transient ischemia. Investig Ophthalmol Vis Sci 39:2132–2139

Rosenbaum DM, Degterev A, David J et al (2010) Necroptosis, a novel form of caspase-independent cell death, contributes to neuronal damage in a retinal ischemia-reperfusion injury model. J Neurosci Res 88:1569–1576

Roth S, Shaikh AR, Hennelly MM et al (2003) Mitogen-activated protein kinases and retinal ischemia. Investig Ophthalmol Vis Sci 44:5383–5395

Sugino T, Nozaki K, Takagi Y et al (2000) Activation of mitogen-activated protein kinases after transient forebrain ischemia in gerbil hippocampus. J Neurosci 20:4506–4514

Tezel G, Yang X, Yang J et al (2004) Role of tumor necrosis factor receptor-1 in the death of retinal ganglion cells following optic nerve crush injury in mice. Brain Res 996:202–212

Wu DC, Ye W, Che XM et al (2000) Activation of mitogen-activated protein kinases after permanent cerebral artery occlusion in mouse brain. J Cere Blood Flow Metab 20:1320–1330

Zhang C, Rosenbaum DM, Shaikh AR et al (2002) Ischemic preconditioning attenuates apoptotic cell death in the rat retina. Investig Ophthalmol Vis Sci 43:3059–3066

Zheng L, Gong B, Hatala DA et al (2007) Retinal ischemia and reperfusion causes capillary degeneration: similarities to diabetes. Investig Ophthalmol Vis Sci 48:361–367

Chapter 91
Cell Fate of Müller Cells During Photoreceptor Regeneration in an *N*-Methyl-*N*-nitrosourea-Induced Retinal Degeneration Model of Zebrafish

Kazuhiro Ogai, Suguru Hisano, Kayo Sugitani, Yoshiki Koriyama and Satoru Kato

Abstract Zebrafish can regenerate several organs such as the tail fin, heart, central nervous system, and photoreceptors. Very recently, a study has demonstrated the photoreceptor regeneration in the alkylating agent *N*-methyl-*N*-nitrosourea (MNU)-induced retinal degeneration (RD) zebrafish model, in which whole photoreceptors are lost within a week after MNU treatment and then regenerated within a month. The research has also shown massive proliferation of Müller cells within a week. To address the question of whether proliferating Müller cells are the source of regenerating photoreceptors, which remains unknown in the MNU-induced zebrafish RD model, we employed a BrdU pulse-chase technique to label the proliferating cells within a week after MNU treatment. As a result of the BrdU pulse-chase technique, a number of $BrdU^+$ cells were observed in the outer nuclear layer as well as the inner nuclear layer. This implies that regenerating photoreceptors are derived from proliferating Müller cells in the zebrafish MNU-induced RD model.

K. Ogai (✉)
Wellness Promotion Science Center, Institute of Medial, Pharmaceutical and Health Sciences, Kanazawa University, 5-11-80 Kodatsuno, Kanazawa, Ishikawa 920-0942, Japan
e-mail: kazuhiro@staff.kanazawa-u.ac.jp

S. Hisano · K. Sugitani
Department of Clinical Laboratory Science, Graduate School of Medical Science, Kanazawa University, 5-11-80 Kodatsuno, Kanazawa, Ishikawa 920-0942, Japan
e-mail: ef.ef.soylatte.ts@gmail.com

K. Sugitani
e-mail: sugitani@staff.kanazawa-u.ac.jp

Y. Koriyama
Graduate School and Faculty of Pharmaceutical Sciences, Suzuka University of Medical Science, 3500-3 Minamitamagaki, Suzuka, Mie 513-8670, Japan
e-mail: koriyama@suzuka-u.ac.jp

S. Kato
Department of Molecular Neurobiology, Graduate School of Medical Science, Kanazawa University, 13-1 Takaramachi, Kanazawa, Ishikawa 920-8640, Japan
e-mail: satoru@med.kanazawa-u.ac.jp

C. Bowes Rickman et al. (eds.), *Retinal Degenerative Diseases,* Advances in Experimental Medicine and Biology 854, DOI 10.1007/978-3-319-17121-0_91

Keywords Zebrafish · Photoreceptor · Regeneration · Müller cells · *N*-methyl-*N*-nitrosourea (MNU) · Cell proliferation

91.1 Introduction

Retinal degeneration (RD) caused by photoreceptor cell death, including retinitis pigmentosa and age-related macular degeneration, is considered as a major cause for visual loss. It has been reported that at least 50 million individuals are suffering from these diseases (Lund et al. 2003), and the prevalence is increasing with the aging of society (Chakravarthy et al. 2010). In mammals, once photoreceptors are lost, they normally fail to regenerate. In contrast, fish show a tremendous regenerative capacity to offset the loss of photoreceptors (Fischer and Bongini 2010; Nagashima et al. 2013). Very recently, a study has demonstrated a reproducible and uniform method to create an RD model in zebrafish, in which fish were treated with an alkylating agent, *N*-methyl-*N*-nitrosourea (MNU) (Tappeiner et al. 2013). In this model, a wide and uniform photoreceptor cell loss was observed within a week after MNU treatment followed by photoreceptor regeneration within a month. As with other zebrafish RD models (e.g., intense light injury and stab wound models), a massive proliferation of Müller cells was generally observed to produce new photoreceptors following MNU treatment. In this study, we attempt to show the cell fate of proliferating Müller cells after MNU treatment to address the question "Are proliferating Müller cells indeed the source of regenerating photoreceptors?" using the 5-bromo-2′-deoxyuridine (BrdU) pulse-chase technique with the zebrafish MNU-induced RD model.

91.2 Materials and Methods

91.2.1 Animals

All experiments described below were approved by the Committee on Animal Experimentation of Kanazawa University, and all attempts were made to minimize pain and the number of fish used. Adult zebrafish (*Danio rerio*; 3–4 cm in body length, 6–12 months after birth, either sex) were used throughout this study. The fish were kept in water at 28 °C unless otherwise stated.

91.2.2 MNU Treatment

MNU treatment of zebrafish was performed as described previously (Tappeiner et al. 2013). In brief, fish were kept in water containing 10 mM phosphate buffer

(pH = 6.3) with a concentration of 150 mg/l of MNU (Toronto Research Chemicals Inc., North York, Canada) for 60 min. After exposure to MNU, fish were washed and kept in fresh water until appropriate time points.

91.2.3 Intraperitoneal Injection of BrdU

Fish were anesthetized by immersion in 0.033 % ethyl 3-aminobenzoate methanesulfonic acid (MS222; Sigma–Aldrich, MO, USA) in PBS, and intraperitoneally injected with 50 µl of 2.5 mg/ml BrdU (Sigma–Aldrich) at 0 (just after MNU treatment), 2, 4, 6, and 8 days post-treatment (dpt), as described previously (Ogai et al. 2012).

91.2.4 Preparing Retinal Sections

At appropriate time points, fish were euthanized by an overdose (0.1 %) of MS-222 for 10 min followed by fixation with 4 % paraformaldehyde in PBS overnight at 4 °C. The cryosections of the retina were then prepared at 12-µm thickness as described previously (Ogai et al. 2012).

91.2.5 Hematoxylin–Eosin (HE) Staining

HE staining was performed to observe the structure of the retina. Sections were stained with Mayer's hematoxylin (Wako Pure Chemical Industries, Osaka, Japan) for 2 min followed by washing and counterstaining with 1 % eosin-Y (Wako Pure Chemical Industries) for 2 min. The cleared sections were then observed using a bright-field microscope (DS-Fi1c; Nikon Instech, Tokyo, Japan).

91.2.6 Immunohistochemistry

The localization of proliferating cells was visualized by immunohistochemistry (Ogai et al. 2012). In brief, antigen retrieval was performed in 10 mM citrate buffer (pH = 6.0) for 5 min at 121 °C or 2 M HCl for 30 min at 37 °C for proliferating cell nuclear antigen (PCNA) or BrdU immunohistochemistry, respectively. Following washing and blocking, the sections were incubated with anti-PCNA (1:500; Sigma–Aldrich) or anti-BrdU (1:500; Sigma–Aldrich) antibody at 4 °C overnight. Visualization was performed with Alexa Fluor 488-conjugated secondary antibody (1:500; Thermo Fisher Scientific, MA, USA) for 60 min at 23 °C. Nuclear staining was performed by 2 µg/ml 4′,6-diamidino-2-phenylindole (DAPI; Wako Pure Chemical Industries). The sections were then observed using a fluorescent microscope (DS-Fi1c).

91.2.7 Statistical Analyses

The data were presented as means ± standard error of the mean. The thickness of outer nuclear layer (ONL) and the number of $PCNA^+$ cells were analyzed by one-way analysis of variance followed by Tukey's *post hoc* test using SigmaPlot (version 12; Systat Software, Inc., CA, USA). A p value of < 0.05 was considered statistically significant.

91.3 Results

91.3.1 MNU Treatment Selectively Depleted Outer Nuclear Layer (ONL) in Zebrafish Retina

First, to confirm the effect of MNU on the zebrafish retina, we obtained retinal sections at 0 (control), 3, 5, 8, 16, 24, and 32 dpt and stained using the HE method. As a result of MNU treatment, the collapse of ONL was observed from 3 to 8 dpt followed by a regeneration of ONL by 32 dpt (Fig. 91.1) in the same manner as previously reported (Tappeiner et al. 2013).

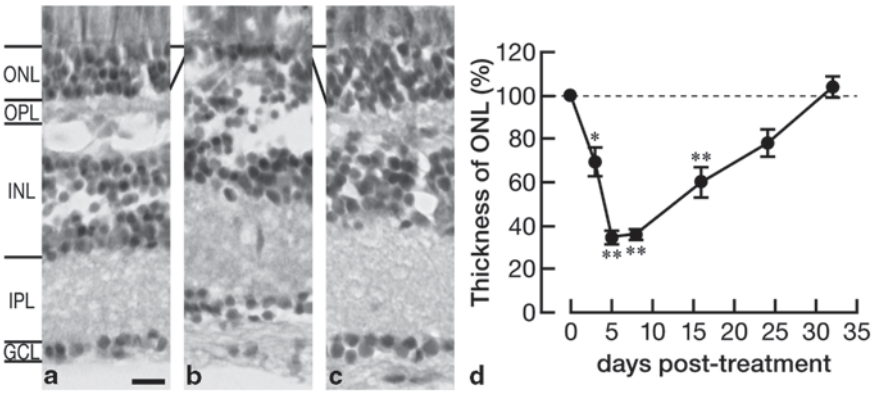

Fig. 91.1 Changes in outer nuclear layer (ONL) thickness after *N*-methyl-*N*-nitrosourea (MNU) treatment in adult zebrafish. (**a–c**) Representative images of Hematoxylin -Eosin staining following MNU treatment. At 8 days post-treatment (dpt), the thickness of ONL was significantly thinner (**b**) than control retina (**a**). The retinal structure at 32 dpt (**c**) was comparable to control retina (**a**). (**d**) Quantification of ONL thickness; $n = 3$ each, $^{*}p < 0.01$, $^{**}p < 0.001$. *OPL* outer plexiform layer, *INL* inner nuclear layer, inner plexiform layer, *GCL* ganglion cell layer. Scale bar in (**a**), 10 μm

91.3.2 MNU Treatment Induced Cell Proliferation in the Inner Nuclear Layer (INL) in Zebrafish Retina

Next, to show cell proliferation after MNU treatment, we stained the sections for PCNA at the same time points as in HE staining. As a result of PCNA staining after the MNU treatment, we observed a massive cell proliferation in INL, putatively Müller cells, within a week that peaked at 5 dpt (Fig. 91.2).

91.3.3 Regenerating Photoreceptors were Derived from Proliferating Müller Cells After MNU Treatment

Given that a massive cell proliferation was observed within a week after MNU treatment and photoreceptor regeneration took place from 10 to 30 dpt, we theorized that regenerating photoreceptors may originate from proliferating Müller cells. To test this theory, we injected BrdU at 0, 2, 4, 6, and 8 dpt (*pulse*) to label proliferating cells within 8 days after MNU treatment when the massive Müller cell proliferation was observed (Fig. 91.2). This was followed by BrdU detection at 32 dpt (*chase*; Fig. 91.3a) when ONL was reconstructed (Fig. 91.1). As a result of the BrdU pulse-chase experiment, we could see a number of $BrdU^+$cells in ONL, as well as INL at 32 dpt (Figs. 91.3b, 91.3c).

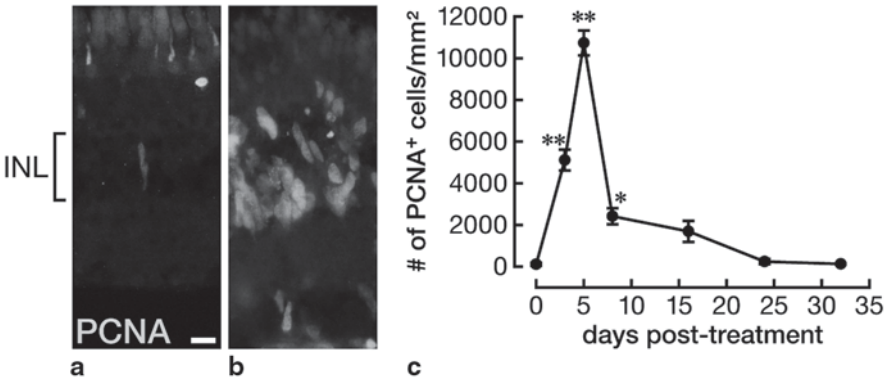

Fig. 91.2 Cell proliferation in zebrafish retina following MNU treatment. (**a**, **b**) Representative images of proliferating cell nuclear antigen (PCNA) immunohistochemistry. In control retina, few $PCNA^+$ cells were observed in INL (**a**), whereas a number of $PCNA^+$ cells were observed at 5 dpt (**b**). (**c**) Quantification of $PCNA^+$ cells after MNU treatment; $n=3$ each, $^{*}p<0.01$, $^{**}p<0.001$. Scale bar in (**a**), 10 μm

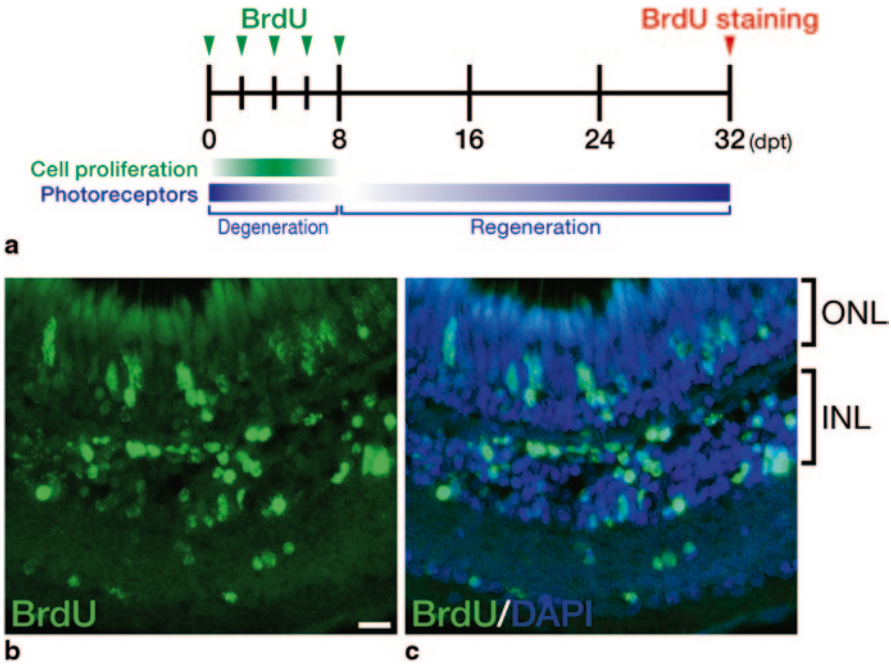

Fig. 91.3 Fate of proliferating cells following MNU treatment. (**a**) Experimental setup. At 0, 2, 4, 6, and 8 dpt, 5-bromo-2′-deoxyuridine (BrdU) was intraperitoneally injected to label proliferating cells during this period. At 32 dpt when the retinal structure was restored (Fig. 91.1), immunohistochemistry was performed against BrdU. (**b**, **c**) Representative images of BrdU immunohistochemistry. A number of $BrdU^+$ cells were observed in ONL as well as INL. Note that the retinal structure was comparable to control retina (Fig. 91.1a). Scale bar in (**b**), 10 μm

91.4 Discussion

Whether genetic or non-genetic (i.e., hereditary or acquired), RD can result in a serious visual loss, which damages the quality of life (Mitchell and Bradley 2006). By using a zebrafish RD model that is capable of regenerating lost photoreceptors, it may be possible to understand not only the degenerative but also the regenerative mechanisms underlying RD. Very recently, Tappeiner et al. (2013) proposed a novel RD model utilizing MNU in zebrafish. MNU has been widely used in RD research in rodents for more than a couple of decades (Smith et al. 1988; Koriyama et al. 2014). MNU can selectively, uniformly, reproducibly, and at any time kill photoreceptors in the retina, which makes it simpler to produce RD models than genetic and/or light-injury RD models (Fausett and Goldman 2006; Pennesi et al. 2012).

In this study, we showed that MNU could kill photoreceptors characterized by the reduction of ONL thickness and that a massive proliferation of Müller cells was observed after MNU treatment, which is consistent with the previous findings (Tappeiner et al. 2013), with a few exceptions. In a previous study, the cell count of ONL

significantly dropped only at 8 dpt, whereas in this study we observed a significant thinning of ONL from 3 to 15 dpt. This discrepancy may be explained by the difference in the method of ONL quantification. The previous study used the cell count of ONL, whereas in this study we used the thickness of ONL. Thinning of ONL occurs not only by cell loss, but also by the reduction of cell size and cell-to-cell distance. However, the cell size and the distance between cells after MNU treatment appeared comparable to that of the control retina (Figs. 91.1a–91.1c). Therefore, we can assume that photoreceptors were indeed lost in this study.

Another difference with the previous study is in time course of cell proliferation. Tappeiner et al. (2013) reported that cell proliferation in INL peaked at 8 dpt, whereas in this study cell proliferation was most active at 5 dpt (Fig. 91.2). At this point, it is difficult to explain the lag in cell proliferation. It is however certain that considerable and rapid proliferation of Müller cells occurs within a week after MNU treatment.

This study further showed that proliferating Müller cells may be a source of regenerating photoreceptors, as a number of $BrdU^+$ cells were observed in ONL as well as INL (Fig. 91.3). This implies that some of the proliferating Müller cells may migrate and differentiate into new photoreceptors (Nagashima et al. 2013), whereas others may remain Müller cells to maintain retinal stem-cell burden and retinal structure.

Notably, in mammalian MNU-induced RD models, Müller cell proliferation took place from 3 to 7 days after MNU treatment but showed no signs of photoreceptor regeneration (Taomoto et al. 1998). It is possible that the major difference in the ability of photoreceptor regeneration between fish and mammals may be laid in the ability of migration and/or differentiation into photoreceptors rather than Müller cell proliferation. Therefore, we hope that investigating such differences in the migration/differentiation abilities of Müller cells may add new insight into therapeutic advances in the treatment of RD in the future.

Acknowledgments This work was supported in part by JSPS KAKENHI Grant Number 25890007 and by the MEXT/JST Tenure Track Promotion Program.

References

Chakravarthy U, Evans J, Rosenfeld PJ (2010) Age related macular degeneration. BMJ 340:c981

Fausett BV, Goldman D (2006) A role for alpha1 tubulin-expressing Müller glia in regeneration of the injured zebrafish retina. J Neurosci 26:6303–6313

Fischer AJ, Bongini R (2010) Turning Müller glia into neural progenitors in the retina. Mol Neurobiol 42:199–209

Koriyama Y, Sugitani K, Ogai K et al (2014) Heat shock protein 70 induction by valproic acid delays photoreceptor cell death by N-methyl-N-nitrosourea in mice. J Neurochem 130(5): 707–719.

Lund RD, Ono SJ, Keegan DJ et al (2003) Retinal transplantation: progress and problems in clinical application. J Leukoc Biol 74:151–160

Mitchell J, Bradley C (2006) Quality of life in age-related macular degeneration: a review of the literature. Health Qual Life Outcomes 4:97

Nagashima M, Barthel LK, Raymond PA (2013) A self-renewing division of zebrafish Müller glial cells generates neuronal progenitors that require N-cadherin to regenerate retinal neurons. Development 140:4510–4521

Ogai K, Hisano S, Mawatari K et al (2012) Upregulation of anti-apoptotic factors in upper motor neurons after spinal cord injury in adult zebrafish. Neurochem Int 61:1202–1211

Pennesi ME, Neuringer M, Courtney RJ (2012) Animal models of age related macular degeneration. Mol Aspects Med 33:487–509

Smith SB, Hashimi W, Yielding KL (1988) Retinal degeneration in the mouse induced transplacentally by N-methyl-N-nitrosourea: effects of constant illumination or total darkness. Exp Eye Res 47:347–359

Taomoto M, Nambu H, Senzaki H et al (1998) Retinal degeneration induced by N-methyl-N-nitrosourea in Syrian golden hamsters. Graefes Arch Clin Exp Ophthalmol 236:688–695

Tappeiner C, Balmer J, Iglicki M et al (2013) Characteristics of rod regeneration in a novel zebrafish retinal degeneration model using N-methyl-N-nitrosourea (MNU). PLoS ONE 8:e71064

Chapter 92
Polymodal Sensory Integration in Retinal Ganglion Cells

David Križaj

Abstract An animal's ability to perceive the external world is conditioned by its capacity to extract and encode specific features of the visual image. The output of the vertebrate retina is not a simple representation of the 2D visual map generated by photon absorptions in the photoreceptor layer. Rather, spatial, temporal, direction selectivity and color "dimensions" of the original image are distributed in the form of parallel output channels mediated by distinct retinal ganglion cell (RGC) populations. We propose that visual information transmitted to the brain includes additional, light-independent, inputs that reflect the functional states of the retina, anterior eye and the body. These may include the local ion microenvironment, glial metabolism and systemic parameters such as intraocular pressure, temperature and immune activation which act on ion channels that are intrinsic to RGCs. We particularly focus on light-independent mechanical inputs that are associated with physical impact, cell swelling and intraocular pressure as excessive mechanical stimuli lead to the counterintuitive experience of "pressure phosphenes" and/or debilitating blinding disease such as glaucoma and diabetic retinopathy. We point at recently discovered retinal mechanosensitive ion channels as examples through which molecular physiology brings together Greek phenomenology, modern neuroscience and medicine. Thus, RGC output represents a unified picture of the embodied context within which vision takes place.

Keywords Vision · Mechanosensation · Greek philosophy · Calcium · TRPV4 · Glaucoma · Phosphenes

D. Križaj (✉)
Departments of Ophthalmology & Visual Sciences, John A. Moran Eye Institute and Neurobiology & Anatomy, Univ. of Utah School of Medicine, Salt Lake City, UT 84132, USA
e-mail: david.krizaj@hsc.utah.edu

C. Bowes Rickman et al. (eds.), *Retinal Degenerative Diseases,* Advances in Experimental Medicine and Biology 854, DOI 10.1007/978-3-319-17121-0_92

92.1 Introduction

Life took advantage of light early on in the evolutionary process as photons were harnessed to drive the cells' energy metabolism through early photosystems and antenna complexes (Land and Nilsson 2012). Because light is also the fastest possible way of transmitting information about the physical environment, in many, perhaps most, vertebrate species, vision emerged as a dominant sensory modality that is essential for orientation within, and communication with, the outside world. The competitive advantages of vision sparked numerous designs of light-detecting pigments, cells and organs, culminating in the arthropod compound eye and the camera-styled eyes and layered retinas of jawed vertebrates (Gehring 2004). The success of the vertebrate retinal design owes much to modular organization of retinal circuits and their adaptability to the demands posed by the variety of ecological niches. At each stage of visual signal transmission, information percolating through retinal circuits appears in the form of increasingly refined aspects of the primary photoreceptor 'bitmap' associated with the space, time, color, direction and movement "dimensions" of the visual stimulus (Masland 2005). However, every level of visual processing might also be impacted by signals that are independent of light. RGCs, for example, may acquire additional inputs from circadian feedback, intraocular pressure (IOP), cardiovascular function and the immune system but may also directly respond to light (Anderson et al. 2010; Xue et al. 2011; He et al. 2012; Della Santina et al. 2013). I thus propose that vision represents an embodied sensory process that integrates information about ambient photons within the complex Gestalt of the entire body.

92.2 Intraocular Pressure, Mechanical Overstimulation and Glaucoma

Every cell is impacted by mechanical stimuli that are inherent in tissue development and/or are contributed by its environment (Nagatomi 2011; Tyler 2012). The response to mechanical forces is conditioned by the types of (compressive, tensile, shear flow) forces and by (cell type-specific) molecular sensors and signaling pathways. Chronic force stimulation can compromise both function and survival of retinal tissue which is softer from tissues that surround it and consequently stretches more when exposed to mechanical strain (e.g., Krizaj et al. 2014). Thus, firing properties and viability of RGCs are impacted by tensile stretch associated with elevations in IOP (Della Santina et al. 2013; El Danaf et al. 2015). If sustained, elevated IOP increases the risk of neurodegeneration and blindness due to developing glaucoma (Bonomi et al. 2001) whereas excessive swelling can compromise RGC viability in diabetic retinopathy and glaucoma (Reichenbach and Bringmann 2010; Pinar-Sueiro et al. 2011). Because other retinal neurons appear to be less susceptible to mechanical stress, RGCs must selectively express pressure-sensitive mechanism(s) the identification of which has been one of the great challenges of contemporary vision research. Interestingly, these very features inherent in the biology of RGCs might have inspired the first known theories of vision.

92.3 Early Theories of Vision are Based on Mechanically Induced Percepts of Light

The phenomenological experience of visual percepts triggered by mechanical indentation of the eye may have inspired the earliest forms of human art (Lewis-Williams and Dowson 1988) and laid the foundation for the earliest known theories of vision and physiology/medicine (Theophrast 1964; Grüsser and Hagner 1990; Gross 1999; Waterfield 2000). The *physiologos* (writer on nature) Alcmaeon of Croton (~450 B.C.) described the optic nerves, proposed they represented the "light-bearing paths" to the brain, identified the brain as the central sensory organ and the seat of understanding, and suggested that sensation allows humans to make reasonable judgments about the external world (tekmairesthai) (Celesia 2001; Huffman 2008). Alcmaeon was the first to report that application of physical pressure to the eye induces perception of light, and used the experience of mechanically induced visual phenomena ("pressure phosphenes") to conclude that vision is based on the transmission of light (fire) within the eye (Beare 1906). [Phosphenes, also called "the prisoner's cinema", are often perceived by people deprived of visible light for prolonged periods of time, meditators, patients with migraine headaches and are used to diagnose the inflamed optic nerve (optic neuritis) (Tyler 1978). Their molecular mechanism is not understood].

As eloquently described in the review by Grüsser and Hagner (1990), another Pythagorean, Empedocles (419–430 B.C.), hypothesized that light is reflected into the eye from objects in the external world and that the eye has two channels that conduct dark and pale impressions towards the brain (i.e., phenomenological analogs of retinal ON and OFF channels). The visual extramission theory was refined by Plato (427−347 B.C.), whose theory, involving complicated interactions between external light and projected light, dominated Western views on vision well into the eighteenth century (Waterfield 2000). Morgagni and Helmholtz suggested that mechanical stimulation of the eye gives rise to visual rather than other (tactile) sensations because of the hard-wired connections to the brain (Gross 1999; Grüsser and Hagner 1990), however the physiological mechanism that drives phosphene generation has never been elucidated. Is it possible that mechanotransducers that subserves phosphene generation corresponds to the pressure-sensitive mechanisms that compromise the viability of RGCs in glaucoma?

92.4 Mechanical Stimuli Drive RGC Physiology Through Mechanosensitive Channels

Mechanosensing ion channels can detect the effects of gravity, sound waves, muscle stretch, acceleration, shear flow, swelling and blood pressure (Kung 2005; Tyler 2012). Sensory stimuli transduced by some of the 28 vertebrate homologs of the Drosophila light-transducing TRP (transient receptor potential) channel include osmotic gradients, mechanical touch, taste, pain, temperature and certain aspects of

hearing/vestibular function (Kung 2005; Sachs 2009). One isoform, TRPV4, is also the closest vertebrate homolog of Inactive and Nanchung—mechanosensitive TRPs that are essential for hearing in *Drosophila* and is expressed in mechanosensitive neurons that include cochlear hair cells, Merkel cells and sensory ganglia (Everaerts et al. 2010). Accordingly, TRPV4$^{-/-}$ mice exhibit mechanical hyperalgesia and behavioral reduction in response to noxious mechanical stimuli and increased mechanosensory thresholds of serosal and mesenteric afferent fibers whereas gain-of-function mutations result in severe dysplasias and neuropathies (Liedtke et al. 2003; Loukin et al. 2010; Zimon et al. 2010). TRPV4 is important for the development of the eye (Wang et al. 2007) and is expressed in both anterior and posterior ocular tissues. Interestingly, TRPV4 expression in the retina is confined to RGCs and glial cells (Krizaj et al. 2014; Ryskamp et al. 2014a; 2015). Either mechanical stimulation or exposure to TRPV4 agonists elicited >100-fold increase in RGC excitability but, when in excess, induced RGC apoptosis and astrogliosis. Consistent with the etiology of glaucoma, genetic ablation of the channel strongly attenuated the RGC response to mechanical stimulation whereas TRPV4 overstimulation spared photoreceptors, bipolar cells and amacrine cells (Ryskamp et al. 2011, 2014a). Thus, by acting as sensors for mechanical stress, TRPV4 channels impel upon retinal output an intrinsic sensitivity to mechanical forces (Krizaj et al. 2014, Ryskamp et al. 2015). In addition to force, TRPV4 is polymodally activated by temperature, endocannabinoids and cell swelling (Everaerts et al. 2010), suggesting that RGCs are likely to use these channels to sense and respond to a wide array of thermal, chemical and mechanical stimuli. The overall picture is complicated by the fact that the RGCs express many different types of TRP channels, which are likely to intercept further facets of the sensory world. For example, canonical TRPC6/7 channels transduce light in ipRGCs (Xue et al. 2011) whereas activation of the TRPV1 nociceptor by endocannabinoids may regulate RGC excitability, interactions with G protein-coupled cannabinoid receptors and calcium homeostasis. (Ryskamp et al. 2014b).

92.5 Conclusion: What is "Seeing?"

In what was one the first connectomics attempts, Sidney Brenner and his colleagues in 1980s heroically reconstructed the nervous system of the nematode *Caenorhabditis elegans* with the expectation that the collage of several thousands of serial EMs will help explain the behavior of the humble worm (White et al. 1986). It turned out that the painstaking work failed to illuminate the biology of *C. elegans* behavior, which is dependent on higher-order interactions between neuronal circuits that mediate sensation, appetitive behavior, locomotion etc. Similar questions plague the modern proponents of connectomics (Seung 2012). We argue that vertebrate vision involves complex physiological operations that deconstruct the original visual map and merge light-induced signals with systemic information. In consequence, the RGC signal, which represents an integration of time-dependent primary and modulatory information, will show itself as a distorted (or rather, informationally

enhanced) output that is likely to frustrate attempts at computational clarity. In any case, the significance of non-visual inputs for daily visual function in diurnal vertebrates remains an exciting challenge for further research. Are they epiphenomena such as pressure phosphenes? Does mechanotransduction contribute to perception? The vertebrate retina is not a camera that translates images into 2D negatives, nor is it Adobe Photoshop that can perform a myriad filtering operations regardless of the machine that powers. Rather, I propose that the retina integrates electrical/cellular signals induced by the absorption of photons with a myriad of intrinsic cellular processes that reflect the circadian, metabolic, age-dependent etc. state of the organism. Because the perceiver's access to visual data streams depends on specific context-dependent circumstances that may include the time of day and bodily state. Perhaps we should view vision as an emergent process that rapidly defeats simplistic quests for mathematic tractability—one that is possessed of an intrinsic sensitivity to the present moment inhabited by the entire organism.

Acknowledgements Supported by the National Institutes of Health, Department of Defense, Glaucoma Research Foundation, HHMI, University of Utah, State of Utah TCIP, the University of Utah Neuroscience Initiative and an unrestricted grant from Research to Prevent Blindness to the Moran Eye Institute at the University of Utah.

References

Anderson DH, Radeke MJ, Gallo NB et al (2010) The pivotal role of the complement system in aging and age-related macular degeneration: hypothesis re-visited. Prog Retin Eye Res 29:95–112

Beare JI (1906) Greek theories of elementary cognition. From Alcmaeon to Aristotle. Clarendon, Oxford

Bonomi L, Marchini G, Marraffa M et al (2001) The relationship between intraocular pressure and glaucoma in a defined population. Ophthalmologica 215:34–38

Celesia GC (2001) Alcmaeon of Croton's observations on health, brain, mind and soul. J Hist Neurosci 21:409–426

Della Santina L, Inman DM, Lupien CB et al (2013) Differential progression of structural and functional alterations in distinct retinal ganglion cell types in a mouse model of glaucoma. J Neurosci 33:17444–17457

El-Danaf RN, Huberman AD (2015) Characteristic patterns of dendritic remodeling in early-stage glaucoma: evidence from genetically identified retinal ganglion cell types. J Neurosci 35(6):2329–2343

Everaerts W, Nilius B, Owsianik G (2010) The vanilloid transient receptor potential channel TRPV4: from structure to disease. Prog Biophys Mol Biol 103:2–17

Gehring WJ (2004) Historical perspective on the development and evolution of eyes and photoreceptors. Int J Dev Biol 48:707–717

Gross CG (1999) Brain, vision, memory: tales in the history of neuroscience. MIT Cambridge, Mass

Grüsser OJ, Hagner M (1990) On the history of deformation phosphenes and the idea of internal light generated in the eye for the purpose of vision. Doc Ophthalmol 74:57–85

Grüsser OJ, Grüsser-Cornehis U, Kusel U et al (1989) Responses of retinal ganglion cells to eyeball deformation: a neurophysiological basis for "pressure phosphenes". Vision Res 29:181–194

He Z, Nguyen CT, Armitage JA et al (2012) Blood pressure modifies retinal susceptibility to intraocular pressure elevation. PLoS ONE 7:e31104

Huffman C (2008) “Alcmaeon”, The Stanford Encyclopedia of Philosophy, Stanford University Press
Križaj D, Ryskamp DA, Tian N et al (2014) From mechanosensitivity to inflammatory responses: new players in the pathology of glaucoma. Curr Eye Res 39:105–119
Land MF, NIlsson DE (2012) Animal eyes. Oxford University Press
Lewis-Williams JD, Dowson TA (1988) The signs of all times: entoptic phenomena in upper palaeolithic art. Curr Anthropol 29:201–245
Liedtke W, Friedman JM, Liedtke W et al (2003) Abnormal osmotic regulation in trpv4-/- mice. Proc Natl Acad Sci U S A 100:13698–13703
Loukin SH, Zhou X, Su Z et al (2010) Wild-type and brachyolymia-causing mutant TRPV4 channels respond directly to stretch force. J Biol Chem 285:27176–27181
Masland RH (2005) Sensory systems: fine-tuning the visual scene. Curr Biol 15:R808–R810
Nagatomi J (2011) Mechanobiology handbook. CRC, Taylor and Francis Group, Boca Raton
Nilius B, Owsianik G (2010) Transient receptor potential channelopathies. Pflugers Arch 460:437–450
Pinar-Sueiro S, Urcola H, Rivas MA et al (2011) Prevention of retinal ganglion cell swelling by systemic brimonidine in a rat experimental glaucoma model. Clin Experiment Ophthalmol 39:799–807
Reichenbach A, Bringmann A (2010) Muller cells in the healthy and diseased retina. Springer
Ryskamp DA, Witkovsky P, Barabas P et al (2011) The polymodal ion channel transient receptor potential vanilloid 4 modulates calcium flux, spiking rate, and apoptosis of mouse retinal ganglion cells. J Neurosci 31:7089–7101
Ryskamp DA, Frye NA, Macaulaey N et al (2014a) Swelling and eicosanoid metabolites differentially gate TRPV4 channels in retinal neurons and glia. J Neurosci 34:15689–15700
Ryskamp DA, Jo AO, Redmon SN et al (2014b) TRPV1 and Endocannabinoids: emerging molecular signals that modulate mammalian vision. Cells 3:914–938
Ryskamp DA, Iuso A, Krizaj D (2015) TRPV4 channels link volume regulation, calcium homeostasis and inflammatory signaling in the retina. Channels 9:70–72
Seung S (2012) Connectome: how the brain’s wiring makes us who we are. Mifflin Harcourt Trade, Houghton
Theophrast (1964) ‘De sensu’ transl. by G.M. Stratton, London: G. Allen and Unwin. 1917. Reprint Amsterdam: E.J. Bonset
Tyler CW (1978) Some new entoptic phenomena. Vis Res 18:1633–1639
Tyler WJ (2012) The mechanobiology of brain function. Nat Rev Neurosci 13:867–878
Wang Y, Fu X, Gaiser S et al (2007) OS-9 regulates the transit and polyubiquitination of TRPV4 in the endoplasmic reticulum. J Biol Chem 282:36561–36570
Waterfield R (2000) The first philosophers. Oxford University Press, UK
White JG, Southgate E, Thomson JN et al (1986) The structure of the nervous system of the nematode Caenorhabditis elegans. Philos Trans R Soc Lond B Biol Sci 314:1–340
Xue T, Do MT, Riccio A et al (2011) Melanopsin signalling in mammalian iris and retina. Nature 479:67–73
Zimoń M, Baets J, Auer-Grumbach M et al (2010) Dominant mutations in the cation channel gene transient receptor potential vanilloid 4 cause an unusual spectrum of neuropathies. Brain 133:1798–1809

Chapter 93
Pigment Epithelium-Derived Factor, a Protective Factor for Photoreceptors *in Vivo*

Federica Polato and S. Patricia Becerra

Abstract Pigment epithelium-derived factor (PEDF) is a natural protein of the retina with demonstrable neurotrophic properties, found in the interphotoreceptor matrix in intimate contact with photoreceptors. This review summarizes the effects of PEDF on photoreceptors in several animal models of retinal degeneration.

Keywords PEDF · Retinal degeneration · Neuroprotection · Photoreceptor · Animal models

93.1 Introduction

Pathological photoreceptor cell death leads to visual loss. Therefore natural inhibitors of cell death can prevent this pathology. PEDF is a natural ocular protein, secreted by the retinal pigment epithelium (RPE). The RPE expresses the *SERPINF1* gene at higher levels compared to the other tissues in the eye, and releases the gene product in a directional fashion into the interphotoreceptor matrix (Becerra et al. 2004). In this extracellular matrix, the protein associates with glycosaminoglycans and becomes available to interact with receptors on the surface of the photoreceptors. PEDF is a member of the serpin superfamily formed by a group of proteins that share common conformation. Although most of the serpin members are serine protease inhibitors, PEDF is grouped with non-inhibitory serpins (Becerra 2006). Its homologous reactive center loop peptide, located towards its carboxy-end, is not used to block protease activity. However, a peptide region from its amino terminal sequence is responsible for neurotrophic effects, which in the 3D structure is distinct

F. Polato (✉) · S. P. Becerra
Section of Protein Structure and Function, Laboratory of Retinal Cell and Molecular Biology, NEI, National Institutes of Health, NIH-NEI BG.6. Room 134. 6 Center Drive MSC 0608, Bethesda, MD 20892-0608, USA
e-mail: polatof@mail.nih.gov

S. P. Becerra
e-mail: becerras@nei.nih.gov

C. Bowes Rickman et al. (eds.), *Retinal Degenerative Diseases,* Advances in Experimental Medicine and Biology 854, DOI 10.1007/978-3-319-17121-0_93

from the homologous serpin reactive loop. The neurotrophic effects of PEDF are independent of its capacity to inhibit serine proteases and depend on interactions with cell-surface receptors. PEDF-R is a cytoprotective receptor for PEDF encoded by the *PNPLA2* gene (patatin like phospholipase A2 family member) that is expressed in the retina and distributed in the inner segments of photoreceptors (Notari et al. 2006; Becerra and Notario 2013; Subramanian et al. 2013). Interactions with PEDF-R are likely to mediate the cytoprotective effects of PEDF in photoreceptors. The efficacy of PEDF in protecting photoreceptor cells against degeneration and apoptosis *in vivo* is reviewed here.

93.2 Biological Function

The PEDF protein exhibits neurotrophic activity and acts on photoreceptor morphogenesis, retinal neuroprotection and neurite outgrowth (Barnstable and Tombran-Tink 2004). The capacity of PEDF to delay photoreceptor cell degeneration and apoptosis is demonstrated in genetic and light-induced damage animal models. PEDF can protect cells of the inner retina and retinal ganglion cell layer from death induced by ischemia and cytotoxic agents. It is also protective of CNS neurons, such as motoneurons, cerebellar granule cells, hippocampal neurons, and cortical neurons, and has demonstrable neurite-outgrowth activities. Here we summarize the effects of PEDF on photoreceptor cells *in vivo* (see also Table 93.1).

93.2.1 The rd1/rd1 Mouse

The *rd1* mouse is an animal model for one variant of recessive human Retinitis Pigmentosa (RP) that carries a homozygous loss of function mutation of the gene encoding the β-subunit of rod photoreceptor cGMP phosphodiesterase 6 (PDE6). The mutation induces cell death of rod photoreceptors, which starts around postnatal day 10 (P10), peaks at P14, and ends almost completely by P21. Cone photoreceptor death starts around P15, with complete degeneration within 6 months (Sancho-Pelluz et al. 2008). Cayouette et al. (1999) evaluated the effects of human recombinant PEDF (rPEDF) in this animal model. *rd1* mice were intravitreally injected with 1 μg rPEDF in one eye at P14. Their contralateral eyes were similarly injected with rβ-galactosidase (1 μg) or left uninjected and used as controls. Photoreceptor degeneration was evaluated 3 or 9 days after administration. At 3 days post-injection (p.i.), the effect of a single PEDF injection on the outer nuclear layer (ONL) height was significant at 120–161 % that of controls. However, the authors did not observe an effect at 9 days p.i. They found that biotin-conjugated PEDF injected in the vitreous of wild type mice cleared from the eye within 24 h, suggesting a transient effect of the injected protein to maintain photoreceptor morphology in *rd1* mice.

Table 93.1 The effects of PEDF on photoreceptor degeneration *in vivo*

Animal model	Genetic or induced damage	Photoreceptor course of degeneration	Method and time of PEDF delivery	Effect of treatment, method and timing for assay	References
rd1 (m)	Loss of function mutation of photoreceptor β-*Pde6B* gene	Rods: start at P10, peak at P14, end at ~ P21. Cones: start at P15, end by 6 months	Intravitreal injection of human rPEDF (1 μg) protein at P14	Thicker ONL; reduced number of TUNEL positive cells at 3 days p.i. (P17)	(Cayouette et al. 1999)
Rds (m)	Null mutation of *Prph2* (Peripherin 2)	Photoreceptors: start at P14, peak after 3 weeks. Complete loss by 12 months	Intravitreal injection of human rPEDF (1 μg) protein at P17	Reduced number of TUNEL positive cells at 3 days p.i. (P20)	(Cayouette et al. 1999)
DKO *rd8* (m) $Ccl2^{-/-}Cx3cr1^{-/-}Crb1^{rd8}$	Constitutive deletion of the *Ccl2* chemokine and *Cx3cr1* chemokine receptor in $Cbr1^{rd8}$ background mice	Photoreceptor degeneration at 6 post-natal weeks	Intravitreal injection of human rPEDF (1 μg) protein at 6 weeks; subconjuctival injection of rPEDF (3 μg) 4 weeks after	Thicker ONL; reduced number of TUNEL positive cells; decreased expression of FasL and Bax; increased expression of Bcl-2 (2 months after the last injection)	(Wang et al. 2013)
RCS (r)	Loss of function mutation of RPE *Mertk* gene	Photoreceptor degeneration between P20 and P60	Subretinal injection of lentiviral SIV-PEDF (human) in 3 weeks old rat	Thicker ONL; reduced loss of photoreceptors (at 2, 8–12 weeks p.i.); decreased TUNEL-positive cells at 2 and 4 weeks p.i.; rescue of functionality (ERG at 4 and 8 weeks p.i.)	(Miyazaki et al. 2003; Murakami et al. 2008)
RCS (r)	Loss of function mutation of RPE *Mertk* gene	Photoreceptor degeneration between P20 and P60	Intravitreal injection of PEDF (2.5 μg)-NP at P21	Thicker ONL; reduced loss of photoreceptors and TUNEL-positive cells (at 4–8 weeks p.i.); rod-opsin expression preserved and rescue of functionality by ERG (at 8 weeks p.i.)	(Akiyama et al. 2012)

Table 93.1 (continued)

Animal model	Genetic or induced damage	Photoreceptor course of degeneration	Method and time of PEDF delivery	Effect of treatment, method and timing for assay	References
Sprague-Dawley rats (r)	Light damage (LD): constant light (CL) exposure (1200–1500 lux) for 3, 7, 10, 14 days	Reduction of ONL thickness (~70%) and null ERG response after 7 days of CL exposure	Intravitreal injection of PEDF (2 μg) or PEDF/bFGF (1 μg/each) in 2–5 month-old rats, at 1 and 2 days pre LD and 0, 1 and 2 days post LD	Thicker ONL; improved ERG response (CL for 3, 7, 10 days)	(Cao et al. 1999)
Lewis rats (r)	Light damage (LD): constant light (CL) exposure (2500 lux) for 24, 96, 168 h	Progressive reduction of ONL thickness and number of photoreceptors after 24, 96 and 168 h of CL exposure	Intravitreal injection of PEDF-expressing or null adenoviral vector (AdPEDF.11 or AdNull.11) 3 days before LD	Thicker ONL; reduced loss of photoreceptors (LD for 96 h) and TUNEL-positive cells (LD for 12 h); improved functionality by ERG (LD for 48 h, recovery 7–28 days)	(Imai et al. 2005)

93.2.2 The rds/rds Mouse

The antiapoptotic effects of rPEDF on photoreceptors were tested in another model for RP, the *rds* mouse, which carries a null mutation in the *Prph2* (peripherin 2) gene (Sancho-Pelluz et al. 2008). In *rds* homozygous mutant mice, retinal degeneration starts at P7 and peaks 3 weeks after birth. Photoreceptors degenerate slowly as compared to *rd1* mice and retinal rod and cone cells are completely lost by 12 months of age (Sanyal et al. 1980). *Rds* mice were intravitreally injected in one eye with human rPEDF (1 μg) at P17 while the contralateral eye, used as a control, was left untreated or administered with rβ-galactosidase (1 μg). The eyes were then collected 3 days p.i. (*i.e.*, P20) to evaluate apoptosis in the ONL. The protective effect of PEDF on photoreceptor apoptosis was significant, with less TUNEL-positive nuclei in the ONL, between 61.5–79.8 % of control eyes, confirming the antiapoptotic activity of PEDF on photoreceptors *in vivo* (Cayouette et al. 1999).

93.2.3 The DKO rd8 Mouse

The *Ccl2/Cx3cr1* double knockout mouse on *Crb1*^{rd8} background (DKO *rd8*) represents a model for progressive focal retinal degeneration, recapitulating some of the features of age-related macular degeneration (AMD), such as RPE alteration, photoreceptor degeneration, immune activation and A2E elevation in the RPE. The mouse was generated by knocking out genes for a chemokine (*Ccl2*) and a chemokine receptor (*Cx3cr1*) created on the C57BL/6N background carrying the *Crb1*^{rd8} mutation (Chu et al. 2013). By 6 weeks of age, all DKO mice show AMD-like retinal lesions, including RPE alteration and photoreceptor degeneration (Chu et al. 2013). Wang et al. (2013) reported that the concentration of PEDF secreted in the conditioned media of primary DKO *rd8* RPE was 84 % decreased relative to wild type (WT). Recombinant human PEDF protein (1 μg) was exogenously administered to 6 week-old DKO *rd8* by intravitreous injection in the right eye, with a subsequent subconjuctival rPEDF (3 μg) injection 4 weeks later. Contralateral eyes were left untreated and used as controls. Four weeks after the last injection, PEDF-mediated protection was observed in the ONL with more than 2-fold reduction of the number of TUNEL-positive nuclei along with increased ONL thickness and significantly lower levels of A2E in the retina in the rPEDF-treated compared to the contralateral eye. The authors also reported reduction in the expression of pro-apoptotic factors such as FasL and Bax, and increased expression of the anti-apoptotic factor Bcl-2 in the retina (Wang et al. 2013).

93.2.4 The RCS Rat

The Royal College of Surgeons (RCS) rat is the first known model of inherited retinal degeneration. Similar to the human disease (Gal et al. 2000), the cause of retinal

degeneration in the RCS rats is a mutation in the receptor tyrosine kinase *Mertk,* (D'Cruz et al. 2000), a gene that is expressed in the RPE. The mutation leads to defective RPE phagocytosis of photoreceptor outer segments followed by progressive loss of photoreceptor cells, which degenerate between P20 and P60 (Mullen and LaVail 1976). Miyazaki et al. (2003) evaluated the effects of PEDF in the retina of RCS rats. Exogenous PEDF was delivered by gene transfer, via subretinal injection of the simian lentiviral vector (SIV) containing the human *SERPINF1* gene in 3-week-old RCS rats. Control animals were left untreated or injected with either SIV-LacZ or vehicle solution. The expression of transduced genes was observed in the RPE at 4 weeks p.i. and persisted at later time points (8, 12, 24 weeks p.i.). Similarly, the number of photoreceptors was preserved in the PEDF-injected eyes, only 4 weeks after gene transduction. The protection was significant compared to control eyes at 8 and 12 weeks. However, the ONL regions furthest from the PEDF injection sites displayed the least protection. The antiapoptotic effect of PEDF is likely responsible for protection from photoreceptor loss in this model, as evidenced by diminished numbers of TUNEL positive nuclei in the ONL of PEDF-transduced eyes relative to controls. PEDF-mediated rescue of the photoreceptors was evaluated by TUNEL assay 4 weeks after the injection, showing that PEDF-treated eyes had reduced numbers of apoptotic photoreceptors compared to controls. Retinal function was also assayed by ERG at 4 and 8 weeks p.i. The authors showed that 8 week-old RCS rats had almost no ERG response; however, PEDF treatment significantly improved the retinal functionality at 4 and 8 weeks after the injection. In conclusion, the gene transfer of human *SERPINF1* in the RPE via lentiviral vectors results in the protection of photoreceptors from death and delayed degeneration in RCS rats (Miyazaki et al. 2003).

The same group (Murakami et al. 2008) showed that the lentivirus-mediated retinal gene transfer of PEDF in RCS rats prevented the nuclear translocation of apoptosis-inducing factor (AIF), resulting in reduced apoptotic loss of their photoreceptors and up-regulated *Bcl-2* expression. They claimed that inhibiting the nuclear translocation of AIF is an essential mechanism of the protective activity of PEDF in this rat model.

The preventive effect of PEDF from photoreceptor degeneration in the RCS rats was also assayed by intravitreal injection of nanoparticles (NP) carrying 2.5 μg of the human protein (PEDF-NP) in the right eye of P21 rats. To evaluate the effects of PEDF-NP on photoreceptor survival, 2 additional groups of 3-week old RCS rats were injected in the right eye with 2.5 μg of PEDF protein or empty NP. Contralateral eyes were either left untreated or injected with phosphate buffered saline (PBS). The protective effect of each treatment was evaluated 4 and 8 weeks p.i. Eyes treated with PEDF-NP had a significant increase in ONL column height and in the number of photoreceptors but reduced TUNEL-positive cells compared to PEDF, empty NP and contralateral eyes. Moreover, PEDF-NP contributed to the preservation of rod-opsin levels and a- and b-wave amplitudes in ERG studies at 8 weeks p.i. (Akiyama et al. 2012).

93.2.5 Light-Induced Damage of Photoreceptors

Constant white light can induce retinal degeneration and is used in established rodentl models to degenerate photoreceptors. In Sprague-Dawley albino rats, exposure to white light (1200–1500 lux) continuously for 7 days reduces the ONL thickness to 12.5–30 % of that of unexposed eyes and eliminates the ERG response. Cao et al. (1999) tested the PEDF-mediated protective effect on photoreceptors damaged with light by intravitreally injecting human PEDF (2 μg) in one eye, using the PBS-injected contralateral eye as a control in rats of 2–5 month old. Injections were at 1 or 2 days pre-light exposure, or 0, 1 or 2 days after constant light (CL) exposure. ERG and histopathology analysis after 14 days of recovery showed that PEDF injected 1 or 2 days before light-induced damage protected photoreceptors from degeneration. When injected 2 days before light-induced damage, PEDF attenuated the reduction in ONL thickness and improved ERG response in eyes exposed to constant light for 3-10 days relative to controls. However, no protection by PEDF was observed after 14 days of CL exposure. Slightly enhanced protective effects have been reported when the eyes were pre-treated with PEDF combined with basic fibroblast growth factor (bFGF) (1 μg each).

Imai et al. (2005) have also assessed PEDF photoreceptor protection from damage induced by constant white light exposure using Lewis albino rats (females of 4–8 weeks). Progressive retinal degeneration, determined as the reduction of ONL thickness and cell number, was observed at 24, 96 and 168 h of continuous light exposure (2500 lux) in untreated rats. PEDF was delivered 3 days before light damage by intravitreal injection of adenoviral vector (AdPEDF.11), which promotes the expression of the gene under the regulation of the CMV promoter. Photoreceptor morphology was evaluated after 96 h of CL exposure and compared among animals injected with AdPEDF.11, untreated or injected with the empty AdNull.11 vector. PEDF rescued ONL thickness and number of photoreceptors as compared to controls. However, the empty vector itself had some protective effect when compared to the uninjected ones. Similarly, PEDF lowered the number of TUNEL-positive nuclei in the ONL (after 12 h of CL exposure) and improved the ERG response (after 48 h of exposure and 7–28 days of recovery after light damage). Animals injected with the empty vector again exhibited significant protection compared to untreated mice. The authors suggested that PEDF induced protection from apoptosis and loss of functionality in photoreceptors damaged by light exposure.

In summary, exogenous administration of the PEDF protein and the *SERPINF1* gene transfer via viral vectors are beneficial in protecting photoreceptors against degeneration and death caused by genetic and/or environmental factors. The mechanisms by which PEDF acts on photoreceptors are beginning to emerge. Overall the data from several groups point to PEDF as an antiapoptotic factor that targets signaling pathways of the Bcl2 family and AIF in degenerating photoreceptors, likely mediated by interactions with PEDF-R (Subramanian et al. 2013) The findings also point to the applicability of the human PEDF sequence in rodent models of retinal degenerations. PEDF holds promise to clinical neuroprotection therapy, and in particular in ocular diseases.

References

Akiyama G, Sakai T, Kuno N et al (2012) Photoreceptor rescue of pigment epithelium-derived factor-impregnated nanoparticles in Royal College of surgeons rats. Mol Vis 18:3079–3086

Barnstable CJ, Tombran-Tink J (2004) Neuroprotective and antiangiogenic actions of PEDF in the eye: molecular targets and therapeutic potential. Prog Ret Eye Res 23:561–577

Becerra SP (2006) Focus on molecules: pigment epithelium-derived factor (PEDF). Exp Eye Res 82:739–740

Becerra SP, Notario V (2013) The effects of PEDF on cancer biology: mechanisms of action and therapeutic potential. Nature Rev Cancer 13:258–271

Becerra SP, Fariss RN, Wu YQ et al (2004) Pigment epithelium-derived factor in the monkey retinal pigment epithelium and interphotoreceptor matrix: apical secretion and distribution. Exp Eye Res 78:223–234

Cao W, Tombran-Tink J, Chen W et al (1999) Pigment epithelium-derived factor protects cultured retinal neurons against hydrogen peroxide-induced cell death. J Neurosci Res 57:789–800

Cayouette M, Smith SB, Becerra SP et al (1999) Pigment epithelium-derived factor delays the death of photoreceptors in mouse models of inherited retinal degenerations. Neurobiol Dis 6:523–532

Chu XK, Wang Y, Ardeljan D et al (2013) Controversial view of a genetically altered mouse model of focal retinal degeneration. Bioengin 4:130–135

D'Cruz PM, Yasumura D, Weir J et al (2000) Mutation of the receptor tyrosine kinase gene Mertk in the retinal dystrophic RCS rat. Hum Mol Genet 9:645–651

Gal A, Li Y, Thompson DA, Weir J et al (2000) Mutations in MERTK, the human orthologue of the RCS rat retinal dystrophy gene, cause retinitis pigmentosa. Nature Genet 26:270–271

Imai D, Yoneya S, Gehlbach PL et al (2005) Intraocular gene transfer of pigment epithelium-derived factor rescues photoreceptors from light-induced cell death. J Cell Physiol 202:570–578

Miyazaki M, Ikeda Y, Yonemitsu Y et al (2003) Simian lentiviral vector-mediated retinal gene transfer of pigment epithelium-derived factor protects retinal degeneration and electrical defect in Royal College of surgeons rats. Gene Ther 10:1503–1511

Mullen RJ, LaVail MM (1976) Inherited retinal dystrophy: primary defect in pigment epithelium determined with experimental rat chimeras. Science 192:799–801

Murakami Y, Ikeda Y, Yonemitsu Y et al (2008) Inhibition of nuclear translocation of apoptosis-inducing factor is an essential mechanism of the neuroprotective activity of pigment epithelium-derived factor in a rat model of retinal degeneration. Am J Pathol 173:1326–1338

Notari L, Baladron V, Aroca-Aguilar JD et al (2006) Identification of a lipase-linked cell membrane receptor for pigment epithelium-derived factor. J Biol Chem 281:38022–38037

Sancho-Pelluz J, Arango-Gonzalez B, Kustermann S et al (2008) Photoreceptor cell death mechanisms in inherited retinal degeneration. Mol Neurobiol 38:253–269

Sanyal S, De Ruiter A, Hawkins RK (1980) Development and degeneration of retina in rds mutant mice: light microscopy. J Comp Neurol 194:193–207

Subramanian P, Locatelli-Hoops S, Kenealey J et al (2013) Pigment epithelium-derived factor (PEDF) prevents retinal cell death via PEDF Receptor (PEDF-R): identification of a functional ligand binding site. J Biol Chem 288:23928–23942

Wang Y, Subramanian P, Shen D et al (2013) Pigment epithelium-derived factor reduces apoptosis and pro-inflammatory cytokine gene expression in a murine model of focal retinal degeneration. ASN Neuro 5:e00126

Part X
Retinal Pigment Epithelium (RPE)

Chapter 94
The mTOR Kinase Inhibitor INK128 Blunts Migration of Cultured Retinal Pigment Epithelial Cells

Melissa A. Calton and Douglas Vollrath

Abstract Retinal pigment epithelium (RPE) cell migration in response to disease has been reported for age-related macular degeneration, proliferative vitreoretinopathy, and proliferative diabetic retinopathy. The complex molecular process of RPE cell migration is regulated in part by growth factors and cytokines, and activation of the PI3/AKT/mTOR signaling pathway. Rapamycin, an allosteric mTOR inhibitor, has been shown to block only one of the primary downstream mTOR effectors, p70 S6 kinase 1, in many cell types. INK128, a selective mTOR ATP binding site competitor, blocks both p70 S6 kinase 1 and a second primary downstream effector, 4E-BP1. We performed scratch assays using differentiated ARPE-19 and primary porcine RPE cells to assess the effect of mTOR inhibition on cell migration. We found that INK128-mediated blocking of both p70 S6 kinase 1 and 4E-BP1 was much more effective at preventing RPE cell migration than rapamycin-mediated inhibition of p70 S6 kinase 1 alone.

Keywords Retinal pigment epithelium · MTOR · Migration · Proliferative vitreoretinopathy · Age-related macular degeneration · ARPE-19 · Rapamycin · INK128

94.1 Introduction

RPE cell migration in response to disease has been reported for age-related macular degeneration (Ho et al. 2011), in addition to proliferative vitreoretinopathy (Campochiaro 1997; Cardillo et al. 1997; Charteris et al. 2002; Chan et al. 2013) and proliferative diabetic retinopathy (de Silva et al. 2008). During disease, RPE

D. Vollrath (✉) · M. A. Calton
Department of Genetics, Stanford University School of Medicine, Stanford, CA 94305-5120, USA
e-mail: vollrath@stanford.edu

M. A. Calton
e-mail: macalton@stanford.edu

C. Bowes Rickman et al. (eds.), *Retinal Degenerative Diseases,* Advances in Experimental Medicine and Biology 854, DOI 10.1007/978-3-319-17121-0_94

cells can migrate into the subretinal space (Zhao et al. 2011) and to a damaged area (Kim et al. 2009; Chan et al. 2010). The complex molecular process of RPE migration is regulated in part by growth factors and cytokines (Chan et al. 2013). In a cell culture model, RPE cell migration was induced by nerve growth factor (NGF) and treatment with rapamycin, an allosteric mTOR inhibitor, blocked migration (Cao et al. 2011). In an *in vivo* mouse model of OXPHOS deficiency, rapamycin slowed mTOR mediated RPE dedifferentiation and hypertrophy while maintaining RPE viability, but was ineffective at preventing RPE cell migration (Zhao et al. 2011). Rapamycin has been shown to block only one of two primary downstream mTOR effectors, p70 S6 kinase 1, in many cell types (Hsieh et al. 2012). In contrast, INK128, a selective mTOR ATP binding site competitor, is able to inhibit the mTOR pathway by blocking two of the primary downstream effectors, p70 S6 kinase 1 and 4E-BP1 (Hsieh et al. 2012). The inhibition of phosphorylation of 4E-BP1 by INK128 has previously been shown to regulate translation of mRNAs involved in pro-invasion/migration in prostate cancer (Hsieh et al. 2012). This suggested that phosphorylation of 4E-BP1 may regulate migration of RPE cells and warranted further investigation.

94.2 Materials and Methods

94.2.1 Cell Culture

Undifferentiated human retinal pigment epithelial cells (ARPE-19 cell line) were cultured as described (Dunn et al. 1996). ARPE-19 cells were differentiated on Matrigel (BD Biosciences) coated plates in DMEM/F12 medium with 15 mM HEPES and L-glutamine (Invitrogen), 1% FBS, antibiotic/antimycotic (Invitrogen), 1 ng/mL bFGF (Invitrogen), 10^{-8} M retinoic acid (Sigma-Aldrich), 10 ng/mL hydrocortisone (Sigma-Aldrich), 0.5X of transferrin insulin selenium supplement (Invitrogen) for 4–6 weeks at 37 °C with 10% CO_2. Medium was changed three times a week. Porcine eyes were purchased from Animal Technologies Inc. The anterior segment, vitreous, and neural retina were removed and the resulting posterior eyecup was incubated in 0.25% trypsin at 37 °C for 1 h. RPE cells were removed from the choroid/sclera by manual pipetting and collected in a centrifuge tube with DMEM-low glucose culture medium (Invitrogen), 10% FBS, and antibiotic/antimycotic (Invitrogen). To obtain a pure RPE population, the cell suspension was placed on top of a 40% Percoll cushion (in PBS) and centrifuged for 10 min at 300 xg. The purified RPE cells were resuspended in culture medium and plated. Cultures were incubated at 37 °C with 5% CO_2 and medium was changed 2–3 times a week.

94.2.2 Reagents and Antibodies

INK128 (Active BioChem) and rapamycin (LC Laboratories) were used at the stated concentrations. Aphidicolin (Sigma-Aldrich) was used at 2 µg/ml to block cell proliferation.

The primary antibodies used include anti-PHOSPHO-S6 (Ser 235/236) (Cell Signaling Technology), anti-S6 (Cell Signaling Technology), anti-4E-BP1 (Cell Signaling Technology), and anti-γ-TUBULIN (Sigma-Aldrich). The secondary antibodies used were goat anti-mouse and goat anti-rabbit (Jackson Immuno Research).

94.2.3 Immunoblot

Protein lysates were prepared as described previously (Strick et al. 2009). Total protein for each sample was quantified with a BCA kit (Pierce Biotechnology) and an equal amount of protein from each sample was separated by 4–15 % gradient SDS-PAGE. Protein transfer and chemiluminescence detection were done as described previously (Liu and Vollrath 2004).

94.2.4 Scratch Assay

In vitro scratch assays were performed as previously described (Liang et al. 2007). Briefly, RPE cells were plated on coated plates to create a confluent monolayer. Prior to the scratch and during image acquisition, the area was marked to establish reference points for capturing multiple images of the same field over a time course. Monolayers were scratched with a p200 pipet tip and changed to scratch assay medium containing 1 % FBS and aphidicolin, with or without rapamycin or INK128. The scratch assay medium was changed every 24 h. The area of the scratch at each time point was determined using ImageJ and compared to the original 0 h scratch time point to determine the percent of scratch closure.

94.3 Results

94.3.1 INK128 Inhibits mTORC1 Activity in Cultured RPE Cells

To determine if INK128 can inhibit mTORC1 activity in RPE cells, we performed a dose response assay in undifferentiated and differentiated ARPE-19 cells, a spontaneously immortalized adult human RPE cell line (Dunn et al. 1996).

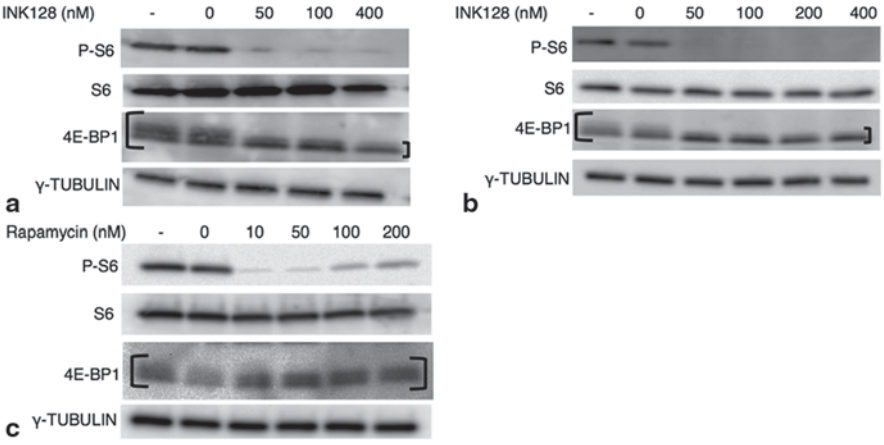

Fig. 94.1 Difference in mTOR effectors inhibited by INK128 or rapamycin in cultured RPE cells. **a** Undifferentiated, and **b** differentiated ARPE-19 cells were treated with INK128 for 24 h, **c** Undifferentiated ARPE-19 cells were treated with rapamycin for 24 h. Markers of mTOR activity P-S6 and 4E-BP1 (antibody detects total protein, independent of phosphorylation) showed a significant reduction in phosphorylated S6 and 4E-BP1 (slower mobility bands) at all doses of INK128, compared to the controls of total S6 protein and a γ-tubulin loading control, respectively. In contrast, rapamycin treatment only reduced S6 phosphorylation.

Immunoblot analysis demonstrates that INK128 is able to inhibit mTORC1 activity by blocking two of the primary downstream effectors, p70 S6 kinase 1 (measured by phosphorylation of S6) and phosphorylation of 4E-BP1 (Fig. 94.1a, b). Rapamycin has been shown to block only one of the primary downstream mTOR effectors, p70 S6 kinase 1, in many cell types (Hsieh et al. 2012) and inhibits PHOSPHO-S6, but not 4E-BP1 phosphorylation in undifferentiated ARPE-19 cells (Fig. 94.1c).

94.3.2 Inhibition of Both mTOR Effectors p70 S6 Kinase 1 and 4E-BP1 in Cultured RPE Cells Correlates with Reduced Cell Migration

In order to determine if mTOR inhibition can limit the migration of RPE cells *in vitro*, we performed a scratch assay and measured percent scratch closure as an indicator of migration. With rapamycin treatment, differentiated APRE-19 cells exhibit similar scratch closure to a medium-only control: 91% closure for rapamycin vs 94% for medium-only after 72 h (Fig. 94.2a). In contrast, after INK128 treatment the RPE cells do not migrate as efficiently and only have 4% scratch closure in differentiated ARPE-19 cells after 72 h (Fig. 94.2a). We also assessed the ability of mTOR inhibition to alter RPE cell migration using cultures of primary porcine

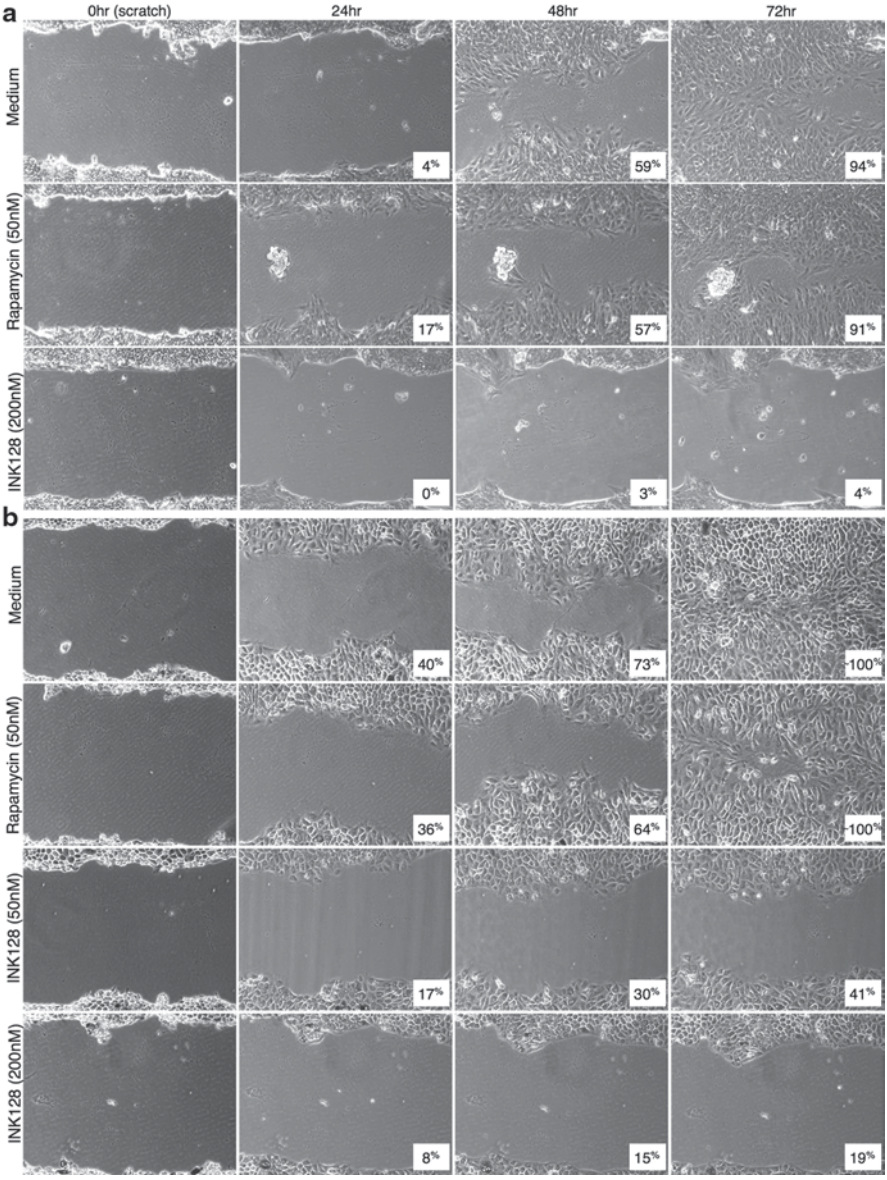

Fig. 94.2 INK128 treatment prevents the migration of RPE cells. A scratch assay was performed in **a** differentiated ARPE-19, and **b** primary porcine RPE cells under medium-only, rapamycin, or INK128 treatment for 72 h. The insets indicate the percentage of scratch closure (compared to 0 h scratch area), which is a measure of migration under the culture conditions used.

RPE (Fig. 94.2b). Similar to our results for ARPE-19, rapamycin treatment does not impede porcine RPE cell scratch closure compared to medium-only after 72 h, whereas treatment with INK128 severly limits the ability of porcine RPE cells to

migrate at both doses tested (Fig. 94.2b). In the porcine RPE cell model, rapamycin treatment appeared to slightly slow migration at 48 h (64% rapamycin vs 73% medium-only), but did not prevent scratch closure. In all conditions tested, the cells were also treated with aphidicolin to block proliferation. Therefore, the scratch closure observed is due to migration of RPE cells. These results suggest that blocking both the mTOR downstream targets 4E-BP1 and p70 S6 kinase 1, but not p70 S6 kinase 1 alone, prevents the migration of RPE cells.

94.4 Discussion

In a previous study, the ablation of OXPHOS in the RPE of mice caused dedifferentiation of the RPE arising from activation of the PI3/AKT/mTOR signaling pathway. The mTOR inhibitor rapamycin slowed dedifferentiation and growth while maintaining RPE viability, but the drug was inadequate in prevention of RPE cell migration (Zhao et al. 2011). In this current study, rapamycin was also ineffective at disrupting RPE migration. In another cell culture study, rapamycin blocked NGF-induced RPE cell migration (Cao et al. 2011). The disparity between the two cell culture studies may result from differences in experimental design. We used a lower dose of rapamycin. We studied monolayers of primary porcine cultures and differentiated ARPE-19 cells, whereas Cao et al. used undifferentiated ARPE-19. Finally, cell migration in our study resulted from a wound made under normal culture conditions, rather than in response to acute administration of a growth factor.

In contrast to rapamycin, we found that INK128 blocks both p70 S6 kinase 1 and 4E-BP1 and prevents the migration of RPE cells in an *in vitro* wound assay. Our results suggest that the migration of RPE cells during disease could be regulated by activation of 4E-BP1. 4E-BP1 is a negative regulator of the key rate-limiting initiation factor for cap-dependent translation, eIF4E.

mTOR phosphorylates 4E-BP1 causing its dissociation from eIF4E, which allows translation initiation complex formation at the 5′ end of mRNAs (Gingras et al. 2001). eIF4E has been shown to bind preferentially to 5′ terminal oligopyrimidine tract (5′ TOP) containing mRNAs (Thoreen et al. 2012). In prostate cancer cells, INK128 treatment revealed specific messages involved in pro-invasion and migration that are not inhibited by rapamycin (Hsieh et al. 2012). This mechanism of translational control may also mediate RPE migration. If so, it will be of great value to identify specific genes regulated by 4E-BP1 in the RPE and investigate their possible roles in regulating RPE migration. INK128 is orally available and currently in eight clinical trials (http://www.cancer.gov/clinicaltrials/search/results?protocolsearchid=9529537). It remains to be determined if this drug can inhibit RPE cell migration in an animal model, as it does in our culture model. Our results may provide insight into retinal degenerative diseases involving RPE cell migration and suggest a new rationale for therapy of these disorders.

Acknowledgments We thank W. Feng for porcine RPE cells and P. Saha for technical assistance. This study was supported by grants from the Thome Memorial Foundation (DV) and Foundation Fighting Blindness (DV), and by a NEI Postdoctoral Training grant T32 EY 20485-4 (MAC).

References

Campochiaro PA (1997) The silicone study. A small piece of the PVR puzzle is put into place. Arch Ophthalmol 115:407–408

Cao G-F, Liu Y, Yang W et al (2011) Rapamycin sensitive mTOR activation mediates nerve growth factor (NGF) induced cell migration and pro-survival effects against hydrogen peroxide in retinal pigment epithelial cells. Biochem Biophys Res Commun 414:499–505

Cardillo JA, Stout JT, LaBree L et al (1997) Post-traumatic proliferative vitreoretinopathy. The epidemiologic profile, onset, risk factors, and visual outcome. Ophthalmology 104:1166–1173

Chan C-M, Huang J-H, Chiang H-S et al (2010) Effects of (-)-epigallocatechin gallate on RPE cell migration and adhesion. Mol Vis 16:586–595

Chan C-M, Chang H-H, Wang V-C et al (2013) Inhibitory effects of resveratrol on PDGF-BB-induced retinal pigment epithelial cell migration via PDGFRß, PI3K/Akt and MAPK pathways. PLoS ONE 8:e56819

Charteris DG, Sethi CS, Lewis GP et al (2002) Proliferative vitreoretinopathy-developments in adjunctive treatment and retinal pathology. Eye (Lond) 16(4):369–374

de Silva DJ, Kwan A, Bunce C et al (2008) Predicting visual outcome following retinectomy for retinal detachment. Br J Ophthalmol 92:954–958

Dunn KC, Aotaki-Keen AE, Putkey FR et al (1996) ARPE-19, a human retinal pigment epithelial cell line with differentiated properties. Exp Eye Res 62:155–169

Gingras AC, Raught B, Sonenberg N (2001) Regulation of translation initiation by FRAP/mTOR. Genes Dev 15:807–826

Ho J, Witkin AJ, Liu J et al (2011) Documentation of intraretinal retinal pigment epithelium migration via high-speed ultrahigh-resolution optical coherence tomography. Ophthalmology 118:687–693

Hsieh AC, Liu Y, Edlind MP et al (2012) The translational landscape of mTOR signalling steers cancer initiation and metastasis. Nature 485:55–61

Kim YH, He S, Kase S et al (2009) Regulated secretion of complement factor H by RPE and its role in RPE migration. Graefes Arch Clin Exp Ophthalmol 247:651–659

Liang C-C, Park AY, Guan J-L (2007) In vitro scratch assay: a convenient and inexpensive method for analysis of cell migration in vitro. Nat Protoc 2:329–333

Liu Y, Vollrath D (2004) Reversal of mutant myocilin non-secretion and cell killing: implications for glaucoma. Hum Mol Genet 13:1193–1204

Strick DJ, Feng W, Vollrath D (2009) Mertk drives myosin II redistribution during retinal pigment epithelial phagocytosis. Investig Ophthalmol Vis Sci 50:2427–2435

Thoreen CC, Chantranupong L, Keys HR et al (2012) A unifying model for mTORC1-mediated regulation of mRNA translation. Nature 485:109–113

Zhao C, Yasumura D, Li X et al (2011) mTOR-mediated dedifferentiation of the retinal pigment epithelium initiates photoreceptor degeneration in mice. J Clin Invest 121:369–383

Chapter 95
Live Imaging of LysoTracker-Labelled Phagolysosomes Tracks Diurnal Phagocytosis of Photoreceptor Outer Segment Fragments in Rat RPE Tissue *Ex Vivo*

Yingyu Mao and Silvia C. Finnemann

Abstract Renewal of rod photoreceptor outer segments in the mammalian eye involves synchronized diurnal shedding after light onset of spent distal outer segment fragments (POS) linked to swift clearance of shed POS from the subretinal space by the adjacent retinal pigment epithelium (RPE). Engulfed POS phagosomes in RPE cells mature to acidified phagolysosomes, which accomplish enzymatic degradation of POS macromolecules. Here, we used an acidophilic fluorophore LysoTracker to label acidic organelles in freshly dissected, live rat RPE tissue flat mounts. We observed that all RPE cells imaged contained numerous acidified POS phagolysosomes whose abundance per cell was dramatically increased 2 h after light onset as compared to either 1 h before or 4 h after light onset. Lack of organelles of similar diameter (of 1–2 μm) in phagocytosis-defective mutant RCS rat RPE confirmed that LysoTracker live imaging detected POS phagolysosomes. Lack of increase in lysosomal membrane protein LAMP-1 in RPE/choroid during the diurnal phagocytic burst suggests that formation of POS phagolysosomes in RPE *in situ* may not involve extra lysosome membrane biogenesis. Taken together, we report a new imaging approach that directly detects POS phagosome acidification and allows rapid tracking and quantification of POS phagocytosis by live RPE tissue *ex situ*.

Keywords Acidification · LAMP-1 · Lysosomes · LysoTracker · Phagolysosomes · Phagosomes · Phagocytosis · Photoreceptor outer segments · RCS · RPE

Abbreviations

POS	Photoreceptor outer segment fragments
RPE	Retinal pigment epithelium

S. C. Finnemann (✉) · Y. Mao
Department of Biological Sciences, Center for Cancer, Genetic Diseases and Gene Regulation, Fordham University, Larkin Hall, 441 East Fordham Road, Bronx, NY 10458, USA
e-mail: finnemann@fordham.edu

C. Bowes Rickman et al. (eds.), *Retinal Degenerative Diseases,* Advances in Experimental Medicine and Biology 854, DOI 10.1007/978-3-319-17121-0_95

95.1 Introduction

Diurnal shedding and clearance of photoreceptor outer segment fragments (POS) by the retinal pigment epithelium (RPE) promotes continuous outer segment renewal that is important for long-term viability and function of vertebrate photoreceptors (Young 1967; Young and Bok 1969). In the mammalian eye, POS shedding and engulfment are precisely synchronized by light and circadian regulation to take place immediately after light onset (LaVail 1976). As a result, numbers of phagosome organelles containing engulfed POS in the RPE *in situ* of wild-type mice and rats reach a daily peak 1–2 h after light onset (LaVail 1976; Nandrot et al. 2004; Nandrot et al. 2007).

The steep decline of detectable POS phagosomes in the RPE after the daily burst of POS uptake implies that phagosomes rapidly mature to acidified phagolysosomes, in which digestive hydrolases efficiently degrade POS components. The daily maturation process of POS phagosomes to phagolysosomes remains incompletely understood. Fusion as well as "kiss-and-run" connections with *bona fide* lysosomes likely both contribute to the acidification of phagolysosomes, which carry the lysosomal membrane marker protein LAMP-1 (Bosch et al. 1993). We hypothesized that digestive organelles of the RPE *in situ* may differ at times of active POS clearance as compared to other times with respect to size, distribution, abundance, or extent of acidification to accomplish timely POS degradation. Labeling with LysoTracker biosensor acidified organelles in live rat RPE tissue in freshly dissected flat mounted eyecups, we observed acidified POS phagosomes in wild-type (but not phagocytosis-defective RCS) rat RPE that dramatically increased in abundance 2 h after light onset. This formation of acidified POS phagolysosomes in wild-type RPE did not correlate with a detectable increase in LAMP-1.

95.2 Materials and Methods

95.2.1 Animals

All procedures involving animals were performed following the ARVO statement for the "Use of Animals in Ophthalmic and Vision Research", and reviewed and approved by the Fordham University Institutional Animal Care and Use Committee. Sprague-Dawley and pink-eyed, tan-hooded RCS rats were raised and housed in 12-h light:12-h dark light conditions and fed *ad libitum*. 28–35-day-old rats were sacrificed by CO_2 asphyxiation following updated AVMA guidelines followed by immediate dissection of posterior eyecups and removal of neural retina.

95.2.2 LysoTracker Live Staining and Imaging

Freshly dissected eyecups were incubated in FluoroBrite™ DMEM with 0.4 µM LysoTracker Green DND-26 and 5 µM DAPI nuclei stain (all Life Technologies) at 37 °C for 15 min, flat-mounted and imaged on a Leica TSP5 confocal microcopy system. Images were compiled and processed using Adobe Photoshop CS4.

95.2.3 Immunoblotting Protein Quantification

Posterior eyecups containing RPE and choroid (R/Ch) and neural retinas (NR) were lysed in 50 mM HEPES, pH 7.4, 150 mM NaCl, 10% glycerol, 1.5 mM $MgCl_2$, 1% Triton X-100 supplemented with protease and phosphatase inhibitor cocktails. Lysates were analyzed by SDS-PAGE and immunoblotting for LAMP-1, PSD95 (both Cell Signaling), and RPE65 (Genetex). Bands were quantified by densitometry using GE ImageQuant TL 7.0.

95.3 Results

95.3.1 Live Imaging of LysoTracker Reveals POS Phagolysosomes and their Diurnal Peak in Abundance After Light Onset in Wild-type But Not Phagocytosis-Defective RCS Rat RPE in Eyecups Ex Vivo

To examine acidified cytoplasmic organelles in the RPE, we used a fluorescent acidophilic biosensor, LysoTracker, to stain and image live RPE tissue in freshly dissected, flat mounted eyecups from rats sacrificed 1 h before, 2 or 4 h after the onset of light. At all time points, we observed that the brightest LysoTracker positive compartments shared a diameter of 1–1.6 µm (Fig. 95.1a–c), which is similar to the size of early phagocytosed POS, suggesting that they are POS phagolysosomes. These acidified compartments were by far most abundant 2 h after light onset matching the diurnal burst of POS engulfment. In contrast, phagocytosis-defective RCS RPE contained almost no phagosomes but numerous small-size acidic compartments that are likely *bona fide* lysosomes (Fig. 95.1d)

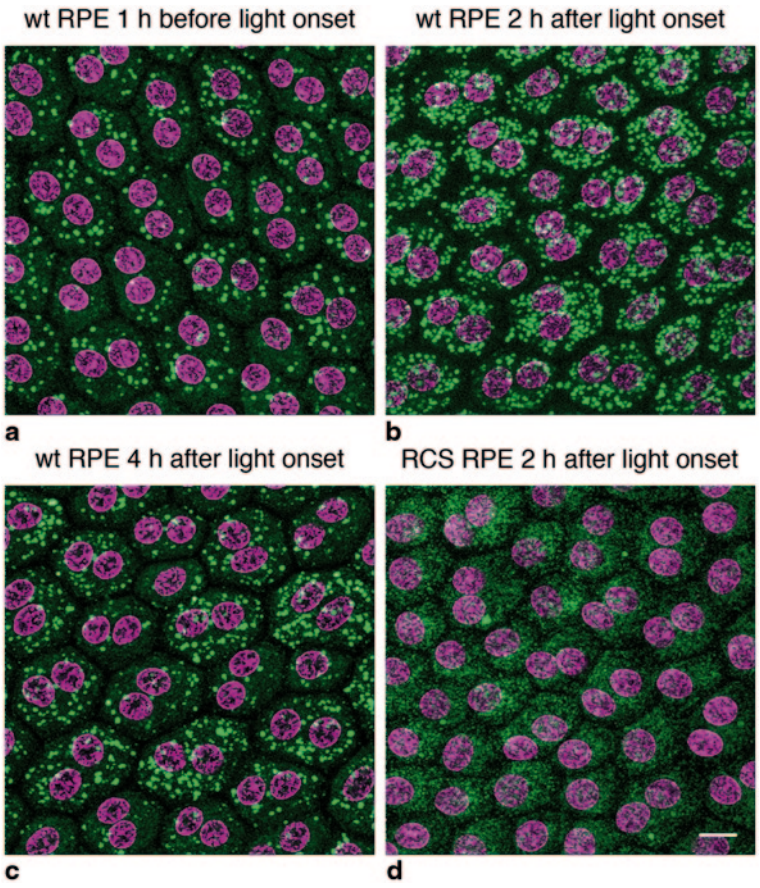

Fig. 95.1 Live imaging reveals diurnal increase of abundance of acidified phagolysosomes in live wild-type but not phagocytosis-defective RCS mutant rat RPE *ex vivo*. LysoTracker (*green*) and nuclei (*pink*) live staining of wild-type (wt) RPE in eyecup flat-mounts harvested at times as indicated, 1 h before (**a**), 2 h (**b**), or 4 h (**c**), after light onset or of RCS RPE 2 h after light onset (**d**). Representative fields of three independent experiments are shown. Images are maximum projections of z-stacks obtained using identical imaging parameters. Scale bar: 10 μm

95.3.2 Levels of Mature LAMP-1 in RPE/Choroid Do Not Change with Light Onset

LAMP-1 is a heavily glycosylated membrane protein that is primarily targeted to lysosomal membranes (Carlsson et al. 1988; Harter and Mellman 1992). The molecular size of rat LAMP-1 polypeptide is ~49 kDa. *N*- and *O*- glycosylation in the Golgi apparatus yields numerous forms of mouse LAMP-1 of 92–140 kDa (Andrejewski et al. 1999). In immunoblots, we detected 95–125 kDa forms in RPE/choroid and 75–95 kDa forms as well as a 49 kDa form (likely the immature precursor)

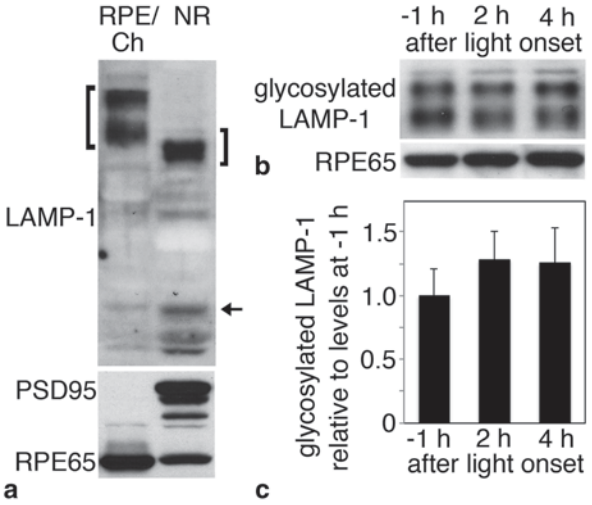

Fig. 95.2 Levels of lysosomal marker protein LAMP-1 do not change after light onset in rat posterior eyecups containing RPE and choroid. **a** Immunoblotting detects LAMP-1 in both RPE/choroid (RPE/Ch) and neural retina (NR) but higher molecular weight bands differ in size indicating differential glycosylation. *Open bracket* indicates glycosylated LAMP-1 in RPE lysate; *close bracket* indicates glycosylated LAMP-1 in retina lysate. *Arrow* indicates unglycosylated LAMP-1. RPE65 and PSD95 were detected on the same blot membrane to indicate enrichment of RPE and neural retina in rat eye fractions, respectively. **b** and **c** Levels of glycosylated LAMP-1 in RPE/choroid do not differ between 1 h before (−1 h), 2 or 4 h after (+2 h, +4 h) light onset. RPE65 detection of the same membrane is shown as loading control. *Bars* indicate relative level of all forms of glycosylated LAMP-1 normalized to RPE65. *Blots* show representative results (**a** and **b**). *Bars* show mean ± SD, of three independent experiments (**c**).

in neural retina (Fig. 95.2a). Levels of glycosylated LAMP-1 are similar in RPE/choroid samples collected before and after light onset (Fig. 95.2b, c), suggesting that POS phagolysosome formation is unlikely to involve a burst of lysosome membrane formation.

95.4 Discussion

In this study, we use LysoTracker biosensor to detect acidified phagosomes in live rat RPE in freshly dissected posterior eyecup flat mounts. To our knowledge, we report the first experimental approach that allows observing acidified phagolysosomes in live RPE tissue. It provides a rapid, simple, and direct assessment of the RPE's phagocytic load that is an ideal complement to established methods analyzing POS phagosomes in RPE tissue after fixation and processing (Young and Bok 1969; Gibbs et al. 2003; Sethna and Finnemann 2013).

We classify the LysoTracker-labelled compartments we observe in wild-type rat RPE as POS phagolysosomes based on (1) their similarity in size to POS phagosomes (Bosch et al. 1993); (2) their increased abundance at the time POS phagosomes peak in the RPE (LaVail 1976; Nandrot et al. 2004); and (3) their absence in phagocytosis-defective RCS RPE (Bok and Hall 1971; Mullen and LaVail 1976). Co-staining of these LysoTracker-positive phagosomes with antibodies specific to either opsin N- or C-terminus, known to differ in stability to RPE lysosomal processing (Esteve-Rudd et al. 2014; Wavre-Shapton et al. 2014), will allow in the future further specification of the content of acidified phagolysosomes and the POS digestion process of the RPE *in situ*.

We found that levels of glycosylated LAMP-1 in tissue extracts enriched in RPE do not increase at the diurnal peak in POS phagosome content in the RPE. Only glycosylated LAMP-1 reaches lysosomes. Thus, levels of glycosylated LAMP-1 are an indirect indicator of the overall quantity of intracellular membranes of lysosomal origin (assuming constant LAMP-1 membrane concentration). Further experiments are ongoing to confirm the preliminary implication of this finding that POS phagolysosomal membranes form largely at the expense of free lysosomal membranes.

Acknowledgments This study was supported by NIH grant EY13295.

References

Andrejewski N, Punnonen EL, Guhde G et al (1999) Normal lysosomal morphology and function in LAMP-1-deficient mice. J Biol Chem 274:12692–12701

Bok D, Hall MO (1971) The role of the pigment epithelium in the etiology of inherited retinal dystrophy in the rat. J Cell Biol 49:664–682

Bosch E, Horwitz J, Bok D (1993) Phagocytosis of outer segments by retinal pigment epithelium: phagosome–lysosome interaction. J Histochem Cytochem 41:253–263

Carlsson SR, Roth J, Piller F et al (1988) Isolation and characterization of human lysosomal membrane glycoproteins, h-lamp-1 and h-lamp-2. Major sialoglycoproteins carrying polylactosaminoglycan. J Biol Chem 263:18911–18919

Esteve-Rudd J, Lopes VS, Jiang M et al (2014) *In vivo* and *in vitro* monitoring of phagosome maturation in retinal pigment epithelium cells. Adv Exp Med Biol 801:85–90

Gibbs D, Kitamoto J, Williams DS (2003) Abnormal phagocytosis by retinal pigmented epithelium that lacks myosin VIIa, the Usher syndrome 1B protein. Proc Natl Acad Sci U S A 100:6481–6486

Harter C, Mellman I (1992) Transport of the lysosomal membrane glycoprotein lgp120 (lgp-A) to lysosomes does not require appearance on the plasma membrane. J Cell Biol 117:311–325

LaVail MM (1976) Rod outer segment disk shedding in rat retina: relationship to cyclic lighting. Science 194:1071–1074

Mullen RJ, LaVail MM (1976) Inherited retinal dystrophy: primary defect in pigment epithelium determined with experimental rat chimeras. Science 192:799–801

Nandrot EF, Kim Y, Brodie SE et al (2004) Loss of synchronized retinal phagocytosis and age-related blindness in mice lacking avb5 integrin. J Exp Med 200:1539–1545

Nandrot EF, Anand M, Almeida D et al (2007) Essential role for MFG-E8 as ligand for avb5 integrin in diurnal retinal phagocytosis. Proc Natl Acad Sci U S A 104:12005–12010

Sethna S, Finnemann SC (2013) Analysis of photoreceptor rod outer segment phagocytosis by RPE cells *in situ*. Methods Mol Biol 935:245–254

Wavre-Shapton ST, Meschede IP, Seabra MC et al (2014) Phagosome maturation during endosome interaction revealed by partial rhodopsin processing in retinal pigment epithelium. J Cell Sci 127(17):3852-3861. doi:10.1242/jcs.154757

Young RW (1967) The renewal of photoreceptor cell outer segments. J Cell Biol 33:61–72

Young RW, Bok D (1969) Participation of the retinal pigment epithelium in the rod outer segment renewal process. J Cell Biol 42:392–403

Chapter 96
Cre Recombinase: You Can't Live with It, and You Can't Live Without It

Yun-Zheng Le, Meili Zhu and Robert E. Anderson

Abstract The development of conditional gene targeting has greatly advanced our knowledge of human retinal diseases, but issues have arisen related to the use of some Cre-expressing mouse lines. In this article, we discuss potential problems associated with transgenic Cre expression-induced degeneration and alteration of rod photoreceptors and retinal pigment epithelium (RPE). Our strategy for circumventing RPE degeneration by induced transient Cre expression uses a single intravitreal doxycycline injection in a tetracycline-inducible RPE-specific Cre mouse line, which results in productive Cre-mediated recombination efficiently in the RPE. As constitutive expression of Cre in the RPE alters RPE biology, this inducible Cre/*lox* system provides an opportunity for conditional gene targeting in the RPE, a tissue that is closely related to photoreceptor degeneration, age-related macular degeneration, and diabetic retinopathy.

Keywords Cre/*lox* · Tetracycline-inducible · Photoreceptor · RPE · Degeneration

Y.-Z. Le (✉)
Departments of Medicine Endocrinology and Cell Biology, and Harold Hamm Diabetes Center, University of Oklahoma Health Sciences Center, 941 S. L. Young Blvd., BSEB 302G, Oklahoma City, OK 73104, USA
e-mail: Yun-Le@ouhsc.edu

M. Zhu
Department of Medicine Endocrinology, University of Oklahoma Health Sciences Center, Oklahoma City, OK 73104, USA

R. E. Anderson
Departments of Cell Biology and Ophthalmology, Dean A. McGee Eye Institute, University of Oklahoma Health Sciences Center, Oklahoma City, OK 73104, USA
e-mail: Robert-Anderson@ouhsc.edu

C. Bowes Rickman et al. (eds.), *Retinal Degenerative Diseases,* Advances in Experimental Medicine and Biology 854, DOI 10.1007/978-3-319-17121-0_96

96.1 Introduction

Cre/*lox* technology has become a method of choice for conditional gene targeting, at least for ocular tissues. While this technology has been successfully used to address many questions in ocular biology and diseases, issues have arisen from the use of Cre-drive lines that have not been discussed sufficiently and which, to some extent, have prevented the effective use of the resources currently available. We will discuss these problems first and then summarize our strategy in circumventing constitutive Cre expression-induced RPE degeneration by transient Cre expression in a tetracycline-inducible RPE-specific Cre mouse line (Fu et al. 2014; Le et al. 2008).

96.2 Problems Associated with Transgenic Cre Expression

Most available Cre-drive lines were generated with the traditional transgenic approach. As a result, these Cre-drive lines exhibited common problems associated with this strategy, including positional and copy number effect (Festenstein et al. 1996; Montavon et al. 2012) that may result in the variation in expression pattern and level among individual animals in transgenic mice. In other cases, transgene insertion affects gene expression in the insertion site, which may produce unwanted phenotypic consequence that interfere with the intended goal of a study (Sundermeier et al. 2014). Cre overexpression directed by rhodopsin promoter has been shown to cause rod photoreceptor degeneration (Jimeno et al. 2006). In our hands, we used short (0.2-kb) and long (4.1-kb) mouse opsin promoters and generated Cre-drive lines, named Short Mouse Opsin Promoter-Cre (SMOPC) line and Long Mouse Opsin Promoter-Cre (LMOPC) lines (Le et al. 2006). All Cre-drive lines, SMOPC1, LMOPC1, and LMOPC2, were capable of carrying out productive Cre-mediated recombination in rods ranging from 42 % (Le et al. 2006) to near 100 % (in LMOPC2 line, data not shown). While the SMOPC1 line and LMOPC1 line did not show any apparent loss of functional and morphological integrity in rod photoreceptors, LMOPC2, which demonstrated a much stronger Cre expression in its retinal extracts (Fig. 96.1), showed a significant loss of photoreceptor outer nuclear layer (ONL) thickness after 10 months of age (Fig. 96.1). As expression of a non-toxic fusion protein, human rhodopsin-green florescent protein (GFP), causes progressive rod photoreceptor degeneration (Chan et al. 2004), perhaps one can argue that rhodopsin promoter-directed Cre overexpression in rods may be a consequence of a negative effect on the host protein transcription/translation/maturation systems conferred by the opsin promoter, which is responsible for the expression of approximately 10 % of total

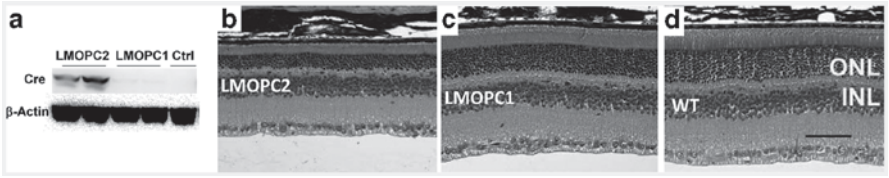

Fig. 96.1 Cre overexpression in rods caused a significant loss of outer nuclear layer (*ONL*) thickness, modified from Le et al. (2006) with permission of the publisher. **a** Western blot analysis showing LMOPC2 mice produced a significantly high level of Cre. **b** Representative haematoxylin eosin (H&E) stained retinal sections from 10-month-old Cre mice and WT controls. Scale bar: 50 μm

retinal proteins. Therefore, the common Cre toxicity may not completely account for photoreceptor degeneration in rod-specific Cre mice. This argument is supported by the observation that there was no apparent cone degeneration in high levels of transgenic Cre expression directed by the promoter of human red/green pigment (Le et al. 2004). Nevertheless, Cre is a site-specific DNA recombinase and Cre overexpression has been shown to cause chromosomal rearrangements in mammals (Loonstra et al. 2001; Schmidt et al. 2000), probably at cryptic recombination sites. This problem may be associated with Cre overexpression induced toxicity in the RPE. Constitutive Cre expression, directed by the promoters of tyrosinase-related protein-1 (TRP1) or human vitelliform macular dystrophy-2 (VMD2), causes RPE dysfunction and concomitant disorganization of RPE layer morphology, large areas of RPE atrophy, photoreceptor dysfunction, and microglial cell activation in the affected areas in an age and Cre dosage dependent manner (He et al. 2014; Thanos et al. 2012).

Cre overexpression induced retinal alteration and degeneration make it very difficult to interpret the data in retinal degeneration studies that utilize "toxic Cre animals" for cell-specific gene deletion. Due to inherent problems associated with transgenic mice, there is a significant difference in the expression level among individual animals within the same Cre transgenic line (Festenstein et al. 1996; Montavon et al. 2012), which makes it almost impossible to distinguish a retinal degeneration phenotype caused by Cre or a target gene, unless the same eye/retina is subjected to analysis for Cre expression and degeneration phenotypes simultaneously. This presents a huge, sometimes impossible challenge, in experimental design. Therefore, conclusions of previous degeneration studies that utilize "toxic Cre mice" may need to be re-validated if Cre-toxicity tests were not met with great stringency. Looking ahead, a better approach for conditional gene targeting will be to use inducible technologies that allow a brief and transient expression of a sufficient level of Cre to be effective and turns its expression off after Cre mediated recombination.

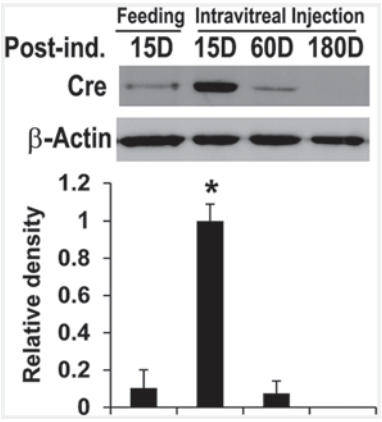

Fig. 96.2 Western blot analysis showing the level of Cre protein in the RPE extracts was significantly reduced in inducible RPE-specific Cre mice 60 days (60D) post-intravitreal Dox induction (ind.), modified from Fu et al. (2014) with permission of the publisher. Error bar: SD; $n=3$. *: $p<0.01$.

96.3 Inducible RPE-Specific Cre Mice

To circumvent the potential toxicity derived from constitutive Cre expression in the RPE, we developed an inducible RPE-specific Cre mouse line with tetracycline inducible gene expression technology (Le et al. 2008). To increase the reproducibility of Cre-mediated recombination, we recently re-examined the inducible conditions with intravitreal delivery of doxycycline (Dox), a tetracycline derivative (Fu et al. 2014), at a concentration (4 μg in 1 μl) that does not cause retinal degeneration (Chang et al. 2000). Intravitreal injection raised the retinal Dox concentration to ~250-fold that of the maximal level in the bloodstream delivered by feeding or intraperitoneal (IP) injection (assuming that the diameter of a mouse eye is 3 mm) (Ruz et al. 2004). As feeding or IP injection depends on the blood circulation to deliver Dox to the eye, the relative retinal Dox concentration delivered by intravitreal Dox injection is likely much higher than that from feeding or IP injection. As a result, intravitreal Dox injection resulted in a burst of Cre expression in the RPE extracts, compared with that induced by feeding (Fig. 96.2). However, Cre protein was diminished quickly with time, and did not cause any apparent alteration in retinal morphology and function (Fu et al. 2014). Since Cre-mediated recombination is permanent *in vivo*, such a brief Cre-expression resulted in approximately 60% of the RPE cells undergoing productive Cre-mediated recombination, with patch areas reaching 100% forever (Fig. 96.3). Therefore, intravitreal Dox delivery with this inducible RPE-specific Cre mouse line provides a new opportunity for conditional gene targeting in the RPE, a tissue that is closely related to photoreceptor degeneration, age-related macular degeneration, and diabetic retinopathy.

Acknowledgement We thank Wei Zheng and Lixin Zheng for Western blot and morphological data with rod-specific Cre mice. Our work was supported by NIH grants GM104934, EY020900, EY00871, and EY21725, grants from Research to Prevent Blindness, Presbyterian Health Foundation, and Oklahoma Center for Adult Stem Cell Research, and an endowment from the Choctaw Nation.

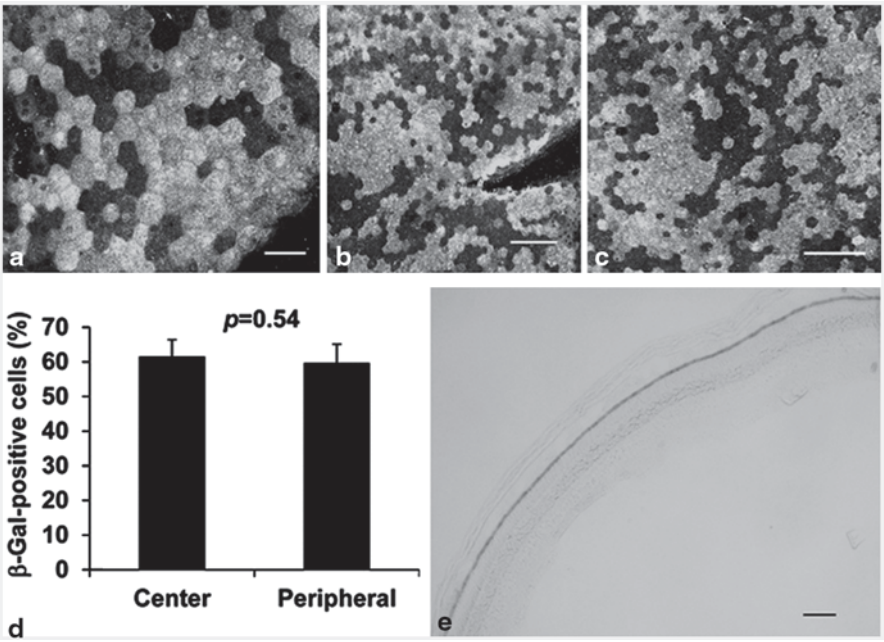

Fig. 96.3 Analysis of productive Cre-mediated recombination by examining the frequency of β-gal-expressing RPE cells in F1 mice derived from inducible RPE-specific Cre and ROSA26 lacZ reporter mice, modified from (Fu et al. 2014) with permission of the publisher. **a**–**d** Representative images and statistical analysis of immunostained RPE flat-mounts for Cre-activated β-gal (*bright*). **a** Enlarged confocal image. Scale bar: 40 μm. **b**–**c** Representative images showing the numbers/frequencies of β-gal-positive cells in central **(b)** and peripheral RPE flat-mounts **(c).** Scale bars: 100 nm. **d** Statistical analysis with t-test. Error bar: SD. $n = 5–6$. **e** Representative image showing homogenous Cre-activated β-gal activity (*dark*) in retinal section of the Cre/β-gal double transgenic mice. Scale bar: 100 μm. Productive-Cre mediated recombination occurred evenly in approximately 60 % of the RPE cells in inducible RPE-specific Cre mice after a single intravitreal Dox injection

References

Chan F, Bradley A, Wensel TG et al (2004) Knock-in human rhodopsin-GFP fusions as mouse models for human disease and targets for gene therapy. Proc Natl Acad Sci U S A 101:9109–9114

Chang MA, Horner JW, Conklin BR et al (2000) Tetracycline-inducible system for photoreceptor-specific gene expression. Invest Ophthalmol Vis Sci 41:4281–4287

Festenstein R, Tolaini M, Corbella P et al (1996) Locus control region function and heterochromatin-induced position effect variegation. Science 271:1123–1125

Fu S, Zhu M, Wang C et al (2014) Efficient induction of productive Cre-mediated recombination in retinal pigment epithelium. Mol Vis 20:480–487

He L, Marioutina M, Dunaief JL et al (2014) Age- and gene-dosage-dependent cre-induced abnormalities in the retinal pigment epithelium. Am J Pathol 184:1660–1667

Jimeno D, Feiner L, Lillo C et al (2006) Analysis of kinesin-2 function in photoreceptor cells using synchronous Cre-loxP knockout of Kif3a with RHO-Cre. Invest Ophthalmol Vis Sci 47:5039–5046

Le Y, Ash JD, Al-Ubaidi MR, Chen Y, Ma J, Anderson RE (2004) Targeted expression of Cre recombinase to cone photoreceptors in transgenic mice. Mol Vis 10:1011–1018

Le Y, Zheng L, Zheng W et al (2006) Mouse opsin promoter controlled expression of Cre recombinase in transgenic mice. Mol Vis 12:389–398

Le YZ, Zheng W, Rao PC et al (2008) Inducible expression of cre recombinase in the retinal pigmented epithelium. Invest Ophthalmol Vis Sci 49:1248–1253

Loonstra A, Vooijs M, Beverloo HB et al (2001) Growth inhibition and DNA damage induced by Cre recombinase in mammalian cells. Proc Natl Acad Sci U S A 98:9209–9214

Montavon T, Thevenet L, Duboule D (2012) Impact of copy number variations (CNVs) on long-range gene regulation at the HoxD locus. Proc Natl Acad Sci U S A 109:20204–20211

Ruz N, Zabala M, Kramer MG et al (2004) Rapid and simple determination of doxycycline in serum by high-performance liquid chromatography. Application to particulate drug delivery systems. J Chromatogr A 1031:295–301

Schmidt EE, Taylor DS, Prigge JR et al (2000) Illegitimate Cre-dependent chromosome rearrangements in transgenic mouse spermatids. Proc Natl Acad Sci U S A 97:13702–13707

Sundermeier TR, Vinberg F, Mustafi D et al (2014) R9AP overexpression alters phototransduction kinetics in iCre75 mice. Invest Ophthalmol Vis Sci 55:1339–1347

Thanos A, Morizane Y, Murakami Y et al (2012) Evidence for baseline retinal pigment epithelium pathology in the Trp1-Cre mouse. Am J Pathol 180:1917–1927

Chapter 97
Efficiency of Membrane Protein Expression Following Infection with Recombinant Adenovirus of Polarized Non-Transformed Human Retinal Pigment Epithelial Cells

Claudia Müller, Timothy A. Blenkinsop, Jeffrey H. Stern and Silvia C. Finnemann

Abstract Transient expression of exogenous proteins facilitates studies of molecular mechanisms and utility for transplantation of retinal pigment epithelial (RPE) cells in culture. Here, we compared expression of the membrane protein β5 integrin-GFP (β5-GFP) in two recently established models of differentiated human RPE, adult RPE stem cell-derived RPE and primary fetal RPE, upon infection with recombinant adenovirus or transfection with DNA in liposomes. We varied viral titer and duration of virus incubation and examined β5-GFP and the tight junction marker ZO-1 in manipulated cells by confocal microscopy. Fewer than 5 % of cells expressed β5-GFP after liposome-mediated transfection. The percentage of cells with detectable β5-GFP exceeded 90 % after adenovirus infection for as little as 1 h. Decreasing virus titer two-fold did not alter the fraction of cells expressing β5-GFP but increased variability of β5-GFP level among cells. In cells with low expression levels, β5-GFP localized mostly to the apical plasma membrane like endogenous

S. C. Finnemann (✉) · C. Müller
Department of Biological Sciences, Center for Cancer, Genetic Diseases and Gene Regulation, Fordham University, Larkin Hall, 441 East Fordham Road, Bronx, NY 10458, USA
e-mail: finnemann@fordham.edu

C. Müller
e-mail: cmuller3@fordham.edu

T. A. Blenkinsop
Department of Development and Regenerative Biology, Icahn School of Medicine at Mount Sinai, 1425 Madison Ave, Icahn Medical Institute, New York, NY 10029, USA
e-mail: timothy.blenkinsop@mssm.edu

J. H. Stern
Neural Stem Cell Institute, Rensselaer, NY 12144, USA

C. Bowes Rickman et al. (eds.), *Retinal Degenerative Diseases,* Advances in Experimental Medicine and Biology 854, DOI 10.1007/978-3-319-17121-0_97

αvβ5 integrin. In cells with high expression levels, β5-GFP localized to the cytoplasm in addition to the apical surface suggesting accumulation in trafficking compartments. Altogether, adenovirus delivery yields efficient exogenous membrane protein expression of correct polarity in differentiated human RPE cells in culture.

Keywords β5 integrin-GFP · Infectivity · Primary human fetal RPE · Protein expression · Recombinant adenovirus · RPE · RPESC-RPE

Abbreviations

β5-GFP	β5 integrin-GFP
hfRPE	Primary human fetal RPE
RPE	Retinal pigment epithelium
RPESC-RPE	Adult retinal pigment epithelium stem cell-derived-RPE
vp	Virus particles

97.1 Introduction

Post-mitotic retinal pigment epithelial (RPE) cells form a polarized monolayer epithelium that fulfills numerous functions each one of which supports photoreceptor long-term function and viability. These include light absorption, transepithelial transport, re-isomerization of all-*trans* retinal, polarized secretion of growth factors, retinal adhesion and the diurnal clearance phagocytosis of shed photoreceptor outer segment tips (Strauss 2005). Impaired RPE-photoreceptor interactions cause retinal dysfunction or retinal degeneration in experimental animal models and contribute to inherited human retinal diseases and age-related macular degeneration.

The availability of RPE cells in culture facilitates studies of RPE functionality and molecular mechanisms otherwise limited by lack of access and sufficient yield to RPE tissue (Mazzoni et al. 2014). Over the past decades several groups have reported protocols to establish and grow polarized non-transformed human RPE cells that retain many characteristics of the RPE in the human eye (Sonoda et al. 2009; Hu and Bok 2010). Among these, adult retinal pigment epithelial stem cell-derived-RPE cells (RPESC-RPE) and primary human fetal RPE cells (hfRPE) are established using stringent, published protocols and seeded for studies at passage 1 or 2 followed by differentiation over several weeks, during which post-confluent monolayers generate pigment, polarize and acquire RPE specific marker proteins (Maminishkis et al. 2006; Blenkinsop et al. 2013).

Mechanistic studies of these novel high quality RPE models greatly benefit from efficient genetic manipulation. Adenovirus vectors are known to infect RPE cells without significant cytotoxicity and recombinant adenovirus-mediated gene transfer has long been used to manipulate gene expression of RPE cells *in vivo* and in culture (Trapani et al. 2014). Utility of virus transduced cells for functional studies requires (1) a large fraction of cells expressing exogenous protein, (2) low variabil-

ity in exogenous protein expression level among transduced cells, and (3) correct subcellular localization of the exogenous protein. Here, we assess these parameters for differentiated, polarized RPESC-RPE and hfRPE cells infected with recombinant adenovirus encoding the transmembrane protein β5 integrin-GFP (β5-GFP).

97.2 Materials and Methods

97.2.1 Human RPE Cell Cultures

RPESC-RPE cells (Salero et al. 2012) were seeded at passage-2 on 6.5-mm Transwell® filters with 0.4 μm pore size (Corning Costar) (Blenkinsop et al. 2013). RPESC-RPE cells were maintained according to published procedures for 6–7 weeks before being used for experiments.

HfRPE cells at passage-0 were provided by Dr. Sheldon Miller (National Eye Institute, National Institutes of Health, Bethesda, MD) and maintained and re-seeded according to published protocols (Maminishkis et al. 2006). HfRPE cells of passage-2 were maintained on glass cover slips in 96-well plates for 4 weeks before being used for experiments.

97.2.2 Adenovirus-Mediated Transduction

Generation of replication-defective, recombinant adenovirus encoding GFP-tagged human β5 integrin was described previously (Nandrot et al. 2012). Adenovirus stock was diluted to 5, 2.5, or 1.25×10^{10} virus particles (vp)/mL in serum-free DMEM and applied to cells for 1 or 15 h followed by incubation in complete medium for 23 or 9 h, respectively, before fixation.

97.2.3 Liposome-Mediated Transfection

pEGFP-N2 expression plasmid encoding β5-GFP was described previously (Nandrot et al. 2012). Cells were transfected with plasmid DNA in the presence of Lipofectamine 2000 as suggested by the manufacturer (Life Technologies). Cells were fixed 24 h after transfection.

97.2.4 Immunofluorescence Staining and Microscopy

RPE cells were fixed with ice-cold methanol for 5 min. Tight junctions were labeled with ZO-1 antibodies and AlexaFluor594-conjugated secondary antibodies

(Life Technologies). Nuclei were counterstained with DAPI. X-y image stacks were acquired on a Leica TSP5 laser-scanning confocal microscopy system) and were compiled using Adobe Photoshop CS4.

97.3 Results

97.3.1 Infectivity of RPESC-RPE Cells

To optimize efficiency of exogenous protein expression following infection with adenovirus in RPESC-RPE cells were exposed to adenovirus particles at different concentrations and for different durations. We used a recombinant, replication defective adenovirus encoding human β5 integrin with a C-terminal GFP tag (β5-GFP). We previously found that this adenovirus promotes expression of β5-GFP protein that forms heterodimeric receptors with endogenous human or rat αv integrin subunits that localize to the cell surface in fibroblasts, RPE cell lines and primary rat and mouse RPE in culture (Nandrot et al. 2012). Moreover, β5-GFP expression rescues the POS recognition deficiency of primary RPE derived from ITGB5$^{-/-}$ mice indicating that αvβ5-GFP receptors function like αvβ5 integrin (Nandrot et al. 2004; Nandrot et al. 2012). Importantly, β5-GFP shows robust green fluorescence that is largely maintained even after cell fixation and indirect immunofluorescence staining procedures.

We first exposed RPESC-RPE cells for 15 h to adenovirus at different concentrations and used confocal microscopy to assess GFP fluorescence in cells fixed 24 h after the start of infection. Figure 97.1a–c illustrates that most RPESC-RPE cells expressed β5-GFP regardless of virus titer. In comparison, delivery of β5-GFP expression plasmid via liposomes was very inefficient (Fig. 97.1d). Quantification of the fraction of RPESC-RPE cells with detectable β5-GFP fluorescence revealed that exposure to 5×10^{10} or 2.5×10^{10} vp/mL resulted in β5-GFP expression by 97% of RPESC-RPE cells (Fig. 97.1e). Exposure to 1.25×10^{10} vp/mL was slightly less efficient yielding 90% of RPESC-RPE cells with visible GFP fluorescence (Fig. 97.1e). However, in cells transduced with adenovirus at 2.5×10^{10} or 5×10^{10} vp/mL fluorescent cells showed uniformly high levels of integrin β5-GFP. Display of x-z confocal sections revealed that β5-GFP in these brightly fluorescent cells localized to sites in the cytoplasm and to the apical surface (Fig. 97.1a and b, x-z displays). In contrast, cells transduced with adenovirus at 1.25×10^{10} vp/mL resulted in a heterogeneous pattern with fluorescence varying significantly among β5-GFP-positive RPESC-RPE cells. Notably, in cells with low or moderate levels of fluorescence, most β5-GFP appeared to localize to the cells' apical surface, while highly fluorescent cells showed cytoplasmic β5-GFP like cells transduced with adenovirus at higher concentration (Fig. 97.1c, x-z display).

We next tested if exposure to adenovirus for a shorter time period would decrease efficiency of transduction of RPESC-RPE cells. Limiting adenovirus expo-

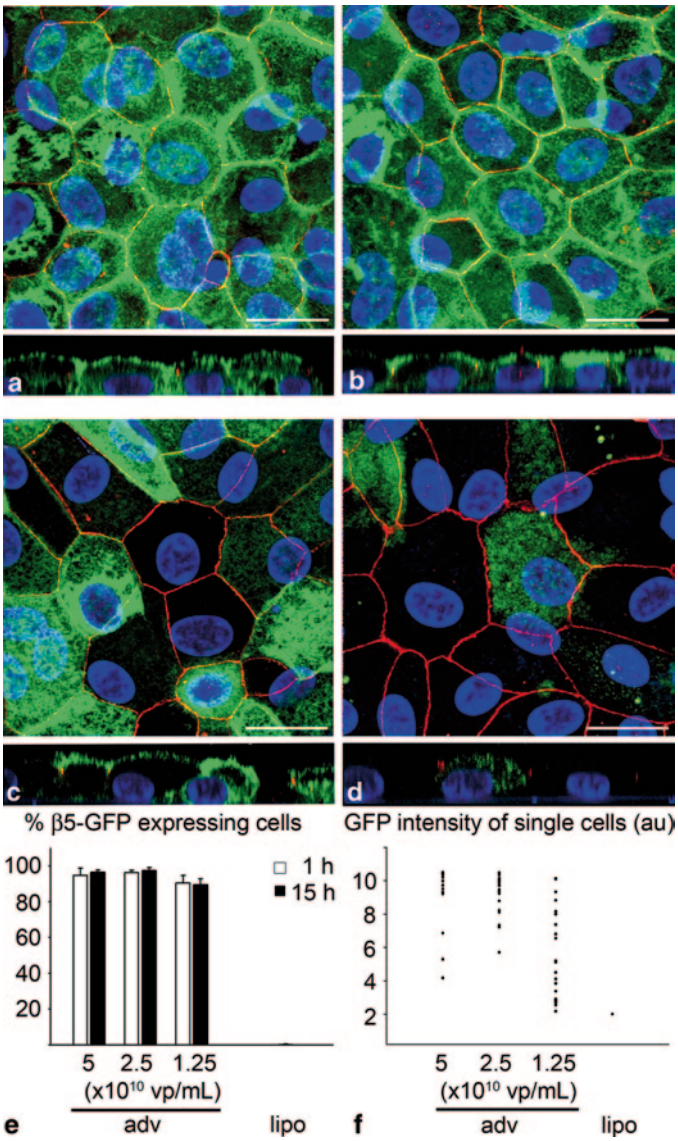

Fig. 97.1 β5-GFP expression by RPESC-RPE cells following adenovirus infection or liposome-mediated plasmid transfection. **a**-**d**: Images show fluorescence microscopy of β5-GFP (*green*), ZO-1 (*red*), and cell nuclei (*blue*) in RPESC-RPE cells after adenovirus infection (adv) or liposome-mediated transfection (lipo). **a**–**c** β5–GFP in RPESC-RPE cells after adenovirus infection (adv) for 15 h at 5×10^{10} vp/mL (**a**) 2.5×10^{10} vp/mL (**b**) or 1.25×10^{10} vp/mL (**c**), or 24 h after liposome-mediated transfection (**d**). The top of each panel shows a maximum projection of a representative image stack, the bottom of each panel shows a select x-z plane. Microscopy settings were adjusted to optimize the dynamic range for each image. Scale bar: 20 µm. **e**: Quantification of RPESC-RPE expressing β5-GFP at any detectable level after exposure to adenovirus for 1 hour (white bars) or 15 hours (black bars) or after liposome-mediated transfection (black bar), as indicated. Bars show mean ± SD, n = 3. **f**: Relative intensity of fluorescence of single cells after infection or transfection as in e and as indicated.

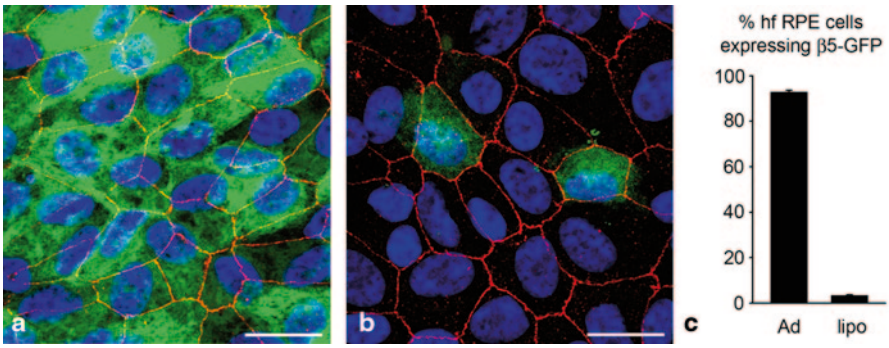

Fig. 97.2 β5-GFP expression by hfRPE cells following adenovirus infection or liposome-mediated plasmid transfection. Images show fluorescence microscopy of β5-GFP (*green*), ZO-1 (*red*), and cell nuclei (*blue*) in hfRPE cells after infection for 15 h with adenovirus at 1.25×10^{10} vp/mL (**a**) or liposome-mediated transfection (**b**). Maximum projections of representative image stacks are shown. Microscopy settings were adjusted to optimize the dynamic range for each image. Scale bar: 20 µm. **c** Quantification of hfRPE expressing β5-GFP at any detectable level after exposure to adenovirus for 15 h (adv) or after liposome-mediated transfection (lipo). Bars show mean ± SD, $n = 3$.

sure to only 1 h did not significantly reduce the percentage of RPESC-RPE cells expressing β5-GFP regardless of virus titer (Fig. 97.1d).

97.3.2 Infectivity of hfRPE Cells

Finally, we tested if highly differentiated, non-transformed hfRPE cells share the high infectivity of RPESC-RPE. Indeed, 93 % of hfRPE cells were fluorescent following 15-h exposure to 1.25×10^{10} vp/mL and most cells were brightly fluorescent (Fig. 97.2a, and c). In contrast, only 3.5 % of hfRPE cells were β5-GFP-positive after liposome-mediated transfection and their fluorescence was uniformly dim (Fig. 97.2b and c).

97.4 Discussion

Our experiments reveal that the two distinct post-confluent, highly differentiated, non-transformed human RPE cell strains we studied, RPESC-RPE and hfRPE, are highly susceptible to adenovirus infection. The finding that exposure to adenovirus for 1 h was as efficient in transducing cells as exposure for 15 h was unexpected. An earlier study found that transduction of confluent human primary RPE cells increased in a linear fashion with infection times of 16–70 h and was negligible if adenovirus was added for only 4 h (da Cruz et al. 1996). It is possible that adenovirus enters RPE cells more efficiently after extended periods of differentiation and polarization as induced in the two model systems we studied.

Acknowledgments We thank Carol Charniga for preparing RPESC-RPE cells and Dr. Sally Temple (both Neural Stem Cell Institute, Rensselaer, NY) for helpful discussions. We also thank Drs. Arvydas Maminishkis and Sheldon Miller for providing passage-0 hfRPE cells and advice on growing primary hfRPE. This work was supported by NIH grant EY13295 (to S.C.F.) and by the Empire State Stem Cell Fund through New York State Department of Health Contract # C028505. Opinions expressed here are solely those of the authors and do not necessarily reflect those of the Empire State Stem Cell Board, the New York State Department of Health, or the State of New York.

References

Blenkinsop TA, Salero E, Stern JH et al (2013) The culture and maintenance of functional retinal pigment epithelial monolayers from adult human eye. Methods Mol Biol 945:45–65

da Cruz L, Rakoczy P, Perricaudet M et al (1996) Dynamics of gene transfer to retinal pigment epithelium. Invest Ophthalmol Vis Sci 37:2447–2454

Hu J, Bok D (2010) Culture of highly differentiated human retinal pigment epithelium for analysis of the polarized uptake, processing, and secretion of retinoids. Methods Mol Biol 652:55–73

Maminishkis A, Chen S, Jalickee S et al (2006) Confluent monolayers of cultured human fetal retinal pigment epithelium exhibit morphology and physiology of native tissue. Invest Ophthalmol Vis Sci 47:3612–3624

Mazzoni F, Safa H, Finnemann SC (2014) Understanding photoreceptor outer segment phagocytosis: use and utility of RPE cells in culture. Exp Eye Res 126:51–60

Nandrot EF, Kim Y, Brodie SE et al (2004) Loss of synchronized retinal phagocytosis and age-related blindness in mice lacking αvβ5 integrin. J Exp Med 200:1539–1545

Nandrot EF, Silva KE, Scelfo C et al (2012) Retinal pigment epithelial cells use a MerTK-dependent mechanism to limit the phagocytic particle binding activity of αvβ5 integrin. Biol Cell 104:326–341

Salero E, Blenkinsop TA, Corneo B et al (2012) Adult human RPE can be activated into a multipotent stem cell that produces mesenchymal derivatives. Cell Stem Cell 10:88–95

Sonoda S, Spee C, Barron E et al (2009) A protocol for the culture and differentiation of highly polarized human retinal pigment epithelial cells. Nat Protoc 4:662–673

Strauss O (2005) The retinal pigment epithelium in visual function. Physiol Rev 85:845–881

Trapani I, Puppo A, Auricchio A (2014) Vector platforms for gene therapy of inherited retinopathies. Prog Retin Eye Res 43:108–128

Chapter 98
Contribution of Ion Channels in Calcium Signaling Regulating Phagocytosis: MaxiK, Cav1.3 and Bestrophin-1

Olaf Strauß, Nadine Reichhart, Nestor Mas Gomez and Claudia Müller

Abstract Mutations in the BEST1 gene lead to a variety of retinal degenerations including Best's vitelliforme macular degeneration. The BEST1 gene product, bestrophin-1, is expressed in the retinal pigment epithelium (RPE). It is likely that mutant bestrophin-1 impairs functions of the RPE which support photoreceptor function and will thus lead to retinal degeneration. However, the RPE function which is influenced by bestrophin-1 is so far not identified. Previously we showed that bestrophin-1 interacts with L-type Ca^{2+}channels of the $Ca_V1.3$ subtype and that the endogenously expressed bestrophin-1 is required for intracellular Ca^{2+}regulation. A hallmark of Best's disease is the fast lipofuscin accumulation occurring already at young ages. Therefore, we addressed the hypothesis that bestrophin-1 might influence phagocytosis of photoreceptor outer segments (POS) by the RPE. Here, siRNA knock-down of bestrophin-1 expression as well as inhibition of L-type Ca^{2+}channel activity modulated the POS phagocytosis *in vitro*. *In vivo* $Ca_V1.3$ expression appeared to be diurnal regulated with a higher expression rate in the afternoon. Compared to wild-type littermates, $Ca_V1.3^{-/-}$ mice showed a shift in the circadian POS phagocytosis with an increased activity in the afternoon. Thus we suggest that mutant bestrophin-1 leads to an impaired regulation of the POS phagocytosis by the RPE which would explain the fast lipofuscin accumulation in Best patients.

O. Strauß (✉) · N. Reichhart
Experimental Ophthalmology, Department of Ophthalmology, Charite University Medicine Berlin, Augustenburger Platz 1, 13353 Berlin, Germany
e-mail: olaf.strauss@charite.de

N. Reichhart
e-mail: Nadine.reichhart@charite.de

N. M. Gomez
Department of Anatomy and Cell Biology, School of Dental Medicine, University of Pennsylvania, Augustenburger Platz 1, 240 South 40th Street, Philadelphia, PA 19104-6030, USA
e-mail: tmspl77@yahoo.es

Claudia Müller
Department of Biological Sciences, Center for Cancer, Genetic Diseases and Gene Regulation, Fordham University Bronx, Bronx, NY 10458, USA
e-mail: mueller_claudi@gmx.de

C. Bowes Rickman et al. (eds.), *Retinal Degenerative Diseases,* Advances in Experimental Medicine and Biology 854, DOI 10.1007/978-3-319-17121-0_98

Keywords BEST1 · Retinal pigment epithelium · Phagocytosis · $Ca_V1.3$ · Ca^{2+} signaling · Vitelliform macular dystrophy · Best disease · Transgenic mice · Bestrophin-1 · MaxiK

98.1 Introduction

Bestrophin-1, the product of the BEST1 gene. Mutations in the BEST1 gene were identified to cause different types of retinal degenerations. The most common type is Best's vitelliforme macular dystrophy (Marquardt et al. 1998; Petrukhin et al. 1998; Marmorstein and Kinnick 2007; Boon et al. 2009). The BEST1 gene product, bestrophin-1, is expressed by the retinal pigment epithelium (RPE) (Marmorstein and Kinnick 2007; Hartzell et al. 2008) which interacts with the photoreceptors of the retina and is essential for visual function (Strauss 2005). Therefore, it is likely that mutant bestrophin-1 impairs RPE function which in turn leads to photoreceptor degeneration.

98.2 Influence of Bestrophin-1 on RPE Cell Function

The RPE maintains the photoreceptor function by diurnal phagocytosis of shed photoreceptor outer segments, transepithelial transport, re-isomerization of all-trans retinal, spatial buffering of ions in the subretinal space, secretion of neurotrophic factors and by light absorption (Strauss 2005).

Several functional properties of bestrophin-1 might be essential for the RPE. Bestrophin-1 was identified as a Ca^{2+}-dependent Cl channel (Marmorstein and Kinnick 2007; Hartzell et al. 2008) which appears endogenously expressed mainly in membranes of ER Ca^{2+} stores (Barro-Soria et al. 2010; Neussert et al. 2010; Strauss et al. 2012; Gomez et al. 2013). However, this localization might not be exclusive. Furthermore, bestrophin-1 influences intracellular Ca^{2+} signaling in the RPE. On one hand bestrophin-1 interacts with L-type Ca^{2+} channels of the $Ca_V1.3$ subtype regulating their surface expression and conductance (Rosenthal et al. 2006; Yu et al. 2008; Reichhart et al. 2010; Milenkovic et al. 2011b). On the other hand bestrophin-1 acts as an intracellular Cl channel which helps to accumulate into or to release Ca^{2+} from cytosolic Ca^{2+} stores by conducting Cl as negatively charged counter-ion for the transmembranal transport of the positively charged Ca^{2+} ions (Gomez et al. 2013).

Best patients show a fast accumulation of lipofuscin (Boon et al. 2009). Since a considerable body of evidence indicate that lipofuscin accumulation cause loss of RPE cells in many types of macular degeneration it is likely that also in Best's disease lipofuscin represents an important risk factor for retinal degeneration (Sparrow et al. 2012). Altered photoreceptor outer segment (POS) phagocytosis can cause lipofuscin accumulation. Furthermore Ca^{2+} signaling involving L-type Ca^{2+} channels

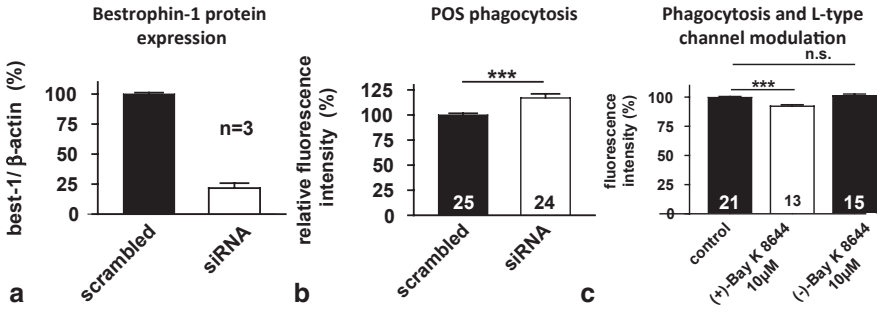

Fig. 98.1 Modulation of POS phagocytosis in cultured porcine RPE. **a** Western-Blot showing the reduction of bestrophin-1 expression after siRNA knock-down. **b** Phagocytosis rates of RPE cells either treated with non-targeting siRNA (scrambled) or bestrophin-1 targeted siRNA. **c** Effect of L-type channel inhibition ((+))BayK8644) or activation ((−)BayK8644 on phagocytosis rate. (mean ± SEM of 3 experiments with $n = 13–25$ samples; *** = p-value < 0.001; modified from Muller et al. 2014)

controls RPE phagocytosis (Karl et al. 2008). Thus an impairment of Ca^{2+} signaling by mutant bestrophin-1 causes altered regulation of phagocytosis, and therefore lipofuscin accumulation.

98.3 Impact of L-type Ca^{2+} Channels and Bestrophin-1 on POS Phagocytosis of the RPE

Data about the impact of ion channels in the phagocytosis regulation further support this hypothesis (Muller et al. 2014). Using a porcine RPE cell culture model the POS phagocytosis was investigated under the influence of ion channel modulation. After siRNA knock-down of bestrophin-1 the POS uptake is increased, which indicates an influence of bestrophin-1 on POS phagocytosis (Fig. 98.1a, b). Here bestrophin-1 is an inhibitor of phagocytic activity. This effect might be either due to inhibitory modulation of L-type channel activity or due to decreased activation of store-operated Ca^{2+} entry (Heth and Marescalchi 1994; Gomez et al. 2013). However, after siRNA knock-down of Orai-1 Ca^{2+} channels which permits the store-operated Ca^{2+} entry, phagocytic activity remains unchanged. Using the dihydropyridine derivative BayK8644 the L-type channel activity can be specifically modulated. The application of L-type channel inhibitor (+)BayK8644 led to a reduced phagocytic activity whereas the application of L-type channel activator (-)BayK8644 had no further effect on POS phagocytosis (Fig. 98.1c). The phagocytosis reduction after L-type channel inhibition shows that L-type channels are required for POS phagocytosis activation. The siRNA knock-down of the L-type channel inhibitor bestrophin-1 would result in increased L-type channel activity and therefore in increased POS phagocytosis. That the L-type channel opener (-) BayK8644 has no effect can be explained by the fact that the substance has also

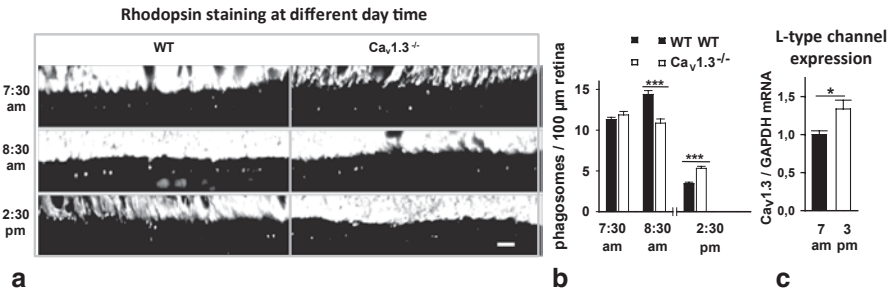

Fig. 98.2 *In vivo* analysis of POS phagocytosis in the $Ca_V1.3$ knock-out mouse. **a** Representative retinal sections prepared from $Ca_V1.3$ knock-out and wild-type mice at different time points of the day; phagosomes in the RPE can be detected by rhodopsin staining (scale bar = 10 µm). **b** Phagocytic activity given in phagosome number at different time points of the day. **c** $Ca_V1.3$ in the RPE at different day times. (mean ± SEM; 30–48 sections from 5 mice per timepoint; * = *p*-value < 0.05, *** = *p*-value < 0.001; modified from Muller et al. 2014)

an impact on the voltage-dependence of L-type channels. A possible activation of L-type channels would be due to increased tyrosine phosphorylation following integrin receptor ligation after POS binding As we showed previously that L-type channels are activated by increased tyrosine phosphorylation after integrin receptor ligation, mechanistically channel activation can follow POS binding to αvβ5 integrin surface receptor during phagocytosis. (Karl et al. 2008).

The data discussed so far were obtained in cultured cells. RPE phagocytosis is a rhythmical regulated process and ion channel expression might vary at different day times. *In vitro* experiments lack that impact. In order to substantiate the above discussed model *in vivo* phagocytosis was investigated in two knock-out mouse animal models deficient for ion channels. Phagocytosis was measured in retinal sections established at different time points during the day. Immunohistological staining against rhodopsin enables the detection of early phagosomes in the RPE. $Ca_V1.3$ knock-out mice showed compared to wild-type littermates lower phagocytic activity at phagocytosis peak in the morning but a higher remaining activity in the afternoon, indicating a bad termination of the process (Fig. 98.2a, 98.2b). Furthermore, $Ca_V1.3$ channels expression rate was higher in the afternoon compared to the morning (Fig. 98.2c). In maxiK knock-out mice the phagocytic activity rises earlier at its peak in the morning but decreases stronger in the afternoon compared to wild-type littermates. In older mice the higher phagocytic activity in the morning results in shorter photoreceptor outer segments. Thus the *in vivo* phagocytosis analysis verified that ion channels play a role in the regulation of phagocytosis but mainly in the regulation of its diurnal activity and probably not in the direct regulation of the process. Since bestrophin-1 is a regulator of the $Ca_V1.3$ channel activity it is likely that bestrophin-1 plays an important role in the diurnal regulation of phagocytosis.

Given that bestrophin-1/L-type channel interaction is involved in the regulation of phagocytosis mutant bestrophin-1 probably disturbs phagocytosis regulation ultimately leading to lipofuscin accumulation. A comparable effect was found in the

5-integrin knock-out mouse model, which shows a loss of circadian phagocytosis rhythm leading to a subsequent strong accumulation of lipofuscin and retinal degeneration (Nandrot et al. 2004). Here it should be mentioned that L-type channels in the RPE are also activated by POS-dependent stimulation of integrin-receptors. Considering the fact that mutant bestrophin-1 is unable to traffic to its physiological important subcellular localization (Milenkovic et al. 2011a) than also in patients a loss of bestrophin-1 function can be considered. As *in vitro* the siRNA knockdown of bestrophin-1 results in a higher phagocytic activity it can be assumed that also in Best patients the loss of function of mutant bestrophin-1 results in higher POS phagocytic activity which might explain the fast lipofuscin accumulation. The investigation of the $Best1^{W93/W93C}$ knock in mice seems to support this conclusion (Zhang et al. 2010). Here at the electron microscopy level irregularities of photoreceptor outer segments and a lipofuscin accumulation were detected which can result from impaired phagocytosis regulation. However, the $Best1^{-/-}$ mouse shows no signs of retinal degeneration. Thus the significance of data from mouse models for the human disease, especially for macular degenerations, should be taken with care.

In summary the ion channels $Ca_V1.3$, bestrophin-1 and maxiK were identified as novel players in the regulation of POS phagocytosis by the RPE *in vitro* and *in vivo*. They are not directly involved in the phagocytosis process. Rather ion channels have an indirect effect by involvement in regulation of the circadian rhythm of the phagocytosis. Mutant bestrophin-1 might disturb this rhythmic activity and lead to lipofuscin accumulation which likely represents an important pathologic event.

Acknowledgements This work was supported by the Deutsche Forschungsgemeinschaft DFG STR480/9−2 and 10−2, the FOR1075.

References

Barro-Soria R, Aldehni F, Almaca J et al (2010) ER-localized bestrophin 1 activates Ca2+-dependent ion channels TMEM16A and SK4 possibly by acting as a counterion channel. Pflugers Arch 459:485–497

Boon CJ, Klevering BJ, Leroy BP et al (2009) The spectrum of ocular phenotypes caused by mutations in the BEST1 gene. Prog Ret Eye Res 28:187–205

Gomez NM, Tamm ER, Strauss O (2013) Role of bestrophin-1 in store-operated calcium entry in retinal pigment epithelium. Pflugers Arch 465:481–495

Hartzell HC, Qu Z, Yu K et al (2008) Molecular physiology of bestrophins: multifunctional membrane proteins linked to best disease and other retinopathies. Physiol Rev 88:639–672

Heth CA, Marescalchi PA (1994) Inositol triphosphate generation in cultured rat retinal pigment epithelium. Investig Ophthalmol Vis Sci 35:409–416

Karl MO, Kroeger W, Wimmers S et al (2008) Endogenous Gas6 and Ca2+ -channel activation modulate phagocytosis by retinal pigment epithelium. Cell Signal 20:1159–1168

Marmorstein AD, Kinnick TR (2007) Focus on molecules: bestrophin (best-1). Exp Eye Res 85:423–424

Marquardt A, Stohr H, Passmore LA et al (1998) Mutations in a novel gene, VMD2, encoding a protein of unknown properties cause juvenile-onset vitelliform macular dystrophy (Best's disease). Hum Mol Genet 7:1517–1525

Milenkovic VM, Rohrl E, Weber BH et al (2011a) Disease-associated missense mutations in bestrophin-1 affect cellular trafficking and anion conductance. J Cell Sci 124:2988–2996
Milenkovic VM, Krejcova S, Reichhart N et al (2011b) Interaction of bestrophin-1 and Ca2+ channel beta-subunits: identification of new binding domains on the bestrophin-1 C-terminus. PloS one 6:e19364
Muller C, Mas Gomez N, Ruth P et al (2014) CaV1.3 L type channels, maxiK Ca(2+)-dependent K(+) channels and bestrophin-1 regulate rhythmic photoreceptor outer segment phagocytosis by retinal pigment epithelial cells. Cell Signal 26:968–978
Nandrot EF, Kim Y, Brodie SE et al (2004) Loss of synchronized retinal phagocytosis and age-related blindness in mice lacking {alpha}v{beta}5 Integrin. J Exp Med 200:1539–1545
Neussert R, Muller C, Milenkovic VM et al (2010) The presence of bestrophin-1 modulates the Ca2+ recruitment from Ca2+ stores in the ER. Pflugers Arch 460:163–175
Petrukhin K, Koisti MJ, Bakall B et al (1998) Identification of the gene responsible for Best macular dystrophy. Nature Genet 19:241–247
Reichhart N, Milenkovic VM, Halsband CA et al (2010) Effect of bestrophin-1 on L-type Ca2+ channel activity depends on the Ca2+ channel beta-subunit. Exp Eye Res 91:630–639
Rosenthal R, Bakall B, Kinnick T et al (2006) Expression of bestrophin-1, the product of the VMD2 gene, modulates voltage-dependent Ca2+ channels in retinal pigment epithelial cells. FASEB J 20:178–180
Sparrow JR, Gregory-Roberts E, Yamamoto K et al (2012) The bisretinoids of retinal pigment epithelium. Prog Ret Eye Res 31:121–135
Strauss O (2005) The retinal pigment epithelium in visual function. Physiol Rev 85:845–881
Strauss O, Neussert R, Muller C et al (2012) A potential cytosolic function of bestrophin-1. Adv Exp Med Biol 723:603–610
Yu K, Xiao Q, Cui G et al (2008) The best disease-linked Cl- channel hBest1 regulates Ca V 1 (L-type) Ca2+ channels via src-homology-binding domains. J Neurosci 28:5660–5670
Zhang YW, Stanton JB, Wu J et al (2010) Suppression of Ca2+ signaling in a mouse model of best disease. Hum Mol Genet 19:1108–1118

Chapter 99
Lysosomal Trafficking Regulator (LYST)

Xiaojie Ji, Bo Chang, Jürgen K. Naggert and Patsy M. Nishina

Abstract Regulation of vesicle trafficking to lysosomes and lysosome-related organelles (LROs) as well as regulation of the size of these organelles are critical to maintain their functions. Disruption of the lysosomal trafficking regulator (LYST) results in Chediak-Higashi syndrome (CHS), a rare autosomal recessive disorder characterized by oculocutaneous albinism, prolonged bleeding, severe immunodeficiency, recurrent bacterial infection, neurologic dysfunction and hemophagocytic lympohistiocytosis (HLH). The classic diagnostic feature of the syndrome is enlarged LROs in all cell types, including lysosomes, melanosomes, cytolytic granules and platelet dense bodies. The most striking CHS ocular pathology observed is an enlargement of melanosomes in the retinal pigment epithelium (RPE), which leads to aberrant distribution of eye pigmentation, and results in photophobia and decreased visual acuity. Understanding the molecular function of LYST and identification of its interacting partners may provide therapeutic targets for CHS and other diseases associated with the regulation of LRO size and/or vesicle trafficking, such as asthma, urticaria and *Leishmania amazonensis* infections.

Keywords Lysosomal trafficking regulator (LYST) · Chediak-Higashi syndrome · Lysosome · Lysosome-related organelles · Melanosome · Vesicle trafficking · Retinal Pigment Epithelium (RPE)

P. M. Nishina (✉) · X. Ji · B. Chang · J. K. Naggert
The Jackson Laboratory, Bar Harbor, ME 04609, USA
e-mail: pmn@jax.org

X. Ji
Graduate School of Biomedical Sciences and Engineering,
University of Maine, 600 Main Street, Orono, USA
e-mail: xiaojie.ji@jax.org

B. Chang
e-mail: bo.chang@jax.org

J. K. Naggert
e-mail: juergen.naggert@jax.org

C. Bowes Rickman et al. (eds.), *Retinal Degenerative Diseases,* Advances in Experimental Medicine and Biology 854, DOI 10.1007/978-3-319-17121-0_99

99.1 Introduction

The gene affected in patients with Chediak-Higashi syndrome, initially identified by positional cloning and YAC complementation almost 20 years ago, was named *Lys*osomal *T*rafficking Regulator (LYST) (Barbosa et al. 1996; Nagle et al. 1996; Perou et al. 1996). The *LYST* gene, also referred to as *CHS/CHS1/Beige*, encodes a large cytoplasmic protein of approximately 430 kDa, whose function remains poorly understood (Ward et al. 2003; Kaplan et al. 2008; Cullinane et al. 2013; Kypri et al. 2013). Structural analysis of LYST does not reveal motifs of definitive function, however, several N-terminal ARM/HEAT repeats, a Pleckstrin homology (PH) domain, a BEACH domain and WD40 repeats near the C-terminus have been predicted (Nagle et al. 1996; Ward et al. 2003; Kaplan et al. 2008; Cullinane et al. 2013).

LYST, a member of the BEACH (named after "*Be*ige and *C*hediak-*H*igashi") family of proteins present in all eukaryotes, shares extensive identity among all mammalian species (Nagle et al. 1996). An 88 % sequence homology is observed between the human and mouse LYST genes with 82 % of amino acid residues being identical (Ward et al. 2000). LYST is widely expressed in most tissues (Perou et al. 1997) and loss-of-function mutations lead to enlarged lysosomes and lysosome-related organelles (LROs) in all cell types (White and Clawson 1979; Burkhardt et al. 1993; Zhao et al. 1994; Introne et al. 1999; Ward et al. 2002; Kaplan et al. 2008). In addition, this organelle enlargement is accompanied with defective protein sorting and plasma membrane repair due to impaired intracellular vesicle trafficking (Huynh et al. 2004; Shiflett et al. 2004; Kaplan et al. 2008).

99.2 Associated Disorders of LYST Mutations

The first case of Chediak-Higashi syndrome (CHS) was reported in 1943 (Lozano et al. 2014). The disease is very rare, with less than 500 cases reported worldwide in the past 20 years (Kaplan et al. 2008). Most patients with CHS (85 – 90 %) are diagnosed in early childhood with severe clinical manifestations, including variable degrees of oculocutaneous albinism and recurrent fatal pyogenic infections (Kaplan et al. 2008; Lozano et al. 2014). Hair color may be blond, gray, or white, often with a distinguishing silvery or metallic sheen (Lozano et al. 2014). CHS patients frequently show aberrantly dispersed eye pigmentation as well, resulting in photophobia and decreased visual acuity (BenEzra et al. 1980; Valenzuela and Morningstar 1981; Kaplan et al. 2008). In addition, other ocular manifestations such as nystagmus and strabismus have also been reported (Lozano et al. 2014). The recurrent bacterial infections due to the dysfunction of polymorphonuclear leukocytes predominantly occur in the respiratory tract, skin and mucous membranes (Padgett et al. 1968; Blume and Wolff 1972; Kaplan et al. 2008; Lozano et al. 2014). Patients

with CHS have platelet defects, which manifest as bruising and mucosal bleeding. Finally, patients also present with progressive neurologic dysfunction, including motor and sensory neuropathies, ataxia, and progressive neurodegeneration. In advanced stages, CHS can also lead to parkinsonism and dementia (Sung and Stadlan 1968; Sung et al. 1969; Hirano et al. 1971; Misra et al. 1991; Tardieu et al. 2005; Kaplan et al. 2008; Lozano et al. 2014).

The majority of children affected by CHS progress to the most life-threatening lymphoproliferative accelerated phase characterized by massive hemophagocytic lympohistiocytosis (HLH), a hallmark of the "childhood" form of CHS. HLH often follows initial exposure to Epstein-Barr virus (EBV) and is characterized by diverse clinical manifestations including fever, lymphadenopathy and liver dysfunction (Lozano et al. 2014). Lymphohistiocytic infiltration of major organs may also be observed. While this condition affects multiple organs and systems, death is generally caused by infection, bleeding or development of HLH, unless treated by bone marrow transplantation (Karim et al. 2002; Kaplan et al. 2008; Lozano et al. 2014). A smaller proportion, 10–15% of patients with CHS, present much milder clinical features, termed the 'adolescent' and 'adult' forms (Karim et al. 2002; Lozano et al. 2014). These forms of CHS manifest as subtle alterations of pigmentation, a lower frequency of infections, mild bleeding tendencies and no accelerated phase. These patients can survive until adulthood but they develop neurologic dysfunctions including intellectual deficits, peripheral neuropathy, balance abnormalities, tremors, parkinsonism and dementia (Sung and Stadlan 1968; Sung et al. 1969; Hirano et al. 1971; Misra et al. 1991; Tardieu et al. 2005; Kaplan et al. 2008; Lozano et al. 2014).

Patients with CHS are prophylactically administered antibiotics to prevent opportunistic infections by pathogens and to control recurrent infections. An effective treatment for hematologic and immunologic complications of the disease has been hematopoietic stem cell transplantation (HSCT) following by prophylactic antibiotics administration. However, to date, there is no clinical evidence that HSCT can prevent the progressive neurologic problems or hypopigmentation associated with the disease (Kaplan et al. 2008; Cullinane et al. 2013; Lozano et al. 2014).

Mutations of *Lyst* or disruption of LYST interacting proteins have also been suggested to be potential factors that contribute to exfoliation syndrome (XFS), a common age-related disease characterized by iris defects, fibrillar accumulations, and aberrantly dispersed pigment throughout the anterior chamber of the eye (Trantow et al. 2009). A body of evidence suggests that the pathologic accumulation of exfoliative material within the iridocorneal angle elevates intraocular pressure (IOP) and leads to glaucoma (Trantow et al. 2009; Trantow et al. 2010). XFS is the most commonly identified cause of secondary open-angle glaucoma. Although, both CHS and XFS are linked to LYST, they share few common pathological features. This may be due in part to the fact that, unlike CHS that is only caused by mutations in LYST, XFS can be caused by mutations in multiple genes. Alternatively, there may be allele specific phenotypes associated with different *LYST* disease alleles.

99.3 Proposed Functions of LYST

The enlarged lysosomes and LROs in all cell types are the hallmark of the subcellular morphology associated with CHS (White and Clawson 1979; Burkhardt et al. 1993; Zhao et al. 1994; Introne et al. 1999; Ward et al. 2002; Kaplan et al. 2008). The mechanism underlying this classic diagnostic feature remains largely elusive and the molecular investigation of the cellular function of LYST and its orthologs are currently underway. These functional studies have initially led to two distinct models for LYST function in the regulation of LRO size (Falkenstein and De Lozanne 2014).

One model suggests that LYST restricts homotypic lysosome fusion. This is supported by many studies suggesting interaction of LYST with fusion regulators in human (Tchernev et al. 2002), mice (Hammel et al. 2010), *Drosophila* (Rahman et al. 2012) and *Dictyostelium* (Harris et al. 2002; Kypri et al. 2007; Kypri et al. 2013). The other model suggests that LYST may contribute to lysosomal membrane fission instead of fusion events. The fission model was first suggested by the observation that *Lyst* overexpression in mice causes a reduction in lysosome size (Perou et al. 1997). Subsequent studies in both mice (Durchfort et al. 2012) and *Dictyostelium* (Charette and Cosson 2007, 2008) support this model by showing that LYST is a positive regulator of post-lysosome fission and abnormal LYST causes reduced rate of lysosome fission.

In a recent paper (Falkenstein and De Lozanne 2014), Falkenstein and De Lozanne proposed that LYST function is likely to be far more complex than either the simple function of lysosomal fusion or fission, and postulated that LYST may regulate fusion through fission mediated recycling of fusion machinery during lysosomal maturation.

Studies in *Saccharomyces cerevisiae* suggest that the LYST homolog, Bph1p, is involved in protein sorting and cell wall formation, but unlike LYST, Bph1p does not affect vacuolar/lysosomal size (Shiflett et al. 2004). Bph1p is also suggested to be involved in vesicular trafficking and defects can lead to altered protein trafficking and thereby, abnormal cell wall formation (Shiflett et al. 2004; Kaplan et al. 2008).

In summary, LYST and its homologs have been predicted to regulate the intracellular LRO size through mechanisms that have yet to be elucidated but are likely to involve lysosomal fusion and fission, as well as vesicular trafficking.

99.4 Significance of Functional Study of LYST

To date, the molecular function of LYST still remains unclear. The function of LYST has been studied in many model systems but each has its own limitation. The beige (*bg*) mouse, first identified in 1967 (Lutzner et al. 1967), is the best studied animal model for CHS and successfully recapitulates most defects in human CHS,

including the distinctive coat color described as beige and abnormal size and distribution of LROs but not HLH (Burkhardt et al. 1993; Kaplan et al. 2008). Even with differences in clinical severity, the animal models will provide essential insight into mechanistic understanding of CHS in terms of vesicle trafficking and LRO formation *in vivo*. RPE cells, essential for normal visual function, and significantly affected in CHS, will serve as a good cell type for functional studies of LYST.

Understanding the function of LYST will be important for creating effective therapies, not only for CHS but also diseases associated with LRO size and/or vesicular trafficking, e.g. diseases such as asthma and urticaria due to abnormal local degranulation by leukocytes and mast cells, and *Leishmania amazonensis* infections (Tchernev et al. 2002; Wilson et al. 2008). Manipulating the expression/activity level of LYST or its interacting partners to regulate lysosomal size would be an attractive strategy to ameliorate or delay the pathological effects of these disorders.

References

Barbosa MD, Nguyen QA, Tchernev VT et al (1996) Identification of the homologous beige and Chediak-Higashi syndrome genes. Nature 382:262–265

BenEzra D, Mengistu F, Cividalli G et al (1980) Chediak-Higashi syndrome: ocular findings. J Pediatr Ophthalmol Strabismus 17:68–74

Blume RS, Wolff SM (1972) The Chediak-Higashi syndrome: studies in four patients and a review of the literature. Medicine (Baltimore) 51:247–280

Burkhardt JK, Wiebel FA, Hester S et al (1993) The giant organelles in beige and Chediak-Higashi fibroblasts are derived from late endosomes and mature lysosomes. J Exp Med 178:1845–1856

Charette SJ, Cosson P (2007) A LYST/beige homolog is involved in biogenesis of Dictyostelium secretory lysosomes. J Cell Sci 120:2338–2343

Charette SJ, Cosson P (2008) Altered composition and secretion of lysosome-derived compartments in Dictyostelium AP-3 mutant cells. Traffic 9:588–596

Cullinane AR, Schaffer AA, Huizing M (2013) The BEACH is hot: a LYST of emerging roles for BEACH-domain containing proteins in human disease. Traffic 14:749–766

Durchfort N, Verhoef S, Vaughn MB et al (2012) The enlarged lysosomes in beige j cells result from decreased lysosome fission and not increased lysosome fusion. Traffic 13:108–119

Falkenstein K, De Lozanne A (2014) Comparison of Dictyostelium LvsB and endosomal fission defect mutants support a fusion regulatory role for LvsB. J Cell Sci 127(Pt. 20):4356–4367

Hammel I, Lagunoff D, Galli SJ (2010) Regulation of secretory granule size by the precise generation and fusion of unit granules. J Cell Mol Med 14:1904–1916

Harris E, Wang N, Wu Wl WL et al (2002) Dictyostelium LvsB mutants model the lysosomal defects associated with Chediak-Higashi syndrome. Mol Biol Cell 13:656–669

Hirano A, Zimmerman HM, Levine S et al (1971) Cytoplasmic inclusions in Chediak-Higashi and Wobbler mink. An electron microscopic study of the nervous system. J Neuropathol Exp Neurol 30:470–487

Huynh C, Roth D, Ward DM et al (2004) Defective lysosomal exocytosis and plasma membrane repair in Chediak-Higashi/beige cells. Proc Natl Acad Sci U S A 101:16795–16800

Introne W, Boissy RE, Gahl WA (1999) Clinical, molecular, and cell biological aspects of Chediak-Higashi syndrome. Mol Genet Metab 68:283–303

Kaplan J, De Domenico I, Ward DM (2008) Chediak-Higashi syndrome. Curr Opin Hematol 15:22–29

Karim MA, Suzuki K, Fukai K et al (2002) Apparent genotype-phenotype correlation in childhood, adolescent, and adult Chediak-Higashi syndrome. Am J Med Genet 108:16–22
Kypri E, Schmauch C, Maniak M et al (2007) The BEACH protein LvsB is localized on lysosomes and postlysosomes and limits their fusion with early endosomes. Traffic 8:774–783
Kypri E, Falkenstein K, De Lozanne A (2013) Antagonistic control of lysosomal fusion by Rab14 and the Lyst-related protein LvsB. Traffic 14:599–609
Lozano ML, Rivera J, Sanchez-Guiu I et al (2014) Towards the targeted management of Chediak-Higashi syndrome. Orphanet J Rare Dis 9:132
Lutzner MA, Lowrie CT, Jordan HW (1967) Giant granules in leukocytes of the beige mouse. J Hered 58:299–300
Misra VP, King RH, Harding AE et al (1991) Peripheral neuropathy in the Chediak-Higashi syndrome. Acta Neuropathol 81:354–358
Nagle DL, Karim MA, Woolf EA et al (1996) Identification and mutation analysis of the complete gene for Chediak-Higashi syndrome. Nat Genet 14:307–311
Padgett GA, Reiquam CW, Henson JB et al (1968) Comparative studies of susceptibility to infection in the Chediak-Higashi syndrome. J Pathol Bacteriol 95:509–522
Perou CM, Moore KJ, Nagle DL et al (1996) Identification of the murine beige gene by YAC complementation and positional cloning. Nat Genet 13:303–308
Perou CM, Leslie JD, Green W et al (1997) The Beige/Chediak-Higashi syndrome gene encodes a widely expressed cytosolic protein. J Biol Chem 272:29790–29794
Rahman M, Haberman A, Tracy C et al (2012) Drosophila mauve mutants reveal a role of LYST homologs late in the maturation of phagosomes and autophagosomes. Traffic 13:1680–1692
Shiflett SL, Vaughn MB, Huynh D et al (2004) Bph1p, the Saccharomyces cerevisiae homologue of CHS1/beige, functions in cell wall formation and protein sorting. Traffic 5:700–710
Sung JH, Stadlan EM (1968) Neuropathological changes in Chediak-Higashi disease. J Neuropathol Exp Neurol 27:156–157
Sung JH, Meyers JP, Stadlan EM et al (1969) Neuropathological changes in Chediak-Higashi disease. J Neuropathol Exp Neurol 28:86–118
Tardieu M, Lacroix C, Neven B et al (2005) Progressive neurologic dysfunctions 20 years after allogeneic bone marrow transplantation for Chediak-Higashi syndrome. Blood 106:40–42
Tchernev VT, Mansfield TA, Giot L et al (2002) The Chediak-Higashi protein interacts with SNARE complex and signal transduction proteins. Mol Med 8:56–64
Trantow CM, Mao M, Petersen GE et al (2009) Lyst mutation in mice recapitulates iris defects of human exfoliation syndrome. Invest Ophthalmol Vis Sci 50:1205–1214
Trantow CM, Hedberg-Buenz A, Iwashita S et al (2010) Elevated oxidative membrane damage associated with genetic modifiers of Lyst-mutant phenotypes. PLoS Genet 6:e1001008
Valenzuela R, Morningstar WA (1981) The ocular pigmentary disturbance of human Chediak-Higashi syndrome. A comparative light- and electron-microscopic study and review of the literature. Am J Clin Pathol 75:591–596
Ward DM, Griffiths GM, Stinchcombe JC et al (2000) Analysis of the lysosomal storage disease Chediak-Higashi syndrome. Traffic 1:816–822
Ward DM, Shiflett SL, Kaplan J (2002) Chediak-Higashi syndrome: a clinical and molecular view of a rare lysosomal storage disorder. Curr Mol Med 2:469–477
Ward DM, Shiflett SL, Huynh D et al (2003) Use of expression constructs to dissect the functional domains of the CHS/beige protein: identification of multiple phenotypes. Traffic 4:403–415
White JG, Clawson CC (1979) The Chediak-Higashi syndrome: ring-shaped lysomomes in circulating monocytes. Am J Pathol 96:781–798
Wilson J, Huynh C, Kennedy KA et al (2008) Control of parasitophorous vacuole expansion by LYST/Beige restricts the intracellular growth of Leishmania amazonensis. PLoS Pathog 4:e1000179
Zhao H, Boissy YL, Abdel-Malek Z et al (1994) On the analysis of the pathophysiology of Chediak-Higashi syndrome. Defects expressed by cultured melanocytes. Lab Invest 71:25–34

Chapter 100
Live-Cell Imaging of Phagosome Motility in Primary Mouse RPE Cells

Roni Hazim, Mei Jiang, Julian Esteve-Rudd, Tanja Diemer, Vanda S. Lopes and David S. Williams

Abstract The retinal pigment epithelium (RPE) is a post-mitotic epithelial monolayer situated between the light-sensitive photoreceptors and the choriocapillaris. Given its vital functions for healthy vision, the RPE is a primary target for insults that result in blinding diseases, including age-related macular degeneration (AMD). One such function is the phagocytosis and digestion of shed photoreceptor outer segments. In the present study, we examined the process of trafficking of outer segment disk membranes in live cultures of primary mouse RPE, using high speed spinning disk confocal microscopy. This approach has enabled us to track phagosomes, and determine parameters of their motility, which are important for their efficient degradation.

Keywords Live-cell imaging · Retinal pigment epithelium · Intracellular trafficking · Photoreceptor outer segment · Phagocytosis

100.1 Introduction

The retinal pigment epithelium (RPE) is a post-mitotic epithelial monolayer of cuboidal cells situated between the light-sensitive photoreceptors and the choriocapillaris (Bok 1993). The RPE performs numerous functions vital to the health of photoreceptors and thus to healthy vision. These functions include recycling of retinoids during the visual cycle, transport of nutrients from the blood to the photoreceptors, and secretion of growth factors, such as vascular endothelial growth

The online version of this chapter 10.1007/978-3-319-17121-0_100 contains supplementary video material, which can be downloaded from: http://extra.springer.com.

Roni Hazim, Mei Jiang authors, Contributed equally

D. S. Williams (✉) · R. Hazim · M. Jiang · J. Esteve-Rudd · T. Diemer · V. S. Lopes
UCLA School of Medicine, Jules Stein Eye Institute, 100 Stein Plaza,
Los Angeles, CA 90095, USA
e-mail: dswilliams@ucla.edu

C. Bowes Rickman et al. (eds.), *Retinal Degenerative Diseases,* Advances in Experimental Medicine and Biology 854, DOI 10.1007/978-3-319-17121-0_100

factor (VEGF) and pigment epithelial-derived factor (PEDF) (Strauss 2005). One of the most critical functions performed by the RPE is the phagocytosis of photoreceptor outer segment (POS) tips (Young and Bok 1969), an event that occurs on a daily cycle (LaVail 1976).

The RPE is a professional phagocyte, internalizing and degrading approximately 10% of each photoreceptor outer segment on a daily basis. Phagosomes containing POS membranes move from the apical region of the RPE towards the basal region (Herman and Steinberg 1982; Gibbs et al. 2003), fusing with degradative organelles such as endosomes and lysosomes along the way (Wavre-Shapton et al. 2014; Bosch et al. 1993). By-products that are not completely degraded tend to form constituents of aggregates, such as lipofuscin or sub-RPE deposits, common features associated with macular degeneration (Brunk and Terman 2002). Given the movement of phagosomes from the apical region, their motility is closely related with their degradation. In an early study, it was shown that colchicine, which disrupts microtubules, inhibited the translocation of phagosomes from the apical region (Herman and Steinberg 1982). More recently, the importance of actin-based motility was demonstrated in mice lacking MYO7A, an unconventional myosin. In those mice, phagosomes were retained longer in the apical region of the RPE, and were degraded more slowly (Gibbs et al. 2003). In the present report, we describe the use of live-cell imaging, using spinning disk confocal microscopy, to study the intracellular trafficking of POS-containing phagosomes within primary mouse RPE cells.

100.2 Isolation and Culture of Primary Mouse RPE

Primary mouse RPE were isolated as previously described (Gibbs et al. 2003). Intact eyes were enucleated from P10-P15 mice and washed 3–4 times by inversion with growth medium (Dulbecco's modified Eagle's medium (DMEM) with 4.5 g/L glucose, L-glutamine, and sodium pyruvate). The eyes were then incubated in a 2% dispase solution for 45 min at 37° C. Following removal of the enzyme solution, the eyes were washed 3 times with growth medium containing 10% fetal bovine serum (FBS) and 20 mM HEPES. The eyes were dissected into eyecups by making an incision along the ora serrata to remove the cornea, iris, lens, and ciliary body. Eyecups were then incubated in growth medium for 20 min at 37° C, as this facilitates the separation of the RPE from the retina and Bruch's membrane. Sheets of RPE were gently scraped from Bruch's membrane and collected in growth medium with 10% FBS. The sheets were then washed 3 times with growth medium and twice with calcium- and magnesium-free Hank's Balanced Salt Solution (HBSS). The cells were then briefly and gently triturated and plated on Lab-Tek chambered coverglass. Live-cell imaging experiments were carried out on 3–7 day old cultures.

100.3 Isolation and Labeling of Mouse POSs

Mouse POSs were isolated as previously described (Gibbs et al. 2003). Mouse retinas were collected under dim red light and homogenized in Ringer's solution (130 mM NaCl, 3.6 mM KCl, 2.4 mM $MgCl_2$, 1.2 mM $CaCl_2$, 10 mM HEPES, and 0.02 mM EDTA). The homogenate was cleared by centrifugation for 30 s at 100 *g*, and then the supernatant was layered on top of a discontinuous Optiprep 8%-10%-15% step gradient in Ringer's solution and spun at 12,000 *g* for 20 min at 4° C. POSs were collected at the 10%/15% interface and diluted 3 times with Ringer's solution. POSs were then pelleted by spinning the solution at 10,300 *g* for 10 min at 4° C. The POSs were then labeled by incubation with 0.1 mg Texas Red-X, succinimidyl ester or 5% (v/v) Alexa Fluor 488 carboxylic acid, succinimidyl ester, mixed isomers in 1 mL 0.1 M $NaHCO_3$, pH 8.3 for 1 h at 4° C. POSs were then washed with Ringer's solution, resuspended in RPE growth medium, and counted using a haemocytometer to determine the yield.

100.4 Live Imaging Using Spinning Disk Confocal Microscopy

Figure 100.1a depicts a schematic diagram of the protocol used for live-cell imaging. We used C57BL/6J mice for both the RPE cells and the POSs. Cultured RPE cells were incubated with $1–5 \times 10^6$ fluorescently-labeled POSs in growth medium with 10 mM HEPES for 20 min at 37° C, washed extensively with growth medium, and then immediately imaged for a maximum of 1 h, using an Ultraview Spinning Disk Confocal Microscope system with a Zeiss Axiovert photomicroscope, including an environment chamber. Movies were acquired at 3 frames per second with the Volocity software (PerkinElmer), using a 63x oil immersion objective and a Hamamatsu EM-CCD camera (see supplementary video). Trajectories of phagosomes were analyzed using the Volocity software (Fig. 100.1b).

Not all phagosomes were moving at a given time, however, the paths of those that were moving typically followed relatively straight lines, with back and forth movements along these lines. This motility is consistent with movements along microtubules, as cargos of plus- and minus-end directed microtubule motors. The paths can be analyzed to assess a variety of phagosome motility parameters. Speed and distance traveled represent two basic parameters. From analysis of the paths of phagosomes that traveled at least 3 μm in a 24-second interval, we found a mean speed of 1.2 ± 0.1 μm/s and a mean total distance traveled of 11.3 ± 1.9 μm, during the 24-sec interval. This speed is typical of transport by microtubule motors (Okada et al. 1995). Transport along actin filaments by myosins is typically many fold slower (Boal 2012), suggesting that the observed motility was dominated by the microtubule motors, kinesin and dynein.

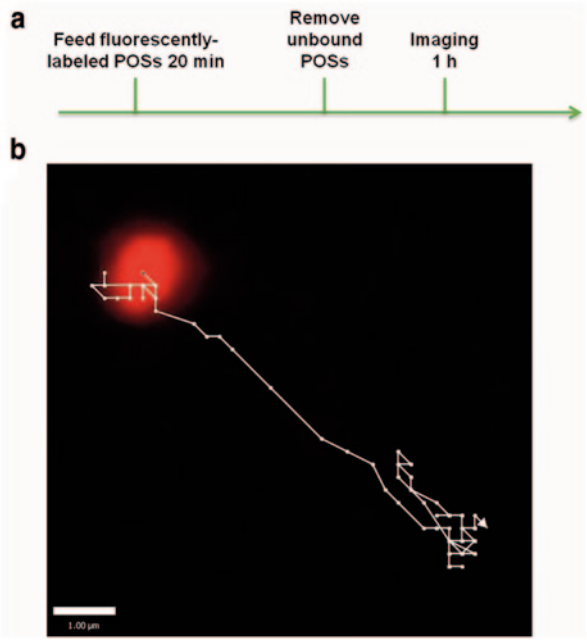

Fig. 100.1 Method for monitoring phagocytosis of photoreceptor outer segments in live RPE. **a** Scheme of phagocytosis assay for live cultures of RPE, **b** Magnified view of a fluorescently-labeled phagosome and its trajectory inside a live RPE cell

100.5 Conclusions

Fluorescently-labeled POS phagosomes can be monitored in live RPE cells, using spinning disk confocal microscopy. Their motility can be determined by tracking their trajectories, thus providing a sensitive, real-time measurement of a critical parameter of RPE health—one, which we are finding in other studies, feeds directly into the efficiency of phagosome degradation, and the propensity for the accumulation of debris and consequent activation of downstream events, such as inflammation and oxidative stress.

Acknowledgements We thank Barry Burgess for technical assistance. This study was supported by NIH R01 grant EY 07042 and P30 grant EY 00331.

References

Boal D (2012) Mechanics of the cell. In: Boal D (eds) Dynamic filaments. Cambridge University, Cambridge

Bok D (1993) The retinal pigment epithelium: a versatile partner in vision. J Cell Sci 17:189–195

Bosch E, Horwitz J, Bok D (1993) Phagocytosis of outer segments by retinal pigment epithelium: phagosome-lysosome interaction. J Histochem Cytochem 41:253–263

Brunk UT, Terman A (2002) Lipofuscins: mechanisms of age-related accumulation and influence on cell function. Free Rad Biol Med 33:611–619

Gibbs D, Kitamoto J, Williams DS (2003) Abnormal phagocytosis by retinal pigmented epithelium that lacks myosin VIIa, the usher syndrome 1B protein. Proc Natl Acad Sci U S A 100:6481–6486

Herman KG, Steinberg RH (1982) Phagosome movement and the diurnal pattern of phagocytosis in the tapetal retinal pigment epithelium of the opossum. Invest Ophthalmol Vis Sci 23: 277–290

LaVail MM (1976) Rod outer segment disk shedding in rat retina: relationship to cyclic lighting. Science 194:1071–1074

Okada Y, Yamazaki H, Sekine-Aizawa Y (1995) The neuron-specific kinesin superfamily protein KIF1A is a unique monomeric motor for anterograde axonal transport of synaptic vesicle precursors. Cell 81:769–780

Strauss O (2005) The retinal pigment epithelium in visual function. Physiol Rev 85:845–881

Wavre-Shapton ST, Meschede IP, Seabra MC (2014) Phagosome maturation during endosomes interaction revealed by partial rhodopsin processing in retinal pigment epithelium. J Cell Sci 127:3852–3861

Young RW, Bok D (1969) Participation of the retinal pigment epithelium in the rod outer segment renewal process. J Cell Biol 42:392–403

Chapter 101
RPE Cell and Sheet Properties in Normal and Diseased Eyes

Alia Rashid, Shagun K. Bhatia, Karina I. Mazzitello, Micah A. Chrenek, Qing Zhang, Jeffrey H. Boatright, Hans E. Grossniklaus, Yi Jiang and John M. Nickerson

Abstract Previous studies of human retinal pigment epithelium (RPE) morphology found spatial differences in density: a high density of cells in the macula, decreasing peripherally. Because the RPE sheet is not perfectly regular, we anticipate that there will be differences between conditions and when and where damage is most likely to begin. The purpose of this study is to establish relationships among RPE morphometrics in age, cell location, and disease of normal human and AMD eyes that highlight irregularities reflecting damage. Cadaveric eyes from 11 normal and 3 age-related macular degeneration (AMD) human donors ranging from 29 to 82 years of age were used. Borders of RPE cells were identified with phalloidin. RPE segmentation and analysis were conducted with CellProfiler. Exploration of spatial point patterns was conducted using the "spatstat" package of R. In the normal human eye, with increasing age, cell size increased, and cells lost their regular hexagonal shape. Cell density was higher in the macula versus periphery. AMD resulted in greater variability in size and shape of the RPE cell. Spatial point analysis revealed an ordered distribution of cells in normal and high spatial disorder in AMD eyes. Morphometrics of the RPE cell readily discriminate among young vs. old and normal vs. diseased in the human eye. The normal RPE sheet is organized in a regular array of cells, but AMD exhibited strong spatial irregularity. These

The first three authors contributed equally to this study.

J. M. Nickerson (✉)
Emory Eye Center, Room B5602, 1365B, Clifton Road, N.E., Atlanta, GA 30322, USA
e-mail: litjn@emory.edu

A. Rashid · S. K. Bhatia · M. A. Chrenek · Q. Zhang · J. H. Boatright · H. E. Grossniklaus
Ophthalmology, Emory University, Atlanta, GA, USA

K. I. Mazzitello
CONICET, Universidad Nacional de Mar del Plata, Mar del Plata 7600, Argentina

Y. Jiang
Mathematics and Statistics, Georgia State University, Atlanta, GA, USA

C. Bowes Rickman et al. (eds.), *Retinal Degenerative Diseases,* Advances in Experimental Medicine and Biology 854, DOI 10.1007/978-3-319-17121-0_101

findings reflect on the robust recovery of the RPE sheet after wounding and the circumstances under which it cannot recover.

Keywords Retinal pigmented epithelium (RPE) · Flatmount · En face · Spatial point patterns · Age related macular degeneration (AMD) · Cadaveric eyes · Spatstat · CellProfiler · Macula · Periphery · Nearest neighbor distance

101.1 Introduction

The retinal pigment epithelium (RPE) layer is located between the neurosensory retina and the choroid. Its main functions are to supply the highly metabolically active retina with nutrients and remove waste products from the photosensory processes of the cones and rods. To correctly function, the RPE layer must remain intact without any holes in the cell layer (Rizzolo 2014). The RPE layer robustly compensates for some damage or death of RPE cells until a certain point (Negi and Marmor 1984; Kalnins et al. 1995; Nagai and Kalnins 1996), but in the advanced stages of some retinal and macular diseases, the RPE layer can break down, leaving empty spaces (Ambati and Fowler 2012; Bhutto and Lutty 2012; van Lookeren et al. 2014). Toxic products are generated near the RPE layer in many eye diseases, such as age-related macular degeneration (AMD) and Stargardt's Disease. As RPE cells age, toxic metabolites continue to accumulate, causing the RPE cells to die (Liang and Godley 2003). With extensive RPE cell death, the epithelial sheet loses its overall stability (Chrenek et al. 2012; Jiang et al. 2013; Jiang et al. 2014), which leads to RPE dysfunction and impaired functioning and damage to the retina, such as that seen in AMD. Epithelial sheets are in general resilient and resistant to damage (Roider et al. 1992), and they maintain barrier function by tiling across the sheet (Jiang et al. 2013). In this study, we hypothesized increased variability in the shape and size of RPE cells and increased spatial irregularity by: (1) region-, (2) age-, and (3) disease.

To test this hypothesis, we analyzed RPE cell shape and size from human cadaveric eyes. Here we report the initial findings from both normal (undiseased) and AMD eyes across a broad age range. We found that RPE cell properties vary fairly consistently according to the region in the eye, age at death, and disease status.

101.2 Methods

Cadaveric human donor eyes ($n = 14$) harvested < 7 h postmortem were dissected to obtain a strip of RPE from the optic nerve through the macula to the ora. We adhered to ARVO guidelines, and the Emory IRB approved the study.

The RPE was flatmounted, stained with AF635-phalloidin, and then imaged using confocal microscopy (Chrenek et al. 2012; Jiang et al. 2013; Jiang et al. 2014). Images (typically 200–400 images, each image with hundreds of cells) were

photomerged using Autopano Pro v2.5 (Kolor, Montmélian, France). RPE segmentation and analysis were amassed with CellProfiler (Lamprecht et al. 2007). Exploration of spatial point patterns was conducted using the "Spatstat" package (Baddeley and Turner 2005) of R.

101.3 Results

101.3.1 Preliminary Findings

In the normal eye, cell density was higher at the macula compared to the far periphery. All parameters showed trends toward more variability in size and shape from macula to periphery. By region, irrespective of age, the macula and mid-periphery exhibited an isometric, small RPE cell, while the far periphery had a less uniform and larger RPE cell.

101.3.2 Aging in the Normal RPE

There was a transition at about 60 years old (yo), when the normal RPE sheet began to deteriorate. The deterioration was location specific. The macula and the far periphery showed significant changes. However, the mid-periphery exhibited no major changes between the younger vs., older eyes (data not shown). In the macula, there was more variability in sidedness (comparing <60 yo to >60 yo), reflected by a reduced percentage of hexagonal cells (43.5 vs. 38.0% respectively, $p = 0.01$).

101.3.3 The AMD Eye

In cadaveric eyes from AMD patients, the disrupted RPE showed great variability in both the size and shape of cells. In the macula of AMD eyes, the RPE exhibited patches of very large cells (Fig. 101.1). Where the RPE was atrophic, the surrounding RPE cells had an aberrant elevated rim. When soft drusen were present, adjacent RPE cells were often larger and stretched.

101.3.4 Regularity in AMD and Normal RPE Sheets

Regularity in spacing was clearly evident in the RPE sheet, with much more uniformity in the normal RPE sheet than in the macula of the AMD patient. Images of each RPE sheet are illustrated in Fig. 101.1. In Fig. 101.2, the cumulative distribution function of the nearest-neighbor distance (the G-function) is compared among the RPE pattern of an AMD eye (red), normal eye (green), and the control: the

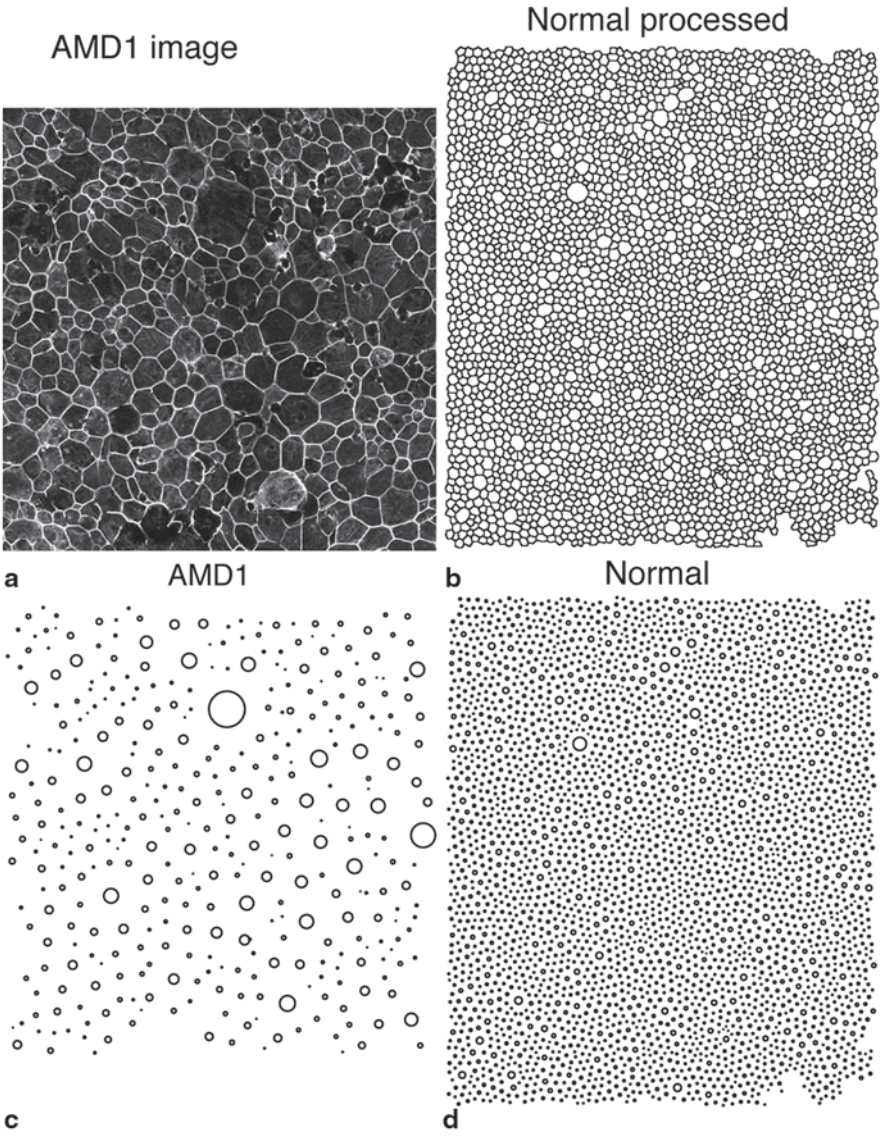

Fig. 101.1 Normal and AMD representative images of the RPE sheet. **a** An image from an AMD eye (AMD1) in the macula. **b** A partially processed image from the macula of a normal individual. The cell borders are now outlined and transformed so that CellProfiler can process the image. **c** Spatial point patterns from the AMD eye in a. **d** Spatial point pattern from the normal eye in b. Sizes of the circles in c and d represent the size of each cell

hexagonal cell lattice with the averaged cell size in the normal eye (blue). We also randomized the normal and the hexagonal lattice (dashed lines) to show the broadening of the distribution function. The plot indicated that the normal RPE pattern is remarkably similar to a hexagonal lattice of cells with a narrow distribution (tight

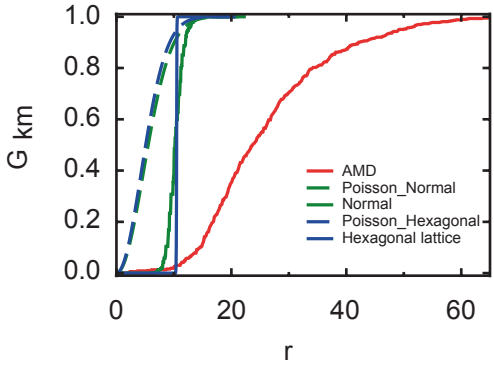

Fig. 101.2 Spatial point analysis by cumulative nearest neighbor distance distribution function. The key point is that G(r) for normal RPE is markedly different from that of AMD RPE, suggesting that the spatial patterns are more regular in normal eyes and become irregular in AMD RPE sheets

size range within 8–12 μ), while the AMD pattern shows a much broader distribution and a strong shift to the right. The latter indicates that the AMD RPE pattern has a larger minimum size, and a much reduced regularity.

101.4 Discussion

101.4.1 The Context of Our findings

The fraction of hexagonal cells on a surface is an indication of the mechanical stability of a tissue: Hexagonal tiling is the most efficient way to cover a plane with a monolayer of cells of equal area with the least total perimeter per cell (Thompson 1942). Sharp deviations from this tiling pattern indicate mechanical stress or a dynamic environment not near equilibrium. Cell death, cell division, and regional differences can affect the regular tiling and these defects compromise the strength and durability of the RPE sheet, and make these spots more vulnerable to neovascularization or the initiation of atrophic lesions (Shirinifard et al. 2012). Tiling defects occur in age-related loss of RPE cells (Watzke et al. 1993), inherited mouse retinal diseases (Jiang et al. 2013), and regional differences (foveal RPE versus equatorial) (Gao and Hollyfield 1992). We have initiated computer simulations of RPE cell death. The simulations seem to reveal testable hypotheses on loss of regularity in spatial point patterns according to a loss of inhibition in cell growth required to fill in holes in the RPE sheet.

101.4.2 The Normal Eye and Aging

The regular shape of RPE cells in the macula implies small and balanced external forces that pull or tug on each cell. The far-peripheral RPE cells were more

irregular, suggesting forces causing uneven tension. The far periphery may be subjected to different amounts of strain due to the nearby ciliary body and the non-uniform, intermittent stress from the ciliary muscles. Alternatively, the RPE cells in the far periphery may be different from those in the macula or mid-periphery (Burke and Hjelmeland 2005). RPE in the macula and far-periphery showed changes in both shape and size with age while the mid-periphery did not. Drusen and basal laminar deposits tend to occur in the macula and far periphery. These are signs of RPE stress; we hypothesize there is more RPE stress in the macula and far periphery than mid-periphery. These models need to be tested that consider differences (e.g., metabolic demands of overlying photoreceptor cells and incidences of hard drusen) among these three locations versus other models of inherently different classes of RPE cells (Burke and Hjelmeland 2005) in these three locations.

101.4.3 The AMD Eye

Understanding normal RPE morphology helps to better understand RPE pathology by discriminating between the effects of age (the most important risk factor of AMD) versus other risk factors (genetics, smoking, type of drusen, and environmental factors). Our preliminary evaluations here may imply that clustered outliers in size and shape of RPE cells are risks for or may initiate progression of AMD. Our studies may help to identify breakdown in the RPE at an earlier stage allowing for more prompt evaluation and treatment.

101.4.4 Spatial Point Patterning

We have found regularity in the spatial patterning of RPE cells that may reflect intercellular interactions. Future studies will help delineate when this regularity occurs/develops, and how it is lost in AMD, including the impact of druse, which distort the pattern in the RPE sheet.

101.4.5 Future Directions

In the near future, we will report full quantitative analysis of changes (per cell and in organization) in RPE with age, region, and disease state. We will correlate en-face metrics with histopathology of the same location cut in cross sections. These analyses should provide insight into the basic biology underlying transition from isometric cells to those that vary widely in shape, size, and function.

Acknowledgments Support provided by Research to Prevent Blindness; NIH R01EY021592, P30EY06360, R01EY016470, R01EY014026, UL1TR000454, and TL1TR000456; Abraham J. and Phyllis Katz Foundation; USAMRAA DOD W81XWH-12-1-0436; The Emory Neurosciences Initiative.

References

Ambati J, Fowler BJ (2012) Mechanisms of age-related macular degeneration. Neuron 75:26–39
Baddeley A, Turner R (2005) Spatstat: an R package for analyzing spatial point patterns. J Statistic Soft 12:1–42
Bhutto I, Lutty G (2012) Understanding age-related macular degeneration (AMD): relationships between the photoreceptor/retinal pigment epithelium/Bruch's membrane/choriocapillaris complex. Mol Aspect Med 33:295–317
Burke JM, Hjelmeland LM (2005) Mosaicism of the retinal pigment epithelium: seeing the small picture. Mol Intervent 5:241–249
Chrenek MA, Dalal N, Gardner C et al (2012) Analysis of the RPE sheet in the rd10 retinal degeneration model. Adv Exp Med Biol 723:641–647
Gao H, Hollyfield JG (1992) Aging of the human retina. Differential loss of neurons and retinal pigment epithelial cells. Investig Ophthalmol Vis Sci 33:1–17
Jiang Y, Qi X, Chrenek MA et al (2013) Functional principal component analysis reveals discriminating categories of retinal pigment epithelial morphology in mice. Investig Ophthalmol Vis Sci 54:7274–7283
Jiang Y, Qi X, Chrenek MA et al (2014) Analysis of mouse RPE sheet morphology gives discriminatory categories. Adv Exp Med Biol 801:601–607
Kalnins VI, Sandig M, Hergott GJ et al (1995) Microfilament organization and wound repair in retinal pigment epithelium. Biochem Cell Biol 73:709–722
Lamprecht MR, Sabatini DM, Carpenter AE (2007) CellProfiler: free, versatile software for automated biological image analysis. Biotechniques 42:71–75
Liang F-Q, Godley BF (2003) Oxidative stress-induced mitochondrial DNA damage in human retinal pigment epithelial cells: a possible mechanism for RPE aging and age-related macular degeneration. Exp Eye Res 76:397–403
Nagai H, Kalnins VI (1996) Normally occurring loss of single cells and repair of resulting defects in retinal pigment epithelium in situ. Exp Eye Res 62:55–61
Negi A, Marmor MF (1984) Healing of photocoagulation lesions affects the rate of subretinal fluid resorption. Ophthalmol 91:1678–1683
Rizzolo LJ (2014) Barrier properties of cultured retinal pigment epithelium. Exp Eye Res 126:16–26
Roider J, Michaud NA, Flotte TJ et al (1992) Response of the retinal pigment epithelium to selective photocoagulation. Arch Ophthalmol 110:1786–1792
Shirinifard A, Glazier JA, Swat M et al (2012) Adhesion failures determine the pattern of choroidal neovascularization in the eye: a computer simulation study. PLoS Comp Biol 8:e1002440
Thompson DW (1942). On Growth and From. A new edition. Cambridge at the University Press. Cambridge, England, UK.
van Lookeren CM, LeCouter J, Yaspan BL et al (2014) Mechanisms of age-related macular degeneration and therapeutic opportunities. J Pathol 232:151–164
Watzke RC, Soldevilla JD, Trune DR (1993) Morphometric analysis of human retinal pigment epithelium: correlation with age and location. Curr Eye Res 12:133–142

Chapter 102
Valproic Acid Induced Human Retinal Pigment Epithelial Cell Death as Well as its Survival after Hydrogen Peroxide Damage is Mediated by P38 Kinase

Piyush C Kothary, Benjamin Rossi and Monte A Del Monte

Abstract Age-related macular degeneration (AMD) is a leading cause of legal blindness in developed countries. Several new drugs are now available to reduce the sight threatening complications of this disease, however, all are useful in only a small fraction of patients and none of them prevents disease development. An understanding of the pathogenesis of the retinal and macular degeneration is the first step in developing preventive and fully effective treatment options for this condition. Lifelong oxidative stress seems to be an etiologic factor. In this study, we used cultured human retinal pigment epithelial cells to study the mechanism of cell death and survival in cells exposed to oxidative stress. Our studies demonstrate that valproic acid (VPA), an epigenetic factor, reduces apoptosis in hRPE cells that were subjected to hydrogen peroxide-induced oxidative injury by alteration in P38 kinase activity. Since VPA has been shown to have therapeutic use in other neuronal diseases, better understanding of the mechanism of this VPA anti-apoptotic activity may enhance its development as a therapeutic agent.

102.1 Introduction

Age-related macular degeneration (AMD) is a leading cause of blindness in the industrial world. Lifelong oxidative stress of human retinal pigment epithelium (hRPE) has been implicated in the pathogenesis of AMD (Kothary et al. 2014) by production of reactive oxygen species (ROS), which can result in damage to hRPE.

P. C. Kothary (✉) · B. Rossi · M. A. Del Monte
Department of Ophthalmology, University of Michigan Medical Center, 1000 Wall Street, Ann Arbor, MI 48105, USA
e-mail: kotha@umich.edu

C. Bowes Rickman et al. (eds.), *Retinal Degenerative Diseases,* Advances in Experimental Medicine and Biology 854, DOI 10.1007/978-3-319-17121-0_102

The hRPE form a single layer of mitotically inactive cells that lie between the choroid and the neural retina. Pigment epithelial cells transport and store toxic nutrients for the photoreceptors and remove waste products such as shed photoreceptor segments. Damage to the RPE can affect the functioning of neurosensory retina.

Valproic acid (VPA), an epigenetic factor, is a drug that is widely used to treat patients with epilepsy (Monti et al. 2009 and it also inhibits growth of some cancer cells. In addition, VPA has been shown to reduce cell death in ARPE19 cells that were subjected to oxidative injury. It is postulated that a cascade of signaling molecules may be involved in beneficial effect of VPA in the treatment of epilepsy and reduced cell death in ARPE 19 cells during oxidative stress.

MAP kinases are involved in cell proliferation and apoptosis (Wang et al. 1998; Kothary et al. 2008). Previous studies have shown that extracellular signal-regulated kinase (ERK) is involved in proliferation where as P38 and STAT 3 (Kothary et al. 2004) are involved in cell death and cell survival (Gutierrez-Uzquiza et al. 2012). In the present study, we have used hydrogen peroxide to induce oxidative stress in hRPE cells and investigated the effect of VPA on hRPE cell viability and P38 production, to determine if these factors may be involved in the molecular mechanisms related to cell survival.

102.2 Materials and Methods

102.2.1 Establishment and Maintenance of hRPE Cell Cultures

hRPE cells were collected from donor human eyes obtained from the Michigan Eye Bank, and differentiated primary cultures were established as described previously (Weng et al. 2009). In brief, cells were grown in an incubator at 37 °C in Ham's F12 nutrient media until confluent, and then trypsinized and plated. The media in the cultured plates was changed every 3 days until experimental reagents were added.

102.2.2 Trypan Blue Exclusion Method

The procedure described in previous publication (Kothary et al. 2006). Briefly, cell media was aspirated and cells were washed twice with F12. 3.0 mL Experimental reagents were added to each well. Plates were incubated at 37 °C for 48 h, and then media was aspirated. Cells were washed with 1 mL PBS and 1 mL Hank's Buffer, and then 750 μL trypsin was added and mixed. After incubating 37 °C for 10 min, cell detachment was verified under a microscope and 10 uL trypan blue dye was added and mixed. Samples of cell mixture from each well were placed on a slide

and transferred to a hemocytometer, where unstained and stained cells were counted in four different fields.

102.2.3 14 C-Methionine Assay

The procedure described in previous publication (Kothary et al. 2010). Briefly, cell media was aspirated and cells were washed twice with F12. Experimental reagents were added, 0.5 mL to each well. After incubating at 37°C for 1 h, 50 μL 14 C-methionine was added. Plates were incubated at 37°C for 24 h, then media was aspirated and cells were washed with 0.5 mL PBS and 200 μL Zwitteragent in 0.2% BSA. Upon mixing, cells in Zwitteragent were transferred to microfuge tubes and 10 μL anti-P38 was added. Plates were refrigerated for 24 h, then 10 μL Protein A was added. After 1 h, tubes were centrifuged at 14,000 rpm for 5 min at 4°C. The supernatant fluid was discarded, and 0.5 mL NaOH was added. Cells in NaOH were transferred to scintillation vials, and 10 mL Ecolite was added. After 1 h, 14 C-methionine incorporation was counted by a scintillation counter.

102.2.4 Nuclear Staining

Nuclear staining of hRPE cells after H_2O_2 and VPA treatment was performed by method described previously described by Weng et al 2009. Nuclear staining showed that H_2O_2 and VPA decreased the hRPE cell number (data not shown).

102.3 Results

102.3.1 Effect of FBS on hRPE Cell Viability

Figure 102.1 shows hRPE cell proliferation is stimulated by increasing concentrations of FBS in a dose dependent manner.

102.3.2 Effect of H_2O_2 and VPA on hRPE Cell Viability

Figure 102.2a shows increasing concentrations of H_2O_2 decrease hRPE cell viability and proliferation to a limited extent.

Figure 102.2b shows increasing concentrations of VPA decrease hRPE cell proliferation.

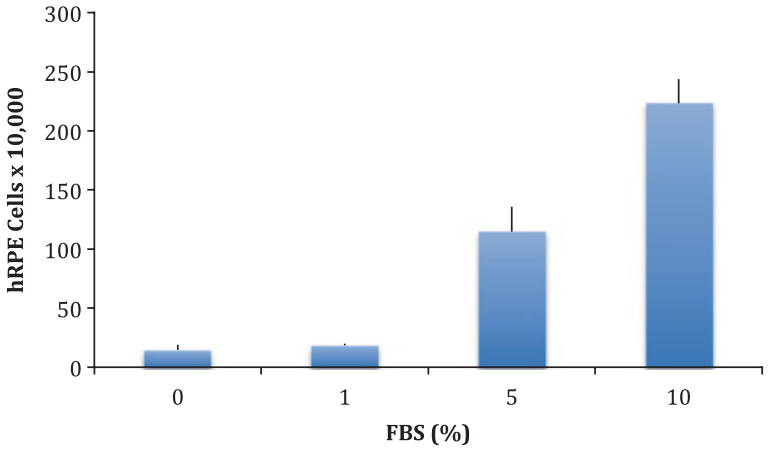

Fig. 102.1 Effect of FBS on hRPE cell viability

102.3.3 Effect of VPA in Presence of H_2O_2 on hRPE Cell Viability

Figure 102.3 shows VPA (1 mM) eliminates the H_2O_2 (1 mM) reduction in hRPE cell proliferation.

102.3.4 Effect of VPA in 14 C-P38 Production

Figure 102.4 shows increasing concentrations of VPA increase 14 C-P38 synthesis in hRPE cells.

102.3.5 Effect of VPA in Presence of H_2O_2 on P38 Production

Figure 102.5 shows VPA (1 mM) eliminates the H_2O_2 (1 mM) induced increased 14 C-P38 synthesis in hRPE cells back to baseline.

102.4 Discussion

AMD affects millions of older people in the industrial world resulting in loss of central reading vision often to legal blindness. AMD is associated with progressive deterioration of the retinal pigment epithelium and lifelong oxidative stress seems to play a role. Therapeutically, invasive surgery e.g. laser photocoagulation of neo-

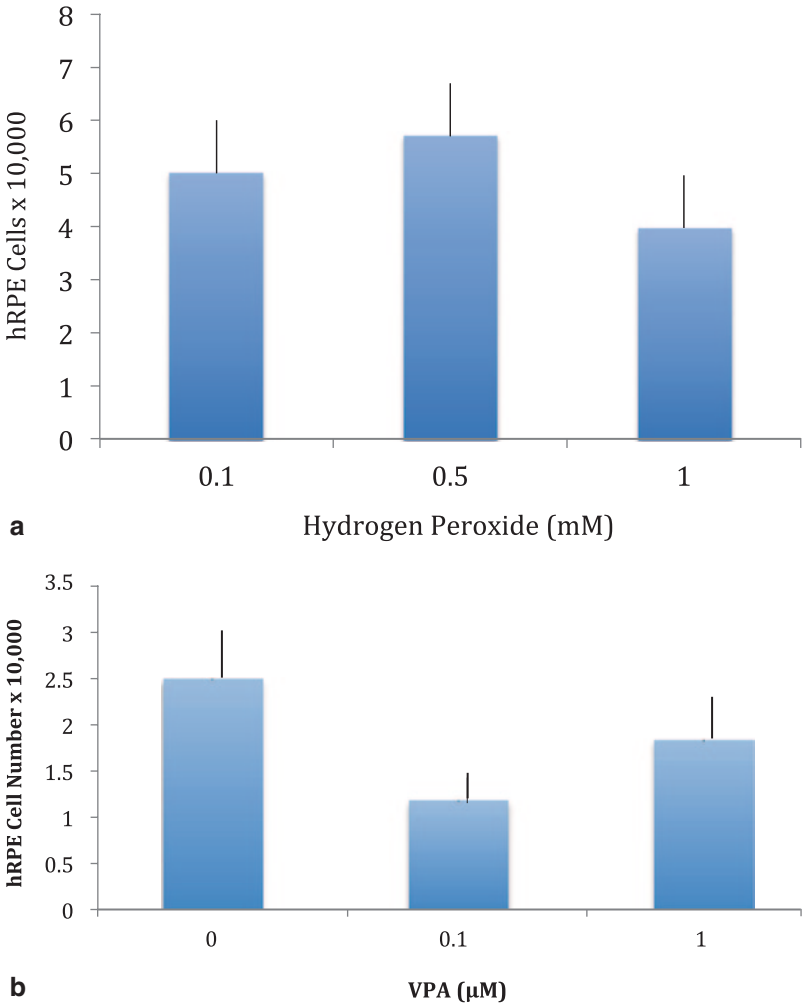

Fig. 102.2 **a** Effect of H_2O_2 on hRPE cell viability, **b** Effect of VPA on hRPE cell viability

vascular membranes, macular translocation surgery and recently discovered anti-VEGF medications have been used to treat these patients for stabilization of vision loss, but no successful preventive or fully restorative treatment has been discovered. Additional investigation of the molecular mechanism of this disease is required to develop better treatments. Therefore, our study aimed at understanding the role of the signaling molecule P38 MAPK in the survival of hRPE may aid in the development of pharmacological treatments for macular degeneration.

We have examined the nature of hydrogen peroxide induced oxidative stress in hRPE cells. Our goal was to determine the molecular expression of P38 in hRPE cells in presence and absence of hydrogen peroxide induced acute oxidative stress

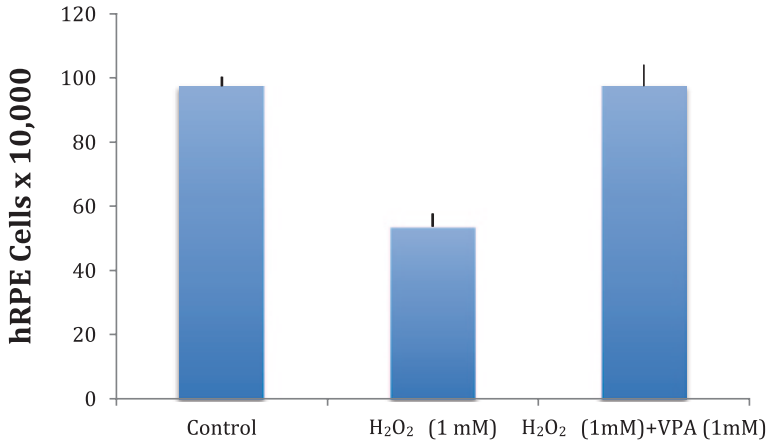

Fig. 102.3 Effect of VPA on H_2O_2 treated hRPE cell viability

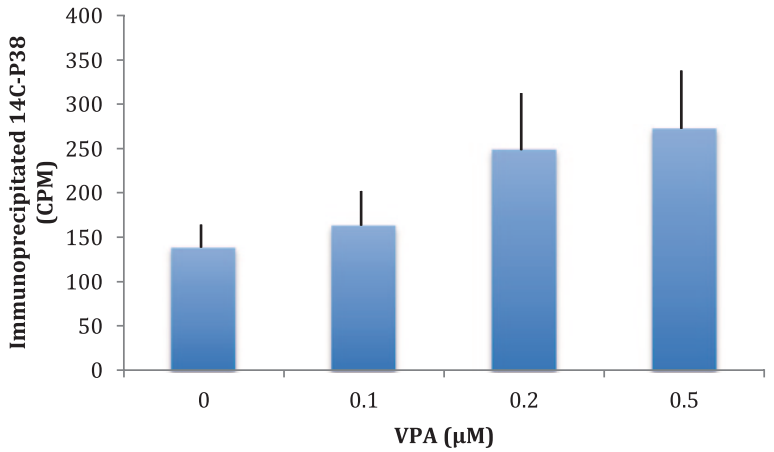

Fig. 102.4 Effect of VPA on 14 C-P38 synthesis in hRPE cells

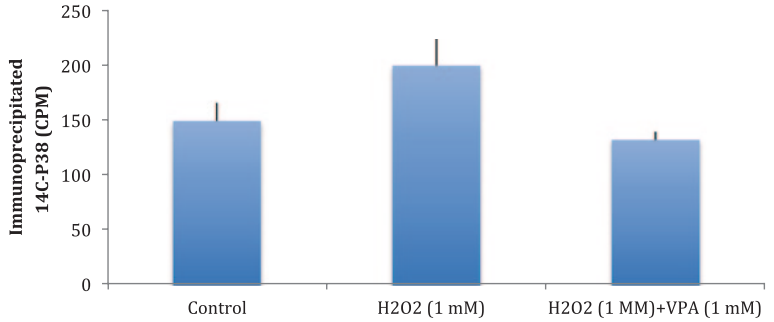

Fig. 102.5 Effect of VPA on 14 C-P38 synthesis in H_2O_2 treated hRPE cells

and the effect of adding VPA, a known inhibitor of oxidative damage, on P38 expression. We have shown that hRPE cells treated with H_2O_2 and VPA separately decreases hRPE cell proliferation and viability and increases P38 production. Xie et al. (2010) has shown that VPA increases P38 synthesis in microglia and that VPA induced microgia cell death is mediate by P38. Previously, we have shown that VPA treatment also increases caspase-3, a marker for apoptosis in hRPE cells.

We found that VPA reduces P38 synthesis and decreases cell death caused by H_2O_2 oxidative stress in cultured differentiated hRPE cells. Our data is in agreement with Gutierrez-Uzquiza et al. (2012) who showed P38 alpha mediates cell survival in response to oxidative stress. Others have shown that P38 activation may be linked mTOR inhibition (Chen et al. 2010; Pocrnich et al. 2009). Further investigation of effect of VPA and H_2O_2 on mTOR expression may clarify the role of mTOR in P38 signaling. P38 may also be up regulating antioxidant gene expression, Gutierrez-Uzquiza et al. 2012).

We conclude that VPA has a pro-survival function in H_2O_2 induced hRPE cell death because of its ability to down regulate P38. VPA is commonly used in the treatment of epilepsy, bipolar disease and cancers. These studies suggest that VPA may also have therapeutic value in the prevention or treatment of AMD as well.

Acknowledgment This study was supported by Skillman Foundation.

References

Chen L, Xu B, Liu L et al (2010) Hydrogen peroxide inhibits mTOR signaling by activation of AMPK alpha leading to apoptosis of neuronal cells. Lab Invest 90:985–993

Gutierrez-Uzquiza A, Arechederra M, Bragado P et al (2012) p38a Mediates cell survival in response to oxidative stress via induction of antioxidant genes. Effect on the p70s6k pathway. J Biol Chem 287:2632–2642

Kothary PC, Del Monte MA (2008) A possible impaired signaling mechanism in human retinal pigment epithelial cells from patients with macular degeneration. Adv Exp Med Biol 613:269–275

Kothary PC, Badhwar J, Weng C et al (2010) Impaired intracellular signaling may allow up-regulation of CTGF-synthesis and secondary peri-retinal fibrosis in human retinal pigment epithelial cells from patients with age-related macular degeneration. Adv Exp Med Biol 664:419–428

Kothary PC, Lahiri R, Kee L et al (2006) Pigment epithelium-derived growth factor inhibits fetal bovine serum stimulated vascular endothelial growth factor synthesis in cultured human retinal pigment epithelial cells. Adv Exp Med Biol 572:513–518

Kothary PC, Lee P, Al-Khersan H, et al (2014) L-Ascorbic acid may protect against oxidative damage in hRPE cells by stimulating intracellular erythropoietin activity. Adv Med Biol 74:115–123

Kothary PC, Pauuw JD, Bansal AK, et al (2004) Inhibition of growth factor stimulated STAT3 by AG490 in human retinal pigment epithelial cells. In: Proceedings of 5th International Symposium on Ocular Pharmacology and Therapeutics, Medimond Srl Bologna, Italy, pp 237–241

Monti B, Polazzi E, Contestabile A (2009) Biochemical, molecular and epigenetic mechanisms of valproic acid neuroprotection. Curr Mol Pharmacol 2:95–109

Pocrnich CE, Liu H, Feng M et al (2009) p38 mitogen-activated protein kinase protects human retinal pigment epithelial cells exposed to oxidative stress. Can J Ophthalmol 44:431–436

Wang Y, Huang S, Sah VP et al (1998) Cardiac Muscle Cell Hypertrophy and Apoptosis Induced by Distinct Members of the p38 Mitogen-activated Protein Kinase Family. J Biol Chem 273:2161–2168

Weng CY, Kothary PC, Verkade AJ et al (2009) MAP kinase pathway is involved in IGF-1-stimulated proliferation of human retinal pigment epithelial cells (hRPE). Curr Eye Res 34:867–876

Xie N, Wang C, Lin Y, Li H et al (2010) The role of p38 MAPK in valproic acid induced microglia apoptosis. Neurosci Let 482:51–56

Chapter 103
Blockade of MerTK Activation by AMPK Inhibits RPE Cell Phagocytosis

Suofu Qin

Abstract Timely removal of shed photoreceptor outer segments by retinal pigment epithelial cells (RPE) plays a key role in biological renewal of these highly peroxidizable structures and in maintenance of retina health. How environmental stress cause RPE cell dysfunction is undefined however. AMP-activated protein kinase (AMPK), a heterotrimer of a catalytic α subunit and regulatory β and γ subunits, maintains energy homeostasis by limiting energy utilization and/or promoting energy production when energy supply is compromised. Intriguingly, AMPK has been shown to be important in functions of RPE cells. In this mini-review, the role and mechanisms of AMPK in controlling RPE cell phagocytosis are discussed.

Keywords AICAR · AMPK · MerTK · Phagocytosis · RPE

103.1 Introduction

The retinal pigment epithelium (RPE) is a monolayer of cuboidal cells where its basal membrane is in contact with Bruch's membrane and apical membrane is associated with the outer segments of retinal photoreceptor cells. The major function of RPE cells is to support the survival and normal functioning of photoreceptors by phagocytizing shed photoreceptor outer segment (POS) membrane discs for photoreceptor renewal (Nguyen-Legros and Hicks 2000). Efficient disposal of shed POS by RPE is essential to prevent RPE and photoreceptor cells from the damaging effects of POS build-up. Phagocytosis of POS by RPE cells occurs by a complex process that includes binding, uptake, and degradation. POS first bind to the vitronectin receptor αvβ5 at the apical membrane of the RPE and initiates a downstream cytoplasmic signaling cascade that results in the reorganization of the RPE plasma membrane and engulfment of POS (Finnemann et al. 1997; Nandrot et al. 2004). POS binding activates and recruits focal adhesion kinase (FAK) to the apical surface of RPE cells (Finnemann 2003). In the meantime, POS binding

S. Qin (✉)
Retinal Disease Research, Department of Biological Sciences, Allergan, Inc., RD3-2D, Irvine, CA 92612, USA
e-mail: qinsuofu@hotmail.com

C. Bowes Rickman et al. (eds.), *Retinal Degenerative Diseases,* Advances in Experimental Medicine and Biology 854, DOI 10.1007/978-3-319-17121-0_103

relocates MER tyrosine kinase (MerTK) to the sites of internalized POS (Feng et al. 2002; Finnemann 2003) whereas MerTK is activated by FAK (Finnemann 2003). Activated MerTK mediates RPE engulfment of POS (Feng et al. 2002). Engulfed POS are degraded in RPE lysosomes (Deguchi et al. 1994).

Age-related macular degeneration (AMD) is an idiopathic retinal degenerative disease that predominates in the elderly in the Western world as a cause of irreversible, profound vision loss (Evans 2001; Qin and Rodrigues 2008). Growing evidence indicates that oxidative stress injury of RPE plays an important role in the etiology of AMD. The RPE is at high risk for oxidative injury due to its location in a highly oxygenated environment, its high levels of light exposure, and generation of reactive oxygen species during POS phagocytosis (Kindzelskii et al. 2004; Yu and Cringle 2005). In the early stage of AMD development, oxidative insult induces a set of profound physiological responses in RPE, leading to dysfunction without initiation of cell death (Honda et al. 2001). Although not much data are available regarding dysregulation of RPE cell phagocytosis by sub-lethal oxidative injury, AMP activated protein kinase (AMPK), a metabolic-sensing Ser/Thr kinase consisting of a catalytic α subunit and regulatory β and γ subunits (Carling 2004), has emerged as an important player in regulating RPE cell functions (Qin 2012). AMPK has been demonstrated to play roles in regulating various RPE cell processes such as survival (Li et al. 2013; Qin and Rodrigues 2010; Yao et al. 2013), immune responses (Qin et al. 2008), migration (Liu et al. 2012), phagocytosis (Qin and De Vries 2008) and permeability (Qin and Rodrigues 2010; Villarroel et al. 2011). In this review, possible mechanisms by which AMPK regulates RPE phagocytosis are discussed.

103.2 Inhibition of RPE Cell Phagocytosis by AMPK Activation

Activation of AMPK by oxidative stress is associated with inhibition of RPE cell phagocytosis (Qin and De Vries 2008). To demonstrate a causal-effect relationship between AMPK activation and phagocytosis inhibition, effects of 5-aminoimidazole-4-carboxamide riboside (AICAR), an AMPK activator that mimics AMP to activate AMPK after its phosphorylation by adenosine kinase, on RPE cell phagocytosis were investigated. AICAR treatment activates AMPK signaling in ARPE19 cells as revealed by increased Thr^{172} phosphorylation of AMPKα and Ser^{79} phosphorylation of acetyl-CoA carboxylase (ACC), an AMPK substrate (Fig. 103.1a). Phosphorylation of AICAR by an adenosine kinase is essential for its activation of AMPKas adenosine kinase inhibitor 5-iodotubercidin completely abrogated activation of AMPK (Fig. 103.1b), revealing that AICAR activates AMPK in RPE cells via directly mimicking AMP effect. Incubation with AICAR inhibits RPE cell phagocytosis by 50% and this inhibition is completely restored by inhibiting AMPK (Fig. 103.1c). Activation of AMPK is therefore directly linked to the inhibition of RPE cell phagocytosis.

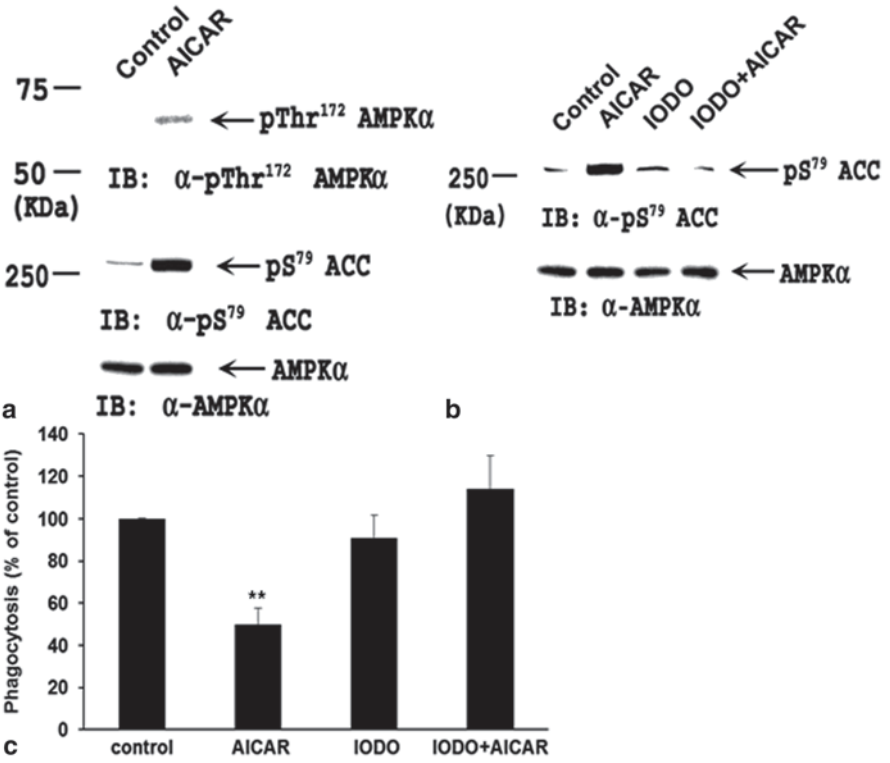

Fig. 103.1 Inhibition of RPE cell phagocytosis by AMPK. **a** AMPK activation by AICAR. Confluent ARPE19 cells were treated with 2 mM AICAR for 30 min. AMPK activation was assessed by immunoblotting with anti-pThr^{172} AMPKα and anti-pS^{79} ACC (Acetyl-CoA carboxylase, AMPK substrate). **b** Inhibition of AMPK activation by IODO. Confluent cells were treated with 0.5 μM iodotubercidin (IODO) for 30 min and then stimulated with 2 mM AICAR for 30 min. **c** Inhibitory effect of AICAR on phagocytosis. Confluent ARPE19 cells in 24-well plate were pre-incubated with 0.5 μM IODO for 30 min prior exposure to 2 mM AICAR for 1h followed by 4 h incubation with 5×10^6 POS particles in 300 μL growth medium in the presence of AICAR. Phagocytosis was determined by flow cytometer

103.3 Abrogation of MerTK Activation by AICAR

FAK and MerTK are two important tyrosine kinases in mediating RPE cell phagocytosis with Fak upstream of MerTK (Finnemann 2003). Phagocytic challenge activates both FAK and MerTK in ARPE19 cells in a time-dependent manner (Fig. 103.2) (Qin and Rodrigues 2012). To address how AMPK regulates RPE cell phagocytic machinery, cells were treated with AICAR before POS addition. AICAR treatment does not alter basal activity of FAK and MerTK. However, AICAR selectively abolishes POS-induced activation of MerTK with no effect on FAK (Fig. 103.2). This observation indicates that activated AMPK limits RPE cell phagocytic activity by abolishing POS-induced activation of MerTK.

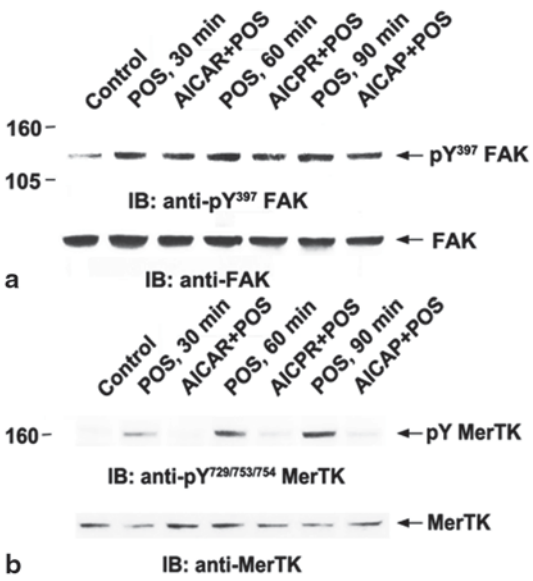

Fig. 103.2 Inhibition of POS-induced MerTK activation by AICAR. Confluent RPE cells were pre-incubated with 2 mM AICAR for 1 h. Cells were incubated with 5×10^6 POS in 300 μL complete medium for various lengths of times with presence of AICAR. Activation of FAK and MerTK was determined by activation-specific anti-pY^{397} FAK **a** and anti-$pY^{729/753/754}$ MerTK antibody **b** respectively

103.4 Regulation of RPE Cell Phagocytosis by AMPK

RPE cells maintain survival and functions of photoreceptors via phagocytizing shed POS. Knockdown of AMPKα2 reduces the ability of RPE cells to phagocytize POS by 40 % whereas there is no effect with knockdown of AMPKα1 (Qin and De Vries 2008). Under stress conditions, sub-lethal oxidative stress-activated AMPKα2 but not AMPKα1 inhibits RPE cell phagocytosis. It is unclear why oxidative stress-induced inhibition of RPE cell phagocytosis is selectively regulated by AMPKα2, however, AMPKα2 rather than AMPKα1 knock-out causes a dramatic decrease in oxidative stress-induced AMPK signaling (Qin and De Vries 2008). Continued RPE phagocytosis of POS may add more insult to the already stressed RPE cells. Thus, reduction of RPE cell phagocytosis by AMPKα2 activation likely protects RPE cells from further photo-toxic damage caused by the oxidized POS. How does AMPK inhibit RPE cell phagocytosis? As proposed in Fig. 103.3, POS binding recruits FAK/MerTK to the membrane and initiates FAK-MerTK signaling cascade, triggering engulfment of POS and subsequent degradation in lysosome. Selective inhibition of POS-induced activation of MerTK by AMPKα2 suggests that AMPKα2 terminates FAK-MerTK signaling cascade by blocking signal relay at MerTK. This isoform-specific role of AMPKα in regulating RPE cell phagocytosis may provide novel therapeutic tools for retinal diseases by developing isoform-selective inhibitors of AMPK. Furthermore, sub-lethal oxidative stress can also inactivate basal and POS-induced activation of FAK and slow down RPE cell capability of phagocytizing POS (Qin and Rodrigues 2012), showing that oxidative stress can regulate phagocytic activity of RPE cells in more than one mechanism.

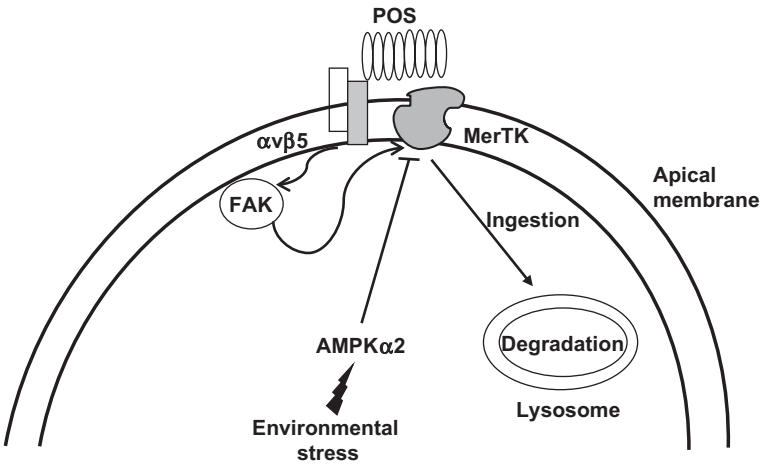

Fig. 103.3 Proposed regulation of RPE cell phagocytosis by AMPK. Phagocytosis starts with binding of POS to αvβ5 initiating a coordinate signal transduction, interaction of αvβ5 with MerTK through FAK that in turn results in engulfment of the bound POS and subsequent degradation in lysosome. Activated AMPK can selectively block activation of MerTK, thereby reducing RPE cell capacity of phagocytizing POS

References

Carling D (2004) The AMP-activated protein kinase cascade–a unifying system for energy control. Trends Biochem Sci 29:18–24

Deguchi J, Yamamoto A, Yoshimori T et al (1994) Acidification of phagosomes and degradation of rod outer segments in rat retinal pigment epithelium. Invest Ophthalmol Vis Sci 35:568–579

Evans JR (2001) Risk factors for age-related macular degeneration. Prog Retin Eye Res 20:227–253

Feng W, Yasumura D, Matthes MT et al (2002) Mertk triggers uptake of photoreceptor outer segments during phagocytosis by cultured retinal pigment epithelial cells. J Biol Chem 277:17016–17022

Finnemann SC (2003) Focal adhesion kinase signaling promotes phagocytosis of integrin-bound photoreceptors. EMBO J 22:4143–4154

Finnemann SC, Bonilha VL, Marmorstein AD et al (1997) Phagocytosis of rod outer segments by retinal pigment epithelial cells requires alpha(v)beta5 integrin for binding but not for internalization. Proc Natl Acad Sci U S A 94:12932–12937

Honda S, Hjelmeland LM, Handa JT (2001) The use of hyperoxia to induce chronic mild oxidative stress in RPE cells in vitro. Mol Vis 7:63–70

Kindzelskii AL, Elner VM, Elner SG et al (2004) Toll-like receptor 4 (TLR4) of retinal pigment epithelial cells participates in transmembrane signaling in response to photoreceptor outer segments. J Gen Physiol 124:139–149

Li KR, Zhang ZQ, Yao J et al (2013) Ginsenoside Rg-1 protects retinal pigment epithelium (RPE) cells from cobalt chloride (CoCl2) and hypoxia assaults. PLoS ONE 8:e84171

Liu Y, Cao GF, Xue J et al (2012) Tumor necrosis factor-alpha (TNF-alpha)-mediated in vitro human retinal pigment epithelial (RPE) cell migration mainly requires Akt/mTOR complex 1 (mTORC1), but not mTOR complex 2 (mTORC2) signaling. Eur J Cell Biol 91:728–737

Nandrot EF, Kim Y, Brodie SE et al (2004) Loss of synchronized retinal phagocytosis and age-related blindness in mice lacking alphavbeta5 integrin. J Exp Med 200:1539–1545

Nguyen-Legros J, Hicks D (2000) Renewal of photoreceptor outer segments and their phagocytosis by the retinal pigment epithelium. Int Rev Cytol 196:245–313

Qin S (2012) Roles for AMP-activated protein kinase in RPE cell function. Adv Exp Med Biol 723:745–751

Qin S, De Vries GW (2008) alpha2 But not alpha1 AMP-activated protein kinase mediates oxidative stress-induced inhibition of retinal pigment epithelium cell phagocytosis of photoreceptor outer segments. J Biol Chem 283:6744–6751

Qin S, Rodrigues GA (2008) Progress and perspectives on the role of RPE cell inflammatory responses in the development of age-related macular degeneration. J Inflamm Res 1:49–65

Qin S, Rodrigues GA (2010) Differential roles of AMPKalpha1 and AMPKalpha2 in regulating 4-HNE-induced RPE cell death and permeability. Exp Eye Res 91:818–824

Qin S, Rodrigues GA (2012) Roles of alphavbeta5, FAK and MerTK in oxidative stress inhibition of RPE cell phagocytosis. Exp Eye Res 94:63–70

Qin S, Ni M, De Vries GW (2008) Implication of S-adenosylhomocysteine hydrolase in inhibition of TNF-alpha- and IL-1beta-induced expression of inflammatory mediators by AICAR in RPE cells. Invest Ophthalmol Vis Sci 49:1274–1281

Villarroel M, Garcia-Ramirez M, Corraliza L et al (2011) Fenofibric acid prevents retinal pigment epithelium disruption induced by interleukin-1beta by suppressing AMP-activated protein kinase (AMPK) activation. Diabetologia 54:1543–1553

Yao J, Bi HE, Sheng Y et al (2013) Ultraviolet (UV) and hydrogen peroxide activate ceramide-ER stress-AMPK signaling axis to promote retinal pigment epithelium (RPE) cell apoptosis. Int J Mol Sci 14:10355–10368

Yu DY, Cringle SJ (2005) Retinal degeneration and local oxygen metabolism. Exp Eye Res 80:745–751

Chapter 104
Modulation of V-ATPase by βA3/A1-Crystallin in Retinal Pigment Epithelial Cells

Mallika Valapala, Yuri Sergeev, Eric Wawrousek, Stacey Hose, J Samuel Zigler and Debasish Sinha

Abstract We have previously demonstrated that βA3/A1-crystallin, a member of the β/γ-crystallin superfamily, is expressed in the astrocytes and retinal pigment epithelial (RPE) cells of the eye. In order to understand the physiological functions of βA3/A1-crystallin in RPE cells, we generated conditional knockout (cKO) mice where *Cryba1*, the gene encoding βA3/A1-crystallin, is deleted specifically from the RPE using the Cre-loxP system. By utilizing the cKO model, we have shown that this protein is required by RPE cells for proper lysosomal degradation of photoreceptor outer segments (OS) that have been internalized in phagosomes and also for the proper functioning of the autophagy process. We also reported that βA3/A1-crystallin is trafficked to lysosomes, where it regulates endolysosomal acidification by modulating the activity of the lysosomal V-ATPase complex. Our results show that the V-ATPase activity in cKO RPE is significantly lower than WT RPE. Since, V-ATPase is important for regulating lysosomal pH, we noticed that endolysosomal pH was higher in the cKO cells compared to the WT cells. Increased lysosomal pH in cKO RPE is also associated with reduced Cathepsin D

M. Valapala (✉) · S. Hose · J. S. Zigler · D. Sinha
Department of Ophthalmology, Johns Hopkins University School of Medicine, Baltimore, MD 21287, USA
e-mail: mvalapa1@jhmi.edu

Y. Sergeev
National Health Institute, Bathesda, MD 20814, USA
e-mail: Yuri.sergeev@nih.gov

E. Wawrousek
National Eye Institute, Bathesda, MD 20892, USA
e-mail: wawrouseke@nei.nih.gov

S. Hose
e-mail: srohrer1@jhmi.edu

J. S. Zigler
e-mail: szigler1@jhmi.edu

D. Sinha
e-mail: debasish@jhmi.edu

C. Bowes Rickman et al. (eds.), *Retinal Degenerative Diseases,* Advances in Experimental Medicine and Biology 854, DOI 10.1007/978-3-319-17121-0_104

activity. Cathepsin D is a major lysosomal aspartic protease involved in the degradation of the OS and hence we believe that reduced proteolytic activity contributes to impaired degradation of OS in the cKO RPE. Reduced lysosomal activity in the cKO RPE also contributes to the incomplete degradation of the autophagosomes. Our results also suggest that βA3/A1-crystallin regulates V-ATPase activity by binding to the V_0 subunit of the V-ATPase complex. Taken together, these results suggest a novel mechanism by which βA3/A1-crystallin regulates lysosomal function by modulating the activity of V-ATPase.

Keywords Retinal pigment epithelial cells · Phagocytosis · Autophagy · Lysosomes · βA3/A1-crystallin

104.1 Introduction

The Retinal Pigmented Epithelium (RPE) is a single layer of pigmented and polarized cells, with the apical surface facing the photoreceptors and the basal side facing Bruch's membrane. It serves many physiological roles that are crucial for maintaining homeostasis of the retina (Strauss 2005). The RPE cells are among the most active phagocytic cell types in the body, phagocytosing 10 % of total photoreceptor volume daily (Kevany and Palczewski 2010). With advancing age, senescent RPE cells accumulate metabolic debris from remnants of incomplete degradation of ingested photoreceptors. This leads to accumulation of lipofuscin, an undegradable byproduct of OS metabolism (Sparrow et al. 2010). Knowledge of the mechanisms that lead to the clearance of cellular material by RPE cells can help us develop strategies that lead to the restoration of the clearance functions in the RPE cells. Autophagy, a process by which cellular constituents are degraded and recycled as part of normal cellular remodeling, is likely to be of particular importance in postmitotic cells with high metabolic demand, such as the RPE. This process begins with the formation of autophagosomes containing engulfed cytoplasmic organelles and protein complexes. The autophagosomes later fuse with the lysosomes to form autophagolysosomes and their contents are degraded by the acid hydrolases present in the lysosomes (Glick et al. 2010; Tong et al. 2010). A disruption of autophagy in postmitototic cells like the RPE, would result in the accumulation of undigested or partially digested cellular aggregates, leading to degenerative cell death of the RPE (Kaarniranta et al. 2013). Therefore, proper functioning of the RPE requires that both phagocytosis and autophagy processes be in balance.

104.2 Importance of Lysosomes in Clearance Functions in the RPE

Lysosomes, which are acidic subcellular organelles, are involved in the terminal events of both autophagy and phagocytosis (Luzio et al. 2007). Although autophagy and phagocytosis are regarded as two separate biological processes, they share many morphological and topological similarities. The termination events in the processing of the phagosome and autophagosome are essentially similar (Deretic 2008). Once formed, both phagosomes and autophagosomes fuse with lysosomes to from mature, acidified degradative organelles, called phagolysosomes and autophagolysosomes, respectively (Deretic 2008). Since lysosomes are a common element in both the processes, impaired lysosomal function is expected to result in dysregulated clearance of both phagosomes and autophagosomes. In a phagocytically active cell like the RPE, the degradative capacity of the lysosomes is indispensable for the proper clearance of ingested outer segments and cellular debri (Kaarniranta et al. 2010). Previous studies have suggested that mutations affecting the activity of lysosomal proteases lead to accumulation of lipofuscin-like material in the RPE. These reports suggest the importance of proper functioning of lysosomal enzymes in the maintenance of physiological functions in the RPE (Siakotos et al. 1978 and Elner 2002). Most lysosomal enzymes in the RPE are known to function in a narrow pH range in the acidic environment of the lysosomal lumen (Liu et al. 2008). The lysosomal endopeptidases, Cathepsin B, D and E are known to be highly important in protein degradation and turnover in a majority of cell types (Luzio et al. 2007). In the RPE cells, cathepsin D is the major protease involved in the lysosomal degradation of the outer segments. The activity of cathepsin D is tightly regulated by lysosomal pH, a rise in pH to 5.0 is known to reduce the activity of Cathepsin D by 80% (Hayasaka et al. 1975) Studies have suggested that chronic use of drugs like chloroquine that alter lysosomal pH induce pathological changes in the RPE. Animals chronically exposed to chloroquine showed increased lysosomal pH and accumulation of phagosomes containing ingested outer segments. Undigested phagosomes and their contents are known to accumulate between Bruch's membrane in RPE in chloroquine-treated animals (Mahon et al. 2004; Peters et al. 2006). These studies suggest a stringent requirement of lysosomal pH for the proper functioning of lysosomal clearance functions in the RPE.

104.3 Mechanisms of Lysosomal Acidification

Lysosomes are acidic organelles involved in the degradation of macromolecules and play important roles in cellular maintenance[7]. The acidity of the lysosomes is generated and maintained by the lysosomal proton pump, vacuolar ATP-ase (V-ATPase). V-ATPase pumps protons into the lysosomal lumen against the electrochemical gradient by utilizing the free energy derived from ATP hydrolysis (Mindell 2012).

V-ATPases are multi-subunit complexes, composed of a cytosolic V_1 domain that catalyzes ATP hydrolysis and an integral V_0 domain that translocates protons from the cytoplasm to the lysosomal lumen. The V_1 domain is composed of eight subunits (A-H) and the V_0 domain is composed of five subunits (a, d, c, c' and c"). In mammals, the 'a' subunit of the V_0 domain is composed of multiple isoforms that have been shown to target V-ATPase to distinct cellular compartments (Mindell 2012).

104.4 Involvement of βA3/A1-Crystallin in the Maintenance of Lysosomal Function in the RPE

We recently reported that βA3/A1-crystallin, a lens structural protein, is expressed in RPE cells and trafficked to lysosomes, where it is involved in degradation of ingested OS and also in autophagy (Valapala et al. 2014). We have recently generated a conditional knockout (cKO) mouse where βA3/A1-crystallin has been deleted specifically from the RPE. In our initial characterization of these animals, we found that while OS discs are ingested, the RPE cells are unable to degrade them and consequently accumulate ingested phagosomes. These mice also show impaired clearance of autophagosomes, hyper-vacuolation and loss of retinal function. These cellular abnormalities in the cKO RPE are also accompanied by an increase in lysosomal pH and a reduction in the activity of lysosomal proteases like cathepsin D. Our studies also suggested that loss of βA3/A1-crystallin inhibits the activity of the lysosomal V-ATPase in the cKO RPE. In order to investigate the mechanisms by which βA3/A1-crystallin modulates the activity of V-ATPase, we performed subcellular fractionation of lysosomes, extracted the lysosomal lumen and membrane fractions. Later, immunoprecipitation was performed using a polyclonal antibody to βA3/A1-crystallin and we immunoprecipitated the V-ATPase subunit ATP6V_0A_1 from the lysosomal membrane fractions in the *Cryba1* floxed (*Cryba1*fl/fl) RPE cells (Fig. 104.1a). Since, the V_0 subunit of the V-ATPase complex regulates its catalytic function; we believe that βA3/A1-crystallin modulates the catalytic efficiency of this complex (Valapala et al. 2014). The exact mechanism by which βA3/A1-crystallin regulates this process is currently under investigation. Furthermore, molecular modeling studies have shown that the molecular surface of the βA3/A1-crystallin complex possesses a distinct binding site for the ATP6V_0A_1 subunit (Fig. 104.1b). Since, the major function of V-ATPase is to generate a pH gradient in the lysosomal compartments, loss of its function significantly alters and lysosomal pH and the activity of the lysosomal proteases in the cKO RPE. Our results show that dysregulated lysosomal degradation in the cKO RPE leads to incomplete degradation and accumulation of autophagosomes (Valapala et al. 2014). In summary, our studies suggest that βA3/A1-crystallin has critical function in the lysosome-mediated processing during both phagocytosis and autophagy in the RPE.

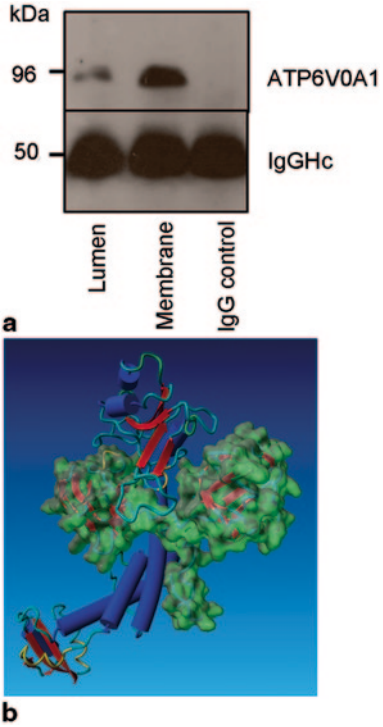

Fig. 104.1 Regulation of lysosomal V-ATPase by βA3/A1-crystallin.**a** Lysosomal fractionation was performed to extract the lysosomal lumen and membrane fractions. Co-immunoprecipitation of these fractions with βA3/A1-crystallin antibody and immunoblotting with ATP6V_0a_1 antibody revealed the pull down of ATP6V_0A_1 predominantly in the membrane fraction. Immunoblotting with IgG heavy chain (IgGHc) served as a loading control. **b** Hypothetical complex of βA3/-crystallin and the N-terminal domain of V_0a_1 obtained by Hex protein docking is shown. Molecular surface of βA3/-crystallin is shown in *green*. The V_0a_1-Nterminus is shown as a ribbon model where β-sheet and α-helical structures are shown by *red arrows* and *blue cylinders*, respectively Reproduced with permission from the journal autophagy

Acknowledgements DS is supported by National Institutes of Health: RO1EY019037-S, Bright focus and Research to Prevent Blindness (an unrestricted grant to The Wilmer Eye Institute).

References

Deretic V (2008) Autophagosome and phagosome. Meth Mol Biol 445:1–10

Elner VM (2002) Retinal pigment epithelial acid lipase activity and lipoprotein receptors: effects of dietary omega-3 fatty acids. Trans Am Ophthalmol Soc 100:301–338

Glick D, Barth S, Macleod KF (2010) Autophagy: cellular and molecular mechanisms. J Path 221:3–12

Hayasaka S, Hara S, Mizuno K (1975) Degradation of rod outer segment proteins by cathepsin D. J Biochem 78:1365–1367

Kaarniranta K, Hyttinen J, Ryhanen T et al (2010) Mechanisms of protein aggregation in the retinal pigment epithelial cells. Front Biosci (Elite Ed) 2:1374–1384
Kaarniranta K, Sinha D, Blasiak J et al (2013) Autophagy and heterophagy dysregulation leads to retinal pigment epithelium dysfunction and development of age-related macular degeneration. Autophagy 9:973–84
Kevany BM, Palczewski K (2010) Phagocytosis of retinal rod and cone photoreceptors. Physiol (Bethesda) 25:8–15.
Liu J, Lu W, Reigada D et al (2008) Restoration of lysosomal pH in RPE cells from cultured human and ABCA4-/- mice: Pharmacologic approaches and functional recovery. Invest Ophthalmol Vis Sci 49:772–780
Luzio JP, Pryor PR, Bright NA (2007) Lysosomes: fusion and function. Nature Reviews Mol Cell Biol 8:622–632
Mahon GJ, Anderson HR, Gardiner TA et al (2004). Chloroquine causes lysosomal dysfunction in neural retina and RPE: implications for retinopathy. Curr Eye Res 28:277–284.
Mindell JA (2012) Lysosomal acidification mechanisms. Annu Rev Physiol 74:69–86
Peters S, Reinthal E, Blitgen-Heinecke P et al (2006). Inhibition of lysosomal degradation in retinal pigment epithelium cells induces exocytosis of phagocytic residual material at the basolateral plasma membrane. Ophthal Res 38:83–88
Siakotos AN, Armstrong D, Koppang N et al (1978) Studies on the retina and the pigment epithelium in hereditary canine ceroid lipofuscinosis, II: the subcellular distribution of lysosomal hydrolases and other enzymes. Invest Ophthalmol Vis Sci 17:618–633
Sparrow JR, Hicks D, Hamel CP (2010) The retinal pigment epithelium in health and disease. Curr. Mol. Med. 10:802–823
Strauss O (2005) The Retinal Pigment Epithelium in Visual Function. Phys Rev 85:841–881
Tong J, Yan X, Yu L (2010) The late stage of autophagy:cellular events and molecular regulation. Protein Cell 1:907–915
Valapala M, Wilson C, Hose S et al (2014) Lysosomal-mediated waste clearance in retinal pigment epithelial cells is regulated by CRYBA1/bA3/A1-crystallin via V-ATPase-MTORC1 signaling. Autophagy 10:480–496

Chapter 105
Proteomic Profiling of Cigarette Smoke Induced Changes in Retinal Pigment Epithelium Cells

Juliane Merl-Pham, Fabian Gruhn and Stefanie M Hauck

Abstract Age-related macular degeneration (AMD) is a medical condition usually affecting older adults and resulting in a loss of vision in the macula, the center of the visual field. The dry form of this disease presents with atrophy of the retinal pigment epithelium, resulting in the detachment of the retina and loss of photoreceptors. Cigarette smoke is one main risk factor for dry AMD and increases the risk of developing the disease by three times. In order to understand the influence of cigarette smoke on retinal pigment epithelial cells, cultured human ARPE-19 cells were treated with cigarette smoke extract for 24 h. Using quantitative mass spectrometry more than 3000 proteins were identified and their respective abundances were compared between cigarette smoke-treated and untreated cells. Altogether 1932 proteins were quantified with at least two unique peptides, with 686 proteins found to be significantly differentially abundant with $p > 0.05$. Of these proteins the abundance of 64 proteins was at least 2-fold down-regulated after cigarette smoke treatment while 120 proteins were 2-fold up-regulated. The analysis of associated biological processes revealed an alteration of proteins involved in RNA processing and transport as well as extracellular matrix remodelling in response to cigarette smoke treatment.

Keywords Age-related macular degeneration · Quantitative mass spectrometry · Cell fractionation · Cigarette smoke · Retinal pigment epithelium

S. M. Hauck (✉) · J. Merl-Pham · F. Gruhn
Research Unit Protein Science, Helmholtz Zentrum München, German Research Center for Environmental Health GmbH, Ingolstaedter Landstr.1, 85764 Munich, Germany
e-mail: hauck@helmholtz-muenchen.de

J. Merl-Pham
e-mail: juliane.merl@helmholtz-muenchen.de

F. Gruhn
e-mail: fabian.gruhn@helmholtz-muenchen.de

C. Bowes Rickman et al. (eds.), *Retinal Degenerative Diseases,* Advances in Experimental Medicine and Biology 854, DOI 10.1007/978-3-319-17121-0_105

105.1 Introduction

Age-related macular degeneration (AMD) is one of the main causes for a loss of vision among the elderly populations in western countries. The prevalence of developing a form of AMD is ~1.5% among the US population 40 years and older, and increases to ~12% for people older than 80 years (Friedman et al. 2004). Hallmark pathology of the dry form of the disease (85–90% of cases) is the formation of deposits between the retinal pigment epithelium (RPE) and the Bruch's membrane and atrophy of the RPE, resulting in the detachment of the retina and loss of photoreceptors. The neovascular form of AMD is mainly characterized by destruction of the RPE and the retina by abnormal choroidal neovascularization (Bhutto and Lutty 2012).

Apart from age, cigarette smoke is one of the main environmental risk factors for AMD and increases the risk of developing the disease by about three times (Lois et al. 2008). It is known that cigarette smoke leads to oxidative stress, antioxidant depletion and complement activation in the affected tissue (Woodell and Rohrer 2014), resulting in atrophy of RPE cells.

In order to improve our so far limited understanding of the tobacco smoke-induced molecular mechanisms underlying this RPE destruction in the context of AMD, we performed quantitative proteomic profiling of cigarette smoke extract (CSE) treated ARPE19 cells in comparison to untreated controls. We identified distinct up- and down-regulated proteins and pathway enrichment analyses revealed significantly altered biological processes in RPE cells in response to CSE treatment.

105.2 Materials and Methods

105.2.1 Cultivation of ARPE19 Cells

Human ARPE19 cells (ATCC) were grown in DMEM medium supplemented with 10% fetal bovine serum on ∅10 cm cell culture dishes (Nunc) at 37 °C in a humidified atmosphere containing 5% CO_2. Before fractionation the cells were grown to 70–80% confluence, washed with PBS and starved for 24 h using smoked or non-smoked medium without FBS.

105.2.2 Preparation of Cigarette Smoke Extracts (CSE)

Stocks of cigarette smoke extract (CSE) for treatment of ARPE19 were prepared as described previously (van Rijt et al. 2012). 100% CSE was sterile filtered through a 0.20-µm filter (Minisart; Sartorius Stedim Biotech), separated into aliquots, and stored at −20 °C for future use. For cell treatment CSE stock was thawed and diluted with DMEM media without FBS to the given concentrations of CSE.

105.2.3 Fractionation of ARPE19 Cells

The cell culture supernatant containing the secreted proteins was removed, sterile filtered through a 0.22-µm filter and subjected to tryptic digest as described in Sect. 105.2.4.

The glycosylated proteins on the ARPE19 surface were biotinylated as described (Wollscheid et al. 2009). Cells were washed and lysed in low-salt lysis buffer and nuclei were separated by centrifugation. Nuclei were step-wise resuspended in high-salt buffer without or with 1% Triton X-100. Extracted nuclear proteins were subjected to tryptic digest.

The supernatant of the centrifugation containing soluble proteins was diluted and biotinylated proteins were bound to equilibrated strep-tactin superflow beads (IBA) at 4 °C for 2 h. The supernatant containing unbound cytoplasmic proteins was subjected to tryptic digest. The beads were washed with buffers containing different detergents prior to protein reduction and carbamidomethylation. After washing, bound proteins were subjected to tryptic digest directly on the affinity matrix (see Sect. 105.2.4).

105.2.4 Sample Preparation for Mass Spectrometric Analysis and Proteomic Profiling

Each 10 µg of secreted, nuclear and cytoplasmic proteins were digested in 100 µl using a modified FASP procedure (Wiśniewski et al. 2009). Samples were collected by centrifugation, acidified with 0.5% trifluoroacetic acid (TFA) and analyzed on an OrbitrapXL.

The purified surface proteins were digested on the affinity matrix. Tryptic peptides were collected by centrifugation. Beads were washed and glycopeptides were eluted using 500 Units PNGaseF (New England Biolabs). Glycopeptides were also collected by centrifugation. Eluates were pooled, acidified with TFA and analyzed on the OrbitrapXL.

The digested peptides were measured by LC-MS/MS as described previously (Merl et al. 2012). The acquired spectra were loaded to Progenesis LC-MS software (version 2.5, Nonlinear) for label free quantification and analyzed as previously described (Hauck et al. 2010), except all features were exported as Mascot generic file (mgf) and used for peptide identification with Mascot (version 2.4) in the Ensembl Human protein database (Version: 2.5, 100607 sequences). A Mascot-integrated decoy database search calculated an average false discovery of $< 1\%$. The Mascot Percolator algorithm was used for the discrimination between correct and incorrect spectrum identifications (Brosch et al. 2009), with a maximum q value of 0.01. Peptides with a minimum percolator score of 15 were re-imported into the software. The different fractions were first analyzed separately and then combined.

105.2.5 Pathway Enrichment Analysis

For network generation, the 184 significantly differentially abundant proteins identified with at least two unique peptides were fed into the Genomatix GeneRanker tool for investigation of significantly overrepresented biological processes ($p < 0.01$) and the TOP10 hits were exported.

105.3 Results

105.3.1 Viability of ARPE19 Cells after 24 h Treatment with Cigarette Smoke Extract

In order to investigate viability and morphology of retinal pigment epithelial cells after treatment with CSE, confluent ARPE19 cells were treated with serum free medium containing different concentrations of CSE for 24 h. Viability and shape of the cells was then monitored under the microscope, with a clear decrease in cell count and viability after treatment with ≥ 30 % CSE (Fig. 105.1). For subsequent proteomic studies a concentration of 20 % CSE was chosen, a dosage below induction of apoptosis in the chosen timeframe.

105.3.2 Proteomic Alterations in ARPE19 Cells in Response to CSE Treatment

Three replicates of ARPE19 cells were treated with serum-free 20 % CSE for 24 h and compared to three replicates of untreated control cells by label-free quantitative LC-MS/MS. As typical mass spectrometric analyses allow for the identification of only up to 1500 proteins in a complex biological sample, we chose to establish a prefractionation workflow based on intra- and extracellular localisation of proteins

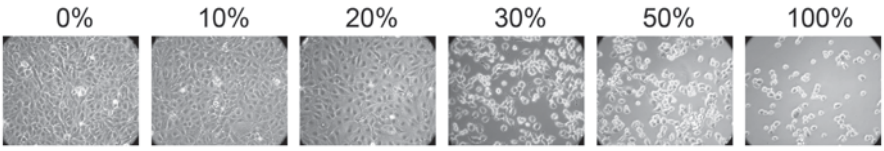

Fig. 105.1 Effect of cigarette smoke treatment on cell viability of ARPE19 cells. Confluent ARPE19 cells were treated with serum free medium containing the given percentage of cigarette smoke extract (CSE) for 24 h. Viability of the cells was then monitored, with a clear decrease in cell count after treatment with ≥ 30 % CSE. For subsequent proteomic studies a concentration of 20 % CSE was chosen

in our cell system of choice, the human ARPE19 cell line. With this setup, more than 3000 proteins could be identified, with 1932 proteins quantified with at least 2 peptides. A coefficient of variation of only 23 % (data not shown) indicated a high reproducibility of the workflow and therefore robust quantification of alterations in protein abundances in response to cigarette smoke treatment.

We found altogether 184 proteins 2-fold changed with a significance cut-off of $p < 0.05$. Of these, 64 proteins were found to be down-regulated after cigarette smoke treatment in comparison to 120 up-regulated proteins.

105.3.3 Pathway Enrichment Analysis

In order to identify significantly affected biological processes in the RPE cells in response to CSE treatment, we analysed these 184 altered proteins using the Generanker pathway enrichment analysis tool. We found altogether 345 affected biological processes with $p > 0.01$; the TOP10 GO-Terms are given in Fig. 105.2 with respective significance values below 0.00001 indicating very high significance. CSE treatment in RPE cells specifically led to alterations of proteins involved in RNA processing and transport (like e.g. SF3B2, HNRNPU and SRRM2) as well as extracellular matrix remodelling (e.g. LTBP3, CTGF and THBS1).

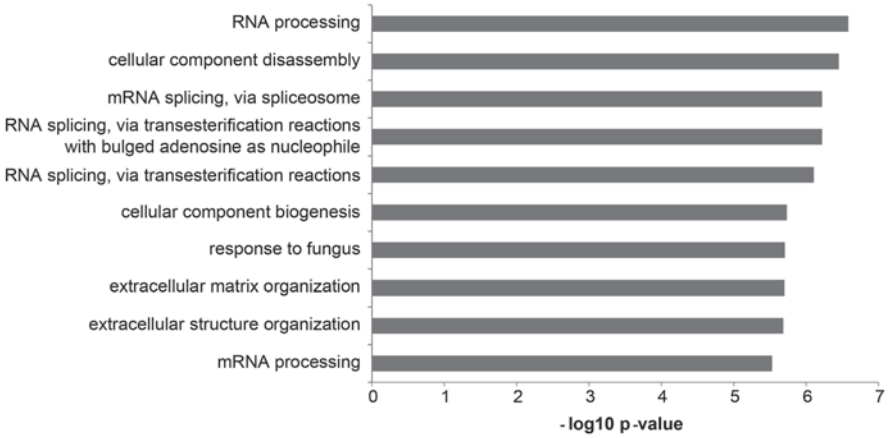

Fig. 105.2 Genomatix Generanker analysis of significantly altered biological processes after 24 h CSE treatment. The significantly altered proteins were fed in the Genomatix Generanker tool, in order to analyse altered biological processes after cigarette smoke treatment. The –log10 of the *p*-value is plotted for the TOP10 significantly altered biological processes

105.4 Discussion

To gain a better understanding of the influence of cigarette smoke treatment on RPE destruction in the context of AMD, we performed proteomic profiling of ARPE19 cells after cigarette smoke exposure in comparison to untreated controls by label-free LC-MS/MS.

We could see a clear dose-dependency looking at the viability and cell-shape of cultivated ARPE19 cells, as described previously (Bertram et al. 2009; Yu et al. 2012), with a clear decrease of cell and cell layer integrity at doses above 30% CSE. As our aim was to quantify differences in protein abundances in affected but still viable cells, we chose a concentration of 20% CSE for subsequent proteomic analysis.

We found approximately 22% of the identified 3000 proteins significantly altered between CSE-treated and untreated cells. Among those proteins we found some, which were already described to be affected by cigarette smoke treatment, like e.g. connective tissue growth factor (Yu et al. 2012), which was 4-fold upregulated and heme oxygenase 1 (Bertram et al. 2009), an indicator for oxidative stress which was 8-fold upregulated. Other proteins were clearly more abundant after CSE treatment without showing significance, like vascular endothelial growth factor (5-fold upregulated) and fibronectin (5-fold upregulated) in agreement with previous results (Bertram et al. 2009; Yu et al. 2012; Chu et al. 2013).

Activation of the complement cascade seems to be a general problem in AMD (Woodell and Rohrer 2014), underlined by the fact, that several complement factor genes were described as AMD risk genes in the past (Gorin 2012). We also found several complement factors upregulated after CSE treatment: CFH was 3-fold upregulated, C2S 2-fold and C1R also 2-fold, but all three were not significantly altered, due to a too high variation between the three replicates. Therefore the complement cascade was not found in the pathway enrichment analysis performed.

The pathway enrichment analysis revealed alterations of proteins involved in RNA processing and transport as well as extracellular matrix (ECM) remodelling in response to cigarette smoke treatment. While it has been shown before that the ECM undergoes severe changes during the different stages of AMD (Nita et al. 2014), including degradation or accumulation of structural components like e.g. fibronectin, little has been described so far on changes in RNA processing and transport in the context of AMD and/or cigarette smoke treatment of RPE cells. A recent study described different splicing patterns in the macula in comparison to peripheral regions of the retina (Li et al. 2014), indicating specific requirements of mRNA splicing and transport in the region primarily affected in AMD. Furthermore, it is speculated that different splicing isoforms of VEGF might influence retinal neovascularization (Carter et al. 2011). In our proteomic screen, we found several heterogeneous nuclear ribonucleoproteins (hnRNPs, e.g. HNRNPA2, HNRNPC) and mRNA splicing factors (e.g. U2AF2, SNRNP70) significantly upregulated after CSE treatment. Interestingly, also several proteins involved in ribosome synthesis and rRNA processing were found altered, like GAR1, NOP58 and DKC1. Recently, association of neurodegeneration and aging with nucleolar stress was described in Parkinson's disease and other neurodegenerative disorders (Parlato and Liss 2014).

We conclude that the described alterations triggered by cigarette smoke treatment might closely reflect AMD-like phenotypes and could lead to a better understanding of disease mechanisms in the future.

Acknowledgements We like to thank Sandra Helm and Silke Becker for technical assistance and Christine von Toerne for constructive discussions, and the Fritz Tobler Foundation for financial support.

References

Bertram KM, Baglole CJ, Phipps RP et al (2009) Molecular regulation of cigarette smoke induced-oxidative stress in human retinal pigment epithelial cells: implications for age-related macular degeneration. Am J Physiol, Cell Physiol 297:C1200–1210

Bhutto I, Lutty G (2012) Understanding age-related macular degeneration (AMD): Relationships between the photoreceptor/retinal pigment epithelium/Bruch's membrane/choriocapillaris complex. Mol Aspect Med 33:295–317

Brosch M, Yu L, Hubbard T et al (2009) Accurate and sensitive peptide identification with mascot percolator. J Proteome Res 8:3176–3181

Carter JG, Cherry J, Williams K et al (2011) Splicing factor polymorphisms, the control of VEGF isoforms and association with angiogenic eye disease. Curr Eye Res 36:328–335

Chu YK, Lee SC, Byeon SH (2013) VEGF rescues cigarette smoking-induced human RPE cell death by increasing autophagic flux: implications of the role of autophagy in advanced age-related macular degeneration. Invest Ophthalmol Vis Sci 54:7329–7337

Friedman DS, O'Colmain BJ, Muñoz B et al (2004) Prevalence of age-related macular degeneration in the United States. Arch Ophthalmol 122:564–572

Gorin MB (2012) Genetic insights into age-related macular degeneration: controversies addressing risk, causality, and therapeutics. Mol Aspects Med 33:467–486

Hauck SM, Dietter J, Kramer RL et al (2010) Deciphering membrane-associated molecular processes in target tissue of autoimmune uveitis by label-free quantitative mass spectrometry. Mol Cell Proteo 9:2292–2305

Li M, Jia C, Kazmierkiewicz KL et al (2014) Comprehensive analysis of gene expression in human retina and supporting tissues. Hum Mol Genet 23 (15):4001–4014

Lois N, Abdelkader E, Reglitz K et al (2008) Environmental tobacco smoke exposure and eye disease. Br J Ophthalmol 92:1304–1310

Merl J, Ueffing M, Hauck SM et al (2012) Direct comparison of MS-based label-free and SILAC quantitative proteome profiling strategies in primary retinal Müller cells. Proteomics 12:1902–1911

Nita M, Strzałka-Mrozik B, Grzybowski A et al (2014) Age-related macular degeneration and changes in the extracellular matrix. Med Sci Monit 20:1003–1016

Parlato R, Liss B (2014) How Parkinson's disease meets nucleolar stress. Biochim Biophys Acta 1842:791–797

Van Rijt SH, Keller IE, John G et al (2012) Acute cigarette smoke exposure impairs proteasome function in the lung. Am J Physiol Lung Cell Mol Physiol 303:L814–823

Wiśniewski JR, Zougman A, Nagaraj N, Mann M (2009) Universal sample preparation method for proteome analysis. Nat Methods 6:359–362

Wollscheid B, Bausch-Fluck D, Henderson C et al (2009) Mass-spectrometric identification and relative quantification of N-linked cell surface glycoproteins. Nat Biotechnol 27:378–386

Woodell A, Rohrer B (2014) A mechanistic review of cigarette smoke and age-related macular degeneration. Adv Exp Med Biol 801:301–307

Yu AL, Birke K, Burger J et al (2012) Biological effects of cigarette smoke in cultured human retinal pigment epithelial cells. PLoS ONE 7:e48501

Chapter 106
Reduced Metabolic Capacity in Aged Primary Retinal Pigment Epithelium (RPE) is Correlated with Increased Susceptibility to Oxidative Stress

Bärbel Rohrer, Mausumi Bandyopadhyay and Craig Beeson

Abstract One of the affected tissues in age-related macular degeneration (AMD) is the retinal pigment epithelium (RPE), a tissue that consists of terminally differentiated cells and that accumulates damage over time. In all tissues, mitochondria (mt), which play an essential role in both cell health (energy) and death (initiator of apoptosis), undergo an aging process through the accumulation of mtDNA damage, changes in mitochondrial dynamics, a reduction in biogenesis, and mitophagy, leading to an overall reduction in mitochondrial energy production and other non-energy-related functions. Here we have compared energy metabolism in primary human RPE cells isolated from aborted fetus or aged donor eyes and grown as stable monolayers. H_2O_2 treatment resulted in the generation of reactive oxygen species and superoxide, an effect that was significantly augmented by age. Mitochondrial metabolism, as analyzed by Seahorse respirometry, revealed reduced mitochondrial oxygen consumption (ATP production) at baseline and a complete loss of reserve capacity in aged cells. Likewise, glycolysis was blunted in aged cells. Taken together, these studies showed that RPE cells derived from aged donor eyes are more susceptible to oxidative stress, and exhibit a loss in mitochondrial respiratory reserve capacity and a reduction in glycolysis. These data suggest that while old cells may have sufficient energy at rest, they cannot mount a stress response requiring additional ATP and reducing agents. In summary, these data support the hypothesis that mitochondria or energy metabolism is a valid target for therapy in AMD.

B. Rohrer(✉) · M. Bandyopadhyay
Department of Ophthalmology, Medical University of South Carolina,
167 Ashley Ave, SEI614, Charleston, SC 29425, USA
e-mail: rohrer@musc.edu

C. Beeson
Department of Drug Discovery and Biomedical Sciences, Medical University of South Carolina,
167 Ashley Ave, SEI614, Charleston, SC 29425, USA

B. Rohrer
Research Service, Ralph H. Johnson VA Medical Center, Charleston, SC, USA

C. Bowes Rickman et al. (eds.), *Retinal Degenerative Diseases,* Advances in Experimental Medicine and Biology 854, DOI 10.1007/978-3-319-17121-0_106

Keywords Retinal pigment epithelium · Mitochondria · ATP production · Oxidative stress

106.1 Introduction

AMD is a slowly progressing multifactorial disease involving genetic abnormalities and environmental insults. Inflammation, oxidative stress and single nucleotide polymorphisms (SNPs) in genes in the complement cascade increase the risk for AMD. RPE cells are affected early and in all forms of AMD. The RPE is composed of a single layer of hexagonal highly pigmented cells, located between the retina and the choroid, forming part of the blood-retina barrier. Its many functions [reviewed by (Strauss 2005)] include: transport of molecules between the subretinal space and the choroidal blood supply; spatial ion buffering; secretion of growth factors, proteases, etc., that control the stability of photoreceptors, Bruch's membrane (BrM) and the choroid; and finally, modulation of the immune response, since the RPE participates in control of immune privilege in the healthy eye or mounting of an immune response in the diseased eye.

The unique phagocytotic function of the RPE, and the need to efficiently recycle the polyunsaturated fatty acid-rich (PUFA) shed outer segments, exposes the RPE to high levels of oxidative stress [reviewed by (Cai et al. 2000)]. Oxidation of PUFA initiates a chain reaction producing many reactive oxygen species (ROS). Furthermore, RPE cells contain many photosensitizers, and exposure to intense visible light induces generation of ROS. To cope with these toxic oxygen intermediates, the RPE has evolved effective defenses against oxidative damage; it is particularly rich in anti-oxidants. Due to this specialization, the RPE can withstand oxidative stress at levels that would typically kill cells. For example, our own work and that published by others has shown that RPE cells grown as monolayers with stable resistance, are resistant to oxidative stress, withstanding H_2O_2 treatment up to a concentration of 1 mM (Bailey et al. 2004; Thurman et al. 2009). However, with increasing age, the RPE antioxidative capability appears to be reduced (Cai et al. 2000). Likewise, old RPE cells appear to exhibit mitochondrial decay, such as mitochondrial fission and loss of mitochondrial morphology, bioenergetic deficiencies, and weakened antioxidant defenses (He and Tombran-Tink 2010), and the aging process overall is coupled to an increase in mitochondrial DNA mutations and mitochondrial disorganization (Miquel et al. 1980). Thus, it is likely that aged RPE cells are more susceptible to oxidative stress (Zarbin 2004). In support of this notion, the NEI-sponsored AREDS study demonstrated that subjects at risk for AMD and those with early AMD benefited from supplements containing high levels of antioxidants and zinc (Bartlett and Eperjesi 2003). While cellular bioenergetics (i.e., ATP production) have been assessed at baseline in human RPE cells (He and Tombran-Tink 2010), little is known about cellular bioenergetics under stress conditions.

106.2 Results

106.2.1 Oxidative Stress is Increased in Cells from Aged Donors

Primary human embryonic RPE cells as well as those isolated from donors (ages 68–72) were grown on Transwell plates as published previously (Bandyopadhyay and Rohrer 2012). Monolayer formation was monitored using transepithelial resistance (TER) measurements to ensure that monolayers of equal levels of differentiation were used (200–300 Ω/cm^2, obtained within 2–3 weeks of reaching confluence). At the time of the experiment, fetal bovine serum was removed from the growth media, which had no effect on the TER of established monolayers (Thurman et al. 2009). Monolayers could then be treated with apical application of 0.5 mM H_2O_2 to induce oxidative stress. Oxidative stress was analyzed by quantifying cytosolic reactive oxygen species (ROS) generation and super oxide production (O_2^-) with dichlorofluorescein diacetate and dihydroethedium, respectively (Fig. 106.1).

At baseline, in untreated cells, aged RPE cells appear to be under significant oxidative stress since ROS levels were significantly elevated by ~6-fold when compared to embryonic cells. Similarly, O_2^- are higher by ~4-fold. Interestingly, while in embryonic RPE cells, ROS levels increased significantly by ~3.5-fold in the H_2O_2-treated monolayers, no further increase over baseline levels could be observed in the aged RPE cells. In contrast, O_2^- levels did not change in cells of either age upon H_2O_2-treated exposure. Lack of cytotoxic effect was confirmed by monolayer morphology and lack of effect on TER [see (Bandyopadhyay and Rohrer 2012) for embryonic cells; data not shown for aged cells].

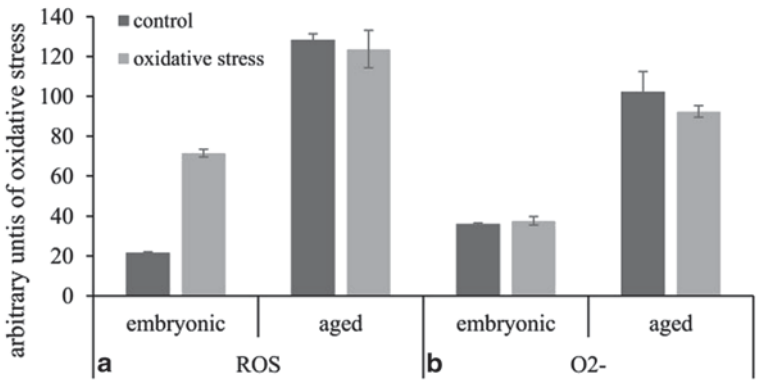

Fig. 106.1 Oxidative stress is increased in aged RPE cells. Cytosolic **a** reactive oxygen species (ROS) and **b** superoxide ($O2^-$) levels was measured using dichlorofluorescein diacetate dye and dihydroethidium, respectively. Both were significantly elevated in aged cells under control condition. Only in embryonic cells could ROS production be increased after exposure to oxidative stress (0.5 mM H_2O_2). Data are expressed as mean ± SEM (n = 3–4 per condition)

106.2.2 Aged RPE Cells have Reduced Mitochondrial and Glycolytic Metabolic Capacity

Cells take up substrates such as oxygen, glucose, fatty acids, etc., and convert them into energy stored as adenosine-triphosphate (ATP). ATP production requires a number of oxidation/reduction reactions involved in glycolysis (converts glucose into pyruvate), the tricarboxylic acid (TCA) cycle (oxidizes pyruvate-derived acetyl-CoA to generate ATP and reducing agents), and oxidative phosphorylation (utilizes NADH and succinate generated in the TCA cycle to establish a proton gradient to power the ATP synthase). As byproducts, heat, lactic acid and CO_2 are released into the extracellular environment. We have published previously on the usefulness of the Seahorse Biosciences XF analyzer (Seahorse Bioscience, Billerica, MD) to track real-time changes in cellular metabolism (Perron et al. 2012). This system uses fluorometric sensors to measure oxygen consumption rates (OCR) and extracellular acidification rates (ECAR) for a single cell layer on the bottom of multiwell plates (Ferrick et al. 2008). Cells were plated in 96-well custom plates and grown in parallel to cells on Transwell plates to determine the time point at which they differentiate and form a monolayer.

Rates were assessed at four stages, basal rate after 15 min of equilibration in the XF instrument, maximal respiratory capacity and mitochondrial oxygen consumption. The latter two parameters were assessed using the following inhibitors: Carbonyl cyanide-4-(trifluoromethoxy)phenylhydrazone (FCCP), a protonophore or an uncoupling agent, since it disrupts ATP synthesis by preventing the buildup of the proton gradient required as the energy source for oxidative phosphorylation; and, sodium azide, a potent inhibitor of mitochondrial respiration that blocks cytochrome c oxidase (complex IV). The normalized OCR (Fig. 106.2a) and ECAR (Fig. 106.2b) values are presented for statistical analysis.

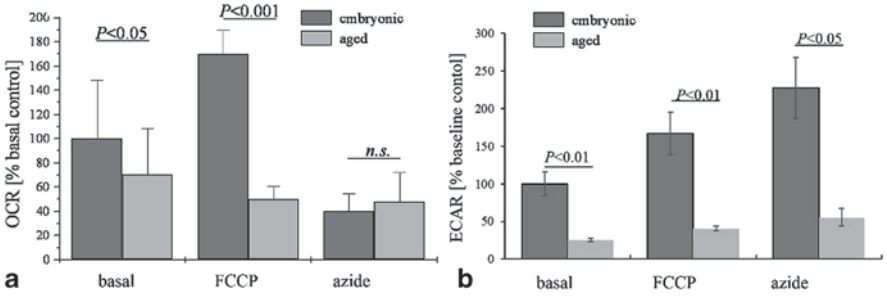

Fig. 106.2 Metabolism in RPE cells. Metabolism was assessed using Seahorse Extracellular Flux assays. Basal rate, maximal respiration (FCCP) and mitochondrial oxygen consumption (*azide*) were assessed in embryonic and aged RPE monolayers. Data are expressed as mean ± SEM ($n = 3–5$ per condition). **a** Summary for oxygen consumption rate (OCR); and **b** extracellular acidification rates (ECAR). Basal mitochondrial metabolism is reduced, but maximal capacity is almost abolished in aged RPE cells, while mitochondrial-dependent O_2 consumption was unaffected. ECAR was significantly reduced in aged cells for all three measures; with both age groups exhibiting an increase in glycolysis when mitochondrial respiration was reduced

RPE cells derived from embryonic donor eyes showed a typical behavior in the OCR analysis (Fig. 106.2a), with oxygen consumption rates being maximally stimulated by FCCP (1.7-fold increase when compared to baseline) and significantly inhibited by azide. In comparison, OCR rates in RPE cells derived from aged donor eyes were only slightly inhibited by azide, and maximal respiratory capacity was completely abolished. On average, basal OCR rates of aged RPE cells were within 30% of those exhibited by embryonic cells, but the maximal respiratory capacity, the additional ATP that can be produced under stress condition, can only be elicited from young but not aged donor cells.

RPE cells, irrespective of the donor age, showed a typical behavior in the ECAR analysis (Fig. 106.2b), in that the glycolytic capacity of the cells increased in response to the agents that interfered with oxidative phosphorylation. In both age-groups, ECAR increased by 60–67% after FCCP and by 118–128% after azide application. However, overall, glycolytic capacity was reduced in aged cells by ~75%.

Finally, it was tested whether OCR and ECAR rates are affected by oxidative stress. Basal respiration was significantly decreased in young RPE cells after H_2O_2-treatment (45 ± 2.8, $P < 0.001$), while rates were not affected in aged RPE cells when compared to untreated cells (13 ± 17.0, $P = 0.6$). Likewise, only the embryonic cells exhibited a drop in ECAR after H_2O_2-exposure (47 ± 7.7, $P < 0.01$), while the rates of aged RPE cells remained unchanged (basal: 8.0 ± 14.0, $P = 0.5$).

106.3 Discussion

Overall, the study was designed to determine the bioenergetics and antioxidant defenses in aged RPE cells. The overall conclusions from this analysis can be summarized as follows: (1) RPE cells from aged donors experience significant oxidative stress at baseline, which cannot be increased after exposure to H_2O_2; and concomitantly, (2) these aged cells have reduced mitochondrial and glycolytic metabolic capacity that cannot be further reduced by oxidative stress. Taken together, these bioenergetic deficiencies coupled with weakened antioxidant defenses may significantly reduce RPE function and contribute to age-related retinal anomalies.

The OCR and ECAR for a given cell type was correlated with the cells requirement for, or its ability to generate, energy and reducing agents. Here, we analyzed RPE cells in an artificial environment in which most of the normal tissue functions (i.e., retinoid metabolism, phagocytosis of rod outer segments, etc.) were eliminated. Stress was induced artificially by exposure of cells to H_2O_2 at a concentration known not to cause damage (Bandyopadhyay and Rohrer 2012). H_2O_2 has been shown previously to reduce state 3 respiration and reduce activity of TCA cycle enzymes (Nulton-Persson and Szweda 2001).

Embryonic RPE cells were found to exhibit a robust increase in oxygen consumption, demonstrating a significant mitochondrial respiratory capacity should additional energy be required. Likewise, embryonic cells appear to consume large

amounts of glucose, based on the ECAR levels, which can be elevated under mitochondrial stress conditions. Overall, between glycolysis and the pentose phosphate pathway (generation of reducing equivalents in the form of NADPH; not analyzed here), the embryonic cells appear to have sufficient reducing agents to maintain a non-oxidized environment. Exposure to H_2O_2 reduced mitochondrial respiration as well as glycolytic capacity, and concomitantly increased the amount of ROS present in the cells. In contrast, old RPE cells have reduced mitochondrial respiration and glycolytic capacity at baseline when compared to embryonic cells, which results in a highly oxidized cellular environment with elevated levels of ROS and O_2^-. This level of oxidative stress did not reduce mitochondrial respiration or alter the already elevated levels of increased amounts of ROS and O_2^- present in the cells; it did, however, further decrease the glycolytic capacity of the cell.

In future experiments, we wish to examine the possibility of ameliorating these bioenergetic deficiencies to increase energy production and bolster the cell's antioxidant defenses to improve RPE cell function and reduce its susceptibility to age-related changes and risk factors of age-related macular degeneration.

Acknowledgments This work was supported in part by the National Institutes of Health (R01EY019320), Veterans Affairs (I01 RX000444), Foundation Fighting Blindness, and an unrestricted grant to MUSC from Research to Prevent Blindness. The authors have no financial conflicts of interest.

References

Bailey TA, Kanuga N, Romero IA et al. (2004) Oxidative stress affects the junctional integrity of retinal pigment epithelial cells. Invest Ophthalmol Vis Sci 45:675–684

Bandyopadhyay M, Rohrer B (2012) Matrix metalloproteinase activity creates pro-angiogenic environment in primary human retinal pigment epithelial cells exposed to complement. Invest Ophthalmol Vis Sci 53:1953–1961

Bartlett H, Eperjesi F (2003) Age-related macular degeneration and nutritional supplementation: a review of randomised controlled trials. Ophthalmic Physiol Opt 23:383–399

Cai J, Nelson KC, Wu M et al. (2000) Oxidative damage and protection of the RPE. Prog Retin Eye Res 19:205–221

Ferrick DA, Neilson A, Beeson C (2008) Advances in measuring cellular bioenergetics using extracellular flux. Drug Discov Today 13:268–274

He Y, Tombran-Tink J (2010) Mitochondrial decay and impairment of antioxidant defenses in aging RPE cells. Adv Exp Med Biol 664:165–183

Miquel J, Economos AC, Fleming J et al. (1980) Mitochondrial role in cell aging. Exp Gerontol 15:575–591

Nulton-Persson AC, Szweda LI (2001) Modulation of mitochondrial function by hydrogen peroxide. J Biol Chem 276:23357–23361

Perron NR, Beeson C, Rohrer B (2012) Early alterations in mitochondrial reserve capacity; a means to predict subsequent photoreceptor cell death. J Bioenerg Biomembr 45:101–9

Strauss O (2005) The retinal pigment epithelium in visual function. Physiol Rev 85:845–881

Thurman JM, Renner B, Kunchithapautham K et al. (2009) Oxidative stress renders retinal pigment epithelial cells susceptible to complement-mediated injury. J Biol Chem 284:16939–16947

Zarbin MA (2004) Current concepts in the pathogenesis of age-related macular degeneration. Arch Ophthalmol 122:598–614

Erratum to: The Potential Use of PGC-1α and PGC-1β to Protect the Retina by Stimulating Mitochondrial Repair

Carolina Abrahan and John D. Ash

Erratum to:
Chapter 53 in: C. Bowes Rickman et al. (eds.), *Retinal Degenerative Diseases*, Advances in Experimental Medicine and Biology 854, DOI 10.1007/978-3-319-17121-0_53

Carolina Abrahan, the author has contributed to the mentioned chapter, however, the name was not mentioned in the files.

The online version of the original chapter can be found under DOI 10.1007/978-3-319-17121-0_53

J. D. Ash (✉)
Department of Ophthalmology, University of Florida, ARB-RG232, 1600 SW Archer Rd, Gainesville, FL 32610, USA
e-mail: jash@ufl.edu

C. Abrahan
Department of Environmental Horticulture Research, University of Florida, Gainesville, FL 32611-0670, USA
e-mail: cabrahan@ufl.edu

C. Bowes Rickman et al. (eds.), *Retinal Degenerative Diseases,* Advances in Experimental Medicine and Biology 854, DOI 10.1007/978-3-319-17121-0_107

Index

C. Bowes Rickman et al. (eds.), *Retinal Degenerative Diseases,* Advances in Experimental Medicine and Biology 854, DOI 10.1007/978-3-319-17121-0

B